
This is a reproduction of a library book that was digitized by Google as part of an ongoing effort to preserve the information in books and make it universally accessible.

GoogleTM books

<https://books.google.com>



Digitized by Google

THE
LONDON, EDINBURGH, AND DUBLIN
PHILOSOPHICAL MAGAZINE
AND
JOURNAL OF SCIENCE.

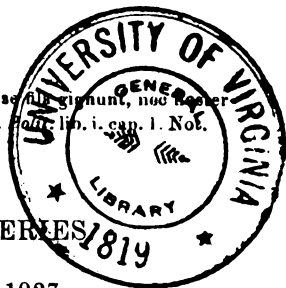
CONDUCTED BY

SIR OLIVER JOSEPH LODGE, D.Sc., LL.D., F.R.S.
SIR JOSEPH JOHN THOMSON, O.M., M.A., Sc.D., LL.D., F.R.S.
JOHN JOLY, M.A., D.Sc., F.R.S., F.G.S.
RICHARD TAUNTON FRANCIS, F.R.S.E.

AND

WILLIAM FRANCIS, F.I.S.

"Nec aranearum sane textus ideo melior quia ex se non gignunt, nec Reptilium
utilior quia ex alienis libamus ut apes." JUST. LIPS.



VOL. IV.—SEVENTH SERIES

JULY—DECEMBER 1927.

LONDON:

TAYLOR AND FRANCIS, RED LION COURT, FLEET STREET.

SOLD BY SMITH AND SON, GLASGOW;—HODGES, FIGGIS, AND CO., DUBLIN;—
AND VEUVÉ BOYVEAU, PARIS.

U. Va. 2-

Sci/Tech. Ctr.

Q

1

1 P5

090118

7th Sm.

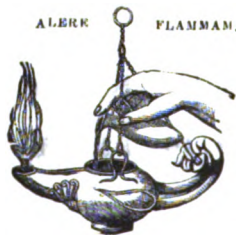
v.4

1027

"Meditationis est perscrutari occulta; contemplationis est admirari perspicua Admiratio generat quaestionem, quaestio investigationem, investigatio inventionem."—*Hugo de S. Victore.*

—“Cur spirent venti, cur terra dehiscat,
Cur mare turgescat, pelago cur tantus amaror,
Cur caput obscura Phœbus ferrugine condat,
Quid toties diros cogat flagrare cometas,
Quid pariat nubes, veniant cur fulmina coelo,
Quo micet igne Iris, superos quis conciat orbes
Tam vario motu.”

J. B. Pinelli ad Mazonium.



CONTENTS OF VOL. IV.

(SEVENTH SERIES).

NUMBER XX.—JULY 1927.

	Page
Dr. A. Ferguson and Mr. I. Vogel on the Storch Equation, a General Dilution Formula, and the Validity of the Law of Mass Action at Limiting Dilutions.....	1
Mr. J. Tutin on a Theoretical Investigation of the Phenomenon of Cavitation in Screw Propellers	17
Mr. T. McHugh on Placing Plane Quadrilaterals in Perspective. Application to Photography	28
Dr. N. K. Sur on the Origin of Terms of the Spectrum of Cobalt ..	36
Dr. K. G. Emeléus and Mr. N. L. Harris on the Geissler Discharge in Argon	49
Miss B. Trevelyan on Comparison of Discharges produced by Two and Three Electrode Systems in Hydrogen.....	64
Mr. R. M. Wilmotte on the Constants of Receiving and Transmitting Antennæ	78
Dr. J. D. Morgan on the Three-Point Spark Gap	91
Dr. R. L. Doan on Refraction of X-Rays by Method of Total Reflexion. (Plate I.)	100
Prof. Wali Mohammad and Mr. S. B. L. Mathur on the Fine Structure of the Spectrum Lines of Cadmium in the Ultra-Violet.....	112
Mr. W. Clarkson on the Lag in Electrical Discharges	121
Mr. G. D. Preston and Dr. E. A. Owen on the Atomic Structure of AuSn. (Plate II.)	133
Mr. T. L. Eckersley on the Transmission of Electric Waves through the Ionized Medium.	147
Dr. K. B. Blodgett on a Method of Measuring the Mean Free Path of Electrons in Ionized Mercury Vapour	165
Mr. P. K. Kichlu and Prof. M. Saha on the Explanation of Spectra of Metals of Group II.—Part II.	193
Mr. W. R. Dean: Note on the Motion of Fluid in a Curved Pipe ..	208
Prof. M. Saha: A Note on the Spectrum of Neon	223
M. Ponte on the Paper "On the Reflecting Power of the Carbon Atom for High-frequency Rays" (Phil Mag. iii. 1927, p. 195) ...	232
Dr. A. Ferguson and Mr. I. Vogel on the Calculation of the Equivalent Conductivity of Strong Electrolytes.—Part I. Aqueous Solutions. (ii.) Application to Data at 0°, 18°, and 25° C.	233
Messrs. A. H. Davis and N. Fleming on the Loud-Speaker as a Source of Sound for Reverberation Work.....	242
Mr. C. W. Davies on the Calculation of Activity Coefficients from Conductivity Measurements	244

	Page
Notices respecting New Books :—	
Dr. R. M. Caven's <i>Atoms and Molecules</i>	250
Prof. T. Levi-Civita's <i>The Absolute Differential Calculus</i>	250
Mr. C. V. Durell's <i>A Concise Geometrical Conics</i>	251
Proceedings of the Geological Society :—	
Mr. E. S. Cobbold on the Stratigraphy and Geological Structure of the Cambrian Area of Comley (Shropshire)	251
Mr. V. G. Glenday and Dr. J. Parkinson on the Kateruk Series and Associated Rocks of the Northern Suk Hills (Kenya Colony)	252
Mr. F. C. Phillips on the Serpentine of the Shetland Islands, and the Associated Rocks and Minerals	253
Dr. F. S. Wallis on the Old Red Sandstone of the Bristol District	254
Mr. J. E. Richey on the Structural Relations of the Mourne Granites (Ireland)	254
Dr. W. F. Whittard on the Stratigraphy of the Valentian Rocks of Shropshire: the Main Outcrop	255

NUMBER XXI.—AUGUST.

Prof. R. D. Kleeman on Properties of Substances in the Condensed State at the Absolute Zero of Temperature	257
Messrs. E. F. Relf and L. F. G. Simmons on a Distant-Reading Instrument for the Measurement of Small Deflexions	269
Mr. D. Meksyn on the Physical Form of Æther	272
Dr. A. Ferguson and Mr. I. Vogel on the Calculation of the Equivalent Conductivity of Strong Electrolytes at Infinite Dilution.—Part I. Aqueous Solutions. (iii.) The Mobilities of the Hydrogen and the Hydroxyl Ions	300
Dr. W. A. Leyshon on the Control of the Frequency of Flashing of a Neon Tube by a Maintained Mechanical Vibrator. (Plates III.–V.)	305
Prof. J. A. Crowther and Mr. J. A. V. Fairbrother on the Action of X-rays on Colloids	325
Prof. J. E. Verschaffelt on the Absolute Zero of Entropy and Internal Energy	335
Prof. J. Joly: Dr. Jeffreys and the Earth's Thermal History	338
Profs. F. H. Hummel and W. R. Morton on the Large Bending of Thin Flexible Strips and the Measurement of their Elasticity	348
Mr. E. L. Warren on the Surface-Tension Balance. (Plate VI.)	358
Prof. J. C. McLennan and Mr. C. D. Niven on Electrical Conductivity at Low Temperatures	386
Dr. K. C. Bailey on the Effect of Radon on the Solubility of Lead Uranate	404
Prof. J. C. McLennan and Dr. A. B. McLay on some New Regularities in Atomic Spectra	407
Notices respecting New Books :—	
Prof. A. S. Eddington's <i>Stars and Atoms</i>	413
Dr. G. L. Clark's <i>Applied X-Rays</i>	414
Prof. A. R. Forsyth's <i>The Calculus of Variations</i>	415
Mr. C. E. Weatherburn's <i>Differential Geometry of Three Dimensions</i>	415
Prof. Sommerfeld's <i>Three Lectures on Atomic Physics</i>	416

NUMBER XXII.—SEPTEMBER.

Prof. R. W. Wood and Mr. A. L. Loomis on the Physical and Biological Effects of High-frequency Sound-waves of Great Intensity. (Plates VII.-XIII.)	417
Prof. O. M. Corbino on the Electronic Theory of the Voltaic Cell	436
Prof. C. V. Raman on the Molecular Scattering of Light in a Binary Liquid-Mixture	447
Mr. A. J. Carr: Note on Green's Lemma and Stokes's Theorem	449
Dr. N. Rashevsky on Light-Quanta and Maxwell's Equations	459
Prof. R. W. Wood: Optical Excitation of Mercury, with Controlled Radiating States and Forbidden Lines. (Plate XIV.)	466
Prof. J. C. McLennan, Dr. A. B. McLay, and Mr. J. H. McLeod on the Structures of the Arc Spectra of Elements of the Oxygen Group	486
Mr. Y. Sugiura on the Application of Schrödinger's Wave Functions to the Calculation of Transition Probabilities for the Principal Series of Sodium	495
Dr. J. Taylor on Ionization by Collision and a "Photoelectric Theory" of the Sparking Potentials. A Reply to Mr. Huxley	505
Prof. L. Vegard on the Structure of Xenotime and the Relation between Chemical Constitution and Crystal Structure. (Plate XV.)	511
Prof. W. J. Walker on Heat Regeneration and Regenerative Cycles	526
Drs. D. M. Wrinch and J. W. Nicholson on a Class of Integral Equations occurring in Physics	531
Prof. R. A. Millikan and Mr. I. S. Bowen on Spectral Relationships of Lines arising from the Atoms of the First Row of the Periodic Table	561
Prof. Sir E. Rutherford on the Structure of the Radioactive Atom and Origin of the α -Rays	580
Prof. Sir E. Rutherford and Dr. J. Chadwick on the Scattering of α -particles by Helium	605
Dr. J. Brentano on Intensity Measurements of X-ray Reflexions from Fine Powders	620
Mr. J. H. Awbery on the Flow of Heat in a Body generating Heat	629
Notices respecting New Books:—	
Dr. C. J. Smithells's Tungsten: A Treatise on its Metallurgy, Properties, and Applications	638
Col. J. W. Gifford's Lens Computing	639
Prof. C. G. Darwin's Recent Developments in Atomic Theory	639
Dr. J. W. Mellor's A Comprehensive Treatise on Inorganic and Theoretical Chemistry. Vol. III. Ti, Zr, Hf, Th, Ge, Sn, Pb, Inert Gases	640
Collected Papers of Sir James Dewar	640

NUMBER XXIII.—OCTOBER.

Dr. R. H. de Waard on a Theory of the Magnetic Properties of Iron and other Metals	641
Messrs. H. Egnér and G. Hägg on the Effect of the Acidity of the Support on the Structure of Monomolecular Films	667
Prof. L. M. Alexander on the Absorption of X-Rays and Multiple Ionization of Atoms	670
Messrs. A. M. Taylor and E. K. Rideal on some Interference Effects in the Near Infra-red	682
Prof. J. M. Cork on the Crystal Structure of some of the Alums. (Plate XVI.)	688

	Page
Mr. J. J. Manley on the Union of Helium with Mercury	699
Miss A. Everett on the Tangent Lens Gauge Generalized	720
Prof. T. H. Havelock: A Note on the Dispersion of Methane.	721
Dr. N. R. Campbell on the Characteristics of Gasfilled Photoelectric Cells.—II.	726
Prof. C. G. Barkla and Dr. S. R. Khastgir on Modified and Unmodified Scattered X-Rays. (J-Phenomenon.—Part VII.)	735
Mr. J. Shearer on a Vacuum Spectrograph and its Use in the Long X-Ray Region. (Plate XVII.)	746
Mr. H. Buckley on the Radiation from the Inside of a Circular Cylinder	753
Prof. H. R. Robinson on Multiple Ionization in X-Ray Levels	763
Mr. G. R. Toshniwal on the Arc Spectrum of Bismuth	774
Prof. W. B. Morton and Mr. W. W. Bruce on the Action in Planetary Orbits	788
Dr. G. N. Antonoff on the Surface Tension of Rock-Salt	792
Dr. E. K. Sandeman on a Theory of the Torque Converter	800
Mr. R. C. Smith on the Viscosity Factor in Emulsification	820
Mr. L. C. Pocock on the Design of Networks for Balancing Telephone Lines	827
Mr. R. T. Lattey on the Dilution Law for Strong Electrolytes	831
Prof. E. L. Harrington on a Concentrated Arc Mercury Lamp. (Plate XVIII.)	836
Dr. E. R. Jones and Mr. C. R. Bury on the Freezing-Points of Concentrated Solutions.—Part II. Solutions of Formic, Acetic, Propionic, and Butyric Acids	841
Mr. W. Clarkson on Discharges and Discharge-Tube Characteristics. Notices respecting New Books:—	849
Tables Annuelles de Constantes et Données Numériques de Chimie, de Physique, et de Technologie. Vol. V.	867
Prof. A. E. H. Love's A Treatise on the Mathematical Theory of Elasticity.	867
Mr. V. T. Saunders's The Polarimeter, a Lecture on the Theory and Practice of Polarimetry	868
Mr. F. Bowman's Elementary Algebra. Part 2	868
Prof. A. M. Whitehead and Mr. B. Russell's Principia Mathematica ...	868
Mr. D. A. E. Garrod's The Upper Palæolithic Age in Great Britain	869
Rev. N. Jones's The Stone Age in Rhodesia	869
Dr. V. F. Hess's Die elektrische Leitfähigkeit der Atmosphäre und ihr Ursachen	870
Collected Researches: National Physical Laboratory	871
M. A. Forestier's L'Energie Rayonnante. Tableaux synoptiques de l'Echelle des Longueurs d'Onde et des principales caractéristiques du rayonnement électromagnétique avec un résumé des théories actuelles.	871
Prof. H. Freundlich's Colloid and Capillary Chemistry	872

NUMBER XXIV.—NOVEMBER.

Messrs. B. Topley and R. Whytlaw-Gray: Experiments on the Rate of Evaporation of Small Spheres as a Method of Determining Diffusion Coefficients.—The Diffusion Coefficient of Iodine	873
Mr. A. F. Dufton on the Warming of Walls.	888
Dr. W. N. Bond on Bubbles and Drops and Stokes' Law. (Plate XIX.)	889

Mr. L. G. H. Huxley on Ionization by Collision	899
Mr. A. O. Bartlett on an Extension of a Property of Artificial Lines	902
Dr. E. T. Paris on Resonance in Pipes Stopped with Imperfect Reflectors	907
Dr. E. C. Wadlow on the Effect of Variable Specific Heats upon the Velocity Generated, and upon the Temperature Drop, in Gases Expanding through Nozzles.	917
Mr. D. F. Martyn on Frequency Variations of the Triode Oscillator.	922
Prof. S. R. Milner on Maxwell's Stress, and its Time Rate of Variation	943
Mr. F. F. P. Bisacre on the Relativistic Rule for the Equipartition of Energy	949
Instructor-Captain T. Y. Baker on the Refraction of Electromagnetic Waves in a Spherically Stratified Medium	955
Mr. C. R. Bury on the Adsorption of Butyric Acid on Water Surfaces	980
Prof. L. Vegard and Mr. K. Sollesnes on the Structure of Isomorphous Substances $N(CH_3)_4I$, $N(CH_3)_4Br$, $N(CH_3)_4Cl$. (Plates XX. & XXI.)	985
Mr. W. Clarkson on Condenser Discharges in Discharge-Tubes.—Part I. Single Condenser Discharges.	1002
Notices respecting New Books:—	
Dr. M. von Laue's <i>La Théorie de la Relativité: Tome II. La Relativité Générale de la Théorie de la Gravitation d'Einstein</i>	1015
von H. Rosenbroch's <i>Microkopische Physiographie der petrographisch wichtigen Mineralien</i>	1016

NUMBER XXV.—NOVEMBER (SUPPLEMENT).

Dr. W. Hume-Rothery on the Metallic State	1017
Mr. H. L. Green on the Application of the Aitken Effect to the Study of Aerosols. (Plate XXII.)	1046
Dr. L. C. Jackson on Atomic Structure and the Magnetic Properties of Coordination Compounds.—Part II.	1070
Dr. R. T. Beatty on Resonant Circuits with Reactive Coupling ...	1081
Messrs. S. A. Higgs and L. C. Tyte on the Effect of Various Flange Systems on the Open-end Correction of a Square Organ Pipe. (Plates XXIII. & XXIV.)	1099
Dr. E. R. Jones and Mr. C. R. Bury on the Freezing-Points of Concentrated Solutions. Part III. Solutions of Phenol	1125
Sir J. J. Thomson on the Electrodeless Discharge through Gases.	1128
Prof. W. M. Hicks on the Analysis of the Copper Spectrum	1161
Mr. I. Waller on the Scattering of Radiation from Atoms	1228
Messrs. L. J. Briggs and H. L. Dryden on Cavitation in Screw Propellers	1237
Mr. H. Glauert on Cavitation in Screw Propellers	1239
Mr. J. Tutin on Cavitation in Screw Propellers	1241
Mr. A. Holmes on the Effect of Radon on the Solubility of Lead Uranate	1242
Notices respecting New Books:—	
Prof. E. Bloch's <i>Thermionic Phenomena</i>	1243
Mr. Bray's <i>Light</i>	1243
Mr. G. O. Blake's <i>History of Radio-Telegraphy and Telephony</i>	1243
Prof. E. C. C. Baly's <i>Spectroscopy</i>	1244

NUMBER XXVI.—DECEMBER.

Prof. A. Press on Thermodynamic Integrating Factors	1245
Prof. A. Press on Consequences of a Matrix Mechanics and a Radiating Harmonic Oscillator without the Quantum Postulate ..	1249
Prof. A. F. Kovarik on the Behaviour of Small Quantities of Radon at Low Temperatures and Low Pressures	1262
Dr. W. A. Caspari on the Crystallography of some Simple Benzene Derivatives	1276
Mr. E. E. Libman on a Theory of Porous Flow	1285
Dr. L. Silberstein on the Transparency of Turbid Media	1291
Prof. F. K. Richtmyer on some Comments on the Classical Theories of the Absorption and Refraction of X-Rays	1296
Mr. W. M. Jones and Prof. E. J. Evans on the Crystal Structure of Cu_3Sn and Cu_3Sb	1302
Miss P. Jones on the Hall Effect in Aluminium Crystals in relation to Crystal Size and Orientation	1312
Mr. J. J. Manley on the Silvering of Glass Plates for Optical Instruments	1322
Dr. G. E. Allan on the Accuracy of the Monochord as a Measurer of Frequency	1324
Dr. A. L. Norbury and Mr. K. Kuwada on the Temperature-Electrical Resistivity Relationship in certain Copper Alpha Solid Solution Alloys	1338
Mr. W. Clarkson on Condenser Discharges in Discharge-Tubes.—Part II. The Intermittent Discharge	1341
Dr. J. Taylor on a new form of Voltmeter for measuring the Average Voltage for Alternating Currents	1356
Notices respecting New Books:—	
Sir N. Shaw's Manual of Meteorology. Vol. I. Meteorology in History ..	1359
Herren H. Ambronn und A. Frey's Das Polarisationmikroskop: seine Anwendung in der Kolloidforschung und in der Färberei	1360
Prof. F. R. Moulton's New Methods in Exterior Ballistics ..	1360
Prof. A. S. Eddington's The Internal Constitution of the Stars ..	1361
Prof. W. J. Dakin's The Elements of General Zoology. A Guide to the Study of Animal Biology, correlating Functions and Structure, with Notes on Practical Exercises	1362
The Scientific Work of the Late Spencer Pickering, F.R.S.	1362
Prof. R. Biswas's Theory of Equations and the Complex Variable	1363
Dr. G. W. C. Kaye's High Vacua	1363
Index	1364

P L A T E S.

- I. Illustrative of Dr. R. L. Doan's Paper on Refraction of X-Rays by Method of Total Reflexion.
- II. Illustrative of Mr. G. D. Preston and Dr. E. A. Owen's Paper on the Atomic Structure of AuSn.
- III.-V. Illustrative of Dr. W. A. Leyshon's Paper on the Control of the Frequency of Flashing of a Neon Tube by a Maintained Mechanical Vibrator.
- VI. Illustrative of Mr. E. L. Warren's Paper on the Surface-Tension Balance.
- VII.-XIII. Illustrative of Prof. R. W. Wood and Mr. A. L. Loomis's Paper on the Physical and Biological Effects of High-frequency Sound-waves of Great Intensity.
- XIV. Illustrative of Prof. R. W. Wood's Paper on Optical Excitation of Mercury, with Controlled Radiating States and Forbidden Lines.
- XV. Illustrative of Prof. L. Vegard's Paper on the Structure of Xenotime and the Relation between Chemical Constitution and Crystal Structure.
- XVI. Illustrative of Prof. J. M. Cork's Paper on the Crystal Structure of some of the Alums.
- XVII. Illustrative of Mr. J. Shearer's Paper on a Vacuum Spectrograph and its Use in the Long X-Ray Region.
- XVIII. Illustrative of Dr. E. L. Harrington's Paper on a Concentrated Arc Mercury Lamp.
- XIX. Illustrative of Dr. W. N. Bond's Paper on Bubbles and Drops and Stokes' Law.
- XX. & XXI. Illustrative of Prof. L. Vegard and Mr. K. Sollesnes's Paper on the Structure of the Isomorphic Substances $N(CH_3)_4I$, $N(CH_3)_4Br$, $N(CH_3)_4Cl$.
- XXII. Illustrative of Mr. H. L. Green's Paper on the Application of the Aitken Effect to the Study of Aerosols.
- XXIII. & XXIV. Illustrative of Messrs. S. A. Higgs and L. C. Tyte's Paper on the Effect of Various Flange Systems on the Open-end Correction of a Square Organ Pipe.

ERRATA.

In the paper by Prof. W. M. Hicks in the Supplement of last month the following errata are necessary:—

Page 1176, line 15, for p. 1165 read p. 1164.

Page 1178, line 26, for B read A.

Page 1181, line 26, for J read K.

Page 1190, in quartet displacements in Z_{23} read $(-17\delta-2\delta_1)$ for $(-4\Delta-2\delta_1)$.

Page 1207, line 8 from bottom, subscript to d should be $_3$.

Page 1213, line 2, dele "with quartic index omitted."

„ line 10 from bottom, for 29037 read 29057, and for $v.P_1$ read $u.P_1$.

THE
LONDON, EDINBURGH, AND DUBLIN
PHILOSOPHICAL MAGAZINE
AND
JOURNAL OF SCIENCE.

[SEVENTH SERIES.]

JULY 1927.

- I. *The Storch Equation, a General Dilution Formula, and the Validity of the Law of Mass Action at Limiting Dilutions.* By ALLAN FERGUSON, M.A., D.Sc., and ISRAEL VOGEL, M.Sc., D.I.C.*

IN the present investigation the authors propose to discuss the application to electrolytes of various types of the Storch equation, either with constant exponent (Storch, *Z. phys. Chem.* 1896, xix. p. 13; Bancroft, *ibid.* 1899, xxxi. p. 188), or in a more general form with the exponent (n) considered as a linear function of the concentration.

The Storch equation,

$$\frac{(Ca)^n}{C(1-\alpha)} = K, \quad (1)$$

may be written

$$n \log (Ca) = \log K + \log C(1-\alpha), \quad (2)$$

and a plot of $\log (Ca)$ against $\log C(1-\alpha)$ yields a rectilinear graph only if n be independent of the concentration †. The slope and intercept of the graph determine n and K , and where the law is followed we have found it possible to determine n correct to four significant figures by using large sheets of precision graph paper.

Equation (1) has, apart from its use by Noyes and his colleagues (see papers in *J. Amer. Chem. Soc.* 1908-13, cf. especially *J. Amer. Chem. Soc.* 1908, xxx. p. 335) and by Bates (*ibid.* 1913, xxxv. p. 519), hardly received the

* Communicated by the Authors.

† α is a symbol for Δ/Δ_0 .

attention which it merits. Our own investigations show that for certain electrolytes the simple Storch equation holds almost to normal concentrations. For others, the simple equation is valid up to concentrations of the order of one hundredth normal, at which point a departure from the linear equation is manifested. This departure often becomes apparent for concentrations at which the so-called viscosity correction is assumed to become sensible. For a third type, the linear equation is departed from at a comparatively early stage. For samples of these types we have been able to show that the assumption that $n (=a+bC)$ is a linear function of the concentration brings them satisfactorily into line*, and we are able to exhibit a general method for the calculation of the constants a , b , and K .

We have deemed it well to make the Storch form the starting-point of our investigation, since it seems to us that this form, especially when exhibited by means of a rectilinear plot, serves admirably to test the validity of Ostwald's dilution formula at limiting dilutions. It has been asserted (Washburn, J. Amer. Chem. Soc. 1918, xl. p. 122) that the theoretical basis of Ostwald's formula is such that any dilution formula which does not yield it as a limiting case is to be rejected on that account, and further, that measurements made at the lowest concentrations show results which can be interpreted only in terms of Ostwald's formula. Concerning these dicta, we would merely say that the first encourages a dangerous tendency to force facts to fit theories, and that it is always possible, even in a simple theoretical deduction, to overlook some factor which may profoundly modify our formulæ. With respect to the second (Weiland, J. Amer. Chem. Soc. 1918, xl. p. 131; Washburn, *ibid.* 1918, xl. p. 150)—and we refer here particularly to Weiland's very careful measurements on potassium chloride at 18° (*loc. cit.*),—we think that their interpretation is erroneous, as we shall later attempt to show.

When we assert that Ostwald's law is, or is not, true at zero concentration, when we define Λ_0 as the equivalent limiting conductance, what do we mean exactly? Surely no more than this: that if the law followed at finite concentrations be assumed to hold good in the limit, we are then led to limiting values of certain constants given by the expressions mentioned above. Emphatically, we do not assert that we should find these values were it possible, for example, to measure the equivalent conductance of a single

* Iodic acid is the one exception.

molecule in an infinite ocean of solvent. Indeed, the theoretical basis of Ostwald's law, statistical as it is in character, becomes as meaningless in the limit as the expression "temperature of a single molecule." The validity of Ostwald's law at limiting concentrations can, we take it, mean nothing more than that over a limited range of low but *finite* concentration the expression $\frac{(C\alpha)^2}{C(1-\alpha)}$ is a constant quantity.

Now this may be tested either directly by experiment at *low* concentrations or by extrapolating the results obtained at higher concentrations. Weiland's results for potassium chloride are usually quoted as showing directly that the law is followed over the range 0.00002 to 0.00007 normal. His results are exhibited in Table I.

TABLE I.
Potassium Chloride, 18°.

Concentration *.	K_E (Weiland).	K_E (Authors).
1.0×10^{-3}	0.02000	0.01921
2.0×10^{-3}	0.02002	0.02016
3.0×10^{-3}	0.02003	0.01994
4.0×10^{-3}	0.02006	0.02002
5.0×10^{-3}	0.02014	0.02014
6.0×10^{-3}	0.02022	0.02022
7.0×10^{-3}	0.02035	0.02033
8.0×10^{-3}	0.02050	0.02051
9.0×10^{-3}	0.02070	0.02065
1.0×10^{-2}	0.02102	0.02103

Now the fundamental criticism of his figures *as they stand* is that over *no* region of finite concentration is the quantity $\frac{(C\alpha)^2}{C(1-\alpha)} = K_E$ constant. This function over the whole range measured is varying continuously with C , although certainly more slowly as the concentration decreases. Unfortunately the variation, owing to errors in Weiland's calculations, is even more pronounced than is indicated in column 2, the values as recalculated by the authors from Weiland's figures

* C will be expressed in gram equivalents per litre throughout this paper.

being given in column 3. The pronounced variation of the quantity K_E over the whole range of concentration completely destroys the value of this, the only direct experimental evidence quoted in support of Ostwald's dilution law for aqueous salt solutions.

Kraus and Parker's experiments (J. Amer. Chem. Soc. 1922, xlv. p. 2429) with iodic acid and Parker's experiments (*ibid.* 1923, xlv. p. 2017) with hydrochloric acid are commonly quoted as affording evidence for the validity of the mass-action law at low concentrations. For iodic acid at 25° we find n equal to 2.000 over a fairly wide range ($C=0.00005$ to $C=0.001$ normal). Hydrochloric acid affords an interesting commentary on our views. Taking Parker's figures at 25° and recalculating them, we find the column headed K_E , in which it will be seen that the constancy is not quite so good as it appears in Parker's original table. In Table II. the value for Λ_0 is, of course, that assumed by Parker, viz. 425.69. If, however, we recalculate Parker's figures, assuming the value for Λ_0 of 425.68 which we have calculated by other methods, we arrive at the column headed K_{E_1} .

TABLE II.

Hydrochloric Acid, 25° C.

Concentration.	K_E (Parker).	K_{E_1} .	K_{E_2} .
5.0×10^{-5}	0.105	0.1063	0.1120
1.0×10^{-4}	0.105	0.1051	0.1090
2.0×10^{-4}	0.105	0.1049	0.1060
5.0×10^{-4}	0.1051	0.1049	0.1054
1.0×10^{-3}	0.1131	0.1132	0.1137
2.0×10^{-3}	0.1421	0.1422	0.1426
3.0×10^{-3}	0.1726	0.1727	0.1705

Now Washburn (J. Amer. Chem. Soc. 1918, xl. p. 124) has said :—"Of course it is true that if one starts with the *a priori* assumption that the Mass-action law will never be obeyed, and then proceeds to determine a Λ_0 value in harmony with this assumption, then naturally it might not be difficult with the aid of this to compute values for the Mass-action expression K_E which would not exhibit any pronounced tendency to conform to the Mass-action law. . . ." Quite true; and *mutatis mutandis* the argument applies if one

assumes the truth of the mass-action law and calculates values of Λ_0 in accordance with that assumption.

Hydrochloric acid admirably illustrates the dangers attendant on any *a priori* assumptions concerning figures obtained at low concentrations. The quantity $(1-\alpha)$ is very nearly zero, and an error of 1 in 10,000 in Λ_0 may burden $(1-\alpha)$ with a systematic 10-per-cent. error, more or less. If, then, one makes *any* assumption whatever with regard to the mass law in calculating Λ_0 , it is more than probable that one will see that assumption reflected in the form of the dilution equation deduced. Thus, if instead of tracing the variations of K_g —in itself a process of doubtful validity—we make a logarithmic plot of equation (2), using Parker's figures for the four points of low concentration, we find a good straight line which yields quite definitely the value $n=2.00$. If, however, still using Parker's experimental figures, we adopt the number 425.68 for Λ_0 , we find that the same four points determine in a perfectly unambiguous way a straight line for which n is 2.02. That is, a change of 1 in 40,000 in the value of Λ_0 produces a change in n of about one per cent. Clearly quantitative arguments based on low concentration results *alone* are exceedingly dangerous; and if the argument is weighted with any assumption *pro* or *con*, the result is more or less a foregone conclusion.

It seems to us that the correct procedure in testing the validity or invalidity of Ostwald's dilution formula is to assume a dilution formula which is a simple generalized form of Ostwald's equation, and to see if the constants of this formula determined over as wide a range of concentration as possible are such as to yield Ostwald's formula at limiting concentrations. The correctness of this procedure is further emphasized by making a determination of the constants at "middle" concentrations, plotting functions of α and C which yield a rectilinear graph. If it be then found that all the points for lower concentrations fall automatically on the straight line, we are *fully* justified in an extrapolation to zero concentration. We emphasize this point, since a rectilinear graph shows very markedly whether the law assumed is a *vera causa*, or merely a good approximation. Conversely, the deduction of constants from a curvilinear graph is at best a dangerous expedient, and one not to be adopted if a rectilinear graph can be drawn.

The Storch equation in the form (2) over low and medium—and sometimes indeed up to high—concentrations gives an admirable straight line. Departures from this straight line,

when they exist, are apparent in regions of *high* concentration. If a straight-line graph be established over a region of medium concentration, in every instance which we have examined—and they are some nineteen in number—we find the law automatically followed by the points of lower concentration down to the minimum concentration measured.

It would be difficult, it seems to us, to devise a more indifferent* test of the validity of Ostwald's law. We assume neither its validity nor its invalidity; our only assumption is that the form of the dilution equation is

$$\frac{(C\alpha)^n}{C(1-\alpha)} = K, \text{ where } n \text{ may or may not be constant, and the}$$

very form itself is tested by the rectilinearity of the plot based on equation (2). If, then, we find that the plot is rectilinear down to the lowest concentrations measured and shows no signs of wavering, and the slope is such that n is equal to 2, so much the better for Ostwald's law. If not, —. Or, if the results are better fitted by $n = a + bC$, then, for the validity of Ostwald's equation, a must be equal to 2.

But what of the value of Λ_0 used in the calculation of α ? Does Washburn's criticism (*ibid.* p. 124) apply here? We do not think so; for again, in the equation

$$\Lambda_0 = \Lambda + BC^{n_0}, \quad . \quad . \quad . \quad . \quad . \quad (3)$$

which we have used for the computation of Λ_0 , we make no assumption whatever as to the validity or invalidity of Ostwald's equation. The rectilinear graphs obtained show that equation (3) is accurately followed over the region of concentration studied, and show—what is of primary importance—that there is no wavering from the law as the concentration falls. Moreover, *the values of n_0 and of B vary from substance to substance, and in a regular manner for related substances* (Ferguson and Vogel, *Phil. Mag.* 1925, 1, p. 971). It follows, therefore, that the usual assumption that n_0 is independent of the nature of the electrolyte must lead to values of Λ_0 of doubtful validity †.

Now, equation (3), which we assume to hold good only over low concentrations, is, as it should be to be logically used to furnish values of Λ_0 for use with the Storch equation, a limiting case of that formula.

* We use the word in its old sense.

† This remark is not without importance in view of the fact that the Debye-Hückel theory leads to a value of n equal to 0.5.

For, putting $\alpha = \Lambda/\Lambda_0$, equation (1) becomes

$$K\Lambda_0^{n-1}(\Lambda_0 - \Lambda) = C^{n-1}\Lambda^n,$$

$$\Lambda_0 = \Lambda + \frac{\Lambda^n}{K\Lambda_0^{n-1}} C^{n-1}.$$

For low values of C the second term on the right-hand side is small. Putting in this small term the approximate value Λ_0 for Λ , we obtain

$$\Lambda_0 = \Lambda + \frac{\Lambda_0}{K} C^{n-1},$$

taking the form (3) with n_0 *approximately* equal to $n-1$ and B *approximately* equal to Λ_0/K . The degree of agreement is shown in Table III. below, in which are exhibited

TABLE III.

Electrolyte.	n_0 .	$1+n_0$.	n .
NaCl	0.4431	1.4431	1.4763
KCl	0.4520	1.4520	1.4867
LiCl	0.4364	1.4364	1.4612
NaNO ₃	0.4458	1.4458	1.4484
KNO ₃	0.4796	1.4796	1.4916
LiNO ₃	0.4253	1.4253	1.4465
NaIO ₃	0.4551	1.4551	1.4877
KIO ₃	0.4604	1.4604	1.4566
LiIO ₃	0.4422	1.4422	1.4715
Ca(NO ₃) ₂ ...	0.4196	1.4196	1.4312
Sr(NO ₃) ₂ ...	0.4582	1.4582	1.4916
Ba(NO ₃) ₂ ...	0.5120	1.5120	1.5436
CuSO ₄	0.5711	1.5711	1.6429
OdSO ₄	0.5511	1.5511	1.6487
HIO ₃	0.9687	1.9687	2.0000
HCl	0.9672	1.9672	2.0158

the values of n_0 (deduced from equation (3)) and of $n_0 + 1$ and of n .

The acceptance of equation (3) as an accurate representation of the facts down to the lowest observed concentrations has important consequences. For if Ostwald's law be valid over any of the regions studied, or be approached as a more or less limiting case, we shall have n_0 constant at a value

Fig. 1.

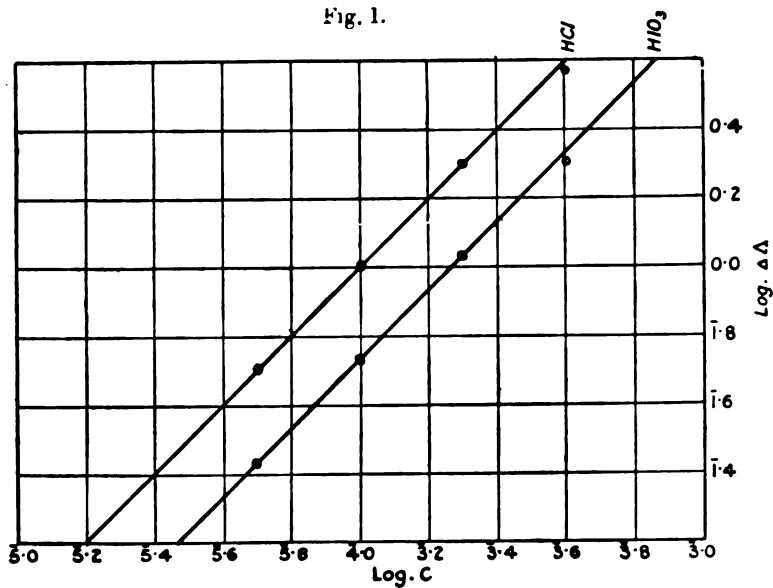
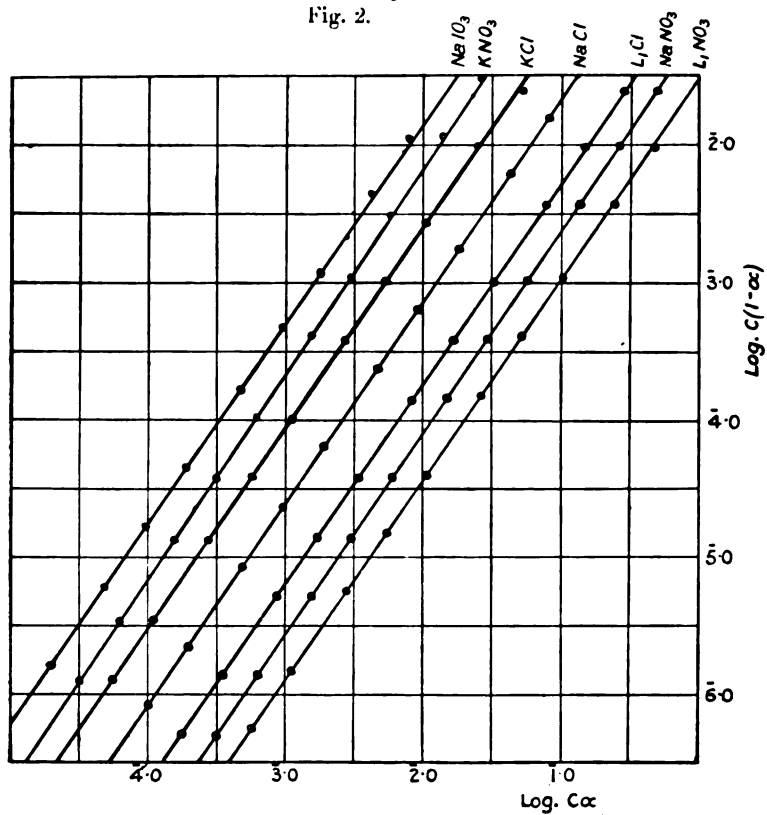


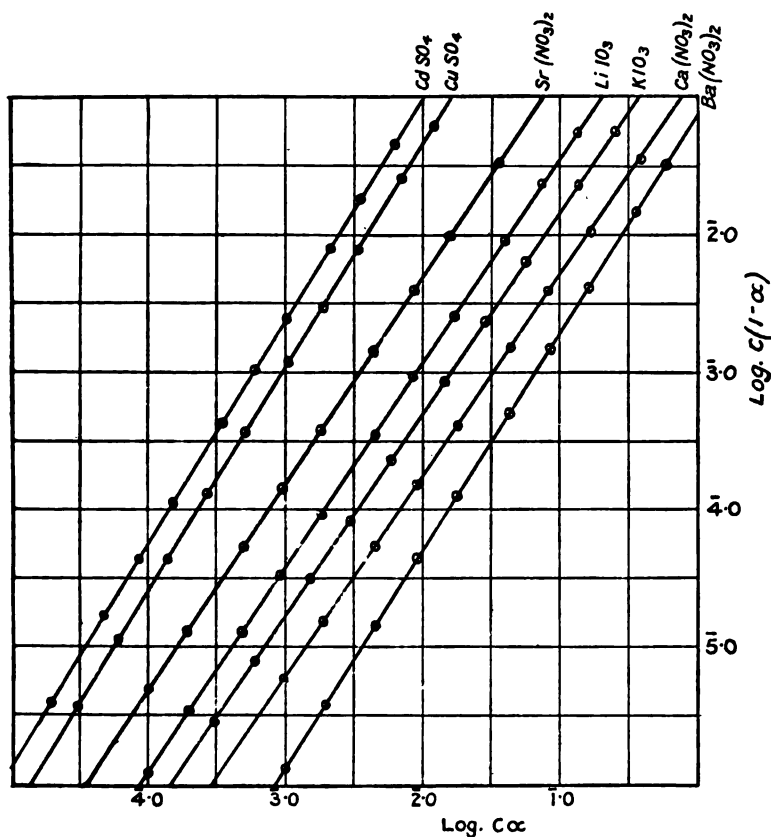
Fig. 2.



approximating to unity, or variable and approaching unity as a limiting value. These facts show that n_0 is constant within the range of experimental error, and Table III. shows that for iodic and hydrochloric acids only is the exponent in the neighbourhood of unity. The rectilinear graphs for these two acids are shown in fig. 1.

We now proceed to test the validity of the simple Storch equation by the logarithmic plot of equation (2). Figs. 2, 3, and 4 exhibit graphically the results for all the

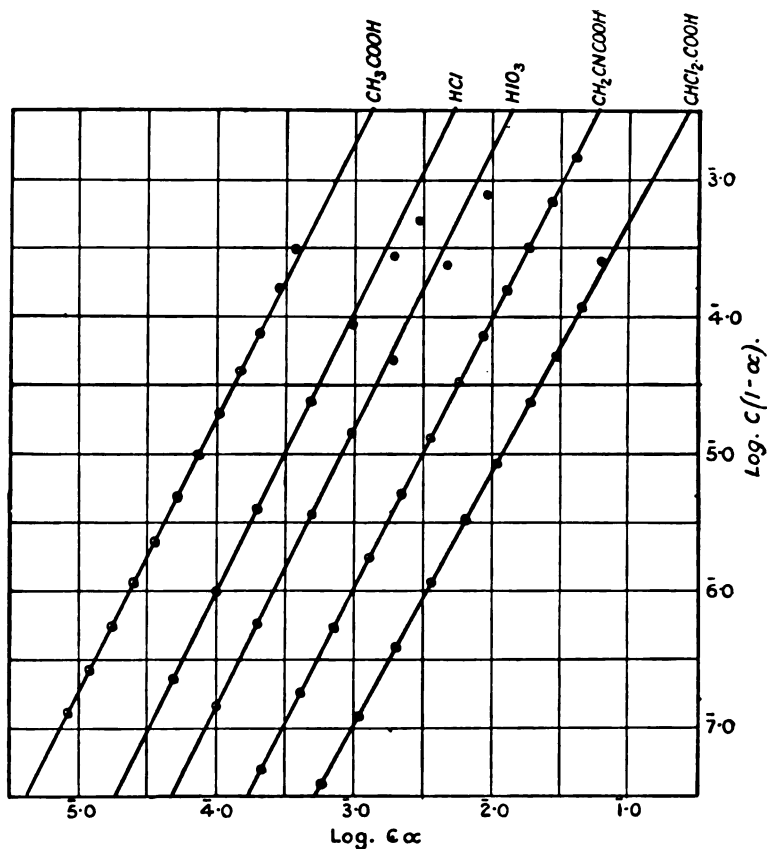
Fig. 3.



substances examined, and the closeness with which the solutions follow this law is measured by the rectilinearity of the line drawn through the observed points shown. Having

determined n from these lines, it is possible to calculate for each concentration a value for K , and any irregularities in the values so computed serve further to test the closeness with which, and the range over which, the law is followed.

Fig. 4.



In Table IV. we exhibit a number of these values for typical electrolytes, and in Table V. we give a conspectus of the values of n , the mean values of K , and the range of validity of the equation for all the electrolytes studied.

The Storch Equation.

TABLE IV.

"Strong" Electrolytes.

Concentration ...	5.0×10^{-3}	1.0×10^{-4}	2.0×10^{-4}	5.0×10^{-4}	1.0×10^{-3}	2.0×10^{-3}	5.0×10^{-3}	1.0×10^{-2}	2.0×10^{-2}	5.0×10^{-2}	1.0×10^{-1}	2.0×10^{-1}	5.0×10^{-1}	1
LiCl	—	1.50	1.57	1.54	1.56	1.55	1.55	1.54	1.55	1.57	1.57	1.67	1.55	1.44
LiNO ₃	—	1.64	1.67	1.66	1.66	1.65	1.63	1.62	1.60	1.61	1.61	1.61	1.56	1.44
Sr(NO ₃) ₂	—	0.68	0.69	0.69	0.68	0.68	0.67	0.67	0.67	0.67	0.68	0.68	0.64	0.58
Ba(NO ₃) ₂	—	0.49	0.50	0.50	0.50	0.49	0.48	0.48	0.48	0.48	0.48	0.47	0.43	—
CuSO ₄	—	0.068	0.070	0.069	0.068	0.066	0.065	0.065	0.066	0.071	0.077	0.086	—	0.112
CdSO ₄	—	0.036	0.058	0.059	0.059	0.058	0.058	0.058	0.059	0.063	0.068	0.075	0.087	0.093
HCl	0.006	0.004	0.003	0.002	0.102	0.129	0.158	—	—	—	—	—	—	—
HIO ₃	0.075	0.073	0.072	0.072	0.075	0.082	0.097	0.113	0.132	0.158	0.180	0.205	—	—

"Intermediate" or "Transition" Electrolytes.

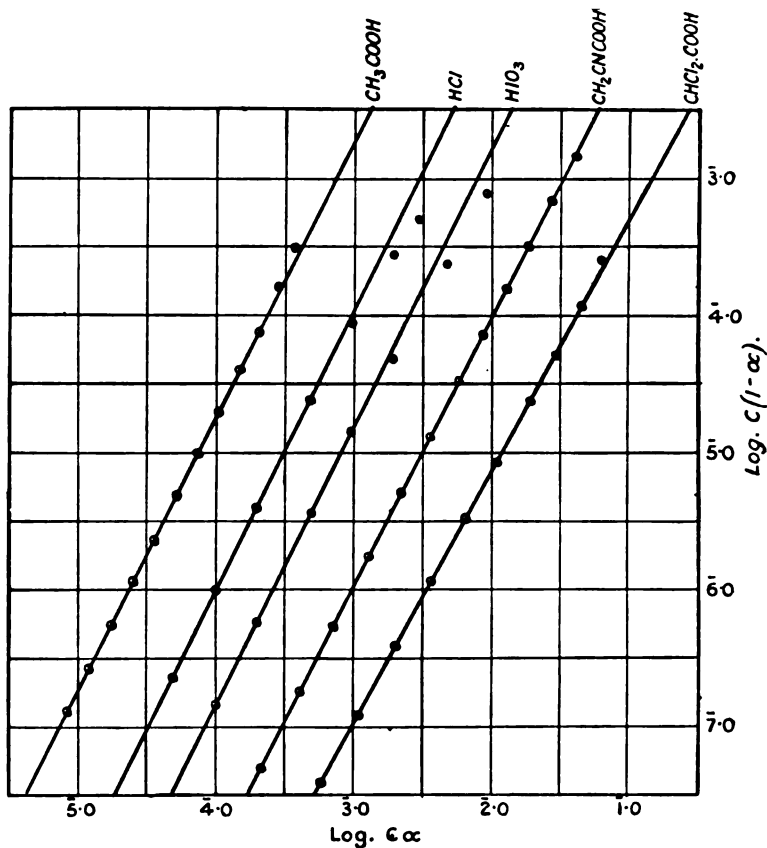
Concentration ...	2.322×10^{-4}	4.645×10^{-4}	9.290×10^{-4}	1.858×10^{-3}	3.716×10^{-3}	7.429×10^{-3}	1.486×10^{-2}	2.973×10^{-2}	5.945×10^{-2}	1.189×10^{-1}	2.378×10^{-1}	4.757×10^{-1}	1
CH ₃ .CN.COOH	0.0044	0.0046	0.0047	0.0047	0.0046	0.0046	0.0046	0.0047	0.0047	0.0047	0.0046	0.0044	—
Concentration ...	—	—	—	1.953×10^{-3}	3.906×10^{-3}	7.813×10^{-3}	1.563×10^{-2}	3.125×10^{-2}	6.250×10^{-2}	1.250×10^{-1}	2.500×10^{-1}	5.000×10^{-1}	1
CHCl ₃ .COOH ...	—	—	—	0.079	0.088	0.091	0.091	0.091	0.089	0.089	0.088	0.082	0.069

"Weak" Electrolytes.

Concentration ...	4.940×10^{-4}	9.879×10^{-4}	1.976×10^{-3}	3.952×10^{-3}	7.904×10^{-3}	1.581×10^{-2}	3.162×10^{-2}	6.323×10^{-2}	1.265×10^{-1}	2.529×10^{-1}	5.058×10^{-1}	1.011
Concentration ...	—	—	—	—	—	—	—	—	—	—	—	—
CH ₃ .COOH	1.86×10^{-4}	1.85×10^{-4}	1.83×10^{-4}	1.85×10^{-4}	1.85×10^{-4}	1.85×10^{-4}	1.85×10^{-4}	1.85×10^{-4}	1.82×10^{-4}	1.77×10^{-4}	1.66×10^{-4}	1.44×10^{-4}

determined n from these lines, it is possible to calculate for each concentration a value for K , and any irregularities in the values so computed serve further to test the closeness with which, and the range over which, the law is followed.

Fig. 4.



In Table IV. we exhibit a number of these values for typical electrolytes, and in Table V. we give a conspectus of the values of n , the mean values of K , and the range of validity of the equation for all the electrolytes studied.

TABLE IV.

"Strong" Electrolytes.

Concentration ...	5.0×10^{-3}	1.0×10^{-1}	2.0×10^{-1}	5.0×10^{-1}	1.0×10^{-2}	2.0×10^{-2}	5.0×10^{-2}	1.0×10^{-1}	2.0×10^{-1}	5.0×10^{-1}	1
LiCl	—	1.50	1.57	1.54	1.56	1.55	1.55	1.54	1.55	1.57	1.57
LiNO ₃	—	1.64	1.67	1.66	1.66	1.65	1.63	1.62	1.60	1.61	1.56
Sr(NO ₃) ₂	—	0.68	0.69	0.69	0.68	0.68	0.67	0.67	0.67	0.68	0.68
Ba(NO ₃) ₂	—	0.49	0.50	0.50	0.50	0.49	0.48	0.48	0.48	0.48	0.43
CuSO ₄	—	0.068	0.070	0.069	0.068	0.066	0.065	0.065	0.066	0.071	0.077
CdSO ₄	—	0.056	0.058	0.059	0.059	0.058	0.058	0.058	0.059	0.063	0.075
HCl	0.0046	0.094	0.093	0.092	0.102	0.129	0.158				
HIO ₃	0.075	0.073	0.072	0.072	0.075	0.082	0.097	0.113	0.132	0.158	0.205

"Intermediate" or "Transition" Electrolytes.

Concentration ...	2.322×10^{-4}	4.645×10^{-4}	9.290×10^{-4}	1.858×10^{-3}	3.716×10^{-3}	7.429×10^{-3}	1.486×10^{-2}	2.973×10^{-2}	5.945×10^{-2}	1.189×10^{-1}	2.378×10^{-1}	4.757×10^{-1}
CH ₃ .CN. COOH	0.0044	0.0046	0.0047	0.0047	0.0046	0.0046	0.0046	0.0047	0.0047	0.0047	0.0046	0.0044
Concentration ...	—	—	—	1.953×10^{-3}	3.906×10^{-3}	7.813×10^{-3}	1.563×10^{-2}	3.125×10^{-2}	6.250×10^{-2}	1.250×10^{-1}	2.500×10^{-1}	5.000×10^{-1}
CHCl ₃ . COOH ...	—	—	—	0.079	0.088	0.091	0.091	0.091	0.089	0.089	0.088	0.082

"Weak" Electrolytes.

Concentration ...	—	4.940×10^{-4}	9.879×10^{-4}	1.976×10^{-3}	3.952×10^{-3}	7.904×10^{-3}	1.581×10^{-2}	3.162×10^{-2}	6.323×10^{-2}	1.265×10^{-1}	2.529×10^{-1}	5.058×10^{-1}
OH ₃ . COOH	—	1.86×10^{-4}	1.85×10^{-4}	1.83×10^{-4}	1.85×10^{-4}	1.85×10^{-4}	1.85×10^{-4}	1.85×10^{-4}	1.85×10^{-4}	1.82×10^{-4}	1.77×10^{-4}	1.66×10^{-4}

TABLE V.

Electrolyte.	<i>n</i> .	K.	Valid up to C=
NaCl	1.4763	1.54	2.0×10^{-2}
KCl.....	1.4867	1.62	1.0×10^{-2}
LiCl.....	1.4612	1.55	5.0×10^{-1}
NaNO ₃	1.4484	1.75	1.0×10^{-2}
KNO ₃	1.4916	1.52	2.0×10^{-1}
LiNO ₃	1.4465	1.65	2.0×10^{-1}
NaIO ₃	1.4877	1.07	5.0×10^{-2}
KIO ₃	1.4566	1.63	5.0×10^{-2}
LiIO ₃	1.4715	1.07	2.0×10^{-2}
Ca(NO ₃) ₂	1.4312	0.99	5.0×10^{-1}
Sr(NO ₃) ₂	1.4916	0.68	2.0×10^{-1}
Ba(NO ₃) ₂	1.5436	0.49	1.0×10^{-1}
CuSO ₄	1.6429	0.068	5.0×10^{-2}
CdSO ₄	1.6487	0.058	5.0×10^{-2}
CHCl ₃ .COOH ...	1.8341	0.088	2.0×10^{-1}
CH ₃ .ON.CO.OH.	1.9574	0.0046	5.0×10^{-1}
HIO ₃	2.0000	0.73	1.0×10^{-3}
HCl.....	2.0155	0.094	1.0×10^{-3}
OH ₃ .COOH	2.0000	0.00000185	1.0×10^{-1}

Some regularities are apparent in Table V. which may here be noted. For the chlorides, nitrates and iodates of sodium, potassium and lithium, and also for the nitrates of calcium, strontium and barium, the coefficient *n* increases with rise in atomic weight, the only exception being potassium iodate.

We may mention here that the experimental figures chosen were those of as high an order of accuracy as possible (Kohlrausch and Maltby, *Wiss. Abh. Techn. Reichs.* 1900, iii. p. 156 : *Ges. Abh.* 1911, ii. p. 826, for NaCl, KCl, LiCl, NaNO₃, KNO₃, and LiNO₃ at 18°; Kohlrausch, *Berl. Ber.* 1900, p. 1002 : *Ges. Abh.* 1911, ii. p. 942, for NaIO₃, KIO₃, and LiIO₃ at 18°; Kohlrausch and Grüneisen, *Berl. Ber.* 1904, p. 1215 : *Ges. Abh.* 1911, ii. p. 1078 : Grüneisen and Steinwehr, *Ges. Abh.* 1911, ii. p. 1223, for Ca(NO₃)₂, Sr(NO₃)₂, Ba(NO₃)₂, CuSO₄, and CdSO₄ at 18°; Kraus and Parker, *J. Amer. Chem. Soc.* 1922, xlv. p. 2429, for iodic acid at 25°; Parker, *ibid.* 1923, xlv. p. 2017, for hydrochloric acid at 25°; Kendall, *Medd. K. Vetens. Nobelinstitut*, Bd. 2, no. 38 (1913), for cyanacetic acid, dichloracetic acid, and acetic acid at 25°). With these figures, and employing

large-scale graph paper, we found it quite feasible to determine our constants correct to four significant figures.

Now, if Weiland's figures (*loc. cit.*) as quoted, using Weiland's value for Λ_0 , be plotted out in this way, it will be seen that, down to the lowest concentrations measured, Weiland's figures follow an accurate Storch equation, in which n is *not* equal to 2.000; and this we believe is the proper manner to test and to interpret his figures.

Turning now to the substances studied for which n is assumed equal to $a + bC$, we can test the equation and determine the constants by a graphical method of a reasonably high order of accuracy, which, however, necessitates rather laborious computations. Briefly, the method is as follows:—

Writing the Storch equation,

$$\left(C \frac{\Lambda}{\Lambda_0}\right)^n = K \left(C - C \frac{\Lambda}{\Lambda_0}\right),$$

and putting

$$C \frac{\Lambda}{\Lambda_0} = Y \quad \text{and} \quad C = X,$$

we have, taking logarithms, and assuming that $n = a + bC$,
 $= a + bX$,

$$a \log Y + bX \log Y = \log (X - Y) + \log K. \quad (4)$$

Taking a convenient point X_0, Y_0 on this curve, we have

$$\log K = a \log Y_0 + bX_0 \log Y_0 - \log (X_0 - Y_0), \quad (5)$$

and eliminating K between (4) and (5), we arrive at

$$a + b \frac{X \log Y - X_0 \log Y_0}{\log Y - \log Y_0} = \frac{\log (X - Y) - \log (X_0 - Y_0)}{\log Y - \log Y_0},$$

yielding the linear plot

$$a + bx = y$$

if

$$x = \frac{X \log Y - X_0 \log Y_0}{\log Y - \log Y_0}$$

and

$$y = \frac{\log (X - Y) - \log (X_0 - Y_0)}{\log Y - \log Y_0}.$$

The method of tabulation is shown in Table VI. for sodium chloride at 18°, while in fig. 5 is shown the rectilinear plot from which the constants a and b have been computed.

TABLE VI.

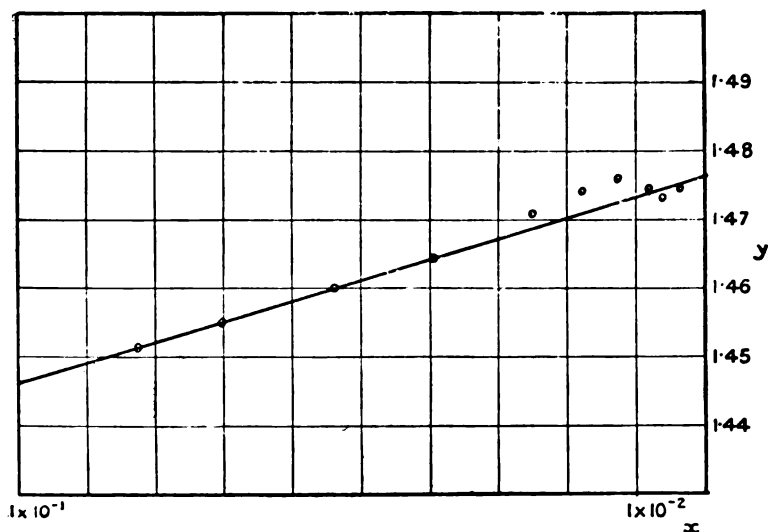
Sodium Chloride, 18° C.

C.	A.	x.	y.	K.
1.0×10^{-4}	108.10	-2.6269×10^{-3}	1.4488	1.455
2.0×10^{-4}	107.82	-3.2721×10^{-3}	1.4747	1.546
5.0×10^{-4}	107.48	-6.2235×10^{-3}	1.4731	1.544
1.0×10^{-3}	106.49	—	—	1.544
2.0×10^{-3}	105.55	-8.1292×10^{-3}	1.4747	1.545
5.0×10^{-3}	103.78	-1.2507×10^{-2}	1.4760	1.546
1.0×10^{-2}	101.95	-1.17614×10^{-2}	1.4742	1.535
2.0×10^{-2}	99.62	-2.4961×10^{-2}	1.4709	1.536
5.0×10^{-2}	95.71	-3.9252×10^{-2}	1.4644	1.546
1.0×10^{-1}	92.02	-5.3885×10^{-2}	1.4600	1.546
2.0×10^{-1}	87.73	-7.0215×10^{-2}	1.4549	1.544
5.0×10^{-1}	80.94	-8.2245×10^{-2}	1.4514	1.546
1	74.35	-5.7390×10^{-2}	1.4546	1.590

$$X_0 = 1.00000 \times 10^{-3}, \quad Y_0 = 9.76793 \times 10^{-4}.$$

$$\frac{(C\alpha)^{1.4764+0.3052C}}{C(1-\alpha)} = K.$$

Fig. 5



In this manner we have shown for various substances that n is a linear function of the concentration, and increases with rise in concentration. A summary of the results for

potassium chloride and lithium chloride (18°) is given in Table VII.*, while in Table VIII. is exhibited the variability

TABLE VII.

Concentration.	KCl.		LiCl.	
	Λ.	K.	Λ.	K.
2.0×10^{-5}	129.51	1.265		
5.0×10^{-5}	129.32	1.451		
1.0×10^{-4}	129.07	1.504	98.14	1.496
2.0×10^{-4}	128.77	1.602	97.85	1.564
5.0×10^{-4}	128.11	1.631	97.19	1.534
1.0×10^{-3}	127.34	1.616	96.52	1.552
2.0×10^{-3}	126.31	1.612	95.62	1.547
5.0×10^{-3}	124.41	1.620	93.92	1.540
1.0×10^{-2}	122.43	1.615	92.14	1.531
2.0×10^{-2}	119.96	1.623	89.91	1.536
5.0×10^{-2}	115.75	1.615	86.12	1.552
1.0×10^{-1}	112.03	1.616	82.42	1.552
2.0×10^{-1}	107.96	1.625	77.93	1.542
5.0×10^{-1}	102.41	1.752	70.71	1.512
1	98.27	2.259	63.36	1.413

$$\text{For KCl } \frac{(C_a)^{1.4863+0.6354 C}}{C(1-a)} = K.$$

$$\text{For LiCl } \frac{(C_a)^{1.4616+0.0484 C}}{C(1-a)} = K.$$

TABLE VIII.

Variation of the Exponent n with Concentration.

Concentration.	NaCl.	KCl.	LiCl.
	n .	n .	n .
1.0×10^{-4}	1.4764	1.4863	1.4616
2.0×10^{-4}	1.4764	1.4863	1.4616
5.0×10^{-4}	1.4766	1.4866	1.4616
1.0×10^{-3}	1.4769	1.4869	1.4616
2.0×10^{-3}	1.4770	1.4876	1.4617
5.0×10^{-3}	1.4779	1.4895	1.4618
1.0×10^{-2}	1.4795	1.4927	1.4621
2.0×10^{-2}	1.4825	1.4990	1.4626
5.0×10^{-2}	1.4917	1.5181	1.4640
1.0×10^{-1}	1.5069	1.5498	1.4664
2.0×10^{-1}	1.5374	1.6134	1.4713
5.0×10^{-1}	1.6290	1.8040	1.4858
1	1.7816	2.1217	1.5100

* Iodic acid (25°) does not appear to conform to this formula.

of the exponent n with concentration. It will be noticed that the value at low concentrations agrees reasonably well with the value deduced from the simple Storch equation.

These results are directly opposed to the conclusions of Noyes and his collaborators (*cf.* Noyes and Falk, J. Amer. Chem. Soc. 1912, xxxiv. p. 479), and especially of Bates (*ibid.* 1913, xxxv. p. 519), who states (*loc. cit.*): "It would appear that in general the value of n continues to increase as the concentration decreases, and that hence the assumption that n does not change appreciably below 0.01 normal is not justified."

The order of accuracy to be expected in comparing observed and calculated values of Λ over the range of validity of this dilution formula is shown in Table IX.*

TABLE IX.
Sodium Chloride, 18°.

$$\frac{(C_{\alpha})^{1.4764+0.3652C}}{C(1-\alpha)} = 1.543.$$

Concentration.	Λ (observed).	Λ (calculated)
1.0×10^{-4}	108.10	108.15
2.0×10^{-4}	107.82	107.82
5.0×10^{-4}	107.18	107.18
1.0×10^{-3}	106.49	106.49
2.0×10^{-3}	105.55	105.56
5.0×10^{-3}	103.78	103.80
1.0×10^{-2}	101.95	101.99
2.0×10^{-2}	99.62	99.66
5.0×10^{-2}	95.71	95.72
1.0×10^{-1}	92.02	92.08
2.0×10^{-1}	87.73	87.67
5.0×10^{-1}	80.94	(80.60)
1	74.35	(73.62)

In brief, taking into account the number and diverse nature of the electrolytes examined (strong, intermediate or transition, weak, uni-uni-, uni-bi-, and bi-bivalent forms have been examined) and the range of concentration considered, our conclusions point to the Storch equation in its simple, or in a generalized, form as the equation which most satisfactorily represents the relation between α ($= \Lambda/\Lambda_0$)

* The method employed for the computation of Λ is briefly described in a note at the end of this paper.

and C over a wide range of concentration. And this relation, which is undoubtedly followed accurately at low concentrations, serves to test Ostwald's law. We do not find that this law is followed as a general rule—of the substances which we have examined, only two out of a total of nineteen show reasonably good agreement with this formula.

NOTE.—Calculation of α from the equation $\frac{(C\alpha)^n}{C(1-\alpha)} = K$, where $n = a + bC$.

This equation may be written in the form

$$\alpha^n = \frac{K}{C^{n-1}} (1-\alpha) = -B\alpha + B, \quad \text{where } B = \frac{K}{C^{n-1}},$$
$$\text{or } \alpha^n + B\alpha - B = 0.$$

The last equation may be readily solved for α , and therefore for A , by the method of iteration described in Whittaker and Robinson, 'The Calculus of Observations,' p. 81 (1926).

One of the authors (I. V.) wishes to acknowledge his indebtedness to the Trustees of the Dixon Fund for a grant with the aid of which part of the expenses of the research have been defrayed.

Imperial College of Science and
Technology, South Kensington.
East London College
(University of London).

II. *A Theoretical Investigation of the Phenomenon of Cavitation in Screw Propellers.* By JOHN TUTIN, M.Sc.*

1. **T**HE phenomenon of cavitation was first observed by Sir John Thornycroft, F.R.S., and S. W. Barnaby, on the trials of the destroyer 'Daring' in 1894†. The propulsive efficiency was abnormally low, and the first five sets of propellers fitted to this vessel failed to propel her at the contract speed. The breakdown in thrust was accompanied by excessive slip and acute vibration. A cure was effected by fitting a sixth set of screws having about fifty per cent. greater blade area.

The phenomenon was attributed to the formation of cavities on the back of the blades. In subsequent experiments on a

* Communicated by the Author.

† Thornycroft and Barnaby, Inst. C.E. 1895.

model propeller in a special vacuum tank, the formation of such cavities was actually observed by Sir Charles Parsons, F.R.S.* In the course of some classical experiments carried out by D. W. Taylor in the Washington Tank, cavities were also observed on the blade face †. This latter phenomenon was both unexpected and surprising, because the slip and the nominal angle of incidence were positive. It was ascribed by Taylor to the water "cascading" from the back of the blade to the face, over the leading edge.

Since the "discovery" of the phenomenon in 1894, a large number of theories of cavitation ‡ have been formulated from time to time, but none of them can be regarded as giving an adequate and reliable explanation of the observed phenomena.

The formation of cavities on propeller blades is described in § 2, and the importance of face cavities is emphasized. The possibility that face cavitation may be due to excessive inflow leads to an investigation in § 3 of the momentum and energy equations of a simple form of propeller. Existing theory is here found to be incorrect, and a new set of equations are derived. In § 4 these results are applied to the blade elements of an actual propeller. A method for determining the real angle of incidence is given, and a simple extension gives the criterion for face cavitation in equation (19).

Finally, in § 5 the problem of eliminating cavitation is considered in the light of the present theory.

Formation of Cavities.

2. The thrust of a screw propeller is the resultant longitudinal component of the excess pressure on the face of the blades and the defect of pressure on the back. Both the pressure on the face and the suction on the back increase as the speed of advance and the revolutions are increased, but whereas an excess pressure may go on increasing indefinitely, the limit of suction at a given point is reached when the absolute pressure is reduced to zero, assuming for the moment an ideal fluid which does not evaporate, and

* Sir Charles Parsons, N.E.C. Inst. 1912-13.

† D. W. Taylor, 'Speed and Power of Ships,' pp. 118-158.

‡ Barnaby, Inst. Nav. Arch. 1897 and 1911. Normand, Inst. C.E. 1905. Wagner, *Jahrbuch S.G.* 1906. Taylor, *loc. cit.* Flamm, Inst. Nav. Arch. 1911. Gumbel, Inst. Nav. Arch. 1913. Mumford, Inst. C.E. 1921. Dyson, 'Screw Propellers,' Chapter on Cavitation. Bauer, *Schiffbautechnische Gesellschaft*, 1923. Horn, *Schiffbautechnische Gesellschaft*, 1926. Foettinger, *V. d. I.* 1926.

which contains no occluded gases. Any further increase in speed and revolutions will produce no further increase in thrust at this point, and will merely extend the boundaries of the region over which the pressure is zero.

In the case of a fluid which evaporates, the limit of pressure will be reached when the absolute pressure is equal to the vapour pressure. The cavity will then contain vapour at a pressure depending solely on the temperature. Further, as in the case of water, if the fluid contains air or other gases in solution, these will escape into the cavity, but it follows from the Law of Partial Pressures, that their presence will not alter the absolute pressure at which the cavity will form. This applies also to any air which may be drawn down from the surface.

Consider, therefore, a particular blade element of a screw propeller, at a given distance from the axis, and let the hydrostatic immersion be h feet. Let h_1 and h_2 denote the hydrostatic equivalents of the atmospheric and vapour pressures, respectively. When the propeller is revolving, the point of incipient cavitation will occur when the pressure drop at some point on the element reaches the value

$$p' = \rho g(h + h_1 - h_2). \quad . \quad . \quad . \quad . \quad (1)$$

For finite values of h , the formation of cavities on the back of a propeller blade at sufficiently high revolutions is clearly inevitable, and a method of calculating the critical speed of rotation at which back cavitation will be incipient can readily be developed from equation (1). [See equation (20).]

However, even extensive cavitation on the back of the blades could not, *per se*, account for the remarkable features of the phenomenon. Cavitation on the back of the blades would certainly result in a decrease in torque, and therefore in an increase in revolutions and slip for a given speed and thrust. Whilst this increase in slip will in most cases result in a moderate loss of propeller efficiency, this is not necessarily so, and, in fact, certain propellers have been known to run at higher efficiency due to the increased slip which accompanied back cavitation.

Normand * states that cavitation proper may result in the power required to attain a given speed being double that required when cavitation is absent. In another well-authenticated instance†, the estimated waste of power due to cavitation at 23 knots would alone have been sufficient to

* *Loc. cit.*

† The 'Drake' class of armoured cruisers.

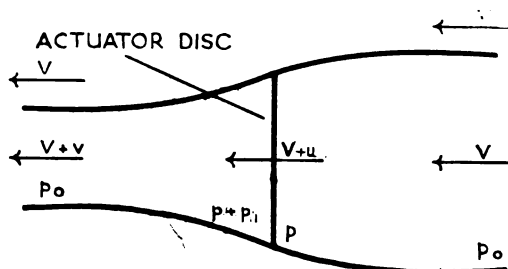
propel the ship at a speed of 14 knots. D. W. Taylor found that at sufficiently high revolutions cavitation became so acute as to cause the thrust to vanish. Hence, some further explanation is required to account for losses of this magnitude.

A possible explanation of the phenomenon readily suggests itself, namely, that under certain conditions there may be excessive acceleration in the fluid ahead of the propeller and consequently abnormally high inflow. This might result in negative angles of incidence, which would account in a very simple manner for the cavities observed by Taylor and attributed by him to cascading at positive angles of incidence.

Momentum Theory.

3. In order to investigate this possibility, however, it is necessary to revert to the fundamental momentum and energy equations governing the action of a screw propeller. In the Froude-Rankine* theory and the Betz-Prandtl† vortex theory, the propeller itself is replaced by an "actuator," which is virtually a propeller consisting of an infinite number of blades, having no boss or hub, so that it becomes effectively a circular disk. It is assumed that the thrust is uniformly distributed over this disk, and the latter, therefore, exerts a discontinuity in pressure on the fluid passing through the disk.

Fig. 1.



Referring to fig. 1, we see that on the hypothesis that it is legitimate to apply Bernoulli's law to the motion before

* Rankine, 'Scientific Papers,' p. 544. R. E. Froude, F.R.S., Inst. Nav. Arch. 1889 & 1911.

† Betz and Prandtl, *Nachr. v. d. Kgl. Gesellschaft des Wissenschaften*, 1919. Glauert, Aero. Research Comm. R. & M. 786 and 869.

and behind the screw disk separately, the Froude-Rankine theory gives

$$p_0 + \frac{1}{2}\rho V^2 = p + \frac{1}{2}\rho(V+u)^2, \quad \dots \quad (2)$$

$$p + p_1 + \frac{1}{2}\rho(V+u)^2 = p_0 + \frac{1}{2}\rho(V+v)^2. \quad \dots \quad (3)$$

Also, equating the rate of increase of axial momentum to the forward thrust,

$$T = p_1 A = \rho A(V+u)v. \quad \dots \quad (4)$$

From equations (2), (3), and (4) the well-known result is obtained

$$u = \frac{1}{2}v. \quad \dots \quad (5)$$

Thus, on the above assumptions, half the added velocity in the slip stream occurs in front of the screw disk and half behind it.

From equations (4) and (5) the inflow velocity u can be determined, and current air-screw research is largely based on the assumption that these equations are correct.

Let us consider, however, the dynamical equilibrium of the system. If it is proposed to apply Bernoulli's law to the inflow and outflow columns separately, it is legitimate to investigate, in the first instance, whether the suction $(p_0 - p)A$, on the forward side of the screw disk, will produce and maintain an inflow velocity u . To satisfy this condition, we must have

$$(p_0 - p)A = \rho A(V+u)u, \quad \dots \quad (6)$$

which is, however, quite incompatible with equation (2). An investigation of the outflow column reveals a similar inconsistency, since in lieu of equation (3) we obtain

$$[(p + p_1) - p_0]A = \rho A(V+u)(v-u). \quad \dots \quad (7)$$

It is, in fact, evident that the actuator is physically incapable of producing the slip-stream flow attributed to it.

Now, the force-momentum relationships expressed in equations (6) and (7) must necessarily hold good. Therefore there must be errors inherent in the energy equations (2) and (3).

In lieu of these, we have :

(a) *Inflow Column*.—Modifying equation (2) to satisfy equation (6) :—

$$p_0 + \frac{1}{2}\rho V^2 = p + \frac{1}{2}\rho(V+u)^2 + \frac{1}{2}\rho u^2, \quad \dots \quad (8)$$

or

$$(p_0 - p)A = \rho A \left(Vu + \frac{1}{2}u^2 + \frac{1}{2}u^2 \right). \quad \dots \quad (9)$$

[useful
work.]

[kinetic
energy of
inflow.]

[energy
dissipated
at screw
disk.]

22 Mr. J. Tulin: *A Theoretical Investigation of the*

(b) *Outflow Column.*—Modifying equation (3) to satisfy equation (7) :—

$$p + p_1 + \frac{1}{2}\rho(V+u)^2 + \frac{1}{2}\rho(v-u)^2 = p_0 + \frac{1}{2}\rho(V+v)^2, \quad (10)$$

or

$$(p + p_1 - p_0)A = A\rho \left[\underset{\substack{\text{[useful] \\ \text{work.}}}}{V(v-u)} + \underset{\substack{\text{[outflow} \\ \text{quota of} \\ \text{kinetic} \\ \text{energy.}}}{\frac{1}{2}(v^2 - u^2)}} - \underset{\substack{\text{[energy} \\ \text{dissipated} \\ \text{at screw} \\ \text{disk.}}}{\frac{1}{2}(v-u)^2}} \right]. \quad (11)$$

(c) *Combined Columns.*—Adding equations (9) and (11) should give the total thrust :

$$T = p_1 A = \rho A \left[Vv + \frac{1}{2}v^2 + (uv - \frac{1}{2}v^2) \right] \quad (12)$$

$$= \rho A (V+u)v. \quad (13)$$

This result is identical with equation (4), as, of course, it should be. Denoting the inflow ratio $\frac{u}{v}$ by d , the inflow velocity becomes

$$u = \frac{1}{2} \sqrt{V^2 + \frac{4Td}{\rho A}} - \frac{1}{2}V. \quad (14)$$

The total dissipation of energy at the screw disk is represented by

$$\frac{1}{2}u^2 + \frac{1}{2}(v-u)^2, \quad (15)$$

and this term indicates an additional loss of energy of about the same order as the loss due to the axial kinetic energy of the slip stream. This additional loss is seen to be required by the dynamical equilibrium of the slip stream. The energy dissipated will, of course, reappear in the slip stream in the form of heat. There are a number of physical problems in which the conditions are analogous, as, for example, inelastic impact.

Efficiency.

$$\text{Actuator Efficiency} = \frac{\text{useful work}}{\text{useful work} + \text{kinetic energy} + \text{heat energy}}, \quad (16)$$

i. e.

$$\eta = \frac{Vv}{Vv + \frac{1}{2}v^2 + \frac{1}{2}u^2 + \frac{1}{2}(v-u)^2} \quad (17)$$

$$= \frac{Vv}{Vv + v^2 - vu + u^2}. \quad (18)$$

Differentiating the above expression, the efficiency is a maximum for a given thrust T , when :

$$u = \frac{1}{6}(4V^2 + 8Vv + 13v^2)^{\frac{1}{2}} - \frac{1}{6}(2V - v).$$

If the ratio $\frac{v}{V}$ is small, this condition reduces to $u = \frac{1}{2}v$, and the maximum efficiency is then

$$\eta_{\max} = \frac{V}{V + \frac{3}{4}v}.$$

The logical conclusion of this investigation is that an actuator cannot be made to deliver thrust by the assumption of a perfect "Bernoulli" flow and a discontinuity of pressure. It follows that the familiar Rankine-Froude theory and the corresponding vortex theory are incorrect. The inflow velocity and ideal efficiency deduced therefrom are misleading. This result is important, because these theories are extensively used in air-screw research in this country, France, Italy, Germany, and U.S.A.

The equations given above constitute a new theory, the main features of which may be summarized as follows :—

(1) There is an inevitable dissipation of energy at the screw disk, in addition to that due to the axial kinetic energy of the slip stream.

(2) The flow is elsewhere stream line and may be assumed to follow Bernoulli's law. Such conditions have been experimentally verified by Stanton* at the National Physical Laboratory, and by Fage† at the Royal Aircraft Establishment, Farnborough.

(3) Denoting the ratio of the inflow to the outflow by the term "inflow ratio," and the ratio of the suction to the total thrust by the term "suction ratio," it follows from equations (6) and (7) that the inflow ratio must be equal to the suction ratio. This may be regarded as a fundamental principle in propeller theory.

(4) In general, the inflow ratio may have any value, provided the above condition is satisfied.

(5) The maximum efficiency is $\frac{V}{V + \frac{3}{4}v}$, when the inflow ratio is $\frac{1}{2}$. This indicates a new line of research, since in order to improve the efficiency of present types of screw propeller we must compel the blade face to do more work ‡.

* Stanton and Marshall, Aero. Res. Comm. R. & M. 460.

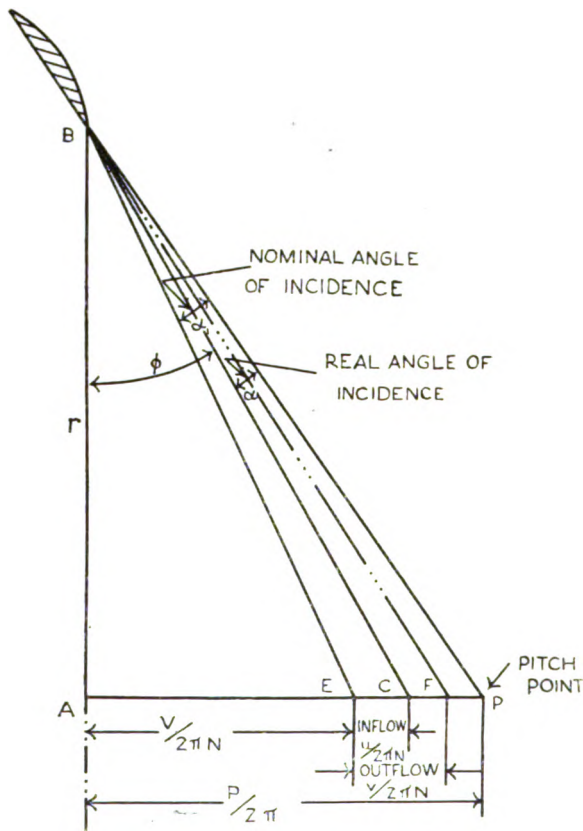
† A. Fage, Aero. Res. Comm. R. & M. 699.

‡ The suction ratio of a normal screw propeller varies from about .7 to 1.0, depending on the thickness and shape of the constituent aerofoils.

Face Cavitation : Inflow Theory.

4. We are now in a position to consider the importance of inflow velocity in its relation to the blade elements of an actual propeller. Assuming in the first instance an isolated aerofoil at a distance r from the axis of rotation, it is evident from fig. 2 that if we know the outflow velocity EF we can

Fig. 2.



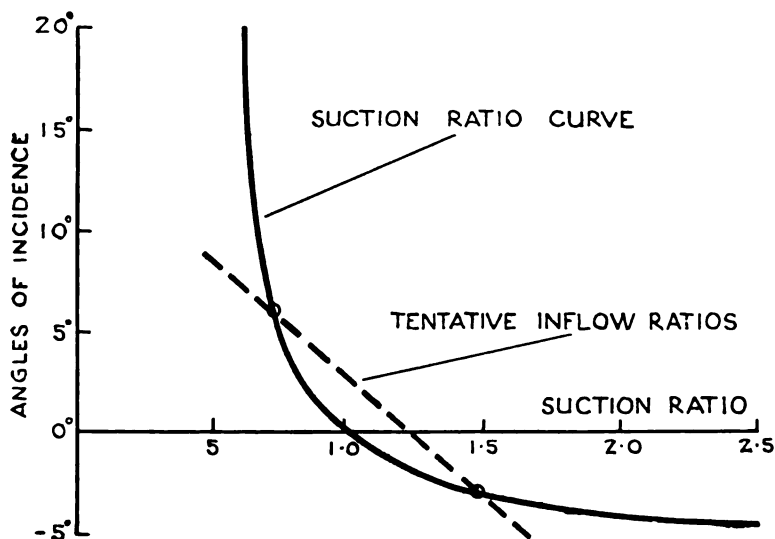
assume a sequence of values of the inflow ratio $\frac{EC}{EF}$, whence

we can obtain a corresponding sequence of values of the angle of incidence α . We must then determine, in order to satisfy equations (6) and (7), the angle or angles for which the inflow ratio is equal to the suction ratio. Extensive

experiment data are already available from which the suction ratio of an aerofoil of given camber ratio over a range of angles of incidence can be derived.

Hence, if the sequence of values of the inflow ratio is plotted on a base of angle of incidence, together with the corresponding values of the suction ratio, as indicated in fig. 3, the solution is given by the points of intersection of the two curves. There are, in general, two solutions, one of which gives a positive and the other a negative angle of incidence. On investigation it is found, however, that in any given case only one solution will give the required thrust, and therefore the real angle of incidence.

Fig. 3.



The inflow history of a normal screw propeller may now be described, assuming the revolutions to be indefinitely increased whilst the speed of advance is kept constant. Referring to fig. 2, at low revolutions the thrust is negative, and the propeller will act as a windmill and deliver torque. Inflow and outflow will both be negative. As revolutions are increased, however, the angle of incidence will eventually coincide with the angle of zero thrust. This point determines the "effective" or "experimental" pitch of the screw. According to the Froude-Rankine and vortex theories, there is no inflow at zero thrust, and therefore the effective pitch should invariably exceed the face pitch, owing to the finite

blade thickness. The present theory shows, however, that although there is necessarily no outflow, there will nevertheless be inflow, and this indicates the possibility of effective pitch being actually less than the face pitch in certain cases. This prediction is confirmed by experiments by Mumford at the Dumbarton Experiment Tank*.

In the vicinity of the point of zero thrust the angle of incidence becomes zero. Inflow and outflow are then necessarily equal and the inflow ratio unity. No additional momentum can be given to the fluid under these conditions after it has passed the screw disk, since the pressure on the blade face at zero angle of incidence is normal.

As the revolutions are further increased, the nominal slip increases and also the thrust. The inflow and outflow, being largely governed by thrust, will also increase. It will be seen that the variation in the angle of incidence will depend on whether the rate of increase of nominal slip is greater or less than the rate of increase of the inflow velocity.

In the light of the above theory, it is not difficult to see how and why an abnormal loss of thrust may arise. When the inflow increases to such an extent as to make the angle of incidence first of all zero and thereafter negative, a cavity may form on the *face* of the blade. When this occurs, it is obvious that the loss of thrust will become acute.

Since face cavitation is incipient when the angle of incidence has become zero, the critical speed at which it will occur can be determined as follows. Let u_0 be the inflow calculated on the assumption that the angle of incidence is zero at *all* thrusts. Then, from equation (14)

$$u_0 = \frac{1}{2} \sqrt{V^2 + \frac{4T}{\rho A}} - \frac{1}{2} V. \quad . \quad . \quad . \quad (19)$$

A curve of u_0 can then be plotted on the same base as nominal slip speed, and the point of intersection of the two curves will give the point of incipient face cavitation.

This criterion of cavitation throws some new light on the behaviour of the phenomenon. For example, in the case of H.M.S. 'Daring,' referred to above, Barnaby assumed that cavitation was incipient at a speed of 24 knots. The nominal slip of the 'Daring's' first pair of screws was, however, excessive over practically the whole range of speeds. For example, at 16 knots it was about 100 per cent. greater than the slip of the sixth pair of screws at 16 knots. Hence cavitation must have set in at a much lower speed than

* Baker and Schaffran, N.E.C. Inst. 1922-1924.

24 knots. The new theory shows that face cavitation was, in fact, incipient at about 13 knots.

In the case of Taylor's special cavitating propeller, on which well-defined cavities were actually observed by stroboscopic methods, investigation now shows that the real angle of incidence was negative over the entire range from 0 to 60 per cent. positive slip. Taylor's "cascading" hypothesis therefore becomes superfluous.

Methods of eliminating Cavitation.

5. It remains to consider, in the light of the above theory, by what means cavitation can be postponed. Equation (1) leads directly to the following criterion for back cavitation :

$$U = \sqrt{\frac{g\rho(h + h_1 - h_2)}{ndk_L(\cos \alpha + \frac{1}{\delta} \sin \alpha)}}, \quad \dots \quad (20)$$

where U is the critical value of the relative velocity, α is the angle of incidence, k_L the lift coefficient of the aerofoil, δ the $\frac{\text{lift}}{\text{drag}}$ ratio of the aerofoil, n the ratio of the maximum suction intensity to the average suction intensity, and d the inflow ratio. Referring to fig. 2, the relative velocity under any given conditions may be determined from the relationship

$$U^2 = (4\pi^2 N^2 r^2) + (V + u)^2. \quad \dots \quad (21)$$

The value of U given by equation (20) is that at which cavitation sets in on the back of the blade element, and by applying the formula to sections of the blade at different distances r from the axis, it is possible to calculate whether cavitation will occur at any point on the back, and if so, to what extent.

If such cavitation is indicated at a particular section, and the revolutions, speed, diameter, and immersion are fixed, it is only possible to effect a cure by reducing either n , d , or k_L . Now n and d are both somewhat inflexible. On the other hand, the lift coefficient k_L is capable of relatively wide variation, by adjusting the camber ratio, and it is therefore possible to determine from equation (20), the maximum permissible camber ratio at any point. Having due regard to considerations of strength, the blade width and thickness can then be adjusted throughout such that back cavitation

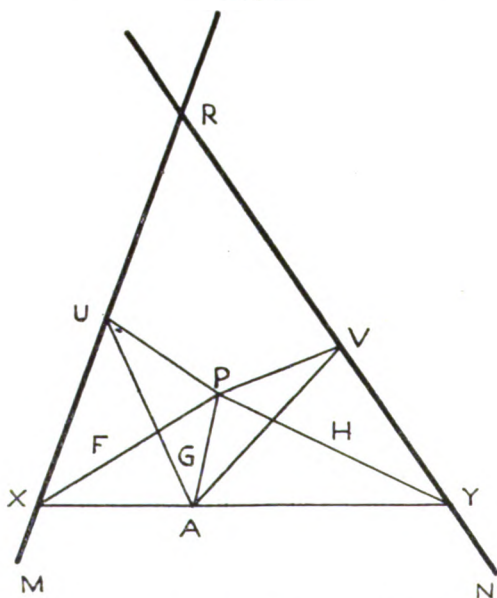
may be prevented without unnecessarily large blade area and excessive frictional losses.

In order to postpone face cavitation, it is desirable not only to eliminate back cavitation, but also to reduce the inflow velocity, as indicated by the inflow-slip criterion of equation (19). This end can be achieved by reducing the suction ratio. Such a redistribution of load from the back of the blade to the face is evidently the only fundamental method of postponing face cavitation.

III. *Placing Plane Quadrilaterals in Perspective. Application to Photography.* By THOS. MCHUGH, B.A.*

LEMMA 1.—RM, RN are two fixed str. lines and A is a fixed pt. through which is drawn a variable str. line meeting them in X, Y. Three str. lines in the plane PF, PG, PH, rigidly attached to one another in any order,

Fig. 1.



are placed so that they (produced through P when necessary) pass through X, A, Y respectively. The pt. P is then determined *uniquely*, and its locus is a circle (through R), fig. 1.

* Communicated by the Author.

Proof. Pts. U, V (fixed) being taken on RM, RN so

$$\widehat{AUM} = \widehat{GPF}, \quad \widehat{AVN} = \widehat{GPH} \quad (\text{fixed angles}),$$

APUX, APVY are each cyclic, and

$$\therefore \widehat{PUR} = \widehat{PAX}, \quad \widehat{PVR} = \widehat{PAY}.$$

$$\therefore \widehat{PUR} + \widehat{PVR} = \widehat{PAX} + \widehat{PAY} = 180^\circ,$$

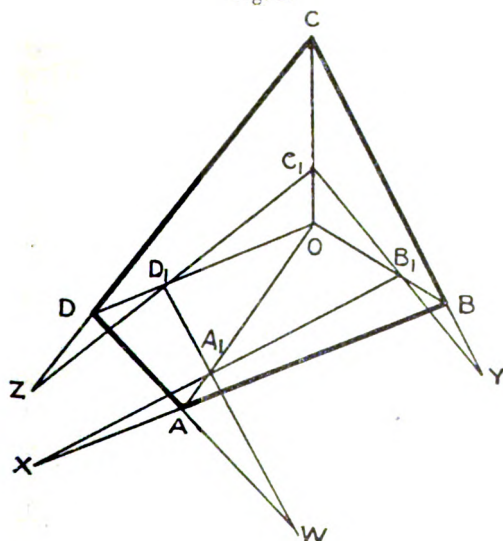
and hence P lies on the fixed \odot through R, U, V. Q.E.D.

Cor. 1. P is always real, and \therefore its locus is so.

Cor. 2. The same theorem holds when \widehat{XAY} is any constant angle ($=180^\circ$, above), but the \odot does not then pass through R.

LEMMA 2.—ABCD, $A_1B_1C_1D_1$ are two given plane quads. Let $A_1B_1C_1D_1$ having definite aspect be placed (*in plano*) with respect to ABCD so that AA_1, BB_1, CC_1, DD_1 concur (at O, say), as in fig. 2. The problem of so placing them is

Fig. 2.



indeterminate, the locus of O being a certain curve on which we can get as many pts. as desired by ruler and compass. Let X, Y, Z, W be intersections of AB, A_1B_1 ; BC, B_1C_1 ; CD, C_1D_1 ; DA, D_1A_1 .

Keeping O and $ABCD$ fixed, and allowing vertices of $A_1B_1C_1D_1$ to move on OA, OB, OC, OD (including the parts produced through O) so that its sides retain their directions, it is clear that $A_1B_1C_1D_1$ retains its shape and aspect. Now shall XY, YZ, ZW, WX (but not XZ or WY) retain their directions.

Proof. Two sides, C_1Z, C_1Y , of the variable triangle C_1ZY , whose vertices move on the fixed concurrent lines CO, CD, CB , have fixed directions (hyp.); \therefore so has third side YZ etc. $Q.E.D.$

LEMMA 3.—If for *any one* position of the varying quad. $A_1B_1C_1D_1$ of Lemma 2, X, Y, Z, W be *collinear*, they are so for *all* positions of $A_1B_1C_1D_1$, and the line of collinearity has a *fixed* direction. In particular, when A_1 falls on A the pts. Y, A, Z will be collinear, and like results hold when B_1 falls on B, C_1 falls on C , and D_1 falls on D .

Cor. 1. If when A_1 falls on A the pts. Y, A, Z be collinear, the pts. X, Y, Z, W will *always* be collinear, and in particular will Z, B, W be so when B_1 falls on B ; W, C, X be so when C_1 falls on C ; X, D, Y be so when D_1 falls on D ; and all the lines of collinearity will be parallel.

LEMMA 4.—The problem referred to in Lemma 2 becomes *determinate* if in addition X, Y, Z, W are to be *collinear*; and then there are as many pts. O as are yielded by the solution of the following problem (clear from results just established) :—

PROBLEM.— $ABCD, A_1B_1C_1D_1$ are two given plane quadrilaterals (fig. 3); required to find in plane of $ABCD$ a quadrilateral $ALMN$ similar to and having same aspect as $A_1B_1C_1D_1$ such that BL, CM, DN concur (at O , say) and that at same time the str. line joining H (intersection of CB, ML) and K (intersection of CD, MN) passes through A .

Analysis. Because BCD, LMN are in perspective, BD, LN, HK concur (at S , say) and conversely. CB, CD are known lines, A a known pt., and the position relatively to each other of the lines MK, MA, MH is known (hyp.);

\therefore by Lemma 1, M lies on a known \odot (through C), (1)

and hence, because ALM is of known species (hyp.),

L , too, lies on a known \odot (2)

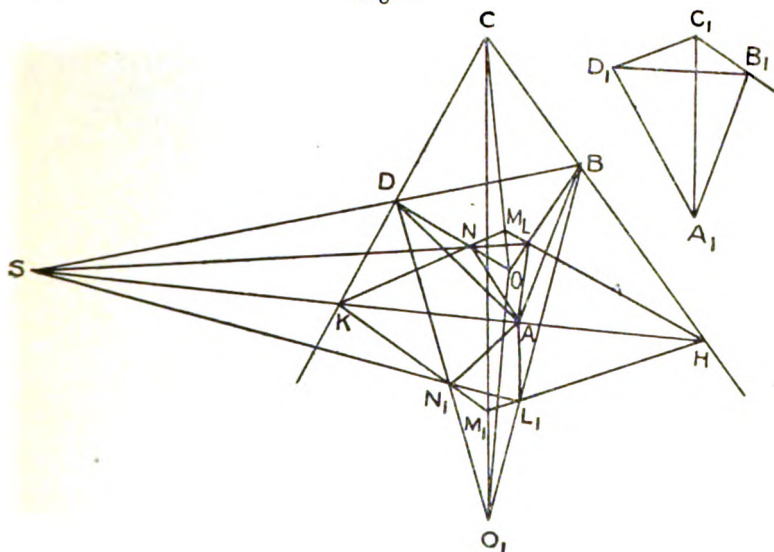
BD, BH are known lines, A a known pt. and the position

relatively to each other, of the lines LS, LA, LH is known (hyp.);

\therefore by Lemma 1, L lies on another known (through B); . . . (3)

\therefore L (and hence ALMN) can be found from (2) and (3).
Q.E.F.

Fig. 3.



Cor. 1. There is *one* and only one real, non-degenerate solution—although apparently *two*—since the \odot^* in (2) and (3) have one common pt., L_0 , say, on CB, which is such that $\widehat{AL_0C} = \widehat{A_1B_1C_1}$. This degenerate case must be excluded. [There is another such degenerate case (not included) corresponding to a position of N on CD, N_0 , say, which is such that $\widehat{AN_0C} = \widehat{A_1D_1C_1}$.] Thus O, ALMN, HAK are *uniquely* determined [*vide* Lemma 4].

[*Another method* consists in finding a figure similar to required one, etc., thus:—Take a str. line SA of any length to correspond to SA of fig. Then, because \widehat{SDA} , \widehat{KDA} are known (hyp.), CD passes through a known pt. on the known \odot SAD. Likewise MN, CB, ML pass through known pts. on the known \odot^* SNA, SBA, SLA respectively. We have

now to construct the quadrilateral MHCK so that each of its sides shall pass through the corresponding one of said pts., so that the angles at M and C shall be equal to known ones, and so that, furthermore, the vertices at H and K shall lie on the basic line SA—which may be done readily by “double points” of involution etc.]

Cor. 2. The analogous problem for any one of the other vertices B, C, D yields the *same* pt. O.

Cor. 3. It is plain that $A_1B_1C_1D_1$ can be placed in similitude with ALMN, having O for centre, in *two* ways (conjointly forming a fig. having central symmetry w. r. to O), and that when it is so placed it (with aspect retained) is in perspective *in plano* with ABCD. There being (*Cor. 1*) only *one* “pt. O”, the problem in Lemma 4 is solved completely. *Two* solutions.

Cor. 4. All quads. *directly* similar to $A_1B_1C_1D_1$, when placed in perspective *in plano* with ABCD, have same centre of perspective, O, and their axes of perspective are lines \parallel HAK.

THEOREM 1.—ALMN etc. being found as above, let it be tilted up unaltered through any angle about HAK for axis. BL, CM, DN still concur.

Proof.

DN (transversal of MKC) divides CM in ratio $-\frac{NK}{MN} \cdot \frac{\overline{DC}}{\overline{KD}}$

and

BL („ „ MHC) „ CM „ „ $-\frac{\overline{LH}}{\overline{ML}} \cdot \frac{\overline{BC}}{\overline{HB}}$,

but those ratios were *equal* before tilting, and they do not change clearly; \therefore BL, DN still divide CM (varying) in same ratio, *i. e.* cut it at *same* pt. Hence BL, CM, DN always concur. Q.E.D. [Otherwise since those lines are intersections of planes SDBLN, MKC, MHC.]

Cor. 1. $\overline{CO} : \overline{CM}$ is constant.

Cor. 2. In particular when angle of tilt about axis HAK = 180° , we get on plane ABCD another quad. $A_1L_1M_1N_1$ —reflexion of ALMN w. r. to HAK—satisfying conditions of Problem but for its *reversed* aspect.

Cor. 3—converse of Th. 1.—If ALMN be a quad. similar to $A_1B_1C_1D_1$ but in a plane different from that of ABCD and such that BL, CM, DN concur (at O, say), and if fig. ALMN be revolved unaltered about intersection of planes ABCD, ALMN—a str. line through A, of course—into the

position of *same* aspect as $A_1B_1C_1D_1$ on plane $ABCD$, that position is a solution of Problem.

Cor. 4. All the quads. satisfying requirements of Cor. 3 are found by revolving $ALMN$ of Problem about the axis HAK [for if there were such a quad. not belonging to this assemblage, we could, (Cor. 3) by revolving it as in Cor. 3 into plane $ABCD$, get another solution of Problem, which is absurd (Cor. 1, Problem)].

Cor. 5. Since $MM_1 \perp HAK$ and $\overline{CO} : \overline{CM} :: \overline{CO_1} : \overline{CM_1}$ (Cor. 1) $OO_1 \perp HAK$. O, O_1 depend only on *shape* of $A_1B_1C_1D_1$.

Cor. 6. In Cor. 3 the locus of O (intersection of BL, CM, DN) is a \odot in space cutting plane $ABCD$ at rt. L' , for M describes such a \odot by Cor. 4, C is fixed and $\overline{CO} : \overline{CM}$ is const. (Cor. 1). Q.E.D. Hence the theorem:—

THEOREM 2.—A pyramid on a given quadrilateral base ($ABCD$) is such that plane sections of required shape ($A_1B_1C_1D_1$) * can be made on it (including part above apex). The locus of its apex (O , say) is a circle whose plane is perpendicular to plane of $ABCD$ and whose centre lies on it. [It is the \odot on OO_1 of above fig. before tilt, as diameter. HAK is \perp plane of \odot .]

Note 1. (i.) Th. 1 etc. may be stated thus:—If one (BCD) of any two triangles (BCD, LMN) in perspective on a plane be kept fixed whilst the other (LMN) revolves about the axis of perspective (HKS), they are in perspective still in space and the centre of perspective (O) moves on a \odot cutting plane of fixed one at rt. L' .

(ii.) The same is true for *polygons* in *complete* perspective *in plano*. [This follows readily from (i.).]

(iii.) In particular (as in Cor. 2, Th. 1) when two figs. are in perspective in plano, so is either of them and the reflexion of the other w. r. to perspective axis.

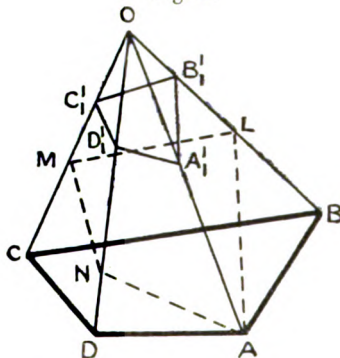
(iv.) When two plane figs. are in perspective in space and one be kept fixed whilst the other is revolved about the intersection of their planes into a new position (*two* such, with different aspects) on plane of the fixed fig., they will be still in perspective (*in plano*).

THEOREM 3.—If $A_1'B_1'C_1'D_1'$ be the quad. $A_1B_1C_1D_1$ placed in a position in perspective in space (fig. 4) with $ABCD$ (fixed), the locus of O (centre of perspective) is \odot cutting plane $ABCD$ at O, O_1 orthogonally (Th. 2). Then shall the intersection of planes $A_1'B_1'C_1'D_1', ABCD$

* See Note 4 below.

be a *fixed* line, which will be an *axis of pure rotation* for $A_1'B_1'C_1'D_1'$. [The section $\parallel A_1'B_1'C_1'D_1'$ through A, of $O(ABCD) \equiv ALMN$, (Cor. 4, Th. 1) which is constant. Hence $\overline{AA_1'} : \overline{A_1'O}$ is constant; so, too, $\overline{BB_1'} : \overline{B_1'O}$ etc., and \therefore (by transversals) the *constant* lines \overline{AB} , $\overline{A_1'B_1'}$ cut one other (produced if necessary) in *constant* segments; so, too, $\overline{B_1'C_1'}$, \overline{BC} , etc. But $ABCD$ is fixed, \therefore etc. Q.E.D.] Compare Note 1.

Fig. 4.



Note 2. (i.) $A_1B_1C_1D_1$ can (Cor. 3, Prob.) be placed with unchanged aspect in *plane* perspective with $ABCD$ in *two* ways ($A_1'B_1'C_1'D_1'$, $A_1''B_1''C_1''D_1''$, say) having common centre of perspective O , but different axes $H'K'$, $H''K''$, which are $\parallel HAK$; and likewise for *changed* aspect in *two other* ways having common centre O_1 , but the axes $H'K'$, $H''K''$ are the same for *both* aspects since the reflexions of $A_1'B_1'C_1'D_1'$, $A_1''B_1''C_1''$, D_1'' w. r. to $H'K'$, $H''K''$ respectively supply [by (iii.), Note 1] the solutions for reversed aspect. Now, revolving $A_1'B_1'C_1'D_1'$ about $H'K'$, and $A_1''B_1''C_1''D_1''$ about $H''K''$, $\overline{AA_1'}$, $\overline{BB_1'}$, $\overline{CC_1'}$, $\overline{DD_1'}$ always concur, and so $\overline{AA_1''}$, $\overline{BB_1''}$, $\overline{CC_1''}$, $\overline{CD_1''}$ [by (ii.), Note 1] —the pts. of concurrency moving on the above circle cutting plane $ABCD$ at rt. L^s at OO_1 . If the planes be kept *parallel* when moving, the pts. of concurrency coincide (at O , say), making (equal) sections *diametrically opposite* to each other w. r. to apex O on the now common pyramid $O(ABCD)$.

We thus have a mode of generating *all* the “quads. $A_1'B_1'C_1'D_1'$ ” of Th. 3.

(ii.) All sections of $O(ABCD)$ [fig. 4] parallel to $A_1'B_1'C_1'D_1'$ cut plane $ABCD$ in \parallel lines and are similar.

Revolving [as in (iv.), Note 1] each into position of same aspect on plane ABCD, we get again the theorem of Cor. 4 of Problem.

Application to Photography.

THEOREM.—Theorem 2 has the practical application:—
“The locus of the pt. at which a camera-man must have the lens of his instrument so as to be able to take a photograph of required shape (quadrilateral) of a given quadrilateral lamina (the corresponding vertices of the quads. being assigned) is a circle in space cutting lamina at rt. angles.”

Thus to take a photograph of ABCD similar to $A_1B_1C_1D_1$ of fig. 3, the lens must be on the \odot cutting plane of papers orthogonally at O, O_1 . Let it be at O, in space. The corresponding pt. M is then determined from Cor. 1, Th. 1, and thence the plane MHK, to which the sensitive plate of camera must be parallel.

Note 3. If one quad. be transverse, or re-entrant, so must the other and in a corresponding way. *Photography* as such demands this, but *Geometry* does not. So that photography (as required) be possible for case just referred to, it is necessary that sections of required shape $A_1B_1C_1D_1$ can be taken of O(ABCD) without having recourse to part produced through O.

Note 4. It is assumed throughout that A corresponds to A_1 , B to B_1 , C to C_1 and D to D_1 .

Note 5. A photo of required triangular shape, of a given triangle, may be taken from any pt. But from no pt. can one of given shape be taken of a plane pentagon. Quadrilaterals supply the interesting cases.

After deducing above theorems I learned that I had been virtually anticipated by Möbius (see Cremona's ‘Elements of Projective Geometry,’ English trans. by Leudesdorf (1893), p. 12, where the subject is presented in another light). For other methods of placing quadrilaterals in perspective, see that treatise, pp. 82–84.

Caltra, Claremorris,
Ireland.

IV. *On the Origin of Terms of the Spectrum of Cobalt.*
 By N. K. SUR, *Department of Physics, University of Allahabad* *.

THE recent work of Russell and Saunders †, Pauli ‡, Heisenberg §, and Hund || on the origin of the fundamental spectral terms of elements of the periodic table marks a definite stage in the development of the theory of complex spectra. Very recently R. H. Fowler and Hartree ¶, Laporte **, McLennan, McLay, and H. G. Smith †† have applied these ideas to account for the nature of the spectral terms of several elements. These ideas have been further developed by Professor Saha ‡‡ to explain not only the nature of the fundamental but also of the other higher terms of the spectrum of Neon and alkaline earths. As pointed out by the writer himself, these ideas can be extended to all elements. The modifications introduced by Dr. Saha have also been fruitful in accounting for the anomalous terms of the alkaline earths. As the fundamental ideas have been discussed by these writers, it is unnecessary to repeat them here. Only a brief explanation of the symbols and the modifications introduced will be given here.

The chief modification introduced by Prof. Saha is in indicating the electron configuration of the atoms of different elements of the periodic table by a method slightly different from the Bohr-Stoner system. This is shown in Chart 1.

We now pass on to a brief discussion of the method of representation in the chart. The number below each level M denotes the total number of electrons required to fill up the level completely. As is evident, instead of splitting a level like L_2 or M_2 into two levels L_{21} , L_{22} or M_{21} , M_{22} containing two and four electrons respectively, we represent them as single levels for optical spectra with their complete quota of electrons. This merely suggests the idea that for optical spectra, as distinguished from

* Communicated by Prof. M. N. Saha, D.Sc., F.I.P.

Saunders and Russell, *Astrophys. Journ.* lxi. p. 38 (1925).

† Pauli, *Zs. f. Phys.* xxxi. p. 765 (1925).

§ Heisenberg, *Zs. f. Phys.* xxxii. p. 841 (1925).

|| Hund, *Zs. f. Phys.* xxxiii. p. 345, and xxxiv. p. 296 (1925).

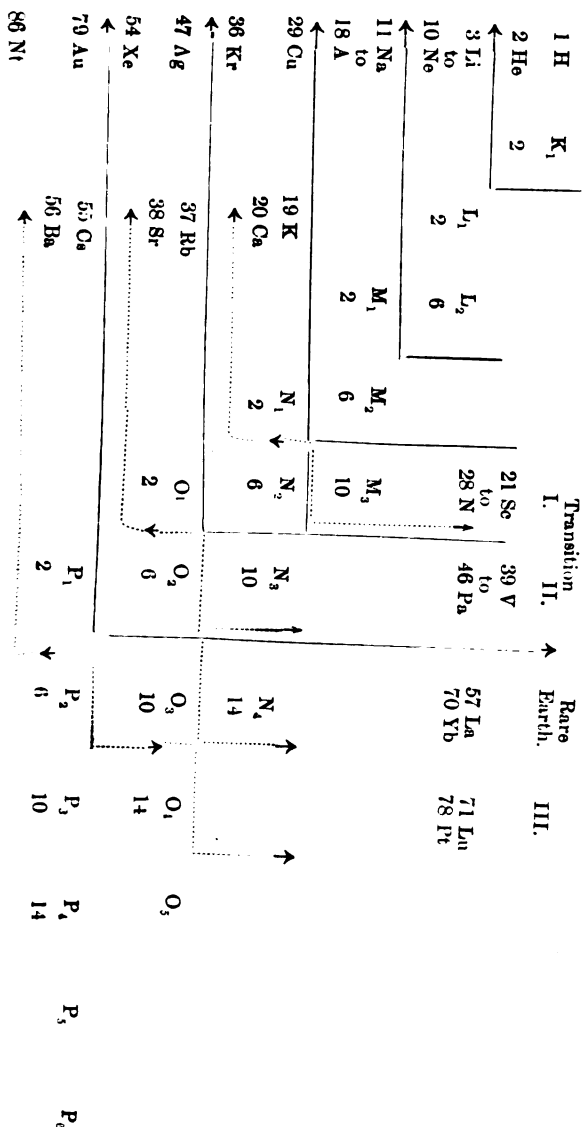
¶ R. H. Fowler and Hartree, *Proc. Roy. Soc.* cxi. p. 83 (1926).

** Laporte, *Journ. Opt. Soc. Amer.* xiii. p. 1 (1926).

†† McLennan, McLay, and Smith, *Proc. Roy. Soc.* lxxvi. p. 112 (1926).

‡‡ Saha, *Phil. Mag.*, June 1927, p. 1265.

CHART I, showing Structure of Atoms.



X-ray spectra, the probability of the occurrence of the electrons in either of the sub-levels M_{21} , M_{22} in which M_2 can be divided is the same. This simplification in the system of representing the levels is of great utility in

unravelling the origin of terms in any optical spectrum, complicated or simple, as will be shown later on.

The chart is self-explanatory as regards the formation of the atoms (3) Li to (10) Ne by successive filling up of L levels, and from (11) Na to (18) Ar by the closing up of M levels. The further successive addition of two fresh electrons leads us to the formation of K and Ca. Any fresh electron now introduced will pass on to the M_3 level. The formation of the atoms of the first transitional group of elements from (21) Sc to (28) Ni is thus accounted for by the simple process of successive introduction of new electrons in the M_3 level, while the N_1 level contains 2 electrons. The only exception is in the case of (24) Cr, which contains 1 electron in the N_1 level and has 5 electrons in the M_3 level. Similarly, we can pass on to other elements. It is also clear from the chart how the atoms of different transitional groups of elements are formed, and how the alkalis and alkaline earths persist throughout the whole system.

The above also explains the reason of assigning N_1 below M_2 in the same vertical column. As mentioned above for the formation of the atoms of K and Ca, we have to bring in two fresh electrons one after the other after the M_2 level has been filled up. These two electrons occupy the N_1 level, and not the M_3 level. Hence the negative energy value of the electron corresponding to N_1 is greater than M_3 , at least for optical levels. For the electrons in the interior of the atom, *i.e.* for X-ray levels, this is, however, not true, and the negative energy in M_3 is larger than the negative energy in N_1 . But for optical levels, the energy in N_1 is sometimes greater, sometimes less, and generally of the same order of magnitude as M_3 . Transition also takes place from M_2 either to M_3 or to N_1 . To indicate this fact, N_1 is put below M_2 and not after M_3 as is usually done. Thus

$$\begin{aligned} (K_1) &> (L_1) > (L_2), (M_1) \\ &> (M_2), (N_1) \\ &> (M_3), (N_2), (O_1) \\ &\text{etc.,} \end{aligned}$$

where (X) denotes the negative value of energy corresponding to the level. But though this is usually the rule, in certain cases, *e.g.* in Sc^+ , the negative energy in the M_3 level is larger than the energy in the N_1 level.

To illustrate the utility of this chart to account for the terms of any optical spectrum, we start with a structure diagram for Potassium K (19):

$$\begin{array}{ccccccc}
 & & & & & & K \\
 & & & & & & 2 \\
 & L_1 & L_2 & & & & \\
 & 2 & 6 & & & & \\
 & & M_1 & M_2 & M_3 & & \\
 & & 2 & 6 & & & \\
 & & & N_1 & N_2 & N_3 & N_4 \\
 & & & 1 & & & \\
 & & & & O_1 & O_2 & O_3 & O_4
 \end{array}$$

According to the fundamental assumption of Pauli, a single electron occupying any orbit by itself is to have a doublet character. Consequently the term which originates when the valence electron is occupying the N_1 level, which is the normal configuration of the electron in the atom, is 2S_1 . We can write it as 1^2S_1 , which denotes that it is the first term of the S series. Transitions of the electron can take place either horizontally or vertically by one step; that is, it may pass on to N_2 , and thence either to M_3 , or to N_2 or to O_1 . When the electron is at N_2 , the terms $1^2P_{1,2}$ originate corresponding to the azimuthal quantum number $K=2$. At N_3 it gives rise to the terms $1^3D_{2,3}$, and at O_1 to 2^2S_1 , which forms the second Rydberg sequence to the S series. It should be noted that transitions cannot usually take place in a slanting direction, such as from N_1 to O_1 , unless the selection principle is violated. Transitions of an electron by three steps such as from $N_1 \rightarrow N_2 \rightarrow O_1 \rightarrow O_2$, are also possible, for it corresponds to $1S-1P+1P-2S+2S-2P$, i. e. from $1S-2P$.

As mentioned above, the structure diagram also gives a rough indication of the values of successive terms. Thus

$$\begin{aligned} 1^2S_1 &> 1^2P_{1,2}, 2^2S_1, \\ &> 1^2D_{2,3}, 2^2P_{1,2}, 3^2S_1, \\ &> 1^2F_{3,4}, 2^2D_{2,3}, 3^2P_{1,2}, 4^2S_1, \end{aligned}$$

and so on. The terms in the same vertical column have also roughly the same order of values.

It is necessary at this stage to discuss in some detail the utility of this structure diagram of atoms in identifying without any ambiguity the terms forming a Rydberg

completed in this case. This is not in accordance with Bohr; but this method of writing the structure diagram clears the point regarding the initial value of m in a Rydberg sequence more in accordance with the usual practice, though Bohr's method gives a uniform notation to both X-ray and optical spectra.

It should be mentioned that the terms like 3^1S_0 and 3^3S_1 , or 4^1S_0 and 4^3S_1 , which originate from the combination of electrons in the same level or levels, do not combine with each other; also two terms like 1^1S_0 and 2^1S_0 show some deviation from an exact Rydberg sequence owing to the presence of 2 electrons in the same level. This deviation is not well pronounced in the case of alkalis.

We have not explained here how to arrive at the terms which result either from the presence of more than one electron in the same level or from a combination of two or more electrons in two different levels; nor have we explained the case of simultaneous displacement of two electrons from their normal position. The nature of small positive or negative terms which result from simultaneous movements of two electrons has been fully discussed by Dr. Saha in a paper communicated to this journal. The other points will be illustrated with reference to Cobalt. But before we pass on to it, we have to explain briefly the symbols which are necessary for this purpose.

By a comparison of the various systems of symbols used by different writers, Laporte* considers Sommerfeld's system of notation to be more convenient than those of others. Hence, while retaining the usual symbol n_{kj}^r of Landé for each spectral term, we adopt Sommerfeld's notation with a slight change as has been done by Prof. Saha. Thus

I_r stands for Sommerfeld's j_s ,

I_k stands for Sommerfeld's j_k ,

and I_j denotes the effective quantum number.

In n_{kj}^r , r stands for the multiplicity of the term, k and j for the azimuthal and inner quantum numbers respectively, and n for the total quantum number.

Thus

$$I_r = j_s = \frac{r-1}{2} = 0, \frac{1}{2}, \frac{2}{2}, \frac{3}{2}, \dots \text{ for singlets, doublets, triplets, etc.,}$$

$$I_k = k-1 = 0, 1, 2, 3 \text{ for } s, p, d, f \dots \text{ terms etc.,}$$

* Laporte, *loc. cit.*

10 in the N_3 level is always 1S_0 . If we combine this 1S_0 term with the terms which arise from the presence of 7 electrons in the M_3 level, the resulting effect is just the same as that due to 7 electrons in the M_3 shell. Thus from Laporte's table we have the following terms from this configuration :

$$^4F \ ^4P \ ^3H \ ^2G \ ^2F \ ^2D \ ^2D \ ^2P.$$

Another possible metastable configuration of the electrons of the Cobalt atom is to have 8 electrons in the M_3 level and 1 in the N_1 level. We find from Laporte's above-mentioned table that the terms due to 8 electrons in the M_3 ring are

$$^3F \ ^3P \ ^1G \ ^1D \ ^1S.$$

To calculate the terms due to the combination of 8 electrons in the M_3 shell and 1 in the N_1 we proceed simply as follows, as Pauli's principle of exclusion does not hold in this case:—

	$I_r = \frac{r-1}{2}$	$I_k = k-1$	
3F	$\frac{2}{2}$	3	$\therefore r = 4, 2; \quad k = 4.$
$1N_1$	$\frac{1}{2}$	$\frac{0}{3}$	\therefore the terms are $^4F, ^2F.$
	$\frac{3}{2}, \frac{1}{2}$		
3P	$\frac{2}{2}$	1	$\therefore r = 4, 2; \quad k = 2.$
$1N_1$	$\frac{1}{2}$	$\frac{0}{1}$	\therefore the terms are $^4P, ^2P.$
	$\frac{3}{2}, \frac{1}{2}$		
1G	0	4	$\therefore r = 2; \quad k = 5.$
1N_1	$\frac{1}{2}$	$\frac{0}{4}$	\therefore the term is $^2G.$
	$\frac{1}{2}$		

Similarly the terms from other combinations are 2D and 2S . Collecting all the terms from these three configurations we write thus:

(a) $9M_3$	$^2\bar{D},$
(b) $7M_3-2N_1$	$^4F \ ^4P : ^2H \ ^2\bar{G} \ ^2F \ ^2\bar{D} \ ^2D \ ^2P,$
(c) $8M_3-1N_1$	$^4F \ ^4P : ^2G \ ^2D \ ^2\bar{S}$ $^2F \ ^2P :$

These three states (a) (b) (c) may be termed as equivalent states. It is not possible to pass from any one of these states to any other by a transition of one step either vertically or

horizontally. So the terms from any one state cannot combine with those from any other. This is exactly borne out by the classification of the spectrum of CoI by Catalan and Bechert*. Also the terms such as F, D, P, etc. from any one state, say (b), cannot enter into combination. To denote this possibility we have dashed the alternate set of terms as shown above. We could have dashed the remaining set of terms and kept 2G , 2D , 2D from state (b) undashed. As the terms from these three states do not combine with each other, we have to dash the terms with the same designation from the other states also. It is therefore merely a matter of convention, the real significance being that S, P or P, D, or D, F terms arising from the same configuration of electrons in an atom possess identical combinatory powers as regards other levels and therefore they cannot combine with each other.

According to the principles developed by Pauli, Heisenberg, and Hund, we note that if in a group of terms resulting from a given electron configuration there are terms having the same value of k but with different multiplicities, the one with the highest multiplicity will be deepest; also if there are terms of the same multiplicity but with different values of k , that with the highest k will be the deepest. Combining these two rules, we find that of the terms from (b) and (c) 4F will be the deepest term in each case. We identify the 4F term from the state $7M_3-2N_1$ with the deepest 4F term as found by Catalan and Bechert, as, according to Bohr and Stoner, this is the most stable configuration of the electrons in the Cobalt atom. The terms next in order are 4F and 2F from $8M_3$ and $1N_1$. That this state is equally probable is shown by the fact that the terms 4F and 2F , both of which result from the combination (${}^3F+1N_1$), appear in the spectrum of Cobalt and their value is very little different from the fundamental 4F . Neither the term ${}^2\bar{D}$ from state (a) nor the other terms from states (b) and (c) have been identified by Catalan and Bechert. We are not in a position to state whether the state (a) exists at all or not. The other terms from (b) and (c) also have not been identified by Catalan and Bechert. Probably they do not appear at all, but as yet we are unable to account for the preference of certain sets of terms over others.

The terms from the states (b) and (c) which correspond

* Catalan and Bechert, *Zs. f. Phys.* xxxii, p. 336 (1925).

to the terms discovered by Catalan and Bechert are shown in Table I.

Next we consider the two equivalent states

$$\begin{array}{ll} (d) & 7M_3-1N_1-1N_2 \\ \text{and} & (e) \quad 8M_3-1N_2. \end{array}$$

The electron configurations in (d) and (e) can result either from a single-step transition of an electron or from three-step transition from (a), (b), and (c). Thus from (a) an electron can pass in two steps to the N_1 level and another can pass on to the N_2 level in one step, resulting in the state (d) $7M_3-1N_1-1N_2$. Similarly the other transformations can be effected. To arrive at terms corresponding to (d) we first find the terms due to the combination of $1N_1$ and $1N_2$, remembering that each electron when occupying a level by itself has a doublet character. Thus:

	$1N_1$	$1N_2$	I_K	
	$\frac{1}{2}$	$\frac{1}{2}$	0	$\therefore r = 3, 1; \quad k = 2.$
	$\frac{1}{2}$	$\frac{1}{2}$	$\frac{1}{1}$	\therefore the terms are
	$\frac{2}{2}$	$\frac{0}{2}$	$\frac{1}{1}$	3P and $^1P.$

Of the terms from $7M_3$ we need only consider the 4F term, as this is the deepest term, and combinations with this term would be more probable than with others. R. H. Fowler and Hartree² have shown that in the spectrum of O^+ , where the orbit given by the running electron has to be combined with the orbits given by $2L_2$, all terms arising from $2L_2$ have to be considered. The most important term is $^3P_{0,1,2}$, and this gives the most important terms. The next combinations are 1S_0 and 1D_2 , and terms arising from these levels are also present. Similarly, taking the 3F term only out of the terms due to 8 electrons in the M_3 level, and, following the process detailed above, we arrive at the following sets of terms:—

$$\begin{aligned} (d) \quad 7M_3-1N_1-1N_2. \\ \quad \quad \quad {}^4F + {}^1P = \begin{cases} {}^6G & {}^6\bar{F} & {}^6D, \\ {}^4G & {}^4\bar{F} & {}^4D, \\ {}^2G & {}^2\bar{F} & {}^2D, \end{cases} \\ \quad \quad \quad {}^4F + {}^1P = \quad {}^4G \quad {}^4\bar{F} \quad {}^4D \\ (e) \quad 8M_3-1N_2. \\ \quad \quad \quad {}^4F + {}^2P = \begin{cases} {}^4G & {}^4F & {}^4D, \\ {}^2G & {}^2F & {}^2D. \end{cases} \end{aligned}$$

* R. H. Fowler and Hartree, Proc. Roy. Soc. cxi. (1926).

We have dashed the F terms to express the fact that these F terms combine with those from the states (a), (b), and (c). The other terms G and D combine with those from (a), (b), and (c) according to the usual rules of the selection principle. As (d) and (e) are equivalent states, the terms from (d) cannot combine with those from (e). Of the terms from (d), 6G should be the deepest, but from the analysis of the spectrum of CoI we find that 6F is the deepest of the group, and 6D , 6G terms are approximately of the same order.

An exception to the selection principle * $\begin{matrix} r+2 \\ r \\ r-2 \end{matrix}$,

governing the combination between terms of different multiplicity, has been noted by Catalan and Bechert. They have discovered a line due to the combination of a doublet F term and a sextet F term, i. e., the line $\lambda = 6143.78$, $F_3^1 - \bar{\phi}_3^1$. Because the 6F or $\bar{\phi}$ term from (d) can combine with the 2F or F^1 term from (e), this apparent anomaly is explained.

As the 4F from (b) is the deepest term, and the next deeper term with which 4F can combine is 6F from (d), resonance lines will also be due to the combination of these two sets of terms, as has been mentioned by Catalan and Bechert; but this will correspond to the line $1S-2p$, $\nu = 15210$ of Calcium, and not to $1S-2P$, $\nu = 23652$, which usually appears with great prominence in the absorption spectrum of the unexcited vapour of the metal.

All the terms from (d) and (e) have been identified by Catalan and Bechert, and are shown in Table I.

Finally, we come to the equivalent states :

$$(f) \quad 7M_3 - 1N_1 - 1O_1,$$

$$(g) \quad 7M_3 - 1N_1 - 1N_3,$$

$$(h) \quad 8M_3 - 1O_1,$$

$$(i) \quad 8M_3 - 1N_3.$$

* It may be emphasized that in the rule for transition given here—i. e. such transitions from a certain state to some other state are possible as are obtained by displacing an electron an odd number of times, the displacement being either vertically or horizontally (but never diagonally).—all apparent deviations from the selection principle are explained. Every one of the two sets of terms arising from such states will combine with the other, if the selection principle for the inner quantum number is satisfied, no matter whatever may be the multiplicity or the azimuthal quantum number of the two sets.

TABLE I.

State and term from structure diagram.	Term designation according to Catalan & Bechert.	Combining terms.
(b) 4F	$f_5^1-f_2^1$	$\left\{ \begin{array}{l} dD^1 \quad eD^2 \quad dF^1 \quad e\bar{F}^2 \quad dG^1 \quad eG^2 \\ dD^1 \quad d\bar{d}^2 \quad e\bar{d}^3 \quad d\bar{f}^1 \quad d\bar{f}^2 \quad e\bar{f}^3 \\ d_g^1 \quad d_g^2 \quad e_g^3 \quad d_{\delta}^1 \quad d_{\phi}^1 \quad d_{\gamma}^1 \end{array} \right.$
(c) 4F	$f_6^2-f_2^2$	$\left\{ \begin{array}{l} dD^1 \quad eD^2 \quad dF^1 \quad e\bar{F}^2 \quad dG^1 \quad dG^2 \\ d_d^1 \quad d_d^2 \quad e_d^3 \quad d\bar{f}^1 \quad d\bar{f}^2 \quad e\bar{f}^3 \\ d_g^1 \quad d_g^2 \quad e_g^3 \quad d_{\delta}^1 \quad d_{\phi}^1 \quad d_{\gamma}^1 \end{array} \right.$
(c) 2F	$F_4^1-F_3^1$	$\left\{ \begin{array}{l} dD^1 \quad eD^2 \quad d\bar{F}^1 \quad e\bar{F}^2 \quad dG^1 \quad dG^2 \\ d_d^1 \quad d_d^2 \quad e_d^3 \quad d\bar{f}^1 \quad d\bar{f}^2 \quad e\bar{f}^3 \\ d_g^1 \quad d_g^2 \quad d_{\phi}^1 \end{array} \right.$
(b) 4P	$p_3^1-p_1^1$	$eD^2 \quad dF^1 \quad d_d^1 \quad d_d^2 \quad e_d^3 \quad d\bar{f}^1 \quad e\bar{f}^3$
(c) 4P	$p_2^2-p_1^2$	$\left\{ \begin{array}{l} dD^1 \quad eD^2 \quad dF^1 \quad e\bar{F}^2 \quad d_d^1 \quad d_d^2 \\ e_d^3 \quad d\bar{f}^1 \quad d\bar{f}^2 \quad e\bar{f}^3 \end{array} \right.$
(c) 2P	$P_2^1?$	$\left\{ \begin{array}{l} dD^1 \quad eD^2 \quad d\bar{F}^1 \quad e\bar{F}^2 \quad d_d^1 \quad d_d^2 \\ e_d^3 \quad d\bar{f}^1 \quad d\bar{f}^2 \quad e\bar{f}^3 \end{array} \right.$
(d) 6F	$\phi_6^1-\phi_2^1$	$dF^1 \quad b_f^1 \quad c_f^2 \quad f_{\phi}^1$
(d) 6D	$\delta_5^1-\delta_1^1$	$b_f^1 \quad c_f^2 \quad f_{\phi}^1$
(d) 6G	$\gamma_7^1-\gamma_2^1$	$b_f^1 \quad c\bar{f}^2 \quad f_{\phi}^1$
(d) ${}^4\bar{F}$ } From $F+{}^3P$.	$f_5^1-f_2^1$	$P^1 \quad cF^1 \quad b_p^1 \quad c_p^2 \quad b_f^1 \quad c_f^2 \quad f_{f3}$
(d) 4G }	$g_6^1-g_3^1$	$cF^1 \quad b_f^1 \quad c_f^2 \quad f_{f3}$
(d) 4D }	$d_4^1-d_1^1$	$c_p^1 \quad cF^1 \quad b_p^1 \quad c_p^2 \quad b_f^1 \quad c_f^2 \quad f_{f3}$
(d) 2G	$G_6^1-G_4^1$	$cF^1 \quad b_f^1 \quad c_f^2 \quad f_{f3}$
(d) ${}^2\bar{F}$	$\bar{F}_4^1-\bar{F}_3^1$	$\left\{ \begin{array}{l} c_p^1 \quad cF^1 \quad b_p^2 \quad c_p^2 \quad b_f^1 \\ c_f^2 \quad f_{f3} \quad d_d^1 \quad d_d^2 \quad e_d^3 \end{array} \right.$
(d) 2D	$D_3^1-D_2^1$	$c_p^1 \quad cF^1 \quad c_p^2 \quad b_f^1 \quad c_f^2$
(d) 4D } From $F+{}^1P$.	$d_4^2-d_1^2$	$cP^1 \quad cF^1 \quad b_p^1 \quad c_p^1 \quad b_f^1 \quad c_f^2 \quad f_{f3}$
(d) 4G }	$g_6^2-g_3^2$	$cF^1 \quad b_f^1 \quad c_f^2 \quad f_{f3}$
(d) 4F }	$f_5^2-f_2^2$	$c_p^1 \quad cF^1 \quad e_p^2 \quad b_f^1 \quad c_f^2 \quad f_{f3}$
(e) 2G	$G_6^2-G_4^2$	$cF^1 \quad b_f^1 \quad c_f^2$
(e) ${}^2\bar{F}$	$\bar{F}_4^2-\bar{F}_3^2$	$cP^1 \quad cF^1 \quad c_p^2 \quad b_f^1 \quad c_f^2$
(e) 2D	$D_3^2-D_2^2$	$cP^1 \quad cF^1 \quad b_p^1 \quad c_p^2 \quad b_f^1 \quad c_f^2$
(e) 4D	$d_4^3-d_1^3$	$c_p^1 \quad cF^1 \quad b_p^1 \quad b_f^1 \quad c_f^2$
(e) ${}^4\bar{F}$	$f_5^3-f_2^3$	$cP^1 \quad cF^1 \quad b_p^1 \quad c_p^2 \quad b_f^1 \quad c_f^2$
(e) 4G	$g_6^3-g_3^3$	$b_f^1 \quad c_f^2$
(f) 6F } From $F+{}^3S_1$.	$\phi_6^1-\phi_1^1$	$d_{\phi}^1 \quad d_{\phi}^1 \quad d_{\nu}^1$
(f) 4F }	$f_5^3-f_2^3$	$\left\{ \begin{array}{l} d\bar{F}^1 \quad dG^1 \quad eG^2 \quad d_d^1 \quad d_d^2 \quad d_f^1 \\ d\bar{f}^2 \quad d_g^1 \quad d_g^2 \quad d_{\delta}^1 \quad d_{\phi}^1 \quad d_{\gamma}^1 \end{array} \right.$

N.B.—In a term like dD^1 , d denotes the state from which the term originates, and D^1 is the term designation according to Catalan and Bechert.

The terms corresponding to these states may be easily found according to the method sketched before. Here we need only consider the terms from (*f*), as they are of special interest in tracing out the Rydberg sequence. The terms due to 1 electron in the N_1 level and 1 in the O_1 level are 3S_1 and 1S_0 respectively. Taking into account the 4F term only from the $7M_3$ state, we get the following terms :

$$\begin{aligned} (f) \quad ^4F + ^3S_1 &= {}^6F, \quad ^4F, \quad ^2F, \\ ^4F + ^1S_0 &= \quad ^4F. \end{aligned}$$

These F terms will be undashed, as they combine with the F terms from (*d*) and (*e*). The terms 6F and 4F from ${}^4F + {}^3S_1$ have been identified as shown in Table I., but the remaining terms 2F and 4F have not been discovered. The state (*b*) $7M_3 - 2N_1$ is equivalent to $7M_3 + {}^1S_0$, and hence ${}^4F + {}^1S_0$ from (*f*) will form a Rydberg sequence to the term ${}^4F + {}^1S_0$ from (*c*). This term has not yet been identified, but its value will roughly be of the same order as 4F from (*f*).

Though the ionization potential of Cobalt cannot be correctly estimated until the term ${}^4F + {}^1S_0$ from (*f*) has been discovered, yet we can have a close estimate of it from the fact that the value of this term is approximately of the same order as ${}^4F + {}^3S_0$ from (*f*). We shall not be much in error if we take ${}^4F + {}^3S_0$ from the state (*f*) as the Rydberg sequence to ${}^4F + {}^1S_0$ from (*b*). The ionization potential is thus obtained as approximately 8.51 volts, which is only a lower limit, the actual value being slightly greater.

This work, therefore, points out that in the analysis of the arc spectrum of Cobalt as yet only a number of fundamental levels and some levels combining with these have been found. No Rydberg sequence has been discovered, but, as will be shown in a separate communication, better progress has been made in the case of Iron, where higher sequences have been correctly guessed by Laporte. Finally, it remains to be settled whether the $9M_3$ state is possible or not; for though according to Bohr and Stoner $7M_3 - 2N_1$ is the most stable configuration of the electrons in the Cobalt atom, the terms due to $8M_3 - 1N_1$ state occur prominently in the arc spectrum of Cobalt. Further work is being done in this direction.

In conclusion I wish to record my best thanks to Professor

Saha for suggesting this problem to me, and for the interest taken in the work.

Allahabad,
October 1926.

Addendum.—It may be mentioned here that some of the doublet terms arising out of the states (*b*) and (*c*) and terms of higher multiplicity from the states (*f*), (*g*), (*h*), etc., have been identified. Further analysis has also led to the identification of the Rydberg Sequence as mentioned before. These results will be published in a separate paper.

Allahabad,
May 1927.

V. *The Geissler Discharge in Argon.* By K. G. EMELÉUS, M.A., Ph.D., Demonstrator in Physics, and N. L. HARRIS, B.Sc., King's College, University of London*.

1. Introduction.

WHEN an exploring electrode, or *collector*, is placed in the path of an electric discharge, its surface becomes covered with a layer often visibly different from the remainder of the ionized gas. The outer boundary of the sheath, which is a region of space-charge, marks the limit of the disturbing effect of the collector. It follows that a study of the current-potential characteristic of the latter will yield precise information about the potential of the surrounding space, and about the number and nature of the ions¹. This method has been applied with considerable success to arcs in mercury vapour and other gases, to glow discharges from a hot filament, and to the scattering of electrons, and its validity and range of application have been dealt with theoretically in some detail². It may also be used, as would be expected, to analyse the glow discharge from a cold cathode, and the present experiments are an extension of preliminary work in this field³.

The number of variables in this type of discharge is large. We have confined our attention for the present to conditions

* Communicated by Prof. E. V. Appleton, D.Sc.

¹ Langmuir, Journ. Franklin Inst. 196, p. 751 (1923).

² Langmuir & Mott-Smith, Phys. Rev. xxviii. p. 727 (1926).

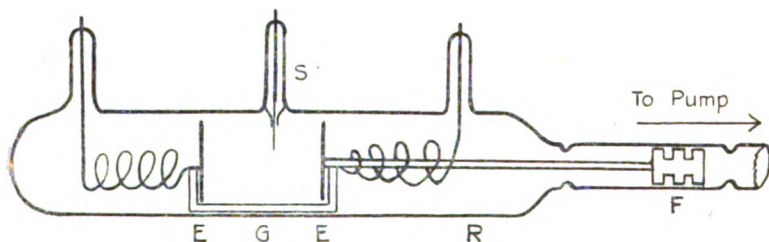
³ Emeléus, Proc. Camb. Phil. Soc. xxiii. p. 531 (1927).

not very different from those corresponding to a normal cathode fall of potential, with a gas-pressure of the order of 1 mm. Hg, potentials of about 250 volts, and current densities of 0.1 milliampere per sq. cm. The cathode dark space is then less than a cm. across, and the region between the diffuse boundary of the negative glow and the anode is almost non-luminous. We have been concerned with the general features of the discharge rather than with their relation to the specific properties of the gas employed (argon).

2. *Experimental Arrangements.*

A discharge-tube was built to the design shown in fig. 1. It had two circular nickel electrodes (E), carried by a bent glass rod (G). One of them was connected by a nickel rod (R) to a piece of soft iron (F), so that the system could be

Fig. 1.



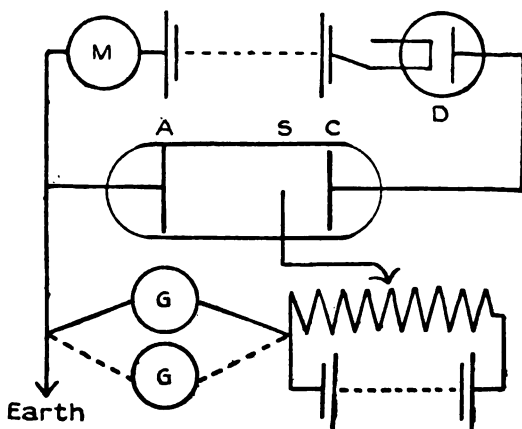
moved bodily by an external electromagnet. Electrical connexion was made with the electrodes by light nickel springs welded to copper strips, which were sealed through side tubes. A length of molybdenum wire (S), 0.2 mm. in diameter, served as collector: all but the last cm. was protected by a glass sheath, and the metal and glass were not in contact near the part exposed to the discharge. It was necessary to use a relatively large exploring electrode to obtain readily measurable currents. The main tube was 4 cm. in diameter, and the distance between the electrodes was 5 cm.

Argon, which had been purified by repeated passage over calcium, and stored over mercury, was admitted after exhausting the tube to a pressure of less than 10^{-4} mm. Hg by a small mercury-vapour pump. Between the reservoir and the discharge-tube it was passed over phosphorus pentoxide, and through a liquid-air trap. The spectroscopic impurities were hydrogen (H_a) and mercury, both of which

are enhanced by argon, but no bands associated with carbon or nitrogen could be detected. With liquid air on a trap between the tube and a McLeod gauge, the pressure did not vary by more than 5 per cent. with the discharge passing continuously for nine hours.

The electrical connexions are shown in fig. 2. The current from a battery of 300 lead accumulators was regulated by a thermionic diode (D) and measured on a multi-range microammeter (M). The collector (S) could be charged to a potential of ± 250 volts relative to the anode (A), and the current to it was measured on one of two galvanometers (G), provided with a variety of shunts, with a range

Fig. 2.



between 10^{-10} amp. and 10^{-3} amp. The apparatus between S and A was carefully insulated, to avoid stray currents.

At the low current densities employed, there is a marked tendency for the cathode dark space to be thicker close to the glass walls of the tube than at the axis. A gap of 2 mm. was therefore left between the rim of the cathode and the glass, which had the effect of making the edge of the dark space flat in the neighbourhood of the collector. This prevented the use of high current densities, when the discharge became intermittent, and passed to the back of the electrode, but was essential in order to obtain uniform conditions over the length of the exploring electrode.

When the discharge was passing, there was a blue negative glow, which was moderately sharply bounded towards the cathode, and faded diffusely into a Faraday dark space

which extended to the anode. An anode glow was sometimes present (§ 4), and the mercury spectrum, if present, was particularly prominent in this part of the tube. 27.15.1927

It has been shown by a variety of methods that the discharge was not oscillatory or intermittent.

3. Method of Analysis.

Simultaneous readings were taken of the current through the tube (i_t), and of the current to the collector (i_c), as the potential (V) of the latter was varied. To allow for slight variations in the main discharge, the ratio i_c/i_t was used in the subsequent analysis; this will not be described in detail, since it has been elaborated in previous papers⁴.

The formulæ used to find the concentrations and temperatures of the slow electrons when they were collected in a retarding field were:—

$$\frac{d \log I}{dV} = \frac{e}{kT} \cdot \cdot \cdot \cdot \cdot (1)$$

and

$$I_0 = Ne(kT/2\pi m)^{\frac{1}{2}} \cdot \cdot \cdot \cdot \cdot (2)$$

where I is the electron current to the collector at potential V , corrected for positive ions, and I_0 is the electron current to it per unit area at the space potential. N , T , and e/m are the concentration, temperature, and specific charge of the electrons, and k is the gas-constant per molecule. The space potential was taken to be that potential of the exploring electrode beyond which the linear relation (1) ceased to hold, and the effective area of the collector was assumed to be that of its cylindrical surface. In some cases when the relation between $\log I$ and V was not linear, the current could be analysed into two components, each of which satisfied equation (1). This has been interpreted as showing the presence of two groups of electrons, each with a definite temperature⁵. No use has been made of that part of the characteristic of the collector which corresponds to reception of electrons in an accelerating field, since the main discharge was then markedly affected by their removal.

The information to be derived by collecting positive ions in an accelerating field is less definite. Dauvillier has shown that there is frequently present in the negative glow radiation which requires for its excitation electrons of energy corresponding to almost the full cathode fall of potential⁶.

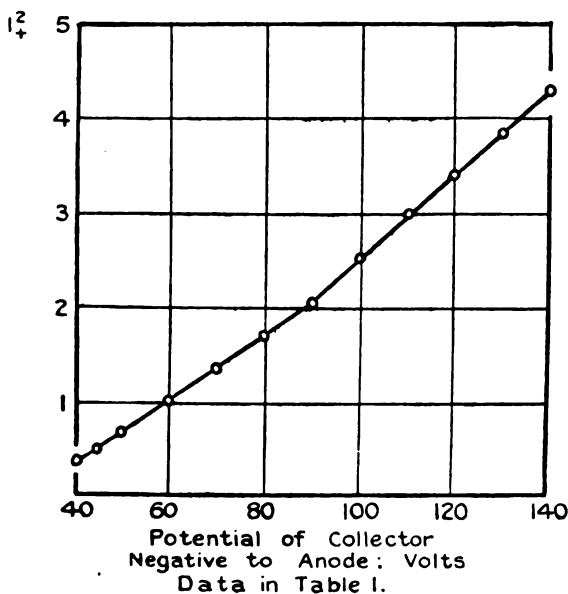
⁴ Langmuir and Mott-Smith, *General Electric Review*, 1924.

⁵ Langmuir, *Phys. Rev.* xxvi. p. 585 (1925).

⁶ Dauvillier, *Journ. de Phys.* vii. p. 369 (1926).

Absorption of soft X-rays, with emission of photo-electrons from the molybdenum, would cause an apparent increase in the positive ion current, but the direct effect of such electrons on the characteristic cannot be predicted with certainty, as they may give rise to secondary electrons on impact on the metal. When the square of the positive ion current was plotted against the potential across the positive ion sheath, almost linear curves were obtained, which often showed two distinct portions. An example of one of these is shown in fig. 3. The break seems to indicate that at the lower potentials "primary" electrons were penetrating the positive ion sheath. The data available are insufficient to correlate the position of the breaks with other conditions in the discharge.

Fig. 3.



A further difficulty arises if we attempt to allow for the effect of collisions made by the positive ions in traversing the sheath, since they were too infrequent to give the ions a drift velocity proportional to the local field. We have therefore employed the cylindrical solution of Poisson's equation in which the effect of collisions is neglected, to obtain an approximate value for the random positive ion current in the discharge⁷. Table I. contains a typical set

⁷ Langmuir and Blodgett, Phys. Rev. xxii. p. 347 (1923).

TABLE I.

Potential between Collector and Space.	121	111	101	91	81	71	61	51	41	31	volts.
I. { Sheath radius.....	*0.91	0.86	0.81	0.80	0.70	0.65	0.60	0.53	0.47	0.40	cm.
Random positive ion current.	1.24	1.25	1.24	1.24	1.24	1.22	1.20	1.21	1.20	1.16	$\left\{ \begin{array}{l} \times 10^{-6} \text{ amp.} \\ \text{per cm.}^2 \end{array} \right.$
II. { Sheath radius.....	0.103	0.100	0.094	0.089	0.083	0.080	0.076	0.073	—	—	cm.
Random positive ion current.	1.04	1.07	1.06	1.05	1.05	0.99	0.95	0.89	—	—	$\left\{ \begin{array}{l} \times 10^{-5} \text{ amp.} \\ \text{per cm.}^2 \end{array} \right.$

Collector just to Anode side of the brightest part of the Negative Glow.

Tube pressure 0.61 mm.; Tube volts 210; Tube current 0.3 milliamp.; Space potential, —19 volts relative to Anode.

I. Values calculated assuming no collisions within the sheath.

II. Values calculated from mobility motion.

* At this potential the visible sheath radius was about 3 mm.

of results obtained for various collecting voltages: a break occurred in the i^2 -V curve at 90 volts. Since there is, in addition, uncertainty as to the temperature of the positive ions, we have not calculated their concentration by equation (2).

In spite of these sources of error, the ratio of the random positive ion and electron currents is about the same as has been found previously, and the results may be relied upon to show in a general way how the positive ion concentration varies along the path of the discharge. Less consistent results are obtained when the characteristics are analysed on the assumption that the positive ions have a mobility motion^{*}, but the distribution curve for their concentration is of the same form. A set of results obtained by this method has been included in Table I.

4. *Experimental Data and Results.*

Experimental data, which have been chosen to illustrate the changes observed as the pressure was varied, are contained in Tables II.-V. and figs. 4-7. It will be seen that in all cases the total electron density (n_e) and random positive ion current (i_+), reach a maximum near the middle of the negative glow, and that the electric field is reversed between the point of maximum concentration and the edge of the cathode dark space. The electron peak does not in general coincide with the positive ion peak, probably because the electron concentrations were obtained from the current at the space potential, when the sheath vanishes, and the data for the positive ions with a sheath the outer radius of which was of the order of a mm. Beyond the edge of the cathode dark space, the characteristic curves changed markedly in form, and have not yet been satisfactorily analysed. The collector throws a shadow towards both anode and cathode, and it may be questioned if reliable information can be obtained about this region by any method in which a probe has to be introduced.

The electric field between the negative glow and the anode changes with pressure. At the three highest pressures there was a positive anode fall of potential of the order of 20 volts, with which was associated an anode glow; the potential was almost constant in the Faraday dark space. At 0.9 mm. there was also a direct field of 8 volts per cm. in the positive side of the negative glow. At 0.19 mm. the field was completely reversed between the anode and the cathode dark space, and there was no anode glow.

^{*} McCurdy, *Phys. Rev.* xxvii. p. 157 (1926).

TABLE II.

Part of Discharge.	Distance from Anode, cms.	Space Potential relative to Anode, volts.	Random Electron Current, amps./cm. ²	Random Positive Ion Current, amps./cm. ²	Fast Group of Electrons.		Slow Group of Electrons.	
					volts.	No./c.c.	volts.	No./c.c.
Faraday Dark Space.	0.52	-24.5	1.18×10^{-5}	1.89×10^{-6}	—	—	4.45	2.59×10^6
	2.38	-23.0	2.24×10^{-5}	1.72×10^{-6}	—	—	4.87	4.59×10^6
	3.88	-23.4	3.24×10^{-5}	2.18×10^{-6}	—	—	4.93	6.70×10^6
	4.28	-27.0	2.66×10^{-5}	2.75×10^{-6}	—	—	3.83	6.21×10^6
Negative Glow.	4.46	-28.3	4.07×10^{-5}	3.64×10^{-6}	—	—	3.33	1.03×10^7
	4.54	-28.2	7.36×10^{-5}	1.34×10^{-6}	—	—	3.11	1.92×10^7
	4.65	-24.7	2.52×10^{-4}	1.05×10^{-6}	—	—	2.74	6.95×10^7
	4.71	-25.9	1.77×10^{-3}	6.09×10^{-6}	4.51	1.47×10^7	1.75	3.93×10^7
	4.75	-16.1	6.20×10^{-3}	3.08×10^{-6}	5.42	2.90×10^7	2.32	1.42×10^7
	4.81	-13.0	1.65×10^{-3}	1.34×10^{-6}	7.67	1.33×10^7	2.43	2.70×10^7

Tube pressure 0.9 mm.; Tube volts 325; Tube current, 1.5 milliamp.
Cathode dark space 0.19 cm. thick.

TABLE III.

Part of Discharge.	Distance from Anode. cms.	Space Potential relative to Anode. volts.	Random Electron Current. amps./cm. ²	Random Positive Ion Current. amps./cm. ³	Fast Group of Electrons.		Slow Group of Electrons.	
					volts.	No./c.c.	Temperature.	Concentration.
Faraday Dark Space.	0.66	-17.5	4.97×10^{-3}	1.47×10^{-6}	—	—	3.46	1.22×10^7
	1.49	-19.5	3.82×10^{-3}	1.52×10^{-6}	—	—	2.11	1.21×10^7
	2.48	-18.8	1.09×10^{-3}	2.14×10^{-6}	—	—	2.19	3.37×10^7
	3.05	-18.25	4.05×10^{-4}	2.60×10^{-6}	—	—	2.05	1.30×10^8
	3.33	-17.8	1.13×10^{-3}	3.34×10^{-6}	—	—	1.37	4.67×10^8
	3.67	-18.0	1.72×10^{-3}	4.82×10^{-6}	—	—	1.24	7.12×10^8
	3.85	-17.9	1.98×10^{-3}	5.00×10^{-6}	—	—	1.33	7.83×10^8
	4.08	-18.4	1.52×10^{-3}	7.51×10^{-6}	—	—	1.03	6.77×10^8
	4.14	-18.2	1.88×10^{-3}	9.42×10^{-6}	3.47	1.02×10^8	0.72	6.89×10^8
	4.28	-18.3	1.43×10^{-3}	7.98×10^{-6}	2.26	1.30×10^8	0.70	6.95×10^8
Negative Glow.	4.33	-17.9	1.59×10^{-3}	7.71×10^{-6}	—	—	1.36	6.25×10^8
	4.45	-16.25	1.32×10^{-3}	4.13×10^{-6}	2.88	2.48×10^8	1.78	4.22×10^8
	4.54	-10.5	1.29×10^{-3}	3.30×10^{-6}	3.97	2.98×10^8	—	—
	4.65	-0.1	1.10×10^{-3}	1.54×10^{-6}	5.02	2.27×10^8	—	—

Tube pressure 0.52 mm.; Tube volts 220; Tube current 0.3 milliamp.

Cathode dark space, 0.35 cm. thick.

TABLE IV.

Part of Discharge.	Distance from Anode.	Space Potential relative to Anode.	Random Electron Current.	Random Positive Ion Current.	Single Group of Electrons.	
					Temperature. volts.	Concentration. No./c.c.
Faraday Dark Space.	3.17	-18.3	1.78×10^{-4}	5.51×10^{-6}	3.10	4.01×10^7
	3.56	-17.5	3.78×10^{-4}	8.60×10^{-6}	3.92	7.72×10^7
Negative Glow.	3.79	-16.8	4.10×10^{-4}	9.60×10^{-6}	3.44	8.97×10^7
	3.98	-16.6	3.07×10^{-4}	6.65×10^{-6}	3.71	6.97×10^7
	4.06	-16.1	3.51×10^{-4}	4.83×10^{-6}	3.92	7.72×10^7
	4.17	-15.7	2.62×10^{-4}	2.13×10^{-6}	4.46	5.42×10^7
	4.28	-15.6	1.38×10^{-4}	9.35×10^{-7}	7.55	2.18×10^7

Tube pressure 0.29 mm.; Tube volts 275; Tube current 0.4 milliamp.

Cathode dark space 0.72 cm. thick.

TABLE V.

Part of Discharge.	Distance from Anode.	Space Potential relative to Anode.	Random Electron Current.	Random Positive Ion Current.	Single Group of Electrons.	
					Temperature. volts.	Concentration. No./c.c.
Faraday Dark Space.	0.35	0.0	8.85×10^{-6}	9.40×10^{-7}	4.48	1.58×10^6
	1.95	+ 5.5	7.11×10^{-6}	9.70×10^{-7}	4.52	7.10×10^6
Negative Glow.	3.05	+ 8.8	1.59×10^{-4}	1.70×10^{-6}	5.10	2.97×10^7
	3.50	+ 11.7	1.72×10^{-4}	1.56×10^{-6}	4.47	4.42×10^7
	3.62	+ 12.6	1.86×10^{-4}	1.44×10^{-6}	4.84	5.14×10^7
	3.74	+ 16.1	1.87×10^{-4}	1.14×10^{-6}	6.52	3.66×10^7
	3.93	+ 21.5	5.92×10^{-5}	1.86×10^{-7}	9.73	4.86×10^6

Tube pressure 0.19 mm.; Tube volts 420; Tube current 0.25 milliamp.

Cathode dark space 1.07 cm. thick.

Fig. 4.—Data in Table II. Pressure 0.9 mm.

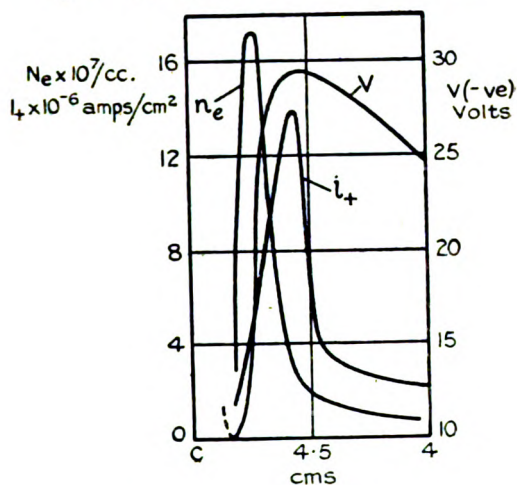


Fig. 5.—Data in Table III. Pressure 0.52 mm.

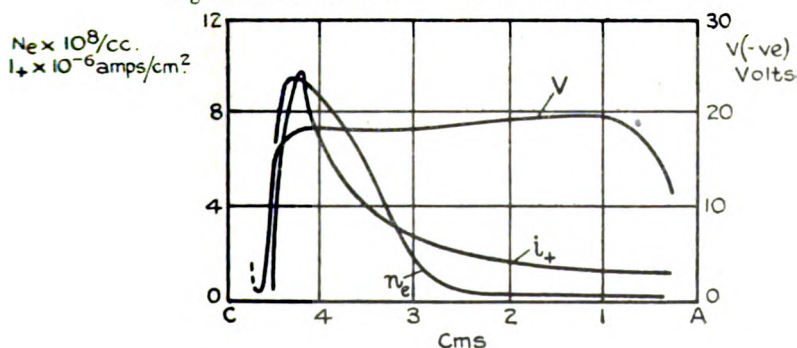


Fig. 6.—Data in Table IV. Pressure 0.29 mm.

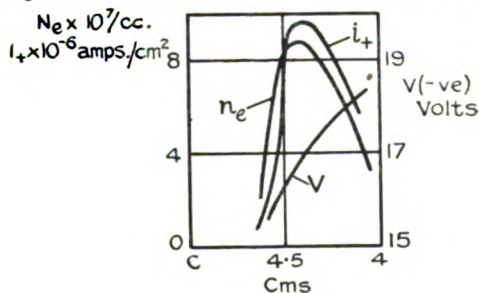
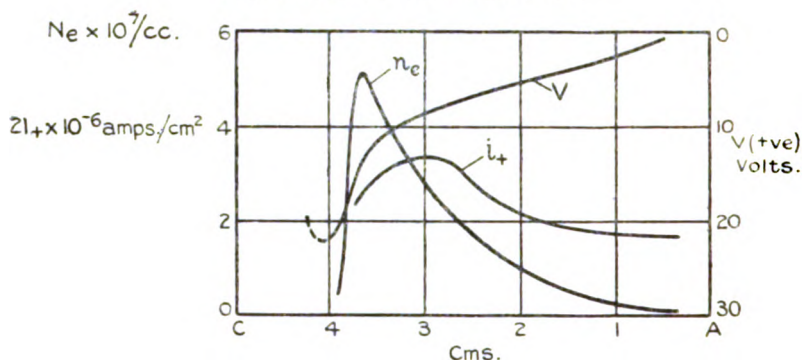


Fig. 7.

Data in Table V. Pressure 0.19 mm.



In Figs. 4-7, V is the space-potential relative to the anode. The abscissæ represent distances from the anode A towards the cathode C. The cathode dark space extended from C to the left-hand limit of the full curves.

The electron temperatures show little change along the Faraday dark space. There is a tendency to increase near the anode, which may be due to superposition of a considerable velocity of drift on the random motion. At 0.52 mm. there was a single fast group of electrons at the edge of the cathode dark space, and an additional slower group in the middle of the negative glow. The single fast group was not recorded at the highest pressure, probably because of the contraction of the negative end of the discharge. At the lowest pressures, only one group was present, as was the case at all pressures in the Faraday dark space.

We shall not give a detailed comparison between our results and those obtained with the older method of using a cold exploring electrode, because of the uncertainty attached to the latter. Reversal of the electric field has, however, been known to occur in the Faraday dark space under conditions similar to those which we have employed⁹, and it has been shown more recently by the present method that it is readily produced in low-voltage arcs in argon¹⁰. The differences between our results and those obtained by similar methods in recent work on glow discharges is to be attributed, in general, to our use of a cold cathode and very small current densities.

⁹ J. J. Thomson, *Phil. Mag.* xviii. p. 441 (1909).

¹⁰ K. T. Compton and Eckart, *Phys. Rev.* xxv. p. 139 (1925).

5. Discussion of Results.

The main features of the present work are the presence or absence of an anode fall of potential, the mechanism of conduction along the Faraday dark space, the origin of the intense ionization in the negative glow, and the nature of the current in the reversed field between the middle of the negative glow and the cathode dark space. We shall consider these individually on the lines proposed by K. T. Compton and others¹¹.

(a) Anode Glow.

In these experiments, the presence of an anode glow has always been associated with a direct local fall of potential rather greater than the ionization potential of argon (15.3 volts), and absence of the glow with a smaller reversed field, whatever the pressure. In the former case, the change from the small electric field in the Faraday dark space to the large direct field at the anode glow must take place in a region of negative space-charge, to satisfy Poisson's relation, but mechanical difficulties have prevented the collector from being brought sufficiently near to the anode to verify this. An anode glow often increases the effective area of the electrode¹², and it probably serves in any event as a source of positive ions for neighbouring parts of the Faraday dark space.

(b) Faraday Dark Space.

Tables II.-V. show that this is almost an equipotential region, except at the lower pressures, and that the concentration of electrons and positive ions increases largely towards the maximum in the negative glow. If the mobility of a positive ion is neglected in comparison with that of an electron, the concentration-gradient is equivalent to an electromotive force whose magnitude is given approximately by

$$E = kT/e \log N_2/N_1, \dots \dots (3)$$

where T is the electron temperature, and N_1 , N_2 the electron concentrations at the points between which E is to be evaluated. When this relation is used to find E between the region of maximum concentration in the negative glow, and the point nearest the anode in the discharges analysed in

¹¹ McCurdy, Phil. Mag. xlviii. p. 898 (1924); K. T. Compton, Turner, and McCurdy, Phys. Rev. xxiv. p. 597 (1924).

¹² Langmuir and Mott-Smith, Gen. Elect. Rev. xxvii. p. 767 (1924).

Tables II.-V., we find for its value about 11, 6, $1\frac{1}{2}$, and 11 volts. The second figure is certainly too large, since the luminosity on the anode was confined to the side remote from the collector, leading to too low an estimate of the concentration of electrons. The last two numbers are almost equal and opposite to the potential differences in the reversed fields. The resultant force on the electrons due to the combined effect of the electric and diffusion fields was therefore little different from zero at the lowest pressures, definitely positive at the highest pressure, and probably positive at 0.52 mm.

An independent estimate of the effective field may be obtained if it is assumed that the electrons have acquired a terminal random velocity; the field to which this is due may then be calculated from a knowledge of the mobility of an electron in argon¹³. This method gives 0.74, 0.18, 0.14, 0.15 volts per cm. respectively for the fields corresponding to figs. 4-7, which are of the order of magnitude indicated by the method of the preceding paragraph. Moreover, the random current of electrons near the anode is sufficient to carry the observed current through the tube, and the number of fast electrons from the cathode dark space which reach the anode must be negligibly small, since the mean free path of a 100 volt electron in argon at a pressure of 1 bar at 74° C. is 69 cm., and 70 per cent. of the collisions result in complete loss of energy¹⁴. Our results therefore afford strong evidence that in this type of discharge the current between the negative glow and the anode is mainly carried by slow electrons moving in combined electric and diffusion fields.

(c) *Negative Glow and Cathode Dark Space.*

The visual edge of the cathode dark space was coincident with the point beyond which characteristics of the usual type were no longer obtained with the collector. Existence of a sharp boundary, although partly a physiological effect¹⁵, is intimately connected with the fact that the dark space is a region of positive space-charge. The maximum of ionization in the negative glow is presumably related to the mean free path of the radiation quanta¹⁶ and fast electrons produced in the cathode dark space.

The reversed field in this part of the tube can be correlated with the local distribution of space-charge. The

¹³ K. T. Compton, *Phys. Rev.* xxii, p. 432 (1923).

¹⁴ Langmuir and Jones, *Science*, lix, p. 761 (1924).

¹⁵ Seeliger and Lindow, *Phys. Zeit.* xxvi, p. 393 (1925).

¹⁶ J. J. Thomson, *Phil. Mag.* xlvi, p. 1 (1924).

curvature of the potential curves in figs. 4, 5, and 7, shows that there is an excess of negative electricity in the middle of the negative glow, which, together with the positive ions in the cathode dark space, will give a component potential gradient opposite in sign to that arising from the surface charges on the electrodes. This will hinder the diffusion of positive ions from the middle of the negative glow towards the cathode, and the magnitude of the resultant electric field does in fact run parallel with that of the concentration gradient, as will be seen by comparison of fig. 4 with fig. 6. On the other hand, both concentration gradient and electric field will exert forces tending to move the slow electrons towards the cathode, and their disappearance must be brought about by recombination, and, probably to a less extent, by diffusion to the walls. This may account for the fact that the brightest part of the glow was observed to be to the cathode side of the region of maximum concentration, and that with very small currents, when the discharge was on the point of extinction and unstable, the negative glow was annular.

The two groups of electrons are comparable with the "secondary" and "ultimate" groups present in discharges from a hot filament at very low pressures¹⁷. The temperature of the group of greater energy increases towards the cathode dark space, but both groups have an average energy well below that required for ionization of the argon by a single impact. The information bearing on their production is meagre. Nevertheless, when taken in conjunction with some measurements which have been made in the discharge from a hot filament in hydrogen¹⁸, our results, though not conclusive, suggest that the current is carried from the cathode dark space to the negative glow by primary electrons, and that the positive ions in the cathode dark space are produced *in situ*¹⁹, and do not have their origin in the negative glow.

6. Summary.

The Geissler discharge between cold electrodes in argon has been studied by means of a cold exploring electrode. The main results, which are probably of general validity for

¹⁷ Langmuir, Phys. Rev. xxvi. p. 585 (1925).

¹⁸ Bramley, Phys. Rev. xxvi. p. 794 (1925).

¹⁹ As, for example, in the theory of J. J. Thomson, Phil. Mag. xlviii. p. 1 (1924).

similar discharges in wide tubes at low potentials and with small current densities, are :—

(i.) The electron concentration and random positive ion current attain a maximum in the middle of the negative glow.

(ii.) The current is carried from the negative glow through the Faraday dark space by slow electrons moving in combined electric and diffusion fields. The average energy of the electrons is very approximately constant in this part of the discharge.

(iii.) The electric field is reversed between the cathode dark space and the middle of the negative glow, and primary electrons are probably present.

The greatest sources of uncertainty are :—

(iv.) The estimation of the concentration of positive ions.

(v.) The detection of primary electrons, which depends on the analysis of the positive ion currents.

It is anticipated that further experiments will make it possible to find the velocity distribution of the primary electrons.

We are indebted to Prof. E. V. Appleton both for very generous provision of apparatus and for valuable criticism and advice.

Wheatstone Laboratory,
King's College, W.C. 2,
6th May, 1927.

VI. *Comparison of Discharges produced by Two and Three Electrode Systems in Hydrogen.* By Miss B. TREVELYAN, B.A.*

IN a previous investigation† of low-voltage glows in hydrogen, the discharge was produced by a stream of electrons from a hot filament, accelerated towards a widely spaced grid placed about two millimetres in front of the filament. The main glow extended through the grid and some way up the tube away from the electrodes.

This discharge is definitely of a different type from that of a three-electrode tube or one containing two electrodes at a distance apart considerably greater than the distance between the walls. The method of employing an auxiliary

* Communicated by Prof. E. V. Appleton, D.Sc.

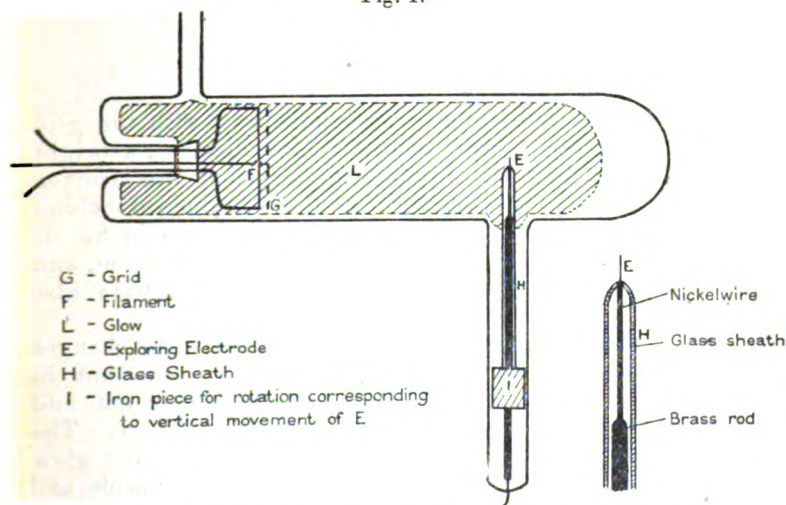
† G. Stead and B. Trevelyan, *Phil. Mag.* xlviii. pp. 978-1006 (1924).

collecting electrode has been used as a means of investigating the distribution of potential, and of determining the concentration and temperature of the electrons in the glow. Some similar measurements have been made with a three-electrode tube. Although the discharge is complicated, it is possible to obtain definite information in both cases, provided that the collecting electrode does not take more than a small fraction of the main current.

Apparatus.

The form of tube used is shown in fig. 1. It was of diameter 3.5 cm., and contained a tungsten filament F capable of carrying up to 3 amperes and a widely spaced grid G made of nickel wire 0.8 mm. in diameter and bent so that there were six parallel wires about 5 mm. apart. The grid was about 2 mm. in front of the filament. The exploring electrode E was a nickel wire 0.17 mm. in diameter and 1.14 mm. long, which was placed about 10 cm. from the grid, and could be moved transversely to the main tube (fig. 1).

Fig. 1.



The three-electrode tube, of the same diameter, had a similar grid and filament, and in addition a nickel ball anode 6.1 mm. in diameter placed about 7 cm. from the grid. The exploring electrode was in this case a circular disk of nickel, 0.85 cm. in diameter, placed parallel to the main discharge, with a guard ring to prevent distortion

of the sheath as far as possible. The disk was at about the same distance from the grid as the anode, and could be moved transversely to the main tube, but in these experiments it was kept fixed about 3 mm. in front of the walls.

Before use, the tube employed was exhausted to a pressure of the order of 10^{-4} mm. Hg. Hydrogen was admitted by means of a palladium tube and mercury vapour excluded as far as possible. This was done for the two-electrode tube by means of liquid air traps, and for the three-electrode tube by means of sodium potassium alloy. The latter method was found to be the more reliable. There were undoubted traces of mercury vapour in the two-electrode tube, but mercury was not detected spectroscopically in the three-electrode tube.

The procedure was as follows :—

The characteristic curves for the respective exploring electrodes were plotted under various conditions, and the space potential, electron concentration, and electron temperature determined by a direct application of Langmuir's analysis*. The space potential was referred in the case of the two-electrode tube to the grid, and in the three-electrode tube to the anode.

Results.

A. Two-Electrode Tube.

Within a certain range of pressures, and with the grid 40–80 volts positive with respect to the filament, a bright purple glow projected beyond the grid; it was convex towards the end of the tube, and also extended behind the filament. The general appearance is shown in fig. 1. The spectrum of the glow showed the Balmer series, and hydrogen secondary spectrum. Mercury lines were also visible.

The length of the glow was very sensitive to changes of pressure, grid potential, and filament current, but in these experiments the last two were kept constant and the length made to vary by change of pressure. The position of the exploring electrode relative to the glow was varied in this way, and the space potential inside and outside the glow could be determined. The range of pressure was from about 0.07 mm. to 0.01 mm., but above 0.05 mm. the glow was diffuse and the boundary indeterminate.

Typical results are given in Tables I. and II., and the general type of characteristic curve in fig. 2. To obtain

* Langmuir, Journ. Frankl. Inst. 196. p. 751 (1923).

TABLE I.
Exploring Electrode level with the walls.

Pressure, mm., of Hg.	Grid Potential relative to filament, volts.	Filament Current, amperes.	Grid Current, milliamperes.	Position of glow.	Space Potential relative to grid, volts.	Electron Concentration per c.c.	*Electron Temperature in volts.
·072	84·7	2·67	1·8	Electrode in glow. Glow was diffuse and filled whole tube.	+15	40×10^6	12·5
·050	84·7	2·69	1·9	As above.	0	34×10^6	12·8
·033	84·7	2·68	2·4	As above.	-8	46×10^6	12·0
·032	84·7	2·68	2·4	As above.	-9	61×10^6	13·7
·029	84·7	2·67	2·8	Glow did not reach end of tube. Elec- trode was at edge of glow.	-4	108×10^6	14·9

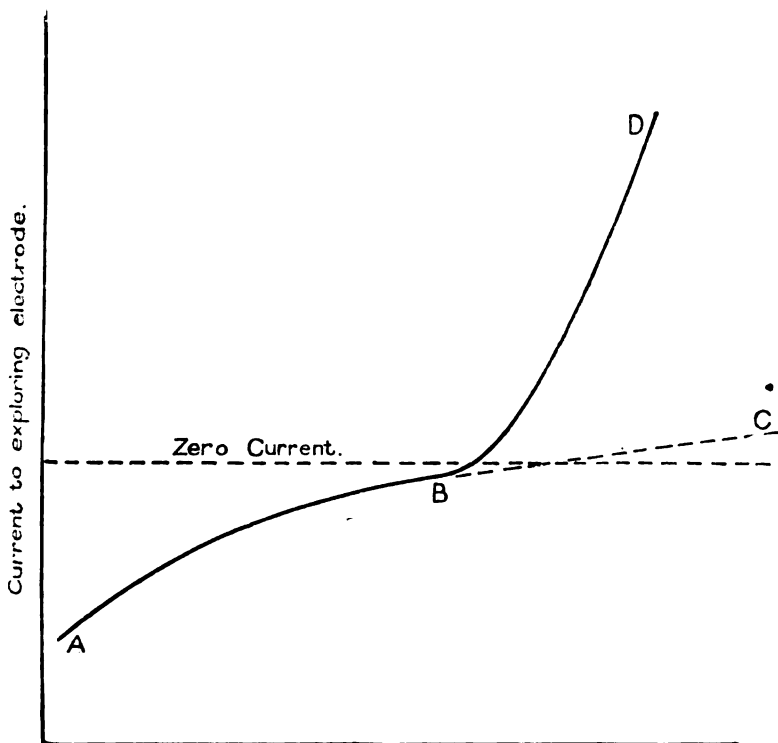
* (Average Energy of Electrons, $Ve = \frac{1}{2}kT$.)

TABLE II.
Exploring Electrode in centre of main tube.

Pressure. mm. Hg.	Grid Potential relative to filament. volts.	Filament Current. amperes.	Grid Current. milliamps.	Position of glow.	Space Potential relative to grid volts.	Electron Concentration per c.c.	Electron Temperature in volts.
·029	85·2	2·60	1·9	End of glow beyond tip of exploring electrode. Tip in glow.	-3	$2·5 \times 10^7$	14·5
·021	85·2	2·60	2·0	Tip at edge of glow.	-10	$1·4 \times 10^7$	16·5
·016	85·2	2·59	2·1	Glow less than 2 cm. behind tip. Tip in dark space beyond glow.	-40	$·76 \times 10^7$	15·3
·009	85·2	2·59	2·4	Glow contracted, end close to grid. Most of tube, and tip in dark space.	-61	$·85 \times 10^7$	8·6

the electron current at a given voltage, the value on the extrapolated part of the curve (BC) was subtracted from that on the part BD, since ABC is taken to represent the positive ion current to the electrode, which is practically linear for a few volts below the space potential.

Fig. 2.



Potential difference between exploring electrode and grid.

The space potential can be located in two ways *:—

(a) By the break in the straight line obtained by plotting values of $\log i$ against V for collection of electrons in a retarding field, where i is the current to the electrode and V the potential of the electrode relative to the grid.

(b) † By the intersection of the straight line obtained by plotting i^2 against V with the V axis when electrons are

* Langmuir and Mott-Smith, General Electric Review, xxvii. p. 451 (1924).

† Langmuir and Mott-Smith, *loc. cit.* p. 455.

being collected in an accelerating field. This gives a value $T/11,600$ volts negative to the space potential, where T is the temperature of the electrons as determined by the slope of the $(\log i)/V$ line. The space potentials were measured relative to the grid.

Results obtained by the first method were generally used in estimating the space potential. The second method gave values slightly higher than those determined from the $\log i$ against V line.

The concentration of the electrons could also be measured in two ways :—

(i.) From the formula,

$$I = \frac{1}{4} ne\bar{v}, \quad \dots \dots \dots (1)$$

where I is the current per unit area of the electrode at the space potential, \bar{v} the average velocity of the electrons, n the number of electrons per c.c.

The formula may also be written as

$$I = ne\sqrt{\frac{e\bar{V}}{3\pi m}}, \quad \dots \dots \dots (2)$$

where $e\bar{V}$ is the average energy of the electrons (as determined from the temperature).

(ii.)* By means of the relation

$$n = \frac{\pi}{\sqrt{2e/m}} \cdot \frac{\sqrt{S}}{Ae}, \quad \dots \dots \dots (3)$$

where S is the slope of the i^2 against V line in accelerating fields, A is the surface area of the electrode, e and m are the charge and mass of the electron.

The two methods gave almost the same values, but the first was more reliable, and values for the concentration under different conditions were obtained from it.

The results may be summarized as follows :—

(a) When the exploring electrode is in the glow, the space potential is approximately that of the grid; but, in some cases, at the higher pressures it is more positive, which suggests that something analogous to striations may occur in this form of discharge, although they are not visible.

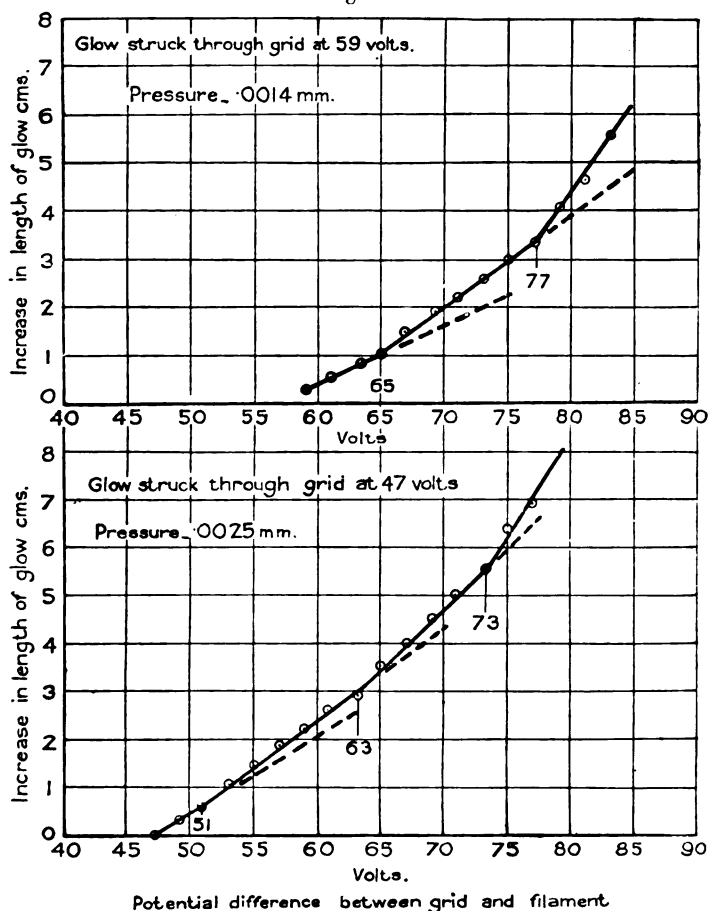
(b) When the electrode is out of the glow, and in the dark space between it and the walls, the space potential becomes rapidly negative to the grid, and probably approaches the potential of the filament at the walls; when the glow is close to the grid, the floating potential of the electrode

* Langmuir and Mott-Smith, *loc. cit.* p. 455.

in the dark space farther up the tube is practically that of the filament.

(c) Further evidence of the presence of the striations is furnished by the curves of fig. 3. These show the change in length of the glow when the grid potential increased, the

Fig. 3.



pressure being kept constant as far as possible. In order to obtain a well defined end to the glow, the experiments were performed at very low pressure, hence mercury vapour may have been present in large proportion compared with the gas. It is seen that there are changes in the slope of the length/grid voltage line which occur at intervals of

about 11 to 15 volts (fig. 3). Grottrian* has found low-voltage striations in mercury vapour, the number depending on the potential difference between filament and anode, an additional 4.9 volts being necessary to bring out a new striation.

(d) Increase of filament current increased the length of the glow. If the pressure was diminished while the discharge was running, the glow contracted and became intrinsically brighter; but if the discharge was first put on at low pressure, the glow ran along to the end of the tube, then immediately recoiled and came to a steady position.

(e) There appears to be one main group of electrons, and these have acquired a Maxwellian distribution. The temperature of the group is high, and on comparing the values in the tables on pages 67 and 68 it may be seen that although the pressure and position of the glow are both changing at the same time, their individual effects on the system may be to a certain extent distinguished from one another. While the electrode is in the glow, in general the temperature tends to increase with diminution of pressure, but as it moves out of the glow, the temperature decreases. At a given pressure, if the filament current increases, the temperature decreases.

(f) As would be expected, the electron concentration increases with increase in emission from the filament. The change of concentration with pressure is somewhat masked by the change of relative position of the glow and electrode. Low pressures and high concentrations are shown in Table II. As the pressure decreases, the main current to the grid increases; hence the concentration of electrons in the glow beyond the grid is likely to increase. At higher pressures, as in Table I., the effect is masked by the fact that there is a large electron concentration in the parts of the glow which have a space potential positive with respect to the grid. Table II. shows that the concentration of electrons falls off rapidly outside the glow, with a simultaneous decrease in electron temperature.

B. *Three-Electrode Tube.*

The discharge obtained in this tube may be considered similar to that of A, but with the field between grid and anode helping the diffusion along the tube. Sufficient data have not yet been acquired to explain completely the appearance and action of the discharge; however, the results

* W. Grottrian, *Zeit. f. Phys.* v. p. 148 (1921).

obtained so far are interesting when compared with those of section A. Further experiments are now in progress in order to elucidate the mechanism of the three-electrode system.

Since, in this tube, the collecting plate was parallel to the direction of the main discharge, it is reasonable to suppose that few of the direct beam of electrons (if these are present) reach it, and that the majority of the electrons collected are those referred to by Langmuir as the secondary and ultimate groups.

Current-voltage curves for the disk were taken under a variety of conditions, when it was about 3 mm. in front of the wall. The electron temperature was obtained as before from the slope of the $\log i$ against V line, and the concentrations by the formula (2).

The results may be summarized as follows :—

Space Potential, Electron Temperature and Concentration.

Gas pressure of the order of 0.02 mm.

A single group of low-temperature electrons (about $10,000^\circ \text{K.}$) appears near the walls, when the field between filament and grid and that between grid and anode are of the same order. When the latter is the greater the single group is again present, but when the former is the greater the $(\log i)/V$ line consists of two straight lines of different slopes, showing that a second group of high-temperature electrons is also present near the walls ($20,000^\circ\text{--}80,000^\circ \text{K.}$). Both groups have an approximately Maxwellian distribution; the concentration of the high temperature group is small, and this group is present alone at low pressures. The concentration of the low-temperature group is a linear function of the potential between grid and anode, when the potential between filament and grid is kept constant (fig. 4).

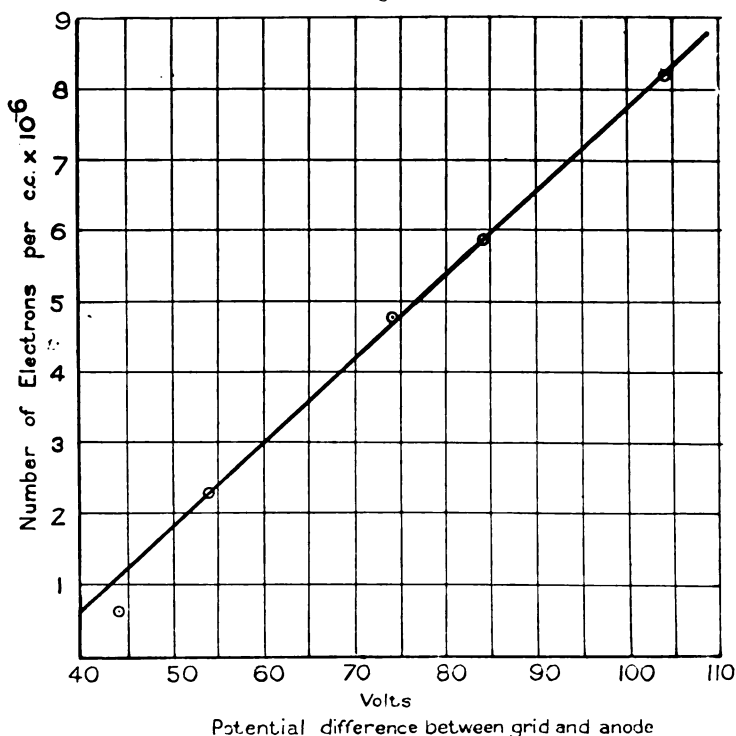
At the higher pressures, concentric glows appear round the anode, these seem to be of the nature of striations; the number of glows increases with the potential between grid and anode.

When the latter is small, and the potential between grid and filament also small, of the order of 40 volts, the space potential near the walls is approximately that of the grid; as both potentials are increased the space potential becomes more nearly that of the anode. An abrupt change occurs corresponding to the formation of a new glow round the anode. A similar abrupt change in the wall charges can

be shown by means of a sounding ball attached to an electroscope, placed near the outside of the tube.

With a large emission from the filament, the grid current is negative (grid collecting positive ions in excess of electrons); the effect is most marked with a large field between grid and anode. A dark space is visible in front of the grid on the opposite side to the filament and extends into the main glow. For smaller filament currents the grid

Fig. 4.



current is positive (excess of electrons). Under these conditions there is therefore a definite value of the filament current corresponding to zero current to the grid, since the latter collects both electrons from the filament and positive ions from the discharge between grid and anode.

Positive Ions.

The nature of the positive ions was roughly determined by approximate measurements of the sheath thickness over

the disk electrode when it was charged so as to collect positive ions. The relation used was *

$$I = 2.33 \times 10^{-6} \sqrt{\frac{m}{M}} \frac{V^{3.2} \left(1 + 0.0247 \sqrt{\frac{I}{V}}\right)}{x^2}, \quad (4)$$

where x was the sheath thickness, m and M the mass of the electron and positive ion respectively, V the difference in potential (expressed in volts) between the two boundaries of the sheath (the disk and glow), I the current per unit area of the electrode (expressed in amps. cm.⁻²), T the temperature of the positive ions in °K. A value of 8000° was taken as roughly representing this temperature.

The values of $\frac{M}{m}$ varied between 1000 and 5000, and were of the right order for hydrogen, but were not sufficiently precise to determine the nature of the carrier (H^+ , H_2^+ , or H_3^+).

General Conclusions.

The current which passes in a discharge is governed by two factors, the applied electric field and the unequal rate of diffusion of the ions, and variation in the conditions of the discharge causes one or other to be predominant. Under conditions which give rise to large concentration of electrons and small potential gradient due to applied field, the current may be carried chiefly by diffusion.

In the two-electrode tube large fields are absent, the main fall of potential occurs between the filament and grid, and the potential of all the luminous region beyond is not far different from that of the grid. There will therefore be practically no resultant field along the glow except that due to local concentration and diffusion effects. When there are no striations, the system may be regarded as consisting roughly of two equipotential surfaces, the walls and filament forming one, and the grid and the glow the other, practically the whole fall of potential occurring in the dark space between them.

By inserting an anode as third electrode, and superposing a field between anode and grid, the system is altered. If the field between grid and filament is not too large, the grid and walls now form an approximately equipotential surface. The former acts as cathode in the main discharge between grid and anode, but here the cathode and anode are far apart

* Langmuir and Mott-Smith, *loc. cit.* p. 452.

and the main luminous region is between them, while in the two-electrode tube the distance between cathode and anode was small compared with the diameter of the tube, and the luminous region was beyond the grid. In one case there is a field along the glow, and in the other the applied field has practically no effect in the luminous part. In the presence of the field, diffusion along the tube is helped, but diffusion towards the walls is hindered.

The greatest difference between the two and three electrode systems lies in the energy of the electrons. In the former, the electron temperatures in the glow are high, and of the order of the ionization potential of hydrogen; in the latter, the temperatures are much lower. This suggests that in the two-electrode system the luminosity was produced by fast electrons able to ionize the gas directly, but in the three-electrode system by less direct means.

It has been shown* that the effect of superposing a drift current on a random current is apparently to increase the temperature of the electrons as measured by an exploring electrode. This may partly account for the high random energies recorded in the two-electrode tube. With the cathode and anode far apart and the glow between them, the temperatures measured near the walls are much lower and of the same order as those observed by Bramley† in the hydrogen discharge. In this case diffusion to the walls is hindered and the observed currents are due to electrons produced near them by primary or secondary processes of ionization.

These experiments have also a bearing on the use of charged plates as "ion-traps," to act as a shield for one part of a tube from the effects of a discharge produced in another part of the same tube. The current to the plates must be governed chiefly by the ionic sheath formed over them, and the influence of potential applied to them will extend only to the outer edge of the sheath. For a flat plate, the relation between the current density I , sheath thickness x , and the potential difference between the plate and the ionized gas is

$$Ix^2 = kV^{3/2}, \quad . \quad . \quad . \quad . \quad . \quad . \quad (5)$$

where k is a constant depending on the charge and mass of the ions. If I is small, x is large, and vice versa. It follows that if x is to be of the order of the dimensions of the tube,

* Langmuir and Mott-Smith, *Phys. Rev.* xxviii. p. 741 (1926).

† Bramley, *Phys. Rev.* xxvi. pp. 794-799 (1925).

in order that the path of the main discharge may be so confined that the latter ceases to pass, a very large potential must be applied to the plates when the current density is large.

In the present experiments the current to the grid must have been largely determined by similar considerations, the discharge beyond the grid being chiefly due to those electrons which succeeded in passing through or between the sheaths formed over the grid wires. The form of these sheaths could not be determined since the discharge was of a different nature on the two sides of the grid.

In Lord Rayleigh's* experiments on the persistence of luminosity in mercury vapour, he subjected the glow to an electric field supplied by two successive charged cylinders. He assumed that the first cylinder had acted as an efficient ion trap, since no current reached the second. This is in agreement with the equation (5) given above, since the current to the first cylinder was small, and the potential difference between it and the anode large. It is interesting to note that, under these conditions, the line spectrum, apart from λ 2537, died out first, the bright glow tapering to a point. This can be ascribed to the line spectrum having its origin in the positive ions which went to form a sheath on the first charged cylinder, the thickness of the sheath increasing as the concentration diminished in accordance with the equation

$$Ix^2 = kV^{3/2}.$$

Another origin has been ascribed to the line λ 2537 and to the continuous spectrum. Both these radiations persist after the line spectrum has died out.

The writer wishes to thank Professor O. W. Richardson for his permission to carry out this work at King's College, London; and Dr. K. G. Emeléus for much valuable help and advice.

* Lord Rayleigh, Proc Roy. Soc. A, cviii. pp. 262-279 (1925).

VII. *On the Constants of Receiving and Transmitting Antennæ.*
 By RAYMOND M. WILMOTTE, B.A., of the National Physical Laboratory*.

ABSTRACT.

THE distribution of current and voltage in a circuit depends on the distribution of the applied E.M.F. in that circuit, and it would be reasonable to suppose that the effective impedance measured at any given point of the circuit would depend on the distribution of the E.M.F.

In the case of an antenna, it is proved theoretically that, if we can assume that the distribution of capacity, inductance, and resistance is the same for transmission as for reception, the effective capacity, inductance, and resistance, as well as the effective height measured at the base, is identical for transmission and reception.

The fundamental assumption is shown not to be strictly correct, particularly as regards the radiation resistance, which is shown to be dependent on the distribution of the applied E.M.F. An experimental study shows that the approximations produce undetectable errors, except in the case of the resistance, in which small differences appear to be detectable.

1. GENERAL CONSIDERATIONS.

IN a paper on "Induced Currents in a Wireless Telegraph Receiving Antenna" †, E. B. Moullin compared the effective heights of receiving and transmitting antennæ and proved them to be equal. He mentioned that it does not appear that this theorem can be proved from general considerations of energy. Moullin's proof is not general, as it applies only to the special case of antennæ with uniformly distributed capacity, inductance, and resistance.

F. M. Colebrook, in a paper which is in the course of publication, has shown that the effective impedance of an antenna is the same for transmission as for reception, but he has also limited the case to that of uniformly distributed constants and applied E.M.F.

We have no reason to assume that the constants are

* Communicated by Sir J. E. Petavel, K.B.E., F.R.S. Communicated by permission of the Radio Research Board.

† E. B. Moullin, "Induced Currents in a Wireless Telegraph Receiving Antenna." *Proc. Camb. Phil. Soc.* vol. xxii. p. 567 (1925).

uniformly distributed, and, in fact, we know that, owing to end-effects and the positions of the various parts relative to earth, the constants of an ordinary antenna are not so distributed.

The following analysis is intended to generalize the results of Moullin and Colebrook by making no assumptions on the law according to which the constants of the antenna are distributed along its length. A fundamental assumption remains, however, that the law of distribution of the constants is the same for transmission as for reception. The validity of this assumption is discussed below in section 3.

2. PROOF.

Consider an element of length δr of an antenna. Let its direction cosines be l, m, n . Suppose the components of the electric intensity of an approaching wave have instantaneous values E_x, E_y, E_z , and that an E.M.F. of instantaneous value V be applied at the foot of the antenna, the frequency of the E.M.F.'s being the same.

We shall write R, L, C for the resistance, self-inductance, and capacity per unit length of the element δr of the antenna.

If v and i are the potentials and current respectively at any point r of the antenna, then the differential equations for the electric conditions at any point are

$$-\frac{dv}{dr} = (R + jLw)i - (lE_x + mE_y + nE_z) \quad . \quad . \quad (1)$$

$$\text{and} \quad -\frac{di}{dr} = jCwv, \quad . \quad . \quad . \quad . \quad . \quad (2)$$

where $j = \sqrt{-1}$ and $w = 2\pi$ (frequency).

It should be noticed that in these two equations R, L, C, E_x, E_y, E_z are any functions of r .

Eliminating v from (1) and (2), we have

$$\frac{d^2i}{dr^2} - \frac{1}{C} \frac{dC}{dr} \frac{di}{dr} - (R + jLw)jCwi = -jCw(lE_x + mE_y + nE_z). \quad . \quad . \quad . \quad (3)$$

To solve this, suppose s is a solution of the equation

$$\frac{d^2i}{dr^2} - \frac{1}{C} \frac{dC}{dr} \frac{di}{dr} - (R + jLw)jCwi = 0 \quad . \quad . \quad . \quad (4)$$

Putting $i = us$, we obtain

$$\frac{d^2u}{dr^2} + \frac{du}{dr} \left(\frac{2}{s} \frac{ds}{dr} - \frac{1}{C} \frac{dC}{dr} \right) = -\frac{jCw}{s} (lE_x + mE_y + nE_z).$$

This is a linear equation in du/dr , and the solution is

$$u = \int \frac{C}{s^2} \int (\ell E_x + m E_y + n E_z) s j \omega dr dr + A \int \frac{C}{s^2} dr + B,$$

where A and B are constants of integration.

$$\text{Let } Q = \int \frac{C}{s^2} \int (\ell E_x + m E_y + n E_z) s j \omega dr dr. \quad . \quad . \quad (5)$$

$$\text{and } P = \int \frac{C}{s^2} dr, \text{ so that } \frac{dP}{dr} = \frac{C}{s^2}. \quad . \quad . \quad (6)$$

Hence we can write

$$i = (Q + AP + B)s. \quad . \quad . \quad . \quad (7)$$

We shall also find the following formula useful :

$$\begin{aligned} Q &= \int \frac{dP}{dr} \int E_r s j \omega dr dr \\ &= \left[P \int E_r s dr - \int P E_r s dr \right] j \omega, \quad . \quad . \quad (8) \end{aligned}$$

$$\text{where } E_r = \ell E_x + m E_y + n E_z.$$

In these equations it should be noticed that the variables P and s are functions of the antenna constants only, while Q is a function of both the antenna constants and of the approaching field.

There now remains to insert the boundary conditions. Let the impedance of the apparatus between the foot of the antenna and earth be Z , and let i_0 be the value of the current at the foot of the antenna, then

$$\begin{aligned} \text{when } r=0, v &= V - Zi_0 \\ i &= i_0, \end{aligned}$$

and, if h is the length of the antenna,

$$\text{when } r=h, i=0.$$

On substituting these boundary conditions, we obtain

$$\begin{aligned} i_0 \left\{ Z - \frac{1}{s_0 C_0 j \omega} \frac{ds_0}{dr} - \frac{1}{(P_0 - P_h) s_0^2 j \omega} \right\} &= V - \frac{(Q_0 - Q_h)}{s_0 (P_0 - P_h) j \omega} \\ &\quad + \frac{s_0}{j C_0 \omega} \frac{dQ_0}{dr}, \quad . \quad . \quad (9) \end{aligned}$$

where s_0, C_0, P_0, Q_0 are the values of s, C, P, Q when $r=0$, and P_h, Q_h are the values of P, Q when $r=h$.

Effective Impedance.

Let us examine equation (9). It will be seen that the right-hand side is a function of applied electric intensities, and the units are those of an E.M.F. Also the coefficient of i_0 is independent of the applied electric intensities, and its units are those of an impedance.

Now, comparing equation (9) with the equation

$$i_0(Z + Z_0) = V + E_0, \quad \dots \quad (10)$$

where Z_0 is the effective impedance of the antenna and E_0 is the equivalent E.M.F. at the base which produces the same current i_0 as the approaching wave, we obtain at once

$$Z_0 = -\frac{1}{s_0 C_0 j\omega} \frac{ds_0}{dr} - \frac{1}{(P_0 - P_A) s_0^2 j\omega} \dots \quad (11)$$

and

$$E_0 = \frac{s_0}{jC_0\omega} \frac{dQ_0}{dr} - \frac{Q_0 - Q_A}{s_0 j\omega (P_0 - P_A)} \dots \quad (12)$$

Equation (11) shows that Z_0 is independent of Z and of the applied E.M.F.'s, while E_0 is a function of both the applied E.M.F.'s and the constants of the antenna. This proves the following proposition:—

If the distribution of the constants along an antenna is unaffected by the applied E.M.F.'s, the effective impedance measured at any point is also unaffected by the applied E.M.F.'s, and is therefore the same for transmission as for reception.

Incidentally, this proposition applies equally well to any form of transmission line.

Effective Height.

In defining the effective height of an antenna we should consider only those parts, or resolved parts of the antenna, which are effective in radiating energy, in the case of a transmitting antenna, or absorbing energy from the approaching wave, in the case of a receiving antenna.

In the case of transmission over a perfectly conducting earth, it is only the resolved parts of the antenna along the vertical axis that are effective in producing an electromagnetic field at a distance, unless the wave-length is comparable to the height of the horizontal portions. If OZ is the vertical axis, the effective height T , of a transmitting

antenna can therefore be generally defined by

$$T_z = \frac{1}{I_0} \int_0^h n I dr, \quad (13)$$

where I, I_0 are the maximum values of i, i_0 .

Substituting equation (7), we have

$$T_z = \frac{\int_0^h n(P - P_h) s dr}{s_0(P_0 - P_h)} (14)$$

In the general case, when the horizontal components have some effect in producing an electromagnetic field, the "effective heights" in the horizontal directions can be defined by

$$T_x = \frac{1}{I_0} \int_0^h l I dr \quad \text{and} \quad T_y = \frac{1}{I_0} \int_0^h m I dr,$$

which will give the results similar to equation (14).

In the case of a receiving antenna, suppose the current produced at the foot by a vertical approaching field E_z is i_0 , and that the same current is produced by an E.M.F. V of the same frequency applied at the foot of the antenna, then the effective height R_z can be defined by

$$R_z = V/E_z. \quad (15)$$

We have similar definitions for R_x and R_y .

In this case the approaching field must be uniform, otherwise the effective height will depend on the distribution of this field, and thus become meaningless.

From equation (9) we can find i_0 in the two cases by first putting $V=0$ and then $E_r=0$. On substituting in equation (15), we have

$$R_z = \frac{\int_0^h n(P - P_h) s dr}{s_0(P_h - P_0)}, \quad (16)$$

and similarly for R_x and R_y .

It will be seen that equations (14) and (16) are identical, and we thus obtain the following proposition:—

If the distribution of the constants along an antenna is unaffected by the applied E.M.F.'s, the effective height is the same for transmission as for reception.

3. VALIDITY OF ASSUMPTIONS.

The whole of the analysis in the previous section depends on the assumption that the distribution of resistance, capacity, and self-inductance is independent of the applied E.M.F.'s. Now, we know that the current distribution must be slightly affected by the distribution of the E.M.F.'s, and the reaction of one part of the antenna on another, whether electric or magnetic, must depend on the distribution of the current.

Suppose the antenna is split up into sections of length l , sufficiently small that the current can be assumed constant in each section. We shall consider the magnetic induction of one section on the next one, assumed to be in the same straight line. From Rosa's* formulæ for straight conductors we obtain for the mutual inductances of two consecutive sections

$$M = 2l \log 2,$$

and for the self-inductance of each section

$$L = 2l \left[\log \left(\frac{2l}{r} \right) - 1 \right],$$

where r , the radius of the conductor, is small compared with the length.

It is seen that L is very much larger than M so long as the wave-length is very large compared with the radius, for this permits conditions to be assumed involving large values of l/r .

These formulæ are not, in the author's opinion, rigorously correct, but, when l is large compared with r , they no doubt give a fair representation of the actual state of affairs.

The electric reaction will give similar results since the integrals involved are similar.

It is therefore not to be expected that small changes in the distribution of current will produce any appreciable difference in the distribution of the effective values of the self-inductance and capacity per unit length of the antenna. This is confirmed by the experimental results described below.

There is, however, a part of the effective impedance, namely the radiation resistance, which may be slightly different when the antenna is used for transmission and when used for reception.

The radiation resistance of an antenna depends on the distribution of current along it and on the field produced by that current, and therefore on the dielectric characteristics

* E. B. Rosa, "Self and Mutual Inductances of Linear Conductors" Bull. Bureau of Standards, vol. iv. p. 301 (1907).

of the surrounding objects. As a general rule, however, the radiation will depend mainly on the three integrals:

$$\frac{1}{I_0} \int_0^h l I dr, \quad \frac{1}{I_0} \int_0^h m I dr, \quad \frac{1}{I_0} \int_0^h n I dr.$$

The greater the value of these integrals, the greater the radiation resistance. Over a perfect earth, for wave-lengths long compared with the height, the last integral will be the most important.

For transmission these integrals, by the definition of effective height (equation 13), are

$$T_x, \quad T_y, \quad T_z. \quad . \quad . \quad . \quad . \quad . \quad (17)$$

For reception, however, the first of these integrals using equation (16) will be found to be

$$\frac{1}{I_0} \int_0^h l s (Q - Q_0) dr - \frac{s_0}{I_0} (Q_0 - Q_h) R_x + R_z. \quad . \quad (18)$$

There will be similar expressions for the other two integrals.

It will be seen that, in general, the radiation resistance is different for transmission and reception.

4. APPLICATION OF FORMULÆ.

In making use of the above formulæ, suppose a value is found for s which is a solution of equation (4). The value of P can be found from the integral (6), while the value of Q is best obtained from equation (8).

The effective resistance is obtained by finding the real part of equation (11), while the imaginary part will give the effective reactance. The effective heights are given by equation (14).

In connexion with the effective impedance, it is usual to represent an antenna by a resistance R_0 , a capacity C_0 , and a self-inductance L_0 , all in series, so that

$$Z_0 = R_0 + L_0 jw + \frac{1}{C_0 jw}.$$

If Lw is the effective reactance equivalent to the reactance of this representation, we have

$$L = - \frac{(1 - L_0 C_0 w^2)}{C_0 w^2};$$

therefore

$$C_0 = \frac{2}{w^3} \left/ \frac{dL}{dw} \right. \quad . \quad . \quad . \quad . \quad . \quad (19)$$

and

$$L_0 = L + \frac{w}{2} \frac{dL}{dw} \quad . \quad . \quad . \quad . \quad . \quad (20)$$

When the frequency is low, it is more usual to measure the effective capacity C of the whole, so that

$$C = \frac{C_0}{1 - L_0 C_0 \omega^2};$$

therefore

$$L_0 = \frac{1}{2C^2 \omega} \frac{dC}{d\omega} \quad \dots \quad (21)$$

and

$$C_0 = \frac{2C^3}{2C + \omega \frac{dC}{d\omega}} \quad \dots \quad (22)$$

Hence, by plotting X or C against ω and finding the differential or the gradient, we can find the effective inductance and capacity at any given point. It should be noticed that equations (21) and (22) break down when the antenna acts as a pure resistance; this occurs at the natural frequency and near odd multiples of the natural frequency of the antenna.

Near even multiples of the natural frequency, $dL/d\omega$ becomes small; the effective impedance of the antenna then resembles more that of a parallel tuned circuit, for which the usual representation is very unsatisfactory. Near these points it is therefore inadvisable to try to split up the effective reactance into a capacity and a self-inductance. In any case such representations are essentially fictitious and of very doubtful value unless the constants of the representative circuit remain unaltered over a considerable range of frequency.

We shall now apply the formulæ obtained above to the well-known case of an antenna having uniformly-distributed resistance, capacity, and self-inductance. In these conditions an obvious solution of equation (4) is

$$s = e^{Kr},$$

where

$$K^2 = (R + jL\omega)jC\omega.$$

Therefore

$$P = - \frac{C e^{-2Kr}}{2K}$$

and

$$Q = - \frac{jC\omega e^{-Kr}}{K^2} E_r.$$

Substituting in equation (11), we have

$$Z_0 = \frac{K}{jCw} \coth(Kh),$$

which is the well-known formula for a uniform transmission line.

Expanding, this becomes

$$Z_0 = R \frac{h}{3} + \frac{1}{hjCw} + \frac{hjLw}{3} + \dots$$

From equation (12) we readily find the effective height to be

$$\begin{aligned} T_z &= \frac{1}{K} \tanh\left(\frac{Kh}{2}\right) \\ &= \frac{h}{2} \left(1 + \frac{h^2 LCw^2}{12} + \dots\right), \end{aligned}$$

as obtained by Moullin*.

To compare the radiation resistance in the two cases of transmission and reception, we have to evaluate $\frac{1}{I_0} \int_0^h I dr$. For transmission, this integral is (equation 17)

$$\frac{I}{K} \tanh\left(\frac{Kh}{2}\right).$$

For reception, the integral—assuming E_r to be uniformly distributed along the antenna—is

$$\frac{1}{K} \tanh\left(\frac{Kh}{2}\right) + \frac{jCw}{K^2} \frac{E_r}{I_0} \left[\frac{2}{K} \tanh\left(\frac{Kh}{2}\right) - h \right];$$

that is,

$$\frac{1}{K} \tanh\left(\frac{Kh}{2}\right) - \frac{jCw}{K \tanh\left(\frac{Kh}{2}\right)} \left[\frac{2}{K} \tanh\left(\frac{Kh}{2}\right) - h \right] (Z + Z_0).$$

We would therefore expect the radiation resistance to be slightly different in the two cases. If $(Z + Z_0)$ is a pure resistance, the resistance will generally be greater for reception than for transmission.

It is interesting to note that the difference is dependent on the value of the impedance Z of the apparatus between the antenna and earth. In fact, when Z is infinite the difference in the radiation resistance is also infinite. The physical interpretation of this is easily found. If Z is infinite the current I_0 at the foot of the antenna will be zero. Thus in

* *Loc. cit.*

the case of transmission there would be no current whatever in the antenna, while, owing to capacity and inductance effects, some currents will flow on reception: this current will produce a re-radiated field. Thus, on reception, some power is re-radiated, although the current at the base may be zero, giving rise to an infinite effective radiation resistance.

Other cases where the constants of the antenna are not uniformly distributed can be treated in a similar way.

5. EXPERIMENTAL VERIFICATION.

In order to ensure that the antenna under measurement had not uniformly distributed constants, loops of wire were added to it until its shape was as shown in fig. 1. A counterpoise earth was used.

Fig. 1.

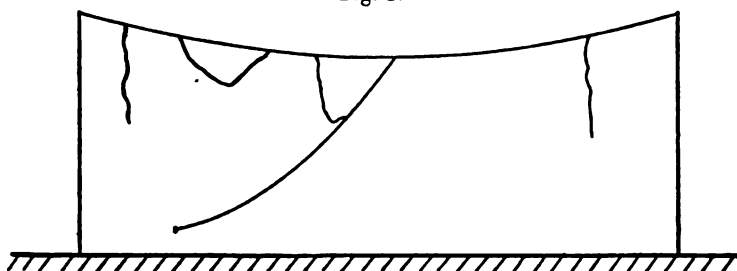
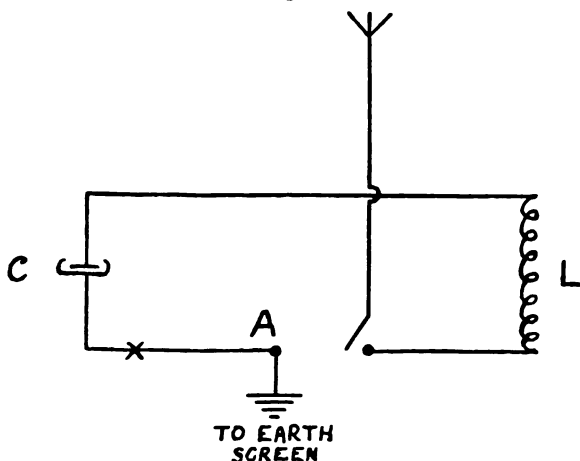


Fig. 2.



The measurements were made by inserting the antenna in series in a circuit (fig. 2) which was measured with and

without the aerial, the counterpoise remaining connected to the point A during all the measurements.

The resistance was measured by the variation of reactance method by varying a very small accurately calibrated condenser in parallel with condenser C.

The measurements were carried out for transmission by inducing from a small power set into the coil L, and for reception by inducing into the antenna from another antenna excited by a larger set about 50 yards distant. A large army hut running within a few feet of the receiving antenna for the whole of its length and situated in between the two antennæ, ensured that the field at the receiving antenna was not uniform. It was ascertained that the direct induction into the coils was small. The two power sets were adjusted to the same frequency by means of the same wave-meter without alteration of setting, so as to eliminate small errors due to frequency adjustments.

Since differences are only to be expected at high frequencies, the wave-lengths used were all under 210 metres. Table I. gives the results of the measurements. The figures for reactance and resistance refer to the antenna alone without the rest of the circuit.

TABLE I.

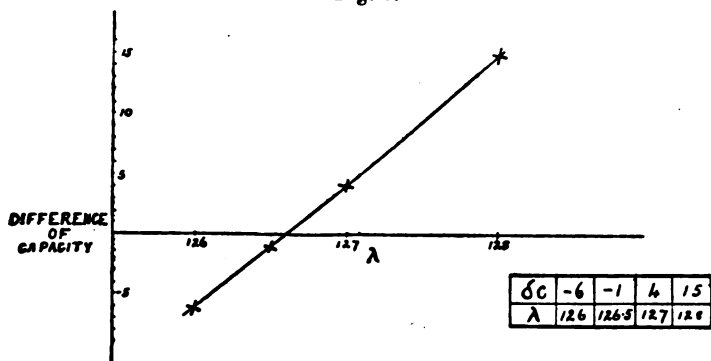
Wave-length in metres.	Reception.			Transmission.		
	Setting of Condenser C.	Reactance in ohms.	Resistance in ohms.	Setting of Condenser C.	Reactance in ohms.	Resistance in ohms.
208.5	119.8	-297	4.2	120	-297	4.2
140.0	283	- 74	5.0	283	- 74	4.9
127.0	186	- 7.8	7.2	186	- 7.8	7.0
114.0	215	+ 89	64	215	+ 89	70

The last results at a wave-length of 114 metres are interesting, for they represent the antenna beginning to act as a rejector circuit. Owing to its shape, the downcoming lead is for a long portion of its length quite close to the earth screen, thus acting as a large capacity. The rest of the antenna acts as a positive impedance at that frequency, so that a rejector circuit is formed. That is the reason for

the sudden rise in the value of the resistance. This condition could be altered by changing the shape of the downcoming lead. This was done and, though no very accurate measurements were taken, the effective resistance decreased to the order of 15 ohms.

From the table we see that the natural wave-length of the antenna is slightly below 127 metres. This, incidentally, is a very accurate way of finding the natural frequency of an antenna without having instruments in series liable to alter the value searched for. The process consists in exciting the circuit by inducing into the coil L and varying the frequency until resonance is obtained with and without the antenna in circuit for the same reading of condenser C . The earth should remain permanently connected to the point A , and it is advisable to disconnect the antenna when it is not in series in the circuit. In practice the exact point

Fig. 3.



is a little troublesome to find, and it is best to plot the differences in the readings of condenser C , with and without the antenna in series, against the frequency for a number of points near the natural frequency, which is then found by interpolation. A typical diagram of results is shown in fig. 3. Readings at higher frequencies were not taken owing to the difficulties of measurement, particularly because of the very high effective resistance which the antenna attained, rendering the deflexion of the ammeter too small to be useful for resistance measurements, which, in any case, are very uncertain at these frequencies and therefore of very doubtful value.

The values obtained are seen from the table to confirm the theoretical deductions. No differences in the condenser settings were detectable, while the resistance appears to be

slightly greater for reception than for transmission, which difference increases with increasing frequency. At 114 metres the resistance was very difficult to measure, but the resistance for transmission appeared to be greater than for reception. This is probably due to the action of the antenna as a rejector circuit, for in that case the greater the resistance within the circuit the smaller the effective resistance.

Too great reliance, however, should not be placed on the small differences of resistance given in the table, as they are within the limits of experimental error. The fact that the errors of measurement due to the arrangement of the circuit are similar for transmission and reception gives, however, greater weight to the reality of the small differences observed.

To test this further, measurements were made near the natural frequency of the antenna ($\lambda = 127$ m.) using thermo-ammeters having different resistances. Since the radiation resistance for reception depends on the value of Z , we should expect the difference to increase with increasing resistance of the ammeters. These differences for different values of thermo-ammeter resistance are given in Table II.

It was found that, owing to the effect of the observer on the large capacity *via* the earth between the screen of the condenser and the counterpoise, and also to the capacity of the coil to earth, the measurements became increasingly difficult as the resistance of the thermo-ammeter was increased.

TABLE II.

Resistance of Thermo-ammeter.	(Resistance for reception) — (resistance for transmission).
1 ohm.	0.2 ohm.
5 ohms.	0.3 ohm.
30 ohms.	0.7 ohm.

The resistance of the rest of the circuit was of the order of 8 ohms.

The differences are small and within the limits of experimental error for absolute values, but probably not for the differences themselves. It should be further noticed that any error caused by reaction back on to the source would

produce an increase in the apparent resistance on the transmission measurements, whereas the resistance on reception was found to be always slightly greater than on transmission.

6. CONCLUSION.

To summarize: we have found theoretically that, if the distribution of the constants of an antenna is the same for transmission as for reception, the effective resistance, reactance, and the effective height are also the same in the two cases. The radiation resistance, however, is slightly different.

Experimental evidence down to about 100 metres wavelength showed that the difference in the reactance in the two cases was undetectable, while there was strong evidence that there was a small difference in the resistance, that for reception being slightly greater than that for transmission.

This investigation was carried out for the Radio Research Board established under the Department of Scientific and Industrial Research, and the author is indebted to the Board for permission to publish this paper.

VIII. *The Three-Point Spark Gap.*

*By J. D. MORGAN, D.Sc.**

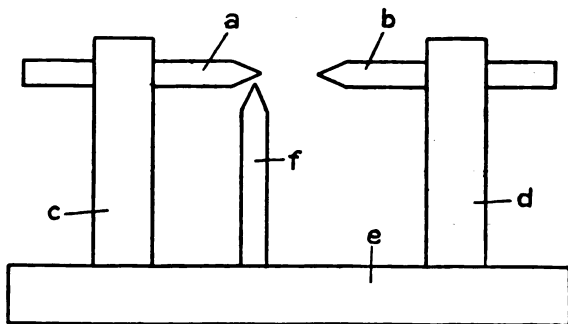
IT is well known that the sparking voltage of a gap is greater—sometimes much greater—when the voltage is applied impulsively, than when it is applied gradually or is sustained. The ratio of the two voltages is commonly termed the impulse ratio. It is also well known that the impulse ratio of a gap can be reduced or irregular sparking made regular by the use of a third point. In its ordinary form the three-point gap comprises a pair of main electrodes forming the main gap, and an insulated third electrode forming between it and one of the main electrodes a small auxiliary gap situated adjacent to the main gap. The efficacy of the small spark across the auxiliary gap depends upon the quantity of electricity passing through it and also upon its position relatively to the main gap. When one of the main electrodes is earthed the auxiliary gap must be arranged near the other electrode. The faint and tiny spark which passes across the auxiliary gap is necessary to the performance of the ordinary three-point gap. A common

* Communicated by Prof. E. Taylor Jones, D.Sc.

form of the three-point gap is shown in fig. 1, where *a* and *b* are the main electrodes carried by metal pillars *c*, *d* on an insulating base *e*, and *f* is the third point forming with *a* the small auxiliary gap. The third point is also carried on the insulating base, but has no connexion with either of the metal pillars. Sometimes the adjacent ends of the main electrodes are made of spherical form.

The problem of the action of the auxiliary spark has received much attention from those whose work involves the use of spark gaps. Until about a year ago no satisfactory explanation of the action of the auxiliary spark appears to have been given. To assert, as was done, that the action is due to ionization was merely to guess at a probability. The most satisfactory solution of the problem yet offered appears

Fig. 1.



to be that due to Mr. Wynn-Williams*. According to Wynn-Williams the action is due to ionization of the gas in the main gap by radiation from the auxiliary spark. In addition to this contribution to the problem, Wynn-Williams also discovered a novel third-point effect. He found that a sharp needle-point held at some distance from, but electrically connected to, one of the electrodes was apparently more effective than the usual auxiliary spark. The same result can be obtained by holding an insulated needle across and in contact with one of the electrodes so that the point is "in view" of the gap. A sharp point like that of a needle is essential to the effect observed by Wynn-Williams. A blunt electrode raised to the same potential has no effect.

The work of Wynn-Williams merits close examination

* "An Investigation into the Theory of the Three-Point Gap." C. E. Wynn-Williams, M.Sc., Phil. Mag. vol. i. Feb. 1926.

and, if possible, further development, and as the validity of at least one of Wynn-Williams's experiments appears to be not beyond doubt, the problem of the three-point gap has been subjected to a further attack on rather different lines from those which he followed.

As already stated, Wynn-Williams found that a sharp needle-point electrically connected to one of the electrodes produced an effect equivalent to that of the auxiliary spark of the ordinary three-point gap, and, presumably because of its greater convenience, he used a needle so connected throughout his major experiments. These undoubtedly support the deduction made from them, but the equivalence of such a needle and an auxiliary spark does not appear to have been established fully. He finds, for example, that the needle-point when activated by a Wimshurst machine has the same effect as when connected to the main gap. It is possible to show, however, that under suitable conditions a needle-point connected to a Wimshurst machine has no effect whatever on the main gap. Further, he seems to suggest that an auxiliary spark produced by a Wimshurst machine or other continuously acting source of electricity has no effect on the main gap, whereas under suitable conditions the contrary can be proved. These facts are sufficient, if any justification were required, to warrant a re-examination of the problem of the three-point gap, in the light of the notable contribution made by Wynn-Williams.

Prof. E. Taylor Jones has for a long time used a gap one of the electrodes of which contains a small quantity of radium placed in a tiny hole on the axis of the gap. The sparking voltage of this gap is remarkably regular, and appears to be in no way improved by any external "third-point" action. This gap demonstrates that direct ionization of the gas in the gap is an effective means of obtaining regular action. It also suggests a line of approach to the problem of the three-point gap.

In the first series of experiments now to be described it was decided to employ a gap of about 2 mm. formed between hemispherical ends of a pair of brass rods of 5 mm. diameter. The electrodes were connected to the opposite terminals of an induction coil actuated by an ordinary vibratory interrupter. It is important to note that one of the electrodes was earthed. Apparently Wynn-Williams did not include this condition in his experiments. Otherwise he would have noticed some of the effects described below. The primary current was adjusted until it was barely sufficient to cause a spark to pass. With the coil in action, but no spark passing at the

gap, a sharp needle connected to one of the poles of a Wimshurst machine was brought to a position about 6 cm. from the gap, and the following effects were observed.

When the high-tension (h.t.) electrode of the gap was of negative sign, and the needle was excited by the positive terminal of the Wimshurst, the gap sparked with perfect regularity. Still keeping the h.t. electrode negative, the needle was transferred to the negative pole of the Wimshurst. Then no sparking occurred at the gap. On reversing the polarity of the h.t. electrode, sparking occurred at the gap when the needle was negatively electrified, but none when the needle was positive. These experiments show that when the needle is excited by a Wimshurst machine, the needle only affects the gap when its polarity is opposite to that of the h.t. electrode of the main gap. The results are only apparent when one of the main gap electrodes is earthed. Without the earth connexion, the effect of polarity on the action of the needle is masked, because the appropriate polarity then always exists at one or the other of the gap electrodes.

In the second series of experiments the needle was connected to the h.t. electrode of the gap. Two facts became evident. It was noticed that when the needle-point was placed near the h.t. electrode, no effect was produced in the gap, and no sparks passed; but when it was placed near the earthed electrode, a spark occurred, so long as the Wynn-Williams condition was satisfied that a straight line could be drawn from the needle-point to any part of the spark path between the main electrodes. Clearly, before the Wynn-Williams effect can be obtained, it is necessary for the needle-point to be subjected to a sufficient potential gradient. Further, it was noticed that the effect of the needle-point on the gap was independent of the polarity of the h.t. electrode. As a check the needle was fixed in the last position, nearer the earthed than the h.t. electrode, and the experiment with the Wimshurst machine was repeated. When connected to the Wimshurst the needle was only operative when of opposite polarity to the h.t. electrode.

Seeing that the action of the needle-point on the gap was, in the first series of experiments, dependent on the polarity of the needle, and, in the second series, independent of polarity, it must be concluded that the action associated with the needle-point was different in the two experiments.

The effect of the discharge from the needle on an electroscope was then examined. It was found that when the needle was connected to either pole of the Wimshurst machine, the electroscope became strongly charged, even

when the needle was held at considerable distance (as much as 25 cm. or more) away from the electroscope. When the needle was connected to the h.t. electrode of the gap, or induction coil, there was but little, if any, charging effect on an uncharged electroscope, but there was a strong discharging effect when the electroscope was charged either positively or negatively. This suggests that in the first series of experiments the effect was due to direct ionization of the gap, whilst in the second the effect was that found and explained by Wynn-Williams. Reference to confirmatory experiments will be deferred while brief consideration is given to the question as to why the Wynn-Williams effect was not obtained in both experiments.

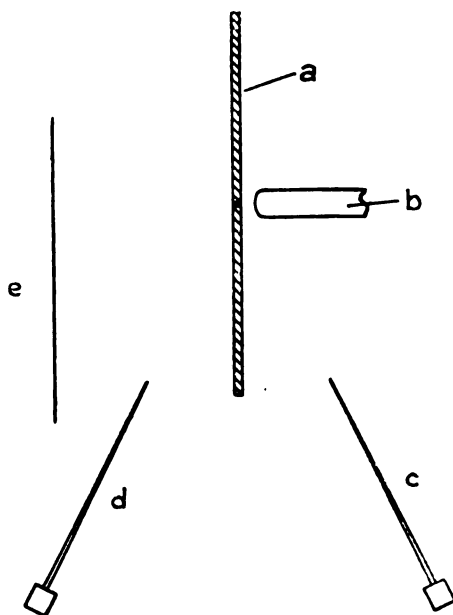
It is surprising and not a little perplexing that the needle-point should behave in a certain manner when connected to the h.t. electrode, and in a different manner when connected to the Wimshurst machine. Assuming that in both experiments the needle-point was subjected to the same potential gradient, the only difference that existed in the conditions of the experiments was that of the manner in which the potential was applied. In the first experiment the voltage, or potential, was applied steadily, whilst in the second it was applied impulsively. Possibly an impulsive action at the needle-point is essential to the Wynn-Williams effect. If so, it ought to be capable of demonstration. To test the matter, the needle-point was first disconnected from the Wimshurst, and the latter was operated until the poles were raised to a sufficiently high potential. With the h.t. electrode negative, a wire attached to the needle was then suddenly brought into contact with the negative pole of the Wimshurst, and momentary sparking occurred at the gap. With the h.t. electrode positive, sudden connexion of the needle with the positive pole of the Wimshurst was also followed by momentary sparking at the gap. Continued connexion of the needle with the Wimshurst in both tests gave the same results as has already been mentioned, namely, no sparking at the gap. It follows that to obtain indirect ionization of the gap by radiation issuing from the needle-point, the latter must be subjected to an impulsive action. In other words, the Wynn-Williams effect is a transitory one, and is not obtained when the needle-point is maintained at a high potential. Under the latter condition the discharge is of the nature of an ionized stream which is only operative on a gap (in which one electrode is earthed) when the stream is of appropriate sign.

Reflection on the results of the experiments led to the

construction of a new form of gap the essential features of which are shown in fig. 2. The use of this gap throws an interesting side light on the question under examination and affords confirmation of the conclusions already reached.

The h.t. electrode *a* is a metal disk of about two inches diameter. This is attached at its edge to the upper end of a vertical insulating pillar. The earthed electrode *b* consists of a metal rod having a hemispherical end adjacent to the disk. This electrode is also carried on an insulating pillar. At the centre of the electrode *a* is formed a tiny hole.

Fig. 2.



Viewing the gap in plan, a needle was placed in or about the position indicated at *c*.

After adjusting the current in the primary winding of the inductance coil so that a spark just failed to occur at the gap between *a* and *b*, the needle was connected by a wire to the electrode *a*. Sparking then occurred at the gap. With the h.t. electrode negative, sparking also occurred when the needle was connected to the positive terminal of a Wimshurst machine. When the needle was connected to the negative terminal of the Wimshurst, the sparking at the gap became

very irregular, and it was found that on closing the back of the hole in the electrode *a* this sparking ceased.

On transferring the needle to the position *d*, and connecting the needle to the electrode *a*, sparking did not occur at the gap, but on bringing an earthed plate into the neighbourhood of the needle and so increasing the potential gradient to the needle-point, some sparking occurred; it was not, however, so regular as when the needle was at *c*. Sparking became quite regular when the needle-point was advanced to a position on or near the axis of the hole in *a*, an earthed plate being held in the neighbourhood of the point as above mentioned. With the needle still at *d* and the h.t. electrode negative, connecting of the needle to the negative terminal of the Wimshurst machine resulted in regular sparking at the gap. Closing of the hole in the electrode *a* caused the sparking to cease. Sparking also ceased when the needle was connected to the positive terminal.

A curious effect was observed when the needle, whilst at *d*, was connected to the negative terminal of the Wimshurst machine, the electrode *a* being connected as already mentioned to the negative terminal of the induction coil. On placing a sheet of mica or an insulated metal plate in the position *e*, or above or below the needle with its plane parallel to the axis of the gap, the sparking at the gap ceased, the needle-point being always "in view" of the hole in *a*, and therefore not obstructed. The plate had no effect when the needle was connected to the electrode *a*.

It is remarkable that when an ionized stream is caused to issue from the needle-point for the purpose of facilitating the passage of sparks in the main gap, the needle must be of opposite polarity to the electrode *a* when placed at the front, or gap side, of that electrode, and of the same polarity when placed at the rear of the electrode. This fact requires further investigation.

The experiments with the gap shown in fig. 2 confirm what was found in the experiments first described, namely, that the action of the needle-point on the main gap when the needle is excited impulsively is different from the action when the needle is excited from a steady source such as a Wimshurst machine.

It is now convenient to consider the main question, and inquire in what manner the auxiliary spark in the three-point gap performs its function when the gap is subjected to the action of an induction coil. The gap shown in fig. 2 enables a decisive answer to be obtained.

Instead of producing the auxiliary spark across a small

H

or auxiliary gap adjacent to the h.t. electrode as in fig. 1, it was more convenient to employ a separate small gap between needle or other suitable electrodes mounted on a handle so that the small gap could easily be presented to different parts of the main gap, one of the electrodes of the small gap being connected to the h.t. electrode of the main gap, or one of the terminals of a Wimshurst machine, and the other to a very small leak, or very high resistance connexion to earth, to insure the requisite discharge of electricity across the small gap.

In the first place it was found that when the small spark was produced by a connexion to either terminal of a Wimshurst machine, and was therefore of the nature of a small but continuous discharge, the spark produced a charging effect on an uncharged electroscope, but the effect was not nearly so strong as that obtained from a needle-point. When the small spark was produced by the induction coil to which the main gap was connected, and was therefore of an intermittent or impulsive character, there was no charging effect on an electroscope. On the contrary, the electroscope, when charged either positively or negatively, was discharged, though the discharging action was not so strong as that obtained when the needle was connected to the coil.

With the small gap connected to the same terminal of the induction coil as the electrode *a* and placed in about the same position as the point of the needle at *c* (fig. 2), perfectly regular sparking occurred at the main gap. The same result was obtained when the small spark occupied a position at the back of *a* on or about the axis of the hole. On moving the small gap to the position *d*, sparking at the main gap ceased. It follows that the action of the small spark was similar to that of the needle-point when the latter was electrified by connexion to the electrode *a*.

The small gap was then connected to each in turn of the terminals of a Wimshurst machine. Unfortunately the results were not very definite. With the electrode *a* negative, and the small gap placed at *c* (fig. 2) and connected to the positive terminal of the machine, rather erratic sparking occurred at the main gap, and none when the small gap was connected to the negative terminal of the machine. On transferring the small gap to the position *d*, the reverse results were obtained. But the erratic or occasional character of the sparking at the main gap when the small sparks were produced by the Wimshurst machine makes it impossible to say that the results were convincing. It was,

therefore, decided to use for the production of the continuous small spark a condenser charged negatively from the induction coil through a thermionic valve. The small spark thus obtained had a fairly strong charging effect on an electroscope. When placed at *d*, the electrode *a* being negative, perfectly regular sparking occurred at the main gap, and the sparking at the main gap ceased when a mica plate was placed at *e*, proving that with the small spark in this position its effect was due to a stream of negative ionization. When placed at *c*, occasional sparking occurred at the main gap, and it was not possible to decide whether this result was due to intermittency in the small gap, producing the same effect as a spark derived directly from the induction coil, or to ultra-violet radiation, it being unlikely that a stream of positive ionization was responsible. If the effect was due to ultra-violet radiation, the experiment showed, as Wynn-Williams appears to have found, that such radiation is not nearly so active as the Entladungstrahlen to which he attributes the properties of the needle-point and auxiliary spark. The Wimshurst machine experiments above described also support the conclusion that ultra-violet radiation is relatively weaker in its action, otherwise the Wimshurst sparks would have given different results.

Notwithstanding the partial success of the experiments with sparks produced by the Wimshurst machine, the evidence obtained from all the experiments adequately supports the conclusion that small sparks obtained from a continuously acting source are different in effect from those obtained intermittently from an induction coil, as in the usual three-point gap, and that the action of the auxiliary sparks in such a gap depends upon a highly active form of radiation due to the impulsive character of the spark. This action is not, however, so strong as that obtained from a needle-point.

Finally, it may be mentioned, though merely as a matter of interest, that a lighted match held in the neighbourhood of the front of the electrode *a* (fig. 2) caused regular sparking at the gap, but had no effect at the back of that electrode, excepting when placed near and opposite the hole, and then it had a slight effect in that an occasional spark passed at the gap.

Summary.

The experiments described confirm the conclusion previously established by Wynn-Williams that the action of the auxiliary spark in a three-point gap is due to ionization

of the gas in the main gap by radiation given off from the auxiliary spark. They also go further, and show that the Wynn-Williams effect is due to an impulsive or transient condition. Moreover, they show that when a needle-point or an auxiliary spark-gap is connected to a steady source of potential, such as a Wimshurst machine, the action of the needle-point or the auxiliary spark on the main gap is then due not to radiation but to an ionized stream.

IX. Refraction of X-Rays by Method of Total Reflexion.
By RICHARD L. DOAN, Ph.D., Ryerson Physical Laboratory, University of Chicago, U.S.A. *

[Plate I.]

THE classical Drude-Lorentz theory of dispersion leads to an expression for the index of refraction of a substance which may be written in the following manner :

$$1 - \mu = \delta = 2.714(10)^{-6} \frac{D}{W} \lambda^2 \sum \frac{n_r \lambda_r^2}{\lambda_r^2 - \lambda^2},$$

where μ = index of refraction for monochromatic radiation of wave-length λ ,

D = density of refracting substance,

W = atomic weight,

n_r = number of electrons per atom of natural frequency $c\lambda_r$.

This theory is based upon the assumption of elastically and isotropically bound electrons which are set into forced vibration by the action of the electromagnetic field of any radiation which is allowed to traverse the substance. The resultant absorption of energy is accompanied by an emission of scattered radiation. If the frequency of the radiation is much higher than the natural frequencies of the electrons, then the latter will scatter as if free and will absorb a minimum amount of energy. But when the natural frequency of a particular group of electrons is approached, the electronic vibrations will increase in amplitude and there will be a greater absorption of energy. The classical theory attempts to account for the dispersion of a substance near an absorption edge simply by an application of the idea of resonance.

* Communicated by the Author.

A quantum theory of X-ray dispersion has recently been developed by R. de L. Kronig*. This theory is of a more empirical nature, in that it introduces known facts concerning atomic absorption coefficients, and an attempt is made to bring the phenomenon of dispersion into close correlation with that of absorption. The picture of elastic and isotropic binding of electrons is rejected as being too specialized and not in accord with available experimental information. It is replaced by the results of a theoretical investigation of Kramers concerning the behaviour of a multiply periodic system under the action of an alternating electric field, and it is from this source that a value for the scattering moment per atom is obtained. The general expression which is deduced for the index of refraction can, after some manipulation, be put into the form

$$1 - \mu = \delta = \frac{NZe^2}{2\pi m\nu^2} + \frac{Nc^4CZ^4}{8\pi^2\nu^4} \ln \left(\frac{\nu_r^2 - \nu^2}{\nu_r^2} \right)^2,$$

in which N and Z are respectively the number of atoms per unit volume and the atomic number of the refracting material, and C is the constant which enters into the expression for the fluorescent absorption coefficient. Its value† is about 0.023 for radiations on the short wave-length side of the K-limit and from one fifth to one eighth of this on the long wave-length side.

For light refracting materials in which no resonance effect is involved the second term on the right, above, becomes negligible and the equation reduces to the ordinary Lorentz form. Differences between the two expressions are therefore to be expected only in the presence of resonance effects.

Experimental Tests of Dispersion Formulas.

Most of the experimental work along this line has been carried out with light substances, and the results obtained are in satisfactory agreement with the theoretical expression :

$$\delta = 2.714(10)^{-6} D \lambda^2 Z / W.$$

The accuracy secured in the measurements has varied from one to five per cent., depending upon the method of experimentation used. Probably the most accurate measurements have been made by Larsson, Siegbahn, and Waller‡ on glass, but other measurements have been made on various

* Journ. Optical Soc. of America, xii. p. 547 (1926).

† See F. K. Richtmeyer, Phys. Rev. xviii. p. 13 (1921).

‡ Die Naturwissenschaften, December, 1924.

materials and for several different X-ray wave-lengths by Bergen Davis and his students*. Some measurements made on iron pyrites should be mentioned as showing the kind of information one may hope to get by studying indices of refraction. In calculating a value for the index of refraction in a case in which resonance occurs, one needs to assume some value for the number of electrons per atom which are situated in the particular frequency-level concerned. If, for instance, the incident radiation has a frequency near that of the K-electrons of the refracting substance, then we need to know the number of K-electrons per atom in order to make use of the theoretical formula. Von Nardroff† carried out this calculation for iron pyrites assuming successive values of one, two, and three for the number of electrons in this level. For copper K α and K β radiation the experimentally determined value of the index of refraction agreed best with the theoretical value when the number of K-electrons was taken as two. This result is interesting in that it shows the possibility of getting independent checks on other methods which have been used to study the distribution of electrons among the various atomic levels.

The experiments described in the present paper were undertaken for the purpose of extending the measurements of indices of refraction to other substances, particularly to those substances in which rather definite resonance effects are to be expected. By comparing the experimental and theoretical values in such cases, one may expect to test further the validity of the theory in the neighbourhood of an absorption edge and also to get an idea of the relative values of the two theories that have already been discussed.

The Experimental Method.

All measurements were made by the method of total reflexion‡. If θ is the glancing angle of incidence of a beam of X-rays on a plane surface and μ is the index of refraction with reference to air, then the critical angle of total reflexion is determined by

$$\begin{aligned} c & \qquad \qquad \qquad \cos \theta = \mu ; \\ \text{then} & \qquad \qquad 1 - \cos \theta_c = 1 - \mu = \delta, \\ \text{or,} & \qquad \qquad 2 \sin^2 \theta / 2 = \delta. \end{aligned}$$

* Proc. National Academy of Science, x. p. 60 (1924); Phys. Rev. xxvii. p. 18 (1925).

† Robert von Nardroff, Phys. Rev. xxiv. p. 143 (1924).

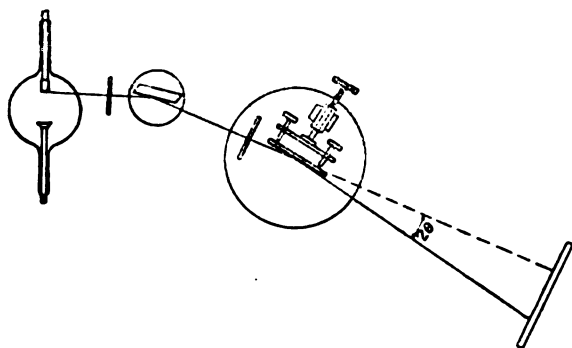
‡ Cf. A. H. Compton, Phil. Mag. xlv. p. 1121 (1923).

For the small angles concerned, the angle may be set equal to the sine, and we get the simple expression which was used in making the calculations,

$$\theta^{\circ} = 2\delta.$$

Most of the surfaces that were used were prepared by depositing various metals on optical glass surfaces by sputtering in *vacuo* from a cathode of the pure metal. Relatively thick films of considerable brilliance and great uniformity were obtained in this way. As a general rule the sputtering was continued for a length of time varying from six to ten times the period required to produce an opaque film. The reflecting power of these surfaces was high and was increased by burnishing before use. The metallic surfaces so prepared were used in connexion with the K-radiation from molybdenum and copper water-cooled Coolidge tubes. Measurements were also made upon the

Fig. 1.



glass surface itself before sputtering and upon a surface of speculum metal polished to optical planeness.

In making the critical angle measurements a surface was mounted on a spectrometer table in such a way that a collimated beam of X-rays, made monochromatic by reflexion from a calcite crystal, fell upon it at a very small glancing angle (fig. 1). Under these conditions a reflected beam was obtained which was in most cases just as sharply defined as the primary beam. Preliminary photographs were first taken to locate the critical angle approximately, after which a photographic plate was mounted at a given distance (about 165 cm. for most of the experiments) from the mirror, and the latter given an effective slow motion of rotation past the critical angle during a continuous exposure.

In the first experiments this effective slow motion took the form of a series of individual exposures at angular intervals of a few seconds of arc, the turning being accomplished by hand, but later this method was replaced by a mechanical device for giving the desired rotation. This consisted of an electromagnet connected through a relay system to a large clock in such a way that the circuit was closed once every two seconds. Each time the circuit was closed a small arm to which was attached a pawl operating in connexion with a ratchet-wheel was drawn over to the core of the magnet, giving rise to an angular motion of the mirror of a fraction of a second of arc. The motion of rotation was thus made uniform and was reduced to such an extent that an angular range of five minutes of arc was covered in about an hour and a half, a period of time adequate to give a good photograph. Some of the photographs obtained are shown in fig. 2 (Pl. I.). It will be observed that the critical angles are quite sharply defined, thus enabling one to make an accurate setting on the extreme position. The sharpness of the critical angle varied in the different cases studied, and the effect of this upon the accuracy of the measurements is discussed below.

Method of Measurement and Considerations of Accuracy.

In more than half of the experiments angular measurements were made directly on the scale of a large spectrometer which was equipped with microscopes and which could be read to seconds of arc. The mounting for the photographic plate was fixed rigidly at the desired distance from the mirror, and this distance remained unchanged during a given experiment. After mounting the plate in position, the mirror was drawn back out of the path of the beam of X-rays and a short exposure was made to give a reference line from which to measure the critical angle. The finished plate was placed upon the table of a comparator and the critical angle measured simply as the distance between the reference line and the point where the reflexion stopped. In order to determine the angle to which this distance corresponded, an "angle plate" exposure was made which consisted in taking two exposures of the reflected beam by turning the mirror through a definite angle, the value of which could be read directly on the spectrometer scale. The distance between these two lines, as measured on the comparator, served as a scale by which the critical angle was determined. In later experiments essentially the same method was used, the only

difference being the substitution of a mirror and illuminated scale for the spectrometer in the initial angular measurements. An interferometer mirror was mounted rigidly on the revolving table by means of a one-inch steel support in such a way that the plane of its surface intersected the plane of the surface upon which experiments were being made in a line which formed the axis of the table. The scale was located at a distance of about ten feet from the mirror, and the telescope was mounted firmly on a stone block. This arrangement was used to calibrate a graduated dial attached through a system of two worm gears to the revolving table. One turn of this dial corresponded to a rotation of $36''$ of arc and its circumference was divided into two hundred parts. In making subsequent angular measurements the lamp and scale method was used only to check the readings of the dial.

The accuracy of measurements such as those described here is affected by three factors. (1) The angular measurement itself is an indirect one, consisting of a spectrometer reading and a comparator reading. Both of these can be made with considerable accuracy, and probably contribute very little to the possible error of the experiments. (2) Width of line. Since measurements were made to the edge of the continuous band at which reflexion ceased, it will be seen that a half-line too much has been included. In most of the experiments the lines had an angular width of from 10 to 14 seconds of arc, and in two or three cases where the sharpness of the critical angle justified the procedure a half of this value was subtracted from the measurement as made to the edge of the band. (3) Sharpness of the critical angle. This factor introduces what is perhaps the largest single source of uncertainty in the measurements. In most of the cases in which the critical angle was small the limiting position was very sharply defined, but this was not always true, particularly for the large angles encountered in the use of the characteristic copper radiation. Since the sharpness of definition varied in the different photographs, the probable accuracy of the measurements is more or less a matter of judgment and is therefore indicated separately for each case. (4) Length of the mirror. In the case of small glancing angles it becomes necessary to consider the length of the mirror as affecting the value of the measured angle. In most of the experiments a mirror 78 mm. in length was used. Let us suppose that in an extreme case the reflexion occurred entirely on one half of the mirror during an angle-plate exposure and that during the critical angle exposure the

mirror was pushed forward so that reflexion occurred entirely on the other half. Obviously any measurements made under these conditions would be in error because the distance from the mirror to the photographic plate is not the same in the two cases. This possible source of error was avoided by making a series of exposures to test the correct position of the mirror. The mounting upon which the latter was fixed was provided with a slow-motion screw having a pitch of $1/100$ inch, and this was equipped with a graduated wheel whose circumference was divided into fifty parts. With this arrangement a given setting of the mirror could be repeated to about $5/1000$ of an inch. The procedure in determining the correct position of the mirror consisted in making a series of short exposures, starting with the mirror back out of the path of the X-ray beam and pushing it forward at intervals of ten divisions of the wheel, the photographic film being shifted a short distance for each exposure. The finished film showed the position at which reflexion just began on one edge of the mirror and also the position at which it ended on the other edge after the mirror had been pushed entirely across the beam. The distance between these two extremes was usually about fifty divisions of the wheel, or about one turn, and in this interval the reflected beam first increased in intensity, reached a maximum, and then decreased. The correct position of the mirror was taken as the mid-point between the two extremes.

Discussion of Results.

Results of the measurements on various surfaces are shown in Table I. Theoretical values of the index of refraction given there were calculated from the Drude-Lorentz dispersion formula, making use of critical absorption limits listed in the fourth edition of Sommerfeld*.

It is possible to check the results obtained by the total reflexion method against those obtained by other methods by making some comparisons in a few cases. The index of refraction of glass for the two wave-lengths listed above has been determined by Larsson, Siegbahn, and Waller, who measured the refraction in an ordinary prism. The agreement between their values and those given in the above table is within experimental error. The refraction of $\text{MoK}\alpha_1$ in silver has been studied by Slack, using a double X-ray spectrometer method in which the primary X-ray beam was

* Arnold Sommerfeld, *Atombau und Spektrallinien*, pp. 295-6.

allowed to enter one surface of a silver prism at normal incidence, refraction taking place upon emergence at the other surface. The agreement between the results arrived at by the two methods is again quite satisfactory, being well within the probable error of measurement by either method.

TABLE I.
Data on Refraction of X-rays by the Total
Reflexion Method.

Line.	λ (A.U.).	Surface.	θ_c .	$\delta(10)^6$ (expt.).	δ (theory).
MoK α_1	0.7078	glass	6 18"	1.67 \pm .03	1.73
"	"	steel	9 35	3.41 \pm .15	4.98
"	"	nickel	10 15	4.42 \pm .15	5.78
"	"	silver	11 42	5.76 \pm .10	5.77
"	"	speculum	10 52	4.96 \pm .10	5.1
CuK α_1	1.537	glass	13 36	7.8 \pm .2	8.14
"	"	copper	20 34	17.74 \pm .3	17.5
"	"	silver	26 42	30.0 \pm 1.5	29.88
"	"	nickel	24 40	25.5 \pm .8
"	"	gold	31 24	41.6 \pm 1.6	40.3
"	"	speculum	23 8	22.4 \pm .4	18.84
CuK β	1.389	copper	19 36	16.25 \pm .4
"	"	nickel	16 9	10.98 \pm .5	32.6

An examination of Table I. shows that for radiation frequencies not too close to an absorption edge the Lorentz dispersion formula represents the facts in a fairly satisfactory manner, although there are some exceptions. Perhaps the most striking example of agreement is in the case of the line CuK α_1 reflected from copper. Here the frequency of radiation is very near to the natural frequency of the K-electrons, and since the absorption edge lies on the short wavelength side of the radiation, the magnitude of the critical angle is considerably diminished. One may calculate values for the index of refraction for this case, assuming successively one, two, and three K-electrons, and the results thus obtained differ from one another by as much as fifteen or twenty per cent. It is interesting to note that the experimental value agrees very closely with the calculation based on two electrons. This agreement is shown below.

Refraction of CuK α_1 in Copper.

Number of K-electrons...	0	1	2	3
$\delta(10)^6$ (theory)	26.1	21.9	17.5	13.2
$\delta(10)^6$ (experiment)			17.74 \pm .3	

The same kind of calculations may be made for silver in connexion with the line $\text{MoK}\alpha_1$, and although the differences are not so large one obtains, on the basis of the measurements here presented, the same kind of information as in the case of copper, and this is also in favour of a two-electron distribution in the K-level.

In the case of refraction of the copper $\text{K}\alpha_1$ line in gold, the binding of the L-electrons must be taken into consideration. Since there are presumably eight electrons distributed among the three L-levels, it is desirable to have some information concerning the method of this distribution in order to make the necessary calculations. In the absence of more definite information in this connexion the calculations have been made following Stoner's suggested distribution of 2 L_1 -, 2 L_2 -, and 4 L_3 -electrons. The value of the index of refraction thus calculated differs from that obtained on the assumption of no resonance by about twenty per cent., but agrees with the experimental measurement.

The expected failure of theory when an absorption edge is approached too closely is demonstrated in the case of $\text{CuK}\beta$ reflected from copper. Here the wave-length of the radiation exceeds that of the absorption limit by only 0.011 Ångström unit, and as a result a calculation made from the theoretical formula gives an index of refraction greater than unity and thus predicts that there should be no reflexion at all. But of course there is some reflexion, and it is possible to find an experimental δ in the usual way. This departure from theory is shown in fig. 3, which is a graphical representation of the dispersion in the vicinity of an absorption edge. The curve is plotted for copper as the refracting substance. Three experimental determinations are indicated on this graph, one of which (for $\lambda = 0.708 \text{ Å.U.}$) has been taken from some measurements made by Slack *. It will be noticed that for two of the cases the experimental points lie on the theoretical curve.

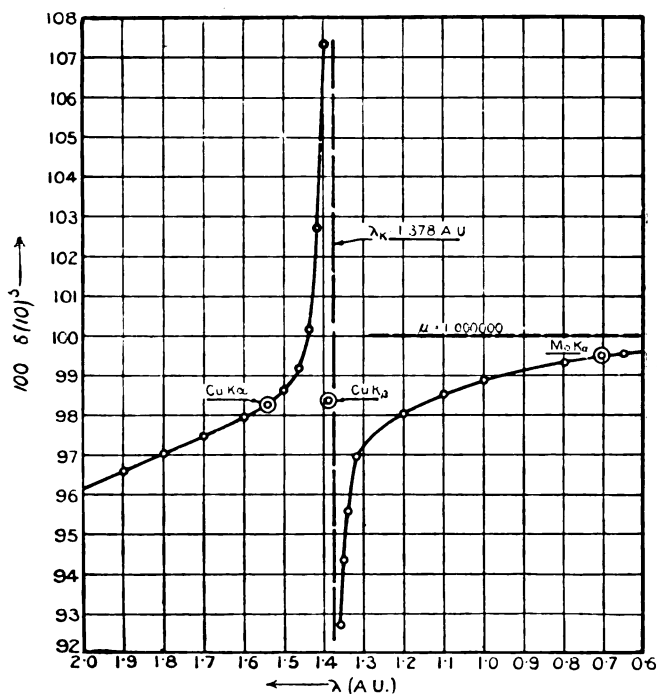
A convenient and interesting method of displaying the results of all measurements made with one particular wave-length is illustrated in fig. 4. As indicated previously, the Lorentz dispersion formula may be written as follows :

$$\frac{\delta}{2.714(10)^{-6} \frac{D}{W} \lambda^2} = \sum \frac{n_r \lambda_r^2}{\lambda_r^2 - \lambda^2}.$$

* C. M. Slack, Phys. Rev. **xxiii**, p. 691 (1926).

Now suppose we inquire as to the behaviour of the quantity on the right as we pass from element to element along the scale of increasing atomic numbers. For the lighter elements, if X-rays of ordinary hardness are used, the value of this summation will be identical with that of the atomic number since λ is negligible compared with λ_r . But with increasing atomic numbers the binding of the K-electrons comes into consideration and a discontinuity is registered at

Fig. 3.

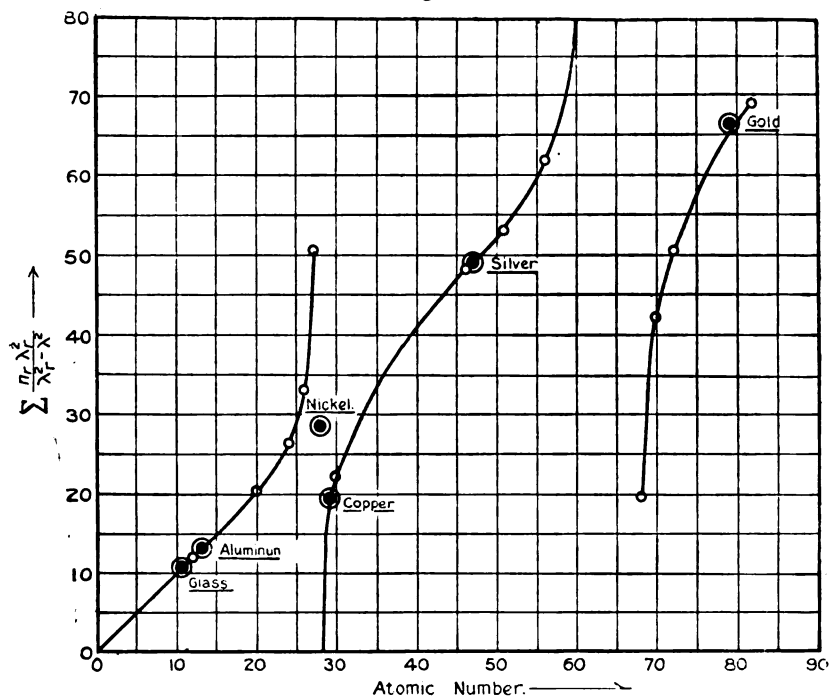


the point where the K critical absorption wave-length of the element lies nearest the wave-length of the radiation. Passing to still higher atomic numbers a similar discontinuity is introduced by the L-electrons. The theoretical curve obtained by plotting the summation against the atomic number is shown in fig. 4 for copper $\text{K}\alpha_1$ radiation ($\lambda = 1.538$). The experimental values given on this curve were obtained by carrying out the calculation indicated on the left side of the above equation, using experimentally determined δ 's. The value for aluminium was taken from

the results of Davis and Slack*. All of the points lie on the curve (or very near it) except that for nickel, whose K-absorption wave-length is 1.489 ångströms.

The low experimental value found for nickel and steel when used with MoK α radiation is somewhat difficult to understand and no ready explanation seems available.

Fig. 4.



In both of these cases the critical angle was as sharply defined as usual, and it is certain that no reflexion at all occurred at angles of a magnitude as great as that predicted by the theory. Before drawing any conclusions as to the meaning of this discrepancy, it is perhaps desirable that the results given here be checked by one of the other methods described above. Of course, so far as the steel is concerned, it always contains a small amount of combined carbon, and the effect of this would be to decrease the value of δ , but such an effect

* Proc. National Academy of Science, x. p. 60 (1924); Phys. Rev. xxvii. p. 18 (1926).

would be far smaller than the observed difference, since the amount of carbon usually does not exceed two per cent. At any rate, the same argument would not apply to the difference found in the case of nickel, for this surface was prepared by sputtering from a pure nickel plate.

Only one of the cases studied is suitable to test the validity of the theory developed by Kronig as against the classical theory of Lorentz. As indicated previously, the two expressions for the index of refraction become identical when no resonance is involved, differing only when an absorption edge is approached. Furthermore, a better test of the quantum expression can be made for radiations of a wave-length less than one ångström because in the derivation of the formula an empirical relation was used for the fluorescent absorption coefficient which applies better to wave-lengths less than an ångström than to those farther up the scale. Therefore, the refraction of $\text{MoK}\alpha_1$ in silver seems to offer the only possibility of testing the formula, and in this case the test is not favourable. The value of δ calculated on the assumption of no resonance comes out to be $6.33(10)^{-6}$, taking into consideration the resonance of the K-electrons, the Lorentz expression gives a value of 5.77 while that of Kronig gives 6.30. (In making this calculation the value of C was taken as $.023/8$ because the radiation used lies on the low frequency side of the K-limit of silver.*) The experimental δ is 5.76. Therefore in this one case the classical theory seems to have preference. However, it would seem that the method of attack used by Kronig is to be preferred from the standpoint of experimentally known facts. The Lorentz formula does not give the kind of variation of the index of refraction near an absorption band that one might expect from absorption data. This is made evident in the fact that the difference between the calculated index in the immediate vicinity of an absorption limit and the index for no resonance is greater on the long wave-length side of the limit than on the short wave-length side. Kronig's formula is not open to this criticism.

Conclusions.

Additional cases have been presented in which the Drude-Lorentz theory of dispersion represents the facts, not only in regions remote from an absorption edge, but also in some instances in which the frequency of the radiation approaches the natural frequency of certain groups of electrons. The

* F. K. Richtmeyer, *Phys. Rev.* January, 1926.

interesting possibility of studying the distribution of electrons among the lower atomic levels has received additional support. The information obtained here is very definite so far as the K-electrons are concerned, but the distribution among the various L-levels is a much more complex problem. However, the determination made for gold shows that it is not impossible to have some measure of success even here. Of course, it will be necessary to increase the accuracy of the measurements by a considerable amount before one can hope to be in a position to decide between various groupings, but there is no reason to believe that this will not be done if the method of attack proves fruitful.

The experiments described in this paper were carried out under the supervision of Professor A. H. Compton, to whom the writer wishes to express his sincere thanks for many valuable suggestions.

Ryerson Physical Laboratory,
The University of Chicago,
September 22, 1926.

X. *On the Fine Structure of the Spectrum Lines of Cadmium in the Ultra-Violet.* By WALI MOHAMMAD, M.A. (Punjab), B.A. (Cantab.), Ph.D. (Göttingen), Professor of Physics, Lucknow University, and S. B. L. MATHUR, M.Sc.*

I. Introduction.

AN accurate knowledge of the fine structure of the spectrum lines of elements is of the greatest importance in the determination of their atomic structure.

The observation of the fine structures discloses the mechanism of the intra-atomic motions as far as the perihelion of the elliptic orbits. It also throws light on the varying orientations of the nucleus. Merton¹, Nagaoka, Sugiura and Mishima², Brunetti³, and others have, by a knowledge of the structure of the spectrum lines, been able to determine the isotopes to which some of the satellites are due. But the contribution of the knowledge of the fine structure of spectrum lines does not end here. Spectroscopy is now in a position to lend support to and to receive support from the theory of relativity, and to furnish facts for discussing the question of the variability

* Communicated by the Authors.

of mass of the electron. Recently Ruark, Mohler and Chenault⁴, Ruark and Chenault⁵, and Joos⁶ have attempted to deduce the energy levels of certain elements from the fine structure of their spectrum lines.

II. *Previous Work.*

Michelson, Janicki, Gehrcke, von Baeyer, Wali Mohammad, Nagaoka, and a host of other workers have, naturally, been attracted to this important branch of spectroscopy; and instrument after instrument of the highest precision has been constructed and most refined methods devised for the investigation of the fine structure.

Almost all the above-named workers have confined their attention to the visible part of the spectrum. This is obviously due to the difficulties experienced in working in the other regions of the spectrum.

Owing to the ease with which a mercury arc can be set up and controlled, all the attempts of investigating the ultra-violet region have been confined to mercury, and the fine structure of some of the mercury lines in the ultra-violet region has been determined by Takamine⁷, Galli and Forsterling⁸, Lucy Wilson⁹, Nagaoka, Sugiura and Mishima¹⁰, and Wood¹¹.

Realizing the need of full information regarding the fine structure of the spectrum lines in the invisible region, the authors have undertaken a systematic investigation of the ultra-violet region, and some of the results obtained by them are reported here.-

III. *Present Work.*

Any method adopted for investigation should provide for the following essentials :

- (i.) A suitable source of illumination.
- (ii.) A suitable instrument of high resolving power.

Regarding (i.), a most suitable source of illumination is offered by an oxy-cathode arc described by Wali Mohammad and successfully used by him and a number of other workers for the investigation of the fine structure. This source possesses the peculiar advantages of yielding lines which are both *sharp* and *bright* and the intensity of which can be controlled with ease.

Regarding (ii.), the instruments available were a Quartz Lummer Plate and a Quartz Fabry and Perot Etalon.

Phil. Mag. S. 7. Vol. 4. No. 20. July 1927.

I

In spite of what has been said about the defects of the Lummer Plate by van Cittert¹² and G. Hansen¹³, it is perhaps the most convenient instrument for use.

IV. *Experimental Arrangement.*

(a) *Source of illumination.*

The source of light was a Wali Mohammad lamp¹⁴, which was fixed up vertically. Briefly stated, the arrangement consisted of a Wehnelt oxy-cathode of platinum and an anode of the substance under investigation, both placed in a water-cooled tube which was exhausted by means of a rotary pump. The oxy-cathode was heated to incandescence, and by applying a steady potential of 220 volts a suitable anode current was allowed to pass between the cathode and the anode, thus melting and evaporating at any desired rate the metal which formed the anode. The current employed for heating the oxy-cathode was usually about 15 amperes; while a thermionic current varying from a fraction of an ampere to several amperes was available.

(b) *Production of the Interference Fringes.*

The upper end of the lamp was closed with a quartz plate or a quartz lens of suitable focal length, which rendered the beam of light emerging from the lamp parallel. This beam was rendered horizontal by means of a specially made tungsten mirror held at 45° to the vertical. The parallel beam thus rendered horizontal fell on a Hilger quartz Lummer-Gehrcke plate of the dimensions :

Length	13 cm.
Thickness	0.46 ,,

and the interference fringes from the upper face of the Lummer plate were focussed upon the slit of a Hilger E quartz spectrograph by means of a quartz fluorite achromat of 40 cm. focal length. A double-image prism was placed in front of the Lummer plate, in order to transmit the beam polarized with the electric vector parallel to the parallel surfaces of the Lummer plate. The fringes were photographed in the usual way in the spectrograph, and Ilford Special Rapid plates were used throughout for the purpose. The time of exposure varied from 3 to 5 minutes only, during which conditions could be kept constant. This arrangement has the advantage that all the lines of the spectrum, in the visible as well

as in the ultra-violet regions, could be photographed simultaneously.

(c) *Calculation of Wave-lengths.*

As the mount supplied by Hilger for the Lummer plate did not allow the interference fringes due to the lower face to be photographed, the elegant method described by McLennan and McLeod¹⁵ for measuring the distance of satellites could not be adopted. Measurements were consequently taken upon the fringe system from the upper face of the Lummer plate, and the fringes of the lowest orders were measured and the mean of several observations taken. In this way the distances between two main line fringes and between a main line fringe and the satellites were determined. Lummer¹⁶, Lummer and Gehrcke¹⁷, von Baeyer¹⁸, Koláček¹⁹, McLennan and McLeod²⁰, Takamine²¹, and more recently Galli and Forsterling²², Worsnop and Flint²³, and P. Kunze²⁴ have each developed a formula of their own, which are all modifications of the original formula given by Lummer. The method adopted by the authors was the calculation of the distance in A.U. between the order of the fringe system of a spectrum line from the dimensions and the optical constants of the quartz Lummer plate. The formula due to von Baeyer; and used also by Nagaoka²⁵ and Simeon²⁶, gives

$$\Delta\lambda = \frac{n\lambda^2}{n^2\lambda - 4t^2\mu d\mu/d\lambda},$$

where

λ = the refractive index of quartz with respect to the ray under investigation,

n = order of the fringe given by

$$n\lambda = 2t\sqrt{\mu^2 - 1},$$

λ = wave-length of the ray,

t = thickness of the Lummer plate,

and $d\mu/d\lambda$ is the dispersion of quartz about λ .

A curve was drawn with the refractive indices of quartz for the extraordinary ray as abscissa and the corresponding wave-lengths in A.U. as ordinates. The data for this were gathered from Landolt and Börnstein's latest tables. Thus not only the refractive index for any wave-length, but also the dispersion of the quartz about that wave-length, could be determined easily from the curve.

The position of a satellite was fixed in the following way :—

Let a = the distance between two main line fringes,
 b = the distance between the satellite and the lower order fringe.

Then if b was $< a/2$, the satellite was positive ;
 but if b was $> a/2$, the satellite was negative ;

and then the distance between the satellite and the higher order fringe was taken.

In either case the wave-length of the satellite was given by

$$\Delta\lambda = \frac{b}{a}.$$

This obviously is an arbitrary method, and the conclusions arrived at are liable to error which can be removed only by some other means ; for example, the use of greater resolving power or the employment of the method of crossed spectra.

V. Preliminary Test.

As a test of the performance of the given Lummer plate as regards its theoretical and actual resolving power, the Cadmium line 4800 was examined and its structure found to be as follows :

$$+0.057 \text{ \AA} ; 0.000 ; -0.037 \text{ \AA} ; -0.085 \text{ \AA}.$$

The results of other workers as well as ours on this line are given below :

$+0.058(\frac{1}{4})$, $0.000(1)$, $-0.034(\frac{1}{4})$, $-0.081(\frac{1}{2})$ Janicki.

$+0.058(6)$, $0.000(10)$, $-0.034(3)$, $-0.081(6)$

Wali Mohammad.

$+0.059(3)$, $0.000(10)$, $-0.033(1)$, $-0.080(2)$ Takamine.

$+0.058(6)$, $0.000(10)$, $-0.034(3)$, $-0.081(3)$ MacNair ²⁷.

$+0.057(6)$, $0.000(10)$, $-0.037(3)$, $-0.085(2)$ Authors.

The agreement is fairly close, and it was safe to conclude that the Lummer plate available gave satisfactory results.

VI. Measurements on Cadmium Lines in the Ultra-Violet Region.

When the results obtained by the authors were nearly ready for publication, a highly interesting and valuable paper giving the results of fine structure of the Cadmium

lines in the ultra-violet region was published by W. A. MacNair in the Philosophical Magazine (Sept. 1926). His values are given side by side with those of the authors for sake of comparison.

The wave-lengths are taken from Exner and Haschek, and the figures in brackets indicate the intensity as visually estimated by the authors.

(1), (2) Lines 3614·62, 3613·11, and 3610·72.

According to Exner and Haschek, there are three lines in this region, with wave-lengths of

3614·62(10),
3613·11(50),
3610·72(500).

The line 3614·62 is faintly visible in only one of the many photographs taken and cannot be seen in any other. MacNair has measured satellites belonging to 3614·62 and 3610·72, and says that line 3613 appears also on one plate, but he gives no structure for the same.

Assuming that satellites are due to lines 3614·62 and 3610·72, the structure of these lines is as follows :

Line 3614·62. $2p_1-3d_3$.

+ 0·034(4),	0·000(10),	- 0·020(2)	Authors.
+ 0·037(2),	0·000(10),	- 0·023(4)	MacNair

Line 3610·5. $2p_1-3d_3$.

0·000(10),	- 0·032(2)	Authors.
0·000(10),	- 0·035	} (3) MacNair.
0·000(10),	- 0·037	

The agreement of the authors' values with those of MacNair is very close indeed. The authors, however, think that the satellites are due to the lines 3613·11 and 3610·72, and not to the line 3614·62, which is too faint to be photographed. They find the structure to be as follows :

Line 3613·11.

0·000(10), - 0·052(4), - 0·020(1).

Line 3610·72.

0·000(10), - 0·035(2).

(3) Line 3500·2. $2p_2-3d$.

This line appears to have only one satellite, while MacNair has found two.

0·000(10), -0·039(7) Authors.
+0·017(2), 0·000(10), -0·010(4) MacNair.

(4) & (5) Line 3467·81. $2p_2-3d_4$.
and Line 3466·37. $2p_2-3d_3$.

According to Exner and Haschek there are two lines very close to each other of wave-length

3467·81(50) and 3466·37(100).

The closeness of the lines makes the assignment of the satellites very difficult, and the conclusions drawn are not without some doubt.

Line 3467·81.

This line appears to be single, and MacNair also finds it single.

Line 3466·37 has the following structure :

+0·033(4), 0·000(10), -0·021(5) Authors.
+0·031(3), 0·000(10), -0·015(5) MacNair.

(6) Line 3403·86. $2p_2-3d_3$.

The authors find two satellites, while MacNair finds only one.

+0·024(9), 0·000(10), -0·023(1) Authors.
+0·017(5), 0·000(10) MacNair.

(7) Line 3261·23. $1·5s-2p_2$.

The satellites of this line are not well separated, and two of them are unusually faint.

The structure is as follows :

+0·033(2), +0·015(2), 0·000(10), -0·016(9), -0·036(8)
Authors.

This line has been investigated by R. W. Wood, who has found only one satellite -0·019.

(8) Line 3252·86. $2p_1-2·5s$.

The structure is as follows :

+0·036(8), 0·000(10) Authors.
+0·031(2), 0·000(10), -0·010(3) MacNair.

The authors believe that, since the satellite appears ill-defined, their results may not be final.

(9) Line 3133·47. $2p_2-2\cdot5s$.

This line gives the following structure :

+ 0·033(6), 0·000(10), -0·028(1)	Authors.
+ 0·024(1), 0·000(10), -0·033(1), -0·012(1)	MacNair.

The satellites of this line are somewhat diffused and ill-defined.

(10) Line 3081·00. $2p_2-2\cdot5s$.

+ 0·015(2), 0·000(10), -0·023(3)	Authors.
+ 0·013(3), 0·000(10), -0·023(2)	MacNair.

The values of MacNair and those of the authors seem to be in very good agreement.

(11) Line 2980·80. $2p_1-4d_2$.

This line appears to be simple. MacNair, too, does not give any satellite.

(12) Line 2980·65. $2p_1-4d_1$.

This line appears simple. MacNair gets a satellite at -0·025(1).

(13) Line 2881·35. $2p_2-4d_3$.

This line appears single. MacNair gets two satellites at -0·021(1) and -0·010(5) respectively.

Exner and Haschek give two lines, as follows :

2881·35 and 2880·89.

The difference in the wave-length of these two lines is so small that in our photographs the fringes produced by these two lines cannot be separated. The authors think that perhaps MacNair might have taken the main line fringe of 2880·78 to be the satellite of 2881·24.

(14) Line 2880·89. $2p_2-4d_2$.

This line shows no satellites.

(15) Line 2837·05. $2p_3-4d_3$.

There is one satellite as follows :

0·000(10), -0·030(5)	Authors.
0·000(10), -0·011(4)	MacNair.

(16) Line 2775·20. $2p_2-3\cdot5s$.

This line has a satellite at -0·027 Å. MacNair has not investigated this line.

VII. *Summary.*

The authors have made an attempt to investigate the structure of the most prominent of Cadmium lines between 4800 and 2775. They find that their results generally are in fair agreement with those of MacNair, who happens to be the only other worker in the field which the authors have investigated. Further results will be communicated in another paper.

References.

1. Merton. Roy. Soc. Proc. A, xci. p. 198 (1915).
2. Merton. Roy. Soc. Proc. xvi. p. 388 (Jan. 2, 1920).
3. Nagaoka, Sugiura, and Mishima. 'Nature,' cxiii. p. 459 (March 29, 1924).
4. Brunetti. *N. Cimento*, July, Aug., Sept. 1924.
5. Ruark and Chenault. 'Nature,' cxiv. p. 575 (1924).
6. Ruark and Chenault. Phil. Mag. i. p. 937 (1925).
7. Joos. *Phys. Zeits.* xxvi. No. 10 (1925).
8. Takamine. Math.-Phys. Soc. Tokyo, Nov. 1915.
9. Galli and Forsterling. *Phys. Zeits.* xviii. p. 155 (April 15, 1917).
10. Lucy Wilson. Astro.-Phys. Journ. p. 340 (Dec. 1917).
11. Nagaoka, Sugiura, and Mishima. 'Japanese Journal of Physics,' ii. p. 121 (1924).
12. Wood. Phil. Mag. p. 761 (October 1925).
13. van Cittert. *Ann. d. Phys.* lxxvii. p. 372 (1925); also *ibid.* xxix. p. 94 (1926).
14. G. Hansen. *Ann. d. Phys.* lxxviii. p. 552 (1925).
15. Wali Mohammad. Astro.-Phys. Journ. xxxix. no. 3 (1914).
16. McLennan and McLeod. Roy. Soc. Proc. A, xc. p. 243 (May 28, 1914).
17. Lummer. *Verh. Deutsch. Phys. Ges.* iii. (1901).
18. Lummer and Gehrcke. *Ann. d. Phys.* x p. 457 (1903).
19. von Baeyer. *Phys. Zeit.* ix. p. 831 (1908).
20. Koláček. *Ann. d. Phys.* xxxix. p. 1431 (1912).
21. McLennan and McLeod. Proc. Roy. Soc. A, xc. p. 243 (1914).
22. Takamine. Proc. Math.-Phys. Tokyo, ix. p. 296 (1915).
23. Galli and Forsterling. *Phys. Zeit.* xviii. p. 155 (1917).
24. Worsnop and Flint. 'Advanced Practical Physics,' p. 358.
25. P. Kunze. *Ann. d. Phys.* lxxix. p. 294.
26. Nagaoka. Proc. Tokyo Math.-Phys. Soc. viii. (ser. 2) p. 296.
27. F. Simeon. Journ. Scientific Instruments, i. No. 10 (July 1924).
28. W. A. MacNair. Phil. Mag. No. 9, p. 613 (Sept. 1926).

XI. *The Lag in Electrical Discharges.* By WILLIAM CLARKSON, M.Sc., A.Inst.P., *The Physical Laboratory of the University, Utrecht**.

ABSTRACT.

THE variation of the "peak" voltage in the inter-mittent discharge in discharge-tubes of scrupulous cleanliness are considered, and possible causes, both in the gas and in the electrodes, are sought for and applied in explanation. Experimental results would agree with a "corona" lag, a theory of which is developed, if a slow "build up" is assumed. This assumption is shown to be justified from results obtained by a method, here described, for measuring the time of duration of a "flash," or condenser discharge. The small preliminary discharges often preceding a "flash" are explained on the same assumption, due to the form of the "corona characteristic." Possible causes of this slow "build up" are discussed, and it is tentatively associated with the apparently inevitable modification of the cathode surface by the filling gas.

1. PEAK POTENTIAL VARIATIONS.

THE characteristic and systematic variation of the "peak" voltage with respect to the statical sparking potential in the intermittent—"flashing"—discharge has been the subject of many references in recent years, by Mauz and Seeliger¹, Taylor and Sayce², and Penning³, for example; but a thorough investigation had not been made, and as a certain degree of confusion had resulted, the need of a solution was apparent if a definite sparking potential as a characteristic property of all discharge tubes was to retain any significance in work on intermittency.

It was the aim, then, of the writer to investigate these variations; but as they could conceivably be due to some irregularities in the tube, such as gas or electrode impurities, or to wall effects, and not inherent properties, it was essential that the work should be carried out in tubes as free as possible from such influences. Fortunately a suitable technique was at the writer's disposal⁴.

Tubes.

A typical tube consisted of a spherical glass bulb, some 10 cm. in diameter, in which were mounted convex nickel electrodes 5 cm. in diameter and about 1 cm. apart, with

* Communicated by Prof. L. S. Ornstein.

their sealed-in leads sheathed with glass up to the back of the electrodes in order to minimize any chance of leakage round the walls of the bulb (and for overrunning).

After having been carefully washed with acid, water and alcohol, and dried, they were exhausted to black vacuum and baked for half an hour or more, and then filled through a liquid-air trap with Neon or Argon to a pressure of some millimetres, the gas having previously stood for several hours in contact with heated calcium, and sealed-off. Finally, by introducing metallic sodium electrolytically through a side-tube, any remaining impurities first were removed and then a bright film of pure metallic sodium deposited on the electrodes.

Properties of the Tubes.

Even in tubes so carefully prepared it was found that the sparking potential only attained constancy after some hours, and also that "polarization" always occurred during use, though only to the extent of a volt or two at the most, this maximum effect not necessarily being attained until after several "flashes." Both of these observations, together with the fact that "polarization" often may be removed simply by passing a "flash" in the reverse direction, indicate electrode changes which at present may be assumed to be an inevitable phenomenon in discharge-tubes, since they have been found to be present despite the most thorough precautions⁴.

Though in the light, as was to be expected, such tubes gave a most marked photoelectric current, this in some cases being of the order of a microampere even at some volts below the sparking potential (fig. 3), in the dark no current could be detected, this proving the nature of the effect and the absence of electrical leakage in the discharge-tube. In general the sparking potential was a volt or two higher in the dark than in the light (fig. 3, A and B).

Measuring Apparatus.

The method employed was similar to that used on previous occasions^{2, 8}, and was retained after due consideration and thorough testing, as capable of giving results most accurately and quickly with a minimum disturbance of the discharge.

The negative side of the circuit was most carefully insulated on paraffin-wax blocks, and the positive side was earthed in several places. The potential was obtained from an M-L anode-converter, this giving any desired voltage up to

600 volts D.C. with remarkable constancy, and the circuit current was regulated by a diode (with variable filament-current) placed in the negative side, and being measured by a shunted micro-ammeter on the earthed side of the circuit, capable of detecting currents down to $0.03 \mu\text{A}$.

Though with high sparking potentials and large filament currents the micro-ammeter did not give a reading corresponding to the actual current at the moment of discharge, this value could easily be found if required.

The electrostatic voltmeter, reading to 400 volts, was quick-acting, coming completely to rest in about ten seconds. As it was most sensitive in the region of 300 volts, dry batteries were placed between it and the accompanying diode in order that this part of the scale could be employed whatever the actual voltages were.

With a small condenser in parallel with the voltmeter (giving a system with a capacity of $0.0016 \mu\text{F}$.), and with careful insulation, the voltmeter leakage could be reduced to 0.2 volt in the time required for a reading. The only time a correction had to be considered was in the case of very slow or "single" flashes.

Results.

The following symbols will be used in this paper:— v_c is the (statical) sparking potential, and would appear to be essentially a constant in any tube. Its connexion with the "corona characteristic" is given later. V_C is the "peak" potential (alternatively, the apparent upper critical voltage or the dynamic sparking potential)* and is the voltage recorded by the measuring apparatus, and ΔV_C is the difference between v and V_C .

Where V_B is the minimum potential recorded, the time of flash (T) is given quite closely by

$$T = \frac{C(V_C - V_B)}{i}, \quad . \quad . \quad . \quad . \quad . \quad . \quad (1)$$

where C is the capacity and i the current in the circuit. It may be stated, however, that as V_B was rarely measured the apparatus was generally modified to measure V_C only, the insulation being improved by this simplification. The time of flash or frequency n is measured directly in this case.

In addition to those described all other available tubes were examined and the variation of V_C observed under the

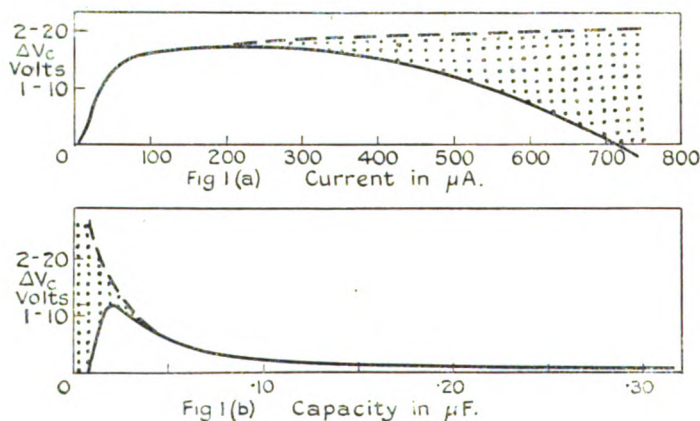
* This title can more aptly be applied to v , the voltage at which build-up" occurs when space-charge is present.

usual conditions, but as the results differed merely in degree and repeatability and not in kind no details are given.

Typical results are given in fig. 1, which shows the relation between ΔV_C and (a) the current, the capacity constant, and (b) the capacity, the current being constant, whether in the light or in darkness.

As fig. 1(a), however, may also represent the variation of ΔV_C with the frequency ($n \propto i$) or the rate of increase of voltage of the condenser ($V_C - V_B/T \propto i$), and fig. 1(b) the variation with the reciprocal of these, it was of interest to combine on one graph (for convenience showing the $T, \Delta V_C$ relation) all the readings taken in the two cases. In general, these points fell on one smooth curve similar in form to fig. 1(b) as prolonged.

Fig. 1.



This last curve did not regularly show the diminution of V_C at the higher frequencies, and this lent additional support to the belief that this phenomenon could be assigned to a separate cause.

It has been shown that corresponding to any small current i in a discharge-tube there is a certain (minimum) voltage v at which a "flash" can occur, this in essence being the sparking-potential for this current. Actually this voltage is the same as that given by the "corona characteristic," and, as fig. 3 will show, though v is almost constant for the smallest currents, in fact being v_c , there is a more or less rapid fall in value as i increases.

As in "flashing" there is a residual current (decreasing with time) after each "flash," due to the "clear-up" of the "space-charge," it is conceivable that with rapid rates of increase of voltage, that is to say at higher frequencies, a current may still be flowing in the tube when the corresponding v , as given by (v, i) the "corona characteristic" or the analogous current and sparking-potential relation existing under the conditions, is reached. The effect of this would be that v , and consequently V_c , would increase as the frequency of the flashes increased, the dotted line (fig. 1) showing a gradual increase with frequency, giving the probable variation of ΔV_c in the absence of this "overlapping" of the discharge.

2. CONSIDERATION OF RESULTS.

Though in practice several influences may be acting at once, on analysis the occurrence of a V_c always higher than v_c may be attributed to two main causes: either (1) the discharge does not immediately start when v_c is reached, or (2) the discharge does commence but some appreciable time is required for the current to attain a high value, *i. e.* to "build-up." In both of these cases, since the voltage across the tube is increasing so long as the circuit current is greater than the current in the discharge-tube (if any), the final voltage V_c is greater than v_c .

Since these causes may be referred to properties either of (a) the filling gas or (b) the electrodes, the following explanations are possible:—

(1 a). Apart from a change in the properties of the gas, this would imply a lack of ionization in a suitable place in the tube at the moment v_c was reached, and V would rise till such ionization did occur, the probability increasing both with time and with voltage. The existence of such a state of affairs in practice has been inferred by many workers, Zuber⁵ for instance, and though not conclusively proven its possibility cannot be disregarded.

(2 a). This would correspond to a "corona lag," and it is obvious that some time, however small, must be taken to establish the discharge. It has been advanced for the case of magneto sparks by Peek⁶ and has been discussed by Campbell⁶.

(1 b) and (2 b). Here the modification of the electrodes, more particularly the cathode, by layers of gas by sorption or sputtering seems the probable cause, and the effect, in the absence of definite data, may be imagined as the

prevention or inhibition of the passage or multiplication of electrons. In 1 *b* the film would have the effect of preventing altogether the production of electrons until higher voltages were reached, and in 2 *b* it would merely act by retarding their passage or liberation in the discharge, perhaps merely acting as a simple resistance. In either case we can imagine the film either as being an inherent or permanent property of an electrode or of being only temporarily established by a discharge and of being removable or, an assumption returned to later, of decaying with time. Cathodic films have been postulated by Zelany⁷ to explain results obtained for spark discharges and for the α -particle counter, and are considered also by Campbell, and on a previous occasion the writer was compelled to postulate them to explain changes in the critical voltage variations in discharge-tubes. Recently they have been submitted to direct examination by Taylor⁴, and though much remains to be done their existence and the fact that they play a role in the discharge cannot be doubted.

Fortunately here causes 1 *a* and 1 *b* can both be rejected at the outset. A positive ΔV_c was observed in circumstances where there certainly was no lack of electrons, as in cases where a photoelectric current was passing (fig. 3), and also, if our explanation is correct, where "overlapping" occurred, in which case of course ΔV_c should have vanished to zero. It is true that 1 *b* could account for the form of the T, ΔV_c graphs, though "polarizations" of 20 volts were highly improbable, but it was soon discredited as rapid "flashes," previously associated with a high V_c , could be obtained with a voltage of v_c providing the circuit current was large enough, the high V_c presumably being due to the particular properties of the usual circuit.

Neglecting "wall-effects" as at the least a very improbable cause, there remained then a "lag" attributable to a slow "build-up," and the following theory was developed which was applicable to either 2 *a* or 2 *b*.

Theory of corona lag.

Let the circuit-current be i ,

and let the initial ($t=0$) current in the tube be i_c

and at the time t be i_t .

Consider the capacity C .

Charging current at time t is $i - i_t$.

Therefore increment of voltage in time t is

$$\Delta V = \frac{1}{C} \left[\int_0^t i dt - \int_0^t i_t dt \right] \dots \dots (2)$$

As the variation of i_t with t is not known direct calculations cannot be made, but sufficiently justifiable assumptions of a general nature can be made for the variation of ΔV_c to be deduced with fair certainty. We may assume that the discharge current will be a function both of the time and of the voltage, increasing rapidly with time, the rate of increase depending on the voltage. We may express i_t then by $\phi(i_0, t, V)$, in which case the voltage (V) at any instant will be given by

$$V = v_c + \Delta V = v_c + \frac{1}{C} \left[it - \int_0^t \phi(i_0, t, V) dt \right]. \quad (3)$$

Two times emerge from a consideration of this relation: first, i_t will equal i at a time τ , when the voltage of course will be V_c ; and second, i_t will be increasing so rapidly at a time θ , that beyond this even a very great increase of i_t will not imply a significant increase in the duration of the discharge which for practical purposes may be said to last a time θ .

The following properties of ΔV_c , τ , and θ can be inferred for the case of a constant C and increasing i . θ will be a maximum for small currents and will decrease as i increases. The ratio, however, of τ/θ will increase rapidly until τ approximates in value to θ . The actual effect on τ will be that it increases rapidly at first, attains a maximum, and thereafter varies as θ .

Furthermore, if i_t varies in the manner assumed here we can simplify equation (2) to read:

$$\Delta V_c = \frac{i\tau}{C}, \quad . \quad . \quad . \quad . \quad . \quad . \quad (4)$$

which would give values of τ which were relatively accurate though a little lower than the actual values. With $\Delta V_c \propto i\tau$, C constant, we may follow the variation of ΔV_c with i , and we find that ΔV_c should increase at first quickly and then slowly as in fig. 1, and that "overlapping" should reduce its value progressively as the initial current is greater. Actual values of τ are calculable since the values of ΔV_c , C , and i are known. To this end a thorough investigation was made of the variation of ΔV_c for small values of i , as it was here that the variation of τ should be most pronounced. A closer study of previous curves (fig. 1) showed that they gave the variation in that region quite well, so they were utilized in the calculations. The form of the ΔV_c curve for small currents together with a curve showing the variation of τ as calculated from such a curve is given in fig. 2.

As will be seen, the form of the curve was that expected from theory, but the actual values of τ were found to be much too large for a "lag" based solely on the known properties of the gas. Values of the order of 0.001-0.01 second were obtained quite frequently, whereas calculations based on the gas constants gave as a maximum value 10^{-4} sec., with values of the order of 10^{-6} sec. as more probable ones.

Short of other experiments confirming the time values and a slow "build-up" proof of a "corona" lag was lacking, though the forms of the curves obtained were in essential agreement with that hypothesis.

3. DURATION OF A CONDENSER DISCHARGE.

So far it had not been proved whether the lag was an inherent property of discharges or merely due to their succession in "flashing." By effecting slight changes in the measuring apparatus, it was found possible to measure the time of duration of a "single flash" and also to gain some insight into the variation of the voltage with time in such a discharge.

A well-insulated key was inserted in the circuit so that the condenser could be charged from the voltage supply to a known potential E and then applied to the tube, the voltmeter being placed directly across the tube with a high resistance (R) of many megohms preceding the divide valve.

In such a circuit, if during the flash the condenser voltage falls instantaneously to V_B , then, unless the initial reading of the voltmeter (V_0) is less than this, no charging-up should be observed. If it takes an appreciable time however, the voltmeter (capacity C) will be charged to an extent depending on the time required to reach the voltage (V_H) finally recorded. Long "lags" or the absence of a flash at all will permit complete mixing of the charges and, if the condenser capacity is large, V_H will approximate to E .

The time taken for the condenser to become discharged to a voltage V_H equals the time (t) for the voltmeter (C) to charge from V_0 to V_H , this being given by

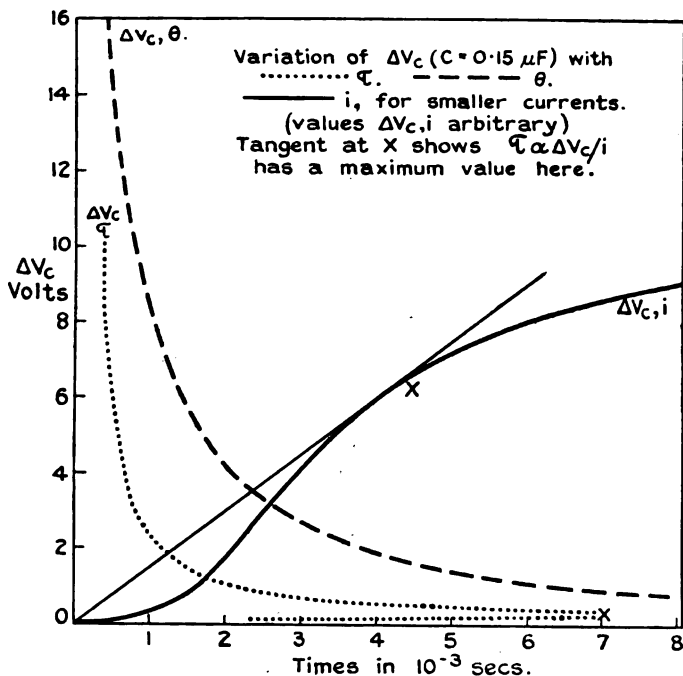
$$t = CR \log_e \left(\frac{E - V_0}{E - V_H} \right), \dots \dots \dots (5)$$

neglecting at this stage the correction for the valve, which in practice may well be done.

Without going into details, it may be said that the results were highly satisfactory. It was found that the time of

duration of the discharge was always appreciable, no instantaneous flashes being observed, and that, though the "lag" varied, it was in a systematic not random fashion. Observations supported the suggestion that the voltage fell at first very slowly and then very rapidly. The curve showing the variation of θ with $E=V_0$ for the same capacity as for τ is given in fig. 2, and it will be seen that despite the inevitable inaccuracies of the results the curves are essentially in agreement.

Fig. 2.



Furthermore, visual evidence of the operation of a factor influencing the "build-up" in the manner postulated was obtained several times when using one tube selected on account of the large "lags" it displayed, as often only a low current ("corona") discharge of appreciable duration occurred instead of the usual brief, intense flash. This was proved to be due to factors in the tube itself and unattributable to leakage or to bad contacts in the circuit. That the retardation could vary was in accordance with many previous observations.

The presence of an excess potential ΔV_c in the intermittent discharge in discharge-tubes could now with confidence be attributed to a "corona" lag of the form postulated.

4. VOLTAGE FLUCTUATIONS PRECEDING DISCHARGES.

These preceding results re-directed the attention of the writer to another, and not unfamiliar phenomenon, exhibited markedly by this tube, namely, that of showing voltage fluctuations, also indicating "corona" discharges, preliminary to "flashes" when "flashing" slowly, that is to say, with small currents.

The tube was examined in the dark, so that even faint discharges could be seen, though the fluctuations had first been observed in daylight; and when necessary the voltmeter was connected to the tube without the insertion of the diode so that the voltage variations could be followed, the microammeter being connected to read either the current through the tube or in the condenser lead.

The following results, taken with the capacity (C) constant, are typical of those obtained.

A discharge occurred as soon as v_c was reached, but even with very small currents this was fluctuating. The intensity of the discharge increased with i with corresponding increases in the voltage fluctuations and in the discharge-tube currents, and with i greater than $0.3 \mu\text{A}$. "flashing" occurred, each "flash" being preceded by a series of "corona" discharges, which, at first drawn-out and faint and merging into one another, became brief and intense with a definite dark "interval" as the "flash" drew near.

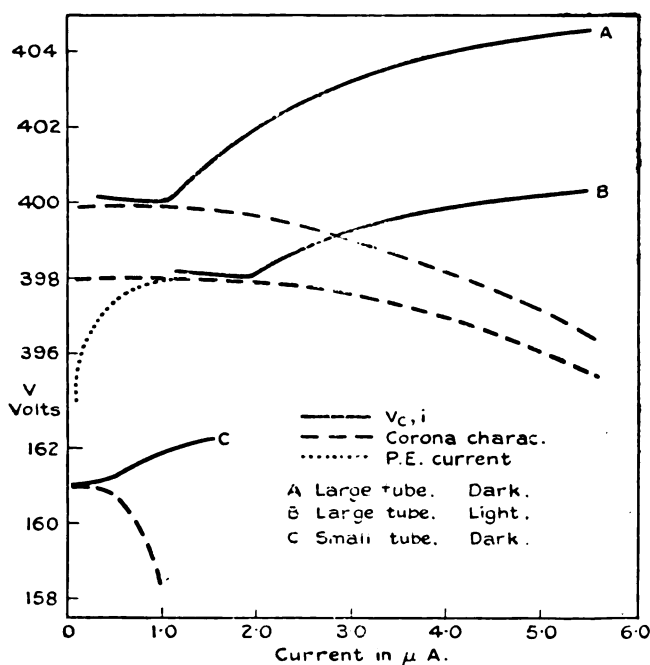
The frequency of these discharges depended on C or i , and the number was reduced as these were increased, so that at $i = 1.0 \mu\text{A}$ they ceased to be observed.

Fig. 3 (A and B) shows the V_c and "corona characteristic" curves in this case, but the slight increase of V_c at smaller currents is schematic, the observations not being very conclusive. "Corona" discharges were observed along the first part of the graph, the probability of a normal "flash" finally occurring increasing with C and i , until at the point where the corona and V_c graphs diverge normal "flashing" supervened, though the slow "build-up" doubtlessly still existed. Fig. 3 C gives the corresponding curves for a small tube distinguished for its small "lags," and it will be seen that their forms are precisely the same,

though the phenomena here were on a reduced scale, preliminary discharges being observed only for very small currents ($< 0.1 \mu\text{A.}$) and small capacities ($< 0.002 \mu\text{F.}$).

Considering what has already been said on the "corona characteristic," it will be seen to be readily conceivable that if the capacity is but small enough, or if the "build-up" is prolonged, the depreciation of the voltage of the condenser may be such that, before the current is very large, the v corresponding to the existing i in the tube is reached and the

Fig. 3.



discharge ceases. The shorter the initial (constant v) portion of the characteristic, the more rapidly v increases with i in the succeeding part, and the greater C or i , the less should be the chance of this occurring.

The observations are in agreement with these predictions.

Reference already has been made to variations in the "lag" with time, for "single flashes" the lag being possibly twice as great at one time as at another, a variation of the same order being produced by light; and further evidence

was obtained in this work, the number of "corona" discharges preliminary to a flash varying from time to time, though in a systematic not random fashion, generally being constant for several flashes in succession. For example, in one case, with $C=0.15\ \mu\text{F.}$ and $i=0.7\ \mu\text{A.}$, the number was ten (at intervals of two seconds) for five flashes, then two for six flashes, and then five for a further set.

In addition to changes with time or use, changes in the retarding agent by the preliminary discharges, perhaps manifested by accompanying changes in the "corona characteristic," must be postulated to account for all the phenomena associated with such discharges, though the precise significance of the results has not yet been definitely decided.

5. CONCLUSION.

Though scarcely falling within the scope of this present paper, reference may be made to the speculations made on the cause of the slow "build-up" and to the conclusions arrived at, though only the briefest outline is attempted and the considerations applied are frankly tentative.

Such an effect must be attributed to a mechanism which limits the rate of increase of the number of electrons at any time, either by resisting the passage of a current, or by reducing the rate of production of electrons in the discharge, the current in practice increasing at less than one-hundredth of the rate anticipated from theory.

Since for calculations of discharge durations, to give results in agreement with observations very improbable values would have to be assumed for the velocity of the ions or for their rate of diffusion, possible causes of the retardation were sought for in the electrodes.

For several reasons it was concluded that the cause could not lie in a permanent modification of the electrode surfaces, by the filling gas (or chance impurities) merely introducing a resistance into the circuit, the idea that thick surface films might be responsible being discredited at the same time.

The retardation could, however, be attributed to (probably temporary) modification of the cathode surface by the filling gas or to variable ("polarization") layers, whose screening action on all or part of the cathode with a consequent stoppage or selective effect on bombarding ions (or emitted electrons?) would explain the reduced emissivity.

There appears to be good support for this hypothesis in evidence from experiments on kindred problems, and

it is quite compatible with the additional phenomena included in this paper.

In conclusion the writer would like to record with gratitude his obligation to Professor Ornstein, whose generous support alone enabled this work to be carried out, to the members of his Staff, and to Dr. J. Taylor for his friendly assistance on all possible occasions.

20th January, 1927.

References.

1. Mauz and Seeliger, *Phys. Zeit.* xxvi. p. 47 (1925).
2. Taylor and Sayce, *Phil. Mag.* li. p. 918 (1925).
3. Penning, *Phys. Zeit.* xxvii. p. 187 (1926).
4. Taylor, *Phil. Mag.* iii. Suppl. p. 753 (1927).
5. Züber, *Ann. d. Phys.* lxxvi. p. 231 (1925).
6. Peek, 'Dielectric Phenomena' (1915). *Campbell, Phil. Mag.* xxxviii. p. 214 (1919).
7. Zeleny, *Phys. Rev.* xxiv. p. 255 (1924).
8. Clarkson, *Proc. Phys. Soc.* xxviii. p. 19 (1925).

XII. *The Atomic Structure of AuSn.* By G. D. PRESTON, B.A., and E. A. OWEN, M.A., D.Sc., *The National Physical Laboratory* *.

[Plate II.]

THIS paper gives the results obtained in an investigation of the structure of the compound AuSn and is a continuation of previous work carried out by the authors on intermetallic compounds †.

The material was examined in the first instance by the powder method and the results were confirmed by the rotating crystal method. The latter part of the paper deals with the Laue method, which yielded further information regarding the structure of the material.

(a) Results obtained by the Powder Method.

In Table I. are given the intensities and the values of $\sin \theta$ for the lines obtained by the powder method. The photographs were taken with a Müller camera, the radiation employed being that emitted by a tube ‡ furnished with a copper anticathode and operated at 8 m.a. and 30,000 volts.

* Communicated by the Authors.

† See *Phil. Mag.* ii. p. 1266 (1926).

‡ See *Journ. Sci. Instr.* iv. Pt. 1, p. 1 (1926).

TABLE I.

Intensity.	Sin θ .	Indices.	λ .	($c=1.275$). a .
7	0.2048	10 $\bar{1}$ 0	α	4.334 Å
18	0.2244	10 $\bar{1}$ 1	β	4.320
6	0.2490	10 $\bar{1}$ 1	α	4.309
14	0.3123	10 $\bar{1}$ 2	β	4.332
15	0.3226	11 $\bar{2}$ 0	β	4.305
1	0.3469	10 $\bar{1}$ 2	α	4.316
2	0.3570	11 $\bar{2}$ 0	α	4.305
22	0.4134	20 $\bar{2}$ 0	α	4.293
22	0.4363	20 $\bar{2}$ 1	α	4.296
22	0.4503	{ 11 $\bar{2}$ 2 20 $\bar{2}$ 2	{ α β	{ 4.338 4.306 }
22	0.4672	10 $\bar{1}$ 3	α	4.313
5	0.4978	20 $\bar{2}$ 2	α	4.310
16	0.5613	{ 21 $\bar{3}$ 1 0004	{ α α	{ 4.319 4.295 }
17	0.5992	{ 10 $\bar{1}$ 4 11 $\bar{2}$ 4	{ α β	{ 4.288 4.314 }
3	0.6150	{ 30 $\bar{3}$ 0 21 $\bar{3}$ 2	{ α α	{ 4.329 4.291 }
4	0.6643	11 $\bar{2}$ 4	α	4.305
18	0.7169	22 $\bar{4}$ 0	α	4.288
19	0.7556	{ 31 $\bar{4}$ 1 40 $\bar{4}$ 1	{ α β	{ 4.310 4.307 }
19	0.7820	21 $\bar{3}$ 4	α	4.304
9	0.7949	31 $\bar{4}$ 2	α	4.302
8	0.8354	40 $\bar{4}$ 1	α	4.311
10	0.8632	10 $\bar{1}$ 6	α	4.315
10	0.8705	40 $\bar{4}$ 2	α	4.307
10	0.9079	{ 32 $\bar{5}$ 1 22 $\bar{4}$ 4	{ α α	{ 4.313 4.303 }
22	0.9340	{ 31 $\bar{4}$ 4 20 $\bar{2}$ 6	{ α α	{ 4.290 4.315 }
10	0.9422	32 $\bar{5}$ 2	α	4.300

Mean $a=4.309 \pm 0.01$ Å.

The exposures occupied about three hours. The figures given in the Table are typical of those obtained on several films, a specimen of which is shown in Pl. II. fig. 1. In calculating the spacings, the values of K_α and K_β wavelengths have been taken as $\lambda_\alpha=1.537$ Å and $\lambda_\beta=1.389$ Å. It will be seen from the Table that the twenty-six observed

lines can all be accounted for by assuming the structure to be a hexagonal lattice of side $a=4.309 \pm 0.01 \text{ \AA}$ and axial ratio $c=1.275$.

The maximum error in the value of a calculated from the observed value of $\sin \theta$ is less than 0.25 per cent. The volume of the unit hexagonal prism is

$$V = \frac{\sqrt{3}}{2} a^2 c = 88.28 \text{ \AA}^3,$$

the observed density is $\rho=11.6$ grammes per c.c., and the molecular weight of AuSn is $M=315.9$ ($O=16$).

If n be the number of molecules associated with the unit cell, then

$$V = \frac{1.65 n M}{\rho},$$

whence we find $n=1.97$, so that within the limits of the error of observation there are two molecules of AuSn associated with the unit hexagonal prism.

The last line in the powder photograph corresponds to indices 3252, and within this region a simple hexagonal structure, the parameters of which are $a=4.309$ and $c=1.275$, should give 56 reflexions. The order in which they would occur is given in column I. of Table II. In column II. are the calculated values of

$$d = a / \sqrt{\frac{4}{3}(h^2 + hk + k^2) + \frac{l^2}{c^2}},$$

and in column III. the values of $d=\lambda/2 \sin \theta$ are given for comparison. Column IV. gives the observed values of the intensities of the lines arranged in descending order, 1 being the most intense and 22 the weakest line in the photograph.

In placing the atoms within the unit we are helped to some extent by consideration of space. The nearest distance between atoms in pure tin is 2.80 \AA , and in pure gold 2.88 \AA . If in the hexagonal prism an atom be placed at the point (000) and another at $(\frac{1}{3} \frac{2}{3} \frac{1}{2})$, the distance between them is

$$a \sqrt{\frac{1}{3} + \frac{c^2}{16}} = 2.842 \text{ \AA},$$

which is almost exactly the mean diameter of a gold and a tin atom.

TABLE II.

	I. Indices.	II. d Calcd.	III. d Obsd.	IV. I Obsd.	V.		VI.	
					I_1 Calcd.	Δ_1	I_2 Calcd.	Δ_2
1	0001	5.49	—	—	0	—	0	—
2	1010	3.73	3.75	7	—	18	4	3
3	1011	3.09	3.09	6	1	5	6	—
4	0002	2.74	—	—	—	—	—	—
5	1012	2.21	2.22	1	2	1	1	—
6	1120	2.15	2.15	2	3	1	2	—
7	1121	2.00	—	—	0	—	0	—
8	2020	1.87	1.86	22	—	3	19	3
9	0003	1.83	—	—	0	—	0	—
10	2021	1.77	1.76	22	8	14	17	5
11	1122	1.70	1.71	22	—	—	—	? β_{2022}
12	1013	1.64	1.64	22	9	13	21	1
13	2022	1.54	1.54	5	6	1	5	—
14	2130	1.41	—	—	—	—	19	6
15	1123	1.39	—	—	0	—	0	—
16	0004	1.37	1.37	16	7	9	16	—
17	2131	1.37						
18	2023	1.31	—	—	18	7	—	—
19	1014	1.29	1.28	17	—	—	23	? β_{1124}
20	2132	1.26	1.25	3	4	1	3	—
21	3030	1.24						
22	3031	1.21	—	—	11	—	9	—
23	1124	1.16	1.16	4	5	1	7	3
24	3032	1.13	—	—	—	—	—	—
25	2133	1.12	—	—	14	11	24	1
26	2024	1.10	—	—	—	—	—	—
27	0005	1.10	—	—	0	—	0	—
28	2240	1.08	1.07	18	16	2	13	5
29	2241	1.06	—	—	0	—	0	—
30	1015	1.05	—	—	24	1	—	—
31	3140	1.04	—	—	—	—	—	—
32	3033	1.03	—	—	0	—	0	—
33	3141	1.02	1.02	19	17	2	25	6 ? β_{4041}
34	2243	1.00	—	—	—	—	—	—
35	2134	.984	.983	19	—	6	22	3
36	1125	.978	—	—	0	—	0	—
37	3142	.969	.967	9	10	1	8	1
38	2025	.947	—	—	—	—	—	—
39	4040	.934	—	—	—	—	—	—
40	2243	.928	—	—	0	—	0	—
41	3034	.922	.920	8	12	4	10	2
42	4041	.920						
43	0006	.916	—	—	—	—	—	—

TABLE II. (continued).

	I. Indices.	II.	III.	IV.	V.		VI.	
		d Calcd.	d Obsd.	I Obsd.	I_1 Calcd.	Δ_1	I_2 Calcd.	Δ_2
44	3143	·901		—	19	6	—	
45	1016	·889	·891	10	22	12	14	4
46	4042	·883	·883	10	22	12	14	4
47	2135	·867		—	21	4	—	
48	3250	·853		—	—	—	—	
49	2244	·847	·847	10	15	5	11	1
50	3251	·846			20	5	—	
51	1126	·843		—	—	—	—	
52	4043	·831		—	—	—	—	
53	3144	827		—	—	—	—	
54	3035	·824		—	0		0	
55	2026	·822	·823	22	25	3	18	4
56	3252	·817	·816	10	13	3	12	2
					151		54	

In calculating the intensities to be expected, atoms of atomic number N_1 have been placed at (000) and $(00\frac{1}{2})$, and atoms N_2 at $(\frac{1}{3}\frac{2}{3}\frac{1}{2})$ and $(\frac{2}{3}\frac{1}{3}\frac{1}{2})$.

The intensity I is given by

$$I \propto d_{hkl}^{2\cdot35} J \cdot (A^2 + B^2),$$

where J is the number of co-operating planes, d_{hkl} is the spacing, and

$$A = \sum N_s \cos 2\pi(hx_s + ky_s + lz_s),$$

$$B = \sum N_s \sin 2\pi(hx_s + ky_s + lz_s).$$

In the present case, substituting the values of (x_s, y_s, z_s) given above, the factor B vanishes and we are left with

$$I \propto d_{hkl}^{2\cdot35} \cdot J \left\{ N_1(1 + \cos \pi l) + 2N_2 \cos \pi(h+k) \cos \pi\left(\frac{h-k}{3} - \frac{l}{2}\right) \right\}^2.$$

The quantity within the brackets vanishes if l is odd and $(h-k)$ is a multiple of 3. The lines 000 l , 112 l , 303 l , and 224 l , should not appear when l is odd. This is confirmed by experiment, none of these lines being observed in the photographs. In columns V. and VI. (Table II.), in which are entered the calculated intensities, these lines are indicated by a 0.

If l is odd and $(h-k)$ is not a multiple of 3, the factor within the brackets becomes $\sqrt{3} N_2$. When l is even, it has one of the following values :

$$2N_1 + 2N_2, \text{ when } (h-k) = 3p, l = 4q;$$

$$2N_1 - 2N_2, \text{ when } (h-k) = 3p, l = 2q \text{ (} q \text{ odd) ;}$$

$$2N_1 + N_2;$$

$$\text{or } 2N_1 - N_2.$$

For tin, $N=50$ and for gold, $N=79$, so the values of I have been computed for the two cases :

$$(1) N_1 = 50, N_2 = 79,$$

$$\text{and } (2) N_1 = 79, N_2 = 50.$$

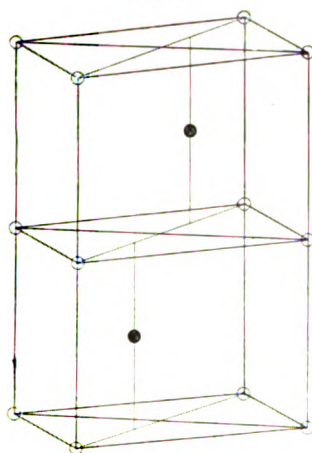
Numbers ranging from 1 to 25 have been assigned in order to the twenty-five most intense lines in each case. The resulting figures appear in columns V. and VI. of Table II. It will be seen that the figures in column V. under I_1 are not so near the observed values as those in column VI. under I_2 . For instance, there is a marked discrepancy in the first two observed lines $10\bar{1}0$, and $10\bar{1}1$. In order to compare the observed and calculated intensities the figures for I_1 and I_2 have been subtracted from those for I giving Δ_1 and Δ_2 . The spaces occupied by a dash have for this purpose been considered to contain the number 25. The sum of the resulting differences is 151 units in the first case when $N_1=50$, whereas in the second case when $N_1=79$ it is only 54 units, which leaves little doubt but that the gold atoms are at the points (000) and $(00\frac{1}{2})$ while the tin atoms are at $(\frac{1}{2}\frac{2}{3}\frac{1}{4})$ and $(\frac{2}{3}\frac{1}{3}\frac{3}{4})$. The errors hardly exceed the accuracy with which the lines in the photograph can be placed in order of intensity. A unit cell of the lattice is shown in fig. 2.

(b) *Results obtained by the Rotating Crystal method.*

The specimen used to obtain the photograph shown in fig. 3 (Pl. II.), was a small chip of material about 1 mm. in cross-section, and 3 mm. long. It was mounted on a spindle situated at the centre of a cylindrical film-holder of radius 3.19 cm., and was rotated during an exposure of two hours in a fine pencil of radiation from a copper anticathode. The photograph thus obtained should be symmetrical about a vertical and a horizontal line drawn through the image of the undeflected spot. Owing, however, to the great opacity

of the material to the soft copper radiation and to the irregular nature of the surfaces of the specimen, some planes are in positions which favour reflexion and others are not, with the result that the symmetry of the photograph is spoiled. For the same reason the relative intensities of the spots are liable to be misleading. The information which can be obtained from the photograph is (1) the value of the glancing angle θ for each spot, and (2) the value of the angle ψ between the axis of rotation and the normal to the reflecting plane.

Fig. 2.



○ Gold

● Tin

If x and y are the co-ordinates of a spot on the photograph referred to rectangular axes OX, OY drawn through the central spot and with OY parallel to the axis of rotation, then θ and ψ are given by the following relations where r is the radius of the camera—

$$\cos 2\theta = \frac{r \cos x/r}{\sqrt{y^2 + r^2}}, \quad \dots \dots \dots (1)$$

$$\sin \theta \cdot \cos \psi = \frac{y}{2 \sqrt{y^2 + r^2}} \cdot \dots \dots \dots (2)$$

TABLE III.

$\sin \theta$.	$\sin \theta \cdot \cos \psi$.	$hki\bar{l}$.	$0\cdot1964\ h$ $+0\cdot1464\ k$ $+0\cdot024\ l$
$\cdot8701$	$\cdot2004$	$4\bar{4}02$	$\cdot2048$
$\cdot8704$	$-\cdot2030$	$\bar{4}40\bar{2}$	$-\cdot2048$
$\cdot8638$	$\cdot2100$	$10\bar{1}6$	$\cdot2108$
$\cdot8652$	$\cdot1825$	$1\bar{0}\bar{1}6$	$\cdot1820$
$\cdot8633$	$\cdot1613$	$01\bar{1}6$	$\cdot1608$
$\cdot8646$	$\cdot1315$	$01\bar{1}\bar{6}$	$\cdot1320$
$\cdot8626$	$\cdot0622$	$1\bar{1}06$	$\cdot0644$
$\cdot8646$	$\cdot0330$	$1\bar{1}0\bar{6}$	$\cdot0366$
$\cdot8626$	$-\cdot0355$	$\bar{1}106$	$-\cdot0356$
$\cdot8640$	$-\cdot0657$	$\bar{1}10\bar{6}$	$-\cdot0644$
$\cdot8620$	$-\cdot1327$	$0\bar{1}16$	$-\cdot1320$
$\cdot8631$	$-\cdot1620$	$0\bar{1}\bar{1}6$	$-\cdot1608$
$\cdot8620$	$-\cdot1835$	$\bar{1}016$	$-\cdot1835$
$\cdot8629$	$-\cdot2108$	$\bar{1}01\bar{6}$	$-\cdot2108$
$\cdot8322$	$\cdot1455$	$3\bar{3}0\bar{4}$	$-\cdot1404$
$\cdot8331$	$-\cdot1569$	$\bar{3}30\bar{4}$	$-\cdot1596$
$\cdot7955$	$\cdot3972$	$\bar{1}432$	$\cdot3940$
$\cdot7941$	$\cdot0008$	$\bar{3}412$	$\cdot0012$
$\cdot7938$	$-\cdot3452$	$\bar{4}312$	$-\cdot3412$
$\cdot7578$	$\cdot0008$	$3\bar{4}1\bar{1}$	$\cdot0012$
$\cdot7447$	$\cdot0008$	$3\bar{4}10$	$\cdot0036$
$\cdot7060$	$\cdot1941$	$\bar{2}4\bar{2}0$	$\cdot1928$
$\cdot7124$	$-\cdot1976$	$24\bar{2}0$	$-\cdot1928$
$\cdot6654$	$\cdot3360$	$11\bar{2}4$	$\cdot3332$
$\cdot6624$	$\cdot2566$	$2\bar{1}\bar{1}4$	$\cdot2560$
$\cdot6659$	$\cdot2380$	$\bar{2}\bar{1}\bar{1}4$	$\cdot2368$
$\cdot6652$	$\cdot0848$	$\bar{1}2\bar{1}4$	$\cdot0868$
$\cdot6617$	$-\cdot0927$	$1\bar{2}14$	$-\cdot0868$
$\cdot6646$	$-\cdot1092$	$1\bar{2}\bar{1}4$	$-\cdot1060$
$\cdot6637$	$-\cdot2590$	$\bar{2}1\bar{1}4$	$-\cdot2560$
$\cdot6617$	$-\cdot3360$	$\bar{1}\bar{1}24$	$-\cdot3332$
$\cdot6633$	$-\cdot3560$	$\bar{1}\bar{1}2\bar{4}$	$-\cdot3524$
$\cdot6170$	$\cdot1515$	$3\bar{3}00$	$\cdot1500$
$\cdot6192$	$-\cdot1535$	$\bar{3}300$	$-\cdot1500$

TABLE III. (continued).

$\sin \theta$.	$\sin \theta \cdot \cos \psi$.	hkl .	$0.1964 h$ $+0.1464 k$ $+0.0024 l$
·6120	·3030	$3\bar{2}12$	·3012
·6134	·2474	$\bar{1}322$	·2476
·6129	·0479	$\bar{2}312$	·0512
·6115	—·0452	$2\bar{3}12$	—·0416
·6106	—·2444	$1\bar{3}2\bar{2}$	—·2476
·6122	—·2970	$321\bar{2}$	—·3012
·5595	·0084	0004	·0096
·5595	—0113	000 $\bar{4}$	—·0096
·3540	·2450	$2\bar{1}\bar{1}0$	·2464
·3587	·0976	$\bar{1}2\bar{1}0$	·0964
·3592	—·1071	$1\bar{2}10$	—·0964
·3464	·2032	1012	·2012
·3472	—·2033	101 $\bar{2}$	—·2012

The measurement of the positions of all the points on the photograph would be an exceedingly laborious work and would not be justified on account of the imperfection of the photograph referred to above. We have accordingly made measurements of fifty spots and propose to show that they are situated on the photograph in the places to be expected from the structure deduced from the powder photograph.

In Table III. columns 1 and 2 are set down the values of $\sin \theta$ and $\sin \theta \cdot \cos \psi$ computed from the measurements of fifty of the most intense spots. The values of $\sin \theta$ have been put down for comparison with the results obtained by the powder method given in Table I.

Let us suppose that the information derived from the powder photograph is correct, and that the structure is hexagonal of side a and axial ratio c .

Then

$$\sin \theta_{hkl} = \frac{\lambda}{2a} \sqrt{\frac{4}{3}(h^2 + hk + k^2) + \frac{l^2}{c^2}},$$

and ψ the angle between the normals to the planes (hkl) and $(h_1k_1l_1)$ is given by :

$$\cos \psi_{hkl} = \frac{\frac{4}{3}[hh_1 + kk_1 + \frac{1}{2}(hk_1 + h_1k)] + \frac{ll_1}{c^2}}{\left[\frac{4}{3}(h^2 + hk + k^2) + \frac{l^2}{c^2}\right]^{1/2} \left[\frac{4}{3}(h_1^2 + h_1k_1 + k_1^2) + \frac{l_1^2}{c^2}\right]^{1/2}}.$$

So, if $(h_1 k_1 l_1)$ is the line in the crystal about which rotation takes place, then

$$\sin \theta \cdot \cos \psi = \frac{\lambda \left[\frac{4}{3} \{ h h_1 + k k_1 + \frac{1}{2} (h k_1 + h_1 k) \} + \frac{l l_1}{c^2} \right]}{2a \left\{ \frac{4}{3} (h_1^2 + h_1 k_1 + k_1^2) + \frac{l_1^2}{c^2} \right\}^{1/2}}$$

$$\equiv Ah + Bk + Cl, \quad (3)$$

where

$$A = \frac{4}{3} \left(h_1 + \frac{k_1}{2} \right) \cdot \frac{\lambda}{2a \sqrt{\frac{4}{3} (h_1^2 + h_1 k_1 + k_1^2) + \frac{l_1^2}{c^2}}},$$

$$B = \frac{4}{3} \left(k_1 + \frac{h_1}{2} \right) \cdot \frac{\lambda}{2a \sqrt{\frac{4}{3} (h_1^2 + h_1 k_1 + k_1^2) + \frac{l_1^2}{c^2}}},$$

$$C = \frac{l_1}{c^2} \cdot \frac{\lambda}{2a \sqrt{\frac{4}{3} (h_1^2 + h_1 k_1 + k_1^2) + \frac{l_1^2}{c^2}}},$$

and

$$A^2 - AB + B^2 + c^2 C^2 \equiv \lambda^2 / 4a^2. \quad . . . (4)$$

In the present case the values of $\sin \theta \cos \psi$ can all be accounted for by putting

$$\sin \theta \cos \psi = 0.1964 h + 0.1464 k + 0.0024 l, \quad . (5)$$

as is shown by the last column of Table III., the appropriate values of hkl being given in column 3.

In Table IV. the mean values of $\sin \theta$ for the 13 different sets of planes to which indices have been assigned in Table III. are collected. The value of c is calculated from the values of $\sin \theta$ for (0004) and (1120) and the values of " a " are then computed for each plane. The resulting mean $4.305 \pm 0.007 \text{ \AA}$ is in good agreement with figure $4.309 \pm 0.01 \text{ \AA}$ obtained from the powder photograph. The values of c are 1.278 and 1.275 respectively. The expression (4) above gives $a = 4.35 \text{ \AA}$, showing that the assumed values of A, B , and C in expression (5) are consistent with a hexagonal structure.

The results obtained by the measurement of the rotating crystal photograph are thus in agreement with those obtained from the powder photograph. This brief analysis of part of the rotating crystal photograph cannot determine the unit of the structure, but it does afford very substantial confirmation of the results arrived at by the powder method.

TABLE IV.

Mean from Table III.	hkl .	($c=1.278$) a
Sin θ .		
·8702	40 $\bar{4}$ 2	4·307 Å°
·8634	10 $\bar{1}$ 6	4·303
·8327	30 $\bar{3}$ 4	4·308
·7945	31 $\bar{4}$ 2	4·302
·7587	31 $\bar{4}$ 1	4·291
·7447	31 $\bar{4}$ 0	4·296
·7092	22 $\bar{4}$ 0	4·335
·6638	11 $\bar{2}$ 4	4·300
·6181	30 $\bar{3}$ 0	4·307
·6121	21 $\bar{3}$ 2	4·309
·5595	0004	4·299
·3573	11 $\bar{2}$ 0	4·301
·3468	10 $\bar{1}$ 2	4·309
Mean	$a = 4.305 \pm 0.007 \text{ Å.}$	

(c) *Results obtained by the Laue Method.*

A small chip of the material was chosen and mounted on the crystal holder of the Müller spectrograph. After a preliminary exposure the necessary adjustment to the crystal was made and the photograph shown in fig. 4 (Pl. II.) was obtained—the incident beam being nearly parallel to the hexagonal axis. An exposure of four hours at 3 to 4 m.a. and 60,000 volts was required to obtain the picture. The symmetry of the arrangement of diffraction spots is more clearly seen in the stereographic projection, fig. 5, and is that of point group D_{6h} . This corresponds to a crystal having the symmetry of groups D_{3h} , C_{6v} , D_6 , or D_{6h}^* . The indices of the spots are most easily determined from the gnomonic projection (fig. 6) from which they can be read off at once. The result is analysed in fig. 7†, where the ordinates are $y = h^2 + hk + k^2$ and the abscissæ $x = l$. For a hexagonal structure with the incident beam parallel to [0001]

$$\lambda = \frac{2lac}{\frac{2}{3}(h^2 + hk + k^2)c^2 + l^2} = \frac{x}{\frac{2}{3}c^2y + x^2} \cdot 2ac,$$

or substituting the values of a and c found from the powder method,

$$\lambda = \frac{10.99x}{2.171y + x^2}.$$

* Wyckoff, 'The Structure of Crystals,' p. 118.

† Bragg, 'X-Rays and Crystal Structure,' p. 284.

Fig. 5.

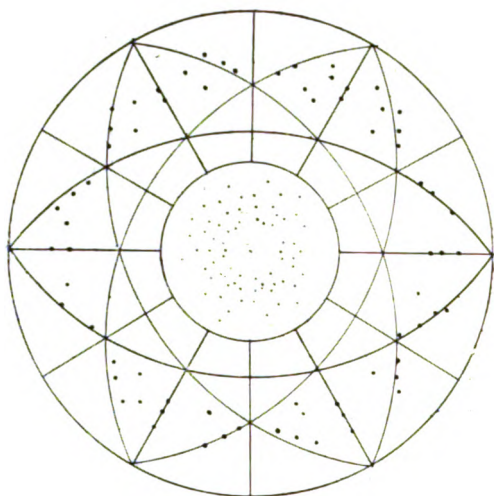
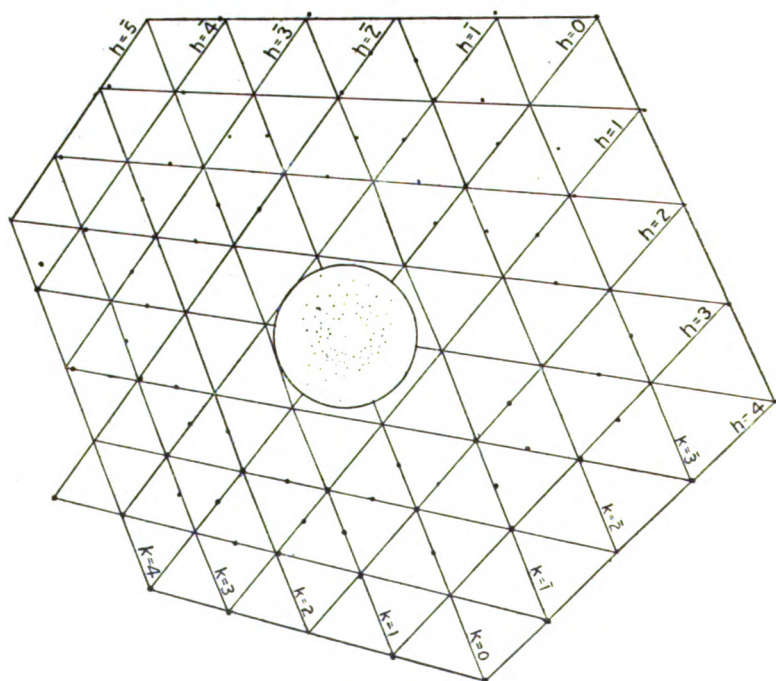


Fig. 6.



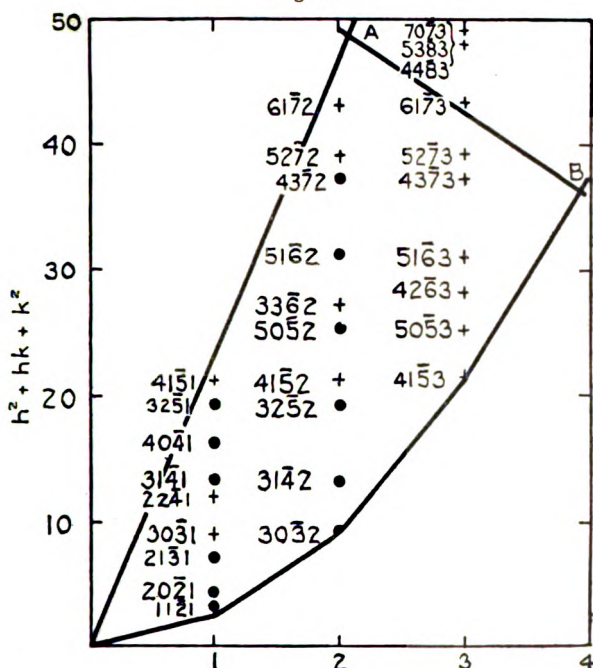
The limiting value of λ for a peak voltage of 60,000 volts is 0.206 Å. This line is shown in fig. 7 and all the observed spots should fall to the right of it. The other limit is set by the size of the photographic plate and is given by

$$\sin \theta = \frac{x/c}{\sqrt{\frac{1}{3}y + x^2/c^2}}.$$

In the case under consideration $\theta_{\max.} = 24^\circ$.

The spots which appear on the photograph are shown by a

Fig. 7.



circle on the diagram, those which are absent by a cross. It has been pointed out above in connexion with the intensities of the reflexions from the powdered material, that when l is odd and $(h-k)=3p$ the intensity factor vanishes if the atoms are in the positions assumed. The first order reflexions from 1121, 3031, 2241, and 4151 should therefore be absent. Of these planes only the first is observed in the Laue photograph, and in this case its presence may be accounted for by 2nd and 4th order reflexions since the indices are small. Further, considering the case when $l=2$, the intensity factor (see above) is small when $(h-k)=3p$ and the planes 3032.

4152, 3352, and 5272 might not appear on the Laue photograph. Of these 3032 only is observed, and its second order reflexion ($l=4$) will be very intense. The plane 6172 falls near the wave-length limit and is not observed for that reason. When $l=3$ the intensity factor again vanishes if $(h-k)=3p$, and is small when $(h-k)$ has other values. No spots for which $l=3$ are observed. If we assume that the intensity of points lying beyond the line AB in fig. 7 is too small to be observed, the points on the photograph are satisfactorily accounted for when the atoms are situated in the positions given above. The mean length of the side of the hexagonal net in fig. 6 gives an axial ratio of 1.30 approximately, which is in agreement with the results obtained by the other methods.

As stated above, the space group is fixed by the symmetry of the Laue photograph to be either D_{3h} , C_{6v} , D_6 , or D_{6h} . Referring to the tables of Astbury and Yardley*, some of these groups may be eliminated. For instance, the presence of the first order reflexions from the planes 1011, 2021, and 4041 † eliminates D_{3h}^2 , C_{6v}^2 , C_{6v}^3 , D_{6v}^2 , and D_{6h}^3 ; the presence of 0004 eliminates D_6^2 , D_6^3 , D_6^4 , and D_6^5 . If we may assume that the X-ray spectra of this material are characterized by the absence when l is odd of first order reflexions from planes ($hh\ 2hl$) none of which have been observed, then the space group must be D_{3h}^4 , C_{6v}^4 , or D_{6h}^4 . The possible positions of atoms within the unit in these groups are ‡:—

$$\begin{array}{l} D_{3h}^4 \} \left\{ \begin{array}{ll} (a) \ 000, \ 00\frac{1}{2}. & (c) \ \frac{1}{3}\ \frac{2}{3}\ \frac{1}{3}, \ \frac{2}{3}\ \frac{1}{3}\ \frac{2}{3}. \\ D_{6h}^4 \} \left\{ \begin{array}{ll} (b) \ 00\frac{1}{4}, \ 00\frac{3}{4}. & (d) \ \frac{1}{3}\ \frac{2}{3}\ \frac{2}{3}, \ \frac{2}{3}\ \frac{1}{3}\ \frac{1}{3}. \\ C_{6v}^4 \quad (a) \ 00u, \ 00u + \frac{1}{2}. & (b) \ \frac{1}{3}\ \frac{2}{3}\ u, \ \frac{2}{3}\ \frac{1}{3}\ u + \frac{1}{2}. \end{array} \right. \end{array}$$

It has been shown above that the intensities of the powder photograph are in good agreement with theory if gold atoms are placed at the points (000) and $(00\frac{1}{2})$ and tin atoms at $(\frac{1}{3}\ \frac{2}{3}\ \frac{1}{3})$ and $(\frac{2}{3}\ \frac{1}{3}\ \frac{2}{3})$, a result in agreement with the possible positions found from symmetry considerations, and the assumption that the planes ($hh\ 2hl$) are absent if l is odd.

Summary.

The atomic structure of the intermetallic compound AuSn has been examined by the powder and the Laue methods, the result of the powder method being confirmed by the rotating crystal method. The analysis shows that AuSn crystallizes

* Phil. Trans. Roy. Soc. A, vol. ccxxiv. pp. 250-252.

† In another film, 1013, 1015 were also observed.

‡ Wyckoff, 'The Analytical Expression of the Results of the Theory of Space Groups,' pp. 159-169.

on a hexagonal lattice of side 4.307 \AA and axial ratio 1.276, the density requiring two molecules of AuSn to be associated with this unit. The space group is found to be D_{3d}^4 , C_{6v}^4 , or D_{6h}^4 , and the intensities of the reflexions agree with a structure in which gold atoms are situated at the points (000) and $(00\frac{1}{2})$ and tin atoms at the points $(\frac{1}{3} \frac{2}{3} \frac{1}{2})$ and $(\frac{2}{3} \frac{1}{3} \frac{1}{2})$.

March 1927.

XIII. *Transmission of Electric Waves through the Ionized Medium.* By T. L. ECKERSLEY, M.A.*

IN a recent paper in the Phil. Mag. the writer showed that the state of ionization had a profound influence on the spreading-out of the electromagnetic waves originating in a localized pulse. The loading of the æther with free ions gives it a dispersive character, with the result that the various frequency components of the pulse are all separated out after a sufficient time; the higher frequencies arrive at any distant point first, the lower frequencies following at progressively later times, giving a disturbance of constantly lowering pitch. A casual examination of the problem might lead one to expect a gradual lowering of the frequency, going on continuously to zero frequency, since all frequencies are represented in the pulse; but contrary to this expectation, it was found that a certain limiting frequency n_0 was reached, this depending on the state of the medium, the value of n_0 being given by the relation:

$$n_0^2 = \frac{Ne^2}{\pi m} \dots \dots \dots (1, 1)$$

It is with the object of inquiring more closely into this characteristic frequency of the medium that the following investigation was undertaken.

At the outset it is better to limit to the consideration of one frequency n say, and to follow the method due to Sommerfeld. We are concerned at the moment with the transmission of waves in the medium, and not with the manner in which the waves get into it, so that we can leave the problems of the reflexion at the surface till a later stage and consider the subsequent history in space and time of a periodic disturbance, just within the boundary of the medium lasting from $t=0$ to $t=\infty$.

The disturbance spreads out into the body of the medium; and it is shown that this disturbance consists of two parts, which may be calculated from certain contour integrals.

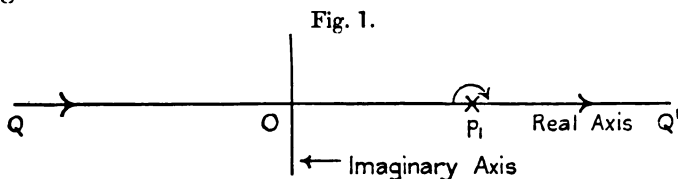
* Communicated by the Author.

In the first place consider :

$$\frac{R}{2\pi} \int_{-\infty}^{+\infty} \frac{e^{-ip_1 t} dp}{p - p_1}, \quad \dots \dots \dots (2, 1)$$

where $p_1 = 2\pi n_1$, n_1 being the frequency of the disturbance, and where the letter R indicates that the real part is to be taken.

The contour is one which passes from $-\infty$ to $+\infty$ along the real axis except at the point p_1 , which is encircled by an infinitesimal semicircle lying in the first quadrant, as in fig. 1.



If t is negative and the imaginary p tends to ∞ , i. e. p tends to $+i\infty$ above the line QQ' , then

$$e^{-ip_1 t} = e^{-i(iR)(-t)} = e^{-Rt}, \quad \dots \dots \dots (3, 1)$$

and the integrand tends to zero exponentially. Now the contour can be transferred to a line parallel to QQ' at $i\infty$ without crossing over any pole of the integrand, and $f(t)$ is therefore zero if $t < 0$; on the other hand, if $t > 0$ the integrand only vanishes when $p = a - i\infty$, the contour cannot be transformed without passing over p_1 and leaving a circle enclosing it. The integral in this case is equal to

$$\frac{R}{2\pi} \int_0^{\infty} \frac{e^{-ip_1 t} dp}{p - p_1} = R e^{ip_1 t}. \quad \dots \dots \dots (4, 1)$$

This integral therefore represents the initial disturbance at $x=0$ say, which is zero for all negative values of t , and equal to $R e^{-ip_1 t}$ for all positive values of t .

Each frequency component of which this integral is composed will travel in the medium with its appropriate phase velocity v_p say, so that at a distance x the integral

$$R \frac{1}{2\pi} \int_{-\infty}^{+\infty} \frac{e^{-ip \left(t - \frac{x}{v_p} \right)} dp}{p - p_1} \quad \dots \dots \dots (5, 1)$$

will represent the complete disturbance due to a given infinite train of waves.

The value of v_p can be determined from the differential equation of transmission.

Thus, if there are N ions per c.c. of charge e and mass m ,

and if f is a frictional force per unit velocity, so that under a steady force the ions move with a mean velocity $\frac{eX}{f}$, then the differential equation for the medium is

$$\frac{\partial^2 z}{\partial x^2} = - \left\{ \frac{p^2}{c^2} \left(1 - \frac{p_0^2}{p^2} \frac{1}{1 + \frac{f^2}{m^2 p^2}} \right) + i 4\pi \frac{p f N e^2}{m^2 p^2 + f^2} \right\} z, \quad (6, 1)$$

if n' is the mean frequency of the collisions,

$$\frac{f}{m p} = \frac{n'}{\pi n_1}, \quad \dots \quad (7, 1)$$

$$p_0^2 = \frac{4\pi N e^2 c^2}{m}, \text{ and is } (2\pi n_0)^2 \quad \dots \quad (8, 1)$$

where n_0 is the critical frequency already described ;

$$\frac{\partial^2 z}{\partial x^2} = - \left\{ \frac{p^2}{c^2} \left(1 - \frac{p_0'^2}{p^2} \right) + \frac{i \sigma_0 p 4\pi}{c \left(1 + \left(\frac{\pi n_1}{n'} \right)^2 \right)} \right\} z, \quad (9, 1)$$

so that

$$\left(\frac{c}{v_p} \right)^2 = (p^2 - p_0'^2) + \frac{i \sigma_0 p 4\pi c}{1 + \left(\frac{\pi n_1}{n'} \right)^2},$$

$$\frac{c}{v_p} = \{ (p^2 - p_0'^2) + i \sigma_1 p \}^{1/2}, \quad \dots \quad (10, 1)$$

where σ_0 is the conductivity, i.e., $\frac{N e^2}{f}$,

where

$$p_0' = \frac{p_0}{1 + \left(\frac{n'}{\pi n_1} \right)^2} \quad \text{and} \quad \sigma_1 = \frac{4\pi c \sigma_0}{1 + \left(\frac{\pi n_1}{n'} \right)^2}, \quad (11, 1)$$

so that the integral representing the disturbance is

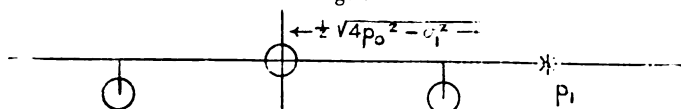
$$\frac{R}{2\pi} \int_{-\infty}^{+\infty} e^{-i p t + \frac{i}{c} \{ (p^2 - p_0'^2) + i \sigma_1 p \}^{1/2} x} \frac{dp}{p - p_1}.$$

The integrand has branch points at the roots of

$$p^2 - p_0'^2 + i \sigma_1 p = 0,$$

$$\text{i. e.} \quad p_{\pm} = \frac{i \sigma_1}{2} \pm \sqrt{\frac{4 p_0'^2 - \sigma_1^2}{4}}. \quad \dots \quad (12, 1)$$

Fig. 2.



These are shown in fig. 2 ; the roots lie symmetrically in the 3rd and 4th quadrants.

Let us suppose that σ_1 is vanishingly small; then two cases arise according as p_1 is less than or greater than p_0 , *i. e.* according as the frequency of the impressed wave is greater or less than the critical frequency.

In either case the integral is zero if $x > ct$, for, as before, we can transform the contour in this case to the locus

$$p = y + iR,$$

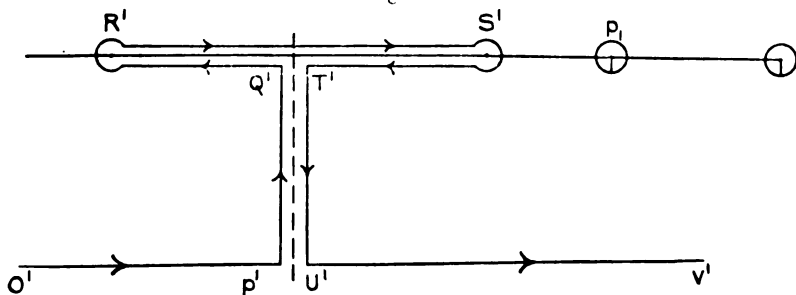
where R is a very large quantity, since all the singularities are in the lower half of the plane, in which case the exponential in the integral tends to $e^{+(R+iy)(t-x/c)}$, which when $x > ct$ can be made as small as we please by increasing R . It therefore follows that c is the limiting velocity of the disturbances, *i. e.* nothing is received at a distant point x

until after a time $t = \frac{x}{c}$.

If, however, $x < ct$, we must transform the contour to one at $-i\infty$.

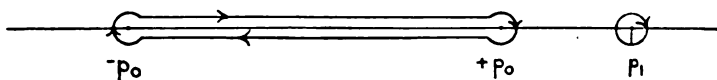
If $p_1 > p_0$, let us join $\pm p_0$ with a cut; then the integrand is regular in the whole plane, and we may transform the contour from

Fig. 3.



together with the circle round p_1 , *i. e.* the original integral is equal to the integral round p_1 and that round the cut joining $\pm p_0$.

Fig. 4.



The former is the residue at p_1 , *i. e.*

$$R e^{-i p_1 t + \frac{i}{c} \left\{ (p_1^2 - p_0^2) + i \right\}^{1/2} x} ; \dots (13, 1)$$

so that

$$\begin{aligned}
 Y &= R e^{-ip_1 t + \frac{i}{c} \{ (p_1^2 - p_0^2) + i \}^{1/2} x} \\
 &+ 2R \int_{-p_0}^{+p_0} e^{-ipt - \frac{i}{c} \{ p^2 - p_0^2 + i \}^{1/2} x} \frac{dp}{p - p_1} \\
 &= 2R \int_{-p_0}^{+p_0} \frac{e^{ipt} \sinh(p_0^2 - p^2)^{1/2} x/c}{p - p_1} dp \\
 &+ R e^{-ip_1 t + i(p_1^2 - p_0^2)^{1/2} x/c}, \dots \dots (14, 1)
 \end{aligned}$$

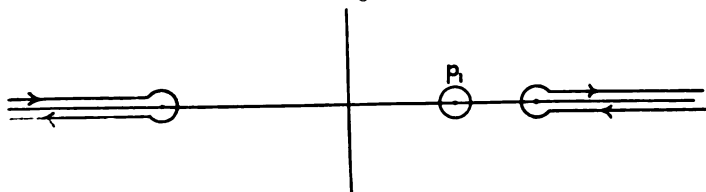
where σ_1 is sufficiently small.

The integrated part consists of a wave of phase-velocity

$$\frac{c}{\left(1 - \left(\frac{p_0}{p_1}\right)^2\right)^{1/2}} \dots \dots (15, 1)$$

Similarly, if $p_0 > p_1$, we can join p_0 with $+\infty$ and $-p_0$ with $-\infty$ and obtain the contour in fig. 5.

Fig. 5.



The integral round p_1 gives rise, as before, to the expression

$$R e^{-ip_1 t - x/c \sqrt{p_0^2 - p_1^2}}; \dots \dots (16, 1)$$

but in this case the phase-velocity is imaginary and gives rise to a large damping coefficient, i. e. $e^{-x/c (p_0^2 - p^2)^{1/2}}$, so that at large distances from the surface of the medium the disturbance has died right out.

The other part of the integral is

$$\frac{R}{2\pi} \int_{-\infty}^{p_0} \frac{e^{-ipt + i \sqrt{p^2 - p_0^2} x/c}}{p - p_1} dp + \frac{R}{2\pi} \int_{p_0}^{\infty} \frac{e^{-ipt - i \sqrt{p^2 - p_0^2} x/c}}{p - p_1} dp \quad (17, 1)$$

$$\begin{aligned}
 &+ \frac{R}{2\pi} \int_{-p_0}^{-\infty} \frac{e^{-ipt - i \sqrt{p^2 - p_0^2} x/c}}{p - p_1} dp + \frac{R}{2\pi} \int_{-\infty}^{-p_0} \frac{e^{-ipt + i \sqrt{p^2 - p_0^2} x/c}}{p - p_1} dp \\
 &= \frac{R}{2\pi} \int_{-\infty}^{p_0} 2i \sin \sqrt{p^2 - p_0^2} x/c \left(\frac{e^{-ipt}}{p - p_1} + \frac{e^{+ipt}}{p + p_1} \right) dp. \quad (18, 1)
 \end{aligned}$$

It will be observed that after a considerable time has elapsed from the beginning of the disturbances, *i. e.* when t is big compared with x/c , both the integrals,

$$\frac{R}{2\pi} \int_{-p_0}^{+p_0} \frac{e^{-ipt}}{p-p_1} \sinh \sqrt{p_0^2 - p^2} x/c dp, \quad \dots \quad (19, 1)$$

$$\frac{R}{2\pi} \int_{-\infty}^{p_0} 2i \sin \sqrt{p_1^2 - p_0^2} x/c \left(\frac{e^{-ipt}}{p-p_1} + \frac{e^{+ipt}}{p+p_1} \right) dp, \quad (20, 1)$$

tend to zero very rapidly as t is increased, so that

$$Re^{-ip_1 t - x/c} \sqrt{p_1^2 - p_0^2}$$

represents the steady state in both cases. The other parts, 1 and 2, represent a disturbance which is only appreciable near the head of the wave, *i. e.* in the neighbourhood of $x=ct$.

Thus, for example, when p_1 is large compared with p_0 , the integral (1) is approximately

$$Z = -\frac{R}{2\pi p_1} \int_{-p_0}^{+p_0} e^{-ipt \pm i \sqrt{p_0^2 - p^2} x/c} dp \quad (21, 1)$$

and

$$p_1 \int Z dx = -\frac{R}{2\pi} \int_{-p_0}^{+p_0} \frac{e^{-ipt \pm i \sqrt{p_0^2 - p^2} x/c}}{\sqrt{p_0^2 - p^2}} dp. \quad (22, 1)$$

Let $y = p/p_0$; range of y is from -1 to $+1$,

$$\begin{aligned} -p_1 \int Z dx &= \frac{R}{2\pi} \int_{-1}^{+1} \frac{e^{-iy p_0 t + i p_0 \sqrt{1-y^2} x/c}}{\sqrt{1-y^2}} dy \\ &= \frac{1}{2\pi} c J_0(p_0 \sqrt{t^2 - x^2/c^2}), \end{aligned}$$

so that

$$Z = -\frac{R}{2\pi p_1} \frac{\partial}{\partial x} c \sqrt{\frac{\pi}{p_0 \sqrt{(t^2 - x^2/c^2)}}} \cdot e^{ip_0 \sqrt{t^2 - x^2/c^2}} \quad (23, 1)$$

approx. when $p_0 \sqrt{t^2 - x^2/c^2}$ is large.

In dealing with the final steady state ($t > x/c$) the disturbance represented by integrals 1 and 2 can be safely neglected. We can now state that "the critical frequency is the frequency at which the nature of the transmission changes from an unattenuated progressive wave to a highly attenuated pulsation or standing wave." The reason for the existence of this limiting frequency, in the case of the pulse already investigated, is now clear. Frequencies lower than n_0 are not

represented because those which were originally present in the pulse are not transmitted by the medium.

§ 2. Physically this failure to transmit the wave must be pictured as caused by a mechanical reaction against the electrons.

For at the critical frequency the magnetic force

$$\frac{1}{ip} \frac{\partial E}{\partial x} \quad (1, 2)$$

in the medium is zero by (14, 1), and no ætherial momentum (i.e. $\frac{EH}{4\pi}$) can be transferred across any plane in the medium perpendicular to the direction of the ray. But the momentum arriving at the surface is $\frac{E^2}{4\pi}$, so that in order to preserve the conservation of momentum at least $\frac{E^2}{4\pi}$ units of momentum per unit time must be given up to the electrons. This quantity may be more, depending as it does on the amount of momentum reversed on reflexion.

According to the solution given, there is a deficit of momentum of amount

$$\geq \frac{E^2}{4\pi} \text{ per unit time. } (2, 2)$$

Since this is a purely electrical problem, it should at least be self-consistent as regards the conservation of momentum and energy. The solution (9, 1) of the equations of propagation must be inaccurate to a certain extent.

According to this solution the ions are only moved in a periodic manner in the Z direction with a velocity amplitude $\frac{eE}{m\nu}$, and there is no material momentum produced in the X direction.

The inaccuracy in the derivation of the previous wave equation is due to the neglect of the action of the magnetic field in the wave front on the moving electrons. It is not difficult to see, even without the aid of mathematics, that this field must produce an average momentum in the X direction. For the electric force Z produces an ionic velocity in the Z direction; this, in conjunction with the magnetic force H, produces a force on the ion in the X direction, which, although zero when averaged over a long period and

incapable of producing any average acceleration of the ion, nevertheless produces an ionic drift in this direction.

The precise details of this drift have been worked out by Sir J. J. Thomson, who has shown that if v_x is the average velocity of drift in the x direction, then, neglecting the relativity variation of mass,

$$c^2 - (c - v_x)^2 = \frac{e^2 c^2 H^2}{m^2 p^2} \quad (7, 2)$$

The value of v_x may be connected up with the critical frequency as follows:—

When v_x is small we can replace $c^2 - (c - v_x)^2$ by $2cv_x$, and we get

$$v_x = \frac{e^2 c H^2}{2m^2 p^2}, \quad (8, 2)$$

and if N is the number of ions per c.c. each of mass m , the average ionic momentum produced is

$$Nmv_x = \frac{Ne^2 H^2}{2mp^2} \quad (9, 2)$$

$$\text{Now} \quad \frac{Ne^2 c^2}{m} = \frac{p_0^2}{4\pi}.$$

$$\therefore Nmv_x = \frac{p_0^2}{2p^2} \cdot \frac{1}{4\pi} \frac{H^2}{c} = \frac{p_0^2}{2p^2} \times (\text{ætherial momentum}). \quad (10, 2)$$

Thus in the neighbourhood of the critical frequency the momentum of the wave is used up in producing ionic momentum, and in this we have the physical explanation of the reason why waves of lesser frequency are not transmitted by the medium, *i.e.* the demand for momentum by the ions is greater than can be supplied by the wave.

The formula (7, 2) was derived by Sir J. J. Thomson on the assumption that the wave propagation was unmodified by the effect of ionic motions, so that $H = E$ in the wave front. But we have seen that this is certainly incorrect in the neighbourhood of the critical frequency where the relation between E and H is

$$H = E \sqrt{1 - \frac{p_0^2}{p^2}} \quad (11, 2)$$

$$\text{or} \quad H = \beta E.$$

It will therefore be well to verify at this stage that the equations on which this result is based are correct when

the motion of the ions in the magnetic field of the wave is taken account of. To do this we must remove the restriction that $H=E$ in the wave front, and assume $H=\beta_1 E$ where $\beta_1=\beta$ if the relations are unmodified, $\beta_1 c$ being the group-velocity. The motion of the ions may then be computed by a similar method to that used by Sir J. J. Thomson, and the conclusion arrived at is that the velocity of drift may be calculated from the formula:

$$\left(1 - \left(\frac{c_1 - v_x}{c_1}\right)^2\right) = \sin^2\left(\frac{eH}{mp} \cos pt\right), \quad (12, 2)$$

where $c_1 = \frac{c}{\beta_1}$ and is the phase-velocity. If $\frac{eH}{mp}$ is small enough, this gives approximately:

$$\frac{dv_x}{dt} = \frac{eHE}{m^2 p^2} \sin pt \cos pt; \quad (13, 2)$$

and since

$$v_z = \frac{m}{eH \sin pt} \frac{dv_x}{dt},$$

$$v_z = \frac{E_0 e}{mp} \cos pt, \quad (14, 2)$$

which is exactly the value in the previous approximate theory, so that to the first order of $\frac{EH_0}{mp}$ the simpler theory is correct. Also, if we assume as a simplification that the positive and negative ions are equal in number and in mass, the total current in the X direction is still zero and the original equations are still valid.

These equations, which were linear, are no longer so when the effect of the magnetic field is taken into account, but they only diverge from linearity when $\frac{EH}{mp}$ is large.

The relation between momentum of the ions and the momentum of the field still holds, for it may easily be shown that

$$Nmv_x = \frac{p_0^2}{2p^2} \cdot \frac{EH}{4\pi}, \quad (15, 2)$$

as before in eq. (10, 2).

The discrepancy as regards the conservation of momentum in the beginning of § 2 may now be cleared up.

For simplicity, consider the case where p/p_0 is small, and

where the electric and magnetic forces in the wave are so small that the deviations from linearity of the equations can be neglected. We have to determine the deficit in ætherial energy in this case.

It has been shown by L. Brillouin * that all but an entirely insignificant part of the energy and momentum in the wave (in the loaded medium) is contained in the region between the surface of the medium and another surface which travels forward with the *group-velocity*:

$$\frac{\partial KV}{\partial K} = U,$$

where $K = \frac{1}{\lambda}$, and V is the phase-velocity.

Now

$$\frac{\partial KV}{\partial K} = \beta c = \sqrt{1 - \frac{p_0^2}{p^2}} c. \quad . \quad . \quad (16, 2)$$

This is equivalent to saying that the head of the wave in the medium travels with the *group-velocity*, not the phase-velocity, or that the energy and momentum in the head of the wave, i. e. between the region

$$x = ct \quad \text{and} \quad x' = Ut,$$

can be neglected. Under these conditions we can calculate the deficit of ætherial energy as follows:—

The electric force in the medium is

$$E = E \sin \left(pt - p \frac{\beta x}{c} \right) \quad \text{and} \quad H = -\beta E,$$

so that the rate of supply of momentum over any surface inside the medium is $\frac{E^2 \beta}{4\pi}$.

Now the rate of increase of momentum at the head-end of the wave is $\frac{EHU}{4\pi c}$.

Since $\frac{EH}{4\pi e}$ is the momentum per unit volume, and the increase of volume (per sq. cm. of area) per unit time is U , this quantity is

$$\frac{EH\beta c}{4\pi c} = \frac{E^2 \beta^2}{4\pi}.$$

* *Annalen der Physik*, No. 10, p. 203 (1914).

There is therefore a deficit of ætherial momentum of amount $\frac{E^2\beta(1-\beta)}{4\pi}$ or $\frac{EH(1-\beta)}{4\pi}$.

When $\frac{p^2}{p_0^2}$ is small, $\beta \simeq 1$ and $1-\beta \simeq \frac{p_0^2}{2p^2}$, and the apparent loss of momentum is

$$\frac{EH}{4\pi} \frac{1}{2} \frac{p_0^2}{p^2}, \quad \dots \dots \dots (17, 2)$$

and the rate of gain of ionic momentum is

$$Nmv_z\beta c = \frac{1}{2} \frac{p_0^2}{p^2} \cdot \frac{EH\beta}{4\pi}, \quad \dots \dots \dots (18, 2)$$

which to the first approximation balances the apparent loss by momentum.

The conservation of energy also holds to the first approximation, for the rate of supply of energy across SS' is

$$\frac{EHc}{4\pi} = \frac{\beta E^2 c}{4\pi}, \quad \dots \dots \dots (19, 2)$$

the rate of gain of energy at the front of the wave

$$\frac{E^2 + H^2}{8\pi} c\beta = \frac{E^2 c\beta}{8\pi} (1 + \beta^2), \quad \dots \dots (20, 2)$$

and the apparent loss of energy is

$$\frac{E^2 c\beta}{8\pi} (2 - (1 + \beta^2)) = \frac{E^2 c\beta}{8\pi} (1 + \beta)(1 - \beta)$$

$$\text{assuming } 1 + \beta = 2 \quad = \frac{E^2 c\beta}{4\pi} (1 - \beta) \text{ approx.}$$

$$= \frac{EHc}{4\pi} (1 - \beta). \quad \dots \dots (21, 2)$$

Now from (12, 2)

$$\bar{v}_x = \frac{1}{4} \frac{e^2 HE}{m^2 p^2} \quad \dots \dots \dots (22, 2)$$

and

$$\bar{v}_x^2 = \frac{E^2 e^2}{m^2 p^2} \sin^2 pt = \frac{E^2 e^2}{2m^2 p^2},$$

$$Nm\bar{v}_x c = Nm\beta \frac{E^2 e^2}{m^2 p^2} \frac{1}{4} = \frac{1}{2} Nmv_x^2.$$

Now

$$Nmv_x c = (1-\beta) \frac{EH}{4\pi} c.$$

$$\therefore \frac{1}{2} N m \bar{v}_x^2 = (1-\beta) \frac{EH}{4\pi} c, \quad . \quad . \quad . \quad (23, 2)$$

and just balances the apparent deficit of energy.

The v_x energy is of the second order in $(1-\beta)$, and can be neglected in comparison with $\frac{1}{2} N m \bar{v}_x^2$.

These solutions are not quite exact, for we have neglected the momentum and energy carried off in the head of the wave (represented by expression (20, 1)), and also neglected the divergence of the solution from true linearity.

For this reason the case where $p \gg p_0$, and v_x/c small, was chosen to illustrate the conservation of energy and momentum, for under these conditions the momentum and energy in the head of the wave are small, and the divergence from true linearity can also be neglected.

But there seems little doubt that the solutions would be exact if we took these minor adjustments into account.

It is clear anyhow that the critical frequency occurs in virtue of the fact that the ions rob the energy and momentum of the main wave, so that it can no longer travel through the medium.

The velocity of drift is in general small compared with the velocity of light unless enormous wave energies are involved, for we have approximately :

$$\frac{v_x}{c} = \frac{1}{2} \frac{p_0^2}{p^2} \frac{HEc^2}{Nm \cdot 4\pi} \quad . \quad . \quad . \quad (24, 2)$$

$$= \frac{1}{2} \frac{p_0^2}{p^2} \frac{M}{Nm}, \quad . \quad . \quad . \quad (25, 2)$$

where M is the electromagnetic mass per unit volume.

So that $v_x \rightarrow c$ in the neighbourhood of the critical frequency only when the electromagnetic mass per unit volume approaches the ionic mass per unit volume ; a simple calculation shows that this requires enormous energy densities in the wave if N has any value comparable with the number of molecules per c.c. in a gas at normal temperature and pressure.

The result is only approximate as the neglect of the velocity variation of mass is serious when velocities approaching that of light are considered.

An exact computation of these effects has been made, but

the mathematical complexity rather obscures the underlying physical relations.

It is significant to compare this relation with that obtained by Compton * and myself † in the case of an individual quantum acting on a single electron which is considered by the former from a purely quantum point of view and the latter from a more or less classical point of view, which show that the velocity of recoil of an electron gets comparable with that of light when the mass ($\frac{h\nu}{2c^2}$ of the quantum)

approaches that of the electron it acts upon. The relation (25, 2) is obviously the same as (5, 6) (p. 280, *Phil. Mag.* July 1926) when generalized so as to apply to an aggregate of electrons instead of an individual one.

§ 3. This critical frequency has another interpretation connected with the quantum theory of the Compton effect.

We have shown that the critical frequency is given by the relation :

$$\frac{Ne^2}{\pi m\nu^2} = 1, \quad (1, 3)$$

and it is shown (Compton, "Scattering and Structure of Radiation," *Phil. Mag.* July 1926) that in order to satisfy the quantum conditions we must have the relation :

$$\frac{h\nu}{H^2/4\pi} = \frac{e^2}{\pi m\nu^2}, \quad (2, 3)$$

where $h\nu$ is the energy of a quantum engaged in an encounter with an electron, and H is the magnetic force in the wave reckoned in the usual classical manner; $\frac{H^2}{4\pi}$ therefore representing the radiant energy per unit volume. The ratio $\frac{4\pi h\nu}{H^2}$ must therefore be of the dimension of a volume, which, for want of a better expression, was termed "the volume of a quantum," V_q , say.

The relation giving the critical frequency can therefore be put in the simple form :

$$V_q N = 1, \quad (3, 3)$$

and since $\frac{1}{N}$ is the average volume occupied by each

* *Phys. Rev.*

† *Phil. Mag.*

electron, we may say that the critical frequency is such that the volume occupied by the quantum at the frequency is equal to the average volume occupied by an electron, or, as we may put it crudely, the quanta and electrons are paired off.

Perhaps the idea of the volume of a quantum is too materialistic a conception to be accepted readily, and it is therefore preferable to use the conception of probability, which is more conformable to the ideas of quantum mechanics. From the quantum point of view, long wave phenomena, such as envisaged here, are undoubtedly cases of statistical mechanics.

We can think of the wave as a well-ordered swarm of quanta encountering a swarm of electrons.

To introduce the idea of probability, consider the quantity :

$$\frac{4\pi N h\nu}{H^2} (4, 3)$$

It is of zero dimensions and is unity when all the quanta per unit volume are paired off with the electrons per unit volume, which suggests that it may be considered as the probability of a direct hit of a quantum in unit volume with one of the electrons in unit volume, or more precisely as the fraction of the number of quanta per unit volume in direct collision with the electrons per unit volume. This conception derives some weight from the following considerations : In each encounter some of the momentum of the quantum is given up to the electron, the amount being expressed by the relation :

$$M_x = \frac{h\nu}{c} (1 - \cos \theta), (5, 3)$$

where M_x is the gain in electron momentum, and θ is the angle of scattering of the individual quanta. On the average the momentum gained by the electrons will be the product of the probability that each quantum will find an objective in an electron and the average momentum given to the electron in an encounter, i. e.

$$\frac{P h\nu}{c} (1 - \cos \theta) f(\theta \phi), (6, 3)$$

where $f(\theta \phi)$ is the distribution of the scattered quanta as a function of θ and ϕ , and P is the probability of a direct hit, which we have tentatively suggested is $\frac{n_0^2}{n^2}$. The average

value of $(1 - \cos \theta)f(\theta\phi)$ is not known exactly, but by the correspondence principle it should agree with the scattered radiation from an electron calculated in the ordinary way. Taking the classical value, this comes out at $1/3$, so that following up this suggestion, electron momentum = $\frac{1}{3} \frac{n_0^2}{n^2} M$ æther on the average say. More generally, Momentum

of electrons = $k \frac{n_0^2}{n^2} M$ æther. Actually to make this agree with (15, 2) we must have $k = \frac{1}{3}$.

In view of the uncertainty of this distribution factor, the agreement, except for the numerical factor, suggests that the interpretation of $\frac{n_0^2}{n^2}$ as the probability factor is correct.

Speaking approximately, the critical frequency occurs when the probability of a direct hit between the quanta in the incoming wave and the electrons is unity, in which case the momentum in each quantum is on the average handed over to one of the electrons, and the momentum of the wave is used up and it can travel no farther.

This interpretation of the quantity

$$\frac{4\pi N h\nu}{H^2} = \frac{n_0^2}{n^2}$$

can also be used to calculate the scattering of X-rays. From the quantum point of view, an encounter between a quantum and an electron raises the latter to an energy level $h\nu$, and after an average time τ , which represents the average life in this excited state, this quantum is scattered.

Now $\frac{N_1}{\tau} = A_{12}N_1$ is Einstein's probability coefficient representing the number of emissions of a scattered quantum per unit time per unit volume where there are N_1 electrons in the excited state. Now N_1 can be computed from the expression (1), the fraction of the total number of quanta in collision for

$$\frac{N_1}{N} = \frac{4\pi h\nu N}{H^2} = \frac{n_0^2}{n^2},$$

where \bar{N} = total number of quanta per unit volume, so that the energy scattered per unit time per unit volume is

$$\frac{n_0^2}{n^2} A_{12} \bar{N} h\nu. \quad . \quad . \quad . \quad . \quad . \quad (7, 3)$$

The rate of supply of energy is $\bar{N} h\nu c$, so the absorption-coefficient is

$$\frac{n_0^2}{n^2} A_{12} \frac{\bar{N} h\nu}{\bar{N} h\nu c} = \frac{n_0^2}{n^2} A_{12}.$$

A_{12} is shown to be

$$\frac{e^2 4\pi^2 n^2}{3m_0 c^3}, \dots \dots \dots (8, 3)$$

so that the absorption-coefficient

$$\frac{n_0^2}{n^2 c} \frac{2e^2 4\pi^2 n^2}{3m_0 c^3} = \frac{8\pi^2}{3} \frac{n_0^2 e^2}{cm_0 c^3}, \dots \dots (9, 3)$$

and since

$$n_0^2 = \frac{Ne^2 c^2}{\pi m_0},$$

$$\alpha = \frac{Ne^2 c^2}{\pi m_0 c} \frac{8\pi^2}{3} \cdot \frac{e^2}{m_0 c^3} = \frac{8\pi Ne^4}{m_0^2 c^2} \dots \dots (10, 3)$$

in agreement with the ordinary values.

§ 4. Frequency Change.

On account of the average velocity produced in the electrons, the frequency of the scattered waves is changed according to the Doppler principle by an amount $\frac{\delta n}{v} = v_x/c$.

In the case where the medium is finely structured compared with the wave-length, it is the reflected wave which is altered in frequency. This change is small except when the ætherial mass (per unit volume) approaches the mass of the electrons per unit volume—a very exceptional case requiring enormous wave energies.

This effect will therefore not be of importance in the investigation of the momentum relations if we confine ourselves to small wave energies where v/c is everywhere small.

Non-Reversible Transmission.

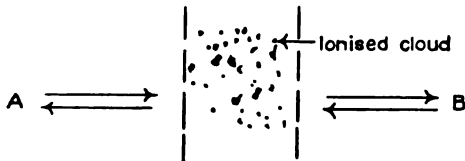
Transmission through this type of medium affords an example of the irreversible effects which have been observed in radio transmission (Proc. I.E.E. vol. lxiii. no. 346, Oct. 1925), where it is shown that there is an apparent difference between East and West transmission and West to East transmission. An example can be constructed as follows:—

Suppose A and B are two sources of electromagnetic

waves. A slab of ionized gas is supposed to be situated between A and B, the ionization being maintained by some external agency—X-ray for example.

Let the critical frequency of this medium be n_0 .

Fig. 6.



If the frequency n of waves emitted by A and B is greater than n_0 , then the medium will be transparent and A can send energy to B, and *vice versa*. If, however, $n < n_0$, the waves will be absorbed in the medium.

If, now, the ionized slab be considered to be moving from left to right with a velocity v , then, referred to axes moving with the slab, the frequency of the waves from A is $n(1 - v/c)$, and from B is $n(1 + v/c)$ (the frequency referred to A and B axes being n).

We will again suppose the critical frequency of the medium (referred to the moving axes) is n_0 , which we are quite at liberty to do. If, now,

$$n(1 + v/c) > n_0 > n(1 - v/c), \quad \dots \quad (1, 4)$$

the medium will be transparent to waves from B, but opaque to those from A, and the system is irreversible. This argument refers to the steady state. In considering the conveyance of an intelligible message from A to B, and *vice versa*, such as we are concerned with in radio telegraphy, for instance, it is insufficient to have only a single steady wave of constant frequency, for this has no character to convey the intelligible message. In general, the message must be considered to be conveyed by a band of frequencies between $n + \delta n$ and $n - \delta n$, say. The above argument, however, applies if the band is so narrow that all the frequencies from A (referred to axes moving with the slab) are less than the critical frequency, and all those from B are greater than this.

Thus

$$(n + \delta n)(1 - v/c) > n_0, \quad \dots \quad (2, 4)$$

$$(n - \delta n)(1 + v/c) < n_0; \quad \dots \quad (3, 4)$$

$$\text{i. e.} \quad \delta n/n > v/c. \quad \dots \quad (4, 4)$$

164 *Transmission of Electric Waves through Ionized Medium.*

The possibility of such irreversible effects seems to be inconsistent with the usually-accepted notions as regards the reversibility of optical phenomena, which appears to be based on a theorem of the following type.

Consider a group of fixed conductors and a series of forces of the types $E_r e^{ipt}$, and a series of corresponding velocity coordinates

$$I_1 e^{ipt}, \dots I_r e^{ipt}. \quad . \quad . \quad . \quad . \quad . \quad (5, 4)$$

Then, if the energy T can be expressed as a homogeneous quadratic function of the I 's, there is a dissipation function of the same type and a normal potential function W , the motion is expressed by the Lagrangian equations of the type :

$$\frac{\partial}{\partial b} \left(\frac{T-W}{\partial I_r} \right) + \frac{\partial(T-W)}{\partial q_r} + \frac{\partial \phi}{\partial I_r} = E_r, \quad . \quad . \quad (6, 4)$$

etc.,

and it follows that

$$\frac{\partial E_r}{\partial I_r} = \frac{\partial E_s}{\partial I_r} \quad . \quad . \quad . \quad . \quad . \quad (7, 4)$$

and the E.M.F. induced in r by unit current in S is equal to the E.M.F. induced in δ by unit current in r , and the effects are reversible in this sense.

This specification implies that the connexions of the system are such that the forces of this specified type $E_r e^{ipt}$ should produce currents only of this specified type, as will be seen on expressing equation (6, 4) explicitly in terms of the velocity coordinates etc. For if we calculate the EM energy from the usual formulæ :

$$\left. \begin{aligned} T &= \frac{1}{2} \iiint (F u_0 + G v_0 + H w_0) dv \\ W^2 &= \frac{1}{2} \iiint (X^2 + Y^2 + Z^2) dv, \end{aligned} \right\} \quad . \quad . \quad (8, 4)$$

where $F G H$ is the vector potential, and $u_0 v_0 w_0$ the total convection current at any point ; and assume that only currents of this type are present, we get expressions for the kinetic and dissipation energies which are homogeneous quadratic functions of the currents as before *.

Thus it is sufficient for a reciprocal relation to have a linear relation between the E.M.F. and currents.

In the example cited of the transmission through a moving dispersive medium, the currents and movements produced in

* Sommerfeld, *Jahrbuch der drahtlosen Telegraphie und Telephonie*, vol. xxvi. book 4, pp. 93-98 (1926).

Mean Free Path of Electrons in Ionized Mercury Vapour. 165

the medium are not linear, and the fact that the reciprocal relation does not hold good in this case does not violate the above theorem.

§ 5. Summarizing, it is shown that in a medium containing free electrons there is a certain critical frequency characterized by the fact that waves of lower frequency than this cannot travel through the medium.

The physical reason for the existence of such a critical frequency is shown to be connected with the fact that the electrons in the medium rob the wave of its momentum, and at the critical frequency also rob this momentum completely so that the wave can travel no further.

This fact is shown to be connected with the theory of Compton scattering, in which an individual quantum gives up its momentum in collision with an electron. The wave is brought to a standstill when all the quanta (per unit volume) are brought into collision with the electrons, which event occurs when the critical frequency is approached.

XIV. *A Method of Measuring the Mean Free Path of Electrons in Ionized Mercury Vapour* *. By KATHARINE B. BLODGETT, Ph.D., General Electric Co., Schenectady, New York †.

Introduction. *

IT has been shown by Stead and Stoner ‡ that in gases at very low pressures glow-discharges of considerable length can be produced in a tube which has electrodes at one end only. The anode is an open grid which is placed immediately in front of the hot cathode so that electrons are accelerated past the grid and ionize the gas in their path along the tube. Stead has used a tube which extended about 35 cm. from the grid, and under suitable conditions the glow could easily be made to reach to the end of it.

If a low accelerating potential is applied to the grid, of the order of 25 volts or less, the glow will not extend to the end of a long tube, but will come to a limit at a distance which is principally determined by the grid

* The experiments described in this paper were made in the Cavendish Laboratory when the writer was a Research Student of Newnham College, Cambridge.

† Communicated by Sir E. Rutherford, O.M., D.Sc., F.R.S.

‡ Stead and Stoner, Proc. Camb. Phil. Soc. xxi. p. 66 (1922).

voltage. This limit is dome-shaped, and, in mercury vapour which is free from contamination by other gases, is very sharply defined. The effect in a darkened room is striking, for the glow can be contracted or extended to great lengths simply by varying the grid voltage, and the space in the tube beyond the sharp limit of the glow appears to be completely dark, as if all sources of luminosity were halted and could not pass beyond that point. The variation of length with voltage is continuous and shows no lag.

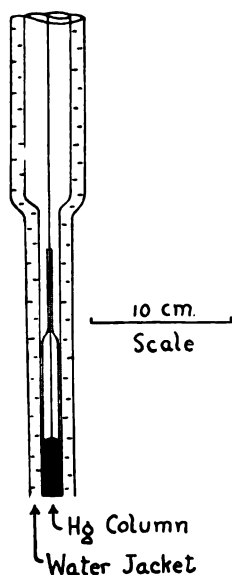
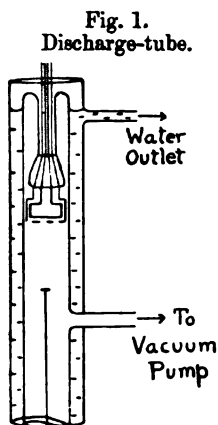
Stead and Stoner pointed out the need for a theory of the glow that would explain the sharp tip, and they put forward a theory based on speculative considerations. More recently, the method devised by Langmuir* for investigating the properties of gaseous discharges has made it possible to revise the theory in the light of experimental data. Langmuir's method consists in measuring the current which is taken up at different voltages by an auxiliary electrode in a discharge, called a collector, and interpreting the data thus obtained with the aid of a theory which he has developed. This paper will describe some results of applying the method of collectors to long glows, which show that these glows supply a means of measuring the mean free path of electrons in an ionized gas.

* *Apparatus.*

The apparatus, which was built with the assistance of Mr. Stead, is drawn to scale in fig. 1. The grid was made of molybdenum wire, 0.2 mm. in diameter, bent into a flat, open zigzag with a spacing of about 3 mm. between consecutive turns, so that the wire presented very little target area to the electrons. It was at the upper end of the tube when the tube stood in a vertical position, with the hot cathode immediately above it in the form of a straight filament of 0.2 mm. tungsten wire stretched across the diameter of the tube about 3 mm. above the grid. The potential drop along the filament was 2.7 to 3.0 volts with heating currents of 3.5 to 4.0 amperes. The area of the grid filled the greater part of the cross-section of the tube which was 3.4 cm. in diameter, and the tube had this diameter for a length of 78 cm. from the grid.

* Langmuir, Journ. Frankl. Inst. cxvi. p. 751 (1923). Langmuir, Gen. Elec. Rev. xxvi. p. 731 (1923). Langmuir and Mott-Smith, Gen. Elec. Rev. xxvii. pp. 449, 538, 616, 762, 810 (1924).

The collector was operated on a glass float which rested on mercury and could be raised or lowered over a range of 60 cm.



The middle section omitted from this drawing is 50 cm. in length.

by lifting a mercury reservoir to which it was connected through a barometric column. This column of mercury also served to make electrical contact from the float to the external circuit and to supply mercury vapour for the discharge. The collector was supported on a length of stout nickel wire, 1.0 mm. in diameter and 78 cm. long, insulated throughout its length by fine glass tubing. The glass float was drawn out into a capillary at the top which was just large enough to receive the nickel wire and hold it firmly in a vertical position; the end of the wire rested on the bottom of the float to support the weight of the nickel, and there, with the aid of a drop of mercury, it made electrical contact with a short lead sealed through the bottom of the float and submerged in the mercury on the other side. With a float of this simple design it was possible to change collectors, using the same float; to facilitate this change the tube was made with a ground-glass joint at the lower end through which the float could be withdrawn.

It became evident in the course of the experiments that it was important that the collector should be set accurately on the axis of the tube. To accomplish this, it was convenient to make use of the slight flexibility of the long nickel wire. With the lower end held rigidly in the float, the upper end could easily be displaced a small amount to one side or the other by inclining the tube through a very small angle from the vertical.

For this purpose the whole apparatus was given freedom to be tipped slightly in any direction, by mounting the long vertical tube and the mercury condensation pump

which was connected to it both on the same stand so that they moved together.

Control of the mercury vapour pressure was secured by means of a glass water-jacket which enclosed the discharge-tube throughout its entire length, with the jacket extending 50 cm. down the lower tube in which the float operated. In addition, the connecting tube leading to the pump was jacketed for 45 cm. of its length. Only circulating water was used, and a thermometer suspended inside the large jacket measured the temperature, which could be held constant to 0.2 degree during a run. The condensation pump was kept running throughout every experiment to keep the mercury vapour pure.

With the water-jacket in place it was no longer possible to exhaust the tube by baking it in the standard manner, and therefore another method had to be employed to rid the surface of the walls of water vapour and other gases. For, in addition to the need for safeguarding the tungsten filament in these experiments, the mercury glow itself called for the cleanest possible conditions inside the tube, since the glow presents a sharp tip only when the mercury vapour is free from contaminating gases. With traces of water vapour present, the glow is faint, and the tip diffuse and indistinct. The appearance of the glow is the surest indication of conditions inside the tube, and a little familiarity with the behaviour of glows in clean and contaminated tubes enables one to tell the condition of the tube at a glance. The method of exhaust employed in these experiments consisted in putting to use the fact that in a glow discharge the walls of the tube become negatively charged, so that positive ions are continually bombarding the walls and thereby dislodging gas molecules from the surface. In other words, a glow will clean its own tube, if given the opportunity to do so by the aid of fast pumping. Campbell * has pointed out that a mercury glow will evolve large quantities of hydrogen from the walls of a tube which has previously been baked just below the softening-point of the glass, indicating that the mechanism of the glow is more effective in this respect than heat treatment. In his experiment the filament wasted rapidly, and broke after 48 hours of running the glow, though the gas was being pumped away all the time. But in the present experiments it was found that if the gas is pumped away sufficiently rapidly as it is evolved, the filament suffers no harmful effects and the walls of the tube are very effectively cleaned. The tube

* Research Staff of the General Electric Company, London (Work conducted by N. R. Campbell), *Phil. Mag.* xli. p. 685 (1921)

may safely be opened to the atmosphere and left open for several days, and then evacuated and cleaned again by this method.

The practice in cleaning the tube after it had been opened to the atmosphere was to run the glow for a few seconds at about 70 volts grid potential, and then shut it off long enough to allow the pump to remove all the gas that had been evolved. At first the glow would be so faint as to be hardly perceptible, partly because of the lowered emission of electrons from the filament in the presence of oxygen, though with the filament raised to such a high temperature that it gave the usual 20 milliamperes emission even in the presence of oxygen, the glow was very faint. As the process of cleaning progressed, by alternately running the glow and pumping out the gas, the glow became brighter and longer, and the tip grew more distinct. For example, at a certain stage of the process the glow would extend for 40 cm. down the tube for a given grid voltage; if, then, the glow was shut off for a minute, it would extend for 45 cm. when it was next turned on. In this way the cleaning process was carried to completion. It was never found practicable in the early stages of the process to keep the glow running and expect the gas to be pumped off as fast as it was evolved, though some care had been taken to make the distance to the pump short, with large enough connecting tubing to ensure fast pumping; perhaps with more ideal conditions the glow could be run in this way. It may be added that at one time, when a trap made of a spiral of small-sized glass tubing was inserted between the discharge-tube and the pump, it was found quite impossible to clean the tube in the ordinary manner with this hindrance in the way, and the trap had to be removed. This is pointed out merely to emphasize the fact that really fast pumping is essential for the success of the process, or the filament will waste and break in the presence of the water vapour, as it did in Campbell's experiments.

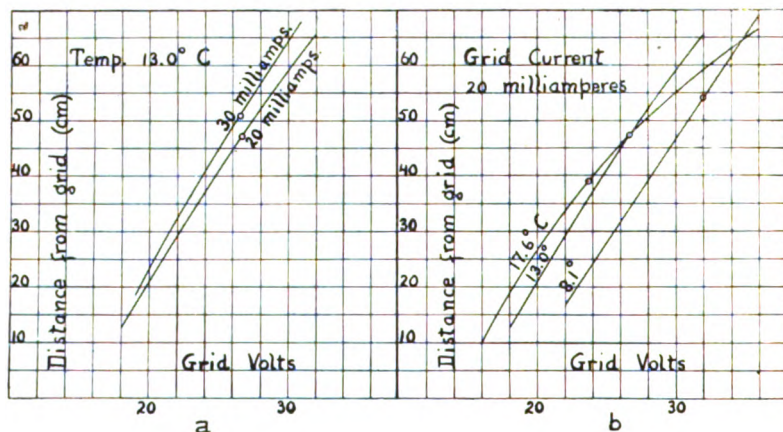
Factors that determine Length of Glow.

Fig. 2 shows the lengths to which a glow in saturated mercury vapour at ordinary temperatures will extend in a tube 3.4 cm. in diameter. These data were taken with the collector removed from the glow. The curves illustrate the low range of grid voltage that is required to produce a glow 65 cm. long, the tip moving 3 or 4 cm. along the tube for every increase in potential of one volt. The current flowing to the grid and the mercury-vapour pressure are

also seen to be factors determining the length; these will be discussed in a later section of this paper. The trend of the curves leaves no doubt that in a longer tube, at low pressures, glows more than a metre in length could be obtained at moderate voltages.

The circle on each curve marks the striking voltage. At this voltage the current jumps discontinuously to a value ten or more times its value immediately before the arc strikes, and at the same time the glow appears to dart out

Fig. 2.
Plots of Length of Hg Glow against Grid Voltage.
Circle on each curve marks striking voltage.



from the filament to the distance which corresponds to this voltage under the conditions of the experiment. It may then be contracted to a third or a quarter of the striking length, but by decreasing the voltage farther the glow is extinguished when it has shrunk to about 10 cm.

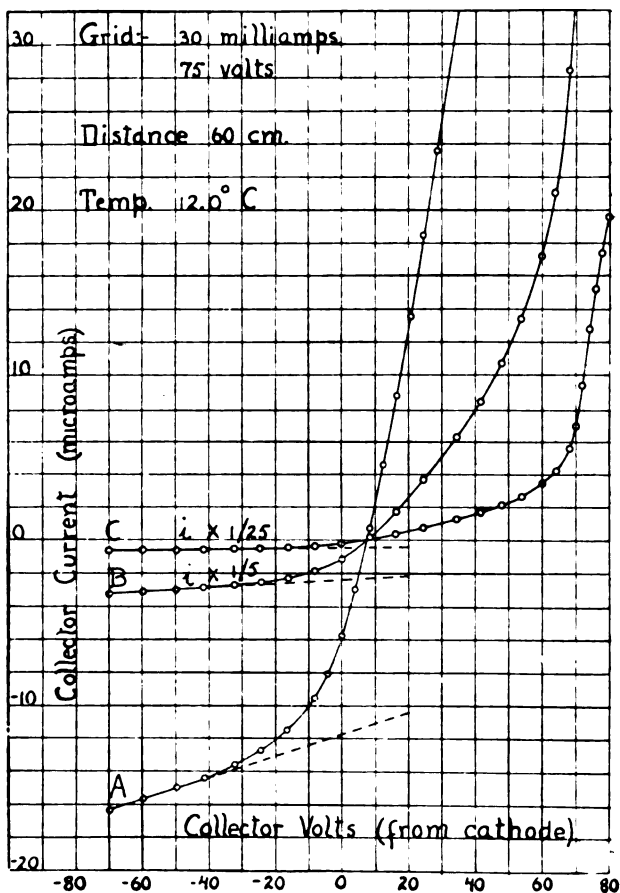
General Nature of Data obtained with Plane Collector.

The collector that was used to take most of the data in this investigation was a plane disk of nickel 0.70 cm. in diameter, mounted in a horizontal position on the upper end of the long vertical lead wire that has been described. The metal face of the disk was toward the cathode, and the back was insulated with mica. A plate of this size could be projected far into the heart of the glow, but could not be used to explore inside the glow anywhere near the tip; for if the plate were withdrawn to a position near the tip

the glow promptly shrank till it no longer passed the plate but appeared to rest on its surface. The plate was always well inside the glow whenever data were taken, except where the contrary is stated. Usually the glow extended the full

Fig. 3.

Typical Current-Voltage Curve drawn to Three Scales of Current.
Data taken with Disk Collector 0.7 cm. in diameter.



length of the large tube in spite of the presence of the collector support down the axis.

The general form which the data take is illustrated in fig. 3. This is a typical plot of the current flowing to a collector with potential differences applied between the collector and the cathode; the potentials were measured

from the negative end of the cathode. The smaller currents were measured with a Nalder Bros. & Co.'s galvanometer, used with light and scale, which gave a deflexion of 2 cm. for 1 microampere.

Fig. 3 shows a current-voltage curve drawn to three different scales of current, so as to give the complete range of the data. The currents in Curve B are plotted on a scale reduced to $1/5$, and in Curve C to $1/25$ of the scale marked on the graph. In plotting the data the convention with regard to sign which Langmuir adopts has been used, *i. e.* "that the sign of a current is positive when positive current flows from the electrode into the space." Currents plotted below the zero line are therefore the positive ion currents which flow to a collector when it is at a negative potential with respect to the space surrounding it. Langmuir has shown that with negative potentials sufficient to repel all electrons the positive ions form a sheath about the collector, and the whole drop in potential becomes concentrated within the sheath. The current is then limited by the positive ion space-charge within the sheath, and is related in magnitude to the sheath thickness by the ordinary space-charge equations. For example, in the case of the present experiments, if the plane collector at a potential 100 volts negative with respect to the mercury glow which surrounds it takes up a positive ion current of 20 microamperes per cm^2 , the sheath thickness becomes 0.44 cm. Whenever such a sheath covers the collector it is always plainly visible as a dark space, since it is a region of no ionization.

Curve C, which gives the complete range of the data plotted in fig. 3, shows how the current rises gradually from a small positive ion current at negative voltages to a much larger electron current at positive voltages, and does not begin to rise rapidly until it approaches the potential of the grid, which in this case was 75 volts. The potential of the glow is approximately that of the grid, since large numbers of electrons begin to reach a collector as soon as it approaches the potential of the space surrounding it. From 75 volts upwards the curve does not reach a current saturation value, such as Langmuir finds for similar curves in a mercury arc, but continues upward indefinitely, and a brightly luminous sheath over the collector indicates that ionization by collision is occurring close to the surface. Meanwhile the current to the grid decreases, as the collector is now acting as a second anode, robbing the grid of some of the anode current.

The intermediate range of the data is best studied in Curve A. This shows how the positive ion current decreases slowly with decreasing negative voltage, according to an approximately linear relationship. The continuation of this part of the curve in a dotted straight line marks the current that would be received if only positive ions were present; but with decreasing negative voltage, electrons begin to reach the collector, and the curve takes an upward trend. Since the space filled by the glow is at the potential of the grid, the electrons which reach the collector in this range must move against a retarding field, and can reach it only according to the energies they possess. It will be seen from the sloping nature of the curve in this range that electrons of all energies are present, and are not readily classified into groups. Some of these electrons are found to have energies higher than that corresponding to the grid potential by which they have been accelerated, as indicated in this instance by the fact that the curve starts upward at a potential about 40 volts lower than that of the cathode. In other words, some few electrons in being accelerated by 75 volts have somehow gained an energy corresponding to 115 volts. This phenomenon of the scattering of electrons has been observed and described by Langmuir*, but has not yet been explained.

The curves in fig. 3 are perfectly typical of all the data that were taken, though the actual magnitudes of the currents varied widely according to the conditions of each experiment. With changes in grid potential the sharp rise in the upper end of the curve was always close to the grid voltage, and the rest of the curve was shifted a corresponding amount to the left or to the right. With increase in grid current there was more intense ionization of the entire glow, and both positive ion and electron currents were increased.

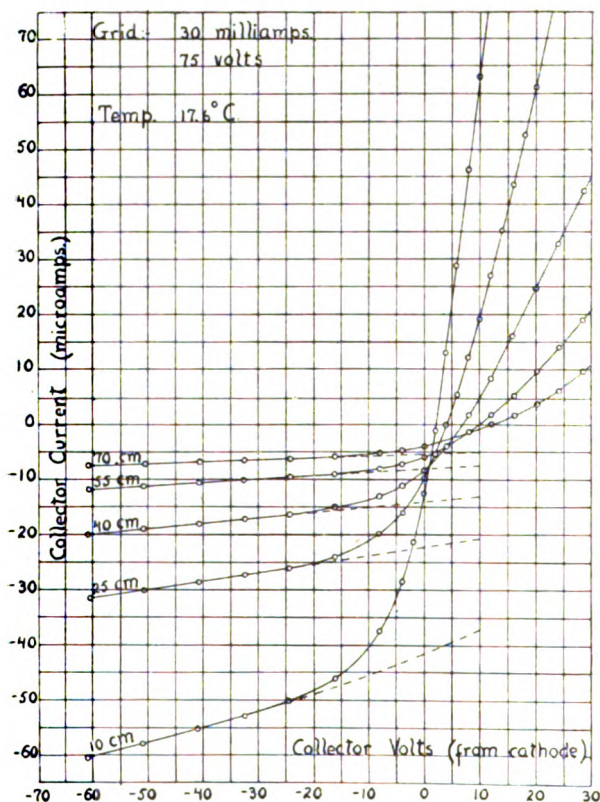
The data in fig. 3 were all taken with the collector at a fixed distance of 60 cm.; all distances were measured from the grid. Fig. 4 shows how the curves varied with the distance of the collector from the grid. The glow conditions were identical in each of the five cases represented in the figure, and only the position of the collector along the axis of the tube was altered. It is clear that the trend of the curves was the same at each distance, and only the magnitude of the currents was different. Though it is impossible to station the collector in the glow close to the tip, there is no reason to doubt that the nature of the data

* Langmuir, *Phys. Rev.* xxvi. p. 585 (1925).

would be exactly the same if they could be obtained practically all the way to the end. In other words, the interior of the glow throughout its length is at approximately the potential of the grid, and one section differs from the next only in the densities of electron and positive ion currents.

Fig. 4.

Current-Voltage Curves for Collector stationed at Different Distances along the same Glow.



Theory of the Glow.

Length of Glow.—An explanation of how such a glow can extend to great lengths and how it can end in a sharp tip is furnished by the theory of positive ion sheaths which cover a negatively-charged surface in the path of a discharge. It is known that the wall of a glass tube enclosing a uniform glow is charged to a negative potential which is nearly as

high as the energy of those electrons which strike it with the highest velocities normal to its surface; the line of reasoning which leads to this knowledge is given in Langmuir's paper. In the case of these experiments, some knowledge of the value of this potential is obtained from curves such as those in fig. 4, for the potential at which the collector receives zero current is that which an *insulated* surface would have that stood normal to the path of the electrons streaming down the tube. Under the conditions of the experiment of fig. 4 this potential is seen to be in the range from +2.1 volts (with respect to the cathode) at 10 cm. to +12.5 volts at 70 cm.; in an experiment at lower vapour-pressure, made at 7.9° C., the range was from -4.8 volts at 10 cm. to -1.3 volts at 70 cm. Since the surface of the wall which actually encloses the glow is not normal but parallel to the electron stream from the cathode, its potentials must be somewhat less negative with respect to the glow than these, for experiments to be described later show that when the collector is turned so that it no longer faces the electron stream coming from the cathode, the electron current is decreased, whereas the positive ion current remains practically unchanged, so that zero current would not be reached on the current-voltage curve until the curve had arrived at higher positive potentials.

Consider, now, what happens with a glow at the anode potential and a wall at only a little more than the cathode potential, so that the wall is negative with respect to the glow and therefore repels electrons from its neighbourhood but gathers positive ions. Throughout the length of the glow the wall thus becomes covered by a sheath of positive ions, and the whole drop in potential between the ionized gas and the wall becomes concentrated within this sheath. It has been pointed out that the thickness of the sheath is determined by the positive ion current density; with the current densities that prevail throughout the greater part of the length of a glow the sheath is not more than 2 or 3 mm. thick, and is often less than this, so that the field of the wall does not extend beyond a distance which is small compared with the tube diameter. Under these circumstances the entire core of the tube is a region of no electrostatic field. This is the region which the observer sees filled with luminous glow, and he also sees that it is separated from the walls by a dark space which is the sheath, unless it happens that the sheath is too thin to be visible.

An electron which is shot through the grid, and enters this core along a path that runs parallel to the axis, will travel

the entire length of the glow with unchanged velocity unless deflected from its path by a collision with a gas molecule or by a magnetic field. On the other hand, an electron which follows a path that makes an angle with the axis will be repelled by the wall as soon as it enters the positive ion sheath, and will be reflected back into the glow unless it possesses a radial velocity sufficient to enable it to penetrate against the retarding field and reach the wall. Thus, as long as electrons remain in the glow, the presence of the positive ion sheath screens them from the field of the wall and affords them a field-free region along which to travel, and when they attempt to leave the glow the field of the wall tends to drive them back into it again. Since both factors act to herd the electrons along the tube, the longitudinal velocities which they receive when they leave the cathode will carry them for long distances.

This state of affairs, however, cannot be maintained for more than a certain distance. For although the glow appears to the eye to be of uniform intensity throughout its length (except at the grid end of the tube, where the light from the filament is too bright to allow the intensity to be estimated), curves such as those in fig. 4 make it clear that there is a marked falling-off in the positive ion current density with increasing distance from the grid. With decreasing positive ion concentration the field of the wall extends farther into the tube, so that the core within which the field is neutralized becomes confined to a narrower region. In other words, the dark sheath becomes thicker, and the glow appears to the observer to have drawn away from the wall. In the limit, at a distance such that the positive ion concentration has fallen to such a low value that it no longer screens the electrons adequately from the field of the wall, this field brings the glow to an end; for the wall beyond this distance then acts as a negatively-charged Faraday cylinder which prevents the electron stream from passing farther down the tube.

Shape of Tip.—On this theory, for a tube of a given diameter the end of the glow is fixed by the distance at which the positive ion concentration has fallen to a certain minimum value. The requirement that the concentration shall not be less than a certain value will also explain why the tip is a blunt-shaped surface and not a long, narrow point. With the glow in a steady state the rate at which ions arrive in any section of its length is equal to the rate at which they are removed. Ions arrive by the formation of new ions as a result of electron collisions and of radiation, and by

diffusion from a neighbouring section; they are removed by recombination with electrons, and by diffusion to the wall or to another section. The observed falling-off in ion concentration along the tube makes it clear that at the grid end of the tube the rate of formation of new ions and the rate of removal by diffusion are both high, whereas far from the grid these rates are both low. If in any region the rate of arrival of ions were to fall so low that it fell below the rate of removal, the glow could not maintain a steady concentration in that region. This is precisely what would happen in the case of a narrow pointed tip, for the formation of new ions takes place only in the path of the electron stream, and this path has been shown to be confined to the luminous core of the tube. Since the rate at which ions could diffuse outward through the surface of a long, narrow point is greater than the rate at which they could be formed within its volume, this shape is impossible for a steady state; a tip which assumed such a state momentarily must promptly "shut up" and take a shape that would meet the requirements of this state. Thus only a blunt-shaped surface is possible.

Experiment that Illustrates.—A picture of how the field in a tube is altered by the striking of a long glow was obtained accidentally with a tube that had a lime-coated Pt strip as a cathode. With a tube of this type the glow makes its appearance in two distinct stages: at voltages below the striking potential of the long glow there appears a luminous blue casing covering the wire of the grid and the grid supports. At low voltages the casing is less than 1 mm. thick, and can be clearly seen outlining the zigzag of the grid and following the nickel supports all the way to the point where they are sealed into the glass; at higher voltages it thickens and projects forward from the grid to a distance of 1 or 2 cm. It is imperceptible when it makes its first appearance at a voltage a little above the ionizing potential, and the accompanying current increase shows no discontinuity. But if, with the glow extending about 2 cm. in front of the grid, the voltage is raised still farther, the glow suddenly "breaks" and fills the entire tube with luminosity of the familiar type.

This short glow illustrates how the electron stream is confined to a short path unless it is able to produce enough ions to screen its path from the field of the wall. As long as the positive ion concentration remains insufficient to neutralize the electron space-charge at the cathode, only a comparatively small stream of electrons is emitted at low

voltages, and the charge on the walls prevents their escape down the tube. At potentials a little above 10·4 volts they acquire enough energy to ionize just before they reach any part of the grid or its supports, and so produce the luminous casing. But as soon as increased emission from the cathode can supply enough electrons to increase the ion concentration to an amount at which this can begin to neutralize the field of the wall, electrons are free to begin passing along the tube, and the higher electron current thus drawn from the cathode will in turn produce more positive ions so that an unstable state of affairs prevails: in other words, the glow breaks. This picture is borne out by observations on the different lengths to which the short glow can be extended before it breaks. The length increases with voltage since more electrons are emitted from the filament and they can produce more ions. But with the cathode as hot as is used in ordinary practice, the glow breaks before it reaches a length of 1 cm. To obtain the longest glows, about 4 cm. in length, the Pt strip must be at the lowest temperature at which it will function as a hot cathode; the emission of electrons is then not sufficient to allow the glow to break until the voltage reaches a high value. This type of glow was never observed with a tungsten filament; and although the vastly greater brightness of this type of cathode makes it much less easy to observe a discharge in its immediate neighbourhood, it is felt with certainty that the glow does not appear, but that the long glow strikes at once with no intermediate stage. It would appear that the difference between the two cases lies in the shape of the cathode, since under the limiting action of space-charge more electrons could pass from a flat strip 1 mm. wide than from a 0·2 mm. filament, so that there would be enough electrons to excite this glow even before the space-charge was wholly neutralized.

Dependence on Current, Voltage, Pressure, and Tube Diameter.—An explanation of how the length of the glow varies with changing conditions, as illustrated in fig. 2, follows at once from the hypothesis that the glow requires more than a minimum concentration of positive ions to maintain itself, and that the tip marks the distance at which the concentration has fallen to this minimum, which will be called the "critical" concentration. With increasing emission from the cathode the number of electrons that are shot through the grid and escape down the tube will be greater, thereby increasing the positive ion concentration at every point, which in turn will allow the glow to extend farther before the concentration falls to the critical value. Raising

the grid voltage increases the velocity with which electrons leave the positive ion sheath at the cathode in all radial directions, and thus adds to the energy available for ionization, so that the result is again a longer glow. The dependence of length on mercury-vapour pressure exhibits the two balancing effects that one would expect—i. e., the current density of electrons that can penetrate a distance through a gas at a given pressure, and the concentration of molecules available for ionization by these electrons. At high pressure the concentration of positive ions is high near the grid, but falls off rapidly with distance along the glow, due to the rapid falling-off in concentration of the electrons which produce the ions; at low pressure, and with the same grid current and voltage, the ion concentration near the grid is lower, but decreases less rapidly with distance. This shows why the curves in fig. 2 (*b*) cross over, since at low pressure more voltage is required to maintain the critical positive ion concentration at a given short distance than is required at high pressure, whereas it is maintained at a given long distance more readily at low pressure. It is seen that the curve marked 13.0° C. has a slight curvature at the upper end, while the curve marked 8.1° C. is perfectly straight in this range; apparently the third curve would cross the second at a little distance farther up, just as both have already crossed the first.

The actual magnitudes of the quantities plotted in fig. 2 are for a tube 3.4 cm. in diameter. In a larger tube the glow would extend farther in each case, for the volume of the glow per unit length would then be greater in proportion to the surface through which ions would be lost out of this volume by diffusion to the wall. It is noticeable that the glow will not readily enter constricted tubing, and was never observed to pass the point at which the lower tube 1.6 cm. in diameter joined the discharge-tube, although this was in a direct line with the discharge.

Positive Ion Current Data.—One would like to measure the critical positive ion current density that the glow requires. It may prove to be possible to determine this quantity by measuring the current densities with a collector somewhere near the tip, and extrapolating from these data. The currents received by the collector measure the number of positive ions that reach the surface of the sheath by virtue of their random motions in the discharge. Therefore the surface area of the sheath and the distribution of random motion of the ions must be known before the current density can be calculated. The area of the collector was 0.385 cm.² in

these experiments, but the surface of the sheath was often two or three times that area.

Table I. gives positive ion current data taken from two widely different sets of experiments. They illustrate the effect of the balancing of electron current density against concentration of Hg molecules, for in the second set of data, at lower pressure than the first set, the positive ion currents are decreased near the grid and increased far away from it. All voltages given in the table are measured from the cathode.

Effect of a Magnetic Field.—In explaining that the tip of a glow cannot be a narrow point because positive ions could not be produced at a sufficiently rapid rate in an electron stream that is very narrow, it was assumed that electron impact is essential for this ionization, and that radiation alone is not sufficient. This assumption was the result of a demonstration by Mr. Stead of the effect of arbitrarily halting the electrons earlier in their course by means of an ordinary bar magnet. Sir J. J. Thomson* has tried the effect of stopping the stream of electrons into the side-arm of a cold cathode discharge-tube by means of a powerful electromagnet placed outside the tube, and finds that the glow extends along a side-arm 50 cm. long with a brightness which does not seem much affected by the magnetic field, although it is extinguished locally in a short layer opposite the magnet. But although this shows that in the intense high-voltage discharges of a cold cathode tube there is sufficient energy of radiation to maintain the glow in a region from which the electron stream has been debarred, there was every indication that this was not the case in the low voltage glows under discussion; for it always happened that when an ordinary bar magnet was brought close to the tube, the glow contracted and could not be excited beyond the point opposite which the magnet was held.

If, however, a much weaker magnetic field is applied to the tube, such that the curved path along which the electrons are made to travel approaches the positive ion sheath which constitutes the boundary of the glow at an angle which is too small to enable the electrons to penetrate to the wall against the retarding field which they meet when they reach this boundary, Langmuir's theory shows that they will be specularly reflected back into the glow. In this case the magnetic field does not succeed in halting the passage of electrons down the tube, but only curves the path into a

* Thomson, Phil. Mag. xlviii. p. 1 (1924).

TABLE I.—Currents with Collector at Negative Potentials in Mercury Glows.
Disk Collector 0.70 cm. in diameter.

Temp. °C.	Grid Volts.	Grid Current (milliamps.).	Collector Volts.	Collector Current (microamps.).				
				10 cm.	25 cm.	40 cm.	55 cm.	70 cm.
17.6	60	30	-71.0	-63.0	-33.2	-21.0	-12.5	-7.8
			-60.7	-60.5	-31.7	-20.0	-11.9	-7.5
			-50.8	-58.0	-30.2	-19.0	-11.3	-7.1
			-40.8	-55.2	-28.7	-18.0	-10.7	-6.8
			-32.4	-53.0	-27.5	-17.2	-10.2	-6.5
			-24.4	-50.2	-26.2	-16.3	-9.7	-6.1
			-16.2	-46.2	-24.0	-15.2	-9.1	-5.8
			-8.0	-37.5	-20.0	-13.2	-8.0	-5.2
			-4.0	-28.5	-16.0	-11.3	-7.2	-4.7
			0	-21.5	-9.7	-8.4	-5.8	-4.1
			-71.0	-37.0	-27.1	-22.2	-17.3	-14.5
			-60.9	-35.3	-26.0	-21.2	-16.5	-13.8
			-50.8	-33.5	-24.7	-20.2	-15.7	-13.2
			-40.7	-30.9	-23.5	-19.1	-14.9	-12.5
			-32.4	-27.9	-22.1	-18.0	-14.1	-11.9
7.9	60	20	-24.3	-23.5	-20.0	-16.7	-13.0	-11.0
			-16.2	-17.0	-16.2	-14.2	-11.0	-9.5
			-12.0	-12.7	-12.7			
			-8.0	-7.2	-7.7	-8.5	-6.2	-6.1
			-4.0	-2.0	0	-2.7	-2.1	-3.0
			0	+17.0	+11.5	+6.2	+4.0	+1.7

series of arcs of a circle, the outline of the path traced out being that of a series of scallops with their cusps pointing toward the wall. The earth's magnetic field is an important instance of this effect. Calculation shows that the horizontal component of this field, of intensity approximately 0.185 gauss, is sufficient to bend the path of 60-volt electrons moving in a vertical direction into a path with radius of curvature 141 cm. This is by no means negligible in comparison with the dimensions of the tube. An electron that is shot into a glow 3 cm. in diameter, with a path that originally follows the axis, and is deflected at once along an arc of this radius of curvature, will meet the boundary of the glow at a distance of 20.5 cm., and, on the theory of specular reflexion at the boundary, will meet it again 41 cm. farther along the tube (distances being measured from the cathode and parallel to the axis). At each reflexion the path will make an angle of $8^{\circ} 22'$ with the boundary. The length of the path will be increased 0.3 per cent. over what it would have been if the electron had followed the axis.

Experiments were made which bear out the reasoning that the wall field causes electrons to continue streaming along the glow even in the presence of the earth's magnetic field, and that if their mean path is increased by being curved it is increased only very slightly. A tube 80 cm. long, which was evacuated by a charcoal tube with liquid air so that it could be moved about, was set in the direction of the earth's magnetic field, and was then set perpendicular to this direction, while the length of the glow was measured for different voltages. No difference could be detected between the two positions by this means. No attempt was made in taking any of the data in this paper to employ means to counteract the earth's field.

Experiments beyond the Glow.

The data plotted in fig. 3 and fig. 4 yield values for electron currents as the algebraic difference of total current and estimated positive ion current. But electron currents can be measured by themselves if the collector is stationed in the dark region beyond the glow. Current-voltage plots obtained with the collector 4 or 5 cm. beyond the tip show that with the collector at negative potentials the current was practically zero; the values actually measured were of the order of 0.2 microamp., and may have been photoelectric currents. With decreasing negative potentials the current curve started upward from zero at precisely the same voltage at which curves taken with the collector *inside* a similar glow

had started to rise, but rose to not nearly such high values. The current varied exactly with the three-halves power of the voltage, if the voltage was measured from the potential at which the curve first began to rise. This current-voltage relationship was measured in one instance up to +140 volts from the cathode. The glow, which in this instance was operating at 18 volts, appeared entirely unaffected by the presence of an electrode at 122 volts higher potential only 5.5 cm. away, which at this voltage was drawing 27.5 microamperes of electron current across the intervening space.

In these experiments the tip of the glow acts, in effect, as a nearly plane thermionic emitter, at a potential which is that of the grid, and at a very high temperature, since the electrons have suffered so wide a scattering of energy as they passed through the glow. However, when the ordinary space-charge equation for thermionic current between parallel planes is corrected for the initial velocities of electrons at a high temperature *, it gives a value for the current which is no longer exactly proportional to $V^{3/2}$. The relationship established by these data awaits further mathematical analysis.

Method of measuring Mean Free Paths.

A common method of measuring the mean free path of particles in a gas is to project the particles with equal velocity into the gas and determine the number of them which arrive per unit time at measured intervals along the path. Then, if N_0 is the initial number projected and N the number arriving at any distance d , the mean free path λ is given by

$$N = N_0 e^{-d/\lambda}.$$

The picture that has been given of the action taking place suggests that some of the electrons travel long distances down the tube without making a collision. It should therefore be possible, by making suitable assumptions with regard to the singling-out of electrons of the same velocity, to use data similar to those shown in fig. 4 to arrive at a value for the mean free path of electrons through ionized mercury vapour.

Experiments with Back Collector.—Before this could be done it was necessary to prove that the electrons to be dealt with actually came directly from the cathode, and were not simply drawn out of the concentration of electrons of random motion in the general glow. Langmuir describes

* Langmuir, Phys. Rev. xxi. p. 419 (1923).

an experiment using a disk-shaped collector mounted in a plane *parallel* to the direction of his electron beam, in which he finds that with the collector in this position the group of electrons of highest energy are absent from his current-curves, although other groups are present in exactly the same quantities as with the collector mounted in the usual plane, i. e. *vertical* to the path of the beam. He calls this group of electrons of highest energy "primary electrons," and defines them as being "those which reach the collector with a large part of the momentum which they acquired in passing through the positive ion sheath" around the cathode. They are the group which undergo scattering of energy. He concludes from his experiment that the primaries move mainly in one direction, while the other groups, which contain the vast majority of the electrons in the discharge, move mainly in all directions.

An adaptation of this idea was employed for the purposes of the present experiments, to find out whether the same distinction between primaries and other electrons holds at 60 cm. from the grid that Langmuir found at 3 or 4 cm. A collector was made from a nickel disk of the same diameter (0.7 cm.) as the one previously used, but completely reversed, with the insulated back toward the cathode; a narrow tongue extending from the edge of the disk was bent back and fastened to the support wire, and then encased in glass. This collector will be called the "back collector," and the one used in all other experiments the "front collector."

The first data obtained with the back collector are illustrated by Curve A in fig. 5(a). These were taken with the back collector used in exactly the same way that the front collector had been used. It was found that the primary current received at +10 volts was reduced to 28 per cent. and at +20 volts to 29 per cent. of what it had been with the front collector under exactly the same glow conditions, whereas the currents of electrons of low energy received near the glow potential, and the positive ion currents, were very nearly the same as before. Though this made it appear certain that the primary electrons were moving mainly in one direction, away from the cathode, the fact that 29 per cent. of the primaries still reached the collector was not wholly satisfactory to the argument. It seemed likely that, since the collector was only 18 cm. from the end of the tube, these might be electrons which had shot straight past the collector on their path *down* the tube, but were then turned back at the end of the tube since

there was no other electrode there to receive them, and returned to the collector.

Fig. 5.

Current-Voltage Plots for Different Collectors in the same Glow.

i_c is collector current.

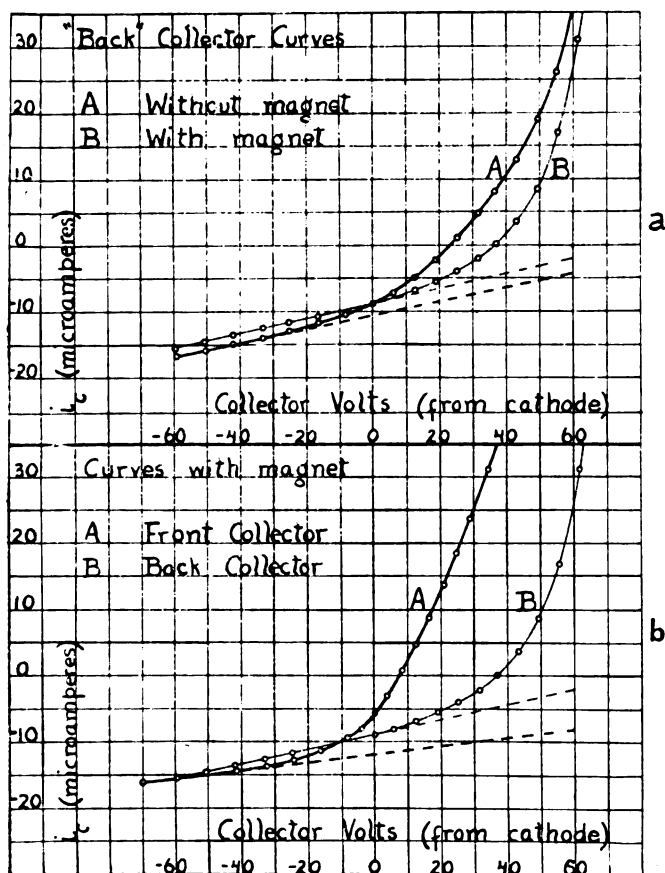
Area of each collector 0.385 cm^2

Distance of each collector 60 cm.

Grid current 30 milliamperes.

Grid potential 75 volts.

Temp. 12.0°C .



In order to test this theory an experiment was tried to see if it was possible to prevent their return by driving them into the walls with a small bar magnet outside the tube, held at a position 10 cm. below the collector. In this position it would not affect them until they had passed the collector; and if their velocities were not in one direction,

it should affect them no more than it did the electrons of low energy which were known to have random velocities. Curve B in fig. 5 (*a*) shows the result of the experiment. The magnet was placed by trial in the position near the tube which gave the greatest current reduction; the current is measured in each case by the difference between the solid and the dotted line. It is seen that the positive ion currents are not very different in the two cases, and above +50 volts the lower curve mounts rapidly toward the upper curve (they meet at +69 volts), showing that the currents of random electrons are the same; but the primary current has been reduced to one-fifth its previous value.

Curve B is plotted again in fig. 5 (*b*) for comparison with the curve of fig. 3, which was taken with the front collector under identical glow conditions. For the sake of comparison this second curve was taken with a magnet also, fixed in the same position; as one would expect, a magnet lower than the collector had no effect upon the currents in this case. The curves show that the current is now reduced to 3.7 per cent. at +10 volts and 6 per cent. at +20 volts. A percentage increase above +10 volts does not necessarily mean that more *primary* electrons are reaching the collector, for Langmuir has shown that there is present in these discharges a small number of electrons of energy a little less than the primaries, which differ from the primaries in having random velocities. He calls these the "secondary electrons," and suggests that they result from collisions of primary electrons with gas molecules.

In addition to establishing the fact that the primary electrons which reach a collector at a distance of 60 cm. come from the direction of the cathode, these data give some knowledge of the sort of path which they may follow. It has been pointed out that an electron which takes a path making an angle with the axis is not thereby removed from the primary current stream unless the angle is wide enough to give the electron a radial velocity sufficient to enable it to reach the wall. If it approaches the boundary of the glow at an angle of only 45° , it must have twice the energy, and at an angle of 30° with the boundary it must have four times the energy that it would need in order to reach the wall at normal incidence. If it lacks this energy, it will be reflected from the boundary first on one side of the tube and then on another side, and will follow a zigzag path down the tube.

The Back Collector curve in fig. 5 (*b*) (Curve B) passes through zero current at +36.5 volts; in this experiment the potential of the glow was approximately 75 volts.

Therefore, even under the conditions of this experiment, which were most unfavourable for a collector surface, if insulated, to acquire a high negative charge, we find that when the collector became equivalent to an insulated surface, its negative potential with respect to the glow amounted to -38.5 volts. Only electrons with energies corresponding to 77 volts or more could reach it if they approached it at an angle of 45° . The relative numbers of these electrons present in the primary current appear from the Front Collector curve (A) in the same diagram; they are the currents received at -2 volts and higher negative voltages. Since actually the wall is in a better position than a back collector to receive electrons that will give it a negative charge, its retarding field will be at least as strong as the field in this illustration. Consequently, electrons with energies that correspond to a fall through the anode potential, or less, cannot reach the wall if they strike the glow boundary at an angle of less than 45° with the boundary surface. There is therefore a wide variety of zigzag paths that these electrons may travel. However, it follows from the same argument that the electrons which travel these paths will not contribute to the primary current that is measured at high retarding potentials, for a 75-volt electron that approaches a collector at an angle of 20° with the normal cannot move against a retarding field of more than 66.2 volts.

Assumptions with regard to Velocities.—Since it is now known that the electrons collected at “0 volts” come in nearly straight paths from the cathode, and since their high energy makes it improbable that they have lost any energy by inelastic collisions on the way, it only remains to question whether reasonable assumptions can be made with regard to singling out electrons of the same velocity, before proceeding to use measurements of primary electron currents to determine the electron mean free path. Langmuir concludes from his experiments on the scattering of primary electrons that the scattering must be due to a direct effect of the primary electrons themselves, and one which is confined to the region actually traversed by them. In addition, the extent of the scattering depends on the magnitude of the primary current; and if this current is small there is no scattering. With the primary current from a filament emitting 5 m.a. (milliamperes) at 50 volts, there was no effect of this kind greater than would be expected as a result of the initial velocities of the electrons and the voltage drop along the filament. Unfortunately the current-voltage

curves taken with a collector at long distances from the cathode do not allow the magnitude of the complete primary current to be distinguished readily from the rest of the electron current, since the curves rise smoothly through the cathode potential with no distinguishing humps in that region. But conjecture shows that the primary current must become very small at increasing distances from the cathode, and is probably never large beyond a distance of 20 cm. away; and, in addition, some of the primary current flows directly to the grid without ever passing down the tube. In this case all the scattering will take place near the cathode, where by far the greatest current density is concentrated; and although the actual grid current is higher than Langmuir's (*i. e.* 20 m.a. or 30 m.a. compared to the 5 m.a. quoted above), the primary current at a moderate distance from the cathode will be no greater in a 20-m.a. discharge than Langmuir measured close to his cathode in a 5-m.a. discharge. On this theory the primary electrons, after passing a distance of a few cms. beyond the grid, will proceed along the tube with unchanged energy until they meet with an inelastic collision. With this assumption it is possible to interpret the current received by the collector at a given voltage when the collector is placed at different distances along the tube, as corresponding to a group of electrons of the same axial velocity. Obviously, only voltages lying in the range where primary electrons are the only electrons collected are suitable for these measurements.

The mean free path λ , that will be calculated from the values of the primary electron current at measured intervals along the tube, will be the mean path between collisions measured in an axial direction; and if any of the electrons in this current follow a zigzag path, λ will need to be increased by a small factor to give the true mean length of path. To estimate the magnitude of this factor, it will be recalled that an electron which describes a zigzag inclined at 20° with the axis will need to have about 9 volts more energy than axial electrons (with 60 to 70 volts energy) in order to be included in the same group with them. Since the electrons that are measured are already near the limit of high energy, the number with that much additional energy is comparatively scant, and, moreover, the path difference at an angle of 20° is only 6.4 per cent., so the factor by which these will alter the average must be small. It may be roughly estimated to be not more than 3 per cent. The path increase caused by the earth's magnetic field has been shown to be negligible.

Similar reasoning shows that this method of measuring λ does not necessarily detect the occurrence of all collisions of electrons with gas molecules. An electron which loses energy, or which is deflected through a small angle without loss of energy, is thereby removed to a group of lower axial velocity. It will therefore be absent from the current measured at the voltage corresponding to the group to which it originally belonged, and its absence will lower the current unless its place is taken by an electron transferred by a similar mechanism from a group with higher axial velocity. Since the supply of electrons with higher energy is low, the chance that such a place will be filled is comparatively small. The chance that it will be filled by an inelastic collision is very much less than that it will be filled by an elastic collision deflecting through a small angle, since the axial velocity change involved is so much less in the latter case. Therefore λ obtained by a method which depends on measuring the fraction of electrons that are missing from a given group at successive intervals along a tube, can be interpreted as meaning fairly closely the mean path of electrons which make no collisions with gas molecules. Since the measurements may, however, include some electrons which have been deflected through very small angles by elastic collisions, the calculated values of λ may be somewhat too high to be accurate values of the mean free path which an electron will describe between collisions of *any kind* with gas molecules.

Data on Mean Free Paths.

The method of obtaining the data was to plot the current-voltage curves for a collector placed at five different distances along the axis of the tube, under identical glow conditions for each of the five curves, and then measure on the graph the electron currents at 0 volts, +5 volts, and +10 volts.

Since λ is given by

$$\lambda = \frac{x_2 - x_1}{\ln \frac{i_1}{i_2}},$$

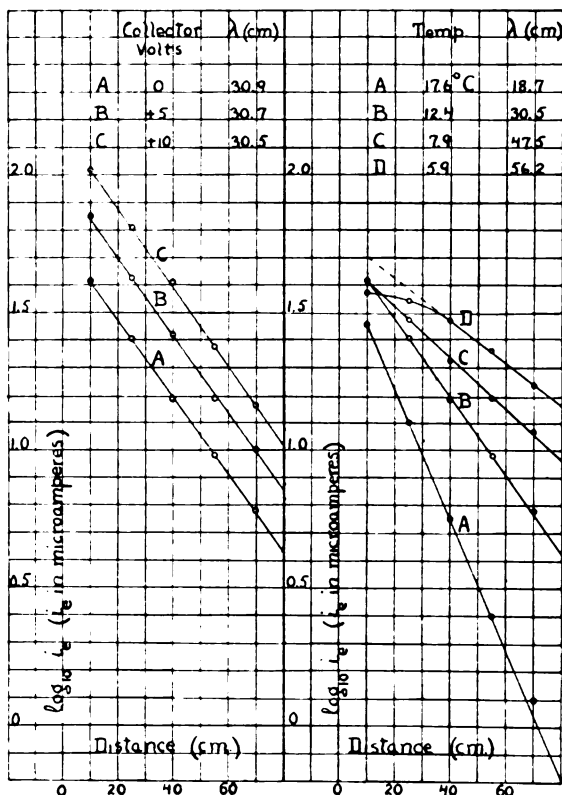
the logarithm of the electron currents was plotted against the distance in the manner illustrated in fig. 6. The points lie along straight lines when plotted in this way, and the values of λ calculated from the slopes are marked on each diagram.

Fig. 6 (a) shows that the points corresponding to 0 volts, +5 volts, and +10 volts lie along lines which have the same slope. This seems to be a justification of the assumptions

Fig. 6.

Plots of Logarithm of Electron Current against Distance from Grid.

- (a) For collector at three voltages in same glow at $12^{\circ}4$ C.
 (b) For collector at 0 volts (cathode voltage) in glows at four pressures of Hg vapour.



made with regard to scattering, since if the scattering process continued along the tube this relationship could hardly hold. The corresponding lines for each of the six sets of curves that were obtained show the three slopes equal in each case within 3 per cent. experimental error, except in the case of the curves at lowest pressure which will be described shortly.

Three sets of curves were taken at $12^{\circ}4$ C. to determine

whether λ is affected by the intensity of ionization in the glow or by the voltage of the electrons. The values obtained are tabulated below.

TABLE II.

Grid current milliamps.	Grid volts.	λ_0 volts. cm.	λ_{+5} volts. cm.	λ_{+10} volts. cm.	λ . Mean.
20	60	30.5	30.8	31.4	30.9
20	80	30.0	30.0	29.7	29.9
30	60	30.9	30.7	30.5	30.7

The values of λ differ among themselves by no more than the experimental error, so that it may be definitely stated that within this range of voltage, and of ionization intensity, λ is determined only by the mercury-vapour pressure. This is in agreement with the observations of Ramsauer * and of Mayer † on other gases, who found that λ varied markedly with the voltage only for slow-speed electrons, corresponding to voltages from about 1 to 25 volts for argon. Experiments were not carried beyond the range given in Table II., as these showed that if changes in λ existed they could not be measured with any certainty without pushing conditions beyond the limit of what a tungsten filament will stand for the length of time required to take these runs. A feature which concerns only the theory of the mechanism of scattering appeared in these data, in the fact that the actual points obtained in the three different cases were so nearly the same that an attempt at plotting a graph of the three lines at 0 volts results in only a confused tangle.

The task of obtaining the curves at different pressures of mercury vapour was enormously facilitated by the knowledge that conditions in the glow, other than the pressure, were of no consequence; for the same glow conditions are not suited to measurements at all pressures, and at 17°·6 C. it was imperative to run the filament at 30 m.a. emission in order to obtain enough electrons to measure at the further end of the tube, whereas at 5°·9 C. this emission was too high. A curve from each set at different temperatures is shown in fig. 6 (b); the two at higher temperature were taken at 30 m.a., and the two at lower temperature at 20 m.a. grid current. All four were at 60 volts grid potential: this is the lowest value at which the glow can generally be forced

* Ramsauer, *Ann. d. Phys.* lxiv. p. 513 (1921), lxvi. p. 546 (1921), lxxii. p. 345 (1923).

† Mayer, *Ann. d. Phys.* lxiv. p. 451 (1921).

past a collector at 70 cm. distance so as to have the collector completely surrounded by the glow.

The four lines in fig. 6 (*b*) all correspond to a collector at 0 volts; that is, connected directly to the negative end of the cathode. The three at higher temperatures are straight, with slopes corresponding to the pressure of saturated mercury vapour at these temperatures; the line at 5°·9 C. curves toward lower values at the upper end. This is taken to mean that when this pressure is reached the primary current has increased to such a value that scattering is not completed close to the filament, but continues for some distance along the tube. This would have the effect of scattering more electrons into the class with velocities corresponding to 0 volts by the time the beam had travelled part way down the tube, than there were in this class when the beam passed a collector stationed at 10 cm. from the grid; and the curve indicates that this may be just what takes place. Although a change of 2°·0 C. seems small to allow this effect to make its appearance between 7°·9 C. and 5°·9 C., the plots show that a considerable increase in primary current has been able to take place in just this range.

Values of λ compared with Pressure of Mercury Vapour.

Table III. gives the values of λ determined in the manner that has been described, with the corresponding pressures of mercury vapour, for the four temperatures that were investigated. The mercury-vapour pressures were calculated from Knudsen's * equation :

$$\log p = 10.5724 - 0.847 \log T - \frac{3342.26}{T},$$

where p is measured in mm. of Hg. The majority of the determinations of mercury-vapour pressure at low temperatures made by Knudsen and other experimenters agree fairly closely with this formula. λ is in each case the mean of the values obtained at the three different collector potentials.

TABLE III.

Temp.	λ .	Pressure.	$p\lambda$.
5.9° C.	56.2 cm.	0.00329 mm.	0.0185
7.9	47.5	.000398	.0189
12.4	30.5	.000605	.0185
17.6	18.7	.000966	.0181

The fourth column shows that the product $p\lambda$ is nearly

* Knudsen, *Ann. d. Phys.* xxix. p. 179 (1909).

constant. From the mean value of $p\lambda$ we obtain a value for λ of 18.5 cm. at 0.001 mm. pressure. The estimated correction of 3 per cent. for zigzag paths would raise this λ to 19.1 cm.

The writer wishes to express her thanks to Sir Ernest Rutherford for his interest in this work, and to Mr. Stead, who set her to investigate the properties of long glows and gave her constantly the benefit of his experience. She is also indebted to Dr. Langmuir for important criticisms and suggestions in the course of writing this paper.

XV. *On the Explanation of Spectra of Metals of Group II.*

—Part II. By P. K. KICHLU and M. SAHA, D.Sc., F.R.S., University of Allahabad, Allahabad (India)*.

IN a previous paper one of us † has discussed the origin of the higher Rydberg sequence terms in the normal spectra of elements of group II. It is well known that besides these normal terms all these elements give a number of anomalous terms. They were noticed by Rydberg ‡ in 1894 in the spectra of Ca and Sr, and Popow § discovered similar groups in the spectra of Ba and Al in 1915. In 1921, Götze || interpreted these groups as a transition between the normal p -group and another group which he called p' (sometimes also called \bar{p} , which notation we shall follow. That the \bar{p} -group was essentially of the same nature as the ordinary p was made clear from investigation of the Zeeman effect of these groups.

Since this time numerous groups of dashed (or barred) terms have been discovered in the spectra of elements of higher groups; but the first indication of the origin of these terms was given by Russell and Saunders ¶, and independently by Wentzel **. Russell and Saunders discovered other groups of $p\bar{p}$ and $d\bar{d}$ combinations in spectra of Ca, Sr, and Ba. These \bar{p} and \bar{d} terms are sometimes negative, and the above-

* Communicated by the Authors.

† M. N. Saha, *Phil. Mag.*, June 1927.

‡ Rydberg, *Wied. Ann.* lii. p. 119 (1891).

§ Popow, *Ann. der Physik*, Bd. xlv. p. 147 (1914).

|| Götze, *Ann. der Physik*, Bd. lxvi. p. 285 (1921).

¶ Russell and Saunders, *Astrophysical Journal*, lxi. p. 38 (1925).

** Wentzel, *Phys. Zeits.* xxiv. p. 106 (1923); xxv. p. 182 (1924).

mentioned authors noted that if a certain number was added to these terms they formed approximately a Rydberg sequence. This number was approximately 13700 in the case of Ca, which is about the same as the difference between the values of the fundamental 2S -term of Ca^+ and the next term in order of value, viz. 2D . From this fact the above-mentioned authors concluded that the anomalous terms arise when the stationary electron of Ca is in the metastable M_2 -level.

In this investigation it will be shown that the conclusion of these authors regarding the origin of \bar{p} -terms is correct in the case of Ca, Sr, and Ba; but from this it is not safe to draw any general conclusion regarding the nature of the dashed terms. As was pointed out in the note on the spectrum of Neon* by the senior author, whenever from any particular distribution of electrons in potential orbits F, D, P terms simultaneously arise, they must then have the same combinatory powers, so that if F and P are treated like ordinary terms, D must be dashed. But we can also dash F and P and treat D as an undashed term. It is purely a matter of convention, in which we have to be guided by our previous knowledge of the history of the spectrum of the element.

Origin of $PP\bar{P}$ -Terms in the Spectrum of Mg, Zn, Cd, etc.

As Bowen† and Millikan have pointed out, $PP\bar{P}$ -terms are known in the spectra of Mg, Zn, and Cd, for which the metastable level of the ionized element is not 2D , but 2P . Bowen and Millikan, by their hot-spark method, were able to discover $PP\bar{P}$ groups in the spectra of Be, B^+ , C^{++} , N^{+++} , O^{++++} , and in Al^+ , Si^{++} , P^{+++} , S^{++++} , Cl^{+++++} , which have got a structure similar to that of Mg. They discovered the most interesting laws regarding the values of these $PP\bar{P}$ -groups, and showed theoretically as well as experimentally that the values of these $PP\bar{P}$ -groups were approximately the same as the value of the fundamental line (${}^1S-{}^1P$) of these elements. Sawyer and Bees, in a note to 'Nature' of Dec. 26, 1925, however, find that in the case of Zn and Cd the values of $PP\bar{P}$ -groups are the mean between the values of (${}^1S-{}^1P$) of the normal element and ${}^2S-{}^2P$ of the ionized element. We shall not dwell upon Bowen and Millikan's explanation of

* M. Saha, Phil. Mag.

† Millikan and Bowen, Phys. Rev. xxv. p. 150 (1925).

more appropriate for expressing actual facts than Bohr's representation of terms by $3S$ (for Mg, M_{11}), $4S$ (for Ca, same as N_{11}), etc., though the latter method of representation has the merit of giving a unitary representation to the X-ray levels as well as optical levels.

The normal terms of Mg are therefore due to combinations :

- (a) $M_1 M_1$ (both the electrons in M_1) giving 1S_0 only, as first pointed out by Pauli*.

$M_1 N_1$, $M_1 O_1$, $M_1 P_1$, ... will give higher Rydberg sequences of 1S_0 -term, and a sequence of 3S_1 -terms beginning with 2^3S_1 (from $M_1 N_1$ in the case of Mg).

- (b) $M_1 M_2$ (one electron is in M_1 , the running electron is in M_2).

Terms obtained : 1P , 3P .

$M_1 N_1$, $M_1 O_2$, $M_1 P_2$, ... give higher Rydberg sequence terms to this set of singlet and triplet P's. The P-sequence begins with the total quantum number 2.

- (c) $M_1 M_3$ (the running electron in M_2).

Terms obtained : 1D , 3D .

$M_1 N_3$, $M_1 O_3$, $M_1 P_3$, ... give the Rydberg sequence. The D-sequence will begin with the total quantum number 3.

In the case of Ca,

- (a) $N_1 N_1$... give us 1S_0 , and
 $N_1 O_1$, $N_1 P_1$, ... give us the 1S and 3S series.

- (b) $N_1 N_2$ give us the first 1P and 3P terms, and
 $N_1 O_2$, $N_1 P_2$ the higher 1P and 3P Rydberg terms.

In the (c) combination the first combination is $N_1 M_3$, and not $N_1 N_3$. As the M_3 -level has at least the same order of value as N_2 , $N_1 M_3$ will give us 1D and 3D terms of the same order of value as the first 1P and 3P terms. This explains the occurrence of large D-terms in the spectrum of Ca, and *mutatis mutandis* in Sr and Ba. Thus in Ca, Sr, and Ba the D-sequence will begin with 2, and not with 3 as in Mg.

If we write out the structure diagrams for Zn and Cd, we see that the normal spectrum will be exactly like that of Mg. No D-terms comparable in value to the first P-terms will occur, and the sequence will begin with the total quantum number $n=3$.

* W. Pauli, Jun., *Zs. für Physik*, Bd. xxxi. p. 765 (1925).

Structure Diagram for Zn (30).

$$\begin{array}{ccccccc} K_1 & & & & & & \\ 2 & & & & & & \\ & L_1 & L_2 & & & & \\ & 2 & 6 & & & & \\ & & M_1 & M_2 & M_3 & & \\ & & 2 & 6 & 10 & & \\ & & & N_1 & N_2 & N_3 & N_4 \end{array}$$

(Both electrons are in N_1 . The next transition is horizontally from N_1 to N_2 . M_2 is completely filled.) A number of anomalous terms is possible from the combination $9M_2, 2N_1N_2$, giving $^3F, ^3D, ^3P, ^1\bar{F}, ^1D, ^1P$, but it is not yet known whether they exist.

Structure Diagram for Cd (48).

$$\begin{array}{ccccccc}
 K_1 & & & & & & \\
 & L_1 & L_2 & & & & \\
 & 2 & 6 & & & & \\
 & & M_1 & M_2 & M_3 & & \\
 & & 2 & 6 & 10 & & \\
 & & & N_1 & N_2 & N_3 & N_4 \\
 & & & 2 & 6 & 10 & \\
 & & & & O_1 & O_2 & O_3
 \end{array}$$

(In normal case other electrons are in O_1 . Transition is horizontally from O_1 to O_2 , giving $O_1 O_2$ as the next state. N_3 is completely filled up. Here also the $9N_3 \cdot 2O_1 O_2$ combination is possible.)

In order to account for the anomalous terms, let us put one electron permanently in the next higher level and move the second electron through the next successive levels. In the case of Mg, Zn, and Cd there is no metastable level diagonally across the fundamental level. Thus, taking the case of Mg, the level M_1 will be kept entirely empty: one electron will be kept permanently at M_2 , the second electron will be moved successively through the $M_2, M_3, N_1, N_2, N_3, \dots$ levels. In Ca, however, the level next to the fundamental is M_3 , so that the fixed electron will be always at M_3 , and the running electron will move through the other possible levels, viz. N_1, M_2, N_2, \dots . For this reason the large D-terms which arise from the combination M_3N_1 may be considered as the first of the anomalous terms in Ca.

Anomalous Terms in Mg, Zn, Cd.

Let us now find out, by applying the combination rules of Pauli, Heisenberg, and Hund, the probable anomalous terms in the spectra of Mg, Zn, and Cd.

(a) $M_2 M_2$ give ${}^3\bar{P}_{0,1,2}$, 1D_2 , 1S_0 .

The P's will be dashed, because $M_1 M_2$ give us ${}^3P_{0,1,2}$, and transition is possible between $(M_1 M_2)$ and $(M_2 M_2)$.

Value of ${}^3\bar{P}_{0,1,2}$.

Let us consider the relative values of the following sequences for Mg :—

$M_1 M_2$ 1^3P	$M_1 N_2$ 2^3P	$M_1 O_2$ 3^3P	$M_1 P_2$ 4^3P	$M_1 Q_2$ 5^3P
$M_2 M_2$ $1^3\bar{P}$	$M_2 N_2$ $2^3\bar{P}$	$M_2 O_2$ $3^3\bar{P}$	$M_2 P_2$ $4^3\bar{P}$	$M_2 Q_2$ $5^3\bar{P}$

Taking corresponding pairs of higher Rydberg terms, say 5^3P and $5^3\bar{P}$, we find that the second electron is in both cases far out. The atomic residue will therefore exert, on the inner of the two valence electrons, approximately the same force in both cases. In other words, we can write symbolically

$$\begin{aligned} (5^3P \rightarrow 5^3\bar{P}) &= (M_1 Q_2) \rightarrow (M_2 Q_2) \\ &= (M_1 \rightarrow M_2) Q_2. \end{aligned}$$

The symbol in the last step denotes that the energy of the electron in the Q_2 position has the same value in both cases because it is far out, hence $5^3P - 5^3\bar{P} = (M_1 \rightarrow M_2)$ of the atomic residue. This atomic residue is, however, the Mg^+ electron, M_1 corresponds to the fundamental 2S of Mg^+ , and M_2 corresponds to the 2P of Mg^+ . We therefore arrive at the rule that for the higher terms

$$({}^3P - {}^3\bar{P}) \text{ of } Mg = ({}^2S - {}^2P) \text{ of } Mg^+.$$

When we pass on, however, to the lower terms like $2^3P - 2^3\bar{P}$, the influence of the atomic residue on the running electron can no longer be regarded as the same in both cases. Hence the above rule will not hold so well. Taking

$$1^3P - 1^3\bar{P} = (M_1 M_2 - M_2 M_2),$$

we find that the transition is obtained by moving one

electron from M_1 to M_2 , the other electron always remaining at M_2 , i. e.,

$$\begin{array}{ccc} M_1 & & M_2 \\ 1 & & 1 \dots \dots {}^3P_2 \\ & \rightarrow & 1, 1 \dots \dots {}^3P_1 \end{array}$$

The difference in energy may be assumed to be approximately the same as is required in the passage of the electron from $M_1 \rightarrow M_2$ from the $M_1 M_1$ -stage :

$$\begin{array}{ccc} M_1 & & M_2 \\ 1, 1 & & \dots \dots {}^1S_0 \\ & \rightarrow & 1 \dots \dots {}^3P_1, {}^1P_1 \end{array}$$

the difference being that in the first case the transition is with the stationary electron at M_2 , in the second case it is with the stationary electron at M_1 . Hence

$$\begin{aligned} 1 {}^3P - 1 {}^3\bar{P} & \text{ is } > {}^1S - {}^1P \text{ of the metal.} \dots \dots (A) \\ \text{and} & < {}^2S - {}^2P \text{ of the ionized metal.} \dots \dots (B) \end{aligned}$$

Rule (A) is given (with = instead of >) by Bowen and Millikan*, whose arguments are almost the same as that given here: rule (B) is given by Sawyer and Beese, who make ${}^3P - {}^3\bar{P}$ equal to the mean value of

$$({}^1S - {}^1P) \text{ of } M \text{ and } ({}^2S - {}^2P) \text{ of } M^+$$

for Zn and Cd. The validity of the above rules will be apparent from the following table:—

TABLE I.

Element.	Value of P—P.	${}^1S - {}^1P$ of M.	${}^2S - {}^2P$ of M^+ .
Mg	35982	35051	35669
Zn	47894	46745	48482
Cd ..	44088	43692	44135
Hg	?	54099	?
Al ⁺	56690	59845	53918
Si ⁺⁺	76986	82878	71280
P ⁺⁺⁺	97037	105190	88649
S ⁺⁺⁺⁺	116985	127144	105266
Cl ⁺⁺⁺⁺⁺	136928	148949	123001

The figures in Table I., as well as theoretical arguments, show that Sawyer and Beese's rule represents facts more accurately than Millikan and Bowen's rule. The 1D_2 , and 1S_0 -terms expected from $M_2 M_2$ -combination has also been recently obtained by one of us in Mg.

* Bowen and Millikan, Phys. Rev. vol. xxv. p. 150 (1925).

Higher negative terms may be obtained by keeping the first electron at M_2 , and allowing the other electron to run through the higher levels M_3, \dots . Though they are not yet known, one typical example may be given:—

Combination $M_4 M_3$ will give us

$$\begin{array}{ccc} {}^3F & {}^3D & {}^3P \\ {}^1F & {}^1D & {}^1P. \end{array}$$

3F will have the highest (*i. e.* lowest negative) value. They may be expected to have the value 1D of $Mg - 35000$, *i. e.* about -20000 for Mg . If they exist, they will combine with the ${}^1D, {}^3D$ terms of Mg .

Origin of Anomalous Terms in Ca, Sr, and Ba.

Bowen and Millikan have pointed out that $P \bar{P}$ -multiplets of the above description have not yet been discovered in the spectra of Ca, Sr , and Ba . The fact receives a clear explanation when we look at the structure diagrams of these elements.

Structure Diagram for $Sr (38)$.

2 K				
8 L				
18 M				
	N_1	N_2	N_3	N_4
	2	6		
		O_1	O_2	O_3
		2		

(Normal terms are obtained by keeping one electron permanently at O_1 and allowing the other to run through O_1, O_2, N_3, \dots ; for anomalous terms, keep the electron at N_2 and let the other run through the levels O_1, N_3, O_2 , etc.)

Structure Diagram for $Ba (56)$.

2 K				
8 L				
18 M				
	N_1	N_2	N_3	N_4
	2	6	10	
		O_1	O_2	O_3
		2	6	
			P_1	P_2
			2	

(To get the normal terms, one of the two electrons is placed at P_1 and the other moves through $P_1, N_4, O_3, P_2, \dots$. The $N_1 P_4$ combination, which is expected to give a large 1F and 3F term, is not yet known with certainty.)

For Ca M_2 is the level next in value to N_1 , and we keep the first electron in this level. The anomalous terms are then obtained by allowing the other electron to run through the other possible levels. We get the following combinations:—

(a) $M_2 M_2$.

Since both electrons are in M_2 -orbit (Pauli's rule will apply), we obtain :

$$^3\bar{F}, ^3\bar{P}, ^1G_4, ^1D_2, ^1S_0.$$

State ($N_1 M_2$) giving $^3D, ^1D$ will not combine with $M_2 M_2$, because $N_1 \rightarrow M_2$ is forbidden. Hence the D-terms arising from this combination will be of the same nature as the D-terms from $M_2 M_2$, i. e. they are not dashed. This enables us to fix the nature of the other terms. $M_2 N_2, M_2 O_2, \dots$ will give us the higher members of the group :

$$\begin{vmatrix} ^3G & ^3\bar{F} & ^3D & ^3\bar{P} & ^3S \\ ^1G & ^1\bar{F} & ^1D & ^1\bar{P} & ^1S \end{vmatrix}.$$

(b) $M_2 N_2$.

This combination gives us

$$\begin{array}{ccc} 2^3F & 2^3\bar{D} & 2^3P \\ 2^1F & 2^1\bar{D} & 2^1P. \end{array}$$

$M_2 O_2, M_2 P_2, \dots$ gives the higher members of the sequence.

(c) $M_2 O_1$.

This combination give us

$$3^3D, 3^1D.$$

These terms will form higher Rydberg sequence of displaced type with the large $^3\bar{D}$ and $^1\bar{D}$. Evidence of their existence has been obtained in the spectrum of Ba. For reasons stated before

$$1^3\bar{D} \text{ of Ca} = 1^3P \text{ of Ca} + ({}^1S - {}^3D) \text{ of Ca} \quad . \quad . \quad (A)$$

$$\text{or} \quad + ({}^1S - {}^1D) \text{ of Ca} \quad . \quad . \quad (B)$$

Relation (A) will be approximately correct, but (B) indicates only an upper limit. The same argument will hold for Sr and Ba. The values of ${}^2S_1 - {}^2D_3$ for Ca^+, Sr^+ and Ba^+ ,

202 Mr. P. K. Kichlu and Prof. M. Saha on the
and $^1S_1-^3D_2$ and $^1S_1-^1D_2$ for Ca, Sr and Ba are shown
below :—

TABLE II.

	M.		M ⁺ .
	($^1S-^3D_2$).	($^1S-^1D_2$).	$^2S_1-^2D_2$.
Ca	20350	21850	13650
Sr	18219	20149	14557
Ba	9215	11395	4884

M=neutral element ; M⁺=ionized atom of the element.

TABLE III.

State.	Present notation.	Russell & Saunders' notation.	Term values.					
			Ca.		Sr.		Ba.	
(a) M ₃ M ₃	$^3\bar{F}_{4, 3, 2}$	19077·9 19510·1 19990·3	432·2 480·2
	$^3\bar{P}_{2, 1, 0}$	<i>p'</i>	10753·0 10839·8 10887·1	86·8 47·3	10250·7 10525·5 10731·8	247·8 206·3	18110·5 18549·3 18820·3	438·8 271·0
	1S_0							
	1D_2	X	8584·9		8964·9		9929·0	
	1G_4							
(b) M ₃ N ₂	$^3F_{4, 3, 2}$	<i>f''</i>	13407·6 13485·9 13573·9	78·3 88·0	12006·0 12335·7 12658·5	329·7 322·8	18372·6 19082·1 19964·8	709·5 882·7
	$^3D_{3, 2, 1}$	<i>d'</i>	11045·3 11085·3 11112·0	40·0 26·7	9365·9 9543·4 9661·1	177·5 117·8	17049·8 17498·1 17837·6	448·3 339·5
	$^3P_{2, 1, 0}$	<i>p''</i>	9964·3 9969·1 9971·0	4·8 1·9	8588·5 8622·2 8633·0	33·7 10·8	16073·1 16325·5 16387·5	252·4 62·0
	1F_3							
	1D_2	Y	8767·0		9836·1		15213·4	
	1P_1			13475·2*	
(c) M ₃ O ₁	$^3D_{3, 2, 1}$			4526†	
	1D_2				

* Identified by Russell and Saunders, *loc. cit.*

† We have for Ba, $^3\bar{D}_{3, 2}-4526=12523·18$ (1), $12972·3$ (8 u);
 $b\ ^3F-4526=14556$ (6r).

In Barium we have followed Paschen's * identification of the D-term. According to Fowler† ${}^2S - {}^2D$ for $Ba^+ = 11990$.

A preliminary comparison with the new terms obtained by Russell and Saunders shows that the above conclusions are well verified. The detailed identification is shown in Table III.

Table III. shows that Russell and Saunders' f'' , p'' , and d' terms can be identified with the 3F , 3P , and 3D terms arising from the $M_3 N_2$ combination. In fact they observe that f'' and p'' are in all respects like ordinary f and p terms. They also follow the usual rule which has been brought to light by Hund ‡ and others, that when from the same combination F, D, and P terms arise, F is usually $> D > P$.

A number of singlet terms have been mentioned by Russell and Saunders, but their nature has not yet been clearly elucidated. We have therefore refrained from trying to identify them with singlet terms 1F_3 , 1D_2 , 1P_1 . But in the case of Ca, we can hazard the identification mentioned in Table III. Of these, $Y = {}^1F_3$ seems to be pretty certain. X may be put $= {}^1D_2$, but it seems to be very difficult to fix up the nature of the "x." Back § finds from Zeeman-effect data that "x" is not a singlet term, but a triplet term, 3F_2 . He has also given 3F_3 , 3F_4 . But he finds that the splitting factor g for Zeeman effect is different ($\frac{3}{2}$) in the case of 3F_2 from the value of g given by Landé's formula ($\frac{3}{2}$), and sees in this a justification of Landé's "Verzweigungs-prinzip." The nature of the large term W, or of Z also, cannot be fixed up from the present data. It may be added that Russell and Saunders have taken only those lines which are given by King from his furnace-spectra data. If the full list of arc lines is taken from Kayser and Konen's '*Handbuch der Spektroskopie*,' vol. vii., it is found that there are many lines yet to be classified.

Values of the Terms.

The identification is rendered more probable from the following theoretical considerations about their values:—

It will be seen that the Barium values of anomalous terms are much larger than Ca or Sr values. Further, the terms arising from $M_3 N_2$ combination have the same order of value as those arising from $M_3 N_1$ combination. Let us consider

* Paschen and Götze, '*Serienspektren*,' Chap. on Barium.

† A. Fowler, '*Series in Line-Spectra*,' p. 137 (1922).

‡ F. Hund, *Zs. für Physik*, Bd. xxxiii. p. 841 (1925).

§ Back, *Zs. für Physik*, Bd. xxxiii. p. 584.

the sequence of terms arising from the following pairs of combinations :—

$M_3 N_2$	$M_3 O_2$	$M_3 P_2$	$M_3 Q_2$	$M_3 R_2$
$1^1D, 3^1D$	$2^1D, 2^3D$	$3^1D, 3^3D$	$4^1D, 4^3D$	$5^1D, 5^3D$
$N_1 N_2$	$N_1 O_2$	$N_1 P_2$	$N_1 Q_2$	$N_1 R_2$
$1^1P, 3^1P$	$2^1P, 2^3P$	$3^1P, 3^3P$	$4^1P, 4^3P$	$5^1P, 5^3P$

Of the set of terms arising from $M_3 X_2$ we have taken only the D's. Compare the values of each corresponding pair in each vertical column.

Now,

$$\begin{aligned} M_3 R_2 &\rightarrow N_1 R_2 = (M_3 \rightarrow N_1) R_2 \\ &= (M_3 - N_1) \text{ of } Ca^+ \text{ approximately} \\ &= ({}^2S - {}^2D) \text{ of } Ca^+. \end{aligned}$$

$$\therefore 5^3D \text{ of } Ca = 5^3P \text{ of } Ca - ({}^2S - {}^2D) \text{ of } Ca^+. \quad \dots \quad (A)$$

The value of 3D and other terms like $f''(b^3F)$ arising from this level will therefore lie between the limits:

	${}^3P_2 - ({}^1S - {}^2D)$	${}^3P_2 - ({}^2S - {}^2D)$	Actual values.	
			f''	3D
For Ca	12139	20338	13485	11085
Sr.....	10888	16480	12335	9543
Ba	17120	23631	19082	17498

1^3D values are thus seen to be slightly lower than the lower limit, and $b1^3F$ values higher than the lower limit. Higher Rydberg terms to the above set have not yet been obtained in sufficient number to enable us to make a satisfactory comparison and to see whether a member like

$$5^3D = 5^3P - ({}^2S - {}^2D) \text{ of } M^+$$

also follows the expected order.

Values of Terms arising from $M_3 M_2$ -levels.

Compare, as before, the set of values arising from the combinations :

$M_3 M_2$	$M_3 N_2$	$M_3 O_2$	$M_3 P_2$	$M_3 Q_2$
1^1P^3P	$2^1P, 2^3P$	$3^1P, 3^3P$	$4^1P, 4^3P$	$5^1P, 5^3P$
$N_1 M_2$	$N_1 N_2$	$N_1 O_2$	$N_1 P_2$	$N_1 Q_2$
$1^1D, 3^1D$	$2^1D, 2^3D$	$3^1D, 3^3D$	$4^1D, 4^3D$	$5^1D, 5^3D$

By the same argument as before the values of the higher terms like $5^3\bar{P}$ will approximately be equal to

$$5^3\bar{D} - ({}^3S - {}^3D) \text{ of } M^+,$$

while the value of $1^3\bar{P}$ will be between $1^3\bar{D} - ({}^1S - {}^1D)$ of M and $1^3\bar{D} - ({}^3S - {}^3D)$ of M^+ . The following table shows the expected values of ${}^4\bar{P}$ compared to the limits calculated as above:—

	Limits.	${}^3\bar{P}$.
Ca.....	7106-15666	10839
Sr.....	7567-13159	10525
Ba.....	21419-27930	18549

The value of ${}^3\bar{P}$ in the case of Ca and Sr is approximately the mean of the limits. But the Ba value of ${}^3\bar{P}$ is less than even the lower limit.

The above comparison explains a feature of the Barium spectrum. The anomalous terms are much larger than the corresponding terms in Ca and Sr. It is easily seen that it is due to the smaller value of the shift numbers ${}^1S - {}^1D$ and ${}^3S - {}^3D$ in the case of Ba. The value of the terms arising from X_3Y_3 and X_3X_3 -levels are of the same order, since 3P and 3D terms have the same order of value. In Barium 3D is much larger than 3P , and we therefore find that the terms arising from X_3X_3 are much larger than the terms arising from X_3Y_3 .

The Rydberg Sequence of Anomalous Terms.

Rydberg sequence has been established satisfactorily up to the fifth term only in the case of $Ca^3\bar{P}$ terms. The comparison of values is given below:—

$1^3\bar{P}$.	$2^3\bar{P}$.	$3^3\bar{P}$.	$4^3\bar{P}$.	$5^3\bar{P}$.
10840	767	-4983	-8313	-10063
${}^3D - ({}^3S - {}^3D)$ 15306	-2097	-7090	-9359	-10649
${}^3D - ({}^1S - {}^3D)$ 7106				

Russell and Saunders find that if 13711 (${}^3S - {}^3D$) be added to the sequence of 3P terms, they form approximately a Rydberg sequence.

Existence of ${}^3\bar{F}$ -terms.

The most important group of terms from the combination M_3M_3 is ${}^3\bar{F}$, which is expected to be larger than ${}^3\bar{P}$, identified with certainty with Russell and Saunders' p' . But these

terms have not yet been identified. The cause is to be traced to its combinatory properties. It can combine with

$${}^3F \quad {}^1F \quad {}^3\bar{D} \quad {}^1\bar{D}$$

arising from combination ($M_3 M_2$), and with the triplet F of the normal spectrum and also with the $N_1 N_2$ terms (Ca). But the terms ${}^3F, {}^1F, {}^3\bar{D}, {}^1\bar{D}$ of combination $M_3 N_2$ have values very nearly equal to ${}^3\bar{F}$, i. e. the difference ${}^3\bar{F} - {}^3F$ would be very small; the lines, if they exist, would be in the far infra-red. Only in the case Ba can we expect 3F to have a sufficiently large value. We have not yet been able to identify the ${}^3\bar{F}$ terms without ambiguity, but the following identification may be provisionally given:—

	$\bar{F}_2(480.2)$ 19990.3	$\bar{F}_3(432.2)$ 19510.1	\bar{F}_4 19077.9
$3^3F_2=7426.8$	(1u) 12563.5		
$3^3F_3=7412.8$?	(2) 12097.3	(1r) 11665.4
$3^3F_4=7398.6$		(1) 12112.0	(6u) 11679.3

The combination with 3F of state $M_2 M_3$ ought to give us strong lines, but they would be hopelessly in the infra-red if these values of ${}^3\bar{F}$ prove to be correct. But we can take the higher Rydberg sequence terms of this 3F , for which Russell and Saunders give the values 4966.3, 4747.5, and 4558.6. We get the following multiplet:—

	\bar{F}_2 19990.3	\bar{F}_3 19510.1	\bar{F}_4 19077.9
$2b^3F_2=4966.3$	(1) 15024.1	(1) 14543.2	
$2b^3F_3=4747.5$?	(1) 14762.8	(1) 14330.5
$2b^3F_4=4558.6$?	?

Probably the last term, viz. 4558, has not been correctly identified, for we have failed to establish it from other sources. The reality of the ${}^3\bar{F}$ for Ba here given is strengthened by

the following further combinations:—

$$\begin{aligned} 19990.3 - q_1 &= 13305.2(1u), \\ 19510.1 - 3F_3 &= 13372.0(2), \quad 19510.1 - q_2 = 12270.0(2), \\ 19510.1 - q_3 &= 12311.2(2), \\ 19077.9 - q_3 &= 11880.9(1u). \end{aligned}$$

Though the existence of the ${}^3\bar{F}$ terms has not yet been established, except in the case of Ba, they form very prominent members in the spectra of Sc^+ , Y^+ , and La^+ . Here ${}^2\text{S} - {}^2\text{D}$ of M^+ (i.e. of Sc^{++} , Y^{++} , La^{++}) is negative, i.e. the ${}^2\text{D}$ -term is larger than ${}^2\text{S}$; hence terms which arise when the stationary electron is at M_3 are much larger than the terms arising out of the combinations N_1X : in other words, though the elements have a structure similar to that of the alkaline earths, the spectrum is just reversed, the anomalous terms become normal terms, and the normal terms become anomalous. Thus in Sc^+ , for which the structure diagram is the same as that for Ca, we have the following terms (since the absolute value is not known, the largest term is given the value 0: the values of the other terms are obtained by subtracting the number placed against each number from the value of the biggest term):—

Sc^+ .

State.	Terms.	Term values.
$\text{N}_1, \text{M}_3, \dots$	${}^3\text{D}$ ${}^1\text{D}$	0, 67.6, 177.8 ?
$\text{M}_1, \text{M}_3, \dots$	${}^3\bar{\text{F}}$ ${}^3\text{P}$	4802, 4883, 4987 12073.8, 12101.3, 12154.1
$\text{M}_3, \text{N}_2, \dots$	${}^3\text{F}$ ${}^3\bar{\text{D}}$ ${}^3\text{P}$	27440.9, 27602.7, 27841.4 27918.1, 28021.6, 28161.5 ?

Thus here ${}^3\bar{\text{F}}$ forms the second biggest set of terms. The same feature is observed in the spectra of Y^+ and La^+ †. The barium spectrum is intermediate in nature between the two groups, Ca and Sr on one hand, Sc^+ , Y^+ , La^+ on the other hand.

* S. Goudsmit, J. van der Mark, and P. Zeeman, Proc. Amst. vol. xxviii. p. 127.

† Y^+ -spectrum: Meggers, Journ. Opt. Sci. Am. vol. xii. p. 418 (1926).
 La^+ : Goudsmit, loc. cit. Goudsmit has apparently taken the terms in the reverse order.

XVI. *Note on the Motion of Fluid in a Curved Pipe.*
 By W. R. DEAN, M.A., *Imperial College of Science* *.

IN this paper the steady motion of incompressible fluid through a pipe of circular cross-section which is coiled in a circle is considered. It is found necessary to approximate by supposing that the curvature of the pipe is small, or that R , the radius of the circle in which the pipe is coiled, is large in comparison with a , the radius of the cross-section. The theory is in good qualitative agreement with experiments conducted by Prof. J. Eustice † on the stream-line motion of water in curved pipes. A quantitative comparison, however, requires a closer approximation than that of this paper; it is found that the theoretical results apply only if $n^2 a / 1440 R$, where n is the Reynolds' number, is small, while in all the experiments the value of this expression is greater than 1. It is probably for this reason that the interesting result established experimentally that at increased velocity of flow the curvature of the stream-lines is increased (so that they follow more nearly the line of the pipe) cannot be obtained from the theory at its present stage; however, an alternative explanation appears possible, and is given in § 13.

2. Fig. 1 shows the system of coordinates that has been found convenient in considering the motion of fluid through a pipe of circular cross section coiled in the form of a circle. The surface of such a pipe is an anchor ring, of which OZ in fig. 1 is the axis. C is the centre of the section of the pipe by a plane that makes an angle θ with a fixed axial plane. CO , the perpendicular drawn from C upon OZ , is of the length R , so that R is the radius of the circle in which the pipe is coiled. The plane through O perpendicular to OZ will be called the "central plane" of the pipe, and the circle traced out by C its "central line." P , any point of the section drawn, is at distance r from C , while CP makes an angle ψ with a line through C parallel to OZ . The position of P is then specified by the orthogonal coordinates r, ψ, θ . The surface of the pipe is given by $r=a$, a being the radius of any section. The components of velocity corresponding to these coordinates are U, V, W ; U is therefore in the direction CP , V perpendicular to U and in the plane of the cross-section, and W perpendicular to this plane. The general direction of flow will be taken to be the direction in which θ increases.

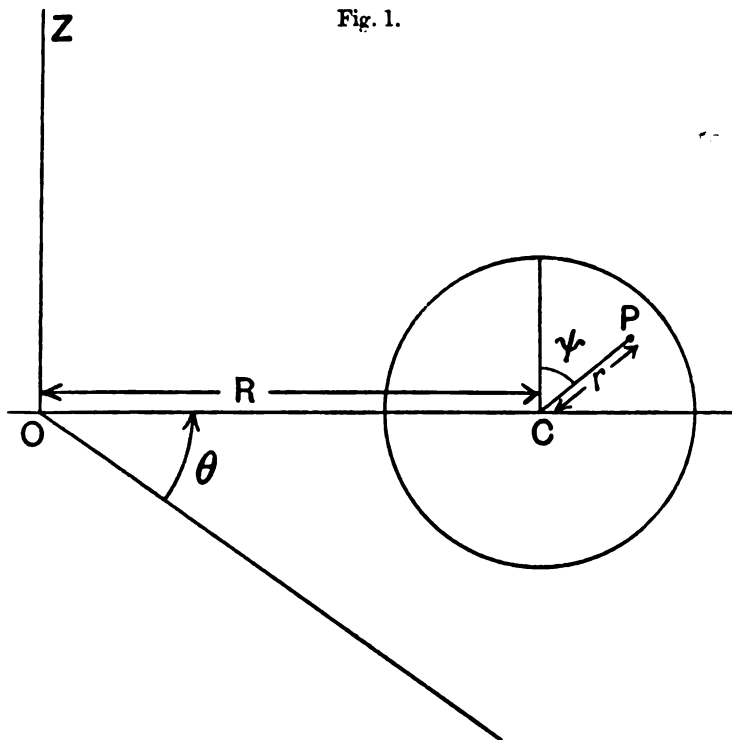
The motion of the fluid is supposed to be due to a fall in pressure along the pipe. There will be a fall in pressure if

* Communicated by Prof. S. Chapman, D.Sc., F.R.S.

† Proc. Roy. Soc. A, vol. lxxxv. p. 119 (1911).

fluid enters the pipe from a container at known pressure at one end and flows along the pipe to a container at lower pressure at the other end. Except near the ends, where

Fig. 1.



there is certain to be some irregularity of flow, we may expect a steady motion in which U , V , and W (but not P , the pressure) are independent of θ .

The equations for such a motion are these :

$$U \frac{\partial U}{\partial r} + \frac{V}{r} \frac{\partial U}{\partial \psi} - \frac{V^2}{r} - \frac{W^2 \sin \psi}{R + r \sin \psi} \\ = -\frac{\partial}{\partial r} \left(\frac{P}{\rho} \right) - \nu \left[\left(\frac{1}{r} \frac{\partial}{\partial \psi} + \frac{\cos \psi}{R + r \sin \psi} \right) \left(\frac{\partial V}{\partial r} + \frac{V}{r} - \frac{1}{r} \frac{\partial U}{\partial \psi} \right) \right], \quad \dots (1)$$

$$U \frac{\partial V}{\partial r} + \frac{V}{r} \frac{\partial V}{\partial \psi} + \frac{UV}{r} - \frac{W^2 \cos \psi}{R + r \sin \psi} \\ = -\frac{1}{r} \frac{\partial}{\partial \psi} \left(\frac{P}{\rho} \right) + \nu \left(\frac{\partial}{\partial r} + \frac{\sin \psi}{R + r \sin \psi} \right) \left(\frac{\partial V}{\partial r} + \frac{V}{r} - \frac{1}{r} \frac{\partial U}{\partial \psi} \right), \quad \dots (2)$$

and

$$\begin{aligned}
 & U \frac{\partial W}{\partial r} + \frac{V}{r} \frac{\partial W}{\partial \psi} + \frac{UW \sin \psi}{R+r \sin \psi} + \frac{VW \cos \psi}{R+r \sin \psi} \\
 &= -\frac{1}{R+r \sin \psi} \frac{\partial}{\partial \theta} \left(\frac{P}{\rho} \right) + \nu \left[\left(\frac{\partial}{\partial r} + \frac{1}{r} \right) \left(\frac{\partial W}{\partial r} + \frac{W \sin \psi}{R+r \sin \psi} \right) \right. \\
 &\quad \left. + \frac{1}{r} \frac{\partial}{\partial \psi} \left(\frac{1}{r} \frac{\partial W}{\partial \psi} + \frac{W \cos \psi}{R+r \sin \psi} \right) \right]. \quad (3)
 \end{aligned}$$

The fluid is supposed incompressible, so that the equation of continuity is

$$\frac{\partial U}{\partial r} + \frac{U}{r} + \frac{U \sin \psi}{R+r \sin \psi} + \frac{1}{r} \frac{\partial V}{\partial \psi} + \frac{V \cos \psi}{R+r \sin \psi} = 0. \quad (4)$$

These four equations reduce to equations for the corresponding motion in spherical polar coordinates if we write $R=0$, and to equations in cylindrical coordinates if we write $1/R=0$ and $\partial/R\partial\theta=\partial/\partial z^*$.

3. We now introduce the assumption that the curvature of the pipe is small: that is, that a/R is small. If the pipe were straight a/R would vanish, and the equations could be satisfied by

$$U=V=0, \quad W=A(a^2-r^2), \quad P/\rho=Cz,$$

where A and C are constants, and z is the distance (measured along the central line) of any section of the pipe from a fixed section. For the slightly curved pipe we assume

$$U=u, \quad V=v, \quad W=A(a^2-r^2)+w, \quad P/\rho=Cz+p/\rho, \quad (5)$$

where u , v , w , and p are all small and of order a/R .

If terms of order a^2/R^2 are ignored, the equation of continuity is

$$\frac{\partial u}{\partial r} + \frac{u}{r} + \frac{1}{r} \frac{\partial v}{\partial \psi} = 0, \quad (6)$$

while the first two equations of motion become

$$-\frac{A^2(a^2-r^2)^2}{R} \sin \psi = -\frac{\partial}{\partial r} \left(\frac{p}{\rho} \right) - \frac{\nu}{r} \frac{\partial}{\partial \psi} \left(\frac{\partial v}{\partial r} + \frac{v}{r} - \frac{1}{r} \frac{\partial u}{\partial \psi} \right), \quad (7)$$

and

$$-\frac{A^2(a^2-r^2)^2}{R} \cos \psi = -\frac{1}{r} \frac{\partial}{\partial \psi} \left(\frac{p}{\rho} \right) + \nu \frac{\partial}{\partial r} \left(\frac{\partial r}{\partial r} + \frac{v}{r} - \frac{1}{r} \frac{\partial u}{\partial \psi} \right). \quad (8)$$

Writing, in conformity with (5), $\partial/R\partial\theta=\partial/\partial z$, we have

* If either substitution is made, the resulting equations are not, however, in the form in which they are usually quoted; the expressions multiplied by ν in equations (1) to (3) are actually the components of $-\text{curl curl } \mathbf{v}$, where \mathbf{v} is the velocity, but this vector is equal to $\nabla^2 \mathbf{v}$ since $\text{div } \mathbf{v}=0$.

from the third equation of motion

$$\begin{aligned} u(-2Ar) = & -\left(1 - \frac{r \sin \psi}{R}\right) \frac{\partial}{\partial z} \left(Cz + \frac{p}{\rho}\right) \\ & + \nu \left(\frac{\partial^2}{\partial r^2} + \frac{1}{r} \frac{\partial}{\partial r} + \frac{1}{r^2} \frac{\partial^2}{\partial \psi^2}\right) \{A(a^2 - r^2) + w\} \\ & + \nu \left(\frac{\partial}{\partial r} + \frac{1}{r}\right) \left\{ \frac{A(a^2 - r^2) \sin \psi}{R} \right\} \\ & + \frac{\nu}{r} \frac{\partial}{\partial \psi} \left\{ \frac{A(a^2 - r^2) \cos \psi}{R} \right\}. \end{aligned}$$

The terms of this equation that are not small must vanish; these are $(-C - 4\nu A)$. We therefore have

$$C = -4\nu A, \quad \dots \dots \dots (9)$$

which gives the relation between pressure gradient and rate of flow in a straight pipe of circular section*. We then have the equation

$$-2Aru = -\frac{\partial}{\partial z} \left(\frac{p}{\rho}\right) - 6\nu A \frac{r \sin \psi}{R} + \nu \left(\frac{\partial^2 w}{\partial r^2} + \frac{1}{r} \frac{\partial w}{\partial r} + \frac{1}{r^2} \frac{\partial^2 w}{\partial \psi^2}\right). \quad \dots \dots (10)$$

The four equations (6), (7), (8), and (10) determine the motion.

4. From equation (10) $\partial p / \partial z$ must be a function of r and ψ , so that p must be of the form $Az + B$, where A and B are functions of r and ψ . If, however, this expression for p is substituted in (7) and (8), it appears that A must be a constant; hence p may be taken to be a function of r and ψ only. If we now write

$$\begin{aligned} u &= u' \sin \psi, & v &= v' \cos \psi, \\ w &= w' \sin \psi, & p/\rho &= p' \sin \psi, \end{aligned}$$

where u' , v' , w' , and p' are functions of r alone, the four fundamental equations become

$$\frac{du'}{dr} + \frac{u'}{r} - \frac{v'}{r} = 0, \quad \dots \dots \dots (11)$$

$$-\frac{A^2(a^2 - r^2)^2}{R} = -\frac{dp'}{dr} + \frac{\nu}{r} \left(\frac{dv'}{dr} + \frac{v'}{r} - \frac{u'}{r}\right), \quad \dots \dots (12)$$

$$-\frac{A^2(a^2 - r^2)^2}{R} = -\frac{p'}{r} + \nu \frac{d}{dr} \left(\frac{dv'}{dr} + \frac{v'}{r} - \frac{u'}{r}\right), \quad \dots \dots (13)$$

and

$$-2Aru' = -6\nu A \frac{r}{R} + \nu \left(\frac{d^2 w'}{dr^2} + \frac{1}{r} \frac{dw'}{dr} - \frac{w'}{r^2}\right). \quad (14)$$

* H. Lamb, 'Hydrodynamics' (4th edition), § 331.

If p' is eliminated from (12) and (13), the following equation results :

$$4A^2r^2(a^2 - r^2)/R\nu = \left(r \frac{d^2}{dr^2} + \frac{d}{dr} - \frac{1}{r} \right) \left(\frac{dv'}{dr} + \frac{v'}{r} - \frac{u'}{r} \right).$$

The solution of this, regarded as a differential equation for $dv'/dr + (v' - u')/r$, is

$$dv'/dr + (v' - u')/r = B/r + Cr + A^2r^2(3a^2 - r^2)/6R\nu, \quad (15)$$

B and C being arbitrary constants. Substituting in equation (15) the value of v' given by (11), we have

$$r \frac{d^2u'}{dr^2} + 3 \frac{du'}{dr} = B/r + Cr + A^2r^2(3a^2 - r^2)/6R\nu,$$

whence

$$u' = D + E/r^2 + (B \log r)/2 + Cr^2/8 + A^2r^4(6a^2 - r^2)/288R\nu,$$

where D and E are arbitrary constants. It follows that

$$v' = D - E/r^2 + B(1 + \log r)/2 + 3Cr^2/8 + A^2r^4(30a^2 - 7r^2)/288R\nu.$$

We must have

$$B = E = 0;$$

otherwise the velocity of the fluid at points of the central line ($r=0$) will not be finite.

It is interesting to notice that another condition is automatically satisfied. When $r=0$ we must have

$$u' = v',$$

and this is the case since each of these expressions is equal to D. It appeared at first sight that the conditions

$$u' = v' = 0, \quad r = 0$$

were necessary, and it is the fact that the conditions

$$w' = p' = 0, \quad r = 0$$

are necessary for a solution of physical significance. For consider two points on the line OC (fig. 1) which are near to, but on opposite sides of, C. At one point $\psi = \pi/2$, $\sin \psi = 1$, while at the other $\psi = 3\pi/2$, $\sin \psi = -1$. There will therefore be a finite difference in pressure, for instance, at these two points, however close they may be together, unless at the centre $p' = 0$. A similar consideration shows that w' must vanish at the centre. But the case of u' and v' is different. Let the component in the plane of the section of the velocity of the fluid at C be of the magnitude V_c and in the direction of the line $\psi = \psi_0$. At any point (r, ψ) in the immediate neighbourhood of C the velocity in the plane

of the section will be given approximately by

$$u = V_c \cos(\psi - \psi_0), \quad v = -V_c \sin(\psi - \psi_0).$$

The component velocities ($u' \sin \psi$, $v' \cos \psi$) found above are of this form only if $u' = v'$, and it has been found that this condition is satisfied. Moreover, it is clear that we must have $\psi_0 = \pi/2$; hence the velocity at the centre of the pipe is of magnitude D and in the direction of the line OC .

At the surface of the pipe, $r = a$, the velocity components u and v , and hence u' and v' , must vanish. Consequently

$$D + Ca^2/8 + 5A^2a^6/288R\nu = 0$$

and

$$D + 3Ca^2/8 + 23A^2a^6/288R\nu = 0,$$

whence

$$C = -A^2a^4/4R\nu, \quad D = A^2a^6/72R\nu.$$

The resulting expressions for the two velocity components are

$$u = A^2 \sin \psi (a^2 - r^2)^2 (4a^2 - r^2) / 288R\nu \quad . \quad . \quad (17)$$

and

$$v = A^2 \cos \psi (a^2 - r^2) (4a^4 - 23a^2r^2 + 7r^4) / 288R\nu. \quad (18)$$

5. Now that u' and v' are known, p' , upon which depends the pressure, is determinate. Before the results of (17) and (18) can be accepted, it must be shown that p' and w' vanish when $r = 0$. From (13)

$$p'/r = A^2(a^2 - r^2)^2/R + \nu \frac{d}{dr} \left(\frac{dv'}{dr} + \frac{v'}{r} - \frac{u'}{r} \right),$$

and since it is clear that the terms on the right-hand side of this equation are finite when $r = 0$, it follows that $p' = 0$ when $r = 0$. From (14) and (17),

$$\frac{d^2w'}{dr^2} + \frac{1}{r} \frac{dw'}{dr} - \frac{w'}{r^2} = \frac{6Ar}{R} - \frac{A^3r}{144R\nu^2} (a^2 - r^2)^2 (4a^2 - r^2).$$

The solution is

$$w' = F/r + Gr + 3Ar^3/4R - \frac{A^3}{1152R\nu^2} (4a^6r^3 - 3a^4r^5 + a^2r^7 - r^9/10).$$

F must vanish, and it is then evident that $w' = 0$ when $r = 0$. The necessary condition that w' and p should vanish at the central line is therefore fulfilled.

The boundary conditions require $w' = 0$, $r = a$; hence

$$w' = -\frac{3Ar}{4R} (a^2 - r^2) + \frac{A^3r}{1152R\nu^2} [4a^6(a^2 - r^2) - 3a^4(a^4 - r^4) + a^2(a^6 - r^6) - (a^8 - r^8)/10]. \quad (19)$$

6. The results of (17), (18), and (19) can be expressed in a more convenient form. Let W_0 be the value of W at the centre of the pipe ; from (5) and (19),

$$W_0 = Aa^2, \quad (20)$$

and is therefore constant. Aa^3/ν , or aW_0/ν , is a non-dimensional constant, the value of which determines the nature of the flow ; we write

$$n = Aa^3/\nu. \quad (21)$$

Finally let

$$r' = r/a. \quad (22)$$

Then

$$U/W_0 = na \sin \psi (1-r'^2)^2 (4-r'^2)/288R, \quad . . . (23)$$

$$V/W_0 = na \cos \psi (1-r'^2)(4-23r'^2+7r'^4)/288R, \quad (24)$$

and

$$W/W_0 = (1-r'^2) \left[1 - \frac{3r \sin \psi}{4R} + \frac{n^2 r \sin \psi}{11520R} \{ 19 - 21r'^2 + 9r'^4 - r'^6 \} \right]. \quad (25)$$

7. It is known* that to cause a given rate of flow a larger pressure gradient is required in a curved pipe than in a straight one, the difference being considerable even when the curvature is small. From this it was anticipated that the difference would be found to depend on the first power of a/R , but the preceding work shows that this is not the case. It is clear that when W is integrated over the whole cross-section the terms involving $\sin \psi$ disappear ; the rate of flow is therefore $\pi a^4 \Delta/2$. The pressure is not, of course, constant over a cross-section of the pipe ; so that there is not a constant pressure gradient as there is in the case of flow through a straight pipe. But it is natural to define as the mean pressure gradient the space-rate of decrease in pressure along the central line of the pipe. Now, it has been pointed out that p , the part of the pressure that varies across the section, must vanish at the central line ; the pressure at any point of this line is therefore $-4\nu Az$, and the mean pressure gradient $4\nu A$. The relation between this quantity and the rate of flow is therefore the same as if the pipe were straight. A closer approximation† than that of this

* This is stated by Eustice, *loc. cit.* p. 119 ; cf. also J. H. Grindley and A. H. Gibson, *Proc. Roy. Soc. A*, vol. lxxx. p. 114 (1908).

† *Note added.*—Work done since this paper was written has shown that it is necessary to retain the terms of order a^2/R^2 .

paper is then required to find the relation between rate of flow and curvature for a given pressure gradient.

8. The motion of the fluid is of special simplicity in the central plane of the pipe. At any point on OC, ψ is either $\pi/2$ or $3\pi/2$; in either case $\cos \psi$, and with it V , vanishes. At any such point the direction of the velocity of the fluid lies in the central plane; hence a particle of the fluid once in this plane does not leave it in the subsequent motion. The motion in one half of the pipe is therefore quite distinct from that in the other.

The differential equation to the stream-lines in the central plane is

$$\frac{dr}{U} = \frac{(R+r)d\theta}{W},$$

but with sufficient accuracy we can ignore r in comparison with R and write $A(a^2 - r^2)$ for W . We then have

$$\begin{aligned} \frac{dr}{Rd\theta} &= \frac{U}{W_0(1-r'^2)} \\ &= na(1-r'^2)(1-r'^2/4)/72R, \end{aligned}$$

or

$$\frac{dr'}{d\theta} = n(1-r'^2)(1-r'^2/4)/72, \quad \dots \quad (26)$$

by substituting for U from (23) and writing $\sin \psi = +1$. This equation will give a first approximation to the stream-lines, but only to those parts of them on the outside of the central line. To get the other parts we must write $\sin \psi = -1$, and the sign of equation (26) must be reversed. Thus, while on the outside of the central line r' increases with θ , the contrary is the case on the inside; but on both sides the general motion of the fluid is the same, namely a continuous movement from the inner to the outer edge of the pipe. It is, in fact, clear from (23) that the direction of the velocity component along OC is the same at all points of OC. It follows from (26) that

$$\theta = \frac{24}{n} \log \left[\frac{(1+r')^2(1-r'/2)}{(1-r')^2(1+r'/2)} \right], \quad \dots \quad (27)$$

if θ is measured from the point where the stream-line crosses the central line $r'=0$. Evidently θ increases steadily with r' , but since θ tends to infinity as the value of r' approaches 1, the stream-line never reaches the outer edge of the pipe. The same expression for θ as in (27), but with the sign reversed, gives the equation to the part of the stream-line on the inside of the central line.

For given r' the value of θ varies inversely as n , and hence inversely as the general velocity of flow. Consequently the angular distance in which a stream-line starting from the centre gets to within a given distance from the outer edge of the pipe is smaller the larger the mean velocity. The relation between θ and r' does not, however, involve a/R , and is therefore independent of the curvature of the pipe.

The table shows the relation between θ and r' on the assumption that θ , measured in degrees, is 50 times the logarithm to base 10 of the function of r' in equation (27). The corresponding value of n is 63.3; for a larger value n' the values of θ in the table must be reduced in the ratio $63.3/n'$.

TABLE.—Relation between r' and θ .

$r' (=r/a)$	0	0.1	0.2	0.3	0.4	0.5	0.6	0.7	0.8	0.85	0.9
θ (degrees)	0	6.6	13.3	20.3	28.0	36.6	46.8	59.5	77.0	89.4	106.8

The form of the whole stream-line is shown in fig. 2, the direction of motion being indicated by the arrow. If the curve drawn is rotated as a whole about O through any angle the curve so obtained is another central stream-line, all these lines being of exactly the same form. In fig. 2 a/R has been assumed, for convenience, to have the large value $1/3$; the r', θ relation is not, as has been seen, affected by the value of a/R , but the approximate results above would not, of course, apply to a pipe with such large curvature.

The figure shows plainly a steady motion of the fluid in the central plane from the inner to the outer edge of the pipe. Since the fluid is assumed incompressible, it is clear enough without further analysis that at a point near the central plane and on the outside of the central line the motion must be directed away from the central plane, while it must be towards the central plane at a point near this plane and inside the central line.

9. The differential equation to any stream-line is

$$\frac{dr}{U} = \frac{r d\psi}{V} = \frac{R d\theta}{A(a^2 - r^2)}, \dots \dots \dots (28)$$

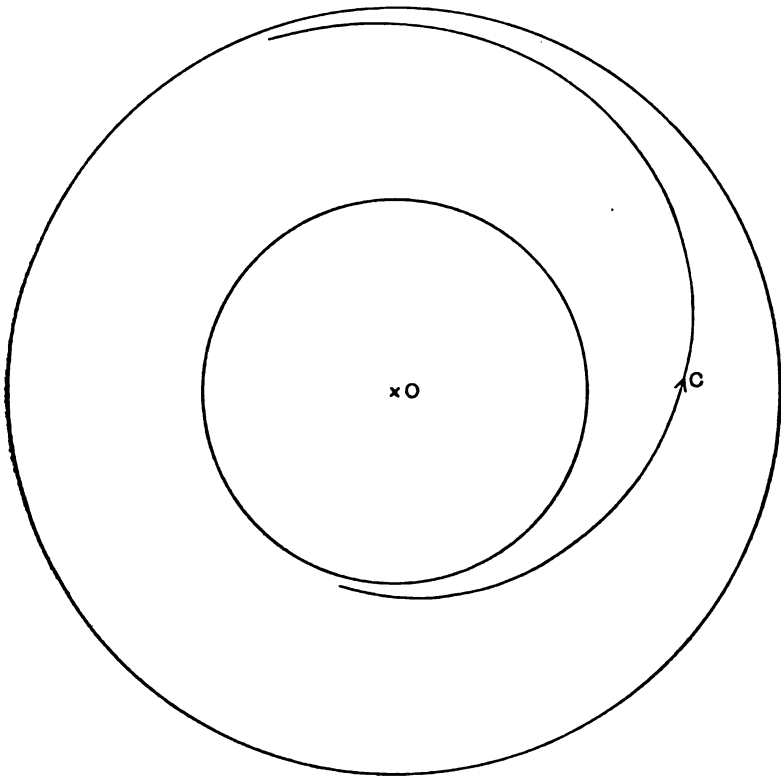
the same approximation as before being made in the last ratio. What is of most interest is the variation in position with regard to the central line of a fluid element as it moves along the pipe; this variation is given by the

relation between r and ψ . From the equality of the first two ratios in (28) we have

$$\frac{dr}{(1-r'^2)(4-r'^2) \sin \psi} = \frac{rd\psi}{(4-23r'^2+7r'^4) \cos \psi},$$

$$\text{or} \quad \tan \psi d\psi = \frac{4-23r'^2+7r'^4}{r'(1-r'^2)(4-r'^2)} dr'.$$

Fig. 2.



Stream-line in the central plane.

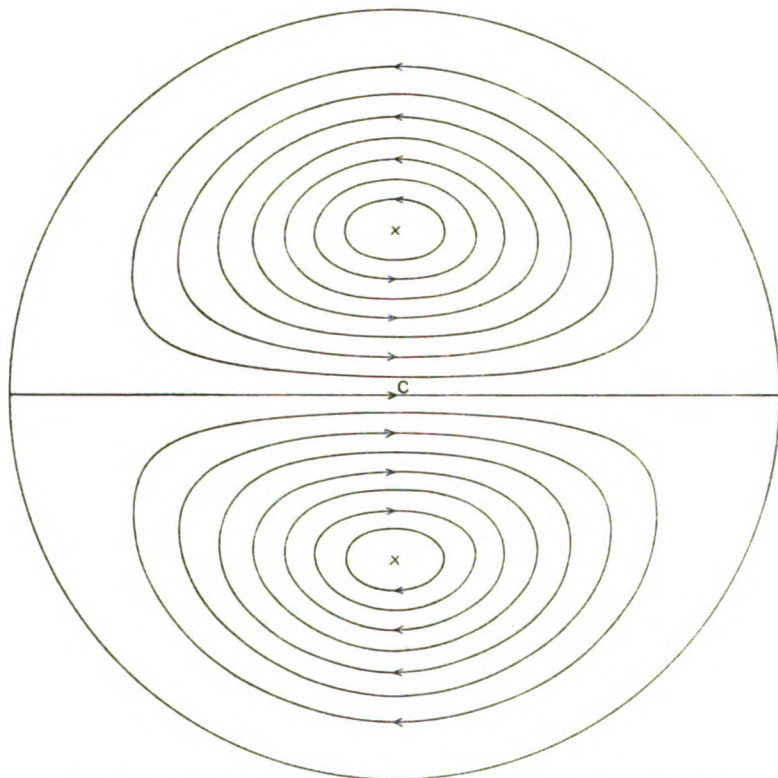
By integration, $\sec \psi = kr'(1-r'^2)^2(1-r'^2/4), \quad (29)$

where k is an arbitrary constant.

The relation between r' and ψ therefore depends neither on a/R nor on n . For any value of k a closed (r', ψ) curve

is obtained. If k is positive, $\sec \psi$ is positive for all values of r' concerned, and the curve is in the upper half of the cross-section. For an equal and opposite value of k the closed curve obtained is the reflexion in OC of the previous curve: it has already been seen that the motions in the two parts into which the pipe is divided by the central plane are independent. A series of the curves is shown in fig. 3. They represent what may loosely be called the

Fig. 3.



Lines showing the movement of fluid elements in the cross-section of the pipe.

projections of the paths of the fluid elements on the cross-section of the pipe; the direction of motion of the elements is shown by the arrows. On this motion is, of course, to be superposed the motion of the elements along the channel; the closed path of the projection corresponds to a helical motion of the fluid element.

From equation (24), V vanishes for all values of ψ when

$$7r'^4 - 23r'^2 + 4 = 0,$$

the only relevant solution of this equation being $r' = 0.429$. At the points where $r' = 0.429$ and ψ is 0 or π , both U and V vanish; these are the points denoted by crosses in fig. 3. The two stream-lines through these points are clearly circles in planes parallel to, and equidistant from, the central plane. The motion of the fluid as a whole can be regarded as made up of what are roughly screw motions in opposite directions about these two circular stream-lines. The general nature of the motion suggested by the theory is now clear.

10. The precise relation between θ and the other variables is of little interest, for the angular distance (θ) in which the projection of a fluid element describes a closed path such as those of fig. 3 must tend to infinity as the minimum distance of the path from C tends to zero. This is clear from the motion of the fluid elements in the central plane, but may be shown directly as follows:—Part of a closed path that is at one point very near to, and above, C must practically coincide with the whole of the upper semicircle of the section of the pipe. θ can be found from the differential equation

$$d\theta = \frac{288r' d\psi}{n \cos \psi (4 - 23r'^2 + 7r'^4)}.$$

Normally the relation between r' and ψ must be known before θ can be found, but for points practically coincident with the boundary we can write $r' = 1$. Then

$$d\theta = -\frac{24}{n} \sec \psi d\psi,$$

and the angular distance in which a fluid element near the boundary goes from the point where $\psi = \alpha$ to that where $\psi = 0$ is proportional to $\log \tan\left(\frac{\pi}{4} + \frac{\alpha}{2}\right)$. This expression is large if α is nearly $\pi/2$.

The only point of interest is that for given r' and $d\psi$, $d\theta$ is inversely proportional to n , and therefore varies inversely with the mean velocity. It has been shown that the form of the closed curves of fig. 3 is independent of the velocity of the fluid, but on the other hand the angular distance in which they are completely described by the projection of a fluid element is inversely proportional to the mean velocity.

11. So far as the general nature of the motion is concerned, the theory is in complete agreement with the experiments of Eustice on the stream-line motion of water in curved pipes of circular cross-section. In the experiments the motion was made visible by the introduction into the stream at various points of dyed water, which was drawn out into thin coloured lines fixed relatively to the pipe. A coloured line in the central plane of the pipe was roughly of the form of the stream-line shown in fig. 2, showing that the fluid elements near the central plane moved steadily across from the inner to the outer edge of the pipe. But when such a line approached the outer edge, it was found to break up into two coloured bands, one of which went round the boundary of the pipe, above the central plane, to the inner edge, while the other described a similar path below the central plane. This is exactly the motion that the theory would suggest. What has been called a coloured line in the central plane consists, of course, of fluid elements both above the plane and below it; it is evident from fig. 3 that according to the theory the coloured matter of a line in the central plane should be divided into two parts. Again the theory accounts for the distinction implied by the above use of the word bands (as opposed to lines). Two fluid elements, both on the same side of the central plane and both near to it, describe (relatively to the section of the pipe) closed paths which are close together. But we have seen that the angular distance in which such a closed path is described tends to infinity (somewhat as a logarithm) as the minimum distance of the path from the central line tends to zero. Thus, if the distance from the central plane of one of the two fluid elements is twice that of the other, the ratio of the angular distances in which they describe their respective closed paths is likely to be in the neighbourhood of $\log 2$. Though originally near together, two such elements will ultimately be far apart. The coloured matter originally concentrated begins therefore to be dispersed as soon as it approaches the outer edge of the pipe.

The motion described above continues: the bands which reach the inner edge then move to the outer edge, remaining near the central plane, and thence round the boundary to the inner edge again. Fig. 5 of Eustice's paper shows in a pipe of small radius of curvature (a/R approximately $1/7$) a coloured line which twice approaches the outer edge and twice the inner edge in an angular distance of less than 2π . The dispersion of the coloured matter must however continue, and the theory suggests, what is found to be the fact, that

the "distinctive character of the colour filament is gradually lost" *.

On the other hand, experiment shows that a coloured line at a sufficient distance from the central plane and, say, above it, is in the form of a helix which is entirely confined to the upper part of the pipe, and that such a line is not dispersed into a band ; in both respects the theory agrees.

12. It is not possible to compare numerically the theory at its present stage with the experimental work. It is usually difficult to make a definite statement as to the limits within which a first approximation such as this is valid ; but a rough idea of the range of validity can be formed from the above expressions for the velocity components. It has been supposed throughout that w is small in comparison with the velocity component W of which it is a part, and therefore the term in the second bracket in the expression for W given by equation (25) must be nearly 1. The expression $r'(19-21r'^2+9r'^4-r'^6)$ is a maximum (for values of r' between 0 and 1) when r' is approximately 0.65, its value being then about 7.6. Hence $n^2a/1440 R$ must be small. Again, U and V have been supposed small in comparison with W . From (23) and (24) this supposition requires $na/72 R$ to be small, but except for relatively small values of n the former condition is the more stringent. But how small $n^2a/1440 R$ must be for a given order of accuracy to be attained it is difficult to say, for w is actually 0 at points of the central line, and what is of most importance is presumably the accuracy of the assumption so far as flow near the centre of the pipe is concerned.

In most of the experiments the values of $n^2a/1440 R$ are, however, greater than 1, so that the theory certainly cannot be applied numerically. The least value of a/R is .005, for a pipe of 1 cm. diameter coiled in a circle of radius 100 cm. The least mean velocity of flow given for this pipe is 6.4 cm. per sec.; the corresponding value of n (the temperature of the water being 18° C.) is over 500, while that of $n^2a/1440 R$ is nearly unity.

13. After a good general agreement between theory and experiment, it is surprising to find what appears to be a complete discrepancy, even although a detailed comparison is out of the question. It is found experimentally that the effect of increasing the mean velocity is that the curvature of the coloured lines is increased : the angular distance in

* *Loc. cit.* p. 123.

which a coloured line in the central plane reaches the outer edge and divides into two bands is found to increase with the velocity. In the limited range wherein the theory applies, the contrary appears to be the case. In § 8 it has been seen that the angular distance in which a central stream-line passes over some given fraction of the radius of the pipe towards the outer edge varies inversely as the mean velocity. A similar result has been found in § 10 in the case of any stream-line*.

The figures in Prof. Eustice's paper make his conclusion quite clear. The most direct of the comparisons of flow in a given pipe at different velocities is that shown in fig. 3 (25)† of his paper, as in the case there illustrated the coloured lines that are compared start from exactly the same point of the cross-section. This figure shows the flow in a pipe of 1 cm. diameter bent in a circle of 25 cm. radius. When the mean velocity is 5.5 cm. per sec. a coloured line starting practically from a point of the central line twice reaches the outer edge and twice the inner edge in an angular distance of little more than $\pi/2$; at twice this velocity a coloured line starting from the same point reaches each edge once only in the same angular distance. The discrepancy may be due merely to the fact that no direct comparison between theory and experiment is possible; but there is another way in which the results might be reconciled. Both theory and experiment agree in that the coloured matter of a central filament is dispersed as soon as it approaches the outer edge of the pipe. Now the coloured matter originally at greatest distance from the central plane suffers the least dispersion, and it must be this matter which preserves the distinctive character of the pair of bands (into which the original single line is divided) after they have been once round the upper or lower half of the boundary. But the angular distance in which either of the bands describes its path from the outer to the inner edge is considerably affected by the distance of closest approach to the central plane of the coloured matter composing it; and this distance will be in effect the maximum distance of the coloured matter of the original filament from the central plane. The original cross-section of the coloured filament is therefore of fundamental importance in deciding how rapidly it will subsequently cross from one edge of the

* In the hope of elucidating this matter the writer has recently considered the flow of fluid through a sinuous channel, but also in this case the departure, in a given distance, of a stream-line from the central line of the channel is directly proportional to the velocity.

† *Loc. cit.* p. 122.

pipe to the other ; the smaller the cross-section the more slowly will the repeated crossings take place. The discrepancy between theory and experiment therefore disappears if it is the case that at increased velocity of flow the cross-sections of the original filaments are sufficiently reduced. In any case it is clear that a numerical comparison between theory and experiment, so far as a filament originally in the central plane is concerned, is impossible unless the cross-section of the filament before dispersion takes place is known.

XVII. *A Note on the Spectrum of Neon.* By MEGHNAD SAHA, D.Sc., F.R.S., Professor of Physics, Allahabad University, Allahabad, India*.

THOUGH the spectral lines of Neon have been completely grouped into series by Paschen, the nature of the series terms was not clearly understood, and a good deal of discussion has been devoted to it. Paschen † discovered

A set of four terms ($s_2 s_3 s_4 s_5$)
of value ranging between 38040–39887 ;

a set of ten terms ($p_1 \dots \dots p_{10}$)
of value ranging between 20958–25671·65 ;

a set of 12 terms ($d_1 d_1' \dots \dots d_6, s_1', s_1'' \dots \dots s''''$)
of value ranging from 11493–12419.

None of these terms, however, constitute the fundamental level of Neon, which must have a very large value corresponding to the observed ionization potential of 21 volts. This level was discovered by Hertz ‡, by means of his vacuum spectrograph. It gives rise to two lines $\lambda=735\cdot7$ and $\lambda=743\cdot5$, separated by a frequency interval of 1428, which is just the difference between the values of Paschen's s_2 and s_4 terms.

From these data, and from a discussion of data on the Zeeman effect of Neon-lines, Goudsmit § has proposed the following new designation of Paschen's terms. Goudsmit's

* Communicated by the Author.

† Paschen, *Ann. d. Physik*, vol. lx. and lxiii.

‡ Hertz, *Zs. für Physik*, vol. xxxii. p. 933.

§ See Goudsmit, *Zs. f. Physik*. vol. xxxii. and Back, vol. xxvii. p. 197.

scheme explains the structure of the Neon spectrum far better than Landé's theory of Spectra of the Second Degree (Spektra der Zweiter Stufe) which he deduced from his 'Verzweigungsprinzip.'

Terms (Paschen's Notation).	Designation according to Goudsmit.	Observed <i>g</i> -factor.	Theoretical <i>g</i> -factor,
Hertz's funda- mental level. }	1S_0	0/0	0/0
s_2	1P_1	1	1
s_3	3P	?	$\frac{0}{0}$
s_4	3P_1	$\frac{3}{2}$	$\frac{3}{2}$
s_5	3P_2	?	$\frac{3}{2}$
p_1	1S_1		$\frac{0}{0}$
p_3	$^1\bar{P}_1$	1	1
p_4	1D_2	1.137	1
p_{10}	3S_1	2	2
p_3	$^3\bar{P}_0$?	$\frac{0}{0}$
p_2	$^3\bar{P}_1$	$\frac{4}{3}$	$\frac{3}{2}$
p_1	$^3\bar{P}_2$	$\frac{2}{3}$	$\frac{3}{2}$
p_7	3D_1	$\frac{2}{3}$	$\frac{1}{2}$
p_6	3D_2	$\frac{7}{6}$	$\frac{7}{6}$
p_9	3D_3	?	$\frac{4}{3}$

The nature of the next group of terms called *d*'s and *s*'s by Paschen has been fixed up by Hund, though their *g*-factor is yet unknown. Most of the lines arising from the combination of these terms with the *p*'s lie in the extreme infra red, so that it would be very difficult to observe their Zeeman effect. It is, however, evident that they cannot all belong to the *d* group, for d_4 has the inner quantum number 4, and no triplet term up to *d* can have such a high inner quantum number. Higher terms like 3F are clearly involved. In this note, the above facts discovered by Hund and Goudsmit are put in new symbols explained by the author in an earlier paper (Saha, Phil. Mag., June 1927).

The number below each term like M denotes the full number of electrons required to close the subgroup completely. A level like L_2 was subdivided into L_{21} , L_{22} , by Stoner with two and four electrons respectively, but this has been omitted.

Chart illustrating the Formation of Atoms.

H He	K ₁ 2				Transition I 21 Sc to 28 Ni	Group II 39 V to 46 Fe	Rare Earths 57 La to 70 Yb	Transition Group III 71 Lu to 78 Pt			
3 Li to 10 Ne		L ₁ 2	L ₂ 6								
11 Na to 18 Ar			M ₁ 2	M ₂ 6	M ₃ 10						
29 Cu to 36 Kr		19 K 20 Ca		N ₁ 2	N ₂ 6	N ₃ 10	N ₄ 14				
47 Ag to 54 Xe		37 Rb 38 Sr			O ₁ 2	O ₂ 6	O ₃ 10	O ₄	O ₅		
79 Au to 86 Hg		55 Cs 56 Ba				P ₁ 2	P ₂ 6	P ₃	P ₄	P ₅	P ₆

Advantage of this Method of Representation.

The first period Li to Ne is formed when the electrons are made to fill the L-levels. The second period (11) Na to (19) Ar when the M₁ and M₂ levels are filled up. It is now known, that if a fresh electron is now brought up, instead of going to M₃, it comes over to N₁, forming K and Ca.

The negative energy value of the electron in position N₁ is therefore larger than the value in position M₃. To represent this state of affairs, we have written N₁ below M₂ and not following M₃, as is usually the custom. We have followed this system all throughout. Thus roughly if by

Phil. Mag. S. 7. Vol. 4. No. 20. July 1927.

Q

through the higher levels denoted by (1), gives rise to the spectral terms written under that level. The diagram also gives a rough indication of the sequence of values of successive terms. Thus

$$\begin{aligned} 1^1S_1 &> 1^1P_{1,2}, 2^1S \\ &> 1^1D_{2,3}, 2^1P_{1,2}, 3^1S_1 \\ &> 1^1F_{3,4}, 2^1D_{2,3}, 3^1P_{1,2}, 4^1S. \end{aligned}$$

Of course these inequalities are only roughly obeyed.

In the construction of the spectra of alkaline earths, we have to keep one electron fixed at N_1 , O_1 or P_1 , as the case may be, and allow the other electron to run through the higher levels. The methods of working have already been discussed in a previous paper communicated to the Philosophical Magazine.

We shall now discuss the spectrum of Neon.

Explanation of the Spectrum of Neon.

K_1
2

L_1 2	L_2 5, 1				
	M_1 (1)	M_2 (1)	M_3 (1)		
		N_1 (1)	N_2 (1)	N_3 (1)	N (1)
			O_1 (1)	O_2 (1)	O_3 (1)
				O_4 (1)	

The normal state of Neon is obtained when all the six electrons are allowed to fill the L_2 -level. It has got $I_k=0$, $I_r=0$, hence it is an 1S_0 -term.

The higher orbits are produced when we keep 5 electrons in L_2 and allow the other to pass through the higher levels. The 5 electrons in L_2 give us a doublet P-level, so that we can construct the terms successively as follows:—

$$\begin{aligned} \text{Running electron } \left. \begin{array}{l} \text{in } M_1 \end{array} \right\} & \begin{array}{l} \text{Combination of } ^1P \text{ with } ^1S_1 \\ I_r = \frac{3}{2}, 0, I_k = |1+0| = 1. \end{array} \end{aligned}$$

Hence we get $^1P_1, ^3P_{0,1,2}$ which are identified by Goudsmit with Paschen's s_2, s_3, s_4, s_5 .

If the running electron is in $N_1, O_1, P_1 \dots \dots$, we shall get the higher Rydberg sequences of these terms.

Running electron } Combination of 2P with 2P .
in M_2 } $I_k = |1 + 1| = 2, 1, 0$.

Hence we expect

$$\begin{array}{ll} c^1S_0 & c^3S_1, \\ c^1\bar{P}_1 & c^3\bar{P}_{0, 1, 2}, \\ c^1D_2 & c^3D_{1, 2, 3}. \end{array}$$

These are the terms which have been obtained by Goudsmit by a similar process, and identified with Paschen's p 's. Now it is quite evident that the p -terms arising from this process will be capable of combining with the previous p -terms (Paschen's s 's). For the process simply means transition of the electron from $M_1 \rightarrow M_2$, and it is perfectly admissible. The present p -terms must therefore be dashed, while the s - and d -terms must remain undashed.

Since all these terms arise from the same level, they have approximately the same scale of values, as observed.

If the electron is in any one of the higher 2-levels, as N_2 or D_2 , or P_2 , they will give rise to the higher Rydberg sequences to the present set, having identical combinatory powers.

Running electron } Combination of 2P with 2D .
in M_2 } We have $I_k = |2 + 1| = 3, 2, 1$.

Hence we expect

$$\begin{array}{ll} d^1P_1 & d^3P_{0, 1, 2}, \\ d^1\bar{D}_2 & d^3\bar{D}_{1, 2, 3}, \\ d^1F_3 & d^3F_{2, 3, 4}. \end{array}$$

We expect twelve terms.

Now Paschen has given exactly twelve terms with

$$j = 0, \text{ for } d_6 \quad \therefore d_6 = c^3P_0.$$

$$j = 1, \text{ for } (d_2 d_5 s_1') = (c^1P_1, c^3P_1, c^3D_1),$$

$$j = 2, \text{ for } (d_1'' d_3 s_1'' s_1''') = (c^1\bar{D}_2, c^3P_2, c^3\bar{D}_2, c^3F_2),$$

$$j = 3, \text{ for } (d_1', d_4, s_1''') = (c^1F_3, c^3\bar{D}_3, c^3F_3),$$

$$j = 4, \text{ for } d_4^1 = c^3F_4.$$

The explanation of these terms is due to Hund, but detailed identification is difficult, and an attempt has been made by writing down the multiplets and comparing the intensities according to that to be expected from the

Sommerfel-Ornstein-Dorgelo scheme. Table I. shows the results of detailed identification.

TABLE I.

Spectral Term.	Term in Paschen's notation.	Term Values.	Inner Quantum Number.
d^1P_1	s_1'	11493.76	1
* $d^1\bar{D}_2$	d_1''	12229.69	2
† d^1F_3	s_1'''	11519.27	3
d^3P_0	d_6	12419.90	0
3P_1	d_5	12405.20	1
3P_2	d_3	12322.24	2
$d^3\bar{D}_1$	d_2	12292.98	1
* $d^3\bar{D}_2$	s_1''	11509.52	2
$d^3\bar{D}_3$	d_1'	12228.26	3
† d^3F_2	s_1''''	11520.80	2
d^3F_3	d_4	12337.35	3
d^3F_4	d_4'	12339.15	4

* The positions of these two terms may be interchanged.

† Positions interchangeable.

The identification is somewhat ambiguous in certain cases. How far the intensity rules are followed will be seen from the following tables. Certain values like (d_1' d_1'') are so close to each other that the lines occurring from them cannot be separated from each other, and the intensity-data in these cases are open to certain amount of doubt. The values of all these terms are of the same order and approximately equal to $\frac{N}{3^2}$. Some of the multiplets with intensities are shown in the following tables.

TABLE II.

The $c^3D - d^3F$ -multiplet.

$c=5L_2M_2$ $d=5L_2M_3$	(p_7) 3D_1	(p_8) 3D_2	(p_9) 0D_3
$(s''')^3F_2$	8136.4 (7) 12287.0	8267.14 (3) 12092.7	
$(d_4)^3F_3$		8865.7 (3) 11276.3	8376.4 (1) 11934.9
$(d_4')^3F_4$			8377.63 (7) 11933.3

TABLE II. (*continued*).
The $c\ ^3D-g\ ^3P$ -multiplet.

$\begin{array}{c} b=5L_2M_2 \\ g=5L_2N_3 \end{array}$	$\begin{array}{c} (p_7) \\ ^3D_1 \\ \bullet \end{array}$	$\begin{array}{c} (p_6) \\ ^3D_2 \end{array}$	$\begin{array}{c} (p_5) \\ ^3D_3 \end{array}$
$(d_6)\ ^3P_0$	5934.46 (7) 16846.0		
$(d_5)\ ^3P_1$?	6000.95 (6) 16659.4	
$(d_3)\ ^3P_2$	5919.04 (2) 16889.9	5987.93 (8) 16695.6	5760.58 (7) 17354.5

The multiplet represents the combination of 3D , and second Rydberg sequence of 3P terms.

The $c\ ^3D-d\ ^3\bar{D}$ -multiplet.

$\begin{array}{c} c \\ d \end{array}$	$\begin{array}{c} (p_7) \\ ^3D_1 \end{array}$	$\begin{array}{c} (p_6) \\ ^3D_2 \end{array}$	$\begin{array}{c} (p_5) \\ ^3D_3 \end{array}$
$(d_2)\ ^3\bar{D}_1$	8681.93 (3) 11515.0	8230.80 (0) 11320.9	
$(s_1'')\ ^3\bar{D}_2$	8128.95 (3) 12298.3	8259.39 (4) 12104.1	7233.12 (1) 12762.8
$(d_1')\ ^3\bar{D}_3$		8720.63 (4) 11385.6	8300.34 (7) 12044.4

Singlet-Combinations.

$\begin{array}{c} c \\ d \end{array}$	$\begin{array}{c} p_{10} \\ S_1 \end{array}$
$(s_1')\ ^1P_1$	7051.29 (5) 14177.9
$(d_6)\ ^3P_0$	7544.08 (6) 13251.8
$(d_5)\ ^3P_1$	7535.78 (8) 13266.4
$(d_3)\ ^3P_2$	7482.85 (9) 13349.5
$(d_2)\ ^3\bar{D}_1$	7472.42 (4) 13378.8

It will thus be seen that the complicated spectrum of Neon is very simply explained on the recent theories of complicated spectra. The theory accounts for not only the fundamental levels, but also for all the higher levels, the Rydberg sequences, and the order of values observed in each case. It also gives a very cogent explanation of the origin of the dashed terms, and explains such transitions as apparently break the selection principle, *e.g.* $\Delta K=2$, or 3.

We can summarize the results as follows :—

Position.	Term.	
(a) $6L_2$,	$1S_0$	
(b) $5L_2, M_1$	$1P_1, 3P_{0,1,2}$	
N_1	Higher Rydberg sequence terms to the above.	
(c) $5L_2, M_2$	$b\ 1S_0$	$b\ 3S_1$
	$b\ 1\bar{P}_1$	$b\ 3\bar{P}_{0,1,2}$
	$b\ 1\bar{D}_2$	$b\ 3D_{1,2,3}$
$5L_2, N_2$ } O_2 }	Same terms but of higher Rydberg sequence.	
(d) $5L_2, M_3$	$c\ 1P_1$	$c\ 3P_{0,1,2}$
	$c\ 1\bar{D}_2$	$c\ 3\bar{D}_{1,2,3}$
	$c\ 1F_3$	$c\ 3F_{2,3,4}$
$5L_2, N_3$ } O_3 }	gives higher Rydberg sequence terms.	

Transitions take place between terms of groups

$$(a) \rightarrow (b) \rightarrow (c) \rightarrow (d) \rightarrow$$

Corresponding to the transition of the electron from

$$L_2 \rightarrow M_1 \rightarrow M_2 \rightarrow M_3.$$

The scheme also explains that the fundamental term $1S_0$ will be rather solitary, *i.e.* will not have terms of higher Rydberg sequence following it.

My thanks are due to Mr. K. Mazumder for drawing the charts.

XVIII. *On the paper "On the Reflecting Power of the Carbon Atom for High-frequency Rays"* (Phil. Mag. iii. 1927, p. 195).

To the Editors of the Philoophical Magazine.

GENTLEMEN,—

IN the paper mentioned above, the formula (6), which I gave on page 199, is only applicable to a pure and very compact powder. If we take the general case of a mixture of powders, of which the density in the briquet under X-rays is δ and which contains the substance to be studied, of density ρ , at the concentration n , one has (with the notations of the paper) :

$$\Delta v = \Delta V \cdot \frac{1}{n} \cdot \frac{\rho}{\delta}.$$

In the formula (6) we must therefore replace μ , absorption coefficient of the powder, by $\mu \cdot \frac{\rho}{n\delta}$ and

$$\frac{E}{I} = \nu \cdot \frac{a}{\pi D} \cdot \phi(\theta) \cdot \frac{1}{2\mu \frac{\rho}{n\delta}} (1 - e^{-2\mu \frac{\rho}{n\delta} \sin \theta}) \lambda^5 N^2 S^2 f^2 *.$$

In the case of a pure powder (*cf.* Compton, 'X-Rays and Electrons,' p. 131), $\mu \frac{\rho}{\delta}$ is the absorption coefficient of a crystal of this substance : it is therefore useless to measure μ , if $e^{-2\mu \frac{\rho}{n\delta} \sin \theta}$ is negligible. But in the case of an impure powder (case of the diamond utilized, which contains a little iron) μ must be measured.

In my paper there is, of course, no correction to be made for relative measurements of f . For the "absolute" experiments, the corrections are, in this case, of little importance. For diamond ($\rho = 3.5$), the sensitive method of analysis given on page 205 enables us to find n . The best values of $\frac{\mu}{\rho}$ for C are probably those of Allen, whose measurements give, for λ KMo, KCu, KFe, $\frac{\mu}{\rho} = 0.68 ; 5.2 ; 9.8$; for Fe, $\frac{\mu}{\rho} = 36.9 ; 330 ; 80$. [The numbers on page 205, taken from Siegbahn, 'The Spectroscopy of X-Rays,' page 248, and Kaye, 'X-Rays,' 2nd ed., page 138, are far too low. *Cf.* Compton,

* In $\Phi(\theta)$, the polarization factor had been written inadvertently $1 + \cos^2 2\theta$, instead of $\frac{1 + \cos^2 2\theta}{2}$. Replace 4 by 8.

loc. cit.] We find in this way $n_0 = 2.2$ g.; $n_{Fe} = .034$ g. (corresponding absorptions, 2.7; 22.6; 24.4). The absorption of rock-salt is $\mu_{NaCl, KMo} = 17.4$. The calculations, redone with these figures, give $f_{C(111)} = 2.6$. n_0 is known at about 10 per cent.: so the accuracy does not exceed 15 per cent. The conclusions are not modified. I hope to be able to repeat these experiments more accurately.

For naphthalene and anthracene the absorptions are, from $\left(\frac{\mu}{\rho}\right)_{C, KCu}$, 5.9 and 6.5. This gives for F_N and F_A 19.5 and 20, and f_C in these substances is 6.7 (Naph.) and 5.9 (Anth.), near 6. It may be pointed out that F may be calculated directly from $E/E_{NaCl(110)}$, which is known, taking an absorption coefficient of 160 for NaCl (KCu), calculated from 17.4 (KMo) by means of the $\lambda^{2.92}$ law. The results are the same.

Believe me yours truly,

30th May, 1927.

M. PONTE.

XIX. *The Calculation of the Equivalent Conductivity of Strong Electrolytes.*—Part I. *Aqueous Solutions.* (ii.) *Application to Data at 0°, 18°, and 25° C.* By ALLAN FERGUSON, M.A., D.Sc., and ISRAEL VOGEL, M.Sc., D.I.C.*

IN Part I. of this series of investigations (Ferguson and Vogel, this Journal, 1925, vol. 1. p. 971) the values of Λ_0 for some thirty-seven strong electrolytes were calculated, using a simple but reliable method for computing B and n in the equation

$$\Lambda_0 = \Lambda + Bn.$$

Contrary to the usual assumption that n is independent of the nature of the electrolyte, it was shown that B and n vary in a regular manner with the nature of the electrolyte and their values are, therefore, important characteristics of each electrolyte. Further, the formula is applicable to uni-uni, uni-bi, and bi-bivalent electrolytes.

The assumption of the constancy of n is fundamental in certain new theories of strong electrolytes. Debye and Hückel, for instance, find that their theory (*Phys. Zeit.* 1923, xxiv. p. 305) leads directly to Kohlrausch's square root formula ("Gesetz")

$$\frac{\Lambda_0 - \Lambda}{\Lambda_0} = B(\frac{1}{2}),$$

where B is determined in terms of certain constants for the

* Communicated by the Authors.

substances concerned and the exponent of C is independent of the nature of the electrolyte. This is directly opposed to the results we have obtained, and we hope later to discuss this point at length.

The methods commonly employed for the determination of Λ_0 lead to markedly different values, and have been the subject of much comment and criticism.

(a) Certain methods such as that depending on the Ostwald-Bredig-Walden rule (Lorenz, *Z. anorg. Chem.* 1919, cviii. pp. 81, 191; 1920, cxii. p. 210) and that suggested by Randall (*J. Amer. Chem. Soc.* 1916, xxxviii. p. 788) are recognized as approximate methods.

(b) Methods have been proposed from time to time which have the Storch equation as basis. That used by Noyes (*J. Amer. Chem. Soc.* 1908, xxx. p. 335), which consists "in plotting the reciprocal of the equivalent conductance ($1/\Lambda$) at the various concentrations (C) against $(C\Lambda)^{n-1}$ and varying the value of n until a linear plot was obtained and then extrapolating for zero concentration," is cumbersome and at most very approximate (*cf.* Abbott and Bray, *J. Amer. Chem. Soc.* 1909, xxxi. p. 729). Bates (*ibid.* 1913, xxxv. p. 519) has described a procedure based on the assumption that the n of the Storch equation

$$(C\alpha)^n = KC(1-\alpha)$$

is variable and decreases with rising concentration (*cf.* also Noyes and Falk, *J. Amer. Chem. Soc.* 1912, xxiv. p. 454, who find the same law of variation of n). This is directly contrary to our own experience, as we find from an examination of nineteen electrolytes of the most varied type that either n is independent of the concentration over a very wide range, or it may be put as equal to $a+bC$, where b is a positive constant in all the instances that we have examined.

(c) The methods which, directly or indirectly, make any assumptions concerning the validity or invalidity of the law of mass action (*cf.* Washburn, *J. Amer. Chem. Soc.* 1918, xl. pp. 122 & 150) are likely to lead to values of Λ_0 weighted by the assumptions made (*cf.* Ferguson and Vogel, this Journal, July 1927).

(d) Various methods have been proposed which are based on the theory of Hertz (*Ann. d. Physik*, 1912, xxxvii. p. 1). These have been chiefly employed by Lorenz and his co-workers (Lorenz, *Z. anorg. Chem.* 1920, cxiii. p. 135; 1921, cxviii. p. 209; Lorenz and Osswald, *ibid.* 1920, cxiv. p. 209; Lorenz and Neu, *ibid.* 1921, cxvi. p. 45; Lorenz and Michael, *ibid.* 1921, cxvi. p. 161; Lorenz and Voigt, *ibid.*

1925, cxlv. p. 277 : Lorenz and Westenberger, *ibid.* 1926, clv. p. 144). It cannot be said that the fundamental postulates of Hertz's theory are well established (*cf.* Auerbach, *Ergebnisse der exakten Naturwissenschaften*, 1922, iv. p. 233), nor have the chief deductions of Lorenz been experimentally verified. The different methods based on Hertz's theory do not, in a large number of cases, give concordant results—these will be referred to later—and the values, in most instances, differ from those deduced by the more generally accepted methods.

(e) By far the best known of the various methods employed are those which use some special form of the equation

$$\Lambda_0 = \Lambda + F(\Lambda, C).$$

Equations of this type have been used by Kohlrausch (*Das Leitvermögen der Elektrolyte*, p. 107 (1916)),

$$\Lambda_0 = \Lambda + bC^{\frac{1}{2}}, \quad (\alpha)$$

$$\Lambda_0 = \Lambda + PC^{\frac{1}{2}}, \quad (\beta)$$

$$\Lambda_0 = \Lambda + k\Lambda^p C^{\frac{1}{2}}, \quad (\gamma)$$

by Lorenz and by Walden (*Z. anorg. Chem.* 1919, cxviii. p. 191; 1921, cxv. p. 49) who use

$$\Delta_0 = \Lambda + mC^{0.45}, \quad (\delta)$$

and by the present writers, who employ

$$\Lambda_0 = \Lambda + BC^n. \quad (\epsilon)$$

Of these equations (β) has long been recognized as giving results of at least as high an order of reliability as those reached by the methods previously discussed. The present writers have shown that n and B can not be assumed constant, but that they vary from electrolyte to electrolyte. They feel, therefore, that the results computed with values of n and B characteristic of each electrolyte are likely to be more reliable than those based on equations (β) and (δ)—equations (α) and (γ) are generally recognized as of a lower order of reliability—and for this reason have extended their calculations to a wider range of experimental data.

The method has now been applied to experimental data at 0°, 18°, and 25°. The data at 0° are due to Walden and Ulich (*Z. phys. Chem.* 1923, cvi. p. 49); the conductivities at round concentrations were interpolated from a large scale Λ - C graph. The results are shown in full in Table I. below as the constancy of the values of Λ_0 over a given range of concentration forms an important feature of these investigations.

TABLE I.

*Concentration.	KCl.		NaCl.		KNO ₃ .	
	Λ .	Λ_0 .	Λ .	Λ_0 .	Λ .	Λ_0 .
2.0×10^{-4}	—	—	—	—	—	—
5.0×10^{-4}	80.65	81.51	66.15	66.72	79.29	79.88
1.0×10^{-3}	80.27	81.51	65.80	66.69	78.95	79.89
2.0×10^{-3}	79.69	81.48	65.26	66.67	78.35	79.83
5.0×10^{-3}	78.50	81.41	64.07	66.64	77.07	79.76
1.0×10^{-2}	77.30	81.51	62.80	66.85	75.75	(80.00)

Concentration.	KIO ₃ .		KClO ₄ .		LiClO ₄ .	
	Λ .	Λ_0 .	Λ .	Λ_0 .	Λ .	Λ_0 .
2.0×10^{-4}	—	—	—	—	54.19	54.31
5.0×10^{-4}	60.20	60.69	76.31	76.84	54.06	54.29
1.0×10^{-3}	59.90	60.70	76.00	76.86	53.85	54.30
2.0×10^{-3}	59.35	60.67	75.45	76.84	53.48	54.28
5.0×10^{-3}	58.10	60.63	74.15	76.80	52.55	54.25
1.0×10^{-2}	56.90	(61.06)	72.67	(76.97)	51.49	(54.50)

Concentration.	K Picrate.	
	Λ .	Λ_0 .
2.0×10^{-4}	54.97	55.17
5.0×10^{-4}	54.75	55.14
1.0×10^{-3}	54.44	55.09
2.0×10^{-3}	53.91	55.00
5.0×10^{-3}	52.79	54.96
1.0×10^{-2}	51.76	(55.41)

* Throughout this series of papers Λ will be expressed in gram equivalents per litre.

Table II. below contains the mean values of Λ_0 at 0°C . together with the values of B and n for these seven electrolytes.

TABLE II.

Electrolyte.	Λ_0 .	B .	n .
KCl	81.48	48.21	0.5296
NaCl	66.68	83.38	0.6569
KNO ₃	79.85	87.51	0.6569
KIO ₃	60.67	111.72	0.7146
KClO ₄	76.84	108.75	0.7013
LiClO ₄	54.29	134.04	0.8242
K Picrate ...	55.07	114.06	0.7476

In Tables III. and IV. are shown the results for some electrolytes at 18° C. (LiClO_4 , K Picrate, Walden and Ulich, *Z. phys. Chem.* 1923, cvi. p. 49; RaBr_2 , Kohlrausch and Henning, *Ges. Abh.* 1911, ii. p. 1108; ZnSO_4 , Kohlrausch and Grüneisen, *ibid.* 1911, ii. p. 1078; CH_3COONa , Lorenz and Osswald, *Z. anorg. Chem.* 1920, cxiv. p. 202).

TABLE III.

Concentration.	LiClO_4 .		K Picrate.		RaBr_2 .	
	Λ .	Λ_0 .	Λ .	Λ_0 .	Λ .	Λ_0 .
1.0×10^{-4}	—	—	—	—	123.7	126.8
2.0×10^{-4}	87.89	88.55	—	—	122.7	126.7
5.0×10^{-4}	87.54	88.37	88.10	89.74	120.9	126.6
1.0×10^{-3}	87.07	88.36	87.50	89.75	119.4	126.8
2.0×10^{-3}	86.31	88.31	86.65	89.74	117.1	126.7
5.0×10^{-3}	84.71	88.28	85.00	89.71	113.4	126.9
1.0×10^{-2}	83.07	(88.62)	83.31	89.79	110.0	(127.6)

Concentration.	ZnSO_4 .		CH_3COONa .	
	Λ .	Λ_0 .	Λ .	Λ_0 .
1.0×10^{-4}	109.53	114.26	—	—
2.0×10^{-4}	107.46	114.27	—	—
5.0×10^{-4}	103.16	114.21	—	—
1.0×10^{-3}	98.39	114.31	74.90	75.98
2.0×10^{-3}	92.05	—	74.27	75.97
5.0×10^{-3}	81.76	—	72.82	75.90
1.0×10^{-2}	72.76	—	71.21	76.04

TABLE IV.

Electrolyte.	Λ_0 .	B.	n.
LiClO_4	88.33	103.32	0.6351
K Picrate	89.74	53.81	0.4596
RaBr_2	126.8	100.9	0.3791
ZnSO_4	114.26	608.5	0.5274
CH_3COONa ...	75.96	95.88	0.6489

Practically the only accurate data for aqueous salt solutions at 25° seem to be those of Lorenz and Michael (*loc. cit.*). Here also the values of Λ at round concentrations were interpolated from a large scale Λ -C plot. The results are given in Tables V. and VI. below, and it will be seen that the consistency of the values of Λ_0 from the lowest concentration measured to about 0.01 N leaves little to be desired.

TABLE V.

Concentration.	KMnO ₄ .		KCl.		NaCl.	
	Λ .	Λ_0 .	Λ .	Λ_0 .	Λ .	Λ_0 .
5.0×10^{-4}	134.16	136.84	148.86	152.28	125.42	128.08
1.0×10^{-3}	133.25	136.85	147.80	152.24	124.45	128.08
2.0×10^{-3}	132.00	136.82	146.55	152.30	123.37	128.06
5.0×10^{-3}	129.67	136.77	144.16	152.26	121.20	128.02
1.0×10^{-2}	127.30	136.82	141.73	152.23	118.95	128.00

Concentration.	KBr.		NaBr.		CH ₃ COONa.	
	Λ .	Λ_0 .	Λ .	Λ_0 .	Λ .	Λ_0 .
5.0×10^{-4}	150.72	153.30	127.37	129.51	—	—
1.0×10^{-3}	149.79	153.28	126.55	129.51	88.22	89.49
2.0×10^{-3}	148.51	153.24	125.39	129.46	87.44	89.44
5.0×10^{-3}	146.15	153.22	123.24	129.47	85.70	89.35
1.0×10^{-2}	143.68	153.26	120.92	129.50	83.79	89.55

TABLE VI.

Electrolyte.	Λ_0 .	B.	".
KCl	152.26	58.82	0.3742
NaCl	128.05	59.50	0.4099
KBr	153.26	72.08	0.4382
NaBr	129.49	72.43	0.4631
KMnO ₄	136.82	66.68	0.4227
CH ₃ COONa..	89.46	119.22	0.6578

For the sake of comparison the values of Λ_0 calculated for these electrolytes by Lorenz and his collaborators are included in Table VII.

TABLE VII.

Electrolyte.	Authors.	* Lorenz and Michael.	† Lorenz and Voigt.
	Λ_0 .	Λ_0 .	Λ_0 .
KMnO ₄	136.82	136.08	—
KCl	152.26	151.03	151.4577
NaCl	128.05	127.32	127.8405
KBr	153.26	152.92	—
NaBr	129.49	129.21	—
CH ₃ COONa.	89.46	† 90.05	91.3063

* Lorenz and Michael, *Z. anorg. Chem.* cxvi. p. 161 (1921).

† Lorenz and Osswald, *ibid.* cxiv. p. 209 (1920).

‡ Lorenz and Voigt, *ibid.* cxlv. p. 277 (1925).

It will be seen that the differences are very much greater than the experimental error involved in the determination of the conductivities. It is significant that although both the calculations of Lorenz and Michael and of Lorenz and Voigt are based on Hertz's theory, different values of Λ_0 are obtained. The results for sodium acetate are somewhat doubtful, as Lifschitz and Beck (*Helv. Chimica Acta*, 1919, ii. p. 133) appear to have exceeded the Λ_0 value here calculated at a dilution of 1024 litres. Mention may be made here of the fact that the results of Lifschitz and Beck are in agreement with the older observations of Ostwald and of Bredig.

The Effect of Temperature on the Constants B and n in the Equation $\Lambda_0 = \Lambda + B C^n$.

From the few results available it appears that the constant B varies irregularly with temperature while n appears to decrease with rise of temperature except in the case of potassium bromide and of sodium acetate.

Calculation of Mobilities at Infinite Dilution.

At 0° C.—The anion transport number of potassium chloride was taken as 0.505 (Walden, *Das Leitvermögen der Lösungen*, i. Teil, p. 236, 1924) and the values of the mobilities thereby computed are exhibited in Table VIII. below.

TABLE VIII.

Cation 0° C.		Anion 0° C.	
Ion.	$\Lambda_0 c^+$.	Ion.	$\Lambda_0 a^-$.
K ⁺	40.3	Cl ⁻	41.2
Na ⁺	25.5	NO ₃ ⁻	39.5
Li ⁺	17.8	IO ₃ ⁻	20.3
Cs ⁺	43.5	ClO ₄ ⁻	36.5
		Picrate ⁻ ...	14.7

At 18° C.—With the aid of the mobilities already calculated in Part I. (*loc. cit.*) Table IX. was constructed.

TABLE IX.

Cation 18° C.		Anion 18° C.	
Ion.	$\Lambda_0 c^+$.	Ion.	$\Lambda_0 a^-$.
$\frac{1}{2}$ Ba ⁺⁺	59.1	ClO ₄ ⁻	54.80
$\frac{1}{2}$ Zn ⁺⁺	46.01	CH ₃ COO ⁻ ..	32.48
		Picrate ⁻ ...	25.14

At 25° C.—Two methods were employed. The first depended on the assumption that the anion transport number of potassium chloride is 0.5030 (Noyes, J. Amer. Chem. Soc. 1912, xxxiv. p. 454). In the second method the mobility at infinite dilution of the permanganate at 25° was calculated from the mobilities at various concentrations experimentally determined by Lorenz and Neu (*Z. anorg. Chem. Soc.* 1921, cxvi. p. 45). It was found that an equation of the form $\mu_0 = \mu + bC^d$, where μ is the mobility at concentration C , μ_0 the mobility at zero concentration, and b and d are constants, represents the relation between the mobility at the lowest measured concentration up to 0.005 N with an accuracy equal to that of the experimental data, and one can therefore extrapolate to zero concentration with some confidence. The results for the permanganate ion are presented in Table X.

TABLE X.

$$\mu_0 = \mu + 100.83 C^{0.7578}.$$

C .	μ .	μ_0 .
5.0×10^{-4}	60.91	61.23
1.0×10^{-3}	60.70	61.24
2.0×10^{-3}	60.31	61.22
5.0×10^{-3}	59.40	61.22
1.0×10^{-2}	58.35	(61.43)
Mean		61.23

Knowing μ_0 for the permanganate ion, the corresponding mobilities of the other ions can be easily calculated. In Table XI. are exhibited the values of μ_0 obtained by both methods, and it will be seen that the agreement is quite satisfactory. Attention must, however, be directed to the fact that the values of the mobilities here deduced differ from those calculated by other investigators: some results are given in Table XII. below.

TABLE XI.

μ .	Method 1.	Method 2.	Mean.
K^+	75.59	75.67	75.63
Na^+	51.38	51.46	51.42
Cl^-	76.67	76.59	76.63
Br^-	77.89	77.81	77.85
MnO_4^-	61.23	61.15	61.19

TABLE XII.

μ_0 .	Authors.	Lorenz and Michael.	* International Critical Tables.
K^+	75.59	74.40	—
Na^+	51.38	50.69	—
Cl^-	76.67	76.63	75.10
Br^-	77.89	78.52	77.44
MnO_4^-	61.19	61.68	—

The values for the conductances at infinite dilution of the dichloracetate, trichloracetate, trichlorbutyrate, *ortho* nitrobenzoate, cyanacetate, 3 : 5 dinitrobenzoate and *ortho* chlorbenzoate deduced in Part I. (*loc. cit.*) are, the authors regret, subject to an error in calculation † ; the corrected values are included in the complete table of mobilities given below.

Cation 0° C. TABLE XIII. Anion 0° C.

Ion.	$\Lambda_0 c^+$.	Ion.	$\Lambda_0 a^-$.
K^+	40.3	Cl^-	41.2
Na^+	25.5	NO_3^-	39.5
Li^+	17.8	IO_3^-	20.3
Cs^+	43.5	ClO_4^-	36.5
		Picrate ⁻	14.7

Cation 18° C.

Anion 18° C.

Ion.	$\Lambda_0 c^+$.	Ion.	$\Lambda_0 a^-$.
K^+	64.60	Cl^-	65.54
Na^+	43.48	NO_3^-	61.83
Li^+	33.53	IO_3^-	34.00
Tl^+	65.53	Br^-	67.70
Cs^+	67.53	I^-	66.06
Ag^+	54.36	F^-	46.77
$\frac{1}{2} Ca^{++}$	52.19	CNS^-	56.48
$\frac{1}{2} Sr^{++}$	51.66	ClO_3^-	54.97
$\frac{1}{2} Ba^{++}$	55.04	ClO_4^-	54.80
$\frac{1}{2} Ra^{++}$	59.1	CH_3COO^-	32.48
$\frac{1}{2} Pb^{++}$	61.61	Picrate ⁻	25.14
$\frac{1}{2} Mg^{++}$	45.78	$\frac{1}{2} SO_4^{--}$	68.25
$\frac{1}{2} Cd^{++}$	46.45	$\frac{1}{2} C_2O_4^{--}$	61.13
$\frac{1}{2} Zn^{++}$	46.01		
$\frac{1}{2} Cu^{++}$	45.91		

* Quoted by Bencowitz and Renshaw, J. Amer. Chem. Soc. xlviii. p. 2146 (1926).

† The mobility of the potassium ion at 18° was subtracted instead of that at 25°.

TABLE XIII. (continued).

Cation 25° C.		Anion 25° C.	
Ion.	$\Lambda_0 c^+$.	Ion.	$\Lambda_0 a^-$.
K^+	75.63	Cl^-	76.63
Na^+	51.42	Br^-	77.85
		MnO_4^-	61.19
		CH_3COO^-	38.04
		Dichloracetate $^-$	46.9
		Trichloracetate $^-$	43.4
		Trichlorbutyrate $^-$	30.9
		<i>Ortho</i> Nitrobenzoate $^-$...	32.4
		Cyanacetate $^-$	41.5
		3:5 Dinitrobenzoate $^-$...	28.3
		<i>Ortho</i> Chlorbenzoate $^-$...	55.4

One of the authors (I. V.) wishes to thank the Trustees of the Dixon Fund for a grant with the aid of which part of the expenses of this investigation have been met.

East London College
(University of London).

The Imperial College of Science
and Technology, South Kensington.

XX. *The Loud-Speaker as a Source of Sound for Reverberation Work.*

To the Editors of the Philosophical Magazine.

GENTLEMEN,—

IN a letter published in the December, 1926, number of the *Philosophical Magazine* Mr. Hart criticises our recent paper* on "*The Loud-Speaker as a Source of Sound for Reverberation Work*," in so far as it concerns the question of Degradation of Acoustical Energy.

Such of our results as we considered reliable, namely, those obtained with the specially constructed condenser microphone, were consistent with the view that at a constant frequency the response of the microphone was proportional to the amplitude of the received sound, and that there was no viscous or similar degradation of sound energy between the loud-speaker and the microphone. Mr. Hart suggests

* *Phil. Mag.* ii. p. 51 (1926).

that degradation may have occurred, its effects being just counterbalanced by lack of proportionality in the response of the microphone. We do not regard this as probable. The width of air gap in our condenser transmitter is about 0.001 inch, and we estimate the maximum amplitude of vibration to be of the order of 0.000001 inch. We find it difficult to believe that with this type of instrument such small displacements could be so far outside the limits of proportionality as to obscure the considerable degradation effect which Mr. Hart appears to expect.

Moreover, Mallett and Dutton*, in experiments at frequencies above 400, kept the output from a source constant and, using a Rayleigh disk as measuring instrument, found the acoustic amplitudes at various distances from the source to obey the usual theory, there being no sign of "degradation."

These experiments relate to frequencies higher than that (100) for which Mr. Hart presents results, and this may explain to some extent why no appreciable degradation was noted. On the other hand, however, when we turn to Mr. Hart's paper †, we feel that the evidence is not altogether convincing. He states that, of the family of curves obtained: "only one, namely, that corresponding to a distance of 40 cms. from the source, can be drawn with certainty." He has drawn this curve and then calculated the curves which would be expected at other distances from the source if the inverse square law of sound intensity were obeyed. Mr. Hart found that "at the higher intensities the experimental points have a strong tendency to lie below these curves—i. e. to indicate unduly low intensities—for distances from the source greater than 40 cms." He concluded therefore that some of the sound energy has been lost from the fundamental frequencies in transmission between 40 cm. and the other distances at which readings were taken.

It appears to us, however, that a curve can be drawn with reasonable certainty through the experimental points obtained at a distance of 70 cm. from the source, and it has the advantage over the work at 40 cm. that results were recorded up to the highest activities at which the source was employed. Using this curve as basis, theoretical curves may be drawn for the various distances from the source by following Mr. Hart's procedure and using the microphone calibration revealed by Mr. Hart's own inverse square calculation. The experimental points then appear to us

* Journ. I. E. E. lxiii. pp. 502, 715 (1925).

† Roy. Soc. Proc. cv. p. 80 (1924).

to agree much more closely with these inverse square law curves, there being no regular deviation to suggest degradation.

In view of this position, therefore, we still feel we were justified in saying in our paper "it must be *assumed* that at this frequency, at any rate, there is no appreciable degradation."

Yours faithfully,

A. H. DAVIS,
N. FLEMING.

March, 1927.

XXI. *The Calculation of Activity Coefficients from Conductivity Measurements.* By C. W. DAVIES, M.Sc., University College of Wales, Aberystwyth*.

THE object of this note is to show that the careful measurement of the conductivities of weak electrolytes provides a valuable means of studying the activity coefficients of ions.

If strong electrolytes may be regarded as completely dissociated in dilute solutions, the diminution in equivalent conductivity that they show with increase in concentration is entirely due to changes in the mobilities of the ions; and in dilute solutions of a weak electrolyte the mobilities of the ions will be expected to show quite similar changes with respect to the total ionic concentration. The true degree of dissociation of a weak electrolyte, at concentration C , will then be given by the ratio Λ/Λ_x , where Λ_x is the sum of the mobilities of cation and anion at ion-concentration $\Lambda/\Lambda_x \cdot C$. This leads to the revised form of the dilution law:

$$\frac{\Lambda^2 \cdot C \cdot f_c \cdot f_a}{\Lambda_x \cdot (\Lambda_x - \Lambda) \cdot f_u} = K, \quad \dots \quad (1)$$

where f_c , f_a , are the activity coefficients of cation and anion respectively, and f_u —the activity coefficient of the undissociated molecules—probably does not differ materially from one in dilute solutions.

In a previous paper† this equation was tested for several organic acids. In the absence of activity data for these acids the activities were calculated by an approximate formula which is not strictly true. More recently the same

* Communicated by the Author.

† J. Phys. Chem. xxix. p. 977 (1925).

equation has been put forward by Sherrill and Noyes * and by MacInnes †, who, however, employed the Debye and Hückel expression ‡ :

$$\log \gamma = -0.5 \sqrt{C_i},$$

for computing the activity coefficients, where $\gamma = \sqrt{f_c \cdot f_a}$, and C_i is the ion-concentration.

Both these methods of calculating activity coefficients may introduce considerable errors §, and moreover are unnecessary; for if accurate conductivity data are available the ratio :

$$\frac{\Lambda^2 \cdot C}{\Lambda_x \cdot (\Lambda_x - \Lambda)} = \frac{K}{f_c \cdot f_a} = K' \quad . \quad . \quad . \quad (2)$$

can be calculated, and will normally be found to increase regularly with increasing concentration. Now for all electrolytes hitherto investigated the mean activity coefficient and the concentration are connected by the limiting law :

$$\log \gamma = -A \sqrt{C_i}, \quad . \quad . \quad . \quad (3)$$

which holds to an ion-concentration of 0.01 N.

From (2) and (3) it follows that

$$\log K' - \log K = 2A \sqrt{C_i}, \quad . \quad . \quad . \quad (4)$$

so that by plotting $\log K'$ against $\sqrt{C_i}$ a straight line is obtained whose slope determines the constant A , and which can be produced to evaluate K , the true dissociation constant. Furthermore, regular deviations from a straight line are found to serve as sensitive indications of abnormal behaviour on the part of the solute.

The value of Λ_x may either (a) be calculated from the empirical formula || :

$$\Lambda_x = \Lambda_\infty - K \cdot \sqrt{C_i} \cdot (\sqrt{\Lambda_\infty^+} + \sqrt{\Lambda_\infty^-}),$$

where Λ_∞^+ , Λ_∞^- are the mobilities of cation and anion; or, (b), if the data are available, the method of Sherrill and

* J. Amer. Chem. Soc. vol. xlviii. p. 1861 (1926).

† *Ibid.* p. 2068 (1926).

‡ *Physik. Zeit.* vol. xxiv. p. 185 (1923).

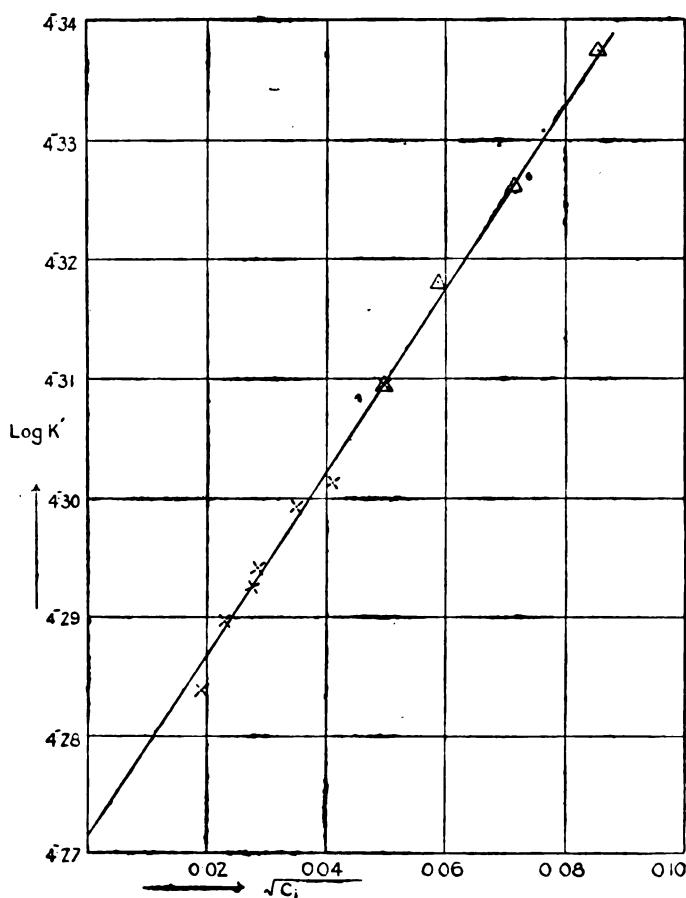
§ The value of the constant is 0.39, not 0.5, for HCl (Randall and Vanselow, J. Amer. Chem. Soc. vol. xlv. p. 2435 (1924); Nonhebel, *Phil. Mag.* [7] ii. p. 1085 (1926)).

|| J. Phys. Chem. xxix. p. 473 (1925). The value of K is 5.24 at 18° C. A rough estimate of the effect of temperature on K gave the value 5.61 at 25°, but the figure $K=5.74$ at 25° is now adopted. This is based on the actual measurements at 25° of Lorenz, Osswald and Michael (*Z. anorg. Chem.* vol. cxiv. p. 209; vol. cxvi. p. 161) and of Parker (J. Amer. Chem. Soc. vol. xlv. p. 2017, 1923).

Noyes and of MacInnes can be used. This depends on the principle that the conductivities of strong electrolytes are additive in dilute solutions so that, for example, Λ_x for acetic acid at the ionic concentration 0.001 is given by $\Lambda_{0.001} \text{HCl} + \Lambda_{0.001} \text{NaAc} - \Lambda_{0.001} \text{NaCl}$.

The latter method has the greater range, for conductivities can be regarded as additive up to a concentration of 0.01 N,

Fig. 1.



whereas the former method only applies to the range $C=0$ to $C=0.002$: within which, of course, both methods should, and do, lead to the same result.

Application to existing data.

There are available only a few series of conductivity measurements with weak electrolytes which claim any great accuracy. Auerbach and Zeglin* have measured sodium formate and formic acid at 18°, and their results yield the data plotted in fig. 1. Triangles are used to show the points obtained by using method (b) described above, for calculating Λ_{∞} . The remaining points were obtained by method (a), the value $\Lambda_{\infty} = 363.5$ being taken for formic acid. The two methods give values in complete agreement, and it is evident that the curve enables the constant A to be evaluated with considerable precision.

The data used are given in Table I., which shows the value of A obtained from the curve, and the values of K, the true dissociation constant, which are obtained when this value of A is introduced into equation (4). Had "A" been given the Debye-Hückel value, K would have shown a regular trend from $0.1785 \cdot 10^{-4}$ in the most concentrated solution to $0.1848 \cdot 10^{-4}$.

TABLE I.

Formic acid at 18°. $A = 0.383$.

C.	A.	K. 10^3 .
0.2534	10.16	0.1869
.1266	14.20	.1868
.06022	20.31	.1875
.03208	27.36	.1868
.01595	37.93	.1861
.008809	50.07	.1872
.004161	70.21	.1872
.003855	72.51	.1866
.001923	97.92	.1871
.001052	124.9	.1859

The only other suitable data on which much reliance can be placed are those of Kendall †. The results obtained from these are summarized in Table II. ‡

* *Z. phys. Chem.* vol. ciii. p. 191 (1922).† *J. Chem. Soc.* vol. ci. p. 1285 (1912).‡ In compiling this table the values of K' calculated by MacInnes (*loc. cit.*) were used.

TABLE II.

Cyanoacetic acid at 25°. $A = 0.372$. o-Nitrobenzoic acid at 25°. $A = 0.381$.

C.	A.	K. 10 ² .	C.	A.	K. 10 ² .
0.05946	88.0	.3541	0.03125	139.7	.6039
0.02972	117.0	.3561	0.01562	179.0	.6095
0.01487	152.5	.3556	0.007812	221.9	.6096
0.007435	193.9	.3557	0.003906	265.0	.6094
0.003716	238.7	.3562	0.001953	303.6	.615
0.001858	282.6	.3578	0.0009765	333.5	.603
0.0009290	320.0	.359			
0.0004645	347.1	.350			

o-Chlorobenzoic acid at 25°. $A = 0.351$. 3.5-Dinitrobenzoic acid at 25°. $A = 0.440$.

C.	A.	K. 10 ² .	C.	A.	K. 10 ² .
0.006662	134.6	.1230	0.003929	175.7	.1508
0.003331	174.0	.1237	0.001965	219.0	.1505
0.001666	218.0	.1236	0.0009824	262.7	.1508
0.0008327	262.6	.1234	0.0004912	301.5	.151

At concentrations below 0.001 N most conductivity measurements with acids are unreliable, owing, probably, to the use of glass cells *. At the higher concentrations, too, irregularities may be expected, since with increasing viscosity of the solution Λ/Λ_r no longer represents the true degree of dissociation. The effect of both these factors can be seen in Table II., but there is an intermediate region in which A can be determined accurately. Where few measurements have been made within this region, as in the case of dinitrobenzoic acid, less reliance can be placed on the result.

Finally, the data of Kendall for acetic acid are shown in Table III. In this case the uncorrected data fail to give a constant value for A , but if A is replaced by the "viscosity corrected" value, $\Lambda \cdot \eta/\eta_0$, a linear curve is obtained in this case also, and A has the value 0.393. The reason for the great importance of the viscosity correction in this case is, of course, that acetic acid is very much weaker than the other acids considered; so that a much greater change in total concentration—and consequently in viscosity—accompanies a given change in ion concentration.

* Kraus and Parker, J. Amer. Chem. Soc. vol. xliv. p. 2429 (1922).

TABLE III.

Acetic acid at 25°. $A = 0.393$.

C	0.07369	0.03685	0.01842	0.009212	0.004608	0.002303
A	6.086	8.591	12.091	16.98	23.81	33.22
[K. 10°].	.1756	.1768	.1778	.1778	.1784	.1788
A. η/η_0 ...	6.138	8.628	12.12	17.00	23.82	33.22
K. 10°1784	.1786	.1782	.1784	.1785	.1788

The method has also been applied to some of the earlier data of Ostwald, Bethmann and Ebersbach *, but with these the points obtained were so scattered as to indicate little except that the acids probably show normal behaviour. Schaller † has measured the conductivity of *o*-Nitrobenzoic acid between 25° and 90° C. Between these temperatures Λ_∞ increases from 382 to 708, and K decreases from 0.0061 to 0.0014. "A" was found to change from 0.5 at 25° to 0.7 at 90°, but this variation is almost covered by the probable error. According to the theories of Milner ‡ and of Debye and Hückel, the increase in A should be about 12 per cent.

Conclusions.

For the acids considered, the constant A varies from 0.35 to 0.44, but until further data are obtained it is impossible to say whether this variability is real. The most reliable series of measurements give: Formic acid, 0.382; Acetic acid, 0.393; Cyanoacetic acid, 0.372: and having regard to the possible sources of error the value $A = 0.38 \pm 0.01$ may be accepted for all the acids investigated.

With this may be compared the value for Hydrochloric acid. Randall and Vanselow find 0.393 from freezing-point measurements; Nonhebel gives 0.39 as the most probable value yielded by E.M.F. measurements at 25°. The divergence of this figure from that required by Debye and Hückel's theory—0.5—is considerable, and Nonhebel has pointed out that it lends support to the Milner theory which requires the value 0.37.

The results obtained in this paper afford further evidence for this view. They may, however, be interpreted in another way, if A is considered not to be constant for all electrolytes but to depend upon the nature of the ions involved. Then

* Kohlrausch-Holborn, 'Leitvermögen der Elektrolyte.'

† *Z. phys. Chem.* vol. xxv. p. 515 (1898).

‡ *Phil. Mag.* xxiii. p. 551 (1912).

the fact that for these acids A has almost constant values, and ones that are lower than those usually accepted for the uni-univalent salts, will be attributed to the influence of the hydrogen ion which is common to them all and which may show an especially small decrease in activity coefficient with rising concentration.

The Edward Davies Chemical
Laboratories, Aberystwyth.
April 3, 1927.

XXII. *Notices respecting New Books.*

Atoms and Molecules. By R. M. CAVEN, D.Sc. (London), F.I.C.
(Blackie & Son Ltd. London & Glasgow. 7s.)

THIS work by Prof. Caven of Glasgow provides a very suitable introduction for first and second year students to the modern theories of Atomic Physics. It begins with an outline of the older Atomic and Molecular theories, and with the older views of valency and chemical constitution. A brief account of the classification of the elements is also given.

After this review of the classical ideas Prof. Caven goes on to give an introduction to the modern ideas of Atomic Physics, and an important chapter is devoted to the Colloidal State.

The treatment in the volume under review is necessarily rather slight, but it can be recommended as providing a satisfactory introduction for the University student.

The Absolute Differential Calculus. By T. LEVI-CIVITA.
(Blackie & Son. Price 21s.)

THE present volume contains a complete translation from the Italian text of Levi-Civita's important work issued in Rome in 1925. It also contains two new chapters which are concerned with the fundamental principles of Einstein's General Theory of Relativity—including, as a limiting case, the so-called Special or Restricted Theory—as an application of the Absolute Calculus.

In this work Levi-Civita has taken the classical laws of mechanics as the starting-point, and he then investigates inductively all the modifications which must be introduced in order to take account of Einstein's ideas. This method is, of course, diametrically opposed to the procedure followed by many writers, who enunciate the postulates of mechanics in tensor form. But the method in this work has its own advantages.

The present work can be heartily recommended and will undoubtedly be very valuable indeed to the large number of students of Relativity who have not been able to read the work

in the original, and the translator, Miss Marjorie Long, formerly Scholar of Girton College, Cambridge, is to be congratulated on the excellence of the translation.

A Concise Geometrical Conics. By C. V. DURELL.
(Macmillan & Co. Price 4s.)

THE present book contains the companion volume to Mr. Durell's volume on Projective Geometry, and it will, no doubt, turn out to be equally useful. It is a feature of the book that a large number of examples and riders have been included, and it will be very valuable to the teacher to have sufficient riders of a more difficult character to draw upon. It is also convenient that Mr. Durell has included alternative methods of proof (by means of projection) of certain theorems in an appendix.

XXIII. *Proceedings of Learned Societies.*

GEOLOGICAL SOCIETY.

[Continued from vol. iii. p. 1350.]

March 23rd, 1927.—Dr. F. A. Bather, M.A., F.R.S., President, in the Chair.

THE following communication was read:—

'The Stratigraphy and Geological Structure of the Cambrian Area of Comley (Shropshire).' By Edgar Sterling Cobbold, F.G.S.

The object of this paper is to place on record the exact positions of the excavations made by the author since 1906, and to describe the stratigraphy and tectonics as revealed by them and by the surface-features.

After a shortened historical account of research the author gives an index-list of the excavations, references to their positions, to the appropriate Reports made to the British Association for the Advancement of Science, and to the faunal horizons seen at each spot. Notes upon some recent excavations and field-work are appended.

Under the heading of stratigraphy, he discusses the sequence and general lithographical characters of the horizons as previously defined, Q. J. G. S. vol. lxxvi (1920) p. 326.

Under the heading of tectonics, evidence is adduced to show that the folding and faulting of the Cambrian fall naturally into four groups: (1) post-Mesonacidian and pre-Paradoxidean,

general direction unknown; (2) post-Paradoxidean and pre-Caradocian, general direction north-north-west to south-south-east; (3) post-Caradocian and pre-Silurian, general direction north-east to south-west, all the result of compressive forces; and (4) post-Silurian, tensional stresses responsible for the Church Stretton Fault. Certain faults affecting the Cambrian are traced up to the Caradocian, but do not affect its outcrop; others affect the Cambrian profoundly, but show slight signs of posthumous movement in post-Ordovician times; and yet others are seen which are regarded as due to the post-Silurian tension.

The facts detailed in the paper enable us to form a fairly consecutive series of views of the deposition and deformation of the Comley Cambrian deposits. These are briefly summarized under fourteen or fifteen headings, and indicate seven diastrophic phases of various intensities. As Prof. Charles Lapworth once said of the bottom of the Cambrian Sea, 'it kept coming up again'.

Special attention is given to the complicated Dairy Hill portion of the area, where recent study and some fresh excavation in 1926 have fully substantiated the inference previously drawn from the Comley Breccia-Bed, that a peak or promontory of Lower Cambrian sandstone remained above water during the accumulations of some 300 feet or more of strata of the *Paradoxides-groomi* Zone.

The paper is illustrated by a geological map of the area on the 6-inch scale, a reproduction of the Dairy Hill portion on the 25-inch scale, an ideal section of the *Paradoxides* Beds while still horizontal, and a sheet of six parallel sections across the area.

April 6th.—Dr. F. A. Bather, M.A., F.R.S., President,
in the Chair.

The following communication was read:—

'The Kateruk Series and Associated Rocks of the Northern Suk Hills (Kenya Colony).' By Vincent G. Glenday, M.A., F.G.S., and John Parkinson, M.A., Sc.D., F.G.S.

The paper describes a series of completely metamorphosed sediments which crop out on or near the Kateruk River, an eastward-flowing tributary of the Turkwal River, situated about 35° 15' long. E. and 2° 37' lat. N., in the north-western part of Kenya Colony. The rocks consist of the metamorphosed representatives of various sedimentary deposits, ashes being included. The constituents indicate a somewhat lower grade of metamorphism than those of the Turoka Series of the south, and it is considered that, although closely related to the latter, the Kateruk Series may eventually prove to be slightly younger. Gabbros, considerably altered, are intrusive in these rocks, and are believed to pass into certain hornblende-schists. On the other hand, some of the latter are thought to be ashes.

April 27th.—Dr. F. A. Bather, M.A., F.R.S., President,
in the Chair.

The following communication was read :—

The Serpentine of the Shetland Islands, and the Associated Rocks and Minerals. By Frank Coles Phillips, M.A.

The Shetland Islands consist mainly of a series of schists and paragneisses, with a strike over the greater part of the area of about north 10° east, and a steep westward dip. Around the eastern and western margins of Mainland occur patches of Old Red Sandstone sediments, and in the north an extensive development of igneous products of that age. A series of older intrusions, ranging from ultrabasic to acid, is found among the metamorphic rocks.

The most basic of these earlier intrusions, chiefly developed in the northernmost islands of Unst and Fetlar, was a dunite, now almost entirely serpentized. This is found mainly around the western and northern margins of the Unst intrusion, and is succeeded on the east by varieties containing rhombic pyroxene and by peridotite. A constant accessory in these rocks is a chrome-spinel, and in places this becomes concentrated as workable deposits of chromite. The ores are of two main types: banded chromite-serpentine and lenticles of massive chromite-rock. Investigation of thin slices shows that the chromite was the earliest-separated constituent from the magma, followed by the silicates, crystallization being in part contemporaneous. The present distribution of the deposits is the result of partial attainment of concentration by aggregation and sinking, complicated by later crushing and faulting. The serpentine is intersected by veins of pyroxenite, largely converted to antigoritic serpentine.

The gabbro, succeeding on the east, is extensively altered, the original pyroxene being uralitized and the felspar converted to a saussuritic aggregate. In Balta and Huney the gabbro is cut by veins of pegmatoid gabbro and albite-zoisite-rock. These changes of serpentization, uralitization, and saussuritization are referred to autometamorphism effected by late-magmatic juvenile water.

Later mineralogical and chemical changes have been brought about by dynamic metamorphism and low-temperature weathering. Extensive carbonation has given rise to segregation-veins of magnesia-lime-iron carbonates, often in well-developed crystals. Talcose schists, the Shetland 'soapstones', are typical products of dynamic metamorphism, the talc being accompanied by magnesian carbonates, representing the excess of magnesia over silica in the original ultrabasic rock compared with that required for the formation of talc. Kämmererite and uvarovite may owe their origin to hydrothermal action; an anthophyllite-schist has been formed, apparently with the introduction of silica. Chrysotile and hornblende-asbestos occur in veins.

May 25th.—Dr. F. A. Bather, M.A., F.R.S., President,
President, in the Chair.

The following communication was read :—

‘The Old Red Sandstone of the Bristol District.’ By
Frederick Stretton Wallis, M.Sc., Ph.D., F.G.S.

The Old Red Sandstone sediments in the immediate neighbourhood of Bristol have been examined and the results recorded from stratigraphical, petrographical, and palæontological standpoints.

Although the total thickness of these deposits is now estimated at 3000 feet, the faunal contents give evidence of the presence of beds of Upper Old Red Sandstone age only, and no apparent unconformity in the strata or mineralogical break has been detected.

Every gradation of deposit between the following types can be found :—Coarse- and fine-grained sandstones, conglomeratic sandstones, siltstones, quartzites, cornstones, pure limestones, and conglomerates. True marls and shales are absent.

It is shown that the material was derived from a pre-Cambrian massif consisting of gneisses, mica- and quartz-schists with abundant quartz augen and volcanic or intrusive rocks, together with a sedimentary series of arenaceous and calcareous (largely silicified) types.

This source was situated north-west of Bristol, and its rocks are shown to have been similar in character to those of the Mona Complex, and especially to the Gwna Beds of that formation. It is not, however, necessary to postulate that the material came from ‘Anglesey’ of the present day. Unfortunately, we do not know even the approximate dimensions of the original complex, and the material may have come from some part of it exposed in Old Red Sandstone times, but now covered by later deposits.

The sediments were transported by a great river, which, flowing through a country affected by heavy seasonal or spasmodic rainfalls, finally reached the sea by a broad delta in the neighbourhood of the Bristol district. Lagoons also formed important physiographical features near the coast.

June 15th.—Dr. F. A. Bather, M.A., F.R.S., President,
in the Chair.

The following communications were read :—

1. ‘The Structural Relations of the Mourne Granites (Ireland);’
By James Ernest Richey, M.C., B.A., F.R.S.E., F.G.S.

The Mourne Mountains are some 13 miles long by about 5 miles wide, and include many peaks of more than 2000 feet in height. The granite-massif of inferred Tertiary age is intruded into Silurian shales, and truncates a north-westerly basic dyke-swarm, of which fact Sir Richard Griffiths was aware in 1835.

The massif is found to consist of at least four distinct intrusions, composed of different granite varieties. The granites all have well-marked, fine-grained intrusive margins, whether in contact with shales or with older granite. Three of these granites form the eastern half of the massif, while the fourth occurs on the west. Eastern and western portions are in contact, but only for about 2 miles, so that the massif as a whole is of hour-glass shape. Exposures are usually good, except where the eastern and western portions join. There is, however, some evidence of the Western Granite being later than the others.

The Western Granite, as shown by the Geological Survey mapping, carried out by Traill in 1870-73, extends outwards on all sides below a slightly domed roof of shales, cappings of which rest upon the granite.

The Eastern Granites are deeply eroded enough to show bounding walls as well as roofs. Floors are nowhere seen. These Eastern Granites are arranged one within the other, with a marked eccentricity towards one side. The outermost granite is the oldest, the innermost the youngest. Relations between the individual roofs and walls are remarkably similar. In each case, a slightly dome-shaped roof turns abruptly into a wall, which is either vertical or steeply inclined outwards. The forms of the granites, so far as seen at the present denudation-levels, are therefore essentially steep-sided, truncated cones, or cylinders, with slightly dome-shaped tops.

Features observed by Traill are that granite-margins transgress the bedding of the Silurian shales, and that the direction of the dip of the shales is unaffected by the intrusion of the granites. The absence of xenoliths, except at actual margins, and the plane surfaces of contacts, are other noteworthy features. The country-rocks have not been pushed to one side, or upwards, as in laccolithic intrusion, nor does overhead stoping appear to have played any part, at least at the present level of observation. It is inferred that the spaces occupied by the various granites have been provided by subterranean cauldron-subsidence of the pre-existing rocks. The intrusion of the Eastern Granites successively one within the other may be then explained by assuming renewed subsidence of the first-subsided block.

2. 'The Stratigraphy of the Valentian Rocks of Shropshire: the Main Outcrop.' By Walter Frederick Whittard, Ph.D., B.Sc., D.I.C., F.G.S.

The Valentian rocks of Shropshire are found in three disconnected outcrops, namely:—

- (i) the Main Outcrop,
- (ii) the Longmynd-Shelve Outcrop,
- (iii) the Breidden Outcrop.

It is the first of these that is described in this paper.

The threefold classification of Salter & Aveline has been adopted,

but their nomenclature has been modified: the rocks are subdivided as follows:—

	<i>Thickness in feet.</i>
(3) Purple Shales	0-400
(2) <i>Pentamerus</i> Beds	0-500
(1) Arenaceous Beds.....	0-200

The Arenaceous Beds extend from near Cardington north-eastwards to the Wrekin, and they consist essentially of conglomerates, grits, and sandstones. Evidence is given for a southerly derivation of the pebbles comprising these beds, and a north-easterly longshore drift is postulated. The Arenaceous Beds attain their maximum development in the Kenley, Church Preen district, and there is reason to suppose that they were partly deposited in an embayment limited by these localities.

The *Pentamerus* Beds are well exposed in several dingles, and detailed descriptions are given of those sections from which graptolites have been collected. The presence of a conglomerate which is restricted to the Wrekin area indicates that the Uriconian rocks were probably exposed here at this time.

The Purple Shales consist almost entirely of purple, maroon, or green mudstones or shales; shelly limestones and calcareous sandstones occur irrespective of horizon. The Onny section is described in detail, and faunal evidence is produced to show that only Purple Shales are exposed in the river-bank. A thin calcareous conglomerate has yielded fossils characteristic of three faunas, of which the Purple Shales fauna alone is indigenous.

The age of the Buildwas Beds is given as the Zone of *Cyrtograptus murchisoni*, a conclusion based on a graptolite assemblage obtained from the Onny River.

The Valentian rocks are displaced by a series of dip-faults, but no folding, other than that caused by slip, has been detected. The unconformable relation of the Silurian rocks to older sediments is fully described, and it is suggested that post-Silurian movements have occurred along the Severn Valley at the region where it is crossed by the Silurian outcrop.

Evidence based on field-data is produced which suggests that the Valentian rocks of the main outcrop were deposited in partly isolated or protected waters.

The few graptolites so far obtained show that only Upper Valentian rocks are exposed; there is no evidence of beds younger than the Zone of *Monograptus crispus*, and most probably the higher zones of the Gala were overlapped by the Wenlock Shales. The rocks of the main outcrop are correlated with the Woolhope and May Hill successions, in which only the highest Valentian rocks are developed.

[The Editors do not hold themselves responsible for the views expressed by their correspondents.]

FIG. 2.

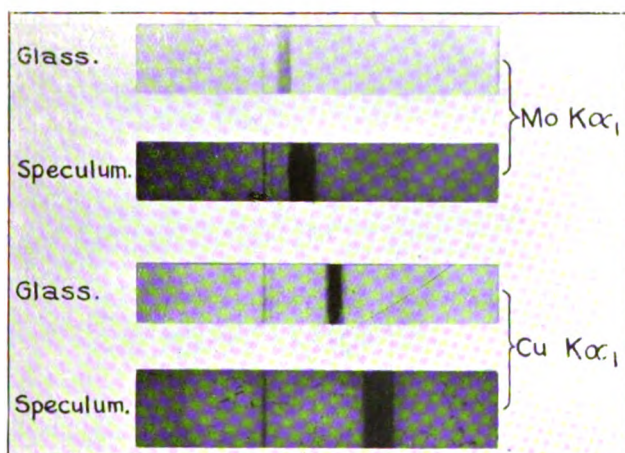


FIG. 1.



FIG. 3.

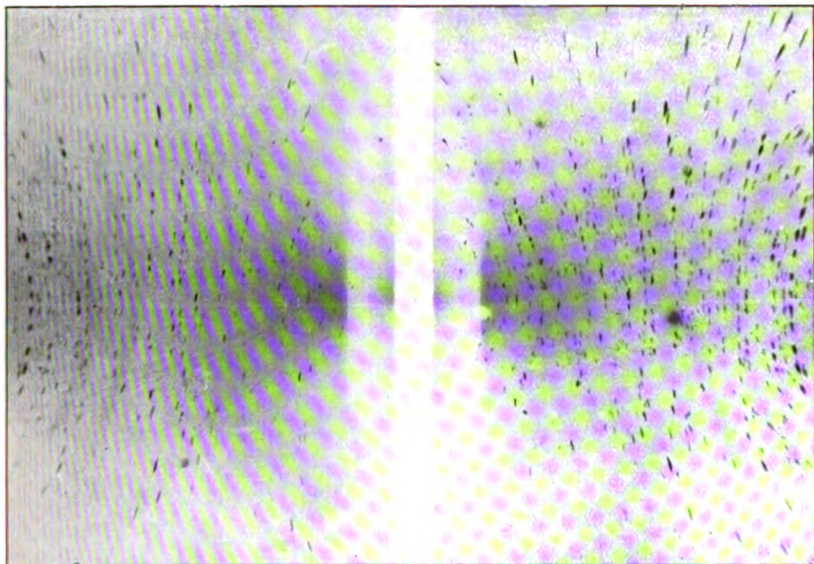
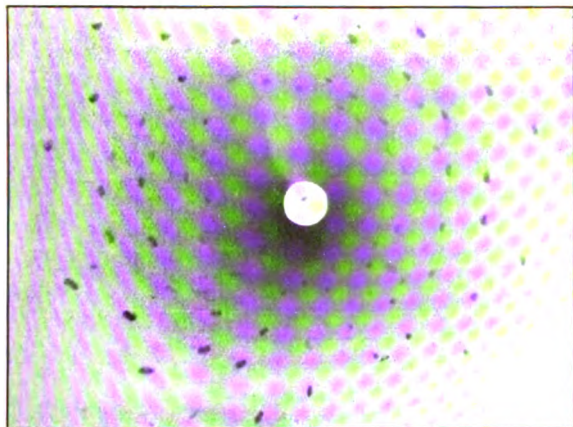


FIG. 4.



THE
LONDON, EDINBURGH, AND DUBLIN
PHILOSOPHICAL MAGAZINE
AND
JOURNAL OF SCIENCE.

[SEVENTH SERIES.]

AUGUST 1927.

XXIV. *Properties of Substances in the Condensed State at the Absolute Zero of Temperature.* By R. D. KLEEMAN, D.Sc., Consulting and Research Physicist and Physical Chemist, Associate Professor of Physics, Union College, Schenectady, N.Y.*

IN a previous paper (Phil. Mag. iii. p. 883, 1927) the writer showed that the internal energy and entropy of a substance or mixture may each be divided into two parts, one of which is externally controllable while the other is not. It was also shown that the controllable entropy and internal energy are each zero when the substance or mixture is in the condensed state at the absolute zero of temperature. This zero was called for convenience the absolute zero of control. It was also shown that the relations

$$\left(\frac{\partial U}{\partial v}\right)_T = 0, \quad \dots \dots \dots (1)$$

$$c_v = \left(\frac{\partial U}{\partial T}\right)_v = 0, \quad \dots \dots \dots (2)$$

$$\dots \dots \dots \left(\frac{\partial S}{\partial v}\right)_T = 0, \quad \dots \dots \dots (3)$$

$$\left(\frac{\partial S}{\partial T}\right)_v = 0 \quad \dots \dots \dots (4)$$

hold under these conditions, where U denotes the controllable internal energy, S the controllable entropy, c_v the specific

* Communicated by the Author.

Phil. Mag. 8. 7. Vol. 4. No. 21. Aug. 1927.

S

heat at the constant volume v , and T the absolute temperature. A number of additional relations will be deduced in this paper from the results already established and well-known thermodynamical formulæ by means of the differential calculus and the postulate that $\frac{\partial^{n+m}p}{\partial v^n \cdot \partial T^m}$ (where p denotes the pressure) cannot be infinite, which follows from our notions of matter. The importance and use of these relations consist in that they must be satisfied by the general relations holding between the various quantities on writing $T=0$ and $v=v_0$, where v_0 denotes the volume of the substance or mixture in the condensed state at the absolute zero of temperature.

1. From thermodynamics we have

$$\left(\frac{\partial U}{\partial v}\right)_T = T \left(\frac{\partial p}{\partial T}\right)_v - p, \quad (5)$$

where U may be taken to refer to the controllable internal energy, since the uncontrollable part, which is not a function of v and T , would disappear through differentiation. On differentiating this equation with respect to T , and n times with respect to v , it becomes

$$\frac{\partial^{n+1}U}{\partial v^n \cdot \partial T} = \left(\frac{\partial^n c_v}{\partial v^n}\right)_T = T \frac{\partial^{n+2}p}{\partial v^n \cdot \partial T^2} (6)$$

The factor of T in this equation is not infinite according to the postulate given, and hence for a substance or mixture in the condensed state at the absolute zero of temperature, or at the absolute zero of control of the substance or mixture, we have

$$\frac{\partial^{n+1}U}{\partial v^n \cdot \partial T} = \left(\frac{\partial^n c_v}{\partial v^n}\right)_T = 0, \quad (7)$$

since $T=0$. The specific heat will possess this property if it can be expressed by the equation

$$c_v = \phi_1(v, T) \cdot \phi_2(T), \quad (8)$$

where $\phi_2(T)=0$ when $T=0$. It possesses then also the property expressed by equation (2). It should be noted, however, that c_v may have the property expressed by equation (7) without having the form given by equation (8).

Every specific heat equation obtained from quantum and other considerations should obey equation (7). A test of the correctness of the assumptions underlying the equation is thereby afforded.

2. Equation (4) may be written

$$\left(\frac{\partial S}{\partial T}\right)_v = \frac{1}{T} \left(\frac{\partial U}{\partial T}\right)_v = \frac{0}{0}$$

at the absolute zero of control according to equation (2), and since $T=0$. By means of the differential calculus the limiting form on the right-hand side of the equation may be written

$$\left(\frac{\partial S}{\partial T}\right)_v = \left(\frac{\partial^2 U}{\partial T^2}\right)_v,$$

and therefore according to equation (4)

$$\left(\frac{\partial^2 U}{\partial T^2}\right)_v = \left(\frac{\partial c_v}{\partial T}\right)_v = 0. \quad . \quad . \quad . \quad (9)$$

We have seen in the paper quoted that equation (2), which is Nernst's specific heat theorem at constant volume, follows directly from thermodynamics. Equation (9) expresses another property of the specific heat, namely, that its first differential with respect to the temperature is zero, which also depends directly on thermodynamics. Experimental evidence of its truth already exists. According to Debye's formula for the specific heat of a monatomic solid *, which is found to agree well with the facts, the specific heat near the absolute zero of temperature is given by

$$c_v = aT^3, \quad . \quad . \quad . \quad . \quad (10)$$

where a is a constant. This equation has been specially investigated by Kammerlingh Onnes and found to be in close agreement with experiment †. It evidently agrees with equation (9). It is highly desirable that experiments be also carried out with mixtures near the absolute zero of temperature, to determine if their specific heats also satisfy equations (2) and (9), as they should if the deductions on which the equations rest are sound.

3. Equation (4) may be written

$$\left(\frac{\partial S}{\partial T}\right)_v = \frac{1}{T} \left(\frac{\partial U}{\partial T}\right)_v = 0,$$

which, on being differentiated with respect to T , becomes

$$\left(\frac{\partial^2 S}{\partial T^2}\right)_v = \frac{1}{T} \left(\frac{\partial^2 U}{\partial T^2}\right)_v - \frac{1}{T^2} \left(\frac{\partial U}{\partial T}\right)_v = \frac{0}{0} - \frac{0}{0},$$

the right-hand side assuming a limiting form on account of

* *Ann. Physik* (4) xxxix. p. 789 (1912).

† *Comm. Phys. Lab.*, Leiden, No. 147 (1915).

equations (2) and (9), and since $T=0$. On obtaining the value of the limiting form by means of the differential calculus the equation becomes

$$\left(\frac{\partial^2 S}{\partial T^2}\right)_v = \frac{1}{2} \left(\frac{\partial^3 U}{\partial T^3}\right)_v \dots \dots \dots (11)$$

It expresses a relation between S and U at the absolute zero of control.

4. On differentiating equation (5) with respect to v it becomes

$$\left(\frac{\partial^2 U}{\partial v^2}\right)_T = T \frac{\partial^2 p}{\partial v \cdot \partial T} - \left(\frac{\partial p}{\partial v}\right)_T.$$

Since $T=0$ and its factor is not infinite according to the postulate given, the equation should be written

$$\left(\frac{\partial^2 U}{\partial v^2}\right)_T = - \left(\frac{\partial p}{\partial v}\right)_T \dots \dots \dots (12)$$

The right-hand side may be evaluated by means of the equation of state, remembering that $T=0$ and $v=v_0$, where v_0 denotes the volume of the substance or mixture in the condensed state at the zero of control. Similarly it can be shown that

$$\left(\frac{\partial^n U}{\partial v^n}\right)_T = - \left(\frac{\partial^{n-1} p}{\partial v^{n-1}}\right)_v \dots \dots \dots (13)$$

5. In general we have

$$\partial S = \frac{1}{T} (\partial U + p \cdot \partial v),$$

which may be written

$$\left(\frac{\partial S}{\partial v}\right)_T = \frac{1}{T} \left(\frac{\partial U}{\partial v} + p\right) = \left(\frac{\partial p}{\partial T}\right)_v \dots \dots \dots (14)$$

by means of equation (5). On differentiating this equation $n-1$ times with respect to v we have

$$\frac{\partial^n S}{\partial v^n} = \frac{\partial^n p}{\partial v^{n-1} \cdot \partial T} \dots \dots \dots (15)$$

The right-hand side of this equation may be evaluated by means of the equation of state. It is of interest to compare this equation with equation (13).

6. For an adiabatic change we have directly that

$$\left(\frac{\partial U}{\partial v}\right)_S = p \dots \dots \dots (16)$$

On eliminating p from this equation by means of equation (5) we obtain

$$\left(\frac{\partial U}{\partial v}\right)_s = \left(\frac{\partial U}{\partial v}\right)_T - \left(\frac{\partial p}{\partial T}\right)_v. \quad \dots (17)$$

For any state of the substance at the absolute zero of temperature we therefore have

$$\left(\frac{\partial U}{\partial v}\right)_s = \left(\frac{\partial U}{\partial v}\right)_T. \quad \dots (18)$$

This equation expresses that an adiabatic change at the absolute zero of temperature is not attended by a change in temperature. Hence the adiabatic corresponding to zero entropy in a diagram expressing the relation between v and T lies entirely on the v -axis. This result follows also from the fact that the entropy corresponding to any point in the space enclosed by the positive v and T axes is larger than that corresponding to the point v_0 on the v axis.

7. From the previous Section it follows directly that

$$\left(\frac{\partial v}{\partial T}\right)_s = \infty, \quad \dots (19)$$

$$\left(\frac{\partial p}{\partial T}\right)_s = \infty, \quad \dots (20)$$

$$\left(\frac{\partial U}{\partial T}\right)_s = \infty, \quad \dots (21)$$

for a substance or mixture at the absolute zero of control.

From thermodynamics we have

$$\left(\frac{\partial S}{\partial v}\right)_p = \left(\frac{\partial p}{\partial T}\right)_s \quad \dots (22)$$

and

$$\left(\frac{\partial v}{\partial T}\right)_s = -\left(\frac{\partial S}{\partial p}\right)_v, \quad \dots (23)$$

and hence at the absolute zero of control we also have

$$\left(\frac{\partial S}{\partial v}\right)_p = \infty, \quad \dots (24)$$

$$\left(\frac{\partial S}{\partial p}\right)_v = -\infty, \quad \dots (25)$$

8. From equations (14) and (3) we have

$$\left(\frac{\partial p}{\partial T}\right)_v = 0 \quad . \quad . \quad . \quad . \quad . \quad (26)$$

at the absolute zero of control.

9. In general

$$\left(\frac{\partial U}{\partial T}\right)_v + \left(\frac{\partial U}{\partial v}\right)_T \left(\frac{\partial v}{\partial T}\right)_s + p \left(\frac{\partial v}{\partial T}\right)_s = \left(\frac{\partial S}{\partial T}\right)_s = 0$$

for an adiabatic transformation, which may be written

$$\left(\frac{\partial U}{\partial T}\right)_v + T \left(\frac{\partial p}{\partial T}\right)_v \left(\frac{\partial v}{\partial T}\right)_s = 0 \quad . \quad . \quad . \quad (27)$$

by means of equation (5). At the absolute zero of control we may write the equation in the form

$$\infty = \left(\frac{\partial v}{\partial T}\right)_s = - \frac{\left(\frac{\partial U}{\partial T}\right)_v}{T \left(\frac{\partial p}{\partial T}\right)_v} = - \frac{0}{0},$$

according to equations (19), (26), and (2). This equation may be written

$$\infty = \left(\frac{\partial v}{\partial T}\right)_s = - \frac{\left(\frac{\partial^2 U}{\partial T^2}\right)_v}{T \left(\frac{\partial^2 p}{\partial T^2}\right)_v + \left(\frac{\partial p}{\partial T}\right)_v} = - \frac{0}{0},$$

by means of the differential calculus, the right-hand side again assuming a limiting form on account of equations (26) and (9), and the equation $T=0$. This equation may therefore be written

$$\infty = \left(\frac{\partial v}{\partial T}\right)_s = - \frac{\left(\frac{\partial^3 U}{\partial T^3}\right)_v}{2 \left(\frac{\partial^2 p}{\partial T^2}\right)_v + T \left(\frac{\partial^3 p}{\partial T^3}\right)_v},$$

by means of the differential calculus. Now in order that the right-hand side of this equation may be ∞ , we must have

$$\left(\frac{\partial^2 p}{\partial T^2}\right)_v = 0, \quad . \quad . \quad . \quad . \quad . \quad (28)$$

whatever the value of $\left(\frac{\partial^3 U}{\partial T^3}\right)_v$ may be

This equation and equation (26) are of considerable importance. Every equation of state has to satisfy them, and they are therefore of use to determine the proper form of the equation of state. Evidently van der Waals' equation does not satisfy these equations, and his equation of state has therefore not the fundamentally correct form. It is an important problem to find an equation of state which will satisfy equations (28) and (26).

As an example of the value of these equations in helping to determine the form of the equation of state, let us write it in the form of the series

$$p = A \frac{RT}{v} + \frac{a_1 + a_2 T + a_3 T^2}{v^2} + \frac{b_1 + b_2 T + b_3 T^2}{v^3}, \quad (29)$$

where $A, a_1, a_2, a_3, b_1, b_2, b_3$ are constants. Equations (28), (26), and the equation $p=0$ give

$$0 = a_1 + \frac{b_1}{v_0},$$

$$0 = AR + \frac{a_2}{v_0} + \frac{b_2}{v_0^2},$$

$$0 = a_3 + \frac{b_3}{v_0},$$

taking into account that $T=0$ and $v=v_0$, the conditions under which the quoted equations hold. The foregoing equations express relations between the constants of the equation of state and v_0 .

10. On differentiating equation (5) twice with respect to T at constant volume, it becomes

$$\frac{\partial^3 U}{\partial v \cdot \partial T^2} = \left(\frac{\partial^2 p}{\partial T^2} \right)_v + T \left(\frac{\partial^3 p}{\partial T^3} \right)_v.$$

On taking into account equation (28), that $\left(\frac{\partial^2 p}{\partial T^2} \right)_v$ is not infinite according to the postulate given, and that $T=0$, the equation becomes

$$\frac{\partial^3 U}{\partial v \cdot \partial T^2} = \frac{\partial^2 c_v}{\partial v \cdot \partial T} = 0. \quad (30)$$

If the specific heat is expressed by the general equation (8) it will satisfy the foregoing equation if either

$$\left(\frac{\partial \phi_1}{\partial v} \right)_T = 0 \quad (31)$$

or

$$\left(\frac{\partial \phi_2}{\partial T} \right)_v = 0. \quad (32)$$

Along the same lines it can be shown that

$$\frac{\partial^{2+n}U}{\partial v \cdot \partial T^{2+n}} = \frac{\partial^{2+n}e_v}{\partial v \cdot \partial T^{2+n}} = (1+n) \left(\frac{\partial^{2+n}p}{\partial T^{2+n}} \right)_v, \quad (33)$$

where n can only have positive and zero values, and the right-hand side can be evaluated by means of the equation of state.

11. On differentiating equation (14) with respect to T and taking account of equation (28), we obtain

$$\frac{\partial^2 S}{\partial v \cdot \partial T} = 0, \quad (34)$$

an equation parallel in form to equation (7) when $n=0$.

Again, on differentiating the same equation $1+n$ times with respect to T we obtain

$$\frac{\partial^{2+n}S}{\partial v \cdot \partial T^{1+n}} = \left(\frac{\partial^{2+n}p}{\partial T^{2+n}} \right)_v, \quad (35)$$

where the right-hand side may be evaluated by means of the equation of state.

12. The equation

$$\left(\frac{\partial p}{\partial T} \right)_v = 0$$

given in Section 8 expresses that $\partial p=0$ on increasing the temperature of the substance at constant volume. Since the pressure is initially zero it follows that it remains zero, and in keeping the volume constant we therefore exercise no constraint. This result will therefore also hold if the volume is unrestricted, or

$$\frac{dp}{dT} = 0, \quad (36)$$

the differential coefficient (which is total) applying to a substance under the pressure of its own vapour.

Along the same lines it can be deduced from equation (28) that

$$\frac{d^2 p}{dT^2} = 0. \quad (37)$$

Thus the equation quoted may be written

$$\left(\frac{\partial^2 p}{\partial T^2} \right)_v = \left(\frac{\partial^2 x}{\partial T^2} \right)_v = 0.$$

It expresses that $\partial x=0$ on increasing the temperature of

the substance at constant volume. Since x is initially zero (equation 26) it remains zero, and we are therefore exercising no constraint in keeping the volume constant. Therefore the constraint may be supposed removed, giving

$$\frac{dx}{dT} = 0,$$

and since we have already seen that the volume constraint may be removed from $\left(\frac{\partial p}{\partial T}\right)_v$, or x , we finally obtain equation (37).

The foregoing equations are of considerable importance. The vapour pressure equation of a substance or mixture, which connects the vapour pressure with the temperature, must satisfy them. They evidently express that near the absolute zero of temperature the vapour pressure p is given by

$$p = a_1 T^{2+a_2}, \quad (38)$$

where a_1 and a_2 are positive quantities depending only on the nature of the substance. This equation could be tested experimentally by means of a special device for measuring low gaseous pressures, such as the one depending on ionization. Its experimental proof would be direct evidence of the fundamental results established in the previous paper on the basis of thermodynamics.

13. In the previous Section we have seen that, keeping the volume of a substance constant on increasing the temperature by ∂T does not act as a constraint. The unrestricted volume therefore does not change on change of temperature, and we may write

$$\left(\frac{\partial v}{\partial T}\right)_p = 0 \quad (39)$$

and

$$\frac{dv}{dT} = 0, \quad (40)$$

since p is zero and remains zero on change of temperature.

It was also shown that keeping the volume constant during the change $\partial^2 T$ did not act as a constraint. The volume therefore did not change, and we may write

$$\left(\frac{\partial^2 v}{\partial T^2}\right)_p = 0, \quad (41)$$

$$\frac{d^2 v}{dT^2} = 0. \quad (42)$$

The equation of state of a substance must obey equations (39) and (41); and the equation connecting its volume with the temperature when in contact with its vapour must obey equations (40) and (42). The volume temperature equation will evidently assume the form

$$v = v_0 + b_1 T^2 + b_2 \dots \dots \dots (43)$$

near the absolute zero of temperature, where b_1 and b_2 are positive constants depending only on the nature of the substance or mixture. This equation may be tested experimentally by measuring the expansion with change in temperature of the solidified substance near the absolute zero of temperature.

It may be noted that if p and v can be expanded in powers of T by Taylor's Theorem, as is very likely, a_2 and b_2 in equations (38) and (43) are each equal to unity.

14. For the entropy of a substance in contact with its vapour we may write

$$\frac{dS}{dT} = \left(\frac{\partial S}{\partial v} \right)_T \frac{dv}{dT} + \left(\frac{\partial S}{\partial T} \right)_v.$$

The differential coefficients on the right-hand side are zero according to equations (3), (4), and (40), and hence we have

$$\frac{dS}{dT} = 0. \dots \dots \dots (44)$$

If the condition is imposed that the pressure is to remain constant, the former equation becomes

$$\left(\frac{\partial S}{\partial T} \right)_p = \left(\frac{\partial S}{\partial v} \right)_T \left(\frac{\partial v}{\partial T} \right)_p + \left(\frac{\partial S}{\partial T} \right)_v.$$

The right-hand side is zero according to equations (3), (4), and (39), and hence we have

$$\left(\frac{\partial S}{\partial T} \right)_p = 0. \dots \dots \dots (45)$$

On differentiating the first equation of this Section totally with respect to T , it becomes

$$\frac{d^2 S}{dT^2} = \frac{d}{dT} \left(\frac{\partial S}{\partial v} \right)_T \frac{dv}{dT} + \left(\frac{\partial S}{\partial v} \right)_T \frac{d^2 v}{dT^2} + \frac{\partial^2 S}{\partial v \partial T} \frac{dv}{dT} + \left(\frac{\partial^2 S}{\partial T^2} \right)_v.$$

According to equations (40), (42), and (11) this equation

may be written

$$\frac{d^2S}{dT^2} = \left(\frac{\partial^2S}{\partial T^2}\right)_v = \frac{1}{2} \left(\frac{\partial^3U}{\partial T^3}\right)_v. \quad (46)$$

Similarly it can be shown that

$$\left(\frac{\partial^2S}{\partial T^2}\right)_p = \frac{1}{2} \left(\frac{\partial^3U}{\partial T^3}\right)_p. \quad (47)$$

15. The change in internal energy of a substance in contact with its vapour is given by

$$\frac{dU}{dT} = \left(\frac{\partial U}{\partial v}\right)_T \frac{dv}{dT} + \left(\frac{\partial U}{\partial T}\right)_v. \quad (48)$$

The right-hand side is zero according to equations (1), (2), and (40), and hence we have

$$\frac{dU}{dT} = 0. \quad (49)$$

If the condition is imposed that the pressure is to remain constant, equation (48) becomes

$$\left(\frac{\partial U}{\partial T}\right)_p = \left(\frac{\partial U}{\partial v}\right)_T \left(\frac{\partial v}{\partial T}\right)_p + \left(\frac{\partial U}{\partial T}\right)_v. \quad (50)$$

The right-hand side is zero according to equations (1), (2), and (39), and hence we have

$$\left(\frac{\partial U}{\partial T}\right)_p = 0. \quad (51)$$

The specific heat c_p at constant pressure is given by

$$c_p = \left(\frac{\partial U}{\partial T}\right)_p + p \left(\frac{\partial v}{\partial T}\right)_p, \quad (52)$$

which becomes

$$c_p = 0 \quad (53)$$

by means of equations (51), (39), and since $p=0$.

The specific heat c of a substance under its vapour pressure is given by

$$c = \frac{dU}{dT} + p \frac{dv}{dT}, \quad (54)$$

which becomes

$$c = 0 \quad (55)$$

by means of equations (49), (40), and since $p=0$.

16. On differentiating equation (48) totally with respect to T it becomes

$$\frac{d^2U}{dT^2} = \frac{d}{dT} \left(\frac{\partial U}{\partial v} \right)_T \frac{dv}{dT} + \left(\frac{\partial U}{\partial v} \right)_T \frac{d^2v}{dT^2} + \frac{\partial^2 U}{\partial v \cdot \partial T} \frac{dv}{dT} + \left(\frac{\partial^2 U}{\partial T^2} \right)_v.$$

The right-hand side is zero according to equations (40), (42), and (9), and hence

$$\frac{d^2U}{dT^2} = 0. \quad . \quad . \quad . \quad . \quad . \quad (56)$$

On differentiating equation (50) with respect to T , keeping the pressure constant, we obtain

$$\left(\frac{\partial^2 U}{\partial T^2} \right)_p = 0 \quad . \quad . \quad . \quad . \quad . \quad (57)$$

according to equations (39), (41), and (9).

Equation (54) on differentiating it totally with respect to T becomes

$$\frac{dc}{dT} = 0, \quad . \quad . \quad . \quad . \quad . \quad (58)$$

taking into account equations (57), (36), and (42).

Equation (52) on differentiating it with respect to T at constant pressure becomes

$$\left(\frac{\partial c_p}{\partial T} \right)_p = 0, \quad . \quad . \quad . \quad . \quad . \quad (59)$$

taking into account equations (57), (26), and (41).

It may be pointed out that the results given in the foregoing Sections, with the exception of those in Sections 1, 4, and 5, cannot be deduced from Nernst's theorem and the third law of thermodynamics, but the general result obtained by the writer is necessary of which they form a part, namely, that the controllable internal energy and entropy of a substance and mixture is zero in the condensed state under the pressure of its vapour at the absolute zero of temperature, and that this zero fulfils the mathematical definition of a minimum according to the differential calculus, which yields equations (1), (2), (3), and (4) on which the deductions made are based. The results in Sections 1, 4, and 5 are deduced directly from well-known thermodynamical formulæ.

The subject may be further developed along similar lines, which will be carried out in subsequent papers.

XXV. *A Distant-reading Instrument for the Measurement of Small Deflections.* By E. F. RELF, A.R.C.Sc., and L. F. G. SIMMONS, M.A., A.R.C.Sc., of the Aerodynamics Department, National Physics Laboratory*.

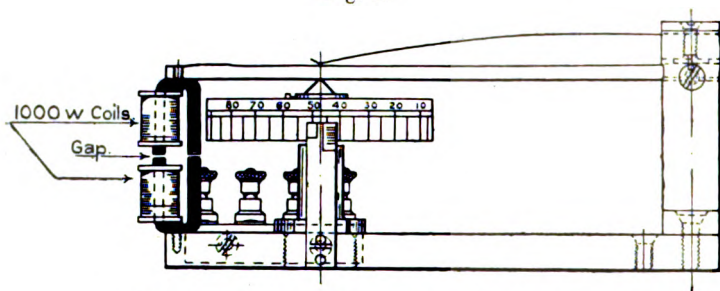
THE apparatus described in this paper was developed in response to a need for an instrument which would indicate at a distance the magnitude of the aerodynamic forces acting on models which were mounted in such a way that direct measurement by balance was impossible, *e. g.* on a whirling arm. The method which has hitherto been used in such cases consists essentially in balancing the force against a calibrated spring, equilibrium of the balance-arm being indicated at a distance by electric contacts. The spring is set to a convenient tension, and the speed of the model through the air varied until balance is obtained. The obvious disadvantage of this method is that it involves access to the model and re-setting of the spring for every reading. The advantage of a method giving, at a distance, a continuous reading proportional to the force acting is obvious, as it would enable a whole series of results at different wind-speeds to be obtained successively and rapidly.

In the search for such a method, various physical properties of materials might conceivably be used to enable the force under measurement to produce an effect at a distance. The most satisfactory method would be one in which an electrical change could be produced without permitting an unduly large movement of the point of application of the force. In America an attempt has been made to use the variation of resistance of a pile of carbon disks compressed by the force. Many difficulties were experienced, and, as far as is known, the only instrument which proved satisfactory was one designed for fairly large forces. An attempt was made at the laboratory to construct a very small carbon pile sensitive to forces of the order $1/100$ lb., but did not promise success, as the instrument was found to be very unreliable, the resistance being dependent upon the previous history of the loading to a considerable extent. Piezo-electric phenomena were also considered, but were rejected on the grounds that even if a crystal could be obtained which would give a sufficient change of potential with the small forces involved, the measurement of a small electrostatic potential is difficult and requires very careful insulation, which could not be easily obtained under conditions contemplated.

* Communicated by the Authors.

It was finally decided that the only practical method of any promise was to cause the force to be determined to deflect a very stiff spring, and to measure this deflexion by an electrical method. The apparatus depends upon the change

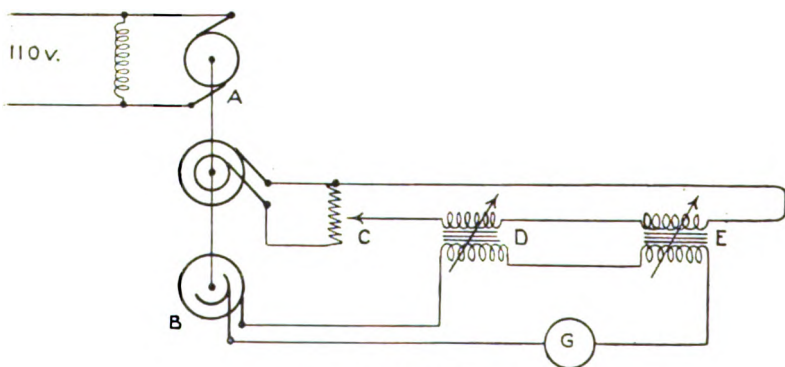
Fig. 1.



Measuring-Gap with Micrometer Adjustment.

in mutual inductance between two coils mounted on an iron core in which there is an air-gap, produced by an alteration in the width of the gap. If two such systems are used, one coil of each being supplied (in series) with alternating current while the other coils are connected so that the induced e.m.f.'s are in opposition, it is evident that a current will flow in the secondary circuit unless the mutual inductances are equal.

Fig. 2.



Circuit Diagram.

The very small alternating currents induced are difficult to measure with accuracy; and even if this could be conveniently done, there is the disadvantage that an alternating current measurement would not indicate which inductance was the greater. The device shown in the circuit diagram (fig. 2)

was accordingly developed so as to permit the use of an ordinary moving-coil galvanometer, and at the same time to indicate the sign of the difference between the gaps. In this figure, A is a rotary converter made by taking two tappings to slip-rings from the armature of a 1/8 H.P. D.C. motor. The shaft of the motor carries a commutator B, which consists of one complete slip-ring and one half-ring (the motor being a two-pole machine). The brushes on the commutator B are mounted so that they can be rotated about the shaft and locked at any position; thus the commutator can be set to make and break once per revolution at any desired phase-angle. The alternating output of the converter is taken to a potentiometer C, so that any desired voltage can be applied to the "primary" windings of the two gaps D and E. The "secondaries" of D and E are connected in opposition, and in series with the commutator B and the moving-coil galvanometer G.

The procedure adopted is as follows:—The gaps D and E are set unequal, so that there is a resultant e.m.f. in the secondary circuit, and the phase-angle of the commutator brushes is adjusted to give maximum deflexion of the galvanometer G. The commutator is thus set to make and break when the secondary current is zero, *i. e.* to give half-wave rectification. In practice the gap D is attached to the apparatus whose displacement is to be measured, while E is operated by a micrometer screw. The measuring-gap D is now set at various positions, *e. g.* by the application of suitable known forces to the balance carrying it, and the readings of the micrometer-gap E taken for balance of the galvanometer. Alternatively, E may be fixed and the deflexion of the galvanometer calibrated against force applied to the apparatus at D. The null method is to be preferred, since, if the gaps D and E are magnetically similar, the null method is independent of frequency, and it is not necessary to take any special precautions to keep the speed of the generator A constant.

It is not essential that the phase-angle of the brushes on the commutator B should be set exactly to the correct position for half-wave rectification. The null method is independent of this setting, but the sensitivity of the device is obviously a maximum when half-wave rectification is obtained. In the direct-deflexion method change of this phase-angle will alter the galvanometer current, but the calibration of the whole apparatus is definite for any commutator setting, provided the frequency and applied voltage are kept constant.

Details of the measuring-gap and micrometer are shown in fig. 1. The coils are 1000-ohm bobbins, commonly used for wireless head-phones. With an applied e.m.f. of about 2 volts from the potentiometer C, and using a reflecting galvanometer giving 1 cm. scale deflexion for 10^{-7} amp., a change of $1/10,000$ inch in either gap gives a scale deflexion of about 5 millimetres.

Some little difficulty was first experienced with the commutator in the galvanometer circuit. This became heated, and set up a small e.m.f. which disturbed the galvanometer zero. The effect was greatly reduced by lubricating the commutator with oil, and was entirely eliminated by constructing a commutator in which the rings and brushes were cut from the same sheet of metal.

The magnetic force in the measuring-gap is measurable under the conditions of sensitivity described above, but would generally be a very small fraction of the force to be measured. It is eliminated in both the null method and the direct-deflexion method by the process of calibration described above. The apparatus cannot be applied to indicate the zero position of a very sensitive balance, since the magnetic force in the gap tends to reduce the stability of the balance. It must also be remembered that the variation of secondary current with gap is not linear, so that the instrument would indicate an incorrect mean if there were a vibration of considerable amplitude in the measuring-gap. It is possible that the calibration could be made nearly linear over a chosen range by suitably shaping the pole-pieces.

XXVI. *The Physical Form of Ether.* By D. MEKSYN*.

I. INTRODUCTION.

1. *On the Character of the Laws of Ether.*

IT is known that between geometrical propositions there are such as cannot be proved but are to be considered as self-evident: these are the so-called axioms of Geometry.

Theoretical Physics presents a somewhat similar case. Its laws are derived by means of mathematical analysis from data of experimental physics, which in their turn are results of measurements.

* Communicated by Prof. H. Levy, D.Sc.

A necessary condition of every measurement is that the unit shall be smaller than the measured quantity: the smaller the standard of measurement is in comparison with the measured quantity, the more precisely the phenomenon can be described. We can measure an event which lasts a day by a clock which indicates minutes and hours, but we are unable to trace a phenomenon which is changing during a minute by means of a clock which marks hours.

Our standards of measurement are finite pieces of matter—atoms, light-waves, and electrons.

Suppose now that we have to deal with a phenomenon which is changing along a length insignificant in comparison with the size of an electron, or during an interval very small in comparison with the time which light takes to pass the electron. It seems that there is no means at our disposal to describe this phenomenon, unless we succeed in splitting up electrons. When physics reaches this stage, the character of its laws must become changed. Instead of being a science which strives to find out the "substance" of phenomena, it becomes a science of a form of phenomena, a kind of Geometry. This takes place when we are dealing with laws of Ether.

Experimental physics at present does not provide us with the necessary information to find out the substance of Ether, electricity and gravitation, and hence there is no need for it in so far as the explanation of results of measurements is concerned.

This has a bearing on the very startling fact that Einstein applying some general considerations succeeded in giving the laws of electricity and gravitation.

2. Some instances of the Form of Ether.

Let us now consider some instances of these considerations. As we shall see, the mechanical action of Ether is due to a kind of four-dimensional displacement of the medium. We do not know the mechanism of this displacement: how does it come about that matter follows the form of this displacement, or by what means it is generated, spread and kept in the medium. The only assumption is that the medium is continuous and incompressible.

Let us find the law of this displacement if we suppose that it is generated from some centre, that it depends for remote points only upon the distance from this centre, and is derived from a potential. (The latter, it seems, is necessary for the stability of the configuration, § 25.)

Phil. Mag. S. 7. Vol. 4. No. 21. Aug. 1927.

T

The law of continuity of an incompressible medium is

$$\frac{\partial \delta x}{\partial x} + \frac{\partial \delta y}{\partial y} + \frac{\partial \delta z}{\partial z} = 0. \quad . \quad . \quad . \quad (1)$$

Now

$$\delta x = \frac{\partial \phi}{\partial x}, \quad \delta y = \frac{\partial \phi}{\partial y}, \quad \delta z = \frac{\partial \phi}{\partial z};$$

hence from (1) we find

$$\frac{\partial^2 \phi}{\partial x^2} + \frac{\partial^2 \phi}{\partial y^2} + \frac{\partial^2 \phi}{\partial z^2} = 0. \quad . \quad . \quad . \quad (2)$$

As the phenomenon has a radial symmetry, (2) becomes

$$\frac{\partial^2 \phi}{\partial r^2} + \frac{2}{r} \frac{\partial \phi}{\partial r} = 0$$

or

$$\phi = \frac{m}{r}.$$

If the form of Ether is represented by a potential function ϕ , the force is given by

$$\frac{\partial \phi}{\partial r} = -\frac{m}{r^2},$$

or we obtain Newton's and Coulomb's laws.

Let the phenomenon be generated from an infinite straight line, and depend for remote points upon the distance from this line.

For this case (2) becomes

$$\frac{\partial^2 \phi}{\partial r^2} + \frac{1}{r} \frac{\partial \phi}{\partial r} = 0$$

or

$$\phi = m l g r,$$

and the force

$$f = \frac{m}{r}.$$

This is the law of gravitation of an infinite material line and the law of a magnetic field of an infinite straight current.

From these instances we see that, whatever may be the cause of a phenomenon, its observed laws are defined by the physical form of the medium, and not by the intrinsic mechanism of phenomena or of the medium undetectable by our measurements.

3. *Ether and Motion.*

In Physics the idea of Ether always comes in connexion with the phenomenon of light or electromagnetic field. It is not considered that the Ether has any bearing on motion of a free material point in space.

Newton's dynamics accepts that a free material point moves in a straight line, because it is the shortest line of the space; it is necessary to apply some force to deflect it from this line because of the law of causality, the force being proportional to some property of a body called its mass, and to the acceleration. The laws of motion centre themselves mainly in the body itself; they are the most simple laws conceivable, but, as a matter of fact, a more detailed examination shows them to be quite incomprehensible.

If a body receives an acceleration, what change has occurred in the interrelation between space and the body? We assume that there is no Ether: the space is void. As the space is quite homogeneous and infinite, and as there is no discrimination between directions or parts of space, there must not be any force applied in order to bring the body from one part of space to another: the law of Motion ought to be according to the law of probability.

We could take up an alternative point of view, and ascribe the laws of Motion to the action of distant masses.

If a material point moves, its distance from distant masses changes, and hence there is a force necessary to produce this change. But here again two cases are possible: either the distant masses are distributed symmetrically in relation to the moving body (then their influence is mutually cancelled and the law of probability persists), or there is no such symmetry (then there must be a marked out direction in which all bodies strive to move, which is contrary to Newton's laws).

It is clear that if a force is necessary to deflect a moving body, it is because motion produces some change in space, and so we come to the conception of Ether.

Ether and Matter (or electrons) are mutually connected parts of one physical system: to every state of matter its state of Ether corresponds; *every Motion of Matter (or electrons) produces a corresponding displacement of Ether.*

It is the latter which defines the laws of Motion of a material body.

Now what is Ether? It will be assumed that free Ether is an absolutely continuous, incompressible, and elastic dynamical substance, *sui generis*, possessing a definite amount of Energy in every unit of volume. It is clear that, whatever the laws of Ether may be, they must be in accordance

with the general laws of equilibrium and Motion of a continuous elastic medium.

From the dynamics of a material point there can be some inferences drawn about deformations of Ether, if the latter is compared with an elastic solid body.

Three kinds of changes can be produced in an elastic solid body without destroying it :—

1. The body can be brought from one state of equilibrium into another. A temporary force is necessary to produce this change, but no force is necessary to keep the body in a state of equilibrium.

2. It can undergo an elastic deformation. Up to a certain limit it is necessary not only to apply a force to bring about this change, but the deformation persists only so long as the force acts, and vanishes together with the force.

3. Above a certain limit the deformation produced in an elastic body persists after the force has been removed.

These three states of a solid body are analogous to three states of Ether.

The first corresponds to a uniform rectilinear motion of a body, the second to an accelerated motion, and the third to electrons and protons, which are permanent four-dimensional deformations of Ether.

4. *The Law of Ether for moving systems.*

Einstein's Principle of Relativity is of great importance to problems connected with moving systems. The idea of this principle is that the laws of Physics are covariant to every system of coordinates, great importance being attached to the use of curvilinear coordinates. It is therefore necessary to inquire as to the bearing which this conception has on the form of Ether. Before it can be done, however, we must make it clear where the kernel of the idea lies.

It seems that the conception of the general Principle of Relativity is either useless or self-contradictory.

As a matter of fact, what is meant by the statement that all laws of Physics are covariant to every system of coordinates? It means that a particular relation, which is the content of a law, does not depend upon a system of coordinates. But, if so, the latter plays only a subsidiary rôle ; it is a matter of convenience, and cannot lead us to any new results.

On the other hand, Einstein, using this method, arrived at a new law of gravitation. Hence it appears that the laws of Physics are not covariant to every system of coordinates.

This difficulty is solved as follows :—

The laws of Physics are represented in the four-dimensional Geometry by mixed space-time quantities ; the covariancy of laws of physics relates to these mixed quantities. On the other hand, at the basis of our experimental knowledge lies the intuitive law, that space and time are distinctly separate entities ; our physical instruments are measuring separately the space and the time-parts of the corresponding four-dimensional quantity, which, taken as a whole, has no observable meaning at all.

Take, for instance, the conception of the four-velocity. Its absolute value for *every motion* is equal to

$$\sqrt{\frac{dx^2}{ds^2} + \frac{dy^2}{ds^2} + \frac{dz^2}{ds^2} - \frac{dt^2}{ds^2}} = \sqrt{-1},$$

where

$$ds^2 = dt^2 - dx^2 - dy^2 - dz^2.$$

It consists of two parts : space-part, $\frac{dx}{ds}, \frac{dy}{ds}, \frac{dz}{ds}$, which represents what we grasp to be the velocity of Motion, and the time-part, which is the kinetic energy of Motion. Or take the electromagnetic six-vector. Its invariant value is

$$H_x^2 + H_y^2 + H_z^2 - E_x^2 - E_y^2 - E_z^2.$$

Two quite different electromagnetic phenomena may have an electromagnetic six-vector of the same absolute value ; the latter is not an observable quantity ; only its separate space- and time-parts, the electric and magnetic forces, have to us a physical reality.

Now, if we change a system of coordinates, it leaves invariant only the four-quantity as a whole, but not separately, its space- and time-parts ; hence we see that, in contradistinction to the three-dimensional geometry of space (solid bodies), in the four-dimensional geometry of Ether, although the laws may be covariant, we are not free to use systems of coordinates, because different system- represent quite different phenomena.

Hence, if we accept that the laws of Physics possess a general covariancy, and at the same time we demand that strict physical laws shall exist for moving systems, we come to the conclusion that :

To every moving system, and a field of gravitation, belongs its metric of Ether, which defines the mechanical and electromagnetic properties of the moving system.

II. DYNAMICS OF A MATERIAL POINT.

5. *Motion and the Metric of Ether.*

The problem of Motion consists of two parts:

1. Given the four-dimensional form of Ether (Metric) to find the Motion of a material point in it.

2. Given the motion of a system to find the corresponding metric of Ether, which is produced by this Motion.

We consider in the present investigation only one particular case—when the Force is derived from a Potential.

The solution of the first problem is given by generalization of the principle of Hamilton.

If ds is an element of the four-track, then the Motion of a free material point is given by the geodesic line of Ether (see also § 14),

$$\delta \int ds = 0, \quad . \quad . \quad . \quad . \quad . \quad . \quad (1)$$

where

$$ds^2 = g_{\mu\nu} dx_\mu dx_\nu.$$

The evaluation of this condition gives the four equations of Motion:

$$\frac{d^2 x_\alpha}{ds^2} + \{\mu\nu, \alpha\} \frac{dx_\mu}{ds} \frac{dx_\nu}{ds} = 0. \quad . \quad . \quad . \quad (2)$$

Comparing (2) with the Classical Laws of Motion, we find that

$$g_{44} = 1 - 2\phi \quad . \quad . \quad . \quad . \quad (3)$$

(or $g_{44} = 1 - \frac{2\phi}{c^2}$ if c is the velocity of light), where ϕ is the Potential function of the Force on a unit of mass of the Material Point.

The equation (3), together with the condition that

$$g = -1, \quad . \quad . \quad . \quad . \quad . \quad (4)$$

gives to the first approximation the Metric which Ether must possess in order to set the material point in the required motion.

We assume that, conversely, if a system has a Motion which can be produced by a force derived from a potential ϕ , the metric of its Ether observed from a system at rest will be given by (3).

6. The same problem of finding the physical metric of Ether can be attacked more directly.

We find in an invariant form the partial differential equation, which must be satisfied by the potential function ϕ .

Let it be

$$f(\phi, \phi_a, \phi_{a\beta}, g_{\mu\nu} \dots) = 0.$$

From this equation we exclude ϕ and all its derivations: we obtain an equivalent system of equations which must be satisfied by $g_{\mu\nu}$.

Solving them, we find the tensor $g_{\mu\nu}$, which, inserted in (2), gives the Motion of the material point.

We consider a few instances for elucidation of these two methods.

7. Hyperbolic Motion.

1. Let a material point be set in motion under the influence of a constant force.

The potential function is

$$\phi = \alpha x. \quad . \quad . \quad . \quad . \quad . \quad . \quad . \quad (5)$$

If the motion proceeds in the direction of the axis X, g_{44} is given by

$$g_{44} = 1 - \frac{2\alpha x}{c^2}. \quad . \quad . \quad . \quad . \quad . \quad . \quad (6)$$

Taking the discriminant of the fundamental form to be equal to $-c^2$, we obtain

$$ds^2 = \left(1 - \frac{2\alpha x}{c^2}\right) c^2 dt^2 - dz^2 - dy^2 - \frac{dx^2}{1 - \frac{2\alpha x}{c^2}}. \quad . \quad (7)$$

2. We consider now this problem from the second point of view.

The potential function represents in four-dimensional space a plane; hence its Gaussian curvature, or the Riemann-Christoffel tensor, is equal to zero. This gives us the required condition for $g_{\mu\nu}$.

We can come to the same condition also as follows:—

The differential equation of ϕ is

$$\frac{\partial^2 \phi}{\partial x_\mu \partial x_\nu} = 0,$$

or, in an invariant form,

$$\phi_{\mu\nu} = 0, \quad . \quad . \quad . \quad . \quad . \quad . \quad (8)$$

where subscripts denote covariant differentiation.

Differentiating covariantly (8) once more, we obtain

$$\phi_{\mu\nu\sigma} = 0, \quad (9)$$

whence it follows :

$$\phi_{\mu\nu\sigma} = \phi_{\mu\sigma\nu} + B_{\mu\nu\sigma}^e \phi_e. \quad (10)$$

As

$$\phi_{\mu\nu\sigma} = \phi_{\mu\nu\sigma} = 0,$$

(10) becomes

$$B_{\mu\nu\sigma}^e \phi_e = 0. \quad (11)$$

Now, for a suitable system of coordinates the Riemann-Christoffel tensor $B_{\mu\nu\sigma}^e$ becomes a differential equation of the second order in $g_{\mu\nu}$, which in their turn are to the first approximation linear functions of ϕ ; hence $B_{\mu\nu\sigma}^e$ is of the second order of ϕ , and therefore it does not depend upon the particular values of the coefficients a in ϕ . On the other hand, ϕ depends upon them. As they can have arbitrary values, (11) will only be satisfied if

$$B_{\mu\nu\sigma}^e = 0, \quad (12)$$

the above-found condition.

We integrate now (12) for two dimensions, assuming that

$$g = -1.$$

From Differential Geometry we have

$$4\sqrt{g}K + 2\frac{\partial}{\partial x_1}\left(\frac{\frac{\partial g_{44}}{\partial x_1}}{\sqrt{g}}\right) + 2\frac{\partial}{\partial x_4}\left(\frac{\frac{\partial g_{44}}{\partial x_4}}{\sqrt{g}}\right) = 0, \quad . (13)$$

where $K = \frac{B_{1212}}{g}$ is the Gaussian curvature.

In our case $K=0$.

If we consider only stationary solutions, (13) becomes

$$\frac{\partial^2 g_{44}}{\partial x_1^2} = 0,$$

or g_{44} is a linear function of X , the above-found result.

8. *Solution of the equations of Motion.*

The motion of a material point is defined from (2), if we insert for $g_{\mu\nu}$ the values given by (7).

The result of these calculations are the two equations of motion :

$$\left. \begin{aligned} \frac{d^2x}{ds^2} + \frac{1}{2} \frac{1}{1-2\alpha x} \left(\frac{dx}{ds} \right)^2 - \alpha &= 0, \\ \frac{d^2t}{ds^2} - \frac{2\alpha}{1-2\alpha x} \frac{dx}{ds} \frac{dt}{ds} &= 0, \end{aligned} \right\} \quad \dots \quad (14)$$

where we take $c=1$ and denote

$$x_1 = x, \quad x_4 = t.$$

From the second equation (14) we obtain the first integral of Motion :

$$(1-2\alpha x) \frac{dt}{ds} = \text{const.} = p. \quad \dots \quad (15)$$

If the initial conditions are $x_0=0$, $v_0=0$, $t_0=0$, then

$$p = 1,$$

and from (15) we find

$$v = \sqrt{(1-2\alpha x)^2 - (1-2\alpha x)^3}. \quad \dots \quad (16)$$

The maximum velocity of the material point is found from

$$\frac{dv}{dx} = 0 \quad \text{or} \quad 1-2\alpha x = \frac{2}{3};$$

this gives for v

$$v = \frac{2}{3\sqrt{3}} = 0.38.$$

This velocity will be attained at a distance

$$x = \frac{1}{6\alpha}.$$

After this point the velocity will decline, and where

$$1-2\alpha x = 0,$$

or at $x = \frac{1}{2\alpha}$, the point will stop.

To find the track we integrate (16), which gives

$$t = \frac{1}{\alpha} \operatorname{tgh}^{-1} \sqrt{2\alpha x},$$

or

$$x = \frac{\operatorname{tgh}^2 \alpha t}{2\alpha}. \quad \dots \quad (17)$$

From the first equation (17) we see that the point will stop at

$$t = \infty.$$

9. Harmonic Motion.

This Motion is given by the potential function

$$\phi = \alpha^2 x^2;$$

hence the element of the four-track is

$$ds^2 = (1 + \alpha^2 x^2) dt^2 - dz^2 - dy^2 - \frac{dx^2}{1 + \alpha^2 x^2}. \quad (18)$$

The form of Ether is given by the condition that the Gaussian curvature is constant.

From (13), taking

$$K = \frac{1}{R^2},$$

$$g = -1,$$

we obtain

$$\frac{\partial^2 g_{44}}{\partial x_1^2} = \frac{2}{R},$$

which gives for g_{44} the above-found expression.

The form of Ether is a "sphere" of the radius $\frac{1}{\alpha}$.

The first integral can be obtained from the fourth equation of Motion, and is

$$g_{44} \frac{dt}{ds} = \text{const.} = p. \quad (19)$$

If the initial conditions are

$$t_0 = 0, \quad x = x_0, \quad v = v_0,$$

integrating (19) once more we obtain

$$x = \frac{x_0 \cos \alpha t}{\sqrt{1 + \alpha^2 x_0^2 \sin^2 \alpha t}}. \quad (20)$$

10. Rotation.

We consider another instance of a harmonic Motion—a uniform rotation.

The fundamental quadratic form is

$$ds^2 = (1 + \alpha^2 r^2) dt^2 - \frac{r^2 d\phi^2}{1 + \alpha^2 r^2} - \frac{dr^2}{1 + \alpha^2 r^2} - dz^2, \quad (21)$$

where we have introduced cylindrical coordinates r, ϕ, z, t .

The integration of the second and fourth equations of Motion gives

$$\left. \begin{aligned} g_{22} \frac{d\phi}{ds} &= \frac{r^2}{1+\alpha^2 r^2} \frac{d\phi}{ds} = h, \\ g_{44} \frac{dt}{ds} &= (1+\alpha^2 r^2) \frac{dt}{ds} = k. \end{aligned} \right\} \dots (22)$$

Combining (22) and (21), we find the connexion between r and ϕ :

$$\frac{2d\phi}{h} \sqrt{-1} = \frac{(1+\alpha^2 r^2)d(r^2)}{r^2 \sqrt{\alpha^2(1+\alpha^2 h^2)r^4 - (k^2 - 1 - 2h^2 \alpha^2)r^2 + h^2}}. \quad (23)$$

The integration of (23) leads to a transcendental equation in ϕ and r , which cannot be solved in finite terms.

If, however, we take only an approximate solution, this expression becomes simplified, and we obtain

$$\left. \begin{aligned} r &= r_0 [1 - r_0^2 \alpha^2 \sin^2 (1 - \alpha^2 r_0^2) \phi], \\ (1 - \alpha^2 r_0^2) \phi + \frac{r_0^2 \alpha^2 \sin^2 (1 - r_0^2 \alpha^2) \phi}{2} &= at. \end{aligned} \right\} \dots (24)$$

11. Einstein's Law of Gravitation.

As the last instance we show how Einstein's law of gravitation for free Ether could be derived from Laplace's equation.

In Galilean coordinates the equation of Laplace is

$$\frac{\partial^2 \phi}{\partial t^2} - \frac{\partial^2 \phi}{\partial x^2} - \frac{\partial^2 \phi}{\partial y^2} - \frac{\partial^2 \phi}{\partial z^2} = 0, \quad \dots (25)$$

and in curvilinear coordinates

$$g^{\mu\nu} \phi_{\mu\nu} = 0, \quad \dots (26)$$

where $\phi_{\mu\nu}$ is the second covariant derivative of the scalar potential ϕ , or

$$g^{\mu\nu} \left(\frac{\partial^2 \phi}{\partial x_\mu \partial x_\nu} - \{\mu\nu, \alpha\} \frac{\partial \phi}{\partial x_\alpha} \right) = 0. \quad \dots (27)$$

To derive Einstein's law we must exclude the first and second derivative of ϕ from (26).

As it is known, it is possible to introduce, without changing the Riemann-Christoffel tensor, such a system of coordinates that for a selected point the first derivatives of $g_{\mu\nu}$ shall vanish, and $\frac{\partial}{\partial x_\alpha} \{\mu\nu, \sigma\}$ shall be increased by an arbitrary quantity $a_{\mu\nu}^\sigma$.

For such coordinates (27) becomes

$$g^{\mu\nu} \frac{\partial^2 \phi}{\partial x_\mu \partial x_\nu} = 0. \quad . \quad . \quad . \quad . \quad . \quad (28)$$

We prove that if ϕ is a solution of (26), $\frac{\partial \phi}{\partial x_a} = \phi_a$ will also be a solution.

We have for the above-mentioned coordinates

$$g^{\mu\nu} (\phi_a)_{\mu\nu} = g^{\mu\nu} \left(\frac{\partial^2 \phi_a}{\partial x_\mu \partial x_\nu} - \frac{\partial}{\partial x_\mu} \{ \alpha\nu, \epsilon \} \phi_\epsilon \right)$$

as the three-index symbol vanishes.

If ϕ satisfies (26), it follows that

$$g^{\mu\nu} \frac{\partial^2 \phi_a}{\partial x_\mu \partial x_\nu} = g^{\mu\nu} \frac{\partial^2 \phi}{\partial x_a \partial x_\mu \partial x_\nu} = \frac{\partial}{\partial x_a} \left(g^{\mu\nu} \frac{\partial^2 \phi}{\partial x_\mu \partial x_\nu} \right) = 0$$

according to (28) and because $\frac{\partial g^{\mu\nu}}{\partial x_a}$ vanishes.

We can also use the arbitrary quantities $a_{\mu\nu}^\sigma$ in such manner as to make vanish

$$g^{\mu\nu} \frac{\partial}{\partial x_\mu} \{ \sigma\nu, \epsilon \} \phi_\epsilon$$

(see A. S. Eddington, 'The Mathematical Theory of Relativity,' pp. 78 and 177) ; hence

$$g^{\mu\nu} (\phi_a)_{\mu\nu} = 0. \quad . \quad . \quad . \quad . \quad . \quad (29)$$

Now the exclusion of derivatives of ϕ from (26) can be made as follows :—

As ϕ is a scalar, the first two subscripts in $\phi_{\mu\nu}$ can be interchanged ; hence (29) becomes

$$g^{\mu\nu} \phi_{\mu\alpha\nu} = 0, \quad . \quad . \quad . \quad . \quad . \quad (30)$$

or interchanging α and ν , we obtain

$$\left. \begin{aligned} g^{\mu\nu} \phi_{\mu\alpha\nu} &= g^{\mu\nu} (\phi_{\mu\nu\alpha} - B_{\mu\nu\alpha}^\epsilon \phi_\epsilon) \\ &= g^{\mu\nu} \phi_{\mu\nu\alpha} - B_{\alpha}^\epsilon \phi_\epsilon. \end{aligned} \right\} \quad . \quad . \quad . \quad (31)$$

Remembering that

$$g^{\mu\nu} \phi_{\mu\nu\alpha} = (g^{\mu\nu} \phi_{\mu\nu})_\alpha = 0,$$

we obtain from (31)

$$B_{\alpha}^\epsilon \phi_\epsilon = 0. \quad . \quad . \quad . \quad . \quad . \quad (32)$$

B_{α}^ϵ depends to the first approximation upon the second

derivatives of $g_{\mu\nu}$, or, what is the same, upon the second derivatives of ϕ , because $g_{\mu\nu}$ are to the first approximation linear functions of ϕ .

Now ϕ_e may include an arbitrary constant which will not be in B_a^e ; therefore, in order to satisfy (32), we must have

$$B_a^e = 0, \quad . \quad . \quad . \quad . \quad . \quad . \quad (33)$$

which is Einstein's law of gravitation.

III. DYNAMICS OF A CONTINUOUS MEDIUM.

12. The Law of Continuity is

$$\left(\rho_0 \frac{dx_\nu}{ds}\right)_\nu = 0, \quad . \quad . \quad . \quad . \quad . \quad . \quad (1)$$

where ρ_0 is the invariant density of the Medium.

We expand (1),

$$\begin{aligned} \left(\rho_0 \frac{dx_\nu}{ds}\right)_\nu &= \frac{\partial}{\partial x_\nu} \left(\rho_0 \frac{dx_\nu}{ds}\right) + \{\epsilon\nu, \nu\} \rho_0 \frac{dx_\epsilon}{ds} \\ &= \frac{\partial}{\partial x_\nu} \left(\rho_0 \frac{dx_\nu}{ds}\right) + \frac{1}{\sqrt{-g}} \frac{\partial \sqrt{-g}}{\partial x_\epsilon} \rho_0 \frac{dx_\epsilon}{ds} \\ &= \frac{1}{\sqrt{-g}} \frac{\partial}{\partial x_\nu} \left(\rho_0 \sqrt{-g} \frac{dx_\nu}{ds}\right) = 0, \end{aligned}$$

which for Galilean coordinates becomes the usual law of continuity.

13. The Law of Motion.

As it is known from the General Theory of Relativity, the law of Motion of a continuous medium is

$$\left(p^{\alpha\nu} + \rho_0 \frac{dx_\alpha}{ds} \frac{dx_\nu}{ds}\right)_\nu = 0, \quad . \quad . \quad . \quad . \quad (2)$$

where $p^{\alpha\nu}$ represents the stress and $\rho_0 \frac{dx_\alpha}{ds} \frac{dx_\nu}{ds}$ the energy tensor of the medium.

Let us find the relation of this law to the law of Motion of a material point in Ether :

$$\frac{d^2 x_\alpha}{ds^2} + \{\mu\nu, \alpha\} \frac{dx_\mu}{ds} \frac{dx_\nu}{ds} = 0. \quad . \quad . \quad . \quad . \quad (3)$$

We denote the left side at (3) by F^a :

$$\frac{d^2 x_a}{ds^2} + \{\mu\nu, \alpha\} \frac{dx_\mu}{ds} \frac{dx_\nu}{ds} = F^a, \quad . . . \quad (3a)$$

and transform it.

We multiply (3a) by $\rho_0 \sqrt{g}$ and transform the first term of the left side

$$\begin{aligned} \sqrt{g} \rho_0 \frac{d^2 x_a}{ds^2} &= \rho_0 \sqrt{g} \frac{\partial}{\partial x_\nu} \left(\frac{dx_a}{ds} \right) \frac{dx_\nu}{ds} \\ &= \frac{\partial}{\partial x_\nu} \left(\rho_0 \sqrt{g} \frac{dx_a}{ds} \frac{dx_\nu}{ds} \right) - \frac{dx_a}{ds} \frac{\partial}{\partial x_\nu} \left(\rho_0 \sqrt{g} \frac{dx_\nu}{ds} \right) \\ &= \frac{\partial}{\partial x_\nu} \left(\rho_0 \sqrt{g} \frac{dx_a}{ds} \frac{dx_\nu}{ds} \right), \quad . . . \quad (4) \end{aligned}$$

as the second term vanishes according to the law of Continuity. Now

$$\begin{aligned} \frac{\partial}{\partial x_\nu} \left(\rho_0 \sqrt{g} \frac{dx_a}{ds} \frac{dx_\nu}{ds} \right) &= \sqrt{g} \frac{\partial}{\partial x_\nu} \left(\rho_0 \frac{dx_a}{ds} \frac{dx_\nu}{ds} \right) + \rho_0 \frac{dx_a}{ds} \frac{dx_\nu}{ds} \frac{\partial \sqrt{g}}{\partial x_\nu} \\ &= \sqrt{g} \frac{\partial}{\partial x_\nu} \left(\rho_0 \frac{dx_a}{ds} \frac{dx_\nu}{ds} \right) + \sqrt{g} \{\nu\mu, \mu\} \rho \frac{dx_a}{ds} \frac{dx_\nu}{ds}. \quad (5) \end{aligned}$$

Combining (5), (4), and (3a), we obtain

$$\left(\rho_0 \frac{dx_a}{ds} \frac{dx_\nu}{ds} \right)_\nu = F^a \rho_0. \quad . . . \quad (6)$$

Combining (6) and (2), we obtain

$$\rho_0 \frac{d^2 x_a}{ds^2} + \rho_0 \{\mu\nu, \alpha\} \frac{dx_\mu}{ds} \frac{dx_\nu}{ds} = -p_\nu^{\alpha\nu}. \quad . . \quad (7)$$

14. Several sequels can be drawn from (7):—

1. If $p_\nu^{\alpha\nu} = 0$, the equation (7) coincides with (3), or, in order that the Motion shall proceed on the geodesic line of the Medium, it is necessary and sufficient that the stress tensor shall be a self-balanced mechanical system.

2. We multiply (7) by $g_{\alpha\beta} \frac{dx_\beta}{ds}$ and obtain

$$g_{\alpha\beta} p_\nu^{\alpha\nu} \frac{dx_\beta}{ds} = 0. \quad . . . \quad (8)$$

This is the law of Energy of the Medium. It is equivalent to the fourth law of Motion of (7), which is sometimes wrongly considered in the General Theory of Relativity to be the Law of Continuity.

3. For Ether at rest and at motion

$$p_{\nu}^{\alpha} = 0 ;$$

hence an electron is moving in an electromagnetic field at the Geodesic line of Ether.

The Law of Energy (8) is identically satisfied for electromagnetic moving systems.

As is known, the Law of Energy breaks down if we apply the formulæ of the Special Theory of Relativity to an accelerated motion of electrons.

IV. ELECTRODYNAMICS.

15. *The Electromagnetic Equations.*

The application of curvilinear coordinates to four-dimensional space presents a difficulty which does not exist in the case of rectilinear coordinates.

As is known, the Lorentz transformations can be derived from the condition that the expression

$$ds^2 = dx_0^2 + dy_0^2 + dz_0^2 + dt_0^2 \quad . \quad . \quad . \quad (1)$$

can be transformed into

$$ds^2 = dx_1^2 + dy_1^2 + dz_1^2 + dt_1^2.$$

If we apply this method to curvilinear coordinates, we must find such a connexion between Galilean and accelerated systems which transform (1) into

$$ds^2 = g_{\alpha\beta} dx_{\alpha} dx_{\beta} \quad . \quad . \quad . \quad . \quad (2)$$

It is known from deformation of surfaces, that this is only possible if the Riemann-Christoffel tensor of (2) vanishes, which generally is not the case. Therefore the form of Ether in general is characterized not by a particular system of coordinates, but by the fundamental tensor $g_{\mu\nu}$.

At the basis of Electrodynamics of moving systems we take Maxwell's equations of the General Theory of Relativity, the fundamental tensor $g_{\mu\nu}$ depends upon the motion of the System.

For convenience' sake, we give here these equations.
If the four-potential is

$$k^\mu = F, G, H, \phi, \quad . \quad . \quad . \quad . \quad . \quad (3)$$

the Electromagnetic Force is given by

$$F_{\mu\nu} = \frac{\partial k_\mu}{\partial x_\nu} - \frac{\partial k_\nu}{\partial x_\mu},$$

$$(F^{\mu\nu})_\nu = I^\mu, \quad . \quad . \quad . \quad . \quad . \quad (4)$$

where

$$I^\mu = \sigma_x, \sigma_y, \sigma_z, \rho$$

is the stream tensor ; the Mechanical Force is

$$h_\mu = F_{\mu\nu} I^\nu, \quad . \quad . \quad . \quad . \quad . \quad (5)$$

the energy tensor

$$E_\mu^\nu = -F^{\nu\alpha} F_{\mu\alpha} + \frac{1}{4} g_\mu^\nu F^{\alpha\beta} F_{\alpha\beta}, \quad . \quad . \quad . \quad . \quad (6)$$

the connexion between E_μ^ν and h_μ is

$$h_\mu = E_{\mu\nu}^\nu \quad . \quad . \quad . \quad . \quad . \quad (7)$$

(see A. Einstein, 'Die Grundlage der Allgemeiner Relativitätstheorie,' § 20).

The two fundamental problems of Electrodynamics of moving systems are :

1. To find the motion of an electron in a given Electromagnetic field.
2. To find the Electromagnetic field of a moving system.

16. *Motion of Electrons.*

We must first make the cause of the mechanical actions of an electric field clear. It greatly resembles the gravitational force, but it is quite a different phenomenon. The mechanical action of a Gravitational field is due to the existing curving of the Ether, which is the physical content of gravitation.

The mechanical action of an electric field is more complicated. The electric field of an electron is self-balanced; therefore, as we shall show later, the Ether of the field is not curved (except for the gravitational effect of its energy), and hence has no mechanical action on the electron itself or on matter which may be in the field.

Now, if the electron is introduced in an external field, the equilibrium is violated; to restore it additional stresses become necessary. They change the electric field of an electron, the external field, and curve the Ether; this evokes the Motion of the electron.

The mechanical force of the field upon the electron is given by (5), where in $F_{\mu\nu}$ ought to be included both the external and the field of the electron. As, however, the latter does not produce a mechanical effect, it can be omitted. The problem of Motion is reduced to the finding of the tensor $g_{\mu\nu}$ corresponding to the mechanical force. If the Force is derived from a potential, the tensor $g_{\mu\nu}$ and the Motion can be obtained by the method given in the dynamics of a material point.

17. Equilibrium of Ether.

We consider the state of the inner field of a moving electron.

The Ether must be in equilibrium whether the electron is at rest or in Motion.

In the first case the conditions of equilibrium are

$$\text{div}_\nu E_\mu^\nu = \frac{\partial E_\mu^\nu}{\partial x_\nu} = 0$$

(see D. Meksyn, *Phil. Mag.* 1926, p. 998). The conditions for Motion are

$$E_{\mu\nu}^\nu = 0, \quad . \quad . \quad . \quad . \quad . \quad . \quad (8)$$

or, expanding (8),

$$\frac{1}{\sqrt{-g}} \frac{\partial}{\partial x_\nu} (E_\mu^\nu \sqrt{-g}) = \frac{1}{2} \frac{\partial g_{\alpha\beta}}{\partial x_\mu} E^{\alpha\beta}. \quad . \quad . \quad (9)$$

The left side represents the divergence of the stress tensor, and is equal to zero if the electron is at rest (or in a uniform rectilinear motion).

If the electron has an accelerated motion, this divergence is balanced by the right side, which represents the mechanical reaction of Ether; it is equal and opposite to the external force acting on the electron.

We take the fundamental form to be

$$ds^2 = \left(1 - \frac{2\phi}{m}\right) dt^2 - \frac{dx^2 + dy^2 + dz^2}{1 - \frac{2\phi}{m}}, \quad . \quad . \quad (10)$$

or to the first approximation

$$g_{11} = g_{22} = g_{33} = -1 - \frac{2\phi}{m},$$

$$g_{44} = 1 - \frac{2\phi}{m}, \quad . \quad . \quad . \quad (11)$$

where m is the mass of the electron, and ϕ is the potential of the external force.

Phil. Mag. S. 7. Vol. 4. No. 21. Aug. 1927.

U

Using (11) and the well-known values of $E^{a\beta}$, we obtain for an electron whose electric field is X, Y, Z ,

$$\frac{1}{2} \frac{\partial g_{a\beta}}{\partial x_\nu} E^{a\beta} = - \frac{(X^2 + Y^2 + Z^2)}{4\pi m} \frac{\partial \phi}{\partial x}.$$

We integrate this expression over the whole field: for hyperbolic motion, as $\frac{\partial \phi}{\partial x}$ is the acceleration it has the same value for the whole field, and hence the required integral will be equal to the first approximation to

$$- \frac{2E^0}{m} \frac{\partial \phi}{\partial x}, \quad (12)$$

where E^0 is the energy of the electron: as, on the other hand, (12) is equal and opposite to the external force $\frac{\partial \phi}{\partial x}$, we obtain

$$m = 2E^0. \quad (13)$$

If we take the fundamental form to be

$$ds^2 = \left(1 - \frac{2\phi}{m}\right) dt^2 - dy^2 - dz^2 - \frac{dx^2}{1 - \frac{2\phi}{m}},$$

we obtain

$$m = \frac{4}{3}E^0, \quad (14)$$

the result given by the Special Theory of Relativity.

18. *An Electron in its own Field.*

We show that the field of an electron exerts no mechanical action upon the electron itself.

As we know, the mechanical force is due to curving of Ether. Therefore we have to prove that no such curving exists in the field, or that $g_{\mu\nu} = \text{const.}$

The equations of equilibrium for rest are

$$\left. \begin{aligned} \frac{\partial E_\nu^\mu}{\partial x_\mu} &= 0, \\ h_\nu &= \frac{\partial E_\nu^\mu}{\partial x_\mu} \end{aligned} \right\}; \quad (15)$$

the first equations hold for Ether, the second for the electron.

The corresponding equations of equilibrium for Motion are

$$\left. \begin{aligned} E_{\mu\nu}^{\nu} &= 0, \\ h_{\mu} &= E_{\mu\nu}^{\nu} \end{aligned} \right\} \dots \dots \dots (16)$$

We expand (16),

$$h_{\mu} = \frac{1}{\sqrt{-g}} \frac{\partial}{\partial x_{\nu}} (E_{\mu}^{\nu} \sqrt{-g}) - \frac{1}{2} \frac{\partial g_{\alpha\beta}}{\partial x_{\mu}} E^{\alpha\beta}. \quad (17)$$

Combining (17) with (15), we find for Ether and the electron the same condition of equilibrium,

$$E_{\mu}^{\nu} \frac{1}{\sqrt{-g}} \frac{\partial \sqrt{-g}}{\partial x_{\nu}} = \frac{1}{2} \frac{\partial g_{\alpha\beta}}{\partial x_{\mu}} E^{\alpha\beta}. \quad (18)$$

We take the fundamental form to be

$$ds^2 = g_{44} dx_4^2 - g_{11}(dx_1^2 + dx_2^2 + dx_3^2) \quad (19)$$

with the condition

$$g_{11} g_{44} = 1 \quad (20)$$

Inserting in (18) the values of $g_{\mu\nu}$ from (19) and the well-known values of $E^{\alpha\beta}$, we obtain

$$E_{\mu}^{\nu} \frac{1}{\sqrt{-g_{11}^2}} \frac{\partial \sqrt{-g_{11}^2}}{\partial x_{\nu}} = \frac{X^2 + Y^2 + Z^2}{4} \left(\frac{\partial g_{11}}{\partial x_{\mu}} + \frac{\partial g_{44}}{\partial x_{\mu}} \right). \quad (21)$$

The right side of (21) is equal to the first approximation to zero; hence

$$E_{\mu}^{\nu} \frac{\partial \sqrt{-g_{11}^2}}{\partial x_{\nu}} = 0. \quad (22)$$

It is a system of four equations which defines the

$$\frac{\partial}{\partial x_{\nu}} \sqrt{-g_{11}^2}.$$

As

$$|E_{\mu}^{\nu}| = \left(\frac{X^2 + Y^2 + Z^2}{2} \right)^{\frac{1}{2}},$$

(22) can only be satisfied if $\frac{\partial \sqrt{-g_{11}^2}}{\partial x_{\nu}}$ or $g_{11} = \text{const.}$, and from (20) follows that $g_{44} = \text{const.}$

19. The Field of a moving system.

We have now to consider the second problem of Electrodynamics: to find the Electromagnetic field of a moving system.

For this purpose we must know the metric of the Ether of this system.

We have seen in Dynamics how this can be done.

When we have the tensor $g_{\mu\nu}$, the electromagnetic field is found from (4), § 15, with the additional condition,

$$k_\mu^\mu = 0. \quad . \quad . \quad . \quad . \quad . \quad (23)$$

Combining the two equations of (4), § 15, we obtain k_μ from

$$g^{\alpha\beta}(k_\mu)_{\alpha\beta} = \mathbf{I}_\mu - \mathbf{G}_\mu^\epsilon k_\epsilon, \quad . \quad . \quad . \quad . \quad (24)$$

and the electromagnetic tensor $F_{\mu\nu}$ from (4), § 15 (see A. S. Eddington, 'The Mathematical Theory of Relativity,' 1923, p. 175).

20. Lorentz transformations for Hyperbolic Motion.

As we have seen, the problem of finding the field of a moving system is reduced to a solution of a partial differential equation of the second order with variable coefficients.

One case, however, exists where the field can be obtained by a mere transformation of coordinates. This case is analogous to a uniform rectilinear motion.

Let x_μ^0 be a Galilean system at rest, and x_μ a system in motion. We express x_μ^0 as a function of x_μ , and insert in

$$ds^2 = dx_1^{02} - dx_2^{02} - dx_3^{02}; \quad . \quad . \quad . \quad (25)$$

the latter must be transformed in

$$ds^2 = g_{\mu\nu} dx_\mu dx_\nu. \quad . \quad . \quad . \quad . \quad (26)$$

This is possible only if the Riemann-Christoffel tensor of (26) vanishes, which case, as we have seen, corresponds to Hyperbolic Motion.

Let us consider an instance where the system is moving along the axis of X.

We have

$$\begin{aligned} ds^2 &= (1 - 2\alpha x) dt^2 - \frac{dx^2}{1 - 2\alpha x} - dy^2 - dz^2 \\ &= dt^{02} - dx^{02} - dy^{02} - dz^{02}. \quad . \quad . \quad . \quad . \quad (27) \end{aligned}$$

The transformations of coordinates are

$$\begin{aligned} x^0 &= -\frac{\sqrt{1-2\alpha x}}{\alpha} \cosh \alpha t, & t^0 &= \frac{\sqrt{1-2\alpha x}}{\alpha} \sinh \alpha t, \\ y^0 &= y, & z^0 &= z; \quad . \quad . \quad . \quad (28) \end{aligned}$$

and hence

$$\left. \begin{aligned} dx^0 &= \frac{\cosh at}{\sqrt{1-2ax}} dx - \sqrt{1-2ax} \sinh at \cdot dt, \\ dt^0 &= \frac{\sinh at}{\sqrt{1-2ax}} dx + \sqrt{1-2ax} \cosh at \cdot dt. \end{aligned} \right\} \quad (29)$$

These expressions can be confirmed by direct insertion in (27).

21. The Electromagnetic Field of Hyperbolic Motion.

We find the Electromagnetic force from the covariant tensor

$$F_{\mu\nu} = \begin{pmatrix} 0 & -\gamma & \beta & -X \\ \gamma & 0 & -\alpha & -Y \\ -\beta & \alpha & 0 & -Z \\ X & Y & Z & 0 \end{pmatrix} \quad (30)$$

If the field in a Galilean space at rest is $F_{\mu\nu}^0$, the field of a moving system will be

$$F_{\mu\nu} = \frac{\partial x_a^0}{\partial x_\mu} \frac{\partial x_\beta^0}{\partial x_\nu} F_{a\beta}^0; \quad (31)$$

or, using (29), we obtain

$$\begin{aligned} X &= X^0, & Y &= \gamma^0 \sqrt{1-2ax} \sinh at + Y^0 \sqrt{1-2ax} \cosh at, \\ Z &= -\beta^0 \sqrt{1-2ax} \sinh at + Z^0 \sqrt{1-2ax} \cosh at, \\ \alpha &= \alpha^0, & \beta &= \frac{\beta^0 \cosh at}{\sqrt{1-2ax}} - \frac{Z^0 \sinh at}{\sqrt{1-2ax}}, \\ \gamma &= \frac{\gamma^0 \cosh at}{\sqrt{1-2ax}} + \frac{Y^0 \sinh at}{\sqrt{1-2ax}}. \end{aligned} \quad (32)$$

If the field of an electron at rest is X^0, Y^0, Z^0 , its field in a hyperbolic motion is found from (34) if we put

$$\alpha^0 = \beta^0 = \gamma^0 = 0.$$

The Field is to the first approximation the same as if the electron would move without acceleration.

The Electromagnetic Momentum is equal to

$$G_x = \frac{\beta Z - \gamma Y}{4\pi} = - \frac{Z^{02} + Y^{02}}{4\pi} \sinh at \cosh at$$

and the reaction of the field upon the electron

$$\frac{\partial G_x}{\partial t} = - \frac{Z^{02} + Y^{02}}{4\pi} \alpha,$$

or, integrating through the whole Field, we find the reaction

$$F = -\frac{4}{3} E^0 \alpha,$$

which is, as we have seen, counterbalanced by the mechanical stress in Ether.

IV. ETHER AND MATTER.

22. Elasticity of Ether.

We consider now the last property of Ether—its Elasticity.

Maxwell's Electrodynamics ascribed the Electromagnetic Field to stresses in Ether; they are, however, usually considered as useful mathematical expressions without a physical meaning behind them.

It stands to reason that in a Medium so different from a solid body as Ether, stresses shall exist, because great forces are required in order to produce a small change in a form of a solid body; on the other hand, we can move in Ether without applying any force at all.

It is one of the confusions of our intuitive knowledge.

To bring into play elastic forces of Ether, the latter must be deformed. Not every motion in Ether brings about this change. A uniform motion does not deform Ether at all, and an accelerated motion produces only a comparatively small deformation. On the other hand, no change in form of a solid body is possible without bringing into play its elastic forces.

23. Strains in Ether.

Let u_μ ($\mu = 1, 2, 3, 4$) be the relative displacement of Ether: then the Strains are

$$e^{\mu\mu} = \frac{\partial u_\mu}{\partial x_\mu}, \quad e_{\mu\nu} = \frac{1}{2} \left(\frac{\partial u_\nu}{\partial x_\mu} + \frac{\partial u_\mu}{\partial x_\nu} \right). \quad . \quad . \quad . \quad (1)$$

Every displacement can be considered as composed of a displacement which is derived from a potential and a rotation.

The first part is equal to

$$u_{\mu} = e_{\mu\nu}x^{\nu}. \quad (2)$$

The potential function is

$$\phi = \frac{1}{2}e_{\mu\nu}x^{\mu}x^{\nu}; \quad (3)$$

hence the relative displacement is

$$u_{\mu} = \frac{\partial \phi}{\partial x^{\mu}}; \quad (4)$$

the strains,

$$e_{\mu\mu} = \frac{\partial^2 \phi}{\partial x^{\mu 2}}; \quad e_{\mu\nu} = \frac{\partial^2 \phi}{\partial x^{\mu} \partial x^{\nu}}, \quad (5)$$

and the dilatation is

$$\Delta = e_{11} + e_{22} + e_{33} + e_{44} = \nabla^2 \phi. \quad (6)$$

Let us find what will be the strains, or the function ϕ , in an infinite incompressible medium, if we assume that the phenomenon has a radial symmetry relative to a point $x_{\mu}^0 = 0$.

For this case (6) becomes

$$\frac{\partial^2 \phi}{\partial r^2} + \frac{3}{r} \frac{\partial \phi}{\partial r} = 0, \quad (6a)$$

or

$$\left. \begin{aligned} \phi &= \frac{m}{r^2}, \\ r &= x_1^2 + x_2^2 + x_3^2 + x_4^2, \end{aligned} \right\} \quad (7)$$

and the strains,

$$e'_{xx} = \frac{2m(3x^2 - y^2 - z^2)}{r^6}, \quad e'_{xy} = \frac{8mxy}{r^6}, \quad (8)$$

for $x_4 = 0$.

24. Stresses in Ether.

We assume that the connexion between Stresses and Strains is given for Ether by Hooke's Law. This Law, as Stokes pointed out, has a bearing on the property of a medium to be thrown into a state of isochronous vibrations.

The connexion between Strains and Stresses depends for an isotropic medium upon two constants, and is

$$\left. \begin{aligned} e_{xx} &= E^{-1} \{X_x - \sigma(Y_y + Z_z + T_t)\}, \\ &. \\ e_{tt} &= E^{-1} \{T_t - \sigma(X_x + Y_y + Z_z)\}, \end{aligned} \right\} \quad (9)$$

$$e_{xy} = \frac{1}{2\mu} X_y, \quad (10)$$

where E is Young's modulus.

As the medium is incompressible, we, adding the four equations (9), obtain

$$\sigma = \frac{1}{3}. \quad (11)$$

Let us find the Strains for an electron at rest.

The Stresses are

$$\left. \begin{aligned} X_x &= \frac{1}{8\pi} (X^2 - Y^2 - Z^2), \\ &\dots \dots \dots \\ T_t &= -\frac{1}{8\pi} (X^2 + Y^2 + Z^2), \\ X_y &= \frac{1}{4\pi} XY; \end{aligned} \right\} \quad (12)$$

inserting (12) in (9) and using (11), we obtain

$$\left. \begin{aligned} e_{xx} &= \frac{m^2}{12\pi E} \frac{3x^2 - y^2 - z^2}{r^6} = \frac{m}{24\pi E} e'_{xx}, \\ e_{xy} &= \frac{1}{8\pi\mu} XY = \frac{m^2}{8\pi\mu} \frac{xy}{r^6}. \end{aligned} \right\} \quad (13)$$

To satisfy the conditions of integrability of the Strains, we must have

$$e_{xy} = \frac{m^2}{8\pi\mu} \frac{xy}{r^6} = \frac{m}{24\pi E} e'_{xy}; \quad (14)$$

whence, using (8), we obtain

$$\mu = \frac{3E}{8}. \quad (15)$$

The Strains are the same as found in § 23.

25. The Strain-Energy Function of Ether and Stability of Electrons.

It is known that an elastic medium possesses a Strain-Energy function,

$$\delta W = X_x \delta e_{xx} + Y_y \delta e_{yy} + \dots + 2X_y \delta e_{xy} + \dots, \quad (16)$$

which is a complete differential.

The inner elastic forces of the medium are derived from a potential,

$$V = \int W dv, \quad (17)$$

where dv is an element of volume.

In order that the medium shall be stable under the action

of these inner forces, it is necessary and sufficient that V shall be a minimum (see G. Kirchhoff, "Mechanik," Vorlesung 27).

We evaluate the function for three dimensions.

Inserting in (16) the values of e_{xx} , e_{xy} ... from (9, 10), we obtain

$$W = \frac{1}{3E} \{ (X_x + Y_y + Z_z)^2 + 4(X_y^2 + X_z^2 + Y_z^2 - X_x Y_x - X_x Z_x - Y_y Z_y) \}. \quad (18)$$

Using Maxwell's expressions for the Stresses (12), we, from (18), find

$$W = \frac{5}{192\pi^2 E} (X^2 + Y^2 + Z^2)^2. \quad \dots \quad (19)$$

As it is known from Thomson's theorem, the energy

$$\int \frac{X^2 + Y^2 + Z^2}{8\pi} dv$$

of an electrostatic Field

$$X = -\frac{\partial \phi}{\partial x}, \quad Y = -\frac{\partial \phi}{\partial y}$$

($\phi = \text{const.}$ on the surface of conductors),

if the charge remains constant, is less than for any other field; hence the electron is in stable equilibrium (§ 18).

26. The Fundamental Form of the Theory of Relativity.

We derive from these considerations one sequel more.

It is known that, in the fundamental form of the Theory of Relativity,

$$ds^2 = dx^2 + dy^2 + dz^2 - c^2 dt^2; \quad \dots \quad (20)$$

the term of time has an opposite sign from the terms of space. This has a bearing on the Law of Constancy of light-propagation.

We show how this could be understood from the Physical Form of Ether.

We have seen that, when electrons are present, Ether is incompressible in four-dimensional space.

Let us however consider such displacements where Ether remains incompressible in the usual sense or only in space; the necessary condition for this is

$$e_{tt} = 0, \quad \text{or} \quad T_t = \frac{1}{3}(X_x + Y_y + Z_z).$$

For an elastic medium the Laws of small motions are

$$\left. \begin{aligned} (\lambda + \mu) \frac{\partial \Delta}{\partial x} + \mu \nabla^2 u + \rho X &= \rho \frac{\partial^2 u}{\partial t^2} \\ \dots \dots \dots \end{aligned} \right\} \dots \quad (21)$$

(see A. Love, 'The Theory of Elasticity,' 1906, p. 131).

In the case of Ether, ρ is the density of its energy, and the dilatation $\Delta = 0$; hence (21) becomes

$$\frac{3E}{8} \nabla^2 u = \frac{\partial^2 u}{\partial t^2}. \quad \dots \quad (22)$$

Now E must be positive (if ρ is positive) in order that the medium shall be stable under the action of its inner forces of Elasticity; hence (22) becomes

$$\nabla^2 u = \frac{1}{c^2} \frac{\partial^2 u}{\partial t^2}, \quad \dots \quad (23)$$

where

$$c^2 = \frac{3E}{8\rho}. \quad \dots \quad (24)$$

The Lorentz transformations can be derived from (23) under the condition that this equation must preserve the same form for every rectilinear uniform motion.

It seems that the *negative sign at the time member of (20) is necessary for Stability of Ether.*

The velocity of light-propagation is given from (24):

$$c = \sqrt{\frac{3E}{8\rho}}. \quad \dots \quad (25)$$

27. Gravitation and the Electrostatic Field of Protons.

The best way of understanding the mutual relation between Electricity and Gravitation (or Motion) is a comparison of Ether with a solid elastic body.

Under the influence of external forces there arise in a solid body two internally-connected phenomena: Elastic stresses and a corresponding change of form.

Ether represents an analogous case where stresses are observed as an electromagnetic field, and a corresponding displacement as gravitation (or mechanical force).

Gravitation and Electricity are two sides of one and the same state of Ether. Electromagnetic Energy must produce a mechanical displacement of Ether or have a

gravitational mass, and, conversely, every mechanical displacement of Ether (Gravitation and Motion) must be accompanied by Electromagnetic stresses.

This explains the influence of Motion and Gravitation upon an Electromagnetic Field, and throws light upon the nature of the Electrostatic field of protons.

As we shall see, it is entirely due to the gravitation of protons and not to their charge.

We know that the Electromagnetic four-potential k_μ of every field satisfies the equations (23), (24), § 19 :

$$k_\mu^\mu = 0, \quad . \quad . \quad . \quad . \quad . \quad (26)$$

$$g^{\alpha\beta}(k_\mu)_{;\beta} = I_\mu - G_\mu^\alpha k_\alpha. \quad . \quad . \quad . \quad (27)$$

We integrate (27) for a proton under the assumption that it has no charge, or $I_\mu = 0$.

From the Theory of Gravitation we have

$$G^{\mu\nu} = -8\pi(T^{\mu\nu} - \frac{1}{2}g^{\mu\nu}T), \quad . \quad . \quad . \quad (28)$$

where

$$T^{\mu\nu} = \rho_0 \frac{dx_\mu}{ds} \frac{dx_\nu}{ds} \quad \text{and} \quad G = 8\pi T = 8\pi\rho_0; \quad . \quad (29)$$

hence

$$G^{\mu\nu} = -8\pi \left(\rho_0 \frac{dx_\mu}{ds} \frac{dx_\nu}{ds} - \frac{1}{2}g^{\mu\nu}\rho_0 \right). \quad . \quad . \quad (30)$$

For Matter at rest, to the first approximation,

$$G_\mu^\nu = 4\pi\rho_0 \quad \text{if} \quad \mu = \nu = 1, 2, 3; \quad . \quad . \quad (31)$$

for $\mu = \nu = 4$,

$$G_4^4 = -4\pi\rho_0, \quad . \quad . \quad . \quad . \quad . \quad (32)$$

and $G_\mu^\nu = 0$ if $\mu \neq \nu$.

For a stationary field, (27) becomes

$$\nabla^2 k_\mu = G_\mu^\alpha k_\alpha, \quad . \quad . \quad . \quad . \quad . \quad (33)$$

or

$$\nabla^2 k_\mu = 4\pi\rho_0 k_\mu \quad \text{for} \quad \mu = 1, 2, 3 \quad . \quad . \quad (34)$$

and

$$\nabla^2 k_4 = -4\pi\rho_0 k_4 \quad \text{for} \quad \mu = 4. \quad . \quad . \quad (35)$$

In the field (34) and (35) are the usual Laplace's equation,

$$\nabla^2 k_\mu = 0. \quad . \quad . \quad . \quad . \quad (36)$$

The solution of (36) for the field is

$$k_\mu = \frac{a_\mu}{r}.$$

300 Dr. Ferguson and Mr. I. Vogel on the Calculation of
Using (26), we obtain

$$a_{\mu} = 0 \quad \text{for } \mu = 1, 2, 3,$$

or the field is purely electrostatic.

We integrate (35) for a particular case of a radial symmetry.

For the field

$$k_4 = \frac{e}{r}, \quad \dots \quad (37)$$

in the inner of the proton, (35) becomes

$$\frac{\partial^2 k_4}{\partial r^2} + \frac{2}{r} \frac{\partial k_4}{\partial r} = -4\pi\rho_0 k_4$$

or

$$\frac{\partial^2 (k_4 r)}{\partial r^2} = -4\pi\rho_0 (k_4 r),$$

the solution of which is

$$k_4 = \frac{A \sin \sqrt{4\pi\rho_0} \cdot r + B \cos \sqrt{4\pi\rho_0} \cdot r}{r}. \quad (38)$$

From the condition that k_4 must be finite, we obtain from (38)

$$k_4 = \frac{A \sin \sqrt{4\pi\rho_0} \cdot r}{r}. \quad (39)$$

At the surface of the proton, (37) and (39) must be equal: this defines A.

We see that, in so far as the outer field of the Proton is concerned, it will be identical with the field of an electron.

XXVII. The Calculation of the Equivalent Conductivity of Strong Electrolytes at Infinite Dilution.—Part I. *Aqueous Solutions.* (iii.) *The Mobilities of the Hydrogen and the Hydroxyl Ions.* By ALLAN FERGUSON, M.A., D.Sc., and ISRAEL VOGEL, M.Sc., D.I.C.*

(a) *The Hydrogen Ion.*

ALTHOUGH the problem of the determination of the mobility of the hydrogen ion at infinite dilution has occupied the attention of investigators for about the last forty years (for complete bibliography see Walden, 'Das Leitvermögen der Lösungen,' 1924; also Parker, J. Amer. Chem. Soc. 1923, xlv. p. 2017), it cannot be said that a

* Communicated by the Authors.

satisfactory value has yet been attained. The accurate measurements of Kraus and Parker (J. Amer. Chem. Soc. 1922, xlv. p. 2429; 1923, xlv. p. 2029) on iodic acid, and of Parker (*ibid.* 1923, xlv. p. 2017) on hydrochloric acid, provide the most reliable data so far published for the calculation of this important constant.

The conductance at infinite dilution for these two acids has now been calculated by the authors' method (Part I. Phil. Mag. 1925, l. p. 971), and the results are shown in Tables I. and II. below.

TABLE I.
Hydrochloric Acid, 25° C.

$$\Lambda_0 = \Lambda + 3061.9 C^{0.96716}.$$

C.	Λ .	Λ_0 .
5.0×10^{-3}	425.49	425.70
1.0×10^{-2}	425.29	425.70
2.0×10^{-2}	424.88	425.69
3.0×10^{-2}	424.48	425.68
4.0×10^{-2}	424.08	425.67
5.0×10^{-2}	423.68	425.65
6.0×10^{-2}	423.30	425.65
7.0×10^{-2}	422.93	425.65
8.0×10^{-2}	422.60	425.70
Mean		425.68

TABLE II.
Iodic Acid, 25° C.

$$\Lambda_0 = \Lambda + 4140.8 C^{0.96866}.$$

C.	Λ .	Λ_0 .
5.0×10^{-5}	389.28	389.56
6.0×10^{-5}	389.23	389.56
7.0×10^{-5}	389.17	389.56
8.0×10^{-5}	389.12	389.56
9.0×10^{-5}	389.06	389.56
1.0×10^{-4}	389.01	389.56
2.0×10^{-4}	388.47	389.55
3.0×10^{-4}	387.93	389.54
4.0×10^{-4}	387.40	389.55
5.0×10^{-4}	386.88	389.51
6.0×10^{-4}	386.36	389.50
7.0×10^{-4}	385.86	389.50
8.0×10^{-4}	385.38	389.52
9.0×10^{-4}	384.92	389.56
$\times 10^{-3}$	384.48	389.52
Mean		389.54

It will be seen that the consistency of Λ_0 for hydrochloric acid over the range 0.00005 N to 0.0008 N and of iodic acid from 0.00005 N to 0.001 N leaves little to be desired. The values of both B and n in the equation $\Lambda_0 = \Lambda + BC^n$ are of interest. B is very much larger than that deduced for salts (*cf.* Part I., §§ (i.) & (ii.) of this series), while n approaches unity. It is also of interest to note that the values of Λ_0 deduced by Kraus and Parker (*loc. cit.*) for iodic acid (389.55) and by Parker (*loc. cit.*) for hydrochloric acid (425.69) are in excellent agreement with the mean value calculated by the present authors.

Having deduced Λ_0 for these acids, the mobility of the hydrogen ion at 25° may now be computed. Unfortunately, no accurate measurements of the conductivities of aqueous iodate solutions at 25° are at present available, and hence the mobility of the iodate ion and therefore of the hydrogen ion cannot be directly calculated. The mobility (μ_0) of the chlorine ion has, however, been computed by the present writers (Part I., § (ii.) *loc. cit.*), and subtracting this value (76.63) from the conductance at infinite dilution for hydrochloric acid (425.68), the value 349.05 is obtained for the mobility of the hydrogen ion at 25°. The mobility of the iodate ion at 25° is accordingly 389.54—349.05, *i. e.* 40.49. Kraus and Parker (*loc. cit.*) deduced 349.93 from the iodic acid measurements, while Parker (*loc. cit.*) obtained 349.89 from the data on hydrochloric acid, the final value for the mobility of the hydrogen ion at 25° accepted by Parker being 349.89 ± 0.05 , which he regarded as a *minimum value*.

It must, however, be noted that Kraus and Parker assume the value of μ_0 for the chlorine ion at 25° to be 75.8 (Noyes and Falk, *J. Amer. Chem. Soc.* 1912, xxxiv. p. 479), a value which differs by more than 1 per cent. from the value (76.67) calculated by the present writers from the conductivity measurements of Lorenz and Michael (*Z. anorg. Chem.* 1921, cxvi. p. 161), the most accurate data for aqueous salt solutions at 25° at present available. Further, in deducing μ_0 for the hydrogen ion at 25° from Λ_0 of iodic acid, they assume that the ratio of the conductances at 25° and at 18° of approximately 0.001 N solutions of potassium iodate is equal to the ratio of the conductances at infinite dilution at these two temperatures. By applying this assumption, Kraus and Parker calculate the value of Λ_0 for potassium iodate at 25°. Here, again, data differing from those at which we have arrived are employed; Λ_0 at 18° for potassium iodate is taken as 98.5 (Noyes and Falk, *loc. cit.*)

(*cf.* Ferguson and Vogel, Part I. *loc. cit.*, 98·54), whilst μ_0 for the potassium ion at 25° is assumed to be 74·8 (Noyes and Falk, *loc. cit.*), the value deduced by the authors (*cf.* Part I., § (ii.) this Journal, p. 233) being 75·63 at 25°.

It was thought important to test this assumption of proportionality, and it seemed that some light could be thrown on the validity of the assumption by applying it to two salts closely related to potassium iodate. The data employed were those of Kohlrausch and Maltby (18°) and of Lorenz and Michael (25°); Λ_0 has already been calculated (*cf.* Part I., §§ (ii.) & (iii.)). The results are given in Table III.

TABLE III.

	$18^\circ\Lambda_{0\cdot001\text{ N.}}$	$18^\circ\Lambda_0$	$25^\circ\Lambda_{0\cdot001\text{ N.}}$	$25^\circ\Lambda_0$	$\frac{25^\circ\Lambda_{0\cdot001\text{ N.}}}{18^\circ\Lambda_{0\cdot001\text{ N.}}}$	$\frac{25^\circ\Lambda_0}{18^\circ\Lambda_0}$
KCl	127·34	130·04	147·80	152·26	1·1607	1·1709
NaCl ...	106·49	109·02	124·55	128·05	1·1696	1·1746

The reason for this discrepancy is not far to seek. From the two equations,

$$25^\circ\Lambda_0 = 25^\circ\Lambda + B(0\cdot001)^n$$

and

$$18^\circ\Lambda_0 = 18^\circ\Lambda + B_1(0\cdot001)^{n_1},$$

we have

$$\frac{25^\circ\Lambda_0}{18^\circ\Lambda_0} = \frac{25^\circ\Lambda + B(0\cdot001)^n}{18^\circ\Lambda + B_1(0\cdot001)^{n_1}},$$

and the ratio used by Kraus and Parker to obtain $25^\circ\Lambda_0$ is obtained by neglecting the "B" terms in the dilution equation. Inspection of the tables showing the values of B and n (Part I., §§ (i.) & (ii.) of this series) will show that the order of magnitude of these constants is such that their neglect, even for a concentration of approximately 0·001 N, is likely to introduce appreciable errors.

(b) *The Hydroxyl Ion.*

The difficulties inherent in the accurate measurement of the conductivities of aqueous solutions of the so-called strong bases have doubtless been responsible for the comparative scarcity of conductivity data in the field (*cf.* Ostwald, *J. prakt. Chem.* 1886, xxxiii. p. 352; 1887, xxxv. p. 112; Bredig, *Z. phys. Chem.* 1894, xiii. p. 289; Winkelblech, *ibid.* 1901, xxvi. p. 428; Calvert, *ibid.* 1901, xxxviii. p. 530; Jones, *Am. Chem. J.* 1901, xxvi. p. 428; Bousfield and Lowry, *Phil. Trans.* 1905, cciv. p. 292; Noyes, *Publ. Carnegie Inst.* 1907, no. 63, p. 262; Frary and Nietz, *J. Amer.*

304 *The Equivalent Conductivity of Strong Electrolytes.*

Chem. Soc. 1915, xxxvii. p. 2263). The only fairly reliable measurements appear to be those of Raikes, Yorke, and Ewart (J. Chem. Soc. 1926, cxxviii. p. 635) on sodium hydroxide solutions at 10°C and 18°C. Their results, however, are not expressed in the generally accepted manner, viz., conductivities at round concentrations, and in order to utilize them in the calculation of the mobility of the hydroxyl ion at infinite dilution, the conductances at round concentration were interpolated from a large scale conductance-concentration graph. While a fairly good curve could be put through the conductance values at 18°, we were unable to do so for the data at 10°.

The conductivity at infinite dilution has been calculated by the authors' method (this Journal, 1925, l. p. 971), and the results are shown in column 3 of Table IV. below. For purposes of comparison, the values of Λ_0 over the same range of concentration computed from the equation

$$\Lambda_0 = \Lambda + 75.7 C^{0.5000}$$

deduced by Raikes, Yorke, and Ewart (*loc. cit.*) are included in the Table.

TABLE IV.

C.	$\Lambda_0 = \Lambda + 64.4 C^{0.4087}$ $\Lambda_0 = \Lambda + 75.7 C^{0.5000}$		
1.0×10^{-3}	215.1	218.9	217.5
2.0×10^{-3}	213.9	218.9	217.3
4.0×10^{-3}	212.1	218.9	216.9
5.0×10^{-3}	211.5	218.9	216.8
8.0×10^{-3}	210.0	218.9	216.8
1.0×10^{-2}	209.3	219.1	216.9

It will be seen that while Λ_0 as deduced by the present authors is constant over the range 0.001—0.01 normal, the values computed from the square root formula show a marked increase at low concentrations. These deviations illustrate clearly the superiority of the general formula

$$\Lambda_0 = \Lambda + BC^n$$

over the very widely-used square root formula.

We arrive thus at the number 218.9 as the most probable value for the conductivity at infinite dilution. The mean value deduced by Raikes, Yorke, and Ewart was 217.0.

In the calculation of the mobility of the hydroxyl ion these authors assume two values for the mobility of the sodium ion at 18°, viz., 43.4 (Noyes and Falk, J. Amer. Chem. Soc. 1912, xxxiv. p. 479) and 43.23 (Washburn, *ibid.* 1918, xl. p. 158) leading to the values 173.6 and 173.8 respectively for the conductance of the hydroxyl ion at infinite

dilution at 18° . If we assume as the most probable value for the mobility of the sodium ion at 18° the value 43.48 deduced in Part I., § (i.) of this series of researches, we find that the conductance of the hydroxyl ion at infinite dilution is 218.9—43.5, i. e. 175.4, a value differing very appreciably from that calculated by Raikes, Yorke, and Ewart.

Summary.

The most probable values for the conductance at infinite dilution of the hydrogen ion at 25° and of the hydroxyl ion at 18° , deduced by the authors' method (Phil. Mag. 1925, l. p. 971), are 349.05 and 175.4 respectively.

One of the authors (I. V.) is indebted to the Trustees of the Dixon Fund for a grant with the aid of which part of the expenses of this investigation has been met.

The Imperial College of Science
and Technology, South Kensington.

East London College
(University of London).

XXVIII. *On the Control of the Frequency of Flashing of a Neon Tube by a Maintained Mechanical Vibrator.* By W. A. LEYSHON. *Ph.D.**

[Plates III.-V.]

CONTENTS.

Section 1. Introduction.

- „ 2. Theory.
- „ 3. Experimental Verification of Theory.
- „ 4. Conclusion.

SECTION 1.—*Introduction.*

THE phenomena which accompany the introduction of an alternating voltage into a circuit maintained in electrical vibration, the periodicity of the undisturbed vibration being equal, or nearly equal, to that of the introduced voltage, have attracted much attention, and have, in particular instances, been considered both theoretically and practically.

If an electric oscillatory circuit is coupled with another maintained by a triode, the well-known “Ziehens” effect is

* Communicated by the Author.

Phil. Mag. S. 7. Vol. 4. No. 21. Aug. 1927.

X

produced on varying the electric constants of the coupled circuit in a suitable manner. The theory of this effect was given for the case of varying inductance by Townsend¹; a general discussion of the problem later by Möller²; Albersheim³ has collected together the published data and theory on this subject.

Butterworth⁴ showed that a mechanical vibrator maintained electrically could, in regard to its reaction on the electrical maintaining system, be replaced by an equivalent electric circuit. He used this theorem in explaining the maintenance of a tuning-fork by a triode^{5, 5A}. Hodgkinson⁶ has also discussed this and similar problems mathematically. Dye used Butterworth's method in a theoretical and experimental study of quartz resonators⁷.

The effect on a triode-maintained oscillatory circuit of the introduction of an alternating voltage of a frequency differing little or not at all from the frequency of the undisturbed vibration, this alternating voltage being derived from a second triode-maintained circuit, has been studied experimentally by Vincent⁸, Appleton⁹, the present writer¹⁰, and others^{11, 12, 13}. Appleton discussed the matter theoretically, and applied his solution of the problem to the case of the reception of wireless signals by an oscillating triode. Recently van der Pol¹⁴ has given a very complete theoretical treatment of the latter problem.

It appears that in all these cases the frequency of vibration of the system as a whole tends to become equal to that of the added voltage, even though the frequency of the undisturbed system may differ quite appreciably from this.

The present paper is concerned with the maintenance of a mechanical vibrator by means of a flashing neon tube. The now well-known circuit for producing flashes was first described, and the simple theory of the circuit given, by Pearson and Anson¹⁵. The control of the frequency of flashing of such a circuit by the introduction of an additional alternating voltage has been mentioned by Bedell and Reich¹⁶ in an application of the circuit for the production of a linear time-base in oscillograph records.

Dye has introduced an alternating voltage derived from a tuning-fork-triode circuit into an Abraham-Bloch multivibrator circuit for control of frequency in his standard multivibrator wavemeter¹⁷. The theory of the multivibrator circuit has been recently given by van der Pol in his paper on Relaxation Oscillations¹⁸.

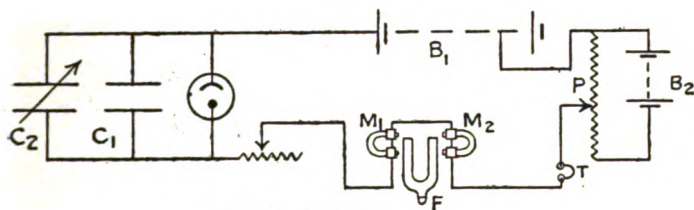
Some direct methods of control of frequency of circuits such as that of the flashing neon tube or the multivibrator

were described in a recent paper in the 'Electrician' ¹⁹; the neon-tube tuning-fork circuit in particular was shown working at the Royal Society Conversazione on June 16th, 1926.

A diagram of the experimental circuit is reproduced in fig. 1.

The electrical vibration in the condenser-neon-tube circuit is very rich in harmonics, since it consists of current impulses of short duration followed by no-current intervals of much longer duration. By means of the tuning-fork the frequency of flashing is kept very nearly constant. Thus the apparatus

Fig. 1.



- B_1, B_2 batteries.
 P potential divider.
 C_1 fixed condenser.
 C_2 variable condenser.
 M_1, M_2 telephone magnets.
 T headphones.

has similar electrical properties to that of the tuning-fork-controlled multivibrator, as described by Dye, but it is of much simpler construction than the latter; the variation with time of the gas-content of the present commercial type of neon tube is a disadvantage, but this difficulty may be overcome in the future ²⁰.

An elementary theory of the action of the tuning-fork in the circuit is developed in the next Section; experimental verifications of the theory are described in Section 3.

SECTION 2.—Theory.

It is first supposed that a sinusoidal voltage of constant amplitude and frequency is introduced into the neon-tube circuit. The differential equation for the circuit is then solved; suitable modifications of the solution are made in order that the introduced voltage may be considered to be due to the motion of the maintained tuning-fork reacting electromagnetically on the circuit.

In the following it is assumed that

- (1) For slow rates of flashing the time of a complete cycle of operations does not differ appreciably from that of a dark period—i. e. the flash is regarded as instantaneous.
- (2) The voltage induced in the neon-tube circuit by the tuning-fork at any instant is proportional to the velocity of the prongs at that instant.
The maximum induced voltage during one particular vibration is proportional to the amplitude of vibration of the tuning-fork.
- (3) The work done against dissipative forces during a complete vibration of the tuning-fork is proportional to the square of the amplitude of that vibration. (Frictional force proportional to velocity.)
- (4) The attracting force acting on the prongs of the fork due to the current in the neon-tube circuit is proportional to the current flowing in that circuit at the instant considered.
- (5) The frequency of vibration of the tuning-fork is not affected to an appreciable extent throughout the range of its maintenance, and its motion is a S.H.M.

In a particular cycle of operations, let

v_0 = amplitude of added sinusoidal voltage ;

$\omega = \frac{2\pi}{T}$, where T = periodic time of vibration of fork ;

t = time which has elapsed since the beginning of the dark period ;

$\phi = \frac{2\pi t'}{T}$, where t' is the interval of time measured from the instant when the fork passes through its position of zero displacement moving towards the attracting coils to the beginning of a dark period.

Then $v_0 \cos (\omega t + \phi)$ is the actual voltage introduced at a particular instant of time when t seconds have elapsed since the beginning of a dark period.

The equations for the circuit are then

$$B - V - v_0 \cos (\omega t + \phi) - Ri - L \frac{di}{dt} = 0, \quad \dots (1)$$

$$\left. \begin{aligned} \int_0^t i \cdot dt &= C(V - V_1), \\ \int_0^T i \cdot dt &= C(V_2 - V_1), \end{aligned} \right\} \quad \dots (2)$$

$$\text{or} \quad i = C \cdot \frac{dV}{dt},$$

where B = battery voltage, V = condenser voltage = voltage across lamp at time t ;

C = capacity of condenser + neon-lamp electrodes ;

R = resistance in series with lamp—including resistance of tuning-fork coils ;

L = inductance of tuning-fork coils (supposed constant) ;

V_1 = lower critical voltage of lamp ;

V_2 = upper „ „ of lamp ;

i = current flowing in the resistance R

[it is supposed that no current flows through the lamp except during the bright period—considered infinitely short in duration].

The differential equation obtained from (1) and (2) is

$$\frac{i}{C} + R \cdot \frac{di}{dt} + L \cdot \frac{d^2i}{dt^2} = wv_0 \sin (wt + \phi) \quad . \quad (3)$$

or

$$\left(\frac{1}{C} + RD + LD^2 \right) i = wv_0 \sin (wt + \phi),$$

where $D = \frac{d}{dt}$.

The solution of this is

$$Ri = A_1 e^{\alpha t} + A_2 e^{\beta t} + \frac{(1 - LCw^2)wRCv_0 \sin (wt + \phi) - w^2 C^2 R^2 v_0 \cos (wt + \phi)}{(1 - LCw^2)^2 + w^2 C^2 R^2}, \quad . \quad . \quad (4)$$

$$\text{where } \alpha = -\frac{R}{2L} + \sqrt{\frac{R^2}{4L^2} - \frac{1}{LC}}$$

$$\text{or } \alpha = -\frac{R}{2L} \left\{ 1 - \left(1 - \frac{4L}{CR^2} \right)^{\frac{1}{2}} \right\};$$

$$\beta = -\frac{R}{2L} - \sqrt{\frac{R^2}{4L^2} - \frac{1}{LC}}$$

$$\text{or } \beta = -\frac{R}{2L} \left\{ 1 + \left(1 - \frac{4L}{CR^2} \right)^{\frac{1}{2}} \right\},$$

A_1, A_2 are constants determined by setting

$$i = \frac{B - V_1 - v_0 \cos \phi}{R}, \quad \frac{di}{dt} = 0 \quad \text{when } t = 0.$$

* Actually, at the beginning of a dark period $i < \frac{B_1 - V_1 - v \cos \phi}{R}$ owing to the presence of inductance in the circuit.

The equation may be written

$$\begin{aligned}
 Ri = & + \frac{1}{1 - \frac{\alpha}{\beta}} \left[B - V_1 - v_0 Q \left(1 - LCw^2 - \frac{w^2 CR}{\beta} \right) \right] e^{\alpha t} \\
 & + \frac{1}{1 - \frac{\beta}{\alpha}} \left[B - V_1 - v_0 Q \left(1 - LCw^2 - \frac{w^2 CR}{\alpha} \right) \right] e^{\beta t} \\
 & + \frac{(1 - LCw^2)wRCv_0 \sin (wt + \phi) - w^2 C^2 R^2 v_0 \cos (wt + \phi)}{(1 - LCw^2)^2 + w^2 C^2 R^2}, \quad \dots \quad (5)
 \end{aligned}$$

where
$$Q = \frac{(1 - LCw^2) \cos \phi + wCR \sin \phi}{(1 - LCw^2)^2 + w^2 C^2 R^2}.$$

It is seen that the second term quickly becomes negligible if $\frac{L}{CR^2}$ is small and $\therefore \frac{R}{L} \gg \frac{1}{CR}$, which was the case in the experiments to be described. Also, if L is negligibly small, the equation becomes

$$Ri = (B - V_1 - v_0 Q') e^{-t/CR} + \frac{wCRv_0 \sin (wt + \phi) - w^2 C^2 R^2 v_0 \cos (wt + \phi)}{1 + w^2 C^2 R^2}, \quad (6)$$

where
$$Q' = \frac{\cos \phi + wCR \sin \phi}{1 + w^2 C^2 R^2}.$$

This is the solution of the differential equation :

$$\frac{i}{c} + R \cdot \frac{di}{dt} = wv_0 \sin (wt + \phi). \quad \dots \quad (7)$$

If, in equation (6), v_0 is made equal to zero, the equation for i becomes

$$Ri = (B - V_1) e^{-t/CR} \quad \dots \quad (8)$$

—the well-known equation for the charging current in an ordinary “flashing” circuit.

From equation (5) the relation between condenser voltage and time is found, remembering that

$$\frac{1}{c} \int_0^t i \cdot dt = V - V_1.$$

We have

$$V - V_1 = K_1(1 - e^{\alpha t}) + K_2(1 - e^{\beta t}) - v_0 P + v_0 Q, \quad \dots \quad (9)$$

where P is the same function of $(\omega t + \phi)$ as Q is of ϕ , and

$$K_1 = -\frac{A_1}{\alpha RC}$$

$$= -\frac{1}{\alpha RC \left(1 - \frac{\alpha}{\beta}\right)} \left[B - V_1 - v_0 Q \left(1 - LC\omega^2 - \frac{\omega^2 CR}{\beta}\right) \right],$$

$$K_2 = -\frac{A_2}{\beta RC}$$

$$= -\frac{1}{\beta RC \left(1 - \frac{\beta}{\alpha}\right)} \left[B - V_1 - v_0 Q \left(1 - LC\omega^2 - \frac{\omega^2 CR}{\alpha}\right) \right];$$

whence

$$V_2 - V_1 = K_1(1 - e^{\alpha T}) + K_2(1 - e^{\beta T}), \quad . \quad . \quad (10)$$

since $P = Q$ when $t = T$.

Neglecting $e^{\beta T}$,

$$T = \frac{1}{\alpha} \cdot \log \frac{K_1 + K_2 - (V_2 - V_1)}{K_1} \quad . \quad . \quad (11)$$

if a steady state is reached in which the period of flashing is equal to the period of the introduced voltage.

If $L = 0$,

$$\beta = -\infty \quad \text{and} \quad T = CR \log \frac{B - V_1 - v_0 Q'}{B - V_2 - v_0 Q'} \quad . \quad . \quad (12)$$

If $v_0 = 0$, this reduces to the well-known equation for the time of a dark period, first given by Pearson and Anson :

$$T = CR \log \frac{B - V_1}{B - V_2} \quad . \quad . \quad . \quad (13)$$

It will be seen from (12) that the effect of the introduced voltage on the period of flashing will be greater for a given value of $v_0 Q$ the more nearly B approaches V_2 .

Again, if Q is positive, the effect of the introduced voltage is to increase the periodic time; if Q is negative the periodic time is diminished; and if $Q = 0$, the time is unaffected by the introduced voltage.

$Q = 0$ when

$$(1 - LC\omega^2) \cos \phi + RC\omega \sin \phi = 0;$$

i. e., when

$$\phi = \tan^{-1} - \frac{(1 - LC\omega^2)}{RC\omega}$$

$$[\phi \approx 0 \text{ or } \pi].$$

Q has a maximum value when

$$-(1 - LC\omega^2) \sin \phi + RC\omega \cos \phi = 0; \quad \dots (14)$$

i.e., when

$$\phi = \tan^{-1} \frac{RC\omega}{1 - LC\omega^2}$$

$$\left[\phi \approx \pm \frac{\pi}{2} \right].$$

Stability of Oscillation.

For stability in a condition of oscillation, after a slight disturbance the system must tend to return to its original condition. For example, if, in the case under discussion, a state of equilibrium has been reached, so that the periodic time of flashing is equal to the periodic time of the introduced voltage, and then ϕ is accidentally increased by some transient disturbance, the resulting effect on the period must be such that the original value of ϕ tends to be restored.

Let us suppose the condition

$$T = \frac{1}{\alpha} \cdot \log \frac{K_1 + K_2 - (V_2 - V_1)}{K_1}$$

to be satisfied, where T = periodic time of introduced voltage, and suppose ϕ lies between 0 and $\frac{\pi}{2}$. This means that the beginning of a dark period occurs *after* the maximum of the introduced voltage.

If a slight increase of ϕ occurs accidentally, the time of the dark period is increased, and the beginning of the next dark period occurs still later; i.e., ϕ is increased. The condition is therefore unstable.

Now suppose ϕ lies between $\frac{\pi}{2}$ and π , and that again the condition

$$T = \frac{1}{\alpha} \log \frac{K_1 + K_2 - (V_2 - V_1)}{K_1}$$

is satisfied.

Here Q is positive, provided that ϕ is

$$< \tan^{-1} \frac{(1 - LC\omega^2)}{RC\omega}.$$

But $\frac{dQ}{d\phi}$, and $\therefore \frac{dT'}{d\phi}$ is now negative.

[T' = time of a dark period.]

Hence an increase in ϕ due to a transient disturbance results in a diminution of the time of the dark period, and therefore in a diminution of ϕ . The condition is stable.

Similarly, it may be shown that a stable condition of oscillation is possible if ϕ lies between

$$\tan^{-1} - \frac{(1 - LCw^2)}{RCw} \quad (\text{where } \phi \approx \pi)$$

and

$$\tan^{-1} \frac{CRw}{1 - LCw^2} \quad \left(\text{where } \phi \approx -\frac{\pi}{2} \right).$$

Thus the period of flashing may be kept constant and equal to that of the introduced voltage for a certain range of C , R , or B by the automatic adjustment of phase between the introduced voltage and the current in the neon-tube circuit.

The range of control of frequency is determined by the maximum value of $v_0 Q$.

In the foregoing it has been assumed that an alternating voltage of constant amplitude has been introduced into the neon-tube circuit.

It is evident that if the voltage is introduced electromagnetically into the circuit by the motion of the prongs of a tuning-fork maintained by the circuit, v_0 will depend upon ϕ , and, further, the condition that work is done on the fork by the neon-tube circuit must be satisfied.

It is supposed that the mechanical force F acting on the prongs of the fork at any instant is proportional to the current i in the neon-tube circuit at that instant; *i. e.*,

$$F = Ni. \quad . \quad . \quad . \quad . \quad . \quad . \quad (15)$$

Then the fork will be maintained in its motion if $\int_0^T F \cdot ds$ is a positive quantity, where s is the displacement of the fork from its zero position.

This may be written

$$\int_0^T Ni \cdot \frac{ds}{dt} \cdot dt,$$

remembering that

$$s = a_0 \sin (wt + \phi),$$

where a_0 = amplitude of vibration of the fork.

314 Dr. Leyshon on Control of Frequency of Flashing

We have for the condition that the fork will be maintained,

$$\int_0^T i \cdot \cos (wt + \phi) \cdot dt \quad \text{must be positive.} \quad (16)$$

Substituting for i from (4),

$$\begin{aligned} & A_1 \int_0^T e^{\alpha t} \cdot \cos \overline{wt + \phi} \cdot dt + A_2 \int_0^T e^{\beta t} \cos \overline{wt + \phi} \cdot dt \\ & + \frac{(1 - LCw^2)wCRv_0}{(1 - LCw^2)^2 + w^2C^2R^2} \int_0^T \sin \overline{wt + \phi} \cdot \cos \overline{wt + \phi} \cdot dt \\ & + \frac{w^2C^2R^2v_0}{(1 - LCw^2)^2 + w^2C^2R^2} \cdot \int_0^T \cos^2 \overline{wt + \phi} \cdot dt \\ & \text{must be positive,} \quad (17) \end{aligned}$$

or

$$\begin{aligned} & A_1 \frac{(1 - e^{\alpha T})}{\alpha^2 + w^2} (-\alpha \cos \phi - w \sin \phi) \\ & + A_2 \frac{(1 - e^{\beta T})}{\beta^2 + w^2} (-\beta \cos \phi - w \sin \phi) \\ & - \frac{w^2C^2R^2v_0}{(1 - LCw^2)^2 + w^2C^2R^2} \cdot \frac{T}{2} \quad \text{must be positive.} \quad (18) \end{aligned}$$

If L is small, the second term may be neglected in comparison with the first.

Thus, since A_1 is positive,

$$-\alpha \cos \phi - w \sin \phi \quad \text{must be positive.}$$

ϕ must therefore lie between

$$\tan^{-1} \frac{CRw}{1 - LCw^2} \quad \left[\phi \approx -\frac{\pi}{2} \right]$$

and

$$\tan^{-1} \frac{\alpha}{w} \quad \left[\phi \approx \pi \right].$$

If $L=0$, ϕ lies between

$$\begin{aligned} & \tan^{-1} CRw \\ & \text{and} \quad \tan^{-1} -\frac{1}{CRw}. \end{aligned}$$

If it is supposed that the dissipative forces in the motion of the tuning-fork itself are proportional to the velocity, then the work done during one vibration is proportional to

the square of the amplitude of vibration of the fork ; and since the value of v_0 , the maximum voltage induced in the neon-tube circuit, is proportional to the amplitude of vibration, then

$$v_0^2 \propto \int_0^T F \cdot ds ;$$

i. e.,

$$v_0^2 \propto (-\alpha \cos \phi - w \sin \phi) \quad . \quad . \quad . \quad (19)$$

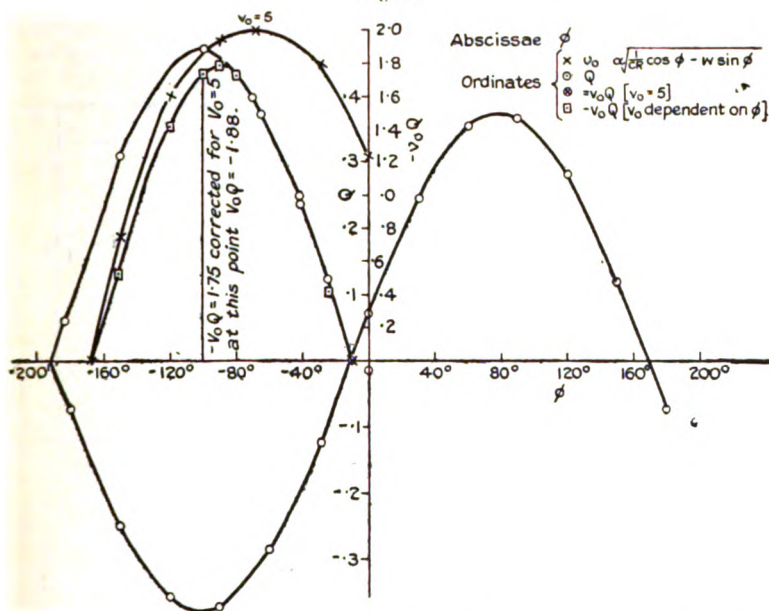
to a first approximation, or

$$v_0 \propto \sqrt{\frac{1}{CR} \cos \phi - w \sin \phi} \quad \text{if } L=0.$$

This gives the relation between v_0 and ϕ^* .

In fig. 2, graphs are given showing the dependence of $v_0 Q$

Fig. 2.



on ϕ , taking approximate values for v_0 (max.), CR, T, and L, to correspond to an experimental case considered in the next Section.

* If the third term of (18) is small compared with the first. v_0^2 is, of course, actually proportional to the sum of the three terms of (18).

In the one case v_0 is considered constant; in the other dependent upon ϕ in the manner shown above.

From equation (18) it is seen that v_0 has its greatest value when $\frac{1}{CR} \cos \phi - w \sin \phi$ has its greatest value; i. e., when $\phi = \tan^{-1} CRw \left(\phi \approx -\frac{\pi}{2} \right)$.

Thus the amplitude of vibration of the fork is (approximately) a maximum when its effect on the period is greatest, and is such that this is shortened by the reaction of the fork on the circuit.

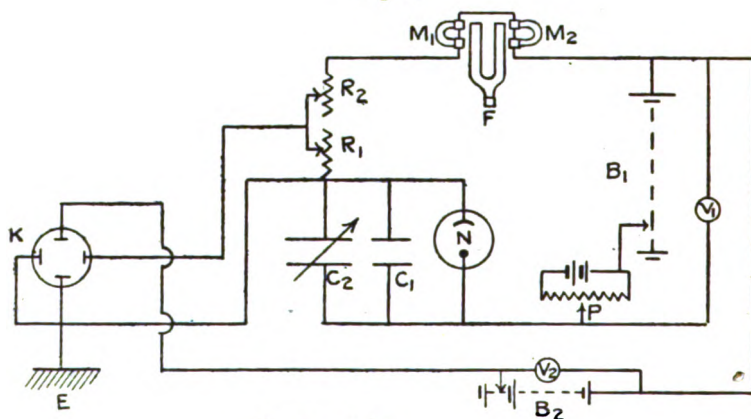
This result is confirmed by experiment.

In the next Section, experiments are described which support the elementary theory outlined in the preceding.

SECTION III.—*Experimental Verification of Theory.*

A fork-controlled neon-tube flashing circuit was set up,

Fig. 3.



- N neon tube.
- C_1, C_2 condensers.
- R_1, R_2 resistances.
- M_1, M_2 telephone magnets.
- F fork.
- B_1, B_2 batteries.
- P potential divider.
- V_1, V_2 voltmeters.
- K cathode-ray oscillograph.

and oscillograph records were obtained of the charging-current and condenser voltage, the apparatus being connected as shown in fig. 3.

The tuning-fork coils were inserted or removed as required by means of a Crawford wireless jack, so that comparisons could readily be made of oscillograph figures with and without the presence of these coils in the circuit.

Records of the oscillograph figures were obtained either by tracing or by means of bromide paper held directly over the fluorescent screen. This latter method was described by Dye in his paper on "An Improved Cathode Ray Tube Method for the Harmonic Comparison of Frequencies" ²¹.

With the tuning-fork coils in circuit, and the tuning-fork free to vibrate, it was found possible to vary one of the constants (battery voltage, resistance, or capacity) of the neon-tube circuit through a considerable range of values, the tuning-fork still being maintained in vibration. As the alteration in value of the electrical constant was made, a corresponding change in the oscillograph figure was seen.

A, B, and C (Pl. III.) are charging current-condenser voltage oscillograph records, obtained with a "Beehive" Osgilby lamp from which the series resistance had been removed.

In A the rate of flashing was increased by the reaction of the vibrating fork on the circuit.

In B the fork had very little effect on the rate of flashing, and was itself not vibrating so strongly.

In C the fork was held so that it could not vibrate.

Records D, E, F (Pl. IV.) are similar oscillograph records obtained with another "Beehive" lamp.

Here D shows the record corresponding to A,

E	"	"	"	B,
F	"	"	"	C,

and G (Pl. IV.) shows the record obtained on removing the tuning-fork coils. (The figure in this case is a straight line corresponding to the equation $B - V - Ri = 0$.)

Record H (Pl. V.) corresponds to A and D, an "I" type lamp (series resistance removed) being used. ~~See page~~

Record J (Pl. V.) shows a figure obtained when the frequency of flashing was one-half the frequency of the fork.

In obtaining these and similar oscillograph figures it was noticed that if (say) the battery voltage was adjusted so that the neon-tube circuit was flashing at a suitable frequency, and the fork was released after being held, the oscillograph figure changed with time, the head of the figure charging backwards and forwards like a serpent, and the rate of

change of the figure becoming slower as the fork gained in amplitude, until finally a steady figure was seen. If telephones were included in the neon-tube circuit, the beats could be heard distinctly.

This phenomenon corresponded to the non-uniform beats observed by Appleton⁹ and by the present writer¹⁰, when an alternating voltage of suitable frequency was introduced into a triode-maintained oscillating circuit.

The oscillograph figures show corresponding values of Ri and $(V - V_1)$ in a rectangular coordinate system, where i =charging current and V =condenser voltage.

Since

$$V - V_1 = \frac{1}{C} \int_0^t i \cdot dt,$$

$$C \cdot \frac{dV}{dt} = i.$$

That is, the figures give the relation between $(V - V_1)$ and its differential coefficient with respect to time.

If, therefore, taking the axis of x as the axis of t and the axis of y as $(V - V_1)$, a line is drawn from the origin having a slope = $\left(\frac{i}{C}\right)_{t=0}$, a point may be taken in this line and

from it another line drawn, the slope of this being equal to the value of $\frac{i}{C}$ obtained from the oscillograph figure corresponding to the value of $(V - V_1)$ for the point chosen. Proceeding similarly with this second line, and so on, the curve (V, t) is obtained as the envelope of the lines so constructed. The curve (i, t) may be readily constructed from this curve and the oscillograph record.

The shape of the (V, t) , (i, t) curves was obtained this way for one of the earlier figures recorded by tracing. These curves are shown in fig. 4.

To check the results, the apparatus was re-set up as shown in fig. 5, the second neon-tube flashing circuit providing a time-base²⁰ for the charging current of the first. The second neon tube was flashing at frequency 256, the first being controlled by a tuning-fork of frequency 512.

Tracings of the figures seen are shown in fig. 6. It will be seen that they are of the same form as those shown in fig. 4.

Fig. 4.

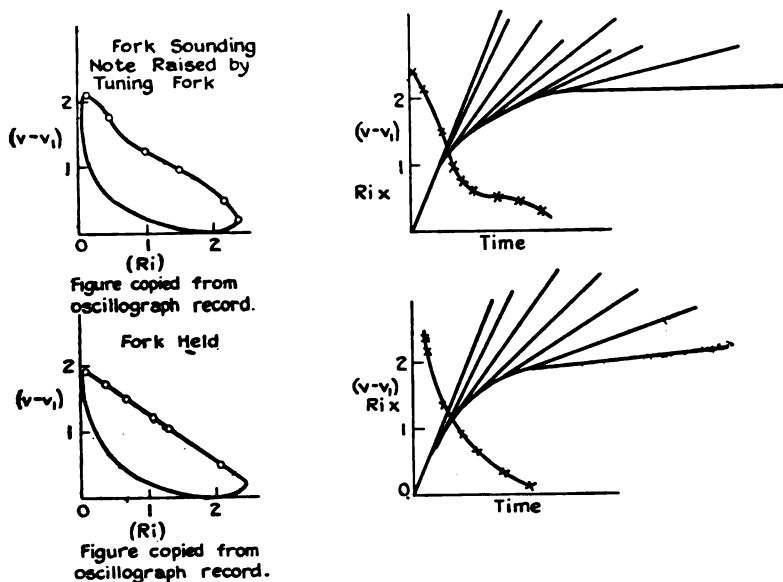
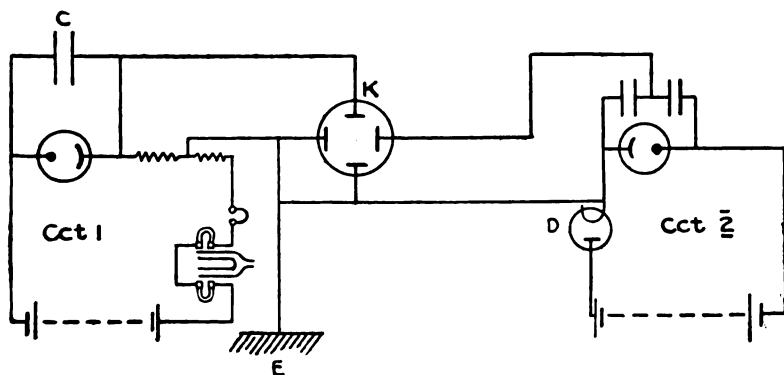


Fig. 5.



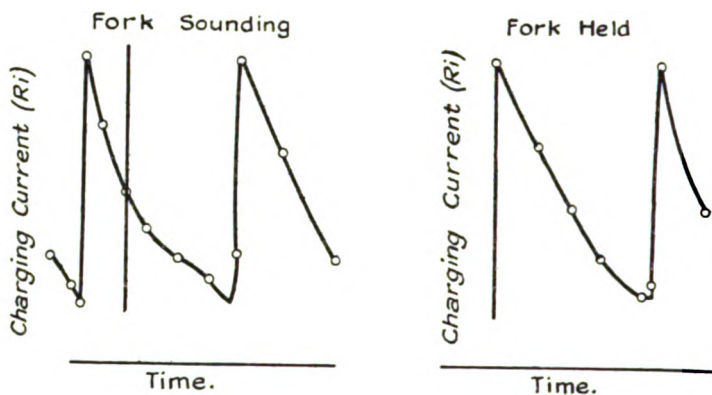
- K cathode-ray oscillograph.
- Cct 2 Neon tube N with condenser C₁, C₂ in series across it, these being charged through the diode D (R triode with grid and filament connected).
- Cct 1 tuning-fork controlled circuit.

Finally, an analysis of the record A was made.

The relation between $(V - V_1)$ and Ri is given by the equation

$$B - V - Ri = v_0 \cos (wt + \phi) + L \frac{di}{dt}. \quad (1)$$

Fig. 6.



The second term on the right-hand side will be of importance only at the beginning of a dark period, since $\frac{di}{dt}$ decreases rapidly with time.

The equation may be written, supposing $L \frac{di}{dt}$ is negligible,

$$V - V_1 + Ri = B - V_1 - v_0 \cos (wt + \phi). \quad (20)$$

When $\cos wt + \phi$ has a maximum or minimum value, the curve approximates to straight lines, given by

$$\text{and } \left. \begin{aligned} V - V_1 + Ri &= B - V_1 - v_0 \\ V - V_1 + Ri &= B - V_1 + v_0 \end{aligned} \right\} \quad (21)$$

The line parallel to these and half-way between them is

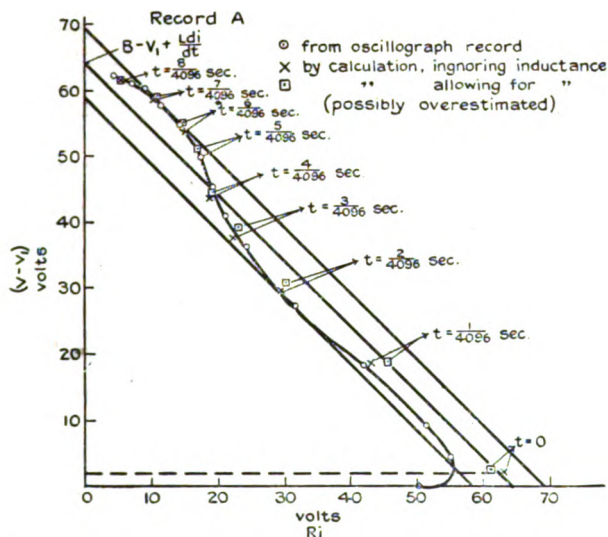
$$V - V_1 + Ri = B - V_1.$$

This cuts the axis of $(V - V_1)$ where $B = V$, a point which cannot, of course, lie on the oscillograph figure, but which gives the value of $(B - V_1)$ if the sensitivity of the oscillograph is known.

The greatest horizontal or vertical distance between the lines represented by equations (21) gives twice the value of v_0 . The value of $(V_2 - V_1)$ is given by the greatest value of $(V - V_1)$ recorded by the oscillograph.

In fig. 7 is shown the graph of $(V - V_1)$ and R_i obtained from record A.

Fig. 7.



The circuit conditions for this record were :—

Total series resistance 88,400 ohms ; oscillograph plates connected across 60,000 ohms.

Parallel capacity $\approx 0.009 \mu F$.

Inductance of tuning-fork coils ≈ 6 henries.

Frequency of tuning-fork 512.

Sensitivity of oscillograph

9.1 volts/cm. for condenser voltage axis.

9.7 " " resistance " "

Using the method outlined above,

$B - V_1$ was found to be 63.75 volts.

$B - V_2$ " " " " 1.75 "

v_0 " " " " 5 "

It was assumed that $\phi = -100^\circ$ (see fig. 2).

Thus $Q = -0.38$, $v_0 Q \text{ max.} = -1.9$, which corresponds roughly to the observed possible range of alteration of B without stopping the fork's vibration.

Phil. Mag. S. 7. Vol. 4. No. 21. Aug. 1927.

Y

Corresponding values of R_i and $V - V_1$ were obtained, using the values given above and equations (5) and (9).

These values are seen to lie very nearly * on the curve obtained experimentally (except at the beginning), thus showing that the elementary theory given accounts for the phenomena at least to a first approximation. It should be noted that the values of L and C were not known very accurately.

From equation (11), T was calculated.

The actual value of T thus found was too great, but according to the calculations the fork should alter the frequency of flashing by an interval of about a minor third. This was in accordance with observation.

The effect of the presence of inductance in the circuit on the relations between (R_i) and $(V - V_1)$ is seen in comparing records E and F.

It will be observed that the critical voltages for the lamp used in obtaining photographs A-C are considerably different from the usual values given for upper and lower critical voltages (160 and 140 volts respectively). The values were about 190 and 127 in this case. For another "Beehive" lamp (used for photographs D-F) the range of alteration of voltage across the lamp was 124-174 volts approximately; for an "I"-type lamp 125-153 volts. In an experiment with the latter there was some indication that the range of alteration of voltage depended on the series resistance†. The variation of the upper and lower critical voltages with circuit conditions has been previously noted by Taylor and Clarkson, Taylor and Stephenson, and Taylor and Sayce²².

Oscillograph figures showing the relation between $(V - V_1)$ and R_i have been obtained when the introduced voltage was derived (through a transformer) from a triode-maintained tuning-fork circuit. It was found that, when the rate of flashing was lowered by the introduced voltage, the figure seen differed in shape from any of those seen in the experiments previously described, and corresponded generally to a

* Using the value $B - V_1 = 63.75$ gave points lying consistently above the experimental curve. A rough estimate of $L \frac{di}{dt}$ when $(\omega t + \phi) = \pm 180$ was obtained, and then was subtracted from 63.75 to obtain a corrected value for $B - V_1$. This corrected value was used in the final calculation.

† Larger ranges of alteration of voltage were found in all cases for larger values of the condenser in parallel with the lamp.

value of ϕ lying between $\frac{\pi}{2}$ and π . The figures were complicated, however, by the harmonics present in the introduced voltage.

It has been found possible to control the frequency of flashing by an introduced voltage derived from a second neon-lamp circuit, the frequency of flashing of the second lamp being equal to or a submultiple of that of the first. Oscillograph figures for these experiments have not yet been obtained.

It should be noted that, in the case of the maintained fork, only a small change occurs in the frequency of the fork when one of the constants of the maintaining circuit is varied over the whole of the range of control of frequency.

In a particular experiment it was found that for a fork of frequency 512 a change in frequency of not more than 0.26 per sec. was obtainable.

SECTION 4.—*Conclusion.*

It is clear from the preceding theoretical and experimental discussion that the action of a tuning-fork in holding constant the frequency of flashing of a neon tube may be considered, to a first approximation, as being due to the introduction of a sinusoidal voltage of constant frequency and variable phase into the neon-tube circuit, this voltage being introduced electromagnetically into the circuit by the motion of the prongs of the fork, and the phase of this voltage adjusting itself so that the frequency of flashing is equal to the frequency of vibration of the fork.

In this case of the fork maintained directly by the neon-tube circuit, the range of control is not so great as it would be if a voltage of constant amplitude (equal to the maximum amplitude of voltage introduced by the fork) and frequency were introduced into the circuit: firstly, because less than one-half of the phase-change possible in the second case can occur in the first case; secondly, because the amplitude of vibration of the fork is dependent on its phase with reference to the current in the neon-tube circuit.

The theory is applicable to the case of vibrators maintained electrostatically—*e.g.*, a piezo-electric crystal in parallel with the condenser.

The fundamental equations are then of exactly the same form as equations (1) and (2), the term $L \frac{di}{dt}$ being omitted.

The solutions for Ri and T are therefore those given by equations (6) and (12), L being set equal to zero in the latter equation.

324 *Control of the Frequency of Flashing of a Neon Tube.*

The essential characteristics of the electrical vibration in the neon-tube circuit are that the voltage amplitude is constant, and the periodic time dependent on the "time constant" of the circuit and the constant voltage applied to the circuit. The periodic time is practically equal to the time of charging of the condenser.

Any other vibration, electrical or mechanical, of similar characteristics will be affected similarly by a sinusoidal (or other periodic) voltage or force of almost the same frequency introduced either independently or by the reaction of a maintained oscillator (electrical or mechanical).

Thus a similar theory to that given in the preceding pages would explain, to a first approximation, the control of frequency of a multivibrator circuit by an introduced sinusoidal voltage.

The experiments described were carried out in the Physics Laboratory of the London (Royal Free Hospital) School of Medicine for Women.

My thanks are due to the Council of the School for a grant from the Waller Memorial Research Fund for the purchase of a cathode-ray oscillograph.

March 1927.

List of References.

1. J. S. Townsend, *Radio Review*, i. no. 8 (May 1920).
2. H. G. Möller, *Jahrb. d. D. Tel.* xvi. pp. 402-431 (Dec. 1920).
3. W. Albersheim, *Archiv. f. Elektrot.* xiv. pp. 23-41 (Nov. 7, 1924).
4. S. Butterworth, *Proc. Phys. Soc.* xxvii. p. 410 (1915).
5. W. H. Eccles, *ibid.* xxxi. p. 269 (1919).
- 5A. S. Butterworth, *ibid.* xxxii. p. 345 (1920).
6. T. G. Hodgkinson, *ibid.* xxxviii. p. 24 (1925).
7. D. W. Dye, *ibid.* xxxviii. p. 399 (1926).
8. J. H. Vincent, *ibid.* xxxii. p. 84 (1920).
9. E. V. Appleton, *Proc. Camb. Phil. Soc.* xxiii. p. 231 (1923).
10. W. A. Leyshon, *Phil. Mag.* xlv. p. 686 (1923).
11. H. G. Möller, *Jahrb. f. drahtl. Tel.* xvii. p. 269 (1921).
12. J. Mercier, *C. R.* clxiv. p. 448 (1922).
13. J. Zenneck, *Jahrb. f. drahtl. Tel.* xxiii. p. 47 (1924).
14. B. van der Pol, *Phil. Mag.* iii. no. 13, p. 65 (1927).
15. S. O. Pearson and A. St. G. Anson, *Phys. Soc. Proc.* xxxiv. pp. 204-212 (1922).
16. F. Bédell and H. J. Reich, 'Science,' lxiii. p. 619 (June 18, 1926).
17. D. W. Dye, *Phil. Trans. Roy. Soc. ser. A*, ccxiv. pp. 259-301 (1924).
18. B. van der Pol, *Phil. Mag.* ii. no. 11, p. 978 (1926).
19. W. H. Eccles and W. A. Leyshon, 'Electrician,' xcvi. no. 2511, p. 65 (1926).
20. R. W. Lohman, *Am. Illmr. Eng. Soc. Trans.* xxi. pp. 478-482 (1926).
21. D. W. Dye, *Proc. Phys. Soc.* xxxvii. part 3 (1925).
22. Taylor & Clarkson, *Phil. Mag.* xlix. p. 336 (1925); Taylor & Stephenson, *ibid.* p. 1081 (1925); Taylor & Sayce, *ibid.* l. p. 916 (1925).

XXIX. *The Action of X-rays on Colloids.* By J. A. CROWTHER, M.A., Sc D., F.Inst.P., *Professor of Physics in the University of Reading*, and J. A. V. FAIRBROTHER, B.Sc.*

Introduction.

THE investigations described in the present paper were undertaken primarily in the hope of obtaining some light on the mechanism of the action of X-rays on living matter. It was hoped that if the nature of this action could be elucidated for some of the simpler inorganic colloids a basis might be found from which to attack the more complex problem presented by the organic colloids which make up such a large proportion of the living cell. The colloidal state is also interesting in itself, and further information as to the electrical condition of the colloid particle might possibly emerge from a detailed study of the action of the rays upon it.

In order to avoid as far as possible complications which might arise from the chemical action of the radiation either on the colloid particles themselves or on the solvent, it was decided to employ in the first place hydrosols of the elements, principally metallic. Preliminary experiments showed that these sols were relatively insensitive to the action of X-rays, and that very large quantities of radiation were required to produce any sensible change in them ; and further that, when exposed in shallow dishes for the long periods required for irradiation, the sols were liable to be affected seriously by factors not directly connected with the radiation, of which impurities in the atmosphere were probably the most important.

Experimental Details.

The source of radiation in all the experiments was a Shearer tube fitted with a molybdenum anticathode, taking a current of 4 m.a. at a P.D. of 55,000 volts, supplied by a large induction coil and a mercury break. The rays emerged through a thin aluminium window, and subsequently passed through a cover-slip of glass 0.15 mm. thick. The mean value of the mass coefficient of absorption in aluminium of the resulting radiation was 4.6. This corresponds to the absorption coefficient of molybdenum K-radiation. The

* Communicated by the Authors.

radiation is no doubt heterogeneous, but a considerable proportion of it must consist of the molybdenum K-radiation.

The colloid to be exposed was contained in a shallow dish, usually of fused quartz, which when filled to a depth of 0.8 cm. held about 2 c.c. of the solution. A covering vessel, the top of which was closed by a glass cover-slip 0.15 mm. thick, was placed over the dish containing the solution, and sealed down with molten paraffin wax. The colloid was thus hermetically sealed throughout the exposure. An equal volume of the same solution was placed in a similar dish and sealed in the same way. This served as a control for the experiment. The colloid after exposure was always compared with the control, and not with the stock solution. It was hoped that any effect which might be due to the mere exposure of the colloid in a shallow vessel would thus be eliminated. The results obtained in this way were found to be consistent.

The radiation was measured by an air-gap ionization chamber, connected to a gold-leaf electrometer, and a standard microfarad condenser. The quantity of radiation required to charge the condenser to a P.D. of 1 volt was taken as a convenient unit for the experiments. Since the volume of air between the electrodes in the ionization chamber was 1 c.c., this represents a dose of 3000 e. units received by the ionization chamber, the aperture of which was placed at 10 cm. from the anticathode of the tube. The surface of the colloidal solution was usually at a distance of 2.0 cm. from the focal spot, so that the dose received by the colloid was 25 times greater, or 75,000 e. The quantity of radiation necessary to produce erythema on the skin is usually reckoned at about 1000 e. The quantity of radiation corresponding to our experimental unit, which will be referred to as 1 mc., is very considerable. The time taken to give a dose of 1 mc. was about 8 minutes.

General Results.

Iron (Bredig solution). Exposures up to 14 mc. produced no apparent change in the appearance of the solution, and no signs of precipitation. The exposed and control solutions were each treated with two drops of very dilute potassium chloride solution. The sol which had been exposed coagulated completely, leaving a colourless liquid. The control showed no coagulation. An additional 6 drops of the same potassium chloride solution were required to produce any visible coagulation in the control. The iron has thus been rendered less stable by the radiation.

Copper (Bredig solution). Coagulation begins when the exposure reaches 11 mc., the amount precipitated increasing with increasing exposure. A dose of 14 mc. precipitates exactly one-half of the colloidal copper from solution. The case of copper is considered in more detail in a later section of the paper.

Silver (Bredig). As prepared by arcing under water this is a dark greenish-black solution. Under prolonged exposure to the radiation, the solution became clearer, and turned distinctly reddish in colour. The change in colour indicates increasing dispersion in the colloid, and increased stability.

Silver. (Collosol Argentum, kindly supplied by the Crookes Laboratories.) This is a protected colloid, and the solution is orange in colour. After exposure to X-rays the colour changed to a dark red. This would indicate increased dispersion. The exposed sol and the control were examined under the ultramicroscope. The control showed a certain amount of aggregation into clusters; the exposed sol contained only single particles. Counts of the relative numbers of particles in the two sols were made by means of a micrometer eyepiece. The average number of particles per square in the eyepiece was 1.16 in the exposed sol, and 0.61 in the control. The exposure was 25 mc.

Gold. (Collosol Aurum, unprotected.) This was a sample of colloidal gold as prepared for Lange's test. Its colour was pink with a distinctly violet tinge. Prolonged exposure to X-rays changed the colour to a clear red. When equal numbers of drops of very dilute electrolytes were added to the two samples, the control precipitated while the exposed remained in solution.

In further experiments a small number of drops of copper sol were added to the gold sol before exposure. After a dose of 5 mc. both the exposed and the control sols were perfectly clear. On warming to boiling-point in quartz test-tubes, the unexposed sol precipitated, while the sol which had been irradiated remained clear.

We may sum up this section by saying that in the case of iron and copper sols the X-rays produce coagulation; in the case of silver and gold the irradiation produces a greater degree of stability in the sol. It may be noted that iron and copper sols are kationic, while gold and silver are anionic.

*A Further Investigation of the Action of X-rays on
Copper Sols.*

Of the colloids investigated, the Bredig copper sol seemed the most suitable for a more detailed study. It is easily prepared in large quantities by arcing under distilled water, and the sol so obtained can be preserved for some months in quartz flasks without any precipitation occurring. The amount of copper in solution at any time can rapidly be determined by titrating with a very dilute solution of nitric acid of known strength, a method due to Paine. Nitric acid dissolves the copper sol without coagulation, and the change in colour from the dark red of the sol to the practically colourless copper nitrate solution is very marked, and gives an excellent end-point for the titration. In this way it was possible to make estimations to an accuracy of about 5 per cent., even with the very small volumes of sol which could be exposed at one time to the radiation (about 2 c.c.).

After exposure to X-rays the sol was transferred to a quartz test-tube and boiled for two minutes. It was then allowed to stand for half an hour and subsequently centrifuged for two minutes, so that any precipitate which might have formed was thrown to the bottom of the test-tube. By means of a pipette 1 c.c. of the clear liquid was withdrawn from the test-tube, and immediately titrated. The sol used as a control was treated in exactly the same manner. The ratio of the volume of acid required to dissolve the copper remaining in suspension in the exposed sol to that required for the control was taken as a measure of the proportion of copper which had not been precipitated by the radiation. Numerous tests showed that consistent results could be obtained by this procedure.

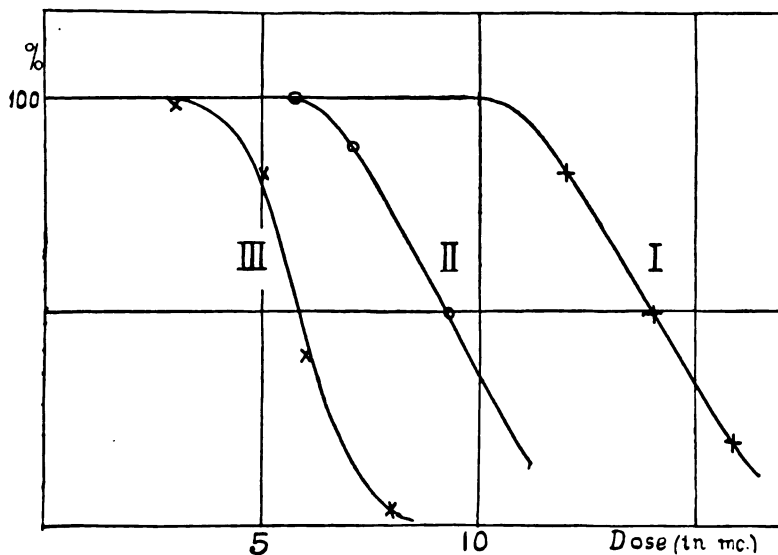
As sols prepared at different times might be expected to vary somewhat in concentration, and size of particles, sufficient sol was prepared for a series of experiments. The copper sol changes in colour for some days after preparation, indicating some change either in the composition or in the size of the particles. The sol was allowed to stand for a week or more before use. The mobility of the sol was then measured by the U-tube method, and was found to be 2.5×10^{-4} cm. per sec. per volt per cm., giving a value for the electrokinetic potential of 0.035 volt. Attempts were also made to determine the size of the particles from the rate of settling of the sol under gravity, using the alternating field method described by Burton*. The experiments were not very satisfactory, as the surface

* Burton and Reid, *Phil. Mag.* vol. 1. p. 1221 (1925).

always became very diffuse before the end of the experiment. The velocity of settling was found to be approximately 4.7×10^{-6} cm. per sec., measuring always the upper boundary of the diffuse layer. This gives the radius of particles as 5.2×10^{-6} cm. This value is probably a minimum. Using the same method for a similar Bredig copper sol, Burton found a value for the radius of the particles of 7.1×10^{-6} cm.

Percentage of Copper remaining in solution after various doses of X-rays.

- I Pure sol.
- II Sol containing 2.4×10^{-6} gm. ferricyanide per c.c.
- III Sol containing 3.9×10^{-6} gm. ferricyanide per c.c.



The copper sol was then exposed, in a series of experiments, to varying doses of X-rays. The results of these exposures are recorded in the curve I of the figure. Coagulation begins when the dose exceeds 10 mc. and the sol is half coagulated with a dose of 14 mc. It is evident that some of the particles require considerably larger quantities of radiation to produce precipitation than others. This is possibly due to a variation in size of the particles. It is possible, however, that it is due to the fact that, owing to absorption in the upper layers, the radiation reaching the lower levels in the sol is distinctly reduced in intensity. It

was impossible to stir the sol during exposure, and the diffusion and chance convection currents may not have been sufficient to maintain a thorough mixing of the solution during the exposure.

A series of experiments were then made in which the sol was "sensitized" before exposure by the addition of minute quantities of some coagulating substance. For this purpose we employed a very dilute solution of potassium ferricyanide. It was found that, with the method of experimentation we adopted, the addition of 7.2×10^{-6} gm. of this salt to 1 c.c. of the copper sol caused the precipitation of half the copper. To two portions of the original copper sol we added quantities of the ferricyanide solution, so as to make the concentration of ferricyanide in the one up to 2.4×10^{-6} gm. per c.c., and in the second up to 3.9 gm. per c.c. These solutions were then given a series of doses of radiation, and the amount of copper remaining in solution was determined as before. The results are shown in curves II and III of the figure, curve II referring to the sol with the smaller proportion of ferricyanide. It will be seen that the amount of radiation required for coagulation becomes smaller as the concentration of ferricyanide increases.

The results, in fact, indicate a numerical equivalence between the radiation and the electrolyte in their coagulating powers. Thus 7.2×10^{-6} gm. of salt in 1 c.c. of sol produce the same coagulation as a dose of 14 mc.; 3.9×10^{-6} gm. reduce the dose of radiation required by 8 mc., and 2.4×10^{-6} gm. reduce the dose by 4.5 mc. The ratio of the quantity of radiation to the amount of salt which produces the same effect is thus 1.95, 2.05, and 1.88 respectively. A concentration of potassium ferricyanide in the sol of 10^{-6} gm. per c.c. is equivalent in its coagulating action to a quantity of radiation measured by 2 mc. in the ionization chamber, *i. e.* to 150,000 e. received by the sol.

Precisely similar results were obtained when the copper sol was sensitized by the addition of small quantities of a negative colloid, such as the unprotected gold sol previously described. It was found that 10^{-5} gm. of gold per c.c. of copper sol was equivalent to 100,000 e. of radiation.

In these experiments the sensitizing agent was added before the exposure, as this is the most convenient way of carrying out the experiment. The effect, however, does not depend on the presence of the sensitizer during the process of irradiation. Practically the same results are obtained if the sol is irradiated first, and the sensitizer is added after the completion of the exposure. Thus if the

pure sol is given 6 mc. of radiation, which leaves it quite clear, and subsequently is mixed with an amount of potassium ferricyanide solution which would, together with the X-rays, have caused the coagulation of half the sol if it had been present at the time of radiation (3.9×10^{-6} per c.c.), 40 per cent. of the copper coagulates. The amount precipitated is thus, within the limits of experimental error, the same as if the salt had been present throughout. Thus the effects of the radiation and the sensitizer, while additive, seem to be completely independent.

Discussion of Results.

The experiments described provide only a preliminary survey of a wide field in which few observations appear to have been made. Fernau* has reported that cerous hydroxide and albumin are coagulated by X-rays, and Wels and Thiele† have found that globulin sols are aggregated by irradiation, a result which so far we have been unable to confirm. In a nearly related subject, Hardy‡ has shown that positively charged globulin sols are coagulated by β -radiation from radium, while negatively charged sols are rendered more disperse. Fernau also records the coagulation of cerous hydroxide by β -radiation.

As a preliminary step to a discussion of the subject, it may be well to record some approximate data on the physical action of X-radiation. A dose of 1 e., by definition, allows the transference of 1 electrostatic unit of electricity across 1 c.c. of air. The number of pairs of ions formed per c.c. in air by the passage of 1 e. is thus $1/4.774 \times 10^{-10}$ or 2.1×10^9 . The number of pairs of ions per gm. of air is thus 1.7×10^{12} . This will also be approximately the number of pairs of ions formed per gm. in water, since for elements of low atomic weight ionization is largely a mass effect. In our experiments, however, the depth of solution employed was sufficient to produce a considerable absorption of the radiation, so that the lower layers received a smaller dose of radiation than the upper. A correction can easily be applied if the coefficient of absorption of the rays is known. For the depths used in our experiments the correcting factor is 0.7. Thus the average number of ions per gm. of sol for a dose of 1 e. received by the surface is 1.2×10^{12} , or 9×10^{16} for our experimental unit dose.

Ionization is, however, a secondary effect produced by the

* Fernau, *Kolloid-Zeit.* xxxiii. p. 89.

† Wels and Thiele, *Arch. ges. Physiol.* ccix. p. 49.

‡ W. Hardy, *Proc. Camb. Phil. Soc.* p. 201 (1903).

action of the photoelectrons ejected by the X-rays. If we assume that the radiation is mainly molybdenum K-radiation, each of these photoelectrons is responsible for about 600 pairs of ions. The number of photoelectrons ejected per gm. of water is thus 1.5×10^{14} for a dose of 1 mc. as recorded by our electroscope. Since the mass absorption coefficient of X-radiation in copper is 45 times that in water, the number of photoelectrons ejected per gm. of copper is 6.7×10^{15} . Taking the radius of the copper particles in the sol as 5.2×10^{-16} cm., the average number of photoelectrons ejected from a particle during a dose of 1 mc. is about 35. Thus during the irradiation necessary to produce coagulation in the copper sol each particle will eject about 500 photoelectrons, and will thus gain a positive charge of 500 e , where e is the electronic charge.

If the stability of the colloid depends on its electrical charge, as is usually assumed, the positive colloids should become more stable, the negative colloids less stable, from the loss of these electrons. This is exactly the reverse of what is indicated by our experiments. The particles will, it is true, receive a certain number of photoelectrons from the surrounding medium, but it is improbable that the number so gained will be more than a small fraction, say 10 per cent., of those which it ejects. The loss of photoelectrons then, so far from being the direct cause of coagulation, appears as an effect which the true coagulating agent must overcome.

The total number of ions produced in 1 c.c. of sol during the exposure required to coagulate the copper sol is $14 \times 9 \times 10^{16}$, or 1.26×10^{18} . The same effect is produced by 7.2×10^{-6} gm. of potassium ferricyanide, which contain 1.2×10^{16} trivalent ferricyanide ions. The total ionization produced by the radiation is thus amply sufficient to neutralize the charges on the colloid particles. That the amount of X-ray ionization required should greatly exceed the electrolytic ionization is only to be expected, since the rate of recombination for the X-ray ions is likely to be large. Only those ions which come within the electrical field of the colloid particles would be likely to be effective, the remainder simply recombining *in situ*.

This conception of the action of the radiation can easily be treated numerically. If we assume that the electrokinetic potential ξ is due to a charge q on a particle of radius r , and that an electrical double layer surrounds the particle of mean thickness δ , and dielectric constant = D , then

$$q = \frac{Dr(r+\delta)\xi}{\delta} = \frac{Dr^2\xi}{\delta} \text{ (approx.)}.$$

If n is the number of ions formed in unit volume of the solution by the amount of radiation required to produce coagulation, and if we assume that all these ions cross the double layer without recombination, the total charge conveyed across the double layer during the exposure will be $ne \times (\text{volume of double layer}) = ne4\pi r^2\delta$ approximately. Thus, assuming that coagulation will take place when the charge q has been neutralized,

$$Dr^2\xi/\delta = 4\pi ner^2\delta; \quad \delta^2 = D\xi/4\pi ne.$$

The ionization at the surface of a copper particle will, however, be greater than that in the bulk of the solution, owing to the greater emission of photoelectrons from the copper. For particles as small as those in colloidal solution the effect will increase with the size of the particle. Taking the radius as 5.2×10^{-6} cm., it can be shown that the ionization at the surface of the particles will be approximately 4 times that in the bulk of the solution. Since the ionization increases with the size of the particle, the coagulating effect of the radiation is not really independent of the radius of the particle, although the radius does not occur explicitly in the formula.

For the copper sol employed in our experiments we have $n = 4 \times 1.26 \times 10^{18}$, $\xi = 0.035$ volt or 1.17×10^{-4} e.s.u., $D = 81$, and $e = 4.774 \times 10^{-10}$ e.s.u. Thus δ , the thickness of the double layer from which the ions are drawn, works out at 5.6×10^{-7} cm., and q , the initial charge on the colloid particle, at 4.4×10^{-7} e.s.u. A more exact calculation, allowing for the charges carried away by the photoelectrons, gives $\delta = 7.2 \times 10^{-7}$ cm.

The value of δ thus obtained is of the order of magnitude generally accepted for the equivalent thickness of the diffuse double layer surrounding a colloid particle. Hevesey*, for example, assumes a value 5×10^{-7} cm. The average electric field in this layer must be of the order of 7×10^4 volts per cm., and it is not unreasonable to suppose that with a field of this order any ions formed in the diffuse double layer would be carried across it without appreciable recombination, even in a liquid medium. There seems, thus, to be some support for the hypothesis that the discharge of the copper colloid is due to the ions formed by the radiation in the diffuse double layer.

The difficulty in accepting this interpretation of the phenomena lies in the fact that, so far, we have not succeeded in

* v. Hevesey, *Kolloid. Zeits.* xxi. p. 129 (1914).

producing coagulation in any negative colloid. We should expect that the presence of free ions would neutralize any electrical double layer, no matter what its sign, whereas the evidence, as far as it goes, indicates that the negatively charged colloids, silver and gold, are rendered somewhat more stable by irradiation. The difficulty is, perhaps, not insuperable. It has been suggested that the metallic particles which form the nucleus of the colloidal micelle are, in the case of the noble metals, actually positively charged, the negative electrokinetic potential being due to an excess of negative charges on the surface of the micelle, where the slipping actually takes place when the particle moves. The ejection of photoelectrons would make the positive nucleus more positive, and thus enable it to hold a larger negative charge. For the copper particles the charge gained by the ejection of negative electrons is smaller than the charge lost by ionization in the diffuse double layer, but the two are of the same order. Since the coefficient of absorption of X-rays is twice as great for gold as for copper, gold will lose electrons at a greater rate than copper, and it is thus quite conceivable that for the gold particles the direct gain of positive charge due to this cause may more than counterbalance the loss of charge due to the ionization currents. Further experiments are in progress to test this suggestion further.

There remains, of course, the further possibility that the action of the radiation may be indirect: that is to say, the X-rays may produce in the sol some chemical substance which in turn acts on the colloidal particles to produce precipitation. Hydrogen peroxide is an obvious suggestion in this connexion. Clark * has, in fact, already put forward the suggestion, in connexion with Fernau's observations on the precipitation of cerous hydroxide, that coagulation is due to the formation and subsequent decomposition of hydrogen peroxide in the solution. Freundlich †, however, states definitely that the addition of hydrogen peroxide to a cerous hydroxide sol has no effect on its stability, so that Clark's suggestion seems to be untenable in this case. Bredig sols of copper and iron are coagulated by quite small quantities of hydrogen peroxide. In order to test the matter further we irradiated a quantity of distilled water under the same conditions as those employed in irradiating the sols. We were unable to detect any trace of hydrogen peroxide in the irradiated water, although the test employed

* Clark, 'Applied X-rays,' p. 78.

† Freundlich, 'Colloid and Capillary Chemistry,' p. 486.

(chromic acid test) would certainly have revealed the presence of as little as one-tenth of the concentration necessary to produce coagulation. It seems improbable, therefore, that hydrogen peroxide plays any appreciable part in the phenomena.

Summary.

It is shown that certain colloidal solutions are affected by exposure to large quantities of X-radiation. Positively charged colloids are coagulated by irradiation, but negatively charged colloids have their stability increased. The effect is studied numerically for a Bredig Copper sol. It is suggested that the coagulation is brought about by the ionization produced in the diffuse double layer surrounding the particles.

The expenses of this research were partly met by a grant from the Government Grants Committee of the Royal Society, to whom we express our best thanks. We are also much indebted to Mr. Ward, and the Crookes Laboratories, for their kindness in supplying us with a number of colloidal solutions.

Department of Physics,
The University of Reading.
May 19, 1927.

XXX. *On the Absolute Zero of Entropy and Internal Energy.*

To the Editors of the Philosophical Magazine.

GENTLEMEN,—

I READ with much interest the paper of Prof. R. D. Kleeman "On the Absolute Zero of Entropy and Internal Energy" in the Phil. Mag. of April 1927. Will you allow me to make some remarks?

1. I do not agree with the author about his conclusion that the conditions $\left(\frac{\partial U}{\partial T}\right)_v = 0$ and $\left(\frac{\partial S}{\partial T}\right)_v = 0$ at $T=0$ are necessary mathematical consequences of the fact that U and S are minimum for $v=\text{const.}$ at the absolute zero of temperature. We know several examples of physical quantities which reach

a minimum value without satisfying the conditions of an analytical minimum, because the variable has no physical meaning beyond the limit for which the quantity reaches the minimum value. So the density δ of a mixture may be a minimum for the concentration $c=0$, because a negative concentration is a physical impossibility, but mathematically

δ has a value for a negative c and $\frac{d\delta}{dc}$ is not necessarily zero.

The same may be—or rather is—the case for the energy and entropy as functions of the absolute temperature; $T=0$ is only a physical limit, and so the values of U and S may be minimum at $T=0$ only because negative temperatures do not exist. Let us take for example the thermal energy of a classical ideal gas: *per definitionem* it is proportional to the

absolute temperature; at $T=0$ it is zero, but $\frac{dU}{dT}$ is not zero, just owing to the choice of the temperature scale. Why

then should $\left(\frac{\partial U}{\partial T}\right)_v$ be necessarily zero at $T=0$ for a con-

densed state? The fact that $c_v = \left(\frac{\partial U}{\partial T}\right)_v = 0$ for the solid state at $T=0$ has not merely a mathematical reason, but is a physical fact which must be accounted for by theoretical considerations (quanta).

For the same reason $\left(\frac{\partial S}{\partial T}\right)_v$ is not necessarily 0 at $T=0$, but when $\left(\frac{\partial S}{\partial T}\right)_v = 0$, then $\left(\frac{\partial U}{\partial T}\right)_v = 0$, for

$$T \left(\frac{\partial S}{\partial T}\right)_v = \left(\frac{\partial U}{\partial T}\right)_v \quad . \quad . \quad . \quad . \quad . \quad (a)$$

2. Nor do I agree with the conclusion $c_{v\infty} = 0$ at $T=0$, for even when $T=0$ the integral term of equation (10) may have a finite value, the integration extending over an infinite increase of the volume.

3. It seems to me that the fact that $\left(\frac{\partial U}{\partial T}\right)_v$ and $\left(\frac{\partial p}{\partial T}\right)_v$ are always positive may not be accounted for by general considerations, and I am not quite sure that one could not imagine systems in which those conditions would not be verified. I think we must consider those conditions as physical facts which we may try to explain by mechanical representations.

Certainly the fact that $\left(\frac{\partial U}{\partial T}\right)_v$ is positive is connected to that other, that adiabatic expansion is attended by a decrease of temperature, but even this is not necessary, and I should say it is a consequence of the first. In other words $\left(\frac{\partial v}{\partial T}\right)_s$ is negative because

$$\left(\frac{\partial U}{\partial T}\right)_v + T \left(\frac{\partial p}{\partial T}\right)_v \left(\frac{\partial v}{\partial T}\right)_s = 0,$$

and $\left(\frac{\partial U}{\partial T}\right)_v$ and $\left(\frac{\partial p}{\partial T}\right)_v$ have positive values.

4. According to equation (a), $\left(\frac{\partial U}{\partial T}\right)_v$ and $\left(\frac{\partial S}{\partial T}\right)_v$ are both positive. Consequently U and S are both minimum (for $v = \text{const.}$) at $T=0$. Besides, according to $\left(\frac{\partial S}{\partial v}\right)_T = \left(\frac{\partial p}{\partial T}\right)_v$, S increases with v even at $T=0$, and so the absolute minimum of entropy (zero of entropy), at which again $\left(\frac{\partial S}{\partial v}\right)_T$ is not necessarily zero, should not correspond to the solid state under pressure 0 at $T=0$, unless this solid state be incompressible, which is to be admitted, as it seems.

As for U , according to $\left(\frac{\partial U}{\partial v}\right)_T = T \left(\frac{\partial p}{\partial T}\right)_v - p$, $\left(\frac{\partial U}{\partial v}\right)_T = -p$ at $T=0$ for the solid state, so that U increases as well by compression as by traction (negative p). By vaporization, even at $T=0$, U increases also and so U is indeed minimum for the solid state under pressure 0. For that state $\left(\frac{\partial U}{\partial v}\right)_T$ is really zero.

But if the solid state at $T=0$ is compressible, the line ab of minimum entropy (see fig. at page 890) ought not to pass through point U_0 : it should pass under that point; and the zeros of entropy and energy would not coincide.

Yours sincerely,

Prof. Dr. J. E. VERSCHAFFELT,

70 St.-Pietersnieuwstraat,
Ghent, April 7, 1927.

Professor of Physics at the
University of Ghent.

XXXI. *Dr. Jeffreys and the Earth's Thermal History.*

By J. JOLY, F.R.S.*

IN a recent number of the 'Geological Magazine' Dr. Jeffreys deals with the subject of the earth's thermal history (Geol. Mag. Nov. 1926, p. 520). In the course of his remarks he refers to a theory of the earth's surface history for which I am responsible †, and repeats certain arguments directed against the fundamental proposition that the alternate accumulation and discharge of heat of radioactive origin was accountable for the cyclical nature of earth-history. He now expresses his arguments as follows:—

"Whenever a physical system of finite extent free to lose heat by radiation from an outer boundary is affected by a steady internal source of heat, the temperature at any point will approach steadily towards some permanent value as a limit, and there will be no possibility of a permanent oscillation of temperature. So long as the system is solid this proposition can be proved easily; fusion, if it occurs, complicates the mathematics, but leaves the result no less evident physically. Joly complicates the issue further by assuming that the outer crust revolves under tidal forces; this introduces the possibility of some oscillation of temperature, but not enough to produce resolidification, and is open to objections on its own account."

In this statement, which Dr. Jeffreys designates his "main conclusion," he is tacitly assuming that no relative motion of the parts of the medium takes place. That this is so will be shown later by several instances of cyclic phenomena arising out of steady supply of heat.

In his earlier paper he writes as follows:—"The basic rocks below the granitic layer also contain radioactive matter, and it is upon the heat generated in them that Prof. Joly relies for his main object, which is to explain periodic variations in temperature within the crust." (Phil. Mag. May 1926, p. 924.)

My comment on this earlier statement was to the effect that it does not describe the conditions I have all along discussed. My "main object" has been to show that there is a periodic accumulation and discharge of heat. But the heat is latent, and there is but little variation of temperature. That Dr. Jeffreys has not entered into the significance of

* Communicated by the Author.

† 'The Surface History of the Earth' (Oxford, 1925).

these conditions is shown by his assumption that the only way periodicity can arise is by a trigonometrical time-factor in the expression for conduction.

A clear statement of what is fundamentally involved in my theory of surface history will render the issues more readily understood. Mr. J. R. Cotter, in his paper "On the Escape of Heat from the Earth's Crust" (*Phil. Mag.* Sept. 1924, p. 458), gives a lucid and concise summary of the thermal conditions as follows:—

"According to Prof. Joly's theory, that portion of the earth's crust immediately beneath the ocean-floor consists of basalt, in which a continual generation of heat takes place, owing to the presence of radioactive materials. Prof. Joly concludes on experimental grounds that the heavier ultra-basic materials which probably underlie this stratum of basalt are much less radioactive. For the purpose of simplifying the investigation, I shall assume that no transmission of heat occurs through that horizon which may be regarded as the lower boundary of the basalt. The modifications which would have to be made in the theory when radioactivity of the underlying rock is taken into account need not here be considered. The temperature of the upper surface of the basalt will be taken to be 0°C. , which is approximately the temperature of the ocean-floor.

"Let us suppose that at some stage in the history of the earth's crust the basalt is solid throughout. As we descend from the upper surface the temperature will rise until at a certain depth the melting-point of basalt is reached. If we denote the melting-point by θ_0 then we can call this horizon the θ_0 geotherm. Below this level the rock is supposed to be everywhere at its melting-point. The temperature will not be quite uniform, but will increase slowly with depth, since the melting-point of basalt rises with increase of pressure. A long period of quiescence will ensue, during which the radioactive heat generated above the θ_0 geotherm will escape by conduction through the ocean-floor, while below this geotherm the heat generated will become latent owing to liquefaction of the rock, the temperature remaining steady all the time. It seems probable that the material in this lower portion would preserve its rigidity till an advanced stage of liquefaction has been reached, being in a condition somewhat like that of a sponge filled with water. A period of activity would now set in, starting with the breakdown of the weakened material owing to the disruptive action of tidal forces. Circulation might begin slowly, but would rapidly increase, because the descending portions would tend

to solidify owing to increase of pressure, so that the increase of density due to solidification would accelerate the rate of descent; while the ascending portions would become more fully liquefied and would rise faster. As soon as circulation became general, a precipitate of solid material would begin to be formed at the bottom of the liquid mass; while at the same time the rest of the medium up to the θ_0 geotherm would become quite fluid, its temperature being nearly uniform and equal to the temperature of the solid deposit—that is, the temperature of the melting-point of basalt at a pressure equal to that of the fluid at its lowest level. Thus the upper part of the fluid would be above the melting-point appropriate to its pressure, and it would begin to melt away and to erode the solid rock above it—that is, it would push the θ_0 geotherm upward. This process would be comparatively rapid at first, but would fall off owing to two causes: first, because as the fluid became shallower owing to the deposit of solid, its temperature would fall, and secondly, because the loss of heat by conduction through the ocean-floor would become accelerated as the geotherms rose. Prof. Joly thinks that the θ_0 geotherm would rise to within a very few miles of the surface. It would, however, finally become stationary, and then descend. At this stage the escape of heat would be very rapid, and the rate of solidification at the bottom would also be rapid. There seems little reason to doubt that the whole would eventually become solid again, and cooling would go on till it recovered its initial condition and initial distribution of temperature. The whole series of changes would form a cycle which would be repeated."

It will be seen that the changes of temperature involved are mainly confined to those arising out of the movement of the θ_0 geotherm and to those due to the change of melting-point with depth. It will also be noticed that only intermittently can the substratum lose heat "from an outer boundary," i.e. attending the upward movement of the θ_0 geotherm. It is just this fact which leads to accumulation of heat and gravitational instability in the depths. Since we must infer from Dr. Jeffreys's references to this matter that he does not accept the general statement as to the importance of latency, and is basing his conclusions upon abstract considerations which do not take account of the conditions actually involved, I think it desirable to deal with the subject more definitely and practically. The main object of the present paper is, then, to show that conditions of cyclic change of state arising out of steady

thermal flux are not only open to our inspection in nature, but are reproducible in various forms in the laboratory. I shall first refer to the well-known and well-investigated phenomena of the geyser.

The conditions responsible for the periodic phenomena of the geyser, as investigated in the first instance by Bunsen and subsequently by others, may be described as follows:—

Heat of volcanic origin, entering steadily from the walls of a deep well, raises the temperature of the water till the boiling-point proper to the depth is nearly attained at all levels. If, then, the boiling-point is finally reached at any particular level, change of state at that level occurs; then follows expulsion of water at the top, reduction of pressure at all levels, and general breakdown of equilibrium. The sudden production of water vapour occasions the explosive ejection of both water and steam in a succession of paroxysmic jets. The water falling back into the well is now everywhere super-cooled respecting the local boiling-point. The steady accession of heat, which continues throughout, once more raises the temperature at all levels till conditions of instability again arise, when the phenomena are repeated.

It will be recalled that Tyndall realized these conditions experimentally and with perfect success ('Heat a Mode of Motion,' p. 124 *et seq.*). He used a vertical tube filled with water, applying a steady source of heat at the lower end. The local change of state at a higher level, which precipitates instability, was represented by a steady additional supply at a higher level. But it is sufficient to supply a steady source of heat to the lower part of the tube.

An interesting paper on the subject of geysers by T. A. Jäger appears in the 'American Journal of Science' (1898, vol. i.). He writes (p. 324): "The accuracy of Bunsen's theory was early confirmed by experiment, and the only mechanism necessary to produce geyser eruptions is a tube filled with water, open above and heated below." He states with reference to the well-known geyser "Old Faithful" of the Yellowstone:—"It takes practically a uniform period, some 65 minutes, to heat the new column to a state of ebullition at its base, and has done so for 28 years of human record; it is fair to assume that the heat-supply is constant." From this it follows that over 240,000 of these "revolutions" had taken place within human record up to the year 1898.

When water flows away at the top of a geyser some must enter from beneath to supply its place, but, as both theory and experiment show, this condition is not essential to the

periodic activity of the geyser. If a geyser basin exists and the cooled water is returned to the tube, the steady heat-supply beneath is sufficient to maintain the "oscillation of temperature" which from Dr. Jeffreys's statement would seem to be impossible.

Let us now imagine that we are dealing with a medium such as constitutes the substratum. It is, we will suppose, in a state of quasi-rigidity. It receives throughout a steady thermal supply. This thermal supply is not the same at all levels. It is, by a curious law affecting a heterogeneous medium of this sort in a gravitational field (*Phil. Mag.* June 1927, p. 1233 *et seq.*), richer in radioactive elements in its higher than in its lower levels. The physical state of the medium is not the same at all levels. In the depths the temperature required for liquefaction is higher than in the upper parts. But the precise distribution of thermal energy cannot be defined. It will depend upon the previous history of the medium.

It is easy to see that as time progresses and energy accumulates a state of instability must arise much the same as that which affects the geyser in the period preceding eruption. Any source of disturbance at this stage may initiate catastrophic breakdown of equilibrium. It may originate in tidal movements gradually augmenting in amplitude as rigidity of the medium diminishes. There will be a critical accumulation of heat which responds to tidal forces to a degree adequate to initiate the breakdown.

When vertical circulation sets in, there can be no break-off till sufficient energy has been discharged to permit of the whole solidifying from beneath upwards and settling down once more into a period of recuperation preceding an ensuing revolution. The depth to which the circulation extends depends upon previous history; *i. e.*, upon the duration of the antecedent storage-period in the great depths. The magnitude of a revolution is so determined.

The phenomena in the geyser and in the substratum are plainly analogous and thermally alike. In the case of the geyser, as in the case of the substratum, there is insufficient loss of heat "from an outer boundary" to control thermal accumulation and consequent instability. Hence it, ultimately, develops cyclic changes analogous to those affecting the substratum. They differ mainly in the nature of the change of state. The refrigerator, too, differs in character. In the one case it is mainly the atmosphere, in the other mainly the ocean which carries away the heat. The like principles affect both. Both appear to be impossible

according to Dr. Jeffreys's statement that cyclic events cannot arise out of a steady thermal supply.

I shall now turn to cyclic phenomena upon a very minute scale—but not the less instructive—arising out of steady thermal flux. I shall first refer to the little device known as an "Air Tester."

It consists of a thin glass bulb opening into a tube sloping downwards, at the lower end of which there is an upward bend opening into a second small bulb. It is sealed, and contains a small quantity of coloured alcohol or ether. The upper bulb is covered with an absorptive fabric which dips into a vessel containing water; so that, owing to evaporation, the surface of this bulb is maintained steadily at a lower temperature than that which prevails in the lower bulb with which it communicates.

The alcohol is intermittently drawn up from the lower to the upper bulb, and after a short delay is discharged down the sloping tube into the lower chamber. From this it is again drawn up into the upper bulb, the intermittent motion continuing with perfect regularity so long as the surrounding atmospheric conditions remain unaltered. The influx of heat into the lower bulb and its withdrawal from the upper bulb may be demonstrated by observing the effect of a pad of loose wool applied to either bulb.

We have here a source and a refrigerator. Heat entering into the lower bulb is expended in increasing the vapour-pressure of the alcohol. Heat abstracted from the upper bulb causes a reduction of vapour-pressure. Both effects tend to bring the alcohol, which fits the connecting tube like a piston, into the upper bulb. So soon as it enters the upper bulb the connexion between the bulbs is opened; there is equalization of pressure throughout, and the alcohol streams back into the lower chamber. Here it fills the bend of the tube, closing the connexion between the two chambers. The difference in vapour-pressure is then re-established, and the phenomena are repeated. Comparing this system with that which is concerned in sustaining the successive revolutions of terrestrial history, we find the development of radioactive heat in the substratum and the change in state of the magma represented by the steady entry of heat into the source and its expenditure in changing the physical state of the working substance. The periodic absorption by the ocean of the accumulated latent heat of liquefaction of the substratum is represented by the periodic condensation and loss of latent heat of the vapour occurring in the refrigerator. There is evidently a physical analogy between the systems.

There is a steady supply of heat entering the system accompanied by cyclical movements of a working substance with and against gravity.

Many years ago, for the purpose of exhibition at a lecture to juveniles on heat-engines, I constructed a simple form of heat-engine of the following kind:—Into a thin glass sphere, about 7 cm. in diameter, a little camphor is introduced. The bulb is then exhausted of air and sealed off. It is next balanced diametrically on pointed trunnions, so that it is free to rotate round a horizontal diameter. A piece of sheet copper is cut to the form of a sector of the sphere. To it is brazed centrally a copper rod, the other end of which can be heated in a Bunsen burner. This sector is separately supported, and can be so arranged as to radiate heat into the sphere either from directly beneath it or in any direction. A screen cuts off the radiant heat of the Bunsen flame.

If we place the radiator directly beneath the axis of rotation, the following effects are produced. The camphor is slowly sublimed and is deposited in brilliant crystals on the inner upper surface of the sphere. This progresses till the camphor has for the most part collected on the upper walls of the bulb. The conditions are then unstable; a small inequality in the distribution of the camphor above causes the bulb to make a half turn, the camphor being brought down into a position immediately over the heater. It is then again evaporated till unstable equilibrium is attained, when there is another half turn. If the bearings are not quite free, and if the whole is shielded from draughts, there may be a long pause, but sooner or later the inversion of the bulb occurs. A slight cross draught shortens the period. Or, by displacing the heater some little way upwards and from immediately beneath the axis of rotation, the same effect is brought about.

Here, again, there is a source and a refrigerator. The motion of the working substance is the result of the vaporization, the absorbed heat becoming latent. Again, we have the analogy of latent heat collected in the substratum till there is change of state, and owing to this change of state the working substance migrating upwards. In the sublimation engine the return movement of the working substance is effected by the rotation of the containing vessel. In the substratum the working substance, owing to its increased density attending solidification, of itself sinks back into the depths. The sublimation engine may be run for hours without attention; the periodic movement of the working substance, from source to refrigerator and again back to the source, in

other words the intermittent discharge of the energy, continuing monotonously. As to the institution of independent and periodic air-currents to shorten the period of unstable equilibrium, we find here the counterpart of periodic tidal intervention whereby the physical breakdown of the energy-laden substratum is accelerated.

The use of the rotating vessel is not essential. It enables a small mass of the working substance to suffice. On a large scale a sufficient accumulation of the sublimed substance upon an overlying refrigerator must of itself break off and descend to the source. This would constitute an experimental reproduction of the substratal conditions in all essential respects ; and possibly as good as any we can hope to attain in the laboratory, having regard to the fact that a low-temperature and low-pressure reproduction of the exact working conditions affecting the substratum is clearly impossible : even could we find a suitable working substance.

As already intimated, Dr. Jeffreys's argument in reality only applies to such systems as admit of no movement of the parts of the medium involved. If there is such movement then, attending steady flow of heat, cyclical events may arise and prevail indefinitely. And this is true even in the complete absence of latency.

A simple case of a heat-engine working on such lines is described by E. H. Griffiths*. There are no valves or similar contrivances. A steady thermal source supplies heat to a glass bulb containing air. This bulb makes air-tight connexion with one arm of a U tube partially filled with mercury. The other arm of the U tube is open.

When the temperature of the air in the bulb rises, the mercury in that arm of the U tube with which it is connected is depressed. The entering air cools rapidly, partly because of the work done, partly because of contact with cold surfaces. Accordingly there is fall of pressure, and the mercury again rises in the U tube. A fresh influx of heated air from the bulb then initiates another down-stroke ; and so on. Here there is a complete cycle in which more work is done upon the down-stroke than upon the up-stroke, at the expense of the steady thermal supply. The cycles continue indefinitely so long as the thermal supply continues.

This system violates Dr. Jeffreys's statement simply because his statement is not applicable to systems where there exists a working substance ; *i. e.*, one which is instrumental in doing

* 'The Thermal Measurement of Energy' (Cambridge, 1906), p. 4 *et seq.*

work at the expense of transported heat received from a steady thermal supply. It is only true of systems in which there are no translatory movements of parts of the medium. It is purely concerned with conductivity, *i. e.* the flux of heat from one part of a medium to another, the medium itself remaining at rest.

In the concluding paragraph of Dr. Jeffreys's statement, quoted from the 'Geological Magazine' (*ante*) and also in his earlier paper in this Journal (Phil. Mag. May 26, 1926), he dwells upon the supposed inadequacy of tidal forces to establish a sufficient displacement of the outer crust of the earth over a molten substratum to effect the discharge of heat accumulated beneath the continents. It is true that in the earlier paper his mathematical investigation of the matter leads him to the result that in this respect the theory may possibly be self-consistent if we assume a molten stratum no more than 20 kms. in depth. Although such a restriction by no means invalidates the theory, as I pointed out at the time (Phil Mag. May 1926, p. 936 *et seq.*), it would appear that this restriction may have arisen out of his simplifying assumptions.

Dr. Jeffreys writes (*loc. cit.* p. 928):—"Let us then investigate the tides in a thin viscous fluid layer just below the surface. The outer crust is supposed thin enough to offer negligible opposition to the motion of the fluid, so that the upper boundary of the fluid will be treated as free." We must infer from this, as well as from the succeeding analysis, that Dr. Jeffreys discards the effects of the compensations of the continents in interfering with tidal movements in a fluid substratum.

Several eminent mathematicians have discussed the question of the movement of the outer crust of the earth over the interior as arising out of oceanic tides—a movement which must result in lengthening the day by a little.

Prof. Eddington has discussed this matter in a recent suggestive address to the Geological Society ('Nature,' Jan. 6th, 1923). He considers the effects of the arrestment of oceanic tidal movements by surface obstacles upon the outer crust of the earth. It is well known, as arising out of the work of Taylor and its extension by Jeffreys, that the dissipation of oceanic tidal energy is mainly accounted for by turbulent motions taking place in certain quite unrestricted areas where the land interferes with tidal translatory movements. Eddington discusses the effects of such interference as, possibly, in a minute degree lengthening the day, even under existing conditions of the substratum. "The frictional

dissipation acts as a brake on the earth's rotation, and we now feel confident that the brake is a surface brake applied at certain points on the earth's surface where the favourable conditions exist. The retarding force is transmitted into the earth's interior and so delays the rotation as a whole ; but unless the material is entirely non-plastic there will be a tendency for the outer layers to slip over the inner layers." He discusses the effects of a minute and variable slipping of the whole crust from east to west over the main part of the interior as helpful in explaining irregularities in the motions of heavenly bodies etc.

Professor Love refers to such effects. In a well-known paper of his (*Proc. R. S. A.* vol. lxxxii. p. 73), "On the Yielding of the Earth to Disturbing Forces," he refers to certain consequences which must ensue if a fluid layer intervenes between the outer and inner regions of the earth. Such a layer, having regard to the existing rigidity of the earth, involves an impossible rigidity of the outer enclosing shell. Molten matter might exist in isolated areas, but cannot form a continuous sheet separating a central body from an enclosing crust. "The conclusion does not negative the possible existence of a layer of comparatively small rigidity ; but if there is such a layer, it must be rigid enough to prevent the finite slipping of the enclosing crust over the central body."

Professor Larmor, in a recent number of 'Nature' (Sept. 11, 1926), refers to this subject. A deep sub-crustal layer in a condition of fluidity is not compatible with the existence of the actual oceanic tides. The lagging tidal pull, if large enough, might cause a westward drift of the fluid surface material as a whole. The principle of Archimedes must assert itself so that there would be no differential effect on the floating continents and mountain ranges—"except in so far as a uniform drift may be obstructed or deflected locally by the more solid roots of the floating continents that are carried along with it."

Here the statement regarding the effect of the Archimedean principle, while, of course, essentially true, seems to leave out of account an ultimate effect arising out of the vertical separation of the centre of gravity of the floating continents from the centre of buoyancy.

Attending the coming into existence of a molten substratum, oceanic tides would cease or be greatly reduced. But the interference of the continents would then be transferred to their compensations "in so far as a uniform drift may be obstructed or deflected locally by the more solid

roots of the floating continents that are carried along with it."

It would appear that Dr. Jeffreys's simplifying assumption—although for mathematical reasons possibly unavoidable—must result in depriving his final conclusion of the significance which he attaches to it. The limitations he deduces have, in fact, been introduced by his own assumptions, which have led him to omit important factors concerned in the genesis of a general shift of the outer crust over the inner parts of the surface of the earth. At times when the existing rigid substratum is replaced by a mobile fluid, the energy of tidal movements prevailing in it becomes more or less dissipated locally in turbulence among the downward-reaching compensations of the continents. The reactionary effect upon the whole outer crust—continents and ocean-floor—is inevitable, and certainly cannot be ignored.

XXXII. *On the Large Bending of Thin Flexible Strips and the Measurement of their Elasticity.* By F. H. HUMMEL, M.Sc., and W. B. MORTON, M.A., *Queen's University, Belfast* *.

§ 1. **T**HE ordinary formulæ which are used when Young's modulus is measured by the bending of straight bars, under an attached load or under their own weight, are limited in their application to cases where the deflexions from the horizontal are small in comparison with the length of the bar. This limitation gives rise to practical difficulties in dealing with very flexible strips, such as a ribbon of thin steel. It seems worth while, therefore, to examine the problem of the large bending of such a strip and, incidentally, the limits within which the approximate formulæ can be used. When the weight of the strip is negligible in comparison with the attached load, the exact solution can be expressed by elliptic functions, but for the bending caused by the weight of the strip itself a method of approximation has to be sought.

The mathematical analysis can be made neater by the introduction of a "characteristic load" in the first problem and a "characteristic length" in the second. For a strip of given length, cross-section, and material the magnitudes l , E , and I determine a force $EI/l^2 = P$, say, irrespective of the weight of the strip. On the other hand, if w is the

* Communicated by the Authors.

weight per unit length, the length $(EI/w)^{\frac{1}{2}} = c$, say, is characteristic of the strip whatever be its length. The bending of a weightless strip is determined by the ratio of the attached load to P , and that of a strip under its own weight by the ratio of its length to c , and the symbols EIw disappear from the analysis.

In each case we suppose the strip to be clamped horizontally at one end. The origin is at this end, xy being measured horizontally and vertically downwards. The inclination of the tangent at any point is denoted by ϕ , and its maximum value at the outer end by α .

§ 2. *Strip of negligible weight bent by terminal load.*

The following results are taken from the theory of the "elastica." The coordinates and the length are expressed by the aid of an auxiliary length, a , and an auxiliary angle, χ , defined by $a = l(P/W)^{\frac{1}{2}}$, where W is the load and P the characteristic load as above defined :

$$\sin \chi = \sin \frac{\pi}{4} \int \sin \left(\frac{\pi}{4} + \frac{1}{2} \phi \right),$$

where ϕ is the inclination of the tangent at the point.

Then

$$x = 2a \sin \left(\frac{\pi}{4} + \frac{1}{2} \alpha \right) \cos \chi,$$

$$y = a \{ (K - F\chi) - 2(E - E\chi) \},$$

with the usual notation of Legendre's functions, the modulus of which is $\sin \left(\frac{\pi}{4} + \frac{1}{2} \alpha \right)$,

$$l = a(K - F\chi).$$

On elimination of a we have

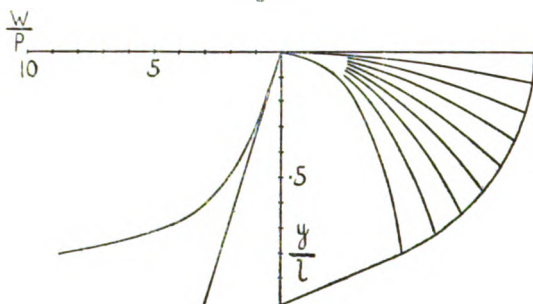
$$x/l = 2 \sin \left(\frac{\pi}{4} + \frac{1}{2} \alpha \right) \cos \chi / (K - F\chi),$$

$$y/l = 1 - 2(E - E\chi) / (K - F\chi).$$

At the terminal point $\phi = \alpha$. Having calculated the corresponding coordinates for a succession of values of α , we can plot the locus described by the end of the strip as the load is continually increased.

The result is shown on fig. 1, where the forms of the rod for $\alpha = 5^\circ, 10^\circ, \dots, 40^\circ$ have also been drawn. It will be seen that the locus makes a finite angle with the horizontal at the lowest point, corresponding to infinite load.

Fig. 1.



It is not hard to show that this angle is $\pi/8$.

For as $\alpha \longrightarrow \pi/2$,

$\chi \longrightarrow \pi/4$,

the modulus $\longrightarrow 1$,

$E\chi \longrightarrow \sin \chi$;

therefore

$$(l-y)/x = (E - E\chi) / \sin\left(\frac{\pi}{4} + \frac{1}{2}\alpha\right) \cos \chi \longrightarrow \sqrt{2} - 1 = \tan \pi/8.$$

On the other side of the vertical are plotted the loads corresponding to the vertical deflexions, expressed as multiples of P . The straight line which touches this graph at the origin shows the loads which would be calculated on the elementary formula,

$$W/P = 3y/l.$$

It will be seen that the agreement is quite good until the drop is about one-quarter of the length of the strip.

A simple relation connects the force P with the horizontal coordinate of the end of the strip and the terminal inclination under given load W .

We have

$$\begin{aligned} P &= Wa^2/l^2 = W/(K - F\chi)^2 \\ &= Wx^2/4l^2 \sin^2\left(\frac{\pi}{4} + \frac{1}{2}\alpha\right) \cos^2 \chi. \end{aligned}$$

In this χ has the value corresponding to $\phi = \alpha$.

$$\text{So} \quad \sin^2 \chi = 1/2 \sin^2 \left(\frac{\pi}{4} + \frac{1}{2} \alpha \right),$$

$$P = W x^2 / 2l^2 \sin \alpha,$$

$$\text{and} \quad EI = Pl^2 = W x^3 / 2 \sin \alpha.$$

If the strip is so much bent that α approaches $\pi/2$, this result gives $EI = \frac{1}{2} W x^3$ very nearly.

§ 3. *Bending of a strip under its own weight.*

Let s be the arc measured from the free end. The equation of moments for the element ds gives the differential equation

$$EI d^2 \phi / ds^2 = -ws \cos \phi.$$

When the characteristic length c is introduced, this becomes

$$d^2 \phi / ds^2 = -s \cos \phi / c^2.$$

The equation is further simplified by taking as independent variable the ratio $\sigma = s/c$; we have then

$$d^2 \phi / d\sigma^2 = -\sigma \cos \phi.$$

Let us try if this can be satisfied by an expansion of ϕ in powers of σ .

$$\text{Put} \quad \phi = \alpha + A_2 \sigma^2 + A_3 \sigma^3 + \dots,$$

in which account has been taken of the terminal conditions $\phi = \alpha$, $d\phi/ds = 0$ when $\sigma = 0$.

Inserting in the equation and disregarding questions of convergency, we get

$$\begin{aligned} 1.2 A_2 + 2.3 A_3 \sigma + \dots \\ = -\sigma \{ \cos \alpha - \sin \alpha (A_2 \sigma^2 + A_3 \sigma^3 + \dots) \\ - \frac{1}{2!} \cos \alpha (A_2 \sigma^2 + A_3 \sigma^3 + \dots)^2 + \dots \}. \end{aligned}$$

On equating coefficients it is found that the only A 's which do not vanish are those whose indices are multiples of three; and each of these is expressed in terms of those preceding it. Thus

$$2.3 A_3 = \cos \alpha,$$

$$5.6 A_6 = \sin \alpha A^3,$$

$$8.9 A_9 = \sin \alpha A^6 + \frac{1}{2} \cos \alpha A_3^2,$$

and so on, the connecting equations becoming rapidly more complicated as the higher powers in the multinomial expansions are taken. If we change the notation and write

B_1 for A_3 , B_2 for A_6 , and so on, then B_n is a homogeneous function of degree n in $\sin \alpha$ and $\cos \alpha$. For purposes of computation it is convenient to transform these into expressions involving sines and cosines of multiples of α . We find sines of even multiples or cosines of odd multiples according as n is even or odd.

The first six expressions are :

$$B_1 = -\cos \alpha / 2 \cdot 3,$$

$$B_2 = -\sin 2\alpha / 2^3 \cdot 3^2 \cdot 5,$$

$$B_3 = (13 \cos \alpha + 7 \cos 3\alpha) / 2^3 \cdot 3^4 \cdot 5,$$

$$B_4 = (94 \sin 2\alpha + 51 \sin 4\alpha) / 2^{11} \cdot 3^3 \cdot 5 \cdot 11,$$

$$B_5 = -(6922 \cos \alpha + 7519 \cos 3\alpha + 3159 \cos 5\alpha) / 2^{13} \cdot 3^6 \cdot 5^3 \cdot 7 \cdot 11,$$

$$B_6 = -(160963 \sin 2\alpha + 169560 \sin 4\alpha + 59439 \sin 6\alpha) / 2^{15} \cdot 3^8 \cdot 5^3 \cdot 7 \cdot 11 \cdot 17.$$

Assuming that a sufficiently accurate value can be obtained from a small number of terms of the series in any given case, we can proceed as follows. Putting $\phi = 0$ and solving the resulting equation for σ by successive approximations, we find the length of strip which, clamped horizontally at one end, will droop so that the slope is α at the other end. The root of the equation is the ratio of this length l to the characteristic length c . Suppose the series to be convergent for the assumed α and for values of σ up to l/c . We now compute ϕ for a number of values of σ in this range, and tabulate $\cos \phi$ and $\sin \phi$. The coordinates of a point on the strip are given by

$$x = c \int_{\sigma}^{l/c} \cos \phi \, d\sigma,$$

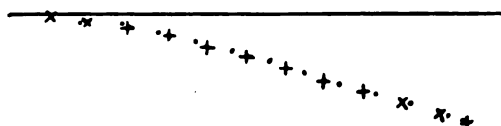
$$y = c \int_{\sigma}^{l/c} \sin \phi \, d\sigma.$$

By using an integraph the graphs of x/c , y/c against σ can be obtained from those of $\cos \phi$, $\sin \phi$, and then the form of the strip is got by plotting together corresponding values of xy .

A comparison with experiment was made by using a strip of pen-steel of length 12 inches. Measurements of (xy) were made at horizontal intervals of an inch, and the terminal slope was found to be $17^\circ 40'$ approximately. When this value is taken for α the ratio l/c comes out to be 1.249; so in order to compare the observed values of the coordinates with those calculated by the method above described, the former are to be multiplied by the factor $1.249/12 = .104$.

The points so obtained are marked with a cross on fig. 2; the points marked with a dot are those obtained by calculation. For purposes of measurement we require merely the co-ordinates of the end-point of the strip. It is then better

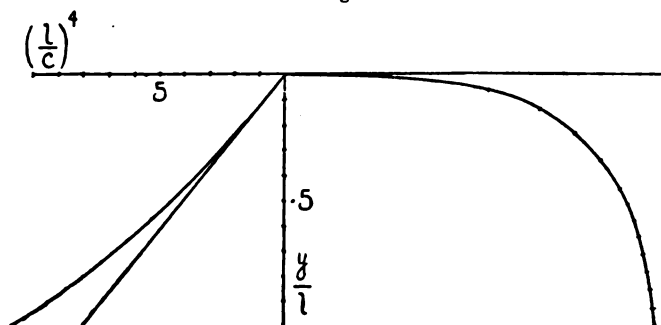
Fig. 2.



to use arithmetical quadrature which can be pushed to any desired degree of accuracy. The process has been carried out for values of α at intervals of 5° from 5° to 45° , with an interval of 0.1 for σ .

The results are shown in the first four columns of the

Fig. 3.



following table, and fig. 3 is the locus described by the end-point as the strip is paid out through the clamp:—

α .	l/c .	α/c .	y/c .	$\frac{1}{8}(6\alpha)^{\frac{2}{3}}$.
5°	·806	·802	·053	·053
10°	1·018	1·008	·133	·133
15°	1·170	1·144	·228	·228
20°	1·298	1·248	·336	·335
25°	1·408	1·322	·452	·451
$27\frac{1}{2}^\circ$	1·460	1·353	·513	·512
30° ..	1·512	1·381	·576	·575
$32\frac{1}{2}^\circ$	1·562	1·402	·641	·640
35°	1·612	1·421	·709	·706
$37\frac{1}{2}^\circ$	1·660	1·434	·778	·775
40°	1·711	1·448	·850	·844
$42\frac{1}{2}^\circ$	1·762	1·456	·924	·915
45°	1·811	1·461	·998	·987

On the other side of the vertical are plotted the values of $(l/c)^4$ to show the departure from the linear relation $(l/c)^4 = 8y/c$ given by the elementary formula.

We have not been able to make any headway with the analytical investigation of the convergency of the series, and so have had to be content with an arithmetical treatment and experimental verification. This is very unsatisfactory from a mathematical point of view, but is perhaps sufficient for practical purposes. It is pretty obvious that the series is convergent for $\sigma < 1$, but it will be seen from the table that this does not carry us to the clamped end, even for $\alpha = 10^\circ$. When the computation is made to include four decimal places, it is found that three terms suffice up to $\alpha = 20^\circ$. For the highest values of σ , a fourth term has to be taken into account from 20° to 35° and a fifth for 40° and 45° .

§ 4. Measurement of Elasticity.

The theory given above can be made available in several ways for the measurement of Young's Modulus. There is an obvious practical advantage in using the bending due to the weight of the strip itself, which perhaps outweighs the unsatisfactory nature of its mathematical basis. For the sake of completeness both cases will be taken together; in each case three different methods may be suggested.

(1) By the coordinates of the end-point. This is the plan followed in the application of the elementary formula to small bending. If we use the vertical drop, y , a graph can be plotted with y/l as abscissa, and as ordinate the ratio of the characteristic force to the actual load, or the characteristic length to the length of the strip, P/W or c/l respectively. These graphs are shown on fig. 4.

(2) By the slope of the chord. For a definite value of P/W in the first case, c/l in the second, the line joining the clamped end to the loaded or free end has a definite inclination to the horizontal. By graphical interpolation the values of the terminal y/x can be found which correspond to a range of values of the ratios in question. If a set of lines be drawn on a vertical sheet placed behind the strip, radiating from the point where the end is clamped (fig. 5), we have only to adjust the load or push the strip through the clamp until its tip lies on one of the lines. Multiplication of W or l by the corresponding factor then gives P or c . Of course the measurements of the former kind will be subjected to the usual inaccuracy if the weight of the strip is not negligible compared with W .

(3) By the terminal slope of the strip. This is a very practicable and convenient way; the strip is nearly straight

Fig. 4.

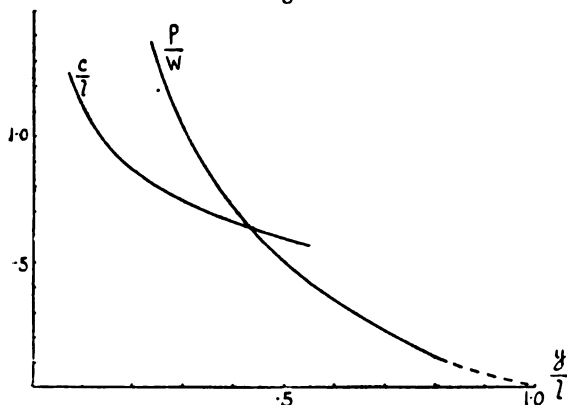


Fig. 5.

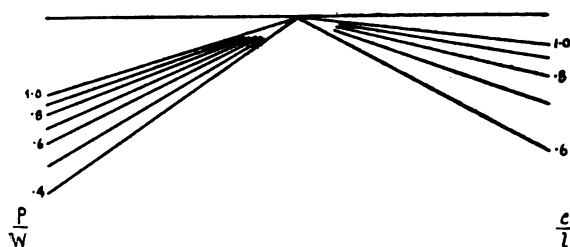
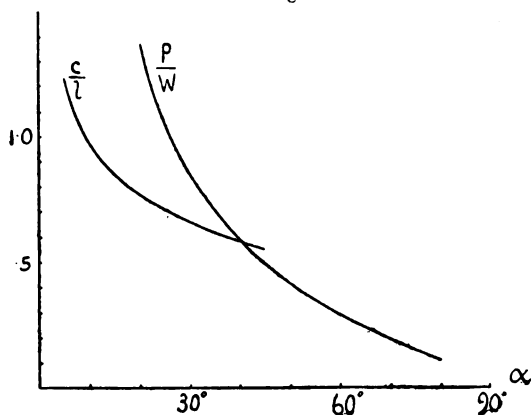


Fig. 6.



for some distance from its end, so that it is easy to set a straight edge parallel to it, or to adjust it to be parallel to a set of lines ruled on a vertical sheet. The connexion between the ratios and the end-slope is shown on fig. 6.

356 Prof. Hummel and Prof. Morton on *Large Bending of*

The following numbers show the results of some measurements made by this method, using a strip of pen-steel bent by its own weight. No special refinements were attempted to secure accuracy. A bracket of angle-iron was fastened at an upper corner of a vertical drawing-board with one of its faces horizontal. The strip was clamped on this face by laying a heavy weight on it. The face was adjusted by a spirit-level. In the first set of readings the end-slope was measured for an even length of strip, and the factor was read off the graph; in the second the length was adjusted so as to give, at the end, one of the special inclinations in the first column of the table of § 3 for which the reciprocal of the ratio is given in the second column.

By measured end-slopes :—

α .	l .	c/l .	c .
14° 30'	12 in.	·862	10·34 in.
22° 0'	14	·742	10·39
31° 0'	16	·650	10·40
40° 40'	18	·580	10·44

Average ...			10·39

By adjusted end-slopes :—

α .	l .	c/l .	c .
15°	12·16 in.	·854	10·38 in.
20°	13·52	·771	10·40
25°	14·72	·711	10·46
30°	15·73	·661	10·42
35°	16·90	·610	10·30
40°	17·86	·584	10·42
45°	18·84	·551	10·36

Average ...			10·39

The dimensions of the section of this strip were 0·635 in. by 0·0117 in., and its weight per inch 0·00210 lb. This gives $E = 2·78 \times 10^7$ lb. per sq. in.

Two curious accidental results may be noticed here which may be used to get approximate values for the characteristic length without using the table or graph. The first is the fact that y is very nearly identical with c when the end-slope is 45° (see table). So to find c it is only necessary to pay out

the strip until the end is parallel to the hypotenuse of a 45° set-square and then measure the vertical drop at the end. The second is found when we extrapolate the relation existing, for small bending, between the drop and the circular measure of the end-slope. We have then

$$y = wl^4/8EI = l^4/8c^3,$$

$$dy/dx = \alpha = wl^3/6EI = l^3/6c^3;$$

on elimination of l ,

$$y/c = \frac{1}{8}(6\alpha)^{\frac{4}{3}}.$$

When this formula is extended to the range of α included in the table, the fifth column is obtained. Comparison with the fourth column shows a close agreement, so that an approximate value of c can be got from measurement of $(y\alpha)$ by use of the formula. None of the other relations, holding between the various magnitudes in the limit of small bending, can be extrapolated to this extent without large errors.

In conclusion, a few results of experience on the experimental side may be added. The end-slope should not be less than about 15° . Each determination should be repeated with the strip turned over and a mean taken. This eliminates the effect of any slight permanent curvature which the strip may have. The experiments showed that such curvature is generally present, and it cannot be corrected by manipulation of the strip. A convenient way of attaching a weight is to make two very small nicks with a file in the sides of the strip near the end. A loop of thread carrying the weight is then passed round the side nicks and brought over on the top side to hang clear from the end of the strip.

As regards approach to the elastic limit, it is to be remembered that the maximum extension and compression are of the order of the half thickness of the strip divided by the radius of curvature; so with a thin strip the strains are small, even with considerable bending.

XXXIII. *The Surface-Tension Balance.* By E. L. WARREN,
Student in Physics at the Royal College of Science, South
Kensington*.

[Plate VI.]

THE determination of the surface-tension of liquids by the capillary ascent method is by no means susceptible to the accuracy usually attributed to it. It is difficult, in the first place, to find a capillary tube of sufficiently uniform cross-section, and when one has been found, the calibration, cleaning, and keeping clean of this tube are no small matters. Moreover, difficulty is experienced in measuring accurately the height of ascent of the liquid in the tube. Furthermore, elaborate thermostatic arrangements are necessary in order to estimate with precision the temperature of the meniscus, and, in consequence, this method is not suitable for the investigation of the variation of surface-tension with temperature. Finally, when every precaution has been taken to overcome these difficulties, it must be remembered that the result obtained represents $T \cos \theta$, where T is the surface-tension and θ the contact angle between the liquid and the walls of the tube, and not simply T . The value of the contact angle is very uncertain: *e.g.*, the value of the contact angle between glass and water is stated by Quincke to be $8-9^\circ$, but by Wilberforce to be 0° . The latter observer used especially clean glass. Seeing that it is impossible to be absolutely sure that the inside of a capillary tube is perfectly clean, the contact angle which actually exists during an experiment may have any value from 0° to 9° , or even greater. Hence an error of possibly more than 1 per cent. may be introduced.

Surface-tension measurements play an important part in modern colloidal work, and for this reason it has become necessary that methods for their determination should be developed which are accurate, rapid, and do not make too great a demand on the instrumental equipment of a technical laboratory. The capillary-ascent method certainly does not satisfy these requirements.

A knowledge of the variation of surface-tension with temperature is of considerable importance. Dr. Ferguson† has stated that the variation of the surface-tension of unassociated liquids with temperature can be expressed very accurately from its freezing-point to its critical temperature

* Communicated by Prof. H. Gregory, Ph.D.

† Ferguson, *Phil. Mag.*, Jan. 1916, p. 37.

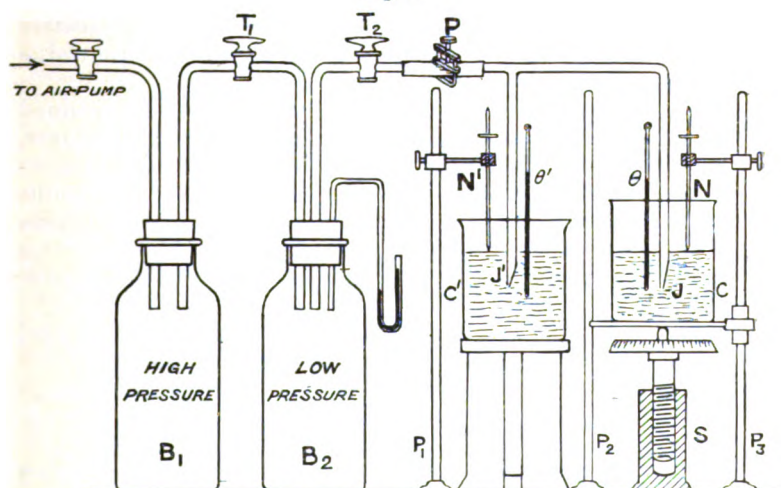
by the equation $T_\theta = T_0(1 - b\theta)^n$, where T_0 and T_θ are the surface-tensions of the liquid at the temperatures 0 and θ respectively, and b the reciprocal of the critical temperature. n is constant for any one liquid. Obviously, then, if we take accurate measurements of the surface-tension of an unassociated liquid over a fairly wide range of temperature, we can calculate b and n , and from b the critical temperature of the liquid.

The method to be discussed is a modification of Jaeger's method, and has been designed primarily for the experimental determination of the temperature-coefficient of surface-tension, and for the investigation of the dependence of the surface-tension of solutions on their concentration. The chief feature of the method is that it enables all such measurements to be expressed in terms of the surface-tension of some appropriate standard liquid such as water.

Description of the Surface-Tension Balance.

The apparatus (see fig. 1) consists of two small circular jets J and J' of the same cross-section, which are in gaseous

Fig. 1.



connexion with each other and with the bottle B_2 . The jets are immersed in liquids in the beakers C and C'. The air in the bottle B_2 is maintained at a pressure of a few millimetres of mercury above that of the atmosphere. The pinch-cock P is opened until bubbles of gas escape at intervals of

about five seconds from one of the jets. The depth of immersion of the jet J is adjusted until the bubbles escape approximately alternately from the two jets. This arrangement enables the surface-tension of the liquid in the beaker C to be balanced against that of the liquid in the second beaker C'. The balance is independent of the pressure maintaining the bubble system. In order that this may be so it is essential that the two jets should be identical in size and shape.

Preparation and Calibration of the Jets.

A piece of ordinary glass tubing about 20 centimetres long was heated in the centre, drawn out until it measured about one millimetre in diameter, and cut into two sections at its narrowest point. In this way, seeing that each orifice was represented by one side of the break, two exactly similar jets were obtained. Many pairs of jets were made before two were obtained which were sufficiently circular, and in the preparation of which the tube had broken in a clean manner in a plane approximately perpendicular to the axis of the tube. The jets finally selected were such that the greatest difference between any two diameters was less than 1 per cent. A difference of as much as 2 per cent. in any two diameters would make a difference of only 1/100 per cent. in the value of the surface-tension.

The mean diameter of each orifice was determined separately. Measurements were taken across six diameters, at orientations increasing by 30° , by means of the cathetometer microscope, used to measure the variation of the depths of immersion of the jets. The values obtained for the mean diameters of the two jets were 1.2123 and 1.2111 millimetres respectively, which, to the degree of accuracy of the measurements, are identical.

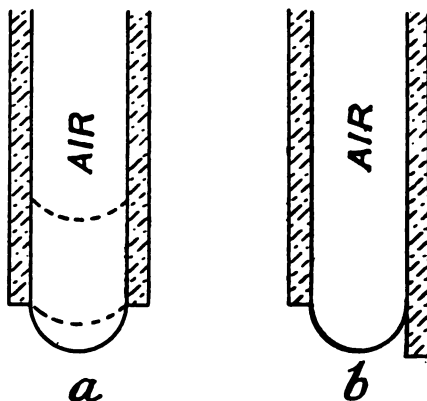
The two jets are clamped vertically in a horizontal steel bar bolted to the tops of the steel pillars P_1 , P_2 , and P_3 .

Formation of the Bubbles.

The air in the bottle B_1 is raised to a pressure of a few centimetres of mercury above that of the atmosphere, and the tap T_1 is opened until the manometer in communication with the second bottle registers a pressure of a few millimetres of mercury in excess of atmospheric pressure. On opening the tap T_2 , the pinchcock P being in adjustment, the meniscus in each tube will be forced slowly down until a bubble is

formed at one of the orifices and escapes. While the meniscus is moving down the interior of the jet its shape will remain the same, but when it reaches the orifice the bubble will slowly increase in size until the section of the meniscus in contact with the edge of the orifice is vertical (see fig. 2*a*). The pressure on the concave side of the meniscus being greater than on the convex side, further increase in the size of the bubble causes it to become unstable and break away from the jet. The meniscus then takes up a position in the tube about three or four centimetres above the orifice, and a new bubble commences to form,

Fig. 2.



Hence the escape of the bubble causes a slight decrease in the level of the free surface of the liquid. This diminution

is equal to about $4 \times \frac{r^2}{R^2}$ millimetres, where r and R are the radii of the orifice and beaker respectively, and is, except where extreme accuracy is required, negligible.

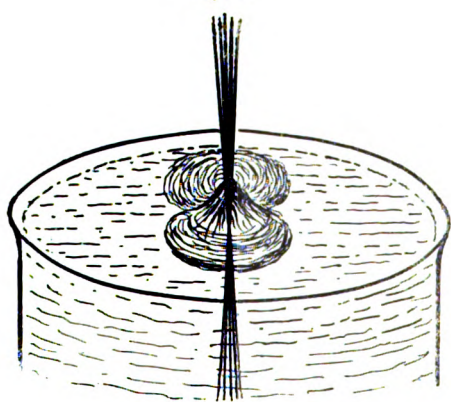
No matter what the contact angle between the liquid and the glass may be, the bubble cannot become unstable until the edge of the meniscus is vertical. If the plane of the orifice is not horizontal, the axis of the jet however being vertical, the shape of the bubble will not be affected, but the effective immersed depth will be equal to the depth of the highest point of the edge of the orifice below the free surface of the liquid (see fig. 2, *b*).

*Adjustment and Measurement of the Depth of Immersion
of the Jets.*

The jet J' is immersed to a depth of two or three centimetres in a suitable liquid in the beaker C' resting on a rigid wooden support. The jet J is immersed in a second liquid in the beaker C. This rests on a metal platform which is capable of sliding up between the two vertical steel pillars P_2 and P_3 . The platform may be moved in a vertical direction by means of a screw S of small pitch. In this way the depth of immersion of the jet may be adjusted with great precision.

This being accomplished, the depth of immersion may be measured with the aid of the screw-pin N. The latter consists of a screw of small pitch terminated at each end by a sharp nickel point. The screw moves vertically through a bracket capable of sliding up the pillar P_3 .

Fig. 3.



On illuminating the surface of the liquid from a large angle of incidence, and viewing the surface in the direction of the reflected rays, the surface appears to be flooded with light. While viewing the surface in this manner the image of the pin can be seen distinctly, and the pin is slowly screwed down until the pin and its image meet. This adjustment may be made with great accuracy, for immediately the pin touches the surface of the liquid a dark patch appears round the point of the pin, due to the curvature of the surface in its vicinity caused by the slight ascent of the liquid up the sides of the pin (see fig. 3). On removing the beaker C the distance from the lower point of the pin and the orifice may

be measured by means of a cathetometer microscope. The depth of immersion of the jet J' is measured in precisely the same manner.

There are two ways of determining the surface-tension of a liquid with the Surface-Tension Balance, viz.:—

1. A suitable liquid of which the surface-tension is known and the liquid under investigation are placed in the beakers C' and C respectively. The balance is set and the depths of immersion of the two jets are measured. The surface-tension of the liquid under investigation can then be calculated.

2. Any convenient liquid is placed in the beaker C' . The liquid under investigation is placed in the beaker C , the balance is set, and the pin N is screwed down until it touches the free surface of the liquid. A cathetometer microscope is set on the upper point of the screwpin. The liquid under investigation is replaced by the standard liquid, the balance is again set, and the pin N readjusted. The movement of the pin is measured by means of the cathetometer microscope. The depth of immersion of the jet with respect to the standard liquid is then measured. Then, if h_1 is the immersed depth with respect to the standard liquid, and x the movement of the pin, the downward sense being counted positive, the immersed depth with respect to the liquid under investigation is equal to $(h_1 + x)$.

If the movement of the pin is small compared with the immersed depth, and is measured accurately, an error of 1 per cent. in the measurement of the immersed depth only involves an error of approximately $\left(\frac{\rho_s - \rho}{\rho}\right)$ per cent., where

ρ and ρ_s are the densities of the liquid under investigation and the standard liquid respectively. This method is that used for measuring the variation of the surface-tension of liquids with temperature, for in this case the liquid under investigation at a certain temperature is adopted as the

standard, and hence $\left(\frac{\rho_s - \rho}{\rho}\right)$ is very small compared with unity : *e.g.*, for water from 0° $\left(\frac{\rho_s - \rho}{\rho}\right)$ per cent. is less than 0.04 per cent.

In order to measure the temperature of the meniscus, a thermometer graduated to tenths of centigrade degrees was suspended in each liquid, so that its bulb was less than one millimetre from the orifice.

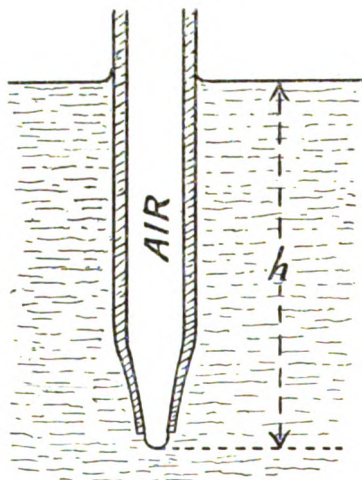
The Surface-Tension Balance is especially suitable as compared with the capillary-rise method for measuring the

surface-tension of solutions. In the latter method the liquid has to pass into a glass tube of which the walls are not perfectly clean and contamination by the dirt or adsorption by the walls of the tube is probable. When the Surface-Tension Balance is used, the breaking away of the bubbles and consequent sudden rush of the solution into the jet ascertains that the jet is kept clean and the solution of uniform strength.

Theory of the Method.

Consider a tube tapering down to an orifice of about one millimetre diameter immersed with its axis vertical in a

Fig. 4.



liquid of density ρ (see fig. 4). Let the pressure of the air in the tube be gradually increased until a bubble is formed at the orifice and is just on the point of breaking away. When this is the case, the edge of the meniscus then being vertical, the meniscus is identical in shape with that due to the capillary ascent of a liquid of zero contact angle in a narrow tube. Let the depth of the apex of the bubble below the surface of the liquid be h . The pressure P_i on the concave side of the meniscus is given by

$$P_i = P + g\rho h + \frac{2T}{R}, \quad . \quad . \quad . \quad (1)$$

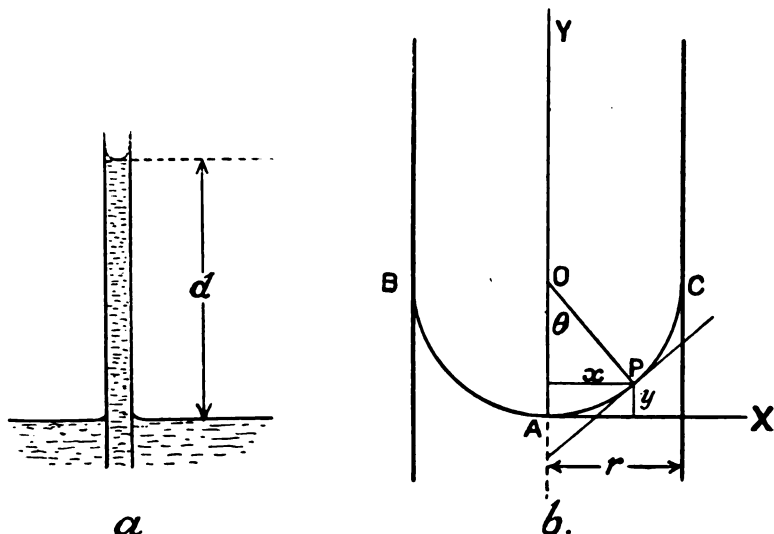
where T is the surface-tension of the liquid, R the radius of

curvature of the meniscus at the vertex, and P the atmospheric pressure.

Consider the capillary-ascent of the liquid in a tube whose radius is equal to that of the orifice. Let us assume that the angle of contact between the liquid and the walls of the tube is zero.

Let fig. 5 (a) represent the liquid in its tube and fig. 5(b)

Fig. 5.



an enlarged diagram of the surface. The excess of the pressure on the concave side over that on the convex side at the point P is equal to $T \left(\frac{1}{R_1} + \frac{1}{R_2} \right)$, where R_1 is the radius of curvature at P of the curve BAC , and R_2 is the length OP of the normal at P , from its point of intersection O by the Y axis, to the surface.

This pressure excess is also equal to $g\rho(y+d)$, where d is the height of ascent of the liquid in the capillary tube, and y is the vertical distance of the point P above the vertex of the meniscus.

Therefore
$$g\rho(y+d) = T \left(\frac{1}{R_1} + \frac{1}{R_2} \right).$$

Writing the specific cohesion a^2 for $\frac{T}{g\rho}$,

$$\frac{1}{R_1} + \frac{1}{R_2} = \frac{y+d}{a^2}.$$

Therefore

$$\frac{1}{x} \frac{d}{dx} (x \sin \theta) = \frac{y+d}{a^2}.$$

The exact solution of this equation is apparently impossible. Approximate solutions have been given by many mathematicians. Poisson * stated that

$$2a^2 = rd \left(1 + \frac{1}{3} \frac{r}{d} - 0.1288 \frac{r^2}{d^2} \right),$$

Mathieu † that

$$2a^2 = rd \left(1 + \frac{1}{3} \frac{r}{d} - \frac{1}{9} \frac{r^2}{d^2} + \dots \right),$$

and Rayleigh ‡, who performed his calculations to a higher degree of accuracy, that

$$2a^2 = rd \left(1 + \frac{1}{3} \frac{r}{d} - 0.1288 \frac{r^2}{d^2} + 0.1312 \frac{r^3}{d^3} \right).$$

The equation

$$2a^2 = rd \left(1 + \frac{1}{3} \frac{r}{d} - 0.1288 \frac{r^2}{d^2} \right) \quad . \quad . \quad . \quad (2)$$

is sufficiently accurate for experimental purposes. At the vertex of the meniscus we have

$$\frac{2T}{R} = g\rho d, \\ 2a^3 = Rd. \quad . \quad . \quad . \quad . \quad . \quad . \quad (3)$$

From equations (2) and (3)

$$R = r \left(1 + \frac{1}{3} \frac{r}{d} - 0.1288 \frac{r^2}{d^2} \right). \quad . \quad . \quad . \quad (4)$$

From (2) to a first approximation

$$\frac{1}{d} = \frac{r}{2a^2},$$

and to a second approximation

$$\frac{1}{d} = \frac{r}{2a^2} \left(1 + \frac{1}{3} \frac{r}{d} \right), \\ \frac{1}{d} = \frac{r}{2a^2} \left(1 + \frac{r^2}{6a^2} \right).$$

* Poisson, 'Nouvelle Théorie de l'Action Capillaire' (1831), Chap. IV.

† Mathieu, 'Théorie de la Capillarité' (1883), Chap. II.

‡ Rayleigh, Proc. Roy. Soc. (A), xcii. p. 184 (1915).

Substituting the more exact value of $\frac{1}{a}$ in the second term and the more approximate value in the third term of equation (4), we have

$$R=r\left(1+\frac{r^2}{6a^2}+\frac{r^4}{36a^4}-0.1288\frac{r^4}{4a^4}\right),$$

$$R=r\left(1+\frac{r^2}{6a^2}-0.0044\frac{r^2}{a^4}\right),$$

or to a sufficient degree of accuracy

$$R=r\left(1+\frac{r^2}{6a^2}\right).$$

Equation (1) can now be written

$$(P_i-P)-g\rho h=\frac{2T}{r\left(1+\frac{r^2}{6a^2}\right)}.$$

Let $(P_i-P)=X$.

Then

$$T=(X-g\rho h)\frac{r}{2}\left(1+\frac{r^2}{6a^2}\right),$$

or

$$T=(X-g\rho h)\frac{r}{2}+(X-g\rho h)\frac{r^3\rho g}{12T}. \quad . \quad . \quad (5)$$

To a first approximation

$$(X-g\rho h)=\frac{2T}{r}.$$

Substituting this value in the second term of equation (5), we have

$$T=(X-g\rho h)\frac{r}{2}+\frac{1}{6}g\rho r^2, \quad . \quad . \quad . \quad (6)$$

where X denotes the excess pressure in the bottle B_2 over that of the atmosphere.

Equation (6) is applicable to the double-jet system described above.

Let r denote the radius of the jets.

Let ρ and T denote the density and surface-tension of the liquid in the beaker C , and h the distance from the surface of this liquid to the vertex of the meniscus when the bubble is about to break away from the jet J . Let ρ' , T' , and h' be the corresponding quantities for the liquid in the beaker C' .

Then from (6)

$$T = (X - g\rho h) \frac{r}{2} + \frac{1}{6} g\rho r^3,$$

$$T' = (X - g\rho' h') \frac{r}{2} + \frac{1}{6} g\rho' r^3.$$

Hence, by subtraction

$$T - T' = g \frac{r}{2} (\rho' h' - \rho h) + \frac{1}{6} g r^3 (\rho - \rho'). \quad (7)$$

Hence, if we know T' we can measure r , h , ρ , h' , and ρ' , and then calculate the value of T .

If we replace the liquid in the beaker C by another liquid of which the quantities corresponding to ρ , h , and T are ρ_s , h_s , and T_s , then from (7)

$$T_s - T' = g \frac{r}{2} (\rho' h' - \rho_s h_s) + \frac{1}{6} g r^3 (\rho_s - \rho').$$

Hence, by subtraction

$$T - T_s = g \frac{r}{2} (\rho_s h_s - \rho h) + \frac{1}{6} g r^3 (\rho - \rho_s). \quad (8)$$

This is the equation which was used to calculate the value given.

It must be remembered that h , h' , and h_s do not represent the immersed depth of the orifice, but the distance from the surface of the liquid to the vertex of the meniscus when the bubble is about to break away.

If h_1 , h'_1 , and h_{s1} are the immersed depths of the jets for the given liquids, then we may say to a sufficient degree of accuracy that

$$h = h_1 + r, \quad h' = h'_1 + r, \quad \text{and} \quad h_s = h_{s1} + r.$$

Experimental Details.

1. Investigation of the Variation of the Surface-Tension of Water with Temperature.

The beaker C' was well lagged with asbestos and filled with pure distilled water. It was found that this water evaporated sufficiently during the time required to complete a determination to appreciably affect the values for the surface-tension obtained. In order to correct for this evaporation, it was assumed that $\frac{dh'}{dt}$, where h' is the immersed depth of the jet J' and t the time, was constant during any particular

determination. Consequently, the time at which the balance was set was recorded.

Round the beaker C a heating coil was wound, the coil being imbedded in asbestos. The beaker was filled with pure distilled water which had been boiled to remove dissolved air and then cooled by a mixture of ice and calcium chloride until it began to freeze. The pressures in B_1 and B_2 and the pinchcock P having been adjusted, the tap T_2 was opened and the beaker was gradually raised until the bubbles were just unable to break away from the jet J, but escaped from the jet J'. Owing to conduction from the surrounding air, the temperature of the water was slowly rising. This caused each successive bubble formed at the orifice J to approach nearer to completion than the previous one, until after one or two minutes the bubbles formed at the jets J and J' respectively were absolutely identical, showing that the surface-tension of the water in the beaker C was balanced against that of the water in the beaker C'. The temperature of the water in the beaker C still very slowly rising, the balance turned and a bubble escaped from the jet J. Immediately the thermometer θ was read, the tap T_2 closed so that the free surface of the water should not be disturbed, the screw-pins N and N' set, the thermometer θ' read, and the time taken, in the order stated. The cathetometer microscope, which by means of a micrometer attachment was graduated to $1/200$ th of a millimetre, was set on the upper end of the pin N and the micrometer reading estimated to $1/1000$ th of a millimetre. Only the micrometer attachment was used to set the microscope during the whole determination. The pin N' was not again adjusted until the end of the determination.

The water was heated to about 5°C. by means of the heating coil. The balance having again been obtained, the thermometer θ was read, the screw-pin N set, and the necessary readings taken. Observations were taken at intervals of five centigrade degrees up to 90° or 95°C. When readings were taken at temperatures above that of the surroundings, a small current was kept flowing through the heating coil during the observations so that the temperature would continue to rise very slowly and the balance set. Above 50°C. it was necessary only to keep sufficient current flowing to keep the temperature of the water constant at the desired temperature, for the evaporation was then sufficiently rapid to finally set the balance.

It was difficult to take readings above 90°C. because the

evaporation then becomes very rapid, and furthermore the residue of dissolved air is evolved and disturbs the surface.

The final observation having been taken, the microscope was set on the upper end of the pin N' and its reading taken. The pin was readjusted, the time taken, and the microscope again set and its reading taken. In this way $\frac{dh'}{dt}$ was determined.

The water in the beaker C was siphoned off, the beaker removed, and the depth of immersion of the jet J for the last observation measured by means of a cathetometer microscope graduated to read 1/20th of a millimetre. (The instrument used to measure the movement of the pins was only constructed to measure distances in the same vertical line.) It can easily be seen that, starting with the lowest temperature, if $x_1, x_2, x_3 \dots x_n$ are the scale readings corresponding to the temperatures $\theta_1, \theta_2, \theta_3 \dots \theta_n$, the depths of immersion of the jet J for these temperatures are given by

$$(h_1 - x_n) + x_1 \text{ for temperature } \theta_1,$$

$$(h_1 - x_n) + x_2 \text{ for temperature } \theta_2,$$

$$\text{etc.} \qquad \text{etc.}$$

$$h_1 \text{ for temperature } \theta_n,$$

θ_n being the highest temperature recorded and h_1 the depth of immersion corresponding to this temperature.

It was found impossible to keep the temperature θ' of the liquid in the beaker C' constant. The temperature θ was corrected accordingly. It was assumed that θ (corrected) $= \theta + (\bar{\theta}' - \theta')$, where $\bar{\theta}'$ is the mean of the temperatures θ' . This would be accurately true if the relation between the surface-tension and temperature was linear. It is approximately so, and for the purposes of a correction may be regarded as so.

2. *Investigation of the Dependence of the Surface-Tension of Solutions of Sodium Chloride on their Concentration.*

The beakers C and C' were filled with distilled water. The height of the beaker C was adjusted by means of the screw S until bubbles escaped approximately alternately from the two jets. The pins N and N' were set on the surface of the liquid in the beakers C and C' respectively, the time was taken, and the thermometers were read. The cathetometer microscope was set on the pin N, and its reading taken. Without in any way disturbing the jet J, the water was siphoned from the beaker C, and the latter was removed

and replaced by a clean dry beaker. This was filled with a solution of sodium chloride, the balance again obtained, the pin N set, and the previous readings repeated. Observations were taken for solutions of all concentrations from 12½ to 300 grams per litre. The results were corrected for the evaporation and variation of the temperature of the liquid in the beaker C' in the manner described in the previous section.

If, the balance having been set, a bubble, after breaking away from the jet, did not burst but remained on the surface of the liquid, the consequent extremely slight rise in the level of the free surface of the liquid was sufficient to prevent subsequent bubbles from escaping from that jet.

RESULTS.

$g = 981.2$ dynes per centimetre per centimetre.

Mean radius of the orifice = 0.06059 centimetre.

Substituting these values in equation (8), we obtain the relation

$$T - T_s = 29.73(\rho_s h_s - \rho h) + 0.60(\rho - \rho_s),$$

where h and h_s are measured in centimetres, ρ and ρ_s in grams per cubic centimetre, and T and T_s in dynes per centimetre.

The following table gives some of the values obtained for the surface-tension of water at 15° C. by different observers:—

TABLE I.

T_{15} Dynes per cm.	Observer.	Method.
73.26	Volkmanu.	Capillary-rise.
73.46	Domké.	
73.38	Richards & Coombs.	
73.55	Brown & Harkins.	
73.45	Ferguson.	Pull on sphere.
73.45	Hall.	Weighing tension in film.
73.76	Sentis.	Capillary tubes.
73.88	Ferguson.	Jaeger's method.
73.72	Dorsey.	Ripples.
74.22	Watson.	
74.22	Kabähne.	Rippled surface used as diffraction grating.
74.30	Perderson.	Waves on jet.
72.78	Bohr.	

The mean of these values, viz. 73.65 dynes per centimetre, was taken as the surface-tension of water at 15° C. in the following results :—

The Variation of the Surface-Tension of Water with Temperature.

A comparison of the results for four sets of observations of the surface-tension of water from the freezing-point to the boiling-point is given in Table III. The second set of observations is given fully in Table II.

The "correction for h " is that necessitated by the evaporation of the water in the beaker C' during the course of the experiment. It was assumed that h'' , the value of h' at the time of the latter setting of the screw-pin N', was that operative during the complete set of observations, and, in order to justify this assumption, the observed values of h were corrected accordingly. Let t_1 be the time at which a certain observation was taken, and t_2 the time of the latter setting of the screw-pin N'.

Then

$$h'' = h' - \frac{dh'}{dt} (t_2 - t_1),$$

where $\frac{dh'}{dt}$ is the rate of decrease of h' with time. That is, we are assuming the depth of immersion of the jet J' to be $\frac{dh'}{dt} (t_2 - t_1)$ smaller than it actually is. We must therefore assume that the depth of immersion of the jet J is an equivalent amount smaller than it actually is.

Let

$$h_c = h - k(t_2 - t_1), \quad . \quad . \quad . \quad . \quad . \quad . \quad (9)$$

where h_c is the corrected value of h .

To a first approximation from equation (7)

$$T - T' = g \frac{r}{2} (\rho' h' - \rho h), \quad . \quad . \quad . \quad . \quad . \quad . \quad (10)$$

$$\begin{aligned} T - T' &= g \frac{r}{2} \left[\rho' \left\{ h'' + \frac{dh'}{dt} (t_2 - t_1) \right\} - \rho \{ h_c + k(t_2 - t_1) \} \right] \\ &= g \frac{r}{2} \left[(\rho' h'' - \rho h_c) + (t_2 - t_1) \left(\rho' \frac{dh}{dt} - \rho k \right) \right]. \end{aligned}$$

It is desired to replace equation (10) by the equation

$$T - T' = g \frac{r}{2} (\rho' h'' - \rho h_c). \quad . \quad . \quad . \quad (11)$$

In order that we may do this,

$$\left(\rho' \cdot \frac{dh'}{dt} - \rho k \right) \text{ must be equal to zero.}$$

Therefore

$$k = \frac{\rho'}{\rho} \cdot \frac{dh'}{dt}.$$

Now $\rho = 1.00$ and ρ' lies between 1.00 and 0.96. In order to apply a small correction we may assume that $\rho' = \rho$.

Therefore

$$k = \frac{dh'}{dt}.$$

Equation (9) then becomes

$$h_c = h - \frac{dh'}{dt} (t_2 - t_1),$$

where

$$\frac{dh'}{dt} = \frac{h' - h''}{t_2 - t_1}.$$

If t_1 and t_2 are the times of the former and latter settings of the screw-pin N' respectively, then $h' - h''$ is the difference between the cathetometer microscope readings for these two settings. In this case, t_1 , t_2 , and $(h' - h'')$ being known, a linear graph was drawn from which $(h - h_c)$ for each observation was read off. In this way " h corrected" was obtained.

Equation (7) now becomes

$$T - T' = g \frac{r}{2} (\rho' h'' - \rho h_c) + \frac{1}{6} g r^2 (\rho - \rho'),$$

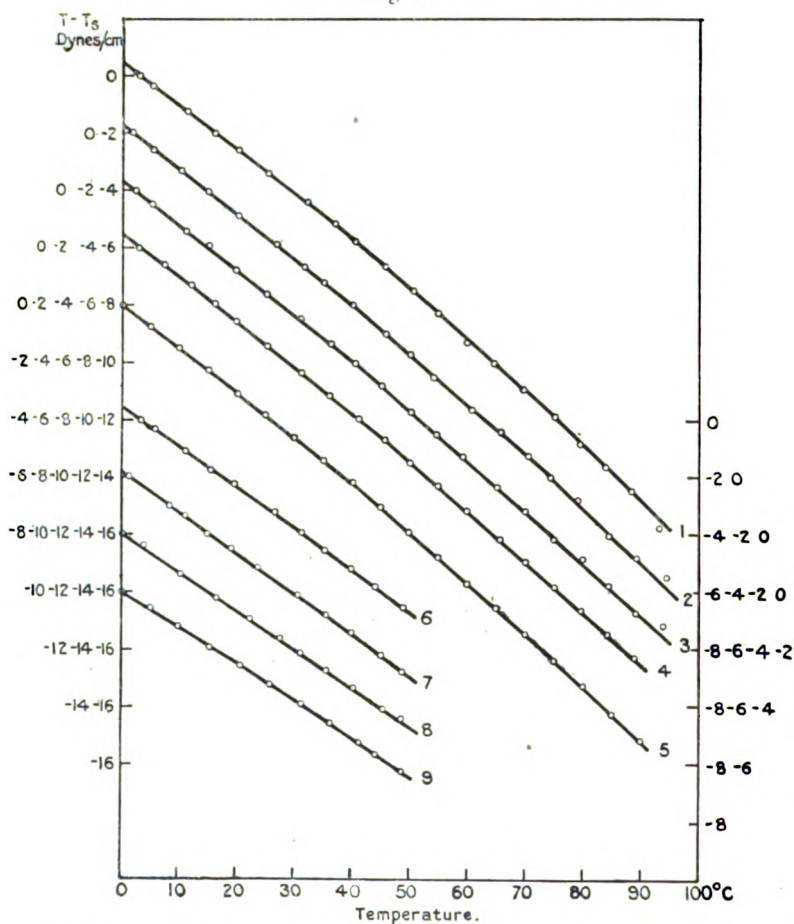
and equation (8) therefore remains unaltered, except that h and h_c must be interpreted as the " h corrected" values instead of the observed values. In assuming that $\rho' = \rho$ we have introduced an error of less than 1/100th per cent.

The values of ρ and h corresponding to the first observation were adopted as the standard values, ρ , h , respectively.

The last column, which represents the differences between the surface-tensions at the first temperature corrected and the subsequent temperature corrected, was plotted against the temperature corrected for each set of observations, and the

curves 1 to 4 were obtained (see fig. 6). It can be seen from these curves that $\frac{d^2T}{d\theta^2}$ is comparatively small, and over ranges 0° to 20° C., 20° to 40° C., 40° to 60° C., 60° to 80° C.,

Fig. 6.



and 80° to 90° C. it may be taken as zero, and a linear law may be assumed without introducing any appreciable error ;

$$\text{i. e.,} \quad T_{\theta_1} = T_{\theta_2} - \frac{dT}{d\theta}(\theta_1 - \theta_2), \quad \dots \quad (12)$$

where $\frac{dT}{d\theta}$ is the rate of decrease of surface-tension with

temperature, and T_{θ_1} and T_{θ_2} are the surface-tensions at the temperatures θ_1 and θ_2 respectively, θ_1 and θ_2 both lying within one of the ranges mentioned. A linear law must not be assumed over any range of 20 centigrade degrees chosen at random, for $\frac{d^2T}{d\theta^2}$ at approximately 40° C. and probably

80° C. is considerable compared with its value in any of the above ranges. More convincing evidence of this fact will be obtained after further analysis of the results.

The figures shown in the columns headed I., II., III., and IV. in Table III. are those derived from the sets of observations I., II., III., and IV. respectively.

Using equation (12), the figures given in the last columns of the four tables of which Table II. is one were corrected to the values they would have had if observations had been taken at temperatures of exactly 0, 5, 10 . . . 90° C. The corrected sets of values are shown in the columns headed "S" of Table III. The deviations of each of the four values of S for each temperature from their mean are shown in the columns headed ΔS . So far we have assumed that no errors were made in the first observation of each set; but this is just as likely to involve errors as any other in that set.

Now the sum of the errors from 0° to 80° C. for each set of observations should be equal to zero (the readings above 80° C. being less consistent than those between 0° and 80 C. were ignored).

Let $a_0, a_5, a_{10}, \dots a_{80}$ be the true values of the errors for any one set of observations corresponding to the temperatures 0°, 5°, 10° . . . 80° C.

Then $\Sigma a = 0$.

$$\begin{aligned} \text{Now} \quad (\Delta S)_0 &= a_0 - a_0, \\ (\Delta S)_5 &= a_5 - a_0, \\ (\Delta S)_{10} &= a_{10} - a_0, \\ &\dots \dots \dots \\ &\dots \dots \dots \\ (\Delta S)_{80} &= a_{80} - a_0. \end{aligned}$$

Therefore $\Sigma(\Delta S) = -na_0$,

where n is the number of observations between 0° and 80° C.,

or
$$a_0 = \frac{-\Sigma(\Delta S)}{n} = \frac{-\Sigma(\Delta S)}{17}.$$

a_0 for each set of observations was calculated, and the true error for each observation was then determined from the relation

$$a_0 = (\Delta S)_\theta + a_0.$$

The mean error is 0.03 dyne per cm. The mean values of S plotted against temperature are shown in curve 5 (see fig. 6). They can be represented approximately by a second degree equation, viz.

$$S = (0.022 + 0.14618\theta + 0.000241\theta^2) \text{ dynes per cm. (13)}$$

The values of S derived from this equation are shown in the column headed " S calculated." It can be seen from the succeeding column that this equation represents the values of S derived directly from the experimental data to 0.04 dyne per centimetre, which is sufficiently accurate for most practical purposes.

On plotting (S observed — S calculated) against the temperature, a well-defined curve was obtained. The values of (S observed + S calculated) obtained from this curve are shown in the column headed " $(S \text{ obs.} - S \text{ calc.})$ corrected." The differences between the sets of figures in these two columns are irregular, and are therefore probably due to errors of measurement made in the course of the experiments. These "experimental errors" were subtracted from the corresponding S observed in order to obtain " S corrected." The surface-tension of water at 15°C. being known, the surface-tension at each of the other temperatures was calculated.

From equation (13) we may state

$$T_\theta = 75.90(1 - 0.001924\theta - 0.00000362\theta^2) \pm 0.04 \text{ dynes per cm.}$$

The variation of the surface-tension of water with temperature cannot be represented accurately by any equation of the form

$$T_\theta = T_0(1 + a\theta + b\theta^2 + c\theta^3 + \dots).$$

The mean "experimental error" involved in the observed values of S is 0.005 dyne per centimetre. Furthermore, these errors have been eliminated. The values of the surface-tension given in the last column of Table III. are therefore consistent to two decimal places; i. e., to 0.005 dyne per centimetre, or less than 1/100th per cent.

TABLE II. (see Curve 2).
 h' at 2.21 p.m. — h' at 4.28 p.m. = 0.0282 cm. Last $h = 2.755$ cm.

Time.	θ' .	θ .	θ corrected.	α .	h .	Correction for h .	h corrected.	ρ .	ρh .	$\rho h - \rho h_0$.	29.73 ($\rho h - \rho h_0$).	0.60 ($\rho_0 - \rho$).	$T_0 - T$.
P.M.													
2.21	19.3	1.5	1.7	0.2390	2.1567	0.0282	2.1285	0.9999	2.1283	0	0	0.00	0
2.20	19.25	5.2	5.45	0.2565	2.1742	0.0263	2.1479	1.0000	2.1479	0.0196	0.58	0.00	0.58
2.36	19.25	10.0	10.25	0.2802	2.1979	0.0249	2.1730	0.9997	2.1723	0.0440	1.31	0.00	1.31
2.42	19.25	14.9	15.15	0.3058	2.2235	0.0236	2.1999	0.9991	2.1979	0.0696	2.07	0.00	2.07
2.47	19.2	19.9	20.2	0.3348	2.2525	0.0225	2.2300	0.9983	2.2262	0.0979	2.91	0.00	2.91
2.46	19.25	26.5	26.75	0.3690	2.2867	0.0205	2.2662	0.9997	2.2587	0.1304	3.88	0.00	3.88
3.2	19.3	31.55	31.75	0.3975	2.3152	0.0192	2.2960	0.9952	2.2850	0.1567	4.66	0.00	4.66
3.9	19.3	34.85	35.05	0.4170	2.3347	0.0177	2.3170	0.9941	2.3033	0.1750	5.20	0.00	5.20
3.15	19.35	39.8	39.95	0.4458	2.3635	0.0163	2.3472	0.9923	2.3291	0.2008	5.97	0.00	5.97
3.20	19.4	45.75	45.85	0.4845	2.4022	0.0152	2.3870	0.9899	2.3629	0.2346	6.97	0.01	6.98
3.29	19.45	50.05	50.1	0.5113	2.4290	0.0132	2.4158	0.9880	2.3868	0.2585	7.69	0.01	7.70
3.40	19.55	54.4	54.35	0.5415	4.4592	0.0107	2.4485	0.9860	2.4142	0.2859	8.50	0.01	8.51
3.45	19.6	61.05	60.95	0.5870	2.5047	0.0096	2.4951	0.9827	2.4519	0.3256	9.62	0.01	9.63
3.50	19.65	65.8	65.65	0.6190	2.5367	0.0084	2.5283	0.9802	2.4782	0.3499	10.40	0.01	10.41
3.55	19.7	70.8	70.6	0.6542	2.5719	0.0073	2.5646	0.9773	2.5064	0.3781	11.24	0.01	11.25
3.59	19.8	74.85	74.55	0.6853	2.6080	0.0065	2.5965	0.9750	2.5316	0.4033	11.99	0.02	12.01
4.4	19.85	79.5	79.15	0.7198	2.6375	0.0063	2.6322	0.9721	2.5588	0.4305	12.80	0.02	12.82
4.7	19.9	85.0	84.6	0.7701	2.6884	0.0047	2.6837	0.9686	2.5994	0.4711	14.01	0.02	14.03
4.12	19.95	89.8	89.35	0.8053	2.7230	0.0035	2.7195	0.9655	2.6257	0.4974	14.79	0.02	14.81
4.17	20.1	95.1	94.5	0.8373	2.7550	0.0024	2.7526	0.9619	2.6477	0.5194	15.44	0.02	15.46

Mean = 19.5

TABLE III.

Temp. in °C.	S in dynes per cm.				ΔS.				Experimental errors a.				S calcu- lated.	S _{obs.} - Scale. corrected.	S _{obs.} - Scale. corrected. b.	S cor- rected.	T.	
	I.		Mean.		I.	II.	III.	IV.	I.	II.	III.	IV.						Numer- ical Mean.
	I.	II.	III.	IV.														
0	0	0	0	0	0	0	0	0	+0.01	-0.03	-0.07	+0.06	0.06	-0.02	-0.02	0	75.94±0.005	
5	0.73	0.78	0.82	0.65	-0.02	+0.03	+0.07	-0.10	+0.02	0	0	-0.04	0.01	0.76	-0.01	0	75.19±	
10	1.52	1.54	1.59	1.43	0	+0.02	+0.07	-0.09	+0.04	-0.01	0	-0.03	0.02	1.51	+0.01	+0.01	74.43	
15	2.28	2.32	2.30	2.21	0	+0.04	+0.02	-0.07	+0.04	+0.01	-0.05	-0.01	0.03	2.27	+0.01	-0.01	73.65	
20	3.03	3.15	3.13	3.01	-0.06	+0.07	+0.05	-0.07	-0.01	+0.04	-0.02	-0.01	0.02	3.04	+0.04	0	72.96	
25	3.80	3.88	3.92	3.82	-0.06	+0.03	+0.07	-0.03	-0.01	0	0	+0.03	0.01	3.83	+0.02	0	72.00	
30	4.51	4.66	4.68	4.61	-0.10	+0.05	+0.07	-0.01	-0.06	+0.02	0	+0.05	0.03	4.62	-0.01	0	71.33	
35	5.32	5.46	5.49	5.40	-0.11	+0.04	+0.07	-0.02	-0.06	+0.01	0	+0.04	0.03	5.43	-0.01	-0.03	70.54	
40	6.14	6.25	6.28	6.18	-0.07	+0.04	+0.07	-0.03	-0.03	+0.01	0	+0.03	0.02	6.25	-0.04	0	69.73	
45	6.98	7.10	7.14	7.01	-0.08	+0.04	+0.08	-0.05	-0.04	+0.01	+0.01	+0.01	0.02	7.09	-0.03	0	68.88	
50	7.83	7.95	8.03	7.88	-0.08	+0.03	+0.11	-0.04	-0.05	0	+0.04	+0.02	0.03	7.93	-0.01	0	68.02	
55	8.70	8.80	8.88	8.73	-0.10	-0.09	+0.08	-0.07	-0.06	+0.06	+0.01	-0.01	0.03	8.79	+0.01	0	67.14	
60	9.72	9.73	9.74	9.62	+0.02	+0.03	+0.04	-0.08	+0.08	0	-0.03	-0.02	0.03	9.66	+0.04	0	66.24	
65	10.52	10.56	10.65	10.46	-0.03	+0.01	+0.10	-0.09	+0.01	-0.02	+0.03	-0.03	0.02	10.54	+0.01	0	65.39	
70	11.43	11.41	11.53	11.34	0	-0.02	+0.10	-0.09	+0.04	-0.05	+0.03	-0.03	0.01	11.43	0	0	64.51	
75	12.25	12.36	12.50	12.21	-0.0	+0.03	+0.17	-0.12	-0.04	0	+0.10	-0.08	0.06	12.34	-0.01	0	63.61	
80	13.35	13.24	13.26	13.15	+0.10	-0.01	+0.01	-0.10	+0.14	-0.04	-0.05	-0.04	0.07	13.26	-0.01	0	62.69	
85	14.27	14.37	14.19	14.05	+0.05	+0.15	-0.03	-0.17	+0.09	+0.12	-0.10	-0.11	0.11	14.19	+0.03	0	61.75	
90	15.22	15.20	15.21	14.96	+0.10	+0.08	+0.09	-0.26	+0.14	+0.05	+0.02	-0.20	0.10	15.13	-0.01	+0.01	60.80	
Algebraic Mean																		
Numerical Mean																		
Numerical Mean..... 0.005																		

The mean value of $\frac{dT}{d\theta}$ obtained from Table III. :

from 0° to 20° C.=0.154 dynes per centimetre per centigrade degree

„ 20° „ 40° C.=0.157 „ „ „ „

„ 40° „ 60° C.=0.174 „ „ „ „

„ 60° „ 80° C.=0.178 „ „ „ „

„ 80° „ 90° C.=0.189 „ „ „ „

Therefore, over the ranges 0° to 40° C., and 40° to 80° C., $\frac{d^2T}{d\theta^2}$ is small, and a linear law may be assumed without introducing any error greater than 0.02 dyne/cm.; but at approximately 40° C. $\frac{d^2T}{d\theta^2}$ is considerable, and over a range of any extent including this temperature a linear law must not, on any account, be assumed.

Variation of the Surface-Tension of Aqueous Solutions of Sodium Chloride with Temperature.

The results of four sets of observations with four solutions of different concentrations are shown in Tables IV. to VII.

The experimental procedure and method of calculation was precisely the same as that adopted in the investigation of the variation of the surface-tension of water with temperature. Owing to the rapidity of evaporation, and the consequent increase in concentration, as the temperature increased, it was not considered advisable to take readings above 50° C.

The densities are those obtained by Karsten (Berlin, 1846). Curves 6 to 9 represent the decrease of surface-tension, $T_s - T$, with temperature for the results recorded in Tables IV. to VII. respectively. These curves can be represented to a considerable degree of accuracy from 0° to 40° C. by linear equations, viz.

Solution of 9.38 grams Sodium Chloride per 100 grams solution.

Surface-Tension $T = 78.63 - 0.1416$ dyne/cm.

Solution of 13.66 grams Sodium Chloride for 100 grams solution.

Surface-Tension $T = 80.19 - 0.1404$ dyne/cm.

Solution of 20.76 grams Sodium Chloride per 100 grams solution.

Surface-Tension $T = 83.00 - 0.1329$ dyne/cm.

Solution of 25.17 grams Sodium Chloride per 100 grams solution.

Surface-Tension $T = 85.00 - 0.1265$ dyne/cm.

The absolute values of the surface-tensions at 0° C. were derived from Table IX.

TABLE IV. (see Curve 6).
 Solution of 9.38 grams Sodium Chloride per 100 grams solution (100 grams per litre at 20.7° C.).
 h' at 11.14 A.M. $-h'$ at 12.36 P.M. = 0.0170 cm. Last $h = 2.545$ cm.

Time.	θ'	θ	θ corrected.	z	h	Correction for h .	h corrected.	ρ	$\rho h - \rho_s h_s$	$\frac{2973 \times}{(\rho h - \rho_s h_s)}$	$0.60 \times$ $(n_s - \rho)$	$T_s - T$
A.M.												
11.14	18.4	3.25	3.35	0.7675	2.3115	0.0170	2.2945	1.0715	2.4586	0	0	0
11.20	18.4	5.6	5.7	0.7772	2.3212	0.0157	2.3055	1.0708	2.4687	0.30	0	0.80
11.25	18.4	10.85	10.95	0.8044	2.3484	0.0147	2.3337	1.0693	2.4954	1.09	0	1.09
11.30	18.4	15.45	15.55	0.8246	2.3686	0.0117	2.3569	1.0678	2.5167	1.73	0	1.73
11.50	18.45	19.45	19.5	0.8430	2.3870	0.0095	2.3775	1.0663	2.5351	2.27	0	2.27
12.0	18.5	26.65	26.65	0.8781	2.4221	0.0074	2.4147	1.0635	2.5680	3.25	0	3.25
P.M.												
12.4	18.5	31.25	31.25	0.9030	2.4470	0.0066	2.4404	1.0617	2.5910	3.91	0.01	3.95
12.9	18.5	35.3	35.3	0.9250	2.4690	0.0055	2.4635	1.0598	2.6108	4.52	0.01	4.53
12.14	18.6	40.0	39.9	0.9497	2.4937	0.0045	2.4892	1.0577	2.6328	5.18	0.01	5.19
12.19	18.6	44.1	44.0	0.9735	2.5175	0.0035	2.5140	1.0556	2.6538	5.80	0.01	5.81
12.24	18.65	49.0	48.85	1.0010	2.5450	0.0024	2.5426	1.0535	2.6786	6.54	0.01	6.55

Mean = 18.5

TABLE V. (see Curve 7).
 Solution of 13.66 grams Sodium Chloride per 100 grams solution (150 grams per litre at 19°C.).
 h' at 1.49 r.m. — h' at 3.24 r.m. = 0.0133 cm. Last $h = 2.12$ cm.

Time.	θ' .	θ .	θ corrected.	x .	h .	Correction for h .	h corrected.	ρ .	ρh .	$\rho h - \rho_s h_s$.	$\frac{29.73 \times}{(\rho h - \rho_s h_s)}$.	$0.60 \times$ $(\rho_s - \rho)$.	$T_s - T$.
P.M. 1.49	18.45	0.8	1.25	0.5536	1.8843	0.0133	1.8710	1.1053	2.0680	0	0	0	0
2.8	18.6	7.95	8.25	0.5855	1.9162	0.0106	1.9056	1.1029	2.1017	0.0337	1.00	0	1.00
2.14	18.7	10.8	11.0	0.5980	1.9287	0.0098	1.9189	1.1018	2.1142	0.0462	1.37	0	1.37
2.21	18.75	14.75	14.9	0.6175	1.9482	0.0088	1.9394	1.1005	2.1343	0.0663	1.97	0	1.97
2.27	18.8	18.9	19.0	0.6362	1.9669	0.0081	1.9588	1.0986	2.1579	0.0839	2.49	0	2.49
2.38	18.9	23.6	23.6	0.6585	1.9892	0.0064	1.9828	1.0965	2.1741	0.1061	3.15	0.01	3.16
2.46	19.0	30.7	30.6	0.6930	2.0237	0.0053	2.0184	1.0931	2.2063	0.1383	4.11	0.01	4.12
2.51	19.0	35.6	35.5	0.7176	2.0483	0.0046	2.0437	1.0908	2.2293	0.1613	4.79	0.01	4.80
2.56	19.1	40.2	40.0	0.7411	2.0718	0.0038	2.0680	1.0887	2.2514	0.1834	5.45	0.01	5.46
3.3	19.15	45.3	45.05	0.7681	2.0988	0.0029	2.0959	1.0861	2.2764	0.2084	6.19	0.01	6.20
3.8	19.25	49.1	48.75	0.7893	0.1200	0.0022	2.1178	1.0842	2.2961	0.2281	6.78	0.01	6.79

Mean = 18.9

TABLE VI. (see Curve 8).

Solution of 20.76 grams Sodium Chloride per 100 grams solution (240 grams per litre at 15° C.).
 h' at 11.25 A.M. $-h'$ at 12.51 P.M. $= 0.0073$ cm. Last $h = 2.115$ cm.

Time.	θ' .	θ .	θ , corrected.	x .	h .	Correction for h .	h corrected.	ρ .	ρh .	$\rho h - \rho_2 h_2$.	$29.73 \times$ $(\rho h - \rho_2 h_2)$.	$0.60 \times$ $(\rho_s - \rho)$.	$T_s - T$.
A.M.													
11.25	15.5	-0.4	-0.25	0.2309	1.8919	0.0081	1.8838	1.1626	2.1901	0	0	0	0
11.31	15.5	3.5	3.65	0.2441	1.9051	0.0067	1.8984	1.1610	2.2040	0.0139	0.41	0	0.41
11.41	15.5	10.05	10.2	0.2765	1.9375	0.0058	1.9317	1.1581	2.2371	0.0470	1.40	0	1.40
11.55	15.55	16.45	16.55	0.3040	1.9750	0.0047	1.9603	1.1551	2.2643	0.0742	2.21	0	2.21
P.M.													
12.2	15.6	22.25	22.3	0.3300	1.9910	0.0041	1.9869	1.1523	2.2895	0.0994	2.95	0.01	2.96
12.8	15.65	27.55	27.55	0.3530	2.0140	0.0036	2.0104	1.1498	2.3116	0.1215	3.61	0.01	3.62
12.18	15.7	31.2	31.15	0.3705	2.0315	0.0027	2.0288	1.1480	2.3291	0.1390	4.13	0.01	4.14
12.24	15.75	35.8	35.7	0.3920	2.0530	0.0022	2.0508	1.1455	2.3492	0.1591	4.73	0.01	4.74
12.29	15.8	40.5	40.35	0.4150	2.0760	0.0018	2.0742	1.1428	2.3704	0.1803	5.26	0.01	5.37
12.34	15.8	45.6	45.45	0.4396	2.1006	0.0013	2.0993	1.1400	2.3932	0.2031	6.04	0.01	6.05
12.43	15.9	48.8	48.55	0.4540	2.1150	0.0006	2.1144	1.1383	2.4068	0.2167	6.44	0.01	6.45

Mean = 15.65

TABLE VII. (see Curve 9).

Solution of 25.17 grams Sodium Chloride=per100 grams solution (300 grams per litre at 15° C.).
 h' at 1.41 P.M. — h' at 3.19 P.M. = 0.0124 cm. Last $h = 2.025$ cm.

Time.	ρ .	ρ .	θ corrected.	z .	h .	Correction for h .	h corrected.	ρ .	r h .	$h - r \rho h_s$.	$2.973 \times$ $(r h - \rho_s h_s)$.	$0.60 \times$ $(\rho_s - \rho)$.	$T_s - T$.
P.M. 1.41	14.75	-0.35	-0.2	0.4161	1.8186	0.0124	1.8062	1.1988	2.1653	0	0	0	0
1.59	14.8	4.85	4.95	0.4335	1.8350	0.0102	1.8248	1.1964	2.1844	0.0191	0.57	0	0.57
2.9	14.8	9.6	9.7	0.4530	1.8555	0.0089	1.8466	1.1943	2.2054	0.0401	1.19	0	1.19
2.25	14.9	15.4	15.4	0.4756	1.8781	0.0068	1.8713	1.1916	2.2298	0.0645	1.92	0	1.92
2.30	14.9	20.6	20.6	0.4965	1.8990	0.0062	1.8928	1.1890	2.2505	0.0852	2.53	0.01	2.54
2.39	14.9	25.7	25.7	0.5180	1.9205	0.0050	1.9155	1.1863	2.2724	0.1071	3.18	0.01	3.19
2.45	14.95	31.45	31.4	0.5425	1.9450	0.0043	1.9407	1.1832	2.2932	0.1309	3.89	0.01	3.90
2.53	15	36.35	36.25	0.5646	1.9761	0.0032	1.9639	1.1805	2.3184	0.1531	4.55	0.01	4.56
3.1	15	41.4	41.3	0.5885	1.9910	0.0022	1.9888	1.1778	2.3424	0.1771	5.26	0.01	5.27
3.5	15.05	44.3	44.15	0.6021	2.0046	0.0017	2.0029	1.1761	2.3556	0.1903	5.66	0.01	5.67
3.10	15.05	48.9	48.75	0.6225	2.0250	0.0010	2.0240	1.1734	2.3750	0.2097	6.23	0.01	6.24

Mean = 14.9

TABLE VIII.

h' at 10.33 A.M. — h' at 12.19 P.M. = 0.0176 cm. Last $h = 1.945$ cm.

Concentration. Grams/litre.	Time.	θ' .	θ .	θ cor- rected.	x .	h .	Cor- rection for h .	h cor- rected.	ρ .	ρh .	$(\rho_2 h_2 - \rho h)$.	$29.73 \times$ $(\rho_2 h_2 - \rho h)$.	$0.80 \times$ $(\rho - \rho_2)$.	$T - T_0$	$T - T_0$ corrected to 20° C.
0	10.33	20.4	20.5		1.2740	2.6555	0.0176	2.6379	0.9982	2.6332	0	0	0	0	0
12½	10.44	20.4	20.5		1.2318	2.6133	0.0158	2.5975	1.0063	2.6139	0.0193	0.57	0	0.57	0.57
25	10.55	20.4	20.6		1.1972	2.5787	0.0141	2.5646	1.0156	2.6046	0.0286	0.85	0.01	0.86	0.87
50	11.10	20.4	20.6		1.1305	2.5120	0.0116	2.5004	1.0327	2.5822	0.0510	1.52	0.02	1.54	1.55
100	11.21	20.4	20.7	same	1.0080	2.3895	0.0098	2.3797	1.0658	2.5363	0.0969	2.88	0.04	2.92	2.94
150	11.35	20.4	20.7	θ .	0.8894	2.2709	0.0074	2.2635	1.0677	2.4846	0.1486	4.42	0.06	4.48	4.50
200	11.46	20.4	20.8		0.7774	2.1589	0.0056	2.1533	1.1288	2.4306	0.2026	6.02	0.08	6.10	6.13
240	11.59	20.4	20.8		0.6885	2.0700	0.0033	2.0667	1.1533	2.3835	0.2497	7.42	0.09	7.51	7.54
300	12.9	20.4	20.9		0.5635	1.9450	0.0017	1.9433	1.1890	2.3106	0.3226	9.59	0.11	9.70	9.73

TABLE IX.

Concentration.		T - T _g at 20° C.				ΔT.			Experimental Errors.				Surface-Tension T at 20° C.
Grams per litre at 20° C.	Grams per 100 grams solution.	X.	XI.	XII.	Mean.	X.	XI.	XII.	X.	XI.	XII.	Arithmetic Mean.	
0	0	0	0	0	0	0	0	0	-0.01	+0.02	-0.01	0.01	72.86
12½	1.24	0.56	0.51	0.57	0.55	+0.01	-0.04	+0.02	0	-0.02	+0.01	0.01	73.41
25	2.46	0.87	0.81	0.87	0.85	+0.02	-0.04	+0.02	+0.01	-0.02	+0.01	0.01	73.71
50	4.84	1.63	1.53	1.55	1.57	+0.06	-0.04	-0.02	+0.05	-0.02	-0.03	0.03	74.43
100	9.38	2.99	2.94	2.94	2.96	+0.03	-0.02	-0.02	+0.02	0	-0.03	0.02	75.82
150	13.66	4.50	4.52	4.50	4.51	-0.01	+0.01	-0.01	-0.02	+0.03	-0.02	0.02	77.37
200	17.71	6.14	6.03	6.13	6.10	+0.04	-0.07	+0.03	+0.03	-0.05	+0.02	0.03	78.96
240	20.80	7.49	7.54	7.54	7.52	-0.03	+0.02	+0.02	-0.04	+0.04	+0.01	0.03	80.38
300	25.21	0.65	9.62	9.73	9.67	-0.02	-0.05	+0.06	-0.03	-0.03	+0.05	0.04	82.53
Sum = +0.10 -0.23 +0.10 Mean = +0.01 -0.02 +0.01													Mean = 0.022

Variation of the Surface-Tension of Aqueous Solutions of Sodium Chloride with Concentration.

A comparison of the results of three sets of observations is shown in Table IX. The third set of observations is given fully in Table VIII.

The method of calculation is similar to that adopted in the investigation of the variation of the surface-tension with temperature. It was assumed that the value of θ' during the last observation in each set was that operative during the complete set, and θ was corrected accordingly. If θ'' is the value of θ' during the last observation, then for any subsequent observation

$$\theta \text{ corrected} = \theta + (\theta'' - \theta').$$

The concentration is recorded in grams of Sodium Chloride per litre at 20° C. and also in grams of Sodium Chloride per 100 grams solution. The deviations ΔT of each of the three values of $(T - T_s)$ at 20° C. for each concentration from their mean value are given, and from these the experimental errors were derived. The mean experimental error is 0.022 dyne per cm. The surface-tension of water at 20° C. being known (see Table III.), the surface-tension at the same temperature of each of the solutions could then be derived.

XXXIV. *Electrical Conductivity at Low Temperatures.* By Professor J. C. McLENNAN, F.R.S., and C. D. NIVEN, M.A.*

CONTENTS.

1. Introduction.
2. Apparatus used in measuring resistances.
3. Preliminary work on methods of making resistances :
 - Method I. used for Lead.
 - Method II. used for Cadmium and Indium.
 - Method III. used for Alkali Metals.
 - Review of these methods.
4. Investigation of resistance-temperature curves of
 - (i.) Beryllium.
 - (ii.) Chromium.
 - (iii.) Rubidium.
 - (iv.) Thorium.
 - (v.) Alloy of Sodium and Potassium.
5. Summary.

1. *Introduction.*

IT has been known for a long time that the electrical resistance of many pure metals is approximately proportional to the absolute temperature. At low temperatures

* Communicated by the Authors. This work was carried out with the aid of a grant of a bursary and scholarship from the National Research Council of Canada to C. D. Niven.

results have shown that this law is far from true. In the case of some metals the resistance suddenly vanishes altogether before the absolute temperature is reached—a phenomenon called by the late Professor H. K. Onnes superconductivity. In the case of other metals the resistance often tends to a constant value. No satisfactory theory has been advanced for such phenomena, and indeed the data on conductivity at low temperatures are so meagre that any theory would be more or less of a speculation at present. Up till now experimenters have been directing their efforts towards proving or disproving the hypothesis that all metals should be superconducting at very low temperatures. Work by Onnes and his collaborators at Leiden, and Meissner at Charlottenburg indicates that superconductivity is a property of only five metals, namely, mercury, lead, tin, thallium, and indium. In the formulation of any theory on conductivity it is necessary to know the form of the resistance-temperature curves at low temperatures, and an endeavour is being made by the authors of this paper to obtain some data that would be of theoretical value. The results up to the present are communicated in the following paragraphs.

2. Apparatus used in measuring resistances.

Before going into the experimental details of how the different resistances were prepared for measurement, it might be as well to mention how the measurements were made. Readings were taken of the resistances when kept at room temperature, and when immersed in liquid air, liquid hydrogen, and liquid helium. Although at the start of the work measurements were made at the temperature of ice, and carbon dioxide snow dissolved in ether, this procedure was discontinued as there was nothing interesting to be found on the resistance-temperature curves by these measurements. The temperature of liquid air was always taken on a tested pentane thermometer as the variations in temperature depending on how old the air was were sufficient to spoil the continuity of a curve. Temperatures below that of liquid helium were obtained by boiling the liquid helium under reduced pressure, the pressure on the boiling liquid giving the temperature by reference to the vapour-pressure curve.

The measuring apparatus used was so far as possible a Mueller Temperature Bridge which is a particular form of Wheatstone Bridge, and has been fully described by Mueller. The method recommended for eliminating lead resistance on this bridge is by the use of four wires—"potentiometer

leads"—and this method was adopted. Resistances which could quite easily be measured on the bridge at normal temperatures had to be measured on a potentiometer at low temperature. The particular instrument used for this purpose was the Cambridge Instrument Company's Vernier Potentiometer. Comparisons were made with a 0.001 ohm standard resistance and by using large currents very small resistances could be measured.

In order to compare the resistances of the different elements measured, the readings at any particular temperature were multiplied by the specific resistance of the metal at room temperature and divided by the measured value of the resistance at room temperature. As no account was taken in this calculation of the metal contracting, there is an error introduced, theoretically: this error is only about 0.1 per cent. at the most. The specific resistances at room temperature were as far as possible taken from Smithsonian Tables, and where values were not given in the Tables, measurements were made to get them.

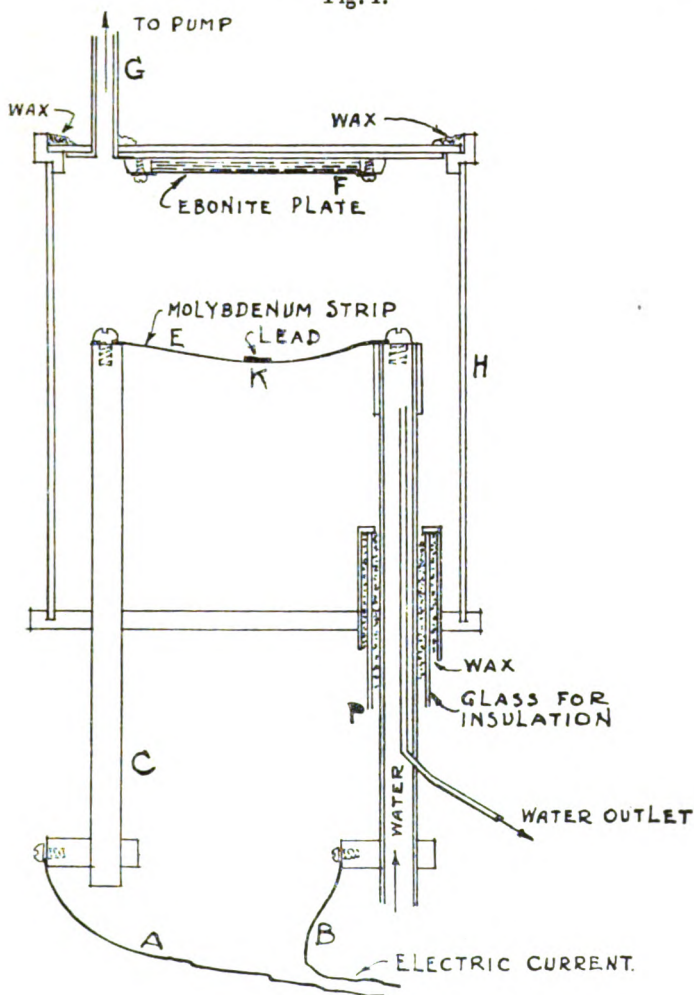
3. *Preliminary work on methods of preparing resistances.*

Before measuring metals which had never been measured before at low temperatures it was considered advisable for a start to take some of the metals which had been investigated by other experimenters and see if we should get the same results as they did. For this preliminary work the elements lead, cadmium, indium, sodium, and potassium were selected, and different methods of making up the resistances exploited.

Method I. used for Lead.—The first metal investigated was lead. Instead of merely taking a wire of lead, it was decided to try and deposit a film on a non-conducting plate, since, if this could be done, it constituted a general method of getting a pure metal in a form that could easily be measured for resistance. In order to make the deposit the small furnace as shown in fig. 1 was employed. The furnace consisted of an evacuated brass vessel through the bottom of which two electrical leads passed; one of these was insulated from the vessel and was therefore watercooled. A molybdenum strip was fixed across the ends of the leads and, when sufficient current was passed through, the molybdenum could be raised to a white heat. In making a deposit the procedure was as follows. The glass or ebonite plate on which the metal was to be deposited was thoroughly cleaned and then clamped to the inside of the

lid of the vessel; a piece of pure lead was placed on the molybdenum strip, the lid was then waxed on to the vessel, and the latter evacuated; when all the oxygen was

Fig. 1.



exhausted the current was put on. Care had to be taken not to put on too heavy a deposit as there was then a tendency for it to peel off; the best deposits were got by passing a current of 35 amperes for about one minute through the particular molybdenum strip in use. Lines

were then carefully drawn up and down the deposit, every alternate line being drawn right through to one end of the plate. In this way a long narrow conducting surface like a zig-zag ribbon was left. In order to provide for contacts, two holes had been bored in the plate before depositing the film and the deposit was left untouched round these holes. The conducting ribbon of deposit terminated at each of these holes. Two comparatively heavy pieces of copper on which the leading-in wires were soldered were then securely clamped on by means of a screw and nut passing through each hole. A spring washer was placed under the nut to allow for contraction in cooling. The first deposits were made on glass, but when these were placed in liquid air the ribbon of lead contracted and broke. It was therefore necessary to get a material other than glass, on which to deposit the film. Such a material had to be an insulator and non-reactive with metals, and it had also to have a coefficient of expansion at any rate as great as the coefficient of expansion of the metal deposited on it. Ebonite seemed to fulfil these requirements, and on being tried proved satisfactory. The resistance of the deposits seemed to alter, growing larger if left over night, and it was concluded that this was due to oxidization; after coating the deposit with collodion this alteration in conductivity ceased. The conductivity of a film of lead deposited on ebonite and thus treated was found to remain unaltered for months even though cooled repeatedly to the temperature of liquid helium and allowed to warm up again.

The resistance of the film thus prepared was found to decrease with temperature according to a linear relation right down as far as the temperature of liquid hydrogen. If the curves in figs. 3 and 4 be looked at it will be observed that had the straight line been continued, the resistance of the lead would have vanished at about 7° K. When the resistance was measured at the temperature of liquid helium, the value was found to be zero. The lead had become superconducting. The question then remained to be answered, did the resistance gradually diminish according to the linear relation or did it suddenly disappear as Professor H. K. Onnes had found for a lead turning? In order to ascertain this, it was decided to try and take readings on a Constantan Resistance Thermometer—which had previously been calibrated in liquid air, liquid hydrogen, and liquid helium—simultaneously with the readings on the lead resistance, while the flask was warming up after having liquid helium in it. The Constantan Resistance Thermometer was read

on the Temperature Bridge, and in the first attempts the lead resistance was measured on the potentiometer. Two difficulties were encountered: in the first place, the potentiometer took too long to read, and in the second place, it seemed as if the temperatures of the two resistances were not really the same. This appeared from the fact that when the flask was warming up after liquefying helium, the constantan resistance reached the temperature of liquid hydrogen before the lead one did. In order to overcome the first difficulty, the potentiometer was abandoned and a very delicate milli-voltmeter substituted. An ammeter was put in series with the lead film resistance. In this way readings would be taken very quickly. The second difficulty was overcome by taking the readings while the flask was being cooled down from liquid hydrogen temperature. The cooling was done very slowly by upsetting the ideal conditions for making liquid helium, for instance, by having the wrong pressure at the expansion nozzle. It was much better to allow the flask to cool down slowly like this for taking the readings than to allow it to heat up slowly by radiation from outside or from the expansion nozzle, as the gas was in circulation all the time and there were therefore no temperature gradients inside the flask to cause the resistances to be at different temperatures. The results obtained were very satisfactory. As the temperature fell the pointer on the millivoltmeter went steadily back until a certain value was reached when suddenly it fell down to zero; by allowing the flask to heat and then by cooling again, this point on the millivoltmeter was crossed several times and the value of the constantan resistance noted each time; the results on the latter resistance always agreed and it corresponded to a temperature of $7^{\circ}5$ K. The late Professor H. K. Onnes found $7^{\circ}2$ K. for the vanishing point of the resistance of the sample of lead turning investigated by him in his special cryostat described in 'Communications from Leiden,' No. 160. The measurements of the lead film are shown in Table I.

Method II. used for Cadmium and Indium.—Another method employed for getting resistances was to roll a rod of the metal into a long strip, then to cut a ribbon of the metal off the side of the strip and wind it on to a glass rod or piece of ebonite. This method was used in the case of cadmium and indium. The method had the disadvantage that only certain metals—namely, those that are malleable—yield to such treatment; and, again, with the large majority of metals, the operation of rolling would so destroy

their crystal structure that their resistance would be altered. It was, therefore, considered necessary to make two resistances of cadmium and "age" one but not the other ; such a precaution was not taken with indium as its melting-point is only 155° C. and the metal rolled very easily.

TABLE I.

CADMIUM—unaged—I.			CADMIUM—aged—I.		
Degrees Kelvin.	Ohms.	Specific Resistance.	Degrees Kelvin.	Ohms.	Specific Resistance.
288	2.703	7.48	293	0.778	7.60
80	0.669	1.81	83	0.192	1.89
20.6	0.068	0.184	20.6	0.0147	0.144
4.2	0.0129	0.035	11.5	15.7×10^{-4}	15.3×10^{-3}
3.8	0.0128	0.035	9.8	9.0	8.8
CADMIUM—aged—II.			9.2	8.5	8.3
Degrees Kelvin.	Ohms.	Specific Resistance.	8.2	6.2	6.1
297	8.71	7.70	4.2	5.2	5.1
81	2.052	1.82	LEAD (film).		
20.6	0.160	0.141	Degrees Kelvin.	Ohms.	Specific Resistance.
4.2	6.2×10^{-3}	5.5×10^{-3}	273	17.93	20.4
3.6	6.1	5.4	82	5.09	5.79
INDIUM.			20.6	0.87	0.99
Degrees Kelvin.	Ohms.	Specific Resistance.	14.4	0.54	0.61
296	0.195	9.10	12.0	0.45	0.51
81	0.046	2.15	10.3	0.40	0.46
20.6	0.012	0.537	7.6	0.35	0.40
4.2	6.9×10^{-3}	0.322	7.5	0.34	0.39
3.38	6.8	0.317	7.4	zero	zero
3.37	zero	zero			

Cadmium.—The strip of cadmium was wound on a piece of pyrex glass; asbestos was used as insulation and the resistance was aged at 200°C . for $3\frac{1}{2}$ hours. The leading-in wires were soldered on. Measurements were made on the aged and on the unaged resistances and the slopes of the curves agreed very well down as far as liquid air, but below that temperature the resistance of the aged cadmium went lower than that of the unaged, until at the temperature of liquid helium the resistance of the unaged was almost seven times that of the aged. There was some doubt at the time that this work was being done as to whether cadmium was superconducting or not, although since then Meissner has definitely shown that it is not. In view of this doubt it was decided to make a much higher resistance and put only a small current through it in measuring the resistance, thus reducing the effect of the magnetic field caused by the flowing current. The resistance was measured in liquid helium with a current of $\cdot 01$ ampere flowing through it, and no diminution of the value was noticed from what it measured with $\cdot 1$ ampere.

By reducing the pressure on the helium the resistance was read down to $3^{\circ}\cdot 6\text{ K}$. but no sign of superconductivity could be observed, and indeed the resistance-temperature curve seemed to be almost parallel to the temperature axis below 8° K . At higher temperatures—between 20° K . and 300° K .—the curve is almost linear and resembles lead in that respect. The residual resistance of cadmium which we obtained agrees well with Meissner's value. By referring to the curve, $\frac{R}{R_0}$ can be calculated and is found equal to

$7\cdot 80 \times 10^{-4}$, while Meissner* gives $7\cdot 60 \times 10^{-4}$ for an "aged" sample of cadmium wire.

Indium.—Although indium did not require to be aged on account of its extreme softness, yet other difficulties in handling it arose. When it was rolled, it spread into such a thin foil that it could hardly be touched without breaking. A ribbon about 2 cm. wide was cut off the edge, laid on a piece of ebonite, and screws passing through four holes in the ebonite at once clamped on four minute copper plates carrying the leads and at the same time held the indium tight against the ebonite. Measurements were made down to the temperature of liquid helium, and then the helium was boiled off under reduced pressure. Improvements had to be made in the pumping system for reducing the pressure

* Meissner, *Zeit. für Phys.* xxxviii, No. 9/10, 1926, p. 647.

before the temperature could be reached at which Professor H. K. Onnes had found indium superconducting, and when these improvements were made we could read temperatures well below 3° K. The pressure at which the resistance of indium vanished was 290 mm. of mercury, which is rather lower than what Professor H. K. Onnes found; this pressure corresponds to a temperature of $3^{\circ}.38$ K. while the pressure given by Onnes corresponds to $3^{\circ}.42$ K. This is a difference of four hundredths of a degree. It is interesting to observe that the resistance-temperature curve for indium is not linear between 20° K. and 300° K. It has a distinct curvature compared with either lead or cadmium, and in this respect resembles the alkali metals.

Method III. used for Sodium and Potassium.—Another method which is practically the same as the one used by Guntz and Bromiewski* was used in the preparation of resistances for metals which, though easily oxidized, yet would distil in vacuo. A fine pyrex glass capillary was drawn out and bent into a U, each arm being about 4 inches long. At either end, the capillary was blown out into a bulb, about 5 mm. in diameter, and into each of these bulbs two tungsten electrodes were sealed. The electrodes projected well into the centre of the bulbs, but did not touch each other. In one of these bulbs a finely drawn-out tube was sealed leading up to a large bulb A, shown in fig. 2. The bulb A was about $2\frac{1}{2}$ cm. in diameter; to this bulb was sealed a tube with a stopcock D and open end E, and also a fine tube leading through a similar bulb B to the bulb C in which the sodium or potassium was placed. The whole apparatus was exhausted by connecting E to a pump, and as soon as a good vacuum was reached the stopcock D was closed and the metal in C was distilled first to B and then to A. The bulbs B and C were then removed. The open end E was then connected to a nitrogen tank with manometer in series; the U-tube and bulb A were immersed in glycerine heated to about 160° C.; the stopcock D was opened, and nitrogen at atmospheric pressure forced the molten metal through the capillary, all oxidation being thus avoided. Finally, the bulb A was fused off.

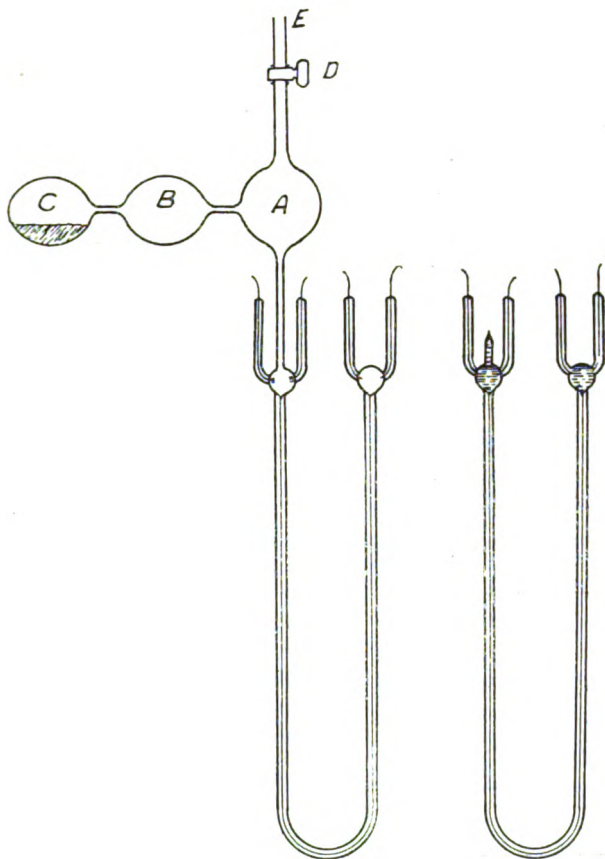
Measurements were made on sodium and potassium down as far as the temperature of liquid hydrogen, and agreed with what other experimenters found.

With regard to the three methods outlined above, it might be remarked that Methods II. and III. are necessarily of

* Guntz and Bromiewski, *Comp. Rend.* 1908, p. 1474.

limited application—one depending on the malleability of the metal and the other on the ability to distil at a low temperature. Method I., which might have been expected to be of more general application, is rather disappointing.

Fig. 2.



Even if the difficulties of the distillation be overcome, the film after it is deposited is liable to be damaged by the contraction of the plate—glass or ebonite—in low temperature work. This trouble was not foreseen when we started making the lead deposit. The results with lead show that the method has possibilities, and when other avenues of attack fail this method might be used.

4. *Investigation of some resistance-temperature curves.*

In addition to repeating the measurements on lead, indium, and cadmium, the resistance-temperature curves of beryllium, chromium, rubidium, thorium, and an alloy of sodium and potassium were investigated. The remainder of this communication will be devoted to describing the work on these metals. The readings for beryllium, chromium, rubidium, and thorium are given in Table II, and those for the sodium-potassium alloy in Table III.

TABLE II.

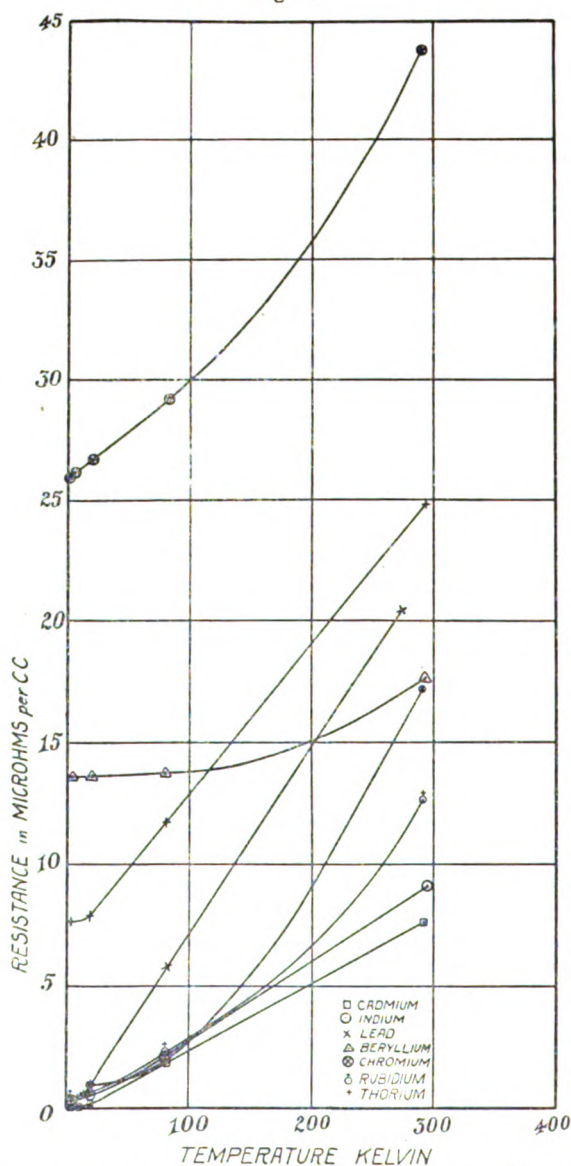
BERYLLIUM.			CHROMIUM—unaged—I.		
Degrees Kelvin.	Ohms.	Specific Resistance.	Degrees Kelvin.	Ohms.	Specific Resistance.
293	8.17×10^{-4}	17.6	290	1.71×10^{-3}	43.8
81	6.39	13.7	83	1.14	29.2
20.6	6.36	13.6	20.6	1.04	26.7
4.2	6.34	13.6	4.2	1.02	26.2
			2.35	1.01	25.9
RUBIDIUM.			CHROMIUM—unaged—II.		
Degrees Kelvin.	Ohms.	Specific Resistance.	Degrees Kelvin.	Ohms.	Specific Resistance.
293	0.735	12.6	290	9.16×10^{-3}	43.8
82	0.134	2.30	83	6.03	28.8
20.6	0.0384	0.658	20.6	5.64	27.0
4.2	0.0208	0.357	4.2	5.58	26.7
2.63	0.0206	0.353	3.01	5.57	26.6
			2.20	5.55	26.5
THORIUM.			CHROMIUM—aged—I.		
Degrees Kelvin.	Ohms.	Specific Resistance.	Degrees Kelvin.	Ohms.	Specific Resistance.
295	1.134	24.83	292	5.59×10^{-3}	17.2
81	0.535	11.72	80	0.655	2.01
20.6	0.357	7.82	20.6	0.260	0.90
4.2	0.348	7.62			
2.93	0.348	7.62			

(i.) *Beryllium*.—The sample of beryllium was obtained from the Beryllium Corporation of America. It would not solder and so clamps had to be used for carrying the terminals. The specific resistance of the sample was taken and found to be 17.6 microhms at 20°C. This indicated that beryllium was a comparatively poor conductor. We also found that its resistance-temperature curve behaved in a rather unexpected manner. Instead of dropping down towards the origin, it remained high, and curved off away from the temperature axis, similar to other metals. The temperature gradient at low temperatures was exceptionally small; in that respect it was comparable with the gradient of cadmium. No sign of superconductivity, when measured in liquid helium under reduced pressure, was detected.

(ii.) *Chromium*.—A sample of chromium was obtained from the General Electric Company of England through the kindness of Mr. C. C. Paterson. This was in the form of a sheet that had been electrolytically deposited. It was very hard and brittle. It was impossible to cut a strip off the side of a sheet with a carborundum saw, owing to the chromium chipping off. Eventually pieces suitable for resistance measurements were obtained by grinding down small pieces of the sheet to strips about $1\frac{1}{2}$ inches long and $\frac{3}{16}$ inch broad. Subsequently strips were successfully obtained by dissolving in acid with the aid of an electrical potential. The sheet chromium was stuck on to a piece of wood with vaseline and painted over the face with vaseline; lines were drawn through the vaseline so as to allow the acid to get into the chromium when the piece of wood was standing in acid. A steel point was made to press against the chromium through the vaseline, and a wire from the positive terminal of the battery led to this point. A second wire from the negative terminal led to a copper plate also standing in the acid. In this way a strip of chromium could be cut off roughly. Its edges could then be ground smooth on a carborundum wheel. In fixing on the leads, solder could not be used as chromium will not solder. The sheet was so brittle that small clamps did not seem desirable. It was decided, therefore, to electroplate small portions at the ends of the chromium strips and then to solder on the leads. The specific resistance measurements were made between steel points.

Chromium presented a problem that appeared to us of great interest. The value given in Smithsonian Tables for the specific resistance of chromium was 2.6 microhms. This indicated that chromium should be an exceptionally good

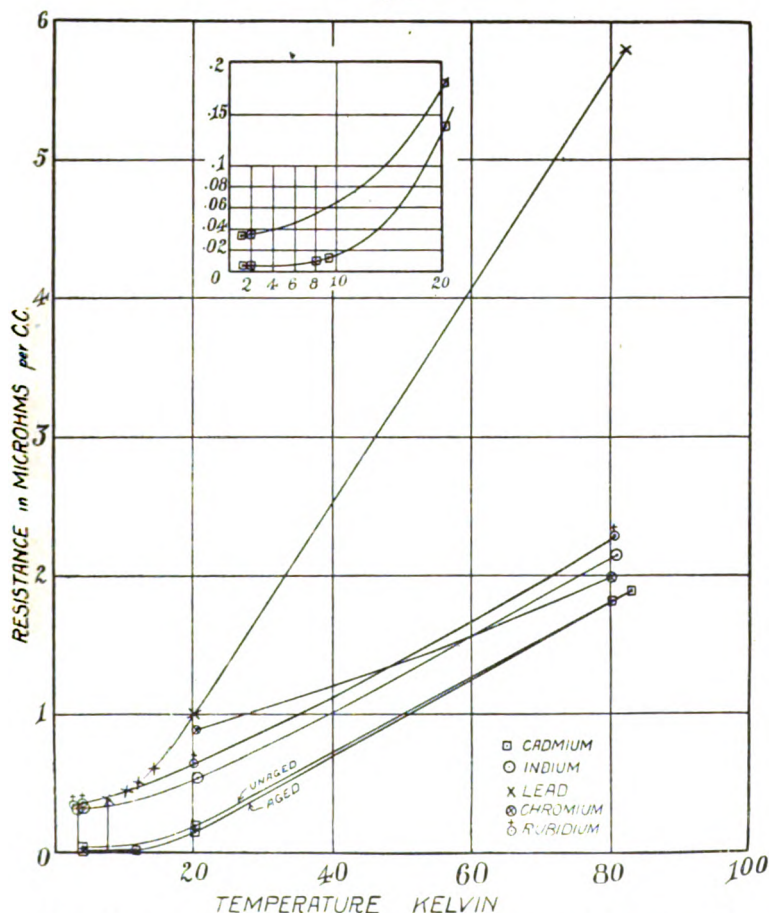
Fig. 3.



conductor, and as recent spectroscopic results showed that chromium should have one electron in the outside system, it appeared as if chromium would behave like an alkali so far as conductivity went. At the start of the work as much

information as possible was collated about this measurement on the specific resistance of chromium. It was done by Shukov, and the abstracts of the original paper (which were in Russian) showed that the work had been done more from a point of view of getting the effect of a nitride of

Fig. 4.



chromium on the resistance. Our value of the specific resistance—which was 44 microhms, and therefore 16 times greater than Shukov's, as a reference to his paper * will show—was possibly due to occluded hydrogen gas in the metal, or to the metal being impure. The metal was tested spectroscopically and found to give only a trace of copper, but the

* *Jurn. Russk. Fizik-Chimichesk. Obschestva*, xlii. pp. 40-41 (1910).

amount was so small that it was not sufficient to account for the high result we obtained. We accordingly decided to heat the chromium to try to drive off the occluded hydrogen gas. This we succeeded in doing.

The furnace in which the chromium was heated consisted of a small quartz tube inside of a coil of nichrome wire. The whole furnace was surrounded by an evacuated glass bulb. The sample was aged for only one hour at the comparatively low temperature thus obtained. It was then taken out and measured for specific resistance at room temperature and also for temperature variation between room temperature and liquid air. The specific resistance was found to be 17.41 microhms and the ratio of the resistance at room temperature to the resistance at liquid air temperature to be 7.3. The strip of chromium was then put back in the furnace and surrounded this time with a tungsten coil and heated for two hours at the much higher temperature thus obtainable. It was taken out and again measured for specific resistance and temperature gradient. This time the specific resistance at room temperature was found to be 17.25 microhms and the ratio of the resistance at room temperature to that at liquid air temperature to be 8.5. The reason for the comparatively high change in the temperature gradient without an appreciable alteration in the specific resistance is not quite understood.

The strip of chromium thus aged was then measured in liquid hydrogen. Unfortunately, owing to trouble with the plant for making the liquid helium, the reading at liquid helium temperature was not obtained; the results down to liquid hydrogen are given, nevertheless, so that the resistance-temperature curves for the aged and unaged strips of chromium may be compared. A glance at the curves shows that to a first approximation the ageing apparently had the effect of moving the whole curve down towards the temperature axis; on closer examination it can be observed that at the temperature of liquid hydrogen the gradient for the aged strip was less than for the unaged. The resistance-temperature curve of chromium has a decided curvature, and in this respect resembles those of the alkali metals and indium; as in the case of other pure metals, the temperature gradient at very low temperatures is small.

(iii.) *Rubidium*.—A U-shaped capillary was filled with the metal exactly as described above in Method III. Although the melting-point of rubidium is $30^{\circ}\text{C}.$, which is above room temperature, yet considerable inconvenience was caused by the thread of metal breaking at low temperatures. The readings for rubidium were taken below $3^{\circ}\text{K}.$; there

was no sign of superconductivity. The resistance-temperature curve showed the distinct curvature found in the curves for the other alkali metals, and the usual small temperature gradient at very low temperatures. The value for the specific resistance was taken from Smithsonian Tables.

(iv.) *Thorium*.—The sample of wire obtained through the kindness of D. Ralph E. Myers, of the Westinghouse Lamp Company, when examined would not solder and so pressure-contacts were employed in measuring the temperature gradient. Readings were taken down to 3° K. The resistance-temperature curve almost obeyed a linear relation right down to liquid hydrogen temperature. At lower temperatures it curved round, having almost a zero gradient at liquid helium temperature. No sign of super-conductivity was observed; the specific resistance was 24·83 microhms at 20° C.; this value as well as the linear form of the resistance-temperature curve pointed to a similarity between lead and thorium.

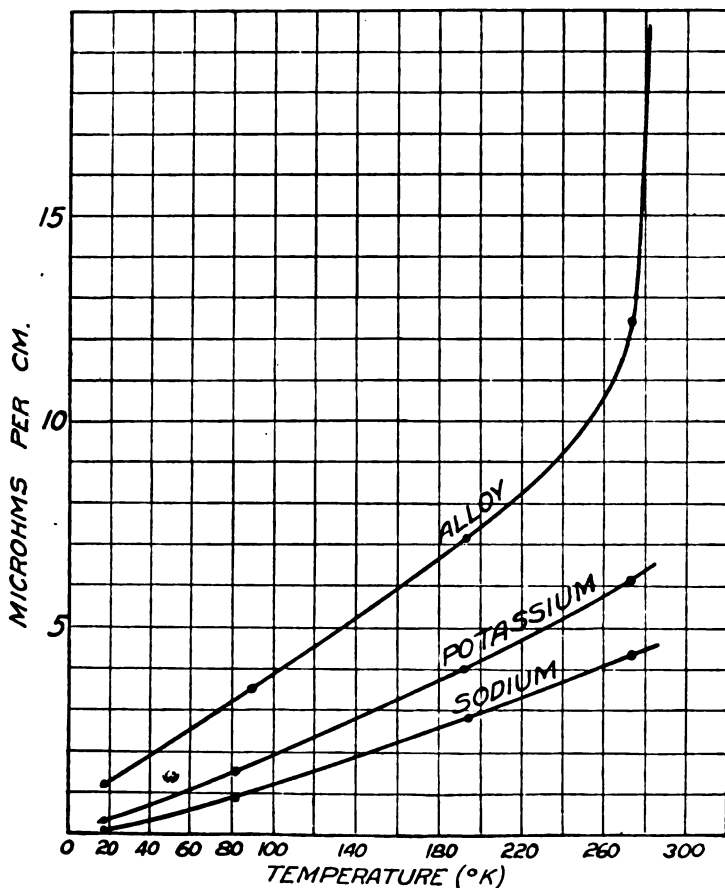
(v.) *Alloy of Sodium and Potassium*.—This work was undertaken to ascertain whether an alloy of sodium and

TABLE III.

SODIUM.			POTASSIUM.		
Degrees Kelvin.	Ohms.	Specific Resistance.	Degrees Kelvin.	Ohms.	Specific Resistance.
273	0·191	4·3	273	0·916	6·1
195	0·127	2·9	191	0·600	4·0
81	0·041	0·91	80	0·240	1·6
20·6	0·004	0·09	20·6	0·045	0·35

ALLOY.		
Degrees Kelvin.	Ohms.	Specific Resistance.
293	3·342	28·6
273	1·481	12·5
192	0·826	7·1
88	0·466	3·6
20·6	0·144	1·2

Fig. 5.



potassium had a resistance curve like that of either of the elements composing it. A U-tube was made as described in Method III. except that it had in addition sealed into the bulb A another distilling-tube to permit sodium as well as potassium to be distilled in, also a small tube to take a little sample of the alloy, and a long capillary to take a measurement of the specific resistance of the alloy. The small sample was used to get the melting-point, which, by reference to the melting-point diagram* for sodium-potassium

* Kurnakow and Puschine, *Zeit. für anorg. Chem.* No. 109, p. 30.

alloys, gave the composition. The results of the experiment are given below. The melting-point of the alloy used indicated an atomic percentage of 55 per cent. potassium and 45 per cent. sodium. This melting-point diagram is of interest in that it suggests that a chemical combination is formed of formula K_2Na .

It can be seen from fig. 5 that the resistance-temperature curve of the alloy obeys a linear relation, very nearly from 20° K. up to its melting-point, while, on the other hand, there is a distinct curvature in the case of the pure metals. A closer study of the curves shows that while at higher temperatures the resistance of the alloy approximates to the sum of the resistances of the pure metals, yet nearer the absolute zero the resistance of the alloy remains high compared with the resistance of either of the pure metals. The observations are in agreement with the theory that at zero degrees absolute the important factor is the phase of the electron in the outermost orbit, while at higher temperatures the thermal agitation eclipses this effect.

5. Summary.

1. The resistance-temperature curves of lead, cadmium, and indium were investigated and the results found confirmed the work of other experimenters.

2. Resistance-temperature curves of samples of beryllium, chromium, rubidium, and thorium were investigated. The results showed that the temperature gradient was small for all pure metals at very low temperatures except for those that were superconducting; and even in the case of the latter the temperature gradient rapidly diminished just before the sudden disappearance of the resistance.

3. The results obtained for chromium showed it to be a fairly poor conductor with a steep temperature gradient at room temperature. The effect of ageing electrolytic chromium was to reduce its specific resistance at room temperature from 44 to 17 microhms; the very high value for the electrolytic chromium was due to occluded gas, and when this was driven off the resistance-temperature curve was moved down towards the temperature axis with very little alteration in its shape.

4. The resistance of rubidium was measured at $2^\circ.63$ K, and no sign of superconductivity was apparent.

5. The resistance-temperature curve of an alloy of sodium and potassium was investigated down to the temperature of liquid hydrogen. It resembled the curves for the pure

metals composing it ; the curve for the alloy indicated a much higher resistance at 0° K. than the residual resistance of either sodium or potassium.

In conclusion we should like to express our indebtedness to Dr. R. Ruedy and Mr. H. S. Wynne-Edwards for examining the chromium spectroscopically and for ageing it in the furnace they were using. The glass-blowing connected with the preparation of the alkali metal resistances was admirably done by Mr. Chappell, glass-blower to the Physics Department of the University of Toronto.

Professor McLennan wishes to take this opportunity of expressing his appreciation of the financial aid given by the National Research Council of Canada and by the Carnegie Corporation, without which this and other low-temperature investigations could not have been undertaken.

The Physical Laboratory,
University of Toronto.
June 29, 1927.

XXXV. *The Effect of Radon on the Solubility of Lead Uranate.*
By KENNETH C. BAILEY, *Sc.D.*, Fellow of Trinity College,
Dublin*.

IN a communication on "Estimates of Geological Time" (Phil. Mag. vol. i. pp. 1055-74, 1926), A. Holmes suggests that the difference existing between the estimates based on the lead-thorium ratio in thorium minerals and those based on the lead-uranium ratio in uranium minerals is due to the fact that, in the latter case, most of the lead produced would probably form lead uranate, which is practically insoluble, while in the former the relatively soluble lead thorate would be formed and partially removed by leaching.

The fact that a compound is insoluble "*in vitro*" does not prove that the same compound will be insoluble when subjected to a radioactive field; and, although the field produced in the case of a uranium mineral is feeble as compared with that available in the laboratory, its action has probably continued over many millions of years—a fact which may well compensate for its lack of intensity. Moreover, such minerals usually contain traces of other compounds,

* Communicated by Prof. J. Joly, D.Sc., F.R.S.

such as chlorides, which might interact with lead uranate under the influence of radiation to form soluble substances.

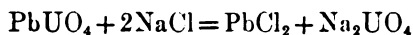
Lead uranate (PbUO_4), whether boiled for some hours with distilled water or left in contact with distilled water for several weeks, remained quite insoluble. The supernatant liquid gave no colour with sodium sulphide, even when evaporated to one-tenth its volume with a few drops of nitric acid, to prevent the deposition of any lead which had gone into solution, and made alkaline before testing. Further, no lead passed into solution when lead uranate was boiled for some hours with a solution of sodium chloride.

Experiments with Radon.

(A) A layer of lead uranate, immersed in a solution of sodium chloride, was subjected to the action of about 160 mcs. of radon until the degradation of the latter to Ra D was approximately complete. The conditions were not very favourable, as the gaseous radon in the upper part of the vessel was separated from the solid lead uranate by a layer of water several cms. thick. α -particles could therefore only reach the lead uranate from the dissolved radon immediately in contact with it.

The solution did not darken on addition of sodium sulphide, but when a portion of it was evaporated to about one-tenth its volume, it gave a dark colour and eventually a slight precipitate with sodium sulphide. A very small amount of lead had evidently been brought into solution.

(B) In order to improve the efficiency of radiation, finely powdered lead uranate was sprinkled over the interior of a glass separating funnel fitted with a ground-glass stopper, and moistened with a strong solution of sodium chloride. The funnel was exhausted, and 120 mcs. of radon admitted and left till degraded to Ra D. The contents were then washed out with distilled water and tested for lead (as before) and for uranium (yellow colour produced by the addition of hydrogen peroxide and sodium hydroxide to the lead-free solution). Both tests were strongly positive, and colorimetric estimation indicated that 0.011 gm. of lead and 0.013 gm. of uranium had gone into solution. The weight of uranium corresponding to 0.011 gm. of lead in the molecule PbUO_4 is 0.0127 gm. This suggests that the reaction



has been promoted by the action of radon, the products on the right-hand side going into solution.

406 *Effect of Rondon on the Solubility of Lead Uranate.*

(C) An experiment was performed under similar conditions to (B) in which the lead uranate was moistened with distilled water, no sodium chloride being added. 115 mcs. of radon were employed.

0.0043 gm. of lead went into solution, but no uranium could be detected in solution. The evidence was not sufficient to indicate the form in which the lead became soluble.

(D) In order to determine whether the entire action is due to α -radiation, lead uranate in contact with sodium chloride solution was subjected for about four months to β - and γ -radiation by placing it about an inch from a glass flask containing radium bromide in solution. A trace of lead, detected only after evaporation of the solution to one-fifth its bulk, went into solution. This experiment made it clear that almost, though not quite, all the reaction produced in (B) was due to α -particles.

A blank experiment with the vessel used in A, B, and C showed that no lead is brought into solution by the action of radiation on the glass.

Calculations of the chemical action due to each α -particle were made on the results of (B) and (C). Such calculations can only be approximate, the most uncertain factor being the fraction of the glass surface actually covered in each experiment with lead uranate.

The number of α -particles per 1000 mcs. per second was taken as 3.5×10^{10} , the average life as 5.55 days, and the mass of the atom of hydrogen (from which the mass of the atom of lead was calculated) as 1.66×10^{-24} gm. An error is introduced by the assumption that the entire action is due to α -particles; but the error has been shown to be small.

Assuming that one-quarter of the glass surface was covered in (B) and one-half in (C) (visual estimation), we find that in (B) each α -particle caused the reaction and entry into solution of about 21,300 molecules of lead uranate, while in (C) each α -particle brought into solution about 4300 atoms of lead.

It is clear, as a result of these experiments, that the lead-uranium ratio in a uranium mineral is likely to be considerably affected by the entering into solution of both lead and uranium under the influence of the radioactive field due to the mineral itself. If we assume that a lead uranate is formed and, under the influence of strong ionization, is brought into solution and removed, then equal numbers of atoms of uranium and lead will disappear; and, as this involves a larger percentage-reduction of the lead than of the uranium present, it follows that estimates of geological time based upon

the lead-uranium ratio will err on the side of insufficiency. If the conditions approximate more closely to those of experiment C than to those of experiment B, the percentage-reduction of lead as compared with that of uranium will be still greater.

The foregoing results show that the "*in vitro*" insolubility of lead uranate cannot be regarded as applying to this compound when associated with the parent substances. If there is leaching at all, we must face the probability that removal of lead has taken place, and at a rate fast compared with the rate of its genesis. Again, where age-long time-periods are involved, it seems doubtful if any differential removal of thorium-lead as compared with uranium-lead can be safely assumed, the time-periods required for the removal of lead in both cases being probably insignificant as compared with the period required for its formation.

I desire to express my thanks to Professor Joly, F.R.S., who suggested this subject for research; to Professor E. A. Werner, Sc.D., for the sample of lead uranate employed; and to Dr. H. H. Poole, Chief Scientific Officer of the Royal Dublin Society, for the radon used in these experiments.

University Chemical Laboratory,
Trinity College, Dublin.

XXXVI. *Some New Regularities in Atomic Spectra.* By
Professor J. C. McLENNAN, F.R.S., and A. B. McLAY,
*Ph.D.**

I. Introduction.

INVESTIGATIONS by the authors and others on the arc spectra of many of the elements in each of the five short periods of six, *i. e.* B to Ne, Al to Ar, etc., have shown that the outermost electrons of each neutral atom in its normal state occupy equivalent n_2 orbits, where $n = 2, 3, \dots$ and 6 respectively for the 1st, 2nd, ... and 5th periods. There are respectively one, two, ... six outermost electrons in the atoms of the elements of each of the B, C, ... Ne groups. For the most easily excited of the higher energy states one of the outermost electrons is displaced to an $(n + 1)_1$ orbit, the rest remaining in their original n_2 orbits.

The configuration of the outermost electrons of the

* Communicated by the Authors.

neutral atoms under consideration when in the above-mentioned states is given in Table I. in the rows A and B respectively. Together with them the spectral terms are given that should characterize each state. In the table the theoretically deepest term is at the left, and the order of the components of any multiple term is indicated by the order of the term subscripts, the left one representing the deepest component.

TABLE I.

Atomic No.	Atoms.	Electron Configuration.		Terms.
			$n_2, (n+1)_1$	
N*	B, Al Ga	A	1 —	2S_1
		B	— 1	$^2P_{12}$
N+1	C, Si Pb	A	2 —	$^3P_{212} \quad ^1D_2 \quad ^1S_0$
		B	1 1	$^3P_{012} \quad ^1P_1$
N+2	N, P Bi	A	3 —	$^4S_2 \quad ^2D_{23} \quad ^2P_{12}$
		B	2 1	$^4P_{123} \quad ^2P_{12} \quad ^2D_{23} \quad ^2S_1$
N+3	O, S Po	A	4 —	$^3P_{210} \quad ^1D_2 \quad ^1S_0$
		B	3 1	$^5S_2 \quad ^3S_1 \quad ^3D_{123} \quad ^1D_2 \quad ^3P_{012} \quad ^1P_1$
N+4	F, Cl At	A	5 —	$^2P_{21}$
		B	4 1	$^4P_{321} \quad ^2P_{21} \quad ^2D_{32} \quad ^2S_1$
N+5	Ne, Ar Xe	A	6 —	1S_0
		B	5 1	$^5P_{210} \quad ^1P_1$

* N=5, 13, 31, 49, and 81 for atoms in the 1st, 2nd 5th short periods respectively.

By an electronic transition resulting in a change of configuration from that given in row B to that in row A in Table I., resonance wave-lengths of the arc spectrum are emitted. The most fundamental resonance line or most easily excited wave-length should be that involving the underlined terms in each spectrum, and hereafter we shall refer to this line only as the resonance line. In nearly all

the arc spectra that are being considered here the resonance line has been identified and shown to be classified by means of the terms underlined in Table I.

While considering the relations between the resonance lines in the various arc spectra the writers observed a well-defined periodicity in the progression of frequency with atomic number in each period, and also a similarity in the periodicities of each of the periods.

We consider that these regularities are well worth pointing out, not only from the standpoint of a practical application of the results to spectral analysis, but also on account of a suggestion their discovery raises of a new problem that should be of considerable interest to theoretical physicists.

II. Results.

The frequency, wherever it has been identified, of the resonance line in each of the arc spectra of the elements that are being considered is given in Table II. In this table the transition, which is the same in all atoms of the same period, of the most loosely-bound electron that results in the emission of the resonance wave-length is indicated, as well as the term classification, which is similar for arc spectra of all atoms of the same chemical group. The values in the arc spectra of the halogen atoms are not those of the resonance line ${}^2P_3 - {}^4P_3$, predicted in Table I. as this has not yet been identified. While the frequency for FI has been classified definitely as ${}^2P_3 - {}^2\bar{P}_3$, those for Cl I, Br I, and I I are uncertain and may be either ${}^2P_3 - {}^2\bar{P}_3$ or ${}^2P_3 - {}^4\bar{P}_3$. The term ${}^4\bar{P}_3$, however, should be a little deeper than either ${}^2\bar{P}_3$ or 4P_3 , so that the frequency values contained in Table II. are probably a little greater than that of the resonance line. Since the arc spectra of Po, Nt, and of the element of atomic number 85 have not yet been analysed, no values are available for the lines required in any of them.

An authority for the value and term classification of each frequency in Table II. is cited in the list of references at the conclusion of the paper.

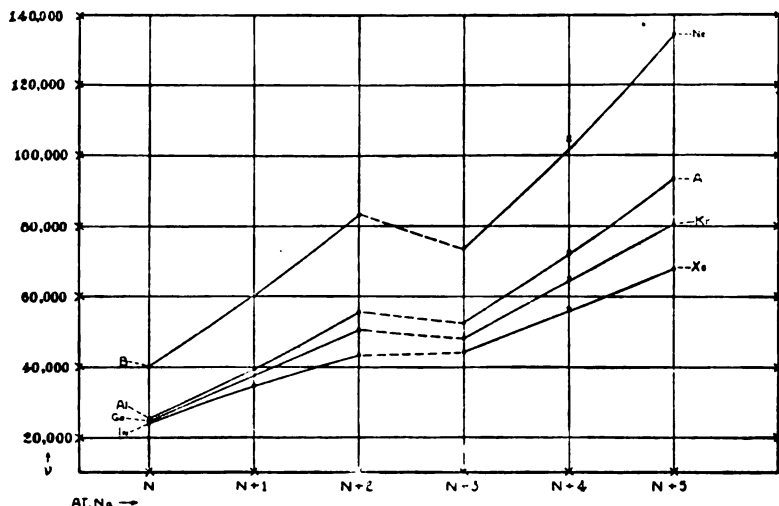
The arrangement of values in Table II. shows the progression of frequency with atomic number in each period, and also shows that it is qualitatively similar in at least each of the first four periods. The results are perhaps more clearly illustrated in fig. 1, where the frequencies, given in Table I., are

TABLE II.

Electron Transition		$3\uparrow \rightarrow 2\downarrow$		$4\downarrow \rightarrow 3\downarrow 2\downarrow$		$5\uparrow \rightarrow 4\downarrow 2\downarrow$		$6\uparrow \rightarrow 5\downarrow 2\downarrow$		$7\uparrow \rightarrow 6\downarrow 2\downarrow$	
Term Class ⁿ .		El ^t .	ν .	El ^t .	ν .	El ^t .	ν .	El ^t .	ν .	El ^t .	ν .
$^2P_1 - ^3S_1$	ν_1 Δr_{21}	B	40,040 20,375	Al	25,348 14,258	Gd	21,788 12,914	In	24,373 10,541	Tl	26,478 8,808
$^3P_0 - ^3P_1$	ν_2 Δr_{32}	C	60,315 22,971	Si	39,606 16,338	Ge	37,702 12,942	Sn	34,914 8,335	Pb	35,287 -2,699
$^4S_2 - ^4P_1$	ν_3 Δr_{43}	N	83,226 -9,526	P	55,944 -3,325	As	50,694 -2,507	Sb	43,249 1,004	Bi	32,588
$^3P_2 - ^5S_2$	ν_4 Δr_{54}	O	73,760 30,976	S	52,619 19,865	Se	48,187 16,715	Te	44,253 11,836	Po	—
$^2P_2 - ^2P_2$ or 4P_2	ν_5 Δr_{65}	F	104,736 29,763	Cl	72,484 21,254	Br	64,902 16,017	I	56,089 11,561	—	—
$^1S_0 - ^3P_1$	ν_6	Ne	134,499	Ar	93,738	Kr	80,919	Xe	63,050	Nt	—

plotted against atomic number and a curve obtained for each period. As we have pointed out, the values for the halogen atoms are a little higher than those needed. Therefore, the curves have not been drawn through the plotted points designated by \times but a little below each one.

Fig. 1.



III. Discussion of Results.

It is immediately evident either from a consideration of the progression of frequencies in Table II. or the curves in fig. 1, that for any of the first four periods

$$\Delta\nu_{21} \div \Delta\nu_{22} < \Delta\nu_{54} \div \Delta\nu_{65},$$

and that there is a discontinuity in the regular progression due to the negative or small positive value of $\Delta\nu_{43}$.

Now the resonance frequencies of the arc spectra of elements of the short periods of atomic numbers N to $N+5$ should be a measure of the relative strength of binding of an outermost electron in an n_2 orbit when one ... six of these orbits are occupied with the atom neutral and in the normal state.

If all equivalent n_2 orbits in an atom were similar then the curves in fig. 1 would be expected to be continuous ones. But in each curve there is a well-defined discontinuity. This discontinuity probably has a close relationship to another well-known feature in the arc spectra of these

elements, namely, that for deep-lying multiple terms of the arc spectra of the elements of atomic numbers N to $N + 2$ the components are in the normal order, while for elements with atomic numbers $N + 3$ to $N + 5$ they are inverted.

It seems probable that both the features mentioned above are due to the fact that n_2 orbits are of two types, that have been designated n_{21} and n_{22} orbits characterized by the inner quantum numbers $j = \frac{1}{2}$ and $j = \frac{3}{2}$ respectively; and that in a neutral atom of atomic number N , $N + 1$, or $N + 2$ the n_{21} orbits are more stable, while in one of atomic number $N + 3$, $N + 4$, or $N + 5$ the n_{22} orbits are more stable. Whether or not the two discontinuities mentioned, that occur between the third and fourth elements of each short period of six, indicate that the maximum number of electrons that can occupy orbits of the n_{21} and n_{22} types is three and three respectively, as against the numbers two and four proposed by Stoner, we are not at present able to say.

IV. Conclusion.

In the preceding sections the relative strength of binding of an outermost electron in an n_2 orbit in neutral atoms that have one ... six equivalent n_2 orbits occupied, has been determined by a consideration of the resonance lines of the arc spectra of a number of elements.

The strength of binding of an outermost n_1 electron when there are one or two of these in an atom has, of course, long been recognized, the latter being more tightly bound than the former.

It would be interesting to determine the binding of equivalent n_3 electrons in ionized atoms and of equivalent n_3 or n_4 electrons in either neutral or ionized atoms, but there are not sufficient data to make this possible at the present time. It is to be hoped that this deficiency will be made up shortly and that further observations of a similar nature to those outlined in the preceding sections will help to throw some further light on the significance of the present results.

References.

- | | |
|--|--------------------|
| | <i>Elements.</i> |
| 1. Fowler, 'Series Spectra,' 1922. | B, Al, Ga, In, Tl. |
| 2. Bowen, Phys. Rev. xxix. 2, p. 231 (1927). | B, C, F. |
| 3. McLennan and McLay, Trans. Roy. Soc. Can. xx. iii. p. 355 (1927). | C, Ge. |
| 4. McLennan and Shaver, Trans. Roy. Soc. Can. xviii. iii. p. 1 (1924). | Si. |

References.

- | | |
|--|------------------|
| | <i>Elements.</i> |
| 5. McLennan and McLay, Trans. Roy. Soc. Can. Sn.
xviii. iii. p. 57 (1924).
Sur, Phil. Mag. iii. 16, p. 736 (1927). | |
| 6. Gieseler and Grotrian, <i>Zeits. f. Phys.</i> xxxix. 5/6, Pb.
p. 77 (1926). | |
| 7. Hopfield, Phys. Rev. xxvii. 6, p. 801 (1926). | N. |
| 8. McLennan and McLay, Trans. Roy. Soc. Can. N, P, As, Sb, Bi.
1927 (in press). | |
| 9. Hopfield, Astr. Jl. lix. p. 114 (1924); 'Nature,' O, S.
cxii. p. 437 (1923).
Laporte, <i>Naturwiss.</i> xii. p. 598 (1924). | |
| 10. McLennan, McLeod, and McLay, Trans. Roy. Soc. Can. Se, Te.
1927 (in press). | |
| 11. Turner, Phys. Rev. xxvii. 4, p. 397 (1926). | Cl, Br, I. |
| 12. Hertz, <i>Naturwiss.</i> xiv. 27, p. 648 (1926). | Ne, Ar, Kr, Xe |
- The Physical Laboratory,
University of Toronto,
June 30th, 1927.

XXXVII. Notices respecting New Books.

Stars and Atoms. By A. S. EDDINGTON, M.A., D.Sc., LL.D.,
F.R.S. Pp. 127 with 11 figures. (Oxford: Clarendon Press,
1927. Price 7s. 6d. net.)

THIS volume contains the substance of three lectures delivered in King's College, London, in 1926, and of an Evening Discourse at the meeting of the British Association in the same year. It deals largely with the author's researches on the internal constitution of the stars, and will serve as a fitting introduction to his larger book, 'The Internal Condition of the Stars,' in which the subject is treated mathematically.

The volume is divided into three lectures, entitled respectively The Interior of a Star; Some Recent Investigations; The Age of the Stars. The basic idea throughout is the interdependence of atomic physics and stellar physics. The progress in our understanding of the conditions which prevail inside a star is dependent upon advances in our knowledge of atoms and radiation. Reciprocally, the clearer understanding which has been thus gained of the conditions in the stars, where matter is under extreme conditions which cannot be duplicated in the laboratory, has contributed in no small measure to the progress of atomic physics.

Professor Eddington's unique power of clear exposition is well known. In this volume he succeeds in conveying to the non-mathematical reader a clear idea as to how mathematical treatment can lead to conclusions about the deep interior of a star, where neither the eye nor the telescope can penetrate. His detective stories, "The Missing Word and the False Clue" and "The

Nonsensical Message," read like real romances, and serve to bring home to the reader some of the difficulties encountered by the way.

The number of really well-written popular books of science is very small. We have no hesitation in classing this volume amongst the best of them. Prof. Eddington writes with an excellent style, and the compelling force of his reasoning, aided by simple illustrations and analogies, renders the volume easy and fascinating to read. Once it is taken up, it will be found difficult to lay it aside before the end is reached.

It is not every scientific worker who has the gift of writing an account in popular language of his own investigations. Professor Eddington has that gift, and we are glad that he has found time to make some of his results available in a book which can be read by a wider circle of readers than his mathematical treatise on the same subject.

Applied X-Rays. By GEORGE L. CLARK, Ph.D. (McGraw-Hill Publishing Co. 255 pp., 99 figs. Price 20s. net.)

MR. CLARK, who writes from the Massachusetts Institute of Technology at Boston, has compressed an extremely large amount of information into his book, and has succeeded in presenting it in logical and attractive fashion. The first two sections of the volume deal, here and there perhaps a little cursorily, with the means of generating X-rays, the measurement of intensity, the absorption and scattering of X-rays, the fundamentals of X-ray spectroscopy, and the protection of the X-ray worker. The chemical and biological effects of X-rays and their radiographic applications, both industrial and medical, are dismissed in two short chapters.

The third and largest section, covering some 150 pages, is devoted to the applications of X-ray crystal analysis. The literature of this subject is now very large, and is growing rapidly, but Mr. Clark makes an enthusiastic and praiseworthy attempt to summarize the situation to date. It is premature to generalize too freely, the technique is still being developed, and the potentialities and limitations of the method are gradually being revealed; but the list of achievements is already sufficiently impressive to warrant high expectations for the future of X-ray spectroscopy in many walks of industry. At the moment, metallurgy would perhaps appear to offer the greatest scope for the X-ray spectroscopist, the physical and chemical properties of many metals and alloys providing tempting and doubtless tantalizing problems.

While this country has every reason to be well satisfied with its contributions to the fundamentals of X-ray crystal analysis, it would not appear from Mr. Clark's book that a like attention has been paid to the industrial applications. Matters are evidently very different both in the States and Germany; but there are grounds for hope that in the near future the situation will rectify itself on this side of the water.

The Calculus of Variations. By A. R. FORSYTH. (Cambridge University Press. Price 50s. net.)

WE have at last before us a work which every physicist whose work has dealt in any way with the Principle of Least Action, and certainly every mathematician, like the present writer, who has been called upon to teach this subject, has longed for. The Calculus of Variations has always consisted, in any possible presentation, of a series of fragmentary investigations aimed at the solution of specific historical problems—for example, the brachistochrone, the solid of least resistance, and so forth. The limitations of validity of these solutions have never been clear. The usual course has been to make a final appeal to Todhunter's History of the Calculus of Variations, which deals with all the more classical problems which invoke this mode of procedure, but with all the limitations of validity pertaining to that time. We consider that, by welding the whole subject together in this volume, as a connected account, Prof. Forsyth has probably done greater service to the mathematician and physicist than he even did in his treatises on the theory of Differential Equations and on Differential Geometry.

Much of the work in this book has hitherto been entirely inaccessible. Some of the most fundamental, really defining the limitations—"grave," as the author repeatedly states,—on some of the solutions commonly accepted, including even the Principle of Least Action—have existed only in manuscript form, as notes of lectures by Weierstrass, who made vast improvements on all the work preceding him. The author has had access to many such sources, and has now really created a new branch of mathematics of a self-contained type. Teachers of mathematics in the Universities will now, for the first time, be able to point the Calculus of Variations out to a pupil as a subject in which further progress is possible in many indicated directions. The book should be a valuable stimulus to many who wish to take up post-graduate research work.

The treatment is exhaustive. We miss nothing with which we were previously familiar, but we always find ourselves able to learn something from the manner in which it is presented. The general format of the book is in the best traditions of the Cambridge University Press.

Differential Geometry of Three Dimensions. By C. E. WEATHERBURN. (Cambridge University Press. Price 12s.)

THE present volume provides an introductory treatise on Differential Geometry, and shows how vector methods may be employed with great advantage. The author is evidently indebted to Forsyth and Eisenhart as well as to the Continental Geometers. But there is a real need for a volume of this sort. It will be found very suitable for first year University students, and a large number of examples are introduced into the work.

The early chapters deal with curvature and torsion, envelopes, developable surfaces, and curvilinear co-ordinates.

Geodesics on Quadric surfaces are next dealt with; and finally, after a discussion of conformal and spherical representations and other cognate topics, the author concludes with a chapter entitled "Further Recent Advances." In this concluding chapter the author gave an account of several important additions to our knowledge of the properties of families of curves and surfaces which he has most recently made. When the book was nearly completed, and the author had decided to avoid introducing the so-called "Beltrami's" differential parameters, in spite of their importance in many directions, he discovered that they were, in fact, individual members of a large family whose significance had hitherto been missed. Accordingly, several of the later sections were re-written, and contain work which cannot be found elsewhere. The value of the book is considerably enhanced; and though the author does not promise this, it may be hoped that further developments in this promising direction may take place and ultimately lead to a supplementary volume. The work can be recommended with confidence to a student with a liking for vectorial notation and treatment who wishes to obtain a thorough knowledge of Modern Differential Geometry.

Three Lectures on Atomic Physics. By A. SOMMERFELD. (Translated by H. L. Brose.) (Methuen & Co. Price 2s. 6d.)

THE present book comprises lectures given in the University of London dealing with the recent developments of the Quantum Theory. In the first Quantum numbers n , k , l , m , etc. are introduced, and a new interpretation of the Hydrogen Spectrum is given. The next lecture deals with the general construction of terms of any Multiplicity, with the definition of primed and unprimed terms and their selection rules, and with Pauli's principles of uniqueness. Finally, the periodic system of the elements is dealt with and also the tetrahedral crystal structure of certain elements of the fourth group.

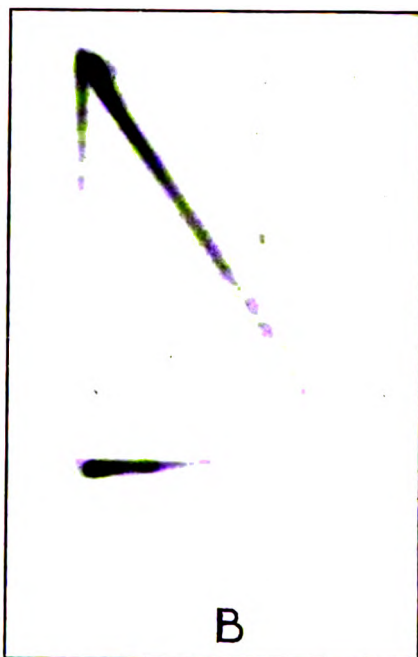
It will be a great advantage to students of Modern Physics to have this little book in its translated form. The lectures were originally given in London, though Prof. Sommerfeld also gave similar lectures elsewhere. As a compendium of current views on the exact position of the Quantum Theory in the mind of one of its most vigorous exponents, they have no parallel. Mr. Brose, the translator, is to be congratulated on the reproduction, in his translation, of the very attractive style which, in a verbal form, delighted those who had the good fortune to hear Prof. Sommerfeld during his visit to England.

[*The Editors do not hold themselves responsible for the views expressed by their correspondents.*]



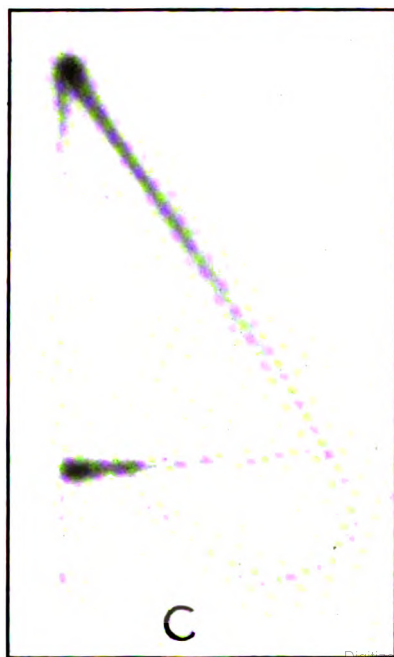
FORK SOUNDING.

Frequency of flashing increased.

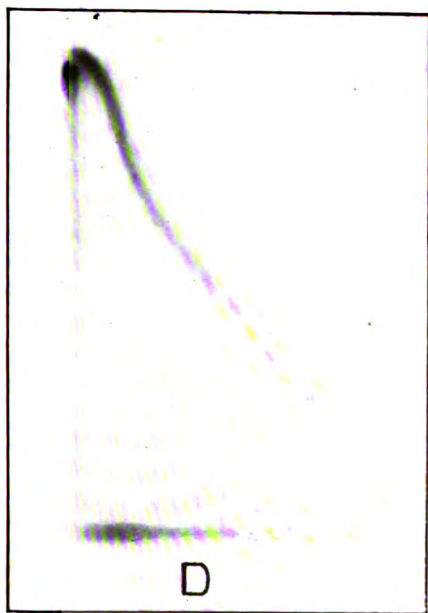


FORK SOUNDING.

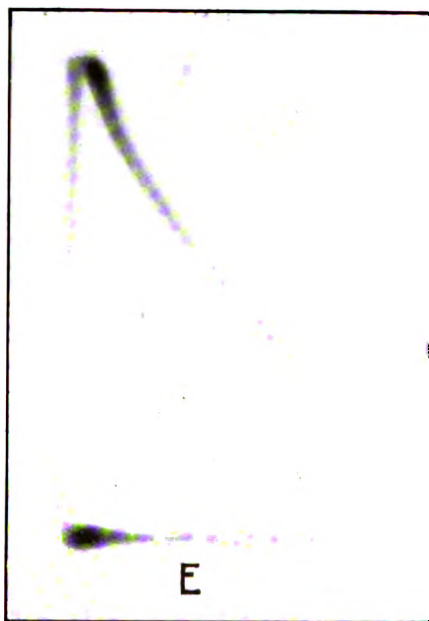
Frequency of flashing affected very little.



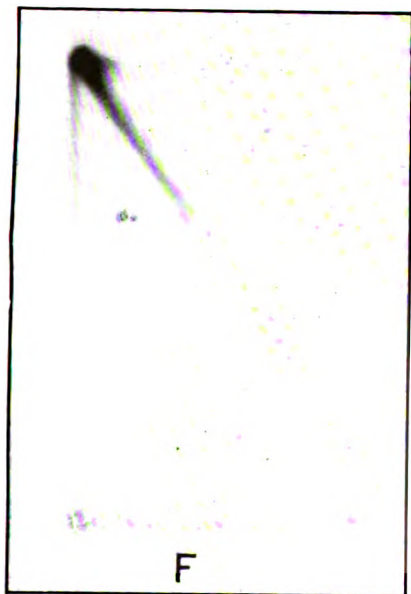
FORK HELD.



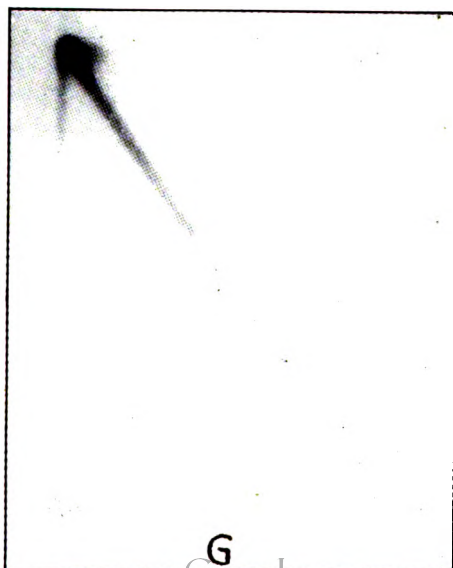
FORK SOUNDING.
Frequency of flashing increased.



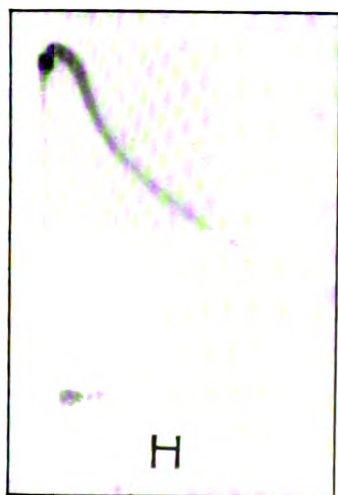
FORK SOUNDING.
Frequency of flashing affected very little



FORK HELD.



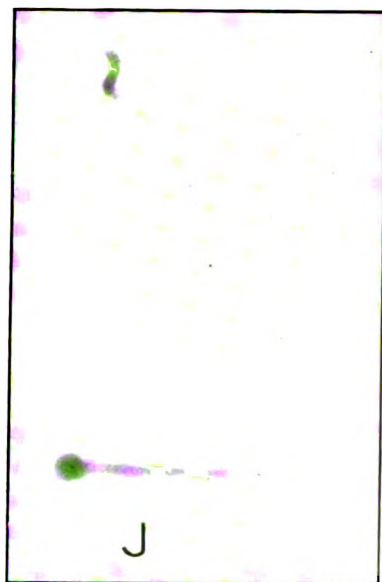
INDUCTANCE REMOVED FROM CIRCUIT.



I-type lamp.

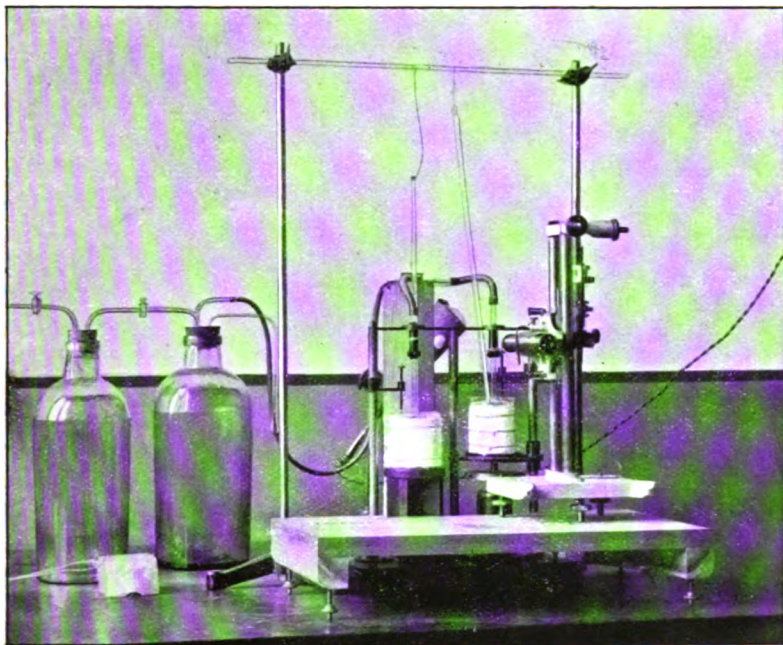
FORK SOUNDING.

Frequency of flashing increased.



FORK SOUNDING.

Frequency of flashing one-half the frequency of the Fork.



THE SURFACE-TENSION BALANCE.

THE
LONDON, EDINBURGH, AND DUBLIN
PHILOSOPHICAL MAGAZINE
AND
JOURNAL OF SCIENCE.

[SEVENTH SERIES.]

SEPTEMBER, 1927.

XXXVIII. *The Physical and Biological Effects of High-frequency Sound-waves of Great Intensity.* By Prof. R. W. WOOD, *For. Mem. R. S.*, and ALFRED L. LOOMIS*. (Communication No. 1 from the Alfred Lee Loomis Laboratory, Tuxedo, N.Y.)

[Plates VII.—XIII.]

Introduction.

IN the present paper we shall give an account of a preliminary survey of what appears to be a wide field for investigation, opened up by the study of the very surprising and remarkable effects obtained with sound-waves of high frequency and great intensity generated in an oil-bath by a piezo-electric oscillator of quartz operated at 50,000 volts and vibrating 300,000 times per second.

The radiation pressure exerted against a glass disk 8 cm. in diameter amounts, under certain circumstances, to 150 grams, and when operating against the free surface of the oil (from which the radiation is totally reflected) raises it in a mound 7 cm. in height, surmounted by a fountain of oil drops, some of which are projected to an elevation of 30 or 40 cm.

The waves can be transmitted along a glass thread 0.2 mm. in diameter and a metre or more in length, and the end of the thread, if squeezed between the thumb and finger, burns a groove in the skin. A tapering glass rod, 0.5 mm. in diameter at the tip, can be thrown into vibration of such

* Communicated by the Authors.

ntensity that a pine chip smokes and emits sparks when pressed against the tip, the rod burning its way rapidly through the wood, leaving a hole with blackened edges. If a glass plate is substituted for the chip, the rod drills its way through the plate, throwing out the displaced material in the form of a fine powder or minute fused globules of glass.

If the waves are passed across the boundary separating two liquids such as oil and water or mercury and water, more or less stable emulsions are formed. Chemical reactions are accelerated, crystallizations started, and other remarkable effects produced by these very intense super-sonic vibrations.

Preliminary experiments with interference fringes formed between a vibrating plate and one at rest indicate that the amplitude of the vibration is of the order of magnitude of a wave-length of light, yet an enormous amount of energy is delivered. The mean energy and acceleration are both proportional to the square of the frequency, and we are here dealing with what Prof. C. V. Boys very tersely describes as "*All acceleration and no motion.*"

The method employed in the generation of the waves is essentially the one developed by Professor Langevin in 1917 for the purpose of locating submarines by the echo of a narrow beam of high-frequency sound-waves. Shortly thereafter experiments along similar lines were inaugurated by the British and American navies.

In Langevin's original apparatus the vibrations of the piezo-electric quartz plate were excited by a Poulsen arc in connexion with suitable condensers and coils. Voltages as high as thirty or forty thousand were applied to the plates, and the amplitude of the waves raised to such a degree that small fish were killed by the radiation and pain of considerable severity was experienced when the hand was thrust into the water in the tank. The Poulsen arc proved troublesome, however, owing to its instability, which made it impossible to keep the electrical vibration in tune with the natural frequency of the quartz plate, and it was speedily supplanted by the vacuum tube, which is used exclusively at the present time.

Since the coefficient of viscosity increases with the square of the frequency, comparatively low frequencies only can be employed when beams of sound are to be projected under water over long distances for signalling or other purposes. Voltages of one or two thousand at frequencies of from 30 to 40 thousand are used for the most part in work of this nature.

In our experiments this limitation is not imposed, since

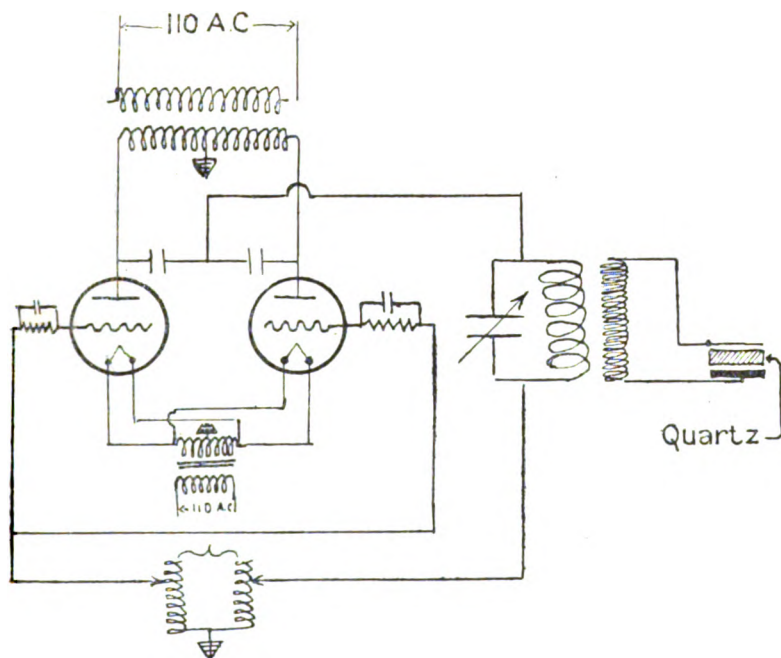
absorption of the radiation by the medium does not interfere to any great degree with the study of effects close to the source, and we operate usually with voltages in the vicinity of 50,000 at frequencies ranging from 200,000 to 500,000.

Description of the Apparatus.

(See Plate VII. fig. 1.)

The apparatus employed in the present work was built in the Research Laboratory of the General Electric Co. at

Fig. 1.



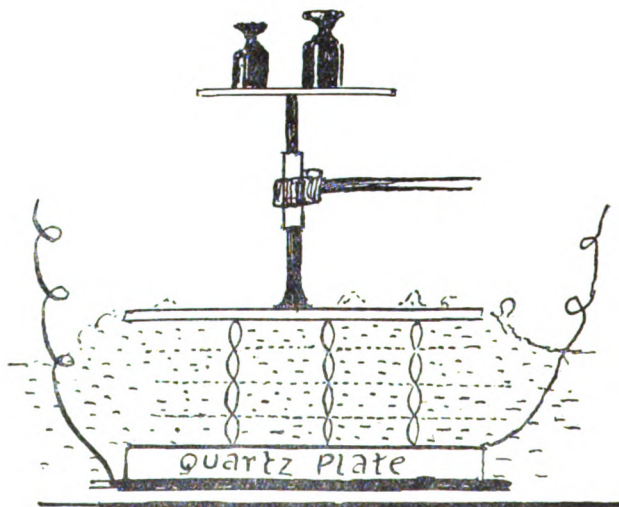
Schenectady. It consists of a two kilowatt oscillator, designed originally for an induction furnace, a bank of oil condensers, giving capacities up to 0.1 microfarad, a large variable air condenser, and several pairs of coaxial coils for raising the voltage. The primary or outer coil consisted of from 7 to 20 turns of Litzendraht cable, the coils varying from 16 to 24 cm. in diameter. The secondary coils were wound on glass cylinders (100 to 250 turns) and mounted within the primaries. Fig. 1 shows in conventional manner the wiring of the various parts. The use of several coils was

found to be necessary as we employed quartz plates varying in thickness from 7 to 14 mm., with which we obtained waves with frequencies ranging from 100,000 to 700,000 cycles per second. The quartz plates were circular disks, and when in operation, one of them rested on a disk of sheet lead at the bottom of a dish of transformer oil. The other electrode consisted of a disk of very thin sheet brass resting on the upper surface of the quartz. The coils for raising the potential and the glass dish with oil, in which the quartz oscillator is immersed, are shown on Plate VIII.

Pressure due to the Radiation.

We have already mentioned the pressure developed against the free surface of the oil above the quartz vibrator as a result

Fig. 2.



of the reflexion of the radiation. In the case of reflexion from plates of glass or metal the magnitude of the effect can be measured. We found that a glass disk 8 cm. in diameter attached to a glass rod and supported as shown in fig. 2 would support a weight of 150 grams. The pressure is a maximum when the distance between the under surface of the plate and the upper surface of the quartz oscillator is a whole number of half wave-lengths. Under this condition the reflected wave strikes the oscillator when its phase is such as to reflect the wave back to the plate. The energy is thus imprisoned

by multiple reflexions between the vibrator and the plate, and the amplitude rises to a very high value, for the same reason that the amplitude of vibration of the stationary waves on a thread attached to a vibrating tuning-fork may be twenty or thirty times the amplitude of the fork when the length of the thread is properly adjusted.

If the rod which supports the glass plate is held in the fingers and the plate pushed down gradually into the oil a strong resistance is encountered periodically, as if the plate were breaking its way through a series of resisting films. In the positions of maximum pressure the energy is reflected back and forth between the oscillator and plate. In the positions of minimum pressure the wave reflected down from the plate meets the oscillator when it is in such a phase as to transmit the reflected wave. That such is the case was shown by the following experiment.

The quartz oscillator was mounted vertically in a large oil bath and a metal vane hung by a bifilar suspension at a short distance to one side of it. With the oscillator functioning, this vane was deflected to one side by the pressure of the radiation. If now a glass plate was immersed in the oil on the opposite side of the oscillator, the deflexion of the vane increased periodically as the glass plate was moved towards the oscillator, *i. e.* it swung back and forth.

This shows us that, to get the maximum amount of energy from the oil into a bath of some other liquid (or into a solid) immersed in the oil, the distance between the bottom of the bath and the upper surface of the oscillator must be so adjusted that the energy builds up between the two by multiple reflexions. A beaker of water, for example, is heated much more rapidly when the above condition is fulfilled. This operation will be referred to in future as adjusting for energy density.

The height of the oil mound raised above the surface over the plate depends in the same way upon the depth of the oil. We have never obtained a smooth uniform mound, as might be expected with low amplitude if the plate were simply expanding and contracting as a whole. With the oscillator operated at low voltage, a number of humps appear on the surface which shift their position with every alteration in the capacity of the condenser. When the frequency of the electrical oscillation is tuned exactly to the natural frequency of the crystal plate the oil mound rises to a height of 7 cm., its summit erupting oil drops like a miniature volcano. Further increase of the power gave a mound 10 cm. in

height, but the quartz plate broke into fragments. A photograph of the oil fountain taken against a very bright background with an exposure of $1/500$ second is reproduced on Plate VII. fig. 2.

Stationary waves on tubes

If a glass tube a metre long and 2 or 3 cm. in diameter, closed at the bottom like a test-tube, is coated on the inside with a layer of a heavy oil, the oil gathers itself together in rings about 3 mm. apart, which line the tube from top to bottom, as soon as the lower end is dipped into the vibrating oil over the quartz plate. The rings appeared to be interrupted in places by another system of waves, and a permanent record of the pattern was secured by substituting paraffin, coloured with aniline red, for the oil and using it in a warm tube. A photograph of a portion of the tube with the rings cut across into a pattern of regularly spaced dots is reproduced on Plate IX. fig. 3.

The wave-length of the oblique system is about 1.5 times that of the horizontal system.

We at first attributed the rings to a stationary system of compressional waves formed by interference between disturbances reflected down from the top of the tube with those coming up from below, but the velocity deduced from the wave-length and frequency was much less than the velocity of sound in glass. The waves turned out to be transverse vibrations, the wave-length being but a small fraction of the diameter of the tube. If a similar glass tube was used without the oil, and the outer surface heated to the softening point in the flame of a blast-lamp while the vibrations were running up and down the tube, the stationary system was permanently recorded in the glass, and could be made visible by casting a shadow of the tube with sunlight (or light from any concentrated source) on a sheet of paper held at a distance of 10 or 15 cm. from the tube. A shadow photograph, made in this way, is represented on Plate IX. fig. 4.

We have made no careful study of the modes of vibration of a tube for high frequencies, and have no explanation for the oblique system of greater apparent wave-length. It seems evident, however, that the velocity of propagation is greater for the waves forming this system than for the others. It was observed also, as the tube cooled down, that the paraffin remained fluid longer in those portions of the tube where the double system registered than at other places, indicating that the internal heating of glass was greater here than elsewhere.

Transverse waves on glass plates, rods and threads.

If a glass rod is cemented with sealing-wax to the centre of a circular glass disk, dusted with lycopodium, a beautiful system of concentric circular rings forms on the plate as soon as the lower end of the rod is brought into contact with the vibrating oil-bath.

These rings are formed at the nodal lines of a system of stationary waves in the plate, formed by the interference of the waves reflected from the rim with those radiating from the centre. If the disk is thicker at the centre than at the rim (we used the base and stem of a broken wine-glass) the distance between the rings is less at the rim than at the centre, from which the inference can be drawn that the waves are transverse vibrations, which is to be expected considering the arrangement of the rod and disk. The velocity is higher at the thick than at the thin portions, consequently the rings are further apart.

If the rod is cemented to the disk at a point situated at a small distance from the centre, we obtain the complicated pattern reproduced as a negative (*i. e.* the lycopodium lines black) on Plate X. fig. 5. Here we evidently have the waves reflected from the rim coming to a focus, which becomes a second source of radiation on the side of the centre opposite to the rod, and a system of radiating interference fringes is formed, as with two similar sources of light. The pattern in the immediate vicinity of the sources is of especial interest.

A beautiful system of circular rings of variable spacing is produced by dusting the inner surface of a champagne glass with lycopodium, and touching the base to the surface of the vibrating oil. At the rim the rings are closer together than near the centre, where the glass is thicker.

Applying the lycopodium method to a glass rod which has been drawn down in a flame to a long tapering point, the diameter varying from 7 to 0.5 mm., gives us a system of rings, the separation of which decreases rapidly as we pass from the thick to the thin portion. This shows that the velocity of propagation is a function of the diameter of the rod, which will of course be true for transverse, but not for longitudinal disturbances. If the rod terminates in a fine point no rings are formed, since in this case the reflexion from the end is negligible and the stationary wave system is not formed.

More permanent rings better suited for wave-length measurements were made by the following method. A

small ball of soft red wax was stuck on the point of the rod held vertically over the oil. This melted and slid down the rod as soon as the lower end was dipped in the oil, owing to heat developed by friction between the vibrating glass and the wax. The wax solidifies in rings above the ball as it descends leaving a permanent record of the wave-length, as shown on Plate X. fig. 6.

In this particular case the rod is drawn down from a glass tube closed at the bottom. The energy abstracted from the oil and thrown into the rod is greater than when a large solid rod forms the collector. Remarkable calorific effects obtained with this type of collector will be described presently.

*Heat developed at Contact-point between vibrating rods
and matter.*

This type of heating was first accidentally observed when taking the temperature of the oil in the erupting mound over the vibrator. Though the mercury registered only 25° , the thermometer tube became so hot at the point where it was held between the thumb and finger that it had to be released. The heat of course is developed by friction between the vibrating glass stem and the skin of the fingers, or rather by the rapid *pounding* of the transverse vibrations, and becomes unbearable only when the glass is squeezed tightly between the thumb and finger. This same heating is observed when any object such as a rod, tube, beaker or flask is held by the fingers and dipped into the vibrating oil-bath. If a glass rod is drawn out into a long thread of the diameter of a horsehair, terminating in a pear-shaped bead, the heat developed, when the end of the thread is squeezed between the fingers and the bead dipped into the oil fountain, is so great that a groove with seared edges is left in the skin. A week later bright red spots similar in appearance to blood-blisters developed, which did not disappear for several weeks. These were perhaps due to an effusion of blood from capillaries deep down in the skin, which were ruptured by the vibration. Still more powerful effects were obtained with rods 0.5 mm. in diameter drawn out from the top of an Erlenmeyer flask the neck of which had been closed by fusion in a blast-lamp. Shown at extreme right of Plate VIII., which also shows rack-and-pinion stand for adjusting a flask of water containing a frog for maximum energy density. A side tube was fused to the flask, by which it was supported in a clamp-stand, furnished with a rack-and-pinion movement, by which the distance between the flat bottom of the flask

and the vibrator could be accurately adjusted for the position necessary for securing the maximum density of the radiation imprisoned between the surfaces. With this condition fulfilled a dry pine-chip, pressed against the top of the glass rod, smoked and emitted an occasional spark, while the rod rapidly burned its way through the wood, leaving a hole with charred edges. The heating, of course occurs only at the point of contact, the remainder of the rod being quite cold.

If a plate of glass is pressed lightly against the top of the rod, the surface of the plate is etched at the point of contact, the microscope showing a curious scalloped pattern. If the pressure is increased the rod drills its way rapidly through the plate, and the microscope shows small globules of molten glass, and finely powdered material.

This method of conducting the vibration along threads of glass yields a valuable technique for the investigation of the biological effects of the high-frequency vibration, which can thus be applied at a small point on a living organism, egg or embryo under the microscope. We have felt the heat at the end of a thread a metre long and 0.2 mm. in diameter. With the flask form of collector, with proper adjustment for the system of stationary waves between the top of the quartz vibrator and bottom of the flask, the energy thrown into the glass thread is often so great that the thread breaks into pieces.

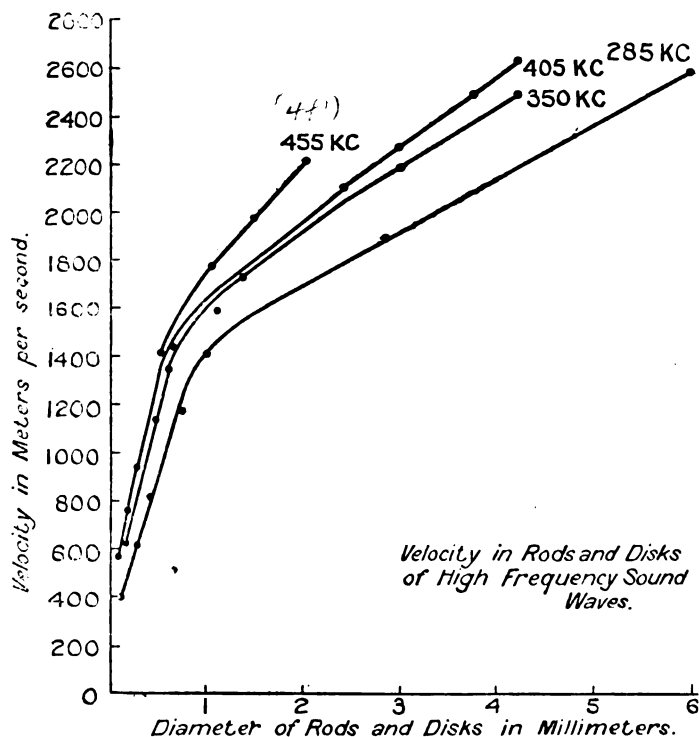
Another form of collector by which energy can be abstracted from the oil and conducted into a rod or thread is shown in fig. 6, Plate X.—a tube of glass closed with a round bottom and drawn down to rod or thread at the opposite end. The sloping wall of the bottom appears to facilitate the production of transverse waves and it was found also, in experimenting with a flat collector made of a thin plate of glass, drawn off into a rod at one corner, that the most vigorous vibrations occurred in the rod when the plate was immersed in the oil in a slightly oblique position and not when it was parallel to the surface of the quartz plate.

Velocity and Dispersion of Transverse Waves in Solids.

By the methods just indicated it is possible to measure the velocity of propagation of the transverse waves if the frequency is known. As has been said, the velocity is a function of the diameter of the rod or the thickness of the plate. Micro-photographs of the rings on rods of 0.15, 0.5 and 1 mm. in diameter are reproduced on Plate XI. fig. 7. Observations made with waves generated by quartz

vibrators of different thicknesses showed that the velocity was also a function of the frequency, as is the case with light traversing a dispersing medium. We investigated the phenomenon of dispersion employing disturbances of four different frequencies—441, 405, 350, and 285 thousand vibrations per second—forming the rings of red wax or lycopodium on rods and threads of glass varying in diameter from 6 mm. to 0.1 mm. The results are shown graphically in the curves reproduced in fig. 3. The velocity, which at

Fig. 3



285 kilocycles is 2600 metres per second in a glass rod 6 mm. in diameter, falls off to 400 metres in the case of a glass thread 0.1 mm. in diameter.

As the diameter of the rod is increased it becomes increasingly difficult to form the rings, and for values of the order of magnitude of the half wave-length it becomes impossible to obtain any record of the transverse waves, even

by the lycopodium method, which is the more sensitive of the two. With very large energy input we several times obtained under these conditions indications of waves of considerably greater wave-length than the transverse ones which we at first believed represented the longitudinal disturbance. Measurements, however, were not in agreement with the known velocity of sound in glass, which is in the neighbourhood of 5000 metres per second.

The dispersion, for a rod of any given diameter, is given by taking the ordinates from the four curves corresponding to the same abscissa, the velocity of propagation increasing with the frequency at first rather rapidly, then more slowly, and finally rapidly again. These values are preliminary only and do not represent a very high degree of accuracy.

Sonic Interferometer and the Velocity of the Waves in Liquids.

Another method was developed for the determination of the velocity in liquids, depending upon the formation of a system of stationary waves between the vibrator and a reflector. We have alluded to the variable periodic pressure exerted upon a plate pushed down through the oil over the vibrator. By counting the number of resisting planes as the plate is lowered through a measured distance, the wave-length can be determined. It is obvious that the accuracy of this method depends upon the precision with which the points of maximum or minimum pressure can be determined. It was found that the best results were secured by employing electrical means for registering the reaction of the reflected waves upon the piezo-electric vibrator, as employed by Professor Pierce of Harvard, and a very compact instrument of low power has been developed in collaboration with Professor J. C. Hubbard, now of Johns Hopkins University, who has already made a series of very satisfactory observations of the velocity of sound in various liquids, solutions, and liquid mixtures. It is possible to obtain results of great accuracy with only a few cubic centimetres of liquid. The results of this work will be reported in a subsequent paper.

As is apparent this method is analogous to the employment of the Fabry and Perot interferometer for determining the wave-length of light, and the apparatus may be termed a Sonic Interferometer. With the plate in the position for maximum pressure, and multiple to-and-fro reflexion of the waves, the condition is similar to that obtaining with a Fabry and Perot instrument illuminated by *parallel rays*

at normal incidence, with its plates at such a distance as to secure the maximum transmission of light. If the wave-length of light or the distance between the plates is slightly altered, the transmission falls to a very low value. Transmission in this case corresponds to the entrance of the energy into a beaker of water tuned for maximum energy density, as previously described. In the usual treatment of the Fabry and Perot interferometer one is apt to overlook the circumstance that under certain conditions transmission of the light is refused, as it is customary to illuminate the instrument by an extended luminous source such as a flame—in which case the amount of light transmitted is independent of wave-length, but transmission is permitted in specified directions only, this limitation giving rise to the rings.

Heating of Liquids and Solids.

The kinematic coefficient of viscosity increases as the square of the frequency. At frequencies from 300 to 400 K.C. the heating of liquids is very pronounced. Thus a test-tube filled with water and immersed in a beaker containing water and cracked ice heats rapidly when the beaker is lowered over the vibrating quartz disk, showing that the energy of the sound-waves (which pass into the water in the test-tube after traversing the intervening glass walls and the ice-water) is converted into heat by absorption, the water in the test-tube rising rapidly in temperature notwithstanding the circumstance that it is surrounded by a layer of water at 0°. The rise of temperature may be as great as one degree every three seconds, the rate depending upon whether the depth of the water and the distance between the vibrator and the bottom of the beaker are adjusted for multiple reflexions of the radiation, as previously described. With 250 c.c. of water the heat developed amounted to about 900 calories per minute—with 150 c.c., 750 cal.; with 100 c.c.; 700 cal.; and with 50 c.c. (in a test-tube) 430 cal.

These results show that though the temperature rise is higher in the case of small volumes of liquid, the total energy abstracted from the radiation increases with the volume of liquid employed.

We have not as yet made any precise determinations of the heating of various liquids by the radiations. Three determinations with 45 c.c. of ethyl alcohol gave 4°·1, 3°·6, and 4°·5 as the temperature elevation for an exposure of 20 seconds. These observations were, however, made

before the necessity of accurate adjustment of the containing vessel had been realized. In work of this nature it will be necessary to devise some method by which it will be possible to throw the same amount (or a measured amount) of energy into the fluids under investigation.

A few observations have also been made of the internal heating of solids. A block of newly formed ice (distilled water frozen in a beaker by ice and salt) was subjected to the action of the sound-waves for two minutes in a beaker of ice water containing numerous small fragments of ice which kept the temperature of the water at 0° . Adjustment for maximum energy density was secured by watching the block of ice which was elevated above its normal position in the water by the radiation pressure. At the end of the exposure the block of ice, on being squeezed between the thumb and fingers, broke up into small fragments showing that liquefaction had taken place throughout the mass, as in the case of so-called "rotten ice" after exposure to the sun's rays.

We found that this experiment could not be duplicated with natural ice (*i. e.* pond ice), and believe that this may be due to the circumstance that in this case we are dealing with a single crystal, whereas in the case of the artificial ice we have a mass of interlocking crystals, the heating taking place at the crystal interfaces.

To eliminate effects due to air bubbles in the ice, distilled water, thoroughly boiled to remove air, and coloured with fluorescein, was covered with a thin layer of paraffin and frozen. The outer portions of the ice block were perfectly transparent, while the central portion was yellowish in colour, somewhat cloudy and devoid of fluorescence, showing that the fluorescein was not in solution. On exposing this block to the radiation for thirty seconds and examining it in sunlight against a black background, it was found to be traversed by innumerable interlacing planes of green fluorescence, caused by the internal melting and consequent solution of the dye. A somewhat analogous effect was noted in one of our earlier experiments, in which a bit of candle (probably stearic acid) was melted on the surface of water in a test-tube and allowed to solidify. Water was then introduced above the solid plug, and the lower end of tube subjected to the vibration. No trace of the radiation appeared in the water above the plug the *under surface* of which melted rapidly and was thrown down into the water as a white emulsion, showing the powerful absorption of the radiation by the solid stearic acid.

It was during an attempt later on to duplicate this experiment with paraffin that we obtained the apparent crystallization of the substance referred to later on in this paper.

Formation of Emulsions and Fogs.

If two non-miscible liquids such as oil and water are simultaneously subjected to the radiation in the same beaker, an emulsion or colloidal solution is formed as a result of the forces acting at the interface between the liquids. This phenomenon was first observed in an earlier arrangement of our apparatus, in which the quartz oscillator operated in a thick layer of oil floating on water. White clouds of finely divided oil were thrown down into the water and occasionally, probably when exact tuning happened to be secured, large masses of oil were projected, with almost explosive violence, down into the water, as a shower of large drops. Stable emulsions resembling milk can be made of stearic acid or paraffin and water. A beaker of water with a layer of mercury at the bottom, under the influence of the vibrations becomes first milky, then brown, and finally black. At the end of twenty-four hours most of the mercury has settled, but a sufficient amount remains in suspension to make the water slightly turbid.

Colloidal solutions of the low melting-point alloys have also been made.

At a liquid-air interface, in the case of less viscous liquids the forces brought into play drive the liquid into the air in the form of a spray of minute droplets, forming a fog. This atomization (to use the popular term) of a liquid by the sound-waves is best shown by pouring a little benzol into a beaker and lowering the beaker into the oil, tuning it for energy density. The beaker fills rapidly with a cloud of white smoke, a benzol fog, the surface of which is in tumultuous motion. A photograph of this phenomenon is reproduced on Plate XII. fig. 10. The beaker was illuminated by sunlight (reflected from a mirror) against a black background, the camera pointing as nearly as possible towards the direction from which the light was coming, to secure the maximum illumination. The filaments rising from the surface are larger droplets moving too rapidly for the camera shutter. Fogs can also be formed over water, but in this case the droplets are larger and settle rapidly.

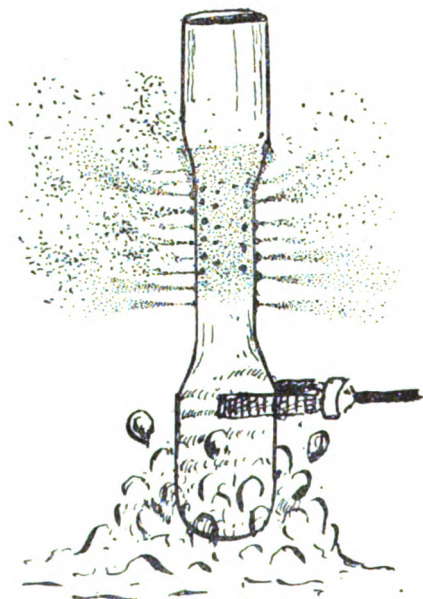
Prof. C. V. Boys has drawn my attention to the analogy between this experiment and a phenomenon produced by the

explosion of a "depth-charge." The first indication of the explosion seen at the surface is the sudden development of a great cloud of fine spray which is projected to a height of ten or fifteen feet. This is followed immediately by the rising mound of water and the great fountain, lifted by the expanding gases. The spray is due to the shock of a "pulse"-wave of almost instantaneous pressure. The spray is never seen following the explosion of a mine, which always contains a large volume of air. This acts as a cushion, and prevents the development of the instantaneous pressure.

A fog of extremely small droplets of heavy transformer oil can be formed by a collector of special construction. This is perhaps the most spectacular experiment of all. A glass tube of about 2.5 cm. diameter is closed at one end, and drawn down to a diameter of about 7 mm. at the other end. The tube is clamped to the rack and pinion stand, and the rounded bottom lowered into the oil, adjustment being made for energy density. This form of collector for compressing the radiation into small volume (if we may use this expression) is the most efficient thus far found. The constricted portion of the tube heats rapidly by internal friction, and if touched with the finger becomes unbearably hot. To distinguish between heating by internal friction and the heat developed when another body is pressed against the vibrating glass it is only necessary to operate the tube for a few seconds, shut off the power and touch the thin constricted portion with the finger. If now, with the tube adjusted for maximum heating and the oscillator working at full power, we apply a little oil with a medicine dropper to the outside of the tube above the narrowed portion, a very surprising thing happens. The oil spreads over the surface and is thrown out in jets of spray resembling smoke and a dense cloud gathers about the tube. If a match flame is brought gradually up to this cloud brilliant flashes of countless small scintillations occur resembling the sparks of the Japanese fireworks, and if the flame is brought closer, the whole cloud goes up in a grand burst of flame and the top of the tube continues to burn fiercely like a torch until the oil supply is exhausted. For some reason not quite clear the oil is unable to run down the thin portion of the tube, gathering in a ring of greater or less width at the top. If the power on the oscillator is reduced or the tube thrown out of adjustment by an up or down movement of a fraction of a millimetre the ring crawls down the tube, rising again as soon as the intensity of the vibration is increased. This driving of the oil layer up the tube is doubtless due to the fact that the energy of

the radiation travelling up the tube is greater than the energy reflected down. It is obvious that the walls of the tube are vibrating as stationary waves, since close inspection shows that the oil in the ring has gathered in more or less regularly arranged dots, and that the jets of spray shoot out from these dots (fig. 4).

Fig. 4.



A photograph of the tube in action is reproduced on Plate XIII., the clouds of spray and the jets being illuminated by sunlight and photographed under the same conditions as with the benzol fog in the beaker. Twenty or more of the small jets of spray are visible in the original photograph shooting out from the tube just below the cloud, and three vertical rows of the oil dots referred to above can be seen without difficulty between the jets.

A fog of metallic mercury was also formed with this type of collector.

With a collector of this type the amplitude of the vibration at the constricted portion frequently becomes so great that the tube is fractured in a curious manner, small irregular pieces of glass breaking away from the tube. A photograph of a tube fractured in this way is reproduced on Plate XI. fig. 8.

Flocculation of Suspended Particles in a Liquid.

In the case of particles exceeding a certain size and of a specific gravity not much greater than that of the liquid in which they are suspended, flocculation occurs the moment the liquid is traversed by the waves, the particles rushing together to form clusters which presently gather into a single dense mass just under the surface. We first noticed this effect when studying the action of the radiation on the unicellular organism *paramecium*, and at the moment interpreted it as a biological effect, but we presently duplicated it with fine sawdust which had soaked until water-logged.

The phenomenon is probably the result of radiation pressure combined with shielding perhaps, or analogous to the attractions observed and studied by Bjerknes in pulsating liquids.

Effects of the waves on Chemical Reactions and Crystallization.

The effects of these high frequency radiations on Chemical reactions is under investigation by Dr. W. T. Richards of Princeton University. In work of this sort it is very necessary to distinguish between effects due to the heating of the liquid as a whole and effects due to the vibration. The liberation of dissolved gases from water has been a matter of common observation by all who have worked with super-sonics. The bubbles appear the moment the vibration is started, long before any sensible rise of temperature is observed, and instead of rising with a uniform velocity they remain suspended in the nodal planes moving up in an irregular manner, with frequent pauses. Distinct evidence has been found that certain chemical reactions are accelerated by the vibrations, the most striking case being the so-called "clock-reaction" in which the termination of the reaction is marked by the sudden change from a clear transparent solution to a deep blue one. In attempting to repeat the experiment, previously made with stearic acid, with paraffin wax, we obtained what appeared to be a crystallization of the paraffin induced by the vibration. The melted paraffin was allowed to solidify on the surface of hot water in a beaker. When the whole was quite cold, the bottom of the beaker was dipped into the vibrating oil. Small opaque white spots immediately appeared in the layer of translucent paraffin, which increased in size, forming irregular clusters. A

Phil. Mag. S. 7. Vol. 4. No. 22. Sept. 1927. 2 F

photograph of the sheet of paraffin (natural size) by transmitted light is reproduced on Plate XI. fig. 9. Under a Zeiss binocular stereoscopic microscope the white spots appeared to be nodules covered with protruding points which suggested a crystalline structure. They have not yet been carefully examined however. Sir W. Bragg, on seeing the photograph, remarked that paraffin crystallized in two modifications, one at the solidifying point, and another at a temperature a few degrees lower.

Dr. Richards failed to get conclusive results on the crystallization of super-saturated solutions of sodium hyposulphate by subjecting the entire amount to the vibrations, but we made one interesting experiment in which the super-sonic waves were carried to the surface of the solution by a bent glass thread. Crystallization immediately started around the tip of the thread, and also around a minute crystal which we dropped on the surface at a distance from the thread, the *type of crystallization* and *rate of growth* being different in the two cases. At the request of the Bureau of Soils, Dept. of Agriculture, we made some experiments on the dispersion of colloids from soils. In soil analysis it is often a long and tedious process to disperse the colloids adsorbed on the soil grains. It was found that the colloids of a "very difficult" soil sample sent for examination were completely dispersed into the water by a few minutes treatment to the super-sonic vibration, while by the usual methods the process of shaking violently and centrifuging has to be repeated twenty or thirty times before the colloid is completely dispersed.

Biological Effects.

Though the effects of these waves upon living matter might more properly be discussed elsewhere, it may not be out of place to mention briefly a few of the observations which we have made as they have some bearing on the physical processes involved.

In marked contrast to the flocculation, or driving together of small particles of suspended matter, which has been mentioned, we have fragmentation, or the tearing to pieces of small and fragile bodies. Filaments of living spirogyra were torn to pieces and the cells ruptured. Small unicellular organisms such as paramecium were rendered immobile by a short treatment to vibration of moderate intensity, subsequently recovering, but were killed by a longer exposure, many of them being torn open. The circumstance that all

are not treated alike is doubtless due to the fact that those which manage to keep out of the nodes of the stationary wave system are less roughly handled by the vibrations. Bacteria apparently are able to survive owing to their small size, for the fragmentation of larger bodies is due to the fact that the forces applied to their surfaces vary in magnitude and direction at different points of the body, while in the case of a bacterium the whole body is subjected to the same treatment.

Red blood corpuscles in physiological salt solution are rapidly destroyed, the turbid liquid becoming as clear as a solution of a red aniline dye.

With vibrations of less intensity the destruction is less complete, a blood count made at the end of each 15 seconds of exposure showing that the percentage destroyed decreases, a point being reached at which no further destruction occurs unless the intensity of the radiation is augmented. This means of course that some of the corpuscles, the recently formed ones perhaps, are more hardy than those of greater age. Small fish and frogs are killed by an exposure of one or two minutes, an observation also made by Langevin at Toulon with his Poulsen arc oscillator (see Plate VIII.) Mice are less sensitive, a twenty-minute exposure not resulting in death, and though at the end of the treatment the animal was barely able to move, the recovery was fairly rapid. Blood counts made with a mouse during exposure showed a diminishing number of corpuscles, until a stationary state (about 60 per cent. normal) was reached. The biologists inform us, however, that the blood count of a mouse is affected by fear, the corpuscles hiding in the liver until the danger is over! We made the count with drops taken from the tip of the tail.

We have not yet determined the cause of death in the case of the fishes and frogs. They were protected against rise of temperature as much as possible by ice fragments, dropped into the water from time to time, but this does not shield them from internal heating, which may be the cause of death, as in the case of small animals introduced into a high-frequency electric field. In the case of a mouse killed by an exposure of two minutes between the plates of an air-condenser operated at about 1000 volts with a frequency of 100 million, we found that the temperature of the body-cavity was over 113°F .

With distilled water or a fairly strong solution of salt in a test-tube between the plates of the condenser, little or no heating occurred; but for small concentrations the heating

was very marked, the maximum being for .8 per cent., which is very nearly the amount found in mammalian blood. At lower frequencies the heating appears to be greater for distilled water, at least with high voltages. We found that one terminal of our 60,000 volt coil could be held in the fingers without the production of any sensation, but if dipped into the open end of a glass tube a metre long and filled with distilled water, caused the water to boil in less than 10 seconds. The introduction of a small amount of salt into the water, prevented the heat entirely in this case, which explains why no thermal discomfort was felt when the wire was held in the hand. The wire must be seized, however, before the current is turned on, otherwise a very vicious arc jumps to the finger producing a burn which is very slow in healing.

XXXIX. *The Electronic Theory of the Voltaic Cell.* By O. M. CORBINO, *Professor of Physics in the University of Rome* *.

EVEN after the recognition on the part of physicists of the actual existence of the Volta effect as an intrinsic property of the metals, in electrochemistry one continues to identify the contact e.m.f. with that of the Peltier effect, which is so much smaller.

It is only in a recent statistical theory of the cell due to Butler †, that the Volta e.m.f. receives its due consideration for the calculation of the total e.m.f.

I propose in this paper to contribute to the clarification of this important question.

From direct experiments, as well as from the study of thermionic and photoelectric phenomena, it results at last definitely ascertained that two metals in contact give rise, also in a perfect vacuum surrounding them, to an electric field, which is, in its external effects, wholly indistinguishable from that which could be obtained by attributing to the two metals two different electrostatical potentials. This field, if the electricity is in equilibrium, must also exist in the region of contact between the two metals, by the effect of a double layer of such a strength as to compensate the different binding energy that the electrons possess relatively to the two metals. The difference of the electrostatical potentials is connected with the different extraction energies W_1 and W_2

* Communicated by the Author.

† J. A. V. Butler, *Phil. Mag.* xlviii. p. 927 (1924).

of the electron by two different metals. Thermodynamics teaches, in fact, that, calling V_1 and V_2 the two potentials and V their difference, the following equation must hold :

$$W_1 - W_2 = eV - eT \frac{dV}{dT},$$

where e is the electron charge and T the absolute temperature.

In this equation V is the Volta effect, while the second term represents the heat corresponding to the Peltier effect, which is, as is known, a very small part of eV . The different binding energy W of the electrons for the various metals, revealed by the thermionic and the photoelectric phenomena, thus justifies the smallness of the Peltier effect, which is considered as an unsurmountable objection against the existence of the Volta effect. Indeed, the work supplied by the quantity of electricity q in overcoming the difference of potential through the contact is mostly employed to give the electrons the necessary energy to leave a metal which attracts them more, and pass to a metal which attracts them less.

Having acknowledged the existence of the Volta effect, it is necessary to re-examine the theory of the cell, to which the difference of electrostatical potential between the electrodes and the electronic shifting which constitutes the current cannot be alien. This is what I purpose to do in the present paper.

Let us suppose that a system of two disks of different metals in electric contact be dipped in one or more electrolytical solutions, containing therefore ions of the two signs. Let it be, for instance, a Daniell cell ($\text{Cu}/\text{CuSO}_4/\text{ZnSO}_4/\text{Zn}$). Under the action of the electrical field existent between the electrodes, the anion SO_4 runs on the positive electrostatic metal, the zinc ; but, instead of neutralizing its charge and getting free, it detaches a zinc ion and remains charged in the liquid as before. At the same time the metallic cation, the copper, issues from the liquid and attaches itself to the cathode, also made of copper. The process therefore leaves unaltered the ion SO_4 and all is reduced to the detaching of one ion Zn from the zinc and upon the entrance of a ion Cu in the copper, while in the outer circuit, through the contact of the two metals, two electrons pass from the zinc to the copper.

It is already acknowledged, even without further details, that a phenomenon, which manifests itself in the aforesaid manner and which can develop itself exactly in the contrary

direction opposing to the cell an outer electromotive force capable of inverting the electrostatical field in the electrolyte, the Volta electrostatical field of the electrodes in contact cannot be alien. The two copper and zinc electrodes connected externally certainly produce a field in the vacuum, and will continue to produce it in the dielectric constituted by the solvent; this field can be perturbed by the other eventual fields which may form themselves in the contacts of the electrolyte with the electrodes; but if, as it occurs in the Daniell cell enclosed in a short circuit, the potential difference ruling in the liquid is slightly different from that which the two electrodes would produce in the vacuum, or in the only dielectric, this means that that perturbation must not be very important. Only the concentration cells, with electrodes not different from one another, and made with the metal while in solution, can have a function independent of the Volta effect of the electrodes.

But clearer illustrations on the mechanism working in the cell and upon the importance that the existence of the Volta effect has in such a mechanism, will be supplied to us by a model of the cell which reproduces with singular correspondence all the theoretical and experimental features.

We will represent a metal with a solution, causing the dissolved body to correspond to the atom-ions of the metal and the water molecules to the electrons. Moreover, we will compare a metal dipped in a solution of one of its salts to a solution saturated in contact with the dissolved body. The inner positive ions of the metal correspond to the molecules of the dissolved body, the conduction electrons of the metal correspond to the molecules of the solvent, *i. e.* to water molecules, and lastly the electrolyte with which the metal is in contact will be represented by the dissolved body in the solid phase present in the solution. The metal may gain or lose only electrons in contact with the other metal or in the vacuum; it may gain or lose only metallic ions, *i. e.* positive ions, through the electrolyte; thus, as the solution may lose or gain only water in contact with other solutions through a semipermeable wall or the vacuum, it may lose or gain only molecules of the dissolved body in contact with the solid phase of the latter. The $\text{Cu-CuSO}_4\text{-ZnSO}_4\text{-Zn}$ combination of the Daniell cell (fig. 1) will therefore correspond to that represented in fig. 2.

In a circular tube there are two saturated solutions of two bodies, A and B, separated in π by a semipermeable fixed wall and in S by a movable piston; on both surfaces of S are collected bodies A and B in a solid state, so as to keep

the corresponding solution saturated also during the slow motion of the piston. Upon the piston S will weigh the two different osmotic pressures of the solutions, and S will move;

Fig. 1.

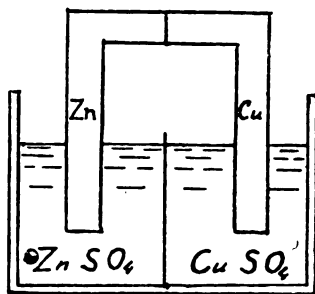
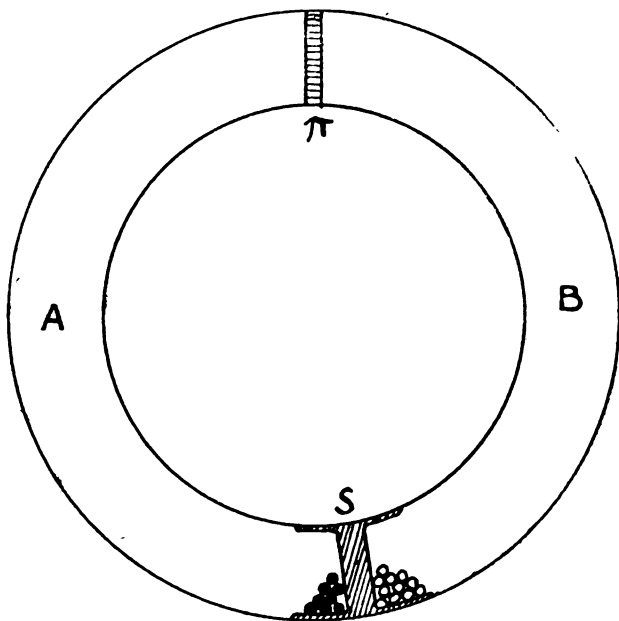


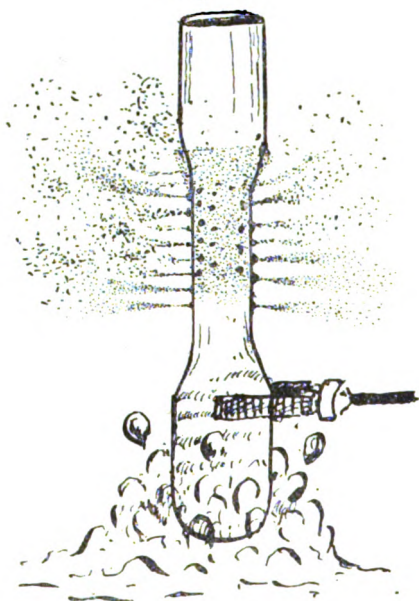
Fig. 2.



to a movement of S, for instance towards the left, will correspond a circulation of pure water across the semi-permeable wall, a diminution of volume of solution A, with a deposit of the dissolved part A, and an increase of the

the radiation travelling up the tube is greater than the energy reflected down. It is obvious that the walls of the tube are vibrating as stationary waves, since close inspection shows that the oil in the ring has gathered in more or less regularly arranged dots, and that the jets of spray shoot out from these dots (fig. 4).

Fig. 4.



A photograph of the tube in action is reproduced on Plate XIII., the clouds of spray and the jets being illuminated by sunlight and photographed under the same conditions as with the benzol fog in the beaker. Twenty or more of the small jets of spray are visible in the original photograph shooting out from the tube just below the cloud, and three vertical rows of the oil dots referred to above can be seen without difficulty between the jets.

A fog of metallic mercury was also formed with this type of collector.

With a collector of this type the amplitude of the vibration at the constricted portion frequently becomes so great that the tube is fractured in a curious manner, small irregular pieces of glass breaking away from the tube. A photograph of a tube fractured in this way is reproduced on Plate XI. fig. 8.

Flocculation of Suspended Particles in a Liquid.

In the case of particles exceeding a certain size and of a specific gravity not much greater than that of the liquid in which they are suspended, flocculation occurs the moment the liquid is traversed by the waves, the particles rushing together to form clusters which presently gather into a single dense mass just under the surface. We first noticed this effect when studying the action of the radiation on the unicellular organism paramecium, and at the moment interpreted it as a biological effect, but we presently duplicated it with fine sawdust which had soaked until water-logged.

The phenomenon is probably the result of radiation pressure combined with shielding perhaps, or analogous to the attractions observed and studied by Bjerknes in pulsating liquids.

Effects of the waves on Chemical Reactions and Crystallization.

The effects of these high frequency radiations on Chemical reactions is under investigation by Dr. W. T. Richards of Princeton University. In work of this sort it is very necessary to distinguish between effects due to the heating of the liquid as a whole and effects due to the vibration. The liberation of dissolved gases from water has been a matter of common observation by all who have worked with super-sonics. The bubbles appear the moment the vibration is started, long before any sensible rise of temperature is observed, and instead of rising with a uniform velocity they remain suspended in the nodal planes moving up in an irregular manner, with frequent pauses. Distinct evidence has been found that certain chemical reactions are accelerated by the vibrations, the most striking case being the so-called "clock-reaction" in which the termination of the reaction is marked by the sudden change from a clear transparent solution to a deep blue one. In attempting to repeat the experiment, previously made with stearic acid, with paraffin wax, we obtained what appeared to be a crystallization of the paraffin induced by the vibration. The melted paraffin was allowed to solidify on the surface of hot water in a beaker. When the whole was quite cold, the bottom of the beaker was dipped into the vibrating oil. Small opaque white spots immediately appeared in the layer of translucent paraffin, which increased in size, forming irregular clusters. A

Phil. Mag. S. 7. Vol. 4. No. 22. Sept. 1927. 2 F

photograph of the sheet of paraffin (natural size) by transmitted light is reproduced on Plate XI. fig. 9. Under a Zeiss binocular stereoscopic microscope the white spots appeared to be nodules covered with protruding points which suggested a crystalline structure. They have not yet been carefully examined however. Sir W. Bragg, on seeing the photograph, remarked that paraffin crystallized in two modifications, one at the solidifying point, and another at a temperature a few degrees lower.

Dr. Richards failed to get conclusive results on the crystallization of super-saturated solutions of sodium hyposulphate by subjecting the entire amount to the vibrations, but we made one interesting experiment in which the super-sonic waves were carried to the surface of the solution by a bent glass thread. Crystallization immediately started around the tip of the thread, and also around a minute crystal which we dropped on the surface at a distance from the thread, the *type of crystallization* and *rate of growth* being different in the two cases. At the request of the Bureau of Soils, Dept. of Agriculture, we made some experiments on the dispersion of colloids from soils. In soil analysis it is often a long and tedious process to disperse the colloids adsorbed on the soil grains. It was found that the colloids of a "very difficult" soil sample sent for examination were completely dispersed into the water by a few minutes treatment to the super-sonic vibration, while by the usual methods the process of shaking violently and centrifuging has to be repeated twenty or thirty times before the colloid is completely dispersed.

Biological Effects.

Though the effects of these waves upon living matter might more properly be discussed elsewhere, it may not be out of place to mention briefly a few of the observations which we have made as they have some bearing on the physical processes involved.

In marked contrast to the flocculation, or driving together of small particles of suspended matter, which has been mentioned, we have fragmentation, or the tearing to pieces of small and fragile bodies. Filaments of living spirogyra were torn to pieces and the cells ruptured. Small unicellular organisms such as paramecium were rendered immobile by a short treatment to vibration of moderate intensity, subsequently recovering, but were killed by a longer exposure, many of them being torn open. The circumstance that all

are not treated alike is doubtless due to the fact that those which manage to keep out of the nodes of the stationary wave system are less roughly handled by the vibrations. Bacteria apparently are able to survive owing to their small size, for the fragmentation of larger bodies is due to the fact that the forces applied to their surfaces vary in magnitude and direction at different points of the body, while in the case of a bacterium the whole body is subjected to the same treatment.

Red blood corpuscles in physiological salt solution are rapidly destroyed, the turbid liquid becoming as clear as a solution of a red aniline dye.

With vibrations of less intensity the destruction is less complete, a blood count made at the end of each 15 seconds of exposure showing that the percentage destroyed decreases, a point being reached at which no further destruction occurs unless the intensity of the radiation is augmented. This means of course that some of the corpuscles, the recently formed ones perhaps, are more hardy than those of greater age. Small fish and frogs are killed by an exposure of one or two minutes, an observation also made by Langevin at Toulon with his Poulsen arc oscillator (see Plate VIII.) Mice are less sensitive, a twenty-minute exposure not resulting in death, and though at the end of the treatment the animal was barely able to move, the recovery was fairly rapid. Blood counts made with a mouse during exposure showed a diminishing number of corpuscles, until a stationary state (about 60 per cent. normal) was reached. The biologists inform us, however, that the blood count of a mouse is affected by fear, the corpuscles hiding in the liver until the danger is over! We made the count with drops taken from the tip of the tail.

We have not yet determined the cause of death in the case of the fishes and frogs. They were protected against rise of temperature as much as possible by ice fragments, dropped into the water from time to time, but this does not shield them from internal heating, which may be the cause of death, as in the case of small animals introduced into a high-frequency electric field. In the case of a mouse killed by an exposure of two minutes between the plates of an air-condenser operated at about 1000 volts with a frequency of 100 million, we found that the temperature of the body-cavity was over 113° F.

With distilled water or a fairly strong solution of salt in a test-tube between the plates of the condenser, little or no heating occurred; but for small concentrations the heating

was very marked, the maximum being for '8 per cent., which is very nearly the amount found in mammalian blood. At lower frequencies the heating appears to be greater for distilled water, at least with high voltages. We found that one terminal of our 60,000 volt coil could be held in the fingers without the production of any sensation, but if dipped into the open end of a glass tube a metre long and filled with distilled water, caused the water to boil in less than 10 seconds. The introduction of a small amount of salt into the water, prevented the heat entirely in this case, which explains why no thermal discomfort was felt when the wire was held in the hand. The wire must be seized, however, before the current is turned on, otherwise a very vicious arc jumps to the finger producing a burn which is very slow in healing.

XXXIX. *The Electronic Theory of the Voltaic Cell.* By O. M. CORBINO, *Professor of Physics in the University of Rome* *.

EVEN after the recognition on the part of physicists of the actual existence of the Volta effect as an intrinsic property of the metals, in electrochemistry one continues to identify the contact e.m.f. with that of the Peltier effect, which is so much smaller.

It is only in a recent statistical theory of the cell due to Butler †, that the Volta e.m.f. receives its due consideration for the calculation of the total e.m.f.

I propose in this paper to contribute to the clarification of this important question.

From direct experiments, as well as from the study of thermionic and photoelectric phenomena, it results at last definitely ascertained that two metals in contact give rise, also in a perfect vacuum surrounding them, to an electric field, which is, in its external effects, wholly indistinguishable from that which could be obtained by attributing to the two metals two different electrostatical potentials. This field, if the electricity is in equilibrium, must also exist in the region of contact between the two metals, by the effect of a double layer of such a strength as to compensate the different binding energy that the electrons possess relatively to the two metals. The difference of the electrostatical potentials is connected with the different extraction energies W_1 and W_2

* Communicated by the Author.

† J. A. V. Butler, *Phil. Mag.* xlviii. p. 927 (1924).

of the electron by two different metals. Thermodynamics teaches, in fact, that, calling V_1 and V_2 the two potentials and V their difference, the following equation must hold :

$$W_1 - W_2 = eV - eT \frac{dV}{dT},$$

where e is the electron charge and T the absolute temperature.

In this equation V is the Volta effect, while the second term represents the heat corresponding to the Peltier effect, which is, as is known, a very small part of eV . The different binding energy W of the electrons for the various metals, revealed by the thermionic and the photoelectric phenomena, thus justifies the smallness of the Peltier effect, which is considered as an unsurmountable objection against the existence of the Volta effect. Indeed, the work supplied by the quantity of electricity q in overcoming the difference of potential through the contact is mostly employed to give the electrons the necessary energy to leave a metal which attracts them more, and pass to a metal which attracts them less.

Having acknowledged the existence of the Volta effect, it is necessary to re-examine the theory of the cell, to which the difference of electrostatical potential between the electrodes and the electronic shifting which constitutes the current cannot be alien. This is what I purpose to do in the present paper.

Let us suppose that a system of two disks of different metals in electric contact be dipped in one or more electrolytical solutions, containing therefore ions of the two signs. Let it be, for instance, a Daniell cell ($\text{Cu}/\text{CuSO}_4/\text{ZnSO}_4/\text{Zn}$). Under the action of the electrical field existent between the electrodes, the anion SO_4 runs on the positive electrostatic metal, the zinc ; but, instead of neutralizing its charge and getting free, it detaches a zinc ion and remains charged in the liquid as before. At the same time the metallic cation, the copper, issues from the liquid and attaches itself to the cathode, also made of copper. The process therefore leaves unaltered the ion SO_4 and all is reduced to the detaching of one ion Zn from the zinc and upon the entrance of a ion Cu in the copper, while in the outer circuit, through the contact of the two metals, two electrons pass from the zinc to the copper.

It is already acknowledged, even without further details, that to a phenomenon, which manifests itself in the aforesaid manner and which can develop itself exactly in the contrary

direction opposing to the cell an outer electromotive force capable of inverting the electrostatical field in the electrolyte, the Volta electrostatical field of the electrodes in contact cannot be alien. The two copper and zinc electrodes connected externally certainly produce a field in the vacuum, and will continue to produce it in the dielectric constituted by the solvent; this field can be perturbed by the other eventual fields which may form themselves in the contacts of the electrolyte with the electrodes; but if, as it occurs in the Daniell cell enclosed in a short circuit, the potential difference ruling in the liquid is slightly different from that which the two electrodes would produce in the vacuum, or in the only dielectric, this means that that perturbation must not be very important. Only the concentration cells, with electrodes not different from one another, and made with the metal while in solution, can have a function independent of the Volta effect of the electrodes.

But clearer illustrations on the mechanism working in the cell and upon the importance that the existence of the Volta effect has in such a mechanism, will be supplied to us by a model of the cell which reproduces with singular correspondence all the theoretical and experimental features.

We will represent a metal with a solution, causing the dissolved body to correspond to the atom-ions of the metal and the water molecules to the electrons. Moreover, we will compare a metal dipped in a solution of one of its salts to a solution saturated in contact with the dissolved body. The inner positive ions of the metal correspond to the molecules of the dissolved body, the conduction electrons of the metal correspond to the molecules of the solvent, *i. e.* to water molecules, and lastly the electrolyte with which the metal is in contact will be represented by the dissolved body in the solid phase present in the solution. The metal may gain or lose only electrons in contact with the other metal or in the vacuum; it may gain or lose only metallic ions, *i. e.* positive ions, through the electrolyte; thus, as the solution may lose or gain only water in contact with other solutions through a semipermeable wall or the vacuum, it may lose or gain only molecules of the dissolved body in contact with the solid phase of the latter. The $\text{Cu-CuSO}_4\text{-ZnSO}_4\text{-Zn}$ combination of the Daniell cell (fig. 1) will therefore correspond to that represented in fig. 2.

In a circular tube there are two saturated solutions of two bodies, A and B, separated in π by a semipermeable fixed wall and in S by a movable piston; on both surfaces of S are collected bodies A and B in a solid state, so as to keep

the corresponding solution saturated also during the slow motion of the piston. Upon the piston S will weigh the two different osmotic pressures of the solutions, and S will move;

Fig. 1.

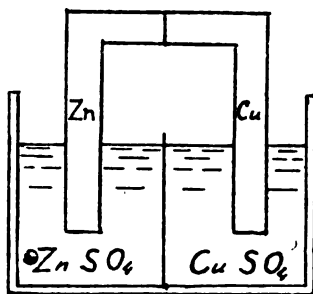
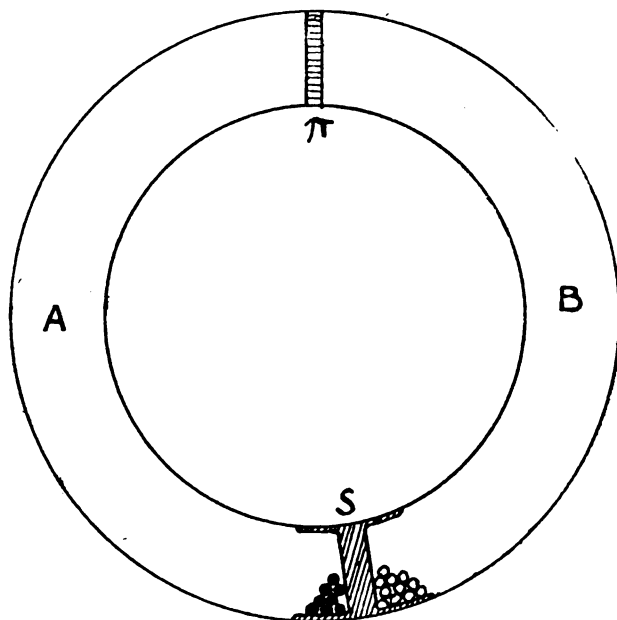


Fig. 2.



to a movement of S, for instance towards the left, will correspond a circulation of pure water across the semi-permeable wall, a diminution of volume of solution A, with a deposit of the dissolved part A, and an increase of the

volume of solution B with the dissolving of body B. The process is continuous until the piston S in its motion reaches wall π , *i. e.* until solution A disappears; of course, if a sufficient quantity of the dissolving body B is available.

A bath in which all the apparatus is dipped serves to maintain the temperature constant.

In perfect correspondence with the model, in the cell of fig. 1 the electrons circulate, outside the cell, from the zinc to the copper through the contact, which, as we have stated, acts as a semipermeable wall; at the same time, the zinc destroys itself in passing to the state of ions Zn in the liquid, while the copper from the state of ion Cu deposits itself as a metal on the copper plate, and this until there are zinc and copper sulphate available. The difference of hydrostatical pressure between A and B corresponds to the difference of the electrostatical potentials between zinc and copper.

So that the analogy with the cell may be closer, we shall suppose that, as the formation of copper from ions and electrons is a *exo-energetic* reaction, also the formation of the solution is so; and therefore the dissolution without osmotic work, *viz.* that which is studied with the calorimeter, will be *esothermal* in virtue of a chemical reaction between the solvent and the dissolved portion, *i. e.* water and calcium salts.

And therefore the origin of the water circulation work in the model will be the forming energy of the volume unit of the two solutions, and precisely the so-called dissolution heat with osmotic work. The portion of this formation-energy corresponding to the work production results, from the theory, as equal to the difference of the osmotic pressures of the two solutions, which, after all, is obtained also directly from the consideration of the working system of the apparatus.

Analogously for the cell will come into play the different inner potentials (photoelectrical potentials) of the two metals, and the variation of energy in the contact of the electrodes with the electrolyte, for the passage of ion Zn into solution, and for that of ion Cu on to the metal. The total available energy will be given by the formation of a certain weight of neutral copper starting from ions Cu which get in from the solution, and by two electrons which enter from the bi-metallic contact, diminished by the energy of corresponding formation of an equivalent weight of neutral zinc. Naturally these formation-energies of the metal are not to be confounded with that of the isolated atom.

The analogy can be followed further. If one opens the

tube of fig. 2 in the place of wall π , by leaving the ends free, the hydrostatical pressures balance and the water circulation stops. Thus, by detaching the two metals of the cell in the place of the electric contact, the field inside the electrolyte is annulled and the motion of the ions stops. And as the two upper and separate parts A, B of the tube might communicate through a tube containing the steam phase, which would reconstitute the circulation, thus an electronical evaporation between Zn and Cu, kept for instance in the vacuum and at a high temperature, would reconstitute the current, for also this communication is equivalent to a contact.

Further : if in the tube of fig. 2 a horizontal stoppage is made both in A and in B, above we shall have the difference of hydrostatical pressure created by the semipermeable wall, while below the liquid pressures will be almost made equal by the movable piston S. From this, one knows the essential function of the semipermeable wall, which creates and tends to maintain the difference of hydrostatic pressure, while the movable piston tends to do away with it ; hence the circulation continues on account of the contra-position of the two.

Analogously, if we cut the upper part of the bimetallic couple horizontally, above we shall have the difference of the electrostatical potential of Volta, while below, between the trunks of Zn and of Cu we shall have a difference of electrostatical potential far smaller. It can be rightly affirmed that the contact of the metals tends to maintain the difference of electrostatical potentials ; the immersion in the liquid tends to lessen it, and therefore the balance is perturbed and a continuous current is determined. This is *Volta's interpretation*.

Of course this does not exclude that the e.m.f. of the cell may be somewhat different from the Volta effect in the vacuum. The exact value of E , owing to the application of the two principles of thermodynamics, must correspond to the total variation of the free energy which occurs in the total circuit, according to the Gibbs-Helmholtz formula, which cannot be contrary to the synthetic interpretation given above, for it is independent of every hypothesis upon the current-production mechanism.

In connexion with the Daniell cell, for which the thermal corrective term of Helmholtz is small, the evaluation of energy $2Ee$ freed in the passage of two electrons, viz. for the shifting in the electrolyte of a bivalent metal ion, can be carried out as follows :—Let it be firstly noted that, upon

ascertaining the formation of a neutral metal where the copper deposits itself, this does not mean that neutral atoms have deposited themselves, for it is quite probable that in the metal there exist only positive ions, deprived of the valence electrons, and an inner thick cloud of conduction electrons; so that, upon constituting the neutral metal, it might well happen that the metal positive ion enters from the electrolyte and *remains as such*, viz. in the state of ion, while the electrons enter from the bimetal contact and mingle themselves in the electronic cloud. Let W_{Zn}^- be the work of photoelectrical extraction of an electron from the zinc, and W_{Cu}^- that of the copper; the cutting off of energy from the contact for the passage of two electrons from the zinc to the copper, neglecting the Peltier effect, will be $2(W_{Cu}^- - W_{Zn}^-)$. In the copper-copper sulphide contact there takes place the passage of one ion Cu from the liquid to the copper, developing a quantity of free energy which we shall call W_{Cu}^+ . The same may be said for the zinc, which will develop, for the passage of ion Zn in the liquid, the quantity of free energy $-W_{Zn}^+$.

We shall therefore have a total of

$$2Ee = 2W_{Cu}^- + W_{Cu}^+ - (2W_{Zn}^- + W_{Zn}^+). \quad . \quad . \quad (1)$$

We can thus have E , e.m.f. of the cell, as a characteristic quotient of it, taken as a whole, between the electrical energy totally developed in the circuit and the quantity of electricity passed.

Let us now try to distribute E among the various contacts which have their place in the circuit. Let it be noted, in the meantime, that (1) can be put under the form :

$$E = \frac{1}{2e} (W_{Cu}^+ - W_{Zn}^+) + \frac{1}{e} (W_{Cu}^- - W_{Zn}^-).$$

But the last term is the Volta effect V . Therefore

$$E = V + \frac{1}{2e} (W_{Cu}^+ - W_{Zn}^+). \quad . \quad . \quad . \quad (2)$$

If, as it happens in the Daniell element, the e.m.f. of the cell is very near the Volta effect between the electrodes, this means that W_{Cu}^+ and W_{Zn}^+ are slightly different from one another, that is to say, that the energies freed in the passage of the ion from the metal to the solution are partially compensated in the two electrodes; or even that the greatest

part of the cell work is given by the passage of the electrons from the zinc to the copper.

This result must not astonish us.

It is therefore necessary to clear a point of considerable importance. Electricity can pass from one metal to another only in the state of electrons; from a metal to an electrolyte only in the state of metal ions. But there is a property common to all the passages. At every contact where there exists on both sides a different connecting energy for electricity, there certainly exists also a difference of electrostatical potential, viz. an outer electrical field, and a double layer at the contact, equivalent to the energy difference; and *vice versâ* at every contact where between the two parts is detected a difference of electrostatical potential with an outer electrical field, there exists a difference of binding energy for electricity between the two parts themselves, and therefore, in a certain sense, a source (positive or negative) of energy for the passage of electricity through the contact. *In this sense no difference can be made between what occurs in each of the three principal contacts of the cell.*

However, if the quantities W_{Cu}^+ and W_{Zn}^+ (variations of free energy for the passage of an ion from the metal to the liquid) are different from zero, there will most likely exist a difference of potential between a metal and liquid and an outer electrical field between them; and besides, as there certainly exists the difference of electrostatical potential between the two metals upon coming into contact, viz. the outer electrical field, there will undoubtedly exist in the contact a metal-electronic seat of energy variations for the passage of electrons from one metal to another.

The only difference between the three contacts is the different kind of electrical ion which can get across them—i. e. the electron for the bimetallic contact, the metallic ion for the contact with the electrolytes; but all of them contribute to the production of current with the corresponding variations of energy and the double layers which arise from them. Therefore it is not at all justifiable to neglect the first and to look at the other two only. *The current arises from the fact that the algebraic sum of the strengths of the three double layers is not zero.*

Considering the formula (1), we have stated that E being near V , it results that W_{Cu}^+ and W_{Zn}^+ are near each other; but each of them might either be very large or very small. To W_{Cu}^+ and W_{Zn}^+ correspond the differences of metal-liquid

potentials, considered in Nernst's formula, and that they can, as he puts it, depend on the concentration of the metal ions in the solution. They should, however, be measured *electrostatically*, and not by the usual means of electrochemistry, which *purposely neglects the differences of electrostatic potential in the contacts of metals*, and is always subjected to the uncertainty of the so-called zero-point of the absolute electrolytical potentials.

So it is customary to attribute to the absolute potential of the normal calomel electrode the value -0.560 volt; then the normal potentials P_M of the various metals are known from the Wilmshire or Potential-Commission Tables; they can be referred to the same zero-point, in respect to which the normal electrode has the absolute potential -0.560 . Therefore the cell formed by metal M , by a salt of its own, in normal solution, and by the normal electrode, has the e.m.f.

$$E = P_M + 0.560,$$

which is independent of the choice of the zero-point.

But for the formula (2), if -0.560 is the true absolute potential of the normal electrode, the following equation must hold:

$$E = M/Hg - \frac{1}{ne} W_M^+ + 0.560,$$

where M/Hg is the Volta effect between the metal and Hg , and n is the valence of the ions M^+ .

We thus obtain as potential difference V_M^+ between the metal and liquid:

$$V_M^+ = \frac{1}{ne} W_M^+ - M/Hg - P_M.$$

And therefore, in the hypotheses made, in order to have the e.m.f. in the metal-electrolyte contact, we must subtract P_M from the Volta effect M/Hg .

The knowledge of the electrostatic potential difference between Cu and $CuSO_4$ would give the exact value of W_{Cu}^+ and the same for the zinc.

And then, having from the photoelectrical data also W_{Cu}^- , W_{Zn}^- , one might reconstitute the total formation-work or the | metal-ions, electrons | mixture which constitutes the neutral metal. These data would be of remarkable interest: they would supply, by the difference between copper and zinc, the e.m.f. of the Daniell cell.

In the ordinary theory of the Daniell cell, we get the right value of the e.m.f., considering, instead of the formation energies of the metals, the variation of energy for the formation of zinc sulphate and the decomposition of copper sulphate; and therefore the difference of the corresponding heats of formation (Zn, O, SO_3 , water), (Cu, O, CuO_2 , water), as determined by Thomsen.

But in this way we introduce elements wholly extraneous to the true functioning of the cell, which is practically independent of the presence of the acid anion SO_4 . Of course these extraneous elements are eliminated by subtracting the two heats of formation.

If the cell contains any other salts instead of sulphates, we must calculate the e.m.f. by means of other thermochemical experiments, still obtaining, by Hess's rule, the same value for the formation-heats of the dissolved homologous salts of Cu and Zn.

With considerably greater simplicity the electronic theory takes into account the formation-energies of the electrodes, which do not depend upon the acid anion, but only, and to a small extent, upon the concentration of the metallic ions in the solution.

In Nernst's theory we find the same simplification and unification of the cells having the same electrodes: indeed, only the dissolution pressure of the metal and the osmotic pressure of the metallic ions in the solution come into account, and not the presence of the acid anion.

They are thus four quantities which characterize the working of the cell: the ionic contribution W_{Cu}^+ and the electronic contribution $2W_{\text{Cu}}^-$ relative to the copper, and the two analogous elements relative to the zinc. The part $2(W_{\text{Cu}}^- - W_{\text{Zn}}^-) = 2eV$, where V is the Volta effect, can be supplied only by the electronic efflux, and the remainder by the electrolyte; and therefore, V being very near E , the greater part of the work obtained is due to the absorption of electrons, which the copper accomplishes from the zinc, viz. to the same cause as the Volta effect, while the displacement-works of the metal ions are mostly compensated.

Conclusion.

Having ascertained the existence of the Volta effect also in the vacuum, and therefore independently of any chemical action, the bimetal couple, *i. e.* copper zinc, forms a natural and perpetual means acting to produce in a space

even of large dimensions an electrostatical field; thus, like a permanent magnet, it forms (with less stability, however) around itself a magnetic field. The origin of the energy of this electrostatical field is simply physical: it arises from the different binding energies of the conduction electrons to the various metals.

In the cell which is obtained by dipping a bimetal couple into a ionized gas, the electrostatical field due to the Volta effect produces a permanent current without supplying an energy of its own, but in so far as there exists an outer source of energy which ionizes the gas. In this case the electrostatical field simply causes, without doing any work, a directing control of the ionic motion, and therefore a current in the wire which connects the two disks; the energy is that of the recombination of the ions. But the field cannot be neglected or ignored. Even in a permanent Pacinotti magnet-dynamo the current is produced by means of the outer mechanical work, but the inductive field is an indispensable condition in order that work may become electrical power.

In hydro-electrical cells the task of the Volta effect is far more important; thus in the Daniell cell the current is produced by means of the formation of neutral copper and the destruction of neutral zinc, and, as has already been seen, in this process one must hold that most of the work obtained is due to the electronic passage, and most of the e.m.f. is upon the contact of the two different metals.

But one might get the extreme case of a cell where the electronic displacement alone can produce electrical current and mechanical work. It will suffice to think of two neutral copper and zinc disks with a large surface, placed at a distance and connected by means of a wire. On account of their approach, there will be produced a current and mechanical work due to the fact that some of the electrons leave the zinc disk to go towards the copper one, which attracts them more strongly. The smallness of the electrostatical capacity prevents the afflux possibility from becoming a great number of electrons; but if, on a block of copper, electrons are caused to run up together on one side, and positive ions on the other, so as to leave the electrostatical potential unchanged, the currents and energies obtained can become much greater. It is this, which, after all, occurs in the hydro-electrical cell. This is why the explanation of the working of the cell on the basis of the Volta effect cannot lead to substantial contradictions, and must, on the contrary, be considered as scientifically correct.

XI. *The Molecular Scattering of Light in a Binary Liquid-Mixture.* By Prof. C. V. RAMAN, F.R.S.*

IN the Philosophical Magazine for March 1927 appears a note under this title by Dr. K. C. Kar, purporting to be a criticism of the theory of light-scattering† in liquid-mixtures developed some years ago by the present writer with Dr. Ramanathan. An examination of the note shows it to be based entirely on a misconception.

In his classical paper on critical opalescence, A. Einstein‡ discussed the scattering of light in liquid-mixtures, considering, however, only the optical effect due to the local fluctuations of composition occurring in the mixture. The object of the paper by the present writer with Dr. Ramanathan in the Philosophical Magazine for January 1923 was, in the first place, to emphasize that the local fluctuations of density in the mixture have also to be taken into account, and in the second place, to show how by considering these two effects together with the influence of the optical anisotropy of the molecules, the observed facts of light-scattering in mixtures may be explained. The formulæ necessary for our purpose were deduced in a perfectly simple and straightforward fashion, in terms of experimentally measurable quantities, from the well-known relation between entropy and thermodynamical probability. It was shown that they furnished a satisfactory explanation of the remarkable changes in the intensity and polarization of the scattered light which occur when the composition of the mixture and its temperature are varied. Subsequent experimental work in the field has fully supported our conclusions§. R. Gans||, who followed us, quotes our formulæ with approval, and indeed has checked their correctness by following a method of derivation differing in detail from ours. He also points out¶, as is indeed quite obvious, that the expression for the fluctuations of composition is obtained in the form given by Einstein only when the specific volume of the mixture is neglected in comparison with that of the vapour. The same result is also clearly seen in our paper, as also in the earlier work of Zernike**. The correction involved is, however, usually quite negligible.

We hardly think that any reader of our paper of 1923 would have found a difficulty in following our arguments or

* Communicated by the Author.

† C. V. Raman and K. R. Ramanathan, *Phil. Mag.* xlv. p. 213 (1923).

‡ A. Einstein, *Ann. d. Physik*, xxxiii. p. 1275 (1910).

§ See, for instance, J. C. K. Rav, *Phys. Rev.* xxii. p. 78 (1923).

|| R. Gans, *Zeit. f. Physik*, xvii. p. 353 (1923).

¶ R. Gans, 'Contribucion estudio de las ciencias, La Plata,' vol. iii. (footnote on page 290, 1923).

** F. Zernike, Doctorate Thesis, Amsterdam (1914).

checking the correctness of the formulæ deduced. Dr. Kar, however, appears to have set out with a fixed idea that there must be some error in our work, and in trying to unearth it falls into various errors himself. Most of his troubles arise from his having failed to notice that the mechanism of the process we follow in our paper is different from that of Einstein, and indeed is somewhat simpler. Whereas Einstein finds merely the work necessary to change the concentration of the mixture by an infinitesimal amount from one value to another, both differing from that of the bulk of the mixture, we, on the other hand, evaluate directly the total work necessary to change the concentration of a small volume of the mixture from its normal (mean) value to one slightly different. For this purpose a volume $m_1 \Delta k v_2$ of the vapour of the second component is withdrawn from the main reservoir, and is then pushed into the smaller reservoir, which has *initially* the same concentration, the latter being altered as the result of the process. The whole volume pushed in is $m_1 \Delta k v_2$, and the partial pressure in the smaller reservoir is initially p_2 , and rises spontaneously and gradually to $p_2 + \Delta p_2$ at the end of the process. The work done in the process is obviously equal to the total volume pushed in, multiplied by the mean of the initial and final pressures. It is not necessary, as Dr. Kar seems to imagine, to compress the vapour initially to a higher pressure. Indeed, if this were done, the process would not be reversible.

When the error indicated above in Dr. Kar's work is set right, there is little in his communication left to comment upon. He refers in his note to a paper by him published in the *Physikalische Zeitschrift*. In view of the fact, however, that this and other writings of his on light-scattering have already been subjected to criticism by Fürth*, by Ornstein and Zernicke†, and by Mitra‡, it would appear that no useful purpose would be served by discussing them further in the pages of the Philosophical Magazine.

210 Bowbazar Street, Calcutta,
31st March, 1927.

Note added in proof, dated 27th July, 1927.—In a paper appearing in the 'Indian Journal of Physics,' vol. ii., the present writer has discussed the relation between light-scattering and osmotic pressure in solutions. The formulæ obtained are in complete agreement with those given in the Philosophical Magazine for January 1923, when the known relation between osmotic pressure and vapour tension is kept in view.

* R. Fürth, *Phys. Zeit.* xxv. p. 111 (1924).

† L. S. Ornstein and F. Zernike, *Phys. Zeit.* xxvii. p. 761 (1926).

‡ M. N. Mitra, *Ind. Journ. Phys.* i. p. 137 (1926).

XLI. *Note on Green's Lemma and Stokes's Theorem.* By A. J. CARR, M.A., Lecturer in Mathematics, Bradford Technical College *.

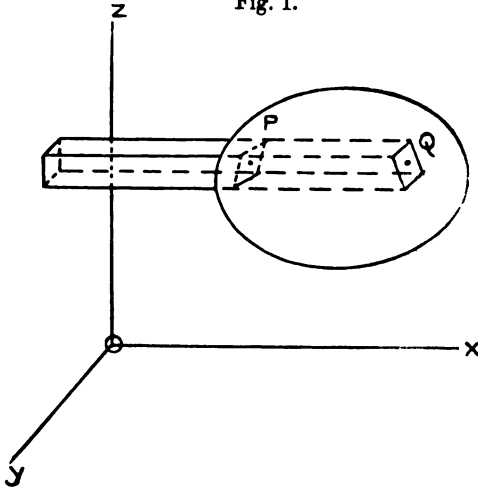
§ 1. MY attention was recently drawn to weak points in the usual proof of Green's Lemma as employed in at least seven treatises on various branches of Applied Mathematics; quite as many have also faulty proofs of Stokes's Theorem. The object of this paper is to expose and also to correct these discrepancies.

I shall deal first with the well-known Green's Lemma, viz.,

$$\iiint_{v_0} \left(\frac{\partial U}{\partial x} + \frac{\partial V}{\partial y} + \frac{\partial W}{\partial z} \right) dx dy dz = \iint_S (lU + mV + nW) dS.$$

Except in treatises on Analysis, this is always proved by

Fig. 1.



taking a figure such as that in the diagram and stating that

$$\begin{aligned} & \iiint \frac{\partial U}{\partial x} dx dy dz \\ &= \iint (U_Q - U_P) dy dz \\ &= \iint [U_Q l_Q dS_Q - U_P (-l_P) dS_P] \\ &= \iint U l dS, \end{aligned}$$

taken over the whole bounding surface.

* Communicated by the Author.

This is undoubtedly true. In fact,

$$\begin{aligned} & \iiint \left(\frac{\partial U}{\partial x} + \frac{\partial V}{\partial y} + \frac{\partial W}{\partial z} \right) dx dy dz \\ &= \iiint \frac{\partial U}{\partial x} dx dy dz + \iiint \frac{\partial V}{\partial y} dx dy dz + \iiint \frac{\partial W}{\partial z} dx dy dz \\ &= \iint_S U dS_1 + \iint_S V dS_2 + \iint_S W dS_3. \end{aligned}$$

But these integrals can *not* be grouped together and written as

$$\iint_S (lU + mV + nW) dS ;$$

for dS_1 is the section made at (x, y, z) on S by a prism $dy dz$ parallel to Ox , dS_2 that made by $dz dx$ parallel to Oy , dS_3 by $dx dy$ parallel to Oz . These are three different elementary areas, for in general it is not possible to subdivide a surface S in such a way that dS always, or indeed ever, projects into $dy dz$, $dz dx$, $dx dy$, on the three co-ordinate planes, so that we cannot say, "Similarly for $\iiint (\partial V / \partial y) dx dy dz$, $\iiint (\partial W / \partial z) dx dy dz$. Hence etc." (v. § 4 *post.*).

§ 2. Green's Lemma is of course true, but the proof should be handled so that the surface is only subdivided in *one* way. To do this we notice that if

$$x = f_1(u, v, w), \quad y = f_2(u, v, w), \quad z = f_3(u, v, w) . \quad (1)$$

where (u, v, w) is any other system of co-ordinates, then a surface whose equation is (say)

$$F(x, y, z) = 0 \quad . \quad . \quad . \quad . \quad . \quad (2)$$

establishes between u, v, w such a relation as

$$w = \phi_1(u, v), \quad . \quad . \quad . \quad . \quad . \quad (3)$$

and on substituting in x, y, z , we find

$$x = \psi_1(u, v), \quad y = \psi_2(u, v), \quad z = \psi_3(u, v). \quad (4)$$

These new equations can therefore replace (2).

Moreover, if another surface

$$F_1(x, y, z) = 0 \quad . \quad . \quad . \quad . \quad . \quad (5)$$

or

$$w = \phi_2(u, v) \quad . \quad . \quad . \quad . \quad . \quad (6)$$

intersect (2) in some curve, the equation of this curve can be put as

$$w = \phi_1(u, v) = \phi_2(u, v),$$

i. e. $v = \lambda(u)$

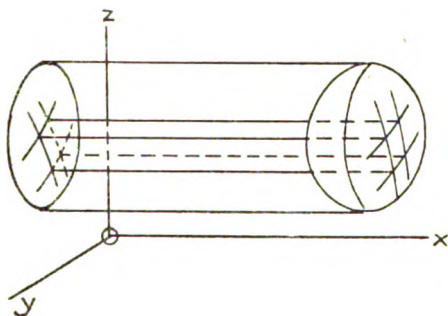
or $u = g(\theta), \quad v = h(\theta);$

whence

$$x = \xi(\theta), \quad y = \eta(\theta), \quad z = \zeta(\theta).$$

As u, v can be represented in a plane, the surface (2) bounded by the curve in which it is cut by (5) is transformed into a region of the (u, v) plane bounded by the corresponding curve. The parallels to $O'u, O'v$ respectively are transformed into the curves on $F=0$, in which this surface is cut by the surfaces $u=\text{const.}, v=\text{const.}$, and this is the single method of subdivision which should replace the three independent ones usually adopted for Green's Lemma. These curves project

Fig. 2.



into curves $u=\text{const.}, v=\text{const.}$ on the yz plane, upon which

$$y = \psi_2(u, v), \quad z = \psi_3(u, v),$$

the bounding curve C_1 being the projection of C , the locus of the points at which parallels to Ox touch the surface. This latter may be supposed the curve above referred to as the intersection of F, F_1 .

The superficial area dS between

$$u = \alpha, \quad u = \alpha + d\alpha, \quad v = \beta, \quad v = \beta + d\beta,$$

projects into $ldS = d\alpha d\beta \cdot \partial(y, z)/\partial(\alpha, \beta)$, and here we can use "similarly" and say that dS projects on the zx and xy planes respectively into $mdS = d\alpha d\beta \cdot \partial(z, x)/\partial(\alpha, \beta)$, $ndS = d\alpha d\beta \cdot \partial(x, y)/\partial(\alpha, \beta)$. If on the yz plane we apply

the intermediate transformation (y', z') , where

$$y' = u, \quad z' = z = \psi_3(u, v) = \psi_3(y', v),$$

so that

$$v = \pi(y', z')$$

or

$$y = \psi_2(y', v) = \pi_1(y', z'), \quad z = z';$$

then

$$ldS = du dv \cdot \partial(y, z) / \partial(u, v)$$

$$= du dv \cdot \frac{\partial(y, z)}{\partial(y', z')} \cdot \frac{\partial(y', z')}{\partial(u, v)}$$

$$= du \frac{\partial \pi_1(y', z')}{\partial y'} \cdot \frac{\partial \psi_3(u, v)}{\partial v} dv$$

$$= du \frac{\partial y}{\partial u} \cdot \frac{\partial z}{\partial v} dv$$

$$= dy_u dz_v.$$

This, of course, is really equivalent to writing

$$z = \psi_3(u, v), \quad \text{i. e.} \quad v = \pi(u, z), \quad y = \psi_2(u, v) = \pi_1(u, z);$$

whence

$$\partial(y, z) / \partial(u, v) = \partial y / \partial u \cdot \partial z / \partial v,$$

since y, z are independent variables inside S_1 , the region on the yz plane bounded by the closed contour C_1 .

Similarly $mdS = dz_u dx_v$, $ndS = dx_u dy_v$, equivalent to what Applied Mathematical writers usually express as $ldS = dx dy$, $mdS = dy dz$, $ndS = dz dx$. But notwithstanding that these last three equations can never be made wholly consistent, we can none the less prove that $\iint_{S_1} \mu dy dz$ is equal to $\iint_{S_1} u d\sigma_1$, where

$$d\sigma_1 = du dv \cdot \partial(y, z) / \partial(u, v) \neq dy dz,$$

for both these integrals are equal to the volume of the cylinder whose "upper" surface is given by $x = \mu(y, z)$, and whose section on the yz plane has been subdivided in two different ways, firstly by parallels to Oy, Oz , secondly by the two systems of curves u, v .

Hence results which are true for the limiting case of an aggregate of elements are not necessarily true for the finite individual elements, however small these be.

§ 3. All this discussion leads to

$$\begin{aligned} I_1 &= \iiint_{V_0} \partial U / \partial x \cdot dx dy dz = \iint dy dz \int_{x_1}^{x_2} \partial U / \partial x \cdot dx \\ &= \iint [U(x_2, y, z) - U(x_1, y, z)] dx dy, \end{aligned}$$

where $x_2 = \mu_2(y, z)$, $x_1 = \mu_1(y, z)$ are the equations to the

"upper" and "lower" parts of S . That is,

$$\begin{aligned} I_1 &= \iint_S U dy dz \text{ extended over the whole exterior surface,} \\ &= \iint_{s_1} U [\mu(y, z), y, z] d\sigma_1 \\ &= \iint_{s_1} U \partial(y, z) / \partial(u, v) \cdot du dv \\ &= \iint_S U l dS; \end{aligned}$$

and

$$\begin{aligned} I &= \iiint_{V_0} (\partial U / \partial x + \partial V / \partial y + \partial W / \partial z) dx dy dz \\ &= I_1 + I_2 + I_3 \\ &= \iint U l dS + \iint V m dS + \iint W n dS \\ &= \iint_S (lU + mV + nW) dS, \end{aligned}$$

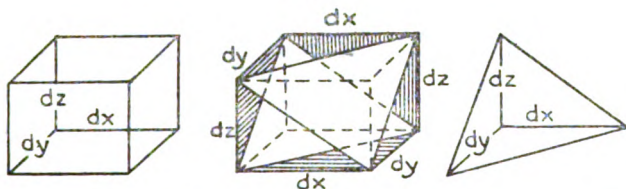
where dS is now the same in each integral.

This method of subdivision would appear to point to the existence in space of n dimensions of the analogue to Green's Lemma for an n -tuple and an $(n-1)$ -tuple integral, viz.,

$$\begin{aligned} &\iint \dots \left(\sum_{r=1}^n \partial U_r / \partial x_r \cdot dx_1 dx_2 \dots dx_n \right) \\ &= \iint \dots \left(\sum_{r=1}^n (-)^{n-r} U_r \frac{\partial(x_1, \dots, x_{r-1}, x_{r+1}, \dots, x_n)}{\partial(u_1, \dots, u_{n-1})} du_1 du_2 \dots du_{n-1} \right). \end{aligned}$$

§4. Again, Stokes's very important theorem is frequently proved by supposing it possible to divide up a surface into elements, each of which projects into rectangles $dy dz$, $dz dx$, $dx dy$ on the three co-ordinate planes. It is easy to see, however, from an elementary parallelepiped that no such surface can exist. True, a triangle can project into triangles of areas $dy dz/2$, $dz dx/2$, $dx dy/2$, but no surface other than a plane can be subdivided into such a set of contiguous triangles, all of which satisfy this condition.

Fig. 3.



However, by striating the surface by the u, v curves we can obtain results which will apply directly to n dimensions,

if we suppose a "diaphragm" given by the variables u, v such that

$$x_r = f_r(u, v) \quad (r=1, 2, \dots, n)$$

and bounded by a closed "contour" C , for which

$$u = \phi_1(\theta), \quad v = \phi_2(\theta).$$

The diaphragm and its bounding contour then transform into a region A of the (uv) plane bounded by a plane curve γ , and

$$\begin{aligned} J_n &= \int_C \sum X dx \\ &= \int_\gamma \left\{ \left(\sum_{r=1}^n X_r \frac{\partial x_r}{\partial u} \right) du + \left(\sum_{r=1}^n X_r \frac{\partial x_r}{\partial v} \right) dv \right\} \\ &= \iint_A \left\{ \frac{\partial}{\partial u} \left(\sum_{r=1}^n X_r \frac{\partial x_r}{\partial v} \right) - \frac{\partial}{\partial v} \left(\sum_{r=1}^n X_r \frac{\partial x_r}{\partial u} \right) \right\} du dv, \end{aligned}$$

applying "Green's Theorem" in two dimensions*. That is,

$$\begin{aligned} J_n &= \iint_A \sum_{r=1}^n \left(\frac{\partial X_r}{\partial u} \frac{\partial x_r}{\partial v} - \frac{\partial X_r}{\partial v} \frac{\partial x_r}{\partial u} \right) du dv \\ &= \iint_A [v, u] du dv, \end{aligned}$$

where $[v, u]$ is the Lagrange bracket-expression for the set of variables (x_r, X_r) . The formula may be left in this shape, but is preferably extended to

$$\begin{aligned} J_n &= \iint_A \sum_{r=1}^n \left(\frac{\partial x_r}{\partial v} \sum_{s=1}^n \frac{\partial X_r}{\partial x_s} \frac{\partial x_s}{\partial u} - \frac{\partial x_r}{\partial u} \sum_{s=1}^n \frac{\partial X_r}{\partial x_s} \frac{\partial x_s}{\partial v} \right) du dv, \\ &= \iint_A \sum_{r=1}^n \sum_{s=1}^n \frac{\partial X}{\partial x_s} \frac{\partial (x_s, x_r)}{\partial (u, v)} du dv, \end{aligned}$$

or again,

$$= \iint_A \sum_{r,s} \left(\frac{\partial X_s}{\partial x_r} - \frac{\partial X_r}{\partial x_s} \right) \frac{\partial (x_r, x_s)}{\partial (u, v)} du dv,$$

the summation being extended over all pairs of the variables.

Putting $x_1 = x, x_2 = y, x_3 = z$; $X_1 = X, X_2 = Y, X_3 = Z$, the special case of three dimensions yields at once the original

* Goursat, 'Mathematical Analysis' (Hedrick's transl. 1904), § 126.

Stokes's theorem, viz.,

$$\begin{aligned} J_3 &= \int_C \left(X \frac{dx}{ds} + Y \frac{dy}{ds} + Z \frac{dz}{ds} \right) ds \\ &= \iint_A \left\{ \left(\frac{\partial Z}{\partial y} - \frac{\partial Y}{\partial z} \right) \frac{\partial(y, z)}{\partial(u, v)} + \left(\frac{\partial X}{\partial z} - \frac{\partial Z}{\partial x} \right) \frac{\partial(z, x)}{\partial(u, v)} \right. \\ &\quad \left. + \left(\frac{\partial Y}{\partial x} - \frac{\partial X}{\partial y} \right) \frac{\partial(x, y)}{\partial(u, v)} \right\} du dv \\ &= \iint_S \left\{ l \left(\frac{\partial Z}{\partial y} - \frac{\partial Y}{\partial z} \right) + m \left(\frac{\partial X}{\partial z} - \frac{\partial Z}{\partial x} \right) \right. \\ &\quad \left. + n \left(\frac{\partial Y}{\partial x} - \frac{\partial X}{\partial y} \right) \right\} dS \quad (v. \S 2). \end{aligned}$$

J_3 may also be exhibited as the sum of three *separate* integrals,

$$\begin{aligned} J_3 &= \iint \left(\frac{\partial Z}{\partial y} - \frac{\partial Y}{\partial z} \right) dy dz + \iint \left(\frac{\partial X}{\partial z} - \frac{\partial Z}{\partial x} \right) dz dx \\ &\quad + \iint \left(\frac{\partial Y}{\partial x} - \frac{\partial X}{\partial y} \right) dx dy. \end{aligned}$$

It is not, however, legitimate to group them under one integral sign, since this implies that dx, dy, dz are taken at the point (x, y, z) , thus forming on the surface an elementary parallelepiped which can in no wise be transformed into an element of surface.

In fact, generally,

$$J_n = \sum_{r,s} \iint \left(\frac{\partial X_s}{\partial x_r} - \frac{\partial X_r}{\partial x_s} \right) dx_r dx_s.$$

§ 5. Since writing the foregoing, I have been reminded that Clerk Maxwell uses a somewhat similar proof*; but on examining his proof, it does not seem to me quite so general as the one given above. For instance, one of his α (or u) curves must coincide with the contour S . But we have seen that this is not at all necessary, it being more convenient to notice that on this contour a relation exists between u, v which transforms it into a plane closed curve on the uv plane. Besides, Maxwell's proof does not draw out the essential fact that Stokes's Theorem is but Green's Theorem in two dimensions for a skew curve bounding a non-planar surface. Goursat† does use this, but his method

* 'Electricity and Magnetism,' vol. i. § 24.

† *Loc. cit.* § 136.

applies only to three dimensions, depending as it does, essentially on the direction-cosines of the normal at a point of the surface and not showing that Stokes's Theorem is reduced to Green's Theorem *entirely* by a transformation to any uv plane.

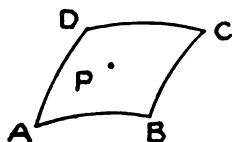
The importance of the n -dimensional form of Stokes's Theorem is seen in such problems as the dynamical one involving the reduction of the relative integral-invariant $\int \Sigma p dq$ to the absolute integral-invariant $\iint [\lambda, \mu] d\mu d\lambda$, where μ, λ do not vary with the time t , but are characteristic solely of the trajectory on which lies the point (q_1, q_2, \dots, q_n) , the sufficient condition for the reduction being the existence of a function $H(q_1, q_2, \dots, q_n, p_1, p_2, \dots, p_n, t)$, such that

$$dq_r/dt = \partial H / \partial p_r, \quad dp_r/dt = -\partial H / \partial q_r^*.$$

Here is implied the $\mu\lambda$ (or uv) transformation, but no proof is given. Indeed, I have not before seen a proof depending on such a transformation. Most proofs in Applied Mathematical treatises rely on striating a surface and then taking three points respectively inside the projections (supposed $dydz, dzdx, dx dy$) of a typical cell whose area is dS .

§ 6. This method, which uses no transformation, can quite adequately and far less erroneously be analysed by taking a point inside the cell itself instead of in its projections, the striating curves being, as before, $u = \text{const.}$, $v = \text{const.}$

Fig. 4.



For take $P(u = \alpha, v = \beta)$ at the centre of a typical cell ABCD, where, on AB, $v = \beta - d\beta/2$, and on BC, $u = \alpha + d\alpha/2$, while on CD, $v = \beta + d\beta/2$, DA being $u = \alpha - d\alpha/2$; also, for brevity, let $f^{(u)} = \partial f(u, v) / \partial u$, etc. Then, since always,

$$\begin{aligned} \int \Sigma X dx &= \int \Sigma [X \cdot x^{(u)} du + X \cdot x^{(v)} dv] \\ &= \int [F_1(u, v) du + F_2(u, v) dv] \quad (\text{say}), \end{aligned}$$

Whittaker, 'Analytical Dynamics,' § 136.

we have

$$\begin{aligned}\int_{AB} \sum_1^n X_r dx_r &= \int_{\alpha-d\alpha/2}^{\alpha+d\alpha/2} F_1(u, \beta-d\beta/2) du \\ &= \int_{\alpha-d\alpha/2}^{\alpha+d\alpha/2} [F_1(\alpha, \beta) + (u-\alpha)F_1^{(\alpha)}(\alpha, \beta) \\ &\quad - (d\beta/2) \cdot F_1^{(\beta)}(\alpha, \beta)] du.\end{aligned}$$

So

$$\begin{aligned}\int_{CD} \sum_1^n X_r dx_r &= \int_{\alpha+d\alpha/2}^{\alpha-d\alpha/2} F_1(u, \beta+d\beta/2) du \\ &= - \int_{\alpha-d\alpha/2}^{\alpha+d\alpha/2} [F_1(\alpha, \beta) + (u-\alpha)F_1^{(\alpha)}(\alpha, \beta) \\ &\quad + (d\beta/2) \cdot F_1^{(\beta)}(\alpha, \beta)] du.\end{aligned}$$

Hence

$$\begin{aligned}\int_{AB} + \int_{CD} &= -d\beta \int_{\alpha-d\alpha/2}^{\alpha+d\alpha/2} F_1^{(\beta)}(\alpha, \beta) du \\ &= -d\beta \cdot F_1^{(\beta)}(\alpha, \beta) d\alpha.\end{aligned}$$

Thus

$$\int_{BC} + \int_{DA} = +d\alpha \cdot F_2^{(\alpha)}(\alpha, \beta) d\beta.$$

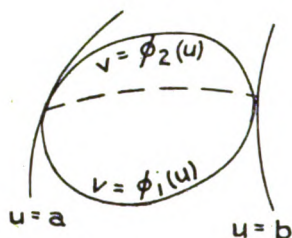
Adding,

$$\begin{aligned}\int_{ABCD} \sum X dx &= [F_2^{(\alpha)}(\alpha, \beta) - F_1^{(\beta)}(\alpha, \beta)] d\alpha d\beta \\ &= \sum_1^n \left\{ \frac{\partial}{\partial \alpha} [X_r \cdot x_r^{(\beta)}] - \frac{\partial}{\partial \beta} [X_r \cdot x_r^{(\alpha)}] \right\} d\alpha d\beta \\ &= \sum_1^n \left\{ \frac{\partial X_r}{\partial \alpha} \frac{\partial x_r}{\partial \beta} - \frac{\partial X_r}{\partial \beta} \frac{\partial x_r}{\partial \alpha} \right\} d\alpha d\beta \\ &= [\beta, \alpha] d\alpha d\beta = f(\alpha, \beta) d\alpha d\beta \quad (\text{say}).\end{aligned}$$

From this point onward the proof proceeds on exactly the same lines as the transformation one. This method, however, seems to me unsatisfactory for an *Applied Mathematics* book, for it entails rigorous discussions of the integrals round irregular partitions at the contour itself, and for n dimensions we cannot determine, except in imagination by analogy with three dimensions, what sort of thing a contour may be,—and in any case such discussion is interesting largely to pure mathematicians, who will find the proof for three dimensions

in Goursat, *loc. cit.* § 124. For if we take $u=a$, $u=b$ to be the bounding curves and let the "lower" and "upper" portions of the contour have equations $v=\phi_1(u)$, $v=\phi_2(u)$

Fig. 5.



respectively, then we only need to put u for x , v for y , and Goursat's discussion of the double integral

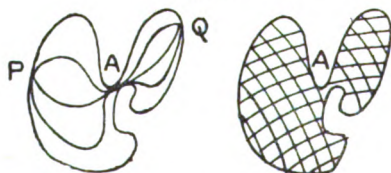
$$\int_a^b dx \int_{y=\phi_1(x)}^{y=\phi_2(x)} f(x, y) dy$$

holds word for word for our integral, viz.,

$$\int_a^b du \int_{v=\phi_1(u)}^{v=\phi_2(u)} f(u, v) dv.$$

The same writer's proof of Stokes's Theorem has already been referred to. That it is three dimensional only is a charge which can also be levelled against that of Jeans* and O. W. Richardson†. Their proof somewhat resembles my second one above, if we write d for $du \cdot \partial/\partial u$ and δ for $dv \cdot \partial/\partial v$, so that $\partial(y, z)/\partial(u, v) \cdot du dv$ becomes $(dy \delta z - dz \delta y)$. Their method, viz. of varying the path of integration from P to Q , would hardly seem to hold good for a curve such as

Fig. 6.



that shown; the various paths would become terribly congested at A . The uv striation method, however, is obviously still sound.

* Math. Theory of Elec. § 439 (3rd ed).

† 'Electron Theory of Matter,' pp. 91-94 (1916).

Summary.

(1) The usual proofs for Green's Lemma and Stokes's Theorem to be found in most Applied Mathematical books are incorrect in that they assume it possible to subdivide a curved surface into elements, each of which has the three projections $dydz$, $dzdx$, xdy . No such element (and, *a fortiori*, surface) can even be realized.

(2) It is easy to substitute a proof which depends on a single change of variables (x, y, z) to (u, v) , thereby transforming a curved surface into a plane one and its skew contour into a plane curve. To the new plane region we apply the two-dimensional form of Green's Theorem.

(3) Alternatively, we can attack Stokes's Theorem directly (as is usually done in text-books), without reference to a plane region.

(4) For Stokes's Theorem, either of these two methods can be extended to n dimensions, a fact which does not hold with respect to any of the proofs I have so far seen. In particular, Eddington * proves Stokes's Theorem for four dimensions as a *tensor* equation. Here, however, no such limitation is imposed.

XLII. *Light-Quanta and Maxwell's Equations.*

By N. RASHEVSKY †.

IN a recent interesting paper, published in this Magazine, Prof. N. P. Kasterin ‡ made an attempt to show that, in spite of the generally accepted opinion, the conception of light corpuscles is compatible with Maxwell's equations and that the form of the light-quantum theory which has been proposed by Sir J. J. Thomson § may be obtained as a particular solution of Maxwell's equations, provided we also consider discontinuous solutions of these equations.

The whole question having an importance of principle, it may be of interest to discuss here somewhat at length some of the difficulties to which Prof. Kasterin's solution leads. It should, however, be emphasized at once that it is not intended by the following to reject the solution of the problem proposed by Prof. Kasterin, but rather to contribute to a clearing of this fundamental question.

As long as we consider Maxwell's theory only as a set

* Math. Theory of Relativity, § 32.

† Communicated by Prof. Dr. A. H. Bucherer.

‡ Phil. Mag. [7] ii. p. 1208 (1926).

§ Phil. Mag. [6] xlviii. p. 737 (1924), and l. p. 1182 (1925).

of mathematical equations, nothing forbids us to admit the possibility of any kind of discontinuities in their solutions. However, the physical interpretation of the equations leads of necessity to a certain interpretation of the discontinuities, and this brings certain difficulties.

Namely, if we say that the equations

$$\text{Curl } \mathbf{M} - \frac{1}{c} \frac{\partial \mathbf{E}}{\partial t} = 0, \quad (1)$$

$$\text{Curl } \mathbf{E} + \frac{1}{c} \frac{\partial \mathbf{M}}{\partial t} = 0, \quad (2)$$

$$\text{div } \mathbf{E} = 0, \quad (3)$$

$$\text{div } \mathbf{M} = 0, \quad (4)$$

hold for the "free æther," while for space containing electric charges equations (1) and (3) acquire the form

$$\text{Curl } \mathbf{M} - \frac{1}{c} \frac{\partial \mathbf{E}}{\partial t} = \frac{\rho \mathbf{v}}{c}, \quad (1a)$$

$$\text{div } \mathbf{E} = \rho, \quad (3a)$$

we to a certain extent *define* hereby what is meant by "free æther," namely the region where $\rho=0$.

The circumstance that (2) and (4) remain in the classical theory unaltered in any case, expresses the fact that the space (or the æther) is *always free of magnetic charges*, in other words that true magnetic charges do not exist.

In the same way (1a) and (3a) must be considered as *defining* the charge density ρ and the current density $\rho \mathbf{v}$, since we can observe and detect a charge and a current *only* by their action, that is *by their field*. In other words, whenever the expression

$$\text{Curl } \mathbf{M} - \frac{1}{c} \frac{\partial \mathbf{E}}{\partial t} \quad (5)$$

$$\text{or} \quad \text{div } \mathbf{E} \quad (6)$$

differs from zero, we say that a current, viz. a charge, is present.

Now, if we consider any solution of (1), (2), (3), and (4), which at certain points or surfaces presents discontinuities, we shall generally find that (5) and (6) will be different from zero at these points or surfaces. Hence the surfaces of discontinuity will behave like surface currents or surface charges. And since, as said above, we *define* a current or a charge by its *behaviour*, we conclude that the assumption of discontinuities in the field is equivalent to the assumption

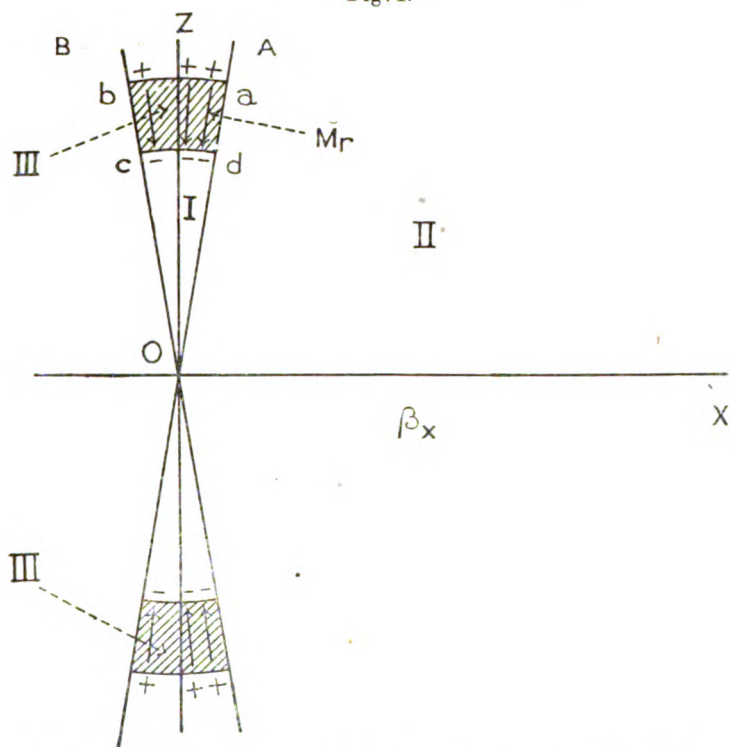
of the presence of currents and charges in this field. Hence we can no longer talk about "free æther."

To a certain extent we may say that the free æther is *per definitionem* continuous.

If we now turn to a particular case considered by Prof. Kasterin, we see that there are three kinds of discontinuities present.

First the discontinuity of the normal component of the magnetic vector at the surface of the ring, constituting the light-quantum, M_r . This physically amounts to assuming *true magnetic charges* to be carried with the quantum, or that the quantum constitutes a magnetic double layer as shown on the figure below, which is essentially the same as

Fig. 1.

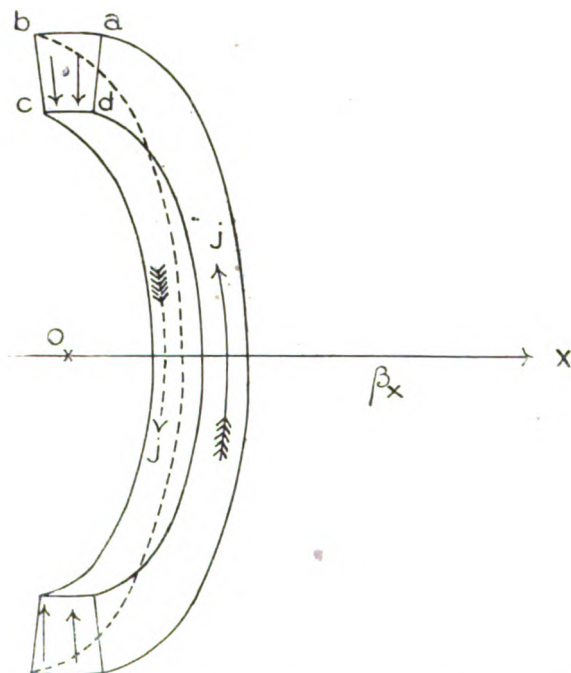


in Prof. Kasterin's paper. This, may be, is after all not such a difficulty as appears at first sight. But there is also a second discontinuity, namely that of the tangential component E_a of the electric vector at the surface $abcd$.

This causes the appearance of the surface-curl of the amount E_a on the boundary of the ring*. Hence on the surface on the ring $\text{Curl } \mathbf{E}$ is not equal to zero, but has a constant value. Therefore we must assume that on the surface $\frac{\partial M}{\partial t}$ is also different from zero, which would contradict the assumption, on which is based the whole deduction of Prof. Kasterin, that the field is independent of time in the system of coordinates moving with the quantum.

It seems therefore necessary to assume the existence of a true magnetic current.

Fig. 2.



A third discontinuity is that of the tangential component of the magnetic vector M_r on the surfaces ad and bc . This gives rise to a surface curl of M , having only the component M_a . This would correspond to a convection current having the direction indicated by the arrows j on fig. 2. The current on the surface ad has therefore an opposite direction, that of bc . It may be remarked that such a

* Cf. M. Abraham, 'Theorie der Elektrizität,' i. § 22 (Teubner: Leipzig & Berlin, 1921).

system of currents would be just equivalent to the magnetic double layer, which we must assume as shown above. Thus it seems to be unnecessary to assume true magnetic charges. But anyhow such a system of surface-currents would not account for the existence of the surface curl of E . And furthermore it is difficult to interpret physically the existence of such a surface electric convection current in the light-quantum.

For either we must assume that the light-quantum carries not only energy but also electric charge, or we must admit that the two opposite currents on the surfaces bc and ad are constituted by two opposite charges, spread continuously over the surface, moving in the same direction. But this would cause an X -component of E to appear in the region III.

Thus we see that the simple solution proposed by Prof. Kasterin does not satisfy entirely Maxwell's equations, if only we confine ourselves to "free æther" not containing any charges. It is of course not proved hereby that a more complicated solution, showing the properties of a light-quantum, may not exist. But it seems that the structure of such a light-quantum will be anyhow far more complicated than that assumed by Sir J. J. Thomson, although it may have the same general features.

The way to escape the difficulties just discussed seems to be to assume that the equations (1)–(4) hold only *inside* the ring, while on the boundary and in outside space neither (1)–(4) nor (1a) and (3a) do hold. In other words, we have to assume that there is *no field* at all outside of III. The difference should be emphasized here between the two statements: the field has a value zero, or there is no field at all. The first one describes a particular state of the æther free of disturbances; while the second means that outside of III there is *no æther at all*. The quantum would thus be a *ring of æther, moving in absolute empty space*. This, however, would make it difficult to account for the waves accompanying the quantum according to Sir J. J. Thomson's theory.

The discussion by Prof. Kasterin on p. 1212 (*l.c.*), which is not quite clear to me, seems to indicate a similar idea. But in such a case there is no reason to consider, as Prof. Kasterin does, the solution $M=E=0$ for the regions I and II. It should be remarked that whatever the possibilities presented by such a conception are, it would lead to a radical change of our conception of charge, and would necessitate an interpretation of (1a) and (3a) which is essentially different from that made at present.

Returning now finally to the principal question, mentioned at the beginning of Prof. Kasterin's paper, as to whether the conception of light-quanta contradicts Maxwell's equations in their usual interpretation, the following may be said.

That the propagation of energy in spherical waves does not necessarily follow from Maxwell's equations is not new. C. W. Oseen* has found a solution, which represents with any required approximation an unidirectional flow of electromagnetic energy.

But even for the solutions represented by the retarded potentials, as used in the electron theory of H. A. Lorentz, the possibility of an unidirectional radiation is not excluded.

In the electron theory we are led to consider expressions of the kind :

$$\phi(x, y, z, t) = \int \frac{\psi(x_1, y_1, z_1, t - \frac{r}{c})}{[r]} dx_1 dy_1 dz_1, \quad (7)$$

$$r = \sqrt{(x-x_1)^2 + (y-y_1)^2 + (z-z_1)^2},$$

where the bracket denotes that the value of r has to be taken for the time $t' = t - \frac{r}{c}$.

Consider the case where ψ is of the form :

$$\psi = \theta(x_1, y_1, z_1) \sin \nu t.$$

If now the region in which θ is different from zero is small, and the distance from this region to the point x, y, z at which we seek the function ϕ is large, then we may consider r in the denominator as constant and have :

$$\begin{aligned} \phi(x, y, z, t) &= \frac{1}{r} \int \theta(x_1, y_1, z_1) \\ &\times \sin \nu \left(t - \frac{\sqrt{(x-x_1)^2 + (y-y_1)^2 + (z-z_1)^2}}{c} \right) dx_1 dy_1 dz_1. \end{aligned} \quad (8)$$

For small ν , $\sin \nu \left(t - \frac{r}{c} \right)$ varies only slowly with x_1, y_1, z_1 and therefore will be nearly constant over the region, where $\theta(x_1, y_1, z_1)$ is appreciably different from zero. We then have :

$$\begin{aligned} \phi(x, y, z, t) &= \frac{\sin \nu \left(t - \frac{r}{c} \right)}{r} \int \theta(x_1, y_1, z_1) dx_1 dy_1 dz_1 \\ &= \text{Const} \frac{\sin \nu \left(t - \frac{r}{c} \right)}{r}, \quad \dots \dots \dots (9) \end{aligned}$$

* *Ann. d. Phys.* lxi. p. 202 (1922).

and ϕ depends only on r : that is, the field is propagated in a spherical wave.

But if ν is very large, or the region in which θ differs from zero is large, we can no longer use (9). We must go back to (8), and we see that the integral is a function in general of x, y, z ; that is, ϕ depends not only on r but also on the direction. The form of this function depends on the choice of $\theta(x_1, y_1, z_1)$, and the possibility is not *a priori* excluded that ϕ will be such a function of x, y, z as will correspond to an unidirectional radiation. Now on the classical electron theory, θ and ν are always such as to justify (9). However, according to the new conception of E. Schrödinger, the electron can no more be considered as sharply limited, and in the lower quantum states the electric charge-density occupies a more extended region*. The electric charge, according to this theory, has also a complicated "internal structure." Furthermore, the light-waves are considered as difference vibrations of waves of much higher frequency. Hence, in Schrödinger's theory there is a tendency to increase the region in which θ is different from zero, as well as to increase ν . Under such conditions the transition from (8) to (9) may appear doubtful and the formula (8) to be preferred, which makes possible highly asymmetric waves, having, maybe, properties similar to light-quanta. If the fundamental waves are directed, the same will be true for waves formed by the difference vibrations.

We may probably construct a similar "energy-parcel" of the electromagnetic waves, as of the waves of Schrödinger's field-scalar ψ .

All this is, of course, very speculative, but as long as the proof of the *impossibility* of the solution of the problem, suggested here, is not given, it seems to be premature to believe in a contradiction between Maxwell's equations and the theory of directed elementary radiation.

Research Department,
Westinghouse Electric and Manufacturing Co.,
East Pittsburgh, Pa.
January 5, 1927

Note added with proof (July 20, 1927).—In the meantime a paper by G. Breit has appeared (Journ. Opt. Soc. of America, xiv. p. 374 (1927)) which in a way seems to confirm the above speculations. Breit shows that unidirectional quanta must be emitted on basis of Schrodinger's wave-mechanics, and this because of the asymmetry of the charge-motion in the atom.

* Cf. especially *Naturwissenschaften*, July 9, 1926, p. 664.
Phil. Mag. 8. 7. Vol. 4. No. 22. Sept. 1927. 2 H

XLIII. Optical Excitation of Mercury, with Controlled Radiating States and Forbidden Lines. By Prof. R. W. WOOD, *For. Mem. R. S.**

[Plate XIV.]

SINCE the appearance of two earlier papers on this subject† a very large amount of experimental work has been done, the publication of which has been delayed owing to the numerous discrepancies and observations requiring further study, which were continually coming to light. Most of the doubtful points have now been cleared up and a number of new and unexpected effects observed, of especial interest being the appearance of the forbidden line 2655·8 (1S-2p₃). That the results reported in my first paper regarding the abnormal increase in the intensity of the line 2655·13 caused by the admission of helium containing a trace of nitrogen, might be explained by the development of the forbidden line (the two being unresolved in my small spectrograph) was suggested to me by Prof. Takamine shortly after the appearance of the paper. This interesting prediction has been repeatedly verified during the past year, the two lines being clearly separated and of variable intensity ratio depending upon the conditions. With optical excitation the forbidden line comes out only in the presence of some inert gas, while Lord Rayleigh‡ has recently photographed it in the luminous vapour outside of the zone of conduction in a mercury vapour vacuum-tube excited by a current of $\frac{1}{10}$ milliampere passed between a hot cathode and an anode plate.

The phenomena discussed in the present paper may be divided into two classes, those which merely verify Bohr's theory of absorption and emission and which can be readily explained by the energy diagram, and other effects of obscure origin which can be explained only with difficulty. It is the study of these that is likely to throw new light on the mechanism of radiation. Some of these effects I have been unable to explain up to the present time.

The apparatus used in the continuation of the work was similar to that formerly employed, except that a magnetic

* Communicated by the Author.

† R. W. Wood, "Controlled Orbital Transfer of Electrons," *Proc. Roy. Soc. cvi.* p. 679 (1924); *Phil. Mag.* October 1925.

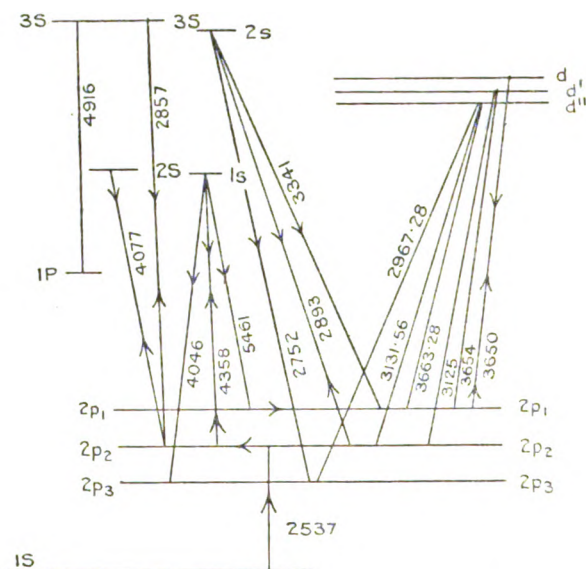
‡ *Proc. Roy. Soc. cxiv.* p. 636 (1927).

field was invariably used to press the discharge in the exciting mercury lamp against the wall facing the resonance tube, and a Y-tube of large bore, surmounting a barometer column of mercury, was used between the vapour pump and the resonance tube in place of a stop-cock, which prevented the contamination of the mercury vapour with vapours from grease. With this improvement the brown deposit on the inner wall of the resonance tube, resulting from prolonged illumination, which formerly gave trouble, has never appeared. It was undoubtedly carbon set free from the vapours of the stop-cock grease by contact with excited mercury atoms, but it adhered to the wall of the quartz tube so strongly that it could be removed only by polishing with pitch and rouge.

A large and very fine quartz spectrograph was used either alone or in conjunction with a quartz Lummer-Gehrke interferometer. With these instruments it has been possible to separate the close lines associated with the d'' and D levels, which were unresolved in the earlier work, a circumstance which made the interpretation of some of the results quite impossible. The resonance tube, of fused quartz, 22 cm. in length and 2.5 cm. in diameter, drawn off obliquely at the bottom to avoid reflected light and secure a black background, was mounted vertically and closed at the top with a right-angle prism of quartz, cemented with Boltwood wax, which gives off no vapour: the tapered portion at the bottom was painted black on the outside as well as the upper portion near the prism. The vertical quartz arc, with anode of tungsten and the cathode bulb immersed in running water, operated with a current of about 2 amperes was mounted close to the resonance tube, or at a sufficient distance to permit of the insertion of absorption cells of quartz filled with bromine or chlorine. The excitation of the mercury atoms in the resonance tube, which is exhausted, or filled with some gas at low pressure, takes place as follows, to cite a single typical process. By the absorption of a quantum of 2537 radiation an electron is brought to the $2p_2$ level, then by the absorption of 4358 raised to $1s$, from which it falls back either to $2p_3$ emitting 4046, or $2p_2$ emitting 4358, or to $2p_1$ emitting 5461. The latter level is metastable and the electron in this level can absorb 3650, being raised to the d level in the process. From here it falls back to $2p_1$ (its only possible transition) and 3650 is re-emitted by the vapour. These transitions are shown in fig. 1, upward pointing arrows indicating absorption transitions, downward pointing, emission.

It thus appears that 3650 is present in the optically excited spectrum as a result of *three* different processes of absorption occurring in succession. If 4358 is removed from the exciting beam by a filter of bromine introduced between the resonance tube and the lamp, the 3650 line disappears, as the second absorption process has been prevented. It is not quite clear why the electrons brought to $2p_1$ by the emission of the three lines originating on the d' d'' and D levels are not efficient for the production of 3650. On reading

Fig. 1.



over the argument advanced in my paper of two years ago I do not find it very convincing, and it may be better for the present to consider the apparent production of 3650 by electrons from $1s$ only, as a point requiring further explanation. As we shall see later on, 3650 is a line quite unique in its behaviour.

As I showed in the former papers the introduction of nitrogen into the resonance tube enhanced many of the lines to an enormous degree, by causing an accumulation of atoms with electrons on the metastable orbit $2p_3$, from which they are unable to return $1s$ and are hence available for the absorption of 4046, 2967, and other lines terminating on this level. This was proven experimentally by showing that 4046

was powerfully absorbed by optically excited mercury vapour in nitrogen at 3 mm. pressure. The green line 5461 is enhanced in this way as much as twenty-fold, while 4046 is enhanced only four-fold. This results from the circumstance that the vapour in the resonance tube has a high coefficient of absorption for 4046 (as a result of transfer of electrons to $2p_3$ by the nitrogen), and since the tube is viewed "end-on" the lower portions contribute very little 4046 radiation, in other words the tube shows self-absorption for this line. This is not true for the other two lines, 4358 and 5461, all portions of the tube contributing equally to the illumination. This was proved by limiting the illumination to a narrow horizontal sheet of rays, by placing a slit between the resonance tube and the lamp, in which case the increment of intensity due to the admission of nitrogen was the same for the three lines.

It is apparent that the intensity ratios of the lines emitted as a result of optical excitation depend upon a number of factors such as (a) the manner in which electrons on an upper level distribute themselves among lower levels (statistical distribution which governs intensity ratios); (b) the relative intensity of the lines in the exciting arc by the absorption of which the electrons are carried to upper levels; (c) transfer of electrons to metastable orbits, as by nitrogen, causing absorption of lines not normally absorbed. (d) An as yet unexplained action of nitrogen in causing the appearance of lines not called for by the energy diagram under the conditions of excitation, an effect probably due to the rayless transfer of electrons from upper to lower levels by collisions of the second type, or possibly, in some cases, caused by what Franck and Cario have named sensitized fluorescence: as an example excitation by bromine filtered light which raises no electrons to $1s$ owing to absence of 4358 and 4046, in consequence of which these lines and the green line are absent, all appearing, however, in great intensity on admitting nitrogen at 3 mm. pressure to the resonance tube.

(e) The intensity of the exciting light. This is an effect which has not yet been carefully studied. That the intensity ratio of the optically excited lines may be modified by removing the exciting lamp to a distance, thus reducing the intensity, may be seen from the following considerations.

Suppose we reduce the intensity by one half, then only one half as many electrons are brought up to $2p_2$ as before and the emission of 2537 is reduced one half, as is usual in fluorescence. All of the other lines (except 3650 and 3021) will be reduced to one quarter of their original value, as there

are but one half as many electrons on $2p_2$ available for the absorption of 4358, and 4358 has also been reduced to one half of its former value. In the case of 3650 and 3021, involving three successive absorptions, we should expect a reduction to $\frac{1}{8}$. This is a point very easily tested by experiment, but at the moment I have no data on the behaviour of 3650 when the lamp is removed to a distance. I have found, however, that a reduction of the intensity of the exciting light in this way reduces the line 2655.13 (a line involving two successive absorptions) much more than the forbidden line 2655.8 where a single absorption only is involved. On referring to my earlier paper I find an observation recorded which is in agreement with this view. It was found that, by applying a magnetic field to the arc, the intensity of 2537 in the optically excited vapour was increased four-fold: the lines 5461, 4358, 4046, 3663, 3654, 3131, 3125, and 2967 (all involving *two* absorptions) were increased eight-fold and the line 3650 (involving three absorptions) was increased sixteen-fold. This is the converse of the case just considered, the application of the magnetic field (by abolishing self-reversal of the exciting lines), corresponding to *increasing* the intensity of the exciting light. It was found also that 3650 was partially reversed in the arc in the absence of a magnetic field, *i. e.* the field caused its enhancement in the exciting light. The question will be more fully taken up in a subsequent paper.

The tremendous increase in the intensity of the optically excited spectrum, caused by the admission of a gas, nitrogen in particular, which was mentioned in the earlier papers has been more fully investigated. Results conflicting with earlier observations and not always easy to duplicate were obtained.

These discrepancies were finally traced to the circumstance that the increment of intensity of the emitted light caused by the nitrogen varied along the path of the exciting beam. Consistent results were obtained as soon as an image of the cross-section of the resonance tube was projected on the slit of the spectroscope with a quartz-fluorite achromat. The light is most intense along the side of the resonance tube facing the lamp, falling off to less than one quarter of this value in some cases as we pass along the diameter to the opposite side of the tube. This is, of course, due to the absorption of the exciting radiations. The decrement in intensity is not the same, however, for all of the emitted spectrum lines, since the coefficient of extinction is not the same for all of the exciting radiations.

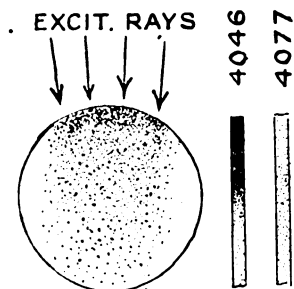
The luminosity distribution of the light in the image of

the cross-section of the tube on the slit and in the lines 4046 and 4077 is shown in fig. 2.

In the earlier investigations no lens was used to form an image on the slit, the collimator being simply pointed down the resonance tube (seen end-on in the right-angle prism which surmounted it). Diaphragms were arranged so that no light scattered by the tube walls entered the spectroscope but, with the frequent re-adjustments made, it is obvious that the spectroscope must sometimes have received light from the more strongly illuminated side of the tube, and sometimes from the less intense portion, therefore no consistency could have been expected in view of the more recent observations.

The photograph reproduced on Plate XIV. fig. 1 was made in this way and will be referred to later.

Fig. 2.



It is evident that with so many factors operating simultaneously it is very difficult to discuss the results of the experiments: facts come to light slowly as a result of comparing a large number of photographs, and little can be done until long experience has made it possible to visualize the energy diagram as a chess-player visualizes the board.

If the total light of the arc is employed matters are almost hopelessly complicated, and we will begin with a discussion of the results obtained with the bromine-filtered excitation, in which case the distribution of electrons over the $2p_1p_2p_3$ levels from $1s$ does not occur. For the present we will confine ourselves to the transitions between the $dd'd''D$ and the $2p_1p_2p_3$ levels, together with the $1P$ level to which electrons may pass from the $d'D$ levels with emission of the yellow lines.

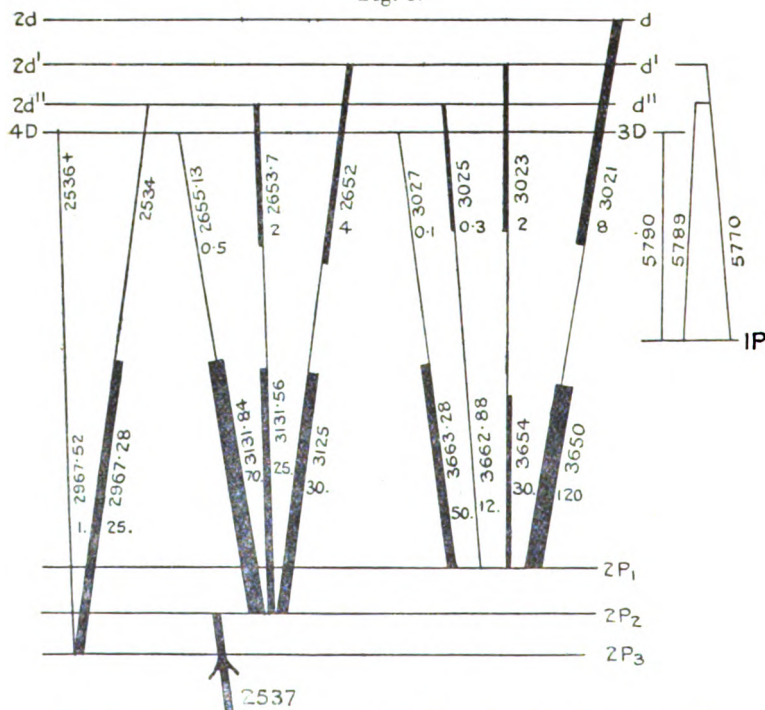
For a discussion of the results it is clear that we must have a record of the relative intensities of the exciting lines emitted by the arc; such a table was given in the earlier

paper, but at the time only the sums of the intensities of the close lines originating on the d'' and D levels were available. As very conflicting statements regarding these intensities were found in the literature, determinations were made with the arc actually employed in the work (*i. e.* water-cooled, and with magnetic field operating). The lines were photographed with a 21 foot concave grating with different times of exposure for each pair of lines. The results are given in the following table, heavy type indicating the bright lines for convenience of reference.

$(2D-2p_1)$	3663·28	4 times intensity of 3662·88 ($d''-2p_1$).
$(2D-2p_2)$	3131·84	3 „ „ „ 3131·56 ($d''-2p_2$).
$(2D-2p_3)$	2967·52	$\frac{1}{20}$ of „ „ 2967·28 ($d''-2p_3$).

With the lamp warm, 3131·56 becomes brighter than 3131·84, which reverses. The extreme faintness of 2967·52 is to be especially noted.

Fig. 3.



A diagram of the energy levels involved and the transitions with which we shall deal is given in fig. 3. As an aid in

visualizing the effects to be expected from given transitions, I have indicated roughly the intensities of the lines in the exciting arc by the widths of the lines joining the levels. As a further aid I have found it advantageous to represent the $d'd''$ and $2d'd''$ levels by the same lines. On the lower portions of the vertical lines joining the energy levels we find the data for the transitions from $2p_1p_2p_3$ to the d levels, and on the upper portions the data for the corresponding transitions to the $2d$ or upper levels. The actual intensities of the lines are given just below the wave-lengths. This type of diagram may seem confusing at first, but it enables us to see at a glance which lines are analogous (*i. e.* 3125 is analogous to 2652), a matter of importance in the study of the action of various gases on the electron transfers.

We will begin with a critical study of the effects of nitrogen on the radiation excited by bromine-filtered light, this being a comparatively simple case. The results are given in the following table for nitrogen at two different pressures, the numerals following the wave-lengths indicating the increment in intensity caused by the nitrogen (in comparison with the intensities emitted when the mercury vapour is *in vacuo*). The third column gives the values when no bromine filter is used.

	Nit. 4 mm.	Nit. 0.25 mm.	Nit. 0.25 mm. (no bromine filter).
3663	8	2	2
3654	2	1	1
3650	30	2	-2
3131	8	4	4
3125	2	1	1
2967	8	16	6

In this table 1 means that the intensity is unchanged, 8 that it has been increased eight-fold, and -2 that it has been reduced to $\frac{1}{2}$ of its value for vacuum.

Actual intensities of two of the lines were as follows : --

	2967.	3131.
Hg in vac.	1	4
Hg in Nit. 3 mm.	8	32
" " " 0.25 mm. ...	16	16

Referring now to the diagram fig 3, we will see how

many of the above changes can be explained. For mercury *in vacuo* we have absorption from the $2p_2$ level only, i. e. lines 3131·84, 3131·56, and 3125. For the present we shall treat the two former as a single line, since they were unresolved in the spectrogram from which the above photometric measurements were made. As a result of 3131 absorption we have 2967, 3131, and 3663 emission, while 3125 absorption gives 3125 and 3654 emission. Line 3650 is absent in so far as the above processes are concerned, though a trace of it may appear on the plate as a result of absorption of 3650 (not entirely removed by bromine filter) by electrons brought to $2p_1$ by the emission of 3663 and 3654 above referred to. Line 2967 will be relatively weak since its component from d'' results from electrons carried to d'' by the relatively weak line 3131·56, while the component from 3D is vanishingly weak since the probability of the transfer $3D-2p_3$ is very small (as shown by the faintness ($\frac{1}{20}$) of this line in the arc.

The addition of nitrogen at 0·25 mm. increases the intensity of 2967 sixteen-fold, 3131 four-fold, and 3663 two-fold.

No change occurs in the case of 3125 and 3654, which indicates that there are as many atoms with electrons on the $2p_2$ level as before the introduction of the nitrogen, in spite of the large number with electrons on $2p_3$.

We will now calculate the expected intensities resulting from the nitrogen.

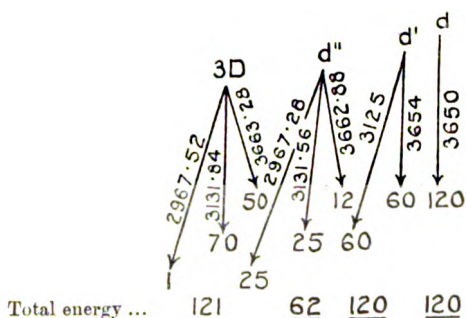
The relative intensities of the exciting lines involved, obtained by combining the relative values given for the d'' and 3D components given above with the relative values recorded in the former paper, are given in the following table :—

	From upper level.	Int.
3D	3663·28	50
d''	3662·88	12
d'	3654	60
d	3650	120
3D	3131·84	70
d''	3131·56	25
d'	3125	60
3D	2967·52	1
d''	2967·28	25

The distribution of energy from the $d d' d'' 3D$ levels to the

$2p_1p_2p_3$ is represented in the following diagram (fig. 4), the total energy from each upper level being recorded below.

Fig. 4.



We first calculate the intensity ratios to be expected for mercury *in vacuo*, taking the sum of the portions contributed by the absorption of 3131.84 and 3131.56. If we consider that the energy expended in raising electrons from $2p_2$ to 3D and d'' by the absorption of these two lines is proportional to the intensities of the lines in the exciting arc we have 3131.84 contributing energy 70, which is divided among the levels $2p_3p_2p_1$ in the proportion $\frac{1}{2}$, 40, and 30 (1, 70, 50, on diagram for 3D), and 3131.56 contributing 25, which is divided in the proportion 10, 10, 5 (25, 25, 12, on diagram for d''). Adding the values for each of the $2p$ levels gives us the following intensity ratios for the (double) lines:—

D	d''	Op. Excit.		Hg. Arc.	
$\frac{1}{2} + 10 = 10.5$	} or	1	2967	26	} or 1
$40 + 10 = 50$		5	3131	95	
$30 + 5 = 35$		3.5	3663	62	

If nitrogen at 0.25 mm. is added, we find that the line 2967 has increased in intensity 16-fold, and from this we can calculate the expected increments of the other lines, thus:—

Assume a sufficient number of atoms with electrons brought by the nitrogen to the metastable level $2p_3$ to give a sixteen-fold increase of (the double line) 2967 by the absorption 2967.28, which raises the electrons to the d'' level. The diagram (fig. 4) for the redistribution among the $2p$ levels shows that if we contribute intensity 15 to 2967 (which may be considered as having a value 1 as a result of

the absorption of 3131 by atoms unaffected by the nitrogen) we must also contribute intensity 15 to 3131·56 and intensity 7·5 to 3662·88. This gives us for the intensities :—

		In Nit.	Vac.
2967	1 + 15	= 16	1
3131	5 + 15	= 20	5
3663	3·5 + 7·5	= 11	3·5

The calculated increment for 3131 is 4, which agrees exactly with the observed four-fold increment. For 3663 the agreement is not so good, a three-fold increment calculated and a two-fold observed. It should be noted that, in setting the absorptions proportional to the intensities of the lines in the exciting arc, we have assumed that the absorption coefficient of the excited vapour for the lines in question is the same. This is of course not justifiable, so that the above computations are to be regarded merely as a rough attempt to follow out the changes in intensity of the various lines.

With 4 mm. of nitrogen in the resonance tube all three lines appear enhanced to the same degree, namely eight-fold. It seems probable that this is, in part at least, the result of the strong absorption of 2967 by the atoms with electrons on $2p_3$, the weakening of this line in comparison with others being analogous to the smaller increment in intensity of 4046 in comparison with 4358 and 5461, previously alluded to.

The enormous increment (thirty-fold) of 3650 results probably from electrons brought down from higher levels to the d level by collisions of the second type, or possibly by something analogous to the sensitized fluorescence of Franck and Cario. The very small value of its intensity *in vacuo* is responsible for the abnormally large value of the increment.

In nitrogen at 0·25, however, the increment is only two-fold. Here also I believe the enhancement to be due to the same cause.

If no bromine filter is used, which causes electrons to be scattered over the $2p_1 p_2 p_3$ levels from $1s$, the presence of 0·25 mm. of nitrogen causes a two-fold decrease in the intensity of 3650, and as we shall see presently this decrease may be as much as four-fold with nitrogen at a lower pressure, 0·05 mm. Referring to the diagram fig. 4, it is seen that we can predict the effect of nitrogen traces on the relative intensity of lines originating on the D and d'' levels.

In vacuo 3131·84 must be much brighter than 3131·56, since it is much brighter in the exciting light, and of all the

electrons raised to D by its absorption, only a very few fall to $2p_3$ (as we know from the small intensity of 2967·52 in the arc). Of the electrons raised to d'' by the absorption of the fainter line 3131·56, many fall to $2p_3$, and are unavailable for the re-emission of 3131·56.

With nitrogen in the tube, however, we have powerful absorption of the strong line 2967·28 which contributes to the emission of 3131·56, while very few electrons are carried from $2p_3$ to D owing to the faintness of the 2967·52 line. Nitrogen should thus enhance 3131·56 enormously.

This prediction was verified by photographing the optically excited vapour with a quartz Lummer-Gehrke plate (interferometer) used in conjunction with a quartz spectrograph, the horizontal fringe system formed by the plate being projected on the wide-open slit of the spectrograph by means of a quartz-fluorite achromatic lens of 40 cm. focus. With the mercury vapour *in vacuo* (Pl. XIV. fig. 4 *a*) the line 2967 does not appear and 3131·84 has about the same intensity as 3125, the displacement of the two fringe systems by the spectrograph being quite evident in the photograph. A mere trace only of 3131·56 appears.

With nitrogen at a very small fraction of a millimetre 2967·28 appears, and 3131·84 and 3131·56 have the same intensity (fig. 4 *b*).

With nitrogen at 1·5 mm. (fig. 4 *c*) 3131·56 is many times brighter than 3131·81, while 2967 is no brighter, if as bright as in case *b*. This is due to the "self-reversal" of 2967·28 by the atoms with electrons on $2p_3$, a phenomenon already described in the case of the line 4046.

All of the above changes are what we should expect from the diagram. In the case of the yellow lines, however, we find a difficulty.

The Yellow Lines.

Observations made visually of the relative intensity of the two yellow lines (by opening the slit of the spectroscope until the two monochromatic rectangles touched each other) showed that, with mercury *in vacuo*, the lines had the same intensity, but that in nitrogen the 5790 line appeared to have about double the intensity of 5770. The enhancement of 5790 was much greater with the exciting light filtered through bromine than when the total radiation of the arc was employed; this indicates that the enhancement results from the electrons on $2p_3$ (brought there by the nitrogen), the removal of 4046 by the bromine leaving more atoms available for the absorption of 2967·28.

Referring now to the diagram, fig. 3, we find a difficulty

at once, since the line 5790 originates on the 3D level, to which electrons can be brought from $2p_3$ only by the absorption of 2967·52, which has only about $\frac{1}{20}$ of the intensity of 2967·28. The absorption of this latter line carries electrons to d'' , and the mercury line 5789 originates on this level, but it is normally so faint that it is difficult to believe that it is responsible for the enhancement observed. The lines 5789 and 5790 would not appear resolved in the spectroscope used. To settle this matter it will be necessary to photograph the yellow lines with the Lummer plate, a matter of some difficulty owing to the long exposure required. If it should turn out that 5789 was in reality greatly enhanced, the phenomenon might perhaps be analogous to the development of the forbidden line 2655·8 which does not appear at all in the arc or spark spectrum, but which comes out in the optically excited spectrum of mercury in nitrogen at 4 mm. with an intensity comparable to that of the other lines. This being the case, it is barely possible that the transfer ($1P-2d''$), which normally is extremely infrequent, may be greatly facilitated. It is, perhaps, more likely that the nitrogen transfers electrons from d' to 3D in a manner analogous to the transfer from $2p_3$ to the metastable level $2p_3$. Such a transfer would decrease the intensity of 5770 and increase that of 5790. It would also tend to decrease 3125 and increase 3131·84. I have frequently detected a decrease of 3125. The slight increment of 3131·84 due to this assumed action of nitrogen would be completely offset by the enormous increment of 3131·56 (resulting from absorption of 2967·28), so that the results obtained with the Lummer plate are not in opposition to this hypothesis. It is possible, too, that the nitrogen transfers electrons from d'' to 3D.

If a filter of chlorine is used in conjunction with bromine no visible light is emitted by the vapour, the excitation being confined to radiations below 2967. The d 3D levels are now free of electrons, but if nitrogen at 3 mm. is added all of the missing lines appear, and the yellow lines now have the same intensity (as is the case with mercury *in vacuo* excited by 3131·84 and 3125). This shows that an emission caused by electrons brought down to d' and 3D from upper levels does not give an enhancement of 5790.

The enhancement of 5790 is not much in evidence until the pressure of the nitrogen is over 2 mm., while .5 mm. is sufficient to greatly enhance all lines depending upon absorption from the $2p_3$ level, which makes it appear probable that

the nitrogen either transfers electrons from d'' to $3D$, in which case 5790 will be enhanced, or increases enormously the probability of the $1P-d''$ transfer which will increase the intensity of 5789.

Development of the HO band : Sensitized fluorescence.

As reported in the earlier papers, the optical excitation of mercury vapour in dry nitrogen gives, in addition to the mercury lines, strong bands, one of which in the vicinity of the mercury line 3125 has been definitely identified with the so-called "water-band" emitted by the oxy-hydrogen flame, and other sources of light in which water vapour is present. This band is now attributed to an HO molecule.

A photograph of the band excited by the light of the mercury arc is reproduced on Plate XIV. fig. 3, in coincidence with the spectrum of an oxy-coal-gas flame. The two mercury lines 3125 and 3131 appear within the band. With continued exposure to the light of the arc the water-band gradually fades away and is replaced by an equally complicated band in the same region but extending beyond the water-band on the short wave-length side.

The distribution of intensity among the lines forming the band is very different in the two types of excitation, a matter which is being investigated in collaboration with Prof. F. W. Loomis and will be reported in a subsequent paper. It is of some interest in view of recent work on the origin of band spectra.

The "Forbidden" line 2655.8 ($1S-2p_3$).

The appearance of this line with an intensity equal to that of its near neighbour 2655.13 ($2p_2-4D$) is a matter of great interest.

I have already mentioned the conditions under which it appears (mercury vapour in nitrogen or a mixture of helium and nitrogen). As yet no study has been made of the conditions most favourable to the appearance of the line, or whether it can be brought out by any other gas than nitrogen. It is shown on the photograph (Pl. XIV. fig. 2) at the right of the group 2652-2655. It apparently does not attain any considerable intensity until the pressure of the nitrogen is sufficient to bring out the "water-band" strongly. The other forbidden line 2270 ($1S-2p_1$) I have not yet observed. It is doubtful whether it can be found in this way, as the number of atoms with electrons on the $2p_1$ orbit

is probably small in comparison with those with electrons on $2p_3$.

As I have stated in the section on the "water-band," continued exposure causes the HO band to disappear and another band of unknown origin (a compound molecule of N and H perhaps) to take its place. The forbidden line becomes weaker when this state is reached, probably due to the presence of hydrogen set free by the action of the excited mercury atoms on the water-vapour. This liberation of hydrogen I have observed with mercury vapour *in vacuo*, sealed from the pump by the mercury Y-tube. The pressure rises quite rapidly as a result of illumination by the Hg arc, and the liberated gas is shown to be hydrogen by a small spectrum tube in circuit with the resonance tube. The oxygen probably combines with the mercury, for I have observed that if air at 1 mm. pressure is admitted to the resonance tube, the emitted light is very feeble at first, rising, however, to the full intensity which it would have in pure nitrogen after a few minutes of illumination.

The intensity of the forbidden line appears to be greater under the conditions specified than by electrical excitation, probably as a result of an enormous concentration of atoms with electrons on $2p_3$. I have hopes of being able to photograph the fine structure of this line with the Lummer plate. If this can be done it will throw a good deal of light on the nature of the 1S level, as the fine structure of but one other line involving this level is known (2537).

Development of Absent Lines by Nitrogen.

If a combined filter of chlorine and bromine is placed between the lamp and the resonance tube, the vapour is excited only by lines of shorter wave-length than 2750.

If the mercury vapour is *in vacuo* we have an invisible emission comprising lines originating on the upper $2dD$ levels to which electrons are carried from $2p_2$ by the absorption of 2652, 2653, and 2655.

If nitrogen at 3 mm. is added to the vapour all of the arc lines are emitted with greater or less intensity, which shows that electrons are either brought down from the upper levels to the lower, or carried up from the $2p$ levels by the nitrogen (activated perhaps by the excited mercury). There seems to be no experimental way of settling between the two processes, for there is no way of bringing electrons up to the $2p$ levels from 1S without at the same time raising

them to the upper levels by the absorption of $2534\cdot8$ ($2p_2-3d''$) and $2536\pm$ ($2p_2-3D$) (the latter line has never been observed on account of its proximity to the $1S-2p_2$ line 2537). To separate 2537 from these lines for illumination is impossible.

The relative intensities of lines developed in this way will depend upon how the electrons are distributed by the nitrogen among the levels intermediate between the $2p$ levels and the upper $2dD$ levels. Self-absorption in the resonance tube may also operate for some lines, as we have electrons on the $2p_2p_2$ levels, as a result of the primary excitation by 2537 and the presence of nitrogen which transfers electrons from $2p_2$ to $2p_2$.

In the absence of this self-absorption, as when employing a very thin layer of radiating vapour, we should expect the intensity ratio of lines originating on the same level ($4046-4358$, 5461 for example) to be the same for all types of excitation and for all conditions. It was found that the lines $3663-3131-2967$ were in the ratio $25-50-25$, while in the arc and by optical excitation the ratio is $25-95-62$.

These ratios are for the lines from D and d'' *unresolved*, as photographed with the spectrograph. Referring to the distribution diagram (fig. 4), we see that the ratio $25:50:25$ will be very nearly realized if we consider that the D level contributes only $\frac{1}{4}$ of its usual amount, *i.e.* to the intensities from d'' , or 25 , 25 , 12 , we add $\frac{1}{4}$, $17\cdot5$, and 12 instead of 1 , 70 , and 50 —obtaining roughly 25 , 43 , 24 .

If this is the correct explanation it means that the nitrogen favours the d'' level in its distribution, the D level receiving only $\frac{1}{4}$ of its usual quota. On one plate, taken with a filter of chlorine only, the three lines in question had the same intensity, 3125 and 3654 (from d') were equal and brighter, while 3650 (from d) was still brighter. This matter will be further investigated as it appears to be of some importance.

The effect of the nitrogen in bringing out the various lines of the spectrum with a chlorine-bromine filter was determined by giving an exposure of 1 hour with the filters interposed and $\frac{1}{4}$ mm. of nitrogen in the resonance tube, and then a series of exposures with the mercury *in vacuo* and no filters, of exposure times 25 mins., 3 mins., 90, 45, 22, 11, and 6 seconds. The slit was opened fairly wide and the densities of the lines in the two cases compared. The numbers following the wave-lengths are the exposure times in seconds, for Hg *in vacuo* and no filter, necessary to give a density equal to that given by an hour's exposure (3600 secs.) with filters and nitrogen in the tube.

1s	5461	22
1s	4358	22
1s	4046	11
2S	4077	90
d''D	3663	22
d'	3654	22
d	3650	45
2s	3341	1500
d''D	3131	45
d'	3125	22
2d	3021	90
d''3D	2967	22
2s	2893	1500
3S	2856	3000
	2803	missing
2s	2752	1200
4D	2655	3000
2d''	2653	1500
2d'	2652	45

The blue-green line was observed visually to come out with considerable intensity with nitrogen at 4 mm., both with and without a bromine filter. Absorption from the $2p_3$ level cannot help in bringing out this line (see diagram, fig. 1), consequently we must ascribe it to electrons brought to 3S from other levels by the nitrogen.

If we were exciting the mercury with 2537 alone, the numbers following the wave-lengths might be taken as representing the efficiency of the nitrogen in developing the lines, allowing of course for self-absorption in the tube, which as in previous cases weakens 4046 with respect to 4358 and 5461 and gives us a diminished efficiency which is of course not real. The very high numbers above 1000 result from the circumstance that direct optical excitation is operating in these cases, as the filters do not absorb the lines below 2800. Thus the lines 3341, 2893, and 2752 result from the absorption of the 2752 radiation by electrons on the $2p_3$ orbit, brought there by the nitrogen.

The line 4077 ($2S-2p_2$), for which the efficiency is 90, is not optically excited however, which seems to indicate that the nitrogen favours the 2S level. The same appears to be true for d and $2d$ levels (3650 and 3021). The large value for 2856 indicates that it must be optically excited, though the chlorine is fairly opaque here.

Very surprising are the last three cases for the closely adjacent $2d/d''4D$ levels. These lines are all optically excited, and we should expect that the relative intensities would be

the same as those observed without the filters. We find, however, that in this case the nitrogen appears to be 33 times as efficient in developing 2653 as in bringing out 2652 and 66 times as efficient for 2655. The intensity increments observed without the filters for several other gases for the three lines were :

	Nit. 3 mm.	CO 0.045 mm.	Argon 1 mm.
2652	1	1	1
2653	4	12	10
2655	1	1	1

In the nitrogen case we have, with the filters (as shown by the diagram, fig. 3), an emission resulting from the absorption of 2534.8 from the $2p_3$ level, and this absorption is the only one operating on the electrons on $2p_3$. Without the filters, however, we have electrons removed from $2p_3$ by the very powerful 4046 and 2967 radiations and scattered over the $2p_1p_2p_3$ from the upper levels to which they have been raised. This may account for the enormous difference observed, but the matter requires further investigation with control experiments. The still greater increase in the case of 2655 is probably due to the development of the 2655.8 forbidden line $1S-2p_3$ mentioned elsewhere.

The Decrease of Intensity of Certain Lines by Gases at Low Pressure.

Certain lines are decreased in intensity in a remarkable manner by the admission of a gas at extremely low pressure to the resonance-tube.

The most interesting case is that of the line 3650, which is decreased four-fold in intensity by nitrogen at 0.05 mm. while all the other lines are either enhanced or unaffected. Photographs showing this effect are reproduced on Plate XIV. fig. 1. A showing the group 3650-3663 for mercury *in vacuo*, and B the same group and same conditions of illumination with 0.05 mm. of nitrogen in the resonance tube. The line 3650, which in A has about four times the intensity of 3654, has faded in B to an intensity exactly equal to that of 3654. As the nitrogen pressure increases the reduction becomes less and finally there is a considerable increment, the changes being as follows :—

Nitrogen pressure...	2	1.25	.43	.2	.1	.05 mm.
Intensity increment or decrement.....	2	1.5	1	-2	-4	-5

A similar decrease of intensity was found for the line 3021 (the line analogous to 3650) from the upper 2 *d* level. The two *d* levels thus appear to be sensitive to very small traces of nitrogen.

A similar decrease in the intensity of 3650 was observed with argon and helium, though not as great as with nitrogen. With CO at 1.25 mm. a six-fold reduction was observed for 3654, 3650, and 3125, while 4358, 3131, and 2967 were unaffected. As the action of carbon monoxide appeared to be peculiar, we will take it up more in detail,

The action of Carbon Monoxide and Argon.

The effect of CO at two different pressures on the various lines is shown in the following table, together with the effect of argon.

	CO ·045 mm.	CO 1.25 mm.	Argon 1 mm.
4358	-1.5	1	3
4077	-2	..	1
4046	-1.5	-2	2
3663	1	-2	2
3654	-2	-6	1
3650	-5	-6	-1.5
3341	1.5	...	2.5
3131	3	1	4
3125	-3	-6	1
3023	-2	...	1
3021	-2	-3	2
2967	3	1	4
2893	1	...	2.5
2653	12	...	10
2652	1	-2	1

The increment of 3131 and 2967 by CO at .045 mm. indicates that electrons have been brought to $2p_2$ by the gas. They appear, however, to be inoperative in causing absorption and re-emission of 4046, since the lines from 1*s* are all reduced in intensity. The line 2967 is evidently absorbed, for we have a threefold increment of the lines from *d*'. It is the behaviour of the 2653 line, from 2*d*', however, which is most striking. This is increased in intensity *twelve-fold*! and results from absorption of 2534 from the $2p_3$ orbit.

The only interpretation of these results that I am able to give at the moment is that, with CO, we have electrons on

$2p_3$, but the probability of absorption from this level with its consequent re-emission decreases as the wave-length increases, in other words quanta of a large energy value (as 2536) are absorbed in great numbers, while those of smaller energy value (as 2967) are absorbed to a lesser degree, and those of still smaller energy (as 4046) not at all. It will be necessary to study the absorption of the excited mercury vapour in CO with the Lummer plate to test the correctness of this interpretation. This will be investigated.

Effect of Nitrogen at Different Pressures.

The effects of nitrogen at different pressures were investigated both with the exciting lamp water-cooled and with magnetic field, and with the the lamp warm and without field. Very different results were obtained in the two cases, which shows how careful we must be in specifying the conditions under which the exciting lamp operates. For example, with the lamp slightly warmed and no field 3650 showed no decrease in intensity with low-pressure nitrogen. It is moreover necessary to make the photographs by projecting an image of the "end-on" resonance tube on the slit of the spectrograph, and make the photometric comparisons with the portion of the image where the light enters the tube. If we compare the increments of intensity for the vapour near the point of exit for the exciting light very different values are obtained, as I have previously pointed out, due to the fact that some of the absorbed rays are rapidly quenched while traversing the tube, while others are not.

The increments and (decrements) obtained with nitrogen over a wide range of pressure are given in the following table.

	Nitrogen pressure :							
	11	4	2	1.25	0.43	0.2	0.1	0.05 mm.
5461	8.5	13	15	12	6	4	2	1.5
4358	6.5	12	12	12	6	4	2	1.5
4046	3	3	4	3	2	2	2	1.5
3663	1.5	3	4	4.45	3	2	1.3	1
3654	1.5	...	1.5	1.5	1	1	1	1
3650	-1.5	3	2	1	1	-2	-4	-5
3131	2.7	6	8	9	6	4	2	2
3125	-1.5	1	1	1	1	1	1	1
2967	1	2.5	4	6	8	8	6	1

These values are to be regarded as provisional however.

It has not been considered worth while, up to the present, to make accurate photometric measurements, owing to the large discrepancies found with rough measurements. Now that the causes of these have been found, accurate measurement will be made.

The much greater increments reported in the earlier paper (thirty-fold for 5461 for example) were found to be due to the circumstance that a magnetic field was not used in these cases. The "core" of the exciting line being removed by absorption, we have a comparatively feeble excitation of mercury *in vacuo*. The addition of nitrogen, by broadening the lines in the usual manner, enables the vapour to utilize frequencies slightly greater and less than the frequency at the centre of the line, and hence causes a greater increment of intensity than in the case of excitation by lines in which the "core" is the most intense part. In other words, the larger increment is seen to be due to the circumstance that, with partially reversed exciting lines, the optical excitation is feeble with mercury *in vacuo*, and it is in comparison with this feeble luminosity that we measure the increment.

Observations made recently under the same conditions and consecutively, with and without the magnetic field, on the increments due to nitrogen at 2 mm. for the region of the resonance-tube where the exciting beam enters, and also at the region of exit, are given in the following table.

	Without mag. field.		With mag. field.	
	Entrance.	Exit.	Entrance.	Exit.
5461	24	18	9	9
4358	18	12	6	6
4046	6	6	2	3
3650	7	4.5	2	1
3131	12	9	6	4.5

XLIV. A Note on the Structures of the Arc Spectra of Elements of the Oxygen Group. By Professor J. C. McLENNAN, F.R.S., A. B. MCLAY, Ph.D., and J. H. MCLEOD, M.A.*

I. Introduction.

THE structure of the arc spectrum of elements of the oxygen group—i. e., O, S, Se, Te, or Po—should, according to the Pauli-Heisenberg-Hund theory, be characterized chiefly by the terms that are given in Table I. and in Table II. In these tables, it will be

* Communicated by the Authors.

TABLE I.

	Electron Configuration.		Term Types.		
	$n_1 n_2 n_3 \dots$	$(n+1)_1 (n+1)_2 \dots$	A.	B.	C.
On Si ...	2 3 —	— —	n^4S	n^2D	n^2P
On Si O ₁ Si	2 4 — 2 3 —	— — 1 —	n^3P $(n+1)^5S$ $(n+1)^3S$	$n^1\overline{D}$ $(n+1)^3D$ $(n+1)^1D$	n^1S $(n+1)^3P$ $(n+1)^1P$
	2 3 1 *	— —	n^5D n^3D	$n^3\overline{G}$ $n^3\overline{F}$ n^3D $n^3\overline{P}$ n^3S $n^1\overline{G}$ $n^1\overline{F}$ n^1D n^1P n^1S	$n^3\overline{F}$ n^3D $n^3\overline{P}$ $n^1\overline{F}$ n^1D n^1P
	2 3 —	— 1	$(n+1)^5P$ $(n+1)^3P$	$(n+1)^3\overline{F}$ $(n+1)^3\overline{D}$ $(n+1)^3P$ $(n+1)^1\overline{F}$ $(n+1)^1D$ $(n+1)^1P$	$(n+1)^3\overline{D}$ $(n+1)^3P$ $(n+1)^3\overline{S}$ $(n+1)^1\overline{D}$ $(n+1)^1P$ $(n+1)^1\overline{S}$

* In the oxygen atom there is no orbit n_3 where $n=2$. Each term in this row should therefore have the prefix $(n+1)$ for O₁.

TABLE II.

	Electron configuration.	Term Types.			
	$n_1 \ n_2 \dots$	D.			
$O_{II} \ S_{II}$ etc.	1 4	n^4P	n^2P	$n^2\bar{D}$	$n^2\bar{S}$
$O_I \ S_I$, etc.	1 5	n_D^3P	n_D^1P		

seen, configurations are given of the six outermost electrons of the neutral atoms, and along with them the type terms to which they give rise. Configurations are also given of the five outermost electrons of the singly ionized atoms in their normal state, together with the type terms corresponding to them. From these latter the terms of the arc spectrum were derived. The number " n " is to be understood as having the values 2, 3, 4, 5, and 6 for O, S, Se, Te, and Po respectively. The terms of the arc spectrum are divided into four groups or systems, three being given in Table I. in the columns designated by A, B, and C, and the fourth in the column in Table II. designated by D. These groups are identified by the particular series limits involved. Each term has been designated in the tables in such a way that it can be unambiguously referred to in the succeeding discussion. It should be mentioned that the deep-lying term n^3P is the first member of each of the three term sequences of which $(n+1)_A^3P$, $(n+1)_B^3P$, and $(n+1)_C^3P$ are respectively the second member. The term n^3P is therefore common to the three systems A, B, and C. Similarly, $n^1\bar{D}$ is common to systems B and C, but $n^1\bar{S}$ belongs only to system C. Although there are really four systems possible in Table II., one based on each term n^4P etc. of the first spark spectrum, the two terms of the arc spectrum given in the table are the only ones that are likely to be observed. The four systems have been grouped therefore for convenience into one—namely, system D.

Higher series members of any term system in Tables I. or II. are obtained when the excited electron occupies an orbit of higher total quantum number—say, $(n+x)$,—and the corresponding terms will then be designated by this number as prefix.

II. *Previous Investigations.*

The arc spectra of oxygen ^{1,2,3,4}, sulphur ^{1,3,4,5}, and selenium ^{1,4} have been analysed to some extent by other investigators.

In O_I the following terms have been identified:— 2^3P ; $(n+1)^3S$, $n=2$ to 10 ; $(n+1)^5S$, $n=2$ to 9 ; $(n+1)^3P$, $n=2$ to 4 ; $(n+1)^5P$, $n=2$ and 3 ; $(n+1)^3D$ and $(n+1)^5D$, $n=2$ to 9 . It is therefore evident that the term system A is very completely known. No terms in the term systems B, C, and D have been finally identified as yet, but it seems that as there are a number of unidentified triplet and singlet lines ^{1,2} that undoubtedly belong to O_I these should be found to lead to terms in these systems. It is interesting to find that Hopfield in a recent note has brought forward evidence that indicates that the famous auroral green line is a so-called forbidden line corresponding to an electron transition between levels represented by two deep-lying terms of the O_I spectrum. This suggests that one or both of the terms 2^1D and 2^1S may be involved.

In S_I the following terms have been observed:— 3^3P ; $(n+1)^3S$, $n=3$ to 5 ; $(n+1)^5S$, $n=3$ to 9 ; 5^3P ; $(n+1)^5P$, $n=3$ and 4 ; $(n+1)^5D$, $n=3$ to 9 ; and $3d^3P$. In this spectrum also the term system A is fairly complete, with the exception of the $(n+1)^3D$ sequence. One of the terms in Table II.—namely, $3d^3P$ —has been found. Here, again, some unidentified sulphur wave-lengths ^{1,3} probably involve terms in the B, C, or D systems.

As Hopfield is continuing his investigations on O_I and S_I , we shall not attempt to extend the analyses of these spectra in this note.

The structure of the spectrum of SeI is not so well known as that of the two former spectra, only the terms 5^3S ; 6^3P ; 5^5P ; $(n+1)^5S$, $n=4$ to 10 ; and $(n+1)^5D$, $n=5$ to 11 , having been identified. The spectra of TeI and PoI have not hitherto been analysed, as far as we are aware.

Some absorption experiments by Zumstein ⁶ had shown that four wave-lengths of the tellurium arc spectrum were absorbed by tellurium vapour, and some others carried out by Miss Allin in this laboratory that a number of wave-lengths were reversed in the spectrum of an underwater spark between terminals of a Te-Au alloy. With this information before us, we attempted to make an analysis of the TeI spectrum, and were able to make some progress. Incidentally, as we will show later, we have been able to extend the analysis of the SeI spectrum.

III. *Results.**Tellurium I.*

In order to aid us in the present investigation, we have re-measured the wave-lengths in the tellurium arc spectrum in the spectral range λ 3200 Å. to λ 1640 Å. The wave-lengths from λ 3200 Å. to 2080 Å. had been observed and measured previously by others, but we believe that our values are more accurate. Those below λ 2080 Å. have been measured for the first time. The wave-lengths with their intensities, frequencies, and the term classification that we have assigned in certain cases are contained in Table III. Three spectrographs were used for the photography of the spectrum, a Hilger E 1 spectrograph of the

TABLE III.

I.	λ (I.Å.).	ν vac.	Classification.
3	3175.15	31485.5	
1	2858.28	34975.8	
6	2769.65	36095.0	$5^1\bar{D}_2-6^3S_1$
6	2530.73	39502.4	$5^3P_1-6^5S_2$
3	2431.71	41110.7	
3	2420.10	41308.0	
17	2385.76	41902.6	$5^3P_1-6^3S_1$
15	2383.24	41946.9	$5^3P_0-6^3S_1$
10	2265.52	44126.3	$5^1\bar{D}_2-a_1$
12	2259.02	44253.2	$5^3P_2-6^5S_2$
10	2255.49	44322.5	$5^1\bar{D}_2-b_2$
9	2208.74	45260.5	$5^1\bar{D}_2-c_2$
8	2159.79	46286.2	
9	2147.19	46557.8	$5^1\bar{D}_2-d_2$
20 R	2142.75	46654.2	$5^3P_2-6^3S_1$
12	2081.03	48037.8	$5^1\bar{D}_2-e_2$
8	2070.9	48273	$5^1\bar{D}_2-f_3$
8	2002.0	49934	$5^3P_1-a_1$
6	2000.2	49979	$5^3P_0-a_1$
7	1994.2	50130	$5^3P_1-b_2$
3	1957.5	51068	$5^3P_1-c_2$
4	1957.1	51078	
2	1954.5	51146	
3	1909.1	52363	$5^3P_1-d_2$
4	1895.5	52738	
6	1859.9	53751	
8	1856.6	53845	$5^3P_1-e_2$
2	1854.3	53906	
6	1853.1	53943	
6	1851.5	53993	
6	1850.0	54037	

TABLE III. (*continued*).

I.	λ (I.A.). λ (I vac.).	ν vac.	Classification.
3	1844.0	54176	
4	1828.9	54673	$5^3P_2-a_1$
6	1825.5	54780	
10	1822.4	54873	$5^3P_2-b_2$
3	1798.4	55605	
6	1796.3	55670	
6	1795.7	55689	
2	1791.8	55610	$5^3P_2-c_2$
4	1790.7	55844	
3	1777.4	56262	
5	1775.0	56338	
3	1773.8	56376	
5	1759.4	56838	
6	1751.0	57110	$5^3P_2-d_2$
3	1733.0	57703	
2	1730.6	57783	
3	1721.2	58099	
3	1712.8	58384	
5	1708.0	58548	
3	1706.7	58593	$5^3P_2-e_2$
6	1700.0	58824	$5^3P_2-f_3$
5	1688.5	59224	
3	1663.1	60129	
5	1655.4	60408	
3	1645.0	60790	

Littrow type with quartz prism for the range λ 3175 Å. to λ 2081 Å., a Hilger E 31 quartz spectrograph for the range λ 2081 Å. to λ 1856 Å., and a Hilger fluorite vacuum spectrograph for the ultraviolet below λ 1856 Å.

An analysis of the wave-lengths of the tellurium arc spectrum has led to the structure summarised in Table IV. The two wave-lengths λ 2259.02 Å. and λ 2142.75 Å. that we have classified as $5^3P_2-6^3S_2$ and $5^3P_2-6^3S_1$ were observed by Zumstein⁶ to be absorbed by tellurium vapour. He also observed in his experiments absorption of λ 2385.76 Å. and λ 2383.24 Å. These we have classified as $5^3P_1-6^3S_1$ and $5^3P_0-6^3S_1$ respectively. Kimura⁷ recently found that the former pair of wave-lengths involving the term 5^3P_2 were absorbed by normal vapour, while the latter pair were not. This would appear to indicate that λ 2385.76 Å. and λ 2383.24 Å. originate in transitions involving metastable states. Whether or not the term 5^3P_0

TABLE IV.

Term.	5^1D_2	$\Delta\nu$	5^3P_1	$\Delta\nu$	5^3P_0	$\Delta\nu$	5^3P_2
Value.	10,558.6	5807.6	4751.0	44.3	4706.7	4706.7	0
6^3S_2	44,253.4	—	(6) 2,530.73 39,502.4			(12) 2,259.02 44,253.2	
	2,400.2						
6^3S_1	46,653.6	(6) 2,769.65 36,095.0	(17) 2,385.76 41,902.6		(15) 2,385.24 41,946.9	(20 R) 2,142.75 46,654.2	
	8,031.3						
a_1	54,684.9	(10) 2,265.52 44,126.3	(8) 2,002.0 49,934		(6) 2,000.2 49,979	(4) 1,828.9 54,678	
	196.2						
b_2	54,881.1	(10) 2,255.49 44,322.5	(7) 1,994.2 50,130			(10) 1,822.4 54,873	
	937.8						
c_2	55,818.9	(9) 2,208.74 45,260.5	(3) 1,957.5 51,068			(2) 1,791.8 55,810	
	1,297.5						
d_2	57,116.4	(9) 2,147.19 46,557.8	(3) 1,909.1 52,363			(6) 1,751.0 51,110	
	1,480.0						
e_2	58,593.4	(12) 2,081.03 48,037.8	(8) 1,856.6 53,845			(3) 1,706.7 58,593	
	236						
f_3	58,832	(8) 2,070.9 48,273				(6) 1,700.0 58,824	

in Table IV. is valid or not is uncertain. The negative difference $5^3P_0 - 5^3P_1 = -44.3$ is rather unusual and only occurs twice, but we have not been able to bring the strong line λ 2383.24 Å. in any other way into the structure of the spectrum. The fact that singlet-quintet inter-combination lines are rarely observed explains the absence of $5^1D_2 - 6^5S_2$.

We have not been able to identify definitely any of the terms of higher energy than 6^3S_1 , because the estimated intensities of the wave-lengths that involve these terms are of little use as a guide in selecting multiplets. This is on account of the fact that the wave-lengths are spread over such a large spectral range. We have therefore designated the terms that we have worked out by small letters *a*, *b*, *c*, etc., with the inner quantum numbers that our analysis has led us to inscribe as subscripts.

Selenium I.

In our investigation of the tellurium arc spectrum we observed five wave-lengths in it that were due to the presence of selenium as an impurity in the tellurium metal we used for arc terminals. We have found that these five wave-lengths are the most fundamental ones of the Se_I spectrum, and have classified them in the first two rows of Table V. Our classification has been strongly supported by the observation made by Kimura⁷ that the four more intense of these five wave-lengths were reversed in a selenium arc.

Another multiplet—namely, that classified as $4^3P - 5^3D$ —is included in the table. The wave-lengths in this multiplet were obtained from tables of measurements by McLennan, Young, and Ireton⁸. The frequency differences, however, are not very exact, so that the correctness of the classification is rather doubtful.

Conclusion.

The addition that we have been able to make to the known structure of the Se_I spectrum and our analysis of the Te_I spectrum have shown that, in so far as they are known, these spectra are similar to those of O_I and S_I . All four spectra have been shown to conform to the theoretical structures predicted for them by the Pauli-Heisenberg-Hund theory. The structure for Po_I is not yet known, as only a very few wave-lengths that belong to its arc spectrum have been observed.

494 *Arc Spectra of Elements of the Oxygen Group.*

TABLE V.

Term.		4^3P_o	$\Delta\nu$	4^3P_1	$\Delta\nu$	4^3P_2
	Value.	2,534	544	1,990	1,990	0
5^3S_2	48,187			(1) 2,164.0 46,196		(3) 2,074.6 48,187
$\Delta\nu$	2,8.4					
5^3S_1	51,001	(8) 2,062.6 48,467		(10) 2,039.7 49,011		(10) 1,960.2 51,000
$\Delta\nu$	10,687					
5^3D_1	61,668	(3) 1,690.4 59,158		(3) 1,674.9 59,705		(2) 1,621.3 61,679
$\Delta\nu$	148					
5^3D_2	61,836			(4) 1,670.8 59,852		(1) 1,617.3 61,831
$\Delta\nu$	407					
5^3D_3	62,243					(2) 1,606.6 62,243

The authors wish to take this opportunity to thank Mr. Crawford and Mr. Clark, who assisted us greatly by photographing the tellurium arc spectrum in the extreme ultra-violet region with the fluorite vacuum spectrograph. To Miss Allin our thanks are also due for contributing the results of her investigations on the under-water spark spectrum of tellurium. Finally, acknowledgment should be made to the National Research Council of Canada for the award of a studentship to one of us, Mr. J. H. McLeod, that made it possible for him to take part in this investigation.

References.

1. Fowler, 'Series Spectra,' 1922.
2. Hopfield, *Astr. Journ.* lix. p. 114 (1924); *Phys. Rev.* xxix. 6, p. 923 (1927).
3. Hopfield, 'Nature,' cxii. p. 437 (1923).
Hopfield and Birge, 'Nature,' cxii. p. 790 (1923).
Laporte, *Naturwiss.* xii. p. 598 (1924).
4. Birge, *J. O. S. A.* viii. p. 233 (1924).
5. Bungartz, *Ann. der Phys.* lxxvi. p. 709 (1925).
Hopfield and Dieke, *Phys. Rev.* xxvi. 5, p. 638 (1926).
6. Zumstein, *Phys. Rev.* xxvii. 5, p. 562 (1926).
7. Kimura, *Jap. Journ. of Phys.* iv. 2, p. 81 (1926-27).
8. McLennan, Young, and Ireton, *Proc. Roy. Soc. A*, xcvi. p. 95 (1920).

XLV. Application of Schrödinger's Wave Functions to the Calculation of Transition Probabilities for the Principal Series of Sodium. By Y. SUGIURA *.

Introduction.

HOYT†, THOMAS‡, and BARTELS§ have tried to calculate the transition probabilities of the series electrons in sodium by the application of the correspondence principle to the orbital model of the sodium atom. In all calculations of this kind only an estimate of the transition probabilities could be obtained, due to the lack of a rational method of averaging between initial and final orbits. The recent development of quantum mechanics of Heisenberg|| and Schrödinger¶ has removed this difficulty, so that it is now possible to calculate rationally the transition probabilities of the series electron not only in hydrogen, but also in higher atoms, as soon as the expression for the potential energy is known.

The rigorous quantum mechanical solution of the problem of an atom with several electrons involves very difficult calculations, but for many purposes a satisfactory treatment may be based on a comparison of the behaviour of the elements with that to be expected from the stationary states of an electron moving in a central field of force. As regards

* Communicated by Prof. N. Bohr, Ph.D.

† F. C. Hoyt, *Phil. Mag.* xvi. p. 135 (1923); *Phys. Rev.* xxv. p. 174; xxvi. p. 749 (1925).

‡ W. Thomas, *Zs. f. Phys.* xxiv. p. 169 (1924).

§ H. Bartels, *Zs. f. Phys.* xxxii. p. 415 (1925).

|| W. Heisenberg, *Zs. f. Phys.* xxxiii. p. 879 (1925), and various papers in *Zs. f. Phys.*

¶ E. Schrödinger, *Ann. d. Phys.* lxxix. p. 361 (1926), and four other papers by the same author in *Ann. d. Phys.*

the latter problem Kramers* has shown quite recently that a rational first approximation to the quantum-mechanical calculation may be obtained by using an orbital model fixed by the usual quantum conditions, if in these half-number values are introduced for the radial and azimuthal quantum numbers. As already shown in a paper by Urey and the writer†, it is in fact possible in case of the X-ray spectra of the heavier elements to construct an interatomic field which allows us to account closely for the observed X-ray terms by means of these conditions.

Relying on the same method of approximation and applying Schrödinger's theory of wave functions, it is attempted in the present paper to calculate the transition probabilities for the principal series of the optical spectrum of sodium. Compared with the problem treated in the previous paper the present problem presents the simplicity that in constructing the central field we may neglect the effects of the spin of the electron and relativity modifications of mechanics. In fact, for the optical terms as well as for the X-ray terms, the doublets arising from these effects are quite small compared with the possible errors involved in our calculation.

§ 1. Central Field in Sodium Atom.

In Table I. are given the values of the spectral terms taking the Rydberg constant R as unity. The term values are compiled from the well-known reports of Siegbahn and Fowler and are denoted in the usual way by the symbol n_k . The field corresponding to these terms is derived by means of the quantum condition‡

$$n - k + \frac{1}{2} = \frac{\sqrt{2}}{\pi} \log_{10} \times \int_{10^{\tau_{\min.}}}^{10^{\tau_{\max.}}} \sqrt{-\frac{1}{2} \left(\frac{\nu}{R} \right) 10^{2\tau} - \frac{1}{2} (k - \frac{1}{2})^2 + Q} d\tau, \quad (1)$$

where for the sake of convenience a logarithmic scale for the radius vector r is used,

$$x = \log_{10} \frac{r}{a_H} \quad \text{and} \quad a_H = \frac{h^2}{4\pi^2 m e^2},$$

* H. A. Kramers, *Zs. f. Phys.* xxxix. p. 828 (1926).

† Y. Sugiura and H. Urey, *Communication Copenhagen Academy, Math.-phys.* vii. p. 13 (1926).

‡ Comp. Sugiura and Urey, *l. c.*

a_H being half the major axis of the electron orbit in the orbital model of the normal state of the hydrogen atom. Further,

$$Q = \frac{r^2}{e^2 a_H} V,$$

where V is the potential energy of the electron in the central field. In order to evaluate Q as a function of x we draw in a Q, x diagram first the curve 10^{2x} and cut the paper along this curve, so that by sliding along the x - and Q -axis by amounts

equal to $\frac{1}{2}\left(\frac{\nu}{R}\right)$ and $\frac{1}{2}(k-\frac{1}{2})^2$ respectively, we can draw the

Q -curve to fit the condition (1) for all n_k terms as closely as possible. The Q -curve thus obtained is shown in the accompanying figure and the accuracy of the computation is illustrated by the last column of Table I. obtained by introducing the function Q given by this curve in (1).

TABLE I.

n_k .	$\left(\frac{\nu}{R}\right)$ obs.	$(n-k)$ calc.
1 ₁	78.8	0.00
2 ₁	4.33	1.01
2 ₂	2.08	0.00
3 ₁	0.378	2.02
3 ₂	0.223	1.00
3 ₃	0.112	0.00
4 ₁	0.143	3.03
4 ₂	0.101	1.99
4 ₃	0.0629	1.00
4 ₄	0.0625	0.00
5 ₁	0.0752	4.02
5 ₂	0.0584	2.98
5 ₃	0.0402	1.99
5 ₄	0.0400	0.99
6 ₁	0.0463	5.02
6 ₂	0.0378	3.96
6 ₃	0.0279	2.98
6 ₄	0.0277	1.98

§2. *Schrödinger's Proper Functions for 3₁, 3₂, and 4₂ Orbits of Sodium.*

In the case of a central field, we have the following expression for Schrödinger's wave equation :

$$\rho^2 \frac{d^2 \chi_{n,k}}{d\rho^2} + 2\rho \frac{d\chi_{n,k}}{d\rho} - \left\{ \frac{\nu_{n,k}}{R} \rho^2 - 2Q + k(k-1) \right\} \chi_{n,k} = 0,$$

$$k = 1, 2, 3 \dots,$$

where $\chi_{n,k}$ is a function of ρ only, ρ being $\frac{r}{a_H}$ and Schrödinger's proper function

$$\Psi_{n,k,m} = \chi_{n,k}(\rho) F_{k,m}(\theta, \phi)$$

for polar coordinates ρ, θ, ϕ . If we can regard a small portion of Q as a part of a parabola, the above differential equation may be written generally as follows :

$$-\frac{d^2 R_{n,k}}{d\rho^2} + \left(A + \frac{B}{\rho} + \frac{C}{\rho^2} \right) R_{n,k} = 0,$$

$$\text{where } R_{n,k} = \rho \chi_{n,k}.$$

Putting

$$x = 2 \sqrt{-A} \rho,$$

we have

$$\frac{d^2 R_{n,k}}{dx^2} + \left(-\frac{1}{4} + \frac{\kappa}{x} + \frac{\frac{1}{2} - \mu^2}{x^2} \right) R_{n,k} = 0,$$

$$\text{where } \kappa = \frac{B}{2\sqrt{-A}} \quad \text{and} \quad \mu^2 = \frac{1}{4} - C.$$

The solution of this differential equation can be expressed in terms of confluent hypergeometric functions $M_{\kappa, \pm\mu}$ * and

$$R_{n,k} = C_1 M_{\kappa, \mu} + C_2 M_{\kappa, -\mu}, \quad \dots \quad (2)$$

where

$$M_{\kappa, \pm\mu} = e^{-\frac{1}{2}x} x^{\frac{1}{2} \pm \mu} \left\{ 1 + \frac{\frac{1}{2} + \mu - \kappa}{1! (1 \pm 2\mu)} x + \frac{(\frac{1}{2} \pm \mu - \kappa)(\frac{3}{2} \pm \mu - \kappa)}{2! (1 \pm 2\mu)(2 \pm 2\mu)} x^2 + \dots \right\},$$

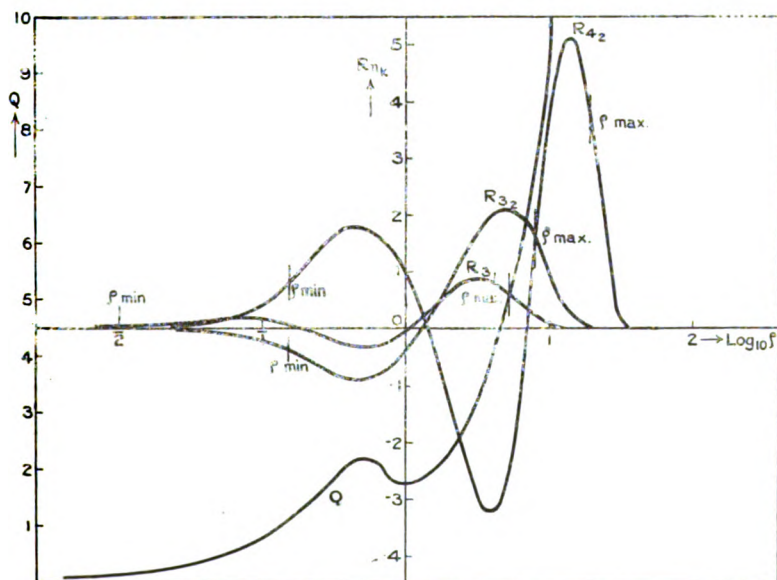
if 2μ is not an integer. For large values of $|x|$ we have generally two asymptotic expressions, one of which is Whittaker's

$$W_{\kappa, \mu} \sim e^{-\frac{1}{2}x} x^{\kappa} \times \left[1 + \sum_{j=1}^{\infty} \frac{\{\mu^2 - (\kappa - \frac{1}{2})^2\} \{\mu^2 - (\kappa - \frac{3}{2})^2\} \dots \{\mu^2 - (\kappa - j + \frac{1}{2})^2\}}{j! x!} \right], \quad \dots \quad (3)$$

* Whittaker and Watson, 'Modern Analysis,' Chap. xvi. p. 337.

while we cannot use the other expression, since it becomes infinity at $x=\infty$ and does not satisfy the boundary condition.

We start to calculate the function $R_{n,k}$ from infinity where the field is determined by Coulomb's law, using the expression (3). At the point where two consecutive different expressions of Q meet, our function $R_{n,k}$ has to satisfy the two conditions: $R_{n,k}$ and $\frac{dR_{n,k}}{d\rho}$ shall have the same value on both sides of the point. By these two conditions we can determine the constants C_1 and C_2 in the expression (2) at



Q: Field curve.

$R_{n,k}$: Schrödinger's proper function of the n_k state.

the one side of every connecting point, if they are known on the other side. We pass, in this way, from infinity to the other boundary at zero and test if the boundary condition at zero is satisfied or not. If the field expression and the term value were not correct, we could not obtain a function $R_{n,k}$ which satisfied all the conditions. We tried to modify the field expression, until we obtained functions $R_{n,k}$ which satisfied the boundary conditions. A slight modification of the field Q in the part, where Q was obtained graphically by (1), was sufficient to give the functions $R_{n,k}$ for the $3_1, 3_2$

and 4_2 states, which satisfied all conditions. R_{3_1} cuts the zero line twice and the tangent at zero is not zero, while R_{3_2} and R_{4_2} cut the zero line once and twice respectively and then tangent at zero is zero, as is to be expected. The curvature of $R_{n,k}$ between extreme radii of the corresponding orbit is positive, while outside of them it is negative as shown in the figure.

§ 3. Transition Probabilities for the Principal Series of Sodium.

As is well known, the spectra of sodium and hydrogen are doublet spectra. We are interested, however, only in the whole intensity of the two components of a doublet, since we can easily determine the relative intensities of the components by the statistic weights of the stationary states. Taking, therefore, the case of a central field, where the doublet system is neglected, the part $F_{k,m}(\theta, \phi)$ of Schrödinger's function $\Psi_{n,k,m}$ which depends upon the angles is the same as in the case of hydrogen, in which the spinning electron effect is neglected:

$$\begin{aligned}\Psi_{n,k,\pm m} &= \chi_{n,k}(\rho) F_{k,m}(\theta, \phi) \\ &= \frac{R_{n,k}(\rho)}{\rho} P_{k-1,m}(\cos \theta) \cos m\phi,\end{aligned}$$

where $P_{k-1,m}(\cos \theta)$ is the associated Legendre function of the $(k-1)$ th degree and m th order.

We can now express Heisenberg's matrix coordinates X, Y, Z by Schrödinger's proper functions as follows:—

$$\left. \begin{matrix} X \\ Y \\ Z \end{matrix} \right\}_{n,k,m;n',k',m'} = \int \begin{matrix} x \\ y \\ z \end{matrix} \Psi_{n,k,m} \bar{\Psi}_{n',k',m'} d\Omega,$$

$$d\Omega = r^2 \sin \theta dr d\theta d\phi,$$

where the integration is to be extended over the whole space. In our special case of the principal series of sodium, leaving apart the doublet system, we have the following three possible cases:—(I.) $n, 2, -1 \rightarrow 3, 1, 0$; (II.) $n, 2, 0 \rightarrow 3, 1, 0$; (III.) $n, 2, 1 \rightarrow 3, 1, 0$ for $n, k, m \rightarrow n', k', m'$. The probabilities of these three transitions are equal; the angular part of the proper functions gives therefore a factor $\frac{1}{3}$ in the square of the amplitudes for each of these transitions. The normalised square of amplitude in the sense of quantum

mechanics, corresponding to the sum of all possible cases, is then given by

$$\sum_{(I)(II)(III)} (X^2 + Y^2 + Z^2)_{n_2, s_1} = a_H^2 \frac{\left(\int_0^\infty \rho R_{n_2} R_{s_1} d\rho \right)^2}{\int_0^\infty R_{n_2}^2 d\rho \int_0^\infty R_{s_1}^2 d\rho} \quad (4)$$

which can be calculated graphically by a planimeter, since R_{n_2} and R_{s_1} are known in the whole region of ρ .

On the other hand, the total energy radiated per unit time from one atom is classically

$$-\frac{dE}{dt} = \frac{2}{3c^3} \sum \overline{\ddot{\Psi}}^2 = \sum \frac{(2\pi\nu)^4}{3c^3} \overline{\Psi}^2, \quad . . . \quad (5)$$

corresponding to linear oscillators with moments

$$\Psi = p \cos 2\pi\nu\tau t,$$

where p is charge times classical amplitude. By the definitions of the classical and the matrix amplitude, we have for a definite state n as a classical expression of amplitude

$$A_n = \sum_r C_r \cos 2\pi(\tau\nu t + \delta_r),$$

which is to be compared with the matrix expression *

$$A_n = A_{nn} + \sum_m (A_{nm} e^{2\pi i\nu_{nm}t} + A_{mn} e^{2\pi i\nu_{mn}t}),$$

or $C_r \cos 2\pi(\tau\nu t + \delta_r)$ corresponds to $A_{nm} e^{2\pi i\nu_{nm}t} + A_{mn} e^{2\pi i\nu_{mn}t}$. When we take the time mean value of the square of amplitude,

$$\frac{1}{2} C_r^2 \text{ corresponds to } 2A_{nm} A_{mn}, \quad . . . \quad (6)$$

so that a factor 4 appears in the quantum mechanical expression for the square of amplitude corresponding to the transition between two states.

According to Einstein's conception of spontaneous transition $P \rightarrow Q$,

$$-\frac{dE}{dt} = \sum_Q A_{PQ} h\nu_{PQ}, \quad . . . \quad (7)$$

and the transition probability $\sum_Q A_{PQ}$ for all possible transitions $P \rightarrow Q$ is given generally by

$$\sum_Q A_{PQ} = \frac{1}{g_P} \sum_{P, Q} A_{PQ}, \quad . . . \quad (8)$$

* O. Klein, *Zs. f. Phys.* xli. p. 433 (1927).

while the number of dispersion electrons f is defined by

$$3f = \tau_P \sum_P A_{QP} = \tau_P \frac{1}{g_Q} \sum_{P,Q} A_{QP}, \quad \dots \quad (9)$$

where $\tau_P = \frac{3mc^3}{8\pi^2 e^2 \nu^2}$; g_P and g_Q are the statistic weights of P and Q states. From (8) and (9) we have Ladenburg's relation *

$$3f = \tau_P \frac{g_P}{g_Q} \sum_Q A_{PQ}. \quad \dots \quad (10)$$

Equating (5) and (7) and taking (4) and (6) into account, the transition probability expressed by Schrödinger's proper functions is

$$\begin{aligned} \sum_Q A_{PQ} &= \frac{1}{g_P} \frac{4(2\pi\nu)^4 e^2}{3\hbar c^2 \nu} a_H^2 \frac{\left(\int_0^\infty \rho R_P R_Q d\rho \right)^2}{\int_0^\infty R_P^2 d\rho \int_0^\infty R_Q^2 d\rho} \\ &= \frac{1}{g_P} 2.682 \cdot 10^9 \cdot \left(\frac{\nu}{R} \right)^3 \frac{\left(\int_0^\infty \rho R_P R_Q d\rho \right)^2}{\int_0^\infty R_P^2 d\rho \int_0^\infty R_Q^2 d\rho}, \quad (11) \end{aligned}$$

because in our case all ν_{PQ} are nearly the same ν . Putting (11) in (10) we have

$$3f_{PQ} = \frac{1}{g_Q} \left(\frac{\nu}{R} \right)^3 \frac{\left(\int_0^\infty \rho R_P R_Q d\rho \right)^2}{\int_0^\infty R_P^2 d\rho \int_0^\infty R_Q^2 d\rho} \quad \dots \quad (12)$$

In our special case of the principal series of sodium $g_P=3$ and $g_Q=1$. Using the expressions (11) and (12), we can calculate the transition probability and the number of dispersion electrons for each line of the principal series of sodium, which are shown in the following table.

TABLE II.

n_2-3_1 .	$\frac{\nu}{R}$.	$\frac{1}{a_H^2} \Sigma (X^2 + Y^2 + Z^2)_{n_2, 3_1}$.	$A_{n_2, 3_1}$ (in sec^{-1}).	f .
3_2-3_1	·1545	18.89	·6228 10^8	·9728
4_2-3_1	·2770	·1562	·0297	·0144
5_2-3_1	·3193	·0152	·0056
6_2-3_1	·3398	·00878	·0028
7_2-3_1	·3511	·00553	·0017
8_2-3_1	·3580	·00371	·0011

Estimated.

* R. Ladenburg, *Zs. f. Phys.* iv. p. 451 (1921).

The values of $A_{n,3}$ for higher members than 5_2-3_1 are estimated by assuming the law $A_{n,k}: n', k' \propto \frac{1}{n^3}$, which is proved theoretically for large values of n in the case of hydrogen, and verified by Trumphy* experimentally in the case of sodium. From the values of $A_{n,3}$, we can compute those of f by the expression (10). The transition probability for each D-line of sodium, deduced from the experimental results of Minkowski†, is $0.64 \cdot 10^8 \text{ sec}^{-1}$, which is only a little larger than the computed value $0.62 \cdot 10^8 \text{ sec}^{-1}$. According to Kuhn‡ and Thomas§, the sum of dispersion electrons for all principal series lines and the continuous absorption should be unity in the one electron problem, and this is, moreover, one of the most important relations in the quantum mechanics. In the case of the sodium atom, the total sum of dispersion electrons ought not, in reality, to be unity, but it is nearly one. When we assume, as in the present calculation, the central field and replace the actual problem of many electrons by one electron problem, we should have one for the value of the total sum of dispersion electrons, as the consequence of the quantum mechanics. In order to get the total sum of the dispersion electrons in our special case, however, we have still to take into account the transition 3_1-2_2 , which is impossible in the actual state of sodium. By a similar method as for 3_1 , 3_2 , and 4_2 states, we can get the wave function for 2_2 state, which gives for the value of the square of matrix amplitude

$$\frac{1}{a_H^2} \Sigma (X^2 + Y^2 + Z^2) = \frac{\left(\int_0^\infty \rho R_{2_2} R_{3_1} d\rho \right)^2}{\int_0^\infty R_{2_2}^2 d\rho \int_0^\infty R_{3_1}^2 d\rho} = 0.0752.$$

Knowing $\left(\frac{\nu}{R}\right)_{3_1, 2_2} = 1.70$, we obtain the contribution in the number of dispersion electrons due to the transition 3_1-2_2 : $f_{3_1, 2_2} = 0.043$, which is to be subtracted from $\sum_{n=3}^\infty f_{n, 3_1} + f$ (continuous). On the other hand, we find $\sum_{n=3}^8 f = 0.998$, so that $\sum_{n=2}^8 f = 0.955$, to which we have still

* B. Trumphy, *Zs. f. Phys.* xxxiv. p. 715 (1925).

† R. Minkowski, *Zs. f. Phys.* xxxvi. p. 839 (1926).

‡ W. Kuhn, *Zs. f. Phys.* xxxiii. p. 408 (1925).

§ W. Thomas, *Naturwissenschaften*, xiii. p. 627 (1925).

504 *Transition Probabilities for Principal Series of Sodium.*

to add some contribution due to higher members of the series and due to the continuous absorption. Since this total sum should be unity our calculation shows that the contribution in f due to the continuous absorption is about 0.04.

Conclusion.

In conformity with the result of Kramers, mentioned in the introduction, we have in this paper found the proper functions in the sense of Schrödinger belonging to 3_1 , 3_2 , and 4_2 states of the sodium atom from the observed term values and the central field obtained by a calculation based on an orbital conception. In this way we could avoid the laborious calculations, which are necessary when the solution of the problem in question is required immediately from the solution of a wave equation. The proper functions thus obtained were then used for the calculation of the transition probabilities and the number of dispersion electrons for the principal series of sodium.

According to Minkowski, as stated above, the transition probability for the D-line $0.64 \cdot 10^8 \text{ sec}^{-1}$ gives already $f_{D_1+D_2} \approx 1$ (f = number of dispersion electrons), which seemed to be too big, since even in the case of sodium $\Sigma f \approx 1$. From our calculations, which give a very rapid decrease of f from the first to the higher members of the principal series in sodium, we can, however, see that Minkowski's result is quite reasonable from the point of view of Kuhn's and Thomas' argument.

Finally, the author wishes to express his best thanks to Professor N. Bohr, Dr. W. Heisenberg, and Dr. O. Klein for their kind interest and valuable advice in the present calculation. Especially he wishes to express his sincere thanks to Professor H. A. Kramers who suggested it to him to carry out this work.

Universitetets Institut for teoretisk Fysik,
København.

XLVI. *Ionization by Collision and a "Photoelectric Theory" of the Sparking Potentials. A Reply to Mr. Huxley. By JAMES TAYLOR, M.Sc., Ph.D., A.Inst.P.; The Physical Institute of the University of Utrecht*.*

IN a recent communication to this Journal H. G. L. Huxley (Phil. Mag. May 1927) has considered a Theory of the Sparking Potentials recently put forward by the present writer (James Taylor, Proc. Roy. Soc. A. vol. cxiv. p. 73, 1927; Phil. Mag. iii. p. 753, 1927). In contradistinction to Townsend's Theory we shall refer to this new hypothesis as the "Photoelectric Theory" of the Sparking Potentials. Huxley brings forward a number of objections to the Photoelectric Theory and concludes that it cannot be satisfactory. The object of the present paper is therefore to consider the objections raised, and at the same time give some account of the circumstances which brought about the enunciation of the theory.

The usual accepted Theory of the Sparking Potentials is that of Townsend "which is based upon his theory of ionization by collision in which both electrons and positive ions are assumed to produce new ions by collision with the molecules of the gas in cases where the pressure is large and the sparking potential is above the minimum."

The Townsend theory of ionization by collision for negative ions or electrons is not universally adopted, but leaving this aside, the objections that can be raised against the Townsend Sparking Potential Theory are:—

(1) The hypothesis that low-speed positive ions produce new ions by collision with the molecules of the gas in which they are moving is open to doubt.

(2) According to this Theory, the sparking potentials should be independent of the nature and condition of the cathode surface, whilst in practice it is found to be largely dependent upon these.

The question (1) of the production of ionization and electrons by the action of low-speed positive ions is one which has called forth much controversy. In some recent work "On the Electric Discharge through Gases at very low pressures," Sir J. J. Thomson (Phil. Mag. xlviii. p. i, 1924) deals somewhat extensively with the question of ionization by collision of positive ions, and raises several objections to the hypothesis that low-speed positive ions are

* Communicated by Prof. L. S. Ornstein.

able to ionize by collision against gas molecules. He discusses other methods by which the ionization in the discharge (often attributed to the above action) may be produced, and puts forward an alternative and very interesting hypothesis according to which the positive ions liberate photoelectrons by the action of the radiation emitted when they are neutralized at the cathode surface. A later paper gives experimental verification of such an action (Sir J. J. Thomson, *Phil. Mag.* ii. p. 675, 1926).

The photoelectric theory of the sparking potentials arose naturally out of the above hypothesis of Sir J. J. Thomson. It was also an expression of the conviction, derived from a study of the Schumann radiations of the electric discharge in rare gases, that it is necessary to attribute a not unimportant part of the mechanism of the discharge to the radiations given out by the gas.

With regard to (2) it has been shown by numerous experimenters that the nature and condition of the electrodes have a very considerable effect upon the value of the sparking potentials obtained (*cp.* Holst and Oosterhuis, *Phil. Mag.* xlv. p. 1117, 1923; Taylor, *loc. cit.*), and that the changes from metal to metal are as large as those from gas to gas. Townsend's Theory, in its unmodified form, fails entirely to account for such changes, and they have often been attributed to impurities in the gas (except for the alkali and alkali earth metals). To test this, the writer carried out experiments in which the conditions were very carefully chosen. The results showed that, with an identical filling gas, changes of the sparking potential (with nickel electrodes) of as much as 65 volts in 170 volts could be brought about by alteration of the cathode surface (Taylor, *Phil. Mag.* iii. p. 762, 1927). Polarization effects in which temporary changes of the sparking potentials were exhibited (*Phil. Mag.* iii. p. 755, 1927) due to change in the electrode surface conditions were also observed. Later work (*Proc. Roy. Soc. loc. cit.*) in which carefully purified argon was used, and in which the electrodes were formed by evaporation of tungsten in vacuum, and were perhaps purer than any electrodes previously used in sparking potential work, showed that the sparking potential was a function of the nature and condition of the cathode surface and varied continuously with changes of the latter. Results with "sodiumated" electrodes (formed by electrolysis through the glass walls of the discharge-tubes) further supported this view.

Any satisfactory theory of the sparking potentials must then be able to account for such important electrode surface

effects. The Townsend theory fails to do this. On the other hand, the photoelectric theory gives a satisfactory explanation.

To proceed to the objections raised by Huxley. The writer was aware of the difficulties in question (see Townsend, Phil. Mag. xlv. p. 44, 1923), and refers to them in one of the papers (Phil. Mag. iii. p. 766, 1927) in the following words:—"Nevertheless there are still difficulties in the light of certain experimental evidence in accepting such a theory as outlined above; it is hoped, however, to continue work in this direction, and a fuller consideration of the theory will be given in a later paper." It was pointed out that experiments were in progress in which both the photoelectric emissivity γ (for the actual radiation emitted by the gas) and the sparking potential v_c were being measured, and it is on this definite experimental control which is being carried out at the present time, that the writer looked to and still looks to giving a conclusive answer as to the value of the hypothesis.

At the same time it is wise to discuss the points raised by Huxley. In paragraph (3) of his paper the discharge between a wire and coaxial cylinder is considered. It is stated that "it is found that the critical force X_1 , at the surface of the wire necessary to initiate the discharge, is independent of the diameter of the outer cylinder provided the latter exceeds a certain value. Experimenters who have studied these phenomena are in general agreement on this point." In the opinion of the present writer the experiments on which this generalization is based have been performed only over a very limited range of conditions. Nevertheless the conclusion may be accepted as approximately correct, and Huxley deduces from it rightly that the function γ , in the writer's hypothesis, should be independent of the force at the negative electrode for this case. (This does not imply, however, that γ is independent of the pressure of the gas.)

In Table (I.) are given some results of Watson quoted by Townsend (*Handbuch der Radiologie*, i., Leipzig, 1920) in connexion with the above generalization relative to the electric force X_1 , at the surface of the wire. When we consider the electric force X at the surface of the outer cylinder it is seen that X/P is of the order of one volt per cm. per mm. The gas for the case considered is air. In the second Table the value of X/P ($= \frac{X_c}{P}$) is about 40 volts per cm. per mm. pressure.

TABLE (I.).

E. A. Watson, 'The Electrician,' vol. xi. Feb. 1910.
Cylinder and wire. Air.

Pressure P. mm.	Diameter wire 2a. mm.	X ₁ . Kilovolts per cm.	X. Kilovolts per cm.	X/P. Volts.
760	0.1	75	0.37	0.5
560	0.136	55	0.37	0.67
360	0.211	34	0.36	1.0
760	0.2	61	0.61	0.8
560	0.27	44.5	0.6	1.08
360	0.42	28.5	0.6	1.67
760	0.5	46.5	1.16	1.52
560	0.68	35.0	1.19	2.12
360	1.055	22.0	1.16	3.22

In above outer cylinder diameter = 20 cm.

TABLE (II.).

P. mm.	Diameter wire, 2a. cm.	C. cm.	X ₁ . Kilovolts per cm.	X _c . Kilovolts per cm.	X _c /P. volts.
760	1.0	0.66	40.0	30.3	40
360	1.0	0.82	23.0	14.0	39
108	1.0	1.12	9.45	4.21	39
25.2	1.0	1.73	3.4	0.98	39

C is the least value of the radius of the outer cylinder for which the condition relative to the critical field holds.

X_c is the field at the surface of the cylinder of radius c cm.

Huxley then considers the sparking potential for parallel plate electrodes, and concludes that in this case there is a large variation of γ with the value of X. This appears to be contradictory to the conclusion, arrived at for the case of cylindrical electrodes, that γ was constant. It is, however, not necessarily the case. We see, from the table given by Huxley, for air, that X/P for the cases considered is between 131 and 440 volts per cm. per mm. In the previous case we saw that this value was of the order of some volts. The experimental evidence is not large, and it was for this reason that the writer avoided such controversial points in the previous papers, hoping rather to control the hypothesis by definite experiment than by plausible considerations. Nevertheless, these differences of X/P for the two cases are striking; and it would appear that the velocity with which the positive ions impinge upon the cathode is much greater for the case of the plane electrodes than for the cylindrical

ones considered. We are thus led to infer that γ (for a given pressure) may be constant provided the field at the surface of the cathode is not above a certain value, or, in other words, provided that the positive ions do not strike against the electrode with too large a velocity. Also it can be assumed that as the velocity of the positive ions increases, so does the function γ .

This effect of increased electronic emission produced by positive ions bombarding a metal target with positive ions of increasing velocity has been recently considered (see for example, Jackson, *Phys. Rev.* xxviii. 3, p. 526, 1926), and it has been shown that the number of electrons grows as the speed of the impinging positive ions is increased. We may imagine then that provided the velocity of the positive ion is sufficiently small the photoelectric effect is simply due to the single neutralization of the ion, but when the velocity is sufficiently increased (due to increase of the surface field), we may consider with Sir J. J. Thomson (*Phil. Mag. loc. cit.*) that

"A positive ion striking against the cathode may alternate from the charged to the uncharged condition, if it has much energy, many times before it loses its charge for the last time; each change from the charged to the uncharged state would be accompanied by the emission of radiation." This action would evidently bring about an increase of γ with the electric field X.

It is further stated that the writer's hypothesis is unable to explain the large difference between the force at the surface of a wire, required to start a negative and a positive discharge. This statement cannot be accepted. The electric field at the cathode is entirely different in the two cases, and the circumstances of the genesis of the electrons from the cathode and the magnification by collision both lead to a difference of field in the required direction.

It may further be pointed out that Huxley's criticisms for the most part imply the acceptance of Townsend's theory of ionization by collision for electrons. In the writer's work the photoelectric hypothesis was fitted into the existing fabric merely as an example of its application, but nowhere was a belief of the authenticity of Townsend's theory of ionization put forward, for this is quite unnecessary from the point of view of the photoelectric hypothesis. In the same way it was suggested that the hypothesis could be fitted into the theory of Holst and Oosterhuis. (These physicists simply maintain a different hypothesis of the production of electrons from the cathode.)

Huxley is correct in his statement therefore (paragraph (4)): "It is no argument therefore in favour of Taylor's hypothesis to be able to state that it can be fitted into the relation obtained by Holst and Oosterhuis." On the other hand, it is no argument in favour of the Townsend Theory.

Turning now to paragraph (5) of Huxley's paper. In this part Dubois' results are mentioned and apparently assumed to be in contradiction to those of the present writer. This is most difficult to understand. If we do assume that Dubois' results are due to saline impurities on the electrodes, it is necessary to give some explanation of their action. An unmodified Townsend Theory fails entirely to give such an explanation, indeed it implies that they are without action at all. On the other hand, if the effect is due "to the action of positive ions in causing electrons to be set free, by bombardment, from impurities on the surface," then we are immediately introducing a foreign hypothesis on top of the original one; and since ordinary electrodes exhibit large variations in the value of the sparking potentials, the effect attributed to the new action becomes of large importance, and the Townsend Theory must be modified to account for it.

Now, it is well known that alkali metal impurities very considerably increase the photoelectric emissivity of a metal surface, and this suggests that the correct explanation is afforded by the Photoelectric Sparking Potential Theory.

"Dubois' conclusions indicate, therefore, that with ordinary metal electrodes the emission from the cathode is negligible compared with the action of the positive ions in ionizing molecules of the gas . . . ; for it is very improbable that the emission from all these metals is the same."

If Dubois' conclusions are correct, and if the action is produced by the change of the photoelectric function γ , there appears to be no reason why γ should not be approximately the same for ordinary metals for the Schumann radiation, which is the radiation chiefly responsible for the photoelectric emission: for, according to Compton and Richardson (Phil. Mag. xxvi. p. 549, 1913), the photoelectric sensitiveness is supposed to be the same for all metals, but for the electronegative metals the curve is shifted bodily towards the region of short wave-lengths. It is obvious then that according to this idea the photoelectric emissivity of metals, whilst differing enormously for visible light (near the threshold frequency), may have no great percentage difference in the region of shorter wave-lengths, that is, in the Schumann radiation region.

Again, it is quite conceivable that ordinary metal electrodes

formed in the same way, may acquire surface films in the discharge, of similar nature and yield similar results.

In conclusion it may be mentioned that Huxley gives no consideration at all, nor any alternative explanation of the experimental results obtained on pure electrodes and gases, and on the surface electrode phenomena described in my papers. He simply neglects the experimental findings altogether.

May 19th, 1927.

XLVII. *The Structure of Xenotime and the Relation between Chemical Constitution and Crystal Structure.* By L. VEGARD, Dr. Philos., Professor of Physics at the University, Oslo*.

[Plate XV.]

Introduction.

§ 1. **I**N two papers† published in 1916 and 1917 I gave results of investigations on the structure of xenotime (YPO_4), by means of the Bragg ionization method. As is well known, the crystal form of this mineral is very analogous to that of the zircon group (zircon, rutile, kassiterite, etc.), but owing to the fact that xenotime usually is more or less transformed into another crystal structure, it was very difficult to obtain reflexions of the various orders for the different faces. Thus in a first series of measurements I found for the face (111) only a fourth-order reflexion, while zircon also gave reflexions from the orders (1, 2, and 3) for the corresponding face. These experimental data consequently led to an arrangement of the oxygen atoms somewhat different from that of zircon.

Repeating the observations by an improved experimental arrangement and on better crystal material, I found that the (111) face also in the case of xenotime gave reflexions of the orders 1, 2, and 3, and then it appeared that xenotime and zircon gave essentially the same spectra for the faces (100) (110) (001) (101) (111).

All experimental data could then be accounted for by giving xenotime the same crystal structure as zircon.

It was at the same time pointed out that this result had far-reaching consequences with regard to the important

* Communicated by the Author.

† L. Vegard, "Results of Crystal Analysis, III. and IV.," *Phil. Mag.* xxxii. p. 505 (1916), and xxxiii. p. 395 (1917).

question as to the mutual relationship between chemical constitution and crystal structure.

The result means that compounds of different chemical properties and composed of atoms of different valencies may take up essentially identical atomic arrangements in the solid state and thus be isomorphous as regards crystal structure and crystal form.

A necessary condition for two compounds to take up the same crystal structure is that the two compounds have the same number of corresponding structural units or that they have chemical formulæ of the form A'_{n_1} , A''_{n_2} $A^i_{n_i}$, and α'_{n_1} , α''_{n_2} , $\alpha^i_{n_i}$, where A or α either may be atoms or groups of atoms (radicals).

In a later paper * it was stated that one of the essential conditions to be fulfilled for isomorphous structures was, that the corresponding structural units fulfil certain conditions with regard to the space they require in the lattice †.

It is, however, also certain that the nature of the chemical binding will play a considerable part in determining the atomic arrangement of the atoms. This is evident from the mere fact that elementary substances appear in a great variety of atomic arrangements (space lattices). That the space filling of the atoms is only one factor among several others is also evident from the fact that the crystal structure may be different for chemically analogous substances, although the lattice in question does not involve any volume conditions to be fulfilled. Thus the alkali and ammonium halogenides appear in two different crystal forms, the rock-salt type and the CsCl type.

On account of the importance attached to the structure of the zircon type of crystals, I determined to carry out an analysis of the same group of crystals by means of the powder method. This redetermination of the structure was first carried out for the minerals zircon, rutile, and kassiterite, and the results were described in a paper already published ‡. It appeared that the structure originally

* L. Vegard, *Vid. Selsk. Skr.* i. No. 16, pp. 12 16 (1922); *Zeitschr. f. Phys.* B. 12, pp. 299-303 (1922).

† Recently the same view as to the connexion between chemical constitution and crystal structure has been taken up by Goldschmidt and his collaborator, who in a series of important papers have applied it to a variety of chemical systems. (*Geochem. Verteilungsgesetze*, IV-VIII, *Vid. Akad. Skr. Mat.-nat. Kl.* Nos. 5 and 7 (1925), No. 1, No. 2, and No. 8 (1926).)

‡ L. Vegard, "Results of Crystal Analysis," *Norsk. Vid. Akad. Skr.* i. No. 11 (1925); *Phil. Mag.* i. p. 1151 (1926).

found for rutile and kassiterite was confirmed by the new investigations. The structure of zircon, however, had to be somewhat modified as regards the position of the oxygen atoms.

The structure originally found for zircon could be referred to the space group C_{4v}^{11} . Now the zircon lattice might be derived from this space group, but we had to specialize the parameters in such a way that new symmetry elements appeared and the space group of the highest symmetry, to which the zircon lattice was to be referred, was that of D_{4h}^{19} .

Also the structure of rutile and kassiterite may be regarded as derived from the space group C_{4v}^{11} by a certain specification, which, however, raises the symmetry to that of the space group D_{4h}^{14} .

Although zircon was considered to be morphologically isomorphous with rutile and kassiterite, they were not exactly "isomorphous" with regard to internal structure.

If the crystal structure could show the chemical constitution, the structure found would mean that rutile and kassiterite had to be written as $(TiO_2)_2$ and $(SnO_2)_2$, while the formula of zircon would be $Zr(SiO_4)$.

Description of the Experiments.

§ 2. In the present paper I am going to give the results of an analysis of the structure of xenotime undertaken by means of the powder method. It appeared to be difficult to find a crystal material which was so little transformed that the xenotime spectrum became dominating on the film. After having tried several pieces, Dr. O. Hassel was so kind as to give me a specimen which gave very good powder diagrams.

As the dimensions of the elementary lattice (a and c) were found in the earlier investigations by means of the ionization method, the lines on the powder diagram belonging to xenotime were easily identified.

In one case there might be some doubt whether a weak line might be referred to xenotime in the tetragonal form or to the transformed state or impurities. The question was settled by means of the previous spectra obtained with the Bragg spectrometer, and to be quite sure I also took a complete diagram with a rotating crystal. I also had the opportunity of comparing my diagram with rotating crystal with one taken by Dr. Hassel. In these complete diagrams as well as in the spectra obtained by the Bragg method, the transformed substance and impurities do not interfere with the reflexion maxima obtained from the crystal faces of untransformed xenotime.

The powder spectrogram of xenotime on which the present analysis is based is shown on the Plate.

The result of the identification of lines is given in Table I. The relative intensities of the lines as they were

TABLE I.—Xenotime (YPO_4).

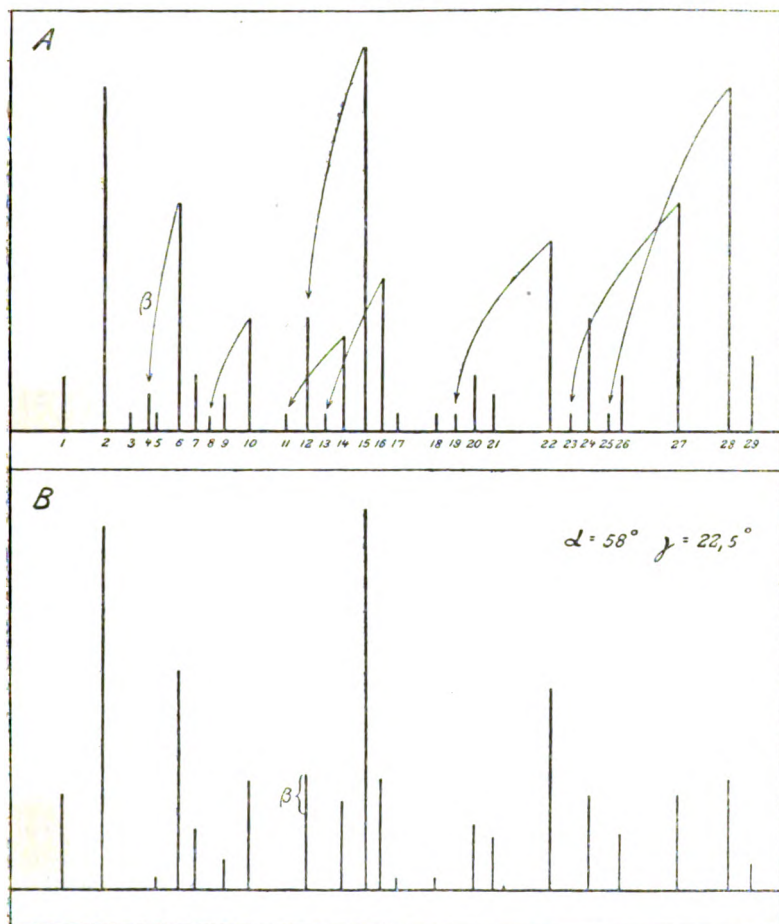
$a=9.735 \text{ \AA.}$ $c=6.013 \text{ \AA.}$ $c/a=0.6177.$ $\alpha=58^\circ.$ $\gamma=22^\circ 5'.$						
No.	ϕ°	$\left(\frac{2a}{\lambda} \sin \phi\right)^2$	$h_1^2 + h_2^2 + \left(\frac{a}{c}\right)^2 h_3^2$	Int.		$h_1 \ h_2 \ h_3$
				Obs.	Cal.	
1	14.520	4.56	4.62	15	25	1 1 1
2	19.393	8.01	8.00	90	95	2 2 0
3	(22.297)	(10.45)	(10.48)	(5)	0	(0 0 2)*
4	24.069	(14.57)	(14.48) β			(2 0 2) β
5	24.758	12.73	12.62	5	3	3 1 1
6	26.579	14.53	14.48	60	57	2 0 2
7	28.006	16.01	16.00	15	16	4 0 0
8	29.040	(20.64)	(20.62) β			(3 3 1) β
9	30.270	18.45	18.48	10	8	2 2 2
10	32.239	20.66	20.62	30	28	3 3 1
11	34.946	(28.75)	(28.62) β			(5 1 1) β
12	{ 36.324	{ (30.74)	{ (30.48) β	30	20 + β	{ (4 2 2) β
	25.49	25.59				1 1 3
13	37.112	(31.90)	(32.00) β			(4 4 0) β
14	38.933	28.67	28.62	25	23	5 1 1
15	40.360	30.45	30.48	100	100	4 2 2
16	41.640	32.05	32.00	40	29	4 4 0
17	42.772	33.52	33.59	5	3	3 1 3
18	45.233	36.60	36.62	5	3	5 3 1
19	46.710	(46.42)	(46.48) β			(6 0 2) β
20	47.940	40.02	40.00	15	17	6 2 0
			{ 41.59 }		7	3 3 3
21	49.072	41.44	{ 41.94 }	10	7	
			42.48		1	0 0 4
22	53.059	46.38	46.48	50	53	4 4 2
			49.59		0	6 0 2
23	54.487	(58.05)	(57.94) β			5 1 3
24	55.963	49.86	49.94	30	25	(4 0 4) β
			50.48		0	2 2 4
25	57.686	(62.58)	(62.48) β			6 2 2
			{ 52.62 }		1	(6 4 2) β
26	{ 58.424	52.69	{ 52.62 }	15	14	5 5 1
			{ 57.94 }		21	7 1 1
27	{ 63.149	57.79	{ 57.59 }	60	4	4 0 4
			60.62		0	5 3 3
			{ 61.94 }		7	7 3 1
28	{ 67.924	62.35	{ 62.48 }	90	22	4 2 4
			64.00		7	6 4 2
29	70.089	64.18		20		8 0 0

* Impurities.

estimated from the spectrogram are given in diagram A of fig. 1.

We now first of all tried whether we could explain the intensities of the lines by means of the structure originally found for zircon and xenotime, but for certain lines there

Fig. 1.



was a disagreement between observed and calculated intensities, which showed—as in the case of zircon—that the atomic arrangement originally found for xenotime had to be somewhat modified. We then naturally tried an atomic arrangement corresponding to the one finally found for zircon.

The coordinates of the basis group of the zircon lattice are given in a previous paper*.

We shall express the coordinates of the basis group of xenotime in the same way as used for zircon, and for the sake of convenience we write down its coordinates. Our unit cell contains 8 molecules. Now all atoms are arranged in face centred lattices, and we merely need to give their coordinates.

$$\left. \begin{array}{l} Y : [\frac{1}{8}, \frac{1}{8}, \frac{1}{8}], \quad [-\frac{1}{8}, -\frac{1}{8}, -\frac{1}{8}]; \\ P : [\frac{1}{8}, \frac{1}{8}, \frac{3}{8}], \quad [-\frac{1}{8}, -\frac{1}{8}, \frac{3}{8}]; \\ O \left\{ \begin{array}{ll} [\frac{1}{8} + \epsilon, \frac{1}{8} + \epsilon, \frac{1}{8} + \eta], & [\frac{1}{8} - \epsilon, \frac{1}{8} - \epsilon, \frac{1}{8} + \eta], \\ [\frac{1}{8} - \epsilon, \frac{1}{8} + \epsilon, \frac{1}{8} - \eta], & [\frac{1}{8} + \epsilon, \frac{1}{8} - \epsilon, \frac{1}{8} - \eta], \\ [-\frac{1}{8} - \epsilon, -\frac{1}{8} - \epsilon, -\frac{1}{8} - \eta], & [-\frac{1}{8} + \epsilon, -\frac{1}{8} + \epsilon, -\frac{1}{8} - \eta], \\ [-\frac{1}{8} + \epsilon, -\frac{1}{8} - \epsilon, -\frac{1}{8} + \eta], & [-\frac{1}{8} - \epsilon, -\frac{1}{8} + \epsilon, -\frac{1}{8} + \eta]. \end{array} \right. \end{array} \right\} \quad (1)$$

We put

$$\left. \begin{array}{l} 2\pi\epsilon = \alpha, \\ 2\pi\eta = \gamma, \end{array} \right\} \dots \dots \dots (2)$$

and the structure factor takes the form :

$$S = \cos A(Y + (-1)^A P + 40 \cos h_1 \alpha \cos h_2 \alpha \cos h_3 \gamma) + 40 \sin A \sin h_1 \alpha \sin h_2 \alpha \sin h_3 \gamma. \quad (3)$$

$$A = 2\pi(h_1 + h_2 + h_3).$$

We distinguish between the three cases :

$$\begin{array}{lll} \Sigma h = 4n, & \cos A = \pm 1, & \sin A = 0; \\ \Sigma h = 4n + 1, & \cos A = \pm \frac{1}{\sqrt{2}}, & \sin A = \pm \frac{1}{\sqrt{2}}; \\ \Sigma h = 4n + 2, & \cos A = 0, & \sin A = \pm 1. \end{array}$$

It should also be remembered that S is to be multiplied with the structure factor characteristic of the face-centred lattice, but this is either 4 or 0; but when we remember that this factor cuts out all reflexions of planes with mixed indices, we need not take this factor into account.

In the case of zircon we deduced directly from the intensities the parameter values:

$$\alpha = 56^\circ, \quad \gamma = 20^\circ.$$

* L. Vegard, *Vid. Selsk. Skr.* i. No. 11 (1925); *Phil. Mag.* i. p. 1151 (1926).

From the condition that one Zr-atom shall have "contact" with eight oxygen atoms, and that the oxygen atoms shall be mutually in "contact," we found the values :

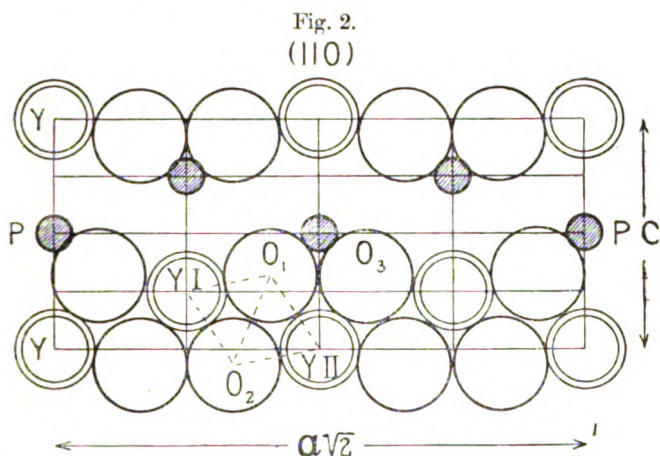
$$\alpha = 58^\circ, \quad \gamma = 19^\circ.3,$$

and within the limit of possible error these values coincide with those directly found from the intensity distribution. Thus there is very good reason to believe that the parameters are in accordance with these contact conditions.

In the case of xenotime the corresponding conditions for the centre distances are :

$$\left. \begin{array}{l} Y_{(I)} - O = Y_{(II)} - O_1 ; \\ O_1 - O_2 = O_1 - O_3. \end{array} \right\} \dots \dots (4)$$

The meaning will be seen from fig. 2.



From these two equations we obtain the parameter values :

$$\begin{array}{ll} \epsilon = 0.161, & \alpha = 58^\circ, \\ \eta = 0.062, & \gamma = 22^\circ.5. \end{array}$$

In addition we tried the following sets of parameter values :

- (1) $\alpha = 60^\circ, \quad \gamma = 30^\circ.$
- (2) $\alpha = 56^\circ, \quad \gamma = 30^\circ.$
- (3) $\alpha = 52^\circ, \quad \gamma = 22^\circ.5.$
- (4) $\alpha = 56^\circ, \quad \gamma = 20^\circ.$

All of these four sets of values give fairly good agreement with observed intensities, but in all cases there are some small discrepancies; thus, in case (1) line No. 14 comes out stronger than 16 contrary to observations. Further, No. 18 comes out too weak.

In case (2) No. 18 is too weak, and No. 27 is too strong as compared with 28.

In case (3) Nos. 5, 7, 17 are too weak, and No. 27 too strong as compared with 28.

In the case (4) Nos. 5, 17 are too weak. In fact we find the best agreement with the parameters $\alpha = 58$ and $\gamma = 22^\circ.5$, which fulfil the above-mentioned "contact" conditions.

The relative intensities calculated by means of these parameters are given in fig. 1 B.

It should be noticed that a faint line No. 3 was observed, which happens to coincide with the position of (002) for xenotime, but the intensity of this line should be identically zero. This faint line No. 3, however, is no doubt due to impurities or to the transformed product of xenotime, for neither the ionization method nor the diagrams taken with rotating crystals show any reflexion corresponding to (002); in these diagrams from faces with definite orientation a line due to impurities or transformed substance would not appear.

From the values found for the parameters we can calculate the "diameters" of each of the constituent atoms. For the centre distances we get:

$$\text{O}-\text{O} = 2.45 \text{ \AA}, \quad \text{Y}-\text{O} = 2.24 \text{ \AA}, \quad \text{P}-\text{O} = 1.66 \text{ \AA}.$$

In Table II. we give the quantities determining the xenotime lattice, and for the sake of comparison we have added those of zircon.

TABLE II.

	Xenotime.	Zircon.
a	9.735 \AA	9.41 \AA
c	6.013 "	6.01 "
c/a	0.6177	0.639
e	0.161	0.161
η	0.062	0.0535
ρ_{O}	1.22 \AA	1.18 \AA
ρ_{Y}	1.02 "	ρ_{Zr} 0.99 "
ρ_{P}	0.44 "	ρ_{Si} 0.49 "

Crystal Structure and Atomic Properties.

§ 3. As the result of these investigations we find that xenotime has actually the same structure as zircon, and very nearly the same dimensions and parameters, and the general conclusions which were drawn from this fact in my paper* published in 1917 have been confirmed.

In the case of zircon we have oxygen attached to two four-valent atoms (Zr Si), in the second case we have one three-valent atom (Y) and one five-valent (P), and these differences involve considerable differences as regards chemical forces and constitution.

In order to explain that the two substances show practically the same atomic arrangement, we have to take two facts into account:—

First of all we notice the most suggestive fact that *the sum of the valencies in both cases is equal to 8*. The sum of the valency electrons is equal to the number (8) which should be characteristic of the "surface" system of the inert gases. This fact suggests that although the valencies are unequal for the atoms of the two minerals, they may in combination form similar electronic systems responsible for the mutual binding of the atoms.

Secondly, the substances fulfil the condition that *corresponding atoms (ions) require nearly the same space in the lattice, or they have about equal "atomic diameters."*

The latter condition is in the present case most essential, for *the lattice puts very strong volume conditions on the dimensions of those atoms which are able to form crystals of the same structure and axis ratio (c/a) as zircon and xenotime.*

The contact conditions previously mentioned † lead to the following equations:

$$\left. \begin{aligned} \epsilon - \frac{1}{2} \left(\frac{c}{a} \right)^2 \eta &= \frac{1}{16} \left\{ 2 + \left(\frac{c}{a} \right)^2 \right\}, \\ \epsilon + \frac{1}{2} \left(\frac{c}{a} \right)^2 (\eta + 4\eta^2) &= \frac{1}{16} \left\{ 3 - \frac{1}{2} \left(\frac{c}{a} \right)^2 \right\}. \end{aligned} \right\} \dots (5)$$

By means of these two equations the parameters ϵ and η are determined as functions of the axis ratio c/a .

Let us now suppose the substance to have the chemical formula ABC_4 , then, as we saw, we can find the diameters of A, B, and C as functions of a and (c/a) . The equations are easily written, but for the sake of brevity we need only

* L. Vegard, Phil. Mag. xxxiii. p. 421 (1917).

† L. Vegard, Vid. Selsk. Skr. i. No. 11 (1925); Phil. Mag. i. p. 1151 (1926).

remark that by introducing the values of the parameters (from 5), we obtain the diameters δ as known functions of a and c/a ; in fact we have

$$\delta = a\phi(c/a),$$

or

$$\frac{\delta_A}{\phi_A\left(\frac{c}{a}\right)} = \frac{\delta_B}{\phi_B\left(\frac{c}{a}\right)} = \frac{\delta_C}{\phi_C\left(\frac{c}{a}\right)} \dots \dots (6a)$$

If the axis ratio c/a is given, $\phi_A(c/a)$, $\phi_B(c/a)$, $\phi_C(c/a)$ are known, and only those atoms which approximately fulfil the condition (6a) can build up a zircon lattice. If the crystals be regarded as isomorphous, they should possess about equal axis ratio c/a ; consequently for substances isomorphous with zircon c/a should be equal to about 0.65, and the atomic diameters should approximately fulfil the relation

$$\frac{\delta_A}{1} = \frac{\delta_B}{0.46} = \frac{\delta_C}{1.2} \dots \dots (6b)$$

If we write rutile TiTiO_4 and kassiterite SnSnO_4 they are seen to be of the form ABO_4 , where $A = B$. But we see that in this case the relation (6) is not fulfilled, and these substances cannot be exactly isomorphous with zircon, which is in fact in accordance with the structures found for these substances. Thus the strong relation which is claimed by the zircon structure explains the fact that this structure is not exactly isomorphous with that of rutile, although they both lead to nearly equal axis ratios and equal symmetry class, so that they may be said to be morphologically isomorphous. Any substitution of atoms between zircon and xenotime on the one side and rutile and kassiterite on the other should be excluded, or mixed crystals should not exist.

From what has been said it should be essential for the formation of the xenotime and zircon lattice that the sum of the valencies of A and B are equal to 8 and that the atomic diameters have approximately a definite ratio. As the rare earth elements are trivalent, and as most of them under comparable conditions have atomic diameters approximately equal to that of Y, we should expect that a number of substances of the form APO_4 , where A is one of the rare earth elements, would form structures isomorphous with that of xenotime.

Now it is to be remembered that the structure found for xenotime is a somewhat unstable one. Xenotime is gradually

changing crystal structure under maintenance of its external form (metamict).

The xenotime structure involves a very close packing of atoms, and in consequence the minerals of this type have a high density. From the measured dimensions of the lattice we find the density of xenotime to be

$$\rho = 4.23.$$

(Abegg, 'Handbuch der anorganischen Chemie,' gives 4.45—4.70. These somewhat higher values are no doubt to be explained by impurities. The values found from the X-ray analysis correspond to the pure substance.)

The dense packing and the unstability of the lattice indicate that the atoms of xenotime do not fulfil the volume conditions of the lattice so well as those of zircon, so the atoms in a similar way as in mixed crystals have to suffer a certain accommodation of their natural atomic (or ionic) diameters. This exercises a certain internal strain, which causes the gradual transformation. This instability will be counterbalanced if we put the substance under high pressure, because we know from thermodynamics that increase of pressure will have a tendency to produce such a state, which requires a small volume.

This would suggest that a mineral like xenotime is formed under high pressure.

Now in his 'Chemische Kristallographie' Groth states that YPO_4 usually contains impurities of the phosphates of the rare earth elements, which indicates that xenotime forms mixed crystals with phosphates of the rare earth elements, or Y atoms are irregularly substituted by atoms of the rare earth elements La, Ce, Pr, ... etc.

When the rare earth elements become dominating, their phosphates are no longer stable in the zircon lattice, but they take up a monocline structure (monazite). It might, however, be possible that the phosphates of the rare earth elements assume zircon structure under high pressures and in certain intervals of temperature.

The results of my early investigations* on mixed crystals of alkali and ammonium haloides present a striking analogy to this case. At ordinary temperature the substances KCl and NH_4Cl *e.g.* have a different crystal structure; but still in the lattice of KCl more than 20 per cent. of the K atoms

* L. Vegard, "Konstitution der Mischkristalle und die Raumbfüllung der Atome," *Vid. Selak. Skr.* i. No. 6 (1921) (Com. Nov. 30, 1920) *Zeitschr. f. Phys.* B. v. p. 17 (1921).

can be substituted with (NH_4) groups, and from the expansion of the lattice I could by means of the additivity law calculate the dimensions of the NH_4Cl lattice of the face centred KCl type. In this case we know that also pure NA_4Cl at temperatures above 159°C. takes up the face-centred KCl structure.

If we limit our considerations to elements A and B, for which the sum of the positive valencies is equal to 8, we are led to regard a large number of combinations of elements with regard to their ability of forming crystals of the zircon type.

As long as we let oxygen be the third element, the volume conditions require that the radius of the positive A ion is equal to about 1 \AA and that of the B ion equal to about $0.4\text{--}0.5 \text{ \AA}$. In the case when both A and B are four-valent (zircon type), we have to consider the possibility that either Zr or Si may be replaced by another four-valent positive ion. Then the following elements come into consideration: C, Ti (rare earth elements), Th, Ge, Sn, Pb.

A substitution of Si with any of these elements would violate the volume conditions (6).

A substitution of Zr should be excluded for the elements Ge, Sn, Ti, which have too small ionic dimensions.

The diameters of the four-valent positive ions of rare earth elements and the ions $\text{Pb} (+4)$ and $\text{Th} (+4)$ according to Goldschmidt* are nearly equal to that of $\text{Zr} (+4)$.

We have therefore to reckon with the possibility that crystals with zircon structure may be formed by substances where Zr in zircon is substituted with Th, Pb, or some of the rare earth elements.

As a matter of fact the Th compound is known as the mineral Thorite (ThSiO_4), which is isomorphous with zircon†, but in the case of thorite the zircon arrangement is unstable and the zircon type of thorite is gradually transformed (metamict form). As in the case of xenotime, this is explained from the fact that the diameter differs from that claimed by volume conditions, and the lattice is only stable at very high pressure.

As to the existence of the lead compound, I find no references in the literature.

When A is three-valent and B five-valent as in the case of xenotime (YPO_4), the atoms B, Al, Se, and the rare earth

* V. M. Goldschmidt, *Det Norske Vid. Akad. Skr.* i. No. 2 (1926).

† See P. Groth, *Chem. Krist.* i. p. 85, and L. Vegard, *Phil. Mag.* xxxii. p. 93 (1916).

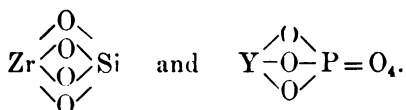
elements may come into consideration, but out of these, as already mentioned, only the rare earth elements approximately fulfil the volume conditions. According to Goldschmidt, Tl as trivalent positive ion has a diameter about equal to that of Y, and therefore from the point of view of volume conditions a compound TIPO_4 might exist in the zircon type of lattice.

If A is two-valent and B is six-valent, a substitution of B with Se (+6) and A by Ca (+2) would approximately fulfil the volume conditions. Further, A might be substituted by Be and B by Cr. Thus the substances CaSeO_4 and BeCrO_4 approximately fulfil the volume conditions required by the zircon structure.

New possibilities would arise when we imagine O substituted by another element, and by means of the volume conditions (6) we should for each substituent of O be able to find out which compounds might possibly possess a structure of the zircon type.

As stated in a previous paper*, similar volume conditions were applied to explain the fact that the anatase structure of TiO_2 only exists in the case of titanium and not for the other elements of the same group. It is of interest to notice that also the structure found for the scheelite group of minerals* leads to fairly strong volume conditions, and by similar considerations we may perhaps understand why a number of analogous substances do not exist with the same crystal structure as that of scheelite.

If we look at the crystal structure of zircon and xenotime from the point of view of their chemical constitution formula, we find that the old way of expressing the chemical constitution would lead to the formulæ:

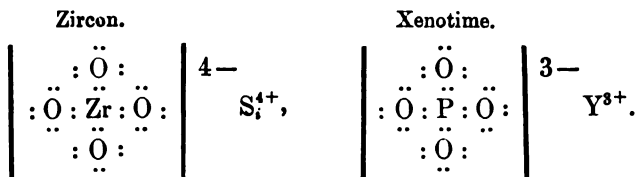


According to these formulæ there should be an essential difference with regard to the chemical constitution of the two substances. In zircon all four oxygen atoms should be equal, while in xenotime one of them should take up a singular position. In the crystal, however, all four oxygen atoms are equal. Either we should have to conclude that the chemical constitution does not come to expression in the

* L. Vegard, *Vid. Selsk. Skr.* i. No. 11 (1925); *Phil. Mag.* i. p. 1151 (1926).

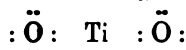
atomic arrangement in the crystal, or we have to find new expressions for the chemical constitution.

Now the way of expressing the chemical constitution, which in later years has been introduced by Werner, Lewis, Langmuir, and Kossel, leads to the following formulæ:



According to these formulæ we have for both minerals a saturated complex of the form MO_4 , with 8 "surface" electrons round each atom, where all oxygen atoms are equal. In the case of zircon the complex carries 4, in the case of xenotime 3 negative elementary charges. These formulæ are thus in perfect agreement with the atomic arrangement in the crystals.

In this connexion it is of interest to notice that the atomic arrangement of rutile (and isomorphous substances) as well as the atomic structure of anatase correspond to a chemical formula $(\text{TiO}_2)_x$. The way in which we write the constitution formula very much depends on the value of x . Putting $x=1$, the constitution formula might be written:



In any case the constitution of TiO_2 and SnO_2 should be essentially different from that of zircon and xenotime, and this difference has found its expression in the crystal structure, in spite of the fact that rutile and zircon on account of analogy as regards form and symmetry properties have been considered as isomorphous. This isomorphism, however, does not apply to internal structure, but merely to external form and morphological symmetry.

Summary of Results.

1. The structure of xenotime has been investigated by means of the powder method and the results verified by comparison with rotating crystal diagrams.
2. The result previously obtained—that xenotime and zircon have practically identical space lattices—has been confirmed.
3. The important consequences, which were drawn in a paper of 1917 from the identity of zircon and xenotime

structure relating to the connexion between chemical constitution and crystal structure, have thus been found valid.

4. In the xenotime lattice all four oxygen atoms are equal, while the old chemical constitution formula would put one of the four oxygen atoms in a singular position. The assumption of the formation of a complex MO_4 with a constitution in accordance with the theories of Werner, Lewis, Langmuir, or Kossel, however, leads to a perfect agreement between the atomic arrangement in the solid state and the constitution formula.

5. In accordance with views expressed in papers published in 1921, one of the factors which may determine the crystal structure is that each atom requires certain space. A great many structures, however, give no volume conditions whatever, and in these cases the nature of the atomic forces is the dominating factor which determines the atomic arrangement. In the case of xenotime, however, the parameter values directly derived from the intensities of the reflexion maxima of the powder diagrams lead to a very close packing of the atoms, and the contact conditions lead to a definite condition with regard to the diameters of those atoms which can form lattices of the zircon type. In this case only substances for which the atoms approximately fulfil the volume conditions of the lattice will be able to form crystals of the zircon type. A number of such possibilities have been mentioned.

6. When the volume conditions are only approximately fulfilled, the lattice is likely to be unstable, but on account of the close packing a lattice of the zircon type may still be stable under very high pressure. Metamict substances like xenotime and thorite have probably been formed under very high pressure. Under ordinary pressure the lattice becomes unstable, and a new more stable lattice is formed under gradual transformation of the minerals.

My sincere thanks are due to Dr. O. Hassel for putting at my disposal a good specimen of xenotime and also photographs of xenotime taken with a rotating crystal. I also wish to express my sincere thanks to Mr. S. Stensholt for his excellent assistance in connexion with these investigations.

Physical Institute,
University, Oslo.
May 11, 1927.

XLVIII. *Heat Regeneration and Regenerative Cycles.* By
WM. J. WALKER, D.Sc., Ph.D., *Professor of Mechanical
Engineering, University of the Witwatersrand, Johannes-
burg* *.

SUMMARY.

THE following paper sets out to investigate the possibilities in heat regenerative cycles, particularly in relation to internal combustion turbine development. A new type of regenerative cycle is proposed, the analysis of which indicates the independence of turbine thermal efficiency on compression ratio. Actually it appears that the thermal efficiency should be higher the lower the compression ratio. The efficiency required of the regenerator unit, however, becomes lower the higher the compression ratio, so that the problem becomes the experimental one of determining the lowest compression ratio at which a regenerator can be designed to meet the conditions imposed.

SO far as thermodynamic cycles are concerned, methods of heat regeneration may be divided into the two classes:—

1. External heat regeneration.
2. Internal heat regeneration.

In the first method the exhaust heat from one prime mover is diverted to another source of supply, such as a steam boiler, and utilized indirectly in another prime mover actuated by the steam produced. The distinctive feature of the method is that the discharged heat is not returned again to take part in a cycle of events similar in all respects to that through which it has just passed.

The second or internal method of heat regeneration has many points of interest, but, possibly owing to somewhat unfortunate ventures in the past in connexion with the development of hot-air engines, it does not appear that any serious attempt has ever been made to investigate its implications in the case of what are now known to be workable thermodynamic cycles for internal combustion engines. The distinctive feature of this method is that some of the rejected heat of a cycle is transferred back again to the fresh charge of working fluid, for the carrying out of the next cycle. The author's investigations into the general nature of this problem have led to certain interesting results which may prove to have some value as a guide to future developments, particularly in gas-turbine evolution.

* Communicated by the Author.

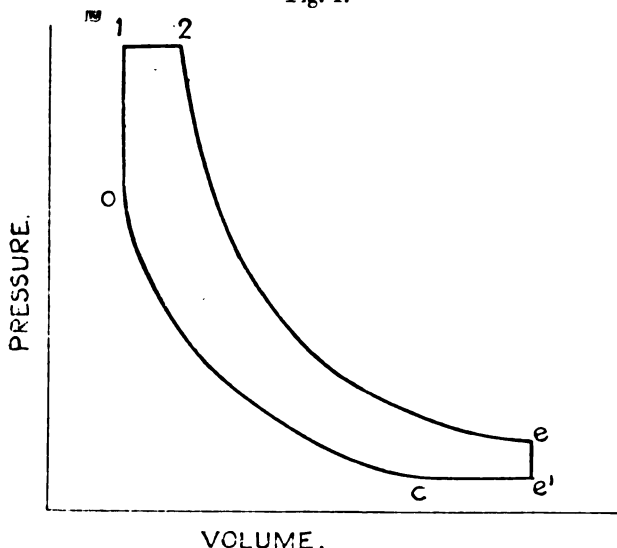
In the classic method of analysing regenerative cycles, each cycle is considered as comprising four general operations as follows in the given order :—

- (a) Isothermal compression at T_2 , say.
- (b) Heat reception.
- (c) Isothermal expansion at $T_1 > T_2$.
- (d) Heat rejection.

If the regenerator efficiency is assumed to be unity, the whole of the heat rejected at (d) is returned during the heat-reception period (b), with the net result that (b) and (d) combined involve neither loss nor gain of heat, and therefore become equivalent to two adiabatic processes. All perfect regenerative cycles of this type have, therefore, the same efficiency as a Carnot cycle between the same temperature limits. Such are the Stirling and Ericsson air cycles with constant volume and constant pressure regeneration respectively. In practice both these cycles failed to realize anything like expectations, because

- (1) They involve external combustion of the fuel ;
- (2) Perfect regeneration cannot be realized ;
- (3) Isothermal compression and expansion are practical impossibilities.

Fig. 1.



Turning now, however, to the possibilities of internal heat regeneration when applied to internal combustion cycles, consider the basic dual combustion cycle of fig. 1. Assuming

that the exhaust gases discharged at temperature T_e are to be used to heat up the supply gases, the most that can be done, theoretically, is to raise the temperature of the latter, by some type of regenerator, also to temperature T_e . In this case, it should be noted, the regenerator does not require to be of unit efficiency, since the exhaust heat discharged is equal to $K_V(T_e - T_{e'}) + K_P(T_{e'} - T_c)$, while, assuming that $T_e < T_1$, that given to the supply gases is $K_V(T_e - T_0)$, which is evidently less. The efficiency of the cycle is given by

$$\begin{aligned}\eta_t &= \frac{\text{Work done}}{\text{Heat received from external sources}} \\ &= \frac{\text{Heat received from external + internal sources} - \text{Heat rejected}}{\text{Heat received from external sources}} \\ &= 1 - \frac{\text{Heat rejected} - \text{Heat received from internal sources}}{\text{Heat received from external sources}} \\ &= 1 - \frac{K_V(T_e - T_{e'}) + K_P(T_{e'} - T_c) - K_V(T_e - T_0)}{K_V(T_1 - T_e) + K_P(T_2 - T_1)} \\ &= 1 - \frac{K_P(T_{e'} - T_c) - K_V(T_{e'} - T_0)}{K_V(T_1 - T_e) + K_P(T_2 - T_1)},\end{aligned}$$

which, substituting all temperatures in terms of T_e , becomes

$$\eta_t = 1 - \frac{m(\beta - 1) - (\beta - r^{m-1})}{\alpha\{r^{m-1} - \rho^m/\beta^{m-1} + m r^{m-1}(\rho - 1)\}}, \quad (1)$$

where

$$r = \text{compression ratio} = \frac{V_e}{V_0},$$

$$\alpha = \text{explosion ratio} = \frac{P_1}{P_0},$$

$$\rho = \text{cut-off ratio} = \frac{V_2}{V_1},$$

$$\beta = \text{extended expansion ratio} = \frac{V_e}{V_c}.$$

For the constant volume cycle, assuming regeneration along these lines to be incorporated, $\rho = 1$ and $\beta = 1$, so that the efficiency from (1) becomes

$$\eta_t = 1 - \frac{1}{\alpha}, \quad . \quad . \quad . \quad . \quad . \quad (2)$$

yielding the somewhat unexpected result that the efficiencies of regenerative cycles of this type are independent of the compression ratio r and the adiabatic index m ; an interesting conclusion in view of the importance of these factors in non-regenerative cycles.

The foregoing has been deduced under the assumption of

constant specific heats of gases. The actual efficiency under variable specific heat conditions is given, to a first and close approximation*, by

$$\eta' = \left(1 - \frac{1}{\alpha}\right) \left\{ 1 - \frac{\lambda T_c}{2} (\alpha + 1) \right\} \\ = 1 - \frac{1}{\alpha} - \frac{\lambda T_c}{2} \left(\frac{\alpha^2 - 1}{\alpha} \right), \quad \dots \quad (3)$$

and evidently increases with α , *i. e.* with the amount of fuel burned per cycle.

It is evident, however, that there are serious practical difficulties in the way of such constant volume regeneration. Constant pressure regeneration is a much more realizable process here, and since it is generally agreed that the constant pressure cycle is the one most applicable to gas-turbine operation, it is natural to investigate such a possibility on the same lines as the foregoing analysis.

It should first be noted that the constant pressure regenerative cycle efficiency cannot be deduced from (1), owing to the discontinuity at point 1 on the cycle, and the consequent uncertainty as to whether or not the regenerated heat will extend its effect past that point. It is obvious from the foregoing that it has been assumed not to have passed that point, *i. e.* T_e is implicitly assumed less than T_1 . If, however, $T_1 < T_e$ and the regenerated heat is added between T_1 and T_2 , the efficiency becomes

$$\eta_i = 1 - \frac{K_V(T_e - T_c) + K_P(T_e - T_c) - K_P(T_e - T_1)}{K_P(T_2 - T_c)}$$

which, by reducing as before, gives

$$\eta_i = 1 - \frac{(\alpha \rho^m / \beta^{m-1} - \beta) + m(\beta - 1) - m(\alpha \rho^n / \beta^{m-1} - \alpha r^{m-1})}{m(\alpha \rho r^{m-1} - \alpha \rho^m / \beta^{m-1})}.$$

For the constant pressure cycle $\alpha = 1$ and $\beta = \rho$, and if this regenerative principle is included, the efficiency becomes

$$\eta_i = 1 - \frac{1}{\rho}, \quad \dots \quad (4)$$

analogous to expression (3).

The corresponding variable specific heat efficiency becomes

$$\eta_i' = 1 - \frac{1}{\rho} - \frac{\lambda T_c}{2} \left(\frac{\rho^2 - 1}{\rho} \right), \quad \dots \quad (5)$$

Although, however, these regenerative cycle efficiencies are independent of compression ratio, such is not the case with the regenerator efficiencies demanded by the systems of regeneration proposed. In the case of the constant volume

* Phil. Mag. Sept. 1917.

cycle, this would evidently be

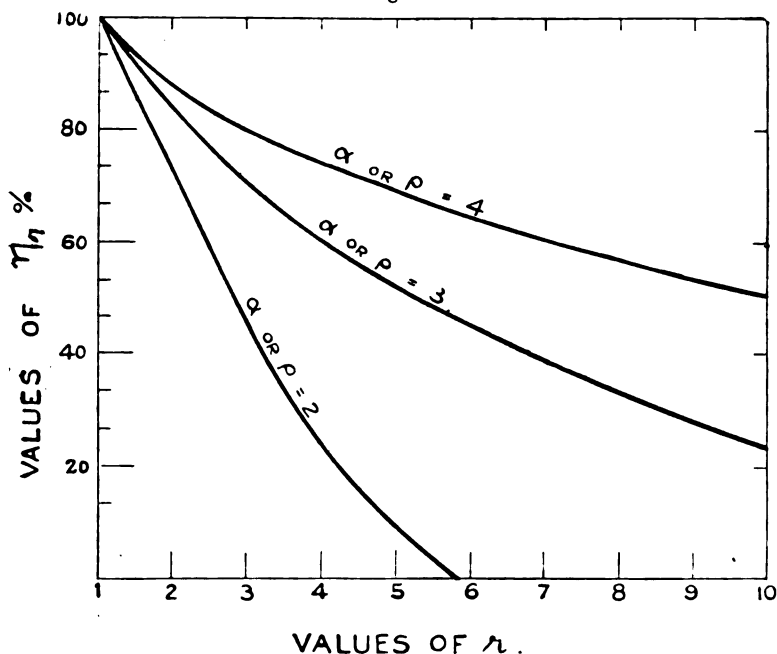
$$\eta_r = \frac{K_V(T_c - T_0)}{K_V(T_c - T_e)} = \frac{\alpha - r^{m-1}}{\alpha - 1} \dots (6)$$

For the constant pressure cycle

$$\eta_r = \frac{K_P(T_c - T_1)}{K_P(T_c - T_e)} = \frac{\rho - r^{m-1}}{\rho - 1} \dots (7)$$

Fig. 2 shows the variation of η_r with the compression ratio r for different values of α and ρ in (6) and (7). Clearly, the higher the compression ratio the lower does

Fig. 2.



the regenerator efficiency require to be to meet the conditions imposed by this method of regeneration.

Should the principle of regeneration here outlined ever become the object of experimental inquiry in connexion with gas-turbine development, the obvious line of approach will be to determine the lowest compression ratio at which the regenerator can meet the conditions imposed. This follows from the fact that, besides conducing to a high mechanical efficiency and to a low value of negative work, a low compression ratio for a given air/fuel ratio will result in a high value of ρ the cut-off ratio, and so yield a high thermal efficiency.

XLIX. A Class of Integral Equations occurring in Physics,
By D. M. WRINCH, M.A., D.Sc., and J. W. NICHOLSON,
M.A., D.Sc., F.R.S.*

THE integral equations and identities to be discussed in this communication are becoming fundamental in certain classes of physical problems. Their "interest" has recently been mainly in relation to problems of seismology. One of the equations is widely known and is usually referred to as the Bateman-Herglotz equation, though its history can be traced much further. It is usually quoted† in the form:—

If

$$\phi(p) = p \int_p^a \frac{f'(\eta) d\eta}{(\eta^2 - p^2)^{1/2}},$$

then

$$f(\eta) = -\frac{2}{\pi} \int_\eta^a \frac{\phi(\lambda) d\lambda}{(\lambda^2 - \eta^2)^{1/2}} + C, \quad \dots \quad (1)$$

where C is some constant. It is used in this form in the application to problems of seismology which are of considerable importance—as emphasized, for example, by Prof. Lamb in his Presidential Address to the British Association in 1925.

The problems of seismology do not, however, exhaust the more immediate uses of this result and others with which it is associated. It is at least of equal importance in problems concerned with the diffraction of waves round certain types of obstacle. But quite apart from these applications, the discussion of this integral equation and the associated equations and identities is of importance in view of the relation between them and the fundamental Bessel-Fourier theorems and equations.

The Bateman-Herglotz equation goes back essentially to Abel‡, whose general result is usually quoted§ in the form:—

If $0 < \sigma < 1$ and

$$\chi(\eta) = \int_\nu^\eta \frac{\phi(\xi) d\xi}{(\eta - \xi)^\sigma}, \quad \dots \quad (2)$$

then

$$\phi(\xi) = \frac{\sin \sigma \pi}{\pi} \frac{\partial}{\partial \xi} \int_\nu^\xi \frac{\chi(\eta) d\eta}{(\xi - \eta)^{1-\sigma}}. \quad \dots \quad (3)$$

* Communicated by the Authors.

† *Vide e. g.* Jeffreys, 'The Earth,' p. 219 (Camb. Univ. Press, 1924).

‡ Collected Works, p. 11; Crelle's Journal, vol. i. p. 153 (1826).

§ Bócher, 'Integral Equations,' p. 8 (Camb. Univ. Press).

Abel generalized this equation from the particular case of $\sigma = \frac{1}{2}$, which he encountered in connexion with the problem of the tautochrone, and though his solution of it was correct the proof was in some ways unsatisfactory. The form given above is appropriate for the case when $\eta > \nu$. There is of course a related equation when $\eta < \nu$ which with its solution may be exhibited as follows :—

If $0 < \sigma < 1$ and

$$\chi(\eta) = \int_{\eta}^{\nu} \frac{\phi(\xi) d\xi}{(\xi - \eta)^{\sigma}}, \quad \dots \dots \dots (4)$$

then

$$\phi(\xi) = -\frac{\sin \sigma \pi}{\pi} \frac{\partial}{\partial \xi} \int_{\xi}^{\nu} \frac{\chi(\eta) d\eta}{(\eta - \xi)^{1-\sigma}}, \quad \dots (5)$$

and it is of this equation that the Bateman-Herglotz equation is a particular case. For, writing $\sigma = \frac{1}{2}$ and

$$\xi = x^2, \quad \eta = y^2, \quad \zeta = z^2, \quad \nu = \gamma^2, \quad \chi(\eta) = g(y)/y, \quad \phi(\xi) = f(x)/2x,$$

it may be written in the form :—

If

$$g(y)/y = \int_{\gamma}^{\nu} \frac{f(z) dz}{(z^2 - y^2)^{1/2}}, \quad \dots \dots \dots (6)$$

then

$$f(x) = -\frac{2}{\pi} \frac{\partial}{\partial x} \int_x^{\gamma} \frac{g(y) dy}{(y^2 - x^2)^{1/2}}. \quad \dots (7)$$

Thus the Bateman-Herglotz equation is a special case of Abel's equation.

In Abel's form as originally quoted it was necessary that $\chi(\nu) = 0$, in order that the equation might have a solution. This restriction was removed by Goursat*, who at the same time provided for the existence of solutions of a discontinuous character. In view of applications to physics and more especially to problems of wave diffraction, Goursat's advance in the study of the equation is of fundamental importance. The restriction nevertheless persists in some of the methods of establishing the equation†.

The first proof published, which can be regarded as free from the main difficulties of Abel's method, was due to Liouville‡, who appears to have been unaware of Abel's work.

* *Acta Math.* xxvii. p. 131 (1903).

† *Cp. e. g.* Bateman, *Phil. Mag.* xix. p. 576 et seq. (1910).

‡ *Journal de l'Ecole Polytechnique*, xxi. p. 1 (1832); *Liouville's Journal*, iv. p. 233 (1839).

That this equation in the special case $\sigma = \frac{1}{2}$ was the fundamental equation regulating the propagation of earthquake waves was first perceived by Herglotz*, who discussed it in a new manner. Subsequently Bateman† independently gave a discussion and in fact rediscovered the theorem.

In the present communication we are concerned with the development of the complete class of integral equations—of which the Bateman-Herglotz equation is a member—and their solutions, and with the interesting identities which present themselves in a systematic survey. It is also shown in the present paper that there is an intimate relation between them and the Bessel-Fourier results.

The Bessel-Fourier results to which we refer comprise the following. Firstly, Fourier's theorem

$$f(x) = \frac{2}{\pi} \int_0^\infty \cos \lambda x d\lambda \int_0^\infty \cos \lambda \mu f(\mu) d\mu \quad . \quad (8)$$

or its equivalent,—if

$$G(\lambda) = \int_0^\infty \cos \lambda \mu f(\mu) d\mu, \quad . \quad . \quad . \quad (9)$$

then

$$f(x) = \frac{2}{\pi} \int_0^\infty \cos \lambda x G(\lambda) d\lambda, \quad . \quad . \quad . \quad (10)$$

exhibiting the function f as the solution of the integral equation (3) for a known form of G , which is known to be unique. Secondly, there is the Bessel-Fourier theorem

$$f(x) = \int_0^\infty \lambda J_0(\lambda x) d\lambda \int_0^\infty \mu J_0(\lambda \mu) f(\mu) d\mu$$

or its equivalent,—if

$$G(\lambda) = \int_0^\infty \mu J_0(\lambda \mu) f(\mu) d\mu,$$

then

$$f(x) = \int_0^\infty \lambda J_0(\lambda x) G(\lambda) d\lambda.$$

Both these theorems are applicable to a function which is continuous except at a finite number of discontinuities provided that it has limited total fluctuation in the range 0 to ∞ .

The Fourier theorem is, of course, a special case of the Bessel-Fourier theorem when stated in the general form

$$f(\rho) = \int_0^\infty \lambda J_n(\lambda \rho) d\lambda \int_0^\infty \mu J_n(\lambda \mu) f(\mu) d\mu \quad (n > -1), \quad (11)$$

which was established for integral values of n by Hankel

* *Phys. Zeit.* viii. p. 145 (1907).

† *Loc. cit.*

and subsequently extended to non-integral values by Sonine* and others. For when $n = -\frac{1}{2}$ it yields

$$f(\rho) = \frac{2}{\pi} \int_0^\infty \frac{\lambda}{(\lambda\rho)^{1/2}} \cos \lambda\rho d\lambda \int_0^\infty \frac{\mu}{(\lambda\mu)^{1/2}} \cos \lambda\mu f(\mu) d\mu$$

or

$$\rho^{1/2} f(\rho) = \frac{2}{\pi} \int_0^\infty \cos \lambda\rho d\lambda \int_0^\infty \cos \lambda\mu \cdot \mu^{1/2} f(\mu) d\mu,$$

which is the Fourier theorem for the function $\rho^{1/2} f(\rho)$. By taking $n = \frac{1}{2}$ we obtain, in the same manner, the sine form of Fourier's theorem.

In deriving the theorems of this paper from these Bessel-Fourier results, the conditions satisfied by the arbitrary functions employed are specified at the outset. And with this point of departure we are, moreover, free from the necessity of proving any "existence" theorems in connexion with the subsequent results.

In addition to the Bessel-Fourier theorem and Fourier's theorem, there exist four useful results which may be regarded as "hybrids" of these two. It was in fact in connexion with these mixed theorems that it became apparent that there was an interesting relation between the equations and identities under discussion and the fundamental Bessel-Fourier theorem. We therefore begin by briefly indicating these hybrids.

Four Mixed Theorems.

If the function $\phi(x)$ satisfy Fourier's cosine formula, then

$$\phi(y) = \frac{2}{\pi} \int_0^\infty \cos \lambda y d\lambda \int_0^\infty \cos \lambda\mu \phi(\mu) d\mu.$$

Thus

$$\phi(by) = \frac{2}{\pi} \int_0^\infty \cos \lambda by d\lambda \int_0^\infty \cos \lambda\mu \phi(\mu) d\mu$$

and

$$\frac{1}{b} \frac{\partial}{\partial y} \phi(by) = -\frac{2}{\pi} \int_0^\infty \lambda \sin \lambda by d\lambda \int_0^\infty \cos \lambda\mu \phi(\mu) d\mu. \quad (12)$$

Now † if $\frac{1}{2} > m > -1$,

$$J_{-m-\frac{1}{2}}(k) = \frac{k^{m+\frac{1}{2}}/\pi^{1/2}}{2^{m-\frac{1}{2}}\Gamma(1+m)} \int_0^\infty \sin(k \cosh q) (\sinh q)^{2m+1} dq. \quad (13)$$

* Sonine, *Math. Ann.* xvi. (1880).

† Sonine, *l. c.*

Thus, multiplying (12) by $(b^2-1)^{\frac{2m+1}{2}}$ and writing

$$b = \cosh q$$

and integrating with respect to q from 0 to ∞ , we get, taking the right-hand side first,

$$\begin{aligned} & \int_0^\infty \left(\frac{\lambda y}{2}\right)^{-\frac{1}{2}-m} J_{-m-\frac{1}{2}}(\lambda y) \lambda d\lambda \int_0^\infty \cos \lambda \mu \phi(\mu) d\mu \\ &= -\frac{\pi^{1/2}}{4\Gamma(1+m)} \frac{\partial}{\partial y} \int_0^\infty \frac{\phi(y \cosh q) (\sinh q)^{2m+1} dq}{\cosh q}, \quad (14) \end{aligned}$$

a theorem whose particular case $m = -\frac{1}{2}$, namely

$$\begin{aligned} & \int_0^\infty \lambda J_0(\lambda y) d\lambda \int_0^\infty \cos \lambda \mu \phi(\mu) d\mu \\ &= -\frac{\partial}{\partial y} \int_0^\infty \phi(y \cosh q) dq / \cosh q, \quad (15) \end{aligned}$$

is of great interest and usefulness.

Again, using Fourier's sine formula we have

$$\frac{1}{a} \frac{\partial}{\partial y} \phi(ay) = \frac{2}{\pi} \int_0^\infty \lambda \cos \lambda ay d\lambda \int_0^\infty \sin \lambda \mu \phi(\mu) d\mu, \quad (16)$$

-and in view of the formula due also to Sonine*,

$$\begin{aligned} & J_{m+\frac{1}{2}}(k) \\ &= \frac{k^{m+\frac{1}{2}}/\pi^{1/2}}{2^{m+\frac{1}{2}}\Gamma(1+m)} \int_0^{\pi/2} \cos(k \sin \phi) (\cos \phi)^{2m+1} d\phi, \quad (m > -1), \end{aligned} \quad (17)$$

if we write

$$a = \sin \theta.$$

Multiply (16) on both sides by $(1-a^2)^{\frac{2m+1}{2}}$ and integrate with respect to θ from 0 to $\pi/2$, and we get

$$\begin{aligned} & \int_0^{\pi/2} \left(\frac{\lambda y}{2}\right)^{-m-\frac{1}{2}} J_{m+\frac{1}{2}}(\lambda y) \cdot \lambda d\lambda \int_0^\infty \sin \lambda \mu \phi(\mu) d\mu \\ &= + \frac{\pi^{1/2}}{\Gamma(1+m)} \frac{\partial}{\partial y} \int_0^{\pi/2} \frac{\phi(y \sin \theta) (\cos \theta)^{2m+1}}{\sin \theta} d\theta, \quad (18) \end{aligned}$$

the second mixed theorem, which in the particular case $m = -\frac{1}{2}$ is of special interest and takes the form

$$\begin{aligned} & \int_0^{\pi/2} \lambda J_0(\lambda y) d\lambda \int_0^\infty \sin \lambda \mu \phi(\mu) d\mu \\ &= \frac{\partial}{\partial y} \int_0^{\pi/2} \phi(y \sin \theta) d\theta / \sin \theta. \quad (19) \end{aligned}$$

* *Loc. cit.*

Again, starting from the cosine form of Fourier's theorem with $\mu f(\mu)$ for the function, we obtain

$$\frac{by}{a} f(by) = \frac{2}{\pi} \int_0^\infty \cos(bayt) dt \int_0^\infty \mu \cos(at) \mu f(\mu) d\mu.$$

Take $a = \frac{1}{b}$ and for any positive value of a

$$\frac{y}{a^2} f\left(\frac{y}{a}\right) = \frac{2}{\pi} \int_0^\infty \cos yt dt \int_0^\infty \mu \cos(at) \mu f(\mu) d\mu. \quad (20)$$

If now we multiply both sides of (20) by $(1-a^2)^{m+\frac{1}{2}}$ and write

$$a = \sin \theta$$

and integrate from $\theta = 0$ to $\theta = \frac{\pi}{2}$, we get

$$\begin{aligned} \int_0^\infty \cos yt dt \int_0^\infty \left(\frac{t\mu}{2}\right)^{-m-\frac{1}{2}} J_{m+\frac{1}{2}}(t\mu) \cdot \mu f(\mu) d\mu \\ = \frac{\pi^{1/2}}{\Gamma(1+m)} y \int_0^{\pi/2} \frac{(\cos \theta)^{2m+1} f(y/\sin \theta)}{\sin^2 \theta} d\theta, \end{aligned} \quad (21)$$

which is the third of the mixed theorems and like the other mixed theorems yields an interesting particular case when $m = -\frac{1}{2}$, namely

$$\int_0^\infty \cos yt dt \int_0^\infty \mu J_0(\mu t) f(\mu) d\mu = y \int_0^{\pi/2} \frac{f(y/\sin \theta)}{\sin^2 \theta} d\theta, \quad (22)$$

or, by the transformation

$$\sin \theta = \operatorname{sech} q,$$

$$\int_0^\infty \cos yt dt \int_0^\infty \mu J_0(\mu t) f(\mu) d\mu = y \int_0^\infty \cosh q f(y \cosh q) dq. \quad (23)$$

After the same manner, starting with the sine formula applied to the function $\mu f(\mu)$, we get

$$\frac{ay}{b} f(ay) = \frac{2}{\pi} \int_0^\infty \sin(bayt) dt \int_0^\infty \mu \sin(bt) \mu f(\mu) d\mu,$$

and taking again $ab = 1$,

$$\frac{y}{b^2} f\left(\frac{y}{b}\right) = \frac{2}{\pi} \int_0^\infty \sin yt dt \int_0^\infty \mu \sin(bt) \mu f(\mu) d\mu,$$

whence, by means of (17), we get the result

$$\int_0^\infty \sin yt \, dt \int_0^\infty \left(\frac{\mu t}{2}\right)^{-\frac{1}{2}-m} J_{m+\frac{1}{2}}(\mu t) \cdot \mu f(\mu) \, d\mu \\ = \frac{\pi^{1/2}}{\Gamma(1+m)} \cdot y \int_0^\infty \frac{(\sinh q)^{2m+1} f(y/\cosh q)}{\cosh^2 q} \, dq, \quad (24)$$

the fourth mixed theorem whose particular case when $m = -\frac{1}{2}$ is

$$\int_0^\infty \sin yt \, dt \int_0^\infty \mu J_0(\mu t) f(\mu) \, d\mu = y \int_0^\infty f(y/\cosh q) \, dq / \cosh^2 q, \quad (25)$$

or, with $\cosh q = \operatorname{cosec} \theta$,

$$\int_0^\infty \sin yt \, dt \int_0^\infty \mu J_0(\mu t) f(\mu) \, d\mu = y \int_0^{\pi/2} f(y \sin \theta) \sin \theta \, d\theta.$$

These four hybrid theorems and more especially their particular cases when $m + \frac{1}{2} = 0$ are of great value in applications to integrals involving the Bessel functions, though derived so simply. Many of the proofs given by Sonine and others of such integrals can be considerably shortened if these results are used. Macdonald* has given similar indications from the Bessel-Fourier theorem itself.

Thus taking as a specific example

$$\phi(\mu) = \mu e^{-p\mu}$$

and applying theorem (15), we get

$$-\frac{\partial}{\partial y} \cdot y \int_0^\infty e^{-py \cosh q} \, dq = \int_0^\infty \lambda J_0(\lambda y) \, dy \int_0^\infty \mu \cos \lambda \mu e^{-p\mu} \, d\mu$$

or

$$\frac{\partial}{\partial y} \cdot [y K_0(py)] = \int_0^\infty \lambda J_0(\lambda y) \left(\frac{\partial}{\partial p} \cdot \frac{p}{p^2 + \lambda^2} \right) d\lambda,$$

whence

$$\frac{\partial}{\partial p} \cdot p K_0(py) = \frac{\partial}{\partial p} \cdot p \int_0^\infty \frac{\lambda J_0(\lambda y) \, d\lambda}{p^2 + \lambda^2},$$

which is true by Basset's theorem †

$$K_0(py) = \int_0^\infty \frac{\lambda J_0(\lambda y) \, d\lambda}{p^2 + \lambda^2}.$$

* Proc. Lond. Math. Soc. vol. xxxv. (1902).

† Due, however, originally to Mehler, *Journal für Math.* lxxiii., as pointed out by Watson.

The further development of such identities is not, however, at present relevant to our purpose.

We now pass on to the derivation of a class of integral equations, including Abel's theorem in its generality, from the Bessel-Fourier and Fourier theorems.

The Fundamental Theorems.

As before, if $\phi(y)$ satisfy Fourier's sine formula,

$$\phi(y) = \frac{2}{\pi} \int_0^\infty \sin \lambda y d\lambda \int_0^\infty \sin \lambda \mu \phi(\mu) d\mu,$$

then

$$\begin{aligned} \phi(ay) &= \frac{2}{\pi} \int_0^\infty \sin \lambda ay d\lambda \int_0^\infty \sin \lambda \mu \phi(\mu) d\mu \\ &= \frac{2b}{\pi} \int_0^\infty \sin \lambda aby dt \int_0^\infty \sin b\mu t \phi(\mu) d\mu, \end{aligned}$$

where b is any positive quantity. If $by=x$, then if we write

$$\phi(\mu) = \mu f(\mu),$$

it follows that

$$\frac{ax}{b^2} \cdot f\left(\frac{ax}{b}\right) = \frac{2}{\pi} \int_0^\infty \sin axt dt \int_0^\infty \sin b\mu t f(\mu) \mu d\mu \quad (26)$$

and

$$\begin{aligned} &\frac{\partial}{\partial x} \cdot \frac{x}{b^2} \left(\frac{1-a^2}{b^2-1} \right)^{\frac{1}{2}-\sigma} f\left(\frac{ax}{b}\right) \\ &= \frac{2}{\pi} \int_0^\infty (1-a^2)^{\frac{1}{2}-\sigma} \sin axt t dt \int_0^\infty (b^2-1)^{\sigma-\frac{1}{2}} \sin b\mu t f(\mu) \mu d\mu. \end{aligned} \quad (27)$$

We now use the formula (13) for $n=\sigma-1$ and the formula (17) for $m=-\sigma$.

Thus writing

$$a = \sin \theta, \quad b = \cosh q,$$

and integrating our equation on both sides, with respect to θ from 0 to $\pi/2$ and with respect to q from 0 to ∞ , we

find

$$\begin{aligned} \frac{\partial}{\partial x} \cdot x \int_0^\infty \frac{(\sinh q)^{2\lambda-1}}{\cosh^2 q} dq \int_0^{\pi/2} \frac{f(x \sin \theta / \cosh q)}{(\cos \theta)^{2\lambda-1}} d\theta \\ = \frac{1}{2} \Gamma(1-\sigma) \Gamma(\sigma) \int_0^\infty J_{\frac{1}{2}-\sigma}(xt) (xt)^{\sigma-\frac{1}{2}} t dt \\ \times \int_0^\infty J_{\frac{1}{2}-\sigma}(\mu t) (\mu t)^{\frac{1}{2}-\sigma} \mu f(\mu) d\mu \\ = \frac{\pi}{2 \sin \sigma \pi} x^{\sigma-\frac{1}{2}} \int_0^\infty t J_{\frac{1}{2}-\sigma}(xt) dt \\ \times \int_0^\infty \mu J_{\frac{1}{2}-\sigma}(\mu t) \mu^{\frac{1}{2}-\sigma} f(\mu) d\mu \\ = \frac{\pi}{2 \sin \sigma \pi} f(x) \end{aligned}$$

by the Bessel Integral Theorem for the function $\mu^{\frac{1}{2}-\sigma} f(\mu)$. Thus we have the fundamental formula

$$\begin{aligned} (A) \quad f(x) = \frac{2}{\pi} \sin \sigma \pi \frac{\partial}{\partial x} \cdot x \int_0^\infty \frac{(\sinh q)^{2\sigma-1}}{\cosh^2 q} dq \\ \times \int_0^\infty \frac{f(x \sin \theta / \cosh q)}{(\cos \theta)^{2\sigma-1}} d\theta. \quad (28) \end{aligned}$$

With the substitutions

$$\cosh q = x/y, \quad \sin \theta = z/y,$$

it becomes

$$\begin{aligned} f(x) = \frac{2}{\pi} \sin \sigma \pi \frac{\partial}{\partial x} \cdot x \int_0^x \frac{dy/x}{(x^2/y^2 - 1)^{1-\sigma}} \int_0^y \frac{f(z) dz/y}{(1 - z^2/y^2)^\sigma} \\ = \frac{2}{\pi} \sin \sigma \pi \frac{\partial}{\partial x} \cdot \int_0^x \frac{y dy}{(x^2 - y^2)^{1-\sigma}} \int_0^y \frac{f(z) dz}{(y^2 - z^2)^\sigma}. \quad (29) \end{aligned}$$

An alternative pair of substitutions,

$$\sin \theta = \lambda/x, \quad \cosh q = \lambda/\mu,$$

leads to

$$\begin{aligned} f(x) = \frac{2}{\pi} \sin \sigma \pi \frac{\partial}{\partial x} \cdot x \int_0^x \frac{d\lambda/x}{(1 - \lambda^2/x^2)^\sigma} \int_0^\lambda \frac{f(\mu) d\mu/\lambda}{(\lambda^2/\mu^2 - 1)^{1-\sigma}} \\ = \frac{2}{\pi} \sin \sigma \pi \frac{\partial}{\partial x} \cdot x^{2\sigma} \int_0^x \frac{d\lambda/\lambda}{(x^2 - \lambda^2)^\sigma} \int_0^\lambda \frac{\mu^{2-2\sigma} f(\mu) d\mu}{(\lambda^2 - \mu^2)^{1-\sigma}}. \quad (30) \end{aligned}$$

After the same manner, if we take Fourier's cosine formula

$$\phi(y) = \frac{2}{\pi} \int_0^\infty \cos \lambda y d\lambda \int_0^\infty \cos \lambda \mu \phi(\mu) d\mu,$$

we may deduce the consequence,

$$\begin{aligned} \frac{\partial}{\partial x} \cdot \frac{x}{a^2} (1-a^2)^{\frac{1}{2}-\sigma} f\left(\frac{bx}{a}\right) &= -\frac{2}{\pi} \int_0^\infty (b^2-1)^{\sigma-\frac{1}{2}} \sin bxt t dt \\ &\times \int_0^\infty (1-a^2)^{\frac{1}{2}-\sigma} \cos a\mu t f(\mu) \cdot \mu d\mu, \end{aligned}$$

and obtain the corresponding equation,

$$\begin{aligned} \text{(B)} \quad f(x)! &= -\frac{2}{\pi} \sin \sigma\pi \frac{\partial}{\partial x} \cdot x \int_0^{\pi/2} \frac{(\cos \theta)^{-2\sigma+1}}{\sin^2 \theta} d\theta \\ &\times \int_0^\infty \frac{f(x \cosh q / \sin \theta)}{(\sinh q)^{1-2\sigma}} dq, \quad (31) \end{aligned}$$

the companion to (28). And with the substitutions

$$\sin \theta = x/y, \quad \cosh q = z/y,$$

it becomes

$$f(x) = -\frac{2}{\pi} \sin \sigma\pi \frac{\partial}{\partial x} \int_x^\infty \frac{y dy}{(y^2-x^2)^\sigma} \int_y^\infty \frac{f(z) dz}{(z^2-y^2)^{1-\sigma}}. \quad (32)$$

An alternative pair of substitutions,

$$\cosh q = \lambda/x, \quad \sin \theta = \lambda/\mu,$$

leads to

$$f(x) = -\frac{2}{\pi} \sin \sigma\pi \frac{\partial}{\partial x} \cdot x^{2-2\sigma} \int_x^\infty \frac{d\lambda/\lambda}{(\lambda^2-x^2)^{1-\sigma}} \int_\lambda^\infty \frac{\mu^{2\sigma} f(\mu) d\mu}{(\mu^2-\lambda^2)^\sigma}. \quad (33)$$

The Application of Theorem A to a function which is zero for parts of its range.

Suppose now that we apply the theorem (A),

$$\begin{aligned} f(x) &= \frac{2}{\pi} \sin \sigma\pi \frac{\partial}{\partial x} \cdot x \int_0^\infty \frac{(\sinh q)^{2\sigma-1}}{\cosh^2 q} dq \\ &\times \int_0^{\pi/2} \frac{f(x \sin \theta / \cosh q) d\theta}{(\cosh \theta)^{2\sigma-1}}, \end{aligned}$$

to a function $f(x)$ which is zero for x between 0 and γ , and zero also for x between δ and ∞ . Then if we perform the

integrations only over the area belonging to a region, in any geometrical representation, defined by

$$0 \leq q \leq \infty, \quad 0 \leq \theta \leq \pi/2,$$

and to cases where

$$\gamma \leq z \sin \theta / \cosh q \leq \delta,$$

we shall be able to deduce that

$$\begin{aligned} \frac{2}{\pi} \sin \sigma \pi \cdot x \int_0^\infty \frac{(\sinh q)^{2\sigma-1}}{\cosh^2 q} dq \int_0^{\pi/2} \frac{f(x \sin \theta / \cosh q) d\theta}{(\cosh \theta)^{2\sigma-1}} \\ = C_1 \quad x < \gamma \\ = C_2 \quad x > \delta, \end{aligned}$$

where C_1 and C_2 are independent of x , and the integrations are of functions equivalent to zero over portions of their range. Moreover, we also have

$$\begin{aligned} \frac{2}{\pi} \sin \sigma \pi \cdot \frac{\partial}{\partial x} x \int_0^\infty \frac{(\sinh q)^{2\sigma-1}}{\cosh^2 q} dq \int_0^{\pi/2} \frac{f(x \sin \theta / \cosh q) d\theta}{(\cos \theta)^{2\sigma-1}} \\ = f(x) \quad \lambda < x < \delta, \end{aligned}$$

where in each case the integrations are performed over the restricted area.

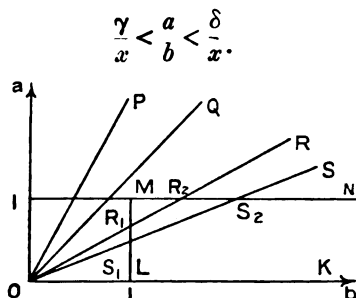
If we write

$$\cosh q = b, \quad \sin \theta = a,$$

and treat a and b as Cartesian coordinates, we have to integrate over the area common to the rectangle

$$a = 0, \quad a = 1, \quad b = 1, \quad b = \infty,$$

and the sector



There are evidently three cases to discuss. And it will be convenient for purposes of exposition to refer to the diagram in which the various lines OP, OQ, OR, OS represent various lines of the form $a/b = \text{constant}$.

Case 1 C. $x < \gamma < \delta$.

In this case the lines

$$\frac{a}{b} = \frac{\gamma}{x}, \quad \frac{a}{b} = \frac{\delta}{x}$$

are represented by OQ and OP respectively, and the sector QOP bounded by these lines and the rectangle KLMN bounded by the lines

$$a = 0, \quad b = 1, \quad a = 1, \quad b = \infty,$$

have no point in common. There is therefore no area over which to integrate, and we therefore merely arrive at the fact that $f(x)$ is zero.

Case 2 C. $\gamma < x < \delta$.

In this case the sector is QOR and it and the rectangle KLMN have in common the triangle R₁MR₂ over which the integration has therefore to be carried out. Thus we have

$$\begin{aligned} \frac{\pi}{2 \sin \sigma \pi} f(x) &= \frac{\partial}{\partial x} \cdot x \int_0^{\cosh^{-1} x/\gamma} \frac{(\sinh q)^{2\sigma-1}}{\cosh^2 q} dq \\ &\times \int_{\sin^{-1}(\gamma \cosh q/x)}^{\pi/2} \frac{f(x \sin \theta / \cosh q)}{(\cos \theta)^{2\sigma-1}} d\theta, \\ \sin \theta &= z/y. \end{aligned}$$

Writing $\cosh q = x/y$, we get

$$\frac{\pi}{2 \sin \sigma \pi} f(x) = \frac{\partial}{\partial x} \cdot \int_{\gamma}^x \frac{y dy}{(x^2 - y^2)^{1-\sigma}} \int_{\gamma}^y \frac{f(x) dz}{(y^2 - z^2)^{\sigma}}, \quad (34)$$

or with

$$x^2 = \xi, \quad y^2 = \eta, \quad z^2 = \zeta, \quad \gamma^2 = \nu, \quad f(x)/x = \phi(\xi),$$

$$\frac{\pi}{\sin \sigma \pi} \phi(\xi) = \frac{\partial}{\partial \xi} \int_{\nu}^{\xi} \frac{d\eta}{(\xi - \eta)^{1-\sigma}} \int_{\nu}^{\eta} \frac{\phi(\zeta) d\zeta}{(\eta - \zeta)^{\sigma}} \quad (\nu \leq \xi).$$

And this result is Abel's theorem for $\xi > \nu$.

For these two equivalent results may also obviously be expressed in the form of integral equations and their solutions. Thus, if

$$g(y) = \int_{\gamma}^y \frac{f(z) dz}{(y^2 - z^2)^{\sigma}},$$

then

$$f(x) = \frac{2 \sin \sigma \pi}{\pi} \frac{\partial}{\partial x} \int_{\gamma}^x \frac{y g(y) dy}{(x^2 - y^2)^{1-\sigma}}. \quad (35)$$

Similarly, if

$$\chi(\eta) = \int_{\gamma}^{\eta} \frac{\phi(\xi) d\xi}{(\eta - \xi)^{\sigma}},$$

then

$$\phi(\xi) = \frac{\sin \sigma \pi}{\pi} \partial \int_{\gamma}^{\xi} \frac{\chi(\eta) d\eta}{(\xi - \eta)^{1-\sigma}}. \quad \dots \quad (36)$$

The above conclusions were reached by integrating over the triangle R_1MR_2 by means of strips parallel to the a -axis. If, however, we integrate over strips parallel to the b -axis, we obtain the theorem—equivalent of course to the theorem previously obtained—

$$\begin{aligned} \frac{\pi}{2 \sin \sigma \pi} f(x) &= \frac{\partial}{\partial x} \cdot x \int_{\sin^{-1}(\gamma/x)}^{\pi/2} \frac{d\theta}{(\cos \theta)^{2\sigma-1}} \\ &\times \int_0^{\cosh^{-1}(x \sin \theta / \gamma)} \frac{f(x \sin \theta / \cosh q)}{(\sinh q)^{1-2\sigma} \cosh^2 q} dq. \end{aligned}$$

Taking new variables λ, μ given by

$$\lambda = x \sin \theta, \quad \mu = \lambda / \cosh q,$$

we find

$$\frac{\pi}{2 \sin \sigma \pi} f(x) = \frac{\partial}{\partial x} \cdot x^{2\sigma} \int_{\gamma}^x \frac{d\lambda / \lambda}{(x^2 - \lambda^2)^{\sigma}} \int_{\gamma}^{\lambda} \frac{\mu^{2-2\sigma} f(\mu) d\mu}{(\lambda^2 - \mu^2)^{1-\sigma}}, \quad (37)$$

or with

$$\begin{aligned} x^2 = s, \quad \lambda^2 = t, \quad \mu^2 = u, \quad \lambda^2 = \rho, \quad f(x)/x = \phi(s), \\ \frac{\pi}{\sin \sigma \pi} \phi(s) = \frac{\partial}{\partial s} \cdot s^{\sigma} \int_{\rho}^s \frac{dt/t}{(s-t)^{\sigma}} \int_{\rho}^t \frac{u^{1-\sigma} \phi(u) du}{(t-u)^{1-\sigma}}. \end{aligned} \quad (38)$$

These results also can be expressed in the form of integral equations and their solutions. Thus, if

$$h(\gamma) = \int_{\gamma}^{\lambda} \frac{\mu^{2-2\sigma} f(\mu) d\mu}{(\lambda^2 - \mu^2)^{1-\sigma}},$$

then

$$f(x) = \frac{2 \sin \sigma \pi}{\pi} \frac{\partial}{\partial x} \cdot x^{2\sigma} \int_{\gamma}^x \frac{h(\lambda) d\lambda / \lambda}{(x^2 - \lambda^2)^{\sigma}}, \quad \dots \quad (39)$$

where σ can have any value between zero and unity, and γ is any constant less than λ . Similarly, if

$$\theta(t) = \int_{\rho}^t \frac{u^{1-\sigma} \phi(u) du}{(t-u)^{1-\sigma}},$$

then

$$\phi(s) = \frac{\sin \sigma \pi}{\pi} \frac{\partial}{\partial s} \cdot s^\sigma \int_\rho^\infty \frac{\theta(t) dt}{(s-t)^\sigma}, \quad . . \quad (40)$$

where σ can range between zero and unity, and ρ is any constant less than t .

The results (39, 40) containing arbitrary constants σ (lying between 0 and 1) and γ (which is less than x) are of considerable generality. If we take the degenerate case when $\sigma = \frac{1}{2}$ and $\gamma = 0$, the resulting equation is of interest. For if we put

$$h(\lambda) = \lambda k(\lambda),$$

(39) becomes :

If

$$k(\lambda) = \int_0^\lambda \frac{\mu f(\mu) d\mu}{(\lambda^2 - \mu^2)^{1/2}},$$

then

$$f(x) = \frac{2}{\pi} \frac{\partial}{\partial x} \cdot x \int_0^x \frac{k(\lambda) d\lambda}{(x^2 - \lambda^2)^{1/2}}.$$

Examples of this theorem are already familiar in physics. Writing

$$\lambda = x \sin \phi, \quad \mu = \lambda \sin \theta,$$

we deduce that if

$$k(\lambda) = \int_0^{\pi/2} f(\lambda \sin \theta) \sin \theta d\theta,$$

then

$$f(x) = \frac{2}{\pi} \frac{\partial}{\partial x} \cdot x \int_0^{\pi/2} k(x \sin \phi) d\phi.$$

A simple case to consider as an illustration of this theorem is

$$f(x) = J_0(x).$$

We then have

$$k(\lambda) \int_0^{\pi/2} J_0(\lambda \sin \theta) \sin \theta d\theta = \sin \lambda / \lambda,$$

by a well-known formula. And

$$\begin{aligned} f(x) &= \frac{2}{\pi} \frac{\partial}{\partial x} \cdot x \int_0^{\pi/2} \sin(x \phi) \frac{d\phi}{x \sin \phi} \\ &= \frac{2}{\pi} \int_0^{\pi/2} \cos(x \sin \phi) d\phi = J_0(x), \end{aligned}$$

and the theorem is verified. As a second illustration let

$$k(\lambda) = \cos a\lambda,$$

where a is constant. Then

$$\begin{aligned} f(x) &= \frac{2}{\pi} \frac{\partial}{\partial x} \cdot x \int_0^{\pi/2} \cos(ax \sin \phi) d\phi \\ &= \frac{2}{\pi} \frac{\partial}{\partial x} \cdot x \frac{\pi}{2} J_0(ax), \end{aligned}$$

or

$$f(x) = \frac{\partial}{\partial x} x J_0(ax) = \frac{\partial}{\partial a} a J_0(ax).$$

Thus

$$\begin{aligned} k(\lambda) &= \int_0^{\pi/2} \frac{\partial}{\partial a} \cdot a J_0(a\lambda \sin \theta) \cdot \sin \theta d\theta \\ &= \frac{\partial}{\partial a} \cdot \left(a \cdot \frac{\sin a\lambda}{a\lambda} \right) = \cos a\lambda, \end{aligned}$$

and the theorem is again verified.

It is also of interest to point out that some remarkable formulæ can be obtained by using the logarithmic Bessel functions for f or k ; and it will in general be found very difficult to establish them in a more direct manner.

Case 3 C. $\gamma < \delta < x$.

The last case when x is greater than γ and δ gives a result of a rather different nature. For, for these values of x , $f(x)$ is zero and therefore we obtain an integral identity satisfied by an arbitrary function.

For the sector ROS and the rectangle KLMN have in common the quadrilateral $R_1R_2S_2S_1$ over which the integration has to be carried out. And we therefore have

$$\begin{aligned} C &= x \int_0^{\cosh^{-1} x/\delta} \frac{(\sinh q)^{2\sigma-1}}{\cosh^2 q} dq \\ &\quad \times \int_{\sin^{-1}(\gamma \cosh q/x)}^{\sin^{-1}(\delta \cosh q/x)} \frac{f(x \sin \theta / \cosh q)}{(\cos \theta)^{2\sigma-1}} d\theta \\ &+ x \int_{\cosh^{-1} x/\delta}^{\cosh^{-1} x/\gamma} \frac{(\sinh q)^{2\sigma-1}}{\cosh^2 q} dq \\ &\quad \int_{\sin^{-1}(\gamma \cosh q/x)}^{\pi/2} \frac{f(x \sin \theta / \cosh q)}{(\cos \theta)^{2\sigma-1}} d\theta, \end{aligned}$$

where C is a constant, independent of x .

Phil. Mag. S. 7. Vol. 4. No. 22. Sept. 1927. 2 N

Using again the same substitutions

$$\cosh q = x/y, \quad \sin \theta = z/y,$$

we get

$$C = \int_{\delta}^x \frac{y dy}{(x^2 - y^2)^{1-\sigma}} \int_{\gamma}^{\delta} \frac{f(z) dz}{(y^2 - z^2)^{\sigma}} \\ + \int_{\gamma}^{\delta} \frac{y dy}{(x^2 - y^2)^{1-\sigma}} \int_{\gamma}^y \frac{f(z) dz}{(y^2 - z^2)^{\sigma}}.$$

This interesting theorem is true for x greater than γ and δ .

To find the value of C we can make $x \rightarrow \infty$. Then the second integral vanishes like $1/x^{2-2\sigma}$. The first becomes with $y = x\mu$,

$$\lim_{x \rightarrow \infty} \int_{\delta}^x \frac{y dy}{(x^2 - y^2)^{1-\sigma}} \int_{\gamma}^{\delta} \frac{f(z) dz}{(y^2 - z^2)^{\sigma}} \\ = \lim_{x \rightarrow \infty} \int_{\delta/x}^1 \frac{\mu d\mu}{(1 - \mu^2)^{1-\sigma}} \int_{\gamma}^{\delta} \frac{f(z) dz}{(\mu^2 - z^2/x^2)^{\sigma}} \\ = \int_0^1 \mu^{1-2\sigma} (1 - \mu^2)^{\sigma-1} d\mu \int_{\gamma}^{\delta} f(z) dz \\ = \frac{1}{2} \int_0^1 (1-t)^{\sigma-1} t^{-\sigma} dt \int_{\gamma}^{\delta} f(z) dz,$$

with $\mu^2 = t$. Since

$$\int_0^1 (1-t)^{m-1} t^{n-1} dt = \Gamma(m) \Gamma(n) / \Gamma(m+n),$$

we may evaluate the t -integral and we obtain

$$C = \frac{1}{2} [\Gamma(\sigma) \Gamma(1-\sigma) / \Gamma(1)] \int_{\gamma}^{\delta} f(z) dz \\ = \frac{\pi}{2 \sin \pi \sigma} \int_{\gamma}^{\delta} f(z) dz.$$

Thus we have the result—when $x > \delta > \gamma$,

$$\int_{\delta}^x \frac{y dy}{(x^2 - y^2)^{1-\sigma}} \int_{\gamma}^{\delta} \frac{f(z) dz}{(y^2 - z^2)^{\sigma}} + \int_{\gamma}^{\delta} \frac{y dy}{(x^2 - y^2)^{1-\sigma}} \int_{\gamma}^y \frac{f(z) dz}{(y^2 - z^2)^{\sigma}} \\ = \frac{\pi}{2 \sin \pi \sigma} \int_{\gamma}^{\delta} f(z) dz. \quad (41)$$

It is perhaps desirable to verify this formula in one individual case, though special cases are, in general, more difficult to prove than the general formula.

Taking first $\sigma = \frac{1}{2}$, $\gamma = 0$, we deduce

$$\begin{aligned} \frac{\pi}{2} \int_0^\delta f(z) dz &= \int_\delta^x \frac{y dy}{(x^2 - y^2)^{1/2}} \int_0^\delta \frac{f(z) dz}{(y^2 - z^2)^{1/2}} \\ &+ \int_0^\delta \frac{y dy}{(x^2 - y^2)^{1/2}} \int_0^y \frac{f(z) dz}{(y^2 - z^2)^{1/2}} \quad (x > \delta), \quad (42) \end{aligned}$$

itself an identity of considerable interest. Then selecting the simplest case $f(z)=1$ for verification, the first integral on the right is

$$\begin{aligned} I_1 &= \int_\delta^x \frac{y dy}{(x^2 - y^2)^{1/2}} \int_0^\delta \frac{dz}{(y^2 - z^2)^{1/2}} \\ &= \int_\delta^x \frac{\sin^{-1}(\delta/y) y dy}{(x^2 - y^2)^{1/2}} \\ &= \left[\sin^{-1} \delta/y - (x^2 - y^2)^{1/2} \right]_\delta^x - \delta \int_\delta^x \frac{(x^2 - y^2)^{1/2} dy}{(y^2 - \delta^2)^{1/2} y} \\ &= \frac{\pi}{2} (x^2 - \delta^2)^{1/2} - \delta \int_\delta^x \left(\frac{x^2 - y^2}{y^2 - \delta^2} \right)^{1/2} \frac{dy}{y}. \end{aligned}$$

With the evaluation of the usual type

$$y^2 = \delta^2 \cos^2 \phi + x^2 \sin^2 \phi,$$

we find

$$I_1 = \frac{\pi}{2} (x^2 - \delta^2)^{1/2} - \delta (x^2 - \delta^2) \int_0^{\pi/2} \frac{\cos^2 \phi d\phi}{\delta^2 \cos^2 \phi + x^2 \sin^2 \phi}.$$

The evaluation of this integral follows well-known lines and we find ultimately that

$$I_1 = \frac{\pi}{2} (x^2 - \delta^2)^{1/2} - \frac{\pi}{2} (x - \delta).$$

Further, the second integral on the right is

$$\begin{aligned} I_2 &= \int_0^\delta \frac{y dy}{(x^2 - y^2)^{1/2}} \int_0^y \frac{dz}{(y^2 - z^2)^{1/2}} \\ &= \frac{\pi}{2} \int_0^\delta \frac{y dy}{(x^2 - y^2)^{1/2}} \\ &= \frac{\pi}{2} \left[-(x^2 - y^2)^{1/2} \right]_0^\delta \\ &= \frac{\pi}{2} [x - (x^2 - \delta^2)^{1/2}]. \end{aligned}$$

Thus

$$I_1 + I_2 = \frac{\pi}{2} \delta = \frac{\pi}{2} \int_0^\delta dx,$$

so that the theorem is verified.

We obtained the above identity by carrying out the integration over the strips parallel to one axis which make up the quadrilateral $R_1 R_2 S_2 S_1$. If we take steps parallel to the other axis we obtain a result which, though equivalent to the former, is of independent interest. Thus we have

$$\begin{aligned} C = x \int_{\sin^{-1}(\gamma/x)}^{\sin^{-1}(\delta/x)} \frac{d\theta}{(\cos \theta)^{2\sigma-1}} \\ \times \int_0^{\cosh^{-1}(x \sin \theta/\gamma)} \frac{f(x \sin \theta/\cosh q)}{\cosh^2 q (\sinh q)^{2\sigma-1}} dq \\ + x \int_{\sin^{-1}(\delta/x)}^{\pi/2} \frac{d\theta}{(\cos \theta)^{2\sigma-1}} \\ \times \int_{\cosh^{-1}(x \sin \theta/\delta)}^{\cosh^{-1}(x \sin \theta/\gamma)} \frac{f(x \sin \theta/\cosh q)}{\cosh^2 q (\sinh q)^{2\sigma-1}} dq, \end{aligned}$$

where C is a constant independent of x . Using again the same substitutions as before, namely,

$$\lambda = x \sin \theta, \quad \mu = \lambda/\cosh q,$$

we find

$$\begin{aligned} C = x^{2\sigma} \int_\gamma^\delta \frac{d\lambda/\lambda}{(x^2 - \lambda^2)^\sigma} \int_\gamma^\lambda \frac{\mu^{2-2\sigma} f(\mu) d\mu}{(\lambda^2 - \mu^2)^{1-\sigma}} \\ + x^{2\sigma} \int_\delta^x \frac{d\lambda/\lambda}{(x^2 - \lambda^2)^\sigma} \int_\gamma^\delta \frac{\mu^{2-2\sigma} f(\mu) d\mu}{(\lambda^2 - \mu^2)^{1-\sigma}}, \end{aligned}$$

with C constant as regards x .

To find the value of C we may for the sake of variety make x tend to δ . Then C , which is a function of γ and δ , is given by

$$C(\gamma, \delta) = \lim_{x \rightarrow \delta} x^{2\sigma} \int_\gamma^\delta \frac{d\lambda/\lambda}{(x^2 - \lambda^2)^\sigma} \int_\gamma^\lambda \frac{\mu^{2-2\sigma} f(\mu) d\mu}{(\lambda^2 - \mu^2)^{1-\sigma}},$$

the second integral evidently being zero when $x = \delta$, and therefore

$$C(\gamma, \delta) = \delta^{2\sigma} \int_\gamma^\delta \frac{d\lambda/\lambda}{(\delta^2 - \lambda^2)^\sigma} \int_\gamma^\lambda \frac{\mu^{2-2\sigma} f(\mu) d\mu}{(\lambda^2 - \mu^2)^{1-\sigma}}.$$

Now using theorem (41) for $x = \delta$, we have

$$\frac{\partial}{\partial \delta} C(\gamma, \delta) = \frac{\pi}{2 \sin \sigma \pi} f(\delta).$$

Thus

$$C(\gamma, \delta) = \frac{\pi}{2 \sin \delta \pi} \int_{\gamma}^{\delta} f(t) dv,$$

the lower limit γ being necessary since C when $\gamma = \delta$ is clearly zero. Thus we have the identity

$$\begin{aligned} \int_{\gamma}^{\delta} \frac{\delta \lambda / \lambda}{(x^2 - \lambda^2)^{\sigma}} \int_{\gamma}^{\lambda} \frac{\mu^{2-2\sigma} f(\mu) d\mu}{(\lambda^2 - \mu^2)^{1-\sigma}} + \int_{\delta}^x \frac{d\lambda / \lambda}{(x^2 - \lambda^2)^{\sigma}} \int_{\gamma}^{\delta} \frac{\mu^{2-2\sigma} f(\mu) d\mu}{(\lambda^2 - \mu^2)^{1-\sigma}} \\ = 2 \frac{\pi}{\sin \sigma \pi} x^{-2\sigma} \int_{\gamma}^{\delta} f(\mu) d\mu. \quad x > \delta > \gamma. \quad (43) \end{aligned}$$

This result containing two arbitrary constants γ and δ which can range up to x and the arbitrary constant σ which may range from zero to unity is of very considerable generality, and contains the necessary analytical machinery appropriate for simple application to problems of mathematical physics whose solution requires specific conditions,—in type, that a function or its derivate takes constant values over certain given boundaries,—to be satisfied. It is applicable to important forms of boundaries not hitherto discussed.

We have discussed the application of the theorem

$$f(x) = \frac{2}{\pi} \sin \sigma \pi \frac{\partial}{\partial x} \cdot x \int_0^{\infty} \frac{(\sinh q)^{2\sigma-1}}{\cosh^2 q} dq \int_0^{\pi/2} \frac{f(x \sin \theta / \cosh q) d\theta}{(\cos \theta)^{2\sigma-1}}$$

to a function $f(x)$ which is zero for x between 0 and γ and between δ and ∞ . To complete the scheme we now apply the theorem to the case of a function $f(x)$ which is zero between γ and δ and not between 0 and γ , nor between δ and ∞ , and companion formulæ may be deduced.

In this case the integrations must be performed over that part of the area

$$0 < q \leq \infty, \quad 0 \leq \theta \leq \pi/2$$

in which

$$\gamma \leq x \sin \theta / \cosh q \leq \delta.$$

In terms of a and b , the area over which the integrations have to be performed is the part of the rectangle KLMN

$$a=0, \quad b=1, \quad a=1, \quad b=\infty.$$

which lies *outside* the sector bounded by the lines

$$\frac{a}{b} = \frac{\gamma}{x}, \quad \frac{a}{b} = \frac{\delta}{x}.$$

We take the various cases in the same order as before and only a brief explanation is necessary to demonstrate the results.

Case 1 D. $x < \gamma < \delta$.

In this case the sector is represented by QOP and in consequence the integration is taken over the whole of the rectangle KLMN and we find that

$$\begin{aligned} \frac{\pi}{2 \sin \sigma \pi} f(x) &= \frac{\partial}{\partial x} \cdot x \int_0^{\infty} \frac{(\sinh q)^{2\sigma-1}}{\cosh^2 q} dq \int_0^{\pi/2} \frac{(fx \sin \theta / \cosh q)}{(\cos \theta)^{2\sigma-1}} d\theta \\ &= \frac{\partial}{\partial x} \int_0^x \frac{y dy}{(x^2 - y^2)^{1-\sigma}} \int_0^y \frac{f(z) dz}{(y^2 - z^2)^{\sigma}} \end{aligned}$$

$$\frac{\pi}{2 \sin \sigma \pi} f(x) = \frac{\partial}{\partial x} \cdot x^{2\sigma} \int_0^x \frac{d\lambda/\lambda}{(x^2 - \lambda^2)^{\sigma}} \int_0^{\lambda} \frac{\mu^{2-2\sigma} f(\mu) d\mu}{(\lambda^2 - \mu^2)^{1-\sigma}},$$

which are, of course, the original theorems (29) and (30).

The next case is more interesting.

Case 2 D. $\gamma < x < \delta$.

In this case the sector is represented by ROQ and the integration is therefore taken over the figure $R_1 R_2 NKL$. For in this area

$$\gamma \nless x \sin \theta / \cosh q \nless \delta.$$

Further, for this range of values $f(x)$ is zero. Therefore we have the identity

$$C = x \int \frac{(\sinh q)^{2\sigma-1}}{\cosh^2 q} dq \int \frac{f(x \sin \theta / \cosh q)}{(\cos \theta)^{2\sigma-1}} d\theta,$$

where the integration is taken over the pentagon $R_1 R_2 NKL$.

Now, taking these integrations by means of strips parallel to the x -axis we have

$$\begin{aligned} C &= x \int_0^{\cosh^{-1}(x/\gamma)} \frac{(\sinh q)^{2\sigma-1} dq}{\cosh^2 q} \int_0^{\sin^{-1}(\gamma \cosh q/x)} \frac{f(x \sin \theta / \cosh q)}{(\cos \theta)^{2\sigma-1}} d\theta \\ &\quad + x \int_{\cosh^{-1}(x/\gamma)}^{\infty} \frac{(\sinh q)^{2\sigma-1} dq}{\cosh^2 q} \int_0^{\pi/2} \frac{f(x \sin \theta / \cosh q)}{(\cos \theta)^{2\sigma-1}} d\theta \\ &= \int_{\gamma}^x \frac{y dy}{(x^2 - y^2)^{1-\sigma}} \int_0^y \frac{f(z) dz}{(y^2 - z^2)^{\sigma}} + \int_0^{\gamma} \frac{y dy}{(x^2 - y^2)^{1-\sigma}} \int_0^y \frac{f(z) dz}{(y^2 - z^2)^{\sigma}}, \end{aligned}$$

writing as before,

$$\cosh q = x/y, \quad \sin \theta = z/y.$$

To find C which depends only on γ and δ but is independent of x we make x tend to γ . Then

$$C = \lim_{x \rightarrow \gamma} \int_0^{\gamma} \frac{y dy}{(x^2 - y^2)^{1-\sigma}} \int_0^y \frac{f(z) dz}{(y^2 - z^2)^{\sigma}},$$

and as before we have

$$\frac{\partial}{\partial \gamma} C(\gamma, \delta) = \frac{\pi}{2 \sin \sigma \pi} f(\delta),$$

and since C is certainly zero if γ is zero, we have

$$C = \frac{\pi}{2 \sin \sigma \pi} \int_0^\gamma f(t) dt.$$

Thus we have the identity

$$\begin{aligned} \int_\gamma^x \frac{y dy}{(x^2 - y^2)^{1-\sigma}} \int_0^y \frac{f(z) dz}{(y^2 - z^2)^\sigma} + \int_0^\gamma \frac{y dy}{(x^2 - y^2)^{1-\sigma}} \int_0^y \frac{f(z) dz}{(y^2 - z^2)^\sigma} \\ = \frac{\pi}{2 \sin \sigma \pi} \int_0^\gamma f(z) dz, \quad \dots \quad (44) \end{aligned}$$

which is true when $x > y$, for almost all arbitrary functions f .

It is also possible as in (37) to carry out the integrations by means of strips parallel to the b -axis. Then we find

$$\begin{aligned} C = x \int_0^{\sin^{-1}(\gamma/x)} \frac{d\theta}{(\cos \theta)^{2\sigma-1}} \int_0^\infty \frac{(\sinh q)^{2\sigma-1}}{\cosh^2 q} dq f(x \sin \theta / \cosh q) \\ + x \int_{\sin^{-1}(\gamma/x)}^{\pi/2} \frac{d\theta}{(\cos \theta)^{2\sigma-1}} \int_{\cosh^{-1}(x \sin \theta / \gamma)}^\infty \frac{(\sinh q)^{2\sigma-1}}{\cosh^2 q} dq \\ \times f(x \sin \theta / \cosh q). \end{aligned}$$

And using as in (37) the substitutions

$$\lambda = x \sin \theta, \quad \mu = \lambda / \cosh q,$$

we obtain

$$\begin{aligned} C = x^{2\sigma} \int_0^\gamma \frac{d\lambda/\lambda}{(x^2 - \lambda^2)^\sigma} \int_0^\lambda \frac{\mu^{2-2\sigma} f(\mu) d\mu}{(\lambda^2 - \mu^2)^{1-\sigma}} \\ + x^{2\sigma} \int_\gamma^x \frac{d\lambda/\lambda}{(x^2 - \lambda^2)^\sigma} \int_0^\gamma \frac{\mu^{2-2\sigma} f(\mu) d\mu}{(\lambda^2 - \mu^2)^{1-\sigma}}. \end{aligned}$$

To find C , we again make x tend to γ . Then we have

$$C = \lim_{x \rightarrow \gamma} x^{2\sigma} \int_0^\gamma \frac{d\lambda/\lambda}{(x^2 - \lambda^2)^\sigma} \int_0^\lambda \frac{\mu^{2-2\sigma} f(\mu) d\mu}{(\lambda^2 - \mu^2)^{1-\sigma}},$$

and using the value as before for $x = \gamma$ we get

$$\frac{\partial C}{\partial \gamma} = \frac{\pi}{2 \sin \sigma \pi} f(\gamma),$$

552 Dr. D. M. Wrinch and Dr. J. W. Nicholson on
and therefore

$$C = \frac{\pi}{2 \sin \sigma \pi} \int_0^\gamma f(\mu) d\mu,$$

C evidently being zero when $\gamma = 0$. Thus our identity above may be written

$$\begin{aligned} x^{2\sigma} \left\{ \int_0^\gamma \frac{d\lambda/\lambda}{(x^2 - \lambda^2)^\sigma} \int_0^\lambda \frac{\mu^{2-2\sigma} f(\mu) d\mu}{(\lambda^2 - \mu^2)^{1-\sigma}} \right. \\ \left. + \int_\gamma^x \frac{d\lambda/\lambda}{(x^2 - \lambda^2)^\sigma} \int_0^\gamma \frac{\mu^{2-2\sigma} f(\mu) d\mu}{(\lambda^2 - \mu^2)^{1-\sigma}} \right\} \\ = \frac{\pi}{2 \sin \sigma \pi} \int_0^\gamma f(\mu) d\mu. \quad \dots \dots \dots (45) \end{aligned}$$

It remains to discuss the case when x is greater than δ and *a fortiori* greater than γ .

Case 3 D. $\gamma < \delta < x$.

In this case the sector bounded by the lines

$$\frac{a}{b} = \frac{\gamma}{x}, \quad \frac{a}{b} = \frac{\delta}{x}$$

may be represented by ROS. The area belonging to the rectangle

$$a=0, \quad b=1, \quad a=1, \quad b=\infty,$$

namely the rectangle KLMN, which lies outside the sector, consists of two parts, the triangle R_1MR_2 and the pentagon S_1S_2NKL . And it is over these two distinct areas that the integration in this case must be performed.

Taking strips parallel to the a -axis we have for the integration over R_1MR_2

$$\begin{aligned} x \iint_{R_1MR_2} \frac{(\sinh q)^{2\sigma-1}}{\cosh^2 q} dq \frac{f(x \sin \theta / \cosh q)}{(\cos \theta)^{2\sigma-1}} d\theta \\ = \int_0^x \frac{y dy}{(x^2 - y^2)^{1-\sigma}} \int_0^y \frac{f(z) dz}{(y^2 - z^2)^\sigma}. \end{aligned}$$

Further, again taking strips parallel to the a -axis we have for the integration over S_1S_2NKL ,

$$\begin{aligned} x \iint_{S_1S_2NKL} \frac{(\sinh q)^{2\sigma-1}}{\cosh^2 q} dq \frac{f(x \sin \theta / \cosh q)}{(\cos \theta)^{2\sigma-1}} d\theta \\ = \int_\gamma^x \frac{y dy}{(x^2 - y^2)^{1-\sigma}} \int_0^y \frac{f(z) dz}{(y^2 - z^2)^\sigma} + \int_0^\gamma \frac{y dy}{(x^2 - y^2)^{1-\sigma}} \int_0^y \frac{f(z) dz}{(y^2 - z^2)^\sigma}. \end{aligned}$$

Thus the theorem stands in the form:—

If $\gamma < \delta < x$, then

$$f(x) = \frac{2}{\pi} \sin \sigma \pi \frac{\partial}{\partial x} \left\{ \int_{\delta}^x \frac{y dy}{(x^2 - y^2)^{1-\sigma}} \int_{\delta}^y \frac{f(z) dz}{(y^2 - z^2)^{\sigma}} \right. \\ \left. + \int_{\gamma}^x \frac{y dy}{(x^2 - y^2)^{1-\sigma}} \int_0^y \frac{f(z) dz}{(y^2 - z^2)^{\sigma}} \right. \\ \left. + \int_0^{\gamma} \frac{y dy}{(x^2 - y^2)^{1-\sigma}} \int_0^y \frac{f(z) dz}{(y^2 - z^2)^{\sigma}} \right\} \quad . \quad . \quad (46)$$

This is also a result of very considerable generality.

Finally, if these integrations were performed by means of strips parallel to the b -axis, we should arrive by analogy with (43) at the result:

If $\gamma < \delta < x$, then

$$f(x) = \frac{2}{\pi} \sin \sigma \pi \frac{\partial}{\partial x} \cdot x^{2\sigma} \left\{ \int_{\delta}^x \frac{d\lambda/\lambda}{(x^2 - \lambda^2)^{\sigma}} \int_{\delta}^{\lambda} \frac{\mu^{2-2\sigma} f(\mu) d\mu}{(\lambda^2 - \mu^2)^{1-\sigma}} \right. \\ \left. + \int_0^{\gamma} \frac{d\lambda/\lambda}{(x^2 - \lambda^2)^{\sigma}} \int_0^{\lambda} \frac{\mu^{2-2\sigma} f(\mu) d\mu}{(\lambda^2 - \mu^2)^{1-\sigma}} \right. \\ \left. + \int_{\gamma}^x \frac{d\lambda/\lambda}{(x^2 - \lambda^2)^{\sigma}} \int_0^{\gamma} \frac{\mu^{2-2\sigma} f(\mu) d\mu}{(\lambda^2 - \mu^2)^{1-\sigma}} \right\} \quad . \quad (47)$$

an alternative form of the same theorem.

The Application of Theorem B to a function which is zero for parts of its range.

The foregoing results consisting of integral equations and identities have been derived from the fundamental theorem

$$(A) \quad f(x) = \frac{2}{\pi} \sin \sigma \pi \frac{\partial}{\partial x} \cdot x \int_0^{\infty} \frac{(\sinh q)^{2\sigma-1}}{\cosh^2 q} dq \\ \times \int_0^{\pi/2} \frac{f(x \sin \theta / \cosh q)}{(\cos \theta)^{2\sigma-1}} d\theta,$$

which was itself derived from Fourier's sine formula,—where $f(x)$ can be zero for certain ranges of x .

Now the structurally related theorem—which has been derived from Fourier's cosine formula—is as follows:

$$(B) \quad f(x) = -\frac{2}{\pi} \sin \sigma \pi \frac{\partial}{\partial x} \cdot x \int_0^{\pi/2} \frac{(\cos \theta)^{1-2\sigma}}{\sin^2 \theta} d\theta \\ \times \int_0^{\infty} \frac{f(x \cosh q / \sin \theta)}{(\sinh q)^{1-2\sigma}} dq,$$

—again with possible zero ranges for f .

It is evident that we may apply this theorem to a function $f(x)$ which is zero for values of x greater than δ and less than γ , provided that we integrate the right-hand side over values of θ and q such that

$$\gamma < x \cosh q / \sin \theta < \delta$$

and

$$0 < \theta < \pi/2, \quad 0 < q < \infty.$$

In fact, using again the substitutions

$$a = \sin \theta, \quad b = \cosh q,$$

integrations have to be performed over the area common to the rectangle

$$a=0, \quad a=1, \quad b=1, \quad b=\infty,$$

and the sector bounded by the lines

$$a/b = x/\gamma, \quad a/b = x/\delta.$$

Case 1 E. $x > \delta > \gamma$.

Taking the various cases in order we find that when $x > \delta > \gamma$ so that the sector is bounded by two lines for which $a/b > 1$, there is no area common to the rectangle KLMN and the sector, which in this case may be represented by POQ. Thus we merely find that $f(x)$ is zero when $x > \delta > \gamma$, as would be anticipated. It will be remarked that there is a close relationship between this case and case 1 C.

Case 2 E. $\delta > x > \gamma$.

In this case, which closely resembles case 2 C, the line OQ represents the line

$$a/b = x/\delta,$$

and OR the line

$$a/b = x/\gamma,$$

so that the area over which the integration has to be performed is the triangle R_1MR_2 . Thus we find

$$-\frac{\pi}{2 \sin \sigma \pi} f(x) = \frac{\partial}{\partial x} \cdot x \int_0^{\cosh^{-1} \delta/x} (\sinh q)^{2\sigma-1} dq \\ \times \int_{\sin^{-1}(x \cosh q/\delta)}^{\pi/2} \frac{f(x \cosh q/\sin \theta)}{\sin^2 \theta (\cos \theta)^{2\sigma-1}} d\theta,$$

and with the substitutions

$$\cosh q = \lambda/x, \quad \sin \theta = \lambda/\mu,$$

it becomes

$$\begin{aligned}
 -\frac{\pi}{2 \sin \sigma \pi} f(x) &= \frac{\partial}{\partial x} \cdot x \int_x^\delta \frac{d\lambda/x}{(\lambda^2/x^2 - 1)^{1-\sigma}} \int_\lambda^\delta \frac{f(\mu) d\mu/\lambda}{(1 - \lambda^2/\mu^2)^\sigma} \\
 &= \frac{\partial}{\partial x} \cdot x^{2-2\sigma} \int_x^\delta \frac{d\lambda/\lambda}{(\lambda^2 - x^2)^{1-\sigma}} \int_\lambda^\delta \frac{\mu^{2\sigma} f(\mu) d\mu}{(\mu^2 - \lambda^2)^\sigma}, \quad (48)
 \end{aligned}$$

or with

$$\begin{aligned}
 x^2 = s, \quad \lambda^2 = t, \quad \mu^2 = u, \quad \delta^2 = \rho, \quad f(x)/x = \phi(s), \\
 -\frac{\pi}{\sin \sigma \pi} \phi(s) = \frac{\partial}{\partial s} \cdot s^{1-\sigma} \int_s^\rho \frac{dt/t}{(t-s)^{1-\sigma}} \int_t^\rho \frac{u^\sigma \phi(u) du}{(u-t)^\sigma}, \quad \text{if } \rho > s.
 \end{aligned} \quad (49)$$

Alternatively, if we carry out the integration by means of strips parallel to the b -axis, we find

$$\begin{aligned}
 -\frac{\pi}{2 \sin \sigma \pi} f(x) &= \frac{\partial}{\partial x} \cdot x \int_{\sin^{-1}(x/\delta)}^{\pi/2} \frac{d\theta}{(\cos \theta)^{2\sigma-1} \sin^2 \theta} \\
 &\quad \times \int_0^{\cosh^{-1}(\delta \sin \theta/x)} \frac{f(x \cosh q/\sin \theta) dq}{(\sinh q)^{1-2\sigma}},
 \end{aligned}$$

and writing as before

$$\sin \theta = x/y, \quad \cosh q = z/y,$$

we deduce, for $x < \delta$

$$\begin{aligned}
 -\frac{\pi}{2 \sin \sigma \pi} f(x) &= \frac{\partial}{\partial x} \cdot x \int_x^\delta \frac{dy/x}{(1 - x^2/y^2)^\sigma} \int_y^\delta \frac{f(z) dz/y}{(z^2/y^2 - 1)^{1-\sigma}} \\
 &= \frac{\partial}{\partial x} \int_x^\delta \frac{y dy}{(y^2 - x^2)^\sigma} \int_y^\delta \frac{f(z) dz}{(z^2 - y^2)^{1-\sigma}}, \quad (50)
 \end{aligned}$$

or with

$$\begin{aligned}
 x^2 = \xi, \quad y^2 = \eta, \quad z^2 = \zeta, \quad \gamma^2 = \nu, \quad f(x)/x = \phi(\xi), \\
 -\frac{\pi}{\sin \sigma \pi} \phi(\xi) = \frac{\partial}{\partial \xi} \int_\xi^\nu \frac{d\eta}{(\eta - \xi)^\sigma} \int_\eta^\nu \frac{\phi(\zeta) d\zeta}{(\zeta - \eta)^{1-\sigma}}. \quad (51)
 \end{aligned}$$

Thus we have from (48, 49) the following integral relations or inversion formulæ:—

(a) If

$$h(\lambda) = \int_\lambda^\delta \frac{\mu^{2\sigma} f(\mu) d\mu}{(\mu^2 - \lambda^2)^\sigma},$$

then

$$f(x) = -\frac{2 \sin \sigma \pi}{\pi} \frac{\partial}{\partial x} \cdot x^{2-2\sigma} \int_x^\delta \frac{h(\lambda) d\lambda/\lambda}{(\lambda^2 - x^2)^{1-\sigma}}. \quad (52)$$

(b) If

$$\theta(t) = \int_t^{\rho} \frac{u^{\sigma} \phi(u) du}{(u-t)^{\sigma}},$$

then

$$\phi(s) = -\frac{\sin \sigma \pi}{\pi} \frac{\partial}{\partial s} \cdot s^{1-\sigma} \int_s^{\rho} \frac{\theta(t) dt/t}{(t-s)^{1-\sigma}} \quad \dots \quad (53)$$

Similarly from (50, 51) we deduce the inversion formulæ :

(c) If

$$g(y) = \int_y^{\delta} \frac{f(z) dz}{(z^2 - y^2)^{1-\sigma}},$$

then

$$f(x) = -\frac{2 \sin \sigma \pi}{\pi} \frac{\partial}{\partial x} \int_x^{\delta} \frac{y g(y) dy}{(y^2 - x^2)^{\sigma}} \quad \dots \quad (54)$$

and

(d) If

$$\chi(\eta) = \int_{\eta}^{\nu} \frac{\phi(\xi) d\xi}{(\xi - \eta)^{1-\sigma}},$$

then

$$\phi(\xi) = -\frac{\sin \sigma \pi}{\pi} \frac{\partial}{\partial \xi} \int_{\xi}^{\nu} \frac{\chi(\eta) d\eta}{(\eta - \xi)^{\sigma}} \quad \dots \quad (55)$$

A particular case is of special importance, namely the case $\sigma = \frac{1}{2}$. Then

$$f(x) = -\frac{2}{\pi} \int_x^{\delta} \frac{y dy}{(y^2 - x^2)^{\frac{1}{2}}} \int_y^{\delta} \frac{f(z) dz}{(z^2 - y^2)^{\frac{1}{2}}},$$

and if

$$g(y) = \int_y^{\delta} \frac{f(z) dz}{(z^2 - y^2)^{\frac{1}{2}}},$$

then

$$f(x) = -\frac{2}{\pi} \frac{\partial}{\partial x} \int_x^{\delta} \frac{y g(y) dy}{(y^2 - x^2)^{\frac{1}{2}}} \quad \dots \quad (56)$$

This is the Bateman-Herglotz equation already mentioned. The other form of these theorems gives

$$f(x) = -\frac{2}{\pi} \frac{\partial}{\partial x} \cdot x \int_x^{\delta} \frac{d\lambda/\lambda}{(\lambda^2 - x^2)^{\frac{1}{2}}} \int_{\lambda}^{\delta} \frac{\mu f(\mu) d\mu}{(\mu^2 - \lambda^2)^{\frac{1}{2}}} \quad \dots \quad (57)$$

and if

$$h(\lambda) = \int_{\lambda}^{\delta} \frac{\mu f(\mu) d\mu}{(\mu^2 - \lambda^2)^{\frac{1}{2}}},$$

then

$$f(x) = -\frac{2}{\pi} \frac{\partial}{\partial x} \cdot x \int_x^{\delta} \frac{h(\lambda) d\lambda/\lambda}{(\lambda^2 - x^2)^{\frac{1}{2}}} \quad \dots \quad (58)$$

In another form the latter formula becomes the degenerate case $\delta = \infty$:—

If

$$h(\lambda) = \int_0^\infty \lambda \cosh u f(\lambda \cosh u) du,$$

then

$$f(x) = -\frac{2}{\pi} \frac{\partial}{\partial x} \cdot \int_0^\infty h(x \cosh v) dv / \cosh v, \quad (59)$$

—an equation discussed by Lamb in relation to hydrodynamics.

As an interesting illustration we take

$$h(\lambda) = \lambda J_0(2\lambda),$$

and we find

$$\begin{aligned} f(x) &= -\frac{2}{\pi} \frac{\partial}{\partial x} \cdot x \int_0^\infty J_0(2x \cosh v) dv \\ &= \frac{1}{\pi} \frac{\partial}{\partial x} \cdot x J_0(x) Y_0(x) \end{aligned}$$

by a well-known formula. Thus

$$\begin{aligned} J_0(2\lambda) &= \frac{1}{\pi} \int_0^\infty \cosh u \frac{\partial}{\partial \lambda} \cdot \{ \lambda J_0(\lambda \cosh u) Y_0(\lambda \cosh u) \} du \\ &= \frac{1}{\pi} \frac{\partial}{\partial \lambda} \cdot \lambda \int_1^\infty \frac{J_0(\lambda t) Y_0(\lambda t) t dt}{(t^2 - 1)^{\frac{1}{2}}}, \quad \dots \dots (60) \end{aligned}$$

a formula of a type which is difficult to prove otherwise.

We have, lastly, to discuss the case when x is less than γ and *a fortiori* less than δ .

Case 3 E. $\delta > \gamma > x$.

In this case the lines

$$a/b = x/\gamma, \quad a/b = x/\delta$$

may be represented by OR and OS and the area over which the integration has to be performed is therefore represented by $R_1 R_2 S_2 S_1$. Thus taking strips parallel to the a -axis

558 Dr. D. M. Wrinch and Dr. J. W. Nicholson on
we find that

$$\begin{aligned}
 -\frac{\pi}{2 \sin \sigma \pi} f(x) &= \frac{\partial}{\partial x} \cdot x \int_0^{\cosh^{-1} \gamma/x} (\sinh q)^{2\sigma-1} dq \\
 &\quad \times \int_{\sin^{-1}(x \cosh q/\delta)}^{\sin^{-1}(x \cosh q/\gamma)} \frac{f(x \cosh q/\sin \theta)}{\sin^2 \theta (\cos \theta)^{2\sigma-1}} d\theta \\
 &+ \frac{\partial}{\partial x} \cdot x \int_{\cosh^{-1} \gamma/x}^{\cosh^{-1} \delta/x} (\sinh q)^{2\sigma-1} dq \\
 &\quad \times \int_{\sin^{-1}(x \cosh q/\delta)}^{\pi/2} \frac{f(x \cosh q/\sin \theta)}{\sin^2 \theta (\cos \theta)^{2\sigma-1}} d\theta,
 \end{aligned}$$

and with the substitutions

$$\cosh q = \lambda/x, \quad \sin \theta = \lambda/\mu,$$

this formula becomes

$$\begin{aligned}
 -\frac{\pi}{2 \sin \sigma \pi} f(x) &= \frac{\partial}{\partial x} \cdot x^{2-2\sigma} \int_x^\gamma \frac{d\lambda/\lambda}{(\lambda^2 - x^2)^{1-\sigma}} \int_\gamma^\delta \frac{\mu^{2\sigma} f(\mu) d\mu}{(\mu^2 - \lambda^2)^\sigma} \\
 &+ \frac{\partial}{\partial x} \cdot x^{2-2\sigma} \int_\gamma^\delta \frac{d\lambda/\lambda}{(\lambda^2 - x^2)^{1-\sigma}} \int_\lambda^\delta \frac{\mu^{2\sigma} f(\mu) d\mu}{(\mu^2 - \lambda^2)^\sigma}.
 \end{aligned}$$

But when $x < \gamma$, $f(x) = 0$. Hence we arrive at an identity

$$\begin{aligned}
 x^{2-2\sigma} \left\{ \int_x^\gamma \frac{d\lambda/\lambda}{(\lambda^2 - x^2)^{1-\sigma}} \int_\gamma^\delta \frac{\mu^{2\sigma} f(\mu) d\mu}{(\mu^2 - \lambda^2)^\sigma} \right. \\
 \left. + \int_\gamma^\delta \frac{d\lambda/\lambda}{(\lambda^2 - x^2)^{1-\sigma}} \int_\lambda^\delta \frac{\mu^{2\sigma} f(\mu) d\mu}{(\mu^2 - \lambda^2)^\sigma} \right\} = C,
 \end{aligned}$$

where C is independent of x .

To find C we may make x tend to γ . Then we have

$$C = \lim_{x \rightarrow \gamma} x^{2-2\sigma} \int_\gamma^\delta \frac{d\lambda/\lambda}{(\lambda^2 - x^2)^{1-\sigma}} \int_\lambda^\delta \frac{\mu^{2\sigma} f(\mu) d\mu}{(\mu^2 - \lambda^2)^\sigma}.$$

Now by theorem (48) it follows that

$$\frac{\partial C}{\partial \gamma} = -\frac{\pi}{2 \sin \sigma \pi} f(\gamma),$$

and therefore

$$C = -\frac{\pi}{2 \sin \sigma \pi} \int_\delta^\gamma f(\mu) d\mu,$$

the lower limit being δ since $C=0$ when $\gamma=\delta$. Thus we

have the identity

$$\begin{aligned} x^{2-2\sigma} \left\{ \int_x^\gamma \frac{d\lambda/\lambda}{(\lambda^2-x^2)^{1-\sigma}} \int_\gamma^\delta \frac{\mu^{2\sigma} f(\mu) d\mu}{(\mu^2-\lambda^2)^\sigma} \right. \\ \left. + \int_\gamma^\delta \frac{d\lambda/\lambda}{(\lambda^2-x^2)^{1-\sigma}} \int_\lambda^\delta \frac{\mu^{2\sigma} f(\mu) d\mu}{(\mu^2-\lambda^2)^\sigma} \right\} \\ = -\frac{\pi}{2 \sin \sigma \pi} \int_\delta^\gamma f(\mu) d\mu = \frac{\pi}{2 \sin \sigma \pi} \int_\gamma^\delta f(\mu) d\mu. \quad (61) \end{aligned}$$

This result has been obtained by integrating strips of the area $R_1 R_2 S_2 S_1$ parallel to the a -axis. Just as in the case of the corresponding D-case we have an equivalent result of a different form for integration by means of strips parallel to the b -axis, namely

$$\begin{aligned} \int_x^\gamma \frac{y dy}{(y^2-x^2)^\sigma} \int_\gamma^\delta \frac{f(z) dz}{(z^2-y^2)^{1-\sigma}} + \int_\gamma^\delta \frac{y dy}{(y^2-x^2)^\sigma} \int_y^\delta \frac{f(z) dz}{(z^2-y^2)^{1-\sigma}} \\ = + \frac{\pi}{2 \sin \pi \sigma} \int_\gamma^\delta f(z) dz. \quad (62) \end{aligned}$$

We do not give a detailed proof of this theorem, since its truth is evident if we compare theorems (61) and (47) and theorem (46) with our final result.

This nearly completes the discussion of the application of the method to a function $f(x)$ which is zero for positive values of x greater than δ or less than γ .

To complete the scheme we have now to apply the theorem to a function $f(x)$ which is zero for values of x between γ and δ .

The detailed consideration of the various cases, when x is greater than δ , when it is between δ and γ , and when it is less than γ , can be left to the reader.

It will be sufficient to record the results.

Case 1 F. $x > \delta > \gamma$.

Thus when $x > \delta$, we shall obtain the original theorems

$$\begin{aligned} \frac{\pi}{2 \sin \sigma \pi} f(x) &= -\frac{\partial}{\partial x} \int_x^\infty \frac{y dy}{(y^2-x^2)^\sigma} \int_y^\infty \frac{f(z) dz}{(z^2-y^2)^{1-\sigma}} \\ \frac{\pi}{2 \sin \sigma \pi} f(x) &= -\frac{\partial}{\partial x} \cdot x^{2-2\sigma} \int_x^\infty \frac{d\lambda/\lambda}{(\lambda^2-x^2)^{1-\sigma}} \int_\lambda^\infty \frac{\mu^{2\sigma} f(\mu) d\mu}{(\mu^2-\lambda^2)^\sigma}. \end{aligned}$$

560 *A Class of Integral Equations occurring in Physics.*

Case 2 F. $\delta > x > \gamma$.

Next when x lies between γ and δ , $f(x)$ is zero and we get an identity, namely

$$\begin{aligned} x^{2-2\sigma} \left\{ \int_{\delta}^{\infty} \frac{d\lambda/\lambda}{(\lambda^2-x^2)^{1-\sigma}} \int_{\lambda}^{\infty} \frac{\mu^{2\sigma} f(\mu) d\mu}{(\mu^2-\lambda^2)^{\sigma}} \right. \\ \left. + \int_x^{\delta} \frac{d\lambda/\lambda}{(\lambda^2-x^2)^{1-\sigma}} \int_{\delta}^{\infty} \frac{\mu^{2\sigma} f(\mu) d\mu}{(\mu^2-\lambda^2)^{\sigma}} \right\} \\ = \frac{\pi}{2 \sin \sigma \pi} \int_{\delta}^{\infty} f(\mu) d\mu. \quad (63) \end{aligned}$$

and the equivalent identity

$$\begin{aligned} \int_x^{\delta} \frac{y dy}{(y^2-x^2)^{\sigma}} \int_y^{\infty} \frac{f(z) dz}{(z^2-y^2)^{1-\sigma}} + \int_{\delta}^{\infty} \frac{y dy}{(\lambda^2-x^2)^{\sigma}} \int_y^{\infty} \frac{f(z) dz}{(z^2-x^2)^{1-\sigma}} \\ = \frac{\pi}{2 \sin \sigma \pi} \int_{\delta}^{\infty} f(z) dz. \quad (64) \end{aligned}$$

Case 3 F. $\delta > \gamma > x$.

Then finally when x is less than γ and δ , we have the theorem

$$\begin{aligned} f(x) = -\frac{2}{\pi} \sin \sigma \pi \frac{\partial}{\partial x} \left\{ \int_x^{\gamma} \frac{y dy}{(y^2-x^2)^{\sigma}} \int_y^{\gamma} \frac{f(z) dz}{(z^2-y^2)^{1-\sigma}} \right. \\ \left. + \int_x^{\delta} \frac{y dy}{(y^2-x^2)^{\sigma}} \int_y^{\infty} \frac{f(z) dz}{(z^2-y^2)^{1-\sigma}} \right. \\ \left. + \int_{\delta}^{\infty} \frac{y dy}{(y^2-x^2)^{\sigma}} \int_y^{\infty} \frac{f(z) dz}{(z^2-y^2)^{1-\sigma}} \right\}, \quad (65) \end{aligned}$$

and the alternative form

$$\begin{aligned} f(x) = -\frac{2}{\pi} \sin \sigma \pi \frac{\partial}{\partial x} \cdot x^{2-2\sigma} \left\{ \int_x^{\gamma} \frac{d\lambda/\lambda}{(\lambda^2-x^2)^{1-\sigma}} \int_{\lambda}^{\gamma} \frac{\mu^{2\sigma} f(\mu) d\mu}{(\mu^2-\lambda^2)^{\sigma}} \right. \\ \left. + \int_{\delta}^{\infty} \frac{d\lambda/\lambda}{(\lambda^2-x^2)^{1-\sigma}} \int_{\lambda}^{\infty} \frac{\mu^{2\sigma} f(\mu) d\mu}{(\mu^2-\lambda^2)^{\sigma}} \right. \\ \left. + \int_x^{\delta} \frac{d\lambda/\lambda}{(\lambda^2-x^2)^{1-\sigma}} \int_{\delta}^{\infty} \frac{\mu^{2\sigma} f(\mu) d\mu}{(\mu^2-\lambda^2)^{\sigma}} \right\}. \quad (66) \end{aligned}$$

This completes the inquiry into the deductions to be drawn from applying the fundamental theorem to a function of x which is zero from γ to δ . Some physical applications of these types of integral equation will be published later.

L. Spectral Relationships of Lines arising from the Atoms of the First Row of the Periodic Table. By R. A. MILLIKAN and I. S. BOWEN.*

I. Spectra of Light Atoms in Many Stages of Stripping.

OUR studies in the field of hot-spark vacuum spectrometry, combined with other work, have now led us to a practically complete understanding of all the radiations that can be emitted by the atoms of the first row of the periodic table in all stages of ionization of their valence electrons.

Thus (1) the complete spectrum of Li_I was already in the literature¹ before our work began.

(2) In the case of Be_I and Be_{II} a small number of lines had been identified by Back, but no term values obtained. We have now classified all the important lines having their origin in either of these two structures, and have obtained the corresponding term values².

(3) In the case of B_I ³, B_{II} ⁴, and B_{III} ⁵ we have identified all the strong lines of all these electronic forms and fixed the corresponding term values.

(4) In the case of carbon, Fowler had worked out most of the lines and term values of C_{II} ⁶. We have completed C_{II} ³ and obtained the identification of all the important lines, and also worked out the term values of C_I ³, C_{III} ⁴, and C_{IV} ⁷; so all of the important lines due to carbon are now classified.

(5) In the case of nitrogen, N_I has been worked out both as to lines and term values by Kiess⁸ and Hopfield⁹. N_{II} was partially obtained by Fowler¹⁰ and the analysis of the strong lines in the extreme ultra-violet was completed by Bowen³. Laporte¹¹, however, has called attention to the necessity of increasing Fowler's term values by about 20,000 frequency units. In N_{III} , Fowler has obtained the identification of five of the lines. The remaining nineteen lines were obtained by Bowen³. In N_{IV} ¹² and N_V ¹³ we have identified a number of the important lines, but the remainder are so faint and fall so far down in the extreme ultra-violet that the corresponding term values have not been obtained.

(6) In the case of oxygen the O_I lines in the visible have long been known¹⁴, and Hopfield¹⁵ has extended into the ultra-violet the study of this spectrum. Also Fowler worked out the lines of O_{II} in the visible and near ultra-violet¹⁶, and Bowen³ has extended the identifications into

* Communicated by the Authors.

the extreme ultra-violet, and corrected errors in preceding term values. The important extreme ultra-violet lines of O_{III} and O_{IV} have been identified by Bowen³, and tentative term values fixed. In O_V and O_{VI} we have identified a number of the important lines¹⁷, but the remainder are unobtainable because faint and below 200 Å.

(7) In the case of F_I , F_{II} , F_{III} , and F_{IV} a few visible lines have been identified by De Bruin¹⁸, while the important ones in the extreme ultra-violet have been worked out by Bowen³, but only tentative values fixed.

(8) In the case of Ne_I , Meissner and Paschen¹⁹ obtained all the important lines and term values in the visible, and Lyman and Saunders²⁰ those in the ultra-violet.

II. *Regular and Irregular Doublet Laws.*

In the working out of the portions of the foregoing spectra for which we have been responsible, the older methods for the identification of lines have been supplemented by the use of new methods arising from the fact that we have been able to extend the most important X-ray laws into the field of optics²¹. Thus, by virtue of the high ionizing power of our hot sparks, we have been able to obtain for the first time in the field of optical spectra a long series of atoms of like electronic structure but of steadily progressing nuclear charge, such as Li_I , Be_{II} , B_{III} , C_{IV} , N_V , O_{VI} , and for this series we have found both of the X-ray laws known as the regular and the irregular doublet laws to hold.

The first of the foregoing laws states that the doublet separation should vary as the fourth power of the effective nuclear charge. It has enabled us to predict the doublet separations of lines to be identified.

The second, or irregular, doublet law has enabled us to predict the exact position in the spectrum of the line to be sought. Furthermore, this last law has not only done the most important service and been of constant use in predicting the position of new lines, but it has enabled us to determine at once the precise nature of the electron jumps involved in the production of unknown lines through the use of the relation which we pointed out as involved in it—namely, that wherever the irregular doublet law holds, the corresponding electron jumps must always be between orbits of the same total quantum number¹².

It was the discovery of these two laws in optics that enabled us to make a definite correlation between optical

and X-ray levels²¹, and forced us definitely to the strange conclusion, published in 1924, that in addition to the relativity cause a non-relativistic cause of doublet separation must exist that yields a separation obeying exactly the relativity formula²².

A cause satisfying this condition as well as the conditions imposed by Landé's work on the anomalous Zeeman effect was found a year later by Uhlenbeck and Goudsmit²³ in the spinning electron. This brilliant idea of the young Dutch physicists has already had extraordinary successes in correlating old phenomena and in interpreting otherwise unexplained effects. It lies at the base of the physical interpretation of the new spectroscopic rules.

III. *The New Spectroscopic Rules.*

Since the very recent formulation by Russell²⁴, Pauli²⁵, Heisenberg²⁶, and Hund²⁷ of the new rules for the determination of the type of spectra arising from different electron configurations, we have found these new rules valuable adjuncts to the laws mentioned in Section II. in the classification of the more complex of our spectra. The detailed statement of these rules and their application to these spectra are given in the Appendix.

These rules were developed by Russell, Pauli, Heisenberg, and Hund from a study of calcium and the other elements of the third row, or the first long period, of the periodic table. The present work has shown that the types of spectra produced by the atoms of the first row of the periodic table are practically those demanded by these rules.

Again the empirical rule, formulated by Hund, that the separations are normal until a shell has become just half filled and then become inverted when more than half full, has been shown in this work to hold also for the elements of the first row. Thus all configurations having one or two p electrons are found here to have normal separations; while with three electrons the separations become very small, and with four or five they widen out again, but with the order of their terms reversed—a behaviour which in Table I. we have represented by giving to the inverted separation a negative sign. In this table we have collected all the separations which have been obtained for the atoms of the first row in all stages of stripping (or ionization). The numbers at the extreme left of the first column represent the number of electrons in p orbits (from 1 up to 6) in the valence shell, *i.e.* the shell of total quantum number 2. The numbers at the tops of

TABLE I.—Fine-structure Separations in the Elements of the first row of the Periodic Table.

No. of p electrons.		No. of s electrons.							
		0.		1.		2.		3.	
1	Li	2P	.338	3P		2P		3P	
	Be		6.61		2.36 .67				
	B		34.4				15.3		
	C		107.4		56.5 22.9		63.1		40.0 20.1
	N		259.1		143.8 61.7		174.2		136.36 31.60
	O		533.8		305.9 134.9		389		
				1P				1P	
2	Be	3P	2.03 1.41	4P		3P		4P	
	B				28.6 21.5		27.7 16		
	C		47.4 29.7		80.5 60.3		82.7 48.8		46.71 33.75
	N		124.5 72.8		185 132		192 116		158.52 105.32
	O		268.2 155.4				394 243		
	F			2P				2P	
					41.6				
	C				110.8				83.12
	N				246				179.99
	O								
	B	1D		2D	< 1	1D		2D	
	C				— 2.3				
	N				— 5.9				
	O				— 10.9				
		1S		2S		1S		2S	
3		4S		5S		3S		5S	
				3S		3S		3S	
	C	2D		3D	— 1.9 < 1	2D		3D	
	N				— 13.7 < 1		< 3		
	O				— 27.8 < 3		— 18		
	F			1D			— 27	1D	
	C	2P		3P	< 1 < 1	2P		3P	
	N		6.9		< 3 — 6.5		< 3		
	O		10		< 5 — 16.3		— 10	1P	
				1P					
4	N	3P		4P	— 44.1 — 18.6	3P		4P	
	O				— 163.4 — 82.1		— 158 — 68		
	F				— 342 — 177		— 344 — 150		— 274.6 — 160
				2P	— 168			2P	
	O				— 384				— 325.6
	F								
	O	1D		2D	— 4	1D		2D	
		1S		2S		1S		2S	
5	F	2P		3P	— 301 — 185	2P	— 407	3P	
	Ne			1P					— 417.45 — 359.35
								1P	
6		1S		3S		1S		2S	

the columns represent the number of valence electrons in s orbits. That this row shows in the fourth column three electrons in s orbits when there are only two ground s electrons, means that two electrons are in the two $2s$ orbits and one in a $3s$ orbit. *It will be seen from glancing down the table that for all the columns, i. e. for all possible numbers of s electrons, as soon as the number of p electrons has passed three, the separations have the negative sign, i. e. the terms have become inverted.*

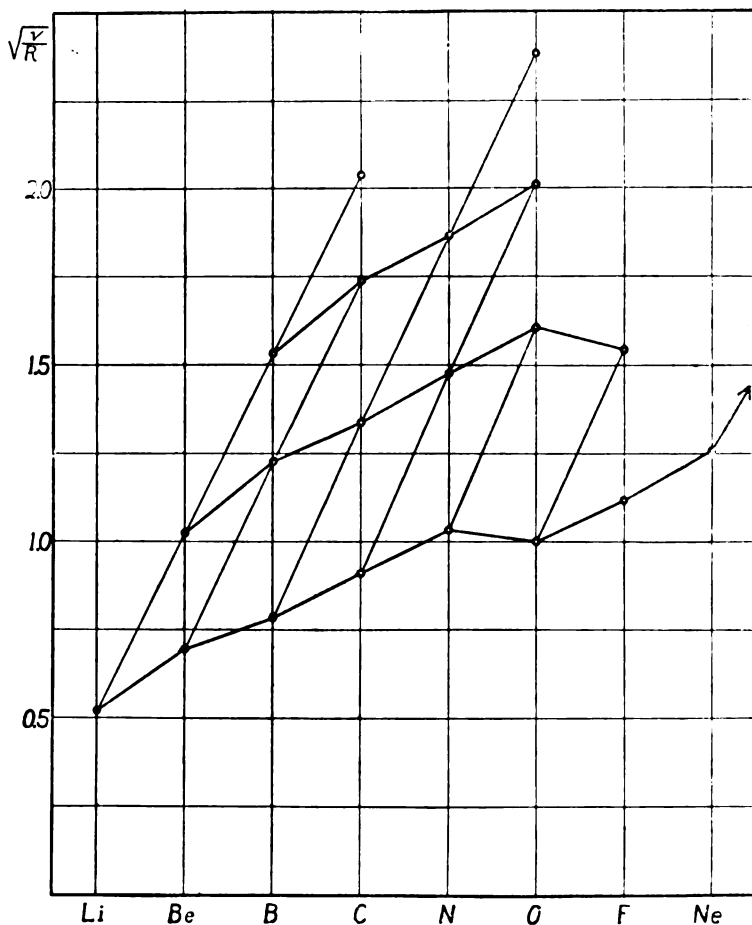
The fact that some squares contain two columns means that the particular configurations involved give rise to either triplet or quartet p terms, which of course have two characteristic separations. The type of the terms is indicated by the symbols at the extreme left within each square.

IV. The Completed Moseley Diagram in the Field of Optics.

In preceding papers we have shown that the Moseley law $\sqrt{\frac{V}{R}} = k(Z - \sigma)$ holds in the field of optics as well as in that of X-rays. This law in Moseley's hands represented merely a linear relation between atomic number Z and the square root of the frequency of a series of *corresponding lines*, and in our first paper²⁸ in this field we attempted to follow Moseley in plotting the relation between Z and what we thought to be a series of corresponding lines in our extreme ultra-violet spectra. More recently it has become customary, in presenting "Moseley straight lines" in the field of X-rays, to plot the relation between Z and the square root of the frequency corresponding to an *energy level, or term*, rather than to a line. Also in all of our own recent proofs of the validity of the Moseley law in the field of optics, it has been a linear relation between the square root of the frequencies of a series of corresponding levels and atomic number that we have exhibited. Indeed, *by this sort of plotting we have been able to show quite generally that a series of atoms of like electronic structure but varying charge always leads to a Moseley straight line.* This result is exhibited very beautifully in the diagram of fig. 1, in which the levels plotted—a small fraction of those we might plot—represent in every case the energy necessary to remove an electron from a p orbit of each of the atoms under consideration. The straight line farthest to the left represents the Moseley diagram for a one-valence electron system of this sort, the next line towards the right the same diagram for a two-electron system of this sort, the next that for a three-valence electron system, the next that

for a four-valence electron system, and so forth. The linear relations here shown are so perfect that the ionizing potentials can be quite accurately obtained for atoms for which they have not yet been determined, and that by simple extrapolation along these lines.

Fig. 1.



The lowest broken line running across the straight lines represents the series of energies necessary to remove an electron from the lowest p orbit in the case of a neutral atom, the next higher broken line the series of energies necessary to remove an electron from the lowest p orbit of a singly-ionized atom, and the broken line above that the series of

energies necessary to remove an electron from the lowest *p* orbit of a doubly-ionized atom. It is, of course, because these lines do not connect atoms of like electronic structure that they are broken instead of straight.

If the Moseley progression be defined as the progression exhibited by the square root of the energy of binding (\sqrt{V}) of a two-*p* electron by all the neutral atoms from hydrogen up to uranium, then the lower broken line of the chart depicts this progression up to neon, while from neon to uranium it is a practically straight line following the direction indicated by the arrow shown at the right side of this figure.

V. Ionizing Potentials.

The ionization potentials—the energy necessary to remove the most lightly bound electron—of all the atoms of the first row in all the degrees of stripping in which it has as yet been possible to obtain the limit of the appropriate series are collected in Table II. Some of these, notably those of

TABLE II.—Ionization Potentials.

	I.	II.	III.	IV.
Li.....	5.371			
Be	9.50	18.141		
B	8.34	24.2	37.786	
C	11.3	24.289	45.5 (45)	64.23
N	14.494	29.56 (24)	47.2 (45)	
O	13.565	34.999 (32)	54.8 (45)	77.0
F	16.9	32.3		
Ne	21.482			

carbon, nitrogen, and oxygen, are of much importance for fixing the temperatures of stars. Indeed, in some cases it has only been by working backwards from stellar temperatures estimated by other methods that rough estimates of these ionization potentials have heretofore been obtained. These previous estimates²⁹ are recorded in italics below the new values obtained from our spectroscopic measurements. The new values will be seen to be from one to twenty-five per cent. higher than the old.

Norman Bridge Laboratory of Physics,
California Institute of Technology,
Pasadena.

APPENDIX.

The Application of the New Spectroscopic Rules to the Spectra of the Atoms of the First Row of the Periodic Table.

The fundamental assumption underlying the modern quantum theory of spectra is that the moments of momentum of all rotary motions within the atom possess the fundamental quantum property of being able to change only by unit steps, *i. e.* all moments of momentum are quantized.

There are three different sorts of moments of momentum to consider. In the first instance, it is the moment of momentum of the individual electron in its orbit which has been quantized. The number of units in this orbital moment of momentum determines the so-called azimuthal quantum number of the orbit, and has heretofore been designated by the letter *k*.

When more than one electron is present within an atom, the total orbital moment of momentum of the whole group is obtained by taking the quantized vector sum of the individual orbital moments. But in this summation process, for reasons not yet fully understood, it is found necessary to reduce the previously assumed value of the azimuthal quantum number by unity. In order to avoid confusion, this new value of the azimuthal quantum number of each electron orbit is now designated by *l*, which means of course that $l = k - 1$. Thus an *s* orbit has a value $l = 0$, a *p* orbit $l = 1$, a *d* orbit $l = 2$, an *f* orbit $l = 3$, etc.

The physical significance of the fact that the vector sum of the *l*'s is quantized to obtain *L* is that the electrons are able to rotate only in orbits of such orientations about the nucleus that this vector sum is a whole number of units of moment of momentum.

In the second instance the moment of momentum of the spin of each electron on its axis is quantized. In order to obtain the following interpretations, it is found necessary to assume, first that the moment of momentum of spin of every individual electron within an atom is always one-half the fundamental unit of moment of momentum, *i. e.* it is $\frac{1}{2} \frac{h}{2\pi}$, and second that all electrons within an atom spin in the same plane, some however spinning in one direction and others in the exactly opposite sense. This last condition means that the total or resultant moment of momentum of spin of all the electrons within an atom is the algebraic sum of the spins of the individual electrons. This total spinning moment

of all the electrons of a given atom is designated by the letter *R*.

In the third instance, in order to obtain the total moment of momentum of the whole atom it is necessary to take the quantized vector sum of the orbital moments, *L*, and of the spin moment, *R*. This is precisely the quantity which was originally called by Sommerfeld the inner quantum number and designated by the letter *J*.

The fundamental quantum condition is now that all possible values of *J* constitute a series of which the successive steps differ by unity. If the value of *R* is an odd number of half units, *i. e.* if there are an odd number of spinning electrons, then all the values of *J* are found to be half integral ($\frac{1}{2}$, $1\frac{1}{2}$, $2\frac{1}{2}$, $3\frac{1}{2}$, etc.), while if the value of *R* is integral, then all the values of *J* are found to be likewise integral (1, 2, 3, etc.). The number of possible values of *J* obtained from a given pair of values of *R* and *L* gives the multiplicity, *i. e.* the number of terms in the fine structure. The maximum of the multiplicity is then $2R + 1$.

The notation now in general use in the formulation of the new rules is as follows:—When the value of *L* built up as above from the vectorial summation of the *l*'s of the individual orbits is 0, the term is by definition an *S* term; when *L*=1 the term is by definition a *P* term; when *L*=2 it is a *D* term; when *L*=3 an *F* term, etc. The value of the maximum multiplicity, as determined by the above formula and involving only *R*, is indicated by a superscript preceding the letter. Thus doublet *S*, triplet *P*, etc. are written 2S , 3P , etc. When it is necessary to differentiate between the different *P* terms, for example, the value of *J* corresponding to each *P* term is written as a subscript, thus: 3P_1 , 3P_2 , etc.; but for convenience in case of half-integral values of *J* it has been decided to use the next higher whole number, thus avoiding using fractional subscripts in the mere naming of the two *P* terms in a doublet, for example.

The word "configuration" will here be used to indicate the number of electrons in each of the different sorts of orbits. Thus s^2p^3 means a configuration of two electrons in *s* orbits and three electrons in *p* orbits, while $s^2p^2\bar{p}$ indicates the configuration in which one of the *p* electrons has been pushed up into a *p* orbit of higher total quantum number.

The foregoing quantization rules predict a much larger number of terms than are actually obtained from a given configuration; and Pauli has formulated an exclusion rule which has a very illuminating physical significance, and

which succeeds in reducing the number of terms to those really observed. It is stated as follows:—No two electrons can be alike in all four of the quantum numbers necessary to describe their motions. These are, namely: (1) total quantum number (n), or *size of orbit*; (2) azimuthal quantum number (k), or *shape of orbit*; (3) projection of orbital moment of momentum upon a fixed direction of reference, or *orientation of orbit*; (4) projection of moment of momentum of spin upon the fixed direction of reference, or *orientation of spin*. These last two are usually called magnetic quantum numbers, since the fixed direction is usually taken as that of a magnetic field, and must be so taken in the analysis of the Zeeman effects.

We shall now apply these rules to the interpretation of the spectra of the simpler atoms.

1. Stripped Atoms, or One-electron Systems.

In the case of the first atom, Li, of the first row the single outer or valence electron may be either in an elliptical orbit 2_1 or a circular orbit 2_2 . In the latter case the orbit is in all of its parts far outside the inner pair of K electrons, so that the effective nuclear charge is very close to $3-2=1$, while in the case of the 2_1 orbit the approach to the nucleus at perihelion is very much closer, and hence the screening of the two K electrons much less perfect. The average binding of the electron in the 2_1 orbit is therefore much greater than that of the electron in the 2_2 orbit, so that the electron jump from the 2_2 to the 2_1 orbit gives rise to the familiar strong line of Li at 6708 Å. The fact that this line is a doublet means that there are two circular (2_2) orbits, P_1 , P_2 , of slightly different energies, from which the electron may jump into the S or 2_1 orbit. The existence of just two levels is seen to be required by the foregoing rules, since by them $l=1$ and, since there is but one electron, $L=1$, and also $R=\frac{1}{2}$, so that J can have just two values, $\frac{1}{2}$ or $1\frac{1}{2}$, depending upon whether the two moments of momentum are added parallel or antiparallel. The theory of the spinning electron thus accounts for the difference in energy of these two orbits merely by the assumption that in one case the electron is spinning in the direction of the orbit, and in the other case in the opposite direction. The foregoing set of rules accounts for the fact that while there are two P levels there is but one S level, since for this level l equals 0, and hence $L=0$, and this can be combined with $R=\frac{1}{2}$ only so as to yield one value of the total moment of momentum J of the atom, viz. $J=\frac{1}{2}$.

The spectra of all the stripped atoms Li I , Be II , B III , C IV , N V , O VI , F VII are of the same type as that of Li , and in our work with them the new rules have not been used, the older methods (Rydberg-Ritz formula) and the regular and irregular doublet laws being sufficient for all identifications.

2. Two-electron Systems.

In the case of the second atom of the row, viz. Be , there are two valence electrons which in the normal or ground state must both be in $2s$, i. e. in s orbits. We shall consider first a configuration in which one of these two s electrons has been moved out to some more remote orbit, such as a p orbit. Here the l 's to be summed vectorially are $l=0$ and $l=1$. Hence $L=1$, also $R=\frac{1}{2}+\frac{1}{2}=1$, or $\frac{1}{2}-\frac{1}{2}=0$. The quantized vector sum of $L=1$ and $R=1$ is $J=0, 1$, or 2 . This is therefore a triplet level, while when $L=1$ and $R=0$, $J=1$. This is therefore a singlet level. This configuration therefore gives rise to triplet or singlet levels and since $L=1$ to triplet P terms (^3P) or singlet P terms (^1P).

If the excited electron had gone to a d orbit ($3d, 4d, 5d$, etc.), then for the two orbits $l=0$ and $l=2$; therefore $L=2$, while, as above, $R=1$ or 0 . This gives either $J=1, 2, 3$ or $J=2$, i. e., as above, it gives rise to triplet or singlet D terms (^3D or ^1D).

Similarly there always result singlet or triplet terms for all positions of one electron, since for the other electron $l=0$ and the type of the term is the same as the type of the orbit of the excited electron.

When the atom has settled down to its ground state, i. e. when both electrons are in the two s orbits, both l 's are 0 , hence $L=0$. Also, so far as the foregoing rules go, $R=\frac{1}{2}+\frac{1}{2}=1$, or $\frac{1}{2}-\frac{1}{2}=0$, and hence $J=1$ or 0 ; but this leads to a predicted number of levels which in the case of two $2s$ orbits is never found in practice, since they are excluded by the Pauli rule, which in this case means that, since the $2s$ electrons have orbits of the same (1) size, (2) shape, and (3) orientation, they cannot be spinning in the same direction, so that $R=\frac{1}{2}-\frac{1}{2}=0$. Hence, since $L=0$, $J=0$, this means that the moment of momentum of the atom equals 0 ; and this requires a singlet term since the maximum possible multiplicity is the number of possible values of J , which is here 1 .

It will be seen from exactly the same sort of analysis that the Pauli rule requires that the moment of momentum of the K shell is always 0 . Similarly it actually always requires

that the moment of momentum of any closed shell is 0; and this means, of course, that it is only the electrons in partially-filled shells which determine the moment of momentum of the atom.

There is another configuration of the two electrons of Be which is of interest in connexion with the Pauli rule, namely when one excited electron has moved up to some higher s orbit. Then, since the two orbits now differ in size, though they are alike in shape, both being s orbits, they may be alike in both orientation and spin, so that $R=1$ or 0, and hence any pair of values of L and R , viz. $L=0$ and $R=1$, or $L=0$ and $R=0$, can give rise only to a single term. In general, however, for all values of L other than its zero value, there result from the quantized vector addition of any of these values with the value $R=1$ three possible values of J , viz. $L+1$, L , and $L-1$, and when L is thus combined with $R=0$, one possible value of J , viz. L . It is then found convenient to classify all terms resulting from $R=1$ as belonging to the triplet system, and all resulting from $R=0$ as belonging to the single system. This notation makes it possible to set up the foregoing general rule, which makes term multiplicity independent of L and dependent upon R alone as stated. The *tour de force* by which this rule has been arrived (ignoring the value $L=0$) finds some physical justification in the fact that combinations (electron jumps) do actually occur most strongly between terms having the same value of R , whether $L=0$ or $L>0$, so that the particular single term arising from $L=0$, $R=1$ does actually belong with the triplet system. With this explanation as to notation we may henceforth always determine maximum multiplicity with the foregoing formula, multiplicity $= 2R + 1$.

Another very interesting configuration is that in which both electrons have been raised into p orbits (the p^2 configuration). Here for each orbit $l=1$, therefore $L=0, 1$, or 2. Also $R=\frac{1}{2}+\frac{1}{2}=1$, or $\frac{1}{2}-\frac{1}{2}=0$. When $L=0$ we have by definition an S term, and when this value of L is combined with $R=0$, there results $J=0$, *i. e.* a singlet S term. When $L=0$ is combined with $R=1$, there results $J=1$, again a single term, which by the above rule, however, belongs to the triplet system, and hence is usually spoken of as a triplet S term. When the values $L=1$ or 2 are combined with $R=0$, there result $J=1$ or 2 respectively, *i. e.* a singlet P term or a singlet D term. And when the values $L=1$ or 2 are combined with $R=1$, there result triplet P or triplet D terms. In a word, then, this configuration gives rise only to singlet

and triplet terms. This might have been found at once from the foregoing rule, that the maximum multiplicity is given by $2R + 1$.

Of the foregoing terms, all save the singlet S, triplet P, and singlet D terms are actually forbidden by the Pauli exclusion rule, as can be seen by working out, a rather tedious process, the possible combinations of the four quantum numbers for each of the two electrons in such a way as to always make at least one of the four different for the two electrons.

In the actual practice of spectroscopy none of the foregoing singlet terms have thus far been located. This is due to the fact that since there are in the case of singlet lines no characteristic frequency differences to search for, singlets are in general very difficult to identify.

The foregoing triplet P terms (P_0, P_1, P_2), which alone remain of the terms corresponding to the configuration of two electrons in p orbits, are actually identical with the three p' terms which we found combining strongly with the triplet P terms of the sp configuration to produce "the flag"—the pp' group—that we found to be characteristic of all two-electron systems formed from atoms of the first two rows of the periodic table; that is, all these pp' groups in two-electron systems of these elements are formed by the removal of both electrons to p orbits and the subsequent return of one of them to an s orbit. In the removal the two electrons may have three different orientations of the plane in which they are both spinning with respect to the L vector, and each of these orientations has a slightly different energy. Similarly, after the return of one of them the plane in which the two are now spinning may have three different orientations with respect to the new L vector. Were it not for the selection principle that J can change only by ± 1 or 0, the jump for the upper group of three states to the lower group of three might be made in nine different ways. The above selection principle reduces these nine to six, which then correspond to the six observed lines of "the flag."

We have now discussed all the levels in two-electron Be that are near enough to the ground-level to give rise to lines of an appreciable strength. The discussion of BeI applies *in toto* to all the two-electron systems, BII , CIII , NIV , OV , FVI .

3. *Three-electron Systems.*

In the case of a three-electron system when two of them are in the ground state, *i. e.* in s orbits for precisely the same reasons stated on p. 572, the Pauli rule requires that these

two electrons spin in opposite directions. Further, the same rule precludes the third electron from being in a $2s$ state, since, if it were, this third s state would have to be identical with one of the other two. In other words, there can never be more than two electrons in an s state of a given total quantum number. This fact was first discovered by Stoner from a considerable amount of experimental data, and was then shown by Pauli to be a consequence of this rule. The ground state of a three-electron system is then two electrons in s orbits and one in a p orbit. But since, as in the case of the two electrons in the K shell, the value of the moment of momentum for these two electrons is zero, the moment of momentum of the atom is determined simply by the p electron. It follows that all the types of spectra possible with a three-electron system when the two s orbits are filled are the same as those of a one-electron system like Li, discussed above, save for the fact that the $2\bar{S}$ term is missing because the $2s$ orbits are full. Here therefore, as in the alkalis, the terms are all doublets.

To take one particular three-electron system which is altogether typical of them all, consider N_{III} . One of the strongest lines to be expected involving the foregoing configuration of two electrons in s orbits and one in a p orbit—a s^2p configuration—is that produced by the jump from s^2d to s^2p . This corresponds to the combination of the doublet D of the s^2d configuration with the doublet P of the s^2p configuration (2D of $s^2d \rightarrow ^2P$ of s^2p). In N_{III} this is the strong line at 374 Å. The next strongest line corresponds to the combination of the doublet S of the $s^2.s$ configuration (two electrons in the $2s$ state and one in an excited s state) with the doublet P of the s^2p configuration (2S of $s^2.s \rightarrow ^2P$ of s^2p). In N_{III} this is the strong doublet line at 452 Å.

Nothing further need be said about the case in which the two $2s$ orbits are filled, although there are weaker lines corresponding to jumps of this single electron between excited states.

But when one of these $2s$ electrons has been pushed up into a p orbit, so that the configuration is one s electron and two p electrons, (sp^2) the two p electrons alone would give rise, as shown on p. 572, to singlet S, triplet P, and singlet D terms. Now a singlet S when combined with one s electron, having the value $l=0$ and $r=\frac{1}{2}$, produces $L=0$, $R=\frac{1}{2}$, which corresponds to doublet S terms (2S). Again, a singlet D combined with one s electron produces $L=2$, $R=\frac{1}{2}$, which corresponds to doublet D terms (2D). Finally,

triplet P terms when combined with one s electron produce $L=1$, $R=\frac{1}{2}$ or $1\frac{1}{2}$, which corresponds to doublet and quartet terms respectively (2P and 4P).

All of these doublet terms combine strongly with the doublet P term of the s^2p configuration. Thus the doublet D combining with the doublet P of the s^2p configuration gives rise to the pair at 991 Å, which are the strongest lines in the whole N_{III} spectrum. Again, the doublet P of the sp^2 configuration combining with the P of the s^2p configuration gives rise to what we have called the pp' "flag" of the three-electron system at 686 Å. Also the doublet S of the sp^2 configuration combining with the doublet P of the s^2p configuration gives rise to the pair of lines at 764 Å.

Another configuration which is found to occur frequently is p^3 , both of the two s electrons having been pushed up into p positions. Analysis similar to the foregoing shows, in view of the Pauli exclusion rule, that the following terms are possibilities: quartet S, doublet P, doublet D. The doublet P of this p^3 configuration combines strongly with the doublet P of the sp^2 configuration to produce the strong pair at 1184 Å. It also combines with the doublet S and the doublet D to give rise to the lines at 1006 Å and 773 Å respectively. Also the quartet S of p^3 combines with the quartet P of sp^2 to give the strong group at 772 Å.

This covers all of the configurations which take part in forming strong lines in N_{III} . Further, the foregoing analysis of course applies to all of the three-electron systems which can be formed from any of the atoms here under consideration: *i. e.* it applies to Bi , C_{II} , and O_{IV} as well as to N_{III} . Also, since all of the lines formed by the changes in the last two configurations above considered are changes in which the total quantum number of all electrons remain unaltered, these lines must all follow the irregular doublet law, a law which was actually a very important factor in their identification.

4. *Four-electron Systems.*

A typical four-electron system is N_{II} . The ground state is, of course, the s^2p^2 configuration. As shown above, the two s electrons have zero momentum; so that the types of terms are identical with those of two electrons in p orbits such as were discussed above under two-electron systems. As shown above (p. 572), this configuration gives rise to a singlet S, a singlet D, and a triplet P.

When one of the p electrons is pushed up into an excited s orbit ($s^2p.s$), the effect of the s^2 is zero, and hence the

type of the terms are those found with one electron in a p and one in an s orbit. These are, as shown above, a singlet P' and a triplet P . The combination of this with the ground configuration gives rise to two singlets (not yet identified) and the pp' group of six lines at 672 Å.

The $s^2p.p$ configuration gives terms of the same type as those we worked out for a two-electron system with both electrons in p orbits, save that in this case these two electrons are not in orbits of the same total quantum number, so that Pauli's exclusion rule no longer applies. Hence all the terms discussed on p. 572 are present, namely singlet S, P, D , and triplet S, P, D . This configuration, in passing over into $s^2p.s$, produces many lines in the visible (for the identification of which A. Fowler has been largely responsible), but none in the region of our activity.

The $s^2p.d$ configuration is unlike any as yet discussed. Its s^2 part can be ignored, thus leaving two orbits for which $l=1$ and $l=2$ respectively. These combine into $L=1, 2$, or 3 . Further, $R=0$ or 1 . The first value of R gives singlets and the last triplets, so that we have singlet P , singlet D , and singlet F terms, also triplet P , triplet D , and triplet F terms. Of all the combinations possible between these terms and those of the s^2p^2 configuration, only one has been found, namely from the triplet P of $s^2p.d$ to triplet P of s^2p^2 . These are the very close lines at 534 Å.

The sp^3 configuration is the p^3 discussed on p. 575 combined with an s electron. Since the moment of momentum of an s orbit is zero, the value of L is unchanged by the addition of the s orbit, and hence the type of the terms is the same as with p^3 alone. The value of R is moved up a half or down a half by the addition of the s orbit, and hence the multiplicity is pushed up one or down one. This means that the quartet S of the p^3 configuration is changed to a triplet S and a quintet S , the doublet P to a singlet P and a triplet P , and the doublet D to a singlet D and a triplet D . Only the triplet S, P , and D terms have been observed, and these through their combination with the triplet P of the s^2p^2 configuration, giving rise to the groups at 645 Å, 916 Å, and 1085 Å respectively.

The only other line of N_{II} observed thus far in the study of the extreme ultra-violet which we have been pursuing with our hot-spark technique is the group at 1276 Å, which is produced by the change from the configuration $s^2p.p$ to sp^3 . This last is of peculiar interest because it represents the jumping of an electron from $3p$ to $2p$ simultaneously with the elevation of another electron from an s to a p orbit.

This is an unusually interesting form of two-electron jump.

In the discussion of N_{II} we have covered in effect all four-electron systems, such as C_I , N_{II} , O_{III} , and F_{IV} .

5. Five-electron Systems.

The typical five-electron system which we shall choose for discussion is O_{II} . The ground state is the s^2p^3 configuration; and since the s^2 has zero momentum, this configuration is precisely the same as the p^3 configuration discussed on p. 575 under the head of a three-electron system. It gives rise to quartet S, doublet P, and doublet D terms.

The first excited state is $s^2p^2.s$, which is identical with the sp^2 configuration discussed on p. 574 under a three-electron system. Its terms are doublet S, doublet D, doublet P, and quartet P. In returning to the ground state the doublet S combines with the doublet P to produce the unresolved pair at 644 Å. The jump 2D to 2P gives the unresolved group at 601 Å. The jump 2P to 2P gives the partially resolved group at 673 Å. The jump 2P to 2D gives the partially resolved group at 617 Å. The jump 4P to 4S gives rise to the three-line group at 539 Å.

The second excited state is $s^2p^2.p$, the terms of which can be obtained by adding to the p^2 terms of a two-electron system (see p. 572) a single p electron. These p^2 terms were 1S , 3P , and 1D , and they change as follows: 1S changes to 2P ; 3P changes (since its former values $L=1$, $R=1$ have changed to $L=0, 1$, and 2 , and $R=\frac{1}{2}$ and $1\frac{1}{2}$) to 2S , 2P , 2D , 4S , 4P , 4D ; and 1D changes (since $L=2$, $R=0$ changes to $L=1, 2, 3$, $R=\frac{1}{2}$) to 2P , 2D , and 2F . The return from this second excited state to the first excited state produces a large number of lines in the visible which are outside the range of our extreme ultra-violet studies, and have actually been identified in the main by A. Fowler.

The third excited state is $s^2p^2.d$, the terms of which can be obtained as above by adding to the p^2 terms of a two-electron system a single d electron. Then 1S changes to 2D ; 3P changes (since its former values $L=1$, $R=1$ have changed to $L=1, 2$, or 3 , $R=\frac{1}{2}$ or $1\frac{1}{2}$) to 2P , 2D , 2F , 4P , 4D , 4F ; and 1D changes (since $L=2$, $R=0$ changes to $L=0, 1, 2, 3, 4$ and $R=\frac{1}{2}$) to 2S , 2P , 2D , 2F , 2G . The return of this third excited state to the second excited state gives rise to a large number of lines in the visible, also identified mainly by A. Fowler. The return from this third excited state to the ground state, however, produces lines which are in the main

field of our studies. They are as follows :—The 2P based on the 3P of the core combines with the 2D of the ground state to produce the unresolved line at 484 Å, and with the 2P of the ground state to produce the unresolved line at 518 Å. The 2D based on the 3P of the core combines with the 2D of the ground state to produce the unresolved line at 481 Å, and with the 2P of the ground state to produce the partially-resolved group at 516 Å. The 2F based on the 3P of the core combines with the 2D of the ground state to produce the unresolved line at 485 Å. The 2P based on the 1D of the core combines with the 2D of the ground state to give the unresolved line at 440 Å. The 2D based on the 1D of the core combines with the 2P of the ground state to give the unresolved line at 470 Å, and with the 2D of the core to give the unresolved line at 442 Å. The 4P based on the 3P of the core combines with the 4S of the ground state to give the unresolved line at 430 Å.

The fourth excited state which we shall consider is sp^4 , *i. e.* one of the two s electrons goes over into one of the p orbits. The simplest way to treat this case is to make use of the general principle that a single vacancy in a shell acts like a single electron in that shell, two vacancies like two electrons, etc., so that since the p can hold but six electrons, p^4 is equivalent to p^2 . This means that sp^4 is the same as p^2s , found on p. 574 to possess the terms 2S , 2D , 2P , and 4P . In returning to the ground state the 2D going back to 2P gives rise to the unresolved strong line at 797 Å, and in going back to 2D to the strong partially-resolved line at 719 Å. Also the 2P going back to 2P produces the partially-resolved group at 581 Å, and in going back to 2D produces the partially-resolved group at 538 Å. Again, the 4P going back to the 4S produces the very strong three-line group at 834 Å.

In the discussion of O_{II} we have covered in effect all five-electron systems such as N_I , O_{II} , F_{III} .

6. Six-electron Systems.

The most completely analysed case of a six-electron system is the arc spectrum of oxygen, the greater part of whose lines in the visible have been identified for thirty years. Recently, too, the ultra-violet lines of O_I have been well classified by Hopfield.

The six-electron system which has become partially known through our studies in hot-spark spectrometry is F_{II} . The ground state is s^2p^4 , which, by virtue of the principle stated in a preceding paragraph, has terms identical with p^2 ,

namely 1S , 3P , 1D . The first excited state is $s^2p^3.s$, which has been fully treated under a four-electron system, and has the terms 5S , 3S , 3P , 1P , 3D , 1D . The only group of lines due to it which we have identified is that produced by the combination of 3S of the first excited state with 3P of the ground state. This gives rise to the group of three resolved lines at 548 Å. The second excited state $s^2p^3.p$ through its return to the first excited state $s^2p^3.s$ should give rise to lines in the visible or near ultra-violet, which, however, have not yet been identified. Also the third excited state $s^2p^3.d$ through its return to $s^2p^3.p$ should also give lines in the visible, but in its return to the ground state s^2p^4 it should give lines in the region of our hot-spark studies. We have, however, not identified with certainty any of this group.

An excited state which actually occurs more frequently than this is the s^2p^5 configuration, and the drop back from this into the ground state then produces the very strong group of lines at 607 Å. The theoretical analysis is here simple, since a p^5 configuration, which corresponds to a vacancy of one in the p shell, is the same as a single p electron configuration. This has a value of $L=1$, $R=\frac{1}{2}$, and when a single s electron is added to this it yields $L=1$, $R=0$ or 1 , *i. e.* singlet and triplet P terms. These should combine with the 1S , 3P , D of the ground state to produce singlet and triplet lines, of which, however, only the triplets mentioned above are found. These should constitute a group of six lines, which they are actually found to be.

7. Seven-electron Systems.

The only possible seven-electron system of this group is F_1 , the ground state of which is s^2p^5 , which is the same as a single p orbit, *i. e.* it gives rise to a 2P term. The most probable excited states are, of course, $s^2p^4.s$, $s^2p^4.p$, $s^2p^4.d$, and since the p^4 is equivalent to p^2 , these are equivalent to the $s^2p^3.s$, $s^2p^3.p$, $s^2p^3.d$, which were treated above under the five-electron system. The 2P of the $s^2p^4.s$ combines with the 2P of the s^2p^5 configuration to produce the four strong lines at 955 Å. Also the observed pair of lines at 807 Å is due to the return from one of the terms of the $s^2p^4.d$ configuration to the 2P term of s^2p^5 .

References.

1. Fowler, 'Series in Line Spectra,' p. 97.
2. Bowen and Millikan, Phys. Rev. xxviii. p. 256 (1926).
3. Bowen, Phys. Rev. xxix. p. 231 (1927).
4. Bowen and Millikan, Phys. Rev. xxvi. p. 310 (1925).

5. Bowen and Millikan, *Proc. Nat. Acad. Sci.* x. p. 199 (1924).
6. A. Fowler, *Proc. Roy. Soc.* cv. p. 299 (1924).
7. Millikan and Bowen, '*Nature*,' cxiv. p. 380 (1924).
8. Kiess, *J. O. S. A. & R. S. I.* xi. p. 1 (1925).
9. Hopfield, *Phys. Rev.* xxvii. p. 801 (1926).
10. A. Fowler, *Proc. Roy. Soc.* cvii. p. 31 (1925).
11. Laporte, *J. O. S. A. & R. S. I.* xiii. p. 13 (1926).
12. Bowen and Millikan, *Phys. Rev.* xxvi. p. 150 (1925); Bowen and Ingram, *Phys. Rev.* xxviii. p. 447 (1926).
13. Bowen and Millikan, *Phys. Rev.* xxiv. p. 212 (1924).
14. A. Fowler, '*Series in Line Spectra*,' p. 166.
15. Hopfield, *Astrophys. J.* lix. p. 114 (1924).
16. A. Fowler, *Proc. Roy. Soc.* cx. p. 476 (1926).
17. Bowen and Millikan, *Phys. Rev.* xxvii. p. 144 (1926).
18. De Bruin, *K. Akad. Amsterdam Proc.* xxxv. p. 751 (1926).
19. Paschen, '*Seriengesetze der Linienspektren*,' p. 30.
20. Lyman and Saunders, *Proc. Nat. Acad. Sci.* xii. p. 92 (1926).
21. Bowen and Millikan, *Phys. Rev.* xxiv. p. 209 (1924).
22. Millikan and Bowen, *Phys. Rev.* xxiv. pp. 209-228 (1924), and especially *Phil. Mag.* xlix. p. 923 (1925).
23. Uhlenbeck and Goudsmit, *Naturwissenschaften.* xiii. p. 953 (1925).
24. Russell and Saunders, *Astrophys. J.* lxi. p. 38 (1925).
25. Pauli, *Zeit. f. Phys.* xxxi. p. 765 (1925).
26. Heisenberg, *Zeit. f. Phys.* xxxii. p. 841 (1925).
27. Hund, *Zeit. f. Phys.* xxxiii. p. 345 (1925).
28. Millikan, *Proc. Nat. Acad. Sci.* vii. p. 289 (1921).
29. Payne, '*Stellar Atmospheres*,' p. 15 (1925).

LI. *Structure of the Radioactive Atom and Origin of the α -Rays.* By Sir ERNEST RUTHERFORD, O.M., P.R.S., *Cavendish Professor of Experimental Physics, University of Cambridge* *.

§1. **I**N the course of the last twenty years, a large amount of accurate data has been accumulated on the emission of energy from radioactive atoms in the form of α , β , and γ rays, and in the majority of cases the average life of the individual elements has been determined. This wealth of data on atomic nuclei, which must have an intimate bearing on the structure of these radioactive atoms, has so far not been utilized as our theories of nuclear structure are embryonic. We are not yet able to do more than guess at the structure even of the lighter and presumably least complex atoms, and for this reason it would appear at first sight that we could not hope to attack, with any chance of success, the problem of the structure of the radioactive nucleus which must contain many more individual units in its constitution than the lighter atoms. However, it has

* Communicated by the Author.

always seemed to me possible that the structure of the heavy nucleus might present certain simple general features which may be either absent or difficult to detect in the lighter atoms. Moreover, in the case of the heavy radioactive atoms we have a great variety of quantitative data with which to test the validity of any working theory.

The simple theory of the origin of the α -rays which I shall outline in this paper had its inception in the endeavour to reconcile apparently conflicting results on the dimensions of the nucleus obtained by different methods. The experiments on the scattering of α -particles have shown that the Coulomb law of force is widely departed from in close collisions of swift α -particles with light atoms, but no deviation has so far been observed for the heavy atoms of high nuclear charge. For example, the scattering by silver and gold of the swiftest α -particles available is in close accord with an inverse square law of electric force, and although the data on uranium, on account of the difficulty of obtaining thin uniform films, are not so definite, yet we could not find any certain indication of the failure of the inverse square law for this element, although the α -particle must have approached within 3.2×10^{-12} cm. from the centre of the uranium nucleus. Since we should anticipate that the law of the inverse square must break down when the α -particle enters the charged region of the nucleus, these experiments appear to indicate that the nucleus of uranium must have a radius less than 3.2×10^{-12} cm. On the other hand, the radioactive data strongly suggest that the nuclear structure must extend to a distance of at least 6×10^{-12} cm. This deduction is based on the following argument. When an α -particle carrying two positive charges is released from the nucleus, it must gain energy in escaping through the repulsive electric field due to the nucleus. The energy gained by the α -particle in passing from a distance r from the nucleus is $2Ze^2/r$, where Ze is the nuclear charge of the residual atom. Even if the α -particle escapes with no initial velocity, its energy cannot be less than this amount. Now the slowest α -particle, which is emitted by Uranium I, has an energy corresponding to 4.07×10^6 electron-volts. Taking the charge on the nucleus after release of the α -particle as $90e$, it follows that the value of r cannot be less than 6.3×10^{-12} cm. and must be greater if the α -particle has any initial velocity. In other words, the dimension of the nucleus computed from radioactive data is at least twice as great as that indicated by a study of the scattering of α -particles.

It does not seem possible to explain away this divergence by assuming that the α -particle leaves the nucleus carrying only one charge, for the change in the atomic number of the element by expulsion of an α -particle shows that it always carries two charges away from the nucleus. On the radioactive data, it seems clear that, if the outer nucleus contains an excess of positive charge, the scattering experiments ought to show a departure from a Coulomb law of force for even slow α -particles. The failure to detect any change in the law of force indicates that either the component parts of the outer nucleus are uncharged or that there is on the average a uniform distribution of positive and negative charges.

The electrical forces from the nucleus on a positively charged body are repulsive and the experimental evidence on the scattering of α -particles by aluminium and magnesium indicates that the attractive forces which come into play due to the distortion or polarization of the main nuclear structure by the charged α -particle only become of importance at distances of about 1×10^{-12} cm. We are thus led to the conclusion that if any constituent particles of the nucleus extend to 6×10^{-12} cm., they must be electrically neutral. If we suppose that neutral particles are in circulation round the central nucleus, they can only be held in equilibrium by attractive forces due to the *distortion* or *polarization* of the particle itself by the electric field or to magnetic forces arising from the central nucleus*. No definite information is available as to the magnetic state of the nucleus, so in the present theory we shall confine ourselves to forces of attraction due to the polarization of the structure of the neutral satellite by the electric forces arising from the main nucleus. It will be seen that this will give rise to attractive forces of the right order of magnitude to retain a satellite in a quantum orbit round the nucleus.

One of the most striking facts in radioactive transformations is the constancy of the speed with which an α -particle is expelled from a given radioactive atom. The recent experiments of Irene Curie on the α -rays from polonium and of G. Briggs on the α -rays from radium C show that the speeds of the issuing rays are identical for each element within the limits of measurements, viz., about 1 in 1000.

* Debye, and in more detail Hardmeier, have calculated the change in scattering of the α -particle by aluminium and magnesium on the assumption that an attractive force varying as $1/r^5$ arises due to the polarization of the nucleus by the α -particle. In the present satellite theory, we are dealing with the different case of the distortion of the neutral satellite due to the field from the nucleus.

This uniformity of speed is a strong indication that the α -particle in the nucleus is circulating in a quantized orbit and is released at a definite characteristic velocity.

§ 2. Suppose a neutral satellite of mass m is moving in a circular orbit of radius r with a velocity v under the influence of an attractive force due to polarization of its structure by the electric field due to a central nucleus of charge Ze .

The attractive forces F on an insulated conducting sphere of radius a due to a point charge Ze at a distance r is given by

$$F = \frac{Z^2 e^2 (2r^2 - a^2)}{r^3 (r^2 - a^2)^{3/2}} \\ = \frac{2Z^2 e^2 a^3}{r^5} \left(1 + \frac{3}{2} \frac{a^2}{r^2} + \dots\right) \quad (1)$$

if a/r is small.

Neglecting for a moment the correction term, the equilibrium of the satellite in a circular n quantum orbit is given by

$$mvr = nh, \\ mv^2/r = 2Z^2 e^2 a^3 / r^5, \quad (2)$$

where h for simplicity is used as a symbol for $2\pi \times$ (Planck's constant).

From these equations

$$r = \sqrt{2} Zea^{3/2} m^{1/2} / nh \quad (3)$$

$$\text{and} \quad \frac{1}{2} mv^2 = n^4 h^4 / 4a^3 m^2 Z^2 e^2 \quad (4)$$

is the kinetic energy of the particle in its orbit.

It will be seen that $r \propto 1/n$, so that the higher the quantum number the smaller the radius of the orbit and the swifter the motion of the particle. The loss of energy w_1 , due to the removal of the satellite from a distance r to an infinite distance against the attractive forces of polarization, is given by

$$w_1 = 2Z^2 e^2 a^3 \int_r^\infty dr / r^5 = Z^2 e^2 a^3 / 2r^4 \quad (5)$$

From equation (2), it is seen that this is one half of the kinetic energy of the particle in its orbit, so that, if the particle for any cause is released from its orbit, it should escape with one half of its original energy of motion. It is clear also that on ordinary mechanics the quantum orbit is unstable since if it is disturbed the particle should escape

from its orbit, but we do not yet know how to interpret instability in quantum mechanics.

For orbits closer to the nucleus, the value of a/r in (1) may become comparable with unity. Making this first order correction, it is easily shown that the energy of the satellite in its orbit is to a first approximation given by

$$\frac{1}{2}mv^2 = \frac{n^4 h^4}{4a^3 m^2 Z^2 e^2} \left(1 - \frac{3}{4} \frac{n^2 h^2}{amZ^2 e^2}\right). \quad (6)$$

The loss of energy w_1 of the particle escaping against the attractive forces is given in this case by

$$w_1 = \frac{a^3 Z^2 e^2}{2r^4} \left(1 + \frac{a^2}{r^2}\right). \quad (7)$$

The energy E of motion of the particle after its escape can be shown to be

$$E = \frac{1}{2}mv^2 - w_1 = \frac{n^4 h^4}{8a^3 m^2 Z^2 e^2} (1 - bn^2), \quad (8)$$

where $b = h^2/maZ^2 e^2$.

§ 3. Application to the α -particle.

We have so far dealt with the case of any neutral satellite which remains uncharged during its escape from the atom. We shall next consider the modifications in the theory in order to account for the velocity of escape of the α -particles from a radioactive atom. For the reasons already given, we shall suppose that the α satellites are electrically neutral circulating in quantum orbits under the attractive forces due to polarization of their structure by the field from the central nuclear charge. Such a neutral α -particle must consist of a helium nucleus which has gained two electrons. These electrons cannot occupy the same positions as in the ordinary helium atom in the free state, for they would then not be part of the main nucleus at all. They must be bound much more closely to the helium nucleus, probably circulating in orbits which are rendered possible only by the distortion of the nuclear structure of the α -particle by the intense electric or magnetic fields due to the central nucleus. In fields below a critical value, the electron orbits may not be possible and consequently a neutral α -particle in escaping from the nuclear structure would be robbed of its two electrons when the field falls to the critical value. It is an essential part of the present

theory that the satellite must lose its two electrons before its complete escape from the nucleus. Such a passage from a neutral to a charged particle is essential in order to fulfil the well established observation that the nuclear charge of an atom is lowered by two units when an α -particle is expelled. It follows also that the electrons liberated from the satellite during its escape must fall back towards the nucleus and be incorporated in its structure*.

It is difficult to estimate the binding forces which hold the electrons in equilibrium in the satellite. They must be strongly bound in order to be retained in the intense nuclear field and probably circulate in the region close to the helium nucleus where we know from scattering experiments the forces are abnormal and much greater than is to be expected on a Coulomb law of force. It may be that the electron orbits become automatically unstable when the distorting forces acting on the satellite fall below a certain value and are released from the satellite. The energy for disruption may be in part acquired from the energy stored in the distorted nucleus, and in part from the energy of motion of the satellite.

If the satellite loses its two electrons at a distance r from an atom of initial charge Ze , the energy acquired in passing through the repulsive field is $2(Z-2)e^2/r$. Consequently if the satellite for some reason is released with its velocity in the orbit of quantum number n , the final energy E of release of the α -particle from the atom of number Z is given approximately by

$$E = 2(Z-2)e^2/r - w_2 + \frac{n^4 h^4}{8a^3 m^2 Z^2 e^2} (1 - bn^2), \quad (9)$$

where w_2 is the kinetic energy lost by the satellite in the process of the removal of the two electrons. The approximations are specified below.

For atoms of the same number Z , the value

$$E = A + Bn^4(1 - bn^2), \quad (10)$$

where A and B are constants, A including the first two terms. In practice, it is convenient for calculation to fix the values of A and B for a standard atomic number by comparison with the experimental data. The number chosen is 84, which includes at least seven groups of α -particles. The

* Fr. Meitner suggested some time ago that some of the α -particles existed in the neutral state within the nucleus in order to account for the observation that in several cases, two β -ray changes follow an α -ray change.

values for atoms of different charge are then deduced by a percentage correction of each constant for Z in equation 9.

The value of r in the first term of equation (9) is dependent to some extent on the atomic number Z . The correction may be estimated in several ways, giving slightly different results.

It is probably best to suppose that the neutral particle loses its electrons when the energy stored in the satellite due to distortion falls below a certain critical value, the same for all α -particles. The expression for this quantity is given in equation (7), where r is taken as the distance from the central nucleus for disruption. Neglecting the term a^2/r^2 , it is seen that $r \propto \sqrt{Z}$, so that the value of the first term in (9) varies as $(Z-2)/\sqrt{Z}$ or to a near approximation \sqrt{Z} .

In the absence of any definite information as to the value of w_2 included in the constant A , we shall apply the correction for atomic number to A as a whole, although this probably somewhat underestimates the true value of the correction. The value of b is seen from (8) to vary as $1/Z^2$.

If Z_0 is the number* of the element used as a standard, the value of E for an element of number Z is given by

$$E = A \sqrt{Z/Z_0} + \frac{BZ_0^3}{Z^2} n^4 \left(1 - \frac{Z_0^2}{Z^2} b n^2 \right). \quad (11)$$

It should be mentioned that in these calculations the retarding forces on the satellite during its escape are integrated from r to ∞ (eq. 7), while in the application to the α -particle, the latter is supposed to lose its electrons at a definite distance from the nucleus when the field falls to a certain value. No information is available as to the relative forces due to polarization in the charged and neutral satellite, but it will be seen that the change in the calculated energy due to this would in practice be included in the constant A , deduced by comparison of the theory with the experimental data.

§ 4. Comparison with experiment.

In order to compare theory with experiment, it is necessary to fix the values of the constants A , B , and b and the value of n by consideration of the energy of the different groups of emitted α -particles. As a result of a large amount of trial calculation, the values of these constants were adjusted

* Since the satellites are electrically neutral, the charge on the central nucleus is given numerically by the atomic number.

to make the best fit with the known energy of the eight groups of α -particles emitted during the uranium-radium series of transformations. Since the energy of the emitted α -particles is dependent only on the nuclear charge of the element and the quantum number of the orbit, the α particles from the thorium and actinium series should fit the same equation with exactly the same value for the constants A, B, and b. Consequently, the theory, if correct, should give the energy of emission of the α -particles from all radioactive elements in terms of only one variable connected with the quantum number n .

In 1921, Geiger * measured with great care the ranges of the α -particles emitted from all the radioactive elements with the exception of Uranium I, Uranium II, and Thorium. He had long before shown that the velocity V of the α -particle is connected with its range R by the equation $V^3 = KR$. Recently G. Briggs† has shown that this relation holds fairly closely for α -particles of range between 7 cm. and 3 cm., i.e. over a range covering practically all the known groups of α -particles.

The results obtained by Geiger are given in Table I. The ranges of the groups of α -particles in air are given for 15° C. and 760 mm. pressure. The probable error in the determination estimated by Geiger is given in column 3. The velocity and energy of the α -particles are determined by the relation $V^3 = KR$, from the known velocity of the α -particles of radium C which have an extrapolated range 6.971 cm. This velocity is known from the experiments of Rutherford and Robinson to be 1.922×10^9 cm./sec.

The energy of emission of the α -particle is most conveniently expressed in electron-volts, i.e. in terms of the potential difference required to give an electron the energy of the α -particle. The energy of the α -particle from radium C, which is taken as a standard of comparison, is 7.662 million volts.

The ranges given for the α -particles from Ur. I and Ur. II are those recently found by Lawrence ‡ by measuring the lengths of the α -ray tracks in a Wilson expansion chamber. They are believed to be correct to within about one per cent. and differ somewhat from the original determination of Geiger and Nuttall §, viz. 2.67 and 3.07 cm. respectively. Before I knew of the results of Lawrence,

* *Zeit. f. Phys.* viii. p. 45 (1921).

† *Proc. Roy. Soc. A*, 114. pp. 313, 341 (1927).

‡ *Trans. Nova Scotia Inst.* 1927.

§ *Phil. Mag.* xxiii. p. 439 (1912).

I had satisfied myself by the scintillation method that the range of the α -particles from Ur. II was greater than that given by Geiger and not less than 3.23 cm.

The data for protoactinium and thorium itself are only approximate.

TABLE I.

Element.	Range in cm. in air at 15° C. and 760 mm.	Mean error in cm.	Velocity in cm./sec. $\times 10^9$.	Energy in volts $\times 10^6$.
Uranium I	2.70	...	1.406	4.07
Uranium II	3.28	...	1.495	4.64
Ionium	3.194	± 0.016	1.482	4.554
Radium	3.389	" 0.009	1.511	4.735
Radon	4.122	" 0.009	1.613	5.397
Radium A	4.722	" 0.010	1.688	5.908
Radium C	6.971	" 0.004	1.922	7.662
Radium F	3.925	" 0.004	1.587	5.223
Protoactinium ...	3.673	" 0.042	1.552	4.998
Radioactinium ...	4.676	" 0.025	1.683	5.871
Actinium X	4.369	" 0.019	1.645	5.610
Actinon	5.789	" 0.017	1.807	6.769
Actinium A	6.584	" 0.010	1.886	7.373
Actinium C	5.511	" 0.006	1.777	6.551
Thorium	2.90	uncertain	1.435	4.27
Radiothorium	4.019	± 0.005	1.600	5.306
Thorium X	4.354	" 0.010	1.643	5.598
Thoron	5.063	" 0.007	1.728	6.291
Thorium A	5.683	" 0.008	1.796	6.685
Thorium C	4.787	" 0.009	1.696	5.963
Thorium C'	8.617	" 0.007	2.063	8.825

The agreement between theory and experiment is shown in Table II. In column 3 is given the quantum number n selected by trial; column 4 the value of $n_1 = n + \frac{1}{2}$ which will be used in calculating the energy of the α -particle (eq. 11); column 5 the calculated value of $Bn_1^4(1 - bn_1^2)$ for atomic number 84; column 6 the same quantity corrected for atomic number; column 7 the value of A corrected for atomic number; column 8 the calculated energy by adding columns 6 and 7; column 9 the observed energy given in Table I.

The value of the constants used in these calculations are for atomic number 84:

$$A = 3.600 \times 10^6 \text{ electron-volts.}$$

$$B = 6.856.$$

$$b = 1.25 \times 10^{-4}.$$

TABLE II.

1	2	3	4	5	6	7	8	9	
Element.	Atomic number.	Quantum number n .	Quantum number $n_1 = n + \frac{1}{2}$.	$Bn_1^4(1 - bn_1^2)$ for at. no. 84 in millions of volts.	$Bn_1^4(1 - bn_1^2)$ at no. in millions of volts.	A corrected for at. no. in millions of volts.	Calculated energy of α -particle in millions of volts.	Observed energy of α -particle in millions of volts.	% Difference, Col. 8 & 9.
Uranium I	92	14	14.5	.295 } .337 }	.245 } .280 }	3.77	4.015	4.07 .	1.4
" "	"	14.5	15	.337 }	.280 }	"	4.05	"	0.5
Uranium II	92	19.5	20	1.042	.873	3.77	4.64	4.64	0.0
Thorium	90	19	19.5	.944	.825	3.729	4.564	4.554	0.0
Radium	88	20	20.5	1.146	1.047	3.687	4.734	4.737	0.1
Radium	86	22.5	23	1.793	1.714	3.643	5.357	5.396	0.8
Radium A	84	24	24.5	2.283	2.283	3.600	5.883	5.910	0.5
Radium O	84	28	28.5	4.062	4.062	3.600	7.662	7.662	0.0
Radium F (To) ..	84	22	22.5	1.644	1.644	3.600	5.244	5.224	0.4
Thorium	90	17	17.5	.618	.539	3.729	4.27	4.27	0.0
Radiothorium	90	22.5	23	1.793	1.569	3.729	5.298	5.306	0.2
Thorium X	88	23.5	24	2.111	1.931	3.687	5.618	5.598	0.4
Thorium	86	25	25.5	2.664	2.549	3.643	6.192	6.191	0.0
Thorium A	84	26	26.5	3.082	3.082	3.600	6.682	6.686	0.0
Thorium C	83	30	30.5	5.283	5.283	3.578	8.913	8.963	0.9
Thorium C'	84	34	34.5	6.239	5.239	3.600	8.839	8.825	0.2
Protoactinium	91	21.5	22	1.510	1.291	3.750	5.041	4.998	0.8
Radioactinium	90	24.5	25	2.471	2.168	3.729	5.897	5.871	0.5
Actinium X	88	23.5	24	2.111	1.931	3.687	5.618	5.610	0.0
Actinon	86	26.5	27	3.301	3.171	3.643	6.814	6.769	0.6
Actinium A	84	27.5	28	3.801	3.801	3.600	7.401	7.373	0.4
Actinium O	83	25.5	26	2.867	2.838	3.578	6.511	6.551	0.6

The reasons for the choice of the particular form of n and its magnitude will be discussed in the next section. It suffices to say here that n may vary by half quantum numbers, *e.g.* 24, 24.50, 25, and $n_1 = n + \frac{1}{2}$ nearly. It will be seen later that the value of n deduced from the experimental data on the α -rays is in excellent accord with the theory and our general knowledge of the dimensions of nuclei.

On the whole there is a very fair agreement between theory and experiment. The calculated values of the energy of emission of at least seven groups of α -particles agree within a small fraction of a per cent. with the observed values, while in a number of other cases the agreement is within the probable experimental error. Although the values of the constants in the equation were chosen to give the best fit with the α -particles from the uranium-radium series, it will be observed that with one exception the agreement for the thorium series is even better.

It might at first sight be thought that a fair agreement between theory and experiment is to be anticipated when n_1 has such a large value and may vary by half units. It must be remembered, however, that the energy-term due to the motion of the satellite varies as the fourth power of the quantum number, and calculation shows that it is very unlikely that the many close coincidences are fortuitous. For example, consider the change in energy of the emission of α -particles from an element of atomic number 84, corresponding to the successive quantum numbers $n_1 = 26, 26.5, 27$. The calculated energies of emission are 6.467, 6.682, 6.913 million volts varying about 3 per cent. from one number to the next. The observed value for the α -particles from thorium A is 6.685 million volts differing very slightly from the calculated value for $n_1 = 26.5$. The case is different for α -particles of low energy, *e.g.* those emitted from Uranium I. and II., where the value of the constant A represents a large part of the total energy. In such cases the quantum number cannot be fixed with the same certainty unless the energy of emission of the α -particles is known with great accuracy.

At this stage it is of little value to discuss in any detail the agreement between theory and experiment. Unfortunately, there still remains some uncertainty as to the correct values of the energies of emission of the groups of α -particles. The velocities of the α -particles have not been determined directly but deduced from measurements of the range of the α -particles in air, and an appreciable error may arise due to

this cause. In some cases, when there is a mixture of α -ray products, it is difficult to be certain of the accuracy of the ranges, however much care is taken in making the observations.

It is important to develop new direct methods of measuring the velocity of emission of the α -particles with the greatest possible precision. If the relative energies of the main groups of α -particles could be determined with certainty to 1/500 or still better to 1/1000, it would then be possible to test the theory in detail.

It should, however, be pointed out that for several elements, notably radon, thorium C, and actinium C, the calculated and observed values differ by considerably more than the experimental error estimated by Geiger. It is not possible to reduce the disagreement notably by adjustment of the constants. It seems clear that if the experimental results are reliable there is a real discrepancy between the theory and experiment.

There is, however, one factor which has been neglected in this calculation. It has been assumed that the forces in the neutral satellite are entirely due to its polarization by the electric field, and no account has been taken of the effect of magnetic forces acting on the satellite. Unfortunately, we have no knowledge of the magnetic state of the satellite or of the radioactive nuclei. Even if the α satellite has no permanent magnetic moment, it is quite possible that the central nuclei may have a magnetic moment which may vary from one nucleus to the next. If we suppose that the nucleus has a magnetic moment, it will exert an attractive force due to the magnetic polarization of the satellite, even if the latter has no permanent magnetic moment itself. No doubt the attractive force due to this cause will vary more rapidly with the distance than the attractive force due to the electric field. If this force is small compared with that due to the electric polarization, the effect of the addition of a magnetic attraction would be analogous to an increase in the nuclear charge. A decrease of the magnetic moment of the nucleus would correspond to the effect of a diminution of the nuclear charge. The marked discrepancy in certain cases between calculation and experiment, if not due to experimental error, may thus possibly be ascribed to a difference in the magnetic moment of the nuclei. At this stage no data are available to estimate the magnitude of this effect, but it may quite likely prove of importance and may have to be taken into account in any complete theory. It would be of great interest if methods could be

found for determining the magnetic moment of radioactive nuclei*.

In this connexion, it is of interest to note that, in the case of the actinium family, the theory in most cases gives a somewhat higher energy for the α -particles than the observed values. This discrepancy would be largely removed if it be supposed that the value of B in equation 11 is about one per cent. less for the nuclei in the actinium group than for the nuclei in the thorium and Ur-Ra group. This would correspond to the effect of an increase of the nuclear charge of about one half per cent., and on the views outlined above would indicate that, with the exception possibly of actinium C, the nuclei of the actinium group have on the average a higher magnetic moment than that for the other two radioactive series. However, any conclusions on these points should be reserved until we are certain of the accuracy of the experimental data.

§ 5. Quantum number of satellites and dimensions of orbits.

In the new or wave mechanics the value of n , where n is the quantum number of an angular momentum on the old calculations, is always replaced by $(n + 1)$ or $n(n + \frac{1}{2})^2$ nearly when n is large†. We should consequently expect the value n^4 in the expression for the energy of motion of the satellite to be replaced by $(n + \frac{1}{2})^4$. It is for this reason we tabulate n_1 in column 4, Table II.

We must now consider the dimensions of the quantum orbits supposed circular. For simplicity of calculation, we shall suppose that the forces on the satellite vary as $1/r^5$ and thus neglect the correction term. Since under these conditions the satellite loses half its orbital kinetic energy in escaping against the attractive forces, the orbital energy of the satellite expelled from radium C, $n=28$, is equal to 8.12 million electron-volts. This corresponds to an orbital velocity 1.98×10^9 cm./sec., which is slightly greater than the ultimate velocity of escape of the α -particle from the nucleus. Substituting the value of V in equation $mvr = nh$ and taking $n=28$ and m =the mass of the helium atom = 6.60×10^{-24} ,

$$r = 2.24 \times 10^{-12} \text{ cm. for an atomic number 84.}$$

* S. Goudsmid and E. Back (*Zeit. f. Phys.* xliii. p. 321, 1927) suggest that the superfine structure in the bismuth optical spectrum may be due to the magnetic moment of the bismuth nucleus. This mechanical moment from which this arises is estimated to be about $9h/2$.

† *Vide* O. W. Richardson, "Present State of Atomic Physics," Proc. Phys. Soc. (1927).

Since $r \propto Z/n$, the value of r for the outermost orbit of Ur I., number 14, is 4.09×10^{-12} cm.

For such an orbit to be possible, this distance must be smaller than the critical distance at which the satellite loses its electrons. Since the value of the constant A , viz. 3.77 million volts for atomic number 92, represents mainly the energy gained by the charged α -particle in escaping through the repulsive field, it can readily be calculated that the critical distance from this nucleus must be less than $r = 6.8 \times 10^{-12}$ cm., corresponding to a quantum number about 8 to 10.

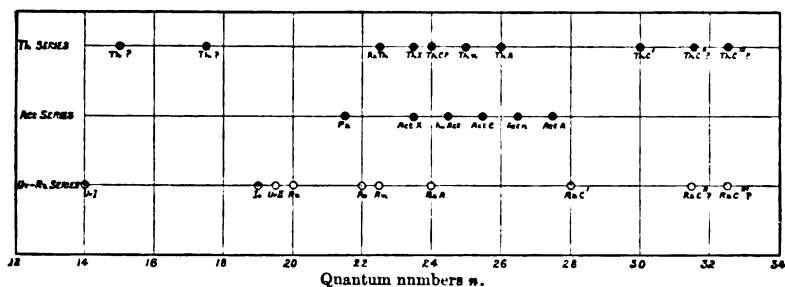
The distances involved are thus in accord with the theory and are of about the magnitude to be expected. There is, however, one difficulty since in some cases, and particularly in the actinium series, half quantum numbers appear. Such half quantum numbers are essential to include all the groups of α -particles of different energies. These half quantum numbers would, of course, disappear if all the quantum numbers are doubled throughout. This, however, is impossible when we take into account the critical distance at which the satellite breaks up. For example, if n is taken as 56 corresponding to the α -particle from radium C, the orbital radius is 4.48×10^{-12} cm., while the outermost uranium orbit $n=28$ has a radius 9.8×10^{-12} cm. This is well outside the critical radius for the satellite, and consequently no such orbit is possible. We may, of course, get over the difficulty by the drastic assumption that the unit of angular momentum is $\frac{1}{2}h$ instead of h , but, apart from this, it seems simplest to suppose that for some reason half quantum numbers are possible, representing subsidiary quantum orbits. We must await a solution of this problem based on the new mechanics to know whether such subsidiary quantum orbits can exist theoretically. We have so far only considered circular orbits, but other more complicated quantum orbits may be possible.

We have made all the calculations on the simple assumption that the quantum numbers are exactly one-half. If, however, we consider the data given in Table II., it will be seen that in the majority of cases, and particularly for the actinium series, the energies calculated on half quantum numbers are on the whole somewhat greater than those observed. If we ascribe the difference entirely to the wrong choice of quantum number, it is easy to estimate that the average quantum number is about $n + .52$ instead of $n + .50$, chosen for calculation. It is probable, however, as already pointed out, that this discrepancy may be accounted for on quite

different grounds. There is some general evidence that the half quantum orbits exhibit some peculiarities not shown by the whole quantum orbits. In § 8 it will be seen that a simple empirical relation exists between the constant of transformation of a nucleus and the quantum number of the satellite which is liberated, both for the thorium and uranium-radium series. There is evidence of a similar general relation for the actinium series, where the orbits are all characterized by half quantum numbers, but the points of the curve are erratic, and the elements actinium X and actinium C do not fit in at all. In addition, radon, which is characterized by a half quantum orbit, is displaced from the main curve for the Ur-Ra series. (See fig. 2.) It may be that on the average these subsidiary orbits are more complex than the normal orbits and do not show in all cases the same simple relations.

The distribution of quantum orbits, which are known from the expulsion of α -particles, is shown graphically in fig. 1 for the three radioactive series of elements.

Fig. 1.



It will be observed that, considering the three series together, all possible orbits, seven in number, are represented between $n=23.5$ and $n=26.5$ inclusive. Between $n=19$ and $n=28$ inclusive, representing 18 possible orbits, only 3 are unrepresented, viz., numbers 20.5, 23, 27. It is noteworthy that not only are the quantum numbers deduced in the actinium series all half, but they are less distributed than for the other two series.

It will be noted also that certain quantum orbits are common to two series of elements, viz., 22 ascribed both to polonium and to radiothorium, 24 to radium A and thorium C, and 23.5 to thorium X and actinium X. If we take into account the long range particles from radium C and

thorium C, probably $n=31$ and $n=32.5$ are common to the radium and thorium series (see § 7).

It is of interest to consider whether other satellites exist in uranium, thorium, and actinium, in addition to those which are liberated in the series of transformations. There is no definite evidence on this important point, but I think it quite possible that a number of other satellites characterized by definite quantum orbits are present in the three elements. If the evidence discussed in § 9 on the connexion between the α - and γ -rays has any validity, it definitely indicates that a number of the satellites are present which in some cases are transferred from one orbit to another without, however, escaping from the nucleus. The evidence so far available, however, does not fix any definite limit to the number of neutral satellites, possibly in some cases of different masses, which may be circulating in quantum orbits round the central nucleus.

§ 6. Dimensions of the satellites.

For the purposes of calculation it has been assumed that the satellite is represented by a conducting insulated sphere of radius a , and the attractive forces have been deduced on this basis. It is important to estimate the magnitude of this radius and to see whether it is consistent with our knowledge of the dimensions of the nucleus. The value of a can be deduced most simply from the constant bn^2 (Equ. 8, 9), which is equal to a^2/r^2 when r is the distance of the satellite from the nucleus. Now we have deduced from the experimental data that $a^2/r^2 = bn^2 = .1015$ for atomic number 84, where r is the radius of the quantum orbit $n=28$, corresponding to the α -particle from radium C. Since $r = 2.24 \times 10^{-12}$ cm. in this case, $a = 7.0 \times 10^{-13}$ cm. We can also deduce the value of a by substituting the values corresponding to the α -particle from radium C in equation 2. This gives $a = 6 \times 10^{-13}$ cm. The two numbers are in fair accord and indicate that the equivalent volume of the satellite assumed spherical is about 1×10^{-36} c. cm.

Now the region surrounding the α -particle where the forces are abnormal has been deduced by Chadwick and Bieler to be spheroidal in shape of semi-axes 8×10^{-13} and 4×10^{-13} cm. The volume of this region, 0.5×10^{-36} c. cm., is of the same order as the polarization volume of the satellite deduced from the theory. This agreement is satisfactory, for the general evidence indicates that the neutralizing electrons in the satellite must be closely bound to the nucleus, probably circulating close to the region where the forces due to the α -particle become abnormal.

§ 7. *Long range particles.*

We have so far confined our attention to the well-known groups of α -particles emitted from the radioactive series. In addition to these main groups, however, it is now known that a relatively very small number of α -particles of definite range are emitted during the disintegration of the active deposits of radium, thorium, and actinium. These are usually ascribed to the "C" bodies, but their exact origin is unknown. It has been found that radium C emits a few particles of range about 9.3 cm. and a still smaller number of range 11.3 cm. Thorium C emits also two groups, one of range about 9.4 cm. and the other of 11.3 cm. In addition, actinium C emits some particles of range about 6.5 cm. As these particles exist in relatively very small numbers—varying from about 1 in 10^4 to 1 in 10^5 of the main groups—it has been difficult to determine their ranges with accuracy, but it seems clear that they are in all cases helium nuclei ejected at high speed.

We may suppose that while the majority of the atoms break up in one way due to the liberation of the satellite from a definite quantum orbit, a small number of the atoms may liberate satellites from other and presumably more deep-seated orbits.

On the theory outlined, each group of α -particles should correspond to a definite quantum orbit and, if the nuclear charge of the disintegrating atom is known, the energy of the issuing α -particles can be calculated in terms of the quantum number. Assuming that the long range α -particles from radium C and thorium C come from an 84 nucleus, the energy and range of the α -particles corresponding to each quantum number are given in the table below.

Quantum number n .	$n + \frac{1}{2}$.	Energy in millions of volts.	Range in cm. at 15°C ., 760 mm.
28	28.5	7.662	6.971 (Rad. C')
28.5	29	7.941	7.36
29	29.5	8.225	7.75
29.5	30	8.530	8.19
30	30.5	8.839	8.617 (Th. C)
30.5	31	9.175	9.14
31	31.5	9.510	9.64
31.5	32	9.868	10.20
32	32.5	10.236	10.76
32.5	33	10.626	11.39
33	33.5	11.020	12.03

The ranges are calculated from the relation $v^3 = KR$ in a

region where the accuracy of this relation has not been tested. The calculated ranges are probably somewhat less than the true ranges for such high-speed particles. Experiments are in progress in this laboratory to determine the ranges of these swift particles with more accuracy and to test whether they can be included in one or more of the groups predicted by the theory.

It is not unlikely that the long range particles from radium C' and thorium C', the ranges of which have been estimated by the scintillation method to be about 9.3 and 9.5 cm. respectively, may prove to be identical in energy corresponding to a quantum orbit $n=31$ in the two elements. The 11.3 particles from the same elements may in a similar way arise from the same quantum orbit $n=32.5$.

With regard to actinium, Bates and Rogers found by the scintillation method that the long range particles from actinium C have a range of 6.49 cm. while the main group has a range 5.511 cm. (Geiger). The range 6.49 cm. corresponds to an energy of the α -particle of 7.30 million volts and may prove to be coincident with the α -particles of actinium A of range 6.584 cm. (Geiger).

§ 8. *Connexion between the radioactive constant and the quantum number.*

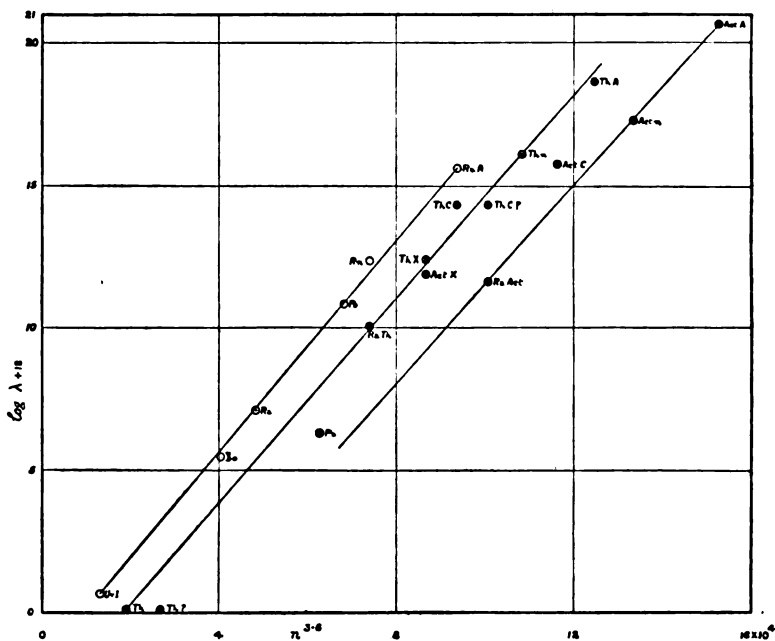
It was long ago shown by Geiger and Nuttall * that the velocity or range of the α -particle in a particular radioactive series increased with the constant of transformation of the element ejecting the α -particle. If the logarithm of the ranges or energies of the α -particles for each radioactive series is plotted against the logarithm of the transformation constant λ , the points lie approximately on a straight line which has a different slope for each radioactive series. This relation has proved very useful in estimating roughly the periods of transformation of elements which cannot be directly determined. When the ranges of the α -particles were redetermined with much more accuracy by Geiger (*loc. cit.*) in 1921, it was found that this rule was only approximate and that there were marked discrepancies, particularly in the actinium series of elements. Lindemann suggested a possible interpretation of the relation observed.

The fact that the energy of the issuing particle must be in part due to the gain of energy in escaping through the repulsive field, makes it doubtful whether the empirical relation found by Geiger has any exact fundamental significance. On the views advanced in this paper, it is to be

* Phil. Mag. xxiii. p. 439 (1912).

anticipated that the radioactive constant λ should be connected not with the final energy of escape of the α -particle, but with the quantum number n characterizing the orbit of the satellite which is liberated, and also, no doubt, with a quantity depending on the constitution of the central nucleus. I find by trial that the radioactive constant λ for each of the elements in one radioactive series can be expressed approximately by a relation of the form $\lambda = ce^{an^{3.6}}$ or $\log \lambda = c + an^{3.6}$, where n is the quantum number of the orbit and c and a are factors which are constant for a particular radioactive series but vary from one series to another. The agreement shown by this relation is illustrated in fig. 2,

Fig. 2.



where the ordinates represent $\log_{10} \lambda + 18$ and the abscissæ are proportional to $n^{3.6}$. For both the uranium and thorium series, the elements, with the exception of radon and thorium C, lie nearly in a straight line. This simple relation is much less obvious for the actinium series, for actinium X and actinium C are much displaced from the straight line drawn through the other products. This peculiarity of actinium has been referred to in § 5, where it is suggested

that this may be connected with the fact that the α -particles from the actinium series are characterized by half or subsidiary quantum numbers. It may be that the difference in the constants c and α for the three series, which presumably depend on the detailed structure of the central nucleus, are in some way connected with differences in the magnetic state of the central nucleus.

It should be pointed out that the line for the Ur-Ra series fits best with the assumption that the α -particle from Ur I is connected with a quantum number 14 rather than 14.5, which happens to fit in a little better with the existing data (Table II). In the case of thorium, the trend of the curve indicates that the α -particle from thorium itself depends on $n=14.5$ or 15 rather than $n=17$, which happens to agree with the very uncertain data on the range of the α -particle from this element. It should also be noted that thorium C does not fit the thorium curve nor does the energy of its α -particle agree with calculation. If we take $n=24.5$ instead of 24 for this element, it fits more closely the thorium curve.

It is, of course, doubtful whether these curves can be extrapolated to give with any certainty the period of transformation corresponding to the long range α -particles from radium C and thorium C. If we extrapolate the Ur-Ra curve, the estimated period of transformation of radium C is much shorter than that deduced from the recent experiments of Jacobsen and Barton. It may be that the relation between λ and n is not so simple as that postulated here, but the rule has I hope some fundamental significance in connecting the average life of the quantum orbit with its quantum number.

The unknown value of λ for Ur II can be deduced from the Ur-Ra curve. Since its rays are characterized by $n=19.5$, while for ionium $n=19.0$, the half-value period should be less than that of ionium and about 100,000 years.

§ 9. *Origin of the gamma rays.*

During the last few years, notably due to the work of Ellis, Ellis and Skinner, Meitner, Thibaud, and Black, a detailed study has been made of the β -ray spectra of radioactive bodies and the frequency of the stronger gamma rays have been deduced. The general evidence indicates that the majority of these γ -rays, some of which have an individual energy of more than 2 million volts, have their origin in the nucleus of the atom, and Ellis has postulated

a system of energy levels in the atom to explain the numerical relations between the stronger gamma rays. The actual mode of excitation of these high frequency gamma rays has already been a matter of doubt. Since the most intense gamma rays usually appear in a β -ray transformation, it was natural at first to suppose that they originated from quantum jumps of electrons in the nuclear system. The possibility, however, that they may be due to movements of massive positively charged particles in the nucleus has often been suggested. The result of recent theoretical investigation, particularly of Kuhn *, seems definitely to exclude the movements of the electron as a source of the gamma rays, for Kuhn has shown on general grounds that if the gamma rays originated from high speed electrons they would not give sharp lines, as are experimentally observed, but broad diffuse bands. On the other hand, as Kuhn points out, if the gamma rays had their origin in the quantum transitions of massive positive particles, this objection would not apply.

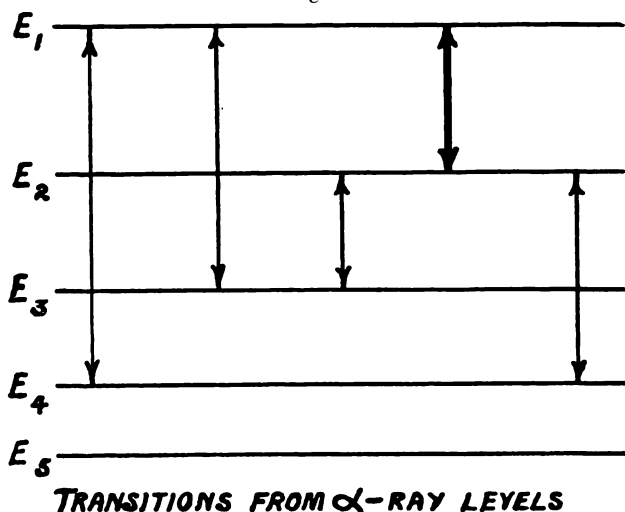
Since in our theory of the origin of the α -particles, we have postulated a number of neutral satellites which circulate in quantum orbits round the nucleus, it is of interest to consider whether the γ -rays have their origin in transitions of the satellite from one quantum level to another. Such a view is not obviously contradicted by the facts, for it is known that not only do γ -rays arise in many cases after β -ray transformations but also in a number of cases, notably radium, actinium X and radioactinium, the emission of γ -rays either accompanies or follows transformations in which only α -particles are emitted.

We may suppose in a general way that as a result of the violent disturbance which follows the emission of an α or β particle from the nuclear structure, one of the satellites becomes unstable, but instead of being ejected from the nucleus drops from one quantum level to another, radiating during the process the difference in the energies of the satellite in equilibrium in these two quantum states. There are a number of possibilities to be considered which are illustrated in the following diagram (fig. 3). Suppose the α satellite in the level E_1 becomes unstable. Considering a large number of atoms some of the satellites may fall to the level E_2 , others to the level E_3 and so on. These will give rise to γ -rays of frequency ν given by $h\nu_1 = E_1 - E_2$, $h\nu_2 = E_1 - E_3$ etc. The relative number of γ -ray quanta of each frequency depends on the probability of each of these transitions. There is also another possibility to consider.

* *Zeit. f. Phys.* xliii. p. 56, 1927 ; xliv. p. 32, 1927.

After the transition for example E_1 to E_2 , the satellite may be only momentarily stable, and after a short interval fall again to lower levels E_4 , E_5 , etc., emitting corresponding γ -rays in the process. It may also happen that more than one satellite may become unstable owing to the disturbance so that two or more systems of γ rays may arise.

Fig. 3.



From comparison of the theory with the energy of emission of α -particles, we have provisionally fixed the energies of the possible quantum levels where α satellites are involved. The energies of some of these levels have been given in Table II. The energy of the possible levels for a radioactive atom of any nuclear charge can be calculated from equation 11. Since, as far as our evidence goes, all levels are possible in the radioactive elements between n about 8 or 10 and $n=30$ or more, including half quanta, there are a large number of possible transitions to select from.

In considering possible transitions, it must be borne in mind that only a few of the possible levels are occupied by satellites even in the parent element uranium, and in the course of its successive transformations a number of these satellites have been removed. Consequently in an atom like radium C, there may be a number of vacant levels in the system which may be occupied either permanently or momentarily by the satellite in its transition.

From consideration of these energy levels, it is at once clear that the differences of the energies in a transition from one level to another are of the right order of magnitude to include not only the γ -rays of highest energy—about 3 million volts—but also by transitions between the lower levels to account for the emission of γ -rays of much lower energy—about 100,000 volts—which are strongly represented in certain γ -ray bodies.

In endeavouring to account for any particular system of γ -rays, we are faced with the difficulty that among such a large group of possible levels, a number of approximate coincidences within experimental error are found between the observed energy of the γ -rays and the energy differences between various levels. In order to guide us in the correct choice, we require to know not only the vacant levels but, from optical analogy, the principles of selection between possible transitions. For example, can transitions occur only between quantum numbers of the same kind whether integral or half quantum numbers? In searching for such criteria, it is clear that a knowledge not only of the frequency of the γ -rays but of their relative intensity is of great importance. For example, it does not seem likely that a weak γ -ray which arises from a transition $E_1 \rightarrow E_2$ could give rise to a γ -ray of stronger intensity due to a transition $E_2 \rightarrow E_3$ and so on. By taking into account the intensities of the γ -rays, the choice of possible levels is obviously much restricted.

I have found that it is possible in these ways to find a scheme of transitions that fits in many cases reasonably well, and, in some cases surprisingly well, with existing γ -ray data. I hope in a subsequent paper to give examples of the agreement between theory and observation. Before, however, any definite decision can be made on the adequacy of this theory of the origin of the γ -rays, it will be necessary to analyse and study in detail the large amount of γ -ray data available for a number of the radioactive elements. The general evidence is, however, sufficiently strong to warrant a very close examination to test the validity of this theory which connects together in such a simple way the two main types of radiation from the radioactive elements.

§ 10. *Structure of the atom.*

On the views put forward in this paper, the nucleus of a heavy atom has certain well defined regions in its structure. At the centre is the controlling charged nucleus of very

small dimensions surrounded at a distance by a number of neutral satellites describing quantum orbits controlled by the electric field from the central nucleus. Some years ago I suggested that the central nucleus was a closely ordered, semi-crystalline arrangement of helium nuclei and electrons. Whatever views may be taken on this point, it is fairly certain that the central nucleus of a heavy element is a very compact structure, occupying a volume of radius not greater than 1×10^{-12} cm. The region around the central nucleus extending to about $r = 1.5 \times 10^{-12}$ cm. is probably occupied by electrons and possibly also charged nuclei of small mass which are held in equilibrium by the attractive forces which arise from the distortion or polarization of the central nucleus. The electrons in this region, circulating round the nucleus, must have velocities close to that of light.

The comparatively large region between $r = 1.5 \times 10^{-12}$ to about 6×10^{-12} cm. may be occupied by a number of neutral satellites held in equilibrium by the polarizing action of the electric field arising from the central nucleus. In the case of the radioactive atoms, we have seen that the satellites must consist in part of neutral helium nuclei which lose their closely bound electrons when the electric field falls below a certain critical value. No definite information is so far available as to the number of these satellites surrounding the nucleus or whether the satellites are all of the same kind. From a study of the relative masses of the isotopes by Aston, it seems not unlikely that neutral satellites of mass 2 or mass 3 and possibly even of mass 1—neutrons—may exist in the strong electric fields of the central nucleus. The radioactive evidence does not help us in this question as only helium nuclei are ejected in the transformations. On the other hand, in the artificial disintegration of elements by bombardment with α -particles, only protons of mass 1 are ejected, but it is difficult to be certain whether the proton which is ejected exists in the nucleus as a charged particle or as part of an electrically neutral combination held in equilibrium at a distance by polarizing forces. It may be that a closer study of the frequency of the disintegrations and the energy of the protons expelled from different elements may throw further light on this question.

We have not so far discussed the important problem whether a central nucleus of identical charge and mass is common to a number of elements or whether it varies regularly in charge and mass from atom to atom. If the central nucleus is a closely ordered and almost crystalline arrangement of its component electrons and protons, it may

be that the number of such stable arrangements is limited in number, and that a given central nucleus may be common to a number of elements. On the theory advanced in this paper, all of the elements belonging to one particular radioactive series have a common nucleus, and it is quite likely that some of the heavier ordinary elements, lead, bismuth and thallium for example, belong to the same nuclear system.

It is of interest to consider the range of atomic number for which α satellites can exist. Taking into account the data given in § 5, it can be shown that for a nuclear charge 84, the innermost orbit corresponding to an 11.3 cm. α -particle and the outermost orbit corresponding to the α -particle from Ur I are included between $r = 1.9 \times 10^{-12}$ and 4.5×10^{-12} cm. Supposing that helium satellites can only exist within the range of electric fields corresponding to these distances, it can be shown, disregarding all questions of stability, that α -satellites are possible but unlikely for atomic number Z as low as 15 and from analogy with the radioactive series should become numerous for Z about 30. It may be significant that the average number of isotopes of the elements increase in a marked manner after about $z = 29$.

Unfortunately we have no corresponding information to estimate when a nucleus can attach a satellite of mass 2, which from isotopic evidence appears to play an important part in nuclear structure. It seems likely that neutral satellites are important constituents of all elements of atomic number greater than 30, but probably cannot exist as a constituent of the very light elements.

We can form the following picture of a radioactive atom. One of the neutral α satellites, which circulates in a quantized orbit round the central nucleus, for some reason becomes unstable and escapes from the nucleus losing its two electrons when the electric field falls to a critical value. It escapes as a doubly charged helium nucleus with a speed depending on its quantum orbit and nuclear charge. The two electrons which are liberated from the satellite, fall in towards the nucleus, probably circulating with nearly the speed of light close to the central nucleus and inside the region occupied by the neutral satellites. Occasionally one of these electrons is hurled from the system, giving rise to a disintegration electron. The disturbance of the neutral satellite system by the liberation of an α -particle or swift electron may lead to its rearrangement, involving the transition of one or more satellites from one quantum orbit to another, emitting in the process γ -rays of frequency determined by quantum relations.

The question whether the γ -rays originate in such quantum transitions of the α satellites as we have outlined is difficult to determine with certainty but the evidence, so far available, does not contradict such an hypothesis. Before more progress can be made it will be necessary to determine the possible energy levels of the satellite system with precision, and on the present theory this will involve a much more accurate determination of the energies of the α -particles expelled in each transformation. At the same time, the frequency of the main γ -rays and their intensities will be required to be known with the utmost precision. In this way, valuable data will be available to test any working hypothesis of the origin of the α and γ rays in radioactive transformations, and thus to help in throwing light on the general problem of the structure of atomic nuclei.

Cavendish Laboratory,
Aug. 10, 1927.

LII. *The Scattering of α -particles by Helium.* By Prof. Sir E. RUTHERFORD, O.M., P.R.S., Cavendish Professor of Experimental Physics, and J. CHADWICK, Ph.D., F.R.S., Fellow of Gonville and Caius College, Cambridge*.

THE study of the collisions of α -particles with hydrogen nuclei has shown that the force between the α -particle and the H nucleus obeys Coulomb's law for large distances of collision, but that it diverges very markedly from this law at close distances. The experiments of Chadwick and Bieler† showed that for distances of collision less than about 4×10^{-13} cm. the force between the two particles increased much more rapidly with decrease of distance than could be accounted for on an inverse square law of force. For example, in one series of experiments the H particles were observed which were projected after collision in directions making angles from 20° to 30° with the direction of the colliding α -particle. When the incident α -particle had a range in air of less than 2.0 cm., the number of H particles projected in this specified direction was about that to be expected if the force between the particles was given by Coulomb's law. With incident α -particles of greater range than this the number of H particles observed became greater than the theoretical number, and the discrepancy rose very

* Communicated by the Authors.

† Chadwick & Bieler, Phil. Mag. xlii. p. 923 (1921).

rapidly as the velocity of the α -particle was further increased. With α -particles of 2.9 cm. range the observed number of H particles was three times the number calculated on inverse square forces, while with α -particles of 6.6 cm. range the observed number was thirty times the calculated number. Not only was the number of H particles projected at small angles by α -particles of high velocity greatly in excess, but the observed variation of the number of H particles with the velocity of the α -particle was in the opposite direction from that predicted by the simple theory.

This divergence from the predictions based on the assumption of Coulomb forces was interpreted by Chadwick and Bieler in the following way. Assuming that the H nucleus could be regarded as a point charge, a model was sought for the He nucleus or α -particle which would account in a general way for all the experimental results. It was shown, by comparison with Darwin's calculations, that the α -particle behaved in these collisions as a body with properties intermediate between those of an elastic sphere and an elastic plate, and it was compared, as a first approximation, with an elastic oblate spheroid of semi-axes about 8×10^{-13} cm. and 4×10^{-13} cm., moving in the direction of its minor axis. A H nucleus projected towards such an α -particle would move under the ordinary electrostatic forces given by Coulomb's law until it reached a spheroidal surface of the above dimensions. It would there encounter a very powerful field of force and recoil as from a hard elastic body. While such a model of α -particle accounted in a rough way for the experimental observations, it was not found possible to obtain a very close comparison owing to the difficulty of calculating the collision relations for an oblate spheroid.

A further line of attack on this question of the field of force in the immediate neighbourhood of the He nucleus can be obtained by the investigation of the collisions of α -particles with helium nuclei. In this case both particles concerned in the collision have the same structure. There is therefore no need to assume a structure for one nucleus in order to deduce that of the other, as was done in the case discussed above.

If E , M , V are the charge, mass, and initial velocity of the α -particle concerned in the collision, v its velocity after impact with the He nucleus at rest, and u the velocity of the He nucleus set in motion by the collision, we have, on the assumption that energy is conserved in these collisions,

$$u = V \cos \theta, \quad v = V \cos \phi, \quad \phi = \pi/2 - \theta,$$

where θ , ϕ are the angles made by the lines of motion of the He nucleus and the α -particle after collision with the initial line of motion of the α -particle.

The assumption that in these collisions the energy is conserved in the translational motion of the particles is amply justified by the experiments of Blackett*. Blackett has obtained Wilson photographs of the collisions of α -particles with He nuclei, in which he has been able to measure accurately the directions of motion of both particles after impact. He finds that the angle $(\theta + \phi)$ is very close to a right angle, the result to be expected for a perfectly elastic collision between two particles of equal mass, one of which is initially at rest.

If we allow a pencil of α -particles to pass through helium and place a zinc sulphide screen in such a way that the particles falling on it travel at an angle ϕ to the direction of the pencil, the scintillations observed on the screen will be due not only to the α -particles scattered through the angle ϕ , but also to those He nuclei set in motion in this direction. The velocities of the particles of both types will be the same, $V \cos \phi$, or the ranges, $R \cos^3 \phi$, where R is the range of the incident α -particle. There is therefore no means of distinguishing between a scattered α -particle and a projected He nucleus. The two types correspond, in general, to collisions of different kinds, for the He nuclei projected at an angle ϕ are the companions of the α -particles scattered through an angle $\pi/2 - \phi$. When $\phi = 45^\circ$, however, both sets of particles arise from the same type of collision.

If we assume that the forces between the particles are given by Coulomb's law, the numbers of the scattered α -particles and the projected He nuclei can be easily calculated. If the α -particle approaches initially along a line at a perpendicular distance p from the He nucleus, it can be shown that

$$p = \tan \theta \cdot \frac{E^2}{V^2} \cdot \frac{2}{M},$$

and the closest distance of approach during the collision is

$$\frac{E^2}{V^2} \cdot \frac{2}{M} \cdot (1 + \sec \theta).$$

If Q be the number of α -particles per second in the incident pencil, and ω the solid angle subtended by the ZnS screen

* Blackett, Roy. Proc. Soc. A, cvii. p. 349 (1925).

placed at an angle ϕ , then the number of α -particles scattered to the screen is

$$Q n t \omega \frac{1}{V^4} \cdot \frac{E^4}{M^2} \cdot 4 \cot \phi \operatorname{cosec}^3 \phi,$$

where n is the number of He atoms per c.c. and t is the length in cm. of the scattering path.

The number of He atoms set in motion in the direction ϕ under the same conditions is

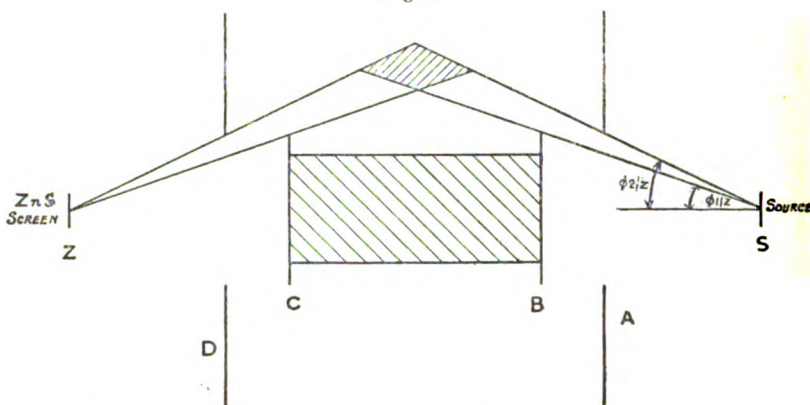
$$Q n t \omega \frac{1}{V^4} \cdot \frac{E^4}{M^2} \cdot 4 \sec^3 \phi.$$

The total number of particles received on the ZnS screen is the sum of these two numbers.

Experimental Method.

The arrangement used in these experiments was the same in principle as that used by Chadwick * for measurement of the scattering of α -particles by metal foils. In the present case we had to deal with scattering in a gas, and certain modifications were made in the arrangement of diaphragms.

Fig. 1.



In all, four diaphragms were necessary, as shown at A, B, C, and D in fig. 1. The diaphragms A and D consisted of graphite sheets containing circular-holes, while diaphragms B and C were small graphite disks. A and B served to define the incident beam of α -particles, an annular ring of limits $\frac{1}{2}\phi_1$ and $\frac{1}{2}\phi_2$, proceeding from the source S, and C and

* Chadwick, Phil. Mag. xl. p. 734 (1920).

D defined the scattered beam received by the zinc sulphide screen Z. The scattering apparatus was on a small scale, and it was necessary to machine and align the parts accurately. The volume of gas which is effective in scattering particles to Z is an annular ring, shown shaded in the figure. If the gas used is helium, the number of α -particles scattered per second to unit area of the ZnS screen is given by

$$\frac{Qntb^2}{16r^2} (\operatorname{cosec}^2 \phi_1 - \operatorname{cosec}^2 \phi_2),$$

where r is the mean distance from the source to the scattering region, and $b = \frac{2E^2}{MV^2}$.

Similarly, the number of those He nuclei which are projected by a collision with an α -particle so as to reach unit area of the screen Z per second is

$$\frac{Qntb^2}{16r^2} (\sec^2 \phi - \sec^2 \phi_2).$$

These latter particles correspond to the α -particles scattered between angles $90^\circ - \phi_1$ and $90^\circ - \phi_2$. The observations carried out within the angular limits ϕ_1 and ϕ_2 measure therefore the scattering within two sets of limits situated at equal intervals from 45° . It is consequently impossible to deduce without ambiguity the complete angular distribution of the α -particles scattered by helium nuclei, for, as has been pointed out, we have no means of distinguishing a scattered α -particle from a projected He nucleus. In some cases, however, even where the law of inverse square is no longer applicable, it is possible to form a rough estimate of the relative importance of the two groups of particles. In the experiments described in this paper we have not attempted to cover the whole range of scattered particles, but we have restricted our attention to the scattering within certain selected angular intervals and we have examined in each region the variation of the scattering as the velocity of the incident α -particles was varied.

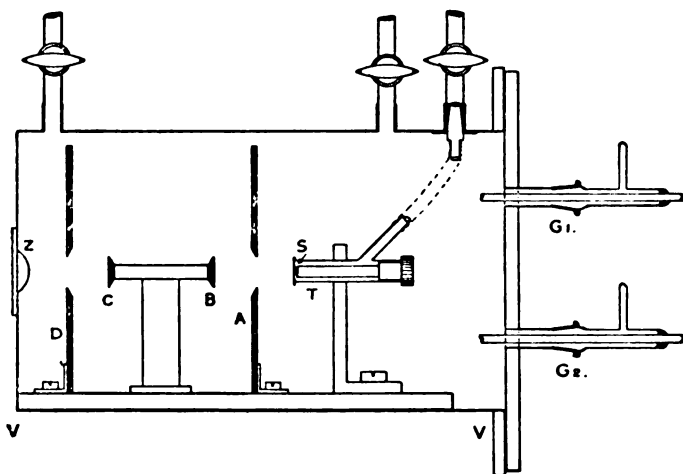
The apparatus employed is shown in fig. 2. The source and diaphragms were carried on a brass plate which fitted into slides fixed to the base of the brass vessel VV. The source, a small disk of 3 to 4 mm. diameter, was enclosed in the brass tube T, the end of which was covered with a thin film of collodion. The diaphragms A and D were mounted on short brass supports, while B and C were attached to the

ends of a lead cylinder of the appropriate length. This cylinder was carried by a thin plate of graphite fixed by means of wax to the brass carrier. The source, the four diaphragms, and the zinc sulphide screen were centred on a common axis.

To reduce extraneous scattering to a minimum, all surfaces exposed to the α -particles emitted by the source were covered, as far as possible, with sheets of pure graphite. In addition, the disks B and C had, in each series of experiments, a diameter at least equal to that of the apertures of diaphragms A and D. Scattering from the edges of the diaphragms to the screen was then usually of very small amount.

The disturbing effect of "contamination" was guarded against by placing the source in the closed tube T. The

Fig. 2.



amount of contamination could be determined at any time during the experiment by rotating in front of the source a graphite disk carried by the ground joint G_1 . The α -particles were then cut off from the scattering region and the scintillations observed on the screen were due to the natural effect together with the contamination effect.

By means of a second ground joint G_2 , an absorbing sheet of mica could be introduced in the path of the incident α -particles. In this way the scattering of α -particles of two different ranges could be compared in the course of one experiment. Further changes in the range of the incident α -particles were made by placing sheets of mica directly over the end of the tube T, in addition to the fixed collodion film.

The source of α -particles was, in most experiments, the active deposit of radium, obtained in the usual way on the brass disk S. In some cases where α -particles of greater range than 7 cm. were required, thorium active deposit was used. After fixing the source in the tube T and placing the carrier holding the diaphragms in position, the box VV was slowly evacuated. The amount of extraneous scattering was then determined by counts of the number of scintillations appearing on the screen Z. Pure helium was then admitted into the box through a long U-tube cooled in liquid air, and the observations of the scattering in this gas were made.

RESULTS.

The results obtained in these experiments are collected in the following tables. The first column gives the mean range of the incident α -particle at the point of scattering, the second column the observed number of scattered α -particles and projected He nuclei per mgn. activity of the source, and the third the corresponding number to be expected on the assumption of inverse square forces. The fourth column gives the ratio of the observed number to the inverse square number.

The number of particles which should be observed if the collisions were governed by inverse square forces was arrived at, for each series of experiments, in two ways: first by calculation from the geometry of the arrangement, and secondly, by observation of the number of α -particles scattered by argon under the same conditions as in the helium experiments. For this purpose the vessel VV was evacuated and filled to a suitable pressure with pure argon. It was assumed that, for the angles of scattering dealt with in these experiments, the forces between the α -particle and the argon nucleus obey Coulomb's law. In the series of experiments at the larger angles of scattering the numbers of scattered particles observed with argon agreed very closely with those calculated from the geometry of the experimental arrangement. At the very small angles of scattering obtaining in some of the experiments the agreement was not so good, and in one case the observed numbers were 15 per cent. higher than the calculated number. In the calculation it was assumed that the source and screen were of dimensions small compared with those of the diaphragms. In the experiments dealing with small angles this was no longer the case, and the discrepancy mentioned above was attributed to this cause. In the following tables

Scattering angles 40° to 50° .

Range of α -particles in cm. of air.	Number of particles.		Ratio.
	Observed.	Calculated.	
6.35	4.4	.21	21
5.3	2.65	.28	10
4.75	2.05	.31	6.6
4.4	1.3	.34	3.9
4.15	.83	.36	2.3
3.3	.44	.49	.9
3.0	.7	.6	1.2
2.6	.95	.7	1.3

Scattering angles 29° to 44° .

8.0	10	.53	19
6.3	6.6	.72	9
5.1	4.2	.96	4.4
4.5	1.7	1.14	1.5
3.0	2.2	1.95	1.1
2.3	3.0	2.8	1.1

Scattering angles 10° to 20° .

6.05	9.3	5.13	1.81
5.3	8.2	6.12	1.34
4.8	7.3	6.96	1.05
4.0	4.6	8.86	.52
3.2	4.0	12.0	.33
2.7	5.7	15.2	.38

Scattering angles 8° to 12° .

6.0	1.3	1.43	.91
4.7	.9	1.97	.46
3.9	.6	2.52	.24
2.6	2.4	4.34	.55
1.9	4.2	6.56	.64

Scattering angles 4° to $7^\circ 30'$.

5.6	1.9	3.1	.61
4.65	1.9	3.96	.48
3.9	4.6	5.0	.92
3.5	6.4	5.8	1.1
3.1	6.8	6.8	1.0
2.75	9.5	8.0	1.2

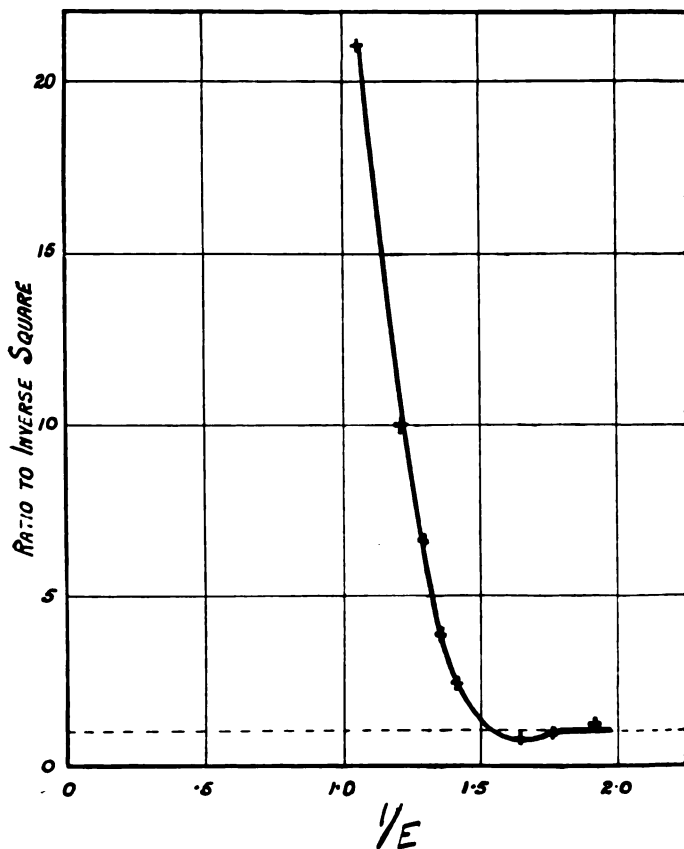
Scattering angles 4° to 6° .

5.65	1.37	1.90	.72
4.7	1.95	2.45	.8
3.6	3.5	3.48	1.0
3.15	3.7	4.16	.9
2.6	6.5	5.5	1.2

the inverse square numbers are therefore deduced from the comparison experiments with argon, rather than from calculation directly from the dimensions of the apparatus.

The results obtained when the particles were observed between the angles of 40° and 50° are shown in the curve of fig. 3, where the ordinates represent the ratio of the

Fig. 3.



observed to the calculated number, and the abscissæ the value of $1/E$, where E is the energy of the incident α -particles. The dotted line for ordinate unity thus represents the relation that would be observed for an inverse square law of force. The ratio is large for the swifter α -particles, falls rapidly to a value just below unity as the

energy of the α -particle decreases, and rises again to about the calculated value. Since within this range of angles the scattered α -particles and the helium nuclei set in motion by recoil are equal in number, this curve also represents the actual variation in number of the projected He nuclei for different speeds of the colliding α -particle. If we compare this curve with the data given by Chadwick and Bieler for the variation in number of project H nuclei between 21° and 31° with the speed of the incident α -particle, we find a marked similarity, not only in the general shape, but also in the magnitude of the divergence from the calculated numbers. Agreement with the calculated numbers is reached at approximately the same conditions in both types of collision.

Taken as a whole, the results given in the above tables indicate that the distribution of projected particles in collisions between α -particles and He nuclei is very similar to that observed when α -particles collide with H nuclei. There is no doubt that, if it were possible to separate the projected nuclei from the scattered α -particles, we should find a similar concentration in the forward direction, which is the more marked the swifter the incident α -particle.

As we have previously remarked, it is not possible to deduce from these experiments the relations between the number of projected He nuclei, the angle of projection, and the speed of the colliding α -particles, as can be done for the collisions in hydrogen. We are to a certain extent limited to finding at what distance of approach between the α -particle and the He nucleus the numbers of projected nuclei plus scattered α -particles become abnormal, for different angles of collision. In this respect the investigation is easier than for collisions in hydrogen, for a wider range of angles is experimentally possible. For example, it was a comparatively simple matter to find the expected deficiency in the number of projected + scattered particles between certain angles of collision, which is the necessary consequence of the excess scattering at other angles*. If we consider the collisions of α -particles of fixed initial velocity, we should expect to find, for very small angles of scattering or angles of projection of the He nucleus close to 90° , that the numbers of particles are normal. As the angle of scattering is increased the numbers should at some angle fall below the inverse square number to a minimum and

* Cf. Rutherford, Guthrie Lecture, Proc. Phys. Soc. Lond. xxxix. p. 359 (1927).

then rise sharply for the larger angles. The experiments on collisions in hydrogen dealt mainly with the excess scattering, and it was difficult experimentally to investigate the regions in which the number of particles should fall below the calculated number, but the present results show this phenomenon very clearly for the collisions of α -particles of 3 to 4 cm. range.

From the above results we are able to make an approximate estimate of the dimensions of the region over which the forces between the α -particle and the He nucleus become normal. Considering the experiments between 40° and 50° , it appears that the forces are given by Coulomb's law when the incident α -particle has a range of less than about 3 cm., that is, until the distance of approach between the centres of the particles becomes less than about 3.5×10^{-13} cm. It is obvious, even from this one series of experiments, that the region of abnormal forces is not spherical, for a comparison of the curve of fig. 3 with the corresponding curve calculated for an elastic sphere, gives a radius for the sphere varying from about 3.5×10^{-13} cm. for the collisions of slow α -particles to about 8×10^{-13} cm. for the fast α -particles. We must conclude, as in the case of the hydrogen collisions, that the region of abnormal forces has a plate-like shape. This indication is strongly confirmed by the experiments at smaller angles of scattering. At these angles the number of projected particles is, if inverse square forces hold, small compared with the number of scattered particles. For example, between 8° and 12° the number of scattered particles should be 108 times the number of projected particles. It is therefore reasonable to assume that, except in the collisions of very fast α -particles, we are here observing mainly the scattered particles and that the projected particles are not important. The experiments at these small angles show a common trend. As the velocity of the α -particle is decreased, the ratio of the number of particles observed to the calculated first falls, sometimes to as low as one-third, and subsequently rises to approximately unity. The investigations at these angles thus deal rather with a deficiency in scattering than with an excess. The same departure from inverse square forces is, however, responsible both for the deficient scattering observed here and for the excess scattering observed at other angles. When we calculate from these experiments the distance of approach between the centres of the colliding particles at which inverse square numbers are finally reached, we find that this distance is much greater than that obtained from the

collisions between 40° and 50° , being about 12 to 15×10^{-13} cm.

It thus appears that for central collisions between an α -particle and a He nucleus the law of force remains normal so long as the distance of approach between the centres of the particles is greater than about 3.5×10^{-13} cm., while for glancing collisions the distance of approach must not be less than about 14×10^{-13} cm. In the collisions of the α -particle with H nuclei the corresponding dimensions of the region of abnormal forces were estimated to be about 4×10^{-13} cm. and 8×10^{-13} cm. The plate-like form of this region is therefore even more apparent in the helium collisions than in the hydrogen collisions.

DISCUSSION.

In this examination of the results we have compared the observed numbers of scattered α -particles and projected nuclei with the numbers to be expected if the forces between the particles are given by Coulomb's law and on the assumption that the rules of classical mechanics are valid. Any divergence from the calculations has been assigned to a departure from the Coulomb law of force.

During the last year the adequacy of classical mechanics to interpret atomic phenomena has been questioned, and a new mechanics has been developed by Heisenberg, Schrödinger, Born, Dirac, and others. The power of this new mechanics has already been demonstrated by the solution of a number of atomic problems, and it has been suggested that the abnormal scattering of α -particles by light elements may be due rather to the failure of the classical mechanics in dealing with such close collisions than to any departure from the inverse square law of force. Recently, however, Oppenheimer* has shown that on certain assumptions the laws of scattering by a central field of force varying as the inverse square have the same form on the new mechanics as on classical mechanics. It appears unlikely that the large divergences observed in the present experiments and in the previous experiments with hydrogen can be explained solely on the basis of the new mechanics. Some departure from the Coulomb law of force is thus indicated. It might still arise that the peculiar distribution of scattering observed was then a consequence of a central field of force, not that of the inverse square, combined with the wave mechanics. Certain criteria have been given by Schrödinger and de Broglie for

* Oppenheimer, *Zs. f. Phys.* xliii. p. 413 (1927).

the conditions under which marked diffraction patterns may be expected to appear in the collisions of particles. These criteria have been interpreted by Blackett* in terms of collision relations founded on classical mechanics, but unfortunately they are not precisely defined, and until some scattering phenomena have been completely explained in this way, so as to furnish the requisite comparative data, it is difficult to decide where diffraction patterns may be expected to disclose themselves in collisions of the type considered here.

It seems reasonable then to ascribe the abnormal scattering of α -particles by hydrogen and helium mainly to a departure from inverse square forces, and to seek an explanation of the plate-like shape of the surface at which this departure occurs in the structure of the nuclei concerned in the collision. The experimental results can be explained in a general way if we introduce a force which increases very rapidly as the distance of collision decreases. This force may be either attractive or repulsive. Such a force was postulated by Chadwick and Bieler to account for the hydrogen collisions, but no evidence of the form or nature of the force was obtained. In order to explain his observations on the scattering of α -particles by aluminium, Bieler† was led to assume that the α -particle was acted on, in addition to the Coulomb force of repulsion, by a force of attraction varying as the inverse fourth power of the distance. By this means he was able to account approximately for his experimental results. More recently, Debye and Hardmeier‡ have suggested that the additional attractive force can be derived from the assumption that the aluminium nucleus consists of charged particles. They suppose that as the α -particle approaches closely to the nucleus there will arise a polarization of the nucleus in the same way as a charged particle in approaching a neutral atom is able to polarize its structure. This polarization will cause an attractive force on the α -particle, which, if the charged particles of the nucleus are held together by inverse square forces, will vary as r^{-6} , where r is the distance from the centre of the nucleus. With reasonable assumptions about the constants involved, Debye and Hardmeier (and later Hardmeier§ in great detail) calculated the scattering by aluminium on this basis, and showed that the experimental results of Bieler and of the present authors could be

* Blackett, Proc. Camb. Phil. Soc. xxiii. p. 698 (1927).

† Bieler, Proc. Camb. Phil. Soc. xxi. p. 686 (1923).

‡ Debye and Hardmeier, *Phys. Zeit.* xxvii. p. 196 (1926).

§ Hardmeier, *Phys. Zeit.* xxviii. p. 181 (1927).

explained. However fruitful this idea may prove in other cases, it does not seem possible to explain the collisions with hydrogen or helium nuclei without some additional assumption about the "shape" of the α -particle. The most striking fact which appears from our experiments is that while for central collisions the departure from inverse square forces occurs at a distance of about 3.5×10^{-13} cm. between the centres of the particles, for glancing collisions the departure occurs at about 14×10^{-13} cm. At this distance the normal forces are relatively small, and any distortional or polarizing forces must be correspondingly small unless the nuclei are supposed to have a greater dimension in this direction than in the direction at right angles.

Whatever may be the origin of the rapidly varying forces acting in close collisions, it appears necessary to assume some plate-like "shape" for the α -particle, that is for the region around the α -particle where these forces become evident. A similar assumption was made by Chadwick and Bieler to explain their experiments on collisions in hydrogen. Regarding the H particle as a point charge, they deduced that the abnormal forces came into action over a spheroidal surface of semi-axes 8×10^{-13} cm. and 4×10^{-13} cm., the short axis being in the line of motion of the α -particle. From the present experiments, where the α -particle collides with a He nucleus, we should expect to find that the forces become abnormal over a region of about twice these dimensions. For glancing collisions in helium the critical distance is, as we have seen, about 14×10^{-13} cm., or roughly twice the major axis of the above spheroid. For the central collisions, however, the distance is about 3.5×10^{-13} cm., actually rather less than the corresponding critical distance for the collisions in hydrogen. Although it is difficult to form any estimate of the effects of distortion, it would appear that the H nucleus or proton must have dimensions comparable with those of the α -particle. This is an unexpected result, for it is usually supposed that the proton has a radius of about 10^{-16} cm. It would, however, be more accurate to say that the region around the proton where the forces are abnormal is comparable in size with the corresponding region for the α -particle, for we can conclude from our experiments nothing about the volume occupied by the actual structure of the nucleus. Allowing for the "size" of the H particle, we may bring the hydrogen and helium results into some rough agreement by assuming that the "shape" of the α -particle is a spheroid of semi-axes about 7×10^{-13} cm. and 2×10^{-13} cm. moving with the short axis in the line of the

motion of α -particle. The assumption of a definite orientation of the α -particle which was made in the interpretation of the hydrogen collisions, though no adequate proof was obtained, is also suggested by the experiments in helium. Here, indeed, it seems almost necessary to assume further that the helium nucleus does not present all possible orientations in the collisions, and to suppose that the abnormal forces also provide a turning couple controlling the relative orientations of the colliding nuclei.

Any explanation of the origin of the forces which are brought to light by these studies of collisions must necessarily be very tentative in character, for it must be remembered that the nuclei are both in motion during the collision and both are in an abnormal state owing to the powerful distorting forces arising from their close approach to each other. It seems unlikely that the usual electrostatic forces, even when modified by the effects of distortion, could provide over such an extensive area forces of the magnitude necessary to explain the observed results. It may perhaps be suggested that the predominant part in these close collisions is the action of magnetic forces. If, as has been suggested in recent years, the electron has a definite magnetic moment associated with it, it is not unreasonable to suppose, with Frenkel *, that the proton also has a magnetic moment. The assumption of such magnetic forces does, indeed, help to explain some of the observed phenomena, though many grave difficulties still remain. Whatever we assume about the intrinsic magnetic moment of the helium nucleus, it is not difficult to show that the effect of the magnetic forces will become prominent at distances of the order of 4×10^{-13} cm., roughly the distance at which the collisions of α -particles in helium and hydrogen become abnormal. The magnetic forces will also increase very rapidly as the distance of approach decreases. It is further interesting to note that, since the deflecting force of a magnetic field on a charged particle is proportional to the speed of the particle, we are able to see in a general way why the abnormality in the scattering of α -particles increases so markedly with rise in velocity of the α -particle. It seems possible that these magnetic forces would be of the right order of magnitude, and the turning couple due to the interaction of the magnetic fields of the two nuclei offers perhaps an explanation of the apparent orientations of the particles during the collisions.

* Frenkel, *Zs. f. Phys.* xxxvii. p. 243 (1926).

While this suggestion of the importance of magnetic forces around nuclei appears to offer a qualitative explanation of our experimental results, the detailed calculation of their effects is very difficult and perhaps, in the present state of our information about the structure of nuclei, somewhat premature.

Summary.

The collisions of α -particles with helium nuclei have been investigated. The results show that, in general, the collision relations for these particles are similar to those holding for the collisions between an α -particle and a hydrogen nucleus. At large distances of collision the forces between the particles are given by Coulomb's law, but at closer distances very strong additional forces come into action. Possible explanations of the origin of these additional forces are discussed, and it is suggested tentatively that they may be due to magnetic fields in the nuclei.

Cavendish Laboratory, Cambridge.

LIII. *Intensity Measurements of X-ray Reflexions from Fine Powders.* By J. BRENTANO, D.Sc., *Lecturer in Physics, Manchester University* *.

SUMMARY.

THE present paper describes an investigation of the intensity of X-ray reflexions of very fine powders of sodium chloride. The intensities were evaluated by photometric measurements made on the powder photographs of sodium chloride, which had been obtained with the type of camera designed by the author.

The intensity of X-ray reflexions by this crystal has been the subject of investigations by Bragg, James and Bosanquet, A. H. Compton, Havighurst, and others. The principal difficulty in the way of obtaining reliable data is due to the existence of extinction both primary and secondary in the crystal. In the present paper the conditions of extinction of X-ray reflexions from extremely fine powders are discussed, and it is pointed out that the only extinction effect which can occur is constant for all reflexions, but is a function of the wave-length. The conditions which have to be satisfied in order to make relative intensity measurements from powders independent of the knowledge of the coefficient of absorption and of extinction are indicated.

The method adopted for the evaluation of the photographic

* Communicated by Prof. W. L. Bragg, F.R.S.

records of sodium chloride is described. The results are compared with the determinations by other authors employing single crystals and relatively coarse powders. The measurements are in general in good agreement, but for the most powerful reflexions the present measurements give somewhat higher values indicating a small amount of primary extinction in the measurements from larger crystals. Reducing a crystal to the state of a "coarse" powder can in general be considered suitable for eliminating secondary, but not primary extinction.

IN another paper by the writer in collaboration with W. E. Dawson reference has been made to intensity measurements of X-ray reflexions obtained from extremely fine sodium chloride particles produced by a chemical reaction of chlorine gas in dry sodium methoxide. It seemed to be of interest to go into a fuller discussion of these determinations in view of the work of Bragg, James and Bosanquet*, and of A. H. Compton† on this substance. In this work the distribution of electrons of the sodium and chlorine atom is derived from measurements of the scattering of X-rays from sodium chloride for various angles. One main difficulty in such determinations comes from extinction effects, which reduce the intensities of the X-ray reflexions, in particular for small angles, which otherwise would have the greatest bearing on the results.

If we define as crystal unit a region of the crystal in which the spacing of subsequent planes is regular or the crystal perfect, this extinction depends on the size of these units and on the regularity of their orientation. Referring in particular to the work of Bragg, in which an extended crystal block was used, a most careful determination of secondary extinction (the terms primary and secondary extinction are used in the sense in which they were introduced by Darwin‡) has been made for the various reflexions and allowance for it introduced in the calculation. Darwin has shown that no direct determination of primary extinction could be made and has suggested the way of eliminating it by observing the reflexions from particles sufficiently small to make it negligible.

* Bragg, James and Bosanquet, *Phil. Mag.* xli. p. 309 (1921); xlii. p. 1 (1921); *Phil. Mag.* xliv. p. 433 (1922).

† A general account of the work of Compton and others is given in A. H. Compton, 'X-rays and Electrons,' D. Van Nostrand & Co., New York, 1926.

‡ Darwin, *Phil. Mag.* xliii. p. 433 (1926). See also Bragg, Darwin and James, *Phil. Mag.* i. p. 897 (1926).

According to Darwin the relative reduction of intensity which the reflected beam suffers through primary extinction can be expressed for a small crystal unit by a factor

$$\frac{\tanh mq}{mq}, \quad (1)$$

where m is the number of reflecting planes, and

$$q = N(e^2/mc^2)F\lambda^2/2 \sin^2 \theta,$$

(N is the number of molecules per 1 cm.^3 , F is the effective number of scattering electrons per molecule; the other letters have the usual significance), a quantity which is proportional to the amplitude reflected from each plane. Applied to rock-salt this leads for the (200) reflexion to a maximum diameter of $2.4 \cdot 10^{-5} \text{ cm.}$ in order to reduce primary extinction to less than 1 per cent.

Compton and Freeman, Compton, Harris, Bates and MacInnes, Bearden, and Havighurst* have followed this course and carried out determinations from powdered rock-salt crystals. The powders used by these authors consisted actually of particles of considerably larger diameter measuring $1 \cdot 10^{-4}$ – $2 \cdot 10^{-3} \text{ cm.}$, but it was assumed that the process of grinding would break up the crystal lattice and make the actual diffracting units much smaller than the crystal particles. Our experiments on gold, where it was shown that gold powder obtained by filing gave considerable extinction, seemed to make it worth while to undertake more careful measurements of the reflexions from the rock-salt particles obtained by chemical reaction which actually approximate to Darwin's condition. The mean diameter of these particles has been found to be $5.5 \cdot 10^{-5} \text{ cm.}$, giving for the (200) reflexion the factor of primary extinction equal to 4 per cent.

A few remarks may be made on the effect of extinction on intensity measurements from powders, in particular as in some recent work these conditions seem not to have been fully considered. Primary extinction, which corresponds to the loss of intensity of the reflected beam due to interference of wave-trains diffracted from different parts of the diffracting unit, can be made negligible in the powder method by reducing the size of the particles to the limits imposed by formula (1). Secondary extinction, which corresponds to the

* Freeman and Compton, 'Nature,' **cx.** p. 38 (1922).

A. H. Compton, *loc. cit.*

J. A. Bearden, *Phys. Rev.* **xxvii.** p. 796 (1926); **xxix.** p. 20 (1927).

Harris, Bates and MacInnes, *Phys. Rev.* **xxviii.** p. 235 (1926).

R. J. Havighurst, *Phys. Rev.* **xxix.** p. 882 (1926).

weakening of the diffracted beam through encountering in different crystal units lattice planes set at the reflecting angle and in which absorption is therefore particularly great, will depend on the chance of a lattice plane having a certain orientation and on its reflecting power*. In the case of refraction from a single crystal of mosaic type, i. e. consisting of a number of units orientated nearly parallel one to another, this will thus depend on the regularity of the crystal and on the intensity of reflexion from the particular lattice. In the case of a powder two effects have to be considered. Secondary extinction in the individual particle, if this is of "mosaic" structure, and secondary extinction due to the X-ray encountering in succession lattice planes set at a reflecting angle situated in different particles. For a powder of particles sufficiently small to show no primary extinction the first effect can be neglected, as the minimum dimensions for a block to show secondary extinction are considerably greater than the minimum dimensions for a unit to show primary extinction.

The second effect depends on the random distribution of the powder particles, as any lattice plane can have any orientation with respect to the X-ray beam. All possible lattice planes which can reflect contribute to it according to their reflecting power and according to the multiplicity factor p , the number p giving the number of times each particular lattice is represented in the crystal. This effect is the same for all reflexions, independent of the angle through which the X-rays are deflected, but depends on the nature of the crystal, the state of the powder, and on the wave-length, since these affect the intensities of the various reflexions and also the total number of spacings which can reflect. The effect can be small for certain crystals and for certain wave-lengths, it cannot be neglected in considering a general case.

In a general way secondary extinction in a sufficiently fine powder is thus a constant for all reflexions and the crystal behaves as if its coefficient of absorption were $\mu' = \mu + \epsilon$, where μ is the ordinary coefficient of absorption and ϵ the coefficient of extinction. Therefore with a powder this interferes with a direct comparison of the incident and of the reflected beams, as all the reflected intensities are affected by extinction and the coefficient ϵ cannot be determined experimentally, except by measuring the absorption

* In the treatment of reflexion from a perfect crystal by Ewald the reflecting power can be associated with an angular range. P. Ewald, *Phys. Zeitschr.* xxvi. p. 29 (1925).

coefficient μ' for the actual powder used. This measurement is difficult and exposed to serious sources of error, as it depends on having a powder layer of known and uniform density. On the other hand, the coefficient μ' is the same for all reflexions.

For the reflexion from a flat layer of powder of such thickness to be totally absorbing, on which a beam of the angular aperture $d\epsilon$ is incident at a glancing angle α and reflected at a glancing angle β , the intensity of the reflected radiation is determined by

$$kI \frac{1}{\mu'(1 + \sin \alpha / \sin \beta)} d\epsilon,$$

where I is the intensity of the incident radiation and k contains those factors which do not depend on absorption and on the geometry of the apparatus. It appears thus that the effect of extinction becomes constant for all reflexions so long as $\sin \alpha / \sin \beta$ is constant. This condition is satisfied in the arrangement described by the author*, with which the records from the layers of fine sodium chloride powder were taken. In it the distance of the powder from the entrance slit of the instrument and from the film resp. the ionization chamber being a and b , the ratio $\sin \alpha / \sin \beta = a/b$ is satisfied for all angles of reflexion. Unequal distances a and b are considered, as they allow in general greater intensities to be used. By employing this method for quantitative measurements the relative values of the intensities become independent of μ' , so that the coefficient of absorption need not be known †.

To test the absence of primary extinction and the allowance introduced for secondary extinction in the determinations of Bragg, James and Bosanquet, the relative values of the F curves corrected for secondary extinction calculated by Bragg can be compared with the values calculated from our measurements when using the same relation between F^2 and the reflected intensities.

The expression based on the classical scattering of the electron gives

$$F^2 \sim P \frac{\sin 2\theta \sin \theta}{p(1 + \cos^2 2\theta)} \lambda^3,$$

* J. Brentano, Proc. Phys. Soc. London, xxxvii. p. 184 (1925).

† Havighurst in adopting our method seems to have overlooked this point, as in considering a case where $a \neq b$ he quotes a formula given by Compton for passing from the observed intensities to absolute values; this formula does not hold good for the conditions of the experiment.

where P corresponds to the integrated reflexion and a term $\sin \theta/p$ appears, as compared with the expression for the reflexion from a single face, in order to account for the particular conditions of the powder method.

Bragg's determinations were carried out with Rh.K α radiation, while we used Cu.K α . As F is a function of $\sin \theta/\lambda$, our values have to be referred to angles θ' such that $\sin \theta'/\sin \theta = \frac{\lambda \text{ RhK}}{\lambda \text{ CuK}} = 0.399$, in order to make them

comparable with the values obtained from rhodium radiation.

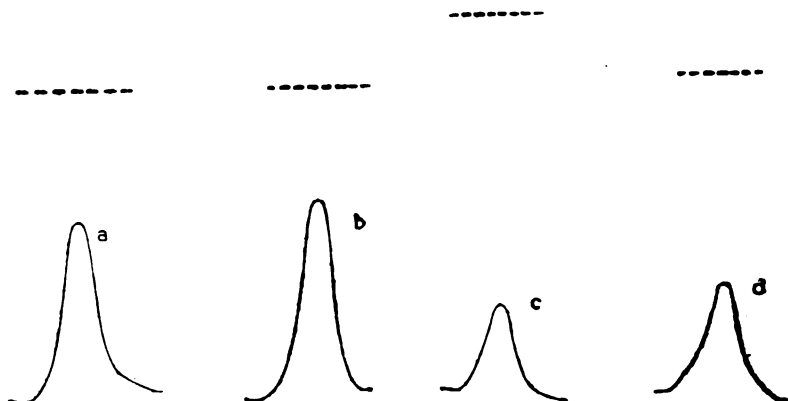
Another way of comparing the determinations is to express the relative values of F as a function of $H^2 = h_1^2 + h_2^2 + h_3^2$ (the sum of the squares of the indices of each reflexion), as the relation between the two quantities is independent of the wave-length.

The reflexions from sodium chloride were recorded photographically and a suitable procedure had to be evolved for their measurement. The blackening records obtained from a self-registering instrument of Moll were not satisfactory for this particular measurement, as the heights of the peaks seemed to be affected by the inertia of the thermopile. A photometer was therefore designed in which the film could be set in any desired position in front of a fine slit by the action of a micrometer-screw. Light illuminating the slit was allowed to fall on a thermopile connected to the galvanometer. Definite portions of the line could thus be measured with the film stationary, and the correct working of the instrument could be checked by interposing zero readings and measurements of the intensity of the source. For smaller angles of deflexion it was found that the integrated intensity could be determined from a measurement of the blackening for the peak of the lines, multiplied by the average width as determined by measuring the area of the record. This of course implied that certain conditions as to the definition of the lines were satisfied. The justification for this procedure was derived from comparing the values obtained in this way with an actual integration of the X-ray intensities corresponding to the various parts of each line.

To ascertain whether the measurements were affected by the width of the slit, records with slits of 0.02 and 0.07 mm. were made. Fig. 1 shows the curves so obtained for the (222) and (422) reflexion plotted on different scales of ordinates in order to make the lines comparable. The contours are very similar and the peak values expressed by I/I_0 , where I_0 is the deflexion for "fog" outside the line

and I is the deflexion on the peak, are in both cases smaller with the wider slit, the reductions being in the ratio 1·16 and 1·17 respectively, showing that the relative values are practically unaffected by the width of the slit. The narrower slit was used in the measurement of the lines. The X-ray intensities were evaluated by blackening marks produced in the ordinary way. Kodak roll-films were used in preference to special X-ray films, and several films superposed in order to have a check for any inequality of the emulsion.

Fig. 1.



Photometry of (222) reflexion with wide slit (a) and with fine slit (b), and (422) reflexion with wide slit (c) and with fine slit (d).

The following tables give the results of the measurements in the form discussed above. Fig. 2 shows them in the form of a graph. The F values for the reflexions from a single crystal are revised F values for which I am indebted to Mr. R. W. James and Miss E. Firth, these values will be published shortly.

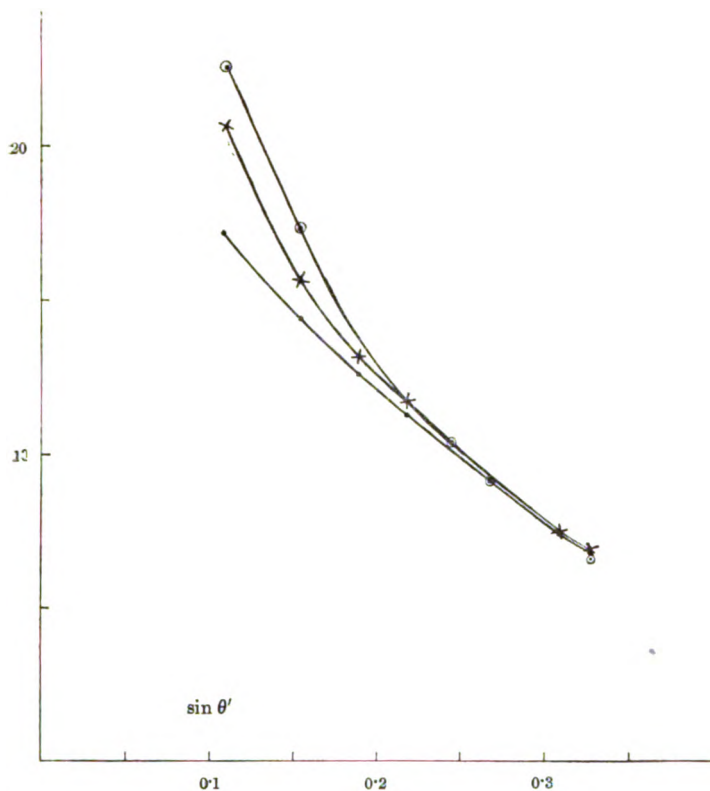
Reflexion from large crystal (James & Miss Firth).

Indices.	H^2 .	F corrected for		$\sin \theta$.
		F uncorrected.	sec. extinction.	
200	4	17·16	20·65	0·109
220	8	14·39	15·62	0·154
222	12	12·59	13·18	0·189
400	16	11·23	11·69	0·218
440	32	77·40	7·46	0·308
600	36	6·84	6·89	0·327

Reflexion from fine powder.

Indices.	H ² .	"Integrated" reflexion. P.	Multiplicity factor. p.	(rel. val.). F.	sin θ .	sin θ' .
200	4	18.3	3	22.6	0.273	0.109
220	8	9.61	6	17.4	0.386	0.154
420	20	2.33	12	10.4	0.611	0.244
422	24	1.54	12	9.16	0.699	0.267
442 (600)...	36	0.91	15	6.46	0.819	0.327

Fig. 2.



F values: ● from single crystal uncorrected.

× from single crystal corrected for secondary extinction.

○ from fine powder.

The F values obtained from the single crystal are absolute determinations, while our values obtained from the powder are relative values and are plotted in arbitrary units, so as

2 S 2

to obtain agreement for $\sin \theta = 0.25$. For this angle the correction for secondary extinction as determined by Bragg becomes sufficiently small; it seems therefore best to make this point coincide in comparing the curves, as the determinations become less accurate for larger angles.

It will be seen that the values are in general in good agreement; for the deflexions at small angles, however, our values are slightly higher, indicating that the reflexions from large crystals were not quite free from primary extinction. Comparing the uncorrected values obtained from a single crystal with the values corrected for secondary extinction and with those obtained from the fine powder, it appears that primary extinction affects the reflexions from a large crystal to a much smaller degree than secondary extinction, for which allowance has been made.

The approximation between the values obtained from large crystals, comparatively coarse powders, and extremely small particles which very nearly satisfy the criterion of negligible secondary extinction show that in all these cases the crystal units are small.

Comparing this with the results obtained with other crystals possessing considerable primary extinction, it appears that rock-salt is an eminently suitable substance for intensity measurements.

To meet the more general case, the conditions for the reflexion of X-rays from powders indicate that in principle the best procedure for obtaining data on intensities consists in taking relative intensity measurements of reflexions from a powder layer of particles sufficiently small to satisfy Darwin's criterion for negligible primary extinction, satisfying thus very simple conditions for the interpretation of the results. If absolute measurements and therefore a comparison with the incident beam is required, the relation can be established by observing one reflexion from a single large crystal and determining the proper coefficient of absorption, using preferably a reflexion for which extinction is negligible.

It is not always easy to obtain powders of so small particles to satisfy the condition of negligible primary extinction, and evidence whether the mechanical treatment of grinding is sufficient to break the lattice into units much smaller than the dimensions of the particles seems not complete.

In the case of rock-salt the crystal units were evidently sufficiently small from the beginning, and the process of grinding, as carried out in the experiments of Havighurst,

was mainly required in order to produce particles small enough to eliminate secondary extinction in the individual particle.

In the case of gold, experiments of Dawson and the author showed that the mechanical treatment of filing was not sufficient to eliminate extinction, and similar conditions were observed by the author on calcite and on zinc carbonate powders, where considerable extinction was found after prolonged grinding. The same is borne out by experiments by Havighurst where exceptionally perfect crystals, obtained by a process of distillation, showed some primary extinction after grinding during several hours.

In conclusion the author wishes to express his thanks to Prof. W. L. Bragg, F.R.S., for expressing valuable criticisms in reading through the manuscript of this paper.

Physical Laboratories,
University of Manchester,
June 30th, 1927,

LIV. *The Flow of Heat in a Body generating Heat.* By
J. H. AWBERY, B.A., B.Sc., *Physics Department, National
Physical Laboratory* *.

Abstract.

THE flow of heat in a body in which heat is at the same time being generated is examined. The differential equation is set out, and forms of solution noted, for cartesian and for polar coordinates.

The problem of the temperature at all points and times, in a sphere generating heat, is solved in detail, when the constant initial temperature is given, the surface being held at a definite temperature from a time zero onwards, and also for the more elaborate case where the initial temperature distribution is an equilibrium one, and the boundary condition is Newton's law of cooling.

Introduction.

SINCE the publication of Fourier's pioneer treatise on the conduction of heat, the methods which he initiated have been applied to a multitude of problems, not only in heat conduction but in all branches of physics, particularly in the theory of the potential.

* Communicated by Sir J. E. Petavel, K.B.E., F.R.S.

In the theory of heat conduction, however, there are a series of problems to be considered, in which the body in which the heat-flow takes place is at the same time the seat of a continuous production of heat. The physical cases in which this occurs are somewhat limited, the most notable being those where an electric current is the source of the heat production; several such cases have been worked out, but, as far as the author is aware, only for the particular case of the steady state, in which the temperatures do not change with time, or else for the case of an infinite solid, with a plane face. Other cases in which conduction problems "with heat generation" have been solved have been dealt with by the method, due to Kelvin, of sources and sinks.

The purpose of the present paper is to examine briefly the modifications necessary to solve such cases analytically, and to give in detail the solution for a sphere.

Fundamental Equation.

By considering the net flow of heat into a small parallelepiped of sides dx , dy , dz , and equating it to zero, it is easily found that the fundamental differential equation of heat conduction takes the form

$$K \left(\frac{d^2\theta}{dx^2} + \frac{d^2\theta}{dy^2} + \frac{d^2\theta}{dz^2} \right) = \rho\sigma \frac{\partial\theta}{\partial t} - Q,$$

where θ is the temperature at the time t and the point (x, y, z) , K is the thermal conductivity, ρ and σ are the density and specific heat of the body, and Q the heat generated per second per unit volume of the body.

It will be convenient to use h^2 as a single symbol for $K/\rho\sigma$, and b^2 for $Q/\rho\sigma$, so that the equation takes the form

$$\frac{d\theta}{dt} = h^2 \nabla^2 \theta + b^2. \quad . \quad . \quad . \quad . \quad (1)$$

Now, although this is not examined in the usual treatises, two cases of it have been thoroughly studied.

(a) When $b^2=0$, it becomes the usual "diffusion equation," and is known to have the useful solutions

$$\theta = \Sigma A e^{mx+ny+pz+qt}, \quad \text{where} \quad h^2(m^2+n^2+p^2) = q,$$

and in which one or more of the exponents may be imaginary and take the form of trigonometrical functions.

(b) If $\frac{d\theta}{dt} = 0$, we have the steady state, and the equation

is that known as Poisson's, considerably studied in electrostatics and gravitation, and, as mentioned above, amenable to treatment by Kelvin's method. One solution is

$$\theta = A - \frac{b^2}{6h^2}(x^2 + y^2 + z^2).$$

In seeking solutions of the general equation (1), it is immediately evident that it cannot be simplified by the common device of assuming that there are solutions of the form (function of time) \times (function of space coordinates), and in fact something of the nature of a particular integral is required.

The assumption that $\theta = \theta' + \theta''$, where $\frac{d\theta'}{dt} = h^2 \nabla^2 \theta'$ and $\frac{d\theta''}{dt} = 0$, leads to $h^2 \nabla^2 \theta'' = b^2$, so that the solution may be taken as the sum of two others, one satisfying the Fourier, and the other Poisson's equation.

It follows that a solution of the equation (1) is

$$\theta = A - \frac{b^2}{6h^2}(x^2 + y^2 + z^2) + \Sigma B e^{mx+ny+pz+qt}, \quad (2)$$

with the same relation as before between m, n, p , and q .

It is evident that this form of solution is available to satisfy any set of boundary conditions for which the problem without heat generation is soluble by means of a series

$$\theta = A + \Sigma B e^{mx+ny+pz+qt},$$

i. e. for most cases whose solutions are known when $b=0$.

Spherical Polar Coordinates.

Turning now to the problems which are more suitably dealt with in polar coordinates, we shall restrict consideration to those where the heat-flow is uniform, so that the temperature is a function of the coordinate r , and independent of angular coordinates.

Either by transformation of the equation (1), or by considering the heat-flow into a spherical shell, the fundamental equation is shown to be

$$\frac{d\theta}{dt} = \frac{h^2}{r^2} \frac{d}{dr} \left(r^2 \frac{d\theta}{dr} \right) + b^2. \quad . \quad . \quad . \quad (3)$$

Taking a new variable $u=r\theta$, this becomes

$$\frac{du}{dt} = b^2 r + h^2 \frac{d^2 u}{dr^2},$$

which is satisfied by $u = u' + u''$

if
$$u' = A + Br - \frac{b^2 r^2}{6h^2}$$

and
$$u'' \text{ satisfies } h^2 \frac{d^2 u''}{dr^2} = \frac{du''}{dt},$$

the latter being identical in form with the Fourier equation.

Temperatures in a sphere, initially at θ_0 , with its surface suddenly held at θ_1 .

We may illustrate the use of these solutions by working out the above problem.

From the last equations we may take

$$u = A + Br - \frac{b^2 r^2}{h^2} + \sum e^{-n^2 k^2 t} (C \cos nr + D \sin nr)$$

or

$$\theta = \frac{u}{r} = \frac{A}{r} + B - \frac{b^2 r^2}{h^2} + \frac{1}{r} \sum e^{-n^2 k^2 t} (C \cos nr + D \sin nr).$$

To apply this to the particular problem, we must evidently take $A=C=0$, to avoid infinite temperatures at the centre of the sphere.

This gives, as the initial condition,

$$\theta_0 = B - \frac{b^2 r^2}{6h^2} + \frac{1}{r} \sum D \sin nr \quad . \quad . \quad . \quad (4)$$

for all values of r .

The surface condition, valid for all positive values of t , is

$$\theta_1 = B - \frac{b^2 a^2}{6h^2} + \frac{1}{a} \sum D e^{-n^2 k^2 t} \sin na.$$

We can comply with the latter equation by taking $na=m\pi$, where m is an integer, so that the sines vanish at $r=a$; then

$$B = \theta_1 + \frac{b^2 a^2}{h^2},$$

and (4) becomes

$$\theta_0 = \theta_1 + \frac{b^2}{6h^2} (a^2 - r^2) + \frac{1}{r} \sum D \sin \frac{m\pi r}{a}$$

an equation for the coefficients D .

In fact, the D 's are the coefficients in the Fourier sine series for

$$r(\theta_0 - \theta_1) + \frac{b^2 r}{6h^2} (r^2 - a^2),$$

so that

$$D_m = \frac{2}{a} \int_0^a \left[r(\theta_0 - \theta_1) - \frac{b^2 a^2 r}{6h^2} + \frac{b^2 r^3}{6h^2} \right] \sin \frac{m\pi r}{a} dr.$$

The integrals of the form $Nr^3 \sin \frac{m\pi r}{a}$ and of $Mr \sin \frac{m\pi r}{a}$ reduce by parts, and the terms involving sines vanish at both limits, so that D_m reduces to

$$(-1)^m \left[\frac{2a^2 b^2}{h^2 m^3 \pi^3} + \frac{2a(\theta_1 - \theta_0)}{m\pi} \right], \quad . \quad . \quad . \quad (5)$$

and the final equation for the temperature is

$$\theta = \theta_1 + \frac{b^2(a^2 - r^2)}{6h^2} + \frac{1}{r} \sum D_m e^{-m^2 \pi^2 h^2 t / a^2} \sin \frac{m\pi r}{a}, \quad . \quad (6)$$

with the above values of D_m .

As particular cases, we notice :

(1) When $t=0$, θ reduces to

$$\theta_1 + \frac{b^2(a^2 - r^2)}{6h^2} + \frac{1}{r} \sum D_m \sin \frac{m\pi r}{a},$$

and since the Fourier series is that of

$$r(\theta_0 - \theta_1) + \frac{b^2 r}{6h^2} (r^2 - a^2),$$

this is θ_0 as it should be.

(2) When $t=\infty$,

$$\theta = \theta_1 + \frac{b^2(a^2 - r^2)}{6h^2},$$

showing what is the excess temperature at any point, after the steady state has been attained. It is also to be noted that at the surface this becomes simply θ_1 , as it is by hypothesis at all times later than $t=0$.

Further, it is obvious that when $t=\infty$, the temperature gradient in the sphere is $-\frac{2b^2 r}{6h^2}$, so that the heat-flow through

the surface, per second, being $-KS \left(\frac{d\theta}{dr} \right)_a$, where S is the area, is

$$\frac{2b^2aK}{h^2} \cdot 4\pi a^2 = \frac{4}{3} \frac{b^2a^3K}{h^2},$$

or, since $b^2 = Q/\rho\sigma$ and $h^2 = K/\rho\sigma$, the heat-flow is $\frac{4}{3} Qa^3$, i. e. $Q \times$ volume of sphere, the result to be anticipated.

(3) When $r=a$, the sines vanish, and $\theta = \theta_1$ simply.

(4) When $r=0$, we have

$$\frac{1}{r} \sin \frac{m\pi r}{a} = \frac{m\pi}{a},$$

and θ takes the form

$$\theta_1 + \frac{b^2a^2}{6h^2} + \Sigma D_m \cdot \frac{m\pi}{a} e^{-m^2\pi^2h^2t/a^2},$$

an expression for the excess at the centre at various times.

(5) When $b^2=0$, the problem simplifies to the case of no heat generation. D_m assumes the simple form $\frac{2a}{m\pi}(\theta_1 - \theta_0)$, and θ is simply

$$\theta_1 + \frac{2a(\theta_1 - \theta_0)}{\pi r} \Sigma \frac{1}{m} e^{-m^2\pi^2h^2t/a^2} \sin \frac{m\pi r}{a}, \quad \dots \quad (7)$$

which is the form (slightly extended) usually given in the text-books*.

Numerical illustration.

The form of D_m is too complicated, and changes too much with variations in the relative values of b and h , to make it profitable to calculate an example fully. We may, however, calculate numerical values for the following problem (which in fact suggested the subject).

Apples when placed on shipboard are usually warm, and have to be cooled down to be carried in cold storage; they also, by their respiration, generate heat. It is required to calculate to what extent they are warmer, after a given time in the refrigerated chamber, than they would be if they generated no heat. The theoretical answer to the latter problem is well known, so that this difference will complete the solution for the actual case. We assume that the apples are initially uniform throughout at θ_0 , and that their skins

* See Carslaw, 'Heat Conduction,' Art. 64, or Byerly, 'Fourier Series and Integrals,' Art. 66.

assume the temperature θ_1 immediately they are introduced into the hold.

The excess temperature referred to is the difference between expressions (6) and (7), viz.,

$$\frac{b^2(a^2-r^2)}{6h^2} + \frac{1}{r} \Sigma (-1)^m \cdot \frac{2a^3b^2}{h^2m^3\pi^3} e^{-m^2\pi^2kt/a^2} \sin \frac{m\pi r}{a} \dots$$

Since the centre of each apple is at the highest temperature, the value there is the only one of interest in the practical problem, and at this point the excess is simply

$$\frac{b^2a^2}{6h^2} + \Sigma (-1)^m \cdot \frac{2a^2b^2}{b^2m^2\pi^2} e^{-m^2\pi^2kt/a^2} \dots \dots (8)$$

The following values were taken for the constants :—

a , the radius of an apple, = 4 cm.,

b^2 = 0·0000133 C.G.S. centigrade units,

h^2 = 0·00155 C.G.S. centigrade units,

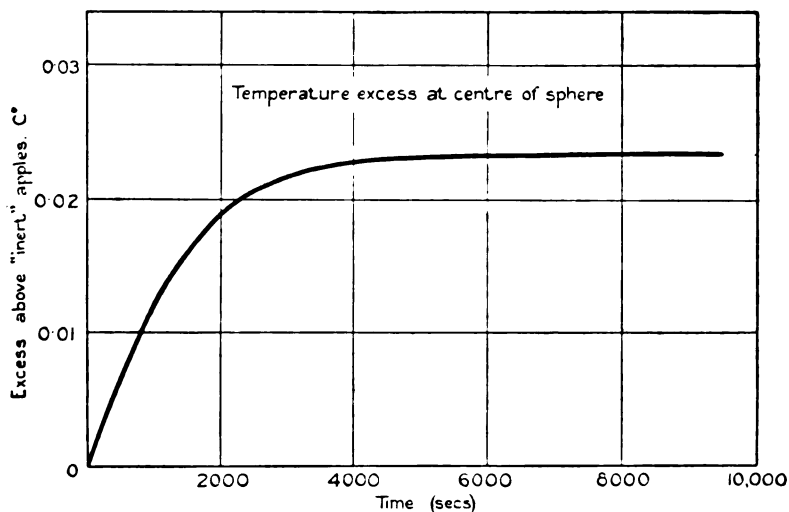
which leads to the following values, which are also plotted in the figure.

Time. (secs.)	Excess temperature at centre, above that of an apple generating no heat. (° C.)
0	0·0000
200	0·0027
400	0·0054
500	0·0067
600	0·0080
1000	0·0125
2000	0·0190
3000	0·0216
4000	0·0226
5000	0·0230
6000	0·0231
7000	0·0232
8000	0·0232
9000	0·0232
10000	0·0232

It is interesting to remark that the value 0·0000 at $t=0$ is a calculated one, the series in equation (8) being actually summed to 0·0232, the value of the first term. It thus provides an excellent check on the algebra and on the numerical work. Its meaning is, of course, that whether

there is heat generation or not, the initial temperature at the centre is assumed fixed at the same value.

As far as this particular problem is concerned, the net result is that the effect of heat generation is negligible. Nevertheless, it appears desirable to place the general equations on record, since it is easy to conceive of cases where the results of these calculations might be required.



Sphere cooling by radiation.

We pass to a second, more practical, problem. It was evident from the beginning that the assumption of a uniform initial temperature throughout was an artificial one, but the result of the previous problem for $t = \infty$ shows what distribution is to be taken, as representing an equilibrium condition. We may also replace the condition of constant temperature at the surface, by the assumption that the sphere loses heat to its surroundings at a rate proportional to the temperature excess above the air. The problem is therefore that of a sphere initially in a state such that its temperature is $\theta_1 + \frac{b^2(a^2 - r^2)}{6h^2}$. At a time zero it is placed in an enclosure

at which it loses heat at a rate $E(\theta_a - \theta_2)$ per sq. cm., E being its emissivity, and θ_a the (variable) surface temperature.

As before, the temperature may be taken as

$$\theta = B - \frac{b^2 r^2}{6h^2} + \frac{1}{r} \sum D e^{-n^2 A^2 t} \sin nr,$$

so that expressions of the initial and boundary conditions are now

$$\theta_1 + \frac{b^2(a^2 - r^2)}{6h^2} = B - \frac{b^2 r^2}{6h^2} + \frac{1}{r} \Sigma D \sin nr, \quad (9)$$

$$\begin{aligned} -K \left[-\frac{2b^2 a}{6h^2} - \frac{1}{a^2} \Sigma D e^{-n^2 h^2 t} \sin na + \frac{1}{a} \Sigma n D e^{-n^2 h^2 t} \cos na \right] \\ = E \left[B - \frac{b^2 a^2}{6h^2} + \frac{1}{a} \Sigma D e^{-n^2 h^2 t} \sin na - \theta_2 \right], \quad (10) \end{aligned}$$

the latter expressing that $-K \left(\frac{\partial \theta}{\partial r} \right)_a = (\theta_a - \theta_2)$, or that heat does not accumulate in the surface.

Equation (10) can only be satisfied if the constant terms, and those involving time, are equated separately.

$$\text{Thus} \quad B = \frac{ab^2(Ea + 2K)}{6Eh^2} + \theta_2$$

$$\tan na = \frac{Kna}{K - Ea}.$$

Thus

$$n = \phi_m/a, \text{ where } \phi_m \text{ is the } m\text{th root of } \tan \phi = \frac{K\phi}{K - Ea}. \quad (11)$$

Substituting these values in (9), it takes the form

$$\theta_1 = \frac{Kab^2}{3Eh^2} + \theta_2 + \frac{1}{r} \Sigma D \sin \frac{\phi r}{a},$$

or putting

$$\theta_1 - \frac{Kab^2}{3Eh^2} - \theta_2 = a \text{ constant } F,$$

$$\Sigma D \sin \phi r/a = Fr.$$

The series on the left is not a Fourier series, owing to the form of ϕ , but it is a series in which an arbitrary function may be expanded. In fact *

$$\begin{aligned} D &= \frac{2}{a} \left[\frac{\phi^2 + \left(\frac{Ea - K}{K} \right)^2}{\phi^2 + \frac{Ea(Ea - K)}{K^2}} \right] \int_0^a Fr \sin \frac{\phi r}{a} dr \\ &= \frac{2F}{a} \left[\frac{\phi^2 K^2 + (Ea - K)^2}{\phi^2 K^2 + Ea(Ea - K)} \right] \left[\frac{a^2 \sin \phi}{\phi^2} - \frac{a^2 \cos \phi}{\phi} \right]. \end{aligned}$$

* See Byerly, *loc. cit.* p. 120.

Since $\tan \phi$ is $\frac{K\phi}{E - E}$, this may be transformed into

$$D = \frac{2a^2EF}{\phi} \frac{[\phi^2K^2 + (Ea - K)^2]^{\frac{1}{2}}}{[\phi^2K^2 + Ea(Ea - K)]}, \quad \dots (12)$$

and the final result is the following somewhat unwieldy one:

$$\theta = \frac{(a^2 - r^2)b^2}{6h^2} + \frac{Kab^2}{3Eh^2} + \theta_2 + \frac{1}{r} \sum D e^{-\phi^2 h^2 / a^2} \sin \frac{\phi r}{a},$$

where the successive D's are given by equation (12), F being an abbreviation for $(\theta_1 - \theta_2) - \frac{Kab^2}{3Eh^2}$, and ϕ being given by the roots of equation (11).

It is difficult to devise checks on the algebra. If the series is correctly expanded, the solution gives the correct answer at $t=0$. At $t=\infty$ it shows an equilibrium condition in which the surface temperature exceeds the surroundings by $\frac{Kab^2}{3Eh^2}$, and this leads, in fact, to a heat-loss per second equal to the rate of generation.

If $b=0$, not only is the heat-loss zero, but the initial temperature becomes the constant θ_1 . In this case θ reduces to $\theta_2 + \frac{1}{r} \sum D e^{-\phi^2 h^2 / a^2} \sin \frac{\phi r}{a}$, and D becomes

$$\frac{2a^2(\theta_1 - \theta_2)}{\phi} \frac{[\phi^2K^2 + (Ea - K)^2]^{\frac{1}{2}}}{[\phi^2K^2 + Ea(Ea - K)]},$$

which agrees with the known result given in Byerly (*loc. cit.* p. 122).

LV. Notices respecting New Books.

Tungsten: a Treatise on its Metallurgy, Properties, and Applications. By Dr. COLIN J. SMITHELLS. Pp. viii + 167, with 33 plates. (London: Chapman & Hall, Ltd. 1926. Price 21s. net.)

THE importance of tungsten for industrial purposes is due to two properties: its low vapour pressure at high temperatures, which makes it possible to take advantage of its high melting-point (which is exceeded only by that of carbon), and its power of hardening metals with which it is alloyed. Its chief uses are for making high-speed steels and for electric light and thermionic valve filaments. It is valuable also for galvanometer suspensions,

on account of its high elasticity, for targets in X-ray tubes, and for electrical contacts in motor-car magnetos, &c. Its properties are remarkable, and special methods have to be employed in working it. Although at room temperatures it is chemically inert, at high temperatures it is readily oxidizable, and in manufacturing processes or practical applications involving high temperatures it must be surrounded by an atmosphere of hydrogen or nitrogen.

In order to obtain tungsten in a ductile condition from the powdered metallic form in which it is initially obtained, it is first pressed into ingots by mechanical pressure; the ingots are then sintered in a furnace so as to be readily handled, formed by passing a heavy current through so as partially to eliminate the voids; swaged at high temperature by a mechanical hammering process, and finally drawn into wires by passing through a series of disks. The wires so obtained are essentially a bundle of crystalline fibres. On heating, recrystallization occurs and the ductility is lost.

Tungsten thus presents many problems of interest to the metallurgist and to the industrial user. Dr. Smithell's book deals with these problems in a very clear and interesting manner and is likely to form a standard work of reference on this subject. Detailed references to original publications are given. The book is well illustrated, and the numerous photo-micrographs may be particularly commended.

Lens Computing. By J. W. GIFFORD. (Macmillan & Co. 7s 6d.)

COLONEL GIFFORD'S book gives a short and concise account of lens computation by trigonometrical trace. After the introductory chapters on achromatism and spherical aberration, the method is applied to doublets and to various kinds of eyepieces—in particular, a modified Huyghenian eyepiece and a new triple erector. Several numerical examples are worked out in detail, including the traces of rays of a doublet and of an Apochromatic triple telescope object-glass.

Recent Developments in Atomic Theory. By C. G. DARWIN. (Humphrey Milford, Oxford University Press, 1927. 1s. net.)

IN this short lecture Prof. Darwin calls attention to three important developments in Atomic physics, the classical experiments of Gerlach and Stern, the rotating electron of Goudsmit and Uhlenbeck, and the Mechanics of Heisenberg for the study of atomic structure. "We hope that with the New Mechanics and the rotating electron a new era has set in which will found a true atomic mechanics."

A Comprehensive Treatise on Inorganic and Theoretical Chemistry.
Vol. III. Ti, Zr, Hf, Th, Ge, Sn, Pb, Inert Gases. Bp J. W.
MELLOR, D.Sc. Pp. x+977, with 255 diagrams. (London :
Longmans, Green & Co. 1927. Price 63s. net.)

THE seventh volume of Dr. Mellor's *Comprehensive Treatise* follows the same general lines as the earlier ones. For each element is given its history, occurrence, extraction, physical and chemical properties, valency and atomic weight, alloys, oxides, salts. At the end of each section detailed references are given to original publications. For lead alone these references total in all nearly 90 pages of close type, from which the thoroughness with which the author has examined chemical literature can be judged. Many of the references bear the date 1926, so that the present volume includes an account of the most recent work.

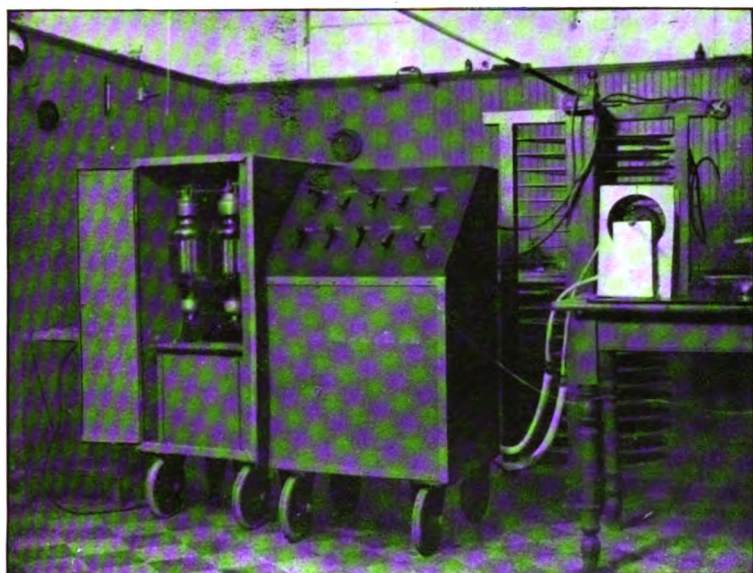
The compilation of such a treatise single-handed is a monumental piece of work; it is, however, more than a mere compilation, for the whole of the material is critically examined and welded together into a homogeneous whole. Dr. Mellor has placed all inorganic chemists under a debt of gratitude to him, and they will all hope that he will be able to carry his monumental task to completion.

Collected Papers of Sir James Dewar. Edited by Lady DEWAR with the assistance of J. D. HAMILTON DICKSON, H. MUNRO ROSS, and E. C. SCOTT DICKSON. Two volumes: pp. xxii+1489, with two plates. (Cambridge University Press. 1927. Price £4 4s. net.)

IN these two volumes are contained all the scientific papers and addresses by Sir James Dewar, together with papers published jointly with other investigators, excepting those in which he was associated with Professor G. D. Liveing. These have already been published in collected form. A few hitherto unpublished investigations are also included. Dewar was a great experimentalist, and in manipulative skill he had few equals. His own work lay largely in the borderlands of science; such as the liquefaction of gases, the production of low temperatures, the study of the properties of matter at such temperatures, high-vacuum technique, phosphorescence, soap-films. With theories he was less concerned. Theories must be built upon observation, but it is rarely that great experimental skill and a high power of theoretical interpretation are combined in the same person. These two volumes will prove of great interest to both categories of investigators; in particular, Dewar's experiments which have a bearing upon inter-molecular forces must prove of great value for the formulation of a theory of such forces. The volumes form a fitting tribute to a long life's work. A name index and a detailed subject index are given at the end of the second volume.

[The Editors do not hold themselves responsible for the
views expressed by their correspondents.]

FIG. 1.

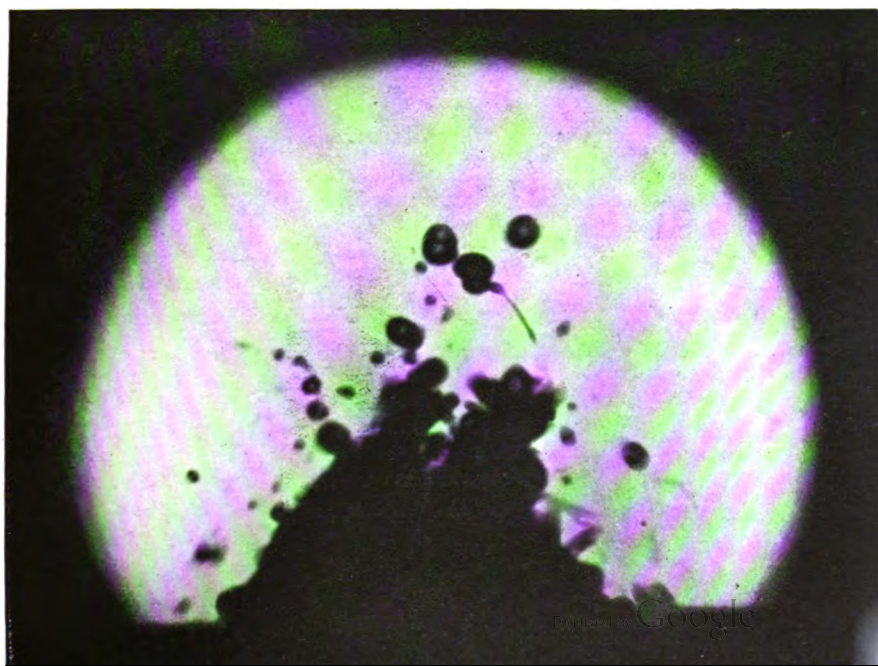


Two 1000 Watt tubes.

Oil condensers.

Variable air condenser
and coils.

FIG. 2.



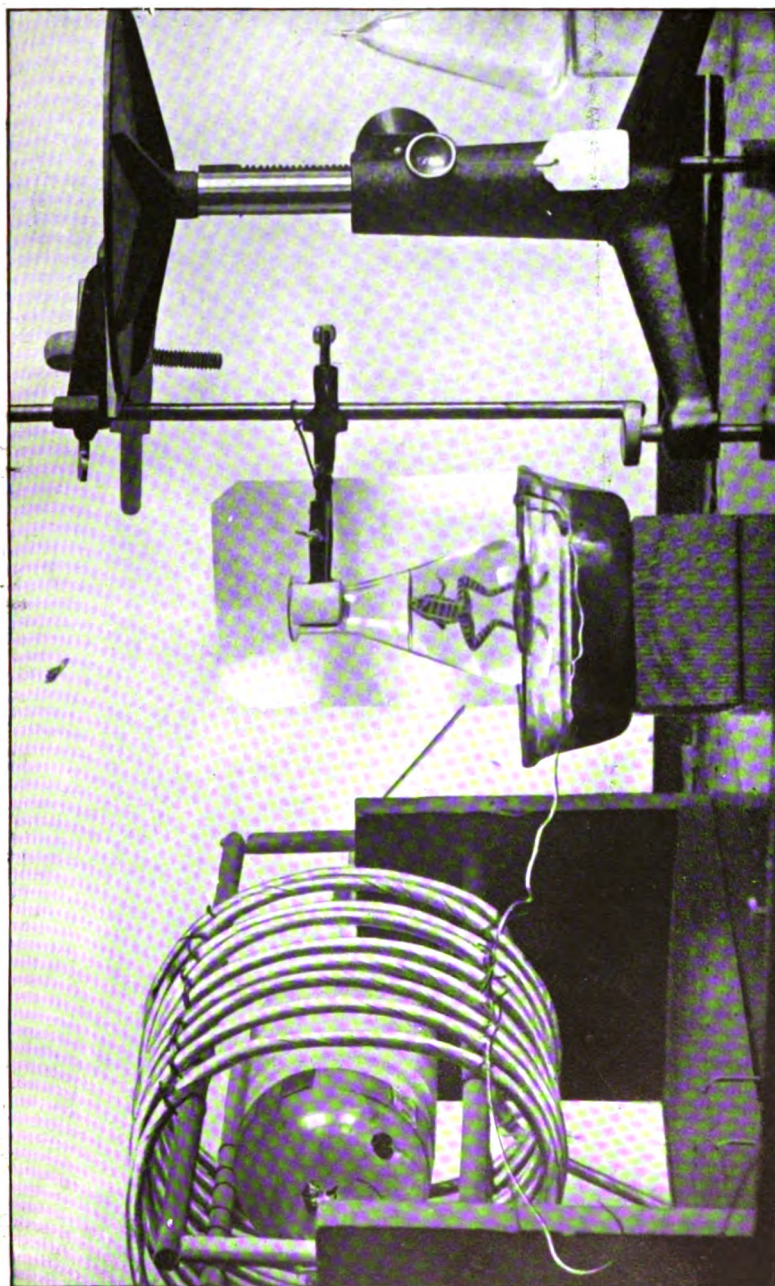


FIG. 3.

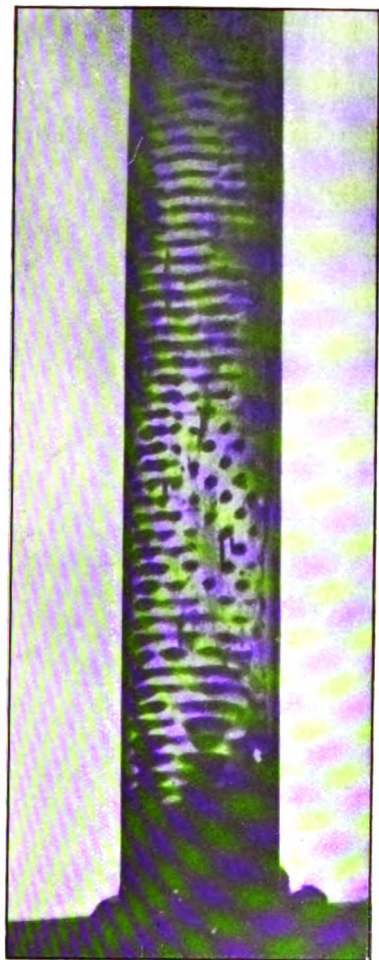


FIG. 4.

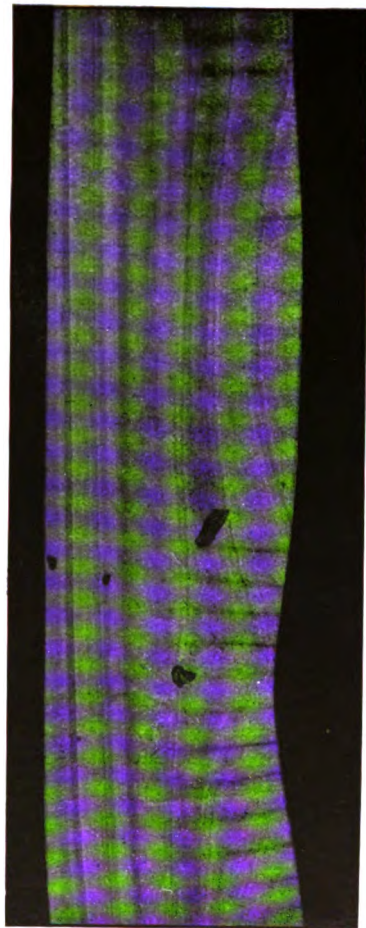


FIG. 6.

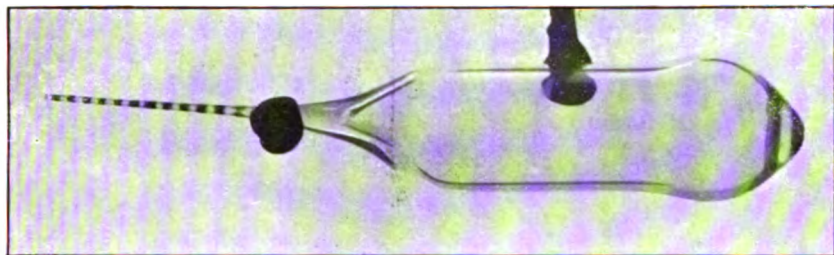


FIG. 5.

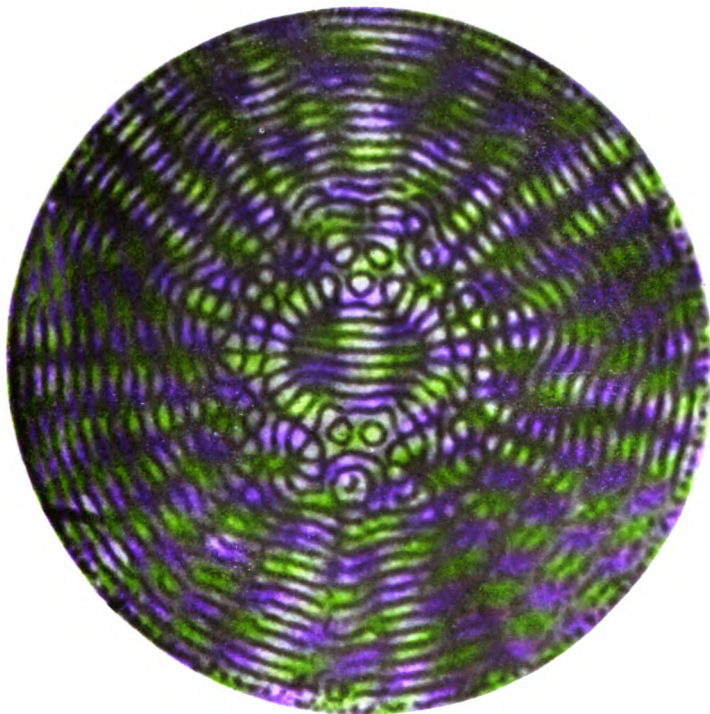


FIG. 7.

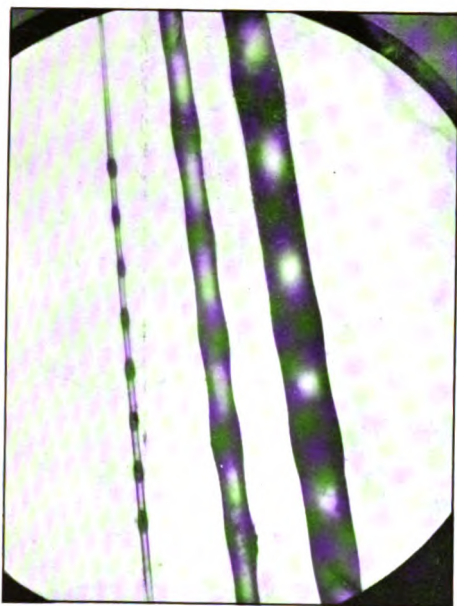


FIG. 8.

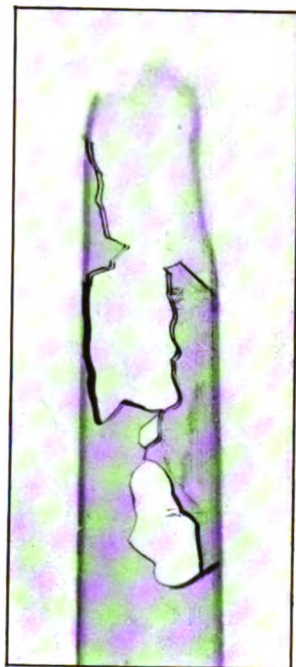


FIG. 9.

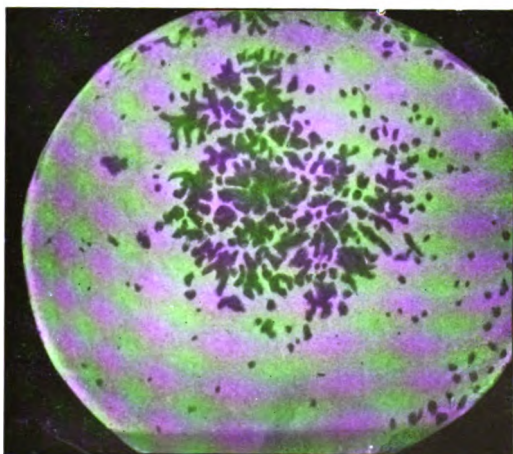
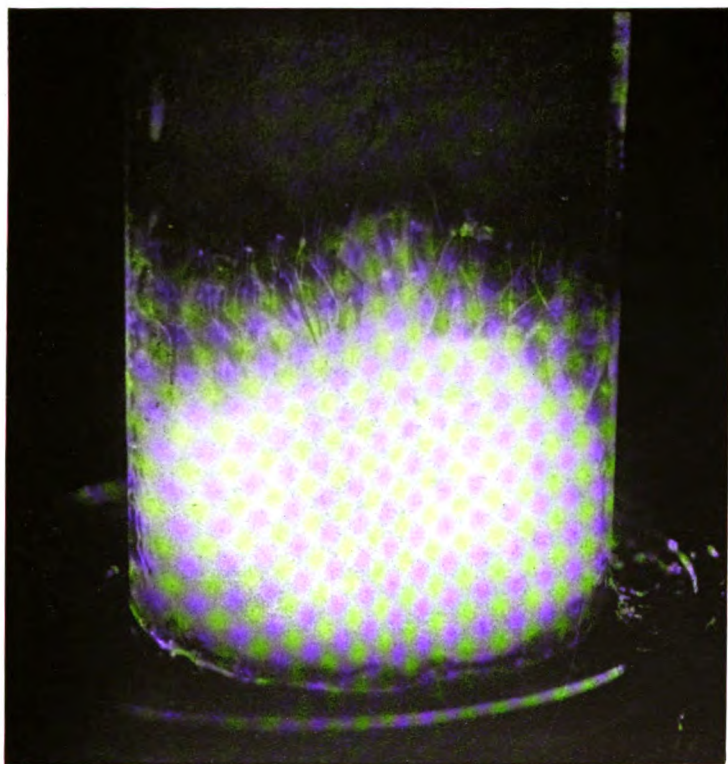


FIG. 10.



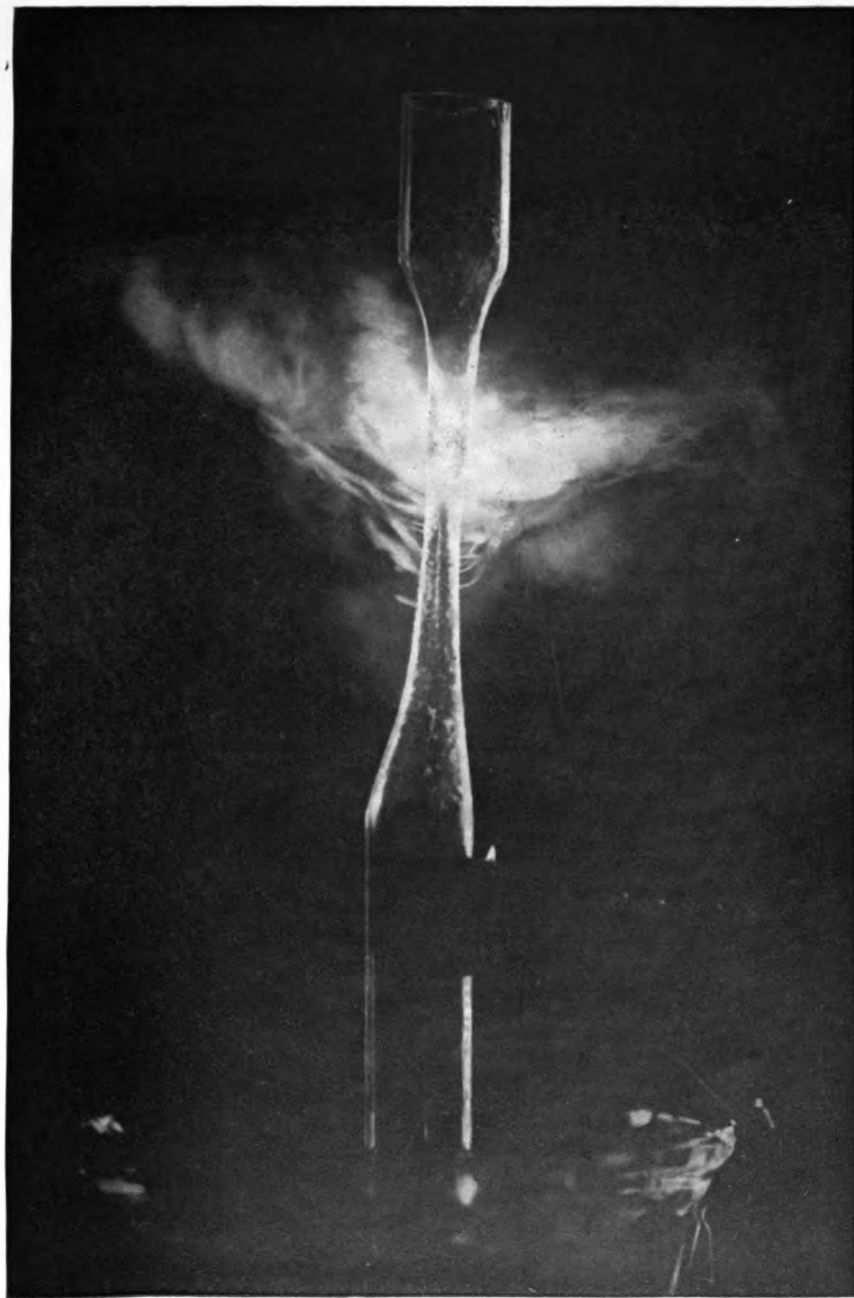


Fig. 1.

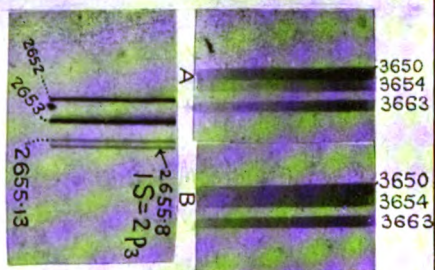


Fig. 2

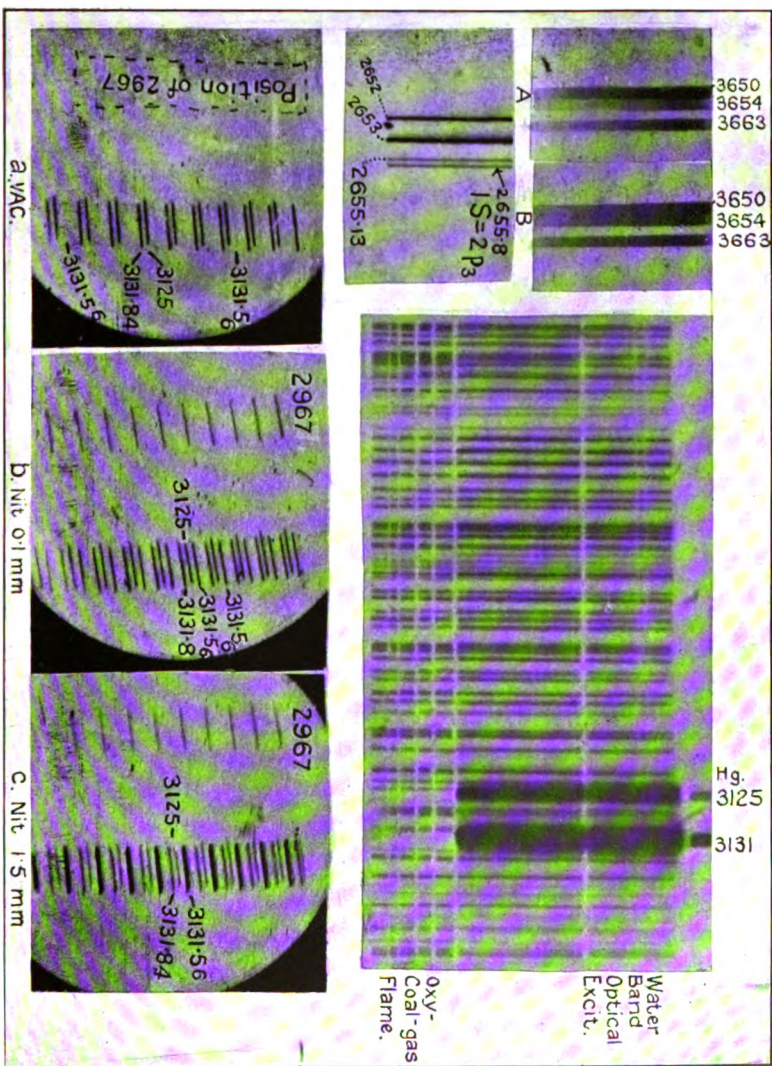
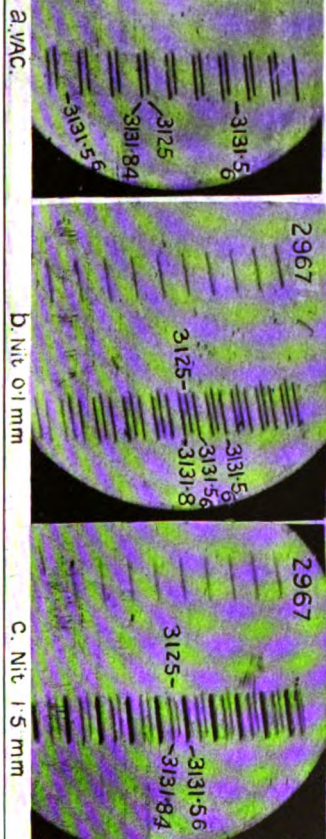
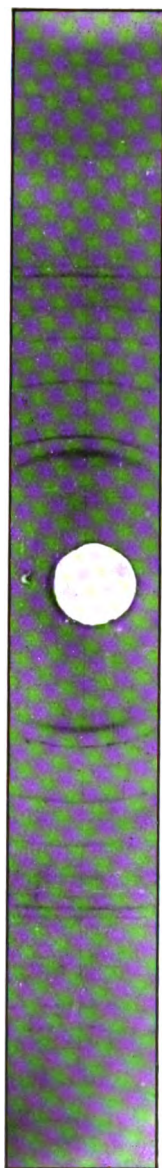


Fig. 3.

Fig. 4.





THE
LONDON, EDINBURGH, AND DUBLIN
PHILOSOPHICAL MAGAZINE
AND
JOURNAL OF SCIENCE.

[SEVENTH SERIES.]

OCTOBER 1927.

LVI. *On a Theory of the Magnetic Properties of Iron and other Metals**. By R. H. DE WAARD, D.Sc. (Utrecht, Holland).†

A. A REMARKABLE PROPERTY OF THE MECHANISM OF
MAGNETIZATION IN FERROMAGNETIC METALS.

CONSIDER a cylindrical bar of some ferromagnetic metal (=a metal showing the phenomenon of magnetic hysteresis), *e.g.* of iron, and let it be placed along the axis of a very long solenoid. When a given electric current is sent through this solenoid, the bar will find itself in a homogeneous magnetic field of known intensity H ‡ which can be changed in any way desired; the magnetization M of the bar (=the magnetic moment per c.c.) may in this way pass through a series of different values. We will suppose the bar so long that, whatever the value of M may be, the demagnetizing force (which is proportional to M) may be neglected.

Let us now start from the "normal" state, where $H=M=0$; we shall then be able, by suitable changes of H , to make M pass through a series of values which

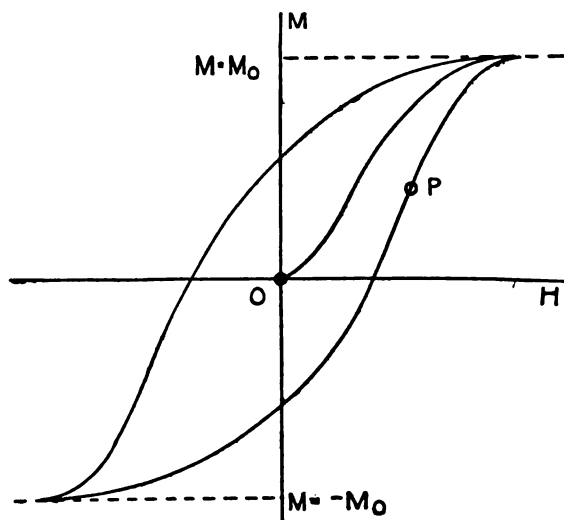
* The principles of the theory worked out in some detail in this paper have been given in the author's Dutch thesis: 'Ferromagnetisme en Kristalstructuur.' Dissert. Utrecht, 1924. A translation in French is found in: *Archives Néerlandaises*, ser. iii. A, tome viii., 1925 ("Ferromagnétisme et structure cristalline").

† Communicated by Prof. L. S. Ornstein.

‡ All magnetic quantities will be expressed by means of the units used by Lorentz in 'The Theory of Electrons' (Leipzig and New York, 1916).

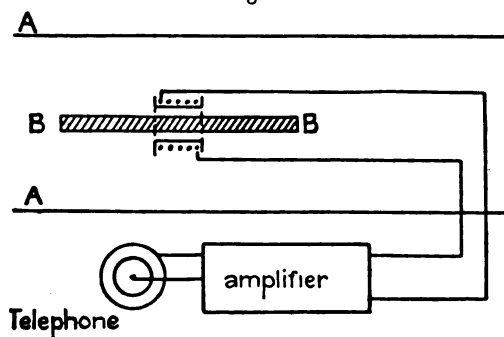
are, in their dependence on H , shown by the well-known curves of hysteresis (fig. 1).

Fig. 1.



An insight into the mechanism of such a process can be obtained from the experiments of Barkhausen*, which show that M is not only changing continuously, but also partly by small jumps. The principle of these experiments is

Fig. 2.



BB, iron bar.

AA, cross-section of the solenoid.

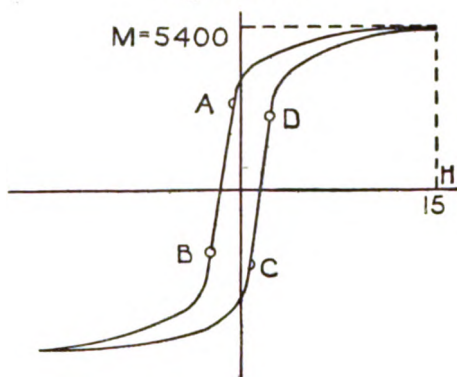
that in a small coil put round a bar like the one considered, every jump of M causes a pulse of induction which can, by means of a triode amplifier, be made detectable in a telephone (fig. 2).

* *Physik. Zs.* 1919, p. 401.

Barkhausen's experiments are repeated and extended by van der Pol *, who points out that in a certain iron bar (wire) whose curve of hysteresis is shown in fig. 3 jumps were observed in the intervals AB and CD

These jumps must be ascribed to sudden changes of the magnetic state of certain sets of iron-crystals, and it is natural to suppose that these changes will consist of an abrupt reversal of the magnetization from positive to negative (resp. from negative to positive) values. *It is, however, easy to show that the shape of a set of crystals*

Fig. 3.—IRON.



which causes a jump of M near A must be extremely prolate and that such a set must be a long row of crystals forming a sort of chain in the direction of the external field.

For convenience we will suppose that the shape of the set is that of a rotational ellipsoid whose axis has the same direction as that of the bar. When, now, the state is realized which is indicated by A in fig. 3, and when for a moment we consider the space occupied by the ellipsoid as an empty space (without changing anything in the magnetic state of the rest of the bar), there will exist a magnetic field H_i inside of it whose intensity is easily calculated (fig. 4).

First there is the external field caused by the solenoid; its intensity

$$H = -0.5$$

can be obtained from fig. 3. Besides that, however, the field should be considered which is caused by the parts

* Proc. Amsterdam, xxiii. p. 980 (1920).

of the bar outside the ellipsoid. The intensity of this field may be written

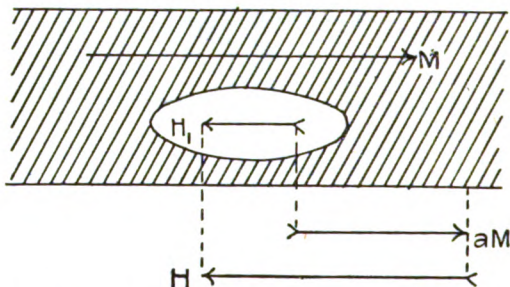
$$aM,$$

when a is the demagnetizing coefficient of the ellipsoid in the direction of the axis. The value of M , as well as that of H_i , can be obtained from fig. 3 ($M=2500$), and consequently one has

$$H_i = -0.5 + 2500a.$$

Thus the set of crystals under consideration which is magnetized in the positive direction finds itself under the influence of a magnetic field of this intensity. When, however, H_i is decreased by a small quantity the magnetization assumes a negative value by a sudden jump.

Fig. 4.



It is now obvious that this would be impossible if H_i were positive, for in this case there would be no question of any tendency to such a reversal. Consequently one has

$$H_i = -0.5 + 2500a < 0,$$

and one must conclude that

$$a < \frac{0.5}{2500} \quad \text{or} \quad a < 0.0002.$$

Now the proportion of the axes of a rotational ellipsoid for which

$$a < 0.0002$$

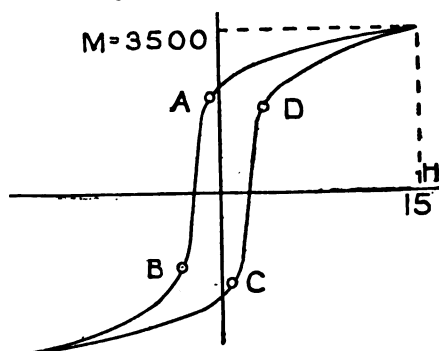
is smaller than 1:100. We have therefore proved that a set of iron-crystals which causes a discontinuity of M in the neighbourhood of A must be a long chain the length of which is certainly longer than 100 cross-diameters. *On first sight such a result looks very strange. It is, however, in perfect accordance with experiments.* Van der Pol also examined a bar of nickel-steel and got in that way the

M-H-curve shown in fig. 5. The same sort of argument as that used for fig. 3 in this case leads to

$$a < \frac{1}{2000} = 0.0005,$$

which corresponds to a proportion of the axes of the ellipsoid smaller than 1:80. Van der Pol was then able to estimate both the length and the cross-section of a set of iron-crystals which gave rise to certain discontinuities of M. In order to find the length of a set he registered,

Fig. 5.—NICKEL-STEEL.



with the help of two galvanometers, the pulses of inductions caused by these discontinuities in two different coils (like the one of fig. 2) which he placed round the bar at some distance one from the other; it appeared that certain discontinuities were still synchronously registered when this distance was as great as 7 cm. Hence the sets of crystals causing these discontinuities must have had a length of at least 7 cm. From the magnitude of the discontinuities it was possible to deduce that the cross-diameter was of the order of 0.05 mm., and these two numbers give rise to a proportion of axes of

$$0.005 : 7 = 1 : 1400,$$

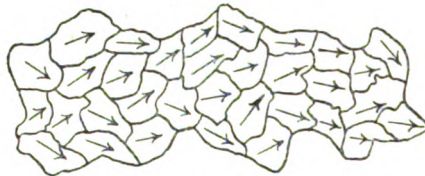
much smaller still than the proportion 1:80 which was *a priori* considered to be improbably small.

In order to make the obtained result more acceptable, we shall proceed to a more detailed consideration of the mechanism of the process of magnetization. We know that an iron bar must be considered as an aggregate of iron-crystals. When such an aggregate is under the

influence of a strong magnetic field H , every crystal will possess a nearly saturated magnetization in the direction of the field (fig. 6 *a*). When now this field is decreased until

Fig. 6 *a*.

$H=0$ the magnetic state of the crystals will to a great extent be determined by the structure of the aggregate, with this condition, that the magnetization will still show a preference for the original direction of H and that in no crystal shall there be already a component of magnetization in the opposite direction (fig. 6 *b*). During further decrement of

Fig. 6 *b*.

H components of magnetization in the negative direction will gradually appear, and this does not only occur continuously, but also, as we have seen, by jumps.

Let us now consider a certain crystal K . This crystal is under the influence of the external field and under that of the surrounding parts of the aggregate. When K is of the same order of magnitude in all directions these surrounding parts will cause inside the space of K a magnetic field of the order of $1/3 M$ (fig. 7 *a*). Together with the external field this gives rise to a field

$$H_i = 1/3 M + H$$

acting on K . When now we keep in mind that a changing of the magnetization of K to a negative value without appreciable changes in the neighbourhood will only be possible when

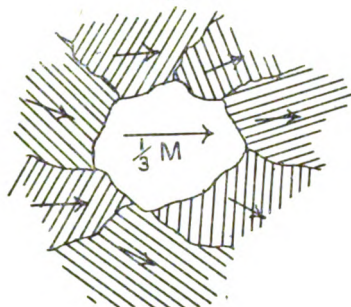
$$H_i < 0,$$

we see that such a change only comes into question when

$$H < -1/3 M.$$

For a simultaneous reversal of the magnetization in a long row R of crystals like K the conditions are much sooner favourable. When, for instance, such a row consists of 50 crystals and when consequently its length is about

Fig. 7 a.



50 times the mean cross-diameter, the surrounding aggregate causes inside R a magnetic field of the order of

$$0.0015 M \text{ (fig. 7 b),}$$

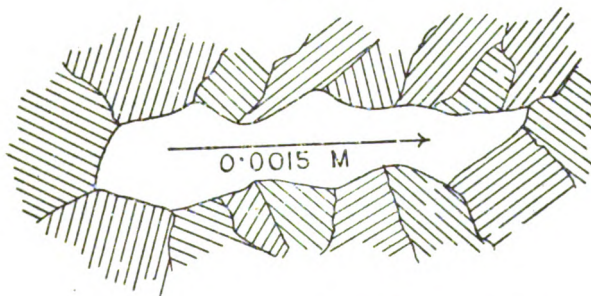
and one has

$$H_i = 0.0015 M + H;$$

therefore a reversal of the magnetization of R may be possible as soon as

$$H < -0.0015 M.$$

Fig. 7 b.



In general we may say that the more prolate the shape of a complex of crystals is, the sooner the complex will show a tendency to a simultaneous and concurrent jump of the magnetizations in the different parts. It is however clear, that the constitution of the different chains with magnetic coherence largely depends on the structure of the aggregate.

The mechanism of the process of magnetization in the interval AB may now be imagined to be that abrupt changes of the magnetization into negative values will in the beginning only occur in extremely prolate sets of crystals, but after a time also in chains of smaller length. There is, however, some reason to suppose that there are also crystals which do not show such a sudden change and whose magnetizations continuously decrease from positive to negative values (apart from small discontinuities caused by real jumps of crystals in the neighbourhood); these changes will as well as the real jumps occur for the greater part in the interval AB. When B is reached it seems probable that no crystal is left with a component of magnetization in the positive direction of H ; and when, by further decrement of H , M is still more decreased, this must be ascribed to a forcing of magnetizations in the negative direction of H . The picture of the mechanism of the process of magnetization given in this section, which is evidently also applicable to the other branch of the curve of hysteresis, will be further illustrated and specified in the following sections.

B. A GENERAL THEORY OF FERROMAGNETISM WITH SIMPLE APPLICATIONS.

§ 1. *Definitions and Fundamental Formulæ.*

The magnetic force H in any point of space is the resultant of two magnetic forces H_e and H_m which are caused by electric currents and magnetized bodies respectively.

We consider a system of ferromagnetic bodies under the influence of the magnetic field of constant or slowly varying electric currents. Such a system represents a certain amount of energy which depends on the currents and on the magnetic state of the bodies. We will assume that the part of this energy depending on M is given by the formula

$$E = -\int (H_e \cdot M) d\tau - \frac{1}{2} \int (H_m \cdot M) d\tau + \frac{1}{2} \int \theta M^2 \cdot d\tau, \quad (1)$$

in which the integrals must be taken over the space occupied by the magnetized bodies. The first term of this equation does not require much explanation: the magnetic moment of an element of volume $d\tau$ with a magnetization M is $M \cdot d\tau$, and the energy of such a magnetic moment with respect to the electric currents (which cause the field H_e) is

$$-(H_e \cdot M) d\tau,$$

when $(H_e \cdot M)$ denotes the scalar product of the vectors H_e and M .

The second and third terms must be considered in mutual connexion. At first sight it might seem that the energy of an element $d\tau$ with respect to the rest of the magnetic bodies is equal to

$$-(H_m \cdot M) d\tau ;$$

in reality, however, it differs from that quantity because H_m is not the magnetic force caused inside $d\tau$ by the surrounding substance only but contains also the magnetic field caused by $d\tau$ itself. When nevertheless we make use of this expression and when we ascribe half of it to the element $d\tau$ and the other half to the rest of the magnetic bodies, we must keep in mind that the third term must account for some compensation. In a given element $d\tau$ this compensation can evidently only depend on M .

Except for this compensation the third term will account for the supposition that (even apart from the energy with respect to its own field) an element $d\tau$ of a magnetic body contains a certain amount of energy in virtue of the fact of its magnetization. The simplest assumption which in this respect can be made is this, that the integrand of the third term

$$\frac{1}{2} \theta M^2 \cdot d\tau$$

is proportional to the square of the local magnetization: θ is a constant which must be expected to have different values in different ferromagnetic substances.

By these remarks the fundamental formula (1) seems to be sufficiently explained.

§ 2. *Application of the Theory to Homogeneous Ellipsoids in Homogeneous Magnetic Fields.*

Consider an ellipsoid consisting of a homogeneous ferromagnetic substance and let it be placed in a homogeneous magnetic field H_e (caused by given electric currents) with one of the axes (Ox) in the direction of this field. When we denote the demagnetizing coefficients in the directions $Ox Oy Oz$ of the axes of the ellipsoid by a , b , and c ($a+b+c=1$) and when we suppose a homogeneous magnetization M throughout the ellipsoid, the components of H_m along the axes are

$$-aM_x, \quad -bM_y, \quad -cM_z,$$

and the energy per cm.³ of the ellipsoid may be written :

$$E = -H_e M_x + \frac{1}{2} (aM_x^2 + bM_y^2 + cM_z^2) + \frac{1}{2} \theta (M_x^2 + M_y^2 + M_z^2).$$

Putting $a + \theta = A, \quad b + \theta = B, \quad c + \theta = C, \quad . \quad . \quad . \quad (2)$

we get $E = -H_e M_x + \frac{1}{2}(AM_x^2 + BM_y^2 + CM_z^2). \quad . \quad . \quad (3)$

With the help of this formula we will now examine how, in different cases, M behaves when H_e is varied. In accordance with a well-known experimental fact in ferromagnetism we will, however, suppose that the absolute value of M is limited and can never exceed a certain magnetization of saturation M_0 . Thus we have the condition:

$$M_x^2 + M_y^2 + M_z^2 \leq M_0^2. \quad . \quad . \quad . \quad (4)$$

Our task is now to find the sets of values of M_x, M_y, M_z which satisfy the condition (4) and for which the energy E has minimum values. This problem is very much simplified when we suppose that the axis Oz of the ellipsoid is shorter than Oy , which is evidently possible without any loss of generality. We then have

$$b \leq c, \text{ and consequently } B \leq C,$$

and it is easily seen that under these circumstances we may put

$$M_z = 0.$$

When, indeed, M has a component perpendicular to Ox the expression

$$\frac{1}{2}(BM_y^2 + CM_z^2)$$

and consequently the energy E can only have minimum values when this component has the direction of the axis Oy . Instead of (3) we thus get the formula

$$E = -M_x H_e + \frac{1}{2}(AM_x^2 + BM_y^2), \quad . \quad . \quad . \quad (3a)$$

which may be written

$$E = \frac{1}{2}A \left(M_x - \frac{H_e}{A} \right)^2 + \frac{1}{2}BM_y^2 - \frac{H_e^2}{2A}.$$

When H_e and E are given, this equation expresses a relation between M_x and M_y which, in a M_x - M_y -diagram,

* A condition of this kind is lacking in the general theory of magnetism given by Helmholtz, 'Vorlesungen über theoretische Physik,' iv. §52, which is based on much the same principles as the one explained in this paper. This theory is for this reason unable to account for the phenomena of ferromagnetism. It cannot explain diamagnetic phenomena either (as is wrongly supposed), since it shows itself in contradiction to these phenomena as soon as stability is considered.

The first of these cases will be treated in some detail. Of the treatment of the other cases, which is very much the same, only the results will be mentioned.

Treatment of Case I. ($B > 0, A < 0$).

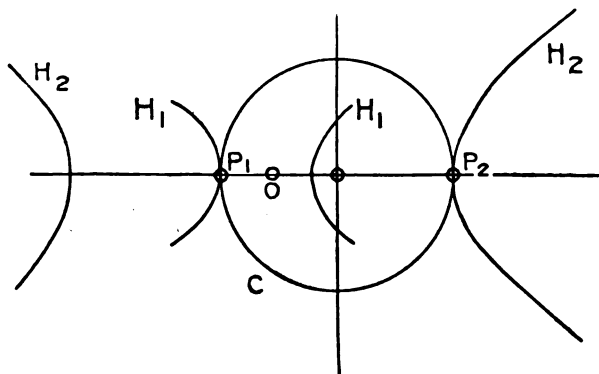
Let H_e have a given positive value : the point $O(\frac{H_e}{A}, 0)$ of fig. 8 is then situated on the left side of the origin. The E-conics determined by the equation (3a) are hyperbolæ of which the axis of M_x is the real axis. The smaller values of E correspond to the more excentric hyperbolæ.

When

$$H_e < -AM_0$$

it is clear that there are two points P_1 and P_2 (fig. 9)

Fig. 9.



satisfying the conditions (a) and (b) mentioned above. These points correspond to the states

$$P_1 : M_x = -M_0, \quad M_y = 0,$$

$$P_2 : M_x = M_0, \quad M_y = 0.$$

When

$$H_e > -AM_0$$

the point P_1 falls out of consideration and the one point P which is left corresponds to the state

$$M_x = M_0, \quad M_y = 0.$$

As analogous results are obtained when H_e is negative, we are led to the following conclusions :—

“ When $H_e > -AM_0$ we must have $M_x = M_0$; the magnetization is then saturated in the positive direction of Ox .

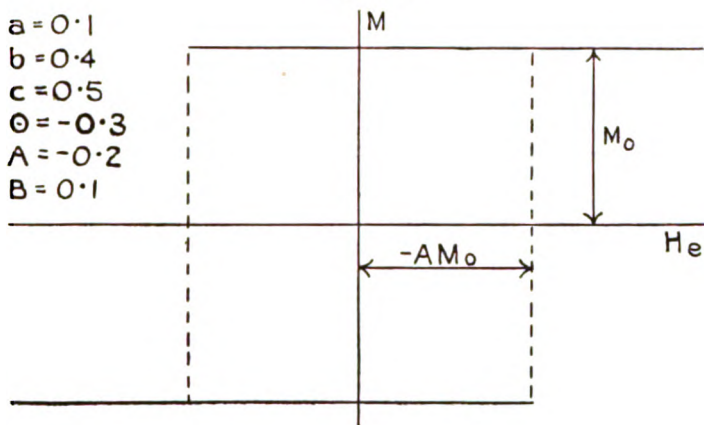
As H decreases this magnetization will persist as long as

$H_e > AM_0$, but as soon as $H_e = AM_0$ it will suddenly change into saturation in the negative direction ($M_x = -M_0$) and then persist as H_e decreases further.

When, on the contrary, H_e is increasing from a value $< AM_0$, the magnetization will again change into positive saturation at the moment that $H_e = -AM_0$.

The behaviour of M_x expressed in these sentences is graphically shown in the M_x - H_e -diagram of fig. 10 a. We

Fig. 10 a.



unit of length on axis of abscissæ
 unit of length on axis of ordinates = 5.

have evidently to do with a case in which the phenomenon of magnetic hysteresis is present in its simplest form. The coercive force is

$$H_e = -AM_0.$$

Cases II. ($B > 0$, $A > 0$) and III. ($B < 0$, $A < B$).

The results of the treatment of these cases are respectively shown in the M_x - H_e -diagram of figs. 11 a and 12 a.

Case IV. ($B < 0$, $A > B$).

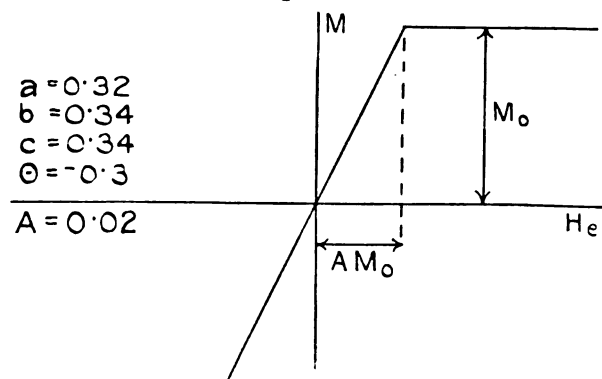
This case is rather uninteresting. When $H_e = 0$, one has

$$M_x = 0, \quad M_y = \pm M_0.$$

When now H_e increases the magnetization keeps its saturation value M_0 , but its direction changes in such a way

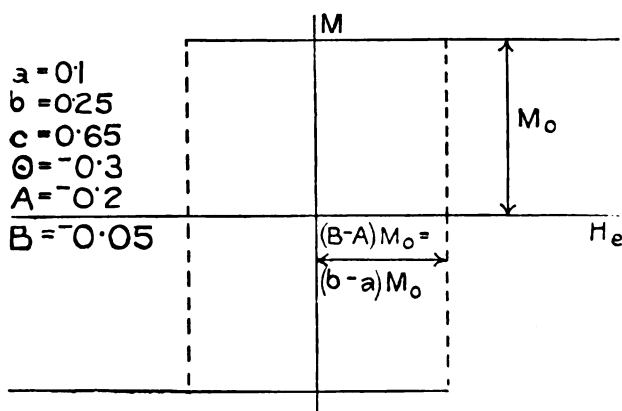
that the angle it includes with the axis Ox continually decreases and becomes zero on the moment that H_e surpasses a certain value. When, after this, H_e decreases, essentially the same states are realized in reversed succession.

Fig. 11 a.



$$\frac{\text{unit of length on axis of abscissæ}}{\text{unit of length on axis of ordinates}} = 25.$$

Fig. 12 a.



$$\frac{\text{unit of length on axis of abscissæ}}{\text{unit of length on axis of ordinates}} = 5.$$

Negative values of H_e evidently lead to analogous results.

In order to make these results comprehensible we will add a few remarks. As $A > B$ we have $a > b$, which implies

that the axis Ox of the ellipsoid considered is, just as the axis Oz (see p. 650), shorter than the axis Oy . Thus the axis Oy is the longest of the three, and in the state without an external field ($H_e=0$) the magnetization is saturated in the positive or in the negative direction of this longest axis. By applying an external field along the axis Ox one can make this magnetization deflect to the x -direction.

As in practice of ferromagnetic measurements, however, use is generally made of long wires or bars to which external fields are applied in the direction of greatest length, a thorough discussion of the case under consideration is of no importance.

Comparative Discussion of the Cases I., II., and III.

A consideration of the cases I., II., and III. immediately shows that the presence or absence of hysteresis only depends on the value of A ; when A is negative there will be hysteresis, and when it is positive there will be none.

Now we know that in virtue of the formula

$$A = a + \theta$$

A depends both on the shape of the ellipsoid considered and on the material of which it is composed; thus the question whether a given ferromagnetic body will show the phenomenon of hysteresis can only be answered when not only the material but also the shape of the body is taken into account.

In practice, however, this is probably never done: it is generally admitted that there exist substances which show magnetic hysteresis and other substances which do not, and that the shape is, in this respect, of no essential importance. Or, in more definite terms: it is generally supposed that in a given substance the behaviour of the magnetization M in any point only depends on that of the local magnetic field,

$$H = H_e + M_m,$$

and that in the relation between M and H the shape of the magnetic body considered does not appear*.

The reason of this generally accepted wrong supposition

* The relation between M and H_e , however, is always supposed to depend and in fact does depend on the shape of the body. Thus in an oblate rotational ellipsoid of iron, magnetized along the axis, the demagnetizing force H_m is so large that an external field H_e of extreme intensity is necessary to bring about a total field H inside the ellipsoid which is large enough to give rise to a reasonable magnetization and a perceptible hysteresis. For this reason measurements of hysteresis are always carried out on long wires or bars.

will be explained in connexion with the formula (4 a) :

$$E = -M_x H_e + \frac{1}{2}(AM_x^2 + BM_y^2).$$

The ordinary conditions of equilibrium are :

$$\frac{\partial E}{\partial M_x} = -H_e + AM_x = 0 \quad \text{or} \quad AM_x = H_e,$$

$$\frac{\partial E}{\partial M_y} = BM_y = 0 \quad \text{or} \quad M_y = 0.$$

When we now neglect the conditions of stability we find

$$H_m = -aM_x,$$

and consequently

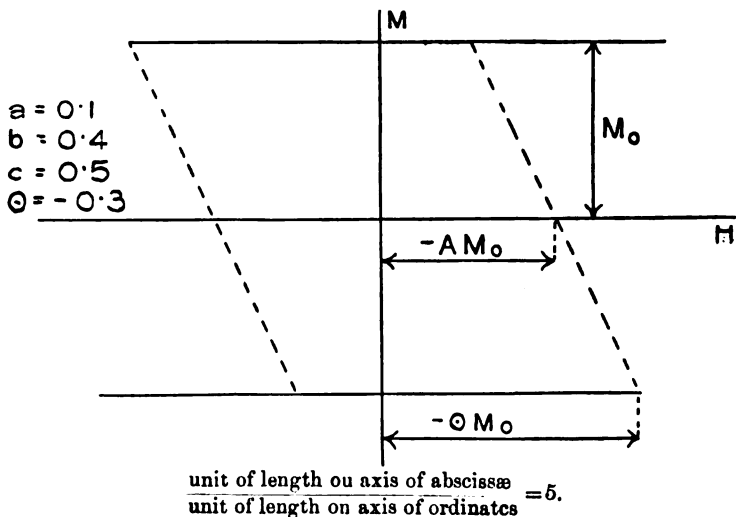
$$H = H_e + H_m = AM_x - aM_x = \theta M_x.$$

Now, in the formula

$$H = \theta M_x$$

there is no quantity which has to do with the shape of the

Fig. 10 b.

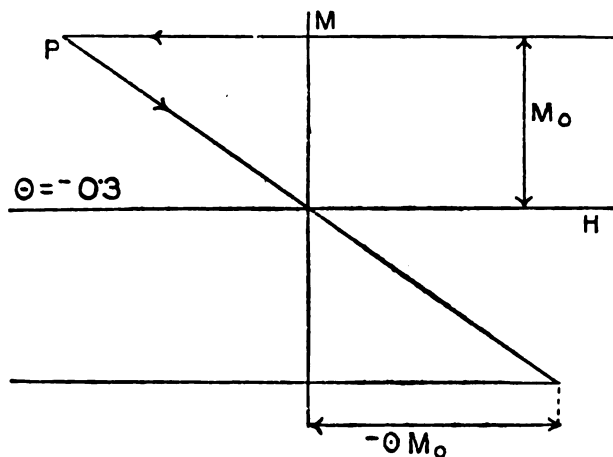


ellipsoid considered; thus, when stability is neglected one gets the impression that in a given ferromagnetic substance (that is to say, when θ is given) the magnetization only depends on the total magnetic field H .

That in reality this is not the case is clearly seen when the M_x - H_e -diagrams of figs. 10 a, 11 a, and 12 a are transformed into M_x - H -diagrams; these M_x - H -diagrams are

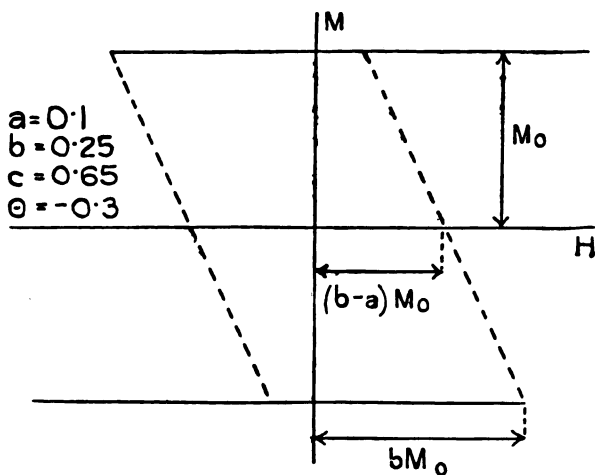
shown in figs. 10 *b*, 11 *b*, and 12 *b*, and are by no means identical. In order to make them as illustrative as possible

Fig. 11 *b*.



unit of length on axis of abscissæ = 5.
unit of length on axis of ordinates = 5.

Fig. 12 *b*.



unit of length on axis of abscissæ = 5.
unit of length on axis of ordinates = 5.

of the influence of the shape of a body on its magnetic properties, they have been drawn in such a way that the

value of θ (or the nature of the substance in question) is the same in the three cases ($\theta = -0.3$). Evidently the occurrence of hysteresis is more probable the more prolate the ellipsoid is.

We thus have been led to the conclusion that certain values of θ may give rise to three different kinds of M_x - H_x -diagrams. This is, however, not the case for every value of θ . When, for instance, θ is positive, A, B, and C are positive as well and we have always to do with a M_x - H_x -diagram like that of fig. 11 b; hysteresis is impossible. When on the contrary $\theta < -1/3$, there is at least one of the coefficients A, B, and C which is < 0 (because at least one of the coefficients a , b , and c is $\leq 1/3$), and there is hysteresis in every case (except in that of a sphere), both of the diagrams 10 a and 12 a being possible*. When $-1/3 < \theta < 0$, every one of the three cases of figs. 10 a, 11 a, and 12 a is possible; presence or absence of hysteresis depend on the shape of the ellipsoid considered.

It will be clear that we have treated in this paragraph the simplest cases† of the simplest theory of ferromagnetism one can think of. Nevertheless these simple cases were in some respects more complicated than is ever admitted in any case occurring in practice. We may therefore conclude that it is absolutely necessary that in the interpretation of experiments on ferromagnetism the following facts are taken into account:—

1. That it is probable that the magnetic properties of bodies (for instance, presence or absence of magnetic hysteresis) will essentially depend on the shape of these bodies; and
2. That there is no reason to believe that the behaviour of the magnetization will merely depend on that of the internal field H .

* See footnote on p. 650. When one would try to describe the phenomena of diamagnetism with the help of the formula $H = \theta M_x$, it would be necessary to introduce strongly negative values of θ ; even for bismuth, the substance with the strongest diamagnetism, one would find $\theta = -560,000$. In the present theory such a value of θ would, however, necessarily lead to the presence of magnetic hysteresis, and the only stable states would be those with saturated magnetization. The theory is therefore unable to explain the phenomena of diamagnetism.

† The conditions of these simple cases have been recently realized in experiments by W. Gerlach (*Zs. f. Physik*, xxxviii. p. 828, 1926) and by K. Honda and S. Kaya (*Sc. Rep. of the Tohoku Imp. Univ.* xv. 6, p. 721, 1926) on the magnetic properties of specimens of iron consisting of single crystals. In a following paper I hope to discuss the results of these experiments in connexion with the present theory.

§ 3. Two Ellipsoids.

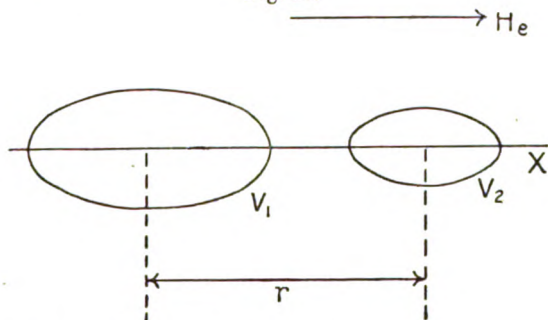
Among the many different views concerning the mechanism of the process of magnetization in ferromagnetic substances there is a very plausible one which we will first briefly explain. It will then be easy to show that in reality it is certainly wrong.

The sort of argument in question is the following :

“An iron bar is an aggregate of a great number of iron crystals. The magnetic state of this bar must consequently be considered as the sum of the magnetic states of these crystals. If the bar shows the phenomenon of magnetic hysteresis the crystals or at least a number of them must do the same, and when the magnetization of such a crystal is plotted against the external field H_e or against the total field H (in a very long bar these fields hardly differ) one has to expect a loop of hysteresis.”

Thus far the argument is correct. It is, however, pursued in such a way that it is believed to be obvious that the

Fig. 13.



crystal will show the same loop when it is loosened from the surrounding substance and independently examined in a magnetic field.

We will show that this supposition is by no means probable. For this purpose we will apply our theory to a system of two uniform ellipsoids, whose longest axes are in the same straight line. We suppose that each of these ellipsoids, when considered on its own, does not show any hysteresis; this will be the case if $0 < A < B < C$. The volumes of the ellipsoids will be denoted by v_1 and v_2 ($v_1 > v_2$). When now the distance r of their centres is so large that the field of the first ellipsoid inside the second one may be considered to be homogeneous, and inversely, and when an external field H_e is applied in the (x -)direction

of the line joining the centres, the total energy may be written :

$$\begin{aligned}
 E = & \frac{v_1}{2} (AM_{1x}^2 + BM_{1y}^2 + CM_{1z}^2) \\
 & + \frac{v_2}{2} (AM_{2x}^2 + BM_{2y}^2 + CM_{2z}^2) \\
 & - \frac{v_1 v_2}{4\pi r^3} (2M_{1x}M_{2x} - M_{1y}M_{2y} - M_{1z}M_{2z}) \\
 & - H_0(v_1 M_{1x} + v_2 M_{2x}).
 \end{aligned}$$

As there are two accessory conditions to be considered,

$M_{1x}^2 + M_{1y}^2 + M_{1z}^2 \leq M_0^2$ and $M_{2x}^2 + M_{2y}^2 + M_{2z}^2 \leq M_0^2$,
it is a rather complicated matter to find the sets of values of

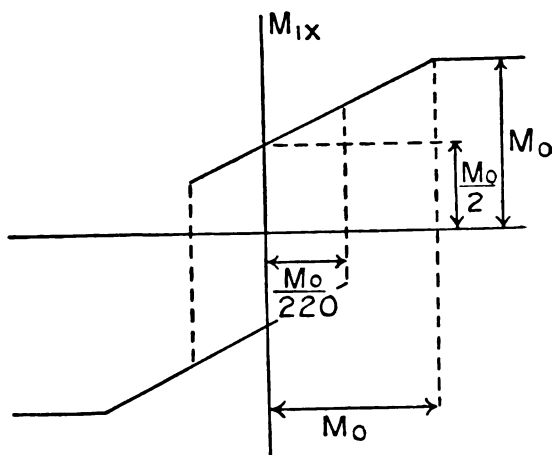
$$M_{1x} \ M_{1y} \ M_{1z} \ M_{2x} \ M_{2y} \ M_{2z}$$

for which E has a minimum value ; we will therefore only give the main results of the analysis :—

“Magnetic hysteresis will be present if

$$A < \frac{\sqrt{v_1 v_2}}{2\pi r^3} ;$$

Fig. 13 a.



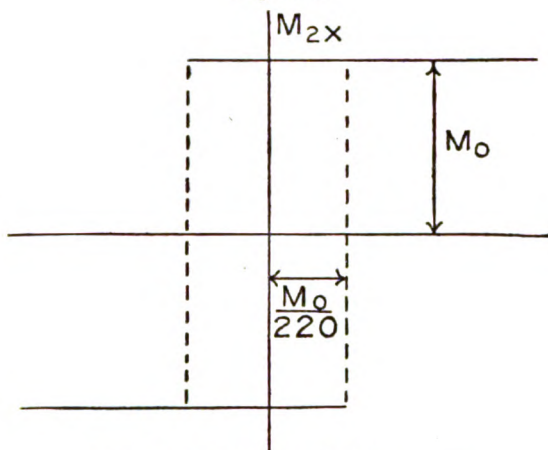
$\frac{\text{unit of length on axis of abscissae}}{\text{unit of length on axis of ordinates}} = 100.$

this is, for instance, the case when

$$\frac{v_1}{2\pi r^3} = 0.09, \quad \frac{v_2}{2\pi r^3} = 0.01, \quad A = 0.02.$$

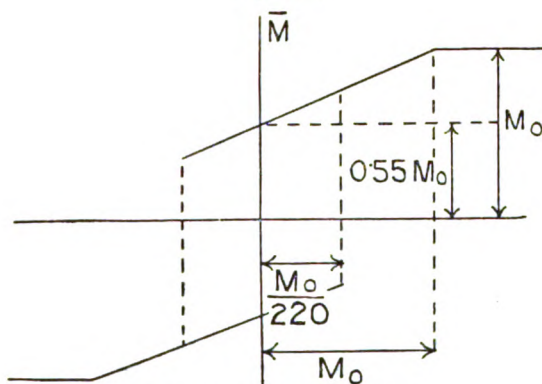
When this case is more closely considered it appears that M_{1x} and M_{2x} depend on H_e in the ways shown in figs. 13 *a*

Fig. 13 *b*.



$\frac{\text{unit of length on axis of abscissæ}}{\text{unit of length on axis of ordinates}} = 100.$

Fig. 13 *c*.



$\frac{\text{unit of length on axis of abscissæ}}{\text{unit of length on axis of ordinates}} = 100.$

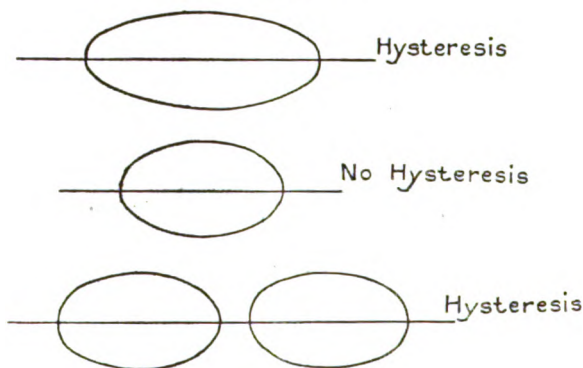
and 13 *b*; the other components of M_1 and M_2 are always $=0$. In fig. 13 *c* the mean magnetization

$$\bar{M} = 0.9M_{1x} + 0.1M_{2x}$$

is shown in its functional dependence on H_e .

We thus see that it is possible that magnetic hysteresis is found in a system of two ellipsoids which do not show any phenomenon of this kind when they are considered separately. After what has been said in § 2, however, this is by no means surprising. In this paragraph we have found that a prolate ellipsoid e_1 of a certain substance may show magnetic hysteresis, while a less prolate ellipsoid e_2 of the same material is free from this property. It can therefore hardly be considered as striking that a system of two ellipsoids e_2 placed one behind the other has a property in common with e_1 which is absent in e_2 (fig. 14).

Fig. 14.



This result is of great importance for our further consideration. It shows that an iron bar may possess the property of magnetic hysteresis even when this phenomenon does not occur in any of the composing crystals. Now, in the following section we shall be obliged to ascribe to a metal like iron a value of θ of such a kind that in a single rotational ellipsoid of this substance a proportion of axes of about 1:100 would be necessary to give rise to any hysteresis; thus it is of interest to know that there is no reason to abandon the theory because needle-shaped crystals of this kind will hardly be present in ordinary iron. The magnetic hysteresis of iron may be just as well caused by the reversal of the magnetization in the long chains of crystals considered in the first section; in their magnetic properties these chains will certainly show some analogy with extremely prolate homogeneous ellipsoids.

C. ESTIMATION OF THE VALUES OF θ FOR IRON, NICKEL,
COBALT, AND SOME SPECIES OF STEEL.

Our aim is to find the values which must be ascribed to the quantity θ in metals like iron, nickel, etc.

In the first place these values must be negative, for in section B we have found that otherwise hysteresis is impossible.

In order to obtain numerical approximations of θ it is necessary to consider more closely the properties of the chains of crystals which have been so frequently mentioned. As to the length of these chains in some iron or nickel wire we must suppose that they will be as long as is consistent with the structure of the wire; or in more definite terms: when there exists, in the wire, a row of crystals which passes through it over a long distance without showing marked discontinuities, it is probable that, in the processes of magnetization and demagnetization along the axis of the wire, this row must be considered as a magnetic unit. The fact that in nickel-steel chains of about 7 cm. of length have been found experimentally is certainly in favour of this view, which has appeared to be probable for theoretical reasons.

At the end of the second section we have pointed out that the magnetic properties of these chains are, to a certain extent, comparable to those of prolate homogeneous ellipsoids. It is, however, clear that when in a chain of crystals and in a homogeneous ellipsoid of about the same shape θ has the same negative value, and when both show the phenomenon of hysteresis, the stronger hysteresis will be found in the ellipsoid. This is easily seen when we keep in mind that during the performance of a loop of hysteresis a series of states are realized which possess only a conditional stability; when in these states perturbations of sufficient amount are applied other states will arise in which the energy has smaller values. It is then at once evident that in a chain of crystals with its inevitable discontinuities a way to the lower stages of energy is more easily found than in a homogeneous ellipsoid of about the same shape, and that in such a chain the magnetization will be more inclined to conform to the external field. When, nevertheless, in the following discussion we shall treat a chain as a homogeneous ellipsoid and when, in that supposition, we shall find an estimation of the value of θ , we must keep in mind that this estimation will be certainly too large and that the real value of θ will be more strongly and perhaps much more strongly negative.

We first consider the jump of M which occurs in the state indicated by the point A in fig. 3. In the first section we have found that this jump must be ascribed to the reversal of the magnetization in a very long chain of crystals. We will suppose that this chain is just as long as the iron wire itself; it is then unnecessary to consider the magnetic state of the surrounding material and we have only to do with the external field, which has, in the moment of the jump, an intensity of -0.6 units*. The magnetization of saturation M_0 being about 5400 units*, this leads, by an application of the case of fig. 10 a , to a value of A of

$$A = a + \theta = \frac{-0.6}{5400} = -0.0001;$$

an application of the case of fig. 12 a would be impossible, because $b - a$ is, in virtue of the prolateness of the chain, of the order of -0.5 instead of -0.0001 .

When we now take into account the fact that a is of the order of 0.0002 (see p. 644) we find

$$\theta \text{ of the order of } -0.0003;$$

it has already been stated, however, that this estimation is certainly too high, and that the real value of θ will be more strongly negative.

We now consider the jump occurring in the state indicated by B , and we suppose that this jump is caused by the reversal of the magnetization in a rotational ellipsoid whose coefficient of demagnetization in the direction of the axis is a ; this direction will be the same as that of the axis of the wire and that of the external field. The surrounding substance will then, in the space occupied by the ellipsoid (see fig. 4) cause a field

$$aM = -2000 a^*,$$

which, in addition to the external field of -2 units*, leads to a total field of

$$-2000 a - 2 \text{ units,}$$

and consequently, by application of the case of fig. 10 a , to the result

$$A = a + \theta = - \frac{2000 a - 2}{5400}$$

or

$$1.4 a + \theta = -0.0004.$$

* This value is obtained from fig. 3.

In the first place, this result shows that

$$\theta < -0.0004,$$

which is quite consistent with the former estimation ; in this case, however, it is necessary to suppose that the chain causing the jump in B has a small α and consequently a considerable prolateness. The absolute necessity of the formation of these long chains was, besides this, included in the small absolute value of θ provided by the first estimation : even if this value were 100 times too small and if in reality θ were -0.03 , even then a homogeneous rotational ellipsoid would only show hysteresis when the proportion of axes were smaller than 1 : 9.

As to the order of magnitude of the real value of θ , we notice that in connexion with the formula

$$\theta < -0.0004,$$

we might suppose that θ is of the order of -0.001 . In this way, however, the lack of homogeneity of the chain considered would not have been taken into account, and consequently it is advisable to suppose that in reality θ is of the order of about -0.001 or -0.01 .

It will be clear that a small absolute value of θ of this kind will correspond to but a very moderate disposition on the part of the crystals to form coherent chains, for these chains must be very long and besides that radical discontinuities must be absent. Thus a considerable number of crystals will not co-operate in any chain and will have their magnetic states changed in a continuous way (apart from small discontinuities induced by primary jumps of the magnetization in chains in the neighbourhood). It is certain that an important part of the changes of the magnetization of the total wire, both inside and outside the intervals AB and CD, must be ascribed just to these crystals.

By application of the same sort of argument as that used in the discussion of the iron wire, estimations of the value of θ have been effectuated for a specimen of nickel-steel examined by van der Pol (see fig. 5), for a piece of very hard steel examined by Ewing*, and for nickel† and cobalt‡. In the last three cases the estimations are based upon curves of hysteresis of which the intervals AB and CD are unknown and had to be determined by comparison with the known intervals in figs. 3 and 5. In all the cases

* 'Magnetic Induction in Iron and other Metals' (New York, 1894), p. 84. † *Ibid.* p. 87. ‡ *Ibid.* p. 89.

mentioned one finds that θ must be of the order of about -0.1 or -0.01 .

These numbers will be considered in connexion with the two other quantities concerning ferromagnetic phenomena given in the following table:—

Metal.	Order of magnitude of θ .	Initial susceptibility.	H_c/M_0 .
Iron	-0.001 to -0.01	185	0.000,25
Nickel-steel	-0.01 to -0.1	—	0.000,57
Hardened steel ...		50	0.003,6
Nickel.....		40	0.001,6
Cobalt.....		75	0.001,3

1. *The initial susceptibility.*

In the fundamental formula (1) the specific properties of the material considered only enter in the term

$$\frac{1}{2} \int \theta M^2 d\tau.$$

It is clear that the smaller the absolute value of θ is, the smaller the influence of this term will be. Thus it is evident that a small absolute value of θ will correspond to a great tendency of the magnetization to conform to the external field, that is to say, to a large initial susceptibility.

As the table shows, this conclusion is in good accordance with experimental data.

2. *The coercive force expressed in terms of the magnetization of saturation (=the quantity H_c/M_0).*

The table shows that the larger absolute values of this quantity correspond to the stronger negative values of θ . This is just what we should expect from theoretical considerations. For we know that in a chain of crystals of given length these stronger negative values of θ give rise to the larger values of the quantity $\frac{H_c}{M_0}$ for the chain (see fig. 10a):

$$\frac{H_c}{M_0} = -A = -a - \theta.$$

Finally an important point in the process of magnetization needs discussion. It has been said that in the cases of figs. 3 and 5, jumps of the magnetization have been observed

by van der Pol in the intervals AB and CD. If our theory is correct it is, however, necessary that greater or smaller jumps also occur beyond these intervals: otherwise AB and CD would be the only parts of the two branches of the curve of hysteresis which do not coincide. Meanwhile it should be observed that not every jump is necessarily connected with a complete reversal of the magnetization in some chain of crystals; it could as well be caused by changes of the direction of the magnetization in some crystals over angles smaller than 90° .

In the cases of figs. 3 and 5, processes of this kind must be expected to occur in the descending branch in the interval on the left of B and in the ascending branch in the interval on the right of D.

LVII. *The Effect of the Acidity of the Support on the Structure of Monomolecular Films.* By HANS EGNÉR and GUNNAR HÄGG*.

FROM the investigations of Langmuir and Adam it is well known that the properties of a monomolecular film spread on water show a sudden change at a certain acidity of the supporting water. Adam† found, for instance, that a film of palmitic acid under low lateral pressure occupied a larger area per molecule when the pH of the water was less than 5.5, than when it was above that point. This critical acidity proved to be almost the same for all films of fatty acids. (On an average corresponding to a hydrogen ion concentration of 10^{-5} N.)

Adam explains this change in area by assuming two different structures of the film. In the case of fatty acids the attraction between the carboxyl groups and the support is supposed to increase as the hydrogen ion concentration in the latter decreases. When this concentration is above 10^{-5} N, the molecules arrange themselves in two levels, one deeper and one higher, the head groups of the higher molecules fitting into the recesses between head and chain of the deeper ones. The results of Adam indicate that in this case the packing is so close that the carbon chains are in contact with one another.

So far as the authors know no attempt has been made to explain just *why* such a sudden change in attraction takes

* Communicated by Prof. F. G. Donnan, F.R.S.

† Proc. Roy. Soc. A, xcix. p. 336 (1921).

place at a certain acidity, *why* this acidity for films of fatty acids corresponds to a pH of about 5, and *why* this critical acidity seems to be practically the same for all fatty acids, although the absolute attraction between these acids and water must vary considerably even for the higher ones. It appeared to us, however, that the questions just asked might be answered, easily and in a quite natural way, if the dissociation equilibria of the film-forming substances are taken into consideration. This will be done in the following brief discussion of the system fatty acid-water, which is the only one for which data are available. As will be pointed out below, there is reason to believe, however, that the same phenomena take place in other systems of the same character.

According to the law of mass action, the relation between pH and the degree of dissociation (α) of an acid is governed by the well-known equation

$$\frac{\alpha}{1-\alpha} = 10^{pH-pK_a},$$

where pK_a is the negative logarithm of its dissociation constant. If we proceed along the pH axis, the transformation from the undissociated to the dissociated form is most rapid when $pH=pK_a$, where the curve shows an inflexion point, and the relative proportion of these two forms is changed from 10 to 1/10, when pH varies from pK_a-1 to pK_a+1 . This rapid change is familiar to most chemists from work with monobasic indicators; their usefulness is limited to a pH -region of about 2 units.

Is the same equation valid for molecules in a monomolecular layer? It is difficult to see why it should not be so. If we look at a single molecule in the layer, its neighbours may exert some influence on its tendency to send out or take in hydrogen ions, but the influence cannot be very strong. In any case, it cannot be nearly so strong as the influence of a polar group inside the same molecule, and in this case we know that the effect of a second carboxyl group is not very great even in a small molecule, it may be dissociated or not. Succinic acid, for example, has a pK_{a1} of 4.2 and a pK_{a2} of 5.6, whereas propionic and butyric acids both have a pK_a of about 4.9.

The dissociation constants of fatty acids with a higher molecular weight than that of Nonylic (Pelargic) acid have not been determined, owing to their very small solubility in water (which for nonylic acid corresponds to a mol fraction of 1.4×10^{-5} , and for myristic acid with 14 carbon atoms

to a mol fraction of ca. 10^{-8}). The following table shows pK_a for the lower acids at 25°C .

TABLE I.

Acid.	pK_a .
Formic.....	3.67
Acetic	4.73
Propionic	4.87
Butyric	4.83
Valeric	4.80
Capric	4.83
Oenanthic	4.88
Caprylic	4.84
Nonyllic	4.96

With the exception of formic acid the constants vary between 4.7 and 5.0, and any tendency towards other values can hardly be discovered. One might expect a tendency towards higher values with increasing molecular weight, but evidently this lies within the experimental errors. Anyhow, it seems perfectly safe to assume that pK_a of the higher acids is quite near 5.0.

According to what was said above we should expect, therefore, that fatty acids should show a marked change in their properties just around a pH of 5.0. As this is what Adam found them to do, it seems reasonable to assume that dissociation phenomena are the *cause* of the transition of the structure of films of fatty acids from close packed heads to close packed chains, to use Adam's nomenclature.

As to the question of *how* the transition takes place, it is easy to understand that the $-\text{CO}_2$ groups would tend to give the molecules a lesser horizontal area than the $-\text{CO}_2\text{H}$ groups. The former also are more symmetrical and have a greater affinity for water than the latter. If two layers are formed as according to Adam, it would be difficult to find any other explanation of this than that the fatty acid anions exist in two tautomeric forms, or that half of them remain in the undissociated form, even at a considerably higher pH than 5, owing to neighbour molecules.

It is probably very difficult to test experimentally the theory set out above. It might be done for other film-forming substances than fatty acids by comparing the pH of the transformation point with pK_a . The dissociation constants of these very substances are, however, as a rule not known, as they naturally are but very sparingly soluble. Another way might be to make measurements of the electric properties of the films according to Guyot and Frumkin.

If the electric moment per square unit of the film is not proportional to the number of molecules per square unit, but shows an irregularity around the critical pH (and probably a considerably higher value above than below that point), this fact would be in favour of our theory, but would not be in accordance with Adam's.

The theory, if correct, would supply a method for determining the dissociation constants of substances able to form monomolecular films. To get pKa , the negative logarithm of that constant, it is only necessary to fix the middle point of the pH -interval inside which the film changes its area. Even other properties of such films than the surface-tension may furnish similar determinations of the dissociation constants, since the change from the dissociated to the undissociated state must affect many other properties.

Summary.

A new theory is proposed, according to which the changes in the properties of monomolecular films with the acidity of the support are closely connected with the dissociation of the film-forming substances. The hydrogen ion concentration at which this change is most rapid is numerically equal to the negative logarithm of the acid dissociation constant of the substance.

It is pointed out that this relation may furnish a means of determining the dissociation constants of sparingly soluble substances.

Stockholm University,
April 1927.

LVIII. *On the Absorption of X-Rays and Multiple Ionization of Atoms.* By LOWELL M. ALEXANDER, Ph.D., Associate Professor of Physics, University of Cincinnati*.

I. INTRODUCTION.

USING different methods of attack, A. H. Compton † and L. de Broglie ‡ have deduced similar theoretical expressions for the atomic fluorescent absorption coefficient τ_a , each equivalent to

$$\tau_a = [K_K Z^4 \lambda^3]^{\lambda < \lambda_K} + [K_L Z^4 \lambda^3]^{\lambda > \lambda_K} \quad . \quad . \quad (1)$$

* Communicated by the Author.

† A. H. Compton, *Phys. Rev.* xiv. p. 249 (1919).

‡ L. de Broglie, *Jour. de Phys. et Rad.* iii. p. 33 (1922); *C. R.* clxxiii. p. 1456 (1921).

where K_K and K_L are constants, Z the atomic number of the absorber, and λ the wave-length of the absorbed X-ray radiation.

On the experimental side, some investigators* find that equation (1) represents their experimental data with sufficient accuracy, while others† adopt fractional exponents instead of integers in equation (1).

The purposes of this article are to present :

- (1) Absorption experiments by the author.
- (2) A critical examination of published absorption-data.
- (3) Proposed new laws of absorption.
- (4) A discussion of multiple ionization of atoms.

Reference will be made to published data as shown :

- B. = Barkla and White, *Phil. Mag.* xxxiv. p. 270 (1917).
H. = C. W. Hewlett, *Phys. Rev.* xvii. p. 284 (1921).
R. = F. K. Richtmyer, *Phys. Rev.* xviii. p. 13 (1921).
O.D.S. = Olson, Dershem, and Storch, *Phys. Rev.* xxi. p. 30 (1923).
R.W. = Richtmyer and Warburton, *Phys. Rev.* xxi. p. 721 Å (1923).
A. = S. J. M. Allen, *Phys. Rev.* xxiv. p. 1 (1924), xxvii. p. 226 (1926), xxviii. p. 907 (1926).
Ar. = L. M. Alexander. This article.

II. EXPERIMENTAL DATA.

Several investigators‡ have remarked that as an absorption discontinuity is being approached on the short wave side, the rate of increase of absorption is considerably less rapid than at shorter wave-lengths. In order to investigate this phenomenon, the author has measured the absorption-coefficient of copper and aluminium over a range of wave-lengths 0.45 to 0.85 Å.

A molybdenum tube and a mechanical rectifier were used, together with Soller§ collimators having an angular aperture of forty minutes of arc. The radiation was reflected from a

* E. A. Owen, *Roy. Soc. Proc.* xciv. p. 510 (1918). F. K. Richtmyer, *Phys. Rev.* xviii. p. 626 (1921).

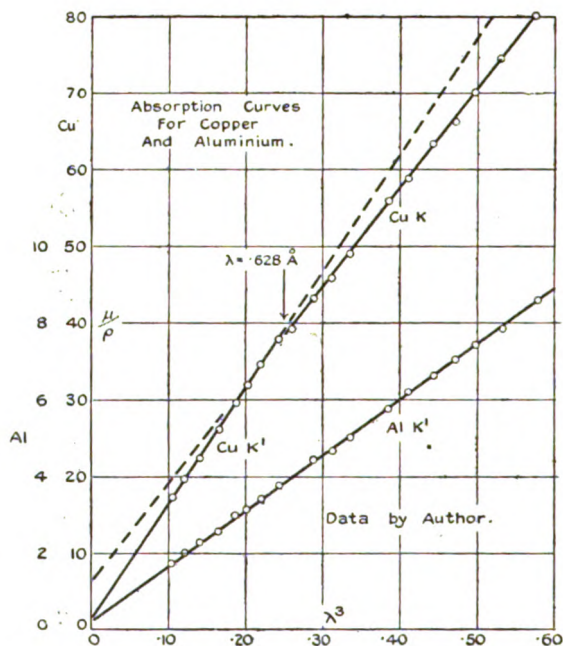
† Bragg and Peirce, *Phil. Mag.* xxviii. p. 626 (1914). Glocker, 'Atomabau' (*Engl. Trans.*), Sommerfeld, p. 188. S. J. M. Allen, *Phys. Rev.* xxvii. p. 226 (1926).

‡ Stoner and Martin, *Roy. Soc. Proc.* cvii. p. 312 (1925). E. A. Owen, *Roy. Soc. Proc.* xciv. p. 510 (1918). F. K. Richtmyer, *Phys. Rev.* xviii. p. 13 (1921).

§ W. Soller, *Phys. Rev.* xxiv. p. 158 (1924).

calcite crystal. Methyl iodide was used in the ionization chamber. The same sheet of copper, or of aluminium, was used throughout the whole range, so that no error was introduced by the necessity of changing sheets during an experiment. These measurements were made in the first order of the spectrum, and the potential of the tube was kept sufficiently low that second-order radiation did not appear. This was determined directly by preliminary tests. Fig. 1 is a plot of the mass absorption-coefficient against the cube of the wave-length.

Fig. 1.



The data for aluminium, when plotted, represent accurately a single and continuous straight line over this range of wave-lengths. On the other hand, the data for copper lie accurately on two straight lines intersecting at 0.628 \AA . This point of intersection I shall call the "KK'-break." The data of greater wave-length than the KK'-break comprise what I shall call K absorption, and those of shorter wave-length are termed K' absorption. Thus, for copper, the law that the mass absorption-coefficient μ/ρ varies as the cube of the wave-length is accurately true within limited ranges of wave-length. If we pass from one of these ranges

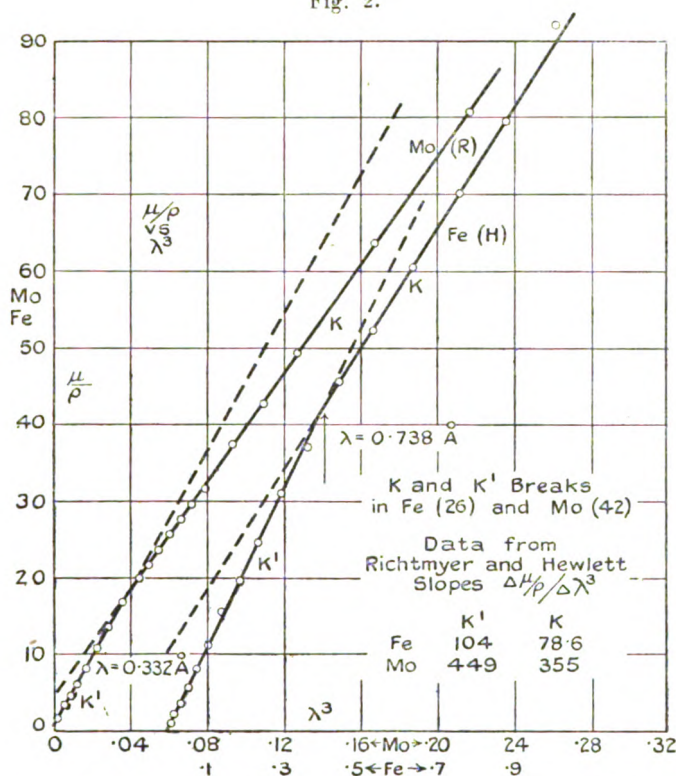
to another, a change in coefficient must be introduced in order to alter the slope of the line, and the slope for the K' absorption is always steeper than that for the K absorption.

III. DATA OF OTHER INVESTIGATORS.

K Absorption.

In order to discover whether such a break in continuity KK' occurs with other metals, the author replotted accurately the K -absorption data of those investigators who used homogeneous X-rays. The mass absorption-coefficient was

Fig. 2.



plotted against the cube of the wave-length from data taken unchanged from published results. In every case where the data extend over sufficient range of wave-lengths such a KK' -break was clearly shown. For brevity two examples are given here, these being selected from many others equally satisfactory. Fig. 2 shows the KK' -break for Mo (42), data

Phil. Mag. S. 7. Vol. 4. No. 23. Oct. 1927.

2 X

by Richtmyer, and for Fe (26), data by Hewlett. Wave-lengths at which these breaks occur are characteristic of the absorbing element.

TABLE I.
Data for KK'-break.

Element and Atomic No.	Observer.	Wave-length of KK'-break in Å units.	$\frac{\nu}{R}$	$\sqrt{\frac{\nu}{R}}$
Fe 26	H.	·738	1235	35·1
Ni 28	A.	·695	1311	36·2
Cu 29.....	Ar.	·628	1451	38·1
	A.	·738	1235	35·1
	A.	·845	1078	32·8
Zn 30.....	A.	·531	1715	41·4
Mo 42	R.	·332	2745	52·4
Ag 47	A.	·272	3350	57·9
	R.	·277	3290	57·4
Sn 50	A.	·241	3781	61·5
W 74	A.	·113	8064	89·8
Pt 78	A.	·101	9022	95·0
Au 79.....	A.	·099	9214	96·0

Table I. gives the values of λ , $\frac{\nu}{R}$, and $\sqrt{\frac{\nu}{R}}$ for the KK'-break in various elements.

L and M Absorption.

When published L and M series absorption data are plotted as above, breaks similar to the KK'-breaks appear. However, the data for L and M series absorption data are too incomplete, and inaccurate, to permit of definite results, but such as could be found clearly indicate such a discontinuity in the slope of two straight-line branches. Furthermore, there is some evidence that more than one such break occurs in the L and M series absorption data.

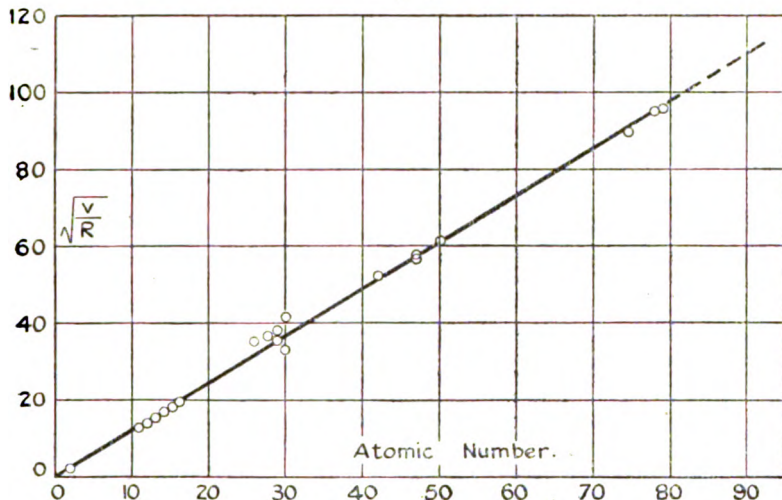
IV. RELATION BETWEEN ENERGY LEVEL OF KK'-BREAKS AND THE ATOMIC NUMBER.

Fig. 3 shows $\sqrt{\frac{\nu}{R}}$ (see Table I.) at the KK'-break plotted against the atomic number of the absorbing element.

The best straight line through these points also passes through the zero point. The equation of this line, which specifies most nearly the frequency at the KK'-break for each element according to atomic number, is :—

$$\frac{\nu}{R} = 1.5 Z^2 \dots \dots \dots (2)$$

Fig. 3.



V. GENERAL LAWS OF ABSORPTION.

Absorption data in the K and L regions are customarily represented by means of the equation,

$$\frac{\mu}{\rho} = k\lambda^3 + \frac{\sigma}{\rho}, \dots \dots \dots (3)$$

where k measures the slope of the line, and σ/ρ the value of μ/ρ for $\lambda=0$, when μ/ρ is plotted as a function of λ^3 .

The coefficients in equation (3) must be re-defined to agree with the results presented here.

$\left(\frac{\sigma}{\rho}\right)'_{\text{K}}$ is here defined as the value of μ/ρ obtained by projecting the straight line representing K' absorption to the μ/ρ axis. $\left(\frac{\sigma}{\rho}\right)_{\text{K}}$ is here defined as the value of μ/ρ obtained by projecting the straight line representing K absorption to the μ/ρ axis. Similarly for the L region.

2 X 2

TABLE II.
 μ/ρ Intercepts.

Absorber.....	1. $\left(\frac{\sigma}{\rho}\right)'_K$	2. $\left(\frac{\sigma}{\rho}\right)_K$	3. $\left(\frac{\sigma}{\rho}\right)'_L$	4. $\left(\frac{\sigma}{\rho}\right)_L$
H 1	·36			
Paraffin	·19			
C 6	·19			
O 8	·16			
Al 13	·20			
S 16	·25			
Fe 26	·22	10·0		
Ni 28	·80	—		
Cu 29	·54	6·0		
Zn 30	·52	2·4	1·0	
Mo 42	·50	4·2	3·0	
Ag 47	·41	2·6	2·0	27·0
Sn 50	—·42	2·8	0·0	12·0
Ba 56	·40	2·0	—	—
W 74	1·3	1·8	0·0	1·8
Pt 78	1·1	1·9	1·0	16·0
Au 79	1·0	1·7	0·9	—
Pb 82	—	—	0·01	21·0

Table II. shows the numerical values of these quantities for the various elements. k'_K is defined as the slope $\left(\frac{\mu}{\rho}/\lambda^3\right)$ of the straight line representing K' absorption. Similarly for k_K , k'_L , and k_L . Numerical values of these quantities for the various elements are shown in columns 3, 5, 7, and 9 of Table III.

Thus we may write in agreement with observed data :

$$\left. \begin{aligned} \frac{\mu}{\rho} &= k'_K \lambda^3 + \left(\frac{\sigma}{\rho}\right)'_K & \text{for } \lambda_{KK'} > \lambda > 0.2 \text{ \AA}, * \\ \frac{\mu}{\rho} &= k_K \lambda^3 + \left(\frac{\sigma}{\rho}\right)_K & \text{for } \lambda_K > \lambda > \lambda_{KK'}, \\ \frac{\mu}{\rho} &= k'_L \lambda^3 + \left(\frac{\sigma}{\rho}\right)'_L & \text{for } \lambda_{LL'} > \lambda > \lambda_K, \\ \frac{\mu}{\rho} &= k_L \lambda^3 + \left(\frac{\sigma}{\rho}\right)_L & \text{for } ? > \lambda > \lambda_{LL'}, \end{aligned} \right\} \quad (4)$$

where λ_K is the wave-length at the K absorption limit and

* The data of those few investigators who have made measurements at wave-lengths less than 0.2 Å show consistent variations in the slope of the $\mu/\rho, \lambda^3$ curves, as if two minute breaks occurred in this range. These breaks, however, occur at approximately the same wave-length for all absorbing elements, and are probably apparatus effects.

TABLE III.

1. Element.	2. Observer.	3. k_K .	4. $C_K \times 10^4$.	5. k_K .	6. $C_K \times 10^4$.	7. k_L .	8. $C_L \times 10^4$.	9. k_L .	10. $C_L \times 10^4$.
H 1	O.D.S.	0.272	[27.40]	—	—	—	—	10.5	12.8
C 6	O.D.S.	0.995	[92.1]	—	—	—	—	—	—
"	H.	1.05	[97.3]	—	—	—	—	—	—
"	A.	1.45	134.2	—	—	—	—	—	—
O 8	O.D.S.	2.78	[108.2]	—	—	—	—	—	—
Al 13	A.	14.4	136.0	—	—	—	—	—	—
"	A.	14.6	138.0	—	—	—	—	—	—
S 16	A.	27.7	135.6	—	—	—	—	—	—
Fe 26	H.	100.0	127.0	78.6	96.2	—	—	—	—
"	R.W.	110.0	134.6	—	—	—	—	—	—
Co 27	R.W.	124.0	137.7	—	—	—	—	—	—
Ni 28	A.	135.5	129.5	—	—	—	—	—	—
"	R.W.	144.0	137.3	—	—	—	—	—	—
Cu 29	B.	152.1	137.0	—	—	—	—	—	—
"	A.	151.0	135.8	—	—	—	—	—	—
"	A.	152.0	136.8	—	—	—	—	—	—
Zn 30	R.W.	153.0	136.0	—	—	—	—	—	—
"	A.	166.7	134.4	—	—	—	—	—	—
Mg 42	A.	172.8	139.3	—	—	—	—	—	—
Ag 47	R.	449.0	138.5	—	—	—	—	—	—
"	A.	670.0	147.5	—	—	—	—	—	—
Su 50	R.	674.0	148.5	—	—	—	—	—	—
Ba 56	A.	750.0	142.8	—	—	—	—	—	—
W 74	A.	883.0	123.4	—	—	—	—	—	—
Pt 78	A.	2080.0	128.0	—	—	—	—	—	—
Au 79	A.	2704.0	142.5	—	—	—	—	—	—
Pb 82	R.	2620.0	132.8	—	—	—	—	—	—
"	A.	—	—	—	—	—	—	—	—
Th 90	A.	—	—	—	—	—	—	—	—
Average			136.0		107.0		19.3		13.5

$\lambda_{KK'}$ is the wave-length at the KK' -break. k and σ/ρ are to be taken from Tables II. and III. These expressions are accurate to 1 per cent. approximately, while the ordinary cube law is in error by 30 per cent. at some wave-lengths.

Both theoretical and experimental results indicate that the fluorescent mass absorption-coefficient τ/ρ is also a function of the atomic number Z and the atomic weight A of the absorbing element. Thus the complete expression, as usually given, is

$$\frac{\tau}{\rho} = \frac{CZ^4\lambda^3}{A}, \quad \dots \dots \dots (5)$$

where C is a constant for different materials, but assumes different values for the K , L , M absorptions in the same metal. In accordance with the results presented here, C assumes the values :

$$\left. \begin{aligned} C_i &= C'_K & \text{for } \lambda_{KK'} > \lambda > 0.2 \text{ \AA}, \\ C_i &= C_K & \text{for } \lambda_K > \lambda > \lambda_{KK'}, \\ C_i &= C'_L & \text{for } \lambda_{LL'} > \lambda > \lambda_K, \\ C_i &= C_L & \text{for } ? > \lambda > \lambda_{LL'}. \end{aligned} \right\} \dots \dots (6)$$

If k_i represents the slope of any of the straight lines obtained experimentally by plotting μ/ρ against λ^3 , the corresponding C_i is computed from the equation,

$$C_i = \frac{k_i A}{Z^4} \dots \dots \dots (7)$$

Columns 4, 6, 8, and 10 of Table III. show the numerical values of the C 's computed from equation (7). It is seen that these values are approximately constant for any given portion of the absorption data. More numerous and, probably, more accurate data are necessary before it can be decided whether C_i is a true constant.

If the C 's be assumed constant for all elements, and the mean value be used, a less accurate but more general formulation of absorption data is given by the equation,

$$\frac{\mu}{\rho} = \frac{C_i Z^4 \lambda^3}{A} + \frac{\sigma}{\rho}, \quad \dots \dots \dots (8)$$

where

$$\begin{aligned} C'_K &= 136 \times 10^{-4}, \\ C_K &= 107 \times 10^{-4}, \\ C'_L &= 19.3 \times 10^{-4}, \\ C_L &= 13.5 \times 10^{-4}. \end{aligned}$$

The values for σ/ρ are to be taken from Table II.

The mass absorption-coefficient μ/ρ may be expressed as atomic absorption coefficient μ_a by the use of the relation,

$$\mu_a = \frac{A}{n} \frac{\mu}{\rho}, \quad \dots \dots \dots (9)$$

where A is the atomic weight and n is Avagadro's number. Thus

$$\mu_a = C_j Z^4 \lambda^3 + \sigma_a, \quad \dots \dots \dots (10)$$

where

$$(C_a)'_K = 2.24 \times 10^{-26},$$

$$(C_a)_K = 1.77 \times 10^{-26},$$

$$(C_a)'_L = 0.318 \times 10^{-26},$$

$$(C_a)_L = 0.223 \times 10^{-26},$$

$$\sigma_a = \frac{\sigma}{\rho} \frac{A}{n}.$$

V1. MULTIPLE IONIZATION.

The sudden change in the slope of the absorption curve which occurs at the KK' -break, the wave-length of which is characteristic of the absorbing element, must represent some energy change in the atom. The only explanation which seems reasonable is that the KK' -break is the point at which double K ionization sets in. From this viewpoint the frequency of the KK' -break marks the point where the quantum of impinging radiation has just sufficient energy to remove the two K electrons as a single act.

The wave-length just at the short-wave side of the K absorption limit marks the point where the quantum of impinging radiation has just sufficient energy to remove the first K electron. The photo-electron under these conditions would have zero velocity at the periphery of the atom. As the frequency of the radiation is increased, the probability of absorption decreases, as is shown by the downward trend of the absorption curve. Also, if the energy of the quantum is entirely transferred to the electron, the speed of the photo-electron should increase regularly with the frequency until the quantum has just sufficient energy to remove both K electrons as a single act. At this point twice as many electrons should be produced, although their speed at the periphery of the atom is again zero. It is not unreasonable to suppose that at higher frequencies the probability of

absorption is decreased slightly, as shown by the increased slope of the $\mu/\rho, \lambda^3$ curve at frequencies higher than that of the KK'-break.

Although the references to double K ionization are for elements of small atomic number where the KK'-break would be difficult to observe, and are disappointingly meagre, yet comparisons may be made between these values and what is here interpreted as double K ionization. I therefore note all such references as are known to me:—

(1) The electron impact measurement of the double K ionization potential of helium (79.5 volts) measured by Franck and Knipping*.

(2) The discovery by Hjalmar of the so-called "spark lines" in the X-ray spectra. Wentzel† attributed these lines to multiple ionization effects.

(3) L. A. Turner‡, using the data of Hjalmar, has computed with certain assumptions the double K ionization energy levels for elements from atomic numbers 11 to 16.

Equation (2) of this article predicts the double K ionization potential of helium to be 81.3 volts as compared with the observed value of 79.5. Franck and Knipping's value for helium and Turner's values for atomic numbers 11 to 16 are plotted in fig. 3.

Table IV. column 4 shows the ratio of ν/R for the KK'-break, computed from equation (2), to the value of ν/R for the K limit in a few elements. According to the ideas presented here, this is the ratio of the energy necessary for the removal of both K electrons as a single act to the energy necessary for the removal of the first K electron. It is usually stated that slightly more than twice as much energy is required for double than for single K ionization. It is certain that this is not true for helium, as the ratio is known to be 3.24. It is seen that the ratio as here computed varies from 3.31 for helium to 1.5 for uranium.

Table IV. column 5 shows the values of ν/R necessary for double K ionization. The experimental value for helium was observed by Franck and Knipping. The other values were computed by Turner. Column 6 shows the ratio of

* Frank and Knipping, *Phys. Zeit.* xx. p. 481 (1919).

† G. Wentzel, *Ann. der Physik*, lxvi. p. 437 (1921), lxxiii. p. 647 (1924).

‡ L. A. Turner, *Phys. Rev.* xxvi. p. 143 (1925).

column 5 to column 3. It is seen that the observed ratio for helium (3.24) compares favourably with the computed

TABLE IV.

1. Atomic Number.	2. ν/R for KK'-break (eq. 2).	3. ν/R for K limit.	4. Ratio $(\nu/R)_{KK'}$ $(\nu/R)_K$.	5. ν/R for double K ionization.	6. Ratio.
2	6.0	1.81	3.31	5.86	3.24
11	181.5	79.04	2.30	159.64	2.02
12	216.0	96.00	2.25	194.06	2.02
13	253.5	114.88	2.21	232.09	2.02
14	294.0	135.6	2.17	273.59	2.02
15	337.5	157.3	2.14	318.94	2.03
16	384.0	182.0	2.11	367.74	2.02
20	600.0	297.4	2.02		
30	1350.0	712.0	1.90		
40	2400.0	1326.0	1.81		
50	3750.0	2149.0	1.74		
60	5400.0	3211.0	1.68		
70	7350.0	4522.0	1.62		
80	9600.0	6113.0	1.57		
90	12150.0	8062.0	1.51		
92	12696.0	8477.0	1.50		

ratio (3.31). However, Turner's computed values give a constant ratio (2.02) for elements of atomic number 11 to 16, whereas column 4 shows a decrease in this ratio as the atomic number increases. Turner computed his multiple ionization terms by making the assumption that the energy of removal of an L electron depends only upon $Z-x$, where x is the number of K electrons present. It is difficult to justify this assumption, except as a first approximation.

The author desires to express his appreciation to Professors L. T. More and R. C. Gowdy for their keen interest and many helpful suggestions in the course of this work.

Cincinnati, Ohio,
August 1, 1926.

LIX. *Some Interference Effects in the Near Infra-red.*

By A. M. TAYLOR and E. K. RIDEAL *.

WHEN examining thin films of crystalline substances in the infra-red spectrum it is usually assumed that the logarithm of the ratio between the intensities of a beam of radiation of a very narrow range of frequencies, before and after transmission through the crystal slice, is a measure of the absorption coefficient for the particular frequency range employed. Some effects to be described show, however, that this ratio of transmitted to incident intensity may be modified by interference phenomena.

A consideration of the intensity I_t of the transmitted beam will lead to the expression

$$I_t = I_0(1 - R_1)(1 - R_2)e^{-\alpha z}, \quad \dots \quad (1)$$

where $\alpha = \frac{4\pi n\nu K}{c}$. In this expression z is the thickness of the crystal slice, n the refractive index for the particular frequency ν , c the velocity of light in free space, and K is an extinction coefficient such that when $4\pi K$ is unity the intensity of the light is reduced to $\frac{1}{e}$ in travelling through one wave-length in the crystal. R_1 and R_2 are the reflexion coefficients at the front and back surfaces of the crystal plate respectively, and

$$R_1 = R_2 = \frac{(n-1)^2 + n^2 K^2}{(n+1)^2 + n^2 K^2}.$$

Havelock¹ has examined the behaviour of R and has shown that K has very little effect in altering the frequency at which R becomes a maximum.

If for a first approximation R_1 and R_2 be put equal to $\frac{(n-1)^2}{(n+1)^2}$, (1) becomes

$$\frac{I_t}{I_0} = \frac{16n^2}{(n+1)^4} e^{-\alpha z}, \quad \dots \quad (2)$$

The usual method of procedure is to plot the experimental values of I_t/I_0 against λ the wave-length of the radiation, and a curve is obtained having one or more minima. These minima correspond with maximum values of α but do not necessarily coincide with them, for on differentiation of (2)

* Communicated by Prof. Alfred W. Porter, F.R.S.

with respect to λ ,

$$\frac{d}{d\lambda} \left(\frac{I_t}{I_0} \right) = \left\{ \left[\frac{32n(1-n)}{(1+n)^5} \cdot \frac{dn}{d\lambda} \right] - z \left[\frac{16n^2}{(1+n)^4} \frac{d\alpha}{d\lambda} \right] \right\} e^{-\alpha z},$$

and the minima must be given by the equation

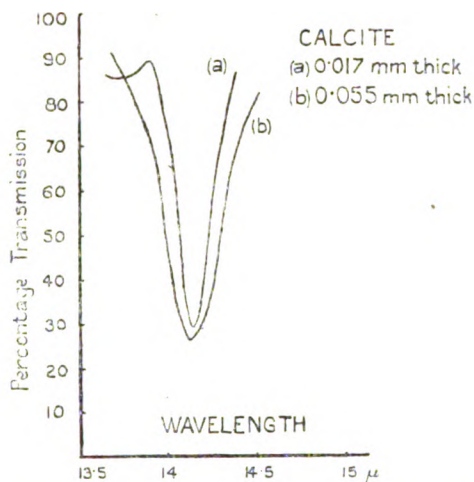
$$\frac{d}{d\lambda} \left(\frac{I_t}{I_0} \right) = 0$$

or

$$\frac{d\alpha}{d\lambda} = \frac{1}{z} \cdot \frac{2(1-n)}{n(1+n)} \cdot \frac{dn}{d\lambda}, \quad \dots \quad (3)$$

whereas the maxima of α are given by $\frac{d\alpha}{d\lambda} = 0$ in the expression for α as a function of λ , when reflexion losses are neglected. For z large the coincidence will be almost exact, but for small values of z the discrepancy may become considerable, especially as $\frac{dn}{d\lambda}$ is large in the neighbourhood of an absorption band.

Fig. 1.



In the examination of the absorption spectrum of the crystalline carbonates Schaefer² and others have made use of very thin specimens for determining the bottom of deep bands. Clearly the thinness of the slice may introduce a correction in the value found for the apparent characteristic frequency. The authors have examined calcite cut perpendicularly to the optic axis, at 14μ , and have found such a shifting of the minimum with thin specimens as expression (3) predicts. Fig. 1 shows the curves obtained for two

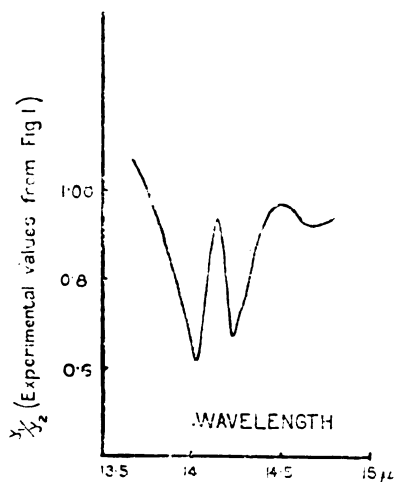
pieces of calcite—(a) 0.017 mm. thick, and (b) 0.055 mm. thick. (a) has a minimum at 14.135μ , whereas that of (b) occurs at 14.125μ . The minimum is shifted in the thinner specimen towards the reflexion maximum found by Schaefer³ at 14.16μ .

This is not the complete account of the effect however, for if $y = \frac{I_t}{I_0}$ at any particular wave-length, then if two different crystals of thickness z_1 and z_2 be examined, from equation (1)

$$\frac{y_1}{y_2} = e^{-a(z_2 - z_1)},$$

so that if y_1/y_2 be plotted against λ a curve will be obtained from which reflexion losses are absent and a minimum of

Fig. 2.



y_1/y_2 should coincide exactly with a maximum of α . Fig. 2 shows the result of plotting the experimental values in this manner, and indicates by the presence of several maxima and minima the superposition of the interference effects to which we have alluded.

A complete examination of the effects of interference would involve a series of beams arising from successive reflexions, but it will be sufficient for this purpose to consider only the first two terms, since all after the first two will be negligible owing to absorption in the crystal.

If the intensity of a beam falling upon the crystal slice at

normal incidence be I_0 , and if the emergent beam consists of two parts I_1 and a twice reflected portion I_2 , consideration of the path of the beams will show that

$$I_1 = I_0(1-R_1)(1-R_2)e^{-\alpha z} \quad . \quad . \quad . \quad (4)$$

and

$$I_2 = I_0(1-R_1)(1-R_2)R_2^2 e^{-3\alpha z}, \quad . \quad . \quad (5)$$

or

$$\frac{I_2}{I_1} = R_2^2 e^{-2\alpha z}. \quad . \quad . \quad . \quad (6)$$

Putting $R_2 = R_1$, then from (4) and (6)

$$\frac{I_2}{I_1} = \frac{R_2}{(1-R_1)^4} \left(\frac{I_1}{I_0} \right)^2, \quad . \quad . \quad . \quad (7)$$

and writing the right-hand side of this equation equal to G^2 , since the amplitude of vibration is proportional to the square root of the intensity, then $\frac{A_2}{A_1} = G$. The amplitude A_t of the transmitted beam is of two parts A_1 and A_2 , so that

$$A_t^2 = A_1^2 + A_2^2 + 2A_1A_2 \cos \phi,$$

where ϕ is the phase angle. Hence the transmitted intensity must be given by

$$I_t = I_1(1+G^2+2G \cos \phi), \quad . \quad . \quad . \quad (8)$$

and finally using equ. (4)

$$\frac{I_t}{I_0} = (1-R_1)(1-R_2)(1+G^2+2G \cos \phi) e^{-\alpha z}. \quad (9)$$

As before, if $y = \frac{I_t}{I_0}$ and two different thicknesses z_1 and z_2 be used,

$$\frac{y_1}{y_2} = e^{-\alpha(z_2-z_1)} \cdot \frac{(1+G_1^2+2G_1 \cos \phi_1)}{(1+G_2^2+2G_2 \cos \phi_2)}. \quad . \quad . \quad (10)$$

The angle ϕ is given by the relation

$$\phi = \frac{4\pi n z}{\lambda},$$

since the path difference between the interfering rays is $2nz$ for normal incidence.

Equation (7) shows that G is small, and hence from (8) I_t and I_1 cannot differ by very large amounts; an estimate of G may be made from (7) by writing I_t for I_1 , whence

$$G = \frac{I_t}{I_0} \frac{R}{(1-R)^2}.$$

For calcite Schaefer and Schubert³ find R about 10 per cent. at a point where I_t/I_0 is about 70 per cent. for a slice 0.07 mm. thick, and from this

$$G = 0.9.$$

This value of G is sufficiently large to cause a pronounced variation in y_1/y_2 as given by expression (10), and the peculiar curve shown in fig. 2 is fully explained as due to interference between the rays concerned.

Far removed from an absorption band α is zero, and equ. (9) shows that interference should be indicated by variations in I_t/I_0 . Such variations are found in the absorption spectrum of calcite and other carbonates², in regions where there can be no vibration frequencies characteristic of the material. If these ripples are due simply to interference the difference between the wave numbers of successive minima should be equal to a constant divided by the refractive index,

$$\left(\frac{1}{\lambda_2} - \frac{1}{\lambda_1}\right) = \frac{1}{2nz}, \quad \dots \dots (11)$$

where n is the mean refractive index between λ_2 and λ_1 . To test this the authors have examined two different thicknesses of calcite cut perpendicularly to the optic axis, and the results are plotted in fig. 3 together with those of Professor Schaefer's examination of a thicker specimen. The character of the ripples obtained in each case shows at once that they are due purely to interference, and a number of bands hitherto attributed to combination terms may be explained in this manner. The refractive index of calcite parallel to the optic axis may be calculated from (11), and the values found from the three sets of measurements are plotted in fig. 4. The results obtained from the three different crystals agree excellently together. The rapid rise of refractive index on the long-wave length side of the fundamental frequency at 7.0μ is particularly noticeable, and is to be expected from the accepted theory of dispersion. The experimental points lie above the curve in the region 11μ to 11.4μ for the reason that the incident beam consisted of a cone of rays of which the axis was parallel to the optic axis of the crystal, so that the extreme rays had a component vibration in the direction of the axis. They were then subject to the influence of the fundamental frequency of the CO_3 group at $11.3\mu^3$, of which the electric vector is along the axis⁴ and in consequence experienced an increased refractive index in this neighbourhood. The refractive

Fig. 3.

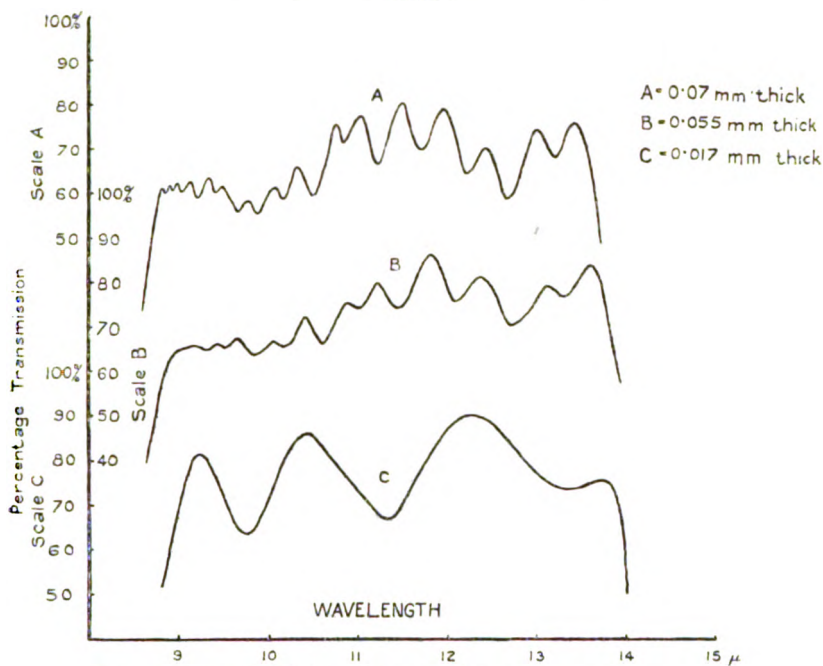
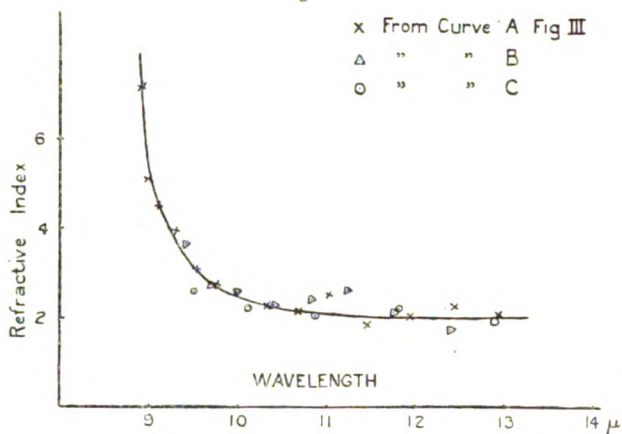


Fig. 4.



index for the ordinary ray is, however, not subject to this increase, and therefore the curve in fig. 4 is drawn so as to neglect these high values.

The apparatus used was that described in a previous paper⁵. Our thanks are due to Professor Schaefer, now of Breslau, who kindly provided the figures of his measurements on calcite of 0.07 mm. thickness.

Laboratory of Physical Chemistry,
Cambridge.

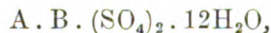
References.

1. Havelock, Proc. Roy. Soc. A, cv. p. 488 (1924).
2. Schaefer, Bormuth & Matossi, *Zeit. für Phys.* xxxix. p. 648 (1926).
3. Schaefer & Schubert, *Ann. der Phys.* l. p. 283 (1916).
4. Kornfeld, *Zeit. für Phys.* xxvi. p. 205 (1924).
5. Rawlins, Taylor & Rideal, *Zeit. für Phys.* xxxix. p. 660 (1926).

LX. *The Crystal Structure of some of the Alums.* By
J. M. CORK, Ph.D., Assistant Professor of Physics,
Michigan University, U.S.A.*

[Plate XVI.]

INTRODUCTION.—The alums make an interesting group of crystals for X-ray analysis. Although the molecule is rather complicated, there are so many isomorphous members in the group, differing from one another simply by the replacement of a single atom, that the solution of the structure is not hopeless, especially regarding the positions of the heavier atoms. They possess the symbolic chemical formula



in which A represents a monovalent metallic ion, B a tri-valent metallic ion, and S, generally sulphur, may be replaced by selenium or tellurium. B is commonly aluminium, chromium or iron; while A may be ammonium, potassium, rubidium, caesium or thallium. All of the alums examined form very perfect crystals of octahedral shape. Crystallographic considerations assign them to the pyritohedral class of the cubic system.

Vegard and Schjelderup† on the basis of spectrometer measurements assigned positions to the atoms in the unit cell so as to make observed and calculated intensities agree. This assignment was made without regard to the space group and led to a complicated and improbable

* Communicated by Professor W. L. Bragg, F.R.S.

† *Annalen d. Physik*, liv. p. 146 (1917).

arrangement. P. Niggli *, using the data of Vegard and Schjelderup, assigned the alums to the space group T_h^2 and suggested possible arrangements. R. W. G. Wyckoff †, by means of Laue and rotation photographs, concluded that the correct assignment of the space group was T_h^6 rather than T_h^2 .

In the present paper new intensity measurements have been made by the X-ray spectrometer upon all orders of the three principal plane sets, (111), (110), and (100), for ammonium, potassium, rubidium, caesium, and thallium-aluminium alums and potassium chrome alum. The dimensions of the unit cell have been accurately determined in each case. In addition, rotation photographs have been taken to verify the space group assignment. Using the method of Fourier analysis, as simplified by Duane, and used so successfully in the case of many relatively simple structures, an attempt has been made to locate the position of some of the heavier atoms in this more complicated structure. In addition, use is made of the atomic structure factor curves to check the agreement between calculated and experimental F values, particularly in the case of high order reflexions, where the effect of the lighter atoms may be neglected. This, together with consideration of the atomic domain, or dimensions required for the particular atoms or groups of atoms in other structures, and the symmetry of space group, limits very markedly the number of possible arrangements.

Lattice Constants.—Four molecules are ascribed to the unit cubic cell. The eight metal atoms take positions at the corners, centre, centre of faces and mid-points of edges of the cell, making a rock-salt arrangement of monovalent and trivalent metals. The lengths of the cube edges obtained are tabulated in Table I. Use was made of as many orders as

TABLE I.
Edge of Unit Cubic Cell for various Alums.

Alum.	Edge of unit cell.
$NH_4Al(SO_4)_2 \cdot 12H_2O$	12·18 Å.
$K \cdot Al \cdot (SO_4)_2 \cdot 12H_2O$	12·14 „
$K \cdot Cr \cdot (SO_4)_2 \cdot 12H_2O$	12·14 „
$Rb \cdot Al \cdot (SO_4)_2 \cdot 12H_2O$	12·20 „
$Cs \cdot Al \cdot (SO_4)_2 \cdot 12H_2O$	12·31 „
$Th \cdot Al \cdot (SO_4)_2 \cdot 12H_2O$	12·21 „

* *Phys. Zeits.* xix. p. 225 (1918).

† *Amer. Journ. of Sci.* v. p. 209 (1923).

possible in each plane set. A slight increase in dimensions is observed as potassium is replaced by rubidium and caesium in turn. Thallium appears to occupy about the same space as rubidium, while the ammonium ion requires only slightly less room. Chromium appears to replace aluminium with a very slight, if any, change in dimensions.

Spectrometric Intensity results.—Intensity measurements were made using a Bragg ionization spectrometer equipped with string electrometer and potentiometer as previously* described. Each integrated reflexion was compared with that from the (400) plane of rocksalt whose value was taken as 100×10^{-6} . Table II. summarizes the data obtained. The reflecting plane is listed in column 1 and the approximate value of the sine of the reflecting angle in column 2, since this varied slightly with the different alums, while columns 3, 5, 7, 9, 11, and 13 contain the experimental values of the integrated reflexions ρ for each alum.

For the case of the ideal mosaic crystal Darwin† has developed a relationship involving the integrated reflexion $\frac{Ew}{I}$, or ρ , and the structure factor F , which may be approximated as follows:—

$$\rho = F^2 \cdot \frac{n^2 \lambda^3 e^4}{4m^2 c^4} \cdot \frac{1 + \cos^2 2\theta}{\sin 2\theta} \cdot \frac{1}{\mu + \alpha \rho} \cdot e^{-B \sin^2 \theta}.$$

In this formula n represents the number of unit cells per cubic centimetre, λ and c the wave-length and velocity of X-rays, e and m the charge and mass of the electron respectively, θ the glancing angle of incidence for X-ray reflexion, α , a constant for a particular crystal specimen, being an indication of the perfection of the crystal, so that $\alpha \rho$ represents the effective increment to the absorption coefficient due to extinction, μ is the linear absorption coefficient, and $e^{-B \sin^2 \theta}$ a temperature factor due to the heat motion of the atoms.

If, as an approximation, α be assumed zero and the temperature factor be taken as unity, then for each value of ρ , a value of the structure factor F may be obtained. The value of the absorption coefficient for ammonium alum was measured experimentally using several thicknesses of the absorber, and that of the other alums found by

* R. W. James, Phil. Mag. xlix. p. 585 (1925).

† Phil. Mag. xxvii. pp. 315, 675 (1915); xliii. p. 800 (1922).

TABLE II.—Intensity of Reflexion and Structure Factor for the various Alums.

Plane.	Sin θ .	$\text{NH}_4\text{Al(SO}_4)_2 \cdot 12\text{H}_2\text{O}$.		$\text{KAl(SO}_4)_2 \cdot 12\text{H}_2\text{O}$.		$\text{KCr(SO}_4)_2 \cdot 12\text{H}_2\text{O}$.		$\text{Rb. Al(SO}_4)_2 \cdot 12\text{H}_2\text{O}$.		$\text{Cs. Al(SO}_4)_2 \cdot 12\text{H}_2\text{O}$.		$\text{Tl. Al(SO}_4)_2 \cdot 12\text{H}_2\text{O}$.	
		$\rho \times 10^6$.	F.	$\rho \times 10^6$.	F.	$\rho \times 10^6$.	F.	$\rho \times 10^6$.	F.	$\rho \times 10^6$.	F.	$\rho \times 10^6$.	F.
111	0.494	70.0	86	8.8	38	21.0	78	1.11	29	17.2	101	6.5	113
200	0.578	13.9	42	8	13	1.6	22	2.11	43	16.0	107	3.36	89
220	0.822	76.3	116	78.8	142	67.2	174	26.2	180	49.0	221	29.2	308
222	0.896	—	—	1.15	19	3.9	47	4.15	79	31.0	192	9.7	195
333	1.161	63.5	125	56.6	15	44.2	170	31.2	233	51.8	268	19.1	295
440	1.492	36.8	111	30.5	125	11.7	102	10.8	158	29.0	231	9.0	236
440	1.645	1.04	19	6.9	62	8.7	90	3.18	90	13.2	164	5.2	186
600	1.909	39.1	129	36.4	154	30.0	174	16.7	223	40.1	310	10.2	283
444	1.982	1.37	25	.05	6	1.45	41	.95	55	5.4	116	1.9	125
800	2.317	.07	6	.33	16	—	—	.69	47	4.05	110	1.48	121
660	2.467	11.5	80	15.6	116	15.4	169	5.52	147	4.05	110	1.48	121
555	2.481	1.0	24	2.68	49	—	—	.99	64	2.9	96	5.05	228
10.00	2.716	3.7	48	5.1	71	3.3	77	1.81	90	.74	51	1.67	135
866	2.977	10.3	86	6.6	86	4.9	96	2.5	122	11.8	217	2.05	164
880	3.289	3.34	52	5.02	79	3.6	88	1.8	101	4.3	140	1.75	162
12.00	3.475	.08	8	—	—	—	—	.47	90	4.1	143	.29	69
777	3.475	3.07	53	.84	34	.46	33	—	—	.94	68	.02	18
888	3.971	—	—	.15	16	.09	16	.06	22	1.1	81	.16	56
14.00	4.057	.18	14	.32	23	—	—	.19	38	.89	74	.16	57
10.10.0	4.112	.25	17	.63	33	.72	52	.08	25	.47	54	.18	61
999	4.470	.50	25	—	—	—	—	.45	—	.46	56	.02	25
16.00	4.638	.60	28	.59	35	—	—	.48	67	.46	59	.13	56
12.12.0	4.945	.23	18	.47	32	—	—	.13	36	.47	61	.11	54
10.10.10	4.967	1.06	39	—	—	.63	55	—	—	.08	26	—	—

computation from this, making use of the data of Windgardth* on atomic absorption coefficients. These values of F are tabulated in columns 4, 6, 8, 10, 12, and 14.

Space Group.—Fig. 1 (Pl. XVI.) shows a rotation photograph taken from caesium alum, using the (100) plane, set with the c axis parallel to the axis of rotation. Similar photographs were taken for the other alums. To distinguish between questionable planes the spectrometer was used. The abnormal spacing characteristic of the space group T_h^6 is, that for planes of indices $\{hko\}$ the spacing is halved if h is odd, for $\{okl\}$ if k is odd, for $\{hol\}$ if l is odd. No reflexions were found contrary to this requirement, thus confirming the assignment of Wyckoff.

There are thus 24 generally equivalent positions. The eight sulphur atoms in each cell must be distributed, one in each small cell, on the trigonal axis. They therefore introduce only one parameter. The sulphate oxygens being 32 in number must be of two kinds, as would be expected if the SO_4 group maintained the tetrahedral form usually assigned it. Eight of the oxygen atoms would thus be arranged similarly to the sulphur atoms, while the remaining 24 would occupy the general positions, introducing in all four more parameters. If the sulphate group, however, maintains in the alums the form it appears to possess in other structures, these 24 atoms would give 3 to each small cell, arranged about the 3-fold axis, forming with the oxygen atom on the axis an equilateral tetrahedron whose base is perpendicular to the 3-fold axis. The oxygen atoms having a diameter of about 2.7 ångströms are thus in close packing array having the sulphur at the centre of mass of the tetrahedron, the sulphur atom being so small that it can well be accommodated by the space before the four oxygens. Thus, if the position of the relatively heavy sulphur atom can be obtained, and the orientation of the tetrahedron along the diagonal, then only the angular position of the tetrahedron thought of as rotating about the 3-fold axis is left undetermined. Similarly the 48 oxygen atoms of the water may be considered as two groups of 24 each in generally equivalent positions. Having located the SO_4 tetrahedron and considering the dimensions of the monovalent and trivalent metal atoms, only certain available space remains for the other oxygen planes normal to the trigonal axes. The 96 hydrogen atoms making 4 sets of 24, occupying generally equivalent

* *Zeit. f. Physik*, viii. p. 363 (1922).

positions, can scarcely be considered, as their scattering power is so small. The space occupied by them must be small. However, in the hexagonal close-packed assemblage of oxygen atoms only 13.94 cubic centimetres per atom is required, whereas in the alum structure, treating the monovalent metal atom as an oxygen atom, about 21.7 cubic centimetres per atom is allowed, so that considerable space is left for the hydrogen atoms, if necessary.

Fourier Analysis of Electron Distribution.—If a set of crystal planes be considered, the distribution of diffracting centres (electrons) in sheets parallel to the planes is a periodic function of the spacing of the plane set and may be expressed by a Fourier series. It has been shown* that the first order amplitude of reflexion from this plane set depends upon the first coefficient of the Fourier series, the second order upon the second coefficient, etc. Conversely, if the amplitude of reflexion of a number of orders for any plane set is known, then it becomes possible to obtain the electron distribution in sheets parallel to the plane. The method has been considerably simplified† and employed in the case of several simple crystals‡. In the form developed by A. H. Compton the sheet electron density P_z for the unit cell at a distance z along a direction perpendicular to the plane set giving the information is given by the series

$$P_z = \frac{Z}{d} + \frac{2}{d} \left(F_1 \cos \frac{2\pi z}{d} + F_2 \cos \frac{4\pi z}{d} + \dots + F_n \cos \frac{2\pi n z}{d} \right),$$

where Z denotes the number of electrons in the unit cell and F_n is the structure factor for the n th-order reflexion from the plane set being considered, and d is the spacing of the planes in the direction considered. By dividing by the number of molecules in the unit cell, the electron distribution within the molecule is given.

The value of F given in Table II., being the square root of a quantity, may be either positive or negative in sign. In this series of alums, however, the correct sign is readily observed, as the origin is taken as the centre of a monovalent metal atom, and when this is replaced by a heavier atom F should increase algebraically. If F decreases

* W. H. Bragg, *Phil. Trans. Roy. Soc. A*, cxcv. p. 253 (1915).

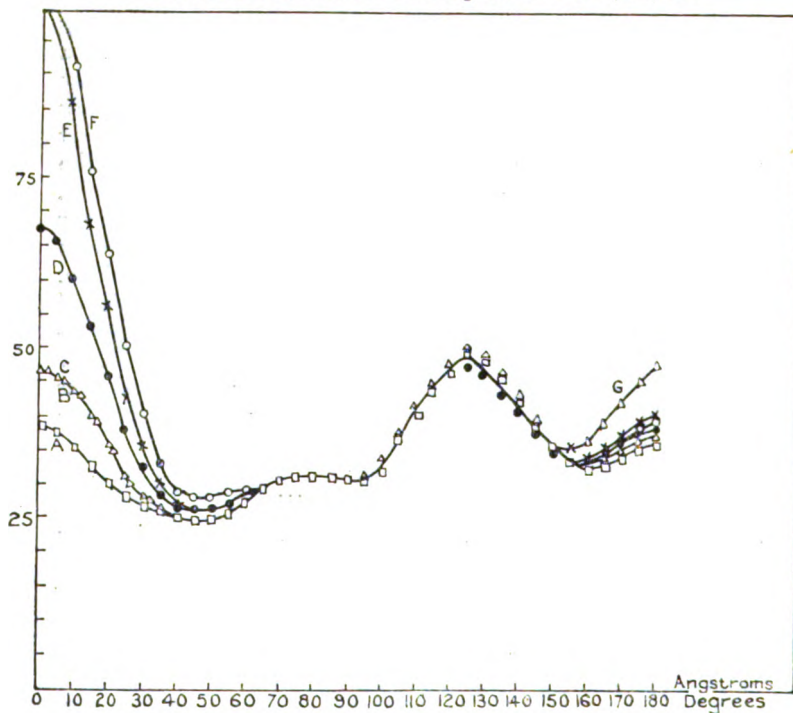
† W. Duane, *Proc. Nat. Acad. Sci.* xi. p. 489 (1925). A. H. Compton, 'Theory of Electrons,' p. 154.

‡ R. J. Havighurst, *Proc. Nat. Acad. Sci.* xi. p. 502 (1925) *et seq.* J. A. Bearden, *Phys. Rev.* vol. xxix. p. 20 (1927). W. L. Bragg and J. West, *Proc. Roy. Soc.* cxi. p. 691 (1926).

numerically when the heavier metal atom is substituted, then it must be negative in sign. For example, for potassium-aluminium alum F_{111} and F_{777} are considered negative. In order to make the series more rapidly convergent, the F values were multiplied by a factor of the form of the Debye temperature factor.

Fig. 2.

Electron Distribution in Planes parallel to the (111) set.



The values of P_z for planes normal to the (111) set for the different alums, computed at intervals of 0.1 ångströms, are shown in fig. 2. This plane set gives alternately layers of monovalent and trivalent metals. Thus if the distance from one monovalent metal layer to the next adjacent similar layer be taken as 360° or 7.06 ångströms for the alums, then the trivalent metal layer will lie at 180° or 3.53 ångströms, and if the sulphur atoms were each at the centres of the small cubes they would lie at 90° or 1.76 ångströms. If, however, the sulphur is displaced

along the diagonal of the small cube any number of degrees, then there will appear sulphur planes of two types. That is, if we imagine a shift of the sulphur of ϕ degrees toward the aluminium, then for a single molecule of alum one plane of $\frac{1}{4}$ atom of sulphur will occur at $90^\circ + \phi$ and another plane of $\frac{1}{4}$ atom at $90^\circ - 3\phi$, and symmetrical positions.

The remarkable similarity of the curves for the different alums indicates clearly the effect of changing either the monovalent or trivalent metal atom. At 0° occurs the electron density on the plane through the centres of monovalent metal atoms. Since number of electrons is represented in the figure by areas, the difference between any two of these curves should give the difference in the number of electrons in the corresponding atoms. Thus the potassium-aluminium curve subtracted from the caesium-aluminium curve gives a difference of 37.4 instead of 36. Similarly, good agreement is obtained in each case except for thallium where the discrepancy is larger. The fact that these curves should agree so well, considering that they represent independent measurements and calculations employing absorption coefficients varying from NH_4 to Tl by a factor of 20, is most striking. The difference between potassium-aluminium and potassium-chromium alum is evident only in the region of 180° , as would be expected. The curves do not at any place drop to zero ordinate values, since as there are so many atoms their fields must overlap. The important question is the interpretation of the peak at about 124° .

If this is the $\frac{3\text{S}}{4}$ sulphur peak it would represent a displacement of the sulphurs along the diagonal from the centre of the small cube of 34° or 1.98 ångströms toward the trivalent metal atom. If this were the case, the position of the corresponding peak could be predicted using the (110) and (100) plane sets. These curves were drawn giving families similar to those shown in fig. 2. The central peak in these curves, however, indicated a smaller shift of the sulphur from the centre of the small cubes than indicated by the (111) set above. This might well be the case if the peaks were not due to the sulphur alone but rather to the region of maximum density of the sulphur and adjacent oxygen layers.

To test this conclusion various positions might be assigned the sulphur atom and the structure factor computed from the atomic structure factor curves of Hartree*. Since the effect

* Phil. Mag. l. p. 289 (1925).

of the oxygen falls off rapidly as the diffracting angle increases compared to sulphur, for high orders of reflexion the oxygen may be neglected as an approximation. The mean of these calculations seemed to assign a position to the sulphur shifted about $26/180$ or 1.55 ångströms from the small cube centre toward the aluminium. The difference between this value and the peak indicated in fig. 2 is readily accountable by the effect of oxygen atoms if the tetrahedron is properly fixed in its angular position on the cube diagonal, and might be of assistance in deciding between possible arrangements.

This position of the sulphur leads to at least two possible configurations for the remaining atoms, both compatible with dimensional requirements and the crystal symmetry, but perhaps not equally reasonable. In one of these configurations the apex of the SO_4 tetrahedron approaches the aluminium. If the following atomic radii* are assumed: oxygen, 2.7 ångströms; sulphur, 0.6 ångström; aluminium, 1.1 ångströms and monovalent metal, 2.7 ångströms, then the distance between hexagonally close packed layers of oxygen or monovalent metal becomes 2.2 ångströms and there is room for sulphur and also approximately aluminium in the interstices between the oxygen. In the above configuration, however, there would be just sufficient room for the oxygen at the apex of the tetrahedron to touch the aluminium. Toward the monovalent metal there would be just room for three groups of three oxygen atoms: the first, that of the SO_4 group, and the other two the six water molecules ascribed to each cell. Since the SO_4 tetrahedron can take only one angular position to account for the apparent larger shift from the (111) curves, and since space limitations are just satisfied by a hexagonal close packing of the three oxygen groups, the position of every oxygen atom would follow.

There are two objections to this arrangement. The aluminium atom would be left in line between two oxygen atoms; and the water of crystallization would be associated entirely with the monovalent metal, whereas it is perhaps more natural to associate water of crystallization with the smaller atom.

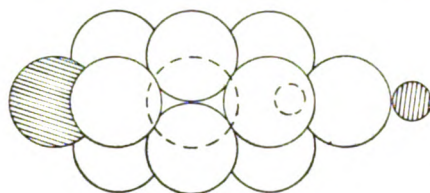
The following alternative arrangement possesses neither of these objections and satisfies the space requirements almost equally well. In this arrangement the SO_4 tetrahedron shifts with its base towards the aluminium. Between the three oxygens of the base of the tetrahedron and the

* W. L. Bragg, *Phil. Mag.* ii. p. 258 (1926).

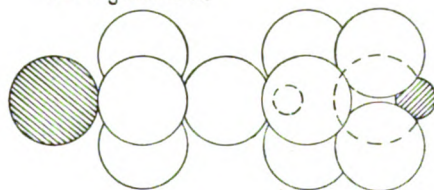
aluminium is a closely packed group of three water oxygens, the other three water oxygens lie between the apex of the tetrahedron and the monovalent metal. Six water molecules are thus associated with each metal atom. Since the angular position of the SO_4 tetrahedron on the trigonal axis is limited to one position to give the increased apparent shift for the (111) plane set, so also would be the position of the six oxygens about the trivalent metal. This would not be the case, however, with the six oxygens about the monovalent

Fig. 3.




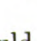
Possible Arrangement of Atoms along the Trigonal Axis.



Arrangement A.



Arrangement B.

-  Monovalent Metal
-  Oxygen
-  Trivalent Metal
-  Sulphur

metal. It would now be possible to write the general equation for the complete structure factor and assigning different parameters to the oxygens in this last general position to compare calculated and experimental F values for low-order reflexions. However, since the extinction factor plays such an important part in these calculations at small reflecting angles, and since its effect in the alums is uncertain, such calculations are deemed hardly worth while.

The two configurations mentioned above are shown in fig. 3. The positions of the various atoms for the second more probable arrangement (B) are as follows :—

Monovalent metal :

$\{000\}$ and three other related positions.

Trivalent metal :

$\{.5, 0, 0\}$ " " " " "

Sulphur :

$\{.322, .322, .322\}$,, seven " " "

SO₄ oxygen—Vertex :

$\{.245, .245, .245\}$,, " " " "

SO₄ oxygen—Base :

$\{.304, .304, .407\}$,, twenty- " " "
three

Water oxygen,

trivalent metal :

$\{.483, .483, .392\}$,, " " " "

monovalent metal :

$\{x, y, z\}$ " " " " "

R. W. G. Wyckoff has pointed out that in the case of the monovalent metal being NH₄, the only arrangement for the four ammonium hydrogens compatible with the space group is their arrangement in line on the trigonal axis. This was regarded as an arrangement so unlikely as to be considered a case in which the symmetry of the space group was not maintained. In the second configuration suggested, the necessary room would be found in the close packing interstices on the trigonal axis.

In order to confirm the arrangement suggested here more members of the alum group should be examined, particularly those in which the sulphur is replaced by a heavier element such as selenium.

This opportunity is taken to express appreciation to Mr. W. H. Taylor for taking the rotation photographs, and to Prof. W. L. Bragg for providing facilities for the work as well as kind advice during the investigation.

*LXI. On the Union of Helium with Mercury**. By
J. J. MANLEY, M.A., *Fellow of Magdalen College, Oxford*†.

1. *Introductory.*

THE wholly unexpected discovery which is the subject of this paper may be conveniently approached by way of a brief review of the experiments which led up to it.

It is well known that when a barometric tube containing its normal column of mercury is moved up and down, electric charges are generated upon the glass. If a little gas be present within the tube a feeble glow is produced, and this is usually accompanied by chemical action and a consequent decrease in pressure. In many cases also the glass walls become stained and ultimately coated with solid matter: this readily happens when the experiment is made with oxygen, nitrogen, or air. But when very pure hydrogen is used, the tube may be oscillated for hours without the production of anything beyond a feeble glow-discharge. If, however, the experiment is greatly prolonged, a narrow annular film having a pearl-like lustre is formed. The substance appears to have but little chemical stability, for on bringing the tube to rest the film gradually vanishes. Chemical analyses showed that in the three cases first cited the solid bodies found within the tube were respectively mercury oxide, a stable nitride of mercury, and a compound containing both mercury and ammonium. The lustrous substance obtained with hydrogen was not analysed: its unexpected transient nature had not been allowed for. But considering the purity of the gas, the chemical cleanness of the tube, and the care taken in purifying the mercury, there can be but little doubt that the substance in question was a hydride of mercury. Possible impurities such as oxygen, nitrogen, or chlorine derived from the glass would each and all form with mercury substances which are at once non-volatile and quite permanent under the ruling conditions.

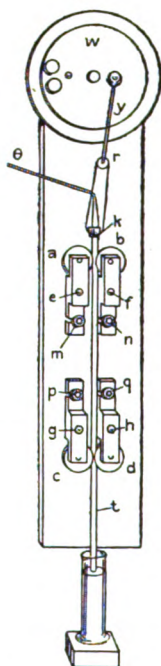
All the experiments just dealt with were made with the apparatus depicted in fig. 1. The barometric tube was set up between rotatable guides and suspended from a large pulley; and this, when driven by a motor, caused the tube to oscillate as required.

* A first paper dealing with mercury helide was communicated to the Royal Society in July 1925. The paper was deposited in the Archives of Burlington House. Also Brit. Assoc. Reports, 1926.

† Communicated by the Author.

This same apparatus was employed for an additional experiment for which pure helium was used. This was done to illustrate the correctness of the views universally held concerning the observed chemical inertness of the gas. Accordingly the tube was actuated for a long time before it was again scrutinized. The result was surprising; for although the lustre of the glass surface was unimpaired,

Fig. 1.



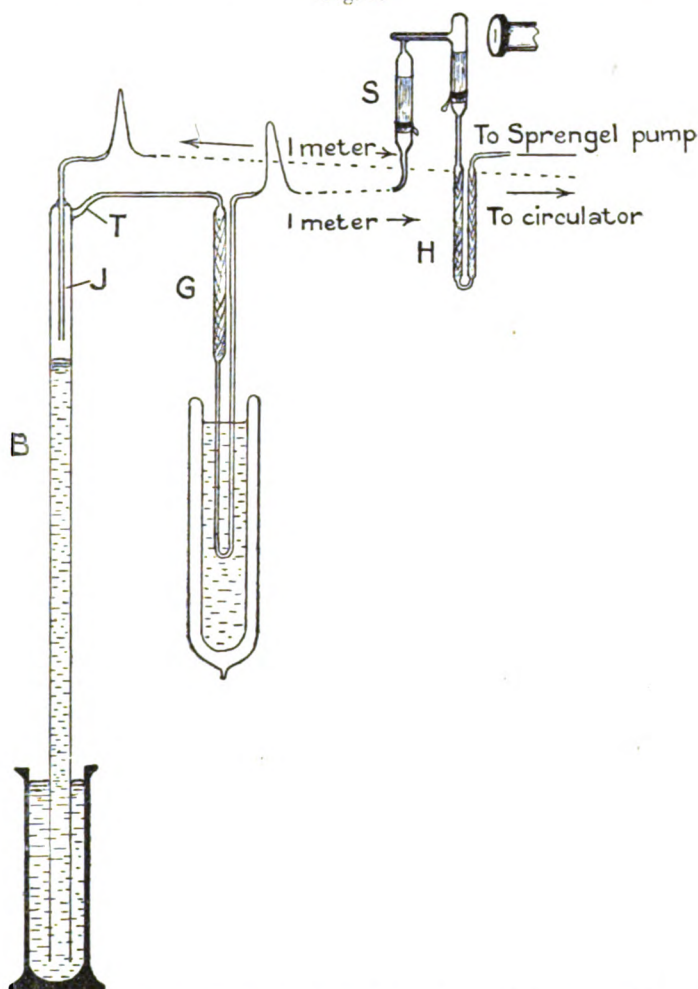
the pressure of the helium had lessened. An *increase* in the pressure could have been explained by assuming (1) that gas had either entered the oscillating tube by making its way along the glass surface from without, or that it had escaped from the mercurial column; and (2) that the remnants of a gas-grown skin had been eroded by the glow-discharge* set up during the experiment. But even these arguments would be untenable, for the intrusion of common gases would result in the formation of solid matter.

In the experiment with helium the initial and final pressures of the gas were respectively 7 and 2.3 mm. The

* Proc. Phys. Soc. xxxvi. p. 288 (1924).

decrease in the original pressure was therefore 67 per cent. It was difficult to account for a change so marked without postulating the formation of a helide of mercury: this view was therefore provisionally accepted, the simple

Fig. 2.



introductory experiments terminated, and plans made for obtaining more complete evidence.

With the simple apparatus of fig. 1 it was obviously impossible to attempt the condensation of the hypothetical helide, and therefore an elaborated form (shown in fig. 2)

was constructed. The new barometric tube was fitted with an injector J and an outlet T; and these, by means of flexible glass capillary tubes 1 m. long, communicated with the corresponding orifices of a circulator* not shown. The chamber G and the U-tube H were filled with gold-leaf: the spectrum tube S was thus guarded against the intrusion of mercury vapour. During each downstroke of the tube B the narrow U-limb attached to G plunged into liquid air. Drying was effected by circulating the helium through a chamber containing purified phosphorus pentoxide. With this apparatus experiments were made as follows.

First, the apparatus was chemically cleaned and dried; then an X-ray vacuum was established, and the gas-grown skins eroded† and removed. Next, pure helium was admitted and circulated for some hours, and then withdrawn. A second portion of pure helium was now introduced and circulated for the purpose of drying. Lastly, the pressure p of the gas when stationary was noted, the circulator restarted, and the motor brought into use. The speed of the latter was such that the barometric tube executed some 7000 or more strokes per hour.

For these experiments p was varied within the limit of 14 and 0.36 mm., and the tube oscillated for many hours; but at no time was any substance discovered within the U-limb of G. It was, however, found that when $p=10$ mm. initially the value slowly decreased to 8 mm.; similarly, when $p=2.57$ mm. a gradual decrease to 2.08 mm. was observed.

These results accord with that obtained in the earliest experiment. The synthesis of mercury helide was probably followed by the formation of a gas-grown skin of the compound; and this skin would be densest upon the surface cooled by liquid air. The evidence for this lies in the fact that as the experiment progressed the mercury green line, as seen in the spectrum-tube, increased in strength; also the intensity was considerably enhanced upon the removal of the liquid air. If the observed increase had been due to free mercury, the intensity of the spectral line would have acquired a maximum value at the minimum pressure of 0.36 mm. It was not so; at that pressure the line was very faint.

From the experiments just detailed three facts emerge.

* Proc. Phys. Soc. xxxviii. p. 129.

† Proc. Phys. Soc. xxxvi. p. 288.

They are :—

- (1) At low pressures and in the presence of a glow-discharge, helium is capable of uniting with mercury.
- (2) The synthesized helide is not condensed, but remains gaseous, even at the temperature of liquid air.
- (3) The helide, in common with other gases, gives rise to gas-grown skins.

It may here be remarked that the formation of a gas-grown skin partially accounts for the decrease in pressure noted during the synthesis.

An attempt was now made to devise more efficient synthesizers. Some of those are described in the next section.

2. Various Synthesizers.

As the helide appeared to be formed in a glow-discharge, synthesizers within which the glow could be produced and varied in intensity were made and tested.

The first of the new synthesizers was a narrow barometric tube surmounted by another 57 cm. long and 22 mm. wide. To the wide portion two external electrodes of tinfoil were attached, the one at the upper end and the other at the lower. The wide limb was also given two side-tubes; these communicated with an apparatus for circulating the contained helium. The spectrum tube S of fig. 2, used for detecting mercury, was, together with its guard-tubes, included in the circuit. With this apparatus many experiments were made, but in no instance was the pressure of the helium changed; also the mercury green line was invariably faint or altogether invisible. The instrument was thus found to be ineffective.

A second synthesizer in which the glow-discharge was produced between parallel electrodes of aluminium, and also a third having mercury electrodes, were equally ineffective; but a fourth, which may now be described, yielded an important result.

The synthesizer which contained 25 c.c. of mercury was a glass tube 35 cm. long and 18 mm. wide placed horizontally in a movable cradle. Its two ends were drawn out to form short narrow limbs, which were bent upward and fused to vertical glass capillary tubes: these last were about 1 m. long, and their upper portions were shaped like a horizontal V. Formed thus, the tubes were not liable to fracture. The capillary tubes communicated, the one with the inlet

and the other with the outlet of the gas circulator. The apparatus was rendered complete by the inclusion of a Sprengel pump, a charcoal chamber which could be immersed in liquid air, and the two gas chambers of a Jamin interferometer. The several sections of the apparatus were in this, as in all other cases, joined by fusion: this is highly important. With the aid of mercury traps it was possible to arrange for the circulating helium to flow serially through the two interferometer chambers, or the contents of one chamber could be isolated and used as a standard of reference for the helium circulating in the other.

To begin with, the apparatus was highly exhausted and then washed out with helium generated from thorianite. The gas on its way in passed through charcoal cooled by liquid air, and was thus purified. The apparatus was again exhausted, then suitably charged with helium, and the gas continuously circulated for a considerable time. In this way traces of air were absorbed and retained by the charcoal cooled by liquid air. The purity of the helium was tested as follows.

First, the circulator was stopped, the reference chamber of the interferometer closed, and the position of a selected fringe adjusted and noted. Next, the circulator was again used, then brought to rest, and the position of the fringe re-observed: as the fringe had not shifted, the gas was homogeneous and ready for use. At this stage the pressure of the helium was measured, the gas re-circulated, and the cradle containing the synthesizer rapidly moved to and fro. By trial it was found that when the cradle executed some 2000 strokes per hour the mercury within the synthesizer remained almost stationary: the motor was therefore adjusted for that speed. It will be observed that in this experiment the required glow-discharge was, as in that with the barometric tube, produced by friction. Proceeding thus, experiments were made with helium at pressures ranging in value from 4.6 to 0.4 mm. Variations in the density of the gas were indicated by the interferometer only when $p = 1.3$ mm. With helium at that pressure, the sighted fringe first shifted negatively by one-half of its width and then for a time remained stationary; but as the experiment progressed, the zero position was regained and then finally entirely over-passed. Taking the width of a fringe as measured by rotating the compensator as $60'$, the observed respective displacements were $-30'$ and $+66'$. The first movement of $-30'$ indicated a *decrease* in the density

of the gas, and the second or +66' an increase. Bearing in mind the fact that the interferometer was connected with the synthesizer by some 3.5 m. of tubing, much of which was of capillary dimensions, the observations are readily and probably correctly interpreted as follows

On starting the experiment, helium begins to combine with mercury vapour; the synthesis proceeds (probably at a diminishing rate) until some small and limiting percentage of helium has been formed. If the experiment is prolonged the total helide is not thereby increased, for here, as in the case of the formation of ozone, a balanced action ultimately obtains. Initially, the known diminution in the pressure of the gas is local, the locality being that of the active synthesizer. In due time, however, the decrease in pressure is manifested throughout, and consequently the density of the helium in the testing chamber of the interferometer is lessened; in response to this change the sighted fringe shifts as stated. Next, as a result of the continued circulation of the gas, the mixture of helium and helide enters the interferometer; the original density of its contents is thus first gradually restored and finally surpassed. Hence the observed second or positive shift of the fringes.

The conclusion here reached was confirmed by another experiment, similar in form, but carried out with a stationary synthesizer armed with external electrodes. In this experiment a spectrometer was used in conjunction with the interferometer. The evidence of the one agreed with that of the other.

Other forms of apparatus were tried, but all, with the exception of that to be described immediately, proved useless. In the next section is given an account of the method adopted for a first quantitative analysis of mercury helide.

3. The Apparatus.

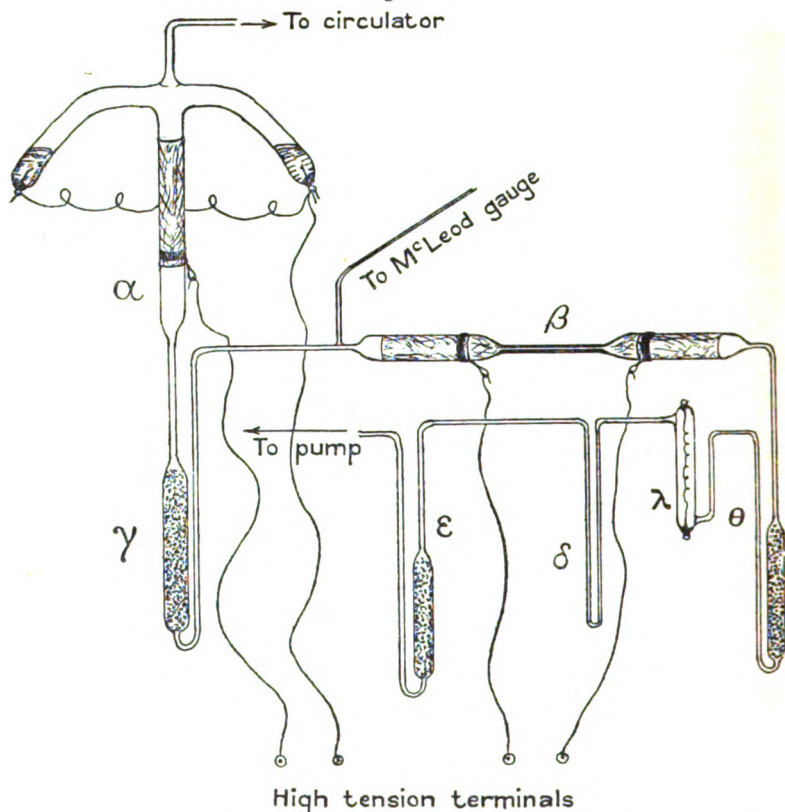
The earliest attempt to determine the chemical composition of the helide was made with the aid of the apparatus shown in fig. 3, wherein α is one synthesizer having both mercury and tinfoil electrodes, and β another fitted only with external electrodes of tinfoil. In this latter the wide portions covered by the electrodes contained platinized asbestos loosely arranged and previously purified. δ is a U-tube of small bore, and γ , ϵ , and θ chambers filled with charcoal. The heater λ was a tube 10 cm. long and 15 mm.

wide, having a spiral of platinum wire. The wire was 0.1 mm. in diameter, and its ends were welded to platinum terminals. The apparatus was prepared for use as follows.

4. Preliminary Treatment.

First, a high vacuum was established and maintained for 6 days. During that time the gas-grown skins upon the

Fig. 3.



interior were electrically eroded and removed; the charcoal chambers were also strongly heated. Next, pure helium was introduced and left undisturbed for 10 days; it was then pumped out, and the new gas-grown skins erupted and ejected. A further charge of helium having been admitted, the circulator was kept in action for a time and the gas examined; the spectrum was quite free from air-lines. Lastly, this helium was also pumped off and a final charge

introduced. The charcoal chambers ϵ and θ were now immersed in liquid air, the helium circulated, and a flame passed to and fro over the limbs extending from ϵ to θ ; also the platinum spiral was raised to a bright red heat. The portion $\epsilon \rightarrow \theta$ was thus rapidly freed from mercury, the absence of which was ascertained spectroscopically. When the helium had acquired a constant pressure (12.1 mm.) the preparations were complete. The synthesis and analysis of the helide were then carried out as described below.

5. *Synthesis of the Helide.*

A maximum quantity of helide was formed by activating the synthesizers with a coil yielding a 1-inch spark. The synthesizers were sometimes used singly and at other times conjointly. When α alone was used, the pressure of the circulating helium remained unaffected; but on bringing β into action alone or in conjunction with α , the pressure declined and finally attained a minimum and constant value. The constancy of the new pressure was taken as indicating the impossibility of carrying the synthesis further. The coil was therefore silenced as a preliminary to the next step.

6. *Decomposition of the Helide.*

Tentative experiments not described here had shown that, on passing the mixture of helium and helide through the active heater λ , the minimum pressure resulting from the action of β gradually gave place to one of larger value, but the new final pressure, although approximating to the original, seldom equalled it. The same experiments also showed that the increasing pressure was invariably accompanied by an accumulation of mercury in the U-tube δ . The method of analysis was therefore as follows

First, the U-tube δ was immersed in liquid air and the pressure of the gas determined; then the spiral λ was raised to and maintained at a bright red heat, the circulator started, and from time to time the pressure p re-determined. When there was no further change in p , a flame was passed over the body of λ and its limbs until the whole of the mercury liberated from the helide had been driven into the lower portion of δ ; the limbs of δ were then closed by softening the glass, and the U-tube with its contents drawn away from the main apparatus and finally prepared for weighing.

7. *Determination of the Weight of the Mercury.*

After δ had been withdrawn the bend was placed in liquid air, the limbs heated, and finally sealed at points some 3 inches above the bend and the superfluous tubing removed. In this way the minute quantity of mercury was collected within a container of small volume. Next, a counterpoise K similar in all respects to δ was made, and its volume repeatedly altered until it differed from that of δ by the negligible quantity of $\cdot 011$ c.c.

We may here observe that in determining the mass, which was less than $0\cdot 3$ mg. of mercury, exceptional difficulties arise; and it will be seen that very inaccurate conclusions may be reached if the containing tube is first weighed, then notched with a cutter and fractured for the removal of its contents prior to a final weighing. The correctness of this view is borne out by the results of an actual experiment, in which notching and fracturing caused the respective losses of $\cdot 0043$ and $\cdot 015$ mg. Such errors were in the present case avoided by opening δ in dry carbon dioxide-free air before commencing the weighings. After the first weighing the mercury was removed by dissolving it in nitric acid, the tube washed out with "conductivity" water, and then dried and re-weighed.

In carrying out the several weighings, all the precautions which I have shown to be necessary and advocated elsewhere were taken: it will therefore suffice if brief mention be made of the following salient points:—

(a) Use was made of a balance having a beam cantilever in type and protected*. For a given temperature the instrument had a constant sensitivity for all loads. The sensitivity, and also the temperature-coefficient of the balance for the load to be imparted, were each determined shortly before the mercury obtained from the helide was weighed. The movements of the balance were observed and measured optically, and for that purpose the apparatus included a plane mirror fixed to the centre of the beam, and a telescope for viewing the pointer of light, which was 6 m. long.

(b) After the tube δ and its counterpoise K had been wiped and suspended from the stirrups, and before their relative weights were determined, both were washed *in situ* by streams of dry and carbon dioxide-free air.

(c) For measuring the several weights, the method of Gauss was used. The weight of δ + mercury and of δ alone

* Thorpe's 'Dictionary of Chemistry,' new edit. Article "Balance."

were the means of several series of weighing duly corrected.

Proceeding as outlined above, it was found that the weight of the combined

$$\text{Mercury} = 0.236_1 \text{ mg.}$$

8. Determination of the Combined Helium.

For the synthesis of mercury helide, pressures ranging from 12.1 to 0.6 mm. were tried. Positive results, as indicated by a decrease in the pressure p , were obtained only when p was approximately 6, 1.9, or 0.6 mm. Accordingly syntheses followed by analyses were effected at each of these pressures, the results summed, and the totals treated as for one complete experiment. The data obtained are given in the following table.

TABLE I.

Exp.	Pressure of Helium.			Diffs. (c) - (b).	Weight of helium in helide.	Total weight of helium in apparatus.
	(a) Initially.	(b) After synthesizing.	(c) After analysing.			
1.	6.24 mm.	5.75 mm.	6.02 mm.	0.27 mm.	0.17 ₈ mg.	0.378 mg.
2.	6.11 "	5.91 "	6.11 "	.20 "	0.12 ₈ "	" "
3.	1.96 "	1.85 "	2.05 "	.20 "	0.12 ₇ "	.121 "
4.	.595 "	.561 "	.595 "	.034 "	0.02 ₃ "	.036 "
5.	.595 "	.561 "	.581 "	.020 "	0.01 ₄ "	" "

Hence total weight of combined

$$\text{Helium} = 0.47_0 \text{ mg.}$$

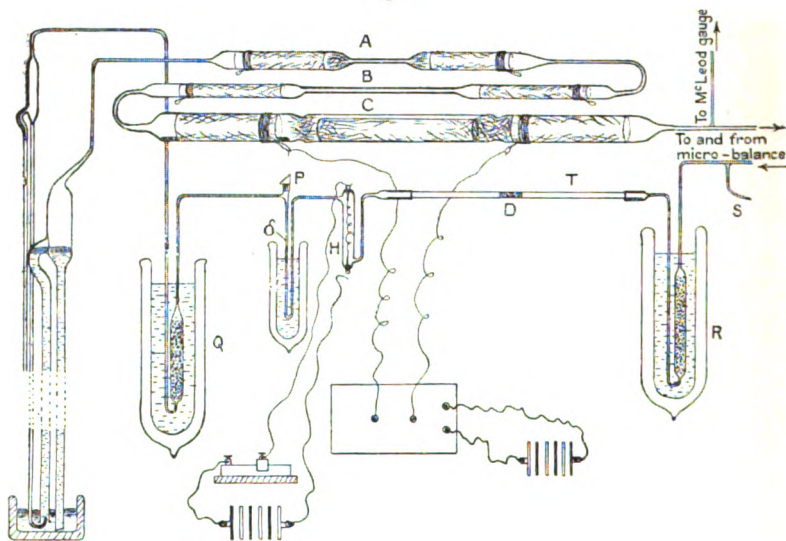
From the above we find that 200.6 parts by weight of mercury combined with 39.94 parts by weight of helium. It therefore appears that the simplest formula for the helide is



In calculating this formula, the view held was that on activating the synthesizers the *formation* of a gaseous helide did not in itself cause any change in volume, and that the diminution in p was consequent upon the growth of a somewhat volatile skin of helide upon the internal surfaces of the apparatus in general. Hence in the presence of a fully-developed skin it was impossible to do more than synthesize an additional but infinitesimal quantity of helide, the pressure of which balanced the tension of the skin. When the gas was circulated and the heater used, the

minute quantity of free helide was decomposed and the tension of the skin left unbalanced. Under these conditions the skin continuously reverted to the gaseous state and was decomposed; and as the decomposition progressed, the original pressure was either partially or wholly restored. Such partial restorations were observed in exps. 1 and 5, and whole ones in exps. 2 and 4. In exp. 3 the final pressure overpassed the initial. This was probably due to the decomposition of some helide remaining at the conclusion of exp. 1.

Fig. 4.



Assumptions other than those just stated appear to lead to formulæ for the helide even less acceptable than that based upon my hypothesis.

We may now describe the apparatus and methods used for another and similar determination.

9. *Second Quantitative Analysis.*

Before proceeding with the second quantitative analysis of mercury helide, important changes were made in the apparatus, and the synthesizers formerly used replaced by three others, A, B, and C; these were constructed and disposed as shown in fig. 4. In the new apparatus the helium in circulating passed in the direction $A \rightarrow B \rightarrow C$.

The synthesizer A was similar in form to, but larger than, β of fig. 3. Its wide limbs were, like those of β , filled with loose platinized asbestos. The second synthesizer, B, differed from A in that it contained no asbestos; also its capillary tube was twice as long and of larger bore. C was a tube 34 mm. wide and 58 cm. long, and within it were placed loose wads of platinized asbestos and a little pure mercury. All the synthesizers were fitted with external electrodes. A new heater, H, displaced λ of fig. 3; also the sensitivity of the spectroscopic test for mercury was greatly increased by the use of a right-angled prism P mounted as shown*. This device gave the spectrometer an end-on view of the vertical tube when the glow-discharge was set up for the test. The apparatus was rendered complete by the inclusion of an Aston micro-balance (not shown in fig. 4) and a silica tube T having a tightly-fitting plug, D, composed of fine and purified asbestos fibre. In this, as in the earlier experiment, all gas-pressures not exceeding 7 mm. were measured with a McLeod gauge having an accuracy of .0001 mm. Larger pressures were determined with a cathetometer. The Sprengel pump and the circulator which formed part of the apparatus were those described in former papers†. The second experiment was commenced only after the complete apparatus had been prepared with all the care observed for the first. The several charges of helium were obtained from powdered thorianite, which was heated in an attached silica tube. On its way in, the gas passed through charcoal cooled by liquid air, and when the final charge of helium had been introduced, the silica tube and its charcoal chamber was sealed off at S. The apparatus was then ready, and the experiment was carried out as follows.

First, the charcoal chambers Q and R were surrounded by liquid air, the circulator started, and the heater and its limbs, including δ , freed from mercury. When the pressure p was constant, the micro-balance was read and the synthesizers activated for 4 hours. During the synthesis, p was but slightly affected. Next, the action of the synthesizers was arrested, the micro-balance re-read, δ immersed in liquid air, and the heater used for 11 hours. Again p varied but little. When the helide had been decomposed, the chamber of the micro-balance and its attachments were by means of mercury traps shut off from the main apparatus, and the compressor operated until the density of the helium as indicated by the micro-balance equalled that previously shown for the mixture

* Proc. Phys. Soc. xxxviii. p. 127.

† Proc. Phys. Soc. xxxvii. p. 142.

of helium and helide; the pressure corresponding to this density was then measured. Finally, the mercury liberated from the helide was collected in the bend of δ , then sealed up and its weight determined. The weighings were carried out with additional refinements lately introduced*. With the aid of those extra refinements the weight of the mercury was, it is believed, determinable with an accuracy of ± 0.0005 mg. The following table contains the summarized data.

TABLE II.

Mean pressure of the gas before the synthesis	= 5.46 mm.
" " " during " " 	= 5.44 "
" " " after the analysis	= 5.46 "
Final mean	= 5.45 ₃ mm.
Weight of mercury derived from the helide	= 0.271 ₄ mg.
" helium present in the apparatus.....	= 1.771 ₆ "
Total weight of helium and helide	= 2.043 mg.
Calculated density of mixture in terms of helium = $\frac{2043}{1771_6}$	= 1.153
Density as measured by the micro-balance	= 1.148

The above observations and data receive a ready explanation on the assumption that in the second quantitative experiment another helide having the empirical formula



was synthesized. The line of argument here adopted is, as will be seen, similar to that used in the case of mercurous chloride, HgCl .

It may however be said that another formula, namely HgHe_2 , is also in harmony with the data of Table II. The mono- and di-helides of mercury differ in their molecular weights by 2 per cent. only, and the total helide present for quantitative analysis was never greater than 3/100 c.c. It will therefore be seen that the effect of substituting HgHe_2 for HgHe is, in so far as the density of the mixture is concerned, inappreciable or nearly so. Hence we may accept the formula HgHe_2 as being more in accord with probability. For this view I am indebted to Dr. Sidgwick.

We have already noted that during the synthesis and analysis the respective mean variation of — and + 0.2 mm. occurred in p . These changes seem to show that a little of

* Proc. Phys. Soc. xxxix. p. 444.

the other helide HgHe_{10} was first formed and subsequently decomposed ; but in the absence of definite proof, this point is not further pressed. All attempts made with the new apparatus to prepare HgHe_{10} in quantities larger than that here suggested ended in failure.

10. *On the Absence of Floating Particles.*

In the first quantitative experiment the decrease in the pressure of the helium, together with the failure of the helide to condense, readily leads to the supposition that the compound might be diffused as floating solid matter ; but in that case it should be possible to remove at least some of the particles by filtration. It was for testing this view that the silica tube with its asbestos plug was inserted between R and H, as shown in fig. 4. The plug was at the outset strongly heated *in vacuo* and also stripped of gas-grown skins. It was in use throughout the second quantitative experiment just described. Had particles been arrested by the filter-plug, additional helide would presumably have been synthesized, and consequently the pressure of the helium would have diminished continuously. Also, on heating the plug, the arrested helide would have been decomposed and additional mercury obtained. Experimentally, the reverse of this was observed ; the pressure was, as already stated, practically unaffected, and when the plug was heated to redness no mercury was detected. Hence we again came to the conclusion that mercury helide is a gaseous and not a solid compound. Two other points yet remain and call for investigation—namely, the question of the possible introduction of mercury (*a*) from the platinum spiral, and (*b*) from the charcoal chambers immersed in liquid air.

11. *On the Absence of Mercurial Impurities.*

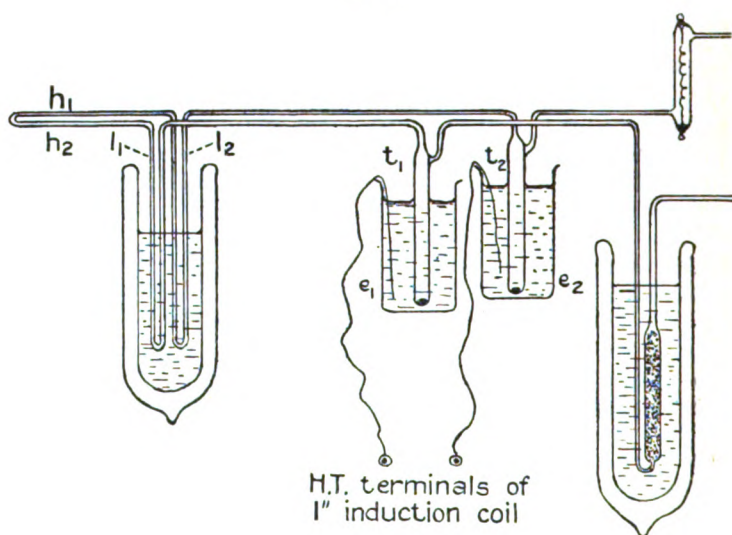
The difficulties of admitting the probability of the union of helium with another element are for the moment so great that we are tempted to accept any explanation other than the true one to account for the appearance of mercury in the U-tube δ . Of the possible explanations, two only call for immediate consideration. It may be urged (1) that the mercury was derived from the platinum spiral of the heater, and (2) that when the synthesizers were active, electric discharges occurred in the charcoal chambers and eroded the solidified mercury, and that resultant particles were then to some extent carried forward into δ by the circulating

helium. With regard to (1), an inferential reply is contained in the preceding sections. It will therefore suffice to note that an essential part of the preparation of the apparatus consisted in circulating the helium and heating the chamber containing the white-hot spiral for some time after mercury could no longer be spectroscopically detected. It will thus be seen that explanation (1) is valueless.

For testing the validity of (2), experiments were made as follows:—

The main apparatus of fig. 4 was opened at a convenient point and the auxiliary apparatus of fig. 5 inserted. The tubes t_1 , t_2 with their mercury contents were given external

Fig. 5.



electrodes e_1 , e_2 of water, as shown. The completed apparatus was first prepared as usual, and then charged with helium at a pressure of approximately 5 mm. Next, the two U-tubes l_1 , l_2 were immersed in liquid air, the helium circulated continuously, and the horizontal limbs h_1 , h_2 heated until they were free from mercury. A bright glow-discharge was now set up and maintained within the auxiliary apparatus for 1 hour. On re-examining the limbs h_1 , h_2 , nothing beyond an occasional glimpse of the mercury line, dim and uncertain, was obtained. A second and similar experiment made after mercury had been distilled

into the U-tubes l_1 , l_2 , and boiling water substituted for cold in the electrode vessels led to an equally negative result. It was thus decisively shown that any mercury entering the liquid air-cooled tubes is completely arrested and retained, even in the absence of impeding charcoal. The tentative explanation (2) is therefore like (1) untenable. But apart from these proofs, it would have been most remarkable had mercury transported at random possessed in two successive instances just those masses required for such precise agreement with related data. Such coincidences are, of course, altogether highly improbable. Some concluding experiments carried out as the result of a suggestion made by Professor Henri, of Zurich, must now be described.

12. Experiments with a Quartz Spectrograph.

During a discussion of the problem, Professor Henri expressed the opinion that mercury helide would give rise to an absorption line in the ultra-violet region, and, further, that the wave-length of the said line would be something like 2500. As such additional evidence was highly desirable, the apparatus of fig. 4 was altered and the twin 1m chambers* of a quartz spectro-photometer substituted for the silica tube T; also the micro-balance was cut out, and the gap thus left closed by a short tube.

For producing the required ultra-violet light, use was made of a 10 in. coil supplied with a current (fed through a motor-driven mercury interrupter) of 9-10 amps. The discharge points were of pure cadmium and the gap was 3 mm. The spark was intensified by a large Leyden jar, and the rays of light rendered parallel with a 2 in. quartz lens. After the light had traversed the spectro-photometer, the two emergent beams entered the slit of a quartz spectrograph and were photographically recorded. The procedure was as follows.

First, the whole apparatus was prepared as for other experiments and then charged with pure helium. Next, the helium was circulated for 2 days and a series of photographs taken. In all these photographs the mercury absorption line 2537 was, as seen in each pair of spectra, equally faint, and in the last instance the line was no weaker than in the first. (This persistence of the line is considered presently.) As the absorption line, though faint, remained unchanged, the inlet and outlet tubes of the lower or reference chamber S

* The gas flowed through the chambers as two parallel and not as two serial streams.

were softened by a flame and so closed. The contents of S thus served as a standard.

With the helium still circulating, the synthesizers were now activating for some hours during each of 5 successive days; also photographs of the twin spectra were periodically taken. It was thus found that the intensity of the mercury absorption line of the sealed reference chamber increased, and ultimately assumed a constant value. In the testing chamber the same line, invariably weak, was in some cases more in evidence than in others. In these experiments the pressure of the helium was varied within the limits of 11.5 and 6.38 mm.

A scrutiny of all the plates for the expected new absorption line showed that in 3 cases only was any such line present. In one of these a line of WL 2276 was found; but as it was common to both spectra, it was judged to be due to extraneous matter. In the other two cases the line was one and the same; it was very weak and not sharply defined, and its WL was 2624*. The line appeared first when the pressure of the helium was 11.5 mm., and again when $p = 6.38$ mm. In each instance the weak mercury absorption line was, as usual, also present. An attempt was now made to obtain a more marked effect; and for that purpose the apparatus was reconstructed so that by means of added mercury traps the testing chamber T could be closed, and then with the aid of an attached Sprengel pump the gaseous contents of the main apparatus M transferred to T and there be retained for spectrographic analysis. From the known volumes of M and T the sensitivity of the test was thus theoretically increased fourfold.

With this apparatus syntheses were effected in the usual way, and the product together with the free helium concentrated and then examined with the spectrograph. All the results were purely negative, and in no case was there any trace of the new absorption line. Whence it appears that if the line 2624 was really due to mercury helide, the conditions under which the compound can exist when traversed by ultra-violet light were obtained by chance, and are at present unknown.

13. *On the Persistence of the Mercury Line 2537.*

Attention has already been drawn to the fact that the mercury absorption line of WL 2537 is invariably present

* This line has been re-measured by Messrs. A. Hilger, who find its WL to be 2638.

in spectra obtained with the test chamber. As the inlet and outlet tubes of the chamber were guarded by U-tubes placed in liquid air, it was not easy to discover from whence the mercury came. For investigating this, the apparatus was again altered and a spectrum tube having external electrodes inserted between the exit of the chamber T and its guard-tube. These changes having been effected, the presence or absence of mercury within the guarded portion of the apparatus could be ascertained (a) by the absorption line 2537 and (b) by the highly characteristic emission line 5461. The following experiments were then made :—

(1) First, the apparatus was highly exhausted, the guard-tubes Q and R (fig. 4) immersed in liquid air, and the whole left at rest. Two days later, the vacuum being high, it was impossible to activate the spectrum tube. A photograph of the twin spectra for the chambers S and T was now taken; this proved that mercury vapour was quite absent from the testing chamber T.

(2) Next, a second photograph was taken whilst the chamber T was strongly heated. In this case also mercury was entirely absent. These results attest the perfect efficiency of the guard-tubes, and at the same time show that whether mercury be present as vapour or in the form of a skin, it is completely withdrawn and prevented from re-entering the chamber and its attached spectrum tube.

(3) Having now freed the testing chamber from mercury, the pure helium was returned to the apparatus and circulated; also photographs of the twin spectra were again periodically taken. All the spectra due to the light passing through T again contained the mercury absorption line 2537. The line, although weak, was invariable. At this stage the heater was used for disintegrating any helide that might be present. The luminosity of the mercury line was not thereby affected.

(4) In the next experiment the circulator, synthesizers, and heater were used for 75 minutes. During this period additional photographs were taken and the spectrum tube frequently viewed with a spectrometer. It was found that the absorption line was but slightly strengthened, whilst the green emission line rapidly increased and finally became very bright*.

The results of the experiments just described led me to conclude that mercury helide in minute quantities is

* To avoid possible misunderstanding, I would remark parenthetically that the oft-mentioned absorption line 2537 was in no case other than what one would designate as "rather weak," "weak," or "very weak."

formed so readily that it is well-nigh impossible to manipulate dry and pure helium over mercury without producing some infinitesimal trace of the compound. The proof for this lies to a large extent in the evidence of the above-cited experiments (3) and (4). That evidence we now briefly review.

14. *Review of Results of Experiments (3) and (4).*

When experiment (3) was started, the chamber T and its spectrum tube were, as I have shown, free from mercury. Soon after commencing the circulation of the helium (the synthesizers being idle), the chosen mercury absorption and emission lines were readily detected, the one by the spectrograph and the other by the spectrometer. That the detected mercury could not have passed through the guard-tubes has been conclusively shown by the experiments of section 11. Hence the most acceptable explanation is found in the assumption that mercury helide is synthesized not only in the fall-tube of the Sprengel pump, but also during the ascent of the bubbles of helium in the barometric column of the circulator*. But if this be the whole truth, we should, according to Prof. Henri, expect to find an absorption band or line appropriate to the helide recorded by the spectrograph; instead of which we obtained, in every case but two, the absorption line characteristic of mercury. Apparently the only possible explanation is that the helide, on traversing the ultra-violet light in the testing chamber, is thereby so quickly resolved into its component elements that in general it fails to leave any legible record of its existence. This explanation receives support from the fact that on using the heater towards the conclusion of experiment (3) the mercury line was not intensified. Had the heater been more effective than the ultra-violet light, the absorption line must have been strengthened. This, as we have already stated, was not the case.

We next note that the evidence of experiment (4) is in complete accord with that of experiment (3). The use of the synthesizers would naturally result in the production of a maximum quantity of helide and a consequent though not necessarily marked intensification of the mercury absorption line. That this line could in no case be other than "weak" is clear from the following.

The volume of the gaseous contents of the apparatus was

* The necessary glow-discharges are, as is well known, produced as the mercury drops in the fall-tube, and again when the liquid in the barometric column of the circulator is disturbed.

at this time approximately 1L. and that of the testing chamber 38 c.c. Taking the weight of the combined mercury as 0.27 mg., and assuming this to be uniformly distributed, the mercury in the testing chamber was not more than $0.27 \times 38/1000$ or 1/100 mg. Of the light coming through the testing chamber, a small fraction only entered the spectrograph to be photographically recorded; and this being so, the invariable weakness of the absorption line is at once understood. In section 12 we observed that the very weak mercury absorption line 2537 of the standard chamber slowly developed and finally became fairly strong and constant. In accordance with the views already expressed, the strengthening of the line was due to a natural and slow decomposition of the helide, accelerated and completed by the passage of ultra-violet light. Brief allusion may now be made to some experiments with argon.

15. *Experiments with Argon.*

With the object of still further testing these conclusions, a series of experiments similar in all respects to those made with helium were performed with argon*. Certain impurities suspected of being present were removed by sparking the gas between "heavy" poles, the one of aluminium and the other of magnesium, as recommended by Merton and Pilley. For an attempted synthesis, the pressure of the argon was varied within the limits of 14 and 2 mm. The pressure of the argon was unchanged, and in no case was mercury discovered in the receiving U-tube of the heater. From this it is quite clear (1) that argon did not combine with mercury, and (2) [and this for the moment is more important] that mercury was neither mechanically or electrically transported into δ . This last affords additional proof that the mercury found in δ during the experiments with helium resulted, as we have already seen, only from the decomposition of the gaseous helides HgHe_{10} and HgHe .

Further confirmation of the correctness of my results may be found in the evidence of those interesting experiments carried out by Boomer in the Cavendish Laboratory. Boomer has shown† that, under the particular conditions he describes, the helides of some five elements, including

* For the argon used in these experiments, I am indebted to Mr. Bolton-King.

† Proc. Roy. Soc. A, cix. p. 198 (1925).

mercury, are probably formed. They appear as solids, and are unstable except at low temperatures.

In conclusion, I desire to thank Prof. Lindemann, Dr. Sidgwick, and Dr. Freeth for their interest and assistance. I have also to acknowledge my indebtedness to Prof. Soddy, through whom Messrs. Brunner Mond & Co. made a generous grant. That grant enabled me to purchase the quartz spectrograph and also a 10 in. coil for testing the prediction made by Prof. V. Henri.

Daubeny Laboratory,
Magdalen College, Oxford.

LXII. *The Tangent Lens Gauge Generalised* *.

By ALICE EVERETT, M.A. †

THIRTY years ago the Philosophical Magazine (vol. xliii. p. 256, 1897) published a description by the late Prof. G. J. Burch, F.R.S., of a simple home-made tool for measuring the curvature of a convex lens, which he named the "Tangent Lens Gauge." It was intended to furnish laboratory exercise for students.

Essentially, it consists of a pair of plate-glass slips joined so as to form a shallow inverted trough which is laid upon the surface under test. The two points of contact, where the plane surfaces touch the sphere, can be seen by reflected light as centres of Newton's ring systems, and the length of the chord joining these points can be measured by the aid of a measuring microscope fitted with a "vertical," or down-tube illuminator. The required radius of curvature is then found by multiplying the chord by a constant factor, and applying a correction, also constant, for refraction. The device is not applicable to concave surfaces.

Recently, in ignorance of Prof. Burch's paper, I chanced to hit upon the same idea, and would here point out that it can be adapted to measure either concave or convex surfaces by employing a tool with spherical, instead of plane, glass faces. A simple arrangement which meets the case is a pair of similar plano-convex lenses fixed edge to edge with their flat faces in one plane. As means of attachment, two parallel, narrow glass strips cemented to the flat faces will serve. These strips should be as far apart as possible, so as

* A previous note appeared in 'The Optician,' Jan. 30, 1925, under a pen-name.

† Communicated by the Author.

to leave the central portions of the lenses free. If this twin combination is placed with its two curved surfaces in contact with the surface under test (it may be secured by plasticene pellets), then the two points of contact, and their distance, d say, apart, can be found as in Burch's method. But the correction for refraction will not be constant in this case.

From the fact that when two spheres touch the point of contact lies on the line of centres, it easily follows that

$$\frac{1}{r} + \frac{1}{R} = \frac{k}{d},$$

where r is the required radius of curvature of the surface under test, R the radius of curvature of either of the twin lenses, and k a constant which can be found by applying the tool to a plane surface. With the usual convention that r is to be taken negatively for concave curvature, the formula is applicable to either a convex or concave surface.

A rough and ready demonstration can be made on spectacle lenses from a test-case, with the naked eye and a pocket scale. The central dark spot of Newton's ring system can easily be seen at the points of contact on applying gentle pressure, though the coloured rings may be invisible. The spot is readily distinguished from dust specks by its sharply circular form.

Riverside,
Sunbury-on-Thames.

LXIII. A Note on the Dispersion of Methane.

By T. H. HAVELOCK, F.R.S.*

1. IT has been commonly assumed, in various connexions, that the hydrides FH , OH_2 , NH_3 , CH_4 may be regarded as neon-like ions F^- , O^{2-} , N^{3-} , C^{4-} deformed or perturbed by one or more hydrogen nuclei. For example, Fajans and Joos† give the following comparison of molecular refractivities :—

Ne.	FH.	OH_2 .	NH_3 .	CH_4 .
1.0	(1.9)	3.76	5.61	6.55

with estimated values for the hypothetical free ions :

F^- .	O^{2-} .	N^{3-} .	C^{4-} .
2.5	7	(22)	(80)

* Communicated by the Author.

† K. Fajans and G. Joos, *Zeit. für Phys.* xxiii. p. 1 (1924).

Phil. Mag. S. 7. Vol. 4. No. 23. Oct. 1927.

3 A

The inference is that CH_4 is a member of this series of hydrides with a structure similar to the other members.

Instead of considering only refractivity, let us take into account also the optical dispersion. We shall use the simplest form of dispersion formula :

$$n^2 - 1 = C_0 / (p_0^2 - p^2) \dots \dots \dots (1)$$

For simple gases under consideration this is sufficient for our purpose, and we take the constants C_0 and p_0 to express approximately the refractivity and dispersion. Cuthbertson has given his experimental results for gases in this form, and we collect his values of the constants in the following table :—

Gas.	$C_0 \times 10^{-27}$.	$p_0^2 \times 10^{-27}$.
Ne	5.1865	38916
FH	—	—
OH_2	5.2540	10697
NH_3	5.9316	8135
CH_4	10.0554	11689.3

. . . (2)

As regards Ne, OH_2 , and NH_3 , we note the approximately constant value of C_0 and the regular decrease in p_0 , both of which points confirm and bring out more clearly the similarity of structure from the optical point of view. No doubt FH would also fit into this scheme; we have no knowledge of its dispersion or refractivity in the gaseous state, but if we assume the estimate 1.9 for its molecular refractivity given by Fajans and Joos, and also assume the value of C_0 to be 5.2×10^{27} , then the corresponding value of p_0^2 is 20703×10^{27} .

On the other hand, for CH_4 we see that the inference from refractivity alone was illusory; C_0 is nearly doubled and p_0 is also increased, and CH_4 clearly does not fall in with the sequence in (2).

In making this comparison in a recent paper*, I remarked that earlier experiments on the dispersion of methane by S. Loria could be expressed by a dispersion formula (1) with $C_0 = 6.314 \times 10^{27}$ and $p_0^2 = 7373.8 \times 10^{27}$; and therefore further experimental evidence seemed desirable. Since then, further work has been published which confirms Cuthbertson's formula in its general character. Friberg†

* Phil. Mag. iii. p. 444 (1927).

† S. Friberg, *Zeit. für Phys.* xli. p. 378 (1927).

has studied the dispersion of ammonia and methane over a large range of wave-length extending from 5462 Å. to 2302 Å. It is true that a simple two-constant formula is not sufficiently accurate for this wide range; but that need not concern us here. Friberg gives for methane a two-constant formula which covers this range surprisingly well, namely

$$\frac{2n^2 + 2}{3n^2 - 1} = 2325.29 - 18.541 \times 10^{-8} \lambda^{-2}. \quad (3)$$

Reduced to the form (1) this gives

$$C_0 = 9.708 \times 10^{27}; \quad p_0^2 = 11284 \times 10^{27}. \quad (4)$$

These values are a little different from Cuthbertson's; but the latter were obtained from the range 6708 Å. to 4800 Å., while Friberg's were found from the extremes of his range. For comparative purposes it is better to use values deduced under similar conditions, and we therefore use Cuthbertson's values throughout as in the table in (2).

2. There are other physical and chemical properties which also suggest that CH₄ is different from the hydrides in this sequence. An investigation of the ionization potential of methane from this point of view has just been made by Pietsch and Wilcke*. They quote the ionization potentials of Ne, FH, OH₂, NH₃ as 21.5, (15), 13.2, and 11.1 volts respectively; while Grimm and others have put that of methane at 9.5 volts, so making it one of this sequence. On the other hand, later experimental values for methane range round 13.9 volts, and Pietsch and Wilcke give the value 14.6 volts.

Reverting to the dispersion formula (1), the frequency p_0 is, on the classical theory, a dominant natural frequency in the ultra-violet. Various attempts have been made lately† to identify p_0 with ionization potential, or in formulæ with several terms with ionization and resonance potentials, when the latter have been transformed into frequencies by the usual quantum relation. It seems more probable that p_0 is near the maximum general absorption on the ultra-violet side of the series limit, and this seems to have been confirmed for the inert gases by Cuthbertson's direct observation of absorption in this region‡. However this may be, it is of

* J. E. Pietsch and G. Wilcke, *Zeit. für Phys.* xliii. p. 342 (1927).

† B. Davies, *Phys. Rev.* xxvi. p. 232 (1925). K. F. Herzfeld and K. L. Wolf, *Ann. der Phys.* lxxvi. p. 71 (1925). R. A. Morton and R. W. Riding, *Phil. Mag.* i. p. 726 (1926).

‡ C. Cuthbertson, *Proc. Roy. Soc. A*, cxiv. p. 650 (1927).

interest to turn the frequencies in the table (2) into potentials by the relation

$$V = 1.234 \times 10^{-4} p/c \text{ volts.} \quad . \quad . \quad . \quad (5)$$

Calling this the dispersion potential, and quoting from Pietsch and Wilcke for the ionization potential, we obtain the following series :—

	Ne.	FH.	OH ₂ .	NH ₃ .	CH ₄ .
V (dis.)	25.4	—	13.5	11.7	14.1
V (ion.)	21.5	—	13.2	11.1	14.6; (13.9)

There is no need to press the comparison too closely, for reasons we have given ; the general similarity of the two series is sufficiently striking to show the analogy between the phenomena.

3. We may conclude that CH₄ does not belong to the neon-like series of hydrides in table (2), and that optically at least it does not behave like a C⁴⁺ ion with four hydrogen nuclei. The atomic binding in the molecule may, of course, be of the homo-polar, or electron-sharing type ; but let us examine the alternative hetero-polar structure of a C⁴⁺ ion with four H⁻ ions. This has been proposed in a recent discussion of chemical valency by Niven*. Reviewing the chemical properties of this sequence, Niven argues that FH consists of F⁻ and H⁺, but that, on the other hand, in methane the carbon atom has lost its 2₁ and 2₂ electrons to the hydrogen atoms to complete their 1₁ systems ; he also considers that OH₂ and NH₃ have the latter type of structure, but the optical and other evidence collected here shows that Ne, FH, OH₂, and NH₃ form a regular sequence, which is definitely broken at CH₄†.

The C⁴⁺ ion has a very small refractivity. If we neglect its direct contribution and also the interaction of the ions, then the refractivity of CH₄ should be that of four H⁻ ions to a first approximation. H⁻ should bear to helium a similar relation to that of F⁻ to neon. Thus if we form a table like (2), but with helium in the first place, H⁻ will be the other member, and we should expect the same value of the constant C₀ and a smaller value of p₀. Using Cuthbertson's

* C. D. Niven, *Phil. Mag.* iii. p. 1314 (1927).

† I find that this has also been advocated by J. H. de Boer and A. E. van Arkel, *Zeit. fur Phys.* xli. p. 27 (1927).

constants for helium, and dividing the constant C_0 for methane by four, we obtain the following table:—

Gas.	$C_0 \times 10^{-27}$.	$p_0^2 \times 10^{-27}$.
He	2.4248	34992
$\frac{1}{4}\text{CH}_4$	2.5138	11689

. . . (6)

These results agree with the view taken of the structure of CH_4 , though no doubt the agreement may possibly prove to be only a coincidence. We have neglected the mutual interaction of the H^- ions; this may be justified for the present comparative use by assuming a tetrahedral structure and using the relevant formulæ given in a previous paper*, so verifying that the effect is relatively small in this case. Just as in table (2), we were not dealing with free ions, but with ions F^- , O^{2-} , and so on, under the influence of hydrogen nuclei, so in CH_4 we have H^- ions under the deforming or contracting influence of a central C^{4+} ion. In a recent paper†, Pauling has given theoretical estimates of the molecular refractivities of hypothetical free ions; his value for H^- is 25.65, and those for F^- , O^{2-} , N^{3-} , and C^{4-} are 2.65, 9.88, 72.6, and 5400 respectively. These give, for instance, a value of 29.6 for CO_3^{--} instead of the value 12.3 assigned by Fajans and Joos; the diminution may be attributed to the influence of the central C^{4+} ion if Pauling's theoretical values are accepted.

Again, the molecular refractivities of OH_2 and NH_3 are 3.7 and 5.5 respectively; these may be compared with the theoretical values 9.88 and 72.6 for the corresponding free ions.

On the present view of the constitution of CH_4 , we deduce a molecular refractivity of 1.61 for H^- in this combination with C^{4+} as the central ion; Pauling's value for the free ion is 25.65.

4. The argument of this note is that a comparison of approximate dispersion formulæ for Ne, FH , OH_2 , NH_3 , CH_4 shows that CH_4 does not belong to this sequence, and that its molecule is not equivalent to a C^{4-} ion with four hydrogen nuclei. A similar conclusion may be drawn from the ionization potentials of this series and from other relevant data. It is shown further that the dispersion formula is not inconsistent with a molecular structure of a C^{4+} ion with four H^- ions.

* Phil. Mag. iii. p. 444 (1927).

† L. Pauling, Proc. Roy. Soc. A. cxiv. p. 181 (1927).

LXIV. *The Characteristics of Gasfilled Photoelectric Cells.*
 —II. By N. R. CAMPBELL. (Communication from the
 Staff of the Research Laboratories of the General Electric
 Company, Ltd., Wembley.)

SUMMARY.

THE theory offered in a previous paper for the "unstable characteristic" of a gasfilled photoelectric cell was false. A new theory is outlined based on the well-studied intermittent "flashing" of neon lamps and similar discharge-tubes. It is shown that the main features of the "characteristic" accord with the ideas derived from this study, and that the complicating factors to which Taylor (with his associates) and Penning have directed attention are more important in the photoelectric cell than in the neon lamp.

Some basis is thus offered for the methods of using the cells described in another recent paper; the correction of the theory does not affect their utility. But minor corrections and improvements of the methods are described.

General Theory of the "Unstable Characteristic."

IN two recent papers* attention was called to (a) the "unstable portion of the characteristic" of a gasfilled discharge-tube, and (b) its use in the detection of illumination. The object of this paper is two-fold; to correct the false interpretation of the facts that was given in the earlier of these papers, and to supplement the facts given in the later.

An attempt was made in (a) (p. 955 *et seq.*) to interpret a certain portion of the curves in fig. 6 as part of the characteristic of the cell, indicating a definite relation between the current through it and the potential between its electrodes; it was suggested that the form of the curve was an indication of the distortion of the field by the space-charge. But it was recorded that the current on this part of the curve was intermittent. This fact destroys completely the interpretation offered; it shows that the relation between the measured current and potential does not indicate a steady state of the cell; and therefore that all attempts to explain the relation in terms of distorted fields, recombination, and so on are beside the point.

Moreover, it should have been clear that the outlines of a

* N. R. Campbell, (a) *Phil. Mag.* iii. p. 945 (1927); (b) *do.* p. 1041 (1927).

correct interpretation had already been provided by the work of J. Taylor (with his associates) and others* on the intermittent discharge through neon lamps and similar vessels. Such vessels are characterized by an upper critical voltage V_s , necessary to start the discharge, and a lower critical voltage V_g , at which the discharge ceases. If they are connected in a circuit containing a source of potential greater than V_s and some device for limiting the mean current \bar{i} to a value much less than that which flows in the discharge, the capacity C between the electrodes will be alternately charged to V_s by the external circuit and discharged almost instantaneously to V_g by the discharge. A voltmeter across the electrodes will read some value \bar{V} , intermediate between V_s and V_g ; n , the frequency of intermittence, will be given by

$$n = \frac{\bar{i}}{C(V_s - V_g)} \cdot \cdot \cdot \cdot \cdot (1)$$

The gasfilled photoelectric cell is similarly characterized by upper and lower critical voltages; accordingly the voltage read on the voltmeter in the experiments of the previous papers should be \bar{V} , determined by the alternating charge and discharge of the condenser formed by the electrodes and their connexions.

According to this simple theory, \bar{V} should be independent of \bar{i} . The characteristics given in fig. 6 of paper (a) have a portion PQ in which V is nearly independent of i and lies between V_s and V_g . Let us suppose that this portion represents the conditions in which the simple theory is nearly true, and let us endeavour to explain the remainder of the characteristic by the introduction of the complicating factors to which Taylor and Penning (*loc. cit.*) have drawn attention.

The facts given have reference to a cell of the "spherical" type, but not that to which fig. 6 refers. Its diameter was greater, namely 10 cm.

The Portion QR.

One of these factors enters if \bar{i} is comparable with the current flowing in the discharge. If $I = f(V)$ is the relation between the current and voltage of the discharge, the current discharging the condenser is $I - \bar{i}$. As \bar{i} increases, V will tend to linger in the neighbourhood of the lower values

* See e.g. J. Taylor and L. A. Sayce, *Phil. Mag.* 1. p. 985 (1925); F. M. Penning, *Phys. Zeit.* xxvii. p. 187 (1926). Most of the earlier literature is cited in these papers.

for which I is small. Accordingly \bar{V} will decrease as \bar{i} increases, until, when $\bar{i} = I_g$, V will be constant and $\bar{V} = V_g$. On these considerations we may explain generally the portion of the characteristic QR, terminating in the steady discharge at R, where $V = V_g$. Along RS $i > I_g$, and \bar{V} is the steady potential given by $i = f(V)$.

The Portion XP.

Along XP the current is always small compared with I ; the variation of \bar{V} with \bar{i} must be due to some influence of \bar{i} upon the recharging of the condenser. Taylor and Penning have shown that, after the discharge ceases, ions and electrons are still left in the vessel; they represent the space-charge that has enabled the discharge to continue at potentials less than V_s . They will increase by some amount q_1 the quantity of electricity that has to be supplied by the external circuit in recharging the condenser, and will make it necessary to write in place of (1),

$$n = \frac{\bar{i}}{C(V_s - V_g) + q_1} \cdot \cdot \cdot \cdot \cdot \quad (2)$$

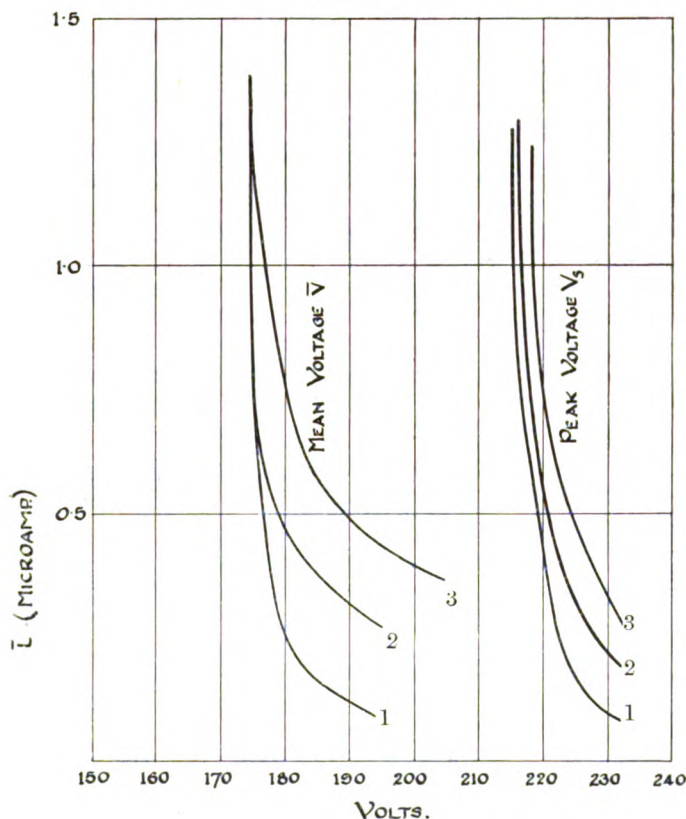
The number and distribution of the charges left can hardly depend on \bar{i} , so long as it is small compared with I ; and if they are completely removed before the discharge starts again, q_1 must be independent of \bar{i} , and no reason is apparent why \bar{V} should vary with \bar{i} . But some measurements of Penning (Table I. *loc. cit.*) indicate that, as \bar{i} is increased, V_s falls; the change in \bar{V} may be due to a change in V_s due to the incomplete removal of the space-charge from the previous discharge.

To examine this explanation, the maximum potential difference between the electrodes was measured with a peak voltmeter in the conditions prevailing along the portion XP; this maximum may be identified with V_s . In fig. 1 both V_s and \bar{V} are plotted against i . The curves 1 refer to the cell in the dark, curves 2 and 3 to the cell under a smaller and a larger illumination. An attempt was also made to measure the minimum potential between the electrodes, but it is much less sharply defined. It was about 82 volts, and no evidence could be found that it varied with \bar{i} or with the illumination. This value is much less than V_g , measured statically, which is 145 volts; the difference is due, of course, to the residual space-charge.

The changes in \bar{V} , whether due to changes in i or in the

illumination, are always accompanied by changes of the same sign in V_s . There is, therefore, some evidence for the explanation offered. It is impossible to decide whether the observed changes in V_s are sufficient to account for those in \bar{V} without knowing the relation between V and the time

Fig. 1.



during the whole period of charge and discharge. But since the changes in \bar{V} are always greater than those in V_s , it would seem that a decrease in V_s must be accompanied by an increase of the proportion of the whole period during which V is in the neighbourhood of its lower limit. Considerations presented later indicate that such an increase is not unreasonable.

But it remains to be explained why V_s should vary with i or with the illumination. The increase with i may be due

to the decrease in the period of recharging, which may be too short for the residual charges to be removed completely; if the positive ions have been brought into the neighbourhood of the cathode, but have not been discharged by it, they will increase the field in its neighbourhood and thus decrease the starting potential. The increase of V_s with illumination would then be due to the more rapid neutralization of these positive ions by electrons emitted from the cathode; illuminations would be equivalent to an increase in the period of recharging. (Actually the whole period increases with the illumination, as is explained below.) But there is some difficulty in accepting this explanation as sufficient, because the period of recharge is so long (at least 0.01 sec.) that it should always be sufficient for the passage of the charges to the electrodes under the action of the field. Even if the secondary ionization produced by their passage is taken into account, it is difficult to prolong the period during which the residual charge may be expected to remain, so that it becomes great enough to produce the observed changes. Perhaps some kind of "polarization," such as Taylor* introduces to explain some of his results, may be present; the positive ions may arrive in the neighbourhood of the cathode, but not be discharged immediately.

The Frequency of Intermittence.

If the considerations presented are sufficient to explain the main features of the curves in fig. 6 of (a), they provide a theoretical basis for the "second method" of using the cells described in (b). We have now to consider the "third method," in which changes in n , not in V , are employed.

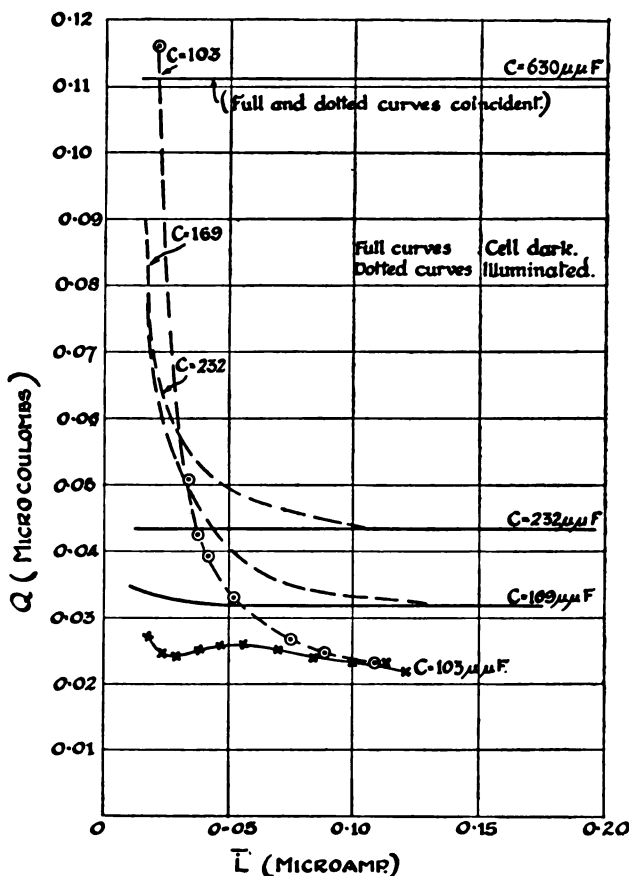
The changes in \bar{V} discussed in the preceding paragraph are accompanied by changes of n , which, of course, increases with \bar{i} . According to (2), even if q_1 is constant, n should not be strictly proportional to \bar{i} , because of the variation in V_s , but in this region no departure from proportionality could be established. n also varies with the illumination, decreasing as the illumination is increased. This change is doubtless partly due to the increase in V_s produced by the illumination; but there must be another cause which becomes more evident when smaller values of \bar{i} than those shown in fig. 1 are investigated.

If \bar{i} is reduced beyond the lowest value shown, n becomes so small that the voltmeter oscillates and there is no steady \bar{V} . At the same time it becomes difficult to determine V_s with the peak voltmeter on account of imperfect insulation. Accordingly, the curves cannot be extended further, but

* J. Taylor, Phil. Mag. iii. p. 753 (1927).

static measurements of the constant potential required to start the discharge show that V_s does not increase appreciably beyond the greatest value shown; the curve for V_s must bend sharply down and become nearly vertical. In this region, which is that to which the "third method" is applicable, changes in n cannot be due to changes in V_s , and it is improbable that they are due to changes in V_g . Some other factor must enter.

Fig. 2.



The facts in this region are best stated in terms of the quantity \bar{i}/n ; according to the general ideas we are discussing, this must be Q , the quantity of electricity passing in each cycle, consisting of a charge and discharge of the condenser C , whatever are the processes occurring during that cycle. Fig. 2 shows Q plotted against i for various values

of the capacity C . The points are inserted on the least regular of the curves to indicate the accuracy of the measurements. The full lines refer to the cell in the dark, the dotted lines to the cell subject to a small illumination, namely that due to a source of 1 candle-power at a temperature of 2600° K. at about 100 metres distance.

In the dark, Q is nearly independent of i . It is quite independent when C is large, but increases slightly when both \bar{i} and C are small. The maximum of Q for $\bar{i} = 0.06$ when $C = 103$ is real; but it does not occur in all cells which show the other features, and it may be neglected in our general survey. If C is reduced further, the ticks in the telephone become very weak and irregular, and it is impossible to obtain consistent values of n . When the cell is illuminated, Q is still independent of \bar{i} for the larger values of \bar{i} , but increases rapidly when \bar{i} is small, the increase being the greater, the less is C . At the smallest values of \bar{i} , Q depends on \bar{i} rather than on C , and is actually rather greater for the smaller capacity. The dark curves must be regarded as corresponding, not to complete darkness, but to some very small illumination. For it is well known that, even when every precaution is taken to exclude light, gasfilled cells always give a small "dark current," which behaves exactly like that due to a small illumination. In the cell to which fig. 2 refers, this dark current was unusually small; other cells, in which it is larger, gave "dark curves" similar in shape to those characteristic of illumination. It is therefore probably legitimate to conclude that, if the dark current were wholly absent, all abnormalities and irregularities would vanish, and Q would be independent of i throughout the range shown.

An outline of an explanation of these facts can be obtained by considering another complication of the simple theory, to which Taylor has drawn attention. In order that the discharge may pass, a space-charge has to be developed in the gas. During its establishment a quantity of electricity, q_2 , must pass through the vessel, which is not necessarily equal to q_1 , the quantity which has to pass in order to remove the space-charge when the discharge ceases. This quantity may be drawn either from the charge contained in the condenser or from the external circuit. If it is drawn from the condenser, there must be a minimum capacity C which enables the discharge to pass. For though q_2 may vary with the capacity, there must presumably be a minimum value $q_{\min.}$, determined by the configuration of the electrodes, beyond

which q_2 cannot fall, however small is C . But if

$$\dot{q}_{\min.} > C(V_s - V_g),$$

the difference of potential across the condenser will have fallen below the value at which the discharge can be maintained before the discharge starts; in such circumstances it could never start. If the discharge is to start at all, q_2 must be drawn from the external circuit.

If q_2 were independent of \bar{i} , Q would still be independent of it. But there is reason to believe that it is not independent when the cell is illuminated. For if the cell is illuminated, there is always a finite current i_0 , namely the greatest current that can be obtained on the Townsend characteristic, which will pass without any occurrence of a discharge. If $\bar{i} < i_0$, the space-charge, on which the discharge depends, will never develop. It is likely that if \bar{i} exceeds i_0 but slightly, the current effective in establishing the space-charge will be $\bar{i} - i_0$ rather than \bar{i} . If we imagine that this effective current has to supply the quantity q_2 , the period τ during which it flows will be $q_2/(\bar{i} - i_0)$, and the total quantity of electricity supplied during this period will be

$$q_2' = q_2 \cdot \frac{\bar{i}}{\bar{i} - i_0} \dots \dots \dots (3)$$

Q will then be given by

$$Q = C(V_s - V_g) + q_1 + q_2',$$

and will increase as \bar{i} diminishes.

According to this theory, for a given illumination the value of \bar{i} at which the dotted curves begin to depart from the full curve in fig. 2 ought to be of the same order as i_0 and nearly independent of C , so long as it is below a certain limit. The second of these expectations is fulfilled. It is difficult to determine the least value of \bar{i} at which the departure begins; but once it begins, the point of departure does not vary greatly with C . But the first is not fulfilled. If i_0 is determined experimentally by raising the potential across the cell and noting the value of i just before the discharge begins, then, in the circumstances of fig. 2, it is certainly 1000 times less than the critical value of \bar{i} ; the maximum Townsend current for this illumination was far below the least which the galvanometer would indicate. But this difficulty is not insuperable. The smaller the illumination, the steeper is the upper end of the Townsend

characteristic ; it is possible that the greatest current obtainable without formal instability, when the illumination is very small, exceeds very greatly any that can be actually observed.

It is not pretended that these considerations clear up the whole matter completely ; they are merely intended to indicate the physical processes upon which any explanation must be based. A complete theory would require an exact understanding of the immensely complicated changes involved in the electric discharge. It is possible that further experiments along these lines would throw light on that interesting and important problem ; but the work on the neon lamp, the ideas from which are the basis of this discussion, has shown how difficult it is to interpret completely any of the measurements. An illustration of this difficulty may be given from fig. 2. According to the theory, the value of Q where it is independent of \bar{i} should be given by (3), if for q_2' is substituted the constant quantity q_2 . The variation of Q with C ought therefore to give the values of $q_1 + q_2$ and of $(V_s - V_g)$. From fig. 2 we find

$$V_s - V_g = 172 \text{ volts ; } q_1 + q_2 = 0.0034 \text{ microcoulomb.}$$

The value of $V_s - V_g$ determined by means of the peak voltmeter potential was 150 volts ; but this value is too great, as it assumes $q_1 = 0$. The value determined statically was 87 volts. Both these values are much smaller than that given by (3), and extension of the measurements to greater values of C shows that (3) is not accurately true, until C becomes of the order of $10^6 \mu\mu\text{ F}$. Either q_1 or q_2 must vary with the capacity, and any simple interpretation of the measurements leads to serious error.

Practical Results.

The primary object of the investigation was, of course, to provide some theoretical basis for the methods of using gas-filled cells described in paper (b) ; it was hoped that they might be made less empirical. This object has not been achieved ; but some corrections to the description of the third method are necessary.

First, it is not desirable (as suggested) to reduce the capacity of the insulated electrode to a minimum. If the capacity is too small (as stated above), the ticks are irregular. The capacity should be the least that gives regular ticks. If the cell is one which gives considerable dark current, this will also be the capacity for which n is a

maximum for a small value of \bar{i} in the dark. The cell of fig. 2 is exceptional in this matter, since it gives a hardly appreciable dark current. The adjustment of the capacity is not at all critical, and may easily be made by means of a small variable air condenser, such as is used in wireless sets; this condenser should be inserted across the telephones and the cell in series.

Second, the constancy of $N_0 - N$, shown in fig. 4 of (b), is not general. It is quite definite with the particular cell and the particular capacity used in obtaining those measurements; but in general $N_0 - N$ for a given illumination decreases somewhat as N_0 increases. It is not difficult to control N_0 with a rheostat so that it is approximately constant and $N_0 - N$ may be taken as a measure of I ; but it is best, if possible, to use the method merely to determine the equality of two illuminations by means of the equality of N .

These corrections do not affect the utility of the method; further use of it confirms the impression that it is unrivalled in convenience when very small illuminations have to be measured.

A modification of it may be mentioned, suitable for illuminations within the range to which the "second method" is suitable. It consists in determining the least current \bar{i} for which any ticks are obtained. If a good thermionic valve and a good rheostat are employed, it is possible to identify illuminations of the order of 1 candle at 5 metres within 5 per cent. by the position of the slider on the rheostat at which the ticks just vanish. The method is therefore rapid and, like the third method, requires no delicate apparatus.

LXV. *Modified and Unmodified Scattered X-Rays. (J-Phenomenon.—Part VII.)* By Prof. C. G. BARKLA, F.R.S., and Dr. S. R. KHASTGIR, University of Edinburgh*.

IN earlier papers we gave a statement of some of the laws governing the production of the modified scattered X-radiation when the primary radiation used was heterogeneous, and the radiations were compared by absorption methods. These laws were contrasted with those obtained by A. H. Compton and others from the study of comparatively homogeneous beams by the crystal diffraction method. The laws were shown to be entirely different from those

* Communicated by the Authors.

governing, or at any rate from those said to govern the Compton effect,—they were simply the laws of the J-phenomenon. In particular, the scattered radiation may be either unmodified or modified as measured by its absorbability in one substance, say aluminium; the change from one to the other is abrupt and it depends upon factors which had previously been considered of little or no importance in their influence on the properties of radiations. More remarkable still the radiation which, when measured in one absorbing substance is a modified radiation, is when its absorbability is measured in another substance, very clearly and precisely an unmodified radiation. In this case the modified and the unmodified radiations are one and the same; only the testing substance is changed. We have illustrated this in a number of ways. There is no haziness about the experimental results; they leave no room for ambiguity.

The evidence of modification as we have observed it, depends upon a relation between the radiation and the testing substance. Such a fact is not provided for by either the classical or the quantum theory; but we have seen in many ways that the property of a radiation depends, in part at least, upon an average quality more closely allied to temperature of the radiation as a whole, and not upon the frequency of its constituents except in so far as they contribute to the average; also corresponding effects are produced in different substances at different average frequencies (or “temperatures”) characteristic of the particular substance.

There is a further factor—possibly the large scale structure or sequence of radiations in the full stream of radiation which is involved; for certain conditions in the radiation are essential to the change in activity at these “temperatures.”

On the classical theory of course, the large scale structure of the scattered radiation is quite different from that of the primary producing it, on account of the super-position of waves from every electron in the scattering substance outside the atomic nuclei. Every wave in the primary radiation produces an irregular succession of waves forming a train of length $l(1 - \cos \theta)$ from each filament of scattering substance of length l in the direction of primary propagation, where θ is the angle between that direction and the direction of propagation of the scattered radiation. It may be that this is the cause of the modification in properties produced by scattering,—that a certain continuity is necessary in the stream of radiation to enable it to attain a certain level of activity. This, however,

can for the present only be regarded as a hypothesis which seems to explain the difference between radiation and radiation. There is a fair amount of evidence in favour of this, but this will be discussed in other papers. At any rate, the modification produced by scattering may or may not be shown in its effect on the absorption in a particular substance. This we have already shown in a number of experiments. The contrast between our results and Compton's* is so marked that it is perhaps necessary to show that there is, at any rate, a close connexion between the two. This connexion, the conditional nature of X-ray phenomena, particularly those associated with quantum rules, and the dependence of what may be called classical and quantum phenomena on the substance intercepting the radiation, are shown very strikingly in the following experiment.

Experiment.

The absorbabilities of primary and scattered radiations were compared in several substances throughout a long range of frequencies of the primary radiation. As indicated before, the simplest method of comparing primary and scattered radiations is to find the ratio of the ionizations produced by the scattered and primary rays, first when those radiations are unintercepted before entering the electroscopes (ratio = S/P), and subsequently after both

* Perhaps the briefest way of emphasizing the difference between our results and Compton's is the following:—

The difference between the absorption coefficients of primary and scattered radiations is only shown (if at all) in definite well-marked steps. Thus if $\left(\frac{\mu}{\rho}\right)_2$ is the absorption coefficient of the radiation scattered at a definite angle θ , and $\left(\frac{\mu}{\rho}\right)_1$ is the absorption coefficient for the corresponding primary radiation,

$$\left(\frac{\mu}{\rho}\right)_2 - \left(\frac{\mu}{\rho}\right)_1 = 0, \text{ or } a, \text{ or } b, \text{ or } c \dots\dots$$

Also for different angles of scattering θ_1 and θ_2 ,

$$\left(\frac{\mu}{\rho}\right)_{\theta_2} - \left(\frac{\mu}{\rho}\right)_{\theta_1} = 0, \text{ or } a, \text{ or } b, \text{ or } c \text{ (frequently 0).}$$

The difference between these results and those of Compton are not only of fundamental importance by reason of their theoretical implications, but the results themselves, in certain regions, are as widely different in magnitude as they could possibly be. For instance, the difference between the primary radiation and that scattered at a small angle is very small on Compton's theory, whereas we usually find the difference to be precisely the same as that between the primary and the radiations scattered at, say, 90° .

beams have traversed the same thickness of some absorbing substance (ratio = S'/P'). It has been shown already that S'/P' may be equal to S/P , indicating equality of absorptions of scattered and primary beams, or S'/P' may be quite markedly less than S/P , indicating greater absorption of the scattered radiation than of the primary, *i. e.* a modified scattered radiation. The change from the unmodified scattering to the modified scattering takes place abruptly; it may, however, be brought about in many different ways.

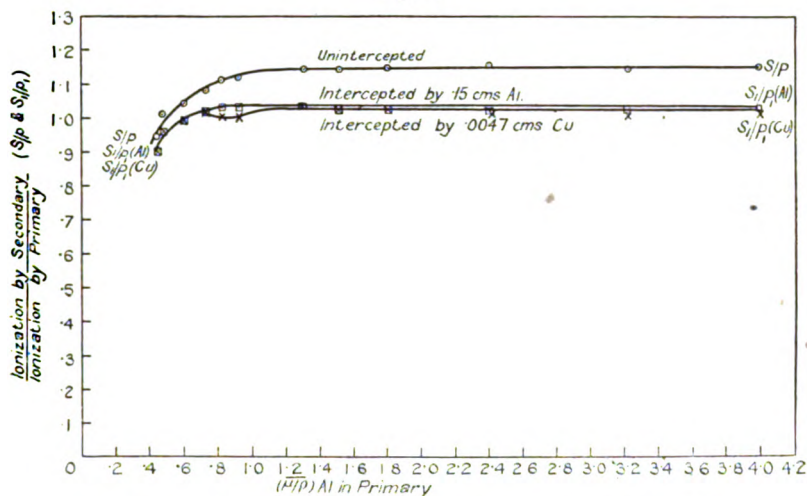
For illustration of these facts, reference should be made to previous papers. What we propose to show now is that while absolutely regular and consistent results may be obtained when the radiations are examined in some substances, two alternative results, which are themselves as widely different as the classical and quantum laws, may be obtained when these radiations are examined in other substances.

A primary beam was partially scattered by transmission through a sheet of paraffin wax as in previous experiments. The scattered radiation at right angles to the primary radiation was definitely more absorbable than the primary radiation when measured in aluminium, copper, or gold. Not only so, but the apparent transformation by scattering—the real transformation in some respects—received quite consistent evidence from the absorption measurements in these three substances. The change in scattering was just of the kind which would be produced by Compton's change of wave-length—if we ignore the relation with wave-length and with scattering angle, which are as already stated. On the other hand, while there was this satisfactory consistency between the results obtained from absorption measurements with these three substances, most striking results were obtained when silver and tin were used as absorbing substances; the interesting feature of these elements being the existence of their K-absorption edges within the limits of the spectrum of the radiation employed. The results obtained with silver and tin were not irregular, they showed a double regularity, for they were either *a* or *b*. Either is interesting, significant, and intelligible*; but the two are totally different, one following the classical laws, the other appearing to follow quantum rules. Yet an otherwise imperceptible change in the radiation determines whether the result shall be (*a*) or (*b*). This is all shown in figs. 1, 2, 3, and 5, in which the ratio of ionizations by scattered

* At least as intelligible as quantum theory.

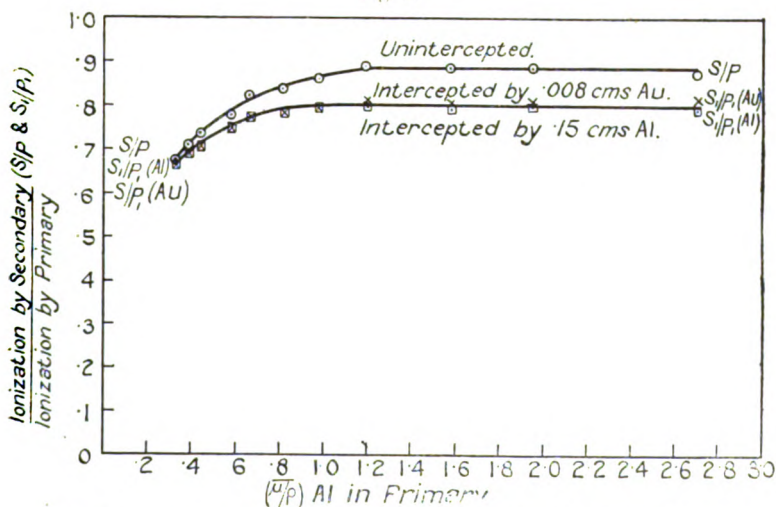
and primary radiations is plotted against the average absorption coefficient of the radiation employed $\left(\frac{\mu}{\rho}\right)^*$.

Fig. 1.



Showing equal amounts of modification as measured in Al and Cu.

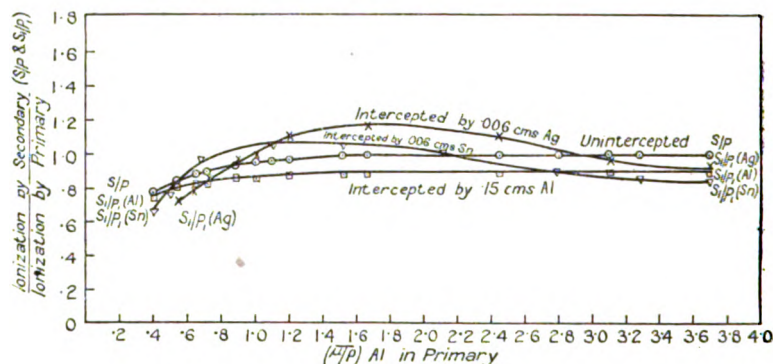
Fig. 2.



Showing equal amounts of modification as measured in Al and Au.

* Calculated as previously from a 50 per cent. diminution of ionization in a short ionization vessel.

Fig. 3.



Showing selective absorptions in Ag and Sn consistent with change in wave-length on scattering.

Proceeding from low to high frequencies (from right to left) it is seen that :—

- (1) The ratio of ionizations produced by scattered and primary radiations was a constant through a long range of frequencies. This is shown by lines marked S/P which are horizontal except for high frequencies. The horizontality is shown by other experiments to extend far beyond the limits of these figures to the right; in fact beyond the value $\left(\frac{\mu}{\rho}\right)_{Al} = 12$;
- (2) when the scattered and primary radiations were transmitted through equal thicknesses of absorbing material, Al, Cu, or Au, the ratio of ionizations (S'/P') was markedly less, showing that the scattered radiation was more strongly absorbed than the primary radiation as usually measured. The values are shown on the curves S'/P' (Al), S'/P' (Cu), S'/P' (Au) in figs. 1 and 2;
- (3) the difference between the absorption coefficients of scattered and primary radiations was a constant through a long range of wave-lengths, *i. e.* $\left(\frac{\mu}{\rho}\right)_2 - \left(\frac{\mu}{\rho}\right)_1 = \text{constant}$ as shown by the horizontality of lines marked S'/P'. Such results have been previously published.

- (4) The fractional change (by scattering) in the absorption coefficient of a radiation of given wave-length was approximately the same in Al, Cu, and Au. This is shown by the fact that when thicknesses of Al, Cu, and Au were chosen to absorb approximately equal amounts of radiation, the ratio S'/P' was the same for these testing substances ;
- (5) the results obtained when silver and tin were used as absorbing substances were of a dual nature. In a series of experiments the absorptions in these substances varied throughout the spectrum precisely as would be expected on the assumption of a change in wave-length by scattering.

Thus (fig. 3) when the wave-length of a primary radiation was fairly long, the absorbability of the scattered radiation in silver was greater than that of the primary, in agreement with the results obtained from absorption measurements in Al, Cu, and Au. As the frequency of the primary was gradually increased, the absorption of this primary radiation in silver began to rise relative to the absorption of the corresponding scattered radiation, and continued to do so until the primary became much more absorbable than the scattered radiation. This is shown by the rise of the values of S'/P' (Ag) in passing from right to left. It is in conformity with the theory of the greater wave-length of the scattered radiation, for as primary and scattered beams increase in frequency, the primary passes the K-absorption edge first ; consequently its absorption rises relative to the absorption of the scattered radiation. With a further increase in frequency, the scattered radiation also passed the K-absorption edge in Ag, and the absorption of scattered radiation rose relative to that of the primary, the ratio of the two absorptions becoming quite normal again as it should away from the region of a K-absorption edge.

Confirmation of this result was obtained by the use of tin as the testing substance, as the K-absorption edge for tin is of higher frequency than that for silver. In this case as the frequency was increased the rise in the absorption of the primary radiation relative to that of the secondary occurred when the radiation was of higher frequency than that showing the corresponding phenomenon in silver (fig. 3). Also the rise in the absorption of the scattered radiation occurred at a correspondingly higher frequency.

All these results must be recognized as overwhelming evidence that the difference of absorbability between the

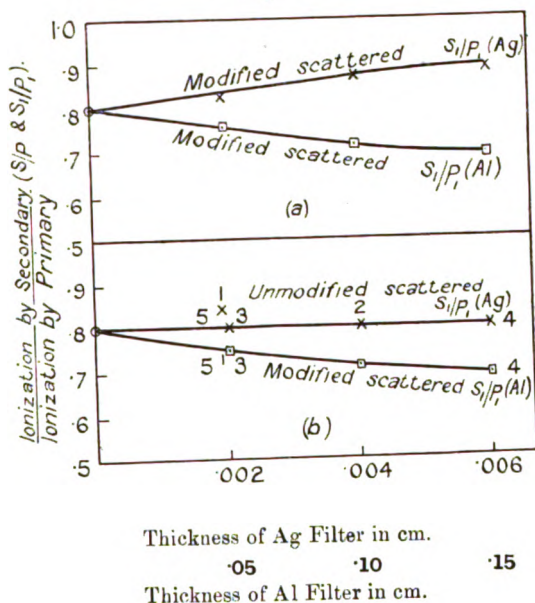
primary and scattered radiation which we observed in these experiments (and many others) was the accompaniment of Compton's "increase in wave-length" by scattering, for the increase in absorbability measured in these various substances was in the proportion expected if due to increase in wave-length; and there was shown even the selective variation in the absorptions of primary and scattered radiations such as would be expected in the neighbourhood of absorption edges in the absorbing substances. It is important to point out, too, that these results were obtained consistently, time after time, in a long series of experiments.

But while experimenting on the absorption of scattered and primary radiations by successive sheets of silver, all evidence of modification by scattering suddenly disappeared, and the scattered radiation became unmodified scattered radiation as far as its relation to silver was concerned: and this new state of things persisted*. On re-examining the absorptions in aluminium however, the scattered radiation was still a modified radiation. Thus fig. 4 shows the ratio S/P for unintercepted beams and S'/P' for various thicknesses of aluminium and of silver placed in the path of both primary and secondary beams. In fig. 4*a* the fall of S'/P' (Al) with increasing thickness of intercepting aluminium, and the rise of S'/P' (Ag) with increasing thickness of silver, show the greater absorbability of the scattered radiation in aluminium, and the smaller absorbability in silver compared with the corresponding absorptions of the primary radiation. This is explained above, as the radiation experimented upon was in the neighbourhood of the K-absorption edge in silver. On repeating the experiment (with a thin sheet of Al in the primary beam before falling on the scattering substance) exactly similar results were obtained in aluminium; silver, too, commenced to give exactly the same results as before, but after filtering by the first sheet of silver (0.002 cm. thick) the sudden change was observed as indicated in fig. 4*b*. (The numbers on the figure indicate the sequence of the observations.) The difference between the absorptions of primary and scattered radiations in silver had abruptly disappeared, and did not return on re-determining the ratio for one sheet of silver. This is shown by the horizontal line S'/P' (Ag) in fig. 4*b*, obtained subsequent to the point marked (1) which was the same as in fig. 4*a*.

* In all the experiments described in this paper the radiation was generated in a Coolidge tube excited by an induction coil with mercury-jet interrupter.

This compelled us to return to a comparison of the scattered and primary radiations through a long range of frequencies as in the experiments, the results of which are recorded in figs. 1, 2, and 3. In order to avoid all possible effects of even a slight variation in the radiation used, the absorptions in aluminium and silver were taken alternately throughout the whole investigation. The experiments with Al as the absorbing substance showed that the scattered radiation was still a modified radiation, modified by exactly the same

Fig. 4.



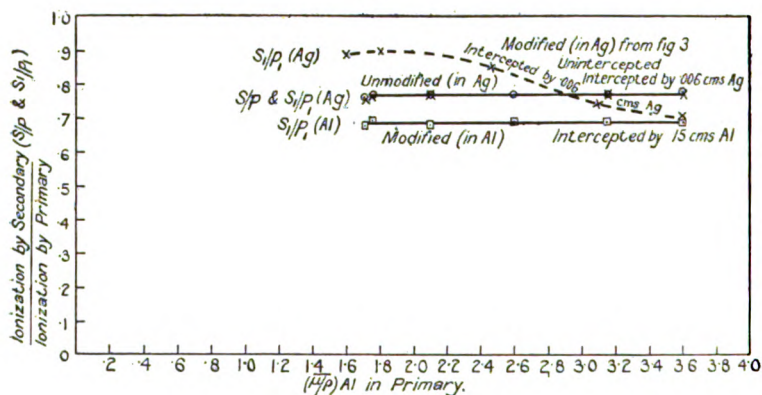
Showing how a scattered radiation which was found to be modified when examined in Al and Ag (fig. 4a) suddenly became unmodified when again examined in Ag, but remained modified as examined in Al (fig. 4b).

amount as in the many previous experiments: thus $S'/P' (Al)$ is below S/P in fig. 5. But when the scattered and primary radiations were absorbed by Ag, all difference between them disappeared— $S'/P' (Ag)$ was precisely equal to S/P . The two are superposed in fig. 5. In order to show the change which had occurred in the absorptions in Ag, the curve $S'/P' (Ag)$ is introduced from fig. 3 in broken line. Thus aluminium absorptions showed no variation from the

modified scattered radiation, whereas silver absorptions showed a complete change from the results of fig. 3 following the quantum rules to those obeying the classical laws.

This is in perfect harmony with our previous statements regarding the J-phenomenon. We have shown that a scattered radiation which is a modified radiation when intercepted by one substance is an unmodified radiation when intercepted by another substance; in this paper, however, it is shown to hold throughout the whole spectrum experimented upon, *i. e.* from low frequencies to high frequencies even including the K-absorption edge of the absorbing substance.

Fig. 5.



Showing scattered radiation, which is modified when intercepted by Al, and is totally unmodified when intercepted by Ag, for radiations of different frequencies. Dotted line shows how under other conditions Ag may show modification by scattering.

These experiments thus show in a much more convincing way what we have already demonstrated over very limited regions, that the evidence of transformation of a radiation by scattering, depends upon a relationship between the scattered radiation and the material used to test the radiation.

In any one substance the modified and the unmodified scattered radiations are alternative results obtained when there is not the slightest indication of variation in other substances. But more important still, the unmodified and the modified scattered radiations as measured in different substances frequently are one and the same radiation unless a radiation may be regarded as changed when the substance placed in its path is changed.

Summary.

The experiments described in this paper show that the scattered radiation, which is quite consistently a modified scattered radiation as measured by its absorption in a number of substances, may be either a modified radiation or an unmodified radiation when its absorptibility is measured in another substance. This has been demonstrated throughout a long range of frequencies including absorption edges in the testing substances.

Thus the unmodified scattered radiation (classical theory) and the modified scattered radiation (quantum rules) in certain circumstances are one and the same radiation, the evidence of modification being dependent upon a relationship between the radiation tested and the testing substance.

This is in harmony with what we have previously stated of the laws governing the J-phenomenon.

The results are entirely at variance with a conception of independent quanta, and illustrate the importance of what we have called "temperature" of the radiation, and upon some other factor, possibly the large-scale structure of the radiation upon which the coherence of that radiation depends.

The authors wish to express their thanks to Mr. W. H. Stevens for his assistance in the experimental work described in this paper.

LXVI. *A Vacuum Spectrograph and its Use in the Long X-Ray Region.* By J. SHEARER, B.A., M.Sc., Evening Lecturer in Natural Philosophy in the University of Melbourne*.

[Plate XVII.]

THE first extensive measurements of X-ray wave-lengths were made in 1913 by Moseley †, who adopted the crystal reflexion method and photograph recording. He found that the absorption, even in hydrogen, of waves longer than 3 Å. was so great as to make a vacuum spectrometer necessary. With it Moseley ‡ measured wave-lengths up to 8 Å. Absorption in the window separating the X-ray tube from the spectrograph becomes increasingly difficult to surmount for waves longer than 10 Å., although celluloid windows have been used § for wave-lengths as long as 18 Å. in the L series of iron.

* Communicated by Prof. T. H. Laby, D.Sc.

† Moseley, *Phil. Mag.* xxvi. p. 1020 (1913).

‡ Moseley, *Phil. Mag.* xxvii. p. 703 (1914).

§ Siegbahn & Thorsæus, *Ark. f. Mat. Astr. o. Fys.* xviii. no. 24 (1924).

Preliminary results were obtained by Thoræus and Siegbahn* with a spectrograph designed without a window. Using a palmitic acid crystal ($2d=71.19 \text{ \AA.}$), they extended the L series to chromium ($L\alpha\text{Cr}=21.69 \text{ \AA.}$).

Redeterminations of values for the elements from zinc to chromium have been made by Thoræus†, who used two types of X-ray tube. In one, a thin wall between cathode and anode perforated by small holes and covered with aluminium foil prevented both a deposit on the anode of tungsten from the filament and also, in the absence of a window, the entrance into the spectrograph of light from the cathode. In the other, a window was used over the slit which served also as anode. The lines Thoræus obtained were very diffuse, being about 2.5 mm. wide.

Later in the same year Thoræus‡ announces the measurement of the oxygen $K\alpha$ (23.73 \AA.) and the vanadium $L\alpha$ (24.2 \AA.) lines.

Dauvillier§ claims to have bridged the spectral gap from 20 \AA. to Millikan's optical limit|| of 136 \AA. He used as crystal a film of melissic acid on lead which behaves as a crystalline body of grating space 87 \AA. ¶ A thin deposit of magnesium on a celluloid film 10^{-5} centimetre thick constituted the window. In the K series** the $K\alpha$ line of oxygen (24.8 \AA.), carbon (45.5 \AA.), and boron (73.5 \AA.) have been measured. No extensions were made to the L and M series, but the N and O series of barium were traced to 71.5 \AA. , and the same series of thorium to 121 \AA. †

Thoræus†† criticises these results on the ground that, in view of the very strong absorption he found for wave-lengths greater than 13 \AA. , there is not sufficient evidence that Dauvillier's lines do not arise from reflexion in higher orders or from other atomic planes. The interpretation given by Dauvillier is rendered more doubtful by the fact that he observed optical reflexion** in this region. Until

* Thoræus & Siegbahn, *Ark. f. Mat. Astr. o. Fys.* xix. A, no. 12 (1925).

† Thoræus, *Phil. Mag.* i. p. 312 (1926).

‡ Thoræus, *Phil. Mag.* ii. p. 1007 (1926).

§ Dauvillier, *C. R.* clxxxiii. p. 656 (1927).

|| Millikan, *Proc. Nat. Acad. Sci.* vii. p. 289 (1921); *Astr. Journ.* liii. p. 150 (1921).

¶ Trillat, *Ann. de Phys.* vi. p. 5 (1926); Dauvillier, *C. R.* clxxxii. p. 1083 (1926).

** Dauvillier, *C. R.* clxxxiii. p. 193 (1926); *Journ. de Phys. et le Rad.* viii. p. 1 (1927).

†† Thoræus, 'Nature,' cxviii. p. 771 (1926).

the K, L, and M spectra of the elements are extended systematically to the elements of low atomic number instead of at random, the interpretation of results in this region will be open to some doubt. The author's own experiments fail to show, with an alternating potential of 240 volts (340 volts maximum) applied to the tube, any photographic action, through 10^{-4} cm. of aluminium foil, on Schumann film placed in the direct beam passing through the slits. Exposures up to 300 milliamp. minutes were used. The shortest waves present would be 36 Å. long.

Before describing a windowless X-ray spectrograph, certain results obtained which disagree with those previously reported for the wave-length of Ni $L\alpha$ and for the grating space of a sugar crystal will be given.

When the author began the experiments outlined in this paper, no spectrograph had been designed that would permit of the elimination of the window by employing the common vacuum in the X-ray tube and spectrograph. With such a spectrograph (described below) the author has photographed the $L\alpha$ line of nickel on Eastman X-ray film (Superspeed) with an exposure of three hours, using a sugar crystal. The line is somewhat diffuse, having a breadth of nearly 0.5 mm., but is considerably sharper than has been observed in work previously published. The following values were obtained from the relation $n\lambda = 2d \sin \theta$, where d = crystal constant and θ = grazing angle:—

Nickel $L\alpha$.

Film.	λ (in Å.).
1	14.5709
2	14.5753
3	14.5747
4	14.5625
5	14.5764
Mean... ..	14.5720

Average Residual = 0.0042 Å. Thoræus's value is 14.528 Å.

A method of measuring θ with precision from a single exposure was adopted. It is described at the end of the paper. These measurements of λ were made relative to $d = 3029.04$ X units for calcite by the following procedure.

In the first place, wave-lengths of the components of the K Ni α doublet were measured in the first- and second-order spectra, a calcite crystal ($d = 3029.04$ X.U.) being used

and the double exposure method. The following are the values :—

Nickel $K\alpha$ doublet.

Film.	Order.	$K\alpha_1$ (X units).	$K\alpha_2$ (X units).
6	1	1654.02	1658.23
	2	1654.20	1658.05
7	1	1653.92	1658.20
	2	1654.43	1658.42
8	1	1653.65	1657.97
	2	1654.10	1657.94
9	1	1653.82	1658.00
	2	1654.06	1657.88
Means.....		1654.03	1658.09
Average Residual ...		0.17	0.15

In the double-exposure method a rotation of the crystal through $(\pi - 2\theta)$, where θ is the grazing angle for the particular line, and of the film through 4θ , would bring the two exposures of the given line into exact super-position. It is an advantage to have the two exposures separated by a small amount (of the order of 1 mm. or less) and to convert this displacement on the film into angular measure. For all exposures the film was held in a holder which bent it into an arc of exactly 10 cm. radius of curvature, and was accurately set at a distance of 10 cm. from the axis of the rotation of the crystal. From the linear displacement of the two lines on the film, therefore, the corresponding angle could be computed. This displacement was measured by a projection method which will be subsequently described in another paper from this laboratory. The lines on the film are curved. When the actual rotation of the film is less than 4θ (as was always the case with these films) the lines are convex to one another and the minimum distance apart is measured. Each film was measured five times. The maximum range in the measurements corresponds to an error of 0.2 X unit, the average residual to an error of 0.02 X unit, which is less than one-fifth the error in the final values of λ .

In all crystal settings the crystal face could be set in the rotation axis with a maximum error of about 0.005 mm., corresponding to an error in λ of 0.3 X unit in the first order and 0.2 X unit in the second order. No systematic error in the results is found which would be accounted for by an error in the position of the crystal face.

Next, the spacing of cane-sugar was determined in terms of the above values of the wave-lengths of $K\alpha_1$ and $K\alpha_2$ of nickel, the third- and fifth-order spectra being used.

Grating space for Sugar (100 face).

Film.	Reference line.	Order.	Spacing ($2d$).
10	$K\alpha_1\alpha_2$	3	21·1602 Å.
	$K\alpha_1$	5	21·1492
	$K\alpha_2$	5	21·1511
11	$K\alpha_1\alpha_2$	3	21·1909
	$K\alpha_1$	5	21·1501
	$K\alpha_2$	5	21·1449
12	$K\alpha_1\alpha_2$	3	21·1343
13	$K\alpha_1\alpha_2$	3	21·1743
Mean			21·1519
Average Residual...			0·0077

Excluding the last two films reduces the Average Residual to 0·0031 Å.; the mean value of $2d$ is hardly affected. Stenström's* value is 21·141 Å. The lower precision in the determination of the sugar constant compared with that attained in the $K\alpha$ wave-length determination is due to the inferiority for X-ray spectroscopy of the sugar crystal and its small dispersion.

In exposing for the Ni $L\alpha$ line, comparatively strong reflexions of the Ni $K\alpha$ doublet were obtained from an atomic plane approximately in the position of the 60 $\bar{1}$ plane.

The corresponding grating space ($\frac{2d}{n}=2\cdot406$ Å.) as calculated from the X-ray photographs could not be reconciled with the data of Becker and Rose †, which give $d=1\cdot749$ Å.

The discrepancy is being investigated in this laboratory.

Difficulty is experienced in long X-ray wave-length measurements by the crystal reflexion method, and arises from:—

(1) Necessity of procuring a crystal with large spacing and small absorption.

* Stenström, *Diss. Lund*, 1919.

† Becker & Rose, *Zeit. f. Phys.* xiv. p. 369 (1923).

(2) Absorption in the window between spectrograph and X-ray tube.

(3) Absorption in the air between the slit and crystal and between the crystal and plate.

(4) The difficulty of obtaining a sufficiently intense source of X-rays.

(5) Absorption in the covering over the photographic plate or film.

(6) Absorption in the gelatine of the photographic film or plate.

These difficulties will be treated separately.

(1) A crystal of cane-sugar fulfils requirements for a limited extension into the spectral gap region.

(2) and (5). The window serves two purposes.

(a) the separation of the X-ray vacuum in the tube from the vacuum in the spectrograph ;

(b) the absorption of light from the cathode that would otherwise enter the spectrograph and fog a naked film.

It is desirable to employ a naked film in order to overcome absorption in a light-tight covering for the film.

(3) The absorption of soft X-rays in air necessitates the employment of a vacuum spectrograph in which the pressure is maintained at at least 0.01 mm.

Difficulties (2), (3), and (5) above were overcome by using an X-ray spectrograph which employs a common vacuum in tube and spectrograph and which permits of the rotation through known angles of the crystal and photographic film from outside the spectrograph while it is evacuated.

The instrument is described below.

(4) A water-cooled nickel target was used ; the L series of nickel lie in the spectral region which is under investigation. With a Wehnelt cathode the tube operated at 15,000 volts and about 10 milliamps. It is described below.

(6) Wave-lengths up to 15 \AA . could be recorded on Eastman X-ray film (Superspeed). With the object of reducing the exposures necessary, Schumann (Hilger) film was also used and subsequently rejected, since the ratio of the intensity of the background of scattered radiation, fog, and pressure marks to that of the lines was greater for Schumann film, which, however, was not new film, than for the Eastman film.

This spectrograph is shown in Pl. XVII. (figs.1 and 2). It

consists of a brass cylindrical box (A) $8\frac{1}{2}$ inches in diameter with a conical bearing of mild steel, case-hardened, let into the base. This bearing carries two concentric cones. To the lower end of the outer (hollow) cone of gun-metal is attached a Watts 6-in. theodolite circle (B) accurately centred and reading with micrometer eyepieces (C) to 5 seconds of arc, and to the upper end an arm carrying a curved film-holder (D) of 10 cm. radius of curvature. An accurate circle was used for recording the rotation of the film as the spectrograph was designed for absolute measurements of the kind which are described above. The innermost cone is solid and of mild steel, case-hardened, supporting on its upper end the crystal table (E), and to the lower end a circle (F) reading to 3 minutes of arc, and an arm (G) for rotating the crystal during exposure. The arm is held by means of a spring against a heart-shaped cam (H) driven by a small motor (I). The angle of sweep of the crystal may be varied over a wide range. The gun-metal conical bearing was carefully turned, and the inner and outer steel bearings turned, then case-hardened, and ground to fit the gun-metal bearing. Castor-oil was used as the lubricant. Either cone could be clamped; the gun-metal one could be rotated with worm and worm-gear (J).

The cylindrical box was closed with a lid, the lower surface of which and the upper surface of the box were ground. Tap-grease in between rendered the lid quite vacuum-tight. The conical bearings when made as described were also vacuum-tight, and remained so during rotation of either cone while the spectrograph was evacuated. To maintain the vacuum, Siegbahn and Thoræus had found it necessary to make a channel around the bearing surfaces of the cones and in the flange under the lid of the spectrograph. In order to reduce leakage of air into the spectrograph, these channels were evacuated by the backing-pump.

The X-ray tube of the Coolidge type is of metal, the general design of which has been previously described in a paper from this laboratory*. It consists of a water-cooled brass tube (K) which carries at one end glass tubing (L) acting as insulator and supporting a metal plate (M), and at the other end a water-cooled Wehnelt cathode which is screwed into the metal tube and sealed, the seal being water-cooled. The water-cooled anode (of copper, nickel-plated) is hollow and is supported by two copper tubes (N) through which the cooling water flows. A front and back slit in a

* Eddy & Turner, Proc. Roy. Soc. A, cxi. p. 117 (1926).

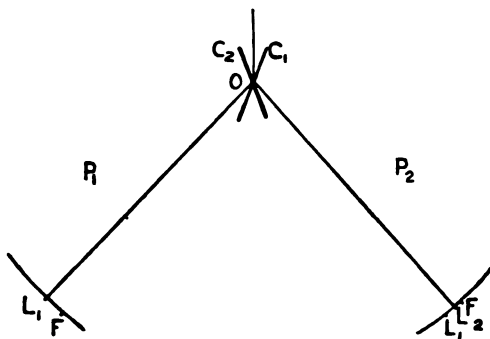
side tube fixed relative to the spectroscope necessitates the employment of an adjustable anode. This adjustment is carried out by softening the wax where the two copper tubes passed through the metal plate, and screwing the anode in or out by means of thread (O).

The use of a Wehnelt cathode reduced the light-intensity to a negligible amount. Further provision for reducing the amount of light entering the spectrograph was made by inserting in the X-ray tube opposite the side tube carrying the slits a thin sheet of copper prepared with a matt surface of copper oxide. The rest of the internal surface of the tube was silver-plated to reduce the emission of occluded gases.

Fogging due to light was absent. Scattered radiation was reduced by using a horizontal back slit that limited the length in the vertical direction of the X-ray beam incident on the crystal.

The pumping system consisted of a mercury condensation pump backed by a Cenco Hyvac (rotary oil) pump.

In order to obviate the necessity of taking two exposures when those exposures were long, a fiducial mark was made on the film. The reading of the circle attached to the film-carrier when this mark is in the plane which passes through the slit and axis of rotation of the crystal may be called the "zero reading" of the circle (Z). It was deduced from observations obtained in the double exposures made for the determination of the lattice constant of sugar which are described above. The fiducial mark is photographed on the film, simultaneously with the exposure for the lines, by the faint scattered radiation which is present during an exposure. The "zero reading" may then be determined as follows :—



R_1, R_2 = circle readings for the 1 and 2 positions P_1, P_2 .
 L_1, L_2 = the lines on film for the two exposures.

In position P₂,

$$d\theta = \angle L_1OL_2, \quad d\theta_1 = \angle L_1OF, \quad d\theta_2 = \angle L_2OF.$$

$$\text{Now} \quad 4\theta = R_2 - R_1 + d\theta.$$

$$\therefore Z = R_1 - d\theta_1 + 2\theta$$

$$= \frac{R_1 + R_2 + d\theta - 2d\theta_1}{2} \quad \text{or} \quad \frac{R_1 + R_2 - d\theta - 2d\theta_2}{2}.$$

A single exposure then suffices for measuring the grazing angle of any line and for calculating its wave-length from the relation $n\lambda = 2d \sin \theta$. As the only assumption made in determining the "zero reading" is that of the equality of the reflexion angles in each of the two symmetrical settings of crystal and film, the precision of absolute determinations of wave-lengths in the L series is not impaired.

I wish to express my gratitude to Professor Laby for the encouragement and assistance that were at all times given, and for the many fruitful suggestions made throughout the course of this work.

My thanks are also due to Miss N. Allen, M.Sc., whose interest in the problem of the crystal structure of sugar was much appreciated.

LXVII. *On the Radiation from the Inside of a Circular Cylinder.* By H. BUCKLEY, M.Sc., F.Inst.P. (From the National Physical Laboratory*.)

IN the *Philosophical Magazine* of July 1920, Bartlett † gives an expression for the amount of heat radiated from the inner walls of a uniformly-heated cylinder on to a coaxial circular area normal to the axis of the cylinder. The main point in his paper is the proof that the radiation from the inner walls of the cylinder between A and B on to the coaxial circular area C (fig. 1) is equal to that which it would receive from a circular disk at B, less what it would receive from a circular disk at A, both disks having the same temperature and emissivity as the walls of the cylinder.

It is due to this point of view that Bartlett's method of considering the problem is at once much simpler and much more powerful than that used by Owen ‡, who obtained the

* Communicated by Sir J. E. Petavel, K.B.E.

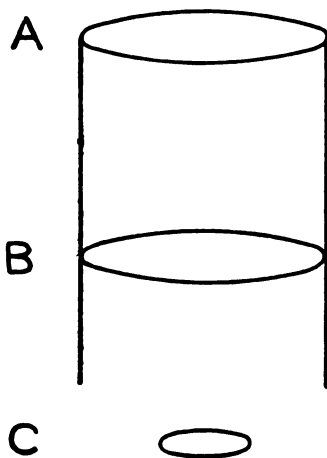
† Bartlett, *Phil. Mag.* xl. p. 111 (1920).

‡ Owen, *Phil. Mag.* xxxix. p. 359 (1920).

same results from first principles by the long and laborious process of quadruple integration over the surfaces of the disk and walls of the cylinder.

Both Bartlett and Owen neglected the occurrence of multiple reflexions between the walls of the cylinder such as would normally occur in practical problems where the emissivity of surfaces are necessarily less than unity. It is possible, however, to use Bartlett's method to calculate the effect of the multiple reflexions in building up the approximation to black-body radiation, which is obtained from the inside of a uniformly-heated cylinder.

Fig. 1.



The present paper in consequence has for its object the determination of the amount of energy radiated from points in the neighbourhood of the end of a uniformly-heated infinite cylinder, account being taken of the multiple reflexions between the cylindrical walls of the cylinder. The problem is of interest particularly in optical pyrometry, where uniformly-heated cylinders have been used as sources of black-body radiation. If such a cylinder be infinitely long, it is obvious that as near an approximation to black-body radiation corresponding to the temperature of the cylinder walls as is desired can be obtained by sighting the optical pyrometer on to a portion of the walls sufficiently far removed from the end.

In practice it is assumed that "black-body" conditions are realized; but there does not appear to be any quantitative assessment of the approximation to those conditions which is actually obtained.

The radiation received by a circular disk from a diffusely-radiating circular disk parallel and coaxial with the receiving disk is given by Walsh* as

$$\frac{\pi E}{2} \{ (a^2 + r^2 + R^2) - \sqrt{(a^2 + r^2 + R^2)^2 - 4r^2 R^2} \},$$

where E is the total radiation emitted by the radiating disk per unit area, a is the distance apart of the disks, and r and R are their radii. In the case where $r = R$ and the positions of the two disks are defined by coordinates x and x_1 measured along the line joining the centres of the disks, this expression reduces to

$$\frac{\pi E}{2} \{ (x - x_1)^2 + 2r^2 - (x - x_1) \sqrt{(x - x_1)^2 + 4r^2} \};$$

$$i. e., \quad \frac{\pi E}{2} \{ (x - x_1)^2 + 2r^2 - (x - x_1) \sqrt{(x - x_1)^2 + 4r^2} \}$$

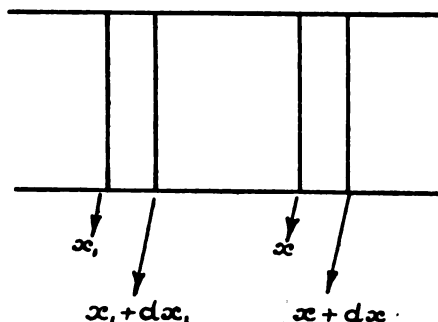
when $x > x_1$

$$\text{and} \quad \frac{\pi E}{2} \{ (x_1 - x)^2 + 2r^2 - (x_1 - x) \sqrt{(x_1 - x)^2 + 4r^2} \}$$

when $x < x_1$.

Consider now a circular cylinder (fig. 2) of radius r and

Fig. 2.



of infinite length emitting perfectly diffuse radiation of amount $\phi(x)$ per unit area at any point x measured from the end of the cylinder.

* Walsh, Proc. Phys. Soc. xxxii. p. 59 (1920). See also Sumpner, Proc. Phys. Soc. xii. p. 10 (1892).

Consider also an elementary annulus of the cylinder of width dx at x so small that the radiation emission may be regarded as sensibly constant over its surface.

Then the radiation received by a disk at x_1 from the annulus at x is given by the difference between the radiations received by the disk at x_1 from disks at x and $x + dx$;

$$\text{i. e.,} \quad -\frac{\pi}{2}\phi(x)\{f(\overline{x+dx \sim x_1}) - f(x \sim x_1)\};$$

$$\text{i. e.,} \quad -\frac{\pi}{2}\phi(x) \frac{d}{dx} f(x \sim x_1) dx,$$

where

$$f(x \sim x_1) = \{(x \sim x_1)^2 + 2r^2 - (x \sim x_1) \sqrt{(x \sim x_1)^2 + 4r^2}\}.$$

Similarly, the radiation received by the elementary annulus at x_1 is given by the difference between the radiations received by disks at x_1 and $x_1 + dx_1$ from the annulus at x ;

$$\text{i. e.,} \quad -\frac{\pi}{2}\phi(x) \left\{ \frac{d}{dx} f(x \sim x_1 + dx_1) - \frac{d}{dx} f(x \sim x_1) \right\} dx;$$

$$\text{i. e.,} \quad -\frac{\pi}{2}\phi(x) \frac{d}{dx_1} \frac{d}{dx} f(x \sim x_1) dx dx_1.$$

Now, the area of the elementary annulus at x_1 is $2\pi r dx_1$. Hence the radiation received per unit area at x_1 from an annulus at x is given by

$$-\frac{\phi(x)}{4r} \frac{d^2}{dx_1 dx} f(x \sim x_1) dx.$$

Thus the radiation per unit area received at x_1 from the whole cylinder is given by

$$-\frac{1}{4r} \int_0^\infty \phi(x) \frac{d^2}{dx_1 dx} f(x \sim x_1) dx.$$

Writing $f(x - x_1)$ for $x > x_1$, $f(x_1 - x)$ for $x < x_1$, and $-\frac{d}{dx}$ for $\frac{d}{dx_1}$ makes this equal to

$$\frac{1}{4r} \left\{ \int_0^{x_1} \phi(x) \frac{d^2}{dx^2} f(x_1 - x) dx + \int_{x_1}^\infty \phi(x) \frac{d^2}{dx^2} f(x - x_1) dx \right\}.$$

For the case of the cylinder in which multiple reflexions occur, if an initial distribution of radiation emission is given, the first reflected distribution may be thus obtained, and from this again the second reflected distribution and so on. The sum of the initial and the reflected distributions gives the final approximation to black-body radiation from the inside of the cylinder.

Assume the walls of the cylinder are maintained at a constant temperature T , that the walls are perfectly diffusing as before, and that the emissivity is ϵ , which is constant throughout the spectrum. Then the reflexion coefficient is $(1-\epsilon)$. Let distances be measured in terms of r , the radius of the cylinder; i. e., put $r=1$. Then $f(x)$ becomes

$$F(x) = \{x^2 + 2 - |x| \sqrt{x^2 + 4}\}.$$

The initial distribution of emitted radiation is $\epsilon\sigma T^4 = \phi_0(x)$. Then the radiation received at any point x_1 from the whole of the cylinder is given by

$$\frac{1}{4} \left\{ \int_0^{x_1} \phi_0(x) \frac{d^2}{dx^2} F(x_1 - x) dx + \int_{x_1}^{\infty} \phi_0(x) \frac{d^2}{dx^2} F(x - x_1) dx \right\},$$

so that the first reflected distribution $\Phi_1(x)$ is

$$\frac{(1-\epsilon)}{4} \left\{ \int_0^{x_1} \phi_0(x) \frac{d^2}{dx^2} F(x_1 - x) dx + \int_{x_1}^{\infty} \phi_0(x) \frac{d^2}{dx^2} F(x - x_1) dx \right\}.$$

Similarly, the second reflected distribution $\Phi_2(x)$ is

$$\frac{(1-\epsilon)}{4} \left\{ \int_0^{x_1} \phi_1(x) \frac{d^2}{dx^2} F(x_1 - x) dx + \int_{x_1}^{\infty} \phi_1(x) \frac{d^2}{dx^2} F(x - x_1) dx \right\},$$

etc., etc.

Adding the distributions

$$\begin{aligned} & \phi_0(x_1) + \phi_1(x_1) + \phi_2(x_1) + \dots \\ &= \phi_0(x) + \frac{(1-\epsilon)}{4} \left[\int_0^{x_1} \{ \phi_0(x) + \phi_1(x) + \phi_2(x) + \dots \} \right. \\ & \quad \left. \frac{d^2}{dx^2} F(x_1 - x) dx + \int_{x_1}^{\infty} \{ \phi_0(x) + \phi_1(x) + \phi_2(x) + \dots \} \right. \\ & \quad \left. \frac{d^2}{dx^2} F(x - x_1) dx \right]. \end{aligned}$$

Now, writing the final distribution as $\Phi(x_1)$,

$$\begin{aligned} \Phi(x_1) = \epsilon\sigma T^4 + \frac{(1-\epsilon)}{4} & \left\{ \int_0^{x_1} \Phi(x) \frac{d^2}{dx^2} F(x_1 - x) dx \right. \\ & \left. + \int_{x_1}^{\infty} \Phi(x) \frac{d^2}{dx^2} F(x - x_1) dx \right\}. \end{aligned}$$

This equation could, of course, have been written down directly, as it merely expresses the fact that in the final steady state the total emission of radiation from any point is equal to the initial emission plus the reflected portion of the radiation received at that point from the whole of the cylinder.

The above equation is an integral equation of the second or Poisson's type. It does not appear to be possible to obtain an exact analytic solution for $\Phi(x)$, but an approximation which can attain whatever accuracy that is desired can be obtained by a method due to Whittaker*.

In Whittaker's paper it is shown, assuming certain existence theorems established by Volterra, that the solution of the integral equation

$$\phi(x) = f(x) - \int_0^x \phi(s) \kappa(x-s) ds,$$

where the nucleus $\kappa(x)$ is supposed to have been expressed approximately by Prony's † method as a series of exponentials of the form

$$\kappa(x) = B_1 e^{\beta_1 x} + B_2 e^{\beta_2 x} + B_3 e^{\beta_3 x} + \dots,$$

is
$$\phi(x) = f(x) - \int_0^x K(x-s) f(s) ds,$$

where
$$K(x) = C_1 e^{\gamma_1 x} + C_2 e^{\gamma_2 x} + C_3 e^{\gamma_3 x} + \dots,$$

in which there are as many exponential terms as there are in $\kappa(x)$.

In the case under consideration $f(x)$ is a constant (viz. $\epsilon \sigma T^4$), so that Whittaker's method suggests that the solution of the integral equation is of the form

$$\Phi(x) = (A_0 + A_1 e^{\alpha_1 x} + A_2 e^{\alpha_2 x} + A_3 e^{\alpha_3 x} + \dots) \sigma T^4.$$

This method has been used for the cases in which the nucleus $\frac{d^2}{dx^2} F(x)$ has been expressed as a single exponential and as the sum of two exponentials.

$$\begin{aligned} \text{Now } \frac{d^2}{dx^2} F(x) &= \frac{d^2}{dx^2} \{x^2 + 2 - x \sqrt{x^2 + 4}\}, \\ &= 2 \left\{ 1 - \frac{x(x^2 + 6)}{(x^2 + 4)^{3/2}} \right\}. \end{aligned}$$

A set of values of $\frac{1}{2} \frac{d^2}{dx^2} F(x)$ is given in the table below for comparison with the corresponding values of e^{-x} , by which it may be seen that the function e^{-x} is a fair approximation to the function $\frac{1}{2} \frac{d^2}{dx^2} F(x)$.

A two-term exponential function $B_1 e^{\beta_1 x} + B_2 e^{\beta_2 x}$ giving an

* Whittaker, Proc. Roy. Soc. xciv. p. 367 (1918).

† Prony, *Journ. de l'École Pol.* Cah. ii. (an iv.), p. 29. See also Whittaker, *loc. cit.*, and Walsh, Proc. Phys. Soc. xxxii. pt. i. p. 26 (1919).

approximation to $\frac{1}{2} \frac{d^2}{dx^2} F(x)$ was obtained by determining the double exponential function, which had the same value as $\frac{1}{2} \frac{d^2}{dx^2} F(x)$ at four points including $x=0$ so that $B_1 + B_2 = 1$, and then slightly adjusting β_1 and β_2 so that

$$\int_0^\infty (B_1 e^{\beta_1 x} + B_2 e^{\beta_2 x}) dx = \frac{1}{2} \int_0^\infty \frac{d^2}{dx^2} F(x) dx = 1;$$

i. e., making $\left(\frac{B_1}{\beta_1} + \frac{B_2}{\beta_2}\right) = -1$.

This adjustment makes the approximation to the radiation emitted from an annulus actually equal to the radiation emitted.

The third column in the table gives the values of $1.21e^{-1.14x} - 0.21e^{-3.40x}$, which, as may be seen, gives a very close approximation to $\frac{1}{2} \frac{d^2}{dx^2} F(x)$ in the region where this function has any value of importance. Fig. 3 enables a graphical comparison of these functions to be made.

x .	e^{-x} .	$\frac{1}{2} \frac{d^2}{dx^2} F(x)$.	$1.21e^{-1.14x} - 0.21e^{-3.40x}$.
0	1.0000	1.0000	1.0000
.10	.9048	.9252	.9302
.25	.7788	.8149	.8202
.50	.6065	.6433	.6459
.75	.4724	.4949	.4982
1.00	.3679	.3737	.3800
1.50	.2231	.2080	.2176
2.00	.1353	.1161	.1235
2.50	.0821	.0668	.0699
3.00	.0498	.0399	.0396
4.00	.0183	.0161	.0127

Assuming, then, that

$$\Phi(x) = (A_0 + A_1 e^{\alpha_1 x} + A_2 e^{\alpha_2 x}) \sigma T^4,$$

it is required to find A_0 , A_1 , A_2 , α_1 , and α_2 from the equation

$$\begin{aligned} & A_0 + A_1 e^{\alpha_1 x_1} + A_2 e^{\alpha_2 x_1} \\ &= \epsilon + \frac{(1-\epsilon)}{2} \int_0^{x_1} (A_0 + A_1 e^{\alpha_1 x} + A_2 e^{\alpha_2 x}) \\ & \quad (B_1 e^{\beta_1(x_1-x)} + B_2 e^{\beta_2(x_1-x)}) dx \\ & \quad + \frac{(1-\epsilon)}{2} \int_{x_1}^\infty (A_0 + A_1 e^{\alpha_1 x} + A_2 e^{\alpha_2 x}) \\ & \quad (B_1 e^{\beta_1(x-x_1)} + B_2 e^{\beta_2(x-x_1)}) dx. \end{aligned}$$

Performing the integrations and equating the constant terms and the coefficients of $e^{\alpha_1 x}$, $e^{\alpha_2 x}$, $e^{\beta_1 x}$ and $e^{\beta_2 x}$ on each side of the equation, it is found that

$$A_0 = \epsilon - A_0(1 - \epsilon) \left(\frac{B_1}{\beta_1} + \frac{B_2}{\beta_2} \right) = \epsilon + A_0(1 - \epsilon),$$

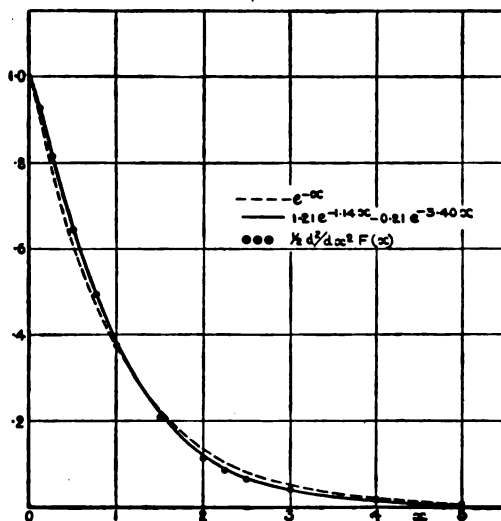
$$1 = (1 - \epsilon) \left\{ \frac{B_1 \beta_1}{\alpha_1^2 - \beta_1^2} + \frac{B_2 \beta_2}{\alpha_1^2 - \beta_2^2} \right\},$$

$$1 = (1 - \epsilon) \left\{ \frac{B_1 \beta_1}{\alpha_2^2 - \beta_1^2} + \frac{B_2 \beta_2}{\alpha_2^2 - \beta_2^2} \right\},$$

$$0 = \frac{1}{\beta_1} - \frac{A_1}{\alpha_1 - \beta_1} - \frac{A_2}{\alpha_2 - \beta_1},$$

$$0 = \frac{1}{\beta_2} - \frac{A_1}{\alpha_1 - \beta_2} - \frac{A_2}{\alpha_2 - \beta_2}.$$

Fig. 3.



Comparison of Single-term and Two-term Exponential Approximations with $\frac{1}{2}d^2/dx^2 F(x)$.

The first equation gives $A_0 = 1$. The second and third equations show that α_1 and α_2 are given by the square roots of the roots of the quadratic equation in z :

$$(1 - \epsilon) \left\{ \frac{B_1 \beta_1}{z - \beta_1^2} + \frac{B_2 \beta_2}{z - \beta_2^2} \right\} = 1.$$

From the fourth and fifth equations the values of A_1 and A_2 can be obtained, using the values of α_1 and α_2 obtained from the second and third, while it can also be shown that $A_1 + A_2 = -(1 - \sqrt{\epsilon})$.

The equations have been solved for the two exponential cases when $\epsilon = 0.75, 0.50, 0.25$, and 0.10 respectively, and the following expressions obtained, giving the distribution of radiation along the cylinders for these values of the emissivity :

$$\epsilon = 0.75, \quad (1 - 0.1399e^{-0.980x} + 0.0059e^{-3.425x})\sigma T^4,$$

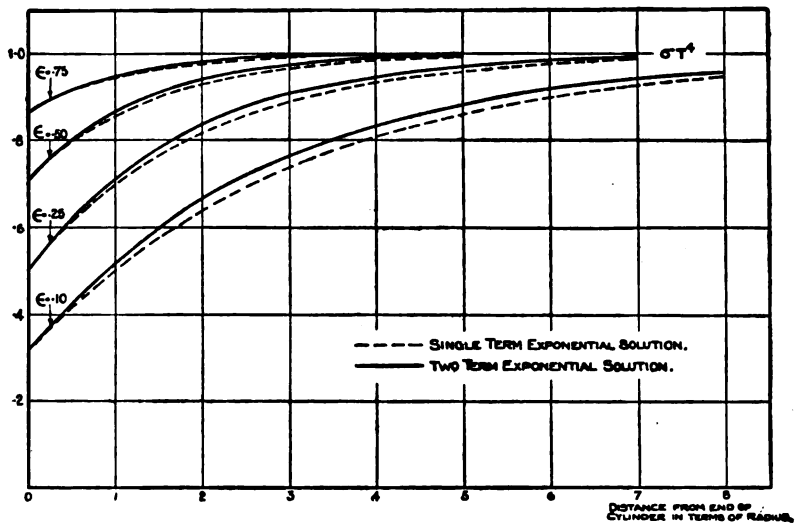
$$\epsilon = 0.50, \quad (1 - 0.3013e^{-0.795x} + 0.0090e^{-3.450x})\sigma T^4,$$

$$\epsilon = 0.25, \quad (1 - 0.5082e^{-0.558x} + 0.0081e^{-3.470x})\sigma T^4,$$

$$\epsilon = 0.10, \quad (1 - 0.6893e^{-0.352x} + 0.0057e^{-3.485x})\sigma T^4.$$

These results are shown graphically by the full-line curves in fig. 4.

Fig. 4.



Distribution of Radiation near the end of a Uniformly-heated Infinite Cylinder.

The solution in the case of the single exponential case is obtained quite simply as $\{1 - (1 - \sqrt{\epsilon})e^{\sqrt{\epsilon}x}\}\sigma T^4$, and the results are also shown on fig. 4 by the dashed-line curves.

It will be noticed that for values of the emissivity greater than 0.50 the single-term exponential solution is very nearly the same as that of the two-term exponential. Considering

762 *Radiation from the Inside of a Circular Cylinder.*

that the single exponential e^{-x} is only a moderately good approximation to $\frac{1}{2} \frac{d^2}{dx^2} F(x)$, and that the results obtained by using it are close to the results obtained by using the quite good approximation given by the two-term exponential solution, it is probable that the slight improvement which could be obtained by using a three-term exponential approximation would not give appreciably different results from those shown by the full-line curves.

It will be noted that at the open end of the cylinder where $x=0$ the same result is obtained, using the single or the two-term experimental approximation to the function $\frac{1}{2} \frac{d^2}{dx^2} F(x)$. This is quite general, and is in consequence of the approximations being adjusted to make

$$\int_0^{\infty} \Sigma B e^{\beta x} dx = 1.$$

So that if $\frac{1}{2} \frac{d^2}{dx^2} F(x)$ be expressed as $\Sigma_1^{\infty} B_n e^{\beta_n x}$, then

$$\Sigma_1^{\infty} A_n = -(1 - \sqrt{\epsilon}),$$

and the value of $\Phi(x)$ at $x=0$ is

$$A_0 + \Sigma_1^{\infty} A_n = \sqrt{\epsilon} \sigma T^4.$$

Since the approximation to $\frac{1}{2} \frac{d^2}{dx^2} F(x)$ can be made as close as is liked, it follows that the value of $\Phi(x)$ at $x=0$ is exact.

Summary.

An expression is derived for the radiation from an annulus to any other annulus, and used to determine the radiation from any point inside an infinite circular cylinder of uniform temperature, multiple reflexion of radiation inside the cylinder being taken into account. The result is obtained in the form of an integral equation of the Poisson type, and an approximate solution is obtained. It is shown that the approximate solution is exact at the end of the cylinder, and that there the radiation emitted from the inside of the cylinder is given by $\sqrt{\epsilon} \sigma T^4$ per unit area, where ϵ is the emissivity of the walls of the cylinder.

The author wishes to express his thanks to Mr. R. A. Frazer for the interest he has taken in this problem and the benefit he has received by discussing it with him.

LXVIII. *Multiple Ionization in X-Ray Levels.* By Prof. H. R. ROBINSON, *University College of South Wales and Monmouthshire* *.

§ 1. **T**HE terms of the X-ray spectra of the elements ("spectra of the first kind") are now very accurately known in the majority of cases. It is some years since the first comprehensive tables of term values were published by (*inter alia*) Sommerfeld and Bohr & Coster. These tables were based largely on emission spectra measured in Siegbahn's laboratory, together with a judicious selection of combinations with known absorption limits. More recent work has, in the main, confirmed the remarkable accuracy of these early tables, though the natural development of spectroscopic research has enabled minor corrections and additions to be made in some instances. Work still remains to be done on the terms of lower frequency, but in the normal X-ray regions the existing data may be regarded as sufficiently complete; the most urgent need is not for increased accuracy in the normal term values, but rather for some detailed knowledge of the terms in atoms which are ionized to different degrees in their X-ray levels.

§ 2. The energies associated with atoms of the latter class are, according to the theory first elaborated by Wentzel †, intimately related to the frequencies of the "non-diagram" lines in X-ray spectra—i. e., those faint lines which cannot be fitted into the accepted scheme of X-ray levels, even by allowing violations of the selection rules. These lines (usually satellites on the high-frequency sides of the normal series lines) are supposed to originate in transitions between states of multiply-ionized atoms; for this reason Wentzel has called them X-ray "spark" lines, although the normal X-ray lines are, in the optical sense, spark lines. Wentzel speaks of spark lines of the first, second, order according as the atom is doubly, triply, ionized—corresponding to the "spectra of the second, third, kind" of Bohr and Coster's notation.

In its broad outlines Wentzel's theory has provided an eminently satisfactory explanation of the origin of spark lines. Support has been brought to the theory by a number of investigations of the conditions necessary for the appearance of the satellites. Coster ‡ first showed, in the course

* Communicated by the Author.

† Wentzel, *Annalen der Physik*, lxi. p. 437 (1921); lxxiii. p. 647 (1924).

‡ Coster, *Phil. Mag.* xliii. p. 1070, xliv. p. 546 (1922).

of a very detailed investigation of X-ray spectra, that the satellites in the L spectrum of silver were practically suppressed if the voltage on the X-ray tube was kept sufficiently low (say about 1 kilovolt above the critical L excitation potentials). Much other indirect evidence of this kind has since been obtained, all indicating that the appearance of the satellites is favoured by the use of vigorous excitation.

§ 3. It cannot, however, be said that there is anything like a complete confirmation of the details of the original scheme propounded by Wentzel. According to this scheme, the K spark lines correspond to the following transitions:—

$$\begin{aligned} K\alpha_3 &= KL \rightarrow L^2, & K\alpha_4 &= K^2 \rightarrow KL, & (\text{First order}), \\ K\alpha_5 &= KL^2 \rightarrow L^3, & K\alpha_6 &= K^2L \rightarrow KL^2 & (\text{Second order}), \\ & & K\alpha' &= KM \rightarrow LM, \end{aligned}$$

the symbol K^2L being used to represent an atom which has lost both K electrons and one L electron, and so on. It will be noticed that no attempt is made to discriminate between the various L and M sub-levels; in any case, as was first shown by Wentzel* in a later paper, there is reason to believe that the multiplicity of these levels is profoundly modified by the multiple ionization of the atom.

Fairly full complements of K spark lines have been measured for only a few of the lighter elements, and the observational data are too meagre to permit of a thorough numerical comparison between experiment and theory. The evidence in favour of the scheme is restricted to the observation, over a very limited range, of certain regularities, predicted by the theory, in the frequency differences $\alpha_5 - \alpha_4$, $\alpha_6 - \alpha_3$, $\alpha_3 - \alpha_1$, for a given element, and the approximate equality of $\alpha_6 - \alpha_4$ for each element with $\alpha_3 - \alpha_1$ for the element of next higher atomic number.

In the case of the spark lines associated with the L series, Wentzel has suggested for the most prominent satellites, $L\alpha_3$ and $L\alpha_4$, the transitions

$$\begin{aligned} L\alpha_3 &= LM \rightarrow M^2, \\ L\alpha_4 &= L^2 \rightarrow LM. \end{aligned}$$

Here, of course, and also in the M series, there is a great variety of levels to select from, and it is difficult to decide, on the available experimental evidence, in favour of any particular scheme of transitions. One great difficulty lies in the nature of the measurements; the spark lines cannot, as

* Wentzel, *Zeits. f. Phys.* xxxi. p. 445 (1925).

a rule, be measured with the same accuracy as the normal series lines. The latter are always heavily over-exposed relatively to the former, and this, naturally, does not make for the accurate measurement of close satellites. It is therefore unlikely that we shall have for some time any appreciably more precise knowledge of the frequencies of the spark lines, or any extension to measurements for the heavier elements, where the separations are still less and the spark lines less prominent.

§ 4 The indirect evidence is also, from the point of view of the scheme, far from satisfactory. There is, in fact, no clear-cut indication of the exact stages of ionization involved in the production of spark lines, or of the manner in which the ionization is brought about. Wentzel's original assumption (abandoned later) of a process of cumulative ionization by successive electron impacts on the same atom seems to be definitely put out of court by the theoretical considerations advanced by Rosseland*. The experimental evidence is also against this theory—all tests, so far, indicate high voltage on the X-ray tube, rather than heavy milliamperage, as the deciding factor in the production of spark lines. Coster's experiments, referred to above, were not carried out under sufficiently definite conditions to furnish a precise estimate of the minimum excitation potential for spark lines. Later experiments have, in a few instances, fixed the critical potentials within narrower limits: the results indicate that, on the theory of multiple ionization by a single electronic impact, Wentzel's scheme requires modification in some of its details. At the same time the results are neither sufficiently numerous nor sufficiently precise to define any more acceptable scheme.

Bäcklin†, investigating the K spectrum of aluminium with different exciting voltages, found that $K\alpha_4$ appeared at a voltage well below the calculated minimum value required for double ionization of the K level. Further, allowing for possible errors in estimating the voltages, it seemed probable that $K\alpha_3$ also appeared below this critical value. The feeble intensity of the spark lines makes the exact measurement of the corresponding critical potentials very difficult; this factor might lead to an over-estimate of the values, but it leaves no loophole for spark lines which appear at unduly low voltages. Another important point brought out by Bäcklin's work was that the ratio of the intensities of $K\alpha_2$

* Rosseland, *Phil. Mag.* xlv. p. 65 (1923).

† Bäcklin, *Zeits. f. Phys.* xxvii. p. 30 (1924).

and $K\alpha_4$ was sensibly independent of the exciting voltage. This would only fit in with Wentzel's original scheme if it could be assumed that simultaneous KL ionization by a single electron occurred much less frequently than simultaneous K^2 ionization (the end state for $K\alpha_4$ being identical with the initial state for $K\alpha_3$). The evidence of Bäcklin's work is therefore strongly against any scheme which requires K^2 states for the explanation of the K spark lines*.

It may be mentioned here that in a recent paper (received after the greater part of the present paper had been written) Saha and Ray† have, on purely theoretical grounds, propounded a scheme for the spark lines which does not involve K^2 states.

Siegbahn and Larsson's‡ observations on the $L\alpha$ satellites of molybdenum are of special interest, and are probably the most accurate available. The critical L_I , L_{II} , L_{III} excitation voltages for molybdenum are approximately 2880, 2620, and 2520 respectively. For normal K excitation the minimum is 19,950 volts. Siegbahn and Larsson find four satellites on the high-frequency side of $L\alpha_{1,2}$ at all voltages above 4000. No new satellites appear between 4000 and 20,000 volts, but a fifth (with possibly, but very doubtfully, a sixth) faint satellite of still higher frequency appears at and above 20,000 volts. No further satellites appear in this region, even at 40,000 volts—the highest potential used.

The satellites lie within the shadow of the intense $L\alpha_1$ line, but the evidence of the photometric analyses of the spectrograms is extraordinarily clear and convincing. The spark lines may be picked out with ease, and some estimate may be obtained of their relative intensities. The following points of primary importance emerge from the study of the spectrograms:—

(1) The intensities of the satellites, relative to that of $L\alpha_1$, are practically unchanged between 4 and 15 kilovolts, and probably up to 20 kilovolts, though no curves are given for the range 15–20 kilovolts.

(2) Not only does a new satellite (or two new satellites) appear, as mentioned above, at 20,000 volts—the *K* excitation limit—but the intensities of all the satellites, relative to that of $L\alpha_1$, increase very appreciably at this stage. Siegbahn

* See, however, Wentzel, *Zeits. f. Phys.* xxxi. p. 450 (1925).

† Saha & Ray, *Phys. Zeitschr.* xxviii. p. 221 (1927).

‡ Siegbahn & Larsson, *Ark. f. Mat. Ast. och Fys.* xviii. no. 18 (1924). Some of the curves are reproduced in Lindh's Report (*Phys. Zeits.* xxviii. p. 93, 1927).

and Larsson have not mentioned this latter point in their discussion. They state at one point that their curves do not correctly represent the relative intensities of the lines, and this contention is certainly justifiable, as $L\alpha_1$ is heavily over-exposed. It seems, however, fair to assume that the marked sudden increase in the strength of the satellites at 20,000 volts is a real effect. Taking the curves as they stand, the relative intensities of the satellites between 20 and 40 kilovolts are at least two and a half times greater than they are below 20 kilovolts. If anything, the satellites appear relatively a little feebler at 40 than at 20 kilovolts; but there is little justification (and no sufficiently attractive pretext) for straining the interpretation of the curves so far as to insist upon this point. It may, then, be taken from the curves that no new satellites, and no marked discontinuities in the intensities of the existing satellites, appear between 20 and 40 kilovolts.

Taking these points in turn :—

(1) It is hardly conceivable that a 4000-volt electron is capable of removing two L electrons from a molybdenum atom. It therefore seems likely that, at all events, the stronger L satellites do not originate in transitions from L^2 states. This is closely analogous with Bäcklin's results for the K spark lines.

(2) I have already referred, in a recent letter to 'Nature'*, to the fact that a rapid increase in the rate of production of atoms in L^2 , LM, states is to be expected after the K critical excitation potential is over-stepped. After the removal of a K electron from an atom, there frequently ensues either (a) the genesis, immediately followed by specially privileged "internal absorption," of a K series X-ray, or (b) a "radiationless" reorganisation of the extra-nuclear electrons, accompanied by the expulsion of a "photo-electron of the second kind," generally from one of the X-ray levels. For the present purpose the exact nature of the process is immaterial, though it is noteworthy that Ellis† (to whom we owe most of our knowledge of the details of the internal conversion of γ rays) leans to the view that his experiments deal with a true internal absorption of radiation. The experimental evidence is less definite in the case of X-rays, where, as Ellis has pointed out, the conditions are not identical with those of his experiments.

* Robinson, 'Nature,' cxviii. p. 224 (1926).

† See, in particular, Ellis & Wooster, Roy. Soc. Proc. A, cxiv. p. 285 (1927).

The point has been discussed in some detail by Smekal *, among others.

So far as the present discussion is concerned, the important point is that, whatever the exact nature of the process by which the potential energy of the excited atom is internally converted, the final result of the process is an atom which is multiply ionized in its X-ray levels. Some of the direct experimental evidence for this will be found summarized in the above-mentioned letter to 'Nature,' and more fully in a recent paper in the 'Proceedings of the Royal Society' †. The effectiveness of this mode of production of multiply-ionized atoms is strongly indicated by the evidence in (2) above, and more particularly by the marked increase in the intensities of the $L\alpha$ satellites above the K excitation limit.

This forms a striking parallel with the fact, predicted by the original Kossel scheme of X-ray spectral series, that the inception of K emission must always be accompanied by a corresponding increase in the L emission. This effect has recently been verified by Stumpen ‡, whose isochromatic curves for the lines of the L series all show distinct upward inflexions of the K excitation voltage.

If any appreciable KL ionization occurred under the conditions of Siegbahn and Larsson's experiments, it would be expected to manifest itself, possibly by the appearance of new L spark lines, and certainly by an increase in the relative intensities of the existing spark lines. The absence of these effects between 20 and 23 kilovolts—and even up to, and presumably beyond §, 40 kilovolts—strongly suggests that ionization of the K level and an L level by the same cathode ray is relatively infrequent—that is, compared with the frequency of the occurrence of L^2 , LM, . . . ionization by "internal absorption of fluorescent X radiation." ||

§ 5. In the meantime a very important contribution to the problem of the spark lines has been made by Coster and Druyvesteyn ¶. It had previously been suggested (originally, I believe, by Coster himself) that the spark

* Smekal, *Ann. der Phys.* lxxxi. p. 391 (1926); *Phys. Zeitschr.* xxvii. p. 831 (1926).

† Robinson & Cassie, *Roy. Soc. Proc. A*, cxiii. p. 282 (1926).

‡ Stumpen, *Zeits. f. Phys.* xxxvi. p. 1 (1926).

§ In Siegbahn & Larsson's work a transformer was used to excite the X-ray tube at the highest voltages, and it seems very likely that the peak voltage may have been high enough for K^2 excitation.

|| The process will be so described for the sake of brevity.

¶ Coster & Druyvesteyn, *Zeits. f. Phys.* xl. p. 765 (1927).

lines would probably be absent from fluorescently excited X-ray spectra; this supposition was apparently confirmed experimentally by Dauvillier*. Coster and Druyvesteyn have now, however, succeeded in exciting K spark lines by fluorescence, using an X-ray tube specially designed to produce intense fluorescent X-radiation in a secondary radiator. Photographs of the K spark lines of iron have been obtained from an iron radiator, placed 5 mm. away from the copper anticathode of the primary tube, with exposures of approximately 400 milliampere-hours at 30 kilovolts. Some idea of the efficiency of the process is given by the authors' statements that under the same conditions the normal $K\alpha$ doublet was well exposed with 8 milliampere-hours, while the direct radiation from the same tube, fitted with an iron anticathode, gave the Fe $K\alpha$ doublet with about $\frac{1}{4}$ milliampere-hour.

Three possible modes of production of doubly-ionized states by the action of X-rays are briefly discussed by Coster and Druyvesteyn. In view of the importance of the problem, these discussions are reproduced, and to some extent amplified, below.

(1) The most direct of all possible processes—the absorption of a quantum of X-radiation, resulting in the simultaneous ejection of two electrons from X-ray levels—is difficult to support by direct experimental evidence. Siegbahn is reported to have observed, in the case of sulphur, a faint absorption discontinuity, corresponding approximately to the frequency required for the simultaneous removal of the two K electrons. So far as I am aware, no detailed confirmation of this report has yet appeared. The discontinuity in question must be extremely faint, or it could hardly have escaped the observation of previous workers on absorption limits. Coster and van der Tuuk† have sought in vain for corresponding effects in argon; Coster and Druyvesteyn, however, point out that effects much larger than that required to account for the observed intensities of the spark lines could very well have escaped detection in the absorption experiments. The maximum intensity of the impulse radiation in the primary beam used to excite the spark lines (copper anticathode, 30 kilovolts) would lie in the region of frequencies corresponding to a little over 20 kilovolts: there would therefore be present very intense radiations of sufficiently high frequencies to produce KL and K^2 states in

* Dauvillier, *C. R.* clxxvii. p. 167 (1923).

† Coster & van der Tuuk, *Zeits. f. Phys.* xxxvii. p. 367 (1926).

single absorption processes. Processes of this kind do not appeal as very likely ones, but the evidence so far available does not rule them completely out.

(2) Double ionization of an atom by a high-speed photo-electron from a neighbouring atom. Quite apart from other and obvious objections to this view, Coster and Druyvesteyn show clearly that the observed intensities of the spark lines are far too high to be accounted for in this way.

(3) A photo-electron expelled with sufficiently high speed from (say) the K level may, on its way out, eject another electron from an X-ray level of the same atom. K^2 , KL, ... states can clearly arise in this way, given a primary X radiation of sufficiently high frequency. A somewhat similar succession of events may readily be visualized in the case of double ionization by a high-speed electron. Coster and Druyvesteyn show that the relative intensities of the spark and normal lines, produced by bombardment of an anticathode with cathode rays of suitable speed, are in rough agreement with the relative numbers of KL and K states predicted by Rosseland's* extension of Sir J. J. Thomson's† theory of ionization by charged particles.

If this view, favoured by Coster and Druyvesteyn, of the processes leading to double ionization is accepted—and it has obvious attractions,—the evidence is again opposed to the attribution of the K spark lines to transitions from K^2 states. The number of such states predicted by the theory is far too small to give the observed intensities of the spark lines. It should, however, be mentioned that this argument tacitly assumes that the proportions of radiationless rearrangements are not vastly different for K and KL states.

Further, a very simple consideration (viz. of the differences between the processes of single ionization by X- and cathode-rays) indicates that, on this view, for a given intensity of the normal K spectrum, the spark lines in the spectrum excited by electronic bombardment should have, very roughly, double the intensities of the same lines in the "fluorescent" spectrum. An intensity difference of this order is, in fact, exhibited by the photometric curves of Coster and Druyvesteyn (*loc. cit.* p. 779), though the comparison is necessarily very rough.

§ 6. The question of the exact mode of generation of doubly-ionized atoms is of the first importance in connexion with projected measurements of the energies associated with

* Rosseland, *loc. cit.*

† Thomson, *Phil. Mag.* xxiii. p. 449 (1912).

the corresponding states. It seems sufficiently clear that only the first mode contemplated in § 5—double ionization in a single absorption act—will give a sharply-defined limiting frequency. If Siegbahn's observation of absorption edges for K^2 states can be confirmed and extended to KL , states, the measurement of these edges may be expected to provide the most accurate determinations of the energies. At present, however, the experimental evidence strongly suggests that double ionization processes of this kind, if indeed they occur at all, do not occur sufficiently often to give well-marked absorption edges under ordinary experimental conditions.

If the process of double ionization occurs in accordance with the scheme of alternative (3) above, as seems highly probable—*i. e.*, in two steps—it will clearly be very difficult to fix the energies with any great accuracy by direct experiment. The details from Coster and Druyvesteyn's paper, quoted in § 5 above, are a sufficient indication of the faintness of the spark lines. Further experiments are promised in which an attempt is to be made to trace the effect upon the spark lines of varying the frequency of the primary beam. The results of these experiments will be awaited with the deepest interest, as a step towards the solution of the problem of the origin of the spark lines. It is, however, obvious from the outset that there are sufficiently formidable experimental difficulties to prevent any accurate determination of critical excitation frequencies for the spark lines. Abrupt variations in the intensities of the spark lines at the critical frequencies are not to be expected, and the photographic method is probably the only one which can be used for detection of lines so feeble as those under investigation. Similar objections would apply to attempts to refine upon the methods of Bäcklin's experiments; it would hardly appear feasible, with the intensities available, to utilize the ionization spectrometer to obtain the isochromatic curves for even the strongest of the spark lines. It would appear that the most that can be hoped from these experiments is a sufficiently close approximation to the critical energies to place beyond doubt the degree and type of ionization in the initial state.

§ 7. The method of measuring the energies of the tertiary photo-electrons ("photo-electrons of the second kind"), which has already been applied to a limited extent in the work of Robinson and Cassie, in many respects offers unique advantages. The chief difficulty lies in the interpretation

of the lines of the corpuscular "spectra," and the method has one other inherent defect: obviously, the only "radiation" available for the expulsion of an electron from the L level of an ionized atom is the K-radiation from the same atom, and so on. The frequencies of the K-radiations are always large in comparison with the critical L excitation frequencies; the disproportion is less marked in the case of the L lines and the M limits, but even here it is sufficient to impair the "resolving power" of the apparatus. For this reason it is not possible to use the method of corpuscular spectrometry quite so effectively in these cases as for the secondary electrons which result from the external absorption of a selected primary radiation. On the other hand, the lines obtained are extremely sharp, and may be measured with very high precision; further, by suitable selection of the source of X-rays, it is always possible to check the measurements by bringing some standard line (corresponding to secondary electrons ejected from a normal level of the target material by a characteristic radiation in the primary beam) into the region of the photographic plate in which the measurements are being made. Most important of all, the process of internal absorption is so remarkably efficient that measurable photographs may be obtained with relatively short exposures, and the definition of the lines is not impaired by the overlapping of lines due to "photo-electrons of the first kind"*. This is in accordance with the evidence deduced from Siegbahn and Larsson's work (§ 4, p. 766), to the effect that internal absorption of X-radiation is by far the most efficient mode of production of multiply-ionized atoms.

The "fluorescent" lines already measured (Robinson and Cassie, *loc. cit.* pp. 284 *et seqq.*) are sufficient to show the possibilities of the method of corpuscular spectrometry, although the measurement of these lines was in this instance subsidiary to another investigation, and no attempt was made to exhaust the series of fluorescent lines for any element. The order of accuracy attained is indicated by the marked differences recorded (for instance) for the energies of the L levels of the ionized copper atom, according to whether the electron is ejected therefrom by internal absorption of $K\alpha_1$ ($L_{III} \rightarrow K$) or $K\beta_1$ ($M_{III} \rightarrow K$).

These experiments were interrupted by the departure of Mr. Cassie and myself from Edinburgh last year.

* *I.e.*, electrons ejected by the fluorescent X-radiation of one atom from the X-ray levels of a neighbouring (originally neutral) atom.

I am now continuing the experimental work with Mr. C. L. Young; we hope, in spite of temporary disturbances occasioned by the necessity for partially gutting and refitting the laboratory, to be able shortly to communicate an extended list of the energy levels of doubly-ionized atoms. It is noteworthy that in the case of internal absorption of K characteristic radiations, the strongest lines so far measured apparently correspond to LM states of the atom concerned, although L^2 states would at first sight appear to be a probable result of the internal absorption of $K\alpha(L \rightarrow K)$. The results of our experiments are thus in excellent accord with the deductions from Siegbahn and Larsson (§ 4, p. 766), that the principal L spark lines originate in transitions from LM and lower states, and not from L^2 states of the atom. The point of particular importance in this connexion is that Siegbahn and Larsson's curves show a marked increase in the intensity, rather than in the type, of the spark spectrum exactly at the point where our experiments indicate an increased production of LM (and LN) states. The new faint satellite(s) found by Siegbahn and Larsson at and above 20,000 volts might conceivably be due to L^2 states produced by internal absorption.

Similarly, the fluorescent corpuscular lines arising from the internal absorption of the L-radiations appear generally to come from atoms which are left in MN, . . . states, though here the interpretation is more ambiguous. The interpretation would in all cases be greatly simplified if it were certain that we had to deal with a true internal absorption of characteristic radiations, in which case valuable guidance could be derived from the known intensity ratios and selection rules, and from the approximately known variations in the intensities of the corpuscular spectra with the frequency of the exciting radiation. It is, unfortunately, quite clear that there are fundamental differences between "internal" and "external" absorption (Robinson, 'Nature,' *loc. cit.*), and much work is still required on the theoretical side of the problem of the radiationless changes. There is also the additional complication of the increased multiplicity of the terms in the ionized atoms (Wentzel, reference in § 3, p. 764). It is evident that a great deal of information is still to be derived from the closer study of the fluorescent lines of the corpuscular spectra—both of the absolute energies of the lines and of their relative intensities,—though it seems probable that the resolving power will have to be increased if the method is to be utilized to the fullest advantage.

Note added in proof.—Reference may be made to two very recent papers which appeared in the *Zeitschrift für Physik* during July 1927. (1) Wentzel has calculated, on wave-mechanical theory, the relative probabilities of different internal rearrangements in an atom initially ionized in the K level; the results of the calculation are in general agreement with the intensities recorded by Robinson and Cassie. (2) Druyvesteyn has communicated the results of new and extensive measurements on spark lines in the K and L series of a number of elements. This work appears to constitute a distinct advance towards the establishment of a satisfactory scheme for the spark lines.

LXIX. *On the Arc Spectrum of Bismuth.* By G. R. TOSHNIWAL, M.Sc., Research Scholar, Allahabad University, Allahabad*.

SUMMARY.

THE arc spectrum of Bismuth has been investigated in the heavy arc and under-water spark, and the lines remeasured between λ 1900 and λ 3550. A discussion of the structure of the spectrum of Bismuth from the standpoint of the theories of complicated spectra is given. It is shown that in Bismuth, owing to its large atomic number, terms arising from the same level are separated by widely different values, and this renders the interpretation of the spectrum rather difficult. A large number of new lines has been obtained and a number of important lines has been carefully remeasured. The new lines include some predicted by Thorsen.

THE arc spectrum of Bismuth is interesting from more than one point of view. Thirty years ago Kayser† and Runge tried to discover regularities, and found that the spectrum consisted of groups of lines having the separations 11418, 4019, and 6223. The last group consisted in some cases of close doublets with the separation 1·91. Ruark, Mohler, Foote, and Chenault‡ investigated the excitation and the ionization potential of the element by the electron bombardment method. They arranged the lines in a number of fundamental levels (denoted by $3d_2$, $3d_1^B$, $3d_1^A$, . . . etc.) and sub-levels (denoted by Greek letters α , β , γ , δ , . . . etc.).

* Communicated by Prof. M. N. Saha, D.Sc., F.R.S.

† Kayser, *Handbuch der Spectroscopie*, ii. p. 576.

‡ Ruark, Mohler, Foote, and Chenault, *Sc. Pap. Bur. Stand.* xix. p. 463 (1923-24).

They added with some hesitation two levels, $1s$ and β , to those given by Kayser and Runge. While this paper was being written there appeared a paper by Thorsen (*Zeitschrift für Physik*, xl.), who tried to discover Rydberg sequences in the spectrum of Bismuth.

On the experimental side, Offermann* gave an accurate measurement of wave-lengths from $\lambda 6134$ to $\lambda 2061$. Randall† has explored the infra-red region from $\lambda 9600$ to $\lambda 22000$ by means of a grating, a thermopile, and a Paschen galvanometer. Walters‡ has measured the wave-lengths in the arc spectrum within the region $\lambda 5600$ to $\lambda 9600$ by means of infra-red photography. Takamine and Nitta have measured the spectrum on the short wave-length side of $\lambda 1990$, and Bloch§ and McLennan|| in the Schumann region down to $\lambda 1400$. The Zeeman effect has been studied by Purvis¶, but the data do not seem to be reliable.

The spectrum of Bismuth has been investigated several times in this laboratory by Dr. N. K. Sur in the furnace and the under-water spark. The results were not published in the expectation of a more extensive investigation. I took up the work started by Dr. Sur and have investigated the spectrum of the 20-21 ampere arc.

The region $\lambda 4800$ to $\lambda 3550$ was photographed by means of a 5-ft. Rowland grating (dispersion 11.12 Å. to a mm.); from $\lambda 3550$ to $\lambda 2170$ was investigated on quartz spectrograph E. I. (Adam Hilger), kindly lent to us by Prof. N. R. Dhar, of the Chemistry Department; and from $\lambda 2170$ to $\lambda 1900$ on the above-mentioned grating and also on a small quartz spectrograph E. 126. Comparison spectra of iron were taken up to $\lambda 2300$, that of the copper arc from $\lambda 2300$ to $\lambda 2170$, and that of the silver spark down to $\lambda 1900$.

My measurements substantially agree with those of Offermann; the differences between the two greater than $\cdot 02$ Å. have been noted down. Offermann's data are used between $\lambda 3500$ – $\lambda 4800$, since my measurements of the plates in this region cannot be accurate in the second decimal place, because of the small dispersion in the first order of the grating. The lines marked by T in this region are new lines, and there is a possible mistake of not more than $\cdot 08$ Å.

* Offermann, Kayser, and Köne., *Handbuch der Spectroscopie*, vol. vi. p. 104.

† Randall, *Astro. Journ.* xxxiv. p. 1 (1911).

‡ Walters, *Sc. Pap. Bur. Stand.* p. 411 (1921).

§ L. and E. Bloch, *C. R.* clxx. p. 320; clxxi. p. 709 (1920).

|| McLennan, Young, and Ireton, *Proc. Roy. Soc.* xcviii. p. 95 (1920).

¶ Purvis, *Proc. Camb. Phil. Soc.* xiv. p. 216 (1907).

Between $\lambda 2170$ and $\lambda 1900$ my measurements differ considerably from those by Eder and Valenta, and recorded by the Bureau of Standards' investigators already mentioned. The order of mistake in this region is not more than $\cdot 08$ A.U.

Besides the lines already recorded in this region, I have discovered a large number of new lines which have been denoted by the letter T. I have looked for the impurity lines of Si, Pb, Ag, Tl, C, Bi, As, Sb, Sn, Zn, etc., and also for air-lines with the aid of the tables given in vols. vi. and vii. of Kayser's 'Handbuch der Spectroskopie.'

Table I. gives a list of the Bismuth arc lines with wave-numbers and classification.

TABLE I.

λ_{air} I. A.	Int.	$\nu_{\text{vac.}}$	Classification.	Remarks.
1902.16	1	52612		
1909.6	2 R	52352	Observed by Sur in absorption.
1913.75	3	52236.3		
1930.42	3 R	51785.0	T.
1953.89	8 R	51163.2	$^4S_2 - J_3$	
1959.48	8 R	51017.3	$^4S_2 - I_2$	Bloch (1959.63).
1973.08	5	50665.7	$^2D_3 - \bar{C}_2$	Bloch, 1973.15.
1976.42	1	50580.1	T.
1984.5	2 U	50374.0	T.
1989.96	5	50235.8		
2001.59	2 U	49944.0	T.
2011.39	1 u	49700.7	T.
2021.21	6 R	49459.3	$^4S_2 - H_2$	Eder, 2020.51 in vac.
2023.99	5 u	49391.3	T.
2033.91	1 U	49150.5	T.
2041.96	8	48956.8	T.
2049.69	7 R	48772.1	Eder, 2049.59 in vac.
2053.52	1 u	48681.2	T.
2057.68	5	48582.8	$^2D_3 - b_2$	T.
2061.70	10 R	48488.1	$^4S_2 - G_3$	Offermann, 2061.73.
2064.79	5	48415.5	T.
2069.70	1	48300.7	T.
2097.63	1 U	47657.6	T.
2110.31	10 R	47371.3	$^4S_2 - F_1$	Offermann, 2110.26.
2133.69	6 R	46852.3	$^2D_2 - N_2$	Offermann, 2133.62.
2134.58	6 R	46832.8	Offermann, 2134.31.
2143.66	1	46634.4	T.
2152.91	6 R	46434.0	Offermann.
2153.53	6 R	46420.7	Offermann.
2156.96	7 R	46347.0	

TABLE I. (continued).

λ_{air} I. A.	Int.	$\nu_{\text{vac.}}$	Classification.	Remarks.
2164.10	4 R	46194.1	Offermann.
2176.62	0 R	45928.4	Ruark etc. give its intensity as 6 R. But a very faint trace of this line appears on only one plate. Ruark etc., 2177.33.
2177.22	4 R	45915.7	$^4S_2 - E_1$	
2189.58	8 R	45656.6	$^2D_2 - M_3$	
2198.26	1 R	45476.3	T.
2202.86	2 RU	45381.3	T.
2203.12	4 u	45376.0	Offermann. Not present on my [plates.]
2214.11	3 R	45150.7	$^2D_2 - L_2$	
2224.24	2	44945.1	Offermann, 2224.21.
2228.23	10 R	44864.6	$^4S_2 - D_2$	
2230.64	10 RU	44816.4	$^4S_2 - C_3$	
2237.84	1 R	44672.0	T. [Tl.?).
2246.77	1 u	44494.5	T.
2249.38	5	44442.9	$^2P_1 - c_2$	T.
2276.57	10 R	43912.2	$^4S_2 - B_2$	
2281.38	6 u	43819.5	Offermann (2281.35).
2288.00	1	43692.8	T.
2289.98	1	43655.0	T.
2293.87	1 u	43582.0	T.?
2297.58	1 v	43510.6	T.
2304.94	1 v	43371.7	T.
2309.73	3 U	43381.7	Offermann, 2309.3.
2313.80	1 R	43205.6	$^4S_2 - a_3$	T.
2316.1	1 U	43162.7	T.
2317.43	1 r	43138.0	T.
2328.19	7 r	42938.6	Offermann, 2328.24.
2329.95	1	42906.2	T.
2333.79	7	42835.6	$^2D_3 - N_2$	
2337.49	1	42767.8	T.
2345.91	5 u	42614.3	T.
2347.89	0 U	42576.4	T.?
2349.10	3	42556.5	$^2D_2 - k_2$	T.
2353.61	1	42474.9	
2354.60	4 u	42457.0	O., 2354.48.
2360.09	1 U	42358.1	$^2P_1 - b_2$	T.
2368.18	1 r	42213.6	T.
2369.21	6 u	42195.2	O., 2369.17.
2379.73	5 u	42008.7	T.
2400.90	10 R	41638.4	$^2D_3 - M_3$	
2409.57	2 U	41488.5	O., 2409.62.
2430.45	3 u	41132.1	$^2D_3 - L_2$	
2433.4	3 U	41082.3	? O.
2435.81	2 U	41041.8	T.
2448.30	8 r	40832.3	$^2D_2 - d_2$	O., 2448.06.
2489.6	3 U	40155.0	O., 2489.4.

TABLE I. (continued).

λ_{air} I. A.	Int.	$\nu_{\text{vac.}}$	Classification.	Remarks.
2499.52	10	39995.6	O., 2499.30.
2515.68	9 R	39738.7	$^2D_2 - J_3$	
2524.53	9 R	39599.5	$^2D_2 - I_2$	
2532.2	5 U	39479.5	O., 2532.5.
2536.56	1 R	39411.63	T. ?, Hg.
2582.20	4	38715.1	O., 2582.15.
2594.12	1	38537.2	$^2D_3 - k_2$	O., 2594.03. My measurement is uncertain, as the line was not visible under microscope.
2600.61	0	38441.04	O. ?
2627.92	8 R	38041.6	$^2D_2 - H_3$	
2696.76	6 R	37070.5	$^2D_2 - G_3$	
2730.45	6 u	36613.2	$^2P_1 - N_2$	O., 2730.51.
2767.88	3	36118.1	T.
2780.52	8 R	35953.9	$^2D_2 - F_1$	
2798.74	6 u	35719.8	$^2D_3 - J_3$	O., 2798.70.
2803.53	4	35658.8	T. (Bi+) ?
2809.64	6 R	35581.4	$^2D_3 - I_3$	
2864.01	7 U	34905.8	$^2P_1 - L_2$	O., 2863.75. My measurement
2883.81	1 u	34666.2	O. ? [uncertain; line very diffuse.
2892.91	1 u	34557.1	O. ?
2897.99	9 R	34496.6	$^2D_2 - E_1$	
2938.32	9 R	34023.1	$^2D_3 - H_2$	
2944.28	0	33954.3	O. ?
2989.05	7 R	33445.8	$^2D_2 - D_2$	
2993.36	6 R	33397.5	$^2D_2 - C_3$	
3024.67	7 R	33052.0	$^2D_3 - G_3$	
3035.18	7 u	32937.5	$^2P_2 - c_2$	O., 3034.91.
3067.73	10 R	32587.9	$^4S_2 - ^4P_1$	
3076.69	2 R	32493.0	$^2D_2 - B_2$	
3093.58	5 u	32315.7	$^2P_1 - k_2$	T.
3144.6	5 U	31791.4	$^2D_2 - a$	T.
3216.8	1 U	31077.8	T.
3239.73	5	30887.9	$^2P_2 - b_2$	T.
3267.97	1 u	30591.2	$^2P_1 - d_1$	T.
3302.55	1.5	30270.9	T.
3361.23	1	29742.5	T.
3382.28	1	29557.4	T.
3397.29	5 R	29426.8	$^2D_3 - D_2$	O., 3397.21.
3402.80	3	29379.2	$^2D_3 - C_3$	T.
3405.63	7 u	29354.7	$^2P_1 - I_2$	O., 3405.23.
3510.96	6 u	28474.2	$^2D_3 - B_2$	O., 3510.85.
3519.18	3	28407.6	T. [Tl. ?].
3596.11	3 R	27799.9	$^2P_1 - H_3$	
3599.94	1	27770.4	T.
3619.37	2	27621.3	T.
3775.75	1	26477.34	

TABLE I. (continued).

λ_{air} I. A.	Int.	vac.	Classification.	Remarks.
3887.94	2	25713.3	$^2\bar{P}_1 - F_1$	
3888.22	2	25711.4	$^2\bar{P}_1 - F_1$	
3912.90	1	25553.2	
4116.35	1	24286.5	T.
4121.52	5	24256.1	$^2\bar{P}_1 - E_1$	
4121.84	5	24254.2	$^2\bar{P}_1 - E_1$	
4127.36	1 <i>u</i>	24221.8	Γ .
4220.83	2	23685.3	Γ .
4254.15	1	23499.9	$^4\bar{P}_1 - \xi$	$\xi = 2475$.
4260.06	1 U	23467.3	T.
4308.17	4	23205.2	$^2\bar{P}_1 - D_2$	
4308.53	4	23203.3	$^2\bar{P}_1 - D_2$	
4492.61	1	22252.6	$^2\bar{P}_1 - B_2$	
4492.97	1	22250.8	$^2\bar{P}_1 - B_2$	
4615.15	1	21661.7	} $^4S_2 - ^2P_1$	
4615.60	1	21659.6		
4692.32	1 <i>u</i>	21305.5	$^4\bar{P}_1 - \phi$	$\phi = 4670$.
4716.38	1	21197.8	T.
4722.19	10	21170.7	$^2D_2 - ^4P_1$	
4722.54	10	21169.1	$^2D_2 - ^4P_1$	
4722.83	10	21167.8	$^2D_2 - ^4P_1$	
4728.96	1	21140.4	T.
4733.78	2 <i>r</i>	21118.9		
5298.36	1 <i>u</i>	18868.5		
5552.23	7 <i>r</i>	18005.8		
5599.41	3	17854.1	$^2\bar{P}_2 - I_2$	
5718.81	2	17481.3		
5742.59	3 <i>r</i>	17408.9		
6134.86	2	16295.8	$^2\bar{P}_2 - H_2$	
6184.99	2 U	16163.7		
6364.75	1 <i>u</i>	15707.2		
6475.73	3	15438.0	} $^4S_2 - ^2D_3$	
6476.24	3	15436.8		
6991.12	4 <i>u</i>	14299.9		
7036.15	2	14208.4	$^2\bar{P}_2 - F_1$	
7335.01	1	13629.5		
7441.25	1 <i>u</i>	13434.9		
7502.33	2	13325.5		
7838.70	3	12753.7		
7840.33	2	12751.1	$^2\bar{P}_2 - E_1$	
8210.83	16	12175.7	$B_2 - \xi$	$\xi = 2475$.
8501.8	1 U	11758.99		
8544.54	2	11700.2	$^2\bar{P}_2 - D_2$	

TABLE I. (continued).

$\lambda_{\text{air I. A.}}$	Int.	$\nu_{\text{vac.}}$	Classification.	Remarks.
8579.74	1	11652.2	$\overline{P}_2 - C_3$	$\xi = 2475.$
8627.9	1 U	11587.1		
8754.88	2	11419.1	$^4S_3 - ^3D_2$	
8761.54	3	11410.4		
8907.81	2	11223.0	$D_2 - \xi$	
9058.62	1	11036.2		
9342.60	1 *	10700.7		
9657.2	300	10352.1		

$\lambda_{\text{Rowland.}}$	Int.	$\nu_{\text{vac.}}$	Classification.	Remarks.
9828.8	20	10171.4	$E_1 - \xi$	$\xi = 2475.$
10106.1	20	9892.3		
10301.7	15	9704.5		
10540.2	8	9484.9		
11073.2	15	9028.4	$D_2 - \phi$	$\phi = 4670.$
11555.5	5	8651.5		
11711.1	100	8536.6		
11994.5	13	8334.9		
12166.5	40	8217.1		
12690.5	30	7877.8		
14331.5	25	6975.7		
2254.2	7	4432.6	$H_2 - \phi$	$\phi = 4670.$

Theoretical Considerations.

Bismuth belongs to the group of five-valence elements (N, P, As, Sb), and it may be recalled that the spectra of none of these elements have been completely elucidated. Fowler * has classified the lines of O^+ , but he could not trace the fundamental levels. Millikan and Bowen † have discovered some of the fundamental levels of O^+ in the extreme ultra-violet, but the mutual relationship between the intercombination systems has not yet been completely established. A discussion of the structure of the spectrum of O^+ from the standpoint of Hund's theory has been given by R. H. Fowler and D. Hartree ‡.

* A. Fowler, P. R. S. (Lond.) A, vol. cx. p. 476 (1926).

† Millikan and Bowen, 'Nature,' Sept. 1926, p. 410.

‡ R. H. Fowler and D. Hartree, P. R. S. (Lond.) A, vol. cxi. p. 83 (1926). For nitrogen, see Kiess, Journ. Opt. Soc. Am. July 1925. For phosphorus, Saltmarsh, Phil. Mag. vol. xlvii. p. 874 (1924).

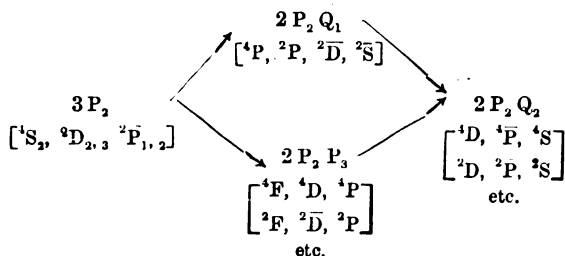
Let us begin with the electronic composition of Bismuth. It may be written as:—

2 K	8 L	18 M	32 N	
	O ₁ 2	O ₂ 6	O ₃ 10	O ₄
		P ₁ 2	P ₃ 3	P ₄
			Q ₁	Q ₂
				R ₁
				R ₂

[For detailed explanation, see a paper by Kichlu and Saha, "On the Explanation of Anomalous Terms in the Spectra of Two-Valence Elements" (Phil. Mag. July 1927).]

The letters K L M N O denote the X-ray levels, and the numbers under them represent the number of electrons in that level. Possible transitions giving rise to line spectra are indicated by arrows.

The combinations and expected terms are shown below:—



Explanation.— $3P_2$ indicates that all the 3-valence electrons are at P_2 -level. $2P_2Q_1$ indicates that one has gone over to Q_1 etc. The terms arising from any combination, as calculated according to the theory of structure of complex spectra, are shown below that combination. Attention is drawn to the fact that in the symbols $3P_2$, $2P_2Q_1$, $2P_2P_3$, etc., P indicates the particular shell in the atom numbered according to the convention, K, L, M, But $2P_{1,2}$ etc. in the brackets indicate spectral terms having P-characteristics. The confusion is regretted, but is unavoidable.

Bismuth being a heavy element will show abnormally wide separations in the values of the terms arising from the same electronic combination. I have therefore started with the theoretical spectrum of Bi^+ , of which the fundamental levels are $3P_{0,1,2}$, $1D_2$, $1S_0$. To calculate the terms of Bi,

I have taken each one of these optical levels, and brought a fresh electron to each of the outer levels, and calculated the possible orbits. This is shown in Chart I., and then the range in value of the terms is discussed below, and their identification is carried out in Table II.

CHART I.

2 P ₂ Q ₁ Combination.	<i>j</i> -value.	Landé's " <i>j</i> ".	Terms.	Identification.
(³ P ₀) ² S _{1/2}	1/2	1	⁴ P ₁	A ₁
(³ P ₁) ² S _{1/2}	1/2	1	² P ₁	E ₁
	3/2	2	⁴ P ₂	D ₂
(³ P ₂) ² S _{1/2}	3/2	2	² P ₂	H ₂
	5/2	3	⁴ P ₃	G ₃
2 P ₂ P ₃ Combination.	<i>j</i> -value.	<i>j</i> +1/2.		
(³ P ₀) ² D _{3/2, 5/2}	3/2	2	X ₂	B ₂
	5/2	3	X ₃	C ₃
(³ P ₁) ² D _{3/2, 5/2}	1/2	1		
	3/2	2	...	I ₂
	5/2	3	...	J ₃
	3/2	2		
	5/2	3		
	7/2	4		
(³ P ₂) ² D _{3/2, 5/2}	1/2	1		
	3/2	2		
	5/2	3		
	7/2	4		
	1/2	1		
	3/2	2		
	5/2	3		
	7/2	4		
	9/2	5	⁴ F ₅	

[To face page 782.

${}^2P_1.$	${}^2\overline{P}_2.$	Term value.
(10927)	-ve	25975

(a) *The Fundamental Levels.*

Five fundamental levels are expected— 4S_2 , $^2D_{2,3}$, $^2P_{1,2}$. It is natural to identify them with the levels discovered by Kayser and Runge, but several discrepancies have to be removed.

A glance at Table II. shows that the first two levels have the same combinatory powers up to the sublevel denoted by "J." The only discrepancy was in the level E. There are two close lines, $\lambda 2177.22$ and $\lambda 2176.62$, and, according to Ruark etc., it is the shorter line which is the more intense and more easily absorbed. But my measurements show that the longer line, $\lambda 2177.22$, is the more intense and is always obtained in absorption, while $\lambda 2176.62$ appears very faintly on one plate only. With this correction, E fits in well under both levels.

Beyond this level the lines which arise from combination with 2S_2 fall in the Schumann region. Bloch has given data for this region, but they do not seem to be reliable.

The third level has the j -value = 3, for it gives fewer combinations. I have specially looked for the lines ($^2D_3 - E$) and ($^2P_1 - C$), but they are definitely absent.

The close levels " 2P_1 " having the separation 1.91 have probably the same inner quantum number 1, and differ only in the "fine quantum number" introduced by Ruark*.

I have provisionally identified the fifth level $^2P_2'$ with Ruark's " β ". This is a bit doubtful.

(b) The next level arise from the combinations

$$\left. \begin{array}{l} 2 P_2 Q_1 \\ 2 P_2 P_3 \end{array} \right\}.$$

We have to identify these levels with the levels denoted by A_1 , B_1 , C_1 , etc., and a mere glance at the chart shows that there is a wide divergence in the scale of values of these terms. We are here encountering terms of the "displaced type," first discovered by Paschen in the spectrum of Neon †, and since confirmed by Grotrian ‡ and Sur §

* Ruark, Phil. Mag. vol. 1. p. 937 (1925); Sommerfeld, Three Lectures on Atomic theories, p. 12.

† Paschen, *Ann. der Physik*, vols. lx. and lxiii.

‡ Grotrian, *Zeits. für Physik*, vol. xxxix.

§ Sur, "On the Spectrum of Pb" (Phil. Mag.); Meissner, *Zeits. für Physik*, vol. xl.

in the spectrum of Pb. We shall take the discussion of this point in detail.

The fundamental terms of Bi^+ are given by the combination $^3\text{P}_2$ giving us the terms

$$^3\text{P}_0 \quad ^3\text{P}_1 \quad ^3\text{P}_2 \quad ^1\text{D}_2 \quad ^1\text{S}_0$$

similar to those of lead. In the case of lead,

$$^3\text{P}_0 - ^3\text{P}_1 = 7817,$$

$$^3\text{P}_1 - ^3\text{P}_2 = 2813.$$

In the case of Bi^+ , we assume that

$$^3\text{P}_0 - ^3\text{P}_1 = 16,000,$$

$$^3\text{P}_1 - ^3\text{P}_2 = 6,000.$$

When we form Bi by bringing another electron, either in position Q_1 or in P_3 , it is comparatively lightly coupled to the inner electrons. We can classify the new terms from $(2\text{P}_2\text{Q}_1)$, and $(2\text{P}_2\text{P}_3)$ in three groups, viz. (1) from $^3\text{P}_0$ -state, (2) from $^3\text{P}_1$ -state, (3) from $^3\text{P}_2$ -state of Bi^+ ; and we expect that these groups are approximately separated by the values $^3\text{P}_0 - ^3\text{P}_1$, $^3\text{P}_1 - ^3\text{P}_2$. These three groups are shown in the tabulated form in Chart I. (p. 782).

In calculating the resultant J-values, we have assigned the Sommerfeld " j "-values to each term. This is shown in column 2. In column 3 the conventional, or Landé j -values, are given. This is Sommerfeld's $(j + \frac{1}{2})$.

It will be seen that we get three terms from $^3\text{P}_0$ -level, viz. $^4\text{P}_1$ and X_2, X_3 . In analogy with Pb, since $^4\text{P}_1$ arises from the electron configuration $(2\text{P}_2\text{Q}_1)$, we may assign to $^4\text{P}_1$ the approximate value $\frac{N}{22}$, and to X_2, X_3 the value $\frac{N}{32}$ $(2\text{P}_2\text{P}_3)$. We have therefore no difficulty in identifying $^4\text{P}_1, \text{X}_2, \text{X}_3$ with A, B, C, respectively.

The $(^3\text{P}_1)^2\text{S}$ terms will be less than $(^3\text{P}_0)^2\text{S}$ or $^4\text{P}_1$ by about 16,000. Hence we may identify these as:—

$$\text{D} = ^4\text{P}_2, \quad \text{E} = ^2\text{P}_1.$$

The $(^3\text{P}_1)^2\text{D}$ -terms will be very small, or may even be negative.

The terms arising from $(^3\text{P}_2)^2\text{S}$ can be easily identified

with G and H. The inner quantum numbers are in perfect agreement.

These identifications leave out the term F with $j=1$, and Thorsen is therefore justified in identifying it as the higher Rydberg member of 4P_1 or A, *i. e.* as $(2 P_2 R_1)$.

In Table III. we give lines which probably form a Rydberg sequence.

TABLE III.

	4S_2 .	2D_2 .	2P_1 .	2P_2 .
X ₁	3067.73 (10 R)	4722.54 (10 R)	(10927) ?	Negative.
	32587.9	21169.1		
	2110.31 (10 R)	2780.52 (8 r)	3887.94 (2)	7036.15 (2)
	47371.3	35953.9	25713.3	14208.4
		2448.30 (8 r)	3267.97 (1 u)	(19086) ?
		40832.3	30591.2	

The lines under the heading 2D_2 are given by the Hicks's formula :—

$$\nu = 47143 - \frac{N}{\left(m + 28143 - \frac{45324}{m}\right)^2}$$

$$m = 2, 3, 4.$$

Thorsen gives $^2D_2 = 47323$. It is due to the fact that he gave the third row incorrectly. The line $\lambda 3267.97$ predicted by Thorsen appeared on my plates. The first line of the 3rd row is given by Thorsen as $\lambda 1913.5$. Dr. Sur has always got the line $\lambda 1909.6$ in absorption. I have been unable to identify the higher members predicted by Thorsen, or members arising from my formula.

The terms arising from $(^6P_0) ^2D_{3/2}$, viz. in the electron configurations $2P_2(P_3)$, $2P_2(Q_3)$, $2P_2(R_3)$... will form a regular Rydberg sequence. The lines provisionally identified are shown in Table IV.

TABLE IV.

	4S_2	2D_2	2D_3	2P_1
X_2	λ 2276.57 (10 R) 43912.2	λ 3076.69 (2 R) 32493.0	λ 3510.96 (6 u) 28474.2	(22252.6)
	λ 1959.48 (8 R) 51017.3	λ 2524.53 (9 R) 39599.5	λ 2809.64 (6 R) 35581.4	λ 3405.63 29358.2
	(53975)	λ 2349.10 (3) 42556.5	λ 2594.03 (1) 38538.2	λ 3039.58 (5 u) 32315.7

The lines under 2D_2 can be represented by the formula

$$\nu = 47314 - \frac{N}{\left(m - 0.08059 - \frac{.59766}{m}\right)^2},$$

$$m = 3, 4, 5.$$

It is seen that the limits calculated from both sets come almost to the same value.

Table V. shows the lines which form a regular Rydberg sequence with terms X_3 arising out of combination 3P_0 $^2D_{5/2}$.

TABLE V.

	4S_2	2D_2	D_3	Term value.
X_3	44816.4 λ 2230.64	33397.5 λ 2993.36	29379.2 λ 3402.80	13746
	51163.2 λ 1953.89	39738.7 λ 2515.68	35719.8 λ 2798.74	7405
	(54032)	42614 λ 2345.91	(38596)	4529

The lines under 3D_2 may easily be grouped under a Rydberg sequence. The last term is somewhat doubtful.

No regular Rydberg sequence except these three is expected. The terms arising out of 3P_1 or 3P_2 will form regular sequences if 16,000 and 6000 approximately are added to them. Hence all terms after the first will become very small or negative. Unless the spectrum is investigated in the Fluorite region, it will be difficult to identify them.

Lines occurring as the result of intercombination between the states $2P, P_3, 2P, Q_3$ and $2P, Q_1, 2P, Q_2$ have been looked for from the existing data, but only the following have been found :—

λ .	ν .	
4254.15	23499.9	A_1-2475
8210.83	12175.7	B_2-2475
8907.81	11223.0	D_2-2475
9828.8	10171.4	E_1-2475

The above was found by Ruark and others; in addition I find the one given below :—

λ .	ν .	
4692.32	21305.5	A_1-4670
11073.2	9028.4	D_2-4670
2254.2	4432.6	H_2-4670

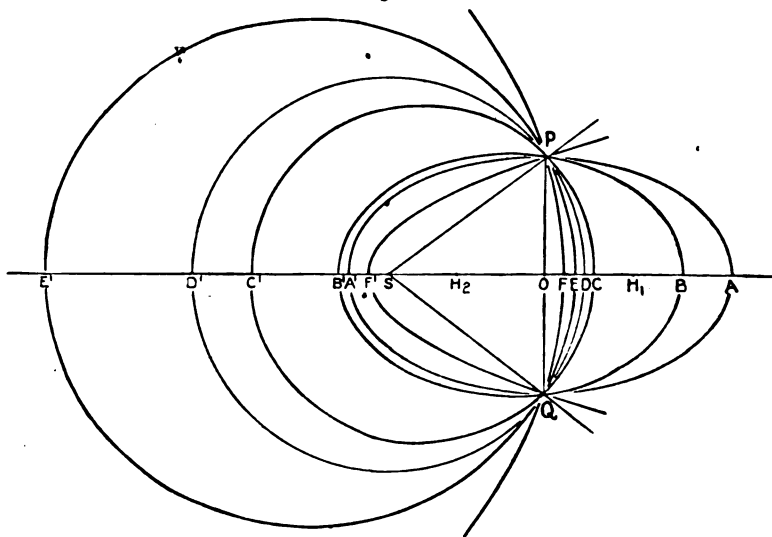
It seems that the existing data are not sufficient to establish the intercombination terms, and hence the region $\lambda 4800$ to $\lambda 8000$ is now being investigated.

In conclusion, I wish to thank Prof. M. N. Saha, under whose direction and guidance this investigation has been carried on. I am also much obliged to Dr. N. K. Sur for his supplying me with some of his unpublished data on Bismuth under-water spark and absorption spectra of Bismuth.

LXX. *On the Action in Planetary Orbits.* By W. B. MORTON, M.A., and W. W. BRUCE, M.Sc., Queen's University, Belfast *.

IN a note which appeared in this Magazine in October 1926† the variation of the action was examined arithmetically for the parabolic trajectory under constant gravity between two points at the same level. In the present note the same thing is done for the path under the law of the inverse square between points at equal distances from the centre of force. The guided paths, like the free ones, are taken to be conics with the centre of force in a focus, and the terminal velocity is kept constant, so that the principle of least action is illustrated.

Fig. 1.



There are four free paths from P to Q in presence of the centre S (fig. 1), forming two ellipses BB', CC'. These have the same length of major axis, so, if H_1H_2 are their empty foci, $PH_1 = PH_2$. The focal chords PH_1, PH_2 intersect the paths again in the segments PBQ, PC'Q, so the other segments PB'Q, PCQ are those which have minimum action.

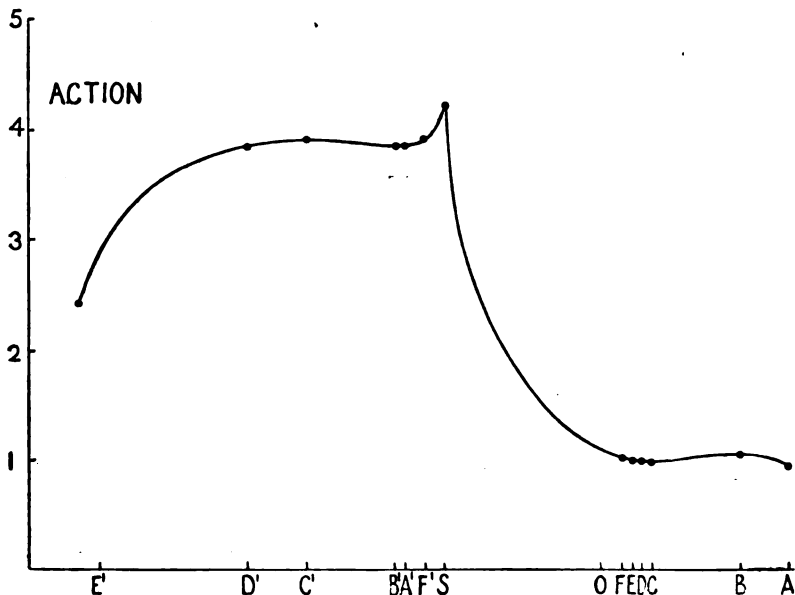
* Communicated by the Authors.

† W. B. Morton, "On the Action in Parabolic Paths under Gravity," Phil. Mag. ii. p. 800 (1926).

It will appear that, with the mode of variation here adopted, the action along the paths by B, C' has a maximum value.

It is evident that as the vertex of the guided path moves from B' to C, through a series of conics with focus at S and passing through PQ, the action must pass somewhere through a maximum, and yet there is no such path for which the variation of the action vanishes in the ordinary sense. The maximum occurs when the conic becomes the pair of lines SP, SQ, and the paradox is explained by the discontinuity in the direction at S when we pass from the line-pair to a near hyperbola. There is a corresponding discontinuity in

Fig. 2.



direction on the curve (fig. 2), in which action is plotted against the position of the vertex of the path.

The species of the conics with which we have to deal are most readily determined by reference to the two orthogonal parabolas F, F'. When the vertex of the curve lies outside the segment FF', the conic is an ellipse; when it lies within FF', a hyperbola. The line PQ is a special hyperbola with vanishing transverse axis, the other focus being the image of S in the line.

The possible elliptic guided paths are limited by the

magnitude of the velocity given to the particle at P; it cannot get further from S along any path than a definite maximum distance at which its kinetic energy is all used up in work against the attraction. There are thus two limiting ellipses (AA', EE' on fig. 1) having this distance as their maximum radius vector on either side of S.

The special case represented on fig. 1, and worked out numerically in what follows, is that in which the triangle SPH₁ is right-angled, with sides as 3 : 4 : 5. It was chosen for the sake of round numbers. It corresponds to a kinetic energy of the particle at P, which is $\frac{3}{4}$ of that which would be gained by a fall from infinity to P. The greatest distance attainable is thus $\frac{7}{4}SP = SA = SE$.

It is easy to express the action-integral in terms of the coordinate r . Let μ be the strength of the centre, $2a_0$ the major axis of the free paths, $2a, \gamma, \delta$ the major axis, greatest radius, and least radius of one of the guided elliptic paths. Then we find

$$A = \int_P^Q v ds = 2\sqrt{(\mu/a_0)} \int (2a_0 - r)^{\frac{1}{2}} (2a - r)^{\frac{1}{2}} (\gamma - r)^{-\frac{1}{2}} (\delta - r)^{-\frac{1}{2}} . dr$$

taken between P and the vertex of the ellipse.

The hyperbolic paths fall into two classes with slightly differing expressions for A:—

(1) Those for which S is on the concave side, with vertices between F and O or between S and F'. Then

$$A = 2\sqrt{(\mu/a_0)} \int (2a_0 - r)^{\frac{1}{2}} (r + 2a)^{\frac{1}{2}} (r + \gamma)^{-\frac{1}{2}} (r - \delta)^{-\frac{1}{2}} . dr.$$

(2) Those for which S is on the convex side, vertices between O and S,

$$A = 2\sqrt{(\mu/a_0)} \int (2a_0 - r)^{\frac{1}{2}} (r - 2a)^{\frac{1}{2}} (r - \gamma)^{-\frac{1}{2}} (r + \delta)^{-\frac{1}{2}} . dr.$$

There are five special cases in which the integral can be expressed by circular functions:—

(1) The limiting paths. Here $\gamma = 2a_0$,

$$\int = 2a_0 \sin^{-1} \sqrt{\{(r - \delta)/(2a - \delta)\} + (r - \delta)^{\frac{1}{2}}(2a - r)^{\frac{1}{2}}}.$$

(2) The free paths, $a = a_0$,

$$\int = 2a_0 \sin^{-1} \sqrt{\{(r - \delta)/(\gamma - \delta)\} + (\gamma - r)^{\frac{1}{2}}(r - \delta)^{\frac{1}{2}}}.$$

(3) The circular path, when $A = v \times \text{arc}$.

(4) The parabolic paths. Here $2a$ and γ become infinite with a ratio of equality and δ is the parameter,

$$\int = (2a_0 - \delta) \sin^{-1} \sqrt{\{(r - \delta)/(2a_0 - \delta)\}} + (2a_0 - r)^{\frac{1}{2}}(r - \delta)^{\frac{1}{2}}.$$

(5) The degenerate hyperbola, which consists of the two straight lines SP, SQ,

$$\int = 2a_0 \sin^{-1} \sqrt{(r/2a_0)} + r^{\frac{1}{2}}(2a_0 - r)^{\frac{1}{2}}.$$

By these formulæ we obtain values of the action for the thirteen positions of the vertex ABCDEFSF'A'B'C'D'E'. For intermediate points the action can be expressed by elliptic functions; but, as is usual in physical questions, the "integrals of the third kind" have an imaginary parameter, and calculation from the formulæ is very laborious. For our purpose it is much simpler to apply arithmetical quadrature to the original formulæ in r . This was done for twenty-two positions of the vertex of the guided path and the graph (fig. 2) plotted from the results. Afterwards, by way of verification, and as an exercise in computation, the elliptic formulæ were used for two points, one between B, C and the other between B', C', chosen so as to give an even value for the modular angle. The points so obtained were found to lie exactly on the curve.

The thirteen special points are marked on the graph, and the axis of abscissæ lettered to correspond.

The unit marked on the vertical axis is the action along the short circular arc from P to Q. It will be noticed that, as in the former case of the parabolic trajectory, the range between the minima C, B' and the maxima B, C' is very small.

The values found for the action at these points are:—

B	1.052,	B'	3.882,
C997,	C'	3.936.

An attempt was made to establish analytically the nature of the stationary values of the Action. The length γ was taken as the independent variable. It was not difficult to show that $dA/d\gamma$ vanishes for the free paths, but the expression for the second differential proved too cumbrous for handling.

LXXI. *On the Surface Tension of Rock-Salt.*By G. N. ANTONOFF, *D.Sc. (Manch.)* *.

THERE is comparatively little known about surface tension of solids, chiefly owing to the want of a suitable method of determining the same. The subject, however, presents an enormous theoretical and practical interest. In its theoretical aspect the knowledge of the surface tension is of importance, because it may throw light on internal structure of solids.

One can say that up to now very little work has been done on the subject. Moreover, up to quite recently the very notion of the surface tension of solids was so vague that one could doubt whether it had any real meaning. Thus, for example, in Chwolson's '*Traité de Physique*,' p. 612 (1906-8), it is assumed that water vapour must have condensed on the walls of the solid to account for its surface tension.

The impetus for the development of this important subject, one may say, was laid down by the work of P. Curie (*Bull. Soc. Min. de France*, viii. p. 145, 1885; also '*Œuvres*,' p. 153). His ideas were very much ahead of his time, and with his premature death they did not find any immediate following, having fallen, so to say, on unprepared ground. Very little work of importance has been done on the subject until quite recently. The literature of the subject can be found, summarized up to 1915, by P. Ehrenfest, *Ann. d. Phys.* (4) xlviii. p. 360 (1915).

And only recently an attempt was made by Max Born to estimate the surface tension of rock-salt, under the assumption that it consists of positive and negative ions held up in equilibrium by purely electrical forces.

These results are described in a paper by M. Born and O. Stern (*Sitz. Preuss. Akad. Wiss.* xlviii. p. 901, 1919). Apart from attractive forces, they assume the existence also of repulsive forces, as a result of experimental evidence regarding the compressibility of rock-salt under external pressure.

In this work it is assumed that the structure of rock-salt is such as revealed by the X-ray analysis.

The surface tension of rock-salt, calculated under the

* Communicated by the Author.

above assumption, was found to be at the absolute zero of temperature

$$150.2 \text{ erg cm.}^{-1} *.$$

Taking into consideration that at the melting-point (above 800°C.) the surface tension of the molten salt is about

$$65.5 \text{ erg cm.}^{-1},$$

the surface tension at ordinary temperature will be about

$$125 \text{ erg cm.}^{-1},$$

assuming that the surface tension is roughly a linear function of temperature.

It may appear at first sight that similar results can be attained from the breaking stress of crystals. The breaking stress of rock-salt is a fairly constant figure and is the same along the three principal axes. The estimates of surface tension from the breaking stress lead, however, to a ridiculously low figure (see my paper, *Phil. Mag.* xliv. p. 62, July 1922). It is quite natural to assume that there are some cracks always present in the crystal.

On the other side there appear to be some doubts as to the actual structure of rock-salt and other substances.

It is known that phenomena of association take place in the liquid state, which makes it probable that something similar will also apply to the solid state. Thus it was stated by Sir William H. Bragg ('*Nature*,' cxi. p. 428) that the ultimate unit of crystal structure or elementary parallelepiped is not a chemical molecule, but is a complex formed by the union of a number of molecules. Or else, the surface structure of the crystal must be different from that at the interior.

The recent work of the writer of this paper (*Phil. Mag.* March 1927) indicates that molecular association in the liquid state with the decrease of temperature proceeds in definite stages according to the law of multiple proportions, and the association factor must reach a very high value by the time the substance becomes solid.

It thus appears that it is not safe to calculate the surface tension on a basis of a theory involving the molecular structure of crystals.

For this reason I made it a point of evolving a method which would give a measure of the molecular field in a more or less direct way.

* According to my usual notations it should be dynes cm.^{-1} . See paper by Ph. A. Guye, *Journ. Chem. Phys.* 5, p. 427 (1907).

Such experiments were already described by myself in my paper (*Phil. Mag.* June 1926), where I give as a figure for surface tension of glass

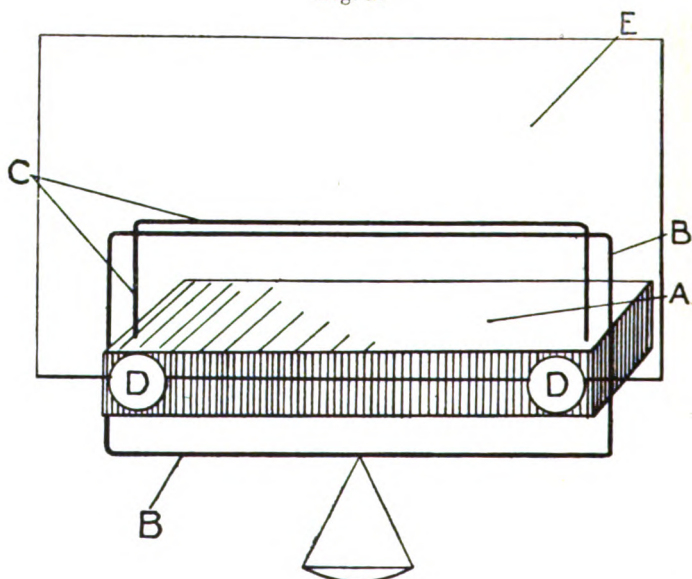
130 dynes per cm.

Now I intend to describe a modified method, which is more suited for measuring the surface tension of rock-salt, and to put forward some theoretical considerations indicating that the constants obtained by my method do actually represent the surface tension.

THE METHOD AND ITS THEORY.

The method consists in preparing suitable pastes * whose surface tensions can be measured by determining the breaking stress of their films. The apparatus used for this purpose is seen on fig. 1. A small table A bears a horizontal rod C

Fig. 1.



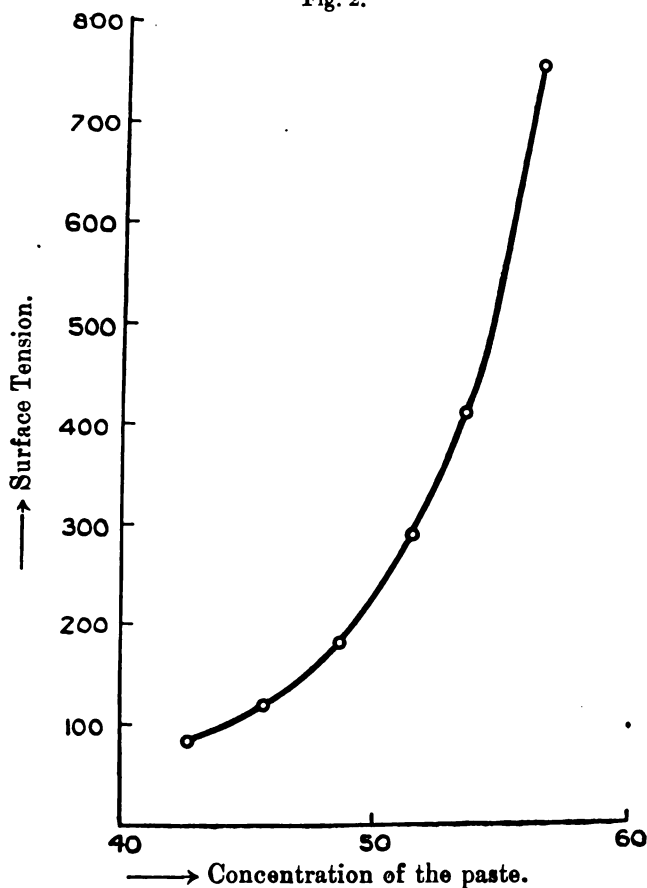
made of thin glass with two ends bent at right angles, fixed in its horizontal surface. Another glass rod B is bent into a quadrangle bearing the tray for weights. The horizontal part of C with the upper horizontal part of B are kept together by the paste used, and B falls on the table when

* *Phil. Mag.* p. 1263, June 1926.

the applied weight exceeds the breaking stress of the film. The frame B is of length exceeding that of table, so that there is no contact between them and no friction during the fall of B.

The vertical front part of the table bears two drawing pins D holding a glass E in front of the apparatus to protect it from breath, as moisture seriously affects the result.

Fig. 2.



The pastes of different concentrations have surface tensions as shown in the drawing (fig. 2).

These pastes are used for determining the surface tension of solids in the following way:—

A tube is taken of material whose surface tension is to be

measured, and the pastes of different concentration are pressed through the same.

It can be seen that the more dilute pastes passing through the tube leave a thin film on the walls of the solid—they wet its surface.

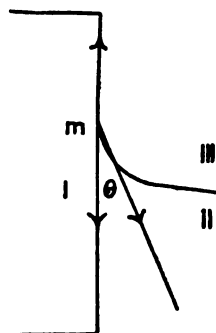
However, as soon as the surface tension of the paste used reaches a certain value, the paste ceases to wet the wall and leaves the tube without adhering to its surface.

The same constant appears in experiments where pastes are made of different constituents.

It appears highly probable that unless other factors intervene, such as solubility or chemical actions, these facts must be connected with surface tension of the solid in some way or another.

This can be made clear in the following way (see fig. 3).

Fig. 3.



In this figure the Medium I represents the solid (glass, rock-salt, etc.), the Medium II the paste, and the Medium III can be disregarded altogether, as representing the air or vacuum.

The notations used are as follows :—

α_1 —the surface tension of the solid (against vacuum or air).

α_{12} —the tension at the interface solid-paste.

α_2 —the surface tension of the paste (against vacuum or air).

According to the elementary theory the following equation must hold true when three media are in contact with one another (see Chwolson, 'Traité de Physique,' p. 612, 1906-8):

$$\cos \theta = \frac{\alpha_{1,3} - \alpha_{1,2}}{\alpha_{2,3}}.$$

Considering that the Medium III can be left out of consideration in this problem, the same expression in our notations will be :

$$\alpha_2 \cos \theta = \alpha_1 - \alpha_{12}.$$

In the experiments described in this paper the angle θ has always increasing values until it reaches 90° at the transition point to be located by these experiments. At this point $\cos \theta$ becomes $=0$, and consequently

$$\alpha_1 = \alpha_{12}.$$

The actual meaning of these experiments is as follows :—

When the interfacial tension is greater than that of the paste, i. e.

$$\alpha_{12} > \alpha_2,$$

the paste adheres to the wall of the solid.

When on the contrary

$$\alpha_{12} < \alpha_2,$$

the paste ceases to wet the solid.

At the transition point

$$\alpha_{12} = \alpha_2,$$

but we have also seen that at the transition point, when $\cos \theta = 90^\circ$,

$$\alpha_1 = \alpha_{12}.$$

It therefore follows that in these conditions the *surface tension of the paste is equal to that of the solid.*

$$\alpha_2 = \alpha_1.$$

It thus appears that the constant obtained by these experiments in this sense is nothing else but the surface tension of the solid itself.

Now it remains to define the actual conditions under which such experiments must be performed.

In my previous paper I did not make any mention of the diameter of the tube to be used.

I found from experience that the tube of the solid must not be too wide.

I take a crystal of rock-salt and bore a hole in it in the direction of one of its principal axes. As rock-salt belongs to the regular system, it does not matter which direction is chosen for the experiment. The hole can be easily made using an ordinary lathe with water as lubricator. Then a glass tube is taken nearly of the same diameter as the

cylindrical hole, and is joined to the rock-salt by means of a sealing mixture (see fig. 4).

The other end of the glass tube adjoined is drawn into a narrow capillary *. The latter is necessary to create suitable resistance to the flow of the paste under influence of external

Fig. 4.



pressure. All these experiments are difficult because it is not easy to prescribe the exact conditions. If the capillary is too narrow, the resistance may be too big, so as to prevent the passage of the paste almost completely. If it is too broad, the experiment becomes impossible, because the passage takes place instantaneously. The right conditions

* This is not shown on the drawing.

can only be found empirically. I may add that the resistance can be sometimes increased by introducing a bubble of air (or several bubbles) into the tube. When the paste with a bubble of air descends in the tube the bubble will appear translucent or transparent, according to whether the paste wets the wall or otherwise.

A much more important point is, what diameter to choose for the tube of the solid.

If this diameter is too big, the experimental device shown in fig. 4 will not work at all.

The external pressure will not extrude the paste from the tube, but the air will rush through the same, leaving a very narrow channel in the middle of the tube.

I found by experience that diameters of the order of magnitude of $\cdot 1$ of an inch suit the experiment very well. In the experiments with glass I have varied the diameter within certain limits, and in all cases I did not find that the constant obtained was thereby affected. However, I avoided very narrow tubes in which special conditions may arise which may affect appreciably the experiment.

Using the pastes, as described in my previous paper, in the device shown in fig. 4, I found for rock-salt as the average of several determinations the value

315 dynes per cm.

It must be borne in mind that in this region the curve (fig. 2) is very steep, and therefore small changes of concentration produce an appreciable change in the surface tension of the paste.

DISCUSSION OF RESULTS.

(1) The method described is not universal. It is limited to certain ranges of values of surface tension, and it is applicable provided there is no dissolving or chemical action of any kind.

It is applicable to most of the crystalline salts, such as rock-salt etc.

(2) The result obtained does not depend on cracks in the crystal, and is a measure of the molecular field exercised by the solid.

✂ If there are any doubts concerning the molecular structure of the solid, the results obtained are thereby not affected at all.

(3) The figures obtained by the method described repeat themselves invariably. No changes of any kind, due to the

time of contact between the paste and the solid, were noticed in the course of these observations.

(4) The theoretical considerations hereinbefore described indicate that the figures obtained do actually represent the surface tension of the solid.

(5) The figure obtained for rock-salt differs considerably from that calculated by Born, which is to be expected from the point of view of the theory laid down in the number of papers *, indicating that molecules must be highly associated in the solid state.

6 Featherstone Buildings,
High Holborn,
London, W.C. 1.

LXXII. *A Theory of the Torque Converter.*

By E. K. SANDEMAN, *Ph.D.* (London), *B.Sc.*, *A.C.G.I.*†

ALTHOUGH descriptions of the Constantinesco Torque Converter have appeared at different times, and at least one detailed description of its mode of operation has been published, no exact theory has ever appeared showing how the design constants are affected by the engine performance and the variations of load. It is the purpose of this paper to show exactly how these quantities are related. The complexity of the problem, considered from an ordinary dynamic standpoint, is considerably reduced by the application of a simple method of electrical analogy.

Any physically realizable mechanical linkwork, consisting, as it must, of elements possessing mass and rigidity, may often be usefully represented by an equivalent electrical network containing inductance and capacity, for which calculations relating to energy transmission give results valid for the mechanical linkwork. *A priori*, there is no advantage in so doing, but it happens that electrical theory relating to wave-propagation has outstripped mechanics, and it is convenient to make use of the shortened processes available.

Consideration of three elementary examples will suffice to make the general principle clear. In fig. 1 are shown three mechanical arrangements and their equivalent electrical circuits. At A, on the left is represented a cam rotated uniformly by any suitable means, and actuating a tappet

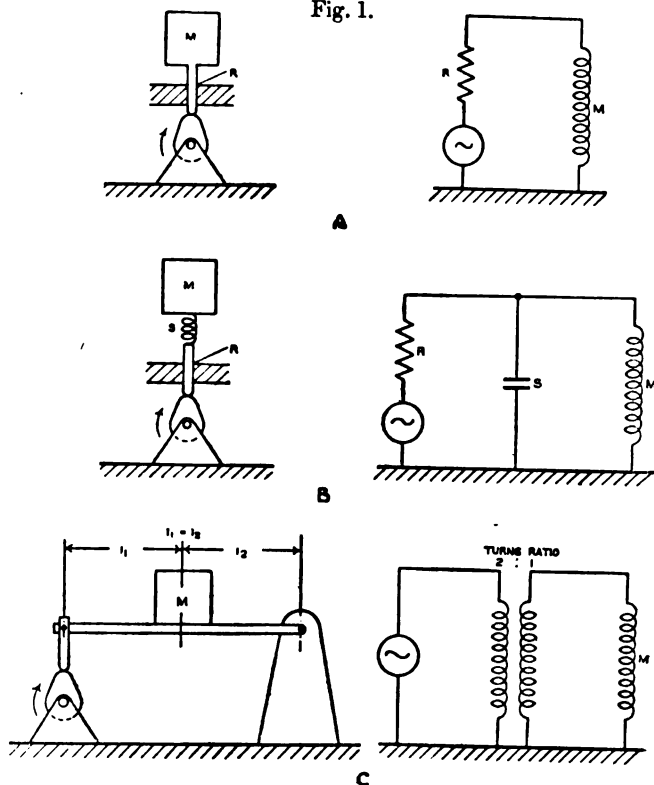
* G. N. Antonoff, *Phil. Mag.* March 1927.

† Communicated by the Author.

sliding between guides, assumed rigidly connected to the same base or earth as the bearing of the cam-shaft.

The top of the tappet is rigidly connected to a mass M . The rotating cam, in association with the lower end of the tappet, becomes a vibration generator, and, provided that the speed of the cam is never great enough to cause the downward acceleration of the tappet to approach that due

Fig. 1.



to gravity, then the form of the cam specifies the "wave-form" of the generator. The equivalent electrical circuit is shown on the right and requires no explanation. It should be noticed that, whereas mechanically the mass is connected only to the vibration generator, electrically it is connected also to earth. It is not easy to generalize, but there are many times when a mechanical earth connexion, or short circuit, corresponds to an electrical open circuit, and when a mechanical free or open circuit corresponds to an electrical short circuit.

At B is a more complex arrangement in which mechanically a spring is inserted in series between the tappet and the mass. Electrically this becomes a shunt element, since the pressure at the top of the tappet has the alternative of compressing the spring and so charging it with potential energy, or else of accelerating the mass and so giving it kinetic energy. Electrically, when two alternative paths are provided for the flow of energy, they are said to be in parallel.

At C is a vibration generator driving a mass by means of a lever, the mass being situated half-way between the fulcrum and the vibration generator. The lever is here a velocity transformer and also a force transformer in the inverse sense. As viewed from the generator, it reduces the impedance of the mass in the ratio of the square of the pressure ratio.

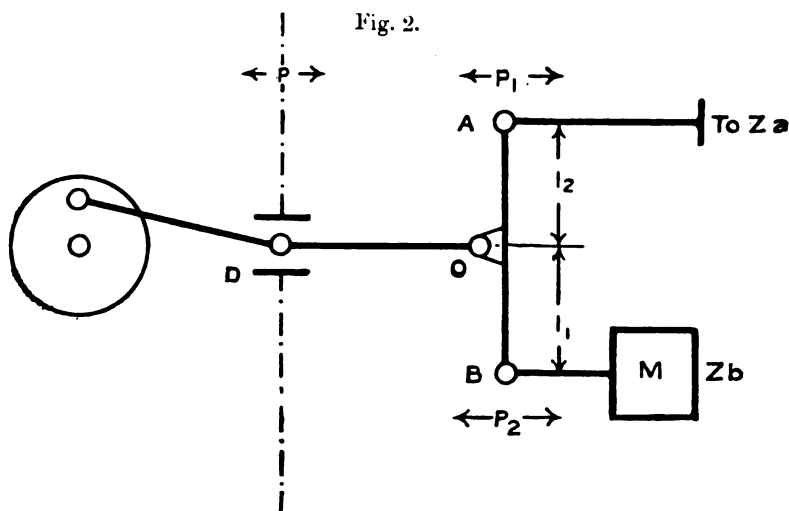
The most important analogous quantities with which we are concerned in mechanics and electrodynamics are tabulated below, together with the units in which the mechanical quantities are expressed. Three sets of units are here given: the C.G.S. system normally employed, the equivalent Foot Pound Second system, and a system which lends itself rather more readily to practice and which employs the pound instead of the poundal as a unit of force. This is used in this paper for obvious reasons.

Electrical.	Mechanical.	C.G.S. Units.	F.P.S. Units.	Practical Units.
Electromotive Force.	Vibromotive Force.	Dynes.	Poundals.	Pounds.
Quantity.	Displacement.	Centimetres.	Feet.	Feet.
Current.	Velocity.	Centimetres per second.	Feet per second.	Feet per second.
Resistance or Impedance.	Resistance or Impedance.	Dynes per centimetre per second.	Poundals per foot per second.	Pounds per foot per second.
Inductance.	Inertia.	Grams.	Pounds.	$\frac{1}{g}$ pounds.
Capacity.	Compliance = $\frac{1}{\text{Elasticity}}$.	Centimetres per dyne.	Feet per poundal.	Feet per pound.
$\frac{1}{\text{Capacity}}$.	Elasticity or Stiffness.	Dynes per centimetre.	Poundals per foot.	Pounds per foot.

With these preliminaries the case of the Torque Converter may be considered.

Ideal Theory of the Torque Converter.

The essential construction of this gear is indicated in fig. 2; a driving-point D has a reciprocating motion imparted to it by means of a crank associated with a fly-wheel rotating approximately uniformly. By means of a



connecting-rod DO this motion is communicated to any point along the length of a lever AB, the end A of which drives a ratchet supplying energy to the load. The other end B is rigidly fastened to a mass M.

Let P = the R.M.S. force applied to the driving-point in pounds (initially this force may be assumed to be sinusoidal),

p_a = the resultant R.M.S. force at A in pounds,

p_b = " " " " B " " "

\dot{x} = the velocity of D in feet per second,

\dot{x}_a = " " " A " " " "

\dot{x}_b = " " " B " " " "

Z = the driving-point impedance in pounds per foot per second,

Z_a = the load impedance in pounds per foot per second,

Z_b = the impedance of the mass M in pounds per foot per second,

$O_A = l_2, \quad O_B = l_1.$

As a simplification it will be assumed that the lever has no mass and that the load impedance Z_a is a pure resistance. (It will appear later that the equations developed are valid for the case where—owing to the action of the ratchet and the discrepancy between harmonic motion and motion of constant velocity—the load impedance is not a pure mechanical impedance.)

Then

$$p_a = \frac{l_1}{l_1 + l_2} P; \quad p_b = \frac{l_2}{l_1 + l_2} P,$$

$$\dot{x}_a = \frac{p_a}{Z_a}; \quad \dot{x}_b = \frac{p_b}{Z_b}.$$

$$\begin{aligned} \therefore \dot{x}_a &= \frac{l_1}{l_1 + l_2} \dot{x}_a + \frac{l_2}{l_1 + l_2} \dot{x}_b \\ &= \frac{l_1}{l_1 + l_2} \cdot \frac{p_a}{Z_a} + \frac{l_2}{l_1 + l_2} \cdot \frac{p_b}{Z_b} \\ &= \left(\frac{l_1}{l_1 + l_2} \right)^2 \frac{P}{Z_a} + \left(\frac{l_2}{l_1 + l_2} \right)^2 \frac{P}{Z_b}. \\ \therefore Z &= \frac{P}{\dot{x}} = \frac{1}{\left(\frac{l_1}{l_1 + l_2} \right)^2 \frac{1}{Z_a} + \left(\frac{l_2}{l_1 + l_2} \right)^2 \frac{1}{Z_b}}. \quad (1) \end{aligned}$$

The above holds for the case where O divides AB internally; it may be shown that, if O divides AB externally, then

$$Z = \frac{1}{\left(\frac{l_1}{l_1 - l_2} \right)^2 \frac{1}{Z_a} + \left(\frac{l_1}{l_1 - l_2} \right)^2 \frac{1}{Z_b}} \quad (1a)$$

If $l_1 = l_2$, then

$$Z = \frac{1}{\frac{1}{4Z_a} + \frac{1}{4Z_b}} \quad (2)$$

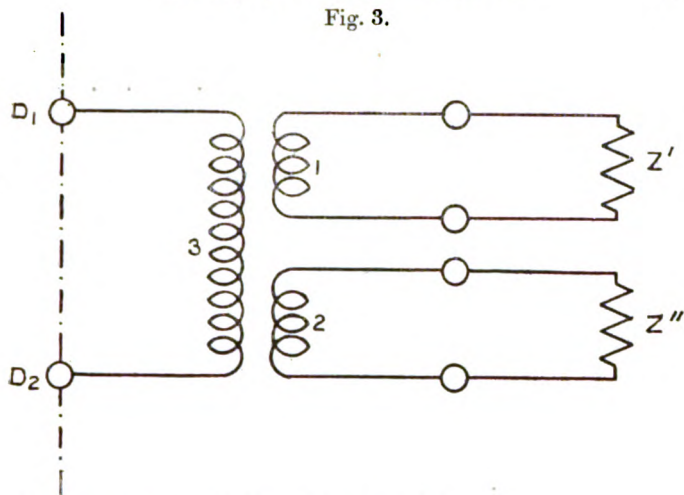
As a check it may be noticed that, if $Z_a = Z_b = X$, then

$$Z = \frac{1}{\frac{1}{4X} + \frac{1}{4X}} = 2X. \quad (3)$$

Electrical Analogy.

Consider an ideal transformer, having three windings, 1, 2, and 3, operating into loads Z' and Z'' , as shown in fig. 3.

Fig. 3.



Let the turns ratio from 3 to 1 be T_1
 and " " " " 3 " 2 " T_2 ,
 and let $T_1 + T_2 = 1$,

V = the R.M.S. voltage applied across the driving-points $D_1 D_2$,

v_1 = the voltage across Z' ,

v_2 = " " " Z'' ,

i = the current in winding 3,

i_1 = " " " " 1,

i_2 = " " " " 2,

Z''' = the impedance across the driving-points $D_1 D_2$.

$$\text{Then } v_1 = \frac{T_1}{T_1 + T_2} \cdot V ; \quad v_2 = \frac{T_2}{T_1 + T_2} V,$$

$$i_1 = \frac{v_1}{Z'} ; \quad i_2 = \frac{v_2}{Z''},$$

$$i = \frac{T_1}{T_1 + T_2} i_1 + \frac{T_2}{T_1 + T_2} i_2$$

$$= \frac{T_1}{T_1 + T_2} \cdot \frac{v_1}{Z'} + \frac{T_2}{T_1 + T_2} \cdot \frac{v_2}{Z''}$$

$$= \left(\frac{T_1}{T_1 + T_2} \right)^2 \frac{V}{Z'} + \left(\frac{T_2}{T_1 + T_2} \right)^2 \frac{V}{Z''},$$

$$Z''' = \frac{V}{i} = \frac{1}{\left(\frac{T_1}{T_1 + T_2} \right)^2 \cdot \frac{1}{Z'} + \left(\frac{T_2}{T_1 + T_2} \right)^2 \frac{1}{Z''}}, \dots (4)$$

which is identically the same form as equation (1).

As a simplification it will be assumed that the lever has no mass and that the load impedance Z_a is a pure resistance. (It will appear later that the equations developed are valid for the case where—owing to the action of the ratchet and the discrepancy between harmonic motion and motion of constant velocity—the load impedance is not a pure mechanical impedance.)

Then

$$\begin{aligned}
 p_a &= \frac{l_1}{l_1 + l_2} P; & p_b &= \frac{l_2}{l_1 + l_2} P, \\
 \dot{x}_a &= \frac{p_a}{Z_a}; & \dot{x}_b &= \frac{p_b}{Z_b}. \\
 \therefore \dot{x}_a &= \frac{l_1}{l_1 + l_2} \dot{x}_a + \frac{l_2}{l_1 + l_2} \dot{x}_b \\
 &= \frac{l_1}{l_1 + l_2} \cdot \frac{p_a}{Z_a} + \frac{l_2}{l_1 + l_2} \cdot \frac{p_b}{Z_b} \\
 &= \left(\frac{l_1}{l_1 + l_2} \right)^2 \frac{P}{Z_a} + \left(\frac{l_2}{l_1 + l_2} \right)^2 \frac{P}{Z_b}. \\
 \therefore Z &= \frac{P}{\dot{x}} = \frac{1}{\left(\frac{l_1}{l_1 + l_2} \right)^2 \frac{1}{Z_a} + \left(\frac{l_2}{l_1 + l_2} \right)^2 \frac{1}{Z_b}}. \quad (1)
 \end{aligned}$$

The above holds for the case where O divides AB internally; it may be shown that, if O divides AB externally, then

$$Z = \frac{1}{\left(\frac{l_1}{l_1 - l_2} \right)^2 \frac{1}{Z_a} + \left(\frac{l_1}{l_1 - l_2} \right)^2 \frac{1}{Z_b}} \quad (1a)$$

If $l_1 = l_2$, then

$$Z = \frac{1}{\frac{1}{4Z_a} + \frac{1}{4Z_b}} \quad (2)$$

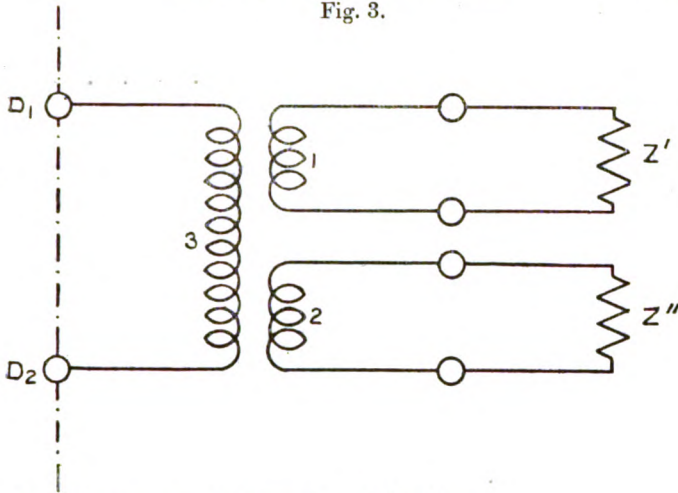
As a check it may be noticed that, if $Z_a = Z_b = X$, then

$$Z = \frac{1}{\frac{1}{4X} + \frac{1}{4X}} = 2X. \quad (3)$$

Electrical Analogy.

Consider an ideal transformer, having three windings, 1, 2, and 3, operating into loads Z' and Z'' , as shown in fig. 3.

Fig. 3.



Let the turns ratio from 3 to 1 be T_1
 and " " " " 3 " 2 " T_2 ,
 and let $T_1 + T_2 = 1$,

V = the R.M.S. voltage applied across the driving-points $D_1 D_2$,

v_1 = the voltage across Z' ,

v_2 = " " " Z'' ,

i = the current in winding 3,

i_1 = " " " " 1,

i_2 = " " " " 2,

Z''' = the impedance across the driving-points $D_1 D_2$.

Then
$$v_1 = \frac{T_1}{T_1 + T_2} \cdot V ; \quad v_2 = \frac{T_2}{T_1 + T_2} V,$$

$$i_1 = \frac{v_1}{Z'} ; \quad i_2 = \frac{v_2}{Z''},$$

$$i = \frac{T_1}{T_1 + T_2} i_1 + \frac{T_2}{T_1 + T_2} i_2$$

$$= \frac{T_1}{T_1 + T_2} \cdot \frac{v_1}{Z'} + \frac{T_2}{T_1 + T_2} \cdot \frac{v_2}{Z''}$$

$$= \left(\frac{T_1}{T_1 + T_2} \right)^2 \frac{V}{Z'} + \left(\frac{T_2}{T_1 + T_2} \right)^2 \frac{V}{Z''},$$

$$Z''' = \frac{V}{i} = \frac{1}{\left(\frac{T_1}{T_1 + T_2} \right)^2 \cdot \frac{1}{Z'} + \left(\frac{T_2}{T_1 + T_2} \right)^2 \cdot \frac{1}{Z''}} \dots \dots (4)$$

which is identically the same form as equation (1).

If $T_1 = T_2$, then (4) simplifies to

$$Z''' = \frac{1}{\frac{1}{4Z'} + \frac{1}{4Z''}} \quad \dots \dots \dots (5)$$

Compare equations (2) and (5) with the well-known relation for impedances in parallel :

$$\frac{1}{R} = \frac{1}{r_1} + \frac{1}{r_2},$$

or

$$R = \frac{1}{\frac{1}{r_1} + \frac{1}{r_2}},$$

Fundamental Principle.

It is therefore apparent that, considering the simplest case, where the driving-point is connected to the middle point of the lever, the first effect of the Constantinesco gear is to multiply the impedance of the load by 4 and to shunt it with an impedance due to the mass which by electrical analogy

$$= \frac{4M\omega}{g} \text{ pounds per foot per second, where}$$

M = the mass in pounds,

g = the acceleration of gravity,

$\omega = 2\pi f$, where f = the frequency of reciprocation in cycles per second.

A secondary effect of equal or greater importance, enabling abnormally large starting torques to be obtained, and due to the combined action of the flywheel and the shunt mass, is discussed later.

Velocity Ratio.

The velocity ratio due to the Constantinesco gear is that between the point D and the point A, and is the square root of the resistance ratio between these points. (See Appendix A.)

$$\text{Velocity Ratio} = \sqrt{\frac{\text{Real part of } Z_1}{\text{Real part of } Z}}.$$

The Load Impedance—First Approximation.

The value of Z_1 depends on the load into which the output of the engine operates, and on any gear ratio which occurs

between A and the load. Imagine, for simplicity, that the gear ratio between A and the output is unity, and let

W = the output power of the engine in horse-power,

550 W = the output power of the engine in foot pounds per second.

Then $Z_1 \dot{x}_1^2 = 550 W$ (since Z_1 is hypothetically a pure resistance).

$$\therefore Z_1 = \frac{550 W}{\dot{x}_1^2} \text{ pounds per foot per second.} \quad (6)$$

(In Appendix B it is shown that if the speed is defined in radians per second angular velocity, then the impedance (resistance) is expressed in pounds feet per radian per second.)

The value of Z is then defined by equation (1). Throughout this discussion the case of an engine driving a road-car is considered, since it is convenient for demonstration purposes, but, provided the load impedance is suitably defined, the explanation holds for any type of load.

Principles of Design.

As is evident from consideration of the conditions at starting, summarized later, the torque converter enables an engine, which only develops appreciable power at high engine speeds, to develop very large torques when operating into large loads. It is evident that in general the smaller the mass the larger will be the engine speed for a given throttle setting, but it is not easy to see what are the determining factors which influence design.

These factors may best be explained by means of two diagrams which will be called the Engine Resistance Diagram (fig. 4) and the Load Resistance Diagram (fig. 5).

The Engine Resistance Diagram.

In Appendix B it is shown that if

W = the power transmitted along a shaft in horse-power,

f = the speed of the shaft in revolutions per second,

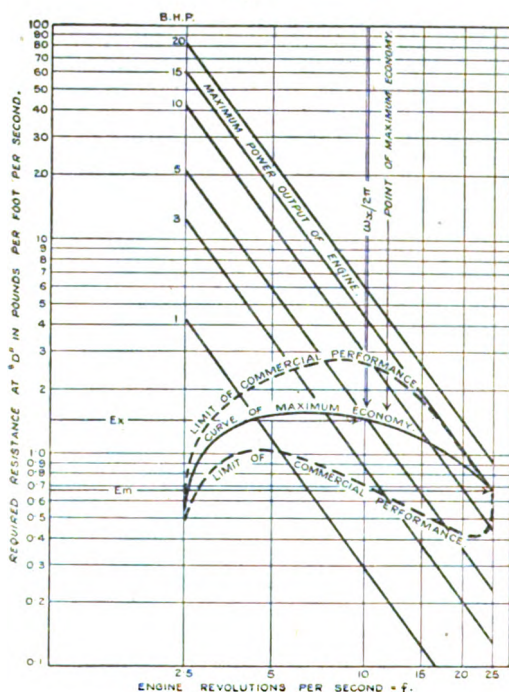
R = the resistance looking into the shaft in pounds feet per radian per second,

$$\text{then} \quad R = \frac{550 W}{4\pi^2 f^2} \quad (8)$$

For any fixed power delivered by any engine there are therefore a series of single values of engine speed corresponding to each value of resistance into which the engine

works. On fig. 4 are shown a series of straight lines relating R and f for different values of horse-power. (It is possible to portray these relations by straight lines since logarithmic scales are employed for both R and f .) Although shown for a limited range of powers, these are perfectly general and have no special reference to any one type of engine. They will be referred to as power lines.

Fig. 4.



For any engine there is an optimum speed at which it is capable of delivering a given power, so that for any one engine there is one point on each of the power lines of the engine diagram corresponding to the optimum load. It may be imagined either that this is the most economical speed, or that it is the most efficient speed. The most economical speed may be defined, for a given horse-power, as that speed at which the running cost per hour is a minimum, while the most efficient speed may be defined, for a given horse-power,

as the speed at which the given power is delivered with minimum petrol consumption. The economy basis appears to be of greatest general importance, although there may be cases where the efficiency basis is the most important.

On fig. 4 are plotted a series of hypothetical points, imagined to represent the performance of an individual engine, corresponding to the speeds at which each power (marked on the power line on which the plotted point lies) is supplied with maximum economy. These points are joined together by a heavy line marked "Curve of Maximum Economy." On each side of this line, and running in the same general direction, are two dotted lines representing the locus of the points on each power curve at which the performance of the engine becomes uncommercial. The distance apart of these lines, measured along the power lines and projected on to the axis of engine speed, then becomes a measure of the flexibility of the engine. The area contained between them evidently contains every condition under which it is desirable the engine should operate. The curve of Maximum Economy then gives the relations between the engine speed and the optimum resistance into which the engine should operate. One point on this curve corresponds to the most economical speed and power of the engine.

The Load-Resistance Diagram.

If R is the load resistance in pounds per foot per second as derived in Appendix D, then W being the power in horse-power and \dot{x} the velocity in feet per second, from Appendix B,

$$W = \frac{R \dot{x}^2}{550}.$$

$$\therefore R = \frac{550 W}{\dot{x}^2}. \quad . \quad . \quad . \quad . \quad . \quad (9)$$

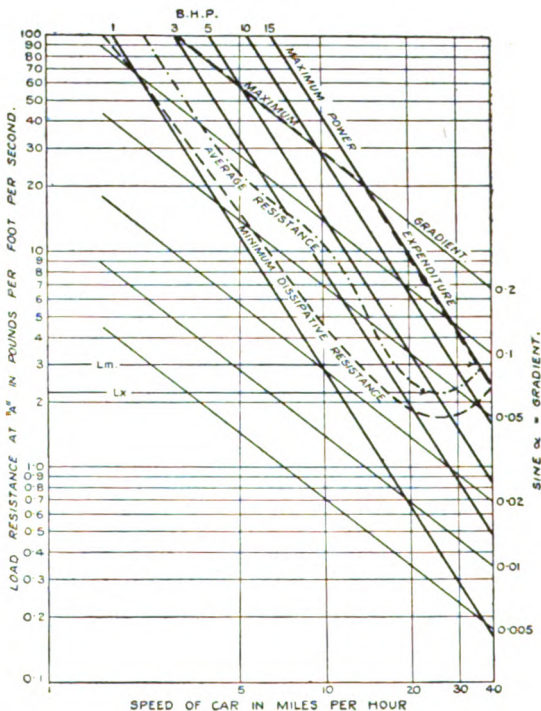
Assuming ρ of Appendix D to be unity for simplicity (*i. e.*, assuming the peripheral velocity of the ratchet = the velocity of the car with regard to the ground-surface) for any fixed value of power delivered to the load, there are a series of single values of resistance at the ratchet-driven rotor. On fig. 5 the heavy lines relate R and \dot{x} for different values of horse-power. These power lines are also perfectly general and have no reference to individual characteristics of apparatus or circumstances.

In Appendix D it is shown that for a given gradient making an angle α with the horizontal the resistance

$$R = \frac{M_c \sin \alpha}{\dot{x}}, \quad (10)$$

where M_c is the weight of the car in pounds—that is, R is inversely proportional to the velocity. On fig. 5 the series of light ruled lines relate R and \dot{x} for different values of gradient for the case of a car weighing 2000 lb.

Fig. 5.



The above lines take no account of the opposing forces brought into play by the passage of the car through air and dissipative losses due to bad road surfaces. The dotted line on fig. 5 marked "Minimum Resistance" may be imagined to determine the speed at which a particular car weighing 2000 lb. is impelled along the level by the expenditure of a given horse-power. It may be regarded either as a curve

between horse-power and speed or between dissipative resistance and speed, and it is the latter which is of immediate interest. By adding the ordinates of the minimum resistance curve to the ordinate of each gradient curve, a new set of gradient curves would be obtained, which would show for each gradient the true relation between horse-power and speed, or resistance and speed. This has not been done here as it constitutes an added complication and is not essential to the explanation. It may be noted that to the eye the position of the maximum gradient curve, representing the steepest gradient to be experienced, would be moved very little by the addition of the minimum resistance curve. It is apparent that the performance of the engine is bounded at the top of the diagram by the "Maximum Gradient" curve and the "Maximum Power Expenditure" curve, and at the bottom of the diagram by the "Minimum Resistance" curve. A curve may now be imagined to be drawn across this area, which passes through the points on each power line corresponding to the speeds at which each power is most frequently used. Such a line has been drawn and has been labelled "Average Resistance."

It is evident that an ideal gear inserted between the load and the engine would make any resistance, appearing within the area of performance on fig. 5, appear as a resistance, facing the engine, corresponding to the intersection of the curve of Maximum Economy on fig. 4 and the common power line, *e. g.* Any resistance on fig. 5 lying on the power line 5 B.H.P. would appear at the point D as a resistance of 1.45, corresponding to the intersection of the curve of Maximum Economy and the power line 5 B.H.P. on fig. 4. This not being possible, it is evidently desirable that every resistance lying within the area of performance on fig. 5 should appear within the area of performance on fig. 4 plotted on the common power line, and should fall as near to the curve of Maximum Economy as possible. Since the Torque Converter contains only two variables, the lever ratio $\left(\frac{l_1}{l_1 + l_2}\right)$ and the mass M , it is evident that the gear can only be arranged to make two points on the area of performance of fig. 5 lie exactly on the curve of Maximum Economy of fig. 4 when seen through the gear.

It is evidently desirable to exercise considerable care in choosing these two points. It is not desired to follow up all the lines of argument which radiate from this centre, and therefore it will be assumed that the two points on each diagram have been chosen.

On the load diagram has been chosen firstly the point at which the maximum horse-power developed, imagined to be 15 B.H.P., is most frequently used, where the 15 B.H.P. power line cuts the Average Resistance curve. The corresponding resistance is L_m .

The second point is that at which the average B.H.P. (5 B.H.P.) is most frequently used. The corresponding resistance is L_x .

On the engine diagram has been chosen firstly the point at which 15 B.H.P. is delivered with maximum economy; the corresponding resistance is E_m and the corresponding engine speed is ω_m .

The second point is that at which 5 B.H.P. is delivered with maximum economy; the corresponding resistance is E_x and the corresponding engine speed is ω_x .

L_m is to be matched to E_m , and L_x to E_x . The value of the shunt mass and O , the point of connexion along AB (fig. 2) can now be determined directly from L_m , E_m , L_x , E_x , ω_m , and ω_x .

When the load resistance at A (fig. 2) is L_m , the impedance facing the engine at D (or O) must be E_m .

Hence, from equations (1) and (1 a)

$$E_m = \frac{1}{\left(\frac{l_1}{l_1 \pm l_2}\right)^2 \frac{1}{L_m} + \left(\frac{l_2}{l_1 \pm l_2}\right)^2 \frac{g}{jM\omega_m}} \quad \dots (11)$$

Similarly,

$$E_x = \frac{1}{\left(\frac{l_1}{l_1 \pm l_2}\right)^2 L_m + \left(\frac{l_2}{l_1 \pm l_2}\right)^2 \frac{g}{jM\omega_m}} \quad \dots (12)$$

Rationalizing equations (11) and (12) and equating reals (the unimals may be neglected in the final count, as these are neutralized in effect by the flywheel), the following equations are obtained:—

$$E_m = \frac{\frac{1}{L_m} \left(\frac{l_1}{l_1 \pm l_2}\right)^2}{\frac{1}{L_m^2} \left(\frac{l_1}{l_1 \pm l_2}\right)^4 + \frac{g^2}{M^2 \omega_m^2} \left(\frac{l_2}{l_1 \pm l_2}\right)^4}, \quad \dots (13)$$

$$E_x = \frac{\frac{1}{L_x^2} \left(\frac{l_1}{l_1 \pm l_2}\right)^2}{\frac{1}{L_x^2} \left(\frac{l_1}{l_1 \pm l_2}\right)^4 + \frac{g^2}{M^2 \omega_x^2} \left(\frac{l_2}{l_1 \pm l_2}\right)^4} \quad \dots (14)$$

The plus signs are derived if equation (1) is used, and the minus signs if equation (1 a) is used.

It should be noted that if AB (fig. 2) is divided internally by O, then

$$\frac{l_2}{l_1+l_2} = 1 - \frac{l_1}{l_1+l_2} \quad \dots \quad (15)$$

If AB is divided externally by O, then

$$\frac{l_2}{l_1-l_2} = \frac{l_1}{l_1-l_2} - 1 \quad \dots \quad (16)$$

There are thus only two unknowns in equations (13) and (14); that is, M and $\left(\frac{l_1}{l_1-l_2}\right)$. It is evident that the value of l_1+l_2 may be fixed from mechanical considerations other than those with which the above equations are concerned.

The simultaneous solution of equations (13) and (14) gives the value of M and the value of $\frac{l_1}{l_1+l_2}$; that is, the value of $\frac{OB}{AB}$ and $\frac{OA}{AB}$.

If the solution to these equations gives an impossible value for M, or one which makes the departures from ideal relationships at slow speeds intolerable, then exact resistance matching at the point first chosen must be abandoned and other more suitable points chosen. Alternatively there may be substituted for M a mechanical network whose reactance frequency curve differs from that of a pure mass.

Having chosen suitable values of M and $\frac{OB}{OA}$, the performance area of fig. 5, as seen through the gear, may be plotted on fig. 4, and this area should lie within the performance area of fig. 4. This can be done by using equation (13), where L_m and ω_m are considered to refer to any point on the periphery of the area of performance on fig. 5, and E_m is the resulting impedance presented towards the engine.

Conditions at Starting.

Constantinesco, in a recent paper before the Royal Society of Arts, has explained what occurs at starting; but for completeness this operation phase is recapitulated. Initially, the car being at rest, the engine is caused to start rotating, and, like the impedance of an air-gap in the electrical case, the impedance of the load is initially infinite, and remains so until the car moves continuously forward. This happens when the forces on the ratchet are sufficient to overcome the back forces brought into play by the binding together of

mutually rotating parts and the unevenness of the road. All the velocity is therefore initially delivered to the shunt mass, and all the power developed by the engine goes into the flywheel. The shunt mass periodically removes a certain fraction of the energy in the flywheel from it during one quarter cycle, and returns it during the next. As the flywheel accelerates under the influence of the continuously supplied power, the velocity of the shunt mass increases and the exchange of energy between the flywheel and the shunt mass becomes greater, and hence the forces brought into play to effect this exchange become greater. The ratchet becomes the fulcrum for the lever which serves as a link between the shunt mass and the flywheel for the mutual energy exchange, so that the reactive forces increase at a rate nearly directly proportional to the engine torque and inversely proportional to the inertia of the flywheel. This rate of increase is very rapid, since the engine flywheel need be little heavier than in a normal car, and it is a matter of common experience how quickly the engine speeds up when the accelerator is depressed on no load.

As soon as the forces on the ratchet reach a value sufficiently large to overcome the reaction forces experienced at zero speed, the car moves forward and continues to accelerate until a condition of equilibrium is reached represented by resistance matching. Assuming the car has been designed on the principles outlined above, the engine will not be running at its most economical speed unless the throttle is set at a definite position corresponding to the value of load resistance experienced. This, of course, depends on the gradient, the road surface, and the friction in the bearings of the car. It is a simple matter to have an indicator on the car to show whether the throttle is in advance or in retard of the most economical position. The chief value of such an indicator would no doubt be to educate the driver to the feel of the car when running under the optimum conditions.

The Load Impedance—Second Approximation.

The relations discussed above are plainly valid for the case where the load resistance connected to the ratchet is a pure resistance.

It is not easy to represent this in terms of ratchet motion, and no attempt will be made to do so.

The practical case appears quite different, since during part of its travel the ratchet is not in contact with the ratchet-driven rotor, and a further complication is introduced

because the rotor moves with practically constant velocity during the time of contact ; this constancy of velocity is due to the large inertia associated with the ratchet-driven rotor, afforded by the mass of the car which is in series with the ratchet-driven rotor. Contact is maintained during a relatively large part of each half cycle, owing to the "give" or compliance (reciprocal elasticity) in the contact. This compliance is in shunt to the rotor resistance, since the v.m.f. in the ratchet may either turn the rotor or charge the compliance with displacement.

Provided the resultant resistance is suitably defined, the relations developed above are also valid for the practical case.

In the practical case the load resistance is defined as the relation between the mean power over a half cycle, and the square of the R.M.S. pressure over a half cycle of the reciprocating motion.

Since the ratchet is double-acting, it may be regarded as a normal impedance containing a number of sources of vibromotive force of frequencies which are multiples of that of the impressed vibromotive force and which form a Fourier series. This is subject to the rider that these v.m.f.'s may be assumed to cause "circulating velocities" which pass mainly through the shunt compliance and the shunt mass and finally cause periodic fluctuations of the engine speed of very small magnitude. No power is dissipated by these circulating velocities. The power necessary to drive these multiple-frequency velocities through the load is derived from the modification of the time-velocity curve of the ratchet (from sinusoidal form), and since they are rectified the power is all usefully expended.

Since the ultimate effect of these multiple frequencies is only a small fluctuation in the speed of the motor (at multiple frequencies), the only velocity of importance at the ratchet is that in phase with the impressed v.m.f., so that the load impedance of interest is a pure resistance.

The power supplied to the ratchet per half period of time T is

$$W = \frac{2}{T} \int_0^{T/2} p_A \dot{x}_A dt, \quad (17)$$

where p_A and \dot{x}_A are the instantaneous values of the pressure and velocity at A (fig. 2).

If p_1 is the R.M.S. force at A , and R_A is the unshunted resistance at A , i. e. in the absence of a shunt compliance,

$$R_A = \frac{p_1^2}{W}.$$

mutually rotating parts and the unevenness of the road. All the velocity is therefore initially delivered to the shunt mass, and all the power developed by the engine goes into the flywheel. The shunt mass periodically removes a certain fraction of the energy in the flywheel from it during one quarter cycle, and returns it during the next. As the flywheel accelerates under the influence of the continuously supplied power, the velocity of the shunt mass increases and the exchange of energy between the flywheel and the shunt mass becomes greater, and hence the forces brought into play to effect this exchange become greater. The ratchet becomes the fulcrum for the lever which serves as a link between the shunt mass and the flywheel for the mutual energy exchange, so that the reactive forces increase at a rate nearly directly proportional to the engine torque and inversely proportional to the inertia of the flywheel. This rate of increase is very rapid, since the engine flywheel need be little heavier than in a normal car, and it is a matter of common experience how quickly the engine speeds up when the accelerator is depressed on no load.

As soon as the forces on the ratchet reach a value sufficiently large to overcome the reaction forces experienced at zero speed, the car moves forward and continues to accelerate until a condition of equilibrium is reached represented by resistance matching. Assuming the car has been designed on the principles outlined above, the engine will not be running at its most economical speed unless the throttle is set at a definite position corresponding to the value of load resistance experienced. This, of course, depends on the gradient, the road surface, and the friction in the bearings of the car. It is a simple matter to have an indicator on the car to show whether the throttle is in advance or in retard of the most economical position. The chief value of such an indicator would no doubt be to educate the driver to the feel of the car when running under the optimum conditions.

The Load Impedance—Second Approximation.

The relations discussed above are plainly valid for the case where the load resistance connected to the ratchet is a pure resistance.

It is not easy to represent this in terms of ratchet motion, and no attempt will be made to do so.

The practical case appears quite different, since during part of its travel the ratchet is not in contact with the ratchet-driven rotor, and a further complication is introduced

because the rotor moves with practically constant velocity during the time of contact ; this constancy of velocity is due to the large inertia associated with the ratchet-driven rotor, afforded by the mass of the car which is in series with the ratchet-driven rotor. Contact is maintained during a relatively large part of each half cycle, owing to the "give" or compliance (reciprocal elasticity) in the contact. This compliance is in shunt to the rotor resistance, since the v.m.f. in the ratchet may either turn the rotor or charge the compliance with displacement.

Provided the resultant resistance is suitably defined, the relations developed above are also valid for the practical case.

In the practical case the load resistance is defined as the relation between the mean power over a half cycle, and the square of the R.M.S. pressure over a half cycle of the reciprocating motion.

Since the ratchet is double-acting, it may be regarded as a normal impedance containing a number of sources of vibromotive force of frequencies which are multiples of that of the impressed vibromotive force and which form a Fourier series. This is subject to the rider that these v.m.f.'s may be assumed to cause "circulating velocities" which pass mainly through the shunt compliance and the shunt mass and finally cause periodic fluctuations of the engine speed of very small magnitude. No power is dissipated by these circulating velocities. The power necessary to drive these multiple-frequency velocities through the load is derived from the modification of the time-velocity curve of the ratchet (from sinusoidal form), and since they are rectified the power is all usefully expended.

Since the ultimate effect of these multiple frequencies is only a small fluctuation in the speed of the motor (at multiple frequencies), the only velocity of importance at the ratchet is that in phase with the impressed v.m.f., so that the load impedance of interest is a pure resistance.

The power supplied to the ratchet per half period of time T is

$$W = \frac{2}{T} \int_0^{T/2} p_A \dot{x}_A dt, \quad \dots \quad (17)$$

where p_A and \dot{x}_A are the instantaneous values of the pressure and velocity at A (fig. 2).

If p_1 is the R.M.S. force at A , and R_A is the unshunted resistance at A , i. e. in the absence of a shunt compliance,

$$R_A = \frac{p_1^2}{W}.$$

This is equivalent to saying that R_A is equal to the direct load resistance at the ratchet-driven rotor. This can be seen to be true, since the system is very closely related to an electrical system consisting of a two-pole (commutator) D.C. generator delivering current to a resistance through a very large inductance. The value of effective resistance is unaltered, either by the wave-form or the presence of the series inductance.

The presence of a shunt reactive element, however, does affect the effective resistance. If C is the shunt compliance in feet per pound, then

$$Z_a = \frac{R_A}{R_A + \frac{1}{jC\omega}} \quad \dots \quad (18)$$

This follows directly from the electrical impedance of a resistance shunted by a condenser. By inserting the value of Z_a so obtained in equation (1) and taking the real part of Z , the resistance into which the engine must operate may be obtained. As explained before, the reactive component of Z may be neglected.

Conclusion.

It has not been attempted to lay down complete principles relating to the basis of design, since these are entirely dependent upon load requirements and the individual characteristics of particular types of prime mover. It is, however, considered that the entire field has been surveyed in sufficient detail to enable the factors affecting design to be weighed and mutually assessed in value, so that a basis for design immediately follows. When this has been established, it is only necessary to apply the ideal theory to arrive at design dimensions.

The author would like to express his very great appreciation of the sympathy given to him, and the suggestions made to him by Mr. R. Appleyard and Mr. A. D. Bloomlein in connexion with the preparation of this paper, to the former of whom its appearance is entirely due. The system of units employed is similar to that used by Mr. A. E. Kennelly and Mr. H. C. Harrison, to the latter of whom the author is indebted for the idea of shunt and series mechanical elements.

APPENDIX A.

Proof that the velocity ratio between two points in a transmission link-work is equal to the square root of the ratio of the real parts of the impedances at those points, in the absence of dissipation.

Let $Z_1 = A \angle \phi$ be the impedance at one point,

$Z_2 = B \angle \psi$ be the impedance at the other point,

\dot{x}_1 and \dot{x}_2 being the velocities into Z_1 and Z_2 respectively.

Then, since there is no dissipation, the power passing each point is the same.

$$\therefore \dot{x}_1^2 A \cos \phi = \dot{x}_2^2 B \cos \psi.$$

$$\begin{aligned} \therefore \frac{\dot{x}_1}{\dot{x}_2} &= \sqrt{\frac{B \cos \psi}{A \cos \phi}} \\ &= \sqrt{\frac{\text{Real part of } Z_2}{\text{Real part of } Z_1}}. \end{aligned}$$

APPENDIX B.

Power Transmission by Shafts.

Let τ = the torque on the shaft in pounds feet,

ω = the angular velocity in radians per second,

\dot{x} = the peripheral velocity of a cylinder in the shaft of unit radius, in feet per second,

p = the force in pounds required to produce a torque τ when acting at unit radius.

Then $\dot{x} = \omega$ and $p = \tau$, and the power transmitted = $p\dot{x} = \tau\omega$ foot pounds per second.

The resistance

$$R = \frac{p}{\dot{x}} = \frac{\tau}{\omega} \text{ pounds feet per radian per second.}$$

The above may be expressed in words:—

Since the torque of a force applied at unit radius is numerically equal to the force, and the peripheral velocity of a shaft of unit radius is numerically equal to its angular velocity, the impedance of the (mechanical) circuit in pounds feet per radian per second is numerically equal to its impedance at unit radius in pounds per foot per second.

Phil. Mag. S. 7. Vol. 4. No. 23. Oct. 1927.

3 G

The power transmitted in horse-power :

$$W = \frac{px}{550} = \frac{\tau\omega}{550} = \frac{R\dot{x}^2}{550} = \frac{R\omega^2}{550}.$$

$$\therefore R = \frac{550 W}{\omega^2} = \frac{550 W}{4\pi^2 f^2} \text{ pounds feet per radian per second,}$$

where f is the speed of rotation in revolutions per second.

APPENDIX C.

Resistance Relations each side of a Crank converting Continuous Rotation into Reciprocating Motion.

The crank is assumed to be of radius r , and the crank-rod to be infinitely long.

ω = the speed of rotation in radians per second = $2\pi \cdot$

f = the frequency of reciprocation,

$\omega r \sin \omega t$ = the instantaneous velocity of the reciprocating end of the connecting-rod,

$\frac{\omega r}{\sqrt{2}}$ = the R.M.S. velocity of reciprocation,

R_D = the resistance on the continuous rotation side in pounds feet per radian per second,

R_R = the impedance on the reciprocating side in pounds per foot per second.

The power on the continuous rotation side = the power on the reciprocating side.

$$\therefore \omega^2 R_D = \frac{\omega^2 r^2}{2} R_R.$$

$$\therefore R_D = \frac{r^2}{2} R_R.$$

APPENDIX D.

Mechanical Resistance of a Mass on a Gradient.

Consider a mass of M pounds on an inclined plane, making an angle α with the horizontal, travelling along the plane under the impetus of a force P at a velocity \dot{x} . Let R be the apparent resistance in the absence of friction.

Then $P = M \sin \alpha$.

The power supplied to the mass

$$= R\dot{x}^2 = P\dot{x}.$$

$$\therefore R = \frac{P}{\dot{x}} = \frac{M}{\dot{x}} \sin \alpha.$$

If the relative peripheral velocities of the active surface of the ratchet-driven rotor, and the road wheels of a car, assumed to take the place of the mass M above is ρ (greater than unity) where the velocity of the road-wheel periphery is the greater, then the resistance looking into the ratchet-driven rotor

$$= \frac{R}{\rho^2}.$$

APPENDIX E.

Effect of Change of Load on Engine Speed.

Under any given running conditions, when the load resistance is increased, for instance, by increase of gradient, the engine will sometimes definitely accelerate and sometimes decelerate without the position of the throttle being altered. This is equivalent to saying that increase of load resistance sometimes produces a decrease in the resistance presented towards the engine, and sometimes an increase.

Referring to equation (13), the resistance presented towards the engine,

$$E_m = \frac{\frac{1}{L_m} \left(\frac{l_1}{l_1 \pm l_2} \right)^2}{\frac{1}{L_m^2} \left(\frac{l_1}{l_1 \pm l_2} \right)^4 + \frac{g^2}{M^2 \omega_m^2} \left(\frac{l_2}{l_1 \pm l_2} \right)^4},$$

where E_m and L_m are now taken to represent respectively general values of resistance presented towards the engine and of load resistance, and ω_m is the corresponding engine speed.

$$\text{Putting } \left(\frac{l_1}{l_1 \pm l_2} \right)^2 = A \quad \text{and} \quad \left(\frac{l_2}{l_1 \pm l_2} \right)^2 = B,$$

$$E_m = \frac{A L_m \times \frac{M^2 \omega_m^2}{g}}{\frac{A^2 M^2 \omega_m^2}{g} + B^2 L_m^2}.$$

$$\text{When } L_m = 0, \quad E_m = 0;$$

$$\text{and when } L_m = \infty, \quad E_m = 0.$$

Differentiating for a maximum, it may be shown that E_m is a maximum when

$$L_m = \frac{A}{B} \cdot \frac{M \omega_m}{g}.$$

Hence, if L_m is less than this value, and increases in value, the resistance will increase and the engine will slow down. If L_m is greater than this value, and increases, the engine will speed up.

LXXIII. *The Viscosity Factor in Emulsification.*
 By R. CHRISTIE SMITH, *Carnegie Teaching Fellow.*

THE idea that liquids have a surface viscosity differing from that of the interior can be traced back to the writings of Descartes and Rumford. To Plateau ('*Statique des Liquides*,' vol. ii.), however, is due the development of the idea. He differentiates between two viscosities of a liquid—an internal viscosity determined in the usual manner by a capillary tube, and a superficial viscosity, on the measurement of which very little quantitative work has been done. Plateau measured the superficial viscosity by means of a magnetic needle floating on the surface of the liquid and taking the relative times for it to swing through a certain arc. He showed that liquids and solutions could be divided into three classes. In the first the superficial viscosity was double the internal, *e. g.* water and most aqueous solutions; in the second the superficial viscosity was a fraction of the internal viscosity, *e. g.* alcohol, turpentine, ether; and in the third the superficial was many times greater than the internal, *e. g.* albumen solutions. Further contributions were made to the subject by G. Luvini (*Phil. Mag.* 1870, xl. p. 190), Tomlinson (*Phil. Trans.* 1871, clxi. p. 51), Marangoni (*Nuovo Cimento*, 1871–72, v.–vi. p. 260, and subsequent papers).

Oberbeck (*Ann. der Physik*, 1880, xi. p. 634) applied the method of the vibrating rod to the measurement of the superficial viscosity, confirming the results of Plateau. His results were further confirmed by Stables and Wilson (*Phil. Mag.* 1883, xv. p. 406), working with the apparatus described by Grotian (*Ann. der Physik*, 1876, clvii. p. 237). In 1890, Lord Rayleigh directed his attention to the subject, and set out to find, if possible, the superficial viscosity of a clean surface. His paper (*Proc. Roy. Soc.* 1890, xlviii. p. 127) contains a description of the method adopted to obtain a clean surface, and he found that as the surface was successively cleaned the superficial viscosity fell in value till equal with the internal, as measured by the time of swing of a needle.

Ramsden (*Proc. Roy. Soc.* 1923, lxxii. p. 156), working from another standpoint altogether, showed that, quite apart from evaporation, solid or highly viscous coatings are formed more or less rapidly on the free surfaces of all proteid

* Communicated by the Author.

solutions, and that similar coatings of viscous matter are formed at the interface of every pair of liquids examined which, without being of high viscosity, are capable of forming persistent emulsions. He gave a long list of substances which gave intense superficial viscosity, but to date no experimental details have been published.

Hillyer (J. A. C. S. 1903, xxv. p. 513) investigated the interdependence of surface tension, viscosity, and emulsifiability. He came to the conclusion that, while in the case of thick liquids, *e. g.* gum solutions of pharmacists, extreme viscosity was a large factor, it did not, as a rule, mean increased emulsifiability.

Clark and Mann (J. Biol. Chem. 1922, lii. p. 157) made an extensive study of emulsifiability, and came to the conclusion that viscosity was not the predominating factor. Clayton ('Theory of Emulsions and Emulsification,' 1923, p. 41) says: "The conclusion that viscosity aids emulsification solely by virtue of the hindrance offered to coalescence of the dispersed globules, and is not the cause of emulsification, has been accepted by the majority of investigators in this field."

While Plateau has been extensively quoted throughout in publications on emulsions, his differentiation between viscosity and superficial viscosity does not appear to have been sufficiently appreciated. While the viscosity as measured by Plateau is that at the air/liquid interface, that of interest in connexion with emulsions is at a liquid/liquid interface, and is therefore appropriately termed the "interfacial viscosity." It therefore appeared that it would be of interest to investigate the relationship between emulsifiability and interfacial viscosity. This has now been done for a variety of substances. In all cases recorded here there are three substances present, *viz.* disperse phase, dispersion medium, and emulsifying agent. It should perhaps be emphasized at this point that Plateau's third class were all solutions which gave great adsorption at the surface layer, whereas in the cases described by the author the film was not adsorbed out from the solution, but is introduced mechanically from the outside. It allows in this manner the interfacial viscosity of films formed by insoluble substances to be determined.

It had been noted by the author that with kaolin as emulsifying agent and water along with pure benzene, benzol, and liquid paraffin, different emulsifiabilities were obtained. The emulsions obtained with benzol and liquid paraffin were comparable (Table I.), but that with pure benzene was considerably poorer.

Table I.

Disperse phase.	Interfacial tension.	Dispersion factor.	Interfacial viscosity.
Pure benzene	33·6	1·13	0·0034
Benzol	22·6	1·39	0·024
Liquid paraffin	44·6	1·34	0·020

Kaolin present in each case.

From the point of view of interfacial tension, it would have been expected that liquid paraffin would have given the poorest emulsion and benzol the best. So a further factor had to be investigated. It will be seen from the table that benzol and liquid paraffin give comparable interfacial viscosities. The interfacial viscosity was measured by the method of Stables and Wilson (*loc. cit.*). In the preliminary experiments a brass disk was used, and subsequently both nickel and glass disks were used without any appreciable difference in results. These disks were suspended so that the interface of the liquids being investigated was half-way up the side. In all the tables given, the interfacial viscosity is simply the logarithmic decrement observed.

It must be noted that the interfacial viscosity here measured must be considerably greater than that detected by Plateau. For instance, in some preliminary experiments using a brass disk the following values were obtained:—

	Log. dec.
Water just level with bottom of disk	0·015
do. more than half-way up	0·018
do. just above top of disk	0·021
Disk completely immersed.....	0·032

It will be seen that in this case the viscosity is that due to the surface friction of the disk, and naturally doubled when completely immersed. When a 0·2 solution of saponin was substituted for water the following results were obtained:—

	Log. dec.
Solution just level with foot	0·30
Almost immersed	0·29
Completely immersed	0·0059

N.B.—These figures are not comparable with those obtained for water above, as the moment of inertia had to be considerably increased to obtain a reading at all.

It is therefore evident that when the disk is swinging in the surface a very appreciable viscosity is manifest. It is not, therefore, in the case of liquids which would be classed under Plateau's first group but those under the third group which will give a viscosity measurable by this method and favourable to emulsification.

The results obtained are set out in Table II. Paraffin and xylene give the best correspondence. Powders which do not form emulsions have been found to give a very slight increase in viscosity. Most of the powders chosen have been selected from the lists given by Hofmann (*Z. phys. chem.* 1913, lxxiii. p. 385) and Reinders (*Z. koll. chem.* 1913, xiii. p. 235) as being those which tended to collect at the interface. It is to be noted, however, that some of the best emulsions have been formed by kaolin which is stated to be preferentially wet by water. In one or two cases solids were found which gave evidence of emulsifying but showed no appreciable interfacial viscosity. Copper sulphide and lead carbonate were outstanding examples of this. On the other hand, aluminium hydroxide and lead chloride gave a high interfacial viscosity but comparatively small emulsification.

The term "emulsifiability" is used throughout this paper as embracing two definite ideas. The first is the ease with which the disperse phase is dispersed, and the second is the stability of the resulting dispersion. A good emulsifying agent must possess both these properties; hence emulsifiability must include both these factors. How they have been combined into one numerical factor is explained under "Experimental."

EXPERIMENTAL.

The apparatus used was very similar to that described by Grotian (*loc. cit.*). A wire about 1.25 m. long supported the cradle C and the disk D. The suspension had two swivels A and B at right angles to each other, and rigid as regards rotatory movements so as to ensure that the disk can hang horizontal. In the cradle C iron rods of different weight may be placed in order to alter the moment of inertia of the system. The moment of inertia of the system was determined by the usual method and found to be 535.2 cgs. units. In some of the preliminary experiments a small disk of 2.8 cm. diameter was used, and also a cylinder 2.8 cm. in diameter and 2.0 cm. in length. For most of the determinations, however, a disk of nickel 7 cm. in diameter and 2 mm. thick was used. The cradle C carried a dumb-bell weighing

TABLE II.

Agent.	Benzene.		Toluene.		Xylene.		Liquid Paraffin.		Petroleum Ether.		Carbon Tetrachloride.	
	D.F.	I.V.	D.F.	I.V.	D.F.	I.V.	D.F.	I.V.	D.F.	I.V.	D.F.	I.V.
Kaolin.....	1.13	.032	1.11	.038	1.30	.10	1.34	.20	1.38	.22	1.14	.0052
Aluminium hydroxide ...	1.00	.019	1.00	.012	1.00	.019	1.00	.06	1.00	.036	1.00	.015
Magnesium hydroxide ...	1.11	.0052	1.20	.0077	1.25	.13	1.33	.096	1.37	.0083	1.03	.010
Fullers' earth.....	1.07	.0036	1.10	No film.	1.17	No film.	1.05	.029	1.34	.0043	1.06	.0017
Kieselguhr.....	1.11	.0044	1.06	.0015	1.18	.006	1.00	.054	1.00	.0049	1.11	.0024
Silica.....	1.00	.0054	1.00	.0010	1.00	.0011	1.00	.010	1.15	.0067	1.00	.0033
Barium sulphate	1.05	.0013	1.00	No film.	1.00	No film.	1.14	.025	1.12	.0013	1.03	.0071
Magnesium oxide	1.00	No film.	1.00	No film.	1.00	No film.	1.05	.006	1.00	No film.	1.04	No film.
Lead chromate	1.15	.024	1.24	.062	1.31	.13	1.26	.022	1.09	.04	—	—
Zinc sulphide	1.03	.0016	1.07	.0014	1.13	.010	1.06	.011	1.06	.0018	—	—
Copper sulphide.....	1.21	.002	1.15	.0024	1.31	.004	1.41	.017	1.13	.0023	—	—
Barium carbonate	1.12	.007	1.09	.013	1.10	.04	1.00	.110	1.09	.013	—	—
Zinc oxide	1.52	.45	1.42	.50	1.52	.25	1.69	.92	1.49	.40	—	—
Zinc carbonate	1.13	.0045	1.11	.002	1.11	.003	1.30	.019	1.12	.004	—	—
Lead chloride.....	1.00	.005	1.00	.003	1.00	.003	1.00	No film.	1.00	No film.	—	—
Lead carbonate	1.14	.50	1.14	.85	1.24	.70	1.34	.34	1.21	.50	—	—

D.F. = Dispersion factor.

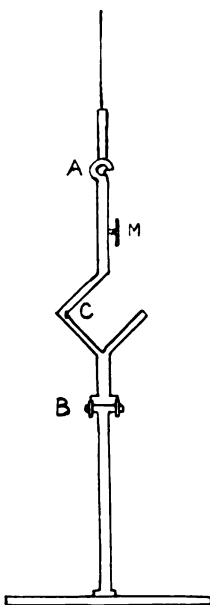
I.V. = Interfacial viscosity = Logarithmic decrement.

I.V. for Water/Benzene = .0010.

I.V. for Water/Liquid paraffin = .0053.

1489 gm. and with a moment of inertia of 52,278 cgs. units. The period of the system was 13.9 sec. A small mirror mounted at M reflected the light from a lamp on to a scale at a distance of about 2 m. The disk was suspended in an oblong photographic dish to prevent rotation of the interfacial film along the disk, as tends to happen with a circular dish. The whole apparatus was enclosed in a box open only at one side in order to exclude draughts.

Fig. 1.



In order to make a determination, water was poured into the photographic dish until the level of its surface was half-way up the suspended disk. Benzene (or other liquid) was then poured in to cover the disk completely. The emulsifying agent (1 gm.) was then carefully sprinkled over the whole surface by means of a piece of muslin. The powder had been previously passed through a sieve of 120 mesh. The solid fell through the benzene and formed a film at the interface. It was found that by leaving the film for 20 to 30 minutes more consistent (and in some cases higher) readings were obtained. No improvement in emulsification could, however, be obtained by allowing the powder to remain at the interface before emulsifying. The results were usually reproducible within 10 per cent. and in many cases 5 per cent., even with different experimenters. Readings were

obtained by setting the disk oscillating horizontally by means of a magnet acting on the iron rod in the cradle. The logarithmic decrement was observed as the magnitude of the swing fell from approximately 24° to 12° . In some cases it was impossible to obtain satisfactory readings by means of the large disk (7 cm.) owing to magnitude of the logarithmic decrement, and it was found necessary to make observations with a smaller disk (2 cm.). The smaller disk gave readings approximately one-tenth of the large disk. All the readings given in Table II. have been corrected to the basis of the large disk.

The test emulsions were made by means of the apparatus described fully elsewhere (*Rev. Gen. Coll.* 1927, v. p. 412). Briefly, a cylindrical tube with a hole in it, fitted to a shaft, has soldered to its lower end a disk of brass to which on the under side are attached vanes covered with copper gauze. On rotating, liquid is drawn through the hole in the shaft and thrown out through the gauze. The whole fits in a boiling-tube and emulsifies conveniently a volume of 40 c.c. Equal quantities (20 c.c.) of water and "oil" were placed along with 0.64 gm. solid (=2 per cent.) in the boiling-tube and emulsified for two minutes with the machine rotating 2000 times per minute. The resulting emulsion was then transferred to a flat-bottomed test-tube and allowed to stand for an hour. If unity represents the volume of the "oil" before emulsification, the "emulsifiability" is taken as the total volume of undispersed "oil" and emulsion after emulsification. This will be greater than 1 and less than 2. The numerical value is seen also to depend on two factors—viz. the amount of the oil dispersed, and the dispersity of the emulsion, and will vary directly with them. It therefore gives a simple numerical method of comparing emulsions. For fuller discussion see paper above mentioned.

Summary.

1. Attention is drawn to the fact that Plateau investigated the phenomenon of surface viscosity.
2. Many experimenters have referred to Plateau's work, but have considered chiefly the viscosity of the dispersion medium.
3. The viscosity of the interfacial film, especially that produced when a solid is introduced into the interface, has now been investigated.
4. It is shown that solids giving good emulsifiability give, as a rule, high interfacial tensions.

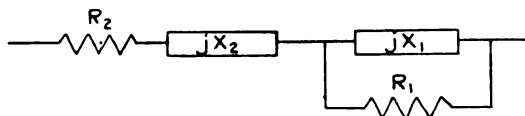
Physical Chemistry Department,
University of Glasgow.

LXXIV. *The Design of Networks for Balancing Telephone Lines.* By L. C. POCOCK, M.Sc.*

THE development of telephone repeaters has brought into prominence a circuit design problem that rarely presented itself before—the problem of building a two-terminal network to have a given impedance frequency characteristic. There are several ways of determining the network, but comparatively little has been published on the subject ; it is the object of this article to describe a quick and easy way of designing a simple network used in a very large number of cases.

The type of network under consideration (fig. 1) is that

Fig. 1.



in which two resistances are in series, and one of them is shunted by a reactance ; in addition a reactance may be required either in series with the line or with the network. The impedance of such a network may be represented by

$$Z = \frac{R_1 R_2 + jX_1(R_1 + R_2)}{R_1 + jX_1} \pm jX_2, \quad \dots \quad (1)$$

where X_1 and X_2 are reactances with proper signs according to their inductive or capacitive nature, and a positive sign before jX_2 means that X_2 is to be in series with the network, while a negative sign means it is to be added in series with the line.

If the impedance of the first member on the right of (1) is denoted by Z_a and plotted in the complex plane for various values of the angular frequency ω , it can be shown that the locus will be the circle having its centre at $R_2 + R_1/2$, and radius $R_1/2$. The second term in (1) represents displacements parallel to the j axis of each point on the circular locus, the amount of the displacement being proportional directly or inversely to ω according as X_2 is inductive or capacitive, and the direction being upwards or downwards according as the sign is positive or negative.

* Communicated by the Author.

The first step in designing a balancing network to have a given frequency characteristic is to plot the given values of Z in the complex plane, marking the values of ω at a number of points ; if, then, it is possible to draw a circle centred on the real axis, through the plots, X_2 is zero. (Subject to the fulfilment of a projection condition to be stated later.) In the general case the plots are not circular, and it can be seen from the shape of the locus whether an inductive or capacitive impedance is required to make the locus circular ; accordingly three or more suitable points on the locus are chosen, and evenly-divided vertical scales are drawn through each, the divisions of each scale being proportional (directly or inversely) to the value of ω at the point ; a circle is then found by trial such that it passes through the same numbered division of each vertical scale, and has its centre on the real axis. The value of X_2 and the corresponding inductance or capacity is readily found from the vertical scales intercepted between the circle and the Z locus ; R_1 and R_2 are found from the position of the centre and the value of the radius of the circle, so that X_1 alone remains unknown.

It is a property of circle diagrams * such as the one under consideration that the frequency variable is distributed round the circle in the manner given by setting up a uniform frequency scale parallel to the j axis and projecting the scale on to the circle, from the point on the circle corresponding to infinite frequency as pole ; it is desirable to verify that the known frequencies round the circle project in this manner into a linear scale perpendicular to the real axis ; when this has been verified, X_1 may be found from the expression,

$$X_1 = \frac{R_1 \sqrt{|Z_a|^2 - R_2^2}}{\sqrt{(R_1 + R_2)^2 - |Z_a|^2}}, \quad \dots \quad (2)$$

where X_1 and $|Z_a|$ are corresponding values at any chosen frequency. The same value of inductance or capacity should be derived from X_1 whatever value of the frequency is used in selecting $|Z_a|$, but no checking of the result except as a precaution against arithmetical error is necessary, provided the circle passes accurately through the prescribed points and the frequency scale projects accurately into a truly linear scale ; in the event of slight departures from this criterion, X_1 may be calculated for three or four points and an average value found for the reactive element.

* Th. Kopeczynski, *Siemens Zeitschrift*, Feb. 1925, p. 75.

Proof.

To prove the expression used in determining X_1 , we shall use the notation of elliptic functions *; but it is the relations between these functions rather than their values as functions of the argument that are made use of, so that they do not appear in the final expression; for simplicity, equation (2) is proved for the case where X_1 is a capacity reactance; in the case of inductance the proof is similar.

From (1) we write more explicitly

$$Z_a = \frac{R_1 + R_2 + jR_1 R_2 C_1 \omega}{1 + jR_1 C_1 \omega}, \quad \dots \quad (3)$$

whence

$$|Z_a| = (R_1 + R_2) \left[\frac{1 + \frac{R_1^2 R_2^2 C_1^2}{(R_1 + R_2)^2} \omega^2}{1 + R_1^2 C_1^2 \omega^2} \right]^{1/2}, \quad \dots \quad (4)$$

which may be rationalized in elliptic functions by the substitutions †

$$sc u = R_1 C_1 \omega, \quad \dots \quad (5)$$

$$k = \left\{ 1 - \frac{R_2^2}{(R_1 + R_2)^2} \right\}^{1/2}; \quad \dots \quad (6)$$

then

$$|Z| = (R_1 + R_2) dn u. \quad \dots \quad (7)$$

Now it is readily shown that

$$sc u = \left[\frac{1 - dn^2 u}{k^2 - 1 + dn^2 u} \right]^{1/2}. \quad \dots \quad (8)$$

Substituting from (6), (7), and (8) in (5) in such a manner as to clear of elliptic functions, we get

$$1/C_1 \omega = R_1 \left[\frac{|Z_a|^2 - R_2^2}{(R_1 + R_2)^2 - |Z_a|^2} \right]^{1/2}, \quad \dots \quad (9)$$

which is equation (2) written explicitly for X_1 as a capacity reactance.

If a considerable number of cases are to be worked out,

* The elliptic functions are $sn u$, $cn u$, $dn u$ ($sc u$ is used for $sn u/cn u$) with an implied parameter (the modulus) k . The relations between these functions are those existing between the trigonometric equivalents $sn u = \sin \theta$, $cn u = \cos \theta$, $dn u = \sqrt{1 - k^2 \sin^2 \theta}$. The elliptic function notation is simpler than the trigonometric, and is more appropriate because the circle diagram used is a simple case of Jacobi's construction. (Dixon, 'Elliptic Functions,' Chap. x. pars. 105 & 107.)

† Dixon, *loc. cit.* par. 89.

tables or curves of the elliptic functions, or their trigonometric equivalents, enable C_1 to be found very easily from (5) and (7) with hardly any numerical calculation at all.

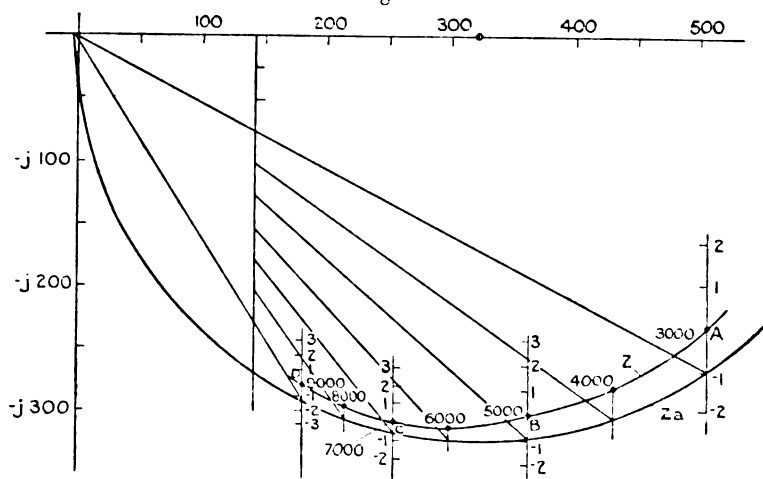
Example.

As an example of this method of designing balancing networks, we shall take an example worked out by Messrs. Robinson and Chamney in illustration of a method developed by them*.

$2\pi f.$	Impedance given.	Calculated network impedance.
3000	$509-j231$	$507-j235$
4000	$432-j281$	$434-j281$
5000	$361-j303$	$366-j303$
6000	$300-j313$	$307-j309$
7000	$254-j309$	$257-j306$
8000	$216-j296$	$217-j297$
9000	$182-j279$	$184-j285$

The required impedance characteristics are shown in the table, and are plotted in the complex plane in fig. 2. The

Fig. 2.



* Inst. P.O. Elect. Engrs., printed paper No. 76, Appendix III. The method adopted is to calculate the slope of the resistance curve at a number of points and plot it against frequency for comparison with standard curves having various values of constant product $C_1 R_1$. C_2 and R_2 are then found by calculating the impedance of the shunted condenser and subtracting from the components of the given impedance characteristic. (See also Dechange, *Bul. Soc. Belge des Electriciens*, Aug. 1924.)

plots are not quite circular, and points A B C D are selected for the vertical scales; a few trials show that a capacity reactance is required for X_1 , and accordingly vertical scales are drawn through A, B, C, and D, and marked with arbitrary divisions proportional to $1/\omega$ in each case.

It is easily found by trial that a circle can be drawn almost exactly through the scale-divisions numbered $y = +1$ with centre at $x = 290$, or a circle can be drawn through the points $y = -1$ with centre at $x = 321$. On applying the test of projecting the points on the circle on to a linear scale, the circle through the points $y = -1$ is found to be the better fit and is therefore adopted. The circle centred at $x = 321$ cuts the real axis at -5 , so that its radius is 326, and therefore $R_1 = 652\omega$. R_2 is -5 ; that is, 5ω added to the line. Measuring the intercept between the Z plot and the circle at $\omega = 5000$ we find it to give $X_2 = +j20$, whence $C_2 = 10$ mf. added in series with the line. Finally, calculating X_1 for the value $\omega = 5000$, we measure the distance from the origin to the 5000 point on the circle giving $|Z_a| = 489$, and evaluating equation (9), we find $X_1 = 749$ or $C_1 = 0.267$ mf.

For comparison with the characteristic to be matched, the network impedance has been calculated giving R_2 and C_2 their negative signs. The values are tabulated in the table with the measured line impedances. Owing to graphical inaccuracies arising out of the small-scale drawing, the calculated resistance values are a trifle high, and though the balance is quite good, it can be improved by subtracting 2ω from the network impedance; that is, changing R_2 from -5 to -7 .

LXXV. *On the Dilution Law for Strong Electrolytes.*

By R. T. LATTEY*.

AN examination of the data for the conductivity of strong electrolytes showed empirically that the following formula has a wide range of application:

$$\lambda_0 - \lambda = A/(B + V^{\frac{1}{2}}), \quad . \quad . \quad . \quad . \quad . \quad (1)$$

where A and B are constants peculiar to the solution in question.

This is obviously in accord with Debye and Hückel's⁽¹⁾ thesis that at great dilutions $\lambda_0 - \lambda$ varies inversely as $V^{\frac{1}{2}}$, and therefore the constant A should be equal to Debye's

* Communicated by the Author.

$\alpha\sqrt{2}$. It is of interest to compare the new formula with some which have been proposed on other grounds; of these, the most general is the form of Storck's equation which has been recently so freely exploited by Vogel and Ferguson ⁽²⁾:

$$\lambda_0 - \lambda = K/V^n, \quad . \quad . \quad . \quad . \quad . \quad (2)$$

where n is usually between 0.4 and 0.8.

There is also the form used by Debye and Hückel and by Onsager ⁽³⁾, viz.:

$$\lambda_0 - \lambda = A/V^{1/2} - AB/V, \quad . \quad . \quad . \quad . \quad . \quad (3)$$

to which the new form must approximate when V is large.

In Table I., Kohlrausch and Maltby's data for KCl (as quoted in Landolt and Börnstein's tables) are compared with values calculated by the three methods referred to, using the constants,

for (1) $\lambda_0 = 130.01$, $A = 89.47$, and $B = 1.82$.

(2) $\lambda_0 = 130.04$, $K = 61.26$, and $n = 0.4520$.

(3) $\lambda_0 = 130.01$, $A = 89.47$, and $AB = 134$.

TABLE I.

V.	(1).	(2).	(3).	K and M.
10000	129.13	129.09	129.16	129.07
5000	128.775	128.725	128.80	128.77
2000	128.09	128.085	128.105	128.11
1000	127.335	127.34	127.345	127.34
500	126.31	126.31	126.31	126.31
200	124.405	124.505	124.395	124.41
100	122.44	122.395	122.43	122.43
50	119.95	119.49	120.07	119.96
20	115.79	114.37	115.40	115.75
10	112.07	109.40	115.14	112.03
5	107.95	100.17	116.84	107.96
2	102.34	85.67	134.27	102.41
1	98.28	68.78	174.57	98.27
0.5	94.60	45.45	271.54	92.60

It will be seen that whereas the new formula gives agreement within less than 1/10 per cent. up to normal solutions, the others break down when V is between 20 and 50.

The new formula has been tested on a variety of data for uni-univalent salts, both in aqueous and other solutions, and has been found satisfactory over far wider ranges than any other formula with which the author is acquainted.

It is proposed here only to discuss uni-univalent salts in

water at 18° C. ; for these the formula is satisfactory in every case examined up to 0.1 N solutions, and in some cases up to greater concentrations.

The data used are those of Kohlrausch, and the results are shown in Table II.

TABLE II.

Salt.	λ_0 found.	λ_0 calcd.	A found.	A calcd.	B.
KBr	132.13	...	92.78	...	2.00
KI	130.69	...	86.69	...	2.00
KCl	130.01	130.01	89.47	89.37	1.82
KNO ₃	126.44	126.43	90.82	90.45	1.015
KSCN	121.24	...	87.46	...	2.00
KClO ₃	119.60	119.485	88.28	88.18	1.177
AgNO ₃	115.88	...	88.41	...	0.940
†KBrO ₃	112.67	112.73	92.58	92.84	1.607
KF	111.34	111.23	81.08	81.70	1.484
NaCl	108.91	108.91	80.55	80.76	1.605
NaNO ₃	105.32	105.33	81.46	81.84	1.345
LiCl	98.90	98.855	78.90	76.92	1.705
KIO ₃	98.48	98.495	80.70	80.84	1.127
*NaClO ₃	98.17	98.385	79.47	79.57	1.423
LiNO ₃	95.23	93.275	78.10	78.00	1.786
*NaBrO ₃	91.70	91.63	84.19	84.23	1.735
NaF	90.08	90.13	73.17	73.09	1.334
NaIO ₃	77.40	77.395	72.37	72.23	1.109
LiIO ₃	67.38	67.34	68.28	68.39	1.138
TiCl	131.33	131.33	91.52 ?	93.82	-2.08
TiNO ₃	127.75	127.75	97.20 ?	94.90	0.4635
HCl	380.56	381.2	109.1 ?	108.35	0.582
HNO ₃	378.34	377.6	108.7 ?	109.45	0.592

* From data by Flügel, *Zt. Phys. Chem.* lxxix. p. 586.

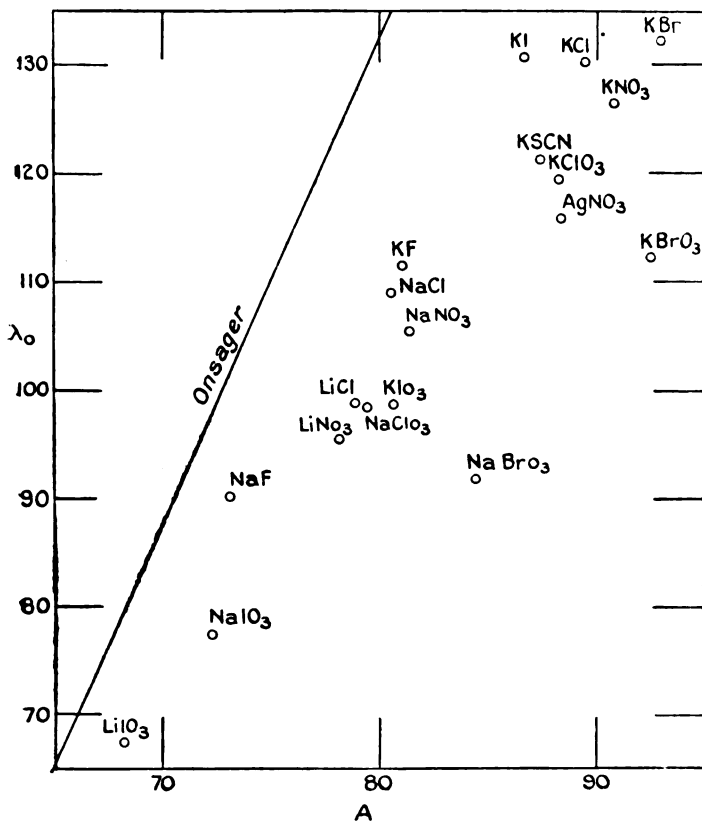
† " " " Hunt, *Journ. Amer. C.S.* xxxi. p. 801.

Now, according to Debye and Hückel ⁽¹⁾, the A can be expressed by $K_1 + K_2 \lambda_0 b$, where K_1 and K_2 are factors depending only on the solvent, while $b = \frac{l_1}{l_2} + \frac{l_2}{l_1}$, where l_1 and l_2 are the mobilities of the ions of the salt in question. Redlich ⁽⁴⁾ has proposed changes in the numerical value of K_2 , while Onsager ⁽³⁾ has propounded a theory by which b is replaced by a factor independent of the salt.

If Debye and Hückel are right, then A should be a linear function of $\lambda_0 b$, while if Onsager is right, A should be a linear function of λ_0 . Figs. 1 and 2 show that neither of these views is supported by the facts. The values of A

are, however, apparently additive: *i. e.*, we can put $A = a_1 + a_2$ where a_1 and a_2 are characteristic of the anion and kation respectively*. In order to assign a series of such values to the ions, it is necessary first to assign an arbitrary value to one ion, and the rest can then be found by subtraction. In fig. 1 it will be seen that the three simple

Fig. 1.



salts KCl, NaCl, and NaF lie approximately on a straight line, and it has therefore been assumed that there is a linear relationship between a and l for the ions K, Na, Cl, and F. The figures so obtained are shown in Table III., and were used in calculating the column headed "A calc." in Table II.

* At any rate so far as aqueous solutions at 18° C. are concerned.

Fig. 2.

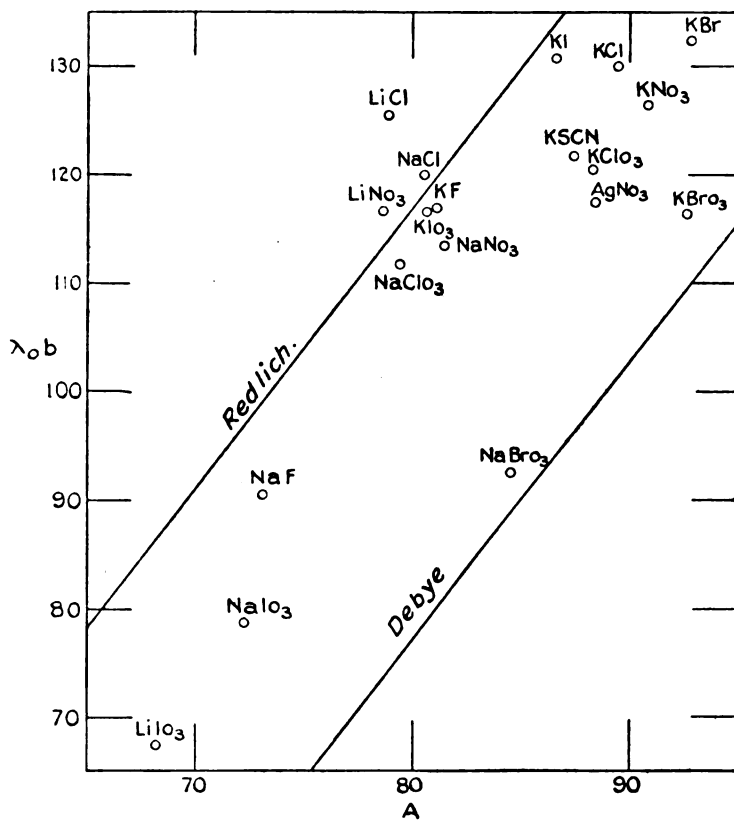


TABLE III.

Ion.	<i>l.</i>	<i>a.</i>	Ion.	<i>l.</i>	<i>a.</i>
Cl	66.405	45.26	Li	32.45	31.66
NO ₃	62.825	46.34	Tl	64.925	48.56
ClO ₃	55.88	44.07	H	314.8	63.1
F	47.625	37.59	Br	68.53	48.67
IO ₃	34.89	36.73	I	67.09	42.58
BrO ₃	49.13	48.73	SCN	57.64	43.35
K	63.605	44.11	Ag	53.06	42.07
Na	42.505	35.50			

Values below the horizontal line depend on a single determination and must be regarded as provisional.

The factor B can, for the present, only be regarded in the nature of a correction term; the value assigned to it is largely affected by small errors in experimental data. A larger mass of data will have to be examined before any generalizations can be attempted.

List of References.

- (1) Debye & Hückel, *Phys. Zeit.* xxiv. pp. 187, 305 (1923); *Trans. Faraday Soc.* 1927.
- (2) Vogel & Ferguson, *Phil. Mag.* l. p. 971 (1925); iv. pp. 1, 232, 300 (1927); *Trans. Faraday Soc.* xxiii. p. 404 (1927).
- (3) Onsager, *Trans. Faraday Soc.* xxiii. p. 341 (1927); *Phys. Zeit.* xxvii. p. 388 (1926).
- (4) Redlich, *Phys. Zeit.* xxvi. p. 99 (1925).

LXXVI. *A Concentrated Arc Mercury Lamp.* By E. L. HARRINGTON, *Ph.D.*, *Professor of Physics, University of Saskatchewan, Saskatoon, Sask., Canada* *.

[Plate XVIII.]

ABOUT four years ago a description† was given of a mercury arc lamp in which the arc was confined wholly to a capillary tube. Suggestions as to operation were made, and some advantages discussed. Certain decided improvements in the lamp itself, extensions in its use and additional observations of its characteristics growing out of its increased use in the laboratory suggest this further discussion.

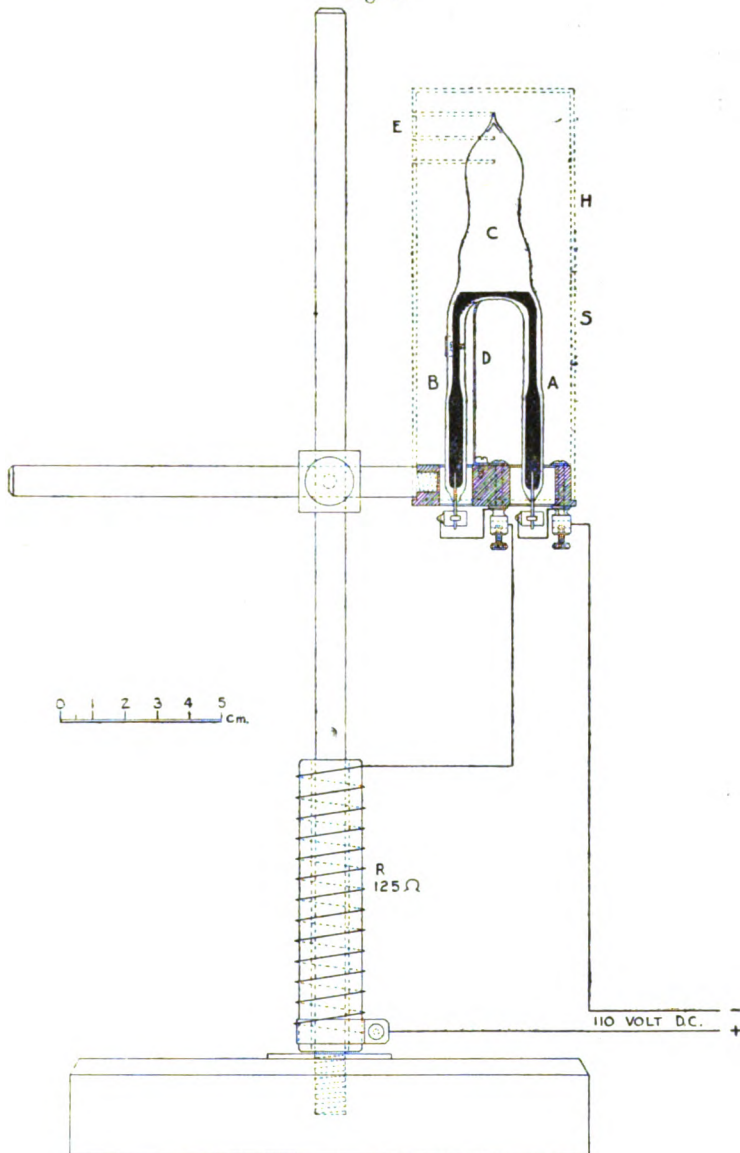
No material changes in dimensions have been made, but the new form, shown in fig. 1, has decided advantages. Its symmetrical form better adapts it for compact mounting in a housing. In this lamp the two legs are exactly alike in construction, being made of pyrex capillary tubing of about 1.5 mm. in bore, and having the lower portions considerably enlarged as shown. The lead-in wires are of tungsten. It has been generally found by those who have used mercury arcs confined either to capillary tubes or to large tubes that the inner tube surfaces become with continued use somewhat less transparent, particularly to the ultraviolet. This effect is especially noticeable in cases where the lamps have been repeatedly overloaded, or where an excess current has been carried for a considerable period. Apparently slight impurities in the mercury accentuate this tendency. With the present lamp having the two legs alike it is possible to interchange the positions of the two legs when one has

* Communicated by the Author.

† Harrington, *J. O. S. A.* and *R. S. I.* vol. vii. p. 689, Sept. 1923.

become discoloured, thereby virtually doubling the life of the lamp. A further advantage of the same sort may be

Fig. 1.



obtained by giving the lamp three or even four legs, if desired.

The housing, H, for the lamp is made of thin brass tubing and is provided with a vertical slit, S, directly in front of the arc capillary and cross slits, E, for ventilation at the top as shown. Such a housing makes the lamp suitable for dark-room use and also protects the eyes of the observers. The lamp is supported by one leg by means of a brass clamp D, the latter being mounted on the fibre base. Connections to the lamp are made by spring clips which are connected to the fixed binding-posts.

For a 120 volt D.C. circuit a series resistance of about 125 ohms and having a carrying capacity of 1 ampere is required. The commercial porcelain tube vitreous enamel-covered resistance units are found highly satisfactory. While the lamp may be operated on any D.C. voltage definitely greater than the lamp voltage (roughly 30 volts, though varying widely with conditions and load) providing the control resistance is properly adjusted, it is best to have a considerable margin to secure definite control. The current required depends upon the size of the capillary tube, but is about 0.7 ampere for the lamp described above.

Preliminary to starting the discharge it must be made certain that the current is actually passing through the lamp and in the direction indicated in fig. 1. With the cover removed, a bunsen flame is applied at the point indicated by A in fig 1, until the mercury column is broken up and the arc started. If owing to interruption of the service or to other cause the arc should go out, it is exceedingly important to make sure that the mercury column is complete and the current flows before again applying the flame, since dangerous pressures might be developed by a continued application of the flame. Vincent and Biggs* have described an electric heater consisting of a resistance wire applied to the capillary. Such an arrangement should make for convenience, but it increases the complexity of the outfit considerably.

It is possible to construct a lamp suitable for A.C. sources by using the mercury arc rectifier type of construction, but the considerable accessory equipment in the way of transformers of special nature required makes it of doubtful general interest, though a commercial company might render a real service to the laboratories by developing and placing on the market a suitable A.C. outfit.

Compared with the commercial diffuse arc mercury lamp, the lamp described above has for laboratory use the very definite advantages of greater convenience, lower initial cost, and lower current consumption. An even more important

* Vincent and Biggs, Jr. Sc. Instr. vol. i. p. 242, May 1924.

advantage lies in the greater richness of the spectra obtainable, as will be shown by the accompanying Plate. The spectrograms are submitted without detailed analysis in view of the rather voluminous literature on the mercury arc spectra already obtainable.

Pl. XVIII. shows the spectra obtainable from the mercury arc under a variety of conditions, using a Hilger Quartz Spectrograph, Type E-3, Size C. Pl. XVIII. (a) was obtained from a Cooper-Hewitt lamp, DP type. The tube of this lamp is of M form, has a total length of about 130 cm., and an external diameter of 2.5 cm. For this spectrogram the current was 4.4 amperes, the tube voltage drop 66 volts, and the time of exposure 30 seconds. The lamp markings indicate that the lamp was designed for 110 volt service and to carry 3.5 amperes. As this spectrogram contains as many lines as are obtainable on say a 2 minute exposure and differs merely in the intensities of the lines shown, it may be taken as typical of the spectra obtainable from a non-concentrated mercury arc discharge in glass.

Pl. XVIII. (b) and (c) were obtained from a pyrex lamp of the type shown in fig. 1, and having a capillary of 1.58 mm. bore. (b) resulted from a 30 second exposure at 26 volts and 0.5 ampere, and (c) from the same exposure but with a 28 volt drop and a current of 1.0 ampere. Here again only the difference in the intensities of the lines are in evidence, so either (b) or (c) may be taken as representative of the spectra obtainable from lamps of this type, when constructed of pyrex glass. A comparison of these with (a) shows that the concentrated arc gives about three times as many lines and much greater intensity than is obtainable from a diffuse arc. It may be observed, also, that the spectra extend further into the ultraviolet, though this may be due principally to the use of pyrex glass which has a somewhat lower transmission limit than ordinary glass*. There appears in these, as well as in the following spectrograms, a faint continuous spectrum background, due to the high temperature of operation.

Pl. XVIII. (d) and (e) were obtained from a lamp of exactly the same design as shown in fig. 1 but constructed of quartz tubing, the capillaries having a 1.32 mm. bore. In (d) the current was 0.48 ampere, the tube voltage 29.0 and the length of exposure 80 sec. (e) was taken with the same lamp and period of exposure, but with a current of 0.98 ampere and a tube voltage of 39. Just as in the above cases, it

* See Luckiesh, 'Ultraviolet Radiation,' p. 82 or 'Science,' p. 281, Sept. 17, 1926.

appears that the increase in the current affects the intensities but not the number of lines appearing. One advantage of using the quartz is apparent in the large increase in the number of lines obtainable, due to the additional extension into the ultraviolet region. There are twice as many as appear in the spectra obtained from a pyrex lamp of the same construction, and about six times as many as are given by a non-concentrated arc in ordinary glass tubing. The spectra of the quartz and of the pyrex lamps appear to be identical in the visible and the near ultraviolet regions.

Another advantage lies in the possibility of operating the lamp at much higher intensities. This is of particular value in making studies in the ultraviolet region, for it has been found that the ultraviolet intensity increases with increasing wattage even more rapidly than that of the visible region, and that in general the shorter the wave-length the higher this rate of increase in intensity *. The particular mode of variation of a line depends upon the series to which the line belongs. Even at ordinary loads the light obtainable has less of an objectionable glare than that obtainable from a diffuse arc, but with a quartz lamp operating at near red-heat the continuous background becomes sufficiently intense to cause the general colour effect to become distinctly less greenish and more yellowish.

Harrison and Forbes †, by a somewhat different method, have made a careful study of the energy distribution in the mercury arc spectra under varying conditions of load, voltage, current, and pressure. Their table of lines, being related to thermopile observations, lists, of course, only a fraction of the lines obtainable by photographic processes. Neither did the lamp used have such a constricted arc as the one under consideration here. In a later work ‡, however, they used a more concentrated arc lamp, which, while of experimental design and not especially suited for laboratory use, gave highly interesting results which have a definite bearing on the lamp described above. Their report lists certain other advantages and characteristics of such lamps of interest to those having need of a highly concentrated mercury arc, either in the physical laboratory or in connexion with photochemical processes §.

* Kuch and Retschinsky, *Ann. d. Physik*, (4) xx. p. 598 (1906).

† Harrison and Forbes, *J. O. S. A. and R. S. I.* x. p. 10. Jan. 1925.

‡ Forbes and Harrison, *J. O. S. A. and R. S. I.* xi. p. 99. August 1925.

§ For a most interesting summary of the quartz lamp characteristics and uses see Buttolph, *Bull. No. 105 A*, Cooper-Hewitt Electrical Company. Luckiesh (*l. c.*) gives extensive information and bibliographies.

LXXVII. *The Freezing-Points of Concentrated Solutions.*—
 Part II. *Solutions of Formic, Acetic, Propionic, and Butyric Acids.* By EDWARD RICHARD JONES, Ph.D.
 (Wales), and CHAS. R. BURY*.

THIS work was undertaken with the object of obtaining reliable values for the activities of a few typical associated substances in aqueous solution.

The experimental methods have been fully described in a previous communication (Phil. Mag. (7) iii. p. 1032, 1927). Two Beckmann thermometers were used: the first, which was used only in one series of experiments with acetic acid (series B), has been standardized to the nearest 0.005° C. by the National Physical Laboratory; the second was standardized by comparison with the first, and was used throughout the rest of this work. The pressure corrections of the two thermometers were 0.0024° and 0.0018° C. per cm. Hg respectively.

Acetic acid was fractionally crystallized three times and then distilled from phosphorus pentoxide (Orton, Edwards, and King, J. C. S. 1911, xcix. (1) p. 1178): about one per cent. of water was added to the product to destroy any anhydride that might have been formed by this treatment. The other three acids used were purified by fractionally distilling pure commercial samples twice. The final product in every case distilled over within a range of half a degree.

TABLE I.—Formic Acid.

<i>m.</i>	θ .	γ .	<i>m.</i>	θ .	γ .
0.2419	0.465	1.014	1.674	3.032	0.973
0.2684	0.515	1.016	1.930	3.475	0.964
0.3362	0.641	1.016	2.089	3.744	0.958
0.4273	0.810	1.017	2.233	3.989	0.953
0.6262	1.173	1.010	2.426	4.312	0.945
0.7599	1.419	1.008	2.675	4.723	0.935
0.9379	1.737	1.001	2.807	4.942	0.931
0.9765	1.807	1.000	2.813	4.948	0.930
1.041	1.924	0.999	3.005	5.254	0.922
1.099	2.028	0.997	3.083	5.385	0.919
1.362	2.490	0.986	3.201	5.576	0.915
1.658	3.006	0.975			

The results are given in Tables I. to IV., in the first columns of which are given the concentrations (*m*) in mols.

* Communicated by the Authors.

TABLE II.—Acetic Acid.

Series A.			Series A (cont.).		
<i>m.</i>	<i>θ.</i>	<i>γ.</i>	<i>m.</i>	<i>θ.</i>	<i>γ.</i>
0·1669	0·314	1·041	2·435	4·199	0·920
0·2653	0·497	1·045	2·533	4·357	0·913
0·3097	0·578	1·040	2·605	4·465	0·910
0·3401	0·636	1·042	2·762	4·704	0·901
0·5432	1·002	1·029	2·885	4·900	0·896
0·6514	1·197	1·024	2·910	4·937	0·894
0·8247	1·505	1·014	3·029	5·113	0·887
0·8510	1·549	1·011	3·259	5·466	0·876
1·126	2·021	0·991	3·329	5·566	0·872
1·243	2·227	0·986	3·330	5·564	0·871
1·396	2·490	0·977	3·348	5·587	0·870
1·642	2·901	0·962			
1·689	2·987	0·961			
1·698	2·998	0·960			
1·812	3·183	0·952			
1·974	3·466	0·948			
2·006	3·507	0·943			
2·114	3·679	0·936			
2·273	3·937	0·928			
2·290	3·974	0·928			

Series B.

0·2811	0·526	1·042
0·8752	1·590	1·008
1·396	2·488	0·977
2·005	3·505	0·943
2·589	4·433	0·910
3·423	5·727	0·870

TABLE III.—Propionic Acid.

<i>m.</i>	<i>θ.</i>	<i>γ.</i>	<i>m.</i>	<i>θ.</i>	<i>γ.</i>
0·2936	0·544	1·088	1·789	2·978	0·912
0·3126	0·577	1·083	2·093	3·411	0·880
0·4211	0·771	1·071	2·134	3·474	0·877
0·5271	0·955	1·056	2·352	3·771	0·854
0·5686	1·028	1·052	2·482	3·948	0·842
0·6606	1·187	1·041	2·676	4·196	0·823
0·8964	1·582	1·011	2·814	4·357	0·808
0·9987	1·756	1·002	2·873	4·436	0·803
1·148	1·994	0·983	3·074	4·673	0·784
1·195	2·068	0·976	3·287	4·919	0·764
1·301	2·238	0·965	3·412	5·054	0·752
1·490	2·531	0·944	3·869	5·528	0·712
1·639	2·753	0·927	3·933	5·583	0·707

TABLE IV.—Butyric Acid.

<i>m.</i>	θ .	γ .	<i>m.</i>	θ .	γ .
0.2826	0.515	1.148	1.824	2.675	0.819
0.4213	0.758	1.123	1.958	2.795	0.790
0.5809	1.028	1.092	2.100	2.888	0.755
0.8160	1.397	1.038	2.513	3.077	0.660
0.9419	1.587	1.011	3.632	3.264	0.472
1.087	1.799	0.981	3.688	3.272	0.466
1.252	2.023	0.945	4.802	3.341	0.361
1.465	2.294	0.899	5.777	3.389	0.302
1.498	2.331	0.891	9.437	3.513	0.186
1.593	2.442	0.871	13.678	3.649	0.129
1.726	2.584	0.842	17.722	3.837	0.100

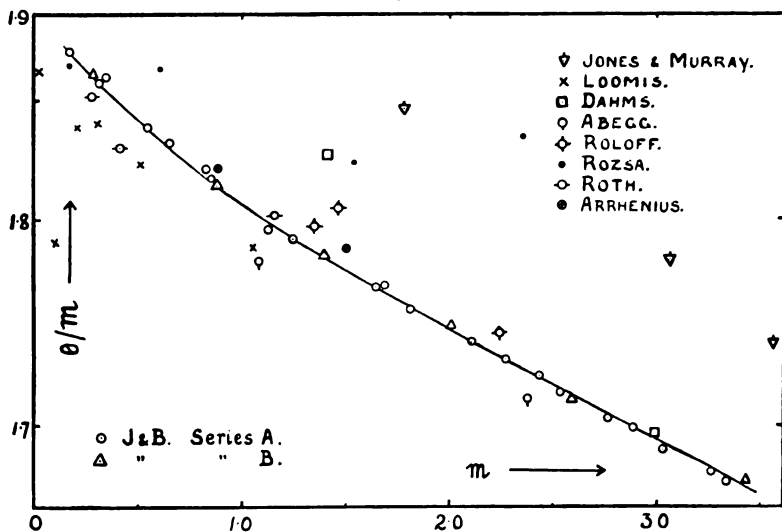
per thousand grams of water as determined by titration with baryta, phenol-phthalein being used as indicator. These concentrations are the mean of two determinations: when duplicate analyses differed by more than 1 in 500, the results were discarded. The baryta was frequently standardized against recrystallised succinic acid. In the second columns are the depressions of the freezing-point of water (θ) corrected for pressure, emergent stem, and thermometer errors, and in the third columns are the activity coefficients (γ).

Previous measurements of the freezing-points of formic acid solutions have been made by Abegg (*Zeit. phys. Chem.* 1894, xv. p. 219), Faucon (*Ann. Chim. Phys.* 1910, xix. (8) p. 70), and Jones and Murray (*Amer. Chem. Journ.* 1903, xxx. p. 198); of acetic acid solutions by Abegg, Arrhenius (*Zeit. phys. Chem.* 1888, ii. p. 491), Dahms (*Weid. Ann.* 1897, lx. p. 119), Faucon, Hausrath (*Ann. d. Physik*, 1902, ix. p. 548), Jones and Murray, Loomis (*Weid. Ann.* 1897, lx. p. 523), Roloff (*Zeit. phys. Chem.* 1895, xviii. p. 582), Roth (*Zeit. phys. Chem.* 1903, xliii. 556), and Rozsa (*Zeit. Electrochemie*, 1911, xvii. p. 934); of propionic acid solutions by Abegg, Faucon, and Peddle and Turner (*Trans. Chem. Soc.* 1911, xcix. (1) p. 685); and of butyric acid solutions by Arrhenius, Faucon, and Peddle and Turner. With the exception of Hausrath's measurements of the freezing-points of very dilute solutions of acetic acid, none of these earlier measurements are of great accuracy. Our results for acetic acid are compared graphically with those determinations by previous investigators that lie in the range of concentrations studied by us in fig. 1, where θ/m is plotted against m . With the other

acids our agreement with previous observers is of the same order.

Lewis and Randall employ the convention that the activity is equal to the concentration when the latter is zero. Calculation of activities, using this convention, involves a rough knowledge of the freezing-points down to zero concentration, which is lacking in the case of weak acids. Serious errors are caused by neglecting ionization in the more dilute solutions and by the treatment of these acids as non-electrolytes (*i.e.* by assuming the curve in fig. 1 extrapolates to $\theta/m = 1.858$, when $m = 0$), though such a course is feasible,

Fig. 1.



and is recommended by Lewis and Randall ('Thermodynamics and the Free Energy of Chemical Substances,' McGraw Hill Book Co., New York, 1923, p. 290) when the experimental data are not very accurate and do not extend to very dilute solutions. On the other hand, the treatment of weak acids by the method employed for strong electrolytes is impossible without accurate data at extreme dilutions, unattainable by modern experimental methods. The convention of Lewis and Randall is therefore inapplicable, and in its place we employ the convention that activity is equal to concentration (expressed as molality) when the latter is unity. This enables a modification of Lewis and Randall's equation to be used, which avoids the difficulty

of evaluating integrals down to zero concentration. Change of convention merely involves multiplying a series of activities at different concentrations by the appropriate constant; and our results can easily be converted when the necessary data for dilute solutions are available. Since the ratio of the activities at two concentrations alone has any practical significance, the convention we have employed in no way affects the utility of our results.

The activity coefficients (γ) given in the third columns of Tables I. to IV. have been calculated from the following simple modification of Lewis and Randall's equation for non-electrolytes (*op. cit.* p. 286):—

$$\log_e \gamma = \log_e \frac{a}{m} = \int_m^{m'} -j d \log_e m - j + 0.00057 \int_m^{m'} \frac{\theta}{m} d\theta + K,$$

$$\text{where } j = 1 - \frac{\theta}{1.858m},$$

and where a is the activity, m' is any convenient concentration, and the integration constant K is given a value, dependent on the value chosen for m' , such that our convention is satisfied.

TABLE V.

m .	γ .		
	Formic Acid.	Propionic Acid.	Butyric Acid.
0.25	1.015	1.091	1.160
0.50	1.013	1.060	1.108
0.75	1.008	1.031	1.054
1.00	(1.000)	(1.000)	(1.000)
1.25	0.991	0.971	0.946
1.50	0.981	0.943	0.892
1.75	0.971	0.917	0.837
2.00	0.961	0.891	0.779
2.50	0.942	0.840	0.664
3.00	0.922	0.791	0.557
3.40	0.907	0.754	0.500
5.00			0.347
7.50			0.235
10.00			0.174
12.50			0.141
15.00			0.118
17.00			0.105

In Table V. are given the activity coefficients of formic,

propionic, and butyric acids, obtained by interpolation at round concentrations. These activity coefficients are strictly valid only at the freezing-points of the solutions: it is desirable to calculate their values at some standard temperature (usually 25°C.), but only in the case of acetic acid are the necessary heat data available. Even here the accuracy of the data probably do not justify calculation of the change of activity with temperature over a large interval, and we have therefore calculated the activity coefficients at 0°C.

TABLE VI.—Acetic Acid.

m .	γ .	\bar{L}_1 .	$\bar{C}_{p_1} - \bar{C}_{p_1}^0$.	γ_{273} .	$1 - \alpha$.
0.005	0.937	—	—	0.942	0.938
0.01	0.971	—	—	0.976	0.956
0.02	0.995	—	—	1.000	0.969
0.05	1.025	—	—	1.030	0.980
0.10	1.035	-0.13	0.01	1.040	0.986
0.20	1.042	-0.28	0.02	1.046	0.990
0.35	1.040	-0.54	0.04	1.044	0.992
0.50	1.032	-0.80	0.05	1.035	0.993
1.00	(1.003)	-1.77	0.11	(1.000)	0.995
1.50	0.971	-2.96	0.19	0.968	0.996
2.00	0.944	-4.25	0.27	0.938	0.997
2.50	0.915	-5.66	0.36	0.906	0.997
3.00	0.891	-7.13	0.46	0.879	0.997
3.40	0.869	-8.45	0.54	0.854	0.998

In the second column of Table VI. are given the activity coefficients of acetic acid at round concentrations at the freezing-points, obtained by interpolation. In the third column are the partial molal heat-contents of water at 17°C. (\bar{L}_1), deduced from the data of Sandonnini (*Atti accad. Lincei*, 1926, (6) iv. p. 63), and in the fourth column are the partial molal heat-capacities ($\bar{C}_{p_1} - \bar{C}_{p_1}^0$) of water deduced from the data of Reiss (*Jahresb.* 1880, p. 91), quoted by Sandonnini. In the fifth column are the activity coefficients at 0°C. (γ_{273}), calculated from the equations of Lewis and Randall (*op. cit.* pp. 289, 349).

There is a clearly-defined maximum in the activity coefficient of formic acid at a concentration of about 0.43 molal, and, apparently, a similar maximum with acetic acid in the most dilute solutions examined. To confirm the

existence of this maximum, we have calculated the activity coefficients of acetic acid at lower concentrations from the freezing-point determinations of Hausrath (*loc. cit.*). The interpolated figures for the activity coefficients at round concentrations, given in Table VI., which are based on Hausrath's data for concentrations below 0.2*m*, and on our own at higher concentrations, show the maximum very clearly. The fall in the value of the activity coefficient at low concentrations is due to ionization. There must also be similar maxima, but at lower concentrations, for the other two acids. The decrease in the value of the activity coefficient at high concentrations, where ionization is negligible, and which is characteristic of all four acids, must be due to some abnormality of the unionized molecules—possibly association.

It is often assumed that the activities of acids which obey Ostwald's dilution law are proportional to the concentrations of the unionized molecules, as deduced from electrical conductivity measurements. Acetic acid is a typical weak acid, and its solutions obey Ostwald's dilution law up to concentrations of one-tenth normal, or considerably higher if the conductivities are corrected for change of viscosity; but the assumption that activity is proportional to the concentration of unionized molecules is far from true, even in hundredth normal solutions. In the sixth column of Table VI. are given the ratios of unionized to total acetic acid ($1-\alpha$): in calculating these, a value of 20.4×10^{-6} , obtained by extrapolation from the data of Noyes (J.A.C.S. 1908, xxx. (1) p. 335) has been used for the dilution law constant. If activity were proportional to the concentration of unionized acid, the ratio $\gamma_{273}:1-\alpha$ should be independent of the concentration: it is obviously not so. The discrepancy must be partly due to the neglect of interionic forces in the usual method of calculating the degree of ionization; but probably a more important factor is the abnormality of the unionized molecules.

Butyric acid is remarkably abnormal; *i. e.* its activity coefficient changes very rapidly with concentration. This fact must be closely connected, thermodynamically, with the close proximity of the freezing-point concentration curve to the critical solution point, which lies in the metastable region within a degree of and below the curve (Faucon, *loc. cit.*). The freezing-point concentration curve is therefore in some ways analogous to the critical isotherm of a gas. There must also be some explanation of this abnormality in terms of the molecular-kinetic hypothesis, and we

think it probable that butyric acid forms micelles, somewhat similar to those formed by the soaps, as has been shown by McBain and his collaborators.

While molecular weights calculated from the freezing-points of concentrated solutions are of no quantitative value, they indicate that butyric acid is very highly associated, and that the degree of association is too great to be explained by the usual hypothesis of association to double or triple molecules.

In dilute solution, butyric acid does not differ greatly from the other three acids, but at a concentration of 1.1 m. it suddenly becomes very abnormal. This behaviour is particularly clear in comparing the curves obtained by plotting j/m against m and used in evaluating activities. This sudden departure from the normal is also characteristic of the soaps (McBain, Randall, and White, J. A. C. S. 1926, xlviii. p. 2517), and is a natural consequence of the law of mass action when applied to the association of simple molecules to form complex molecules containing a large number of single molecules, such as these micelles are.

The soaps and butyric acid have one feature in common which is probably essential for micelle formation: they both consist of long molecules, one end of which—the hydrocarbon end—has little attraction for water, while the other end—the COONa or $-\text{COOH}$ group—has considerable attraction. In other respects there is little resemblance between the soaps and butyric acid: the former are strong electrolytes and form ionic micelles, while butyric acid is a weak electrolyte and less than 1 per cent. ionized at concentrations where micelles exist.

We hope shortly to offer further evidence in favour of this hypothesis.

One of us (E. R. J.) wishes to acknowledge his indebtedness to the Department of Scientific and Industrial Research for a maintenance grant during the session 1925–26, and to the University of Wales for a Postgraduate Studentship during the session 1926–27.

Edward Davies Chemical Laboratories,
University College of Wales, Aberystwyth.
May 26th, 1927.

LXXVIII. *Discharges and Discharge-Tube Characteristics.*
 By WILLIAM CLARKSON, M.Sc., A.Inst.P., Armstrong
 College, Newcastle-on-Tyne *.

Introduction.

THESE experiments, carried out in the session 1925-26, were undertaken on account of certain observations made during a study of "flashing" in Argon-Nitrogen tubes over a wide range of pressures⁶, these observations showing that "flashing" must be of universal occurrence in electrical discharge-systems, in virtue of the fact that all such systems possess "sparking" and "extinction" potentials, and have capacity.

It was found possible to obtain discharges of two kinds: "flashes" in which the characteristic was only finally reached, and discharges in which the characteristic itself was traversed, only dynamic equilibrium being attainable in the former type.

An examination of discharge-tube "characteristics" proved that discharges of quite unique appearance were associated with each stage at whatever pressure, the positive column being present, and further that valuable information could also be gained from observing the appearance of "flashes," either directly or in a rotating mirror, the latter serving to resolve the phases of complex discharges.

The following paper gives the general association of discharges with discharge-tube characteristics; but though it was possible to correlate many references in the literature of the subject¹ to the discharges observed, so much has been done, especially in publications in German, that the need no longer exists^{2,3,10}.

A reference to some of the ideas employed may not be out of place here, especially as many are not being fully developed till later. The idea of a "threshold current"¹² was constantly utilized, the "sparking potential" under dynamic conditions being taken to decrease with the "initial current," but the full significance of this was not demonstrable until the correspondence of the "statical sparking potential characteristic" with the "corona characteristic" was discovered⁴. Also, though a "slow build-up" was implied by many phenomena, this could not receive closer attention till recently, when the "corona-lag" was investigated⁵, and here the effect

* Communicated by Prof. G. W. Todd, D.Sc.

of the "clear-up" has been limited in the main to the problem of "overlapping" in "flashing."

These ideas will be treated in more detail after the "characteristics" have been considered, and then an account of representative experiments will be given.

Tubes and Apparatus.

For the most part the experiments described here were carried out on two tubes, air, nitrogen, or argon-nitrogen mixture (this giving lower sparking potentials) being employed in a dry, though not a pure, state. It was not considered necessary to use absolutely pure gases, and later experiments have proved that the results obtained also apply to tubes of scrupulous purity. Though pressures up to a few millimetres were generally used, the range was extended to half an atmosphere, without, however, exceptional phenomena being encountered.

It was desired to have tubes of large cathode area, so that the extent of the negative glow could be studied, tubes that were free from wall effects, assuming these to have an influence, and with the discharge always taking place in the same region, this preventing the rapid change in critical constants so noticeable in tubes where the discharge can occur in different places. Movement of the discharge also inhibits visual examination. To this end the smaller tube was made with electrodes placed axially in a cylindrical tube some five centimetres in diameter. The electrodes were 10 cm. long, and consisted of brass rods one cm. in diameter, with hemispherical ends; their separation never being more than a few mms. This tube was especially good for mirror observations and for the variations of the negative glow. Later, a second tube was made, with convex brass electrodes 15 cm. in diameter, the upper electrode being movable. The maximum separation was 15 cm.

The electrodes were smooth and highly polished, but though all the apparatus was chemically clean initially, a high degree of electrode cleanliness could not be maintained, probably owing to the active nature of the gases present, particularly oxygen.

All discharges in these tubes were axial and the tubes were satisfactory in every way.

Constant potential up to one thousand volts was generally obtainable, batteries and an M.L. Anode-converter being used; but often, as when using a diode at saturation current, or when slight voltage variations did not matter, the 480 D.C. mains could also be employed.

Though resistances were often used, a diode (valve with grid and plate connected) was often employed to give a constant current system. In this respect the work differed greatly from previous work in which only a constant resistance had been used.

Voltages were measured with an electrostatic voltmeter, normal range 200–600 volts, but this was altered when necessary by putting batteries in series. When maximum and minimum voltages were being measured a diode also was included, as previously⁶, and a small capacity placed across the voltmeter to lessen the effect of leakage.

GENERAL CONSIDERATIONS.

Current-voltage characteristics.

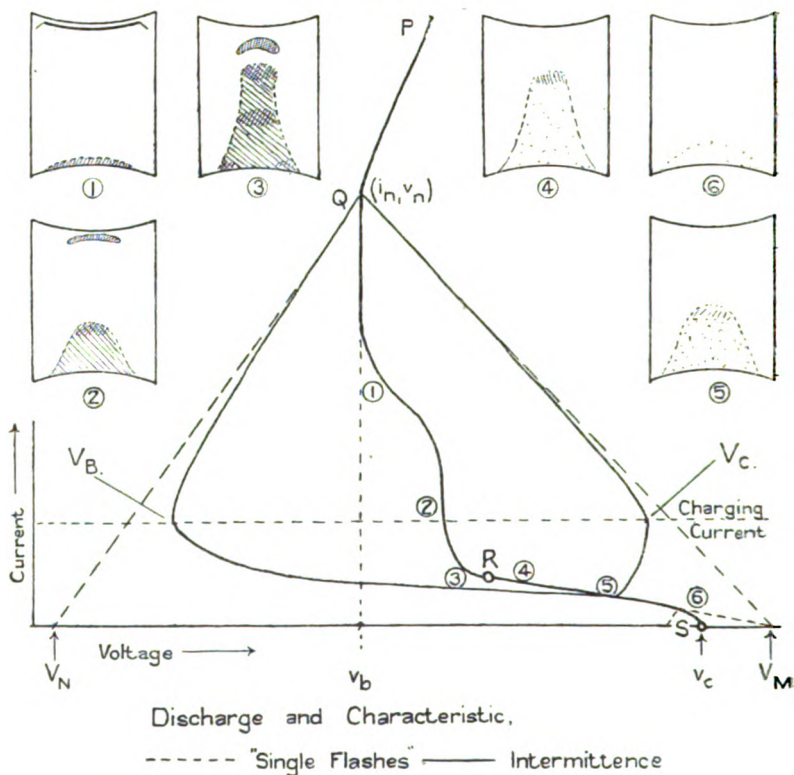
As this is a property of discharge-tubes that will constantly be referred to in this paper, its form in the tubes just described must first be considered. Under all conditions the characteristic was invariably of the form given (schematically) in fig. 1, though the actual values of the voltage or the current depended not only on the pressure and nature of the gas and on the electrode separation, but also on the state of the electrodes.

The characteristic (fig. 1) fell naturally into two sections: PQR the "stable" region and RS the "corona" region. PQ is the normal characteristic, Q giving the minimum voltage v_b at which the discharge could be sustained. From Q the voltage increased with increase of current. With decrease of the current, though the voltage might be constant for a certain range, below this range a fairly quick rise (10–50 volts) occurred until another constant range was reached (down to R). At R another short quick rise in voltage took place, the "corona" characteristic was entered, and generally intermittence set in, even with minimum capacity. Indeed, in these tubes the "corona" region was seldom stable enough for the voltages to be measured; but sufficient results were obtained to show that the characteristic, as expected, was of the same form as in other tubes, and that the flattening of the characteristic at R was continued in a gentle curve to the region of the statical sparking potential S, at which value the voltage remained constant down to the lowest appreciable currents.

The "corona" characteristic has also been referred to as the "threshold characteristic"⁴, because it represents the minimum current (or space charge) from which, at the voltage e sent, the current can increase (build-up). The fact that,

in these experiments, a greater residual space charge or current was accompanied by a lower dynamic sparking potential is in accord with this view of the "corona" characteristic, and though it cannot be proved, it seems highly probable that the statical threshold current conditions hold fairly closely even in rapid intermittence, even though the equilibrium here is dynamic. This view will be accepted provisionally in this paper, just as the "stable" characteristic will be assumed to hold also.

Fig. 1.



Single Flashes.

The course of a single "flash" or condenser discharge may now be followed. If a condenser charged to a voltage V_M is applied to a discharge tube a strong discharge occurs (save in certain circumstances) and the voltage falls to a value (V_N), lower than v_b . The intensity of the "flash" and the extent of the negative glow depend on the size of the capacity and can serve as indicators of the current attained. Since the

discharge starts at some point ($i=0, v=V_M$) on or to the right of the corona characteristic and finishes at some point to the left ($0, V_N$), it must have intersected the stable characteristic, and further, since it starts and ends with zero current, the current must undergo a period of increase and then of decrease. If we assume that the maximum current is attained, as is probable, at the "stable" characteristic, the intercept in each case may be determined at least approximately.

With a capacity (C) across the tube a steady current is caused to flow and the point i_n, v_n on the characteristic is attained. If now the circuit is broken the discharge ceases but the voltage of the capacity has fallen to a value V_N . The difference between v_n and V_N is a measure of the "clear-up" for that point on the characteristic. In this way the whole characteristic may be examined for small capacities, and to a less extent for large ones, for though nearly all the characteristic is stable for small capacities the minimum current at which a discharge can be maintained increases with the magnitude of the capacity. When we know the i_n, v_n corresponding to the V_N for the single flash, we have some idea of the point at which the stable characteristic was reached.

Experimental results gave that $v_n - V_N$ increased as i_n, v_n increased, a lower final voltage thus implying a higher maximum current, the capacity of course being constant.

If a diagram is drawn, as in fig. 2, V_M, v_n , and V_N may all be inserted, and if they are joined a schematic plan of the path of the discharge is obtained, neglecting for the moment the problem of "clear-up" mechanism, a point to be returned to later. The straight lines are merely diagrammatic.

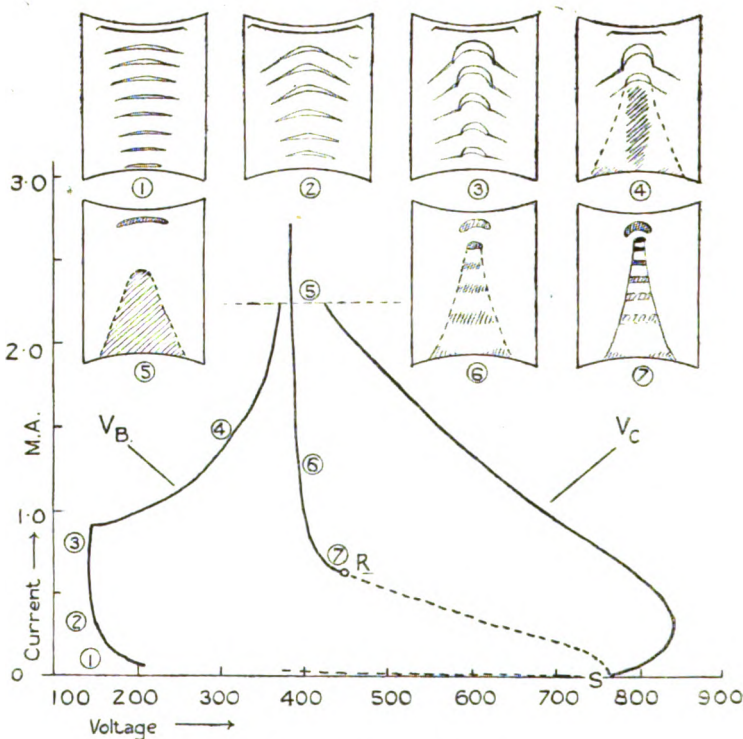
"Dynamic characteristics."

The following views have been implied in this account. The characteristic is assumed to lie between two regions where only dynamic equilibrium can be attained, but whereas to the right the factors tending to increase the number of ions predominate, to the left the reverse is the case, the characteristic forming the boundary where the influences are equal and statical conditions hold. P-Q determines the maximum (steady?) current possible at any voltage, as imposed by the tube constants, and QRS determines the minimum value, this only being stable when the current is limited by the external circuit, since in all cases the current will attain a maximum value.

Another assumption⁵ that will be made is that concerning

the variation of current with time, a variation of which fig. 1 can give no idea. Here it is assumed that the current takes some little time to attain its maximum value, increasing at first slowly and then more and more quickly, a reverse process taking place on "extinction." These are necessary assumptions for the explaining of "corona" lags and many other properties of condenser discharges.

Fig. 2.



Intermittent Discharge ($C = 5 \times 10^{-6} \mu F$)

Nitrogen, 4 mms. press.

By "extinction" is meant the leaving of the characteristic for the region of the unsustained discharge. "Extinction" must occur when a condenser discharge reaches the characteristic between Q and S, as further passage of current must reduce the voltage below that value required by the sustained discharge. If this is the sole mechanism of extinction, it would imply that the discharge could not

"go-out" in the section P-Q, as here it should be possible to traverse the characteristic down to Q before this occurred. If this traversal was rapid enough (a questionable point), though the maximum current as determined by the characteristic would be carried, excess of space charge representative of the higher current might still be present when Q was reached, in which case "clear-up" phenomena would be explained. Certainly the region P-Q is traversed when a suitable resistance is in series with the condenser.

It would appear, however, that "extinction" actually can occur even in discharges where there is a charging current greater than Q. "Hysteresis" has been invoked to account for this and for the fact that "extinction" occurs in cases when a steady current is suddenly reduced—a case parallel to that of condenser discharges. An objection to "extinction" on PQ is that it implies that the tube can carry "clear-up" currents greater than the maximum currents permitted by the characteristic, in which one would have to postulate that the characteristic gave merely the maximum steady current or that the normal characteristic did not apply to flashes where lags in the cathode fall were so pronounced.

In this paper it will be accepted that "extinction" occurs at the intercept, such an assumption being easier to handle and not seriously affecting the experimental conclusions.

Intermittence.

Each individual discharge in intermittence may be taken to present the features of a single "flash" modified by a charging current, this causing the condenser voltage to increase whenever the current in the tube is less than this current in the circuit, that is to say, in the first stages of "build-up" and the last ones of "clear-up"⁵, when of course maximum and minimum voltages (V_C and V_B) will be attained, though the general variation may be inferred from several ways; but it is impossible accurately to determine i_m , r_n in the absence of an exact value for V_M . Fig. 1 gives the new discharge path implied, and it will be seen that if the rate of charge of the condenser is great enough (i large or C small), and the "clear-up" current sufficiently large, it is possible for a current still to be flowing when the corresponding voltage v_m on the characteristic is reached. If the intercept is on the "corona" section another "flash" will occur, but if it is on the "stable" section at a point for which a steady current is possible for the capacity with the given charging current, a continuous discharge will ensue,

even though this may not happen until after several "flashes." It is easily seen that for this condition to be attained the charging current must be greater than the minimum steady current—an experimental fact in intermittence.

EXPERIMENTAL.

Appearance of Steady discharges.

An account of the voltage-current variations of the full characteristic has already been given. Generally the current was varied by altering the filament current of the diode regulating the circuit current, the voltages being given by the electrostatic voltmeter across the tube, with or without a diode in series with it. The electrode separation was always great enough for a positive column to be present at some stage of the discharge and, as already has been said, the visual appearance of the discharge was a sure index to its relative position on the characteristic; so a general account may be given that will apply to both tubes under whatever conditions.

At the smallest currents, at r_c on the "corona" characteristic, the only visible evidence of a discharge was a faint glow at the anode, this glow increasing in brightness and depth as the current increased and often developing a bright head¹, which at the final stages became an elliptical bulb. At R, the transition to the stable characteristic was made, and the positive column, in the few cases where this stage could be maintained, filled the interelectrode space with a confused glow.

The transition was marked by the sudden appearance of a strong though limited negative glow, this glow being cupped round the end of a positive column similar to, though more distinct than, that preceding the transition. With increase of the current this column decreased in length and in distinctness, and the negative glow moved to the cathode and occupied a greater and greater amount of its surface. At last, when Q was reached, even the last traces of an anode glow had generally disappeared and only a bright, thin negative glow remained. From this point the discharge merely gained in intensity as i was increased, save at higher pressures when the usual steady strie appeared. The length of the column in a tube was of course also determined by the inter-electrode distance, and its distinctness by the pressure, the definition increasing as the pressure increased. The discharges typical of "flashes" are discussed later.

Though such phenomena made it possible to study discharges by visual observation alone, this method was of limited application in that it could not differentiate the actual phases in a discharge or series of discharges. Consequently a rotating mirror was utilized. A silvered microscope slip, polished on the outside, affixed to an electric motor of regulatable speed proved quite adequate.

When the discharge was very narrow, as in the rod tube, or if a slit was used, "flashes" up to many thousands per second could be resolved. Thus the mirror served to detect intermittence, though head-phones and a wavemeter were also employed to this end. Frequencies giving notes beyond audio-limit were frequently encountered.

"Flashes" and Intermittence.

It was found that condenser discharges in these tubes could be classified in two groups: those which ended on the "corona" characteristic ("corona" flashes), and those ending on the stable characteristic ("normal" flashes and sparks).

The spark was the form of the normal "flash" for high current densities, occurring with large capacities or at high gas pressures, the positive column here becoming extremely localised. Its intense nature was demonstrated by pitting of the electrodes, and in more extreme cases by the complete discharge of the condenser. Its other properties will be dealt with when discussing the normal form of "flash."

The presence of a positive column in "flashes" showed that this phenomenon was also manifested in traversing the region to the right of and between the "corona" and stable characteristics. Such a column was always striated, the number of striations being related to the voltage across the tube, that is to say increasing with pressure and electrode separation, and suggested that the striæ were, to a first approximation, about an ionizing potential apart. In many ways they were reminiscent of the striæ observed under certain conditions on the corona characteristic in the rare gases, but such striæ were never seen in these experiments.

The striæ were best observed in not too slow "flashing" as they were continuously in evidence, but in all cases the duration of "flashes" was too short for the variation of the striæ with time to be studied directly. Fig. 2 shows their change in shape when a constant capacity and a steadily increasing charging current was employed, which here implies also greater initial currents in the tube and the accompanying lower dynamic sparking potential, and from this an idea of their dependence on voltage and current may

be deduced. We may attribute the striæ observed to the slower portion of the build-"up," since it is here that they will exist for the longest time and despite a probably lower intensity will have a greater visual effect. In the corona striæ just mentioned the striæ were flatter and thinner at small currents, but became increasingly domed and lenticular as the current increased, and we may expect the same changes in the inter-characteristic region.

The same variations with tube-current and voltage for "flashing" striæ will be observed in fig. 2, but it will be seen that more extreme forms were developed; thus the final form consisted of a cup-like "core" with side "wings." According to the views advanced in this paper, the condenser voltage would only slightly increase in attaining V_C when large initial currents were present and the striæ exhibited would be those corresponding to all the stages from small currents up to quite large ones at but a slightly higher voltage. These would appear superimposed and would be of the form observed, the "wings" corresponding to the initial stages and the intense "dome" to the final stages.

Even in the initial stages of "sparks," when the "core" of the discharge was just a glowing column these "wings" were still observable, an observation in complete accord with the opinions just advanced.

If a sequence of two discharges occurred at different initial voltages their difference was immediately demonstrated by the appearance of two (superimposed) sets of striæ in the tube, the presence of a steady stage being recognizable in a like manner, even without the assistance of the rotating mirror.

Fig. 2 shows the variations of V_C and V_B , and the appearance of the discharge for a small capacity, that of the large tube alone, with the current increasing from zero up to the value at which the discharge became continuous (0-5) after which the current was reduced until intermittence again set in (5-7). Three stages of "flashing" were recognizable: (0-1) a region of "corona" flashes, these always occurring when the charging current was not great enough for the discharge to win clear of the "corona" characteristic; (1-3) the region of the "striations"; and (3-5) a "final" stage¹¹. From (0-1) the voltage readings for V_C and V_B were somewhat erratic and in consequence have merely been indicated. From (1-3) the "flashing" was quite regular, a steadily increasing frequency being recorded as the current was increased; but though V_B changed very little, V_C at first rose rapidly, and then as the charging current became still greater, gradually

diminished. At this stage the frequency was of the order of a thousand or so per second. A sudden change in pitch and an abrupt increase in V_B heralded the next stage (3-5). V_B increased rapidly at first and then slowly attained a value rather greater than v_b ,— V_c still falling, though without evidence of discontinuity,—until finally there was only about 20 volts difference between them. The frequency was now generally at or beyond the audio-limit.

With further increase of the current the discharge became steady, and it was seen that a point about midway on the vertical part of the stable characteristic above R had been attained. As has already been said, the voltage did not change much as the current was reduced until this had almost attained its minimum value, at which stage it rose and intermittence supervened.

These phenomena can readily be explained on the assumptions already outlined in this paper.

V_c varies according to two factors, the charging current and the "initial" current in the discharge. The second effect cannot be present until a certain frequency is attained, after which it plays a dominant role, and the initial voltage v_m traverses the whole of the "corona" characteristic as the frequency increases. The extent of the negative glow showed, as is to be expected, that the intercept on the "stable" characteristic at first increased and then decreased, V_B not suffering much change until (5) was reached. The sudden rise of V_B would be explained by the intercept moving onto the region between Q and R; it would rapidly leave the more horizontal part and would finally reach the more constant voltage part. The appearance of the discharge supports this explanation.

As the difference between V_c and V_B was very small at the "final" stages, the time spent near or at the stable characteristic would represent an increasing fraction of the time of discharge, and we may expect the phenomena of this region to come into greater prominence at this stage, and the positive column to increase with the charging current on account of the steadily decreasing intercept. Such a region is, of course, not easy to study, as the discharge is in the neighbourhood of both sections of the characteristic all the time, but the discharges discussed here certainly were intermittent and not merely pulsatory.

Interrupted "Steady discharges."

Very interesting observations were made during a study of discharges, whether finally steady or intermittent, before

they had attained regularity. The charging circuit was made and broken at regular intervals at a frequency suitable for the rotating mirror, a mercury interrupter being used for this purpose.

Where the current was such that only intermittence could occur it was seen that, as expected, the "flashes" were not necessarily alike until after several had taken place. The first "flash" was the strongest as it commenced at r_c , and if "overlapping" was present to any appreciable extent, this was followed by a succession of fainter "flashes" at steadily decreasing time intervals, until finally they occurred regularly and had the same brightness, showing that a constant dynamic sparking potential had been attained. Naturally this was only observable in full when a sufficient number of "flashes" could take place between breaks, that is when the "flashing" was of high enough frequency.

The phenomena when the current was large enough to result in a steady discharge were very illuminating. Though a large capacity only gave "flashes," the discharge showed two "flashes" as C was reduced, the first strong though not reaching so high a current as for the larger capacity, and the second weaker. This was then followed by a steady discharge, the point R having presumably been reached during the "clean-up." With smaller capacities only one "flash" was necessary before steadiness was reached, smaller maximum currents being recorded. The presence of a gap between the "flash" and the steady discharge (a noticeable feature in all these cases) would agree with the explanation that the stable characteristic was departed from and returned to again (at R), and though it could conceivably represent the traversal of the characteristic, this is believed to be a distinct case and will be considered later. Such an explanation would scarcely account for the time interval observed.

"Flashes" ending in a discharge, whether constant or transient, on the characteristic, were generally readily distinguishable, the negative glow at low currents being of limited area and standing off the cathode, so that two cathode glows were seen on looking at the discharge, even though the positive column was masked by the striæ. Their extent and brightness gave a very fair idea of their relative duration.

Induction-coil discharges.

Similar phenomena were obtained on the large tube with pressures up to half an atmosphere, a large induction coil being used as a transformer for the alternating mains. An

Amrad "S" tube was found to make a very satisfactory rectifier. In these cases the "normal" characteristic gave the usual striated positive column for all currents greater than Q .

In the rotating mirror the discharge was seen to consist of a spark⁹, or series of sparks if the condenser was large, followed by a gap (clear-up), and then the gradual emergence of striæ from the anode. The current at this stage was increasing, as the increasing negative glow clearly showed, but whether the characteristic was retraversed when the current decreased seemed to depend very much on conditions. It is probable that the rate of reduction was the determining factor. It is of interest that oscillograph records of such a discharge in a mercury lamp⁸ suggest that a similar explanation may be applied to that case also.

Special study was made of the gap between the "flash" and the steady discharge, as it was initially thought that this was due to a retraversing of the characteristic until the tube current equalled the charging current; but the evidence suggested that this was not so, neither anode nor negative glow being present.

When an ordinary induction coil was used the difference between the currents in opposite directions was most interestingly shown, the one giving merely a series of sparks but the other finally ending in a steady discharge.

Discharge of Capacity through Resistance.

Though reasons have been advanced for supposing that "extinction" often occurred at the point of intersection of the characteristic, definite evidence of the traversal of the characteristic from this point under certain circumstances will also be given. This traversal was particularly in evidence in condenser discharges through a resistance, both for single "flashes" and for intermittence. Indeed the characteristic itself was occasionally studied in this way, a large (10μ . F.) condenser being charged to a high potential and discharged through the tube in series with a suitable high resistance, such a discharge of course resembling the discharge of a battery on decreasing potential.

In such a system though the passage of a current must lower the potential of the condenser, the same does not apply to the potential across the tube, as this is able to increase under certain circumstances, for, since the

potential fall along the resistance is determined by the current, which in turn is fixed by the tube characteristic, its value will also decrease with time. If this rate of fall is greater than that of the condenser, the tube potential will increase. The action of the resistance is thus to permit an accommodation of the voltage across the tube to the tube characteristic, as was clearly demonstrated when, for such a system, the charging circuit was suddenly broken.

The phenomenon of these "flash-steady" discharges was also observable in intermittence where a resistance of suitable size was interposed between the condenser and the discharge-tube, the possibility of this form being obtained and the duration of the "steady" portion increasing with the capacity and the resistance. The fact that there was often an abrupt transition from normal "flashing" to the "flash-steady" form at a certain stage of the increase of capacity suggested that the two forms were quite distinct, though at other times it did appear to be possible to effect the transition more gradually. Visual observation showed also that the resistance sensibly limited the current attained, the time of the "flash" thus being increased, so that altogether discharges of appreciable duration were produced; in fact, it was possible to have intermittent discharges in which the dark interval was very small in comparison with this period. In the case where the resistance is in the condenser arm, a further influence will be that the "flash" will be due to the capacity of the tube alone until the voltage has dropped to a value much less than that of the condenser.

Tubes of low conductivity were not studied, but previous work showed that "flashes" of longer duration also occurred in these tubes, particularly with the larger capacities⁷.

It will be seen that all these factors increase the possibility of a stable state being attained. Indeed they have been utilized in work on this question⁷.

One problem arising from the study of such discharges was whether the normal characteristic was traversed in all cases at the end of a "flash," and to what extent, the duration of such a traversal of course being calculable, in the case where no resistance was employed, from the voltage fall and the average current. Usually the time required in these experiments was so short that it would not have been observable, and thus there was no visible proof that this did not always occur. Before any change could be noticed in a mirror it would be necessary for a

small current stage to be reached, and this from the positive glow present was what happened in "flash-steady" discharges, the restricted negative glow accompanying this stage also being a prominent feature. A gap between the "flash" and the "steady" sections would indicate that extinction had occurred, the clear-up region giving small currents with an absence of a distinctive discharge, but only when it could be proved that the charging current was greater than that at Q (fig. 1) was it possible to have direct evidence suggesting that extinction might occur on the normal characteristic and that traversal of the characteristic did not usually take place.

Inductances.

The effect of large inductances in the condenser arm was also examined. As expected, due to the potential absorbed as the current changed, they encouraged the production of a series of "flashes" of decreasing intensity, damping out the "build-up" and quickly restoring the voltage during "clear-up." The number of "flashes" in each discharge changed as the capacity was altered, and it is certain that the "flashes" represented discharges of the tube capacity in a great number of cases. Such a possibility has already been considered and further comments are therefore unnecessary.

Pulsatory and similar discharges.

Though in these tubes the discharge was confined to the middle of the electrodes and "fatigue" effects could not effect a large movement of the discharge, rotating mirror examination showed that great fluctuations of the negative glow occurred even in discharges which apparently were quite steady. The specific part these might play in instability at lower currents was not studied, but it is probable that they were not without influence.

Sometimes when the discharge had nominally become steady, as in fig. 2, the mirror showed that the discharge was definitely pulsatory, the positive column and the negative glow going through a regular sequence of changes, the discharge varying from merely a strong negative glow to the restricted glow and strong positive column (the range between Q and R?). The frequency varied as in normal "flashing," with C and i , but the slow frequencies gave the greatest changes in appearance. These discharges appeared never to be extinguished and were quite distinct from "flashing," giving no sound in headphones or wave-meter, rapid and extreme changes of current thus being

absent. Though the discharge became steady in the sense given in the preceding paragraph, no discontinuity occurred with increase of current.

It is significant that when "flashing" was studied in the case where this was observed a variety of "flash-steady" discharge was seen with the larger currents. In the mirror the "flash" was followed by a regular movement of the negative glow from the cathode until finally it merged into a positive column and the discharge ceased. Such discharges were not to be confused with the behaviour of the negative glow in "clear-up"³, or the occurrence of a second incipient "flash." Corona "flashes" were more readily obtained in these cases also.

These effects are reminiscent of those obtained with resistance in the capacity circuit, or for limited conductivity, and may be attributed to electrode effects producing discharges very similar to those "preliminary discharges" described in connexion with the "corona lag."⁵ In many ways the resemblance between these pulsatory discharges at the vertical region of the "stable" characteristic, and "corona flashes" at the vertical region of the "corona" characteristic, was very close, but it is similarly not easy to explain them without invoking great changes in the characteristic unless it is assumed that they really were intermittent. We may assume that the voltage would always be about constant, and that the characteristic was never much departed from owing to the strong retardation. The discharges would then be those of the characteristic and the "dark interval" would be inappreciable as in many "corona" discharges. The "flash-steady" discharge would also be explainable on this basis.

It is certain that more rapid and extreme discharges of this nature, such as would occur with smaller retardations, would affect telephones, and indeed blurred notes that could be attributed to such discharges were occasionally heard. Such notes may be heard in some "flash-steady" discharges near the critical resistance. It is always possible, of course, for discharges determined by the capacity of the tube to be superimposed on "flashes" due to a condenser, as in the cases previously given.

"Steady" striated column.

It was not always easy to study the striated positive column at the lowest steady currents, as this region of the characteristic was often very unstable even on the capacity of the tube alone. This was probably due to the

action of impurities either in the gas or on the electrodes, a slight trace of oxygen in nitrogen having an appreciable effect in this direction, even without seriously affecting the voltages.

Fig. 2 gives an illustration of the form this discharge could take, and though the final form was not always obtainable, this must in part be attributed to the instability referred to, though it is true that great differences in definition existed in different cases. Once the hazy column had assumed a definite form increase in current merely caused the details of the column to become more clearly defined, the end striæ taking the form of flat plates at regular intervals. At the lowest currents they increased in number as well, as the voltage increased, and the cone became crossed with thin flat striæ which decreased in distinctness towards the anode. The negative glow now almost enclosed the tip of the positive column.

Where a mixture of gases was present the striæ showed stages of clearness and vagueness as the voltage changed, the colour of the striæ depending on the gases present.

The mirror was used to determine whether the striæ were moving striæ, but rather unsatisfactory results were obtained. The striæ at the tip of the column seemed always to be steady, but those near the anode were fluctuating in a regular manner. Occasionally they were seen to flow, but this was due to a change in current, just as the fluctuations could be due to variations of the discharge due to "fatigue" effects.

Where the rod tube was employed the discharge moved into the weakest field and very unsymmetrical columns were obtained¹⁰. The field also had a great effect on the form of the striæ in "flashing." With a pointed cathode and a plane anode the "wings" almost disappeared¹¹, but with a reversal of these conditions they formed one large dome with the rest of "core," the striæ increasing rapidly in size with nearness to the cathode. This is the form present when a "flash" takes place from a limited area of the anode.

In conclusion the author would like to express his sense of obligation to Professor Todd, Armstrong College, for his constant support in his researches, and to the Board of Scientific and Industrial Research, whose award of an Investigatorship permitted these and other researches to be carried out.

SUMMARY.

An account is given of discharges in gases up to half an atmosphere pressure, the positive column being present. The appearances of the discharges are employed in explanation.

1. A common volt-ampere characteristic was found, a unique discharge being associated with each stage at whatever pressure.

2. A condenser discharge is considered as a jump from the "corona" characteristic to the "stable" characteristic, "build-up" occurring from the first and "clear-up" beyond the second. The characteristic is thus considered as a statical boundary between two regions where only dynamic equilibrium is possible.

3. "Threshold current" phenomena and "clear-up" effects are discussed, and are employed to explain dynamic sparking potentials.

4. The various ways in which a discharge can become steady are developed and the problem of "extinction" considered.

5. The variations of striæ in "flashing" are recorded and associated with the lag in the "build-up."

6. These assumptions are applied to discharges of many kinds observed or in references.

References.

1. De la Rue and Müller, *Phil. Trans.* 1878-80.
2. Valle, *Phys. Zeit.* 1926; also Zelany, *Phys. Review*, 1924.
3. Penning, *Phys. Zeit.* xxvii. p. 187 (1926).
4. Taylor, *Phil. Mag.* iii. p. 368 (1927).
5. Clarkson, *Phil. Mag.* iv. p. 121 (1927).
6. Clarkson, *Proc. Phys. Soc.* xxxviii. p. 10 (1925).
7. Taylor and Clarkson, *Phil. Mag.* xlix. p. 336 (1925).
Taylor and Sayce, *Phil. Mag.* l. p. 916 (1925).
8. Newman, *Phil. Mag.* xlvii. p. 939 (1924).
9. Aston, *Proc. Camb. Phil. Soc.* xix. p. 300 (1916-19).
10. Pedersen, *Ann. d. Phys.* lxxi. p. 317 (1923), and lxxv. p. 826 (1925).
11. Finch and Cowen, *Proc. Roy. Soc.* iii. p. 257 (1926).
12. Appleton, Emeléus, and Barnett, *Proc. Camb. Phil. Soc.* xxii. p. 447 (1925).

LXXIX. *Notices respecting New Books.*

Tables Annuelles de Constantes et Données Numériques de Chimie, de Physique, et de Technologie. Vol. V. Années 1917-1922. Deuxième Partie. Pp. lii+805 to 1934. (Paris: Gauthier-Villars et Cie. 1926.)

THIS volume completes the publication of data for the period 1917-1922. The arrears of publication arising from the war are gradually being overhauled, and the next volume, dealing with the years 1923-1924, should shortly be ready. A detailed index for the first five volumes is also in course of preparation. The volume for the years 1925-1926 is promised for 1928, and thereafter the publication will become once more an annual one.

The arrangement of the present volume is similar to that of preceding volumes with few exceptions. Photochemistry has been given a separate section. The section dealing with photography has been considerably expanded and contains a mine of information. The method of classification of alloys in the metallurgy section has been changed.

The tables are not in any sense critical; that is not their purpose. They provide a valuable reference medium for numerical data in all branches of science, and no well-equipped scientific library can afford to be without them. It may be added that eighteen countries have contributed to the cost of preparation, through subventions from the Government, scientific or technical societies, and industrial firms.

A Treatise on the Mathematical Theory of Elasticity. By A. E. H. LOVE, M.A., D.Sc., F.R.S. Fourth Edition. Pp. xviii+643. (Cambridge University Press. 1927. Price 40s. net.)

THE third edition of Prof. Love's well-known and standard treatise on the Mathematical Theory of Elasticity appeared in 1920. The new matter included in the present edition is not very extensive, amounting only to about 20 pages. The most important additions are: (i.) a simplified treatment of the equilibrium of a sphere, leading by elementary methods to the most important geophysical applications; (ii.) a discussion of the theory of the bending of a rectangular plate by pressure applied to one face; (iii.) a discussion of the theory of large deformations of plates and shells; (iv.) an account of the process by which stress-strain relations are deduced from the molecular theory of a crystalline solid. Other minor additions or revisions have been made where necessary.

The numbering of the articles in the earlier editions has been retained—a procedure which is to be commended. Articles added in earlier editions were designated with the suffix A or B:

those added in the present edition have been marked with suffixes beginning with C. Under (i.) above, renumbering of some articles was necessary. In this connexion it may be pointed out that in § 180 the reference to § 184 should have been changed to § 177.

The frequent revision of a standard work of this nature is desirable, so that the results of new researches may be incorporated. Prof. Love has been very successful in doing this without unduly increasing the size of the book. It is likely to remain the standard work on the subject for many years.

The Polarimeter, a Lecture on the Theory and Practice of Polarimetry.

By V. T. SAUNDERS. (Adam Hilger. 1s. 6d.)

THE author gives an interesting historical account of the development of the polarimeter from the earliest efforts to the standard instruments of the present day. The Lippich type of polarimeter is described in detail. "The Polarimeter has exerted a great influence upon the progress and development of the theory of organic chemistry," and in this connexion reference is made to Pasteur's work on tartaric acids, to the use of the instrument in the sugar and other industries, and lastly to its practical application in biological research.

Elementary Algebra. Part 2. By F. BOWMAN. (Longmans, Green & Co. 1927. 6s.)

THE second part of this work deals with the three primary series binomial, exponential, and logarithmic, with an introductory account of the convergence of series in general. The chapter on Graphs brings under consideration algebraic functions of higher degree, the circle and radius of curvature, confocal conics and Cassini curves, followed by the treatment of complex numbers and con-formal representation. The final chapters are devoted to the solution of equations of the third and fourth degrees, to determinants of any order, and the solution of simultaneous equations. The numerous examples and exercises—about one thousand, mostly with answers—will be found very useful to the student.

Principia Mathematica. By A. M. WHITEHEAD and B. RUSSELL. Volume 2, 45s.; volume 3, 23s. 2nd Edition. (Cambridge University Press.)

THE Cambridge University Press has now completed the second edition of the important work, 'Principia Mathematica,' by Prof. Whitehead and Mr. Bertrand Russell. This work has remained since its publication in 1906 the most important work on the foundations of Mathematics, and in all probability it will continue

to be so for some considerable time. The volumes at present under review are concerned with Cardinal Arithmetic, Relation Arithmetic, Series, and Quantity. These two volumes constitute, as before, a triumph of printing.

The Upper Palæolithic Age in Great Britain. By D. A. E. GARROD, B.Sc. Pp. 211, with 49 figures. (Oxford: Clarendon Press. 1926. Price 10s. 6d. net.)

A VERY useful service has been rendered by the author in collecting together records of the Upper Palæolithic industries of Great Britain. Hitherto the literature relating to them has been buried for the most part in various scientific journals, some of which are not easy of access. In addition, authors have varied considerably in their system of nomenclature, and the collections themselves are scattered through various museums and private collections.

A systematic review of the available material was therefore necessary in order to correlate the whole of the material and to gain the correct perspective. The author has performed her task well, and this volume will be invaluable to the investigator who attempts to compare the palæolithic industries of Great Britain with those of other countries.

A full account is given of the Upper Palæolithic cave-sites and of the different implements, bone and other objects and fauna found in them. This is followed by a description of open-air finds referable to Upper Palæolithic times and of epipaleolithic cultures. A chronological table of Upper Palæolithic sites and a complete bibliography and index enhance the usefulness of the volume for purposes of reference.

The Stone Age in Rhodesia. By NEVILLE JONES Pp. xiv + 120, with frontispiece in colour and 40 figures. (Oxford: University Press. 1926 Price 12s. 6d. net.)

SOUTH AFRICA promises to provide an unrivalled field as a scene of prehistoric study. At present very little has been done to investigate the relics of palæolithic times. The late Dr. Péringuey, Director of the South African Museum, Cape Town, and the late Mr. J. P. Johnson in the Union, and the Rev. Neville Jones in Southern Rhodesia have made the most important contributions. The purpose of the present volume is to place on record all that is so far known of the Stone Age in Rhodesia and to stimulate interest in a study which, in the opinion of the author, only lacks popularity by reason of its being so little comprehended.

Difficulties of classification in South Africa, when an attempt is made to correlate with the classifications of finds in Europe, arise

from the different materials employed—there is, for instance, no flint in South Africa,—from the absence in general of definite geological evidence, and the almost complete lack of any skeletal remains of man. There can be no question, however, that whether or not South Africa and Europe were originally contemporary in culture, South Africa subsequently lagged behind and remained Aurignacian in culture until the use of iron was introduced by Bantu immigrants, probably not more than 1000 years ago. Nevertheless, the various European cultures have their equivalents in South Africa, and the author has for convenience adopted the corresponding names, without implying that the periods in the two areas were contemporaneous. One implement of special interest which occurs abundantly in Rhodesia, and is also found in many other localities in South Africa, but rarely in Europe, is the chopping-axe or cleaver. The author brings forward strong evidence to prove that it is a finished implement.

The author gives an account not only of human remains and of stone implements, but also of Bushman paintings and their significance. A list of localities in Rhodesia where implements have been found will be of value to other investigators. It is to be hoped that this volume will prove a stimulus to others in South Africa to investigate the numerous relics of earlier times with which the country abounds.

Die elektrische Leitfähigkeit der Atmosphäre und ihre Ursachen.

By Dr. VICTOR F. HESS (Sammlung Vieweg, Heft. 84-85). Pp. viii+174, with 14 figures. (Braunschweig: Friedr. Vieweg & Sohn. 1926. Price 9.50 r.m.)

THE phenomena connected with the electrical conductivity of the atmosphere are of importance to the physicist, the meteorologist, the geophysicist, the geologist, and the astronomer. The well-written monograph by Dr. Hess dealing with this subject is therefore welcome. It covers in general the literature of the subject up to the end of 1925, but in dealing with the penetrating radiation in the atmosphere and with the ionization of the upper layers of the atmosphere, the literature up to March 1926 has been covered. Full references are given to all the more important original publications. A detailed account is given of the investigations of the penetrating radiation of supposed cosmic origin; as a pioneer investigator in this field, Dr. Hess's account is of particular value.

The German text-books on atmospheric electricity of Gockel and of Mache and Schweidler have long been out of date. Dr. Hess foreshadows in a preface a new text-book by Prof. Benndorf and himself. We are pleased to know that such a volume is in preparation. Meanwhile, the present monograph, dealing more particularly with the phenomena connected with

ionization in the atmosphere, forms a valuable contribution to the existing literature on this subject. There are two good French works dealing with atmospheric electricity, but there is a singular deficiency of English works on the subject.

Collected Researches: National Physical Laboratory. Vol. xix. 1926. Pp. v + 443. (London: H.M. Stationery Office, 1926. Price 18s. 6d. net.)

THIS volume contains reprints of 31 papers by members of the Staff of the National Physical Laboratory. The dates of publication of the originals range from 1917 to 1925, and the inclusion of the year 1926 in the title of the volume is therefore somewhat misleading. The papers are all concerned with physical subjects, and the originals were published mostly in the Proceedings of the Royal Society, Proceedings of the Physical Society, Philosophical Magazine, Transactions of the Faraday Society, and the Journal of the Röntgen Society. The varied subjects of the papers and the importance of many of them emphasize the number and value of the researches undertaken at the Laboratory. Each paper is prefaced by an abstract of its contents, a plan which is much to be commended. The printing has been carried out by the Royal Society printers, and is of the high quality customary of their work.

L'Energie Rayonnante. Tableaux synoptiques de l'Echelle des Longueurs d'Onde et des principales caractéristiques du rayonnement électromagnétique avec un résumé des théories actuelles. By A. FORESTIER. 2nd Edition. Pp. 75. (Paris: Librairie Scientifique Albert Blanchard. 1926. Price 20 f.)

THIS volume is concerned with the essential unity of Röntgen rays, infra-red, luminous, and ultra-violet waves, and Hertzian waves, and contains a large amount of useful information in tabular form, together with a brief theoretical outline. The introduction contains a brief sketch of Maxwell's theory and of the electron theory of Lorentz, followed by a summary of the fundamental constants. The first table deals with Hertzian or wireless waves; the second with the infra-red to ultra-violet regions. This section includes Planck's formula, photoelectric phenomena, Rutherford's atom, Bohr's theory, and Sommerfeld's theory of the fine structure of spectral lines, followed by numerical data. The third table is concerned with X-rays, including diffraction by crystals, and Moseley's law. The fourth table deals with radioactivity. The spectroscopy of gamma rays and the junction between Hertzian and infra-red rays are dealt with in a final section, covering recent work.

The volume should be useful to the student, showing, as it

does, in a simple manner the inter-relationships of electromagnetic waves of different wave-lengths. The more advanced student will also find it of value for purposes of reference.

Colloid and Capillary Chemistry. By Prof. HERBERT FREUNDLICH, Ph.D. Translated from the third German edition by H. Stafford Hatfield, B.Sc., Ph.D. Pp. xv + 883, with 157 figures. (London: Methuen & Co. 1926. Price 50s. net.)

THIS translation of the important text-book by Freundlich on colloid chemistry is very welcome, for there is no English text-book which covers the ground in so complete a manner. The third German edition, from which the translation was made, was a reprint of the second, new matter being added in an appendix. It is to be regretted that the translator has not incorporated the additions, which amount to 30 pages, into the body of the work. Continual reference to notes at the end is annoying to the reader, particularly when there is no reference in the text to these notes.

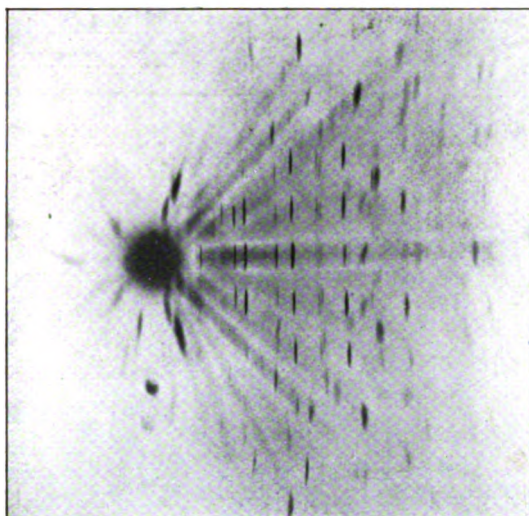
Colloid chemistry can be approached from two directions. Starting from a simple system of two phases with a common interface, the one phase can be imagined more and more finely divided and distributed throughout the other with increase of the interface. Or we may start from a pure solution and suppose the size of the particles continually increases until we come into the region of colloid chemistry. These two avenues of approach are fully dealt with in the first portion of the work. The phenomena at interfaces, or capillary chemistry, is treated in great detail. This method of treatment has the advantage that the laws governing the complicated phenomena of colloid chemistry, such as adsorption, influence of solubility, electrical effects, &c., can be more easily developed in connexion with the simpler phenomena of capillary chemistry. The processes of crystallization are fully dealt with under the heading of "The Interface Solid-Liquid." Separate sections are devoted to the kinetics of the formation of a new phase and to the Brownian movement. The latter forms the second avenue of approach.

The second portion of the book deals with colloidal disperse systems under the headings Colloidal solutions; sols (byophobic and byophilic) and gels; mist and smoke; foams; disperse structures with solid dispersion media. Experimental facts are fully described and, where possible, theoretical interpretations are preserved.

The volume is well printed and has excellent subject and author indexes at the end.

[The Editors do not hold themselves responsible for the views expressed by their correspondents.]

FIG. 1.



Rotation photograph for Cæsium Alum.

FIG. 1.

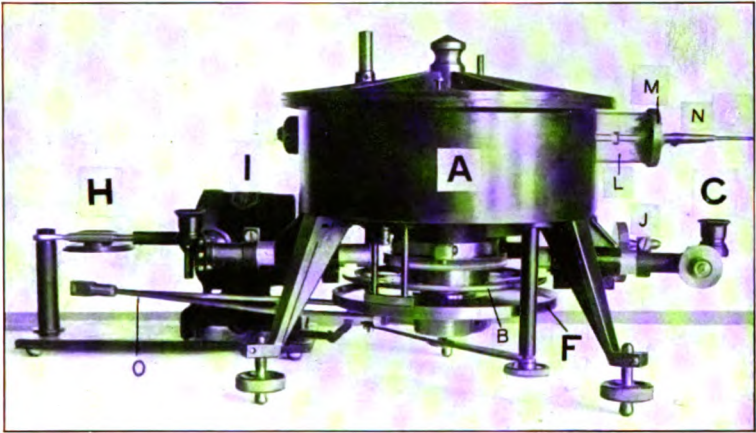
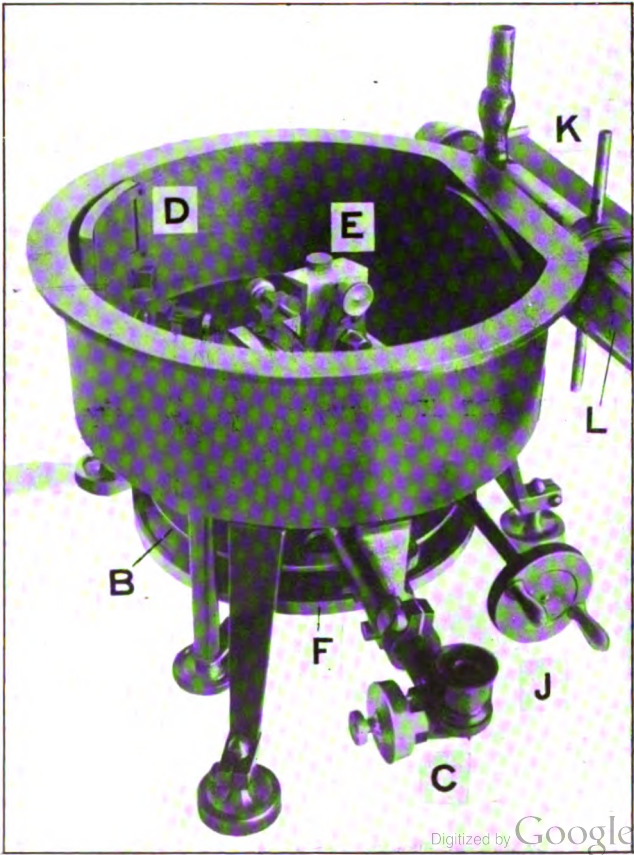
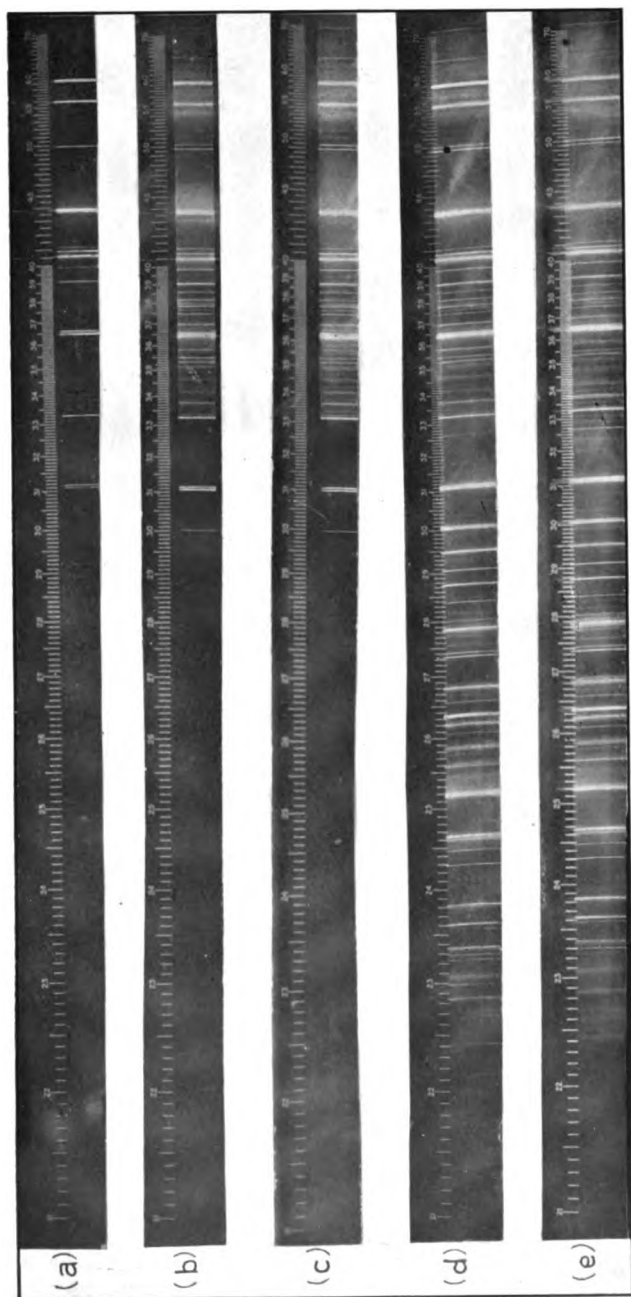


FIG. 2.





- (a) Non-concentrated Mercury Arc in Soft Glass.
- (b) Concentrated Mercury Arc in Pyrex Glass.
- (c) Same as (b) except at Wattage Twice as High.
- (d) Concentrated Mercury Arc in Transparent Quartz.
- (e) Same as (d) except at Wattage Twice as High.

THE
LONDON, EDINBURGH, AND DUBLIN
PHILOSOPHICAL MAGAZINE
AND
JOURNAL OF SCIENCE.

[SEVENTH SERIES.]

NOVEMBER 1927.

LXXX. *Experiments on the Rate of Evaporation of Small Spheres as a Method of Determining Diffusion Coefficients. —The Diffusion Coefficient of Iodine.* By BRYAN TOPLEY and ROBERT WHYTLAW-GRAY *.

Introduction.

EVAPORATION into a still atmosphere from the surface of a sphere of volatile material is a process governed by diffusion. The object of this communication is to describe an experimental method whereby observations of the rate of evaporation may be utilized to determine the diffusion coefficient. The method applies to the case of liquids and solids whose saturated vapour pressure does not exceed about 1 mm. at the temperature of the experiment, and requires the vapour pressure to be known with accuracy.

Stefan's general theory of diffusion ⁽¹⁾ applied to the evaporation of a sphere of finite size suspended freely at the centre of a spherical shell of absorbing material which maintains a zero concentration of the vapour at the surface of the absorbing material, leads to the result :

$$dm/dt = \frac{4\pi M \cdot D \cdot P}{\left(\frac{1}{r} - \frac{1}{r_0}\right)RT} \cdot \log_e \left\{ \frac{1}{1-p/P} \right\},$$

* Communicated by the Authors.

Phil. Mag. S. 7. Vol. 4. No. 24. Nov. 1927.

3 L

where dm/dt = the rate of evaporation in gms. per second.

M = the molecular weight of the vapour.

D = the diffusion coefficient of the vapour in gms. per second per sq. cm. at the total pressure P .

p = the saturation pressure of the vapour in dynes per sq. cm.

P = the total (constant) pressure of the atmosphere between the sphere and the absorbent in dynes per sq. cm.

r = the radius of the evaporating sphere.

r_0 = the radius of the spherical shell of absorbent.

R = the gas constant in ergs per degree.

T = the absolute temperature.

By differentiating, this can be re-written in terms of the surface of the sphere:

$$\int_{S_1}^{S_2} \left(1 - \frac{\sqrt{S}}{2r_0\sqrt{\pi}}\right) dS \\ = \frac{8\pi M \cdot D \cdot P}{\rho \cdot RT} \cdot \left(\log_e \left\{ \frac{1}{1-p/P} \right\}\right) \cdot (t_2 - t_1),$$

where S = the surface area, in cm. sq., of the sphere at t secs.

ρ = the density at T° of the sphere.

Thus, on plotting $\left[S - \frac{\sqrt{S^3}}{3r_0\sqrt{\pi}}\right]$ against t , a straight line

should be obtained, the slope of which determines the diffusion coefficient.

It was noticed originally by Sresnewsky⁽²⁾ that the rate of evaporation of a spherical droplet in air is directly proportional to its radius, and not to its surface; this was confirmed by Morse⁽³⁾, using solid spheres of iodine resting on the pan of a microbalance. Langmuir, in a paper discussing Morse's experiments, argued that if the evaporation of a small object in still air is controlled by diffusion and is analogous to the loss of heat from bodies of the same shape, then the rate of loss of mass of a freely-suspended sphere of volatile material should be given by the formula:

$$-\frac{dm}{dt} = \frac{4\pi M \cdot D}{RT} \cdot p \cdot r.$$

The equation deduced from Stefan's theory reduces to this expression for small values of the ratio p/P , and when r becomes infinite. Using this formula, Langmuir⁽⁴⁾ calculated the value of D for iodine diffusing in air at atmospheric pressure, and at 20° from Morse's experiments, obtaining as a rough approximation the value $\cdot 07$; this, he pointed out, is of the same order as the diffusion coefficient of other substances of high molecular weight, and therefore the result lends support to the view that evaporation under these conditions is determined by diffusion only. The equation,

$$\left[S - \frac{\sqrt{S^3}}{3r_0\sqrt{\pi}} \right]_{s_2}^{s_1} = \frac{8\pi M \cdot D \cdot P}{\rho RT} \cdot \left(\log_e \left\{ \frac{1}{1-p/P} \right\} \right) \cdot (t_2 - t_1),$$

applied to a pure substance evaporating symmetrically into a still atmosphere at constant temperature, relates the rate of evaporation to the diffusion coefficient at the pressure P and to the saturated vapour pressure of the pure substance in question; hence the experimental measurement, under carefully controlled conditions, of the rate of evaporation should serve to determine the diffusion coefficient if the vapour pressure is known; alternatively, the vapour pressure if an independent measure of the diffusion coefficient is available. A correction which takes account of the self-cooling of the evaporating sphere is discussed later.

When the radius of the sphere is small compared with the distance of the absorbent, the term $\frac{\sqrt{S^3}}{3r_0\sqrt{\pi}}$ can be neglected; so that for small values of the ratio p/P the equation becomes

$$-\frac{dS}{dt} = \frac{8\pi M \cdot D}{\rho \cdot RT} \cdot p.$$

As a close approximation, therefore, dS/dt should remain constant as the sphere evaporates. That this is true in practice was shown by Langmuir in connexion with Morse's experiments already mentioned, and in addition it has been found to hold for droplets of various pure liquids (see Whytlaw-Gray and Whitaker⁽⁵⁾).

A complete test of the relationship involves verifying experimentally the magnitude of the constant $\frac{8\pi M}{\rho \cdot RT}$; for this purpose measurements are required on a substance for which both the vapour pressure and the diffusion coefficient are known. The number of slightly volatile substances for

which sufficiently accurate data for the vapour pressure exist is very limited ; iodine, however, seemed to be a favourable case, since the vapour pressure is known with accuracy in the region of room temperature, and is such that the evaporation takes place at a rate convenient for measurement. Moreover, the chemical reactivity of iodine vapour makes it experimentally easy to measure the diffusion coefficient independently. For this reason it was decided to repeat Morse's experiments under strictly controlled conditions.

The experimental work consisted of two parts : first, the measurement of the rate of evaporation of small spheres of iodine at four temperatures ; and second, the independent determination of the diffusion coefficient at the same temperatures.

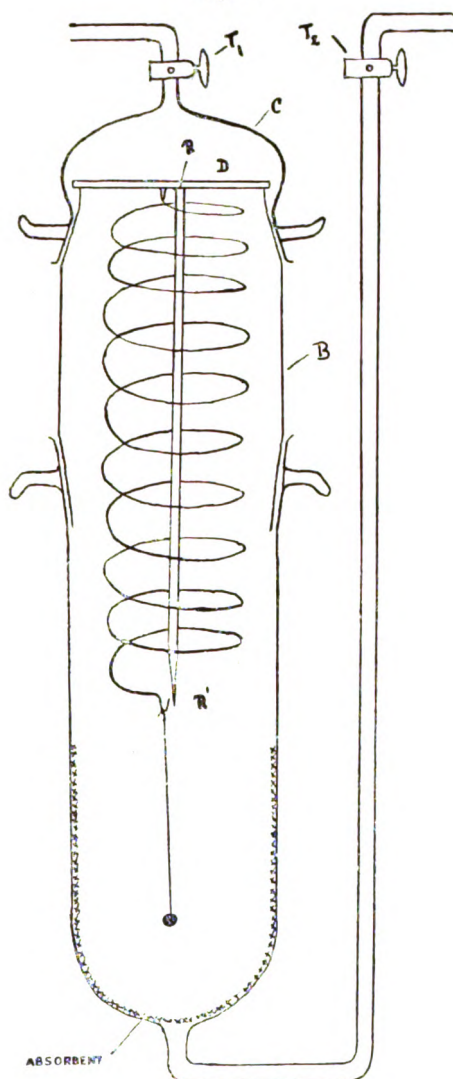
Measurement of the Rate of Evaporation of Iodine Spheres.

The diagram (fig. 1) shows the experimental arrangement used ; the essential part of the apparatus is a silica spiral spring made in the way described by H. Greville Smith ⁽⁶⁾. The spring, together with a reference rod RR', is sealed to the cross-bar D. The glass spring-balance case is made in three parts for ease of manipulation ; the cap C and the lower part of the cylindrical case are accurately ground on to the middle portion B. The particular spring used in the majority of the experiments was deliberately made comparatively insensitive, for two reasons : it was required to carry a relatively large load (up to 60 mgm.), and it was desired that the iodine sphere should evaporate completely without too great a change in the position of the sphere relative to the absorbent. A sensitivity of between 1 and 1.5 mgm. weight change for 1 mm. change in extension of the spring was found convenient ; the largest sphere investigated had an initial weight of 15 mgm., and the change in position when this evaporated completely was about 10 mm.

The spring was calibrated by the successive addition of aluminium wire weights, each of approximately 5 mgm. These were weighed separately on a Bender-Holbein micro-balance, in terms of a set of N.P.L. standardized weights. In addition they were compared among themselves by observing the extension produced by hanging each weight in turn on a spiral spring ; this was repeated with a second spring. In this way the sensitivity of the spring actually used was found for the required range of extension relative to the reference point R'. Settings were made by a microscope supplied by the Cambridge Scientific Instrument Co.,

alternately on the reference point and on the hook which terminates the spiral spring.

Fig. 1.



The spring-balance case was carried by a stand designed to allow the balance to be lowered very smoothly under the

surface of the water of a large thermostat fitted with a plate-glass window. The stand, thermostat, and micrometer microscope were mounted on a heavy marble slab, which in turn was supported on thick rubber bungs, to lessen vibration. The temperature was controlled to $1/200^{\circ}$ by a sensitive Lowry regulator. The taps T_1 and T_2 were closed after the spring balance had been in the thermostat long enough for temperature equilibrium to be established; the pressure P of the air in the balance case was taken as equal to the barometric height read at that moment.

The Iodine Spheres.—Ordinary "Resublimed" iodine was further purified by grinding with KI and subliming off the iodine (twice), and then re-subliming a third time at as low a temperature as possible. The spheres were obtained in the following way: a fine silica fibre was dipped repeatedly in the just molten iodine, until from 50 to 100 mgm. had solidified on the end of the fibre in an irregular-shaped lump. This was fused into a drop of molten iodine by touching it momentarily with the tip of a fine flame; this has the effect of causing a sudden vaporization of the greater part of the iodine, the remainder melting in the atmosphere of iodine vapour to a more or less spherical droplet, which solidifies to a small sphere; it was found that a good approximation to a spherical droplet could be obtained up to a weight of about 25 mgm.; droplets larger than this tended to fall off while still molten, or to become pear-shaped.

There exists the possibility that iodine solidifies from the molten state in an unstable form which subsequently changes over into the ordinary stable form; the point was directly tested by experiments in a dilatometer, and some evidence was obtained for a small change in density in solidified iodine during the first few hours after its solidification. Sufficient time was allowed to elapse before beginning the evaporation for this change to be completed.

A thin layer of fused potassium hydroxide was used to absorb the iodine vapour; this adjusts the partial pressure of water-vapour in the spring-balance case to that of the lowest hydrate of KOH; the iodine spheres were thus evaporating in air with less than the normal amount of water-vapour, while the independent determinations of D carried out in tubes refer to the air of the laboratory, since metallic absorbents were used. This, however, could scarcely make a sufficient difference to be observed. In a few experiments copper gauze was used instead of potassium hydroxide; no difference could be traced to the change.

The correction for the self-cooling of the evaporating sphere

must now be considered. In the present experiments the vapour pressure of the iodine at the highest temperature (30°) is less than 0.5 mm., and the pressure of the air through which the iodine diffuses is atmospheric, so that

$P \cdot \log_e \left\{ \frac{1}{1-p/P} \right\}$ may be taken as equal to p with sufficient accuracy. The diffusion coefficient is then calculated from

$$\frac{\left[S - \frac{\sqrt{S^3}}{3r_0\sqrt{\pi}} \right]_{S_1}^{S_2}}{(t_2 - t_1)} = \frac{8\pi M}{\rho \cdot RT} \cdot (D \cdot p).$$

The left-hand side of this equation is an experimentally measured quantity, which should be constant over the "life" of the evaporating sphere, provided that p remains constant; this depends upon whether the cooling of the sphere below the thermostat temperature is independent of the surface area of the sphere.

The extent of the self-cooling is readily calculated by equating the rate at which heat flows into the sphere to the rate at which heat is being rendered latent by the evaporation

$$dH/dt = -\frac{dS}{dt} \cdot \sqrt{S} \cdot \frac{\rho}{4\sqrt{\pi}} \cdot \frac{\lambda}{M},$$

where dH/dt = the rate at which the sphere is absorbing heat, in calories per second,

λ = the latent heat of evaporation, in calories per gm. molecule.

Heat can reach the sphere in three ways :

- (1) By conduction through the gas ;
- (2) by conduction through the suspending fibre ;
- (3) by radiation from the absorbent.

The complete equation is then

$$-\frac{dS}{dt} \cdot \sqrt{S} \cdot \frac{\rho\lambda}{M \cdot 4\sqrt{\pi}} = [T_2 - T_1] \left\{ \frac{4\pi k}{2\sqrt{\pi} - \frac{1}{r_0}} + \frac{\gamma\pi a^2}{r_0} \right\} + S \cdot 2\pi \int_0^\infty \{ f(\nu, T_2) - f(\nu, T_1) \} \nu d\nu$$

where T_1 = the temperature of the sphere.

T_2 = the temperature of the absorbent.

k = the specific conductivity of the gas through which diffusion takes place.

a = the radius of the suspending fibre.

γ = the thermal conductivity of the material of the fibre.

α_ν = the absorption coefficient of the material of the sphere for radiation of frequency ν .

$f(\nu, T)$ = the Planck radiation function.

The term $\frac{\gamma \pi a^2}{r_0} \cdot [T_2 - T_1]$ representing the conduction through the fibre is not quite exact, since the temperature gradient in the gas surrounding the fibre is not linear. If the (silica) fibre is sufficiently fine, the conduction through the fibre may be neglected except when the sphere becomes very small, as is shown by the calculation given after the data of Exp. 32 (Table I.).

The term representing the effect of radiation assumes

TABLE I.

Exp. 32. Temp. 30.05°C . P=761.1 mm.

S (cm. ²).	$\left[S - \frac{\sqrt{S^3}}{3r_0\sqrt{\pi}} \right]$.	$\frac{(t_2 - t_1)}{\text{seconds.}}$	$\frac{\left[S - \frac{\sqrt{S^3}}{3r_0\sqrt{\pi}} \right]_{S_1}}{(t_2 - t_1)_{S_2}}$.
·05134	·05025	0	
·04843	·04743	1140	2.47×10^{-6}
·04289	·04204	3180	2.58 "
·03070	·03019	7920	2.53 "
·02520	·02482	10020	2.54 "
·01465	·01448	14040	2.55 "
·00830	·00823	16920	2.48 "

$$\text{Average value} = 2.525 \times 10^{-8}$$

Hence $(Dp) = 49.26$

and $(T_2 - T_1) = 0.481^\circ$, \therefore Temp. of sphere = 29.57°C .
taking $k = 6.12 \times 10^{-6}$ and $p = 0.451 \text{ mm}$.

taking $k = 6.12 \times 10^{-6}$ and $p = 0.451$ mm.
for air at 30.05°C .

and $\left. \begin{array}{l} \lambda = 15100 \text{ cal.} \\ \rho = 4.93 \end{array} \right\} \text{ for iodine at } 30.05^\circ \text{ C.}$

\therefore D corrected to P=760 mm. = .0820.

$$dH/dt = 8.498 \times 10^{-6} \text{ calorie/per second,}$$

for $S = .00830 \text{ cm}^2$.

Maximum value of conduction through the silica fibre

$$= 6.798 \times 10^{-8} \text{ cal. per sec.,}$$

taking $a = .005$ cm.

 $\gamma = .0036.$

TABLE I. (continued).

Exp. 28. Temp. 20.00° C. $p = 757.8$ mm.

S (cm. ²).	$\left[s - \frac{\sqrt{s^3}}{3r_0\sqrt{\pi}} \right]$.	$(t_2 - t_1)$ seconds.	$\frac{\left[s - \frac{\sqrt{s^3}}{3r_0\sqrt{\pi}} \right]_2^1}{(t_2 - t_1)}$.
·09061	·08805	0	
·08841	·08594	1800	1.17×10^{-8}
·08600	·08363	3840	1.15 "
·08095	·07878	8100	1.14 "
·07411	·07209	13560	1.18 "
·07108	·06930	16350	1.15 "
·06455	·06301	21840	1.15 "
·05591	·05467	29169	1.14 "
·04698	·04602	36960	1.14 "
·03550	·03487	46410	1.15 "
·02336	·02791	52980	1.14 "

Average value = 1.15×10^{-8}

Hence (Dp) = 21.66. ∴ Temp. of sphere = 19.775° C.
 and $(T_2 - T_1) = 0.225^\circ$, and $p = 1961$ mm.
 taking $k = 5.969 \times 10^{-5}$ for air at 20.00° C.
 and $\lambda = 15100$ cal. } for iodine at 20.00° C.
 $\rho = 4.93$

∴ D corrected to P = 760 mm. = .0824.

$dH/dt = 1.456 \times 10^{-5}$ calorie per second,

for S = .09061 cm.²

Maximum amount of heat radiation to the sphere
 = 2.98×10^{-6} cal. per sec.

selective absorption by the sphere of certain frequencies ; it cannot be evaluated without a knowledge of the infra-red absorption of iodine. However, by taking $\alpha_r = \alpha = 1$, an upper limit is obtained for the rate at which heat can reach the sphere in the form of radiation for a given temperature difference ; since if the sphere behaves as a perfectly black body, the net rate of absorption of radiation is given by

$$S \cdot \sigma \cdot [T_2^4 - T_1^4],$$

where σ = Stefan's constant = $1.38 \cdot 10^{-12}$ cal.cm.⁻²sec.⁻¹.

The greatest value that $(T_2 - T_1)$ can have in a given experiment must be less than that obtained by calculating it on the assumption that only conduction through the gas is operating to carry heat to the sphere. In this way an upper limit is found for the relative magnitude of the radiation term. The data of Exp. 28 (Table I.) show that

even when the sphere is comparatively large the radiation is not very important, and it diminishes with S . Since iodine is a bad conductor of electricity, it is probable that the absorption coefficient for infra-red radiation of the wave-lengths which are important at room temperature is much less than unity, and consequently the importance of the radiation term is still further diminished.

As applied to these experiments with iodine, the equation can now be simplified to

$$[T_2 - T_1] = \left\{ \left[S - \frac{\sqrt{S^3}}{3r_0\sqrt{\pi}} \right]_{s_2}^{s_1} / (t_2 - t_1) \right\} \times \frac{\lambda \cdot \rho}{8\pi M \cdot k} = \frac{(D \cdot p)\lambda}{RT_2 k}$$

It is concluded, therefore, that the lowering of temperature is independent of the size of the sphere over the range for which measurements are made. This conclusion is borne out by the results tabulated below for two typical experiments,

in which the observed values of $\left\{ \left[S - \frac{\sqrt{S^3}}{3r_0\sqrt{\pi}} \right]_{s_2}^{s_1} / (t_2 - t_1) \right\}$

are seen to be constant while the sphere evaporates down to about one-tenth of its initial mass. The correction for the self-cooling of the sphere is then obtained by first calculating the value of the product (pD) from the experimental line; the lowering in temperature $(T_2 - T_1)$ is found from this value of (pD) . The value of p appropriate to the *corrected* temperature of the sphere is then used to calculate D .

This leaves out of account the small change in D itself resulting from the fact that the atmosphere through which diffusion takes place is at a temperature varying between T_2 and T_1 ; but the difference produced by this is outside the experimental accuracy of the method. The possible effect of convection set up by the cooled sphere is discussed later.

The fluctuations about a mean of the figures in the last column in Exps. 32 and 28 are caused mainly by errors in setting the microscope, produced by slight irregularities in the glass of the spring-balance case. In any particular experiment the mean is probably accurate to within 0.5 per cent.

Strictly, the sphere should be kept at the centre of a spherical spell of absorbent: actually, since in these experiments the iodine sphere moves upwards as the spring contracts during the evaporation by as much as 1 cm., the absorbent was placed on the inside of the cylindrical case, the absorbent layer being continued to a height well above the sphere. It was calculated for the particular apparatus.

used that the cylindrical layer of absorbent with its hemispherical cap was equivalent, sufficiently nearly, to a sphere of radius 2 cm.

The vapour pressure of iodine at the different temperatures employed has been found by interpolation from the data of Baxter, Hickley, and Holmes⁽⁷⁾.

The density of solid iodine has been taken as 4.93, as a mean value for the four temperatures (International Critical Tables). The values for the diffusion constant (fully corrected) are contained in Table II.

TABLE II.

Evaporation of Iodine Spheres.

Temperature 30.05°.	Temperature 25.05°.
D at 760 mm.	D at 760 mm.
.0840	.0815
.0851	.0817
.0854	.0822
.0851	.0815
.0832	.0819
.0820	.0834
.0847	.0829
.0873	.0840
	.0824
Average0846	Average0824
Temperature 20.00°.	Temperature 14.00°.
D at 760 mm.	D at 760 mm.
.0817	.0760
.0822	.0789
.0829	.0820
.0823	.0779
.0831	.0782
.0824	
Average0824	Average0786

The Diffusion Coefficient of Iodine.

The data in the literature for the diffusion coefficient of iodine vapour in air are scanty and somewhat discordant. Apart from the rough calculation made by Langmuir from Morse's experiments, the only diffusion measurements in air appear to be those of E. Mack⁽⁸⁾, who found the value $D = .108$ in air at 25° and 760 mm. It seemed difficult to reconcile this figure with the experiments of Mullaly and Jacques⁽⁹⁾ on the rate of diffusion of iodine vapour in pure nitrogen, at pressures ranging from 9 to 19 mm. and at 20°.

Mack, making allowance for the difference between the cross-section of the average air molecule and the nitrogen molecule, calculated that the diffusion coefficient to be expected in the air at 25° and 760 mm. would be '075. The discrepancy is unexpectedly large. The method adopted in Mack's experiments was to allow the iodine vapour to diffuse from the surface of solid iodine contained in a small glass cup; the ground edge of the cup was placed in contact with the ground edge of a glass tube through which the diffusion took place to an absorbing medium (soda-lime or charcoal) at the other end of the tube. The weight of iodine evaporating in a known time was found from the loss in weight of the glass cup containing the iodine. An attempt was made to repeat these experiments, but it was found impossible to get concordant results; an appreciable leakage of iodine vapour takes place at the junction of the edge of the cup and the edge of the diffusion tube, because of the large gradient in the partial pressure of iodine vapour across the junction. When the diffusion tube was surrounded by a closely-fitting sleeve of copper foil, the escaping iodine produced a deposit of cuprous iodide on the copper opposite to the junction of the iodine cup and the tube; the formation of this protective layer and the consequent decrease in the gradient of iodine vapour concentration across the junction explains the observation that the apparent rate of diffusion diminished as the duration of the experiment was increased. Possibly the high value for D found by Mack was caused by a similar leakage.

The experimental arrangement was therefore modified as follows:—Iodine vapour from the surface of iodine fused into a glass cup diffuses downwards through a silica tube, being absorbed at the bottom by a suitable absorbent; the diffusion tube and iodine cup are enclosed in a copper tube fitted with a tap and kept in a thermostat. The weight of iodine diffusing in a known time is found by weighing the silica tube plus absorbent before and after the experiment. Since the absorbent has to be weighed, soda-lime is unsuitable; charcoal suffers from the disadvantage that it gives up adsorbed air as it adsorbs iodine; suitable absorbents were found to be silver powder (prepared electrolytically, and by reduction of silver nitrate solution with formaldehyde) and copper powder.

The diffusion coefficient is calculated from Stefan's formula :

$$D = \frac{m \cdot l}{q \cdot t} \cdot \frac{1}{c \log_e \left(\frac{c}{c - c_s} \right)},$$

where m = the mass in gms. of iodine diffusing in t seconds

μl = the length of the diffusion tube in cms.

q = the cross-section of the tube in cm.^2

c = the total (constant) concentration of the gas in the tube, in gm. molecules per c.c.

c_s = the partial concentration of saturated iodine vapour in gm. molecules per c.c.

Two different silica tubes were used :

(1) $q = 2.758 \text{ cm.}^2$ Length = 15.5 cm.

(2) $q = 2.560 \text{ cm.}^2$ Length = 9.5 cm.

The actual value of l in any particular experiment was less than the length of the tube used by the depth of the layer of absorbent at the bottom of the tube, and was measured to the nearest 1/100th cm.

The extent of adsorption of iodine vapour on to the inside of the silica tube during the diffusion was tested by blank experiments in which the iodine cup was left in position on the tube for the usual duration of an experiment, but no absorbent was placed inside. The gain in weight amounted to about 1/10th mgm., while the weight of iodine diffusing in an experiment was usually 10 to 15 mgms. To eliminate this error arising from adsorption, diffusion was allowed to go on for some hours before weighing the tube plus absorbent for the first time, thus saturating the silica surface before the experiment.

The results are given below in Table III. The diffusion coefficients have been reduced to the values which they would have at 760 mm. of air. Except in the last two experiments, the diffusion was done at atmospheric pressure. The last two experiments, at 14° and 38 mm. air pressure, are in agreement with the mean of those done at atmospheric pressure and at the same temperature ; since the actual rate of evaporation of the iodine is 20 times as great at 38 mm. as at atmospheric pressure, and any surface cooling of the solid iodine would be greatly magnified, the concordance between the results at the two pressures shows that any such cooling is negligible.

The experiments themselves supply evidence that all the iodine is removed as soon as it diffuses on to the surface of the metal absorbent, so maintaining there a zero concentration of iodine vapour : first, the period of diffusion was lengthened in a few cases (so that the amount of iodine absorbed was increased) without producing a decrease in

the value obtained for D. Thus the progressive saturation of the active surface does not proceed beyond a safe limit. Second, the different forms of silver and copper absorbent lead to the same numerical result for D.

TABLE III.
Experiments in Tubes.

Temperature 30·05°.			Temperature 25·05°.		
Absorbent.	Tube.	D at 760 mm.	Absorbent.	Tube.	D at 760 mm.
Electrolytic Silver. }	(2)	·0850	Reduced Silver	(1)	·0802
" ...	(2)	·0854	Electrolytic Silver. }	(1)	·0797
" ...	(2)	·0867	" ...	(1)	·0789
" ...	(2)	·0855	" ...	(1)	·0786
Reduced Silver	(2)	·0852	" ...	(2)	·0793
" "	(2)	·0870	" ...	(2)	·0830
" "	(2)	·0849	" ...	(2)	·0796
Copper Filings	(2)	·0853	Reduced Silver	(2)	·0807
Average		·0856	" "	(2)	·0827
Average			Average		
Temperature 20·00°.			Temperature 14·00°.		
Absorbent.	Tube.	D at 760 mm.	Absorbent.	Tube.	D at 760 mm.
Electrolytic Silver. }	(2)	·0781	Reduced Silver	(2)	·0763
" ...	(2)	·0801	" "	(2)	·0735
" ...	(2)	·0794	" "	(2)	·0755
" ...	(2)	·0787	" "	(2)	·0724
Copper Filings	(2)	·0815	" "	(2)	·0750
" "	(2)	·0774	" "	(2)	·0745
Average		·0792	" "	(2)	·0761
Average			Average		
			(38 mm.)		
			Average		
			·0748		

TABLE IV.

Temperature °C.	D from "tube" experiments at P = 760 mm.	D from "sphere" experiments at P = 760 mm.	Mean value of D at 760 mm.
30·05°	·0856	·0846	·0851
25·05°	·0804	·0824	·0814
20·00°	·0792	·0824	·0808
14·00°	·0748	·0786	·0767

Discussion of Results, and Sources of Error.

The experiments with evaporating spheres and the experiments in tubes are compared in Table IV. At $30\cdot05^{\circ}$, $25\cdot05^{\circ}$, and $20\cdot00^{\circ}$ the discrepancy between the two values for D is not much greater than would be anticipated from the variations in the results of individual experiments recorded in Tables II. and III. The variation in the results for the iodine spheres is probably to be attributed to two main causes first: the difficulty of obtaining a perfect sphere, and second, the effect of vibration of the apparatus, which upsets the symmetry of the diffusion gradient. Both of these would tend to make the value of D too large. In the tube experiments the main source of error is inaccuracy in the weighings.

The figure $\cdot0786$, obtained from the evaporation of spheres at $14\cdot00^{\circ}$, is very probably too high because the longer duration of the experiments at this temperature made it impossible to complete an experiment during a part of the day when the laboratory was comparatively free from vibration through local traffic.

An important point is that the discrepancy between the "sphere" experiments and the "tube" experiments does not increase at the higher temperatures, although the degree of self-cooling is greater; this must mean that the correction for self-cooling is adequate, and that any convection currents set up by the cooling of the sphere are not sufficient to affect seriously the results. The fact that (both for the "sphere" and the "tube" experiments) the decrease in D between $25\cdot05^{\circ}$ and $20\cdot00^{\circ}$ is too small may be due to an error in the relative values assumed for the vapour pressure of iodine at these temperatures: Baxter, Hickley, and Holmes do not give measurements for the vapour pressure between 15° and 30° , and this gap was covered by interpolation, after smoothing their experimental data by means of the Ramsay and Young formula against Knudsen's formula for the vapour pressure of mercury as a reference substance.

The results of these experiments are not sufficiently exact to give an accurate measure of the temperature coefficient of the rate of diffusion, but an approximate figure may be obtained; assuming that D varies as T^n , then from the mean values of D in the last column of Table IV., $n=2\cdot0$.

It is concluded from these experiments that the method of allowing small spheres suspended from a silica micro-balance to evaporate under definite conditions is capable of giving results for the diffusion coefficient accurate to about 2 or 3 per cent., and under favourable conditions (*e.g.* with

liquid drops, which are more accurately spherical, and with greater freedom from vibration) to within 1 per cent.

We have pleasure in expressing our thanks to Dr. F. R. Goss for the use of a Bender-Holbein microbalance, and to Messrs. Brunner and Mond for a grant which defrayed part of the cost of the apparatus.

References.

- (1) J. Stefan, *Wien. Ber.* lxx. p. 323 (1872).
- (2) Sresnewsky, *Beibl. Ann. Phys. Chemie*, vii. p. 888 (1883).
- (3) Morse, *Proc. Am. Acad. Arts Sci.* xlv. p. 363 (1910).
- (4) Langmuir, *Phys. Rev.* xii. p. 368 (1918).
- (5) Whytlaw-Gray & Whitaker, *Proc. Leeds Phil. Soc.* i. p. 97 (1926).
- (6) H. Greville Smith, 'Nature,' cxvi. p. 14 (1925).
- (7) Baxter, Hickley, & Holmes, *J. A. C. S.* xxix. p. 127 (1907).
- (8) E. Mack, *J. A. C. S.* xlvii. p. 2468 (1925).
- (9) Mullaly & Jacques, *Phil. Mag.* lxxviii. p. 1105 (1924).

Summary.

(1) An experimental arrangement is described for measuring the rate of evaporation of freely-suspended spheres of volatile material.

(2) The calculation of the diffusion coefficient of the vapour, and the correction for the self-cooling of the sphere, are discussed.

(3) The diffusion coefficient of iodine vapour in air has been measured over the temperature range from 14° to 30°.

The University, Leeds.

LXXXI. *The Warming of Walls.* By A. F. DUFTON, M.A.,
D.I.C. (*The Building Research Station*) *.

1. **I**T is well known that some rooms are not readily warmed. Complete analysis of the warming of a room is not easy. The influence, however, of the fabric of a wall is shown by the time taken to warm the surface when heat is supplied to it at a constant rate.

2. For simplicity a homogeneous wall (of thickness d , conductivity k and diffusivity h) initially at uniform temperature is considered. The rate of heating chosen is $2T k/d$, twice that necessary to maintain the desired temperature difference T between the faces of the wall, and the temperature of the second face is assumed to be constant.

* Communicated by the Author.

In time t the temperature of the wall at distance x from the heated surface increases by

$$T \left\{ 2 - \frac{2x}{d} - \frac{16}{\pi^2} \sum_0^{\infty} (2n+1)^{-2} e^{-(2n+1)^2 \pi^2 k t / 4d^2} \cos (2n+1) \pi x / 2d \right\}.$$

The rise at the surface, the limit of this as x tends to zero, is

$$T \left\{ 2 - \frac{16}{\pi^2} \sum_0^{\infty} (2n+1)^{-2} e^{-(2n+1)^2 \pi^2 k t / 4d^2} \right\}$$

and attains the value T when

$$\frac{16}{\pi^2} \sum_0^{\infty} (2n+1)^{-2} e^{-(2n+1)^2 \pi^2 k t / 4d^2} = 1,$$

approximately after a time $d^2/5h$.

For a nine-inch brick wall the time is 6 hours : for a (one inch) wall of wood affording the same insulation 10 minutes.

3. The warming of a laminated wall depends largely upon the material at the heated surface. A room with masonry walls is much more readily warmed if lined with wood or other insulation of small thermal capacity.

LXXXII. *Bubbles and Drops and Stokes' Law.* By W. N. BOND, M.A., D.Sc., F.Inst.P., Lecturer in Physics, University of Reading*.

[Plate XIX.]

Summary.

THIS paper extends Stokes' calculations for the slow rectilinear motion of a solid sphere through viscous fluid, in the way he outlined, to the case where the sphere is composed of fluid. Experiments on the rate of rise of air bubbles in water-glass and in golden syrup, and on the velocity of the fluid in the neighbourhood of the bubbles in the former liquid, are in substantial agreement with the prediction that the bubble should rise one and a half times as fast as it would if it were solid. A smaller number of experiments on air bubbles and drops of syrup in castor oil also show reasonable agreement with theory. But those on water bubbles in castor oil indicate an effect due to surface contamination.

* Communicated by the Author.

Incidentally, the measured velocities of the fluid near steel spheres give a reasonably good check on Ladenburg's correction for the effect of the walls of the containing vessel.

INTRODUCTION.

STOKES' * mathematical investigation of the slow motion of a solid sphere through viscous liquid is well known. It has been the basis of a most useful method of determining viscosities †, as well as of a method of estimating the diameter of very small spheres ‡.

There is good evidence to show that, as Stokes assumed, there is no slip of the fluid at the surface of a solid sphere, except when surrounded by a gas at low pressure. When, however, the slow motion of a spherical gas bubble (or drop of liquid) through another fluid is concerned, there will probably be in general a finite tangential velocity of the fluid just inside and outside the spherical surface. The circulation of the fluid inside the sphere would therefore have to be taken into account in deducing the terminal velocity of a rising gas bubble or rising or falling liquid drop. Further, it is likely that the spherical surface of contact between the two fluids might itself offer a resistance to such tangential velocities (at any rate if the surface were contaminated). These two facts are specifically mentioned by Stokes §, though he does not complete the working-out of the theory.

This paper contains : firstly, a development of the theory given by Stokes ; secondly, an account of experiments on the terminal velocity of rising air bubbles and falling drops of liquid ; and thirdly, an account of measurements of the velocity of the surrounding liquid in the neighbourhood of rising air bubbles.

THEORY.

When a solid sphere of radius a moves with a uniform velocity V_{∞} through a large extent of fluid of density ρ and viscosity μ , then, provided we have ||

$$\frac{V_{\infty} a \rho}{\mu} < 0.6, \quad (1)$$

* 'Mathematical and Physical Papers,' iii. pp. 55-59.

† Gibson & Jacobs, Journ. Chem. Soc. cxvii. p. 473 (1920).

‡ J. J. Thomson, Phil. Mag. (5) xlvi. p. 528 (1898). Millikan, 'The Electron,' p. 46 etc.

§ *Loc. cit.* pp. 61-62.

|| H. D. Arnold. See Millikan, 'The Electron,' p. 96.

turbulence will not occur and the kinetic energy of the liquid may be neglected. The general nature of this result may be predicted by dimensional considerations; and a similar condition should also be required for the flow inside a drop or bubble to be purely viscous. These conditions are supposed fulfilled in all the following theory.

In place of considering a falling drop or rising bubble, we will suppose the drop or bubble at rest and the liquid moving. Taking polar coordinates, with origin at the centre of the sphere and axis towards the arriving fluid, we have for the surrounding fluid a stream function of the form *

$$\psi = (Ar^{-1} + Br + Cr^2 + Dr^4) \sin^2 \theta. \quad . \quad . \quad (2)$$

The components of the fluid velocity resolved in an axial plane along and perpendicular to the radius are respectively

$$\left. \begin{aligned} R &= 2(Ar^{-3} + Br^{-1} + C + Dr^2) \cos \theta, \\ \Theta &= (Ar^{-3} - Br^{-1} - 2C - 4Dr^2) \sin \theta. \end{aligned} \right\} \quad . \quad . \quad (3)$$

The components in the directions r, θ of the pressure of the sphere on the fluid are respectively

$$\left. \begin{aligned} P_r &= (12Aa^{-4} + 6Ba^{-2} + 12Da) \mu \cos \theta, \\ T_\theta &= (6Aa^{-4} + 6Da) \mu \sin \theta, \end{aligned} \right\} \quad . \quad . \quad (4)$$

and the resultant force exerted by the outer fluid on the sphere on account of the motion is

$$-8\pi\mu B. \quad . \quad . \quad . \quad . \quad . \quad (5)$$

A set of equations similar to (2), (3), and (4), but with A, B, μ , etc. replaced by dashed letters, applies to the fluid inside. The conditions at a distance require

$$D = 0, \quad C = -\frac{1}{2}V_\infty;$$

and for the velocity not to be infinite at the origin we have

$$A' = 0, \quad B' = 0.$$

The other constants are determined by the conditions of no radial velocity at the surface, continuity of tangential velocity, and equality of the tangential component of pressure.

Thus, when $r=a$, we have

$$R = 0, \quad R' = 0, \quad \Theta = \Theta', \quad T_\theta = T_\theta'.$$

(The last of these conditions will not be true if the surface

* Stokes, *loc. cit.* pp. 55, 56, 59, and 31.

itself resists tangential stresses, the effect being as if the viscosity of the fluid inside had been increased. Also the normal component of pressure at the spherical surface is not the same in the two liquids, so the sphere will be very slightly distorted.)

Hence we obtain

$$A = -\frac{\mu'}{\mu + \mu'} \cdot \frac{a^3 V_\infty}{4}, \quad B = \frac{2\mu + 3\mu'}{\mu + \mu'} \cdot \frac{a V_\infty}{4},$$

$$C' = \frac{\mu}{\mu + \mu'} \cdot \frac{V_\infty}{4}, \quad D' = -\frac{\mu}{\mu + \mu'} \cdot \frac{V_\infty}{4a^2}.$$

It will be convenient to transform equations (3) and (5), and at the same time to return to the case where the sphere moves through liquid which is at rest at a distance.

We then obtain for the liquid outside, when the centre of the sphere is just passing the origin,

$$\left. \begin{aligned} R &= V_\infty \left\{ k \left(\frac{3}{2} \frac{a}{r} - \frac{1}{2} \frac{a^3}{r^3} \right) + (1-k) \frac{a^3}{r^3} \right\} \cos \theta, \\ \Theta &= V_\infty \left\{ k \left(-\frac{3}{4} \frac{a}{r} - \frac{1}{4} \frac{a^3}{r^3} \right) + (1-k) \left(\frac{1}{2} \frac{a^3}{r^3} \right) \right\} \sin \theta. \end{aligned} \right\} \quad (6)$$

The force on the sphere due to the motion becomes

$$6\pi k V_\infty a \mu, \quad . \quad . \quad . \quad . \quad . \quad . \quad (7)$$

and equating this to the gravitational force $\frac{4}{3}\pi a^3(\rho' - \rho)g$, the velocity of free fall becomes

$$V_\infty = \frac{1}{k} \left\{ \frac{2}{9} \frac{(\rho' - \rho)ga^2}{\mu} \right\} \quad . \quad . \quad . \quad . \quad . \quad (8)$$

where ρ' and ρ are the densities of the fluid inside and outside.

The equations (6), (7), and (8) do not assume continuity of tangential force and velocity at the surface of the sphere. But by assuming these conditions, used above to deduce A and B, we obtain

$$k = \frac{2/3 + \mu'/\mu}{1 + \mu'/\mu} \quad . \quad . \quad . \quad . \quad . \quad (9)$$

Equations (6) to (9) show that when μ' is large compared with μ , $k=1$ and the whole reduces to the case of a solid sphere, with no tangential velocity at the surface of the sphere. When, however, μ'/μ becomes small, we have $k=\frac{2}{3}$, and the sphere moves one and a half times as fast as a solid sphere of the same density. The terms in a^3/r^3 have now vanished, and there is no tangential component of pressure at the surface of the sphere.

Before describing the experiments, the effect of the walls of the vessel containing the fluid must be considered. When a solid sphere falls down the centre of liquid contained in a vertical cylinder, the mean velocity during the middle third of the path, V , may (according to Ladenburg *) be used to deduce V_∞ thus:

$$V_\infty = V \left(1 + 2.4 \frac{a}{R} \right) \left(1 + 3.3 \frac{a}{h} \right), \quad . \quad . \quad (10)$$

where R is the radius and h the total length of the cylinder of liquid. Since it is only the terms in a/r in equations (6) which represent appreciable velocities at a distance, these are the only terms that will contribute measurably to the wall correction. Hence for a drop or bubble we may use a modified correction:

$$V_\infty = V \left(1 + 2.4 k \frac{a}{R} \right) \left(1 + 3.3 k \frac{a}{h} \right). \quad . \quad . \quad (11)$$

EXPERIMENTS I. *Terminal Velocities.*

In these experiments a vertical brass box of internal cross-section 4.75 cm. square was used, the total length of liquid column being generally about 13 cm. Two adjacent sides of the box had plate glass windows fitted, and at the centre of the base was a glass tube for the production of air bubbles of suitable size. The rate of rise of the air bubbles (or of the movement of liquid drops) was measured with a travelling microscope. The diameter of the bubbles was found both by a horizontal travel of the microscope and also by multiplying the velocity of the bubble by the time it took to move a distance equal to its own diameter. Various forms of illumination were used, but chiefly a white central background with the sides dark. The temperature of the liquid was read with a sensitive thermometer at one corner of the box; and the viscosity of the liquid was found by timing the rate of fall of ball bearings (of various sizes) before and after each measurement on a bubble or drop.

The substantial accuracy of the wall correction and the constancy of the viscosity at different rates of shear were thus verified. Any slight lack of homogeneity of the liquid was made to have little effect, by the bubble and steel sphere traversing the same part of the liquid. The condition of equation (1) was satisfied in all experiments for the surrounding liquid, and also in all cases $V_\infty a \rho' / \mu'$ was small compared with unity.

* Ladenburg, *Ann. der Physik*, (4) xxii. p. 287 (1907); xxiii. p. 447 (1907).

Most of the experiments were carried out using air bubbles rising in commercial "water-glass" (sodium silicate), in water-glass slightly diluted with water, and in commercial "golden syrup." The viscosities of these liquids were from about 2000 to 400 c.g.s.

Discarding some of the first less accurate observations (which fluctuated more, but had about the same mean value), the results of these tests were as follows:—

Values of $1/k$.

Air in Water-glass.	Air in diluted Water-glass.	Air in Golden syrup.
1.58	1.13	1.47
1.41	1.46	1.43
1.45	1.40	1.42
1.49	1.31	1.39
1.30	1.67	1.46
1.50	1.56	1.41
1.38	1.37	
Means ...	1.44	1.43

The general mean of all the measurements gives $1/k = 1.43$. This does not differ from the theoretical value of 1.50 (μ'/μ very small) by more than can be accounted for by the fluctuation of the results. But these fluctuations, though partly due to experimental errors, may quite possibly have been contributed to by varying amounts of contamination of the surface of the bubble. (It may be remarked in passing that the above values of $1/k$ had been determined before the theoretical value of 1.50 had been deduced.)

Later, a smaller set of experiments was carried out using air, water, and golden syrup in castor oil. The very small air bubbles gave a value of approximately $1/k = 1.5$. The other results were as follows:—

Values of $1/k$.

Water in Castor oil.	Golden syrup in Castor oil.
1.16	—
1.12	—
1.23	1.08
1.13	0.99
1.14	1.11
Means ...	1.16

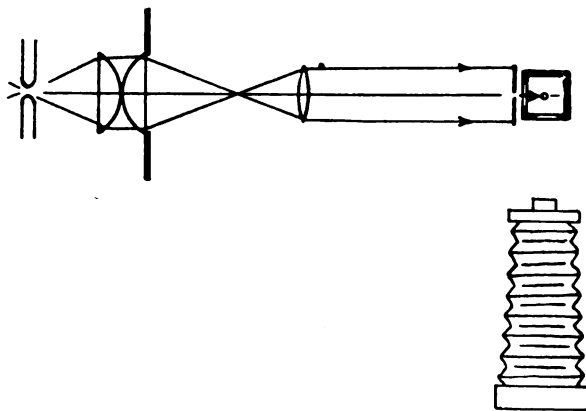
These would have been expected to be about 1.50 and

1.00 respectively. It must be presumed that surface contamination has prevented frictionless motion over the surface of the water-drop, and has on the other hand possibly allowed some slip at the surface of the drop of golden syrup.

EXPERIMENTS II. *Motion of the Fluid near the Bubble.*

The vessel used in the previous experiments was now filled with "water-glass" in which a number of very small air bubbles had been produced. A horizontal parallel beam of light from an arc lamp fell normally on one of the two glass windows, passing through a narrow vertical slit fixed centrally on the window. In this way light fell only on all the small air bubbles in a vertical plane passing through the centre of the rising bubble experimented on. The motion of the bubble and of the very small bubbles in this plane was recorded photographically, using a camera facing the second window (shown diagrammatically in plan in fig. 1). Fig. 2

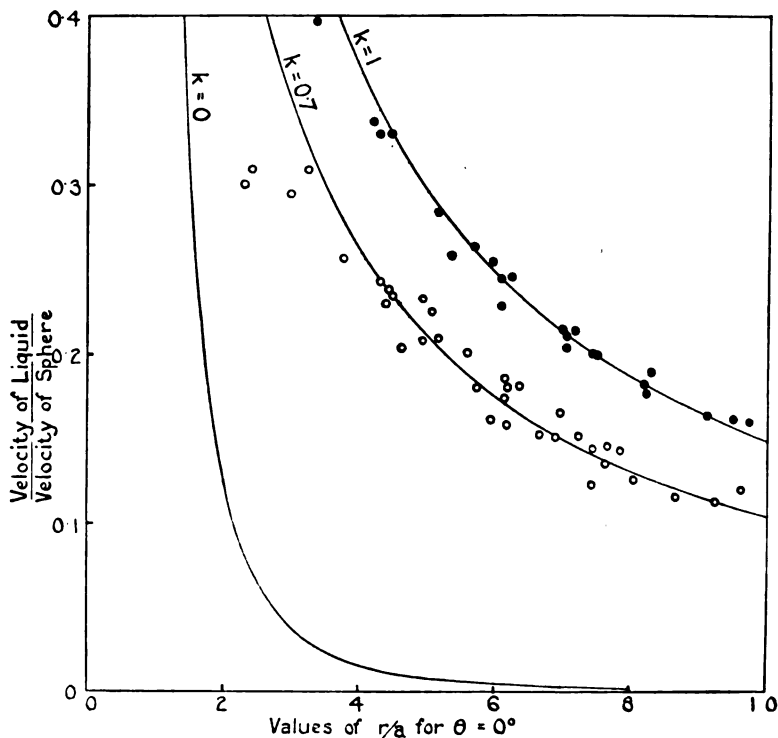
Fig. 1.



(Pl. XIX.) illustrates the type of result, successive exposures being made at equal intervals of time on the same plate. In this way exposures were made on three rising air bubbles and on a steel sphere slightly larger, and on one slightly smaller, than the bubbles. The diameters of the steel spheres were obtained previously, and also one of the air bubbles was measured by microscope. Using the measured camera

magnification, the diameters of image were deduced. As the form of illumination necessitated by this experiment was not suitable for obtaining a photographic record of the sizes of the spheres or bubbles themselves, a separate exposure was made near one end of four of the plates (fig 2, Pl. XIX.), showing the sphere or bubble in front of a white background. The diameters of the images thus obtained gave a satisfactory check with those predicted.

Fig. 3.



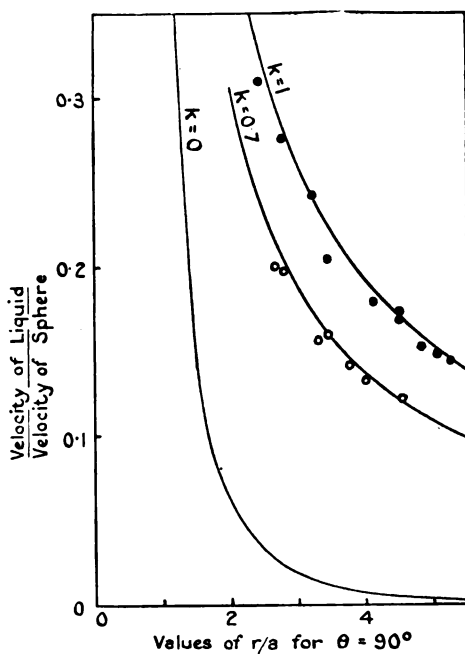
From the five photographs the velocity of the liquid at different distances from the spheres, at angles $\theta=0^\circ$ and $\theta=90^\circ$, was obtained as a multiple of the velocity of the sphere. On comparing the results obtained from the two steel spheres with those predicted by the usual theory (equations (6) with $1/k=1$), it was found necessary in each case to add a constant velocity to all the observations to obtain agreement. This velocity was slightly less than that

predicted by Ladenburg's results (equation 10), but showed evidence of increasing slightly near the sphere and probably reaching his value at the sphere.

The upper curves in figs. 3 and 4 are those predicted ($1/k=1$); and the results obtained from the steel spheres, after the addition of the above velocity on account of the wall correction, are indicated by dark dots.

The corresponding results for the air-bubble photographs were corrected according to the modified equation (11), assuming the value $1/k=1.43$ previously obtained experi-

Fig. 4.



mentally (i. e., $k=0.70$). These are represented by the circles in figs. 3 and 4. The curves passing through these circles were obtained from equations (6), again assuming $1/k=1.43$.

The agreement between observation and the curves is quite good. (Even if the unmodified correction, equation (10), be used, all the air-bubble observations come

lower in these figures than the lowest steel observations at an equal value of r/a .)

The lowest curves in figs. 3 and 4 represent the velocity distribution for irrotational flow, obtained by putting $k=0$ in equations (6).

Thus the form of equations (6) has been verified, the value of k previously obtained found to be in agreement with the results, and incidentally a check has been obtained of Ladenburg's correction.

In conclusion the author would like to thank Prof. J. A. Crowther for the facilities that have made this work possible, and for the interest he has taken in the work; to Mr. J. S. Burgess, the laboratory steward, thanks are also due for his continued kind help in regard to apparatus.

Note added on October 8th, 1927.—From the above results it will be evident that when Stokes' Law is used to estimate the diameter of small drops of liquid, as in Millikan's determination of the electronic charge, e , a correction may have to be applied on account of the circulation of the liquid inside the drop. Thus, *unless skin friction decreases the effect*, we have to the required approximation

$$e \text{ (corrected)} = e \left(1 - \frac{\mu}{2\mu'} \right).$$

Values of e obtained using mercury drops in air might therefore need reducing by a maximum of slightly more than $\frac{1}{2}$ per cent. I have not found data to deduce the maximum possible error in the case of Millikan's experiments using watch oil in air (though it seems likely that the maximum error might be only about $\frac{1}{10}$ per cent.).

This possible source of error does not seem to have been pointed out, and therefore it appears that it may not have been entirely eliminated.—W. N. B.

LXXXIII. *Ionization by Collision.* By L. G. H. HUXLEY,
B.A., Lecturer and Demonstrator, Electrical Laboratory,
Oxford*.

IN a previous number of this Journal (Phil. Mag. Sept. 1927, p. 505) J. Taylor has given a reply to my remarks on his "Photoelectric Theory of Sparking," in my communication entitled "Ionization by Collision" (Phil. Mag. May 1927, p. 1056), and, in addition, he also raises objections to the Theory of Sparking formulated by Townsend. It is proposed here both to consider these objections and to comment on the replies.

Taylor makes three distinctly different kinds of objection, which may be considered separately.

1. With regard to the theory of ionization by the collisions of electrons with molecules of the gas, Taylor raises an objection without giving reasons, stating that "the Townsend Theory of Ionization by collision for negative ions or electrons is not universally adopted"; and again, later, we find, with reference to the same hypothesis, "the photoelectric hypothesis was fitted into the existing fabric merely as an example of its application, but nowhere was a belief of the authenticity of Townsend's theory put forward."

It is to be presumed that Taylor, in proposing a theory of Sparking Potentials, assigns some action to the electrons; and it would be interesting to learn more precisely what is his theory of the action of the electrons and his reasons against the existing theory, which has so much experimental evidence to recommend it. To quote a definite experiment, it would be interesting to know how to explain the increase of conductivity obtained in pure helium by Bazzoni, as shown by Curve A, fig. 3 (Phil. Mag. Dec. 1916, p. 571).

2. Taylor's second objection is to the hypothesis that positive ions can ionize molecules of a gas in cases where the potential difference between the electrodes is of the order of the minimum sparking potential. He finds support for this objection in a paper by Sir J. J. Thomson (Phil. Mag. July 1924, p. 1), where reasons are proposed for believing that positive ions, unless they possess energies of several thousands of volts, do not ionize molecules of the gas. For instance, it is stated that to ionize a molecule of a gas having an ionizing potential of 10 volts, a hydrogen atom would require at least an energy corresponding to 4500 volts and an

* Communicated by Prof. J. S. Townsend, F.R.S.

oxygen atom 72,000 volts. In view of other phenomena, this certainly does not seem at all probable. For instance, the phenomena of thermo-luminescence in gases are adequately explained on the assumption that a gas molecule can produce the same effect on impact with another molecule as an electron having energy of the same order of magnitude. To quote Andrade ('The Structure of the Atom,' 3rd edit. p. 341) : "Now, it is reasonable to assume—by which we mean that the deductions from this assumption fit in well with observed facts, since there is no *a priori* inevitability about it—that the impact of another atom, provided it had the same energy, can produce the same effect as the impact of an electron."

Nor is it unreasonable to assume that a positively-charged molecule or atom can produce a similar effect. Since experiment shows that luminosity can be produced in the case of the alkali metals in the Bunsen flame, and that the energy to be communicated by the impacting body lies in the region of 3 volts, on Sir J. J. Thomson's hypothesis, a hydrogen atom in a Bunsen flame to produce this luminescence would require an energy in the neighbourhood of 2000 volts. The fraction of such atoms at 1700°C. whose translational energies exceed 2000 volts is of the order e^{-6000} , a number which is so minute as to merit no further consideration. The presence of free electrons in flames has long been known*, and may obviously be explained by the same assumption. In fact, the generally-accepted theory of the luminescence and conductivity of hot gases is an extension of the hypothesis of the action of the positive ions to uncharged particles of the same order of mass.

It must again be emphasized that the main features of the electrical discharge in gases between concentric cylinders can most simply and accurately be explained on the hypothesis of ionization of gas molecules by collision with positive ions.

In my previous paper it was shown that the properties of the corona discharge indicate that, on Taylor's hypothesis, γ (the coefficient which occurs in Taylor's hypothesis) is constant, while the properties of discharges between parallel plates show a large variation of γ with the value of X (the electric force at the surface of the cathode). Taylor agrees with this conclusion, and shows that this result is still in accordance with his hypothesis; for in the one case X is small and γ might quite well have fallen to a constant value,

* Harold A. Wilson, 'The Electrical Properties of Flames and of Incandescent Solids,' p. 89 (University of London Press).

while in the other case X is much larger and γ could in this region vary with X . It must be urged, however, that Townsend ('Electricity in Gases,' p. 368) was able to derive a formula connecting the critical force necessary to initiate a corona discharge in air with the diameter of the wire and the pressure, by using the numerical results yielded by experiments on sparking in uniform fields; so the theory indicates that the effects produced by electrons and positive ions are the same in both cases.

3. Taylor's third objection is to an "unmodified" Townsend Theory, which it is stated fails entirely to account for certain variations in sparking potentials due to electrode effects; but he omits to mention the fact that the electrode effects are actually dealt with in the treatise on Electricity in Gases. Townsend discusses two different effects of the positive ions—namely, the effect of positive ions in ionizing molecules of the gas, and their effect in setting free electrons from the negative electrode. He deals separately with these two possible effects of positive ions, and gives two formulæ, one involving only the effect of positive ions in ionizing molecules of the gas, and another involving only the effect of electronic emission from the cathode due to impinging positive ions. The following extracts from the treatise 'Electricity in Gases' serve to illustrate this point. On p. 330 we find a paragraph entitled "Effect of electrons set free from the negative electrode," in which the alternative theory of spark production is formulated. The two possible effects of positive ions are discussed, and it is stated at the end of paragraph 230 that "there are no reliable experiments to show the relative values of these two effects in a discharge for a given value of the product pS , but for simplicity it may be assumed that the gas effect predominates when pS exceeds the value corresponding to the minimum sparking potential." The effect of the alkali metals on the potentials in discharge-tubes is dealt with on p. 409, where the following statement is made: "The small cathode fall of potential is probably due to the fact that under the action of the radiation from the discharge or of the impacts of the positive ions, the alkali metals emit large numbers of electrons as compared with the numbers that would be emitted under similar circumstances from ordinary metals."

It is difficult to see why Taylor fails to find an explanation of electrode effects in the treatise on Electricity in Gases.

Dubois's results were quoted in contradiction to Taylor's; for with uncontaminated electrodes the one seemed to find

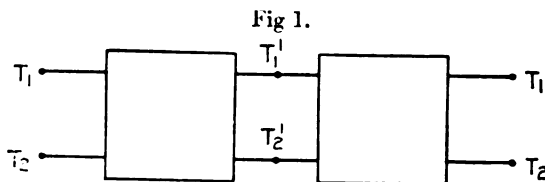
constancy in the sparking potential, while the other finds regular variations. It may be that Taylor's effect is more noticeable in the rare gases, with which Dubois does not deal. Having read Dubois's thesis, I was quite aware of his explanation of his results with saline contamination, and as far as the theory is concerned, he states that he reviews the existing theory, and gives one formula in which Townsend's two formulæ are combined.

Electrical Laboratory, Oxford.

LXXXIV. *An Extension of a Property of Artificial Lines.*

By A. C. BARTLETT, B.A.* (Communication from the Research Staff of the General Electric Co., Wembley.)

IF any artificial line section having input and output terminals $T_1 T_2, T_1' T_2'$ has within it a pair of terminals $T_1' T_2'$, so that it may be represented, as in fig. 1, by two equal



asymmetrical networks placed back to back, then, if the second half be removed, the impedance of the network remaining, measured at the terminals $T_1 T_2$, is

$$Z_0 \tanh \frac{\theta}{2} \text{ if } T_1' T_2' \text{ be short-circuited,}$$

$$\text{and } Z_0 \coth \frac{\theta}{2} \text{ if } T_1' T_2' \text{ be open-circuited,}$$

where Z_0 and θ are the characteristic impedance and propagation constant of the artificial line section.

As an example, take the T section shown in fig. 2 (a). In fig. 2 (b) a half-section is shown, and it is seen that

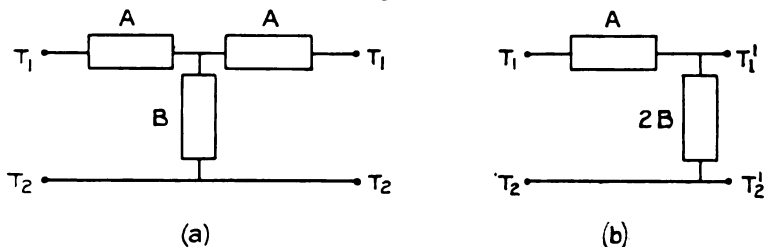
$$Z_0 \coth \frac{\theta}{2} = A + 2B$$

$$\text{and } Z_0 \tanh \frac{\theta}{2} = A.$$

* Communicated by C. C. Paterson.

It will be shown that this is a special case of a more general theorem which may be stated thus:—If an artificial line section has within it n terminals $T_1' T_2' \dots T_n'$, such that, if these terminals are open, the artificial line section

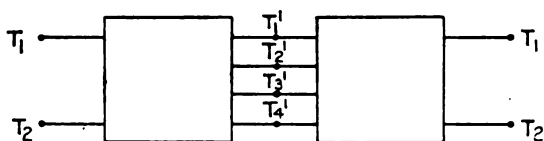
Fig. 2.



is cut into two exactly similar halves, the impedance of one-half measured at the terminals $T_1 T_2$ with $T_1', T_2' \dots T_n'$ free is $Z_0 \coth \frac{\theta}{2}$, and with $T_1', T_2' \dots T_n'$ all connected together is $Z_0 \tanh \frac{\theta}{2}$.

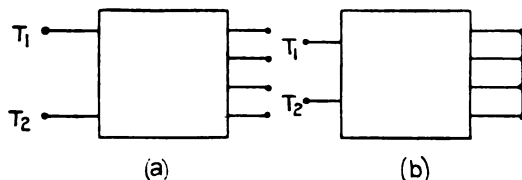
Thus, if fig. 3 represents the artificial line section (taking

Fig. 3.



$n=4$), then $Z_0 \coth \frac{\theta}{2}$ is the impedance of fig. 4 (a) and $Z_0 \tanh \frac{\theta}{2}$ of fig. 4 (b).

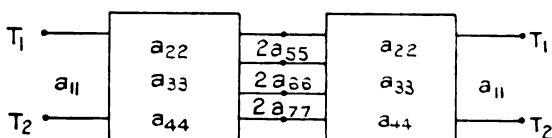
Fig. 4.



The proof, though simple, is rather long. To simplify

matters, suppose, as above, that $n=4$, and let the artificial line section be as shown diagrammatically in fig. 5.

Fig. 5.



Let a_{11} be the sum of the impedances round the terminal meshes; let a_{22} , a_{33} , and a_{44} be the sums of impedances round meshes inside each half-section; $2a_{55}$, $2a_{66}$, and $2a_{77}$ be the same for the meshes common to the two half-sections. In addition, there will be the mutual impedances a_{12} etc. between the meshes a_{11} and a_{22} etc. in each half.

Then the characteristic impedance will be given by *

$$Z_0^2 = \Delta / \frac{\partial^2 \Delta}{\partial a_{11} \partial a_{11}},$$

where Δ is the axi-symmetric determinant

$$\begin{vmatrix} a_{11} & a_{12} & a_{13} & a_{14} & a_{15} & a_{16} & a_{17} & 0 & 0 & 0 & 0 \\ a_{21} & a_{22} & a_{23} & a_{24} & a_{25} & a_{26} & a_{27} & 0 & 0 & 0 & 0 \\ a_{31} & a_{32} & a_{33} & a_{34} & a_{35} & a_{36} & a_{37} & 0 & 0 & 0 & 0 \\ a_{41} & a_{42} & a_{43} & a_{44} & a_{45} & a_{46} & a_{47} & 0 & 0 & 0 & 0 \\ a_{51} & a_{52} & a_{53} & a_{54} & 2a_{55} & 2a_{56} & 2a_{57} & a_{58} & a_{59} & a_{510} & a_{511} \\ a_{61} & a_{62} & a_{63} & a_{64} & 2a_{65} & 2a_{66} & 2a_{67} & a_{68} & a_{69} & a_{610} & a_{611} \\ a_{71} & a_{72} & a_{73} & a_{74} & 2a_{75} & 2a_{76} & 2a_{77} & a_{78} & a_{79} & a_{710} & a_{711} \\ 0 & 0 & 0 & 0 & a_{45} & a_{46} & a_{47} & a_{41} & a_{42} & a_{43} & a_{44} \\ 0 & 0 & 0 & 0 & a_{35} & a_{36} & a_{37} & a_{34} & a_{33} & a_{32} & a_{31} \\ 0 & 0 & 0 & 0 & a_{25} & a_{26} & a_{27} & a_{24} & a_{23} & a_{22} & a_{21} \\ 0 & 0 & 0 & 0 & a_{15} & a_{16} & a_{17} & a_{14} & a_{13} & a_{12} & a_{11} \end{vmatrix},$$

in which

$$a_{rs} = a_{sr}.$$

This determinant, which is partially centro-symmetric, can be simplified in the following way:—To the first row add the last row, to the second row add the last but one row, and similarly for the third and fourth rows. Next, in the resulting determinant:—From the last column subtract the first column, from the last but one column subtract the second column, and treat similarly the last but two and last but three columns. It is then found that the determinant

* Cf. J. I. E. E. pp. 223-227, Feb. 1927. Equation (20).

breaks up into the product of two other determinants giving

$$\Delta = 2^3 \Delta' \Delta'',$$

where $\Delta' =$

$$\begin{vmatrix} a_{11}, & a_{12}, & a_{13}, & a_{14}, & a_{15}, & a_{16}, & a_{17} \\ a_{21}, & a_{22}, & a_{23}, & a_{24}, & a_{25}, & a_{26}, & a_{27} \\ a_{31}, & a_{32}, & a_{33}, & a_{34}, & a_{35}, & a_{36}, & a_{37} \\ a_{41}, & a_{42}, & a_{43}, & a_{44}, & a_{45}, & a_{46}, & a_{47} \\ a_{51}, & a_{52}, & a_{53}, & a_{54}, & a_{55}, & a_{56}, & a_{57} \\ a_{61}, & a_{62}, & a_{63}, & a_{64}, & a_{65}, & a_{66}, & a_{67} \\ a_{71}, & a_{72}, & a_{73}, & a_{74}, & a_{75}, & a_{76}, & a_{77} \end{vmatrix}$$

and $\Delta'' =$

$$\begin{vmatrix} a_{11}, & a_{12}, & a_{13}, & a_{14} \\ a_{21}, & a_{22}, & a_{23}, & a_{24} \\ a_{31}, & a_{32}, & a_{33}, & a_{34} \\ a_{41}, & a_{42}, & a_{43}, & a_{44} \end{vmatrix},$$

Similarly,

$$\frac{\partial^2 \Delta}{\partial a_{11} \partial a_{11}} = 2^3 \frac{\partial \Delta'}{\partial a_{11}} \cdot \frac{\partial \Delta''}{\partial a_{11}},$$

so that

$$Z_0^2 = \frac{\Delta'}{\partial \Delta' / \partial a_{11}} \cdot \frac{\Delta''}{\partial \Delta'' / \partial a_{11}}.$$

But $\Delta' / \frac{\partial \Delta'}{\partial a_{11}}$ is seen to be the impedance of the first half of the network of fig. 5 with all the terminals $T_1' T_2' T_3' T_4'$ connected together, while $\Delta'' / \frac{\partial \Delta''}{\partial a_{11}}$ is the impedance of the same network with $T_1' T_2' T_3' T_4'$ all free.

Since their product is equal to Z_0^2 ,

$$\Delta' / \frac{\partial \Delta'}{\partial a_{11}} \quad \text{and} \quad \Delta'' / \frac{\partial \Delta''}{\partial a_{11}}$$

may be written as

$$Z_0 \tanh \frac{\phi}{2} \quad \text{and} \quad Z_0 \coth \frac{\phi}{2}.$$

By using the identity

$$Z_0 \sinh \phi = 2 / \left(1/Z_0 \tanh \frac{\phi}{2} - 1/Z_0 \coth \frac{\phi}{2} \right),$$

and inserting values in the right-hand side, $Z_0 \sinh \phi$ can be found; if this is done, it will be found after reduction to be equal to Δ divided by the determinant obtained by omitting from Δ the first row and last column. But this is the receiving-end impedance of the original artificial line

section short-circuited at the receiving end, and is equal to $Z_0 \sinh \theta$; hence

$$\phi = \theta,$$

and the theorem is proved for this case.

The method, however, is quite general, and therefore the general theorem holds.

A number of simple corollaries follow for artificial line sections that can be bisected in the manner above:—

1. An exactly equivalent bridge section can be constructed.
2. By making bridge sections in which for one pair of arms any ladder network made up of any numerical multiples of $Z_0 \tanh \frac{\theta}{2}$ and $Z_0 \coth \frac{\theta}{2}$ is used, while for the other pair of arms the reciprocal of this network with respect to Z_0 is used, an indefinite number of bridge sections can be constructed having the same Z_0 as the original section but different propagation constants.

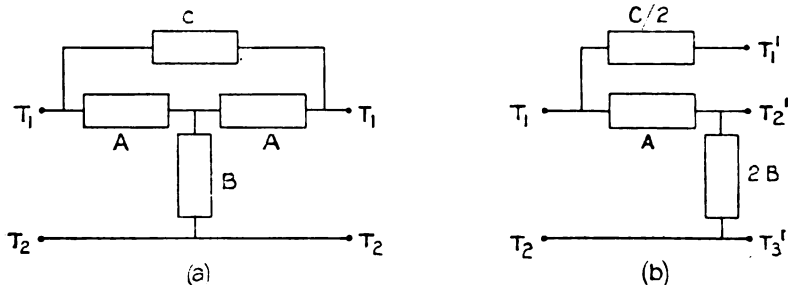
3. If the original section is modified by opening any of the terminals $T_1', T_2' \dots T_n'$ and inserting any series impedances, then, if Z_0' and θ' are the constants of the modified section,

$$Z_0 \coth \frac{\theta}{2} = Z_0' \coth \frac{\theta'}{2}.$$

4. If the original section is modified by connecting any pairs of the terminals $T_1', T_2' \dots T_n'$ by any impedances, then, if Z_0' and θ' are the constants of the modified section,

$$Z_0 \tanh \frac{\theta}{2} = Z_0' \tanh \frac{\theta'}{2}.$$

Fig. 6.



As a special case, consider the three-element artificial line section shown in fig. 6 (a). A half-section is shown in fig. 6 (b), three terminals, $T_1' T_2' T_3'$, being required for the bisection.

Thus for this artificial line section it can be seen from inspection that

$$Z_0 \coth \frac{\theta}{2} = A + 2B,$$

$$Z_0 \tanh \frac{\theta}{2} = \frac{1}{\frac{1}{A} + \frac{1}{C/2}} = \frac{AC}{2A + C};$$

and therefore

$$Z_0^2 = \frac{AC(A + 2B)}{2A + C}.$$

This theorem for any artificial line to which it applies usually affords the simplest method of obtaining the constants in terms of the elements of the section.

From any artificial line section of the type considered, another can be derived by taking the two half-sections and connecting T_1' of one half-section to T_n' of the other half, T_2' to T_{n-1}' , etc. For this derived section the determinant Δ is completely centro-symmetric. The application, however, of the theorem that any centro-symmetric determinant is the product of two determinants does not appear to lead to any simple physical interpretation, though it does simplify the calculation of the constants.

LXXXV. *On Resonance in Pipes Stopped with Imperfect Reflectors.* By E. T. PARIS, D.Sc., F.Inst.P.*

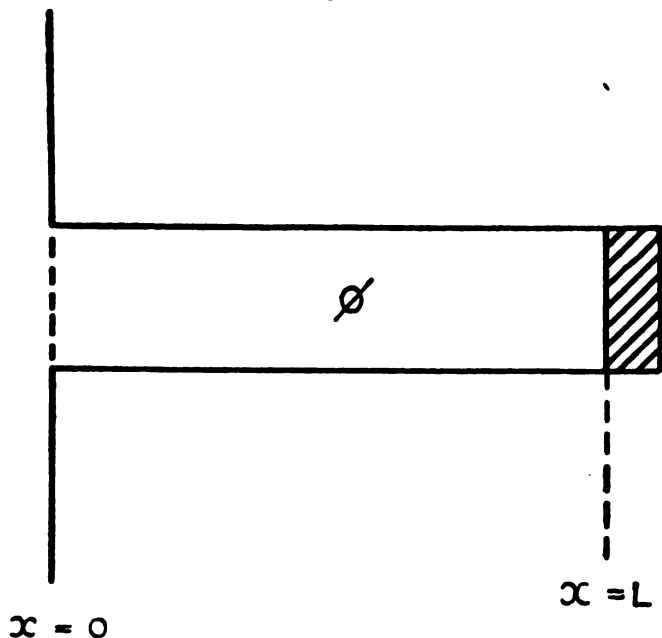
THE problem investigated in the following paper is that of resonance in a straight cylindrical pipe closed at one end by some material or mechanism which absorbs sound-energy. The pipe is supposed to have rigid walls and a diameter neither so great compared with the wave-length of the source that transverse vibrations are excited, nor so small that there is appreciable loss of energy from the operation of viscous forces. Thus the motion of the air within the pipe, due to a pure-tone source of sound, can be represented by two plane-waves of suitable amplitudes and phases travelling in opposite directions parallel to the axis of the pipe.

The first case to be considered will be that of a pipe under the influence of an external simple source of sound, the strength of which (measured in c.c. per sec.) varies with

* Communicated by the Author.

time in a simple harmonic manner. It will be supposed that the pipe is provided with an infinite plane reflecting flange lying in the plane $x=0$ (fig. 1), and that the source of sound is at such a distance from the pipe that the amplitude of the velocity-potential due to it is sensibly constant over the mouth of the pipe. This potential will be denoted by $2F\epsilon^{ikat}$.

Fig. 1.



To allow for the escape of sound-energy from the open end, a velocity-potential may be assumed within the pipe of the form $A(\beta\epsilon^{-ikx} + \epsilon^{ikx})\epsilon^{ikat}$, where β is the coefficient of reflexion at the open end. To this potential must be added a second potential, $2F \cos kx \cdot \epsilon^{ikat}$, to sustain the pressure-variations at the open end due to the external source of sound. Thus the total potential within the pipe is of the form

$$\phi = \{(F + \beta A)\epsilon^{-ikx} + (F + A)\epsilon^{ikx}\}\epsilon^{ikat}. \quad . \quad . \quad (1)$$

The value of A must be adjusted so as to make ϕ comply with the requirements of the problem in those parts of the pipe away from the open end.

It will now be supposed that the pipe is closed at $x=L$ by some material or mechanism which absorbs sound-energy. In order to investigate the resulting velocity-potential within the pipe, use will be made of the Webster-Stewart conception of "acoustical impedance"*. According to Stewart the impedance of an acoustical receiver is the ratio $\delta p/(dq/dt)$, where δp is the pressure-variation at the receiver due to the source, and dq/dt is the rate of volume-displacement of air at the receiving surface. If ϕ is the velocity-potential (due to the source) at the receiver, $\delta p = \rho(d\phi/dt)$, so that acoustical impedance is the ratio $\rho\phi/q$ if both ϕ and q vary as e^{ikt} . To avoid an unnecessary repetition of ρ , impedance will here be taken to be the ratio ϕ/q , and its reciprocal, q/ϕ , will be denoted by Ω . It is convenient to have a name for Ω , and it will be referred to as "acoustical admittance."

Thus, if Ω is the admittance of the receiving-surface closing the pipe at $x=L$, and dq/dt is the rate of volume-displacement of air across the plane $x=L$, the condition to be satisfied by ϕ when $x=L$ is

$$-\sigma \frac{\partial \phi}{\partial x} = \frac{dq}{dt} = \Omega \frac{\partial \phi}{\partial t}, \quad \dots \dots (2)$$

σ being the cross-sectional area of the pipe. By combining (2) with (1), we find that

$$F + A = \mu e^{-2ikL}(F + \beta A), \quad \dots \dots (3)$$

where

$$\mu = \frac{1 - (a\Omega/\sigma)}{1 + (a\Omega/\sigma)}. \quad \dots \dots (4)$$

Thus

$$A = -\frac{1 - \mu e^{-2ikL}}{1 - \beta \mu e^{-2ikL}} F. \quad \dots \dots (5)$$

and

$$\left. \begin{aligned} F + \beta A &= \frac{1 - \beta}{1 - \beta \mu e^{-2ikL}} F, \\ F + A &= \frac{1 - \beta}{1 - \beta \mu e^{-2ikL}} \mu e^{-2ikL} F. \end{aligned} \right\} \dots \dots (6)$$

So that the total potential within the pipe is

$$\begin{aligned} \phi &= \frac{(1 - \beta)F}{1 - \beta \mu e^{-2ikL}} \{e^{-ikx} + \mu e^{-2ikL} e^{ikx}\} e^{ikt} \\ &= \frac{(1 - \beta)F}{1 - \beta \mu e^{-2ikL}} \{e^{-ik(x-L)} + \mu e^{ik(x-L)}\} e^{ikt}, \quad \dots \dots (7) \end{aligned}$$

* For an account of the recent development of impedance methods in acoustics, see I. B. Crandall's 'Theory of Vibrating Systems and Sound' (Macmillan, 1926).

representing two trains of plane-waves travelling in opposite directions along the axis of the pipe. If the amplitude of the wave travelling from the open to the closed end is unity, the amplitude of the reflected wave is $|\mu|$.

Let $\beta = \beta_0 e^{-ika}$, $\mu = \mu_0 e^{-ik\delta}$, where β_0 and μ_0 are real. Then

$$\begin{aligned}\phi &= \frac{(1-\beta)F}{e^{ikL} - \beta_0 \mu_0 e^{-ik(L+a+\delta)}} \{e^{-ik(x-L)} + \mu e^{ik(x-L)}\} e^{ikat} \\ &= \frac{(1-\beta)F e^{ik(a+\delta)}}{e^{ikL'} - \beta_0 \mu_0 e^{-ikL'}} \{e^{-ik(x-L)} + \mu e^{ik(x-L)}\} e^{ikat}, \quad \dots (8)\end{aligned}$$

where $L' = L + \frac{1}{2}(\alpha + \delta)$.

To find the condition for resonance, consider the effect of varying L when the wave-length of the sound and the diameter of the pipe are kept constant. The square of the amplitude of the vibration within the pipe will be inversely proportional to the square of the modulus of the denominator of the right-hand member of (8); that is, to

$$\begin{aligned}&|e^{ikL'} - \beta_0 \mu_0 e^{-ikL'}|^2 \\ &= 1 + \beta_0^2 \mu_0^2 - 2\beta_0 \mu_0 \cos 2kL'. \quad \dots (9)\end{aligned}$$

This will be a maximum or a minimum when $\sin 2kL' = 0$, or $2kL' = n\pi$, when n is an integer. Thus when $L' = n(\lambda/4)$ the energy of the vibration in the pipe* is either a maximum or a minimum, and it is easily seen from (9) that maxima occur when $L' = 0, \lambda/2, \lambda, 3\lambda/2$, etc., and minima when $L' = \lambda/4, 3\lambda/4, 5\lambda/4$, etc.

The case of a pipe stopped by a complete reflector is arrived at by putting $\Omega = 0$, and hence, by (4), $\mu = 1$. Thus, for a stopped pipe, the condition for resonance is

$$L' = L + \frac{1}{2}\alpha = \lambda/2, \lambda, 3\lambda/2, \text{ etc.}$$

The relation of L' to the customary "reduced length" of a stopped pipe can be seen by considering more closely the meaning of α .

The value of β for a flanged open end is †

$$\beta = - \frac{1 - ik\sigma \left(\frac{1}{c_0} - \frac{ik}{2\pi} \right)}{1 + ik\sigma \left(\frac{1}{c_0} - \frac{ik}{2\pi} \right)} \dots (10)$$

Where c_0 is "the conductance of the open end of the pipe," which, in the case of a circular cross-section, is approximately

* *I. e.*, the average energy per unit length of pipe, not the total energy.

† *Cf.* Phil. Mag. ii. p. 756 (1926).

equal to $3.8 \times$ the radius *. To find α we have

$$\beta = - \frac{\left\{ \left(1 - \frac{\sigma k^2}{2\pi} \right) - ik\sigma/c_0 \right\} \left\{ 1 + \frac{\sigma k^2}{2\pi} \right\} - ik\sigma/c_0}{\left(1 + \frac{\sigma k^2}{2\pi} \right)^2 + \left(\frac{\sigma k}{c_0} \right)^2}$$

$$= - \frac{\left\{ \left(1 - \frac{\sigma k^2}{2\pi} \right)^2 - \left(\frac{\sigma k}{c_0} \right)^2 \right\} - 2i \frac{\sigma k}{c_0}}{\left(1 + \left(\frac{\sigma k^2}{2\pi} \right)^2 + \left(\frac{\sigma k}{c_0} \right)^2 \right)}. \dots \dots (11)$$

So that

$$-k\alpha = \tan^{-1} \left\{ - \frac{2\sigma k/c_0}{\left(1 - \frac{\sigma k^2}{2\pi} \right)^2 - \left(\frac{\sigma k}{c_0} \right)^2} \right\}. \dots (12)$$

In the case of a pipe having a diameter small compared with the wave-length, the quantity $\left\{ \left(1 - \frac{\sigma k^2}{2\pi} \right)^2 - \left(\frac{\sigma k}{c_0} \right)^2 \right\}$ is always positive, and hence $\tan(-k\alpha)$ is negative. Thus

$$-k\alpha = \pi - \tan^{-1} \left\{ \frac{2\sigma k/c_0}{\left(1 - \frac{\sigma k^2}{2\pi} \right)^2 - \left(\frac{\sigma k}{c_0} \right)^2} \right\}. \dots (13)$$

and

$$\alpha = \frac{\lambda}{2\pi} \tan^{-1} \left\{ \frac{2\sigma k/c_0}{\left(1 - \frac{\sigma k^2}{2\pi} \right)^2 - \left(\frac{\sigma k}{c_0} \right)^2} \right\} - \frac{\lambda}{2}. \dots (14)$$

Let

$$2\alpha' = \frac{\lambda}{2\pi} \tan^{-1} \left\{ \frac{2\sigma k/c_0}{\left(1 - \frac{\sigma k^2}{2\pi} \right)^2 - \left(\frac{\sigma k}{c_0} \right)^2} \right\}. \dots (15)$$

Then

$$\alpha = 2\alpha' - \frac{\lambda}{2}. \dots \dots (16)$$

and

$$L' = L + \frac{1}{2}\alpha = L + \alpha' - \frac{\lambda}{4}. \dots \dots (17)$$

Thus resonance occurs in a narrow stopped pipe when $L + \alpha' - \lambda/4 = 0, \lambda/2, 4\lambda, 3\lambda/2$, etc.; that is, when $L + \alpha' = \lambda/4$,

* *Ibid.* p. 757.

$3\lambda/4$, $5\lambda/4$, etc., which agrees with the well-known facts if α' is the usual "correction for an open end." The expression for α' in (15) reduces to the approximate relation, $\alpha' = \sigma/c_0$, when the diameter of the pipe is very small compared with the wave-length*.

To return to the case when the pipe is stopped with an admittance Ω at $x=L$, we see that resonance occurs when $L + \alpha' + \frac{1}{2}\delta = \lambda/4, 3\lambda/4, 5\lambda/4$, etc.; that is, when the "reduced length" of the pipe ($L + \alpha'$) plus the distance $\frac{1}{2}\delta$, which depends on the change of phase at reflexion at the stopped end, is equal to an odd number of quarter wave-lengths.

Some special cases may be mentioned. If the pipe is stopped at $x=L$ by a mass of non-porous material, there is no change of phase at reflexion and $\delta=0$, so that the reduced length ($L + \alpha'$) gives greatest resonance no matter how much sound-energy is absorbed at the stopped end. This case is, however, somewhat difficult to realize in practice on account of the necessarily finite thickness of the layer of material used to stop the pipe†.

If the material is porous, there may be change of phase at reflexion, in which case $\delta \neq 0$. The difference in the lengths of a pipe adjusted to resonance when stopped with porous and non-porous materials might, in fact, be used to measure δ and hence the change of phase at reflexion.

As an example of a somewhat different kind, reference may be made to the Boys pattern double resonator‡ (fig. 2). The pipe in this case is closed by a rigid plate in which there is a small aperture forming the entrance to a Helmholtz resonator. The theory of the Helmholtz resonator shows that its admittance is given by

$$\Omega = \frac{c}{2h - i\Delta}, \quad \dots \dots (18)$$

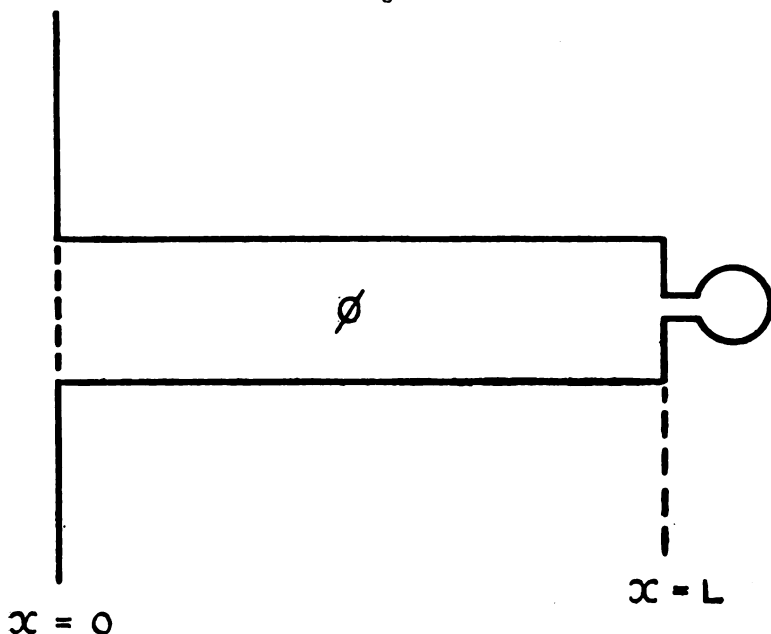
where c is the conductance of the orifice, h is the damping coefficient, and $\Delta = \omega_0(\omega_0/\omega - \omega/\omega_0)$, ω_0 being equal to 2π times the resonance-frequency of the resonator, and ω to 2π times the frequency of the incident sound-waves. Thus in

* Cf. Rayleigh, 'Theory of Sound,' ii. (2nd ed.) p. 200.

† If the pipe is stopped by a thin diaphragm the appropriate value of Ω is $(\sigma\rho/m)/(2h - i\Delta)$, in which ρ is the density of air, m is the equivalent mass of the diaphragm, h is its damping factor and $\Delta = \omega_0(\omega_0/\omega - \omega/\omega_0)$, where $\omega_0 = 2 \times$ the resonance frequency of the diaphragm and $\omega = 2\pi \times$ the frequency of the sound.

‡ The theory of this resonator is dealt with in Phil. Mag. ii. pp. 751-769 (1926).

Fig. 2.



the case of a Boys resonator *

$$\mu = \frac{1 - \frac{ac}{\sigma(2h - i\Delta)}}{1 + \frac{ac}{\sigma(2h - i\Delta)}} \quad \dots \quad (19)$$

Hence

$$\mu_0^2 = \frac{\left\{ \Delta^2 + 4h^2 - \left(\frac{ac}{\sigma} \right)^2 \right\}^2 + 4\Delta^2 \left(\frac{ac}{\sigma} \right)^2}{\left\{ \left(2h + \frac{ac}{\sigma} \right)^2 + \Delta^2 \right\}^2}, \quad \dots \quad (20)$$

$$\delta = \frac{\lambda}{4\pi} \tan^{-1} \left\{ \frac{2\Delta \left(\frac{ac}{\sigma} \right)}{\Delta^2 + 4h^2 - \left(\frac{ac}{\sigma} \right)^2} \right\}. \quad \dots \quad (21)$$

The expression (20) is interesting, for it shows that if $\Delta=0$, that is if the Helmholtz resonator is exactly in unison with the incident sound, and also if $2h = \frac{ac}{\sigma}$, then

* μ has not the same meaning as in the earlier paper. It is used to denote the reciprocal of μ as previously used.

$\mu_0=0$; that is, the sound-waves passing down the pipe from the open end are completely absorbed at $x=L$. The admittance at $x=L$ in this case is therefore equal to that of an infinite pipe of cross-section σ . These conditions are not difficult to fulfil. At 512 vibrations per second, for example, it is possible to make a Helmholtz resonator with $h=80$ sec.⁻¹ and $c=0.125$ cm. Thus for complete absorption we should have $\sigma = \frac{ac}{2h} = \frac{33760 \times 0.125}{2 \times 80} = 26.4$ cm.² If the pipe is

circular $\sigma = \pi R^2$, and therefore $R = \sqrt{26.4/\pi} = 2.9$ cm.

This result is independent of L , the length of the pipe, and appears to be of wider application than to the theory of resonance in pipes. It suggests that by means of a certain distribution of resonators over the face of a flat reflecting wall complete absorption of normally incident sound of a certain wave-length could be secured by a suitable choice of the dimensions of the resonators.

From the expression (21), and the condition that $L + \alpha' + \frac{1}{2}\delta$ must be equal to an odd number of quarter wave-lengths, the values of L which will make the energy of the vibration in the pipe a maximum can be found. If $\Delta=0$, then $\delta=0$, so that if the incident sound and the Helmholtz resonator are in tune, best resonance (for this frequency) is obtained when the reduced length of the pipe is an odd number of quarter wave-lengths.

The case when the source of sound is inside the pipe will now be briefly considered. Let the source lie in the plane $x=0$ and let the strength be $U\epsilon^{ik\alpha t}$ c.c. per sec., such as might be provided by a piston closely fitting into the tube and driven by suitable mechanism, or by a telephone diaphragm driven by alternating current.

The potential within the pipe is

$$\phi = (A\epsilon^{-ikx} + B\epsilon^{ikx})\epsilon^{ik\alpha t}, \quad (22)$$

and we must have

$$-\sigma \frac{\partial \phi}{\partial x} = U\epsilon^{ik\alpha t} \text{ when } x=0, \quad (23)$$

whence

$$B = A - U/ik\sigma. \quad (24)$$

Also when $x=L$,

$$-\sigma \frac{\partial \phi}{\partial x} = \Omega \frac{\partial \phi}{\partial t}. \quad (25)$$

Therefore

$$A - \frac{U}{ik\sigma} = \mu A e^{-2ikL}, \quad (26)$$

where μ has the same meaning as previously.

Thus

$$\left. \begin{aligned} A &= \frac{U/ik\sigma}{1 - \mu e^{-2ikL}}, \\ B &= \frac{U/ik\sigma}{1 - \mu e^{-2ikL}} \mu e^{-2ikL}. \end{aligned} \right\} (27)$$

So that

$$\begin{aligned} \phi &= \frac{U/ik\sigma}{1 - \mu e^{-2ikL}} \{e^{-ikx} + \mu e^{-2ikL} e^{ikx}\} e^{ikat} \\ &= \frac{U/ik\sigma}{e^{ikL} - \mu e^{-ikL}} \{e^{-ik(x-L)} + \mu e^{ik(x-L)}\} e^{ikat}. \quad . . . (28) \end{aligned}$$

If, as before, $\mu = \mu_0 e^{-ik\delta}$,

$$\phi = \frac{U/ik\sigma}{e^{ikL'} - \mu_0 e^{-ikL'}} \{e^{-ik(x-L')} + \mu_0 e^{ik(x-L')}\} e^{ikat}, \quad . . . (29)$$

where $L' = L + \frac{1}{2}\delta$.

The square of the amplitude of the vibration in the pipe is inversely proportional to

$$\begin{aligned} &|e^{ikL'} - \mu_0 e^{-ikL'}|^2 \\ &= (1 + \mu_0)^2 - 2\mu_0 \cos 2kL'. \quad (30) \end{aligned}$$

The energy of the vibration is therefore a minimum or a maximum when $\sin 2kL' = 0$, or $L' = n\frac{\lambda}{4}$. It is easily seen that resonance occurs, i.e., the energy is a maximum, when n is even, that is when $L' = \frac{\lambda}{2}, \lambda$, etc.

If the pipe is closed by a rigid plate at $x=L$, $\Omega=0$ and $\mu=1$. Hence, by (29), the amplitude of the vibration in the pipe is inversely proportional to $\sin kL'$, and becomes (theoretically) infinite when $\sin kL'=0$; that is, when $L' = \frac{\lambda}{2}, \lambda$, etc. This may be taken as indicating that the amplitudes become so great that the approximate equations of sound-propagation on which the theory given above is founded are no longer applicable.

Equations (7) and (28) find an application in connexion with the theory of the stationary-wave method of measuring sound-absorption at normal incidence. The principle of this

method can be illustrated by considering the case of plane-waves incident normally on the flat surface of sound-absorbing material. Let the reflecting surface lie in the plane $x=0$, and μ be the coefficient of reflexion. Then the amplitude of the incident waves being supposed equal to unity, the potential of the incident and reflected waves will be

$$\phi = (\epsilon^{-ikx} + \mu\epsilon^{ikx})\epsilon^{ikatt}. \quad . \quad . \quad . \quad (31)$$

It is clear that this potential will give rise to a series of positions of maximum and minimum pressure-variation in front of the reflecting surface, and that (if $\mu = \mu_0\epsilon^{-ik\delta}$) the ratio of maximum and minimum will be $(1+\mu_0)/(1-\mu_0)$. If this ratio is measured with an acoustical instrument and is found to be, say, m , then $\mu_0 = (m-1)/(m+1)$. The proportion of the incident sound-energy which is absorbed, namely $(1-\mu_0^2)$, can therefore be determined in terms of the observed ratio m . If Ω' is the acoustical admittance per unit area of the reflecting surface at normal incidence, then, since ϕ must satisfy the condition

$$-\frac{\partial\phi}{\partial x} = \Omega' \frac{\partial\phi}{\partial t} \text{ when } x=0, \quad . \quad . \quad . \quad (32)$$

we find that $\mu = (1 - a\Omega')/(1 + a\Omega')$.

In practice, in order to produce plane-waves incident normally on a reflecting surface, recourse is had to a pipe stopped at one end with a disk of the material to be tested. The other end of the pipe may be left open and a source may be placed near it, or, alternatively, the source may be actually mounted in the other end of the pipe. The two arrangements correspond to the two cases considered above, and the resulting potential inside the pipe is given by equations (7) and (28) respectively. It will be seen from these equations that the form of the potential inside the pipe is the same in both cases, and depends only on the value of the admittance placed at $x=L$. The potential is that due to two sets of plane-waves travelling in opposite directions; and if the amplitude of that travelling in the direction x -positive is unity, then the amplitude of that travelling in the direction x -negative is μ_0 , $\mu (= \mu_0\epsilon^{-ik\delta})$ being the coefficient of reflexion at $x=L$. There are thus positions of maximum and minimum pressure-amplitude inside the pipe, just as there are in front of an infinite plane-reflecting face. Also we see from (4) that $\mu = (1 - a\Omega')/(1 + a\Omega')$, where Ω' is written for Ω/σ and is the admittance per unit area of the reflecting surface. Thus μ has the same meaning as in (31).

It may be noted that the ratio of maximum to minimum pressure-amplitude inside the pipe (though not, of course, the amplitudes themselves) is independent of L , the length of the pipe. This point appears to have been the subject of a certain amount of misconception. Eckhardt and Chrisler *, for example, in recent work with the stationary-wave method, brought the pipe into resonance with the source at each frequency at which observations were made, appearing to think that the measurements would otherwise be unreliable. Also Tuma †, who was the first to use the method, brought the pipe into resonance before making observations. Such a procedure seems to be unnecessary.

Summary.

The theory of pipes stopped with imperfect reflectors is discussed and the conditions for resonance are deduced. Some special cases are dealt with, including that of a Boys pattern double resonator, and the conditions necessary for complete absorption (*i. e.* no reflexion) of sound by a resonator placed at the end of a stopped pipe are found. Some of the results obtained have an application to the theory of the measurement of sound-absorption by the stationary-wave method.

Biggin Hill, Kent.
June 1927.

LXXXVI. *The Effect of Variable Specific Heats upon the Velocity Generated, and upon the Temperature Drop, in Gases Expanding through Nozzles.* By E. C. WADLOW, *Ph.D., B.Sc.* ‡

EQUATIONS for calculating the velocity generated, and the weight of gas discharged, when a gas initially at a high pressure is allowed to expand through a nozzle to a lower pressure, taking into consideration the increase of specific heat with temperature, have been given by Dr. W. J. Walker §.

* 'Scientific Papers of the Bureau of Standards,' No. 526 (April, 1928)

† *Wien. Sitzungber. d. K. Akad. d. Wissenschaften*, iii. pt. 2A, pp. 402-410 (1902).

‡ Communicated by the Author.

§ *Phil. Mag.* xliii. pp. 589-593 (1922).

The formulæ giving the velocity generated are based upon the fundamental equation

$$V^2 = 2gK_p \int_{T_2}^{T_1} dT, \quad (1)$$

where

V = Velocity generated. Feet per second,

$g = 32.2$ feet per sec. per sec.,

K_p = Specific heat of gas at constant pressure. Ft. lb. per lb. per °C.

T_1 = Initial temperature °C. abs.

T_2 = Final temperature °C. abs.

If the relationship between specific heat and temperature is given by

$$\left. \begin{aligned} K_p &= A + ST \\ K_v &= B + ST \end{aligned} \right\}, \quad (2)$$

the relationship between velocity generated and temperature is given by

$$V^2 = 2g \left[A(T_1 - T_2) + \frac{S}{2}(T_1^2 - T_2^2) \right]. \quad . . (3)$$

Similarly, if

$$\left. \begin{aligned} K_p &= A + ST + S'T^2 \\ K_v &= B + ST + S'T^2 \end{aligned} \right\}, \quad (4)$$

the velocity generated is given by

$$V^2 = 2g \left[A(T_1 - T_2) + \frac{S}{2}(T_1^2 - T_2^2) + \frac{S'}{3}(T_1^3 - T_2^3) \right]. \quad . (5)$$

Owing to the difficulty of measuring T_2 when the velocity of the gas issuing from the nozzle is high, equations (3) and (5) cannot be used directly to calculate, from experimental observations, the actual velocity generated during the expansion, although the numerical values of g , A , S , S' and T_1 may be known or measured with fair accuracy.

With a view to overcoming this difficulty, equations (3) and (5) have been transformed by Dr. Walker to the following forms, respectively:

$$V = \left[2g \frac{m}{m-1} p_1 v_1 \left\{ 1 - \left(\frac{p_0}{p_1} \right)^{\frac{m-1}{m}} \right\} \right]^{\frac{1}{2}} \left\{ 1 + \frac{\lambda T_1}{4m} \left(1 - \left(\frac{p_0}{p_1} \right)^{\frac{m-1}{m}} \right) \right\}. \quad . (6)$$

and

$$V = \left[2g \frac{m}{m-1} p_1 v_1 \left\{ 1 - \left(\frac{p_0}{p_1} \right)^{\frac{m-1}{m}} \right\} \right]^{\frac{1}{2}} \left\{ 1 + \left(\lambda T_1 + \frac{\lambda'}{2} T_1^2 \right) \left[\frac{1 - \left(\frac{p_0}{p_1} \right)^{\frac{m-1}{m}}}{4m} \right] \right\} \quad (7)$$

where

$$m = \frac{A}{B}, \quad \lambda = \frac{S}{B}, \quad \lambda' = \frac{S'}{B}.$$

p_1 = Initial pressure. Lb. per square foot.

v_1 = Initial specific volume. Cubic ft. per lb.

p_0 = Final pressure. Lb. per square foot.

T_1 = Initial temperature, °C. abs.

Thus the velocity may be calculated from observations of the initial and final pressures, initial temperature, and physical constants for the gas under consideration, all of which may be measured fairly accurately without difficulty.

For many purposes, however, a knowledge of the theoretical temperature of the gas at the end of the expansion is desirable, and this is particularly so when this quantity is to be used as a standard for comparison with values obtained by measurement or by indirect methods. A knowledge of this temperature also enables equations (3) and (5) to be employed, without further transformation, for calculating the theoretical velocity generated.

It is the object of the following to supplement the equations of Dr. Walker by giving formulæ for the calculation of the temperature of the gas at the end of an adiabatic expansion, and thus to provide an alternative method of calculating the theoretical velocity generated.

The most general case is obtained by assuming the relationship between specific heats and temperature of the gas to be given by (4). The adiabatic equation may then be written

$$p v^m e^{\lambda T + \frac{\lambda'}{2} T^2} = \text{constant}, \quad \dots \quad (8)$$

where the symbols have the meanings previously assigned to them, and in addition, e is the base of natural logarithms. Therefore

$$p_1 v_1^m e^{\lambda T_1 + \frac{\lambda'}{2} T_1^2} = p_2 v_2^m e^{\lambda T_2 + \frac{\lambda'}{2} T_2^2}. \quad \dots \quad (9)$$

Also

$$pv = RT. \quad . \quad . \quad . \quad . \quad . \quad . \quad (10)$$

Putting

$$v = \frac{RT}{p}$$

in (9) and simplifying,

$$p_1^{1-m} T_1^m e^{\lambda T_1 + \frac{\lambda'}{2} T_1^2} = p_2^{1-m} T_2^m e^{\lambda T_2 + \frac{\lambda'}{2} T_2^2}, \quad . \quad . \quad (11)$$

or

$$\left(\frac{p_2}{p_1}\right)^{\frac{1-m}{m}} = \frac{T_1}{T_2} e^{\frac{\lambda}{m}(T_1 - T_2) + \frac{\lambda'}{2m}(T_1^2 - T_2^2)} \quad . \quad . \quad (12)$$

Expanding the exponential, and writing x for $\left(\frac{p_2}{p_1}\right)^{\frac{1-m}{m}}$ or $\left(\frac{p_1}{p_2}\right)^{\frac{m-1}{m}}$, we have

$$T_2 x = T_1 \left[1 + \frac{\lambda}{m}(T_1 - T_2) + \frac{\lambda'}{2m}(T_1^2 - T_2^2) + \left\{ \frac{\lambda}{m}(T_1 - T_2) \right\}^2 + \dots \right] \quad . \quad (13)$$

Neglecting terms involving squares and higher powers of $\left(\frac{\lambda}{m}\right)$ and of $\left(\frac{\lambda'}{m}\right)$, we have

$$T_2 x = T_1 + \frac{\lambda}{m} T_1^2 - \frac{\lambda}{m} T_1 T_2 + \frac{\lambda'}{2m} T_1^3 - \frac{\lambda'}{2m} T_1 T_2^2, \quad . \quad (14)$$

or

$$T_2 \left(x + \frac{\lambda}{m} T_1 + \frac{\lambda'}{2m} T_1 T_2 \right) = T_1 \left(1 + \frac{\lambda}{m} T_1 + \frac{\lambda'}{2m} T_1^2 \right), \quad . \quad (15)$$

or

$$T_2 = T_1 \left[\frac{1 + \frac{\lambda}{m} T_1 + \frac{\lambda'}{2m} T_1^2}{x + \frac{\lambda}{m} T_1 + \frac{\lambda'}{2m} T_1 T_2} \right], \quad . \quad . \quad . \quad (16)$$

or, since $T_2 = \frac{T_1}{x}$ nearly,

$$T_2 = T_1 \left[\frac{1 + \frac{\lambda}{m} T_1 + \frac{\lambda'}{2m} T_1^2}{x + \frac{\lambda}{m} T_1 + \frac{\lambda'}{2mx} T_1^2} \right] \quad . \quad . \quad . \quad (17)$$

A more convenient and, for most purposes, sufficiently

accurate formula is obtained by neglecting all terms involving λ' , and terms involving squares and higher powers of $\left(\frac{2}{m}\right)$.

We then have

$$T_2 = T_1 \left[\frac{1 + \frac{\lambda}{m} T_1}{x + \frac{\lambda}{m} T_1} \right] \cdot \cdot \cdot \cdot (18)$$

Equations (17) and (18) may be simplified by writing

$$\alpha = \frac{\lambda}{m}, \quad \beta = \frac{\lambda'}{2m},$$

when they become

$$T_2 = T_1 \left[\frac{1 + \alpha T_1 + \beta T_1^2}{x + \alpha T_1 + \frac{\beta}{x} T_1^2} \right] \cdot \cdot \cdot \cdot (17 a)$$

and

$$T_2 = T_1 \left[\frac{1 + \alpha T_1}{x + \alpha T_1} \right] \cdot \cdot \cdot \cdot (18 a)$$

respectively.

The values of α and β for a number of gases which find application industrially have been calculated from data given by Partington and Shilling*. These hold for a temperature range of 0° C. to 2000° C., and are given in Table I.

TABLE I.

Gas.	α .	β .
Air	0·000,024,5	0·000,000,022,4
Oxygen	0·000,024,5	0·000,000,022,4
Nitrogen	0·000,024,5	0·000,000,022,4
Carbon Monoxide ...	0·000,024,5	0·000,000,022,4
Carbon Dioxide ...	0·000,592	-0·000,000,067
Hydrogen	0·000,105	zero.
Steam	-0·000,132	0·000,000,129

The velocity generated may now be obtained either by substituting T_2 from (17 a) in (5) or T_2 from (18 a) in (3). For most purposes it is sufficiently accurate to use (18 a) and (3), and decidedly more convenient arithmetically.

* 'The Specific Heats of Gases,' pp. 201-209. Benn Bros., Ltd.
Phil. Mag. S. 7. Vol. 4. No. 24. Nov. 1927. 3 O

Regarding the calculation of the velocity generated during adiabatic expansion, with variable specific heats, there is little to choose between the equations of Dr. Walker and the method employed here. Both require the same number of initial measurements and the accuracy of both is dependent upon the accuracy with which the numerical values of the relevant properties of the gases are known.

The equations are likely to be most useful in connexion with the design of internal combustion turbines. The maximum pressures and temperatures which can be foreseen are in the neighbourhood of 300 lb. per square inch and $2500^{\circ}\text{C. abs.}$, respectively. The field is such, therefore, that changes of specific heat with temperature are all important, and changes with pressure will be so small as to be safely neglected.

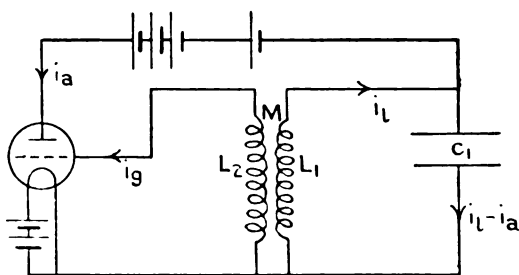
LXXXVII. On Frequency Variations of the Triode Oscillator.

By DAVID F. MARTYN, *B.Sc., A.R.C.Sc., Research Student, University of Glasgow* *.

(1) Introduction.

IT is well known that the frequency of the oscillations generated by the simple oscillator of fig. 1 does not depend solely on the values of the inductance L_1 and the capacity C_1 . Thus small changes, of the order of 2 or 3 per cent., may be produced by alteration of the filament

Fig. 1.



current or anode voltage of the valve, or by altering the coupling between the coils L_1 and L_2 .

These variations have been examined experimentally by several investigators, notably by Eccles and Vincent †. So

* Communicated by Professor E. Taylor Jones, D.Sc.

† Proc. Roy. Soc. xcvi. and xcvi. (1920).

far no satisfactory explanation of the phenomena has been offered*.

The purpose of the present paper is to record various new effects which have been obtained experimentally, and to put forward a theory which appears to be capable of explaining the observed phenomena.

(2) Apparatus.

In all the experiments to be described below the simple oscillator of fig. 1 was used. Two different pairs of generating coils were used. One pair had each a coefficient of self induction of 0.03125 henries. The coefficient of mutual induction between the coils of this pair could be varied from 0.02182 henries downwards. This pair of coils will hereafter be denoted as Coils I. The other pair of coils were considerably larger. One of this pair (A) had a coefficient of self induction of 0.665 henries, while that of the other (B) was 1.49 henries. The mutual inductance between these coils was fixed and had a value of 0.752 henries. This pair will be denoted as Coils II.

The frequency variations normally obtained with Coils I. were of the order of magnitude noticed by other observers; i.e., about 3 per cent. They were detected by a heterodyne method, a second oscillator being loosely coupled to the main oscillator, and the changes in the beat frequency observed.

In the case of Coils II. very large frequency changes were obtained in the circumstances to be described later. These changes extended sometimes over a range of three octaves. In these cases, the frequency being audible, the changes were measured by comparison with a monochord and standard tuning-fork.

(3) Variation of Frequency with Filament Current.

Using Coils II. and a Mullard P.M. 6 valve, the following results were obtained (fig. 2):—In the figure the ordinate represents frequency in cycles per second, and the abscissa filament current in milliamperes. The oscillating circuit L_1C_1 consisted of the coil (A) in parallel with a condenser of capacity 0.03 microfarad.

It is seen from the graph that in each case when oscillations commence they have very nearly the natural frequency

$$\frac{1}{2\pi \sqrt{L_1 C_1}}.$$

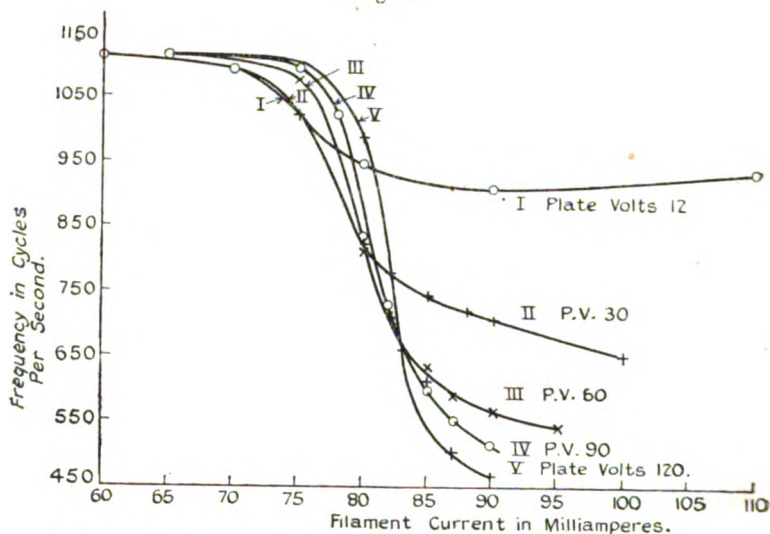
The general effect of increase of filament

* See, however, note at end of paper.

current is to produce a decrease of frequency. This decrease is greater for high values of plate voltage. For very low plate voltages a minimum frequency is obtained. This minimum occurs at a high value of the filament current.

The initial rate of decrease of frequency is slower for high than for low plate voltages. As the filament current increases, however, a point is soon reached at which the rate of decrease of frequency for high plate voltage becomes much greater than that for low plate voltages. As the filament current reaches its maximum, the curves tend to straighten out, the rate of change of frequency with filament current again becoming small.

Fig. 2.



The variations of frequency extend over more than two octaves for high plate voltages.

Similar types of curves were obtained, using valves of very different characteristics.

Using Coils I., similar types of variation were observed, but the total frequency changes were smaller in magnitude, being, say, 3 per cent. when the same capacity (0.03 mfd.) as formerly was used. Since these coils were movable, it was possible to examine the effect of variation of coupling on the character of the frequency-filament current curves.

It was found that if loose coupling was used, then the minimum frequency could be obtained at higher values of

the plate voltage than was possible when using close coupling. Further, the minimum was now obtained for a lower value of filament current, and the total range of the frequency variations was reduced.

The attainment of this minimum frequency is important from the practical point of view. Eccles and Vincent * have pointed out that, in order to obtain a constant frequency from a triode oscillator, it is desirable to set the filament current to the value which gives the minimum frequency. Small changes in filament current will then produce the smallest possible change of frequency. Eccles and Vincent indicate that this minimum frequency can always be obtained by the use of a weak enough coupling. On the other hand, recently Obata † has invariably failed to obtain the minimum frequency, although using several different types of valve. The results of the writer, as described above, indicate that the value of the plate voltage plays an important part in determining the position of the minimum frequency. Thus it is often possible to obtain the minimum while using the closest coupling, provided that the plate voltage is sufficiently low. On the other hand, when using loose coupling, the minimum is not obtained if too high a value of plate voltage is used. The conditions necessary for the production of a minimum frequency are further examined in the sequel, when the theoretical explanation of the frequency changes is considered.

The variation of the oscillatory current which occurred in the coil L_1 when the filament current was altered was also examined. It was found that normally the effect of increase of filament current was to produce an increase of the oscillatory current. Whenever a minimum occurred on the frequency-filament current curve, however, there simultaneously occurred a minimum on the curve connecting oscillatory current and filament current. This effect has been previously noted by Vincent ‡. It was further observed that a minimum occurred at the same place on the curve connecting oscillatory grid current and filament current.

After a valve has been run for some time at a high filament current, then in some cases the minimum frequency on the frequency-filament current curve is no longer obtainable. In general, the older a valve is, and the longer it has been in use, the more difficult it is to obtain the minimum frequency.

* *Loc. cit.*

† *Proc. Phys.-Math. Soc. Japan, Jan. 1927.*

‡ *Loc. cit.*

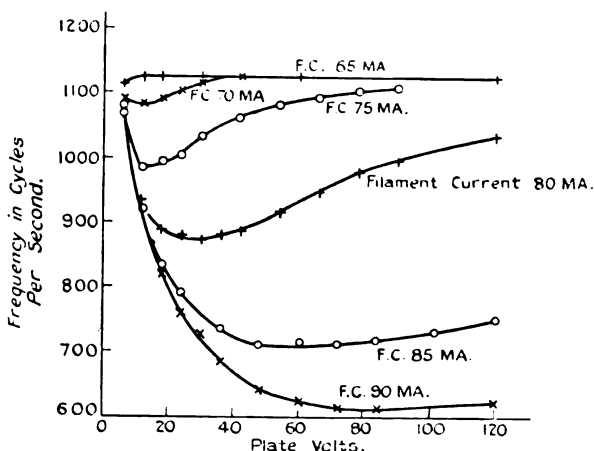
(4) *Variation of Frequency with Plate Voltage.*

Typical curves illustrating the variation of frequency with plate voltage are given in fig. 3. These results were obtained with Coils II., the condenser of capacity 0.03 mfd. being connected across coil A. The valve used was a Mullard P.M. 6. Curves are plotted for values of the filament current ranging from 65 to 90 milliamperes.

As the plate voltage is increased from zero, oscillations commence at about six volts with a frequency slightly below

the value $\frac{1}{2\pi\sqrt{L_1C_1}}$. Further increase of plate voltage

Fig. 3.



produces a decrease in frequency. At a certain value of plate voltage a minimum frequency occurs, and further increase of voltage produces a rise in frequency. The total frequency change, which may amount to as much as two octaves, is greater for higher values of the filament current. A further effect of using a higher filament current is to move the position of minimum frequency to the right of the graph, so that the minimum occurs at a higher value of plate voltage. For very low filament current values the curve shows an initial rise. In these cases it appears that the minimum has passed off the scale to the left. It is no longer obtainable because oscillations cannot be made to occur at a sufficiently low plate voltage.

Similar types of curves were obtained using quite different makes of valves.

The experiments were repeated using Coils I. The results were of the same character as those obtained with Coils II. ; but the frequency variations were of a smaller order of magnitude, being at most 2 per cent. when using the same value of capacity C_1 .

The effect of variation of coupling on the character of the frequency-plate voltage curves was investigated. It was found in every case that the effect of loosening the coupling was to reduce the rate at which the frequency changed with respect to plate voltage. Further, with looser coupling, in every case the position of minimum frequency on the frequency-plate volts curve was shifted to the right: i. e., with looser coupling the minimum frequency occurred at a higher value of the plate potential.

The amplitude of the oscillatory currents in L_1 and L_2 was found to increase steadily as the plate voltage was increased. No minimum amplitude occurred at any point on the curve.

(5) Conditions Favourable to Greatest Frequency Variation.

In all the experiments which were conducted on frequency variations, whether produced by change of filament current or of plate voltage, it was observed that the largest percentage changes of frequency were obtained in the following conditions :—

- (1) When the capacity of the condenser C_1 was as small as possible. For example, with Coils I. the total possible frequency change could be increased from 3 per cent. to about 50 per cent. by reduction of the capacity C_1 from 0.03 mfd. to 0.002 mfd.
- (2) When the coupling between the coils L_1 and L_2 was as close as possible.
- (3) When the self inductance of the grid coil L_2 was as large as possible.
- (4) When the "impedance" of the valve used was as low as possible.

(6) Variation of Frequency with Coupling.

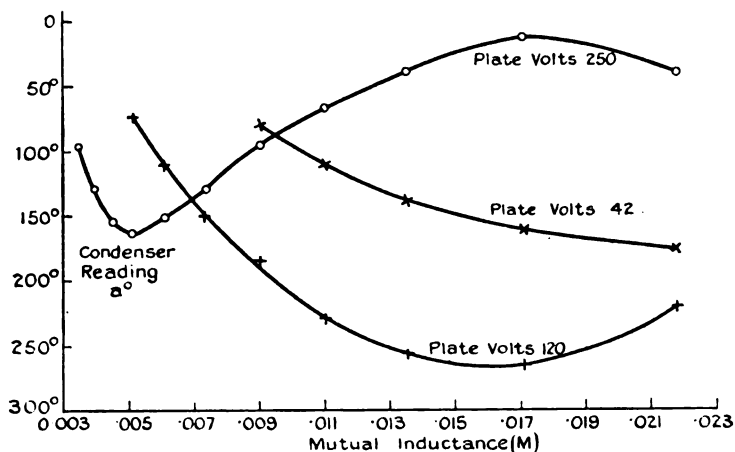
For the purpose of examining the effect of variation of coupling on frequency, Coils I. were used. The condenser C_1 had a capacity of 0.04 mfd. The frequency changes were measured by the beat method. A small variable condenser included in the circuit of the standard oscillator was adjusted so as to bring the standard oscillator into unison with the main oscillator. An increase in the dial reading a°

of this condenser corresponds to a decrease in frequency of the oscillator under consideration.

Fig. 4 shows the types of frequency variation obtained. The ordinate represents the condenser reading a° , and the abscissa the value of the mutual inductance between the coils. Curves are given for different values of the plate voltage.

Three distinct types of frequency variation occur, according to the value of the plate voltage.

Fig. 4.



For low values of plate voltage the frequency steadily decreases as M increases (type a .)

For medium values of plate voltage a minimum frequency occurs (type b).

For high values of plate voltage a minimum frequency occurs at a low value of M , and a maximum frequency also occurs at a high value of M (type c).

In one instance only, a second minimum was observed at a very high value of M (type c'). In all other respects this case conformed to type c .

The total range of frequency variation is about 2 per cent. The above types of curves were obtained with several different valves. In each case the filament current used was the normal value for the valve in question. Similar curves were obtained at higher and lower values of filament current, provided that the values of the plate voltage were altered to correspond. Thus, when using lower values of

filament current, the typical curves *a*, *b*, and *c* were obtained for lower plate voltages than were necessary in the case considered.

(7) *Theory of Frequency Variations.—Introductory.*

In the generally accepted theory of the production of triode oscillations by the arrangement shown in fig. 1, the following assumptions are made:—

- (1) That no self, mutual, or inter-electrode capacities are present, the only capacity considered being that of the condenser C_1 .
- (2) That no current of electrons flows in the valve between the filament and the grid at any time.
- (3) That the anode current i_a is given by the simple expression—

$$i_a = k_1 v_a + k_2 v_g,$$

where v_a and v_g are the anode and grid potentials respectively at any instant, and k_1 and k_2 are constants for a definite value of the filament current.

If, further, for the moment, we neglect the resistances present in the circuit, then it is easy to show that undamped oscillations of frequency $\frac{1}{2\pi \sqrt{L_1 C_1}}$ will be produced, provided:

$$k_2 M = k_1 L_1,$$

the latter relation being known as the “condition of maintenance.” On this theory, the frequency of the oscillations should depend solely on the values of L_1 and C_1 , and no variation should be produced by alteration of the conditions of working of the valve. The theory has been extended by Eccles* to the case where resistances are included in series with both L_1 and C_1 .

If R denotes the resistance in series with L_1 , and S that in series with C_1 , then he finds that the pulsatace “ p ” of the oscillations is given by the expression:

$$p^2 = \frac{1 + k_1 S}{L_1 C_1 - R C_1^2 (R + S + k_1 R S)},$$

while $k_2 M = k_1 L_1 + C_1 (k_1 R S + R + S)$

is the condition of maintenance.

The above expression for “ p ” contains the quantity k_1 . The value of k_1 is dependent on the values of the filament

* Proc. Phys. Soc. xxxi. p. 137 (1919).

current and plate voltage of the valve. Hence we should expect changes in frequency to be produced by alterations in the values of these latter quantities. k_1 has usually a value of about 10^{-6} mho, however, so that the magnitude of the changes will be very small unless the resistances are large. In the case of the apparatus used by the writer the resistances were very small. Thus S was sensibly zero, and R not more than 5 ohms for Coils I. The observed frequency variation was, say, 3 per cent., or about 500 times greater than that possible by the above formula.

A further advance in the theory of the oscillations has been made by Appleton and Greaves*. They expressed the anode current i_a in the form of a power series in v_a by consideration of the "oscillation characteristic" of the valve. As a result of this procedure they succeeded in taking account of the curvature of the valve characteristics, and of the harmonics thereby produced. The presence of these harmonics affected the frequency of the fundamental, and an expression for the fundamental frequency in the form of a series was obtained. Here again, however, the frequency variation accounted for by the theory is of a much smaller order of magnitude than that observed practically.

It appears, therefore, that we must take still other factors into account if we wish to explain the observed frequency variations. All of the experiments described above were carried out at audio-frequencies. Hence we should expect the very small inter-electrode and stray capacities to have no appreciable influence on the frequency in these cases.

There still remains to be considered the question of grid current. It has been customary in theoretical analyses of the problem to assume that this current is infinitesimally small, probably because of the great complication of the analysis which otherwise ensues. When the question of grid current is considered, however, even in its simplest aspect, it appears at once that we have here a factor capable of accounting for a frequency variation of the required order of magnitude. Before considering the theory of the production of oscillations, taking account of grid current, some experimental observations on grid current are given.

(8) *Observations on Grid Current.*

First, Coils II. were used, with a condenser of 0.04 mfd. across Coil A. A current-measuring instrument was inserted between the grid coil and the grid terminal of the

* Phil. Mag. xlv. p. 401 (1923).

valve. The filament current was then increased until oscillations commenced. At once a grid current of twenty microamperes was observed. As the filament current increased, this current increased. As soon as the frequency began to fall appreciably, the grid current commenced to increase more rapidly, until when the frequency had fallen two octaves, the grid current was as much as ten milliamperes.

It has recently been stated* that it is always possible (*e.g.*, by the use of negative grid bias) to make grid current zero while oscillations are occurring. If this statement is correct, it should be possible by this means to attain a very constant frequency, by reason of the elimination of what we are considering to be the chief source of frequency variation; viz., grid current. Accordingly it is of importance to test this statement strictly.

Using Coils II., it was not possible in any circumstances to arrange that the grid-current reading was zero at any time when oscillations were occurring.

With Coils I. the coupling was reduced to the lowest value which permitted of the oscillations being maintained. At this point the oscillations could be heard only faintly, and a delicate galvanometer in the grid circuit registered zero. The question at once arose whether actually no grid current flowed, or whether the galvanometer was not sensitive enough to detect the minute current which was flowing. To test this point, a well-insulated condenser of capacity 2 mfd. was connected in series between the galvanometer and the grid of the valve. The coupling was adjusted, as before, so that oscillations were just maintained, and the galvanometer reading was zero. The oscillations continued for a period of about a minute, and then suddenly died out. If, now, the terminals of the condenser were electrically connected momentarily, then oscillations recommenced, only to die out once more after a lapse of a minute. When a condenser of smaller capacity than 2 mfd. was used, the oscillations died out in a correspondingly shorter interval of time.

It was evident that a very minute grid current was always flowing. This current charged the condenser gradually until the grid received a negative bias large enough to stop the oscillations. It is further evident that if at any instant a negative bias was attained great enough to stop grid current, and yet permitting oscillations to occur, then the

* E. B. Moullin, 'Radio-Frequency Measurements,' p. 7.

bias on the grid would remain constant and the oscillations would continue indefinitely.

We may therefore conclude that it does not appear to be possible for oscillations to occur without flow of current to the grid.

(9) *Theory of Generation of Oscillations, taking account of Grid Current.*

In fig. 1, i_g represents the value of the grid current flowing at any instant, while i_l is the instantaneous value of the current in L_1 . If we neglect for the moment the resistances present, then we may write down at once the following equations of the circuit:—

$$v_a = M \frac{di_g}{dt} - L_1 \frac{di_l}{dt}, \quad . \quad . \quad . \quad . \quad . \quad (1)$$

$$v_g = M \frac{di_l}{dt} - L_2 \frac{di_g}{dt}, \quad . \quad . \quad . \quad . \quad . \quad (2)$$

$$i_l - i_a = C \frac{dv_a}{dt}. \quad . \quad . \quad . \quad . \quad . \quad (3)$$

As a first approximation, we shall assume that i_a and i_g are each linear functions of v_a and v_g . Hence we have:—

$$i_a = k_1 v_a + k_2 v_g, \quad . \quad . \quad . \quad . \quad . \quad (4)$$

$$i_g = k_3 v_g + k_4 v_a. \quad . \quad . \quad . \quad . \quad . \quad (5)$$

By elimination between these five equations, we obtain the following differential equation giving i_l :—

$$k_3 C_1 (L_1 L_2 - M^2) \frac{d^3 i_l}{dt^3} + \{ (L_1 L_2 - M^2) (k_1 k_3 - k_2 k_4) + L_1 C_1 \} \frac{d^2 i_l}{dt^2} + \left(L_1 k_1 + L_2 k_3 - M \overline{k_2 + k_4} \right) \frac{di_l}{dt} + i_l = 0. \quad . \quad (6)$$

k_4 is usually very small compared with k_3 , and will be neglected to simplify the algebra.

If undamped sinoidal oscillations are produced, then we may write:

$$i_l = \hat{I}_l \sin pt.$$

Substituting this value of i_l in equation (6) and equating to zero the coefficients of $\sin pt$ and $\cos pt$, we obtain two equations for p^2 :

$$p^2 = \frac{L_1 k_1 + L_2 k_3 - M k_2}{k_3 C_1 (L_1 L_2 - M^2)} \quad . \quad . \quad . \quad . \quad (7)$$

$$= \frac{1}{L_1 C_1 + k_1 k_3 (L_1 L_2 - M^2)} \quad . \quad . \quad . \quad . \quad (8)$$

The condition of maintenance is necessarily contained in these two equations.

In addition, another solution of equation (6) exists, of the form :

$$i_t = Ae^{-at} ;$$

α is a very large quantity, having a value normally of, say, 10^6 sec.^{-1} . Hence this solution gives rise to a transient which dies out almost instantaneously when oscillations commence, and will therefore be neglected.

It is evident from equation (8) that the frequency of the oscillations generated is less than the natural frequency of the circuit $\frac{1}{2\pi\sqrt{L_1C_1}}$. The amount of this lowering is dependent upon the magnitude of the expression

$$k_1k_3(L_1L_2-M^2).$$

If we take the approximate numerical value of this expression for an extreme case, using Coils II. with a large grid current flowing, we find that it has a value equal to about four times that of L_1C_1 . This indicates a fall of frequency of about two octaves, which is precisely the order of the maximum observed frequency change.

If, now, keeping the same values for k_1 , k_3 , and C_1 , we substitute the values for L_1 , L_2 , and M appropriate for Coils I., we find that the maximum variation of frequency should be about 3 per cent. This, again, is the order of the maximum frequency variation observed with Coils I.

The quantity k_3 , which is difficult to measure experimentally, may be eliminated from equation (8) by the aid of equation (7). Thus

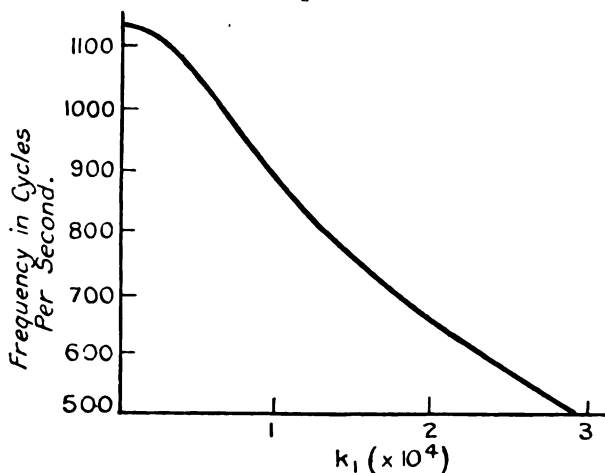
$$\begin{aligned} & k_1k_3(L_1L_2-M^2) \\ &= \frac{1}{2L_2} \left\{ -C_1M^2 + k_1^2(L_1L_2-M^2)(\mu M - L_1) \right. \\ & \quad \left. + \sqrt{C_1^2M^4 + k_1^4(L_1L_2-M^2)^2(\mu M - L_1)^2} \right. \\ & \quad \left. + 2C_1k_1^2(L_1L_2-M^2)(\mu M - L_1)(2L_1L_2-M^2) \right\}. \end{aligned} \quad \dots (9)$$

In this expression k_3 has been replaced by μk_1 , where μ is the "amplification factor" of the valve, a quantity which is appreciably constant over a wide range.

This gives now an expression for the frequency in terms of L_1 , L_2 , M , C_1 , the constant of the valve μ , and k_1 . Hence

in any particular case we may plot a curve showing the relation between frequency and k_1 . Fig. 5 illustrates the curve so obtained for Coils II. and a Mullard P.M. 6 valve.

Fig. 5.



(10) *Condition of Maintenance.*

Elimination of " p " from equations (7) and (8) leads to the equation :

$$\begin{aligned}
 & -k_3 C_1 M^2 \\
 & = L_1^2 k_1 C_1 - M L_1 C_1 k_2 + k_1 k_3 (L_1 L_2 - M^2) (k_1 L_1 + k_3 L_2 - k_2 M).
 \end{aligned}
 \quad \dots (10)$$

This is the condition for the maintenance of the oscillations. For cases where the variations of frequency are small this reduces to

$$k_3 M^2 = k_1 L_1 (\mu M - L_1). \quad \dots (11)$$

It is of interest to compare this condition with that obtained on the assumption that grid current is zero—viz. :

$$k_1 (\mu M - L_1) = 0.$$

It is difficult to see how this latter equation could ever be satisfied in ordinary circumstances. Thus, in any common case, M might have a value one-quarter that of L_1 , and μ might be, say, ten. μM is then considerably greater than L_1 . We have to imagine that the oscillations keep on

increasing until μ has decreased greatly to a value which will satisfy the relationship $\mu M = L_1$. Experience indicates that μ is sensibly constant, even over the bends of the valve characteristics, where k_1 and k_2 have changed greatly in value. On the other hand, if we consider equation (11) it is easy to see the course of events. When oscillations commence, the grid current increases until k_2 has a value such that $\frac{k_2 M^2}{k_1 L_1}$ is numerically equal to the difference between μM and L_1 .

(11) *Conditions for Maximum Frequency Variation.*

Maximum frequency changes will be obtained when the ratio $\frac{k_1 k_2 (L_1 L_2 - M^2)}{L_1 C_1}$ is as large as possible. From equation (9) we see at once that this condition requires that C_1 shall be as small as possible. When C_1 is small, we have:

$$\frac{k_1 k_2 (L_1 L_2 - M^2)}{L_1 C_1} = \frac{k_1^2}{C_1} \left(1 - \frac{M^2}{L_1 L_2} \right) (\mu M - L_1). \quad (12)$$

The quantity $\frac{M^2}{L_1 L_2}$ is always less than unity, and it may be kept small by making L_2 large. Hence we see from equation (12) that the largest frequency variations will be obtained when

- (1) C_1 is as small as possible,
- (2) M and L_2 are as large as possible compared with L_1 ,
- (3) k_1 (the reciprocal of the valve impedance) is as large as possible.

These conclusions are in perfect agreement with the experimental results previously described. In particular it becomes evident at once why the variations of frequency normally observed with Coils II. were much greater than those obtained with Coils I.

Unlimited decrease of C_1 is impossible by reason of the self-capacity of the coil L_1 . Again, it is always possible to obtain a valve with a high value of k_1 ; but this is invariably accompanied by a low amplification factor. To obtain maximum frequency variations, therefore, a valve must be chosen for which $k_1^2 \mu$ is as large as possible.

Unlimited increase of L_2 is impossible by reason of the self-capacity of the latter coil. Thus the natural period

of coil L_2 , must never be allowed to become an appreciable fraction of the periodicity of the oscillations, or the theory considered above becomes invalid.

(12) *Conditions for Minimum Frequency Change.*

For minimum frequency change, equation (12), which has been deduced on the assumption that C_1 is very small, becomes invalid. Making use, however, of the condition of maintenance for small frequency changes (equation 11), we may write :

$$\frac{k_1 k_2 (L_1 L_2 - M^2)}{L_1 C_1} = \frac{k_1^2}{C_1} \left(\frac{L_1 L_2}{M^2} - 1 \right) (\mu M - L_1). \quad (13)$$

$(\mu M - L_1)$, which is always positive in sign, will be made very small by decreasing M and μ and increasing L_1 . In these circumstances, $\left(\frac{L_1 L_2}{M^2} - 1 \right)$ will be kept small provided L_2 is made very small. k_1 must be small and C_1 large.

The conditions for minimum frequency variation are therefore exactly the reverse of those given above for maximum variation.

(13) *Non-linearity of Characteristics.*

Up till now we have assumed that the characteristics of the valve could be represented by straight lines. In most practical cases, however, the amplitude of the oscillations is such that the upper or lower bends of the characteristics are reached. It is necessary, therefore, to investigate how this will affect the frequency and the maintenance condition of the oscillations. Taking account of the curvature of the characteristics, we re-write equations (4) and (5) in the forms :

$$i_a = a_0 + a(v_a + \mu v_g) + b(v_a + \mu v_g)^2 + c(v_a + \mu v_g)^3 + \dots, \quad (4')$$

$$i_g = a'_0 + a'(v_a + \mu' v_g) + b'(v_a + \mu' v_g)^2 + c'(v_a + \mu' v_g)^3 + \dots \quad (5')$$

Substituting in these two equations

$$v_a = V \sin pt \quad \text{and} \quad v_g = V' \sin (pt + \eta),$$

and neglecting all frequencies other than "p", we obtain

$$i_a = V \left\{ a + \frac{3}{4} c (V^2 + 2\mu^2 V'^2) \right\} \sin pt \\ + \mu V' \left\{ a' + \frac{3}{4} c' (\mu^2 V'^2 + 2V^2) \right\} \sin (pt + \eta) \quad (4'')$$

and

$$i_g = V \left\{ a' + \frac{3}{4} c' (V^2 + 2\mu'^2 V'^2) \right\} \sin pt \\ + \mu' V' \left\{ a' + \frac{3}{4} c' (\mu'^2 V'^2 + 2V^2) \right\} \sin (pt + \eta). \quad (5'')$$

Combining these two latter equations with equations (1), (2), and (3), we arrive at the same solution (equations 7 & 8) as was previously obtained, provided we replace k_1 , k_2 , k_3 , and k_4 in the former solution by the expressions:

$$(\alpha) \quad \{a + \frac{3}{4}c(V^2 + 2\mu^2 V'^2) + \dots\},$$

$$(\beta) \quad \mu \{a + \frac{3}{4}c(\mu^2 V'^2 + 2V^2) + \dots\},$$

$$(\gamma) \quad \mu' \{a' + \frac{3}{4}c'(\mu'^2 V'^2 + 2V^2) + \dots\},$$

$$(\delta) \quad \{a' + \frac{3}{4}c'(V^2 + 2\mu'^2 V'^2) + \dots\}, \text{ respectively.}$$

In neglecting all frequencies other than " p ", we have assumed that the effect of harmonics on the frequency of the fundamental is negligible, being of the second order.

We see, therefore, that the frequency of the oscillations is dependent upon their amplitude. Physically we may interpret the expressions (α) , (β) , etc., as representing the "effective" slope of the characteristic over the working range. We shall therefore expect the formulæ previously developed for the frequency of the oscillations to apply, even when working on the bends of the characteristics, provided we replace k_1 etc. by this effective slope. Obvious difficulties would attend accurate measurement of this quantity. For our purpose below, however, the position is simpler, since it is only necessary to have a qualitative knowledge of the effective slope, and to know when it increases or decreases.

EXPLANATION OF EXPERIMENTAL RESULTS.

(14) *Variation of Frequency with Filament Current.*

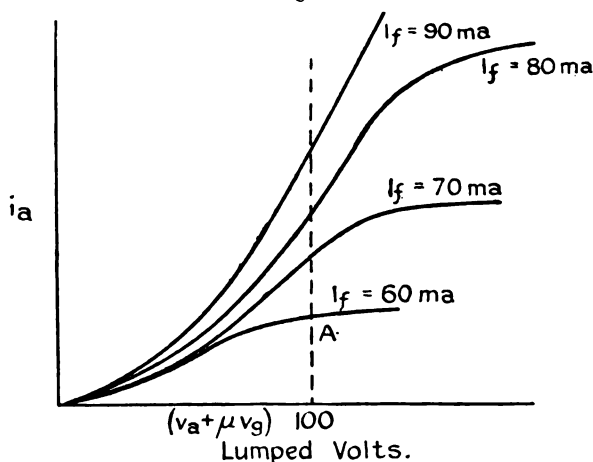
From consideration of equations (8) and (9) it is plain that, provided the values of L_1 , L_2 , M , and C_1 be kept constant, then the only way in which we can change the frequency of the oscillations is by alteration of the value of k_1 . (It is here assumed that μ is always constant, which will be sufficiently correct provided the particular valve used is not changed.) The problem of variation of frequency with filament current reduces, therefore, to the question of how k_1 is affected by variation of filament current. In general, the effect of increase of filament current on the shape of the "lumped" * valve characteristic is to raise the upper or saturation bend, and hence to increase the length of the straight part of the curve. The slope of

* Eccles, Proc. Phys. Soc. xxxii. p. 92 (1920).

the straight part is also slightly increased. A typical set of "lumped" characteristics at various values of filament current are shown in fig. 6.

We may now trace the effect of increase of filament current on the frequency of the oscillations. Imagine the plate potential to be set at 100 volts, and oscillations to commence when the filament current is 60 milliamperes. Then oscillations of small amplitude occur about the representative point A. At this point the slope of the curve (i. e., k_1) is small. Hence the oscillation frequency is not far below

Fig. 6.



the value $\frac{1}{2\pi \sqrt{L_1 C_1}}$. As the filament current increases, the

representative point passes farther and farther on to the straight part of the curve; hence k_1 increases and the frequency decreases. At the same time the amplitude of the oscillations increases, and the oscillating point may pass a considerable distance along the volts axis in the negative direction. Eventually a stage is reached at which the saturation bend becomes so high that it is not reached by the oscillating point.

If we commence with a higher plate voltage, then we need to make a correspondingly larger increase in filament current before getting on to the straight part of the characteristic. Hence with high plate voltages the initial rate of decrease of frequency is slow.

At high plate voltages the negative excursion of the oscillating point is less. Hence the effective slope of

the characteristic is greater, and the total frequency change greater at high plate voltages.

When the filament current becomes so great that the oscillating point ceases to reach the upper bend of the characteristic, the rate of decrease of frequency again falls off.

The Frequency Minimum.

For the production of a minimum frequency on the frequency-filament current curve the chief necessary condition is that the oscillating point shall not reach the saturation bend of the characteristic. For if the bend is reached, then increase of filament current, by raising the position of the bend, will increase the effective slope k_1 , and so decrease the frequency continuously.

There is experimental evidence to show that, for high values of filament current, the effect of increase of filament current is to flatten out the bottom bend of the characteristic. This is probably accounted for by the strong "space-charge" present. In these circumstances, owing to the flattening of the bottom bend, the effect of increase of filament current is to reduce the effective slope of the characteristic, and consequently to raise the frequency of the oscillations. For the same reason the amplitude of the oscillations is reduced simultaneously.

It is now clear why loose coupling, low plate voltage, and high filament current are favourable conditions for the production of a minimum frequency. All of these conditions tend to ensure that the oscillating point shall not reach the upper bend. At the same time, a high filament current is necessary in order to produce a large emission of electrons, with the consequent flattening of the bottom bend. Further, it is now clear why a valve, after working for some time at high filament current, may fail to give rise to a minimum frequency. The filament has "aged," and the emission is no longer sufficient to give rise to the effect.

(15) Variation of Frequency with Plate Voltage.

In this case also the variations of frequency may all be traced to variation of k_1 . Let us imagine (fig. 6) that oscillations are started at a low plate voltage. Here k_1 has a low value, and the oscillations have very nearly the frequency $\frac{1}{2\pi\sqrt{L_1C_1}}$. Increase of plate voltage removes the representative point away from the bottom bend,

so that k_1 increases and the frequency falls. Eventually, as the plate voltage is increased, the representative point approaches the upper bend, and the frequency commences to rise. If the amplitude of the oscillations is such that the oscillating point can reach both bends at once, then the minimum frequency occurs at a value of plate voltage about midway between the bends. Hence increase of filament current raises the position of this minimum frequency.

If the amplitude of the oscillations is small, then the oscillating point will not normally reach the upper bend of the characteristic. Hence increase of plate voltage will produce a continuous fall in frequency until a high voltage is reached sufficiently near to the upper bend. Hence the minimum frequency, for oscillations of small amplitude, will occur at a higher value of plate voltage than that for large oscillations. This explains why reduction of the coupling has the effect of shifting the position of the frequency minimum to a higher value of plate voltage. For higher values of filament current the length of the straight part of the characteristic is greater. Hence the effective slope k_1 is greater and the total frequency lowering greater.

(16) *Variation of Frequency with Coupling.*

The theoretical effect of coupling on the frequency is given by equation (13). For small frequency variations, by differentiation we get

$$\frac{dp}{dM} = \frac{k_1^2 L_1 p^3}{2M^3} \{ \mu M^3 + \mu L_1 L_2 M - 2L_1^2 L_2 \}. \quad (14)$$

Taking the numerical values for L_1 etc., appropriate for Coils I., and plotting the function for different values of M , we obtain the following results. For low values of M , $\frac{dp}{dM}$ is negative. It is zero at a value of M about the middle of the scale, and positive for high values of M . This corresponds to the experimental curve type (b) (fig. 4). This type therefore, obtained at medium values of plate voltage, is the type of curve normally to be expected on theoretical grounds.

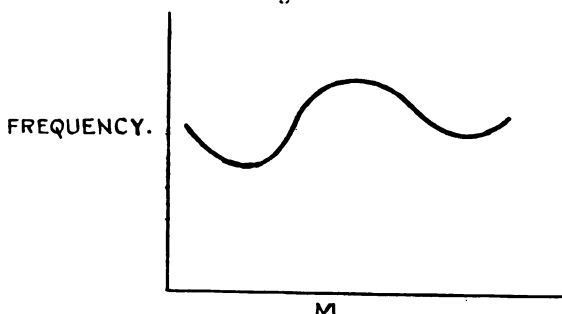
In order to explain types (a) and (c), we require to consider the amplitude of the oscillations. It is well known that, if M be steadily increased, then the amplitude of the oscillations first increases from zero, reaches a maximum value, and thereafter decreases. If the representative point is near to one of the bends on the characteristic,

then increase of amplitude sends the oscillating point round this bend, so reduces the value of the effective slope k_1 , and increases the frequency. Hence if the plate voltage is such that the representative point is near to a bend in the characteristic, then the frequency will vary in exactly the same manner as the amplitude.

We see, therefore, that when we alter the value of M we have two influences operating to produce a change of frequency.

One influence, that due to equation (14), tends to produce a minimum frequency at about the middle of the curve, while the other, that due to change of amplitude, tends to produce a maximum frequency at the same position. The resultant of these two effects will produce a frequency variation of the type shown in fig. 7. This curve was

Fig. 7.



obtained experimentally in only one case, while using a high plate voltage (type c' above). Adjustment of the plate voltage to a value approximately midway between the bends of the characteristic tends to eliminate the effect due to change of amplitude (type b).

Type (a) is produced by proximity to the bottom bend of the characteristic. The amplitude at low values of M is in this case insufficient to produce an initial minimum.

Type (c) is that usually produced by proximity to the upper or saturation bend of the characteristic.

(17) Possible Applications.

Several applications of the effects described above suggest themselves. Thus it is possible to amplify small changes of current into very large changes of frequency. This effect may be utilized in order to measure small high-frequency currents. The current to be measured is applied to the filament of the valve, either through a transformer,

or directly, with choke coils in series with the filament battery. Since it is possible to produce a change of frequency of several octaves by an alteration of only a few milliamperes in filament current, the method appears capable of great sensitivity. It possesses the advantages of giving a reading independent of frequency, and of introducing a negligibly small impedance into the circuit carrying the current to be measured. It remains to be seen if the filament emission remains sufficiently constant to ensure reasonable permanence of calibration.

The writer has not yet had the opportunity to make a thorough examination of the possibilities of the method, but intends doing so as soon as circumstances permit.

Summary.

Frequency variations due to changes in filament current, plate voltage, and coupling are investigated experimentally. Variations as great as two octaves or more are described. The most important cause of frequency variations is found to be the flow of grid current. The conditions for maximum and for minimum frequency change are worked out. The experimental results are then explained in detail by means of the theory.

In conclusion, I wish to express my sincere thanks to Professor E. Taylor Jones for his very kind interest and advice, and to the University of Glasgow for the facilities to carry out the above research.

Natural Philosophy Department,
University of Glasgow.
July 1927.

[*Addendum.*—While this paper was going through the press the attention of the author was drawn to a paper by Strecker (*Jahrb. Draht. Teleq.* xxii. (1923)) on the same subject. This valuable paper had escaped the notice of the present writer since no reference to it had appeared in 'Science Abstracts.' In this paper Strecker considers the effect of grid current, and arrives at equations equivalent to nos. 6, 7, and 8 above. In his work Strecker has confined his attention to oscillations of very small amplitude, and with the results which he obtains in these circumstances the present writer is in entire agreement. In the present paper, however, oscillations of large amplitude are considered, and for this reason the method of treatment and the nature of the experimental results differ considerably from those of Strecker.]

LXXXVIII. *On Maxwell's Stress, and its Time Rate of Variation.* By S. R. MILNER, D.Sc., F.R.S., Professor of Physics, The University, Sheffield*.

IN the electromagnetic field three functions of \mathbf{e} and \mathbf{h} are known to which dynamical meanings can be ascribed. They are †

$$W = \frac{1}{2}(e^2 + h^2), \quad . \quad . \quad . \quad . \quad . \quad (1)$$

the energy density,

$$\mathbf{G} = \frac{1}{c}[\mathbf{e}\mathbf{h}], \quad . \quad . \quad . \quad . \quad . \quad (2)$$

the momentum density, and Maxwell's stress system defined by

$$\Pi_n = \frac{1}{2}(e^2 + h^2)\mathbf{n} - (\mathbf{e}\mathbf{n})\mathbf{e} - (\mathbf{h}\mathbf{n})\mathbf{h}. \quad . \quad . \quad . \quad (3)$$

Π_n stands for the stress exerted across any unit plane whose normal is \mathbf{n} , positive values indicating pressures. The justification for calling this function of \mathbf{e} , \mathbf{h} , and \mathbf{n} a stress system is found in the following relation between Π_n and \mathbf{G} , which can be derived from the fundamental equations:

$$\frac{\partial G_x}{\partial t} = -\left(\frac{\partial \Pi_{xx}}{\partial x} + \frac{\partial \Pi_{yx}}{\partial y} + \frac{\partial \Pi_{zx}}{\partial z}\right), \text{ etc.} \quad . \quad . \quad (4)$$

This shows that the time rate of increase of the electromagnetic momentum in a fixed unit volume is equal to the resultant force which would be exerted by Π_n on that volume if Π_n were an ordinary mechanical stress.

Maxwell, I believe, did not doubt the existence of a mechanical stress actually operating on the medium, or, as we should now say preferably, on the field. Later writers have questioned its actuality. The fact is that Π_n satisfies one condition which we postulate as a property of a mechanical stress, but it does not satisfy another and an equally necessary one. Π_n is by definition a quantity at a *fixed point* in the observer's space; it varies with the time, but it is not conceived as a quantity which *moves*. Consequently, although it accounts in accordance with dynamical principles for the variation of the momentum of the field, it is incapable of doing work and accounting for the time variation of the energy ‡. An expression for the rate of increase of the

* Communicated by the Author.

† In this paper Heaviside units are used; [...] denotes the vector product; scalar products are not marked with special signs, round brackets and dots being used with the ordinary meanings.

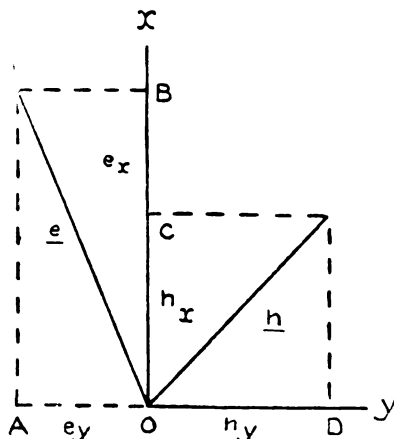
‡ To do this a *moving stress* is required, and this differs in its magnitude from Maxwell's Π_n . Cf. E. Cunningham, Proc. Roy. Soc. A, lxxxiii. p. 110 (1910); S. R. Milner, *loc. cit.* cxiv. p. 23 (1927).

energy in a fixed unit volume can indeed be found, but it comes out, not in terms of Π_n , but of \mathbf{G} , viz. Poynting's theorem :

$$\frac{\partial W}{\partial t} = -c^2 \left(\frac{\partial G_x}{\partial x} + \frac{\partial G_y}{\partial y} + \frac{\partial G_z}{\partial z} \right) (5)$$

In spite of the fact that it does not satisfy fully the dynamical requirements of a stress, Π_n is a useful and important function of \mathbf{e} and \mathbf{h} , which can be imagined as operating at each point of an electromagnetic field and producing the changes which take place there. It is difficult to visualize Π_n in its vectorial form (3); it is easy, however, if we consider it as a system of principal stresses, each of which has a definite magnitude and acts along one of three rectangular axes suitably oriented at each point of the field.

Fig. 1.



Consider any point of the field and take the plane containing \mathbf{e} and \mathbf{h} as that of xy . Draw axes Ox , Oy in this plane such that the rectangles AB , CD (fig. 1) are equal; i. e., such that

$$e_x e_y + h_x h_y = 0.$$

Then Ox , Oy , and the perpendicular Oz are the principal axes of Maxwell's stress at the point. Only when \mathbf{n} is along one of these directions is the stress normal to the area on which it acts. Π_1 , Π_2 , Π_3 being the principal stresses along Ox , Oy , Oz , it may easily be shown that

$$\left. \begin{aligned} -\Pi_1 &= +\Pi_2 = \frac{1}{2} \{ (e^2 + h^2)^2 - 4[\mathbf{eh}]^2 \}^{\frac{1}{2}} \\ &= (W^2 - c^2 G^2)^{\frac{1}{2}}, \\ \Pi_3 &= \frac{1}{2} (e^2 + h^2) = W. \end{aligned} \right\} . . . (6)$$

Π_1 is a tension, Π_2 and Π_3 are pressures, Π_2 being numerically equal to Π_1 . The figure formed by three perpendicular lines, suitably oriented at each point of the field, together with the magnitude of the principal stresses along them, forms a complete geometrical representation of a three-dimensional symmetrical tensor of the second rank in the same way that a line of given magnitude and orientation represents an ordinary vector.

Instead of the principal stresses, it is more convenient to use two variables simply related to them, which we may call "stress vectors," defined thus:

$$\left. \begin{aligned} p &= (\Pi_3 - \Pi_1)^{\frac{1}{2}} \text{ acting along } Ox, \\ q &= (\Pi_3 - \Pi_2)^{\frac{1}{2}} \quad \quad \quad \quad \quad Oy. \end{aligned} \right\} \quad \cdot \quad \cdot \quad \cdot \quad (7)$$

\mathbf{p} and \mathbf{q} are vectors of the same type as \mathbf{e} and \mathbf{h} , which are by definition at right angles to each other, whether \mathbf{e} and \mathbf{h} are or are not. They specify completely the dynamical variables by

$$\left. \begin{aligned} -\Pi_1 &= +\Pi_2 = \frac{1}{2}(p^2 - q^2), \\ \Pi_3 &= W = \frac{1}{2}(p^2 + q^2), \\ \mathbf{G} &= \frac{1}{c} [\mathbf{pq}], \end{aligned} \right\} \quad \cdot \quad \cdot \quad \cdot \quad \cdot \quad (8)$$

and are also related to \mathbf{e} and \mathbf{h} by the equations

$$\left. \begin{aligned} \mathbf{p} &= \mathbf{e} \cos \alpha + \mathbf{h} \sin \alpha, \\ \mathbf{q} &= -\mathbf{e} \sin \alpha + \mathbf{h} \cos \alpha, \end{aligned} \right\} \quad \cdot \quad \cdot \quad \cdot \quad \cdot \quad (9)$$

where

$$\tan 2\alpha = \frac{2(\mathbf{e} \cdot \mathbf{h})}{e^2 - h^2} \quad \cdot \quad \cdot \quad \cdot \quad \cdot \quad \cdot \quad (10)$$

The fact that the time rates of increase of W and \mathbf{G} can be expressed in terms of the space variations of \mathbf{G} and Π_n (eqs. (5) and (4)) suggests a search for an expression for the time rate of variation of Π_n . If this could be obtained in terms of W , \mathbf{G} , and Π_n , the three equations would form a closed chain, giving a complete formulation of the electromagnetic laws in terms of dynamically interpretable quantities. It appears, however, that in the most general field (where \mathbf{e} and \mathbf{h} are not perpendicular) this cannot be done until another variable has been introduced into the equations. W , \mathbf{G} , and Π_n together specify only 5 independent variables between them—*e. g.*, the magnitudes of p and q , together with 3 direction cosines to fix the orientation of the rectangular stress axes. The complete field, on the other hand, at each point requires 6 independent variables

to express it—*e. g.*, the magnitudes of e and h , with 4 direction cosines to fix their lines of action. Introducing the α of equation (10) as a sixth variable, we see that \mathbf{p} , \mathbf{q} , and α will fully specify all quantities, both dynamical and electromagnetic (except electric charges), in the field.

The time variation of Maxwell's stress appears to be most simply expressed by formulæ stating separately the time rates of increase of p^2 and q^2 (which fix the magnitudes of the principal stresses), and the angular velocity with which the system of stress axes is rotating*.

On substituting from (9) in the fundamental equations

$$\dot{\mathbf{e}} = c \operatorname{curl} \mathbf{h}, \quad \dot{\mathbf{h}} = -c \operatorname{curl} \mathbf{e},$$

we obtain equivalent ones in terms of p , q , and α :

$$\begin{aligned} \dot{\mathbf{p}} - \mathbf{q}\dot{\alpha} &= c(\operatorname{curl} \mathbf{q} - [\mathbf{p}\nabla\alpha]), \quad \dots (a) \\ \dot{\mathbf{q}} + \mathbf{p}\dot{\alpha} &= -c(\operatorname{curl} \mathbf{p} + [\mathbf{q}\nabla\alpha]), \quad \dots (b) \end{aligned} \quad (11)$$

Since \mathbf{p} and \mathbf{q} are everywhere perpendicular, α can be eliminated by multiplying scalarly by \mathbf{p} and \mathbf{q} , giving

$$\left. \begin{aligned} \frac{\partial}{\partial t}(\tfrac{1}{2}p^2) &= c\mathbf{p} \operatorname{curl} \mathbf{q}, \\ \frac{\partial}{\partial t}(\tfrac{1}{2}q^2) &= -c\mathbf{q} \operatorname{curl} \mathbf{p}. \end{aligned} \right\} \dots \dots (12)$$

These are just the same relations as exist between \mathbf{e} and \mathbf{h} , although \mathbf{p} and \mathbf{q} are vectors quite different from \mathbf{e} and \mathbf{h} in both magnitude and direction.

Although α does not appear in (12), it cannot be eliminated from expressions for the rotation of the stress axes. A complete set of equations can, however, be derived, three to give at a fixed point the component velocities of angular rotation of the stress system about its own axes in terms of the space derivatives of \mathbf{p} , \mathbf{q} , and α , and a fourth the time rate of increase of α in terms of space derivatives of \mathbf{p} and \mathbf{q} .

The equation for $\dot{\alpha}$ may readily be obtained by multiplying (11 a) by \mathbf{q} and (11 b) by \mathbf{p} and adding. Since

$$\mathbf{q}[\mathbf{p}\nabla\alpha] + \mathbf{p}[\mathbf{q}\nabla\alpha] = 0 \quad \text{and} \quad \mathbf{q}\dot{\mathbf{p}} + \mathbf{p}\dot{\mathbf{q}} = 0,$$

we obtain at once

$$\frac{\partial \alpha}{\partial t} = c \frac{(\mathbf{q} \operatorname{curl} \mathbf{q} - \mathbf{p} \operatorname{curl} \mathbf{p})}{p^2 - q^2}. \quad \dots (13)$$

To obtain the rotations, use for the moment the special

* The attempt to express $\frac{\partial \Pi_n}{\partial t}$ direct leads to great complications.

axes Ox , Oy , Oz of fig. 1, which are along the directions of \mathbf{p} , \mathbf{q} and $[\mathbf{pq}]$ respectively. On these axes

$$p_x = p, \quad p_y = p_z = 0, \quad q_y = q, \quad q_x = q_z = 0.$$

If we write $d\theta_{yz}$, $d\theta_{zx}$, $d\theta_{xy}$ for the infinitesimal angles through which the directions of \mathbf{p} , \mathbf{q} and $[\mathbf{pq}]$ have rotated at a neighbouring point of space or time, where the components of \mathbf{p} and \mathbf{q} are $p_x + dp_x$, etc., we have by simple geometry

$$\begin{aligned} dp_x &= dp, & dp_y &= p d\theta_{xy}, & dp_z &= -p d\theta_{zx}, \\ dq_x &= -q d\theta_{xy}, & dq_y &= dq, & dq_z &= q d\theta_{yz}. \end{aligned}$$

We can consequently write for the component angular velocities of the stress system

$$\begin{aligned} \omega_x &= \frac{\partial \theta_{yz}}{\partial t} = \frac{1}{q} \frac{\partial q_z}{\partial t}, \\ \omega_y &= \frac{\partial \theta_{zx}}{\partial t} = -\frac{1}{p} \frac{\partial p_z}{\partial t}, \\ \omega_z &= \frac{\partial \theta_{xy}}{\partial t} = \frac{1}{p} \frac{\partial p_y}{\partial t} = -\frac{1}{q} \frac{\partial q_x}{\partial t}. \end{aligned}$$

Since \mathbf{p} , \mathbf{q} , and $[\mathbf{pq}]$ are perpendicular, these equations can be written in vectorial form independent of the special axes :

$$\left. \begin{aligned} q^2 \cdot \mathbf{p} \omega &= [\mathbf{pq}] \dot{\mathbf{q}}, & . & . & (a) \\ p^2 \cdot \mathbf{q} \omega &= -[\mathbf{pq}] \dot{\mathbf{p}}, & . & . & (b) \\ [\mathbf{pq}] \omega &= \mathbf{q} \dot{\mathbf{p}} - \mathbf{p} \dot{\mathbf{q}}, & . & . & (c) \end{aligned} \right\} . . . (14)$$

ω stands here for the vector angular velocity of the system of stress axes. (14 a) gives, on substituting from (11 b) for $\dot{\mathbf{q}}$ *,

$$q^2 \cdot \mathbf{p} \omega = c(-[\mathbf{pq}] \text{curl } \mathbf{p} + q^2 \cdot \mathbf{p} \nabla \alpha). \quad (15 a)$$

Similarly, from (14 b),

$$p^2 \cdot \mathbf{q} \omega = c(-[\mathbf{pq}] \text{curl } \mathbf{q} + p^2 \cdot \mathbf{q} \nabla \alpha), \quad (15 b)$$

and from (14 c)

$$\begin{aligned} [\mathbf{pq}] \omega &= c(\mathbf{q} \text{curl } \mathbf{q} - \mathbf{q}[\mathbf{p} \nabla \alpha]) + q^2 \dot{\alpha} \\ &= c\left(\frac{p^2 \cdot \mathbf{q} \text{curl } \mathbf{q} - q^2 \cdot \mathbf{p} \text{curl } \mathbf{p}}{p^2 - q^2} + [\mathbf{pq}] \nabla \alpha\right). \end{aligned} \quad (15 c)$$

on substituting for $\dot{\alpha}$ from (13).

(15 a, b, c) determine the three scalar products of ω with \mathbf{p} , \mathbf{q} , and $[\mathbf{pq}]$ respectively—i. e., the component angular

* Since $[\mathbf{pq}][\mathbf{q} \nabla \alpha] = -\nabla \alpha [\mathbf{q}[\mathbf{pq}]]$ and $[\mathbf{q}[\mathbf{pq}]] = q^2 \cdot \mathbf{p}$.

948 *Maxwell's Stress, and its Time Rate of Variation.*

velocity of the stress system about each of its own axes is derived in terms of the space variations of the stress vectors and of α . The complete angular velocity is thus determined.

The point of chief interest about these equations is the remarkable way in which $\nabla\alpha$ enters into them. They may be written in the form

$$\left. \begin{aligned} \mathbf{p}(\omega - c\nabla\alpha) &= -c \frac{[\mathbf{p}\mathbf{q}] \text{curl } \mathbf{p}}{q^2}, \\ \mathbf{q}(\omega - c\nabla\alpha) &= -c \frac{[\mathbf{p}\mathbf{q}] \text{curl } \mathbf{q}}{p^2}, \\ [\mathbf{p}\mathbf{q}](\omega - c\nabla\alpha) &= c \frac{p^2 \cdot \mathbf{q} \text{curl } \mathbf{q} - q^2 \cdot \mathbf{p} \text{curl } \mathbf{p}}{p^2 - q^2}. \end{aligned} \right\} \dots (16)$$

or, still more simply, denoting by suffixes components on the special axes defined by the stress,

$$\left. \begin{aligned} (\omega - c\nabla\alpha)_x &= -\frac{c}{q} \text{curl}_x \mathbf{p}, \\ (\omega - c\nabla\alpha)_y &= -\frac{c}{p} \text{curl}_y \mathbf{q}, \\ (\omega - c\nabla\alpha)_z &= c \frac{p \text{curl}_y \mathbf{q} - q \text{curl}_x \mathbf{p}}{p^2 - q^2}. \end{aligned} \right\} \dots (17)$$

Write $\omega' = \omega - c\nabla\alpha$, so that $\omega = \omega' + c\nabla\alpha$. ω' is expressed solely in terms of \mathbf{p} , \mathbf{q} , and their space derivatives, i. e., is completely defined by the stress. In a field in which $\alpha=0$ everywhere (a restriction which implies that \mathbf{e} and \mathbf{h} shall be everywhere perpendicular to each other), ω' is the full rotation which the stress system possesses. In the more general field, however, in which \mathbf{e} and \mathbf{h} are not perpendicular, to obtain the actual angular velocity of the stress axes, there has to be added to ω' an additional rotation, $c\nabla\alpha$. α is a scalar variable which, as has been pointed out, is entirely independent of the stress. It is simply related to $(\mathbf{e}\mathbf{h})$, and from the electromagnetic point of view forms a measure at each point of the extent to which the field deviates from the condition that \mathbf{e} and \mathbf{h} are perpendicular. We see now that it has also a certain dynamical significance; α is a potential whose gradient (multiplied by c) constitutes a velocity of rotation of the stress axes which exists in the general field independently of and superposed on that (ω') produced by the stress itself. The presence of this "intrinsic" rotation, as it may be called, sharply distinguishes the properties of fields in which

e and **h** are not perpendicular and fields in which they are. The matter may be put in this way. Consider any "orthogonal" field (**h** \perp **e** everywhere). A knowledge of the stress system at each point enables its rate of increase (in free space) to be determined completely, and with it the whole subsequent changes in the field. In a non-orthogonal field this is not the case. There is now present at each point an intrinsic rotation of the stress system depending for its amount on the extent to which the field deviates from orthogonality, and the changes in the field can only be fully predicted from a knowledge of the stress system when the effect of this rotation is taken into account.

LXXXIX. *The Relativistic Rule for the Equipartition of Energy.* By F. F. P. BISACRE, O.B.E., M.A.*

THE well-known rule of equipartition of energy in a gas is that each degree of freedom carries energy, $\frac{1}{2}RT$.

If classical mechanics be abandoned in favour of the mechanics of the special theory of relativity, this rule must be modified for high temperatures. It is of some interest, perhaps, to examine the nature of the modification needed. The modification turns out to be a very simple one that is accurately expressible in terms of Bessel Functions of the second kind.

Consider a mass of gas, consisting of n particles, each of proper mass, m , and being at temperature T .

Assume that the potential energy is negligible so that the whole energy (*i. e.*, the kinetic energy and the "internal" energy) of the system is given by

$$E = mc^2 \sum_i \left\{ 1 - \frac{\dot{x}_i^2 + \dot{y}_i^2 + \dot{z}_i^2}{c^2} \right\}^{-\frac{1}{2}}, \quad i = 1, 2, \dots, n \quad (1)$$

in the usual notation.

The kinetic energy, κ , is given by

$$\kappa = E - mnc^2 \quad . \quad . \quad . \quad . \quad . \quad . \quad (2)$$

Plot a 3-dimensional velocity diagram having one representative point per particle. The coordinates of a point give the component speeds of the particle it stands for.

The radius vector, r , gives the magnitude of the resultant velocity of the particle; hence $r < c$: in fact, the whole velocity diagram lies inside a sphere of radius c .

* Communicated by the Author.

Let ϵ be the whole energy of a single particle, then

$$\epsilon = mc^2 \left\{ 1 - \frac{v^2}{c^2} \right\}^{-\frac{1}{2}}, \quad (3)$$

so that the representative points of all particles having energy ϵ must lie on the spherical surface of radius

$$r = c \left\{ 1 - \frac{m^2 c^4}{\epsilon^2} \right\}^{\frac{1}{2}}, \quad (4)$$

and consequently all particles having energy between ϵ and $\epsilon + \delta\epsilon$ have representative points lying between the spherical surfaces of radii r and $r + \delta r$, where

$$\delta r = m^2 c^3 \epsilon^{-3} \left\{ 1 - \frac{m^2 c^4}{\epsilon^2} \right\}^{-\frac{1}{2}} \delta\epsilon. \quad (5)$$

Since the velocity cannot exceed c , we must carefully reconsider the usual conception of "equal probability." I follow Cunningham* in this:—

"If nothing is known of a given particle save that it is in a certain region of space, it is assumed that all positions within that region are equally likely to be the actual position of the particle; or, again, it is assumed that for a given particle of which nothing is known to restrict its velocity, all velocities are equally probable, no matter how great. Now, in the case of the velocity it is obvious that the principle of relativity cannot admit this as a reasonable assumption, since the continual addition of velocities never leads to a velocity greater than that of light; and so the question may be asked: 'What criteria of equal probability are consistent with the principle?'"

In classical theory, if $\delta\tau$ is an element of volume of the velocity diagram corresponding to $u, u + \delta u; v, v + \delta v; w, w + \delta w$, and we find n representative points in this volume, then we must suppose that, if nothing is known to restrict the velocity, we shall find the same number of points in another volume the same size at some other place in the diagram, u', v', w' .

This rule cannot hold where the velocity cannot be greater than c .

"A general criterion may be laid down applying to all cases.

"Any two states of a self-contained system which can be transformed into one another by a Lorentz transformation are to be considered as equally probable."

By comparing a particle with a small velocity (u, v, w)

* E. Cunningham, 'The Principle of Relativity,' p. 208 (1921).

with one obtained from it by a Lorentz transformation, it follows that, other things being equal, it is just as probable that the velocity of any particular particle will be represented by a point within the volume $\delta\tau$, near the origin, as within $\delta\tau'$ elsewhere, where

$$\delta\tau' = \delta\tau \cdot \beta^{-4}$$

$$\text{and } \beta = \left[1 - \frac{v^2}{c^2}\right]^{-\frac{1}{2}} = \epsilon/mc^2 \text{ by (3),}$$

where v is the resultant velocity, i. e. the radius, r .

Dividing up the space enclosed by the spherical surface $r=c$ into cells of equal probability and distributing the points in the most probable way so as to keep the total number constant and the total energy they represent constant, we find, in the usual way *, that the number of representative points lying in the cell of volume $\tau\beta^{-4}$ is $Ae^{-\gamma\epsilon}$, where A and γ are constants and ϵ is the energy corresponding to a point in the cell.

The number of such cells in the spherical shell of radii r and $r + \delta r$ is

$$\frac{4\pi r^2 \cdot \delta r \cdot \beta^4}{\tau}.$$

If δn is the number of representative points lying within this shell,

$$\delta n = \frac{4\pi r^2 \cdot \delta r \cdot \beta^4}{\tau} \cdot Ae^{-\gamma\epsilon} = Br^2\beta^4 e^{-\gamma\epsilon} \delta r,$$

where B is a constant, and δn is the number of particles having energy lying between ϵ and $\epsilon + \delta\epsilon$.

Substituting known values for β , r , and δr , we get

$$\delta n = \frac{B}{m^2 c} \left\{1 - \frac{m^2 c^4}{\epsilon^2}\right\}^{\frac{1}{2}} \epsilon e^{-\gamma\epsilon} \delta\epsilon;$$

$$\text{i. e., } n = \frac{B}{m^2 c} \int_{mc^2}^{\infty} \left\{1 - \frac{m^2 c^4}{\epsilon^2}\right\}^{\frac{1}{2}} \epsilon e^{-\gamma\epsilon} d\epsilon = \frac{B}{m^2 c} \cdot I_d$$

$$\text{and } E = \frac{B}{m^2 c} \int_{mc^2}^{\infty} \left\{1 - \frac{m^2 c^4}{\epsilon^2}\right\}^{\frac{1}{2}} \epsilon e^{-\gamma\epsilon} d\epsilon = \frac{B}{m^2 c} \cdot I_n.$$

$$\therefore E = n I_n / I_d.$$

The ordinary kinetic energy, κ , is given by

$$\kappa = n \left\{ \frac{I_n}{I_d} - mc^2 \right\}.$$

There are $3n$ degrees of freedom; hence, if $\bar{\epsilon}$ is the quota,

$$\bar{\epsilon} = \frac{1}{3} \left\{ \frac{I_n}{I_d} - mc^2 \right\} \dots \dots \dots (6)$$

* J. H. Jeans, 'The Dynamical Theory of Gases,' p. 45 *et seq.* (1921).

It remains to evaluate the integrals.

The substitutions

$$\epsilon = mc^2 x \quad \text{and} \quad \alpha = \gamma mc^2$$

lead to

$$I_n/I_d = mc^2 \cdot F(\alpha)/\psi(\alpha),$$

where

$$F(\alpha) = \int_1^\infty \left\{ 1 - \frac{1}{x^2} \right\}^{\frac{1}{2}} x^2 e^{-\alpha x} dx$$

and

$$\psi(\alpha) = \int_1^\infty \left\{ 1 - \frac{1}{x^2} \right\}^{\frac{1}{2}} x e^{-\alpha x} dx.$$

Now *

$$F(\alpha) = \left[\int_1^\infty (x^2 - 1)^{-\frac{1}{2}} x^3 e^{-\alpha x} dx - \int_1^\infty (x^2 - 1)^{-\frac{1}{2}} x e^{-\alpha x} dx \right]$$

and

$$\psi(\alpha) = \left[\int_1^\infty (x^2 - 1)^{-\frac{1}{2}} x^2 e^{-\alpha x} dx - \int_1^\infty (x^2 - 1)^{-\frac{1}{2}} e^{-\alpha x} dx \right],$$

and each of these integrals can be obtained from

$$f(\alpha) = \int_1^\infty (x^2 - 1)^{-\frac{1}{2}} e^{-\alpha x} dx$$

by differentiation; in fact

$$F(\alpha) = [f'(\alpha) - f'''(\alpha)]$$

$$\text{and} \quad \psi(\alpha) = [f''(\alpha) - f(\alpha)],$$

where accents denote differentiation with respect to α .

By putting $\cosh \theta$ for x we can reduce $f(\alpha)$ to

$$f(\alpha) = \int_0^\infty e^{-\alpha \cosh \theta} d\theta, \quad (7)$$

which is the Bessel function of the second kind, defined by

$$f(\alpha) = K_0(\alpha) = (\log_e 2 - 0.577 \dots) J_0(i\alpha) - J_0(i\alpha) \log_e \alpha + \left[\frac{\alpha^2}{2^2} + \dots \right],$$

and is Heine's function. It satisfies the related Bessel equation :

$$\frac{d^2 w}{d\alpha^2} + \frac{1}{\alpha} \frac{dw}{d\alpha} - w = 0. \quad (8)$$

* I am indebted to Dr. John Dougall for the suggestion to split up the integrals in this way.

The function is tabulated on pp. 127, 128 of Jahnke and Emde's 'Funktionentafeln'—so is the function $K_1(\alpha)$, which is the same as $-\frac{dK_0}{d\alpha}$, i. e. as $-f'(\alpha)$.

We have, then,

$$F(\alpha)/\psi(\alpha) = \left[\frac{K_0(\alpha)}{K_1(\alpha)} + \frac{2}{\alpha} \right] \dots \dots \dots (8a)$$

by using equation (8) to express $K_0''(\alpha)$ and $K_0'''(\alpha)$, in terms of $K_0(\alpha)$ and $K_0'(\alpha)$, i. e. $-K_1(\alpha)$.

The result is that

$$\bar{\epsilon} = \frac{mc^2}{3} \left[\frac{K_0(\alpha)}{K_1(\alpha)} + \frac{2}{\alpha} - 1 \right], \dots \dots \dots (9)$$

where

$$\alpha = \gamma mc^2.$$

The asymptotic value of $K_0(\alpha)$ is given by

$$K_0(\alpha) \approx \sqrt{\frac{\pi}{2}} \cdot \frac{e^{-\alpha}}{\sqrt{\alpha}} \left\{ 1 - \frac{1}{8\alpha} + \dots \right\}$$

from which it appears that

$$\bar{\epsilon} = \frac{1}{2\gamma} \text{ when } \alpha \text{ is large.}$$

Now c is large when T is small, so that this is the classical result, and we know that, when T is small, $\bar{\epsilon} = \frac{1}{2}RT$, so that γ is $1/RT$, which formula we shall assume to hold good for all values of T .

$$\bar{\epsilon} = \frac{1}{2}RT,$$

$$\therefore \gamma = 1/RT.$$

The general result is, then,

$$\bar{\epsilon} = \frac{mc^2}{3} \left[\frac{K_0(\alpha)}{K_1(\alpha)} + \frac{2}{\alpha} - 1 \right], \dots \dots \dots (10)$$

where

$$\alpha = \frac{mc^2}{RT}.$$

For a given gas and temperature, α is calculable, and values of $K_0(\alpha)$ and $K_1(\alpha)$ are given in Jahnke and Emde's Tables.

When α is small, the important term in the Bessel function is the logarithm of α , and we get

$$K_0(\alpha) \approx -\log \alpha$$

$$\text{and } K_1(\alpha) \approx 1/\alpha.$$

$$\therefore \bar{\epsilon} \rightarrow 2/3\gamma,$$

since $\alpha \log \alpha \rightarrow 0$ as $\alpha \rightarrow 0$.

We thus have

$$\left. \begin{aligned} \bar{\epsilon} &\rightarrow \frac{3}{2}RT \text{ as } T \rightarrow \infty, \\ \bar{\epsilon} &\rightarrow \frac{1}{2}RT \text{ as } T \rightarrow 0. \end{aligned} \right\} \dots \dots \dots (11)$$

CONCLUSION.

It is sometimes stated that the classical rule, $\frac{1}{2}RT$, is "inevitable," whatever system of dynamics be used, so long as continuity is preserved—to break away from the classical rule discontinuities are *essential*. This is plainly not true. In breaking away from classical *kinematics*, the criterion of equal probability comes in question, so that the simple exponential rule is no longer applicable. If one tries to apply the simple exponential rule to this problem, one reaches the absurdity that the energy of the gas is *finite* as $T \rightarrow \infty$. Cunningham's modified probability rule avoids this, and these results go to show the essential reasonableness of his rule.

Even in a field free from gravitational forces, the classical rule is merely an approximation (though, of course, a very good one) to a much more complicated law. The specific heat, even of an *ideal* gas, must show an upward tendency (of the amount indicated by the above results) which arises purely from the limitations imposed by the nature of space-time.

March 1, 1927.

Note added in proof.—It may be held that the proper probability rule to take involves not β^4 but β^3 (see Cunningham, 'The Principle of Relativity,' 1921, p. 209, §5).

If this rule be taken,

$$\frac{1}{mc^2} \frac{E}{n} = \frac{1}{mc^2} \frac{I_n}{I_d} = \frac{(\alpha^2 + 6)K_1(\alpha) + 3\alpha K_0(\alpha)}{2\alpha K_1(\alpha) + \alpha^2 K_0(\alpha)}$$

giving

$$\bar{\epsilon} = 1/2\gamma \text{ when } \alpha \text{ is large}$$

$$\text{and } \bar{\epsilon} = 1/\gamma \text{ when } \alpha \text{ is small ;}$$

$$\text{i. e., } \bar{\epsilon} \rightarrow \frac{1}{2}RT \text{ as } T \rightarrow 0$$

$$\text{and } \bar{\epsilon} \rightarrow RT \text{ as } T \rightarrow \infty.$$

*XC. On the Refraction of Electro-Magnetic Waves in a Spherically Stratified Medium. By Instructor-Captain T. Y. BAKER, R.N. (ret.) **

IN a material medium the velocity of electro-magnetic waves is affected by physical conditions such as density, degree of ionization, etc., that exist at the different points. It is generally held that in no case can the velocity of the wave-fronts exceed that of light *in vacuo*, so that the ratio of the velocity at any point in the medium to that *in vacuo* is a fraction. The inverse of this fraction is termed the refractive index at the point.

It is also held that energy is transmitted through a medium or through the æther in the form of transverse vibrations in which the wave-fronts move forward in directions always at right-angles to themselves, and the family of surfaces to which consecutive wave-fronts give rise are cut orthogonally by a set of curves which ordinarily are termed rays.

In considering the transmission of radiant energy it is in many cases more convenient to do so in terms of the rays rather than in terms of the wave-fronts.

As the different portions of the wave-fronts pass through different parts of a heterogeneous medium the velocities of those portions will change in accordance with the distribution of refractive index, giving rise to alterations in the shapes of the wave-fronts and consequently to the shapes of the rays.

A heterogeneous medium that is of special interest is one which is stratified, as far as refractive index is concerned, in concentric spherical layers. The earth's atmosphere approximates to something of this nature, though the change from night to day, altering, as it presumably does, the state of ionization, probably causes the stratification to be eccentric.

The consideration of the nature of the distribution of refractive index is not the only factor that governs the transmission of radiant energy through the atmosphere. Where the paths of the rays impinge upon the earth's surface there is possibly something in the nature of surface reflexion; where they pass from one layer into another where there is a rapid drop in refractive index there may be something analogous to what happens when a train of waves in the visible spectrum passes an air-glass surface. In such case part of the energy is transmitted from one medium to the

* Communicated by the Author.

other, part is reflected. For normal incidence the fraction of reflected energy is $\left(\frac{n-1}{n+1}\right)^2$ for oblique incidence the fraction is given by Fresnel's formula

$$\frac{1}{2} \left\{ \frac{\sin^2 (i-i')}{\sin^2 (i+i')} + \frac{\tan^2 (i-i')}{\tan^2 (i+i')} \right\},$$

i and i' being the angles of the incidence of the ray with the normal in the two media.

There must also be considered, in order to bring the investigation into line with actual facts, what proportion of the energy is absorbed by the medium as the waves pass through it, and lastly, as the energy passes close to the surface of the earth, there must be considered the diffraction effects that are produced in the shadow.

All these considerations make the investigation of the paths of light-waves and wireless waves exceedingly complicated, and it is only the hypothetical cases in which some of the governing factors are omitted that rigorous mathematical treatment is possible.

In this paper such a course has been followed. Nothing but straight forward refraction is considered ; that is to say the waves are supposed to move everywhere at right-angles to themselves with velocities inversely proportional to the refractive index. All diffraction effects, all absorption effects, all surface reflexion effects, whether at the earth's surface, or possibly at the Heaviside layer, are left out of account, and the investigation which follows aims at showing what kind of physical effects in the reception of wireless signals, or in the distance and depression of the visible sea-horizon, will be found in this hypothetical atmosphere. No attempt is made to discuss the physical conditions such as density, degree of ionization, etc., at any point that produce the particular refractive index at that point, except that it is assumed that refractive index is a function of wave-length, and that consequently the distribution of refractive index with height is not necessarily the same for one wave-length as for another.

With those limitations there is investigated for this hypothetical atmosphere what must be the nature of the distribution of refractive index that will allow of a transmission of energy completely round the earth, and that will give rise to such phenomena as the skip distance. Within the region of the visible spectrum the refractive effects that give rise to a triple horizon, sometimes termed mirage, are considered.

The following nomenclature will be used throughout :—

r : the distance of any point from the centre of stratification.

p : perpendicular from the centre upon the tangent to the ray at any point.

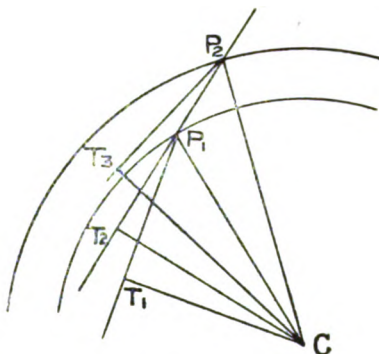
ϕ : the angle at any point between the tangent to the ray and the radius vector to the point.

n : the refractive index at any point.

R : the radius of the earth.

In fig. 1 are shown two surfaces separating media of refractive indices n_1, n_2, n_3 and a ray T_1P_2 is incident at the point P_1 making an angle T_1P_1C with the radius, *i.e.* with the normal at P_1 .

Fig. 1.



The ray then passes through the layer of constant refractive index n_2 until it strikes the next interface at P_2 , making an angle P_1P_2C with the normal, and is again refracted.

The points T_1, T_2, T_3 are the feet of the perpendiculars from the centre on the ray in each layer.

The equations of refraction are :

$$n_1 \sin T_1P_1C = n_2 \sin T_2P_1C,$$

$$n_2 \sin T_2P_2C = n_3 \sin T_3P_2C,$$

whence

$$n_1 T_1C/P_1C = n_2 T_2C/P_1C,$$

and

$$n_2 T_2C/P_2C = n_3 T_3C/P_2C,$$

or

$$n_1 T_1C = n_2 T_2C = n_3 T_3C =, \text{ etc.}$$

And generally, if the layers are made infinitely thin, $n \cdot TC$

is constant, the lines $T_1 P_1, T_2 P_2$, etc., becoming ultimately successive tangents to the curved path of the ray.

Consequently for a ray in a spherically stratified medium $np = \text{constant} = k$ say.

Hence, if n be known as a function of $r (=f(r))$, the equation of the ray is

$$np = pf(r) = k \quad . \quad . \quad . \quad . \quad . \quad . \quad (i.)$$

This is the general equation of any ray whatever in a spherically stratified medium.

The radius of curvature, ρ , being $\frac{rdr}{dp}$, it follows that

$$\rho = r / \frac{dr}{dn} = -rn/p \frac{dn}{dr}.$$

In a particular case the waves in question may be waves of visible light travelling in a nearly horizontal direction over the surface of the sea. This will be the case when investigating the depression of the visible horizon from a point at a comparatively small height above sea-level. It is clear that in such case the rays must be very nearly horizontal for the whole of their length, and the ratio of r to p differs from unity only by very small amounts. The value of n for such light is known to be only very slightly greater than unity, and consequently the curvature of the ray at different points along its path is very nearly proportional to $\frac{dn}{dr}$. It

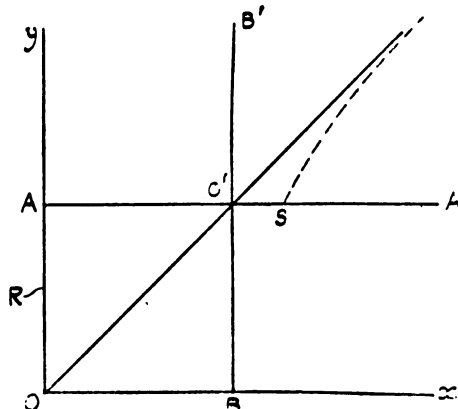
is a customary practice in surveying to deal with the refraction by assuming that the ray is hollow towards the earth's surface and has a radius of about seven times the earth's radius. This is only consistent with what has been said above, provided the refractive index between sea-level and the point of observation diminishes at a uniform rate, a condition of affairs that is by no means always the case.

Reverting to equation (i.) suppose the ray is at some point P_1 (fig. 2) in its path travelling horizontally. Then at this point p_1 and r_1 are equal; and let the ray subsequently reach some higher level r_2 at a point P_2 where it is again horizontal. Then the equation $np=k$ gives rise to the relationship $n_1r_1=n_2r_2$, where n_1 and n_2 are refractive indices at P_1 and P_2 .

The ray has travelled from P_1 to P_2 and clearly cannot have been horizontal for the whole of its length, since it has gone from a lower level to a higher one. At an intermediate point Q it must be travelling upwards, and since

In fig. 3 the pecked lines represent the value of nr , starting from the level AA' where $OA=R$, the earth's radius.

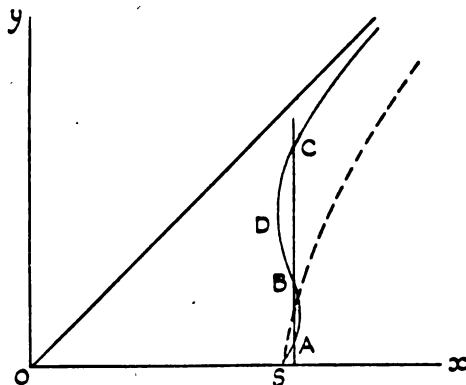
Fig. 3.



It is obvious that the curve can never cross the line OO' at 45° through the origin, for if it did we should have a point at which the velocity was greater than the velocity of light *in vacuo*, which is contrary to the initial assumptions.

Hence the line OO' becomes the asymptote to the curve.

Fig. 4.



The starting point S of the curve must be slightly to the right of O' (for visible light $n=1.0003$ approximately), and it is convenient at this point to re-draw the figure as fig. 4, taking $O'A'$ and $O'B'$ as axes and drawing everything on a much larger scale.

It is clear that in order to construct the track of any ray through the atmosphere, the value of n must be known in terms of the height above sea-level. This is known, of course, if the shape of the curve is known in fig. 4, and it is therefore of interest to consider the kind of curve that may be expected.

For visible light at all events $n-1$ drops uniformly with the density of the air, and as the density certainly diminishes as the height increases n becomes smaller and smaller and the curve gets continually closer to the asymptote.

The customary type of curve is that shown in the pecked line in fig. 4, but the curve shown in full line is not inconsistent with the assumption that n must diminish as the height increases. Whenever a curve of this shape occurs, then by drawing a line ABC parallel to OY to cut the curve in A, B, and C we find three separate levels for which nr has the same value. The figure shows that nr has the same value at A and B and is greater intermediately. The conditions are therefore suitable for a ray starting at r_1 (A) ultimately to reach a level r_2 (B), and thereafter to be confined entirely within the zone between these two heights.

On the other hand, a ray which is horizontal at a height r_2 cannot possibly reach the level r_3 of C, since intermediately nr has a lower value and np would be smaller still. There is therefore no possibility of a ray which is horizontal at the level r_2 getting across the zone r_2 to r_3 , but if a ray starts off at a sufficient inclination it will do so.

In fig. 4, D is the point for which nr is a minimum ($=n_4r_4$).

If a ray starts from the level r_1 at an inclination ϕ_1 with the vertical, then the constant of the equation of the ray is $n_1p_1=n_1r_1\sin\phi_1$.

If the ray just becomes horizontal at the level r_4 we have

$$n_1r_1\sin\phi_1=n_4r_4$$

$$\text{or} \quad \sin\phi_1=n_4r_4/n_1r_1.$$

Thus, any ray starting nearer to the horizontal than the above will become horizontal at a lower level than D and will return to lower levels. Any ray nearer the vertical will pass through the zone r_4 , and with a curve for nr as shown in fig. 4 this ray will ultimately escape into the space beyond the earth's atmosphere.

The general conclusions to be drawn from the above statements are that if the curve for nr starts to the right from S, representing sea-level, no radiant energy can return

to sea-level unless the curve throws back to the left of the ordinate through S. Unless this throw-back exists radiation emitted at any inclination above the horizontal *must* escape from the atmosphere.

Now the general state of affairs with wave-lengths ordinarily used in wireless is that a considerable amount of such radiation does not escape but is retained within the atmosphere and is ultimately absorbed. With wireless waves, therefore, the general state of affairs is that the throw-back exists.

With the much shorter wave-lengths of visible light the conditions seem to be pretty well the reverse. The normal state of the nr -curve is that shown in fig. 4 in pecked line, but undoubtedly the throw-back does sometimes exist, for it seems impossible to explain by any other means the optical phenomenon of the triple horizon that is referred to later.

The shape of the curve shown in fig. 4 apparently furnishes an explanation of many of the phenomena of the reception of wireless signals.

It suffices to explain how a wave starting from a station can travel completely round the earth and be picked up again close to the transmitting station. It does not seem to be in the least degree necessary to suppose that such radiant energy travels round the earth with a series of alternate reflexions at the earth's surface and at the Heaviside layer. For suppose that the shape of the nr -curve in fig. 4 is a vertical straight line for the first three or four thousand feet. It is quite clear that a vertical plane-wave, say three thousand feet high, will, if it travels round the earth as a vertical plane-wave, have moved for the upper portion of the wave a distance $2\pi r$ and for the lower part $2\pi R$; and that since velocities at all points of the wave are inversely proportional to n the condition $nr = \text{constant}$ for the whole of the three thousand feet is a sufficient condition that wave-front will travel as a vertical plane-wave right round the earth.

Another phenomenon that can be explained by the shape of the nr -curve is that of there being frequently a blank space—the “skip distance”—over which there is a no reception of wireless waves. Signals are received at, say, 100 miles, and are then not picked up again until 1000 miles or more from the station.

In fig. 5 is shown a suitable nr -curve for such a result to be obtained. A is at the level of the transmitting station conveniently taken as sea-level. The curve throws back

and cuts the vertical through A at the point B (radial distance r_1).

We thus have $n_1 r_1 = n_0 R$ and nr intermediately greater than either of these values. After B, the curve subsequently becomes vertical again at E, re-crosses the vertical through A at C, and goes off asymptotically to the 45° line through the origin.

Fig. 5.

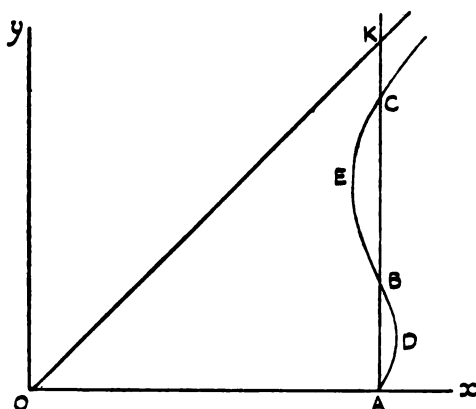
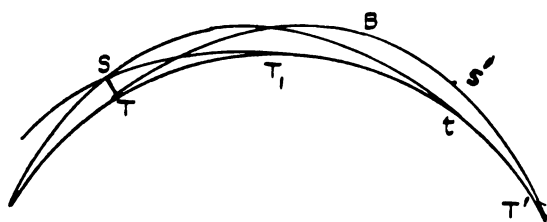


Fig. 6.



Consider now a ray starting from the station horizontally from T, fig. 6. That ray has an equation represented by $np = n_0 R$. Now

$$p = 1 / \left\{ u^2 + \left(\frac{du}{d\theta} \right)^2 \right\}^{\frac{1}{2}},$$

where $u = 1/r$. Hence

$$n = n_0 R \left\{ u^2 + \left(\frac{du}{d\theta} \right)^2 \right\}^{\frac{1}{2}},$$

and θ has the ordinary meaning when using polar co-ordinates, giving

$$\left(\frac{du}{d\theta}\right)^2 = \frac{n^2}{n_0^2 R^2} - u^2,$$

or

$$\theta = \int \frac{n_0 R du}{\{n^2 - u^2 n_0^2 R^2\}^{\frac{1}{2}}}.$$

Consequently the ray reaches the sea-level again and is there horizontal at an angular distance θ , given by

$$\theta = z \int_R^{r_1} \frac{n_0 R dr}{r \{n^2 r^2 - n_0^2 R^2\}^{\frac{1}{2}}},$$

an integrable equation if n is known in terms of the height.

Without an exact knowledge of the refractive index in terms of the height the integration cannot be carried out, but it is to be noticed that the denominator of the integrand, viz. $r\{n^2 r^2 - n_0^2 R^2\}^{\frac{1}{2}}$ becomes smaller at any level as nr approaches $n_0 R$.

Prescribing, therefore, that the ray is to reach the level of B, the greater the bulge between A and B in fig. 5 the closer to T will be the point T' at which the ray returns to earth again. The flattening of the bulge extends the distance at which the wave returns to earth, but this process must not be pushed to the limit of making BA absolutely flat and vertical, for in such case the point where the throw-back of the nr -curve occurs is not at B but at a point immediately above A. In other words, with such an atmosphere a ray starting from A horizontally travels round the earth at sea-level, and becomes a particular ray of the plane vertical wave-motion previously considered. The ray-path TBT' (fig. 6) is thus drawn for a definite throw-back height B (fig. 5) and a definite bulge ADB.

On the downward part of the wave-path there can be found a point S' of a height above sea-level corresponding to the upper end S of the transmitting aerial.

Slide the ray-path backwards round the earth until S' coincides with S and T' then takes up a position T₁.

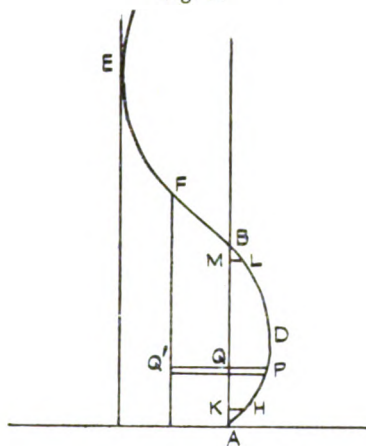
The atmosphere being stratified in concentric layers ST₁ is a possible ray-path, and a ray emitted from S in the suitable downward direction will reach sea-level at T₁. Any ray starting from S in a direction more nearly horizontal than ST₁ must have a larger value of p at the point S than the ray ST₁ has. Such a ray has consequently a larger constant np and cannot therefore reach sea-level at all.

The point T_1 is thus the farthest distance from the transmitting station at which the signals can be received. Beyond T_1 there will be no reception until some greater distance is reached. Slide the ray-path forward again until it passes through S and touches the sea-level the second time in t . This point t is a place at which a signal from S sent out in a suitable upward direction can be heard, and the space T_1t is a blank region (with a possible modification) over which there is no reception.

A ray starting from T in an upwardly-inclined direction has for the constant of its equation $n_0 R \sin \phi_0$, where ϕ_0 is the angle which the ray makes with the vertical at T . Let it be assumed that this inclination is only slightly above the horizontal, so that $\sin \phi_0$ is only very slightly less than unity.

Between B and E (fig. 7) it will be possible to find a point

Fig. 7.



F such that nr for this point, which is less than nr for B or nr for A , is equal to $n_0 R \sin \phi_0$. Thus the inclined ray starting from T in the direction ϕ_0 will become horizontal at the height of F and will afterwards return downwards and reach sea-level again at the inclination ϕ_0 with the vertical.

A similar integration formula can be applied to determine the place at which this ray returns, but the integration is extended over a bigger range of height.

The denominator of the integrand now becomes $r\{n^2 r^2 - n_0^2 R^2 \sin^2 \phi_0\}^{\frac{1}{2}}$, and for any particular value r the quantity under the square root has a greater value, according

to the figure, than the quantity $r\{n^2r^2 - n_0^2R^2\}$ for the integration of the previous ray. Thus for the integration of this inclined ray the range of integration is greater but the integrand is less, and it cannot be generally said that the inclined ray comes down nearer to T than the horizontal ray, or *vice versa*.

As the inclination of the ray is increased the culminating point of the ray rises, but the limit is reached when F arrives at E where nr has a minimum value. Any inclination of the emitted ray nearer to the vertical gives, for the equation $nr = K$, such a value of K that at no point in the atmosphere can the ray become horizontal, and the ray can therefore never return again to earth but will escape completely from the atmosphere.

It appears, therefore, from this reasoning

- (i.) That transmission round the earth can only occur if the nr -curve throws back to smaller values than n_0R ;
- (ii.) that the critical emission direction is given by

$\sin \phi = \frac{(nr)_{\min.}}{n_0R}$. No ray emitted at a steeper inclination can ever return to earth, and the shape of the curve above E is absolutely immaterial so far as any of the received waves are concerned.

Explanations of wireless phenomena generally seem to be based upon some sort of idea that the ray received is either the "direct wave" as ST_1 at T_1 or the "reflected wave" as $S'T'$ at T' , and usually in such explanation it is assumed that the reflected wave has gone up to the level of the Heavyside layer, generally taken to be from 70 km. to 120 km., and in some way reflected at that level. The possibilities of the waves reaching such heights must, of course, not be lost sight of, but it does not seem to be in the least degree necessary that they should all go so high. The points B and E might be so low and the points D and E so close to the line AB that reception would be possible over all parts of the globe without any ray travelling higher than a couple of kilometres—or even less.

It is not intended in this paper to do much more than offer a geometrical explanation of some phenomena of wireless transmission. It is recognized that such explanation cannot be complete; that the complications of diffraction, interference, and polarization must inevitably be present and

make the fitting of the parameters of the geometrical equations to observations somewhat uncertain. But in spite of these difficulties this geometrical aspect of wireless refraction seems to be reasonable, particularly when dealing with rays not too near the earth, and to lead to certain generalizations that are probably near the truth.

One of these generalizations is concerned with the type of value that n would necessarily have to have if the "reflected wave" had always to go to the height of the Heaviside layer, say to 300,000 feet above sea-level. At such a place p will equal 20,300,000 feet, taking 20,000,000 feet as a round number representing the earth's radius with sufficient accuracy. If the ray started off at an inclination ϕ_0 with the horizontal, we should have $n \times 20,300,000 = n_0 \sin \phi_0 \times 20,000,000$, so that $n_0 = 1.015 n \operatorname{cosec} \phi_0$.

Suppose now that it were possible for a ray to be emitted at an angle of 45° with the vertical and subsequently to return to earth, we should then have

$$\begin{aligned} n_0 &= 1.015 \times 1.414 n \\ &= 1.435 n. \end{aligned}$$

Now n , the refractive index at the culminating point, cannot be less than unity, so that the equation would involve a refractive index at the sea-level of at least 1.435, a figure probably far too great.

The fact is, unless one is prepared to accept quite high values for the refractive index at sea-level, the direction of emission of these rays which travel to the reception station must be confined to a few degrees above the horizontal, and it should be noted here that the higher the level of E in fig. 5 the greater must the sea-level value of n be.

Another generalization can be drawn from the integral which has already been discussed. The variable part is a denominator term frequently of very small dimensions. In order that this term can be computed with any degree of precision it is essential that the refractive index should be known with a precision that is greater still. To permit of that integral being evaluated with any semblance of reality the refractive index must be known to five or six decimal places and for a considerable number of levels up to the culminating level for the critical ray.

The values of n are not so known at the present time, and it seems almost impossible to obtain them by any direct means except possibly within the range of the visible spectrum.

Without such precision in the values of the refractive

index any attempt to compute the skip distance is farcical, but in order to illustrate the methods of doing so a fictitious atmosphere has been compiled which does not pretend to be any more than a blind guess at what the refractive index *might* be.

In making up this table of refractive indices regard had to be paid to ensuring a smoothness of values even when taken down to very small differences, and the easiest way of preserving this smoothness seemed to be to find a formula which when plotted had the suitable geometrical characteristics: that is to say, it had to represent a curve crossing the vertical at A, B, and C (fig. 5), and ultimately asymptotic to the line OK. Further, in making up the formula, regard had to be paid to the fact that it must be single valued in height, and that it should be as simple as possible to compute from.

The first consideration was the choice for n_0 , which was taken to be 1.015. This figure allows the point E to be placed if required as high as 300,000 feet, but as will be seen later the point was made to come out considerably lower. In making up the formula it was convenient to make up the Cartesian equation of a curve in the form $x=f(y)$, for which the vertical and horizontal lines through A were taken as axes of coordinates. To reduce numbers to reasonable magnitudes the unit of length was taken to be one-thousandth part of the earth's radius, say 20,000 feet or about 6 kilometres. The radius of the earth being 1000, $n_0 R = 1015$, and the asymptote OO' of fig. 3 then cuts the axis $y=0$ at $x=-15$ and the axis $x=0$ at $y=15$.

Below this point, $y=15$, must come the three crossing points, and these were ultimately taken to be $y=0$, $y=4$, and $y=9$.

It was found that the equation

$$x = y - 15 + \frac{990}{y^2 + 2y + 66}$$

was an equation which fulfilled the geometrical conditions, and from this formula the value of nr and n in the attached tables are computed.

Vertical tangents to this curve occur at $y=1.60121$ where $x=0.39601$, and at $y=6.58740$ where $x=-.33548$.

The value of nr along $x=0$ is 1015 and the minimum value of nr is 1014.66452.

Hence the critical angle of emission is given by

$$\begin{aligned} \sin \phi_0 &= 1014.66452/1015 \\ &= 0.99967, \end{aligned}$$

making $\phi_0 = 88^\circ 32'$.

With this atmosphere it is thus the fact that no rays emitted from sea-level at a greater inclination above the horizon than about $1\frac{1}{2}^\circ$ can be retained within the atmosphere, and the extreme height attained by any ray is round about 132,000 feet. Further, all rays emitted from the station which are retained within the atmosphere must culminate at heights lying between 80,000 feet ($y=4$) and 132,000 feet ($y=6.58740$).

The equation of the ray emitted horizontally from sea-level is $np=1015$, and the distance TT' (fig. 6) is given by

$$\theta = 2 \int_{1000}^{1004} \frac{1015 dr}{r\{n^2r^2 - n_0^2R^2\}^{\frac{1}{2}}}.$$

In evaluating this integral the factor r in the denominator varies between 1000 and 1004, so that a reasonably close approximation will be obtained if the integral is written

$$\int_{1000}^{1004} \frac{2.026 dr}{\{n^2r^2 - (1015)^2\}^{\frac{1}{2}}}.$$

Again, the quantity $n^2r^2 - (1015)^2$ has factors $nr-1015$ and $nr+1015$. The largest value of nr is 1015.39601 and the smallest 1015. The second factor can therefore be replaced without serious inaccuracy by 2030.15, whose square root is 45.057, and the integral becomes

$$\int_{1000}^{1004} \frac{.045057 dr}{(nr - 1015)^{\frac{1}{2}}}.$$

A way of looking at this integral that conveys an idea of how it depends upon the shape of the curve can be derived from fig. 7. P is a point on the curve at distance r from the earth's centre, and PQ is $nr-1015$.

Hence the integral is $.045057 \int \frac{dr}{\sqrt{PQ}}$, the integration extending from A to B .

At both ends of the integration the integrand becomes infinite since the PQ becomes zero, and the greatest care must be taken when performing the integration by approximate methods.

One convenient method is as follows:—Cut off from the range of integration two parts, AHK and BLM , by lines KH and ML not too far away from A and B respectively, and treat the parts of the curve between A and H and B and L as straight lines.

Then the total integration can be broken into three parts:

(a) over the range A to K, (b) over the range K to M, and (c) over the range M to B.

For (a) we can transfer the variable to y measured vertically from A instead of r measured from the centre, and the integrand will be $\frac{1}{\sqrt{my}}$, where $m = \tan HAK$. We thus have over the area AHK:

$$\begin{aligned} \text{Integral} &= \cdot 045057 \int_0^{AK} \frac{dy}{\sqrt{my}}, \\ &= \frac{\cdot 045057}{\sqrt{m}} \int_0^{AK} \frac{dy}{\sqrt{y}}, \\ &= \frac{\cdot 045057}{\sqrt{m}} \times 2 \sqrt{AK}, \\ &= \frac{\cdot 090114}{\sqrt{m}} \sqrt{AK}. \end{aligned}$$

In a similar manner, the part (c) of the integrand

$$= \frac{\cdot 090114}{\sqrt{m'}} \sqrt{BM},$$

where m' is the corresponding slope of the tangent at B.

It will be seen from this that as the inclination to the vertical of the tangents at A and B becomes smaller the integrals (a) and (c) become larger, and that if the curve either at A or at B touched the vertical AB the integral would become infinite. For the central portion between K and M the integrand nowhere becomes infinite, and ordinary methods of approximate integration are suitable.

The values of nr for $n = 1000, 1001, 1002, 1003, 1004$ are 1015, 1015·034782, 1015·38018, 1015·22222, and 1015; and it will be seen from these figures that one must have accuracy in the first three decimal places to obtain accuracy in the integration. When the value of r has been divided into nr it becomes immediately clear that the determination of the point T', at which the ray TBT' of fig. 6 returns to sea-level, involves an accurate knowledge of the fifth and sixth decimal places in the value of n .

It is important that this point should be made quite clear. *It is quite impossible to attempt to compute the track of a ray through the atmosphere for an electro-magnetic wave that starts off in a known direction from a known point unless the refractive index for all levels that it will reach is known with accuracy to about the fifth decimal place.* Whether it is possible to

measure the refractive index with that accuracy does not form part of this paper.

The values of $nr-1015$ near the point of A are :

r .	$nr-1015$.
1000	0
1000.1	0.0524
1000.2	0.1007
1000.3	0.1448
1000.4	0.1849
1000.5	0.2212

At the other end the values of $nr-1015$ are :

r .	$nr-1015$.
1003.5	0.1129
1003.6	0.0902
1003.7	0.0675
1003.8	0.0449
1003.9	0.0223
1004.0	0.0000

The figures show that the curves are reasonably straight at the ends for a space of 0.2, and that the values of m and m' are approximately 0.55 and 0.22.

Integrating the middle portion by Simpson's Rule, we obtain :

$$\begin{aligned}\theta(a) &= 0.0544 \\ \theta(b) &= 0.3353 \\ \theta(c) &= 0.0859\end{aligned}$$

$$\text{Total} = 0.4756 \text{ or } 1635 \text{ sea miles.}$$

Hence a ray starting horizontally at sea-level reaches sea-level again at a point 1635 miles away.

Take, for purposes of illustration, a height ST (fig. 6) of 500 feet, which is in the units we are using 0.025.

The angular distance TT, as obtained by integration of the same formula between limits 1000 and 1000.025. Integration here must be of the type (a), and the value is $\frac{.090114 \times \sqrt{.025}}{\sqrt{0.55}} = .0192$, or 65 sea miles.

Consequently the distance T_1t of fig. 6 is 1505 miles, and this will be the skip distance unless any of the inclined rays starting from the transmitting station descend within this space.

All the rays emitted from the station culminate within the space $r=1004$ to $r=1006.5874$.

The point of descent for an inclined ray is given by

$$\theta = 2 \int_{R}^{\cdot} \frac{R n_0 \sin \phi_0 dr}{r \sqrt{n^2 r^2 - n_0^2 R^2 \sin^2 \phi_0}},$$

where the range of integration extends at the most from 1000 to 1006.5874.

The same preliminary approximation, involving treating r and $\sqrt{nr + n_0 R \sin \phi_0}$ as constants, can be made and the equation then becomes

$$\theta = \int_{1000}^{\cdot} \frac{.045057 dr}{(nr - 1015 \sin \phi_0)^{\frac{1}{2}}}.$$

The angle ϕ_0 is in any case greater than $88\frac{1}{2}^\circ$. No appreciable loss of accuracy is entailed by writing $\sin \phi_0$ as unity, except in the denominator term.

Written in this way it is clear that the integral can be interpreted by means of fig. 7.

A ray which culminates at F will have a value for ϕ_0 easily calculated, and $nr - n_0 R \sin \phi_0$ now becomes the distance PQ'.

The altered limits of integration obviously can affect the integral, either to make it larger or to make it smaller.

The increase in the length from PQ to PQ' is a reducing factor but the increase in range of integration tends to make the value larger, and especially should it be noted that the shape of the nr -curve shows that the value m' in (c) is becoming smaller as the culminating height becomes greater. Ultimately the reduction in the integral due to increased values of PQ' must be overbalanced by the increase due to the end values, and finally when F reaches E the integral will be infinite.

The maximum height (E) which any rays starting from the earth's surface can reach and yet return to the earth's surface is a circular asymptote, and the ray must in theory travel an infinite distance before it starts to descend and another infinite distance before it reaches sea-level again. In the neighbourhood of E nr is sensibly constant, which is the condition for a vertical wave travelling at constant height round the earth.

From the above reasoning it can be seen that as the inclination above the horizontal of a ray starting from T is increased, the point of descent to the earth's surface may move from T' towards T or may move away from T. It is entirely a question of the distribution of refractive index with height, and it is extraordinarily sensitive to small

changes in the refractive index distribution. If the point moves towards T it may even go as far as T_1 and wash out the whole of the skip distance; or it may go part of the way and diminish the skip distance T_1t that was found for rays horizontal at sea-level. The skip distance is therefore limited by T_1 at the one end, and at the other by either t or some point at which an inclined ray comes down.

But in any case, as the inclination gets larger and larger and approaches the critical angle, the *point of descent must ultimately pass beyond T' and cover continuously the whole of the earth's circumference beyond that point.*

There is thus no second skip distance, as there would be if reception were confined to those rays that are horizontal at the earth's surface.

Let us now investigate whether the faked atmosphere has a skip distance or not.

It will be convenient to integrate

$$\int_{1000}^{\cdot 045057dr} \frac{\cdot 045057dr}{(nr - 1015 \sin \phi_0)^{\frac{1}{2}}}$$

up to limits 1004.5, 1005, 1005.5, 1006, and 1006.5.

In theory the minimum distance of the point of descent could be obtained by the calculus of variation, but this would involve the computation of $\int_{PQ} dr$, and as PQ is supposed to be known only in terms of numerical values the labour involved would be too great.

It is therefore preferable to plot a curve for the five ranges given above and determine the minimum by inspection of the curve.

The values of x for

$$x = y - 15 + \frac{990}{y^2 + 2y + 66},$$

when y has values 4.5, 5.0, 5.5, 6.0, 6.5, are

$$\begin{aligned} & -0.106299, \quad -0.198020, \quad -0.269231, \quad -0.315784, \quad . \\ & \quad \quad \quad -0.335052, \end{aligned}$$

and the values of nr are

$$\begin{aligned} & 1014.893701, \quad 1014.801980, \quad 1014.730769, \quad 1014.684216, \\ & \quad \quad \quad 1014.664948. \end{aligned}$$

Integrating the equation

$$\theta = \int_{1000}^{\cdot 045057dr} \frac{\cdot 045057dr}{\{nr - n_0 R \sin \phi_0\}^{\frac{1}{2}}}$$

to the appropriate upper limit, and with the appropriate values of $n_0 R \sin \phi_0$, we obtain the following values :—

Inclination of ray.	Range to point of descent.	Height of culminating point.
$\phi = 90^\circ$	= 1635 miles.	80,000 feet.
$89^\circ 10'$	1585 „	90,000 „
$88^\circ 53'$	1693 „	100,000 „
$88^\circ 41'$	1920 „	110,000 „
$88^\circ 34'$	2270 „	120,000 „
$88^\circ 33'$	3370 „	130,000 „
$88^\circ 32'$	—	132,000 „ approx.

It will be seen that the horizontal ray is not the one which determines the skip distance, the point of descent initially approaching the transmitting station as the inclination is raised above the horizontal direction, and the turning point is reached at about 1580 miles. The inclination of this ray is about $0^\circ 45'$ above the horizontal, and the culminating point at about 87,000 feet. Thereafter the point of descent recedes, and consequently all points beyond 1580 miles from T can receive rays starting from T. Rays starting from S will be received about 70 miles nearer.

Hence the near reception will extend to about 65 miles, and the skip distance will be about 1450 miles.

Examination of the figures in the above integration leads to the conclusion that only a very small alteration in the shape of the nr -curve is required to wash out the whole of the skip distance. Give the part ADB (fig. 5) a little more bulge, and the point of descent for the horizontal ray is brought closer in. The increased bulge naturally leads to the curve crossing the vertical at B more squarely, and this in its turn will reduce the end values of the integrals for the inclined rays. Thus it will be seen that only quite small alterations in the refractive index distribution are necessary to cut out the skip distance altogether and give continuous reception all the way from the starting point.

Now presumably the refractive index distribution depends upon the wave-length, much in the same way as a piece of glass has different refractive indices for the red and blue ends of the spectrum. There is then no impossibility in the atmosphere giving rise to a skip distance for one wave-length and not for another.

One further point should be noted. If the nr -curve started

off to the left of the vertical instead of the right, as it would do if the point B (fig. 5) was at the level of the earth's surface, then no ray starting horizontally would get any distance at all; there would be no skip distance but continuous reception by inclined rays right away from the start.

There would still be a critical angle of emission given by $\sin \phi_0 = \frac{(nr)_{\min.}}{n_0 R}$, and only rays starting off below this direction could possibly return to earth again.

In the fictitious atmosphere that has been used to illustrate the methods of integration the points B and C were taken at the arbitrary heights of 80,000 and 180,000 feet and, resulting from the formula by means of which the table of values for n was compiled, all the rays by which reception takes place culminate between heights of 80,000 and 132,000 feet. There is no reason to assume that these two heights are in any way connected with the Heaviside layer. It would, in fact, have been just as easy to make up an atmosphere in which B and E both lay below 10,000 feet, and in which wireless transmission would take place along rays which did not approach anywhere near the Heaviside layer. It should be noted also that the higher the point C is placed the greater the need for having a refractive index at the earth's surface which is considerably more than unity. Conversely the smaller the refractive index at the earth's surface the lower must be point C if the wireless wave is to be bound to the atmosphere.

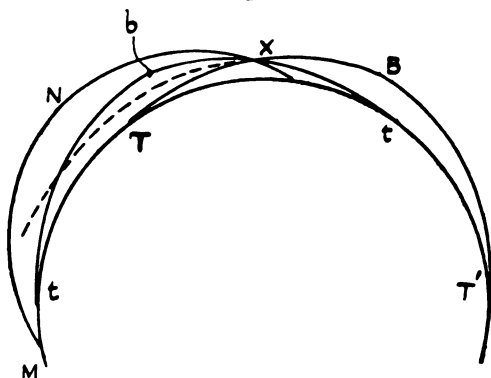
No attempt is made in the above work to explain the physical causes of such a distribution of refractive index, nor has any account been taken of the reflexion and diffraction of the waves by the earth's surface or of the scattering of energy by the medium. Such physical effects certainly exist. They complicate the problem of determining the transference of radiant energy, but it does not seem to be imperative to take account of them in order to have a reasonable explanation of most of the phenomena of wireless transmission and reception.

The shape of the curve of nr has important bearings also on the passage of visible light through the atmosphere. The value for n at the earth's surface is much lower (1.000293) and the phenomenon of the earth-bound ray has to take place, if at all, within a hundred feet or so. In point of fact, the normal case for the refractive index of visible light is that of fig. 3, and it is only in exceptional cases that a throw-back of the curve occurs to the left of the vertical. When such is the case, a ray of light which is horizontal at

T (fig. 8) becomes horizontal again at B, and comes down again to the earth's surface at T', the distance TT' depending as before upon the value of the integral $\int_R^r \frac{dr}{\{nr - n_0R\}^{\frac{1}{2}}}$ up to the level of B.

Now the height AK up to the asymptote (fig. 5) is only 0.293 in the units used, *i.e.*, something under 6000 feet, but the point B must be much lower than that. Probably it is seldom more than a couple of hundred feet above sea-level. A man viewing the sea-horizon from the point B

Fig. 8.



will receive the rays truly horizontally and the earth will to him appear flat.

For observations made between T and B the horizon will appear depressed, the maximum amount occurring at D where D is at the height of the point D in fig. 5.

Now, through any point X on TB an exactly similar curve *tbt'* could be drawn which started horizontally at *t* became horizontal again at *b* and at X was moving downwards. Hence the man at X will receive two rays, one coming to him inclined upwards and another inclined equally downwards, both of which have started tangentially to the earth's surface.

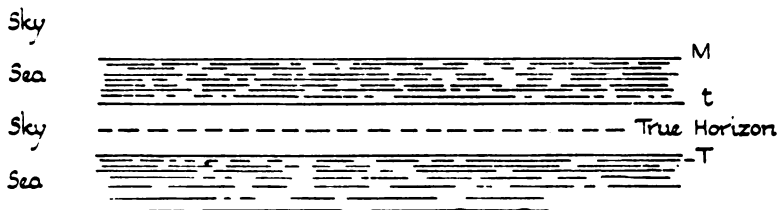
For each of them the equation is $pn = n_0R$, and since *n* is the same for both rays at the point X (radial distance *r*) the values of *p* must be the same at this point, this giving equal inclinations above and below the horizontal.

Any ray which reaches X between these two directions

must by the geometry of the figure have a larger value for p , and consequently a larger value for np . Thus the constant in the equation $np = K$ for this ray is greater than $n_0 R$, and by the assumption as regards the shape of the nr -curve for the atmosphere this value is reached for some height that is above the earth's surface.

The observer will thus see, as his eye travels upwards from the sea below him, sea up to the direction XT. There will there be a sharp dividing-line separating sea from sky and a space of clear sky between the direction XT and the direction Xbt. Above that direction he sees sea again, and this continues until the direction is reached in which a ray having started off at the critical angle has made an infinite number of revolutions round the earth to the circular asymptote, and subsequently another infinite number until it reaches his eye on the downward path. Actually, of course,

Fig. 9.



it does no such thing, the absorption by the atmosphere being far too great, so that the limit is set not by the critical angle but by the range of visibility, and the third line which separates sky from air is an indistinct one corresponding to a ray inclined at M, the extreme range of visibility which culminates at N higher than b or B and reaches his eye in a downward direction.

The appearance of the sea-horizon as seen from X is thus that shown in fig. 9, and the true horizontal occurs half-way between the lines t and T and is shown in pecked line.

It is hardly necessary to compile a table of refractive indices that will serve to compute the angular distance between T and t . It is sufficient to state that owing to the very low refractive index for visible light the heights of B and E in fig. 5 can only be of the order of a hundred feet or so, and that in consequence the distances from X of T, t , and M in fig. 8 can be only a few miles, and the angular separation of the three horizons only a matter of a minute or two at the most. The phenomenon of the triple horizon

is well known to anyone who has had to take astronomical observations for navigation purposes. It is generally referred to as mirage without any very satisfactory explanation of how it is caused. Not infrequently the navigator assumes that the detached strip of sea is a layer of low-lying haze or cloud.

As the point X moves upwards towards B the two horizons t and T merge into one another and at the point B have just disappeared. It is therefore wrong to say, as was done above, that the observer at B sees the earth as flat. He sees it hollow, the line dividing sea from sky being that of M, which is the indistinct line coming from the extreme range of visibility. As the observer goes higher still he ultimately reaches a height at which he is at the culminating point of an inclined ray which started from the extreme range of visibility. He then has a "dip" value of zero and for greater heights the sea-horizon is depressed below the horizontal. It appears, therefore, that a formula for the dip proportional to the square-root of the height as is taken in all mathematical tables is quite wide of the mark when the particular atmospheric conditions occur that give rise to a throw-back in the *nr*-curve.

It is of course known that cases occur in which the dip tables are in error by considerable amounts, although on the average they probably are near enough. In a series of observations carried out some years ago by an American naval officer off the coast of California, errors of the dip tables up to nine minutes were observed. In actual practice a few minutes error in measurement of the sun's altitude results in an equal number of miles error in determination of the ship's position; and as it is only when out of sight of land that astronomical observation becomes necessary the safety of a ship is never endangered. For surveying work, or in cable-laying ships, however, the matter is different, and the only way to avoid the dip errors is either to observe several stars in different azimuths or to measure the dip at the time by special apparatus which measures the angular distance from the front to the back horizon.

Table of Values for Refractive Index.

In this table the unit of length is taken to be 1/1000 part of the earth's radius, approximately 20,000 feet or 6 kilometres. The formula used to construct the "*nr*"-curve is $x = y - 15 + \frac{990}{y^2 + 29 + 66}$, being the height above the earth's surface, and $nr = 1015 + x$.

TABLE.

<i>y.</i>	<i>nr.</i>	<i>n.</i>
0	1015·0	1·015
0·1	1015·06242	1·0149509
0·2	·10066	1·0148977
0·3	·14480	1·0148403
0·4	·18495	1·0147790
0·5	·22119	1·0147138
0·6	·25364	1·0146448
0·7	·28241	1·0145722
0·8	·30762	1·0144960
0·9	·32938	1·0144164
1·0	·34783	1·0143335
1·1	·36307	1·0142474
1·2	·37526	1·0141583
1·3	·38451	1·0140662
1·4	·39096	1·0139714
1·5	·39484	1·0138740
1·6	·39599	1·0137740
1·7	·39484	1·0136716
1·8	·39143	1·0135670
1·9	·38590	1·0134603
2·0	·37839	1·0133517
2·1	·36900	1·0132412
2·2	·35789	1·0131290
2·3	·34520	1·0130153
2·4	·33103	1·0129000
2·5	·31553	1·0127835
2·6	·29882	1·0126659
2·7	·28101	1·0125471
2·8	·26224	1·0124274
2·9	·24260	1·0123069
3·0	·22222	1·0121856
3·1	·20121	1·0120638
3·2	·17967	1·0119415
3·3	·15771	1·0118187
3·4	·13542	1·0116956
3·5	·11290	1·0115724
3·6	·09025	1·0114491
3·7	·06755	1·0113257
3·8	·04489	1·0112023
3·9	·02235	1·0110792
4·0	·00000	1·0109562
4·1	1014·97793	1·0108335
4·2	·95619	1·0107112
4·3	·93482	1·0105893
4·4	·91402	1·0104679
4·5	·89370	1·0103471

TABLE (continued).

<i>y.</i>	<i>nr.</i>	<i>n.</i>
4.6	1014.87397	1.0102270
4.7	.85489	1.0101074
4.8	.83650	1.0099886
4.9	.81885	1.0098705
5.0	.80198	1.0097532
5.1	.78594	1.0096368
5.2	.77077	1.0095213
5.3	.75649	1.0094066
5.4	.74315	1.0092930
5.5	.73077	1.0091803
5.6	.71938	1.0090686
5.7	.70901	1.0089560
5.8	.69968	1.0088484
5.9	.69140	1.0087398
6.0	.68422	1.0086324
6.1	.67811	1.0085261
6.2	.67530	1.0084231
6.3	.66924	1.0083169
6.4	.66653	1.0082139
6.5	.66495	1.0081123
6.6	.66452	1.0080116
6.7	.66524	1.0079122
6.8	.66713	1.0078140
6.9	.67019	1.0077170
7.0	.67442	1.0076211

NOTE.—The figures given above are *not* measured values of the refractive index but are computed from a formula. The only justification for carrying the figures to a number of decimal places much in excess of anything that has ever been measured lies in the explanation given on p. 970.

The thanks of the author are due to the Admiralty for permission to publish this paper.

XCI. *The Adsorption of Butyric Acid on Water Surfaces.*

By C. R. BURY*.

SEVERAL authors have already calculated from surface-tension measurements the amount of butyric acid adsorbed on water surfaces: in the absence of activity data, they have assumed the activity of butyric acid to be proportional to its concentration, or to the concentration of its unionized molecules. Recent measurements of the freezing-points of butyric-acid solutions (Jones and Bury, *Phil. Mag.* (7) iv. p. 843, 1927) have shown this assumption to be unjustifiable; and it therefore seems desirable to

* Communicated by the Author.

recalculate the adsorption, making use of the activities deduced by these authors.

The most interesting surface-tension measurements are those of the air-solution surface by Drucker (*Zeit. Phys. Chem.* lii. p. 649, 1905): though possibly less accurate than more recent measurements by Szyszkowski (*Zeit. Phys. Chem.* lxiv. p. 395, 1908), they cover the whole range from pure water to pure acid. In Table I. are given the concentrations of butyric acid in gram molecules per 1000 grams solution (C) and their relative surface tensions at 25° (σ/σ_0), taken from his paper. From these have been calculated the concentrations in gram molecules per 1000 grams water (m) and the absolute surface tensions in dynes per cm. (σ), using Volkmann's value for pure water (*Wied. Ann.* lvi. p. 457, 1895). Activity coefficients (γ) have been obtained by interpolation from the data of Jones and Bury, and from these the activities ($\alpha = \gamma m$).

TABLE I.

C.	log C.	γ .	m .	α .	log α .	σ/σ_0 .	σ .
0			0			1.000	71.78
0.01583	-1.8005		0.01585			0.963	69.12
0.03561	-1.4485		0.03571			0.900	64.60
0.08247	-1.0837		0.08308			0.828	59.43
0.1187	-0.9255		0.1199			0.778	55.85
0.2675	-0.5727	1.149	0.2740	0.3148	-0.5020	0.659	47.30
0.4353	-0.3612	1.117	0.4527	0.5057	-0.2961	0.577	41.42
0.9802	-0.0087	0.983	1.073	1.055	+0.0231	0.456	32.74
2.834	+0.4524	0.454	3.777	1.715	+0.2342	0.389	27.92
6.920	+0.8401	0.100	17.72	1.772	+0.2485	—	(27.0) *
9.015	+0.9549		43.76			0.374	26.85
11.38	+1.0561					0.361	25.91

* Interpolated from the γ -log C graph.

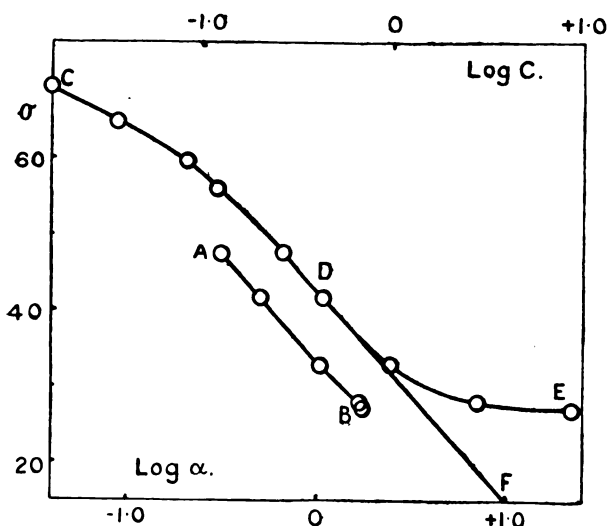
The line AB in the figure represents Drucker's surface tensions plotted against log α : within the limits of experimental error, it is straight over the whole range of concentrations (0.27-17.7 m.) for which activity data are available. From Gibbs's equation, which can be written in the form

$$\Gamma = -\frac{1}{2.303RT} \frac{d\sigma}{d \log \alpha},$$

where Γ is the amount of butyric acid adsorbed at the

water-air surface as defined by Gibbs (Scientific Papers, 1906, vol. i. p. 234), R is the gas constant, and T the absolute temperature, it follows that Γ is proportional to the slope of this line, and is therefore constant over the whole range. Its numerical value is 4.75×10^{-10} gram molecules per $(\text{cm.})^2$, which corresponds to an area of $34.7 \times 10^{-16} (\text{cm.})^2$ per molecule. There is a possible error of about 2 per cent. in these figures, due to the graphical method of calculation employed.

Fig. 1.



Substances which form monomolecular layers or are strongly adsorbed at the surface of a solvent appear always to form very abnormal solutions in that solvent; it is therefore dangerous to use any but experimentally determined activities in calculations of this type. Thus, if activity was assumed to be proportional to concentration, Γ would be proportional to the slope of the line CDE in the figure, which represents surface tensions plotted against $\log C$. Adsorption would then increase with concentration up to the point of inflexion (D) at 0.35 per gram molecules per 1000 grams solution, and then decrease. There would possibly be a small range of concentrations in the

immediate neighbourhood of the point of inflexion over which Γ was constant, but this could hardly be regarded as evidence of the formation of a saturated surface layer.

Szyszkowski (*loc. cit.*) found that the relation between surface tension and concentration of solutions of certain fatty acids could be expressed by an equation of the type

$$\sigma = \sigma_0 - 0.411 \sigma_0 \log \left(\frac{C}{0.0475} + 1 \right),$$

where σ_0 is the surface tension of pure water. The numerical constants have been evaluated by Szyszkowski from Drucker's experimental data for butyric acid at 25°. This equation is represented by the line CDF in the figure; it obviously fails to represent the experimental data at high concentrations. Langmuir's well-known argument as to the formation of monomolecular surface layers by soluble fatty acids (*J. Amer. Chem. Soc.* xxxix. p. 1883, 1917) is based on two assumptions: that activity is proportional to concentration, and that Szyszkowski's equation is valid at high concentrations. The errors introduced by the two assumptions practically cancel out: *i. e.*, the lines AB and DF on the figure are almost parallel.

A number of calculations by previous investigators and by myself are summarized in Table II., where Γ is the maximum adsorption and A the minimum area occupied by a molecule of butyric acid. My own calculations have been made by the method described above, using the activities of Jones and Bury. The activities are strictly valid only at the freezing-point; their use at higher temperatures must lead to underestimation of A, but this is probably negligible. It is therefore probable that the increase of A with temperature, which is obvious from the measurements of Drucker and Szyszkowski, is real, and not entirely due to the errors of experiment and calculation. The difference between the results of these two observers is attributed by the latter to the greater purity of his acid.

A saturated surface layer does not appear to us to be formed at a benzene-water interface. The curve obtained, even when activities are used, has the same form as the curve CDE in the figure. In the absence of any information in the original paper as to the temperature at which the surface-tension measurements were made, I have assumed, in my calculation, that this was 20° C.

TABLE II.

Surface.	Surface-tension measurements by	T.	$\Gamma \times 10^{10}$, $\Delta \times 10^{16}$. Calculated by		
Water-air	(Szyszkowski's equation.)			31	Langmuir *.
"	?	?	4.53	36.3	Harkins & King †.
"	?	?		32	Harkins & McLaughlin ‡.
"	Drucker *.	25°	4.75	34.7	Bury.
"	"	35°	4.68	35.3	"
"	Szyszkowski *.	2-3°	5.45	30.3	"
"	"	18-19°	5.34	30.9	"
"	"	25°	5.16	32.0	"
Water-benzene.	Harkins & King †.	?	4.60	35.9	Harkins & King †.
"	"			32	Harkins & McLaughlin ‡.
"	"		4.89	33.8	Bury.
Water-hexane...	Harkins & McLaughlin ‡.	20°		32	Harkins & McLaughlin ‡.
"	"		5.97	27.6	Bury.

* *Loc. cit.* † J. Amer. Chem. Soc. xli. p. 970 (1919).

‡ J. Amer. Chem. Soc. xlvii. p. 1610 (1925).

In conclusion, butyric acid forms saturated surface layers at the water-air surface, in which the area occupied by a molecule of acid is independent of concentration over wide ranges, but appears to increase slightly with temperature. The area occupied by a molecule at the water-hexane interface is appreciably smaller than at the water-air surface, but still larger than that occupied by the higher, insoluble, fatty acids and alcohols. There is no evidence of the formation of a saturated surface layer at the water-benzene interface.

Edward Davies Chemical Laboratories,
University College of Wales,
Aberystwyth.
August 22nd, 1927.

XCII. *The Structure of the Isomorphic Substances* $\text{N}(\text{CH}_3)_4\text{I}$, $\text{N}(\text{CH}_3)_4\text{Br}$, $\text{N}(\text{CH}_3)_4\text{Cl}$. By L. VEGARD, *Dr. Philos., Professor of Physics, Oslo*, and KARL SOLLESNES, *Research Student at the Physical Laboratory, Oslo* *.

[Plates XX. & XXI.]

Introduction.

§ 1. **T**HE structure of the tetramethylammonium iodide $\text{N}(\text{CH}_3)_4\text{I}$ was treated by one of us in two previous papers.

In a paper published in 1917 † the structure was investigated by the Bragg ionization method. The dimensions of the unit cell were determined and found to contain two molecules, and the atoms were found to be arranged in a way which corresponds to the space group D_{4h}^1 .

In a paper recently published ‡ by one of us, together with T. Berge, results were given of investigations on the structure of $\text{N}(\text{CH}_3)_4\text{I}$ by means of the powder method. The main results stated above as to the magnitude of the unit cell and the space group of the atomic arrangement were confirmed, but in order to obtain a satisfactory agreement between observed and calculated intensities of the powder diagrams, certain changes of the parameters had to be made.

In $\text{N}(\text{CH}_3)_4\text{I}$ the reflecting power of nitrogen is very small as compared with that of iodine, and consequently the intensities of the spectral lines are very little influenced by the position of nitrogen atoms

From the investigations of the iodine compound alone, we are left in some uncertainty as to the position of the nitrogen atoms. The influence of these atoms, however, should be more prominent in the isomorphic compounds of bromine and chlorine, and for this reason it was of great importance to extend the investigations also to these two substances.

It appeared to be somewhat difficult to obtain good powder diagrams from the chlorine compounds, because it was very hygroscopic. The difficulty was overcome by introducing the powder into a capillary tube covered with a glass cap, which could be removed after the tubes were put into the X-ray camera. In this way we finally obtained good spectrograms for both the Br and Cl compound. Reproductions of the films are given in the plate (Pl. XX.).

* Communicated by the Authors.

† L. Vegard, "Results of Crystal Analysis.—IV." *Phil. Mag.* **xxiii**, p. 395 (1917) (I.).

‡ L. Vegard & T. Berge, *Det. Norske Vid. Akad. Skr.* i. No. 10 (1926) (II.).

Phil. Mag. S. 7. Vol. 4. No. 24. Nov. 1927.

3 S

Specification of the Lattice.

§ 2. The lines appearing on the film were easily identified from the analogy with the iodine compound already analysed. For all three compounds the unit cell contains two molecules. (See Tables II. and III.)

In order to find accurate values for the dimensions of the lattice, the powder was mixed with some rock-salt, and from the rock-salt lines the correction terms for the film were found. A number of the stronger lines were carefully measured, and the values of a and c calculated by the method of least squares. The results are given in Table I.

TABLE I.

	a .	c .	c/a .
$N(CH_3)_4I$	7.91 Å.	5.74 Å.	0.7256
$N(CH_3)_4Br$	7.708 „	5.501 „	0.7137
$N(CH_3)_4Cl$	7.588 „	5.374 „	0.7082

The intensities of the observed lines as they were estimated from the spectrograms are given in Tables II., III., and IV., and in figs. 1 and 2 (A) for the Cl and Br compounds respectively. For the sake of completeness, a similar diagram is given in fig. 3 for the iodine compound.

TABLE II.— $N(CH_3)_4Cl$.

No.	$h_1 h_2 h_3$.	$h_1^2 + h_2^2 + h_3^2 \left(\frac{a}{c}\right)^2$.	$\left(\frac{2a}{\lambda} \sin \phi\right)^2$.	I obs.	I cal.
	1 0 0	1			
1	$\begin{Bmatrix} 0 & 0 & 1 \\ 1 & 1 & 0 \end{Bmatrix}$	$\begin{Bmatrix} 1.99 \\ 2.00 \end{Bmatrix}$			
2	(1 0 1) β	2.99	3.026	8	9.6
3	1 0 1	2.99	(3.31)		
4	(1 1 1) β	(3.31)	(3.33)		
5	$\begin{Bmatrix} 1 & 1 & 1 \\ 2 & 0 & 0 \end{Bmatrix}$	$\begin{Bmatrix} 3.99 \\ 4.00 \end{Bmatrix}$	4.009	100	100
	2 1 0	5.00	—	—	0
6	(2 1 1) β	(5.79)	5.79		0.1
7	2 0 1	5.99			
8	2 1 1	6.99	7.00	70	53.2
9	(1 0 2) β	(7.43)	7.37		
10	$\begin{Bmatrix} 0 & 0 & 2 \\ 2 & 2 & 0 \end{Bmatrix}$	$\begin{Bmatrix} 7.97 \\ 8.00 \end{Bmatrix}$	7.938	4	4.7
11	(2 2 1) β	(8.27)	(8.28)		

TABLE II. (*continued*).

No.	$h_1 h_2 h_3$.	$h_1^2 + h_2^2 + h_3^2 \left(\frac{a}{c}\right)^2$.	$\left(\frac{2a}{\lambda} \sin \phi\right)^2$.	I obs.	I cal.
12	1 0 2	8.97	8.951	28	20.1
	3 0 0	9.00	—	—	0
13	$\left\{ \begin{array}{l} 2\ 2\ 1 \\ 3\ 1\ 0 \end{array} \right.$	$\left\{ \begin{array}{l} 9.99 \\ 10.00 \end{array} \right.$	9.993	20	16.4 2.0
	3 0 1	10.93			
14	$\left\{ \begin{array}{l} 2\ 0\ 2 \\ 3\ 1\ 1 \end{array} \right.$	$\left\{ \begin{array}{l} 11.97 \\ 11.99 \end{array} \right.$	11.991	20	13.7
15	2 1 2	12.97	12.964	5	2.5
	3 2 0	13.00	—	—	0
16	(3 0 2) β	(14.06)	14.01		
17	3 2 1	14.99	14.936	5	3
18	$\left\{ \begin{array}{l} 2\ 2\ 2 \\ 4\ 0\ 0 \end{array} \right.$	$\left\{ \begin{array}{l} 15.97 \\ 16.00 \end{array} \right.$	15.91	8	10.3
19	3 0 2	16.97	16.974	28	32
	4 1 0	17.00	—	—	0
20	$\left\{ \begin{array}{l} 0\ 0\ 3 \\ 3\ 1\ 2 \\ 4\ 0\ 1 \\ 3\ 3\ 0 \end{array} \right.$	$\left\{ \begin{array}{l} 17.94 \\ 17.97 \\ 17.99 \\ 18.00 \end{array} \right.$	17.993	16	17
21	$\left\{ \begin{array}{l} 1\ 0\ 3 \\ 4\ 1\ 1 \end{array} \right.$	$\left\{ \begin{array}{l} 18.94 \\ 18.99 \end{array} \right.$	18.98	25	24.5
22	$\left\{ \begin{array}{l} 1\ 1\ 3 \\ 3\ 3\ 1 \\ 4\ 2\ 0 \end{array} \right.$	$\left\{ \begin{array}{l} 19.94 \\ 19.99 \\ 20.00 \end{array} \right.$	19.98	12	10.7
23	3 2 2	20.97	20.91	20	18.8
24	$\left\{ \begin{array}{l} 2\ 0\ 3 \\ 4\ 2\ 1 \end{array} \right.$	$\left\{ \begin{array}{l} 21.94 \\ 21.99 \end{array} \right.$	21.93	8	8.2
25	2 1 3	22.94	22.91	4	3.8
	4 0 2	23.97			0.2
26	4 1 2	24.97	24.94	2	0.7
	5 0 0	25.00	—	—	0
	3 4 0	25.00	—	—	0
27	$\left\{ \begin{array}{l} 2\ 2\ 3 \\ 3\ 3\ 2 \\ 5\ 1\ 0 \end{array} \right.$	$\left\{ \begin{array}{l} 25.94 \\ 25.97 \\ 26.00 \end{array} \right.$	25.93	25	18.7
28	$\left\{ \begin{array}{l} 3\ 0\ 3 \\ 5\ 0\ 1 \\ 3\ 4\ 1 \end{array} \right.$	$\left\{ \begin{array}{l} 26.94 \\ 26.99 \\ 26.99 \end{array} \right.$	26.96	3	3.5
29	$\left\{ \begin{array}{l} 3\ 1\ 3 \\ 4\ 2\ 2 \\ 5\ 1\ 1 \end{array} \right.$	$\left\{ \begin{array}{l} 27.94 \\ 27.97 \\ 27.99 \end{array} \right.$	28.01	20	16.1
	5 2 0	29	—	—	0
30	$\left\{ \begin{array}{l} 3\ 2\ 3 \\ 5\ 2\ 1 \end{array} \right.$	$\left\{ \begin{array}{l} 30.94 \\ 30.99 \end{array} \right.$	30.95	15	11.1
	0 0 4	31.90			
	4 4 0	32.00	31.98	3	2
31	$\left\{ \begin{array}{l} 1\ 0\ 4 \\ 4\ 3\ 2 \\ 5\ 0\ 2 \end{array} \right.$	$\left\{ \begin{array}{l} 32.90 \\ 32.97 \\ 32.97 \end{array} \right.$	33.00	25	16.3

TABLE II. (continued).

No.	$h_1 h_2 h_3$	$h_1^2 + h_2^2 + h_3^2 \left(\frac{a}{c}\right)^2$	$\left(\frac{2a}{\lambda} \sin \phi\right)^2$	1 obs.	1 cal.
32	$\begin{Bmatrix} 1 & 1 & 4 \\ 4 & 0 & 3 \\ 5 & 1 & 2 \end{Bmatrix}$	$\begin{Bmatrix} 33.90 \\ 33.94 \\ 33.97 \end{Bmatrix}$	33.92	25	12
33	$\begin{Bmatrix} 4 & 4 & 1 \\ 5 & 3 & 0 \end{Bmatrix}$	$\begin{Bmatrix} 33.99 \\ 34.00 \end{Bmatrix}$			
34	$\begin{Bmatrix} 4 & 1 & 3 \end{Bmatrix}$	34.94	34.94	5	3
35	$\begin{Bmatrix} 2 & 0 & 4 \\ 3 & 3 & 3 \end{Bmatrix}$	$\begin{Bmatrix} 35.90 \\ 35.94 \end{Bmatrix}$	36.01	25	19
36	$\begin{Bmatrix} 5 & 3 & 1 \\ 6 & 0 & 0 \end{Bmatrix}$	$\begin{Bmatrix} 35.99 \\ 36.00 \end{Bmatrix}$			
37	$\begin{Bmatrix} 2 & 1 & 4 \\ 5 & 2 & 2 \\ 6 & 1 & 0 \end{Bmatrix}$	$\begin{Bmatrix} 36.90 \\ 36.97 \\ 37.00 \end{Bmatrix}$	36.94	$\begin{Bmatrix} 4 \\ - \end{Bmatrix}$	$\begin{Bmatrix} 1.8 \\ 0 \end{Bmatrix}$
38	$\begin{Bmatrix} 4 & 2 & 3 \\ 6 & 0 & 1 \\ 6 & 1 & 1 \end{Bmatrix}$	$\begin{Bmatrix} 37.94 \\ 37.99 \\ 38.99 \end{Bmatrix}$	38.00	30	$\begin{Bmatrix} 22.8 \\ 1.5 \end{Bmatrix}$
39	$\begin{Bmatrix} 2 & 2 & 4 \\ 4 & 4 & 2 \\ 6 & 2 & 0 \end{Bmatrix}$	$\begin{Bmatrix} 39.90 \\ 39.97 \\ 40.00 \end{Bmatrix}$	40.05	15	9.2
40	$\begin{Bmatrix} 3 & 0 & 4 \\ 3 & 1 & 4 \end{Bmatrix}$	$\begin{Bmatrix} 40.90 \\ 41.90 \end{Bmatrix}$	$\begin{Bmatrix} 40.85 \\ 41.93 \end{Bmatrix}$	$\begin{Bmatrix} 7 \\ 18 \end{Bmatrix}$	$\begin{Bmatrix} 4.4 \\ 12.6 \end{Bmatrix}$

TABLE III.—N(CH₃)₄Br.

No.	$h_1 h_2 h_3$	$h_1^2 + h_2^2 + h_3^2 \left(\frac{a}{c}\right)^2$	$\left(\frac{2a}{\lambda} \sin \phi\right)^2$	1 obs.	1 cal.
	1 0 0	1			
1	$\begin{Bmatrix} 0 & 0 & 1 \\ 1 & 1 & 0 \end{Bmatrix}$	$\begin{Bmatrix} 1.96 \\ 2.00 \end{Bmatrix}$	1.94		
2	(1 0 1) β	(2.40)	(2.36)		
3	1 0 1	2.96	2.94	20	20
4	(1 1 1) β	(3.30)	(3.31)		
5	$\begin{Bmatrix} 1 & 1 & 1 \\ 2 & 0 & 0 \end{Bmatrix}$	$\begin{Bmatrix} 3.96 \\ 4.00 \end{Bmatrix}$	3.95	100	100
	2 1 0	5.00	—	—	0
6	(2 1 1) β	(5.75)	(5.75)		
7	2 0 1	5.96	5.93	5	5
8	2 1 1	6.96	6.94	60	49.2
9	(1 0 2) β	(7.31)	(7.32)		
10	$\begin{Bmatrix} 0 & 0 & 2 \\ 2 & 2 & 0 \end{Bmatrix}$	$\begin{Bmatrix} 7.85 \\ 8.00 \end{Bmatrix}$	7.953	7	9.4
11	(2 2 1) β	(8.23)	(8.27)		
12	1 0 2	8.85	8.832	45	26.7
	3 0 0	9.00	0	—	0
3	$\begin{Bmatrix} 2 & 2 & 1 \\ 3 & 1 & 0 \end{Bmatrix}$	$\begin{Bmatrix} 9.96 \\ 10.00 \end{Bmatrix}$	9.94	42	24.8
	3 0 1	10.96	—	—	0

TABLE III. (continued).

No.	$h_1 h_2 h_3$	$h_1^2 + h_2^2 + h_3^2 \left(\frac{a}{c}\right)^2$	$\left(\frac{2a}{\lambda} \sin \phi\right)^2$	I obs.	I cal.
14	$\begin{Bmatrix} 2 & 0 & 2 \\ 3 & 1 & 1 \end{Bmatrix}$	$\begin{Bmatrix} 11.85 \\ 11.96 \end{Bmatrix}$	11.925	36	20.2
15	$\begin{Bmatrix} 2 & 1 & 2 \\ 3 & 2 & 0 \end{Bmatrix}$	$\begin{Bmatrix} 12.85 \\ 13.00 \end{Bmatrix}$	$\begin{Bmatrix} 12.847 \\ - \end{Bmatrix}$	$\begin{Bmatrix} 30 \\ - \end{Bmatrix}$	$\begin{Bmatrix} 14 \\ 0 \end{Bmatrix}$
16	$(3 \ 0 \ 2)\beta$	(13.93)	(13.97)		
17	$\begin{Bmatrix} 3 & 2 & 1 \\ 2 & 2 & 2 \end{Bmatrix}$	$\begin{Bmatrix} 14.963 \\ 15.85 \end{Bmatrix}$	$\begin{Bmatrix} 14.934 \\ 15.90 \end{Bmatrix}$	$\begin{Bmatrix} 10 \\ - \end{Bmatrix}$	$\begin{Bmatrix} 7.3 \\ 1 \end{Bmatrix}$
18	$\begin{Bmatrix} 4 & 0 & 0 \\ 3 & 0 & 2 \end{Bmatrix}$	$\begin{Bmatrix} 16.00 \\ 16.85 \end{Bmatrix}$	$\begin{Bmatrix} - \\ 16.872 \end{Bmatrix}$	$\begin{Bmatrix} 10 \\ 35 \end{Bmatrix}$	$\begin{Bmatrix} 9.7 \\ 28 \end{Bmatrix}$
19	$\begin{Bmatrix} 4 & 1 & 0 \\ 0 & 0 & 3 \end{Bmatrix}$	$\begin{Bmatrix} 17.00 \\ 17.667 \end{Bmatrix}$	$\begin{Bmatrix} - \\ 17.85 \end{Bmatrix}$	$\begin{Bmatrix} - \\ - \end{Bmatrix}$	$\begin{Bmatrix} 0 \\ - \end{Bmatrix}$
20	$\begin{Bmatrix} 3 & 1 & 2 \\ 4 & 0 & 1 \\ 3 & 3 & 0 \end{Bmatrix}$	$\begin{Bmatrix} 17.85 \\ 17.903 \\ 18.00 \end{Bmatrix}$	17.974	$\begin{Bmatrix} - \\ - \\ 15 \end{Bmatrix}$	$\begin{Bmatrix} 1.3 \\ 2 \\ 11.8 \end{Bmatrix}$
21	$\begin{Bmatrix} 1 & 0 & 3 \\ 4 & 1 & 1 \end{Bmatrix}$	$\begin{Bmatrix} 18.67 \\ 18.96 \end{Bmatrix}$	18.896	28	$\begin{Bmatrix} 4.4 \\ 20.40 \end{Bmatrix}$
22	$\begin{Bmatrix} 1 & 1 & 3 \\ 3 & 3 & 1 \\ 4 & 2 & 0 \end{Bmatrix}$	$\begin{Bmatrix} 19.67 \\ 19.96 \\ 20.00 \end{Bmatrix}$	$\begin{Bmatrix} 19.94 \\ - \end{Bmatrix}$	$\begin{Bmatrix} 7 \\ 12 \end{Bmatrix}$	$\begin{Bmatrix} 6.8 \\ 8.9 \end{Bmatrix}$
23	$\begin{Bmatrix} 3 & 2 & 2 \\ 2 & 0 & 3 \end{Bmatrix}$	$\begin{Bmatrix} 20.85 \\ 21.67 \end{Bmatrix}$	$\begin{Bmatrix} 20.87 \\ 21.81 \end{Bmatrix}$	$\begin{Bmatrix} 32 \\ 10 \end{Bmatrix}$	$\begin{Bmatrix} 24 \\ 4.3 \end{Bmatrix}$
24	$\begin{Bmatrix} 4 & 2 & 1 \\ 2 & 1 & 3 \end{Bmatrix}$	$\begin{Bmatrix} 21.96 \\ 22.67 \end{Bmatrix}$	$\begin{Bmatrix} - \\ 22.71 \end{Bmatrix}$	$\begin{Bmatrix} - \\ 10 \end{Bmatrix}$	$\begin{Bmatrix} 9.5 \\ 10.2 \end{Bmatrix}$
25	$\begin{Bmatrix} 4 & 0 & 2 \\ 4 & 1 & 2 \end{Bmatrix}$	$\begin{Bmatrix} 23.85 \\ 24.85 \end{Bmatrix}$	$\begin{Bmatrix} - \\ 24.85 \end{Bmatrix}$	$\begin{Bmatrix} - \\ 10 \end{Bmatrix}$	$\begin{Bmatrix} 0.1 \\ 6 \end{Bmatrix}$
26	$\begin{Bmatrix} 5 & 0 & 0 \\ 3 & 4 & 0 \end{Bmatrix}$	$\begin{Bmatrix} 25.00 \\ 25.00 \end{Bmatrix}$	$\begin{Bmatrix} - \\ - \end{Bmatrix}$	$\begin{Bmatrix} - \\ - \end{Bmatrix}$	$\begin{Bmatrix} 0 \\ 0 \end{Bmatrix}$
27	$\begin{Bmatrix} 2 & 2 & 3 \\ 3 & 3 & 2 \\ 5 & 1 & 0 \end{Bmatrix}$	$\begin{Bmatrix} 25.67 \\ 25.85 \\ 26.00 \end{Bmatrix}$	$\begin{Bmatrix} 25.79 \\ - \\ - \end{Bmatrix}$	$\begin{Bmatrix} 10 \\ - \\ - \end{Bmatrix}$	$\begin{Bmatrix} 9.8 \\ 1.5 \\ 1.9 \end{Bmatrix}$
28	$\begin{Bmatrix} 3 & 0 & 3 \\ 5 & 0 & 1 \\ 3 & 4 & 1 \end{Bmatrix}$	$\begin{Bmatrix} 26.67 \\ 26.96 \\ 26.96 \end{Bmatrix}$	$\begin{Bmatrix} 27.06 \\ - \\ - \end{Bmatrix}$	$\begin{Bmatrix} - \\ - \\ 7 \end{Bmatrix}$	$\begin{Bmatrix} 2.2 \\ - \\ 6.8 \end{Bmatrix}$
29	$\begin{Bmatrix} 3 & 1 & 3 \\ 4 & 2 & 2 \\ 5 & 1 & 1 \end{Bmatrix}$	$\begin{Bmatrix} 27.67 \\ 27.85 \\ 27.96 \end{Bmatrix}$	$\begin{Bmatrix} 27.98 \\ - \\ - \end{Bmatrix}$	$\begin{Bmatrix} 23 \\ - \\ - \end{Bmatrix}$	$\begin{Bmatrix} 1.7 \\ 1.4 \\ 14.5 \end{Bmatrix}$
30	$\begin{Bmatrix} 5 & 2 & 0 \\ 3 & 2 & 3 \\ 5 & 2 & 1 \end{Bmatrix}$	$\begin{Bmatrix} 29 \\ 30.67 \\ 30.96 \end{Bmatrix}$	$\begin{Bmatrix} - \\ 30.71 \\ - \end{Bmatrix}$	$\begin{Bmatrix} - \\ 14 \\ - \end{Bmatrix}$	$\begin{Bmatrix} 0 \\ 5.2 \\ 9.7 \end{Bmatrix}$
31	$\begin{Bmatrix} 0 & 0 & 4 \\ 4 & 4 & 0 \\ 1 & 0 & 4 \end{Bmatrix}$	$\begin{Bmatrix} 31.41 \\ 32.00 \\ 32.41 \end{Bmatrix}$	$\begin{Bmatrix} - \\ 31.95 \\ - \end{Bmatrix}$	$\begin{Bmatrix} - \\ 2 \\ - \end{Bmatrix}$	$\begin{Bmatrix} 1.9 \\ 3.1 \\ - \end{Bmatrix}$
32	$\begin{Bmatrix} 4 & 3 & 2 \\ 5 & 0 & 2 \\ 1 & 1 & 4 \end{Bmatrix}$	$\begin{Bmatrix} 32.85 \\ 32.85 \\ 33.11 \end{Bmatrix}$	$\begin{Bmatrix} 32.90 \\ - \\ 32.52 \end{Bmatrix}$	$\begin{Bmatrix} 35 \\ - \\ 7 \end{Bmatrix}$	$\begin{Bmatrix} 21.6 \\ - \\ 4.7 \end{Bmatrix}$
33	$\begin{Bmatrix} 4 & 0 & 3 \\ 5 & 1 & 2 \\ 4 & 4 & 1 \end{Bmatrix}$	$\begin{Bmatrix} 33.67 \\ 33.85 \\ 33.96 \end{Bmatrix}$	$\begin{Bmatrix} 34.00 \\ - \\ - \end{Bmatrix}$	$\begin{Bmatrix} - \\ 7 \\ - \end{Bmatrix}$	$\begin{Bmatrix} 3.3 \\ - \\ 3 \end{Bmatrix}$
33	$\begin{Bmatrix} 5 & 3 & 0 \\ 4 & 4 & 1 \end{Bmatrix}$	$\begin{Bmatrix} 34.00 \\ 34.00 \end{Bmatrix}$	$\begin{Bmatrix} 34.00 \\ - \end{Bmatrix}$	$\begin{Bmatrix} 7 \\ - \end{Bmatrix}$	$\begin{Bmatrix} 5.7 \\ - \end{Bmatrix}$

TABLE III. (continued).

No.	$h_1 h_2 h_3$.	$h_1^2 + h_2^2 + h_3^2 \left(\frac{a}{c}\right)^2$.	$\left(\frac{2a}{\lambda \sin \phi}\right)^2$.	I obs.	I cal.
34	4 1 3	34.67	34.80	8	6.5
35	$\left\{ \begin{array}{l} 2 \ 0 \ 4 \\ 3 \ 3 \ 3 \end{array} \right\}$	$\left\{ \begin{array}{l} 35.41 \\ 35.67 \end{array} \right\}$	35.59	7	4.5
36	$\left\{ \begin{array}{l} 5 \ 3 \ 1 \\ 6 \ 0 \ 0 \end{array} \right\}$	$\left\{ \begin{array}{l} 35.96 \\ 36.00 \end{array} \right\}$	36.04	25	$\left\{ \begin{array}{l} 14.7 \\ 1.0 \end{array} \right\}$
37	$\left\{ \begin{array}{l} 2 \ 1 \ 4 \\ 5 \ 2 \ 2 \\ 6 \ 1 \ 0 \end{array} \right\}$	$\left\{ \begin{array}{l} 36.41 \\ 36.85 \\ 37.00 \end{array} \right\}$	36.88	10	$\left\{ \begin{array}{l} 6 \\ 0 \end{array} \right\}$
38	$\left\{ \begin{array}{l} 4 \ 2 \ 3 \\ 6 \ 0 \ 1 \end{array} \right\}$	$\left\{ \begin{array}{l} 37.67 \\ 37.96 \end{array} \right\}$	37.67	25	15
	6 1 1	38.96	38.90	4	3.2
	2 2 4	39.41	—	—	1.7
39	$\left\{ \begin{array}{l} 4 \ 4 \ 2 \\ 6 \ 2 \ 0 \end{array} \right\}$	$\left\{ \begin{array}{l} 39.85 \\ 40.00 \end{array} \right\}$	40.06	15	$\left\{ \begin{array}{l} 0.7 \\ 8.7 \end{array} \right\}$
	3 0 4	40.41	—	—	1.0
40	3 1 4	41.41	41.40	25	14.8

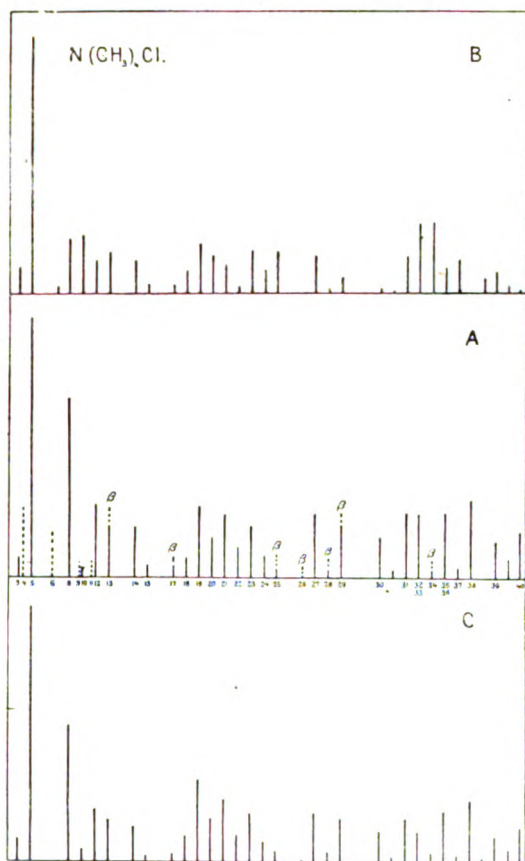
TABLE IV.—N(CH₂)₄l.

$h_1 h_2 h_3$.	I cal.	I cal.	$h_1 h_2 h_3$.	I cal.	I cal.
$\left\{ \begin{array}{l} 0 \ 0 \ 1 \\ 1 \ 1 \ 0 \end{array} \right\}$	15	25	$\left\{ \begin{array}{l} 3 \ 3 \ 1 \\ 4 \ 2 \ 0 \end{array} \right\}$	12	$\left\{ \begin{array}{l} 5.4 \\ 8.1 \end{array} \right\}$
1 0 1	15	20.4	3 2 2	25	23.9
$\left\{ \begin{array}{l} 1 \ 1 \ 1 \\ 2 \ 0 \ 0 \end{array} \right\}$	100	100	2 0 3	—	1.4
2 1 0	—	0	$\left\{ \begin{array}{l} 4 \ 2 \ 1 \\ 2 \ 1 \ 3 \end{array} \right\}$	30	$\left\{ \begin{array}{l} 12 \\ 15.6 \end{array} \right\}$
2 0 1	12	12.4	$\left\{ \begin{array}{l} 4 \ 1 \ 2 \\ 5 \ 0 \ 0 \end{array} \right\}$	15	$\left\{ \begin{array}{l} 8.6 \\ 0 \end{array} \right\}$
2 1 1	45	38.0	$\left\{ \begin{array}{l} 3 \ 4 \ 0 \\ 2 \ 2 \ 3 \end{array} \right\}$	—	$\left\{ \begin{array}{l} 0 \\ 3.9 \end{array} \right\}$
2 2 0	15	12.3	5 1 0	10	$\left\{ \begin{array}{l} 4.16 \\ 6.6 \end{array} \right\}$
1 0 2	30	26.7	$\left\{ \begin{array}{l} 3 \ 0 \ 3 \\ 5 \ 0 \ 1 \end{array} \right\}$	10	12.1
3 0 0	—	0	3 4 1	15	$\left\{ \begin{array}{l} 3.68 \\ 15.0 \end{array} \right\}$
$\left\{ \begin{array}{l} 2 \ 2 \ 1 \\ 3 \ 1 \ 0 \end{array} \right\}$	40	30.7	$\left\{ \begin{array}{l} 4 \ 2 \ 2 \\ 5 \ 1 \ 1 \end{array} \right\}$	—	0
2 0 2	—	1.6	5 2 0	—	0
3 1 1	30	27.3	$\left\{ \begin{array}{l} 3 \ 2 \ 3 \\ 5 \ 2 \ 1 \end{array} \right\}$	10	$\left\{ \begin{array}{l} 11.38 \\ 6.36 \end{array} \right\}$
2 1 2	30	20.7	$\left\{ \begin{array}{l} 0 \ 0 \ 4 \\ 4 \ 4 \ 0 \end{array} \right\}$	—	$\left\{ \begin{array}{l} 1.61 \\ 2 \end{array} \right\}$
3 2 0	—	0	1 0 4	—	1
3 2 1	6	6.8	$\left\{ \begin{array}{l} 4 \ 3 \ 2 \\ 5 \ 0 \ 2 \end{array} \right\}$	30	$\left\{ \begin{array}{l} 12.94 \\ 8.35 \end{array} \right\}$
$\left\{ \begin{array}{l} 2 \ 2 \ 2 \\ 4 \ 0 \ 0 \end{array} \right\}$	6	$\left\{ \begin{array}{l} 2.6 \\ 9 \end{array} \right\}$	$\left\{ \begin{array}{l} 1 \ 1 \ 4 \\ 4 \ 0 \ 3 \end{array} \right\}$	—	$\left\{ \begin{array}{l} 5 \\ 1.5 \end{array} \right\}$
3 0 2	25	22.7	4 4 1	—	4.33
4 1 0	—	0	$\left\{ \begin{array}{l} 5 \ 3 \ 0 \\ 4 \ 1 \ 3 \end{array} \right\}$	22	$\left\{ \begin{array}{l} 6.89 \\ 10.14 \end{array} \right\}$
$\left\{ \begin{array}{l} 4 \ 0 \ 1 \\ 3 \ 3 \ 0 \end{array} \right\}$	22	$\left\{ \begin{array}{l} 4.83 \\ 9.71 \end{array} \right\}$			
1 0 3	—	$\left\{ \begin{array}{l} 9.55 \\ 16.6 \end{array} \right\}$			
$\left\{ \begin{array}{l} 4 \ 1 \ 1 \\ 1 \ 1 \ 3 \end{array} \right\}$	15	$\left\{ \begin{array}{l} 2.7 \end{array} \right\}$			

We then proceeded to calculate the intensities of the lines on the basis of the atomic arrangement previously found * for the iodine compound.

Introducing the same angular parameters for all three compounds, we found the intensities given in (B) figs. 1 and 2. In fig. 3 (B) are given the corresponding intensities

Fig. 1.



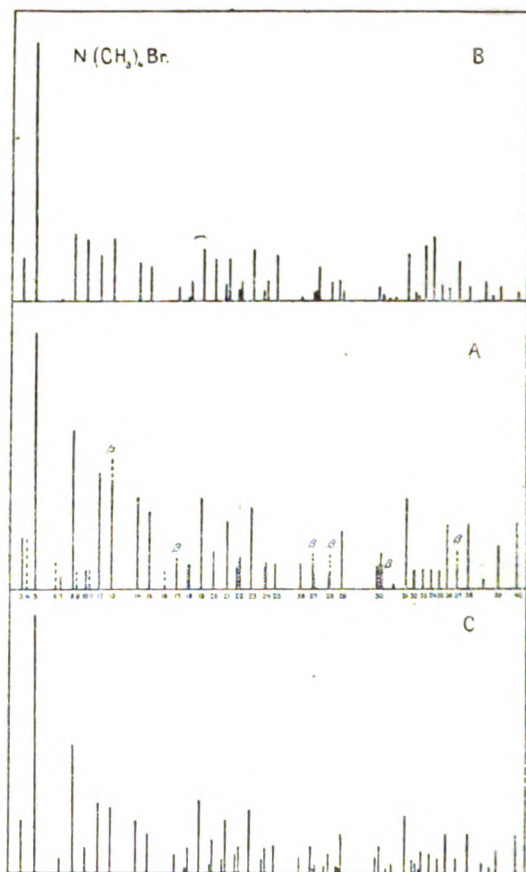
for the iodine compound. Comparing observed and calculated intensities we find that the agreement, which, as stated in a previous paper, is fairly good in the case of the I compound, becomes less good in the case of the Br compound, and still worse in the case of the Cl compound.

* *Loc. cit.* (II.).

After having tried various changes of the position of the atoms, we finally found that the following re-arrangement led to a satisfactory agreement between observed and calculated intensities.

In the lattice previously found the N-atoms were fixed with one parameter. With the particular value found for

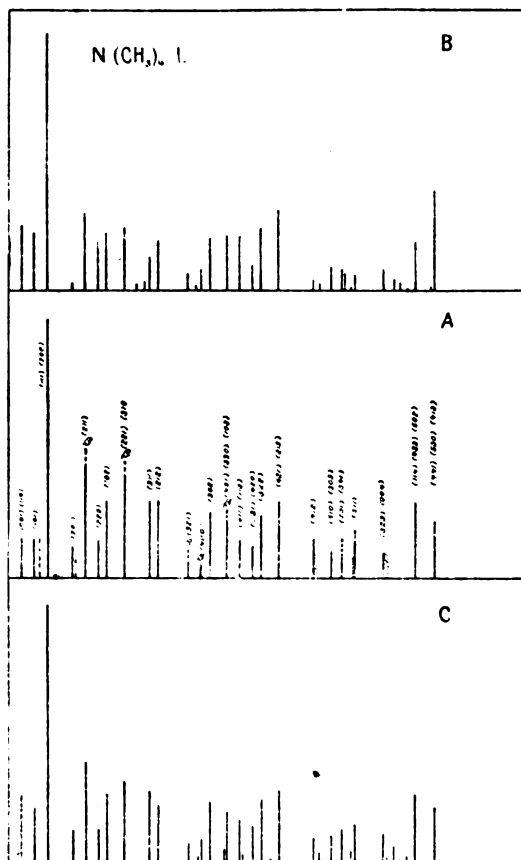
Fig. 2.



the parameter it appeared that the two nitrogen atoms contained in the unit cell were very nearly situated in a plane perpendicular to the *c*-axis. The C-atoms formed tetrahedral groups with their centres in level with those of the corresponding nitrogen atoms.

The re-arrangement of the atoms which had to be introduced mainly consisted in moving the nitrogen atoms a distance $a/2$ parallel to a , so that they were placed in the centres of the carbon tetrahedra. We now further assumed that the two nitrogen atoms contained in the unit cell were exactly placed in a plane perpendicular to the c -axis. The

Fig. 3.

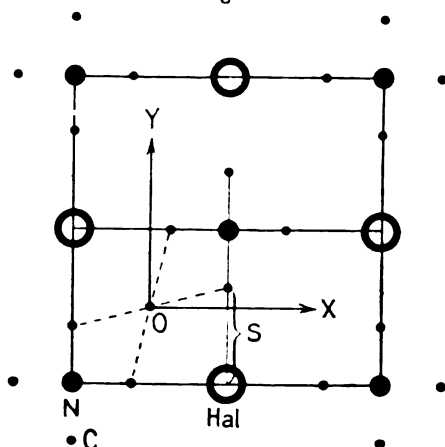


positions of the N-atoms are thus fixed without any parameter.

This change of position of the N-atoms does not involve any change of the space group of the lattice, and we may also say that the nitrogen atoms occupy the position of the space group D_{4h}^7 , which has no parameter.

We now naturally take the plane of the nitrogen atoms as (X-Y) plane of the coordinate system.

Fig. 4.



Taking the symmetry centrum (O) midway between the two neighbouring N-atoms (fig. 4) as origin of the coordinates, the positions of the atoms may now be written in the form :

$$\left. \begin{aligned} \text{N} : & \pm \left[\left[\frac{1}{4}, \frac{1}{4}, 0 \right] \right] \\ \text{Cl, Br or I} : & \pm \left[\left[\frac{1}{4}, -\frac{1}{4}, p \right] \right] \\ \text{C} : & \pm \left\{ \begin{aligned} & \left[\left[\frac{1}{4}, \left(-\frac{1}{4} + s \right), -r \right] \right] \\ & \left[\left[\frac{1}{4}, \left(-\frac{1}{4} - s \right), -r \right] \right] \\ & \left[\left[\frac{1}{4} + s, -\frac{1}{4}, -r \right] \right] \\ & \left[\left[\frac{1}{4} - s, -\frac{1}{4}, -r \right] \right] \end{aligned} \right\} \dots (1) \end{aligned} \right\}$$

Indicating the number of electrons associated with one of the halogen atoms by A and disregarding the reflexion power of the hydrogen atoms, the structure factor takes the simple form :

$$\left. \begin{aligned} h_1 + h_2 &= 2n, \\ S &= N(-1)^{h_1} + A \cos h_3 \alpha + 2C \cos h_3 \gamma [\cos h_1 \delta + \cos h_2 \delta] \\ h_1 + h_2 &= 2n + 1, \\ S &= -A \sin h_3 \alpha + 2C \sin h_3 \gamma [\cos h_1 \delta + \cos h_2 \delta] \end{aligned} \right\} \dots (2) *$$

* After this result was obtained we found that P. Niggli (*Zeitschr. f. Kristall.* liii. p. 210, 1922), in discussing Vegard's original atomic arrangement, has suggested that possibly the N-atoms might take up that position of the space group which is fixed without parameters.

where

$$\alpha = 2\pi p,$$

$$\gamma = 2\pi r,$$

$$\delta = 2\pi s.$$

Comparing the parameters here introduced with those of the previous paper (II.), we have to remember that

$$p = 1/4 + p',$$

$$r = 1/4 - r',$$

where p' and r' are the corresponding parameters previously used.

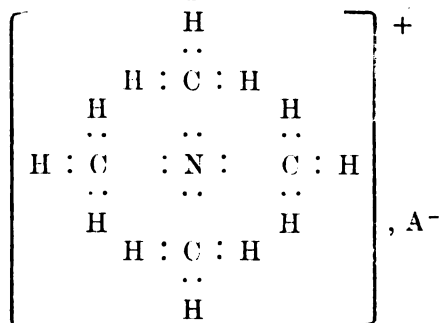
In order to find the typical intensity distribution, we calculate the intensities by means of the simplified formula :

$$J = \frac{vs^2}{h_1^2 + h_2^2 + \left(\frac{a}{c}\right)^2 h_3^2} \quad \dots \quad (3)$$

The atomic arrangement previously found and described in the papers referred to (I. and II.) was most simply described by means of molecular elements $N(CH_3)_4I$, where the N- and I-atoms are situated on the same fourfold axis. When the N-atoms are put into the centres of the C-tetrahedra, and we get the arrangement here described, the molecular elements lose their significance, and we have a type of arrangement more like that of rock-salt. This fact would indicate that the crystals under consideration are forming lattices with polar binding (ionic lattices), where the halogen forms the negative ion, and the complex $N(CH_3)_4$ as a whole the positive ion.

In the formula for the structure factor we should put A equal to $N + 1$, where N is the atomic number of the halogen atom. With regard to the group $N(CH_3)_4^+$, the calculations show that it cannot be treated as a single centre with a weight equal to the sum of the electrons, but we have to regard each atom as a separate centre with its own electrons. An exact calculation of the reflexion power of the group would involve a knowledge of the way in which the electrons on an average are distributed within the complex, which we do not possess at the present time. Assuming a homœopolar binding of the atoms inside the complex, and assuming that the constitution formula may be written so as to express the tendency of the N- and C-atoms to surround themselves with groups of 8 electrons, and the tendency of the H-atoms to be attached by means of pairs (helium group), the constitution

996 Prof. Vegard and Mr. Sollesnes on the Structure of
formula of our substances might be written :



This constitution, however, as far as the "binding" electron systems is concerned, may merely have a formal significance. As a matter of fact, we found that a very good agreement between observed and calculated intensities is obtained by assuming the electrons to be associated with their respective nuclei, and it makes little difference for the calculated intensities whether we assume the halogen to be an ion or a neutral atom. Our final intensity values were calculated on the assumption that the reflecting power of the halogen is proportional to $(N+1)$ and that of C and N proportional to the respective atomic numbers.

In order to obtain approximate values of the parameters, we have also disregarded the reflexion power of the hydrogen atoms, for, as the reflexion power of each atom is very small, and as the H-atoms are spread out throughout the interior of the elementary cell, they should not very essentially affect the typical intensity distribution of the lines.

The parameter values of the halogen and C-atoms, which we found for the three compounds, are given in Table V.

TABLE V.

		$\text{N}(\text{CH}_3)_4\text{Cl}$	$\text{N}(\text{CH}_3)_4\text{Br}$	$\text{N}(\text{CH}_3)_4\text{I}$
Halogen	p	0.361	0.375	0.394
	a	130°	135°	142°
Carbon	r	0.156	0.153	0.164
	γ	56° (56°·3)	56° (55°)	60° (59°·1)
	s	0.339	0.339	0.347
	δ	122°·5 (122°·1)	122°·5 (122°)	125°
Centre distance,				
N - C		1.48 Å.	1.49 Å.	1.51 Å.

The intensity distribution calculated in this way is given in Tables II., III., IV., and is graphically represented in (C) figs. 1, 2, and 3. We notice that the agreement between observed and calculated intensities is remarkably good for all three compounds.

The arrangement of the atoms N, C, and halogen corresponding to these parameters is illustrated in fig. 5 (Pl. XXI.), which shows a stereoscopic reproduction of a model of the lattice.

If we calculate the centre distances between the N- and the surrounding C-atoms, we find a value of about 1.5 Å., corresponding to the centre distance between neutral nitrogen and carbon atom in contact. We may thus regard the group NC_4 as forming a close packing of neutral atoms.

The Dimensions and Arrangement of the Hydrogen Atoms.

§ 3. Assuming the halogen to occupy the large space characteristic of univalent negative ions, we find that they have no direct contact with the NC_4 -group. In order to explain the lattice as a packing of spheres, we must, as already found in our previous investigations, give a certain diameter to the hydrogen atom. As the N- and C-atoms are in contact, the hydrogen atoms must fill the space round the NC_4 -group, and by means of "contacts" with the C-atoms and halogen ions, establish the stability of the lattice.

On account of the small reflexion power of hydrogen, it is hardly possible to determine exactly the position of the hydrogen atoms by means of the X-ray data alone, but as we may regard the atomic centres of N, C, and halogen as known, it might be possible to find the arrangement and dimensions of the hydrogen atoms from the assumption that the lattice may be regarded as a packing of spheres.

The elementary cell contains 24 hydrogen atoms. From the space group D_{2h}^{25} , we find that these atoms may either be divided into three groups of 8 atoms, or into two groups—one containing 3 and one containing 16 atoms. The first possibility does not seem to lead to any satisfactory arrangement, when all hydrogen atoms shall have equal diameters.

In order to fix the position and diameter of hydrogen, we must give definite diameters to N, C and the halogen ions.

The values used are given in Table VI. In the case of N and C the diameters are supposed to be those of the neutral atoms, but as the centre distances N—C are not exactly equal for all three compounds, we have to introduce corresponding variations of the diameters.

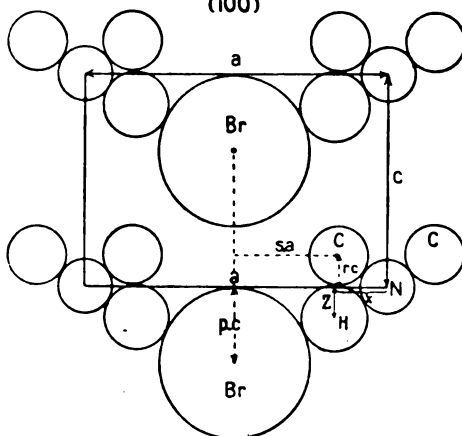
The group of 8 atoms have their centres in (1 0 0) planes through the N-atoms. Their position is fixed by two parameters (x' , z') giving the coordinates relative to an N-atom. These atoms may be placed in such a way that they have contact with both C and N and with the negative halogen ion. The position is illustrated in fig. 6, and from these three contact conditions the parameters x , z and the radius can be found.

The results, which were found by means of a graphical method, are given in Table VI.

In the group of 16 hydrogen atoms, each atom has three parameters (x , y , z) (referred to the centre of an N-atom).

Fig. 6.

(100)



By studying the space to be reserved for these atoms we found that each atom might have contact with two other H-atoms, one C-atom, and one halogen atom. This makes in all four contact conditions, which lead to the following equations:—

- I. $[x - a(\frac{1}{2} - s)]^2 + y^2 + (z - cr)^2 = (r_c + r_H)^2$,
- II. $(\frac{1}{2}a - x)^2 + y^2 + [(1 - p)c - z]^2 = (r_{H\perp} + r_H)^2$,
- III. $2(\frac{1}{2}a - x - y)^2 = (2r_H)^2$,
- IV. $2(x - y)^2 + [(1 - 2r)c - 2z]^2 = (2r_H)^2$.

From these four equations we should be able to find the four unknowns x , y , z , and r_H . A direct solution of these equations would be somewhat troublesome, and we have

used a method with trial and error. From the model of the space lattice we can easily find certain limits for the values of r_H . We then introduce a probable value of r_H , calculate ($x y z$) by three of the equations, and use the fourth as a test. In this way we found the parameters and dimensions given in Table VI.

A stereoscopic reproduction of a model showing the arrangement of the H-atoms relative to the NC_4 -group and the halogen is given in fig. 7 (Pl. XXI.).

TABLE VI.*

	$N(CH_3)_4Cl.$	$N(CH_3)_4Br.$	$N(CH_3)_4I.$
$r_{Hal. (ion)}$	1.82 Å.	1.96 Å.	2.15 Å.
r_N	0.71 "	0.71 "	0.72 "
r_C	0.77 "	0.78 "	0.79 "
Groups of 8 H-atoms. $\left\{ \begin{array}{l} x/a \dots\dots \\ z/c \dots\dots \\ r_H \dots\dots \end{array} \right.$	$\left\{ \begin{array}{l} 0.184 \\ 0.140 \\ 0.86 \text{ Å.} \end{array} \right.$	$\left\{ \begin{array}{l} 0.183 \\ 0.182 \\ 0.85 \text{ Å.} \end{array} \right.$	$\left\{ \begin{array}{l} 0.177 \\ 0.122 \\ 0.85 \text{ Å.} \end{array} \right.$
Groups of 16 H-atoms. $\left\{ \begin{array}{l} x/u \dots\dots \\ y/a \dots\dots \\ z/c \dots\dots \\ r_H \dots\dots \end{array} \right.$	$\left\{ \begin{array}{l} 0.224 \\ 0.117 \\ 0.386 \\ 0.85 \text{ Å.} \end{array} \right.$	$\left\{ \begin{array}{l} 0.215 \\ 0.127 \\ 0.373 \\ 0.85 \text{ Å.} \end{array} \right.$	$\left\{ \begin{array}{l} 0.197 \\ 0.180 \\ 0.356 \\ 0.87 \text{ Å.} \end{array} \right.$

We notice the remarkable fact that the *radius of the H-atoms comes out nearly equal for both groups of H-atoms and for all three compounds and equal to 0.85 Å.*

The mere fact that the centre distance N—C, deduced from X-ray data, corresponds to that of contact between these two atoms, shows—as already mentioned—that the hydrogen atoms must require a space for themselves.

In order to verify this conclusion we have calculated the intensities on the assumption that CH_3 is forming spherical groups in contact with N and halogen, but the result was not in agreement with observations. If we shall regard the structure as a packing of spheres, *the hydrogen atom must be given the fairly large diameter of about 1.70 Å.*

If we would drop the idea of a radius for the H-atoms and only consider the dimensions of the group CH_3 , this group could not be given a spherical shape if stability is to be secured by mutual contacts, but, as stated by one of us in a

* By the calculation of the numbers given in Table VI. we have used values of the parameters ($\gamma \delta$) of the C-atoms, which are given in the brackets of Table V.

previous paper (II.), the CH_3 -group should be given some other shape, *e. g.* that of a rotational body like an egg.

Although we cannot claim any great accuracy as regards the parameters of the hydrogen atoms, still the fact that we have obtained a nearly constant value for the hydrogen diameter indicates that they cannot be far from the true values.

If so, the present substances should give us a means of fixing more accurately how the electrons of the complex $\text{N}(\text{CH}_3)_4^+$ are distributed among the atoms. The procedure would be to calculate the intensities for a number of different possible distributions and compare them with observations.

It would especially be of interest to find out whether the hydrogen atom reflects with a power corresponding to *one* or to *two* electrons associated with it. In the latter case hydrogen might be regarded as an univalent negative ion with an electron system like that of the neutral helium atom.

Such an investigation would lead to a considerable calculating work and will be left for a later publication.

The morphotropic relation between the substitution products $\text{N}(\text{CH}_3)_4$ hal. and their mother substances NH_4 hal. was studied by one of us in the paper of 1917 (I.). This relation is not at all so simple as the comparison between the topic parameters would suggest. The number of molecules in the unit cell is different for the mother substance (4) and for the substitution product (2). Comparing the dimensions of the unit cells there is apparently no simple connexion. If, however, we determine the dimensions (a' , c') of a similarly shaped cell containing only one molecule and compare it with the side of a cube containing one molecule of the mother substance, a simple relation comes out, which is apparent from Table VII.

TABLE VII.

	a' .	c' .		a'_M .
$\text{N}(\text{CH}_3)_4\text{I}$	6.278	4.556	NH_4I	4.54
$\text{N}(\text{CH}_3)_4\text{Br}$	6.118	4.366	NH_4Br	4.328
$\text{N}(\text{CH}_3)_4\text{Cl}$	6.023	4.265	NH_4Cl	4.143

The side of the cube of one molecule for the mother substance (a'_M) is approximately equal to the height (c') of the prism containing one molecule of the substitution product.

In this connexion it is of interest to notice that the ammonium salts can appear in a form of the (CsCl) type,

where the unit cell contains one molecule, but the sides of these cubes for the same substance are smaller than a' . They were found* to be 3.88 Å. and 4.07 Å. for the Cl and Br compounds respectively.

Thus we see that the volume occupied by one molecule very much depends on the atomic arrangement, and it is then not easily understood why the dimension in the c -direction of the one-molecular cell should be practically unchanged by a substitution which essentially alters the atomic arrangement.

Summary of Results.

1. Investigations undertaken in 1917 on the structure of $N(CH_3)_4I$ have been continued by using the powder method and extended to the bromine and chlorine compounds.

2. The correctness of the dimensions of the unit cell and of the space group (D_{4h}^7) originally found for the structure of $N(CH_3)_4I$ has been confirmed.

3. The investigation of the bromine and chlorine compound, where the reflecting power of the halogen atoms is less dominating than in the case of the iodine compound, has made it possible to fix more accurately the position of the nitrogen and carbon atoms.

4. The nitrogen and carbon atoms form groups NC_4 , where N is placed in the centre of a tetrahedron of C-atoms. The centre distance N—C of these groups is found to be 1.50 Å., corresponding to that of neutral atoms.

5. If we regard the crystal as a packing of spheres, the hydrogen atoms must be given a definite diameter. In order to obtain the same diameter for all hydrogen atoms in the crystal we have to assume one group of 8 and one group of 16 H-atoms inside the unit cell. From the volume conditions we can calculate the parameters and diameter for each group of H-atoms. Both groups give the same value, 1.70 Å., for the diameter of the H-atom.

6. The determination of the positions of the H-atoms from volume conditions may give us a possibility of determining the number of electrons connected with each H-atom in the space lattice of the crystals.

7. The arrangement of the atoms suggests that the crystal has an ionic constitution $N(CH_3)_4^+ - Hal.$

Physical Institut, Oslo.

July 4, 1927.

* L. Vegard, *Zeitschr. f. Phys.* v. p. 21 (1921).

XCIII. Condenser Discharges in Discharge-Tubes.—Part I.
Single Condenser Discharges. By WILLIAM CLARKSON,
M.Sc., A.Inst.P., The Physical Institute of the University
of Utrecht.*

1. INTRODUCTION.

FOLLOWING a sequence of observations on the volt-ampere characteristics in discharges⁽¹⁾, this paper applies the observed phenomena to condenser and intermittent discharges through gases to explain their critical voltage relations.

Each condenser discharge is considered as presenting the following sequence of phenomena:—The “striking” of the discharge, the consequent “build-up” of current, the “extinction,” and the “clear-up” of space-charge.

It has been demonstrated recently that the potential at which a discharge “strikes” is variable according to the current and space-charge in the tube. The idea of a “threshold current” was utilized by the author to explain the progressive lowering of the “striking” potential with increase in frequency in intermittence⁽¹⁾. It has been shown that the “threshold-current” characteristic is identical with the corona characteristic⁽²⁾. This identity is assumed here also for dynamic discharge conditions, since this simplifies presentation.

It was well known that a “lag” could take place at the “striking” of a discharge; but whether it occurred before or after this initiation of a self-sustained discharge has been much discussed⁽³⁾. It was recently shown that a “lag” occurred even in very clean discharge-tubes. The attribution of this “lag” to a slow “build-up” permitted the peak-voltage phenomena in “intermittence” to be explained⁽⁴⁾.

The “clear-up” of both steady and condenser discharges has been studied in detail here, for the variation of the minimum potential in both single “flashes”⁽⁵⁾ and “intermittence”⁽⁶⁾ has been attributed to this phenomenon.

2. TUBES AND APPARATUS.

The type of tube used here has been described previously⁽⁴⁾. The electrodes were of nickel, convex, about 5 cm. in diameter and 1 cm. apart. The tubes were thoroughly cleaned and baked-out before filling with purified gas: after filling, the electrodes were sodiated electrolytically.

Tubes containing neon at pressures of 4 mm. and of

* Communicated by Prof. Ornstein.

8 mm., and with argon at 10 mm., were employed. The discharge phenomena observed were alike in all cases, and did not differ essentially from the phenomena observed on previous occasions.

The measuring apparatus has also been described. A quick-acting electrostatic voltmeter was used for voltage measurements, and a shunted galvanometer for the currents. The circuit current was controlled by a diode valve.

3. CONDENSER-DISCHARGE CHARACTERISTICS.

a. *The Volt-ampere Characteristic.*—The characteristics found were of the usual form, as shown in fig. 1 (*a*), where SR is the corona characteristic, RQP the “stable” characteristic, and the stage beyond Q the “normal” characteristic.

The currents corresponding to the corona characteristic were the minimum (i_n), for the applied voltage (v_n), at which a self-sustained discharge was possible. Space-charge was a factor of great importance here. v_n was constant, at the value of the sparking potential (v_c), for currents of a few microamperes, but then fell rapidly as i_n increased.

The corona characteristic has also been referred to as the “threshold-current” characteristic, since, under stable conditions at least ⁽²⁾, it determines the potential at which a discharge “strikes” and at which a “build-up” is possible (v_m, i_m).

The normal characteristic gives the maximum current sustainable at the applied voltage.

We may assume that on “build-up” the current increases, from a point v_m, i_m , until another point on the characteristic, v_n, i_n , is realized. Extinction will then occur ⁽¹⁾.

Experiments show that on the “extinction” of a steady discharge the voltage falls by an amount variable with conditions. This is referred to as the “clear-up” of space-charge.

Referring to a diagram of the characteristic, with voltage as ordinate and current as abscissa, we see that “build-up” must occur in the region to the right of the characteristic, and “clear-up” in the region to the left. These are regions of instability, and only realizable dynamically (see later).

Considering that multiplication of ions is possible for all except small voltages, the characteristic is definable as the boundary where the factors tending to increase the number of ions are exactly counterbalanced by those tending to reduce the number. To the right the former factors predominate, to the left the latter.

We may assume that all points to the right of the

characteristic are realizable; but we find that the same assumption applied to the region to the left, would imply that currents at v_n greater than the corresponding i_n were possible for points on the normal characteristic. The normal characteristic may give the maximum current sustainable with an abnormal cathode fall only, in which case we may suppose that greater currents may be attainable under other space-charge conditions. Though the attempts made to realize these conditions by photo-electric means proved inconclusive, the P.E. characteristics given by Campbell⁽⁷⁾ offer support to the idea. Certainly, if only normal cathode falls were possible, v_n would remain constant at v_b , and this problem would not arise.

Intermittence and corresponding experiments, and the fact that the "clear-up" associated with the characteristic increases regularly with current, suggest that the normal characteristic is not necessarily traversed towards Q from r_n , i_n in flashes. Below Q, of course, "extinction" must occur, since the voltage, necessarily decreasing, is already a minimum for the self-sustained discharge.

b. *V, I Diagrams.*—Fig. 1 (a) shows the current-voltage relations assumed in this paper for single condenser discharges. From the striking of the discharge at (nominally)

zero current, a voltage $V_M \Rightarrow v_C$ being necessary, the current increases steadily, with a corresponding decrease of the condenser potential, until a voltage, v_n , determined by the current and the space-charge distribution at which the discharge is no longer self-sustainable, is reached. "Extinction" occurs here and the current falls to zero, the condenser voltage being meanwhile lowered to a final value V_N (the "tracks" drawn in fig. 1 (a) are diagrammatic, not experimental).

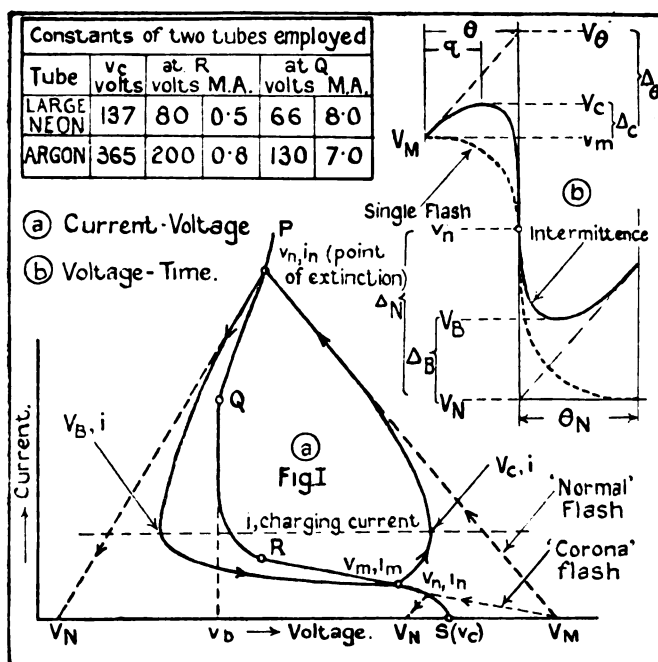
In addition to the assumption that "extinction" occurs at v_n , i_n , as would be determined by the characteristic under static conditions, it is further assumed that the "clear-up" at the characteristic is representative of that of "flashes" also. Both these are necessary experimental assumptions. They probably give results not only qualitatively correct, but quantitatively of the right order.

One point must be stressed at this stage. To define any stage in a discharge accurately, in addition to the values of voltage and current, as given in the diagram, the space-charge distribution must also be known. This is indeterminate, and is variable. It must be connected with the

time duration of the discharge, another factor that cannot be included in such a diagram, though since this is measurable we are not without some insight into the conditions actually obtaining during the discharge.

Only points on the characteristic, for steady discharges, where the space-charge conditions are reproducible, are therefore definite. All others are indeterminate; and in

Fig. 1.



condenser discharges, particularly in intermittence, it may be said that no points are fully definable. It is for this reason that the assumptions as to the significance of the (statical) characteristic in discharges, in "striking" and "extinction," are necessary. They are made with full cognizance of the above facts. It is doubtful whether we may speak of an unvarying characteristic in discharges at all; but, in any case, the usual volt-ampere characteristic presents the only concrete approximation that may be utilized.

4. "CLEAR-UP" AT CHARACTERISTIC.

The clear-up of space-charge presents many points of intrinsic interest, and the writer decided to attempt as thorough a quantitative examination as was possible.

a. *Method*.—A condenser, shunted by the electrostatic voltmeter, was placed across the tube, through which a steady current was then passed. Some point (v_n, i_n) on the characteristic was thus attained. When the current circuit was suddenly broken the discharge ceased, but not before a quantity of electricity, Q , sufficient to lower the condenser voltage to V_N , $Q = C(v_n - V_N)$, had been transferred. Given constant conditions it was found that V_N had a definite value for any one current and capacity.

It was obviously not possible to study the whole of the characteristic in this way, as the range over which steady currents were possible depended on the capacity; but from qualitative results, obtained with a diode in the condenser circuit (intermittence thus being prevented), it was seen that the conclusions drawn from the original method were of general applicability.

b. *Results*.—All these tubes showed the same general clear-up properties. $\Delta_N (= v_n - V_N)$, increased with increase of i_n , and decreased with increase of C . As far as could be determined, the corona characteristic and stable characteristic gave a continuous Δ_N, i curve.

Fig. 2 (*b*) shows the variation of Δ_N (large neon tube) for capacities from $0.0022 \mu F.$ – $0.9 \mu F.$, and for currents (roughly) from 0.1 – 50.0 M.A., i_n being plotted on a log scale. It will be seen that the rate of increase of Δ_N falls off with increase of current, and that V_N approaches asymptotically a small limiting value. This is more easily demonstrable with small capacities, the currents required for larger capacities being beyond the practical range, being about two amperes for a capacity of $1.0 \mu F.$

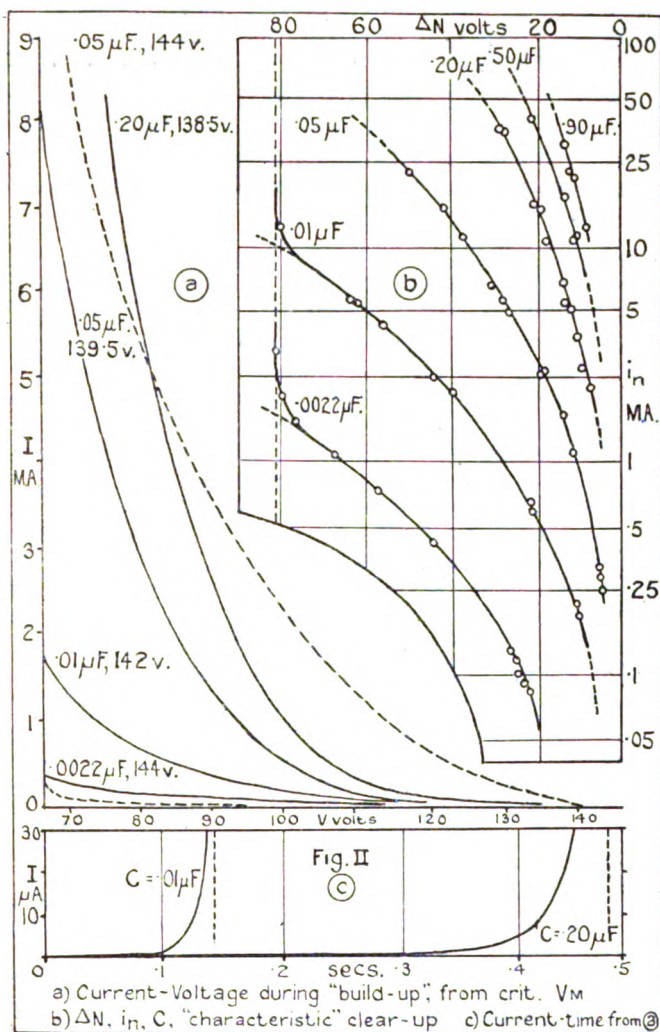
As the variations of v_n with i_n were small enough to be neglected, fig. 2 (*b*) actually gives the Δ_N, C, i_n variations for a constant initial voltage. Their relation is given accurately by the empirical expression

$$\Delta_N = k \frac{i_n^x}{C^y} \dots \dots \dots (1)$$

In this case x and y were approximately of the same magnitude (0.5 and 0.55 respectively), and k had a value of 0.07 .

It was found that the same expression applied to similar clear-up curves for the other tubes. The argon-filled tube, for instance, gave $k=0.19$, and both x and y equalled 0.42 .

Fig. 2.



Though it cannot definitely be stated at this stage that this relation is common to all discharge-tubes, whatever the electrode disposition etc., certain definite statements concerning clear-up may be made.

Since in the four tubes examined x and y always had values of the order of 0.5, it is proposed to simplify treatment by assuming this value throughout. Thus we may say from equation 1 that Δ_N varied as $\sqrt{i_n/C}$.

The quantity transference is given from equation (1) by

$$Q = ki_n^x C^{1-y}, \quad \text{approx. } \propto \sqrt{i_n C}. \quad (2)$$

The fact that Q varies with C , i constant, indicates that it is not a constant quantity determined by the initial current, but that it also varies with voltage. Multiplication of ions during clear-up is thus involved, and these effects must be considered.

c. *General Considerations.*—Visual observation of the phenomenon of clear-up in intermittence shows that the positive column disappears almost immediately ⁽⁶⁾⁽¹⁾. Practically all the clear-up period is occupied by the diffusion of the negative glow towards the anode. It is possible that this period is characterized by currents of the order of corona characteristic currents. Whether the current experiences a discontinuity or sudden decrease at the moment of extinction, however, cannot be inferred.

Considerations previously applied to "build-up," ⁽⁴⁾ are extended to clear-up in the following treatment. Space-charge distribution is perforce neglected.

During any time in clear-up there will occur multiplication, recombination, and diffusion of ions. We may assume that the rate of change of space-charge falls rapidly with reduction of V . Current-voltage characteristics obtained for photo-electric currents (constant illumination) in the clear-up region, showed that I increased continuously with V . The rate of increase became greater as V approached v_b , a change of, say, 20 volts in this region bringing about a twentyfold change of current.

The rate of clear-up will be approximately constant at constant voltage.

If the current is assumed to depend on the amount of space-charge present in the inter-electrode space, a somewhat exponential time-current curve will result.

For the case where there is a capacity across the tube, the voltage during clear-up will fall at a rate determined by the current, most rapidly at first when I is a maximum, and then much more slowly, as the ensuing reduction in potential will have caused a correspondingly rapid diminution of current. The space-charge will persist longer at higher potentials.

The variation of Δ_N with C and i_n may now be considered.

At a constant rate of clear-up (i_n constant, and therefore Q constant), Δ_N should vary inversely as C , but as the rate of clear-up increases rapidly with diminution of V (*i.e.* with reduction of C), Δ_N will actually vary much more slowly than i/C . The same argument applies to changes with i_n (C constant), the change in rate of clear-up causing Δ_N to vary much less rapidly than the current i_n . We may further expect that the result of corresponding changes in i_n and C will be of the same order; and this, indeed, is the case, though the significance of the square-root relation ($\Delta_N \propto \sqrt{i_n/C}$) lies in the quantitative relations.

The relation between Δ_N and the voltage during clear-up was clearly demonstrated in V_N, i_n curves in cases where v_n changed rapidly with i_n (above Q , fig. 1, *a*). The curves showed a pronounced change in slope at Q , Δ_N increasing rapidly. The constants x and y were also found to change.

The variation of Q under different conditions is contained in the foregoing discussion.

d. *Times*.—It has been shown that with the voltage across the electrode zero, clear-up occurs in a time less than 10^{-6} second⁽⁸⁾; and since with V near v_b the time is large (∞ at v_b), it appears that a wide variation of time of clear-up with voltage is possible.

An idea of the relative variation of the time of clear-up may be obtained from a consideration of the quantity transference and the ratio of the average to the initial current. Quantitative results are impossible, since the actual value of the average current, though probably of the same order of magnitude as corona currents, is not known.

One effect of a lowering of V_N will be to reduce the relative duration of the final (the small current) stage in clear-up. The ratio initial current to average current will thus decrease as Δ_N increases, the actual value of the average current depending of course on i_n .

If we express this ratio by R , we have from equation (2) that

$$T \propto R\sqrt{C/i_n}, \dots \dots \dots (3)$$

or from equation (1) that T varies inversely as Δ_N , for R varies with Δ_N also.

The previous considerations are in agreement with this. We may expect that T (i_n constant, C variable) will increase as C increases, but with C constant and i_n variable will decrease, since Q varies much less slowly than i_n , and the average current varies (approximately) as i_n itself. We

may expect T to be (approx.) constant for constant V_N , since the relations during the clear-up will be the same, provided that i_n and C vary similarly, as in this case.

In the absence of a direct method of measuring these times, quantitative values were obtained for intermittence experiments. For the large neon-filled tube times of the order of 0.010–0.020 second were calculated for $\Delta_N = 40$ –50 volts. If we accept these results, the limits of time in fig. 2 (b) are about 0.005–0.05 second. These are reasonable values. R is of the order of 30.

5. SINGLE-CONDENSER DISCHARGES.

a. *Method.*—The variation of the final voltage (V_N) with variation of the capacity (C), and the initial voltage (V_M), for single flashes, was examined by having the condenser, shunted by the voltmeter, arranged with a suitable key so that it could first be charged to a certain potential and then discharged through the tube. Capacities ranging from 0.002–1.0 μ F. were employed.

b. *Results.*—Results similar to those recorded in the previous work on the subject⁽⁶⁾ were obtained for all tubes employed: a fully-developed (normal) discharge did not occur until V_M was definitely, often considerably, higher than v_c ; V_N decreased with increase of $\Delta_M (= V_M - v_c)$, and the rate of change of V_N with Δ_M varied in the same manner. It was found, however, that this did not affect the validity of the definition of v_c as the “sparking potential,” for observations in the dark showed that some form of

charge always occurred with $V_M \Rightarrow v_c$; below the critical V_M they merely were of the corona form.

The full sequence of phenomena as presented most clearly, here with C of the order of 0.01 μ F., is described below.

At values of V_M just greater than v_c the discharge was scarcely visible. It consisted of a faint corona glow which welled out from the anode only after an appreciable lag. This lag became less and less in evidence as Δ_M increased, and the discharges became progressively brighter and of shorter duration. Though at first scarcely distinguishable from v_c , V_N decreased more and more rapidly as the critical V_M was approached. At a voltage just less than this critical voltage a bright corona flash of short duration was obtained, but at a voltage just greater the flash was normal and the

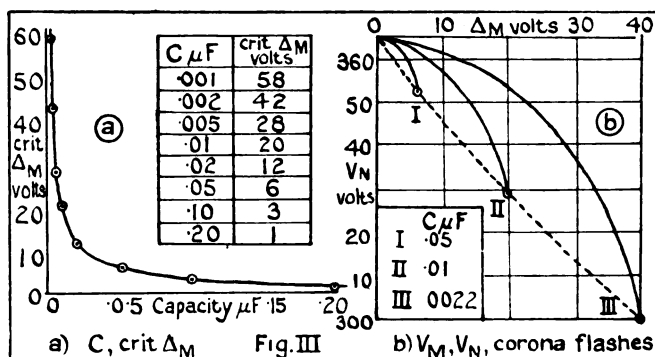
value of V_N fell considerably. It was often clearly seen, however, that the initial stages of these flashes were still corona glows.

In the previous work on the subject, V_N variations were explained from the various quantity transferences to be assumed as occurring for various capacities under different voltage and current conditions. With the assumptions made here as to the "extinction" and "clear-up" in flashes, these considerations assume a more precise significance. Further, actual values of i_n may be found from clear-up graphs when C and V_N are known.

Corona Flashes.

Fig. 3 shows the V_M , V_N variations (argon-filled tube) for various values of capacity. The curves are of the form just described for $C=0.01 \mu F.$, only the actual range of

Fig. 3.



variations changing with C (fig. 3, *b*). The critical V_M varied in a hyperbolic manner with C (fig. 3, *a*), the V_M , C curve being asymptotic to v_c . ΔM was about 20 volts with $C=0.001 \mu F.$ V_M , V_N curves for other capacities could be constructed from these, since the form of the curve, the critical V_M , and the limiting value of V_N , were known in each case.

The curves show that with C constant i_n increased with ΔM , since in all cases a lower V_N was associated with a higher V_M . Also that for V_M constant i_n increased with C , V_N here decreasing. The rapid changes of V_N in corona flashes are attributable primarily to the large decrease of voltage associated with increase of current, normal flashes

showing much less change, as v^* was approximately constant and only clear-up effects could vary.

These results showed that considerable lags were present at the initiation of discharges. Only when the current increased very slowly could the voltage be diminished sufficiently for extinction to occur on the early stages of the corona characteristic. Visual observation of the fainter flashes showed that lags of the order of 0.1–1.0 second occurred before the glow became bright. The lag decreased rapidly with increase of Δ_M .

Table I. gives the minimum value of θ , the time of duration of the discharge, for a wide range of values of Δ_M , three capacities being employed. θ was calculated from the quantity transference $C(V_M - v_n)$ and the maximum current i_n . V_N being known, i_n was found from the corona characteristic of the tube, due allowance being made for the depreciation of voltage due to clear-up.

TABLE I.

Capacity μ F.....	.10	.02			.0022				
Δ_M volts3	3.5	4.5	8.0	9.5	14	23	32	40
Min. $\theta \times 10^{-3}$ sec.	1.7	1.4	1.1	.45	.44	.18	.13	.09	.08

The Δ_M, θ curves were continuous and of hyperbolic form. The times calculated were all of appreciable magnitude. This is in excellent qualitative agreement with previous results. Quantitative comparison would demand that the average current was obtained; but that cannot be done with the accuracy required.

The hyperbolic form of the C , crit. V_M graphs (fig. 3, *a*) may be explained from these results. The time for v_c to be reached decreased with increase of Δ_M , but the current attained in this time increased. It is thus probable that the quantity transferred in this time will be at least approximately constant for a certain range of capacities.

"Normal" Flashes.

a. V_N, i_n, C , relations.—Experiments showed that in normal flashes, C constant, V_N increased with increase of Δ_M , as in corona flashes, and with Δ_M constant increased regularly with C , with the exception of the smallest capacities.

A minimum value of V_N of the order of 15 volts was recorded, as in the "characteristic clear-up." The maximum value of V_N was near to, though here always less than, v_b .

These V_M, V_N curves showed that i_n increased with, though less slowly than, C . With i_n directly proportional to C , V_N would be almost constant. The corresponding curves with C constant showed that i_n also increased continuously with C . Table II. illustrates the results obtained with the large neon-filled tube. They are in good agreement with the observed extent of the negative glow.

TABLE II.—Variation of i_n (M.A.) with C and Δ_M .

Δ_M volts.	Capacity μ F.			
	·0022	·01	·05	·20
10	·34	2·2	12	55
30	·61	3·8	22	79
50	·97	5·6	34	99

The currents associated with high values of C and Δ_M explain the occurrence of sparks in these cases. In connexion with sparking, it may be mentioned that the value of V_N did not immediately change to zero, but showed a progressive lowering with increase of C or V_M .

The table also clearly demonstrates the presence of lags, as only limited currents were attained in most cases.

b. *V, I Time, relations.*—These relations were obtained from the value of i_n at the critical V_M .

At a voltage just less than the critical V_M the discharge ends on the corona characteristic, and at a voltage just higher, on the normal characteristic. Consequently the current-voltage relations in this latter discharge should be obtained by joining V_M , 0, and v_n, i_n , by a curve just grazing the corona characteristic. The precise form of the curve, however, is not implied.

The time of discharge, θ , may be obtained from such by integrating $1/I, V$ graphs. In this case it is permissible to join the given points by a smooth curve, since I probably increases in a continuous manner. Instead of $V, 0$ being used however, it is obviously necessary to assume that I has some small initial value. The term "Zero" is permissible in descriptive treatment only.

The times calculated in this way with an initial current of 0.001 – $0.0001 \mu\text{A.}$, for capacities ranging from 0.002 – $0.20 \mu\text{F.}$, showed a variation of θ with V_M of precisely similar form to that previously obtained. The construction employed would thus appear to be justified, even though the actual values obtained were generally larger (up to $\times 2$) than the probably more correct ones.

Fig. 2 gives the V, I , curves implied, for all but the smallest currents; actually the voltage was almost constant until currents of the order of $0.01 \mu\text{A.}$ were attained. As is to be expected, in the presence of appreciable lags the greater part of the voltage-fall occurs before large currents are reached.

Fig. 2 (c) gives representative current-time curves. The presence of a "slow build-up" is strikingly demonstrated, the relative time to attain $10 \mu\text{A.}$ being from 0.85 – 0.95θ . The corresponding voltage fall with the smallest capacity was 20 volts. Calculations of the ratio of the maximum to the average current gave 100 – 1000 as representative values. No direct relation is, of course, to be expected, since the ratio depends on the lag, and is only indirectly connected with the final current.

Fig. 2 (a) shows how the "rate of build-up" increases with voltage.

It must be pointed out that though these results do not preclude the existence of a short initial "time" lag⁽³⁾, no direct evidence of such a lag has appeared up to the present.

By adopting the appropriate values for θ , it was possible to construct the I, V curves for values of V_M other than the critical one. The resultant curves differed from the original ones only in showing a much more rapid build-up (fig. 2, a).

The construction used above determines the relations of corona as well as normal flashes at the critical V_M , the only difference being that in the former case only the data up to the moment that the corona characteristic is reached are to be taken. Qualitatively the results agreed with those of Table I. As suggested, an appreciable curtailment of θ was apparent. Though the form of the curve has been obtained, nothing is to be gained by applying the ideas gained to all the corona flashes, though mention may be made that, as the ratios of the maximum to the average currents obtained here were of the order of 4 – 10 , the time-results could with confidence be multiplied by some such (variable) factor. Such a treatment would not invalidate any of the conclusions drawn. It gives results in much better agreement with observed values.

SUMMARY.

1. The role of the volt-ampere characteristic and the sequence of phenomena in the condenser discharges in discharge-tubes are considered.

2. The fall of voltage (Δ_N) during "clear-up" associated with various points on the characteristic (v_n, i_n), is studied with different capacities (C). Δ_N is found to be proportional to $\sqrt{i_n/C}$, and the time of clear-up, θ_N , to $1/\Delta_N$.

3. Such relations are qualitatively explainable from a rapid increase of clear-up with reduction of voltage.

4. The variation of the final voltage (V_N) with the capacity (C) and the initial voltage (V_M), corona and normal flashes, and the transition V_M , are studied. The maximum currents (i_n) attained are deduced from V_N and clear-up curves. i_n increases with C and V. Numerical values are given.

5. Corona flashes demonstrate a slow build-up. Their times of duration (θ) are obtained qualitatively.

6. The data at the transition V_M is employed to determine the actual current-voltage relations during discharge, and also to determine the duration of build-up (θ).

7. Current-time curves are of somewhat exponential form with a very slow increase of current initially. The rate of build-up increases rapidly with voltage.

References.

- (1) Clarkson, Phil. Mag. (pending).
- (2) Taylor, Phil. Mag. iii. p. 368 (1927).
- (3) Zelany, Zuber, Peek, and others. See reference (4).
- (4) Clarkson, Phil. Mag. iv. p. 121 (1927).
- (5) Taylor & Stephenson, Phil. Mag. xlix. p. 1081 (1925).
- (6) Penning, *Phys. Zeit.* xxvii. p. 187 (1926).
- (7) Campbell, Phil. Mag. iii. p. 925 (1927).
- (8) Oschwald & Tarrant, Proc. Phys. Soc. xxxvi. p. 262 (1924).

XCIV. Notices respecting New Books.

La Théorie de la Relativité: Tome II. La Relativité Générale de la Théorie de la Gravitation d'Einstein. Par M. VON LAUE, Professeur de Physique Théoretique à l'Université de Berlin. Traduction faite d'après la quatrième édition allemande, revue et augmentée par l'auteur, par Gustav Létang. Pp. xvi + 318. (Paris: Gauthier-Villars et Cie. 1926. Price 78 francs.)

THE treatise of Dr. von Laue on the theory of relativity is one of the best that has been written, and the appearance of a French translation, assuring it a wider circulation, is to be welcomed.

Written by a physicist primarily for physicists, special care has been taken to smooth the difficulties of those who approach the theory for the first time, and to remove objections against the theory on the part of some who have failed properly to understand it, owing to an insufficient knowledge of non-Euclidean geometry and tensor calculus. A large portion of the volume is therefore occupied with matter introductory to the theory proper: an account is given of earlier theories of gravitation and of the physical ideas at the basis of the generalised principle of relativity. Two chapters deal with tensor calculus and non-Euclidean geometry. The deduction of the fundamental laws of physics, including electromagnetism, dynamics, and gravitation, is followed by the application of these laws to particular cases. The final chapters deal with the rigorous solution of the equations of the field, and with special developments of the theory. The physical insight of the author will appeal particularly to those who approach the theory from the physical rather than from the mathematical point of view.

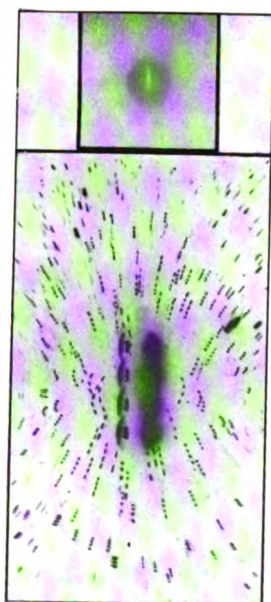
Microscopische Physiographie der petrographisch wichtigen Mineralien. Begründet von H. ROSENBROCH. Bd. I. *Erste Hälfte-Untersuchungsmethoden.* Fünfte, völlig umgestaltete Auflage, von Dr. E. A. WÜLFING. Pp. xxiv + 848, with 680 text-figures and 15 plates. (Stuttgart: E. Schweizerbart'sche Verlagsbuchhandlung. 1921-24. n.p.)

THE new edition of the great classical work by Rosenbuch on microscopical petrography contains nearly 400 more pages than the previous edition, which appeared in 1904. The first edition, published in 1873, contained only 111 pages, and each succeeding edition has shown an increase both in the number of pages and in the number of text-figures. This indicates the rapid development of the subject. It contains a comprehensive account of optical theory, including both geometrical and physical optics with special attention to crystal optics. The general theory of the microscope receives very thorough treatment, and many different types of petrological microscopes are described, as well as various accessories. A full account is given of various experimental methods with numerous practical details.

The present edition was issued in three portions, which appeared at intervals. It is now available in collected form. On account of its completeness and accuracy, it is a manual which no worker in the field of microscopical petrography can afford to be without.

[The Editors do not hold themselves responsible for the views expressed by their correspondents.]

FIG. 2



Above: Air bubble rising in "Water-glass."
Below: Negative showing movement of bubble
and liquid.

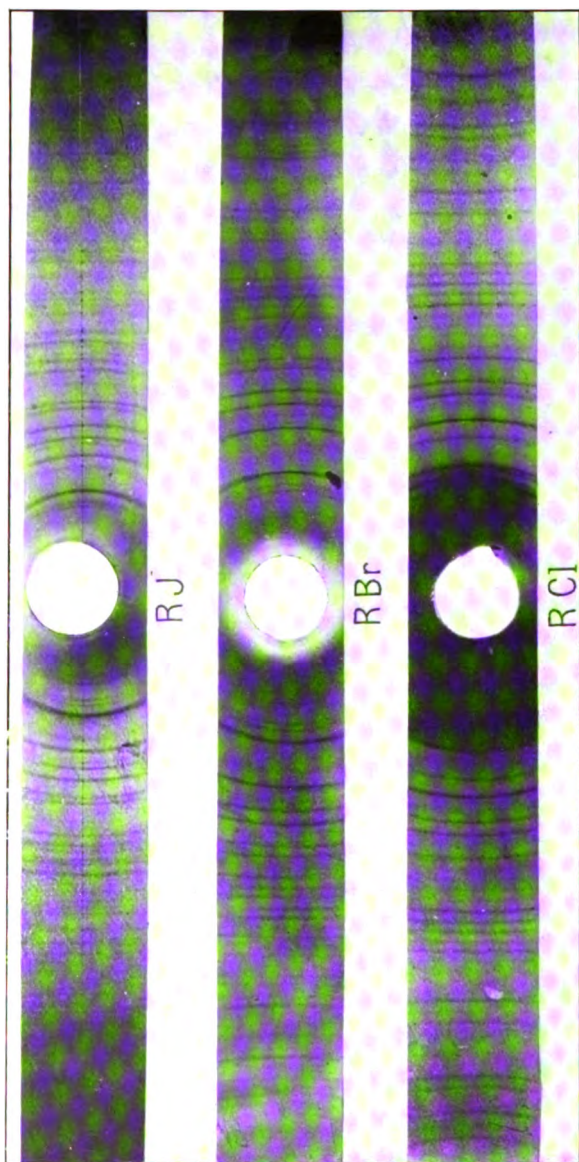


FIG. 5.

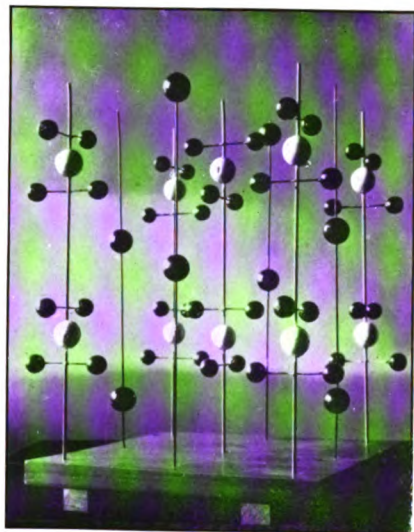
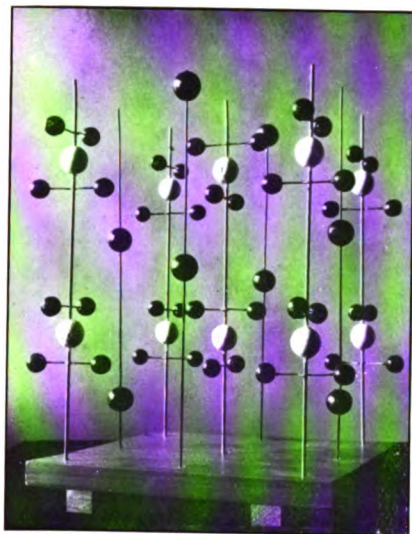
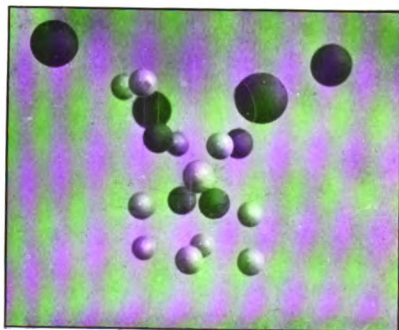
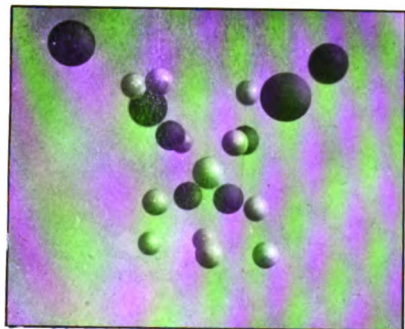


FIG. 7.



THE
LONDON, EDINBURGH, AND DUBLIN
PHILOSOPHICAL MAGAZINE
AND
JOURNAL OF SCIENCE.

[SEVENTH SERIES.]

SUPPLEMENT, NOVEMBER 1927.

XCV. *The Metallic State.*
By WILLIAM HUME-ROTHERY, M.A., Ph.D.*

Introduction.

THE various theories of the metallic state have previously considered chiefly the thermal and electrical properties, since it is in connexion with these that the metals show their chief characteristics. The object of the present paper is to discuss the applications of these theories to some of the other properties of metals in the solid state, and the electrical properties will only be referred to incidentally.

SECTION I.

IN the first place it may be well to summarize critically the principal theories of the metallic state, since the descriptions of these are widely scattered throughout the

* Communicated by Prof. F. A. Lindemann, F.R.S.

literature, and are not easily accessible. The theories may be conveniently grouped under the following headings:—

1. *The Free Electron or Electron Gas Theory**, according to which the characteristics of metals are due to the presence of free electrons in the space between the atoms. These electrons are supposed to behave like a perfect gas, and on this assumption most of the electrical phenomena may be explained with fair accuracy. In particular, if the law of equipartition of energy be assumed, the theory leads to a correct value for the Wiedemann-Franz ratio. The objection to the theory is that the thermal and electrical properties indicate quite different numbers of free electrons, and that the supra-conductivity at very low temperatures is not accounted for. On these and other grounds the theory has been effectively criticized by Lindemann†. It is, however, still accepted in many quarters.

2. *The Di-Pole Theory of Thomson*‡.—On this theory the atoms of some substances, including metals, contain electrical doublets, or pairs of equal and opposite electrical charges at a small distance apart. From this point of view the part played by the electric force is to polarize the metal, or to form chains of the di-poles. When once these chains are formed, the electrons are passed along by the forces exerted by the doublets, and the electrons which move are not those in the doublets themselves. The arrangement of the doublets is upset by the thermal agitations, and on this assumption the theory gives a general explanation of the electrical phenomena including the supra-conductivity at low temperatures which was not explained by the older electron gas theory. The large amount of polarization required is, however, contrary to what we should expect if we accept modern atomic theory, and is also contrary to the values obtained by Born for the degree of polarization of ions. On these and on other grounds the theory is no longer generally accepted.

3. *The Theory of Wien and Gruneisen*§.—This theory

* Drude, *Ann. d. Phys.* i. p. 566, iii. p. 369 (1900). The subsequent literature is very extensive.

† Phil. Mag. xxix. p. 125 (1915).

‡ 'The Corpuscular Theory of Matter,' p. 86 and Phil. Mag. xxx. p. 192 (1915).

§ See Gruneisen, *Verh. d. Deut. Phys. Ges.* xv. p. 186 (1913); also Beckman, *Phys. Zeit.* xvi. p. 59 (1915).

is based partly on the theoretical work of Wien *, and partly on the empirical discovery that the ratio of the specific resistance to the absolute temperature increases at low temperatures in exact proportion to the atomic heat †. The fundamental assumptions are that the electrons are still moving freely between the atoms, but that the lengths of their free paths are determined solely by the amplitude of the atomic vibrations. From quantum considerations Wien assumes that the length of the free path is inversely proportional to the square of the amplitude of the atomic vibrations. The electron velocity is regarded as independent of the temperature, and remaining unchanged even at the absolute zero. As extended by Gruneisen the theory was the first to give any quantitative explanation of the decrease in electrical resistance under pressure, which was accounted for on the assumption that the increased pressure increased the frequency, and hence diminished the amplitude of the atomic vibrations, and that this effect more than outweighed the reduction in distance between the atomic centres. Quantitatively the theory gave a pressure coefficient of resistance of the right sign for all the normal metals ‡, and almost exact agreement for copper, silver, gold, and aluminium, but not such good agreement for the other metals, especially those of low melting-points. The theoretical treatment is, however, open to criticism in that it draws on both of the fundamentally-opposed theories of Wien and the electron gas theory §, and also that the fundamental treatment of Wien assumes the energy quanta to be located in the individual atoms instead of in elastic waves.

4. *The Electron Lattice Theory of Lindemann* ||.—This theory rejects the whole conception of electrons moving freely as in a gas, and considers them as behaving like a perfect solid and being situated on a space lattice interpenetrating that of the atoms. It is assumed that though attracted according to the inverse square law by the ions at distances greater than the atom's radius, the electrons are repelled at distances less than a certain value r_0 , and hence that at some critical distance the attractive and repulsive forces balance and the electron is free to move. The theory does not predict the Wiedemann-Franz ratio,

* *Sitzber. d. Berlin. Akad.* p. 184 (1913).

† *Ibid.* p. 306 (1911).

‡ Bismuth is abnormal.

§ See Bridgman, *Proc. Am. Acad.* lii. p. 640 (1917).

|| *Phil. Mag.* xxix. p. 126 (1915).

but does not contradict it. The great advantage of the theory is that the electrical and thermal properties are no longer in conflict, since an electron lattice can be shown to behave as an ionic lattice would do at a very low temperature, and in this way a high heat conductivity is accounted for without attributing any measurable heat capacity to the electrons. The theory has been criticized on the grounds of improbability on the one hand, and of instability of the resulting structure on the other.

5. *The Theory of Bridgman* *.—The idea of this theory was to retain as much as possible of the electron gas theory, and yet avoid the discrepancies between the thermal and electrical requirements. It is assumed that the electrons pass freely *through* the atoms, with velocities given by the equipartition value as in the older theory, the resistance being caused by the difficulty of passing from one atom to another. The electrons carrying the current are small in number compared with the atoms, but constant in number, and at low temperatures, when the atoms are in "contact," the electrons pass freely from one atom to the other. But at higher temperatures gaps appear between the atoms, and these gaps cause the resistance in the same way that the collisions caused the resistance in the older theories. The bulk of the dynamical arguments of the older theory can be applied to the Bridgman theory, substituting "gaps" for "collisions"; but a much longer free path is possible, since the gaps do not necessarily appear between every two atoms, for there may be several atoms in a long string before the gap is met with, and in this way the thermal and electrical requirements are reconciled. Bridgman's results for the effect of pressure on the Wiedemann-Franz ratio were not in agreement with his earlier view of thermal conductivity as due entirely to electrons, and he later regarded a considerable portion of the conductivity as due to the atoms, the energy being passed in a series of waves from atom to atom, much as an impulse will travel down a row of billiard balls in contact. In this respect the theory is fundamentally opposed to that of Lindemann, in which the thermal conductivity of the atomic lattice is considered negligible at ordinary temperatures. Bridgman, in fact, criticizes the Lindemann view on the grounds that, whilst the electron lattice by itself will have a high thermal conductivity if the Debye

* *Phys. Rev.* ix: p. 269 (1917); xvii. p. 161 (1921); xix. p. 115 (1922).

elastic wave theory be accepted, the same conclusion is not justified when the electron lattice is interpenetrated by that of the atoms. On the whole the balance of evidence favours the Lindemann view, since it seems probable that the atomic and electron lattices with widely differing frequencies would not interfere with one another; whilst if the Bridgman theory is accepted, it is strange that salts should have such a low conductivity when their constituent ions are closer than the atoms in a metal. It is also by no means clear why the heat conductivity of metals is almost independent of temperature if the Bridgman view is adopted. The later developments of the Bridgman theory are more complex, and he now regards the electrons as passing between the atoms in some metals, and through the atoms in others. The theory undoubtedly suffers from drawing on rather fundamentally opposed conceptions; for, as pointed out by Bridgman, a motion through the atom with no resistance is only likely to occur in some kind of a quantized orbit, and it is hardly likely that the resulting velocity would vary according to the older equipartition value; whilst the assumption that the electrons are few in number compared with the atoms, and yet constant in number, is most improbable. If the free electrons are not equal in number to, or some simple multiple of, the numbers of atoms, we should expect their number to be a variable given by an equation of the type $n = n_0 e^{-Q/RT}$, which would give a wrong temperature coefficient.

The above theories are all more or less in agreement with the electrical properties of the metals, and it is doubtful whether a consideration of these properties alone will enable a final selection to be made.

SECTION II.

The first of the other properties which it is desired to consider here is the compressibility, and in order to make the argument clear, it is again necessary to refer to the previous work.

The modern theory of compressibility is due chiefly to Born*, and was developed originally for simple ionized salts such as the alkali halides, in which the ions in the crystal are regarded as bound together by electrostatic attractions varying inversely as the square of their distance

* *Ann. d. Physik*, lxi. p. 87 (1920).

apart. The oppositely-charged ions are thus drawn together until the attraction is balanced by a non-electrostatic repulsion, due presumably to the fields of force produced by the electrons revolving in their orbits. The fundamental argument used by Born is to represent the potential energy of a unit cube by an expression of the type $\Phi = -\frac{a}{\delta} + \frac{b}{\delta^n}$,

where the first term refers to the electrostatic attraction and the second to the non-electrostatic repulsion, which is assumed to vary as an inverse power of the distance *.

In this equation the first term is definitely established, the inverse square law for the electrostatic attraction having been proved experimentally by Born from measurements of dielectric capacity and refractive index for long wave-lengths, and by Slater † from accurate compressibility data. The factor a can then be calculated for a series of point charges if the lattice type is known.

The second term is, however, much less satisfactory. Qualitatively with large values of n it gives a repulsion increasing very rapidly at small distances, in agreement with what is required, but it has little real justification. From measurements of compressibility it was found by Born that $n=9$ (approximately) for most of the alkali halides, except for the lithium salts for which $n=5$. For calcium fluoride $n=7.5$, whilst for magnesium oxide $n=4.1$, according to data given by Hund ‡. According to the very accurate work of Slater, the simple Born theory of a repulsion according to an equation of the type $\frac{b}{\delta^n}$ is definitely not in agreement with the facts, and

there is indeed little reason that it should be. From the figures given above it can be seen that with the typical alkali halide, sodium fluoride, the value of n is about 9, whilst for magnesium oxide, which has the same crystal structure, the value of n is only about 4. Now, if our views on atomic structure are correct, Na^+ and Mg^{++} ions, whilst differing in dimensions, are identical in electronic structure, and differ only in the nuclear charges, which are 11 and 12 respectively. Similarly, the F' and O'' ions are identical except for the unit difference in nuclear charge. Since

* In the more elaborate extensions of the theory an additional term is introduced to allow for the polarization of the ions in each other's fields, but this is omitted here for simplicity.

† *Phys. Rev.* xxiii. p. 488 (1924).

‡ *Z. Physik*, xxxiv. p. 833 (1925).

$n=9$ approximately for all alkali halides, it is unlikely that a difference of one unit in the nuclear charge would cause such a profound alteration in the value of n for sodium chloride and magnesium oxide, and it would seem much more probable that n is really a complex function of the distance, and that the great difference between the values of n in the two cases is due to the fact that ions are pulled much closer together in magnesium oxide, owing to the increased electrostatic forces, which at constant distance are as 4:1 in magnesium oxide and sodium chloride respectively.

In attempting to apply the above theory to the compressibility of metals, the electron lattice theory is clearly the most attractive, the obvious suggestion being to consider the electrons as taking the place of the negative ions. This point of view has been adopted by Bridgman, especially for the face-centred cubic calcium, which he regards as having the calcium fluoride type of structure with electrons replacing the negative fluorine ions. The compressibility results may be summarized as follows:—

(1) The absolute compressibilities of the alkali and alkaline earth metals are much greater than those of their salts; *e.g.*,

Potassium chloride $K = 4.0 \times 10^{-6}$.

Potassium metal $K = 35 \times 10^{-6}$.

For other metals the compressibilities are greater than those found for salts, except for some metals of high melting-point for which measurements with the corresponding salts have not yet been made.

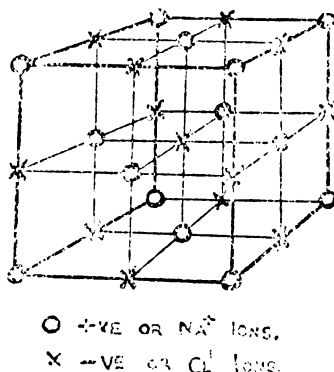
(2) The application of the simple Born Theory leads to a value of the right dimensions for the compressibility, but any attempt to use a Born term $\frac{b}{\delta^n}$ for the energy due to the non-electrostatic repulsion leads to values of n much smaller than those deduced and confirmed by Born for the corresponding ions in salts.

We thus appear to have reached a point at which the electron lattice theory, whilst satisfactory from some points of view, seems to fail when applied in detail. It is the object of the remaining sections of this paper to show that this apparent failure is due to the omission of some important factors, and that, when properly applied, the electron lattice theory is able to give a picture of the metallic state which is in general agreement with the observed facts.

SECTION III.

The first and most obvious objection to the above application of the electron lattice theory to the compressibility, is that it appears incompatible with the electrical conductivity. Thus if we take a univalent face-centred cubic metal as having the sodium chloride type of lattice shown in fig. 1, the Born theory considers the positive and negative ions as attracting one another until the electrostatic attraction is balanced by the non-electrostatic repulsive force. For convenience such ions will be referred to as "in contact"; but this is not to be taken as implying the existence of any sharp bounding surface. If, therefore, the attraction and

Fig. 1.—The Sodium Chloride Structure.



If a univalent face-centred cubic metal has this structure, the positive metallic ions are shown as circles, O, and the negative electrons as crosses, X.

repulsion are balanced when the electrons are in the positions shown in fig. 1, it is clear that they cannot move through the metal without passing very much closer to the atoms, when repulsion would occur; a similar objection arises if we regard metallic calcium as having the calcium fluoride structure with electrons replacing fluorine ions.

The explanation of this anomaly is to be found in a consideration of the dimensions concerned. In the sodium chloride lattice, for example, we imagine each negatively-charged chlorine (Cl^-) ion to attract its six neighbouring positively-charged sodium (Na^+) ions, until the attractive and repulsive forces counterbalance when the chlorine ion is in contact with its six neighbours. *Now this is only possible if the ions are of comparable size.* If the one ion is very

much smaller than the other, the closing-together process will be stopped, not by the contact of the unlike ions, but by the contact of the like ions of the larger size. In the simple case of the sodium chloride lattice, if r_1 and r_2 are the radii of the positive and negative ions, r_1 being the greater, and if these are assumed constant in the case of contact between ions of like and unlike charges*, the critical value is clearly given by

$$\frac{2r_1}{\sqrt{2}} = r_1 + r_2.$$

If $\frac{2r_1}{\sqrt{2}} < r_1 + r_2$, then the closing-up process is stopped by the contact of unlike ions; whilst if $\frac{2r_1}{\sqrt{2}} > r_1 + r_2$, the closing-

up process is stopped by the contact of like ions. In this way we may still adopt the point of view of the simple theory of the ionic lattice, and consider the oppositely-charged ions (or ions and electrons) as attracting one another, and yet understand why the resulting structures have such profoundly different properties in the two cases in which the closing-up process is stopped by the contact of unlike ions as in the simple salts, or of like ions as in the metals.

Now, if this conception be true, the possibility of finding relations between the interatomic distance in salts and metals at once arises. Any general relation is not to be expected for the following reasons. (1) It is by no means certain that the "radius" of an ion is the same when it is surrounded by different numbers of atoms in different orientations. (2) If the above picture of the metallic state is correct, the attractive forces pulling the atoms together are not always the same. Thus in sodium chloride the repulsion is between Na^+ and Cl^- ions, and acts against a direct electrostatic pull between the same two ions. But in a univalent face-centred cubic metal X the repulsion is between two X^+ ions, whilst the force holding those together is not a direct attraction between these ions, but is due to the components of the pulls due to the electrons, and the attractions will clearly be different if the face-centred atomic lattice has the electrons in different positions. Thus in the sodium chloride, zinc sulphide, and calcium fluoride structures the positive ions are all on face-centred cubic

* This assumption is, of course, really unjustified, and is only made to illustrate the way in which the argument applies to a definite structure.

lattices, but the positions of the negative ions vary. In the same way a given atomic lattice in a metal may correspond to different positions of the electrons, and the resulting attractions will differ. But in favourable cases with similar atomic arrangements relations may be traced. The work on the crystal structure of the alkali halides indicates very clearly that in these crystals the ions have radii * which are constant both when each is surrounded by six neighbours as in the sodium chloride type of lattice, and when surrounded by eight neighbours as in the caesium chloride type of lattice. Now, the alkali metals crystallize in the body-centred cubic structure, with each atom, or ion, surrounded by eight others, and we may reasonably compare these with the above alkali halides. The actual figures are shown in Table I. In order to avoid confusing the argument, the derivation of the ions in the halide crystals is given in a separate appendix.

TABLE I.

Radius of metallic ion in salts.		One-half closest approach in metal.	Ratio.
Lithium	1.641 Å.	1.515 Å.	1.45
Sodium	1.257	1.86	1.48
Potassium	1.552	2.25	1.45
Rubidium.....	1.689	2.45†	1.45
Cæsium.....	1.974	2.64†	1.34

With the exception of caesium, for which the constants are imperfectly known, the interatomic distance in the metals bears a practically constant ratio to the diameter of the corresponding ions in the halide crystals, in complete agreement with the picture given above. The distances are of course greater in the metals, since here the ions in contact have similar charges and are only held together by the components of the attractions to the electrons.

We may now see how the above conception can be applied to the compressibility data of Bridgman. The simple dimensional argument used by the latter will still apply, since we are again using the conception of the crystal being

* Here, again, the term radius is not to be taken as implying a sharp boundary surface, but simply implies the distance at which the attractive and repulsive forces balance one another.

† These figures are derived from density determinations, as no direct X-ray measurements on the metal are available. The remaining figures are all from direct X-ray analysis.

built up by the attractions and repulsions of the different ions, and the simple argument does not consider which ions the repulsion is between, but merely places it as a function of the lattice constant, and considers the compressibility as being built up from the lattice constant and the electronic charge e . We should, however, expect the initial com-

pressibility of metals $\left(\frac{1}{v_0} \frac{\partial v}{\partial \rho}\right)_{\tau=v_0}$ to be greater than that of

salts, since in the salts, where the attraction is between oppositely-charged ions in direct contact, the closing-up process (which is simply reinforced by external pressure) will clearly have proceeded further than in the metals, where the contact is between similarly charged ions, and the attraction is an oblique one towards the smaller electrons. This is, of course, in agreement with the facts. But the simple Born theory of the halide crystals will require modification before it can be applied to the metals, in order to take into account the fact that the particles are no longer held in contact by attractive and repulsive forces acting in the same directions and between the same particles. We can quite understand, therefore, that where, as in Bridgman's work, no such modification is made, the empirical values for the coefficient n of the repulsive

force $\frac{b}{\delta^n}$ will be quite different in the metals and salts.

If the Born theory for the salts is applied directly to the metals without considering the above points, we should

expect the empirical value of n , in the term $\frac{b}{\delta^n}$, to be less in

the metals, since here the contact is between the like ions where the electrostatic and non-electrostatic repulsions reinforce one another, and the repulsion, when expressed as a function of the distance, will be spread out more gradually; i.e., n will be smaller in agreement with the facts. But for the theory to be applied strictly, it will be necessary to determine the position of the electron lattice, and to take into account the fact that the attraction and repulsion act in different directions between different particles, in contrast to the salts, where the attraction and repulsion are between the same particles. This would result in an alteration in the relative values of the constants a and b in the equation

$\Phi = -\frac{a}{\delta} + \frac{b}{\delta^n}$, quite apart from the question of the validity

of a term of the type $\frac{b}{\delta^n}$. We are further able to understand why so many of the metals crystallize in one of the close-packed structures (cubic or hexagonal), the electrons occupying the "holes" between the larger atoms, since this will in general allow the closing-up process to proceed to its greatest extent, giving the least potential energy. This tendency is, in fact, shown by many of the gem-stones consisting of relatively large oxygen ions and small metal ions*.

The electron lattice theory therefore gives us a clear picture as to the way in which the crystal lattice is built up, and is in general agreement with the compressibility data, but before considering the other properties, it may be well to see how the other theories can be applied.

SECTION IV.

The principal difficulty with all the other theories is to see how the crystal lattice is built up. Generally speaking, crystals may be considered as being formed in three different ways. (1) There is first of all the simple ionic type of lattice described above. In some cases the ions are monatomic as in sodium chloride, whilst in others, such as calcium carbonate or sodium nitrate, they are more complex. Whatever may be the defects of the quantitative methods of Born, there can be no doubt that his theory gives a clear picture of the way in which these lattices are built up, and, as shown above, the same conception can be applied to the metals. (2) The second class of crystal may be regarded as formed by direct non-polar chemical combination of the atoms; *i.e.*, by the sharing of electrons between two or more atoms. An example of this kind of crystal is the diamond. The typical characteristics of this kind of crystal are hardness and brittleness, and usually high melting-point, although if the sharing involves much distortion of the orbits, the melting-point may be lower. (3) The third class of crystals includes the bulk of the compounds of organic chemistry; and here the crystal forces are regarded as being of magnetic origin. The molecules are considered to contain electrons spinning in opposite directions, and thus producing magnetic fields which tend to take up a definite orientation. The characteristics of this type are in general low melting-point and brittleness.

Now, if we adopt the Free Electron Gas theory, it is clear that the forces producing the crystal must be due to the

* See Bragg, Chem. Soc. Annual Reports, p. 275, 1926.

atoms (or ions) and not to the free electrons, which are, *ex hypothesi*, moving in all directions. Unless, therefore, we consider the crystal lattice as being produced in some quite unknown manner, we can only regard it as being formed by the sharing of the non-valency electrons or by the magnetic fields due to these. The softness and plasticity of the metallic crystals are definitely against the former supposition, whilst the plasticity and high melting-points of so many of the metals are against the latter. A similar objection applies to the theory of Wien and Gruneisen.

If the di-pole theory of Thomson is adopted, the difficulty is even greater, for here we have to allow for an actual movement of the atoms (or ions) in the crystal. It is difficult to see how this movement can occur if the formation of the crystal lattice is due to the sharing of electrons, or to the magnetic fields produced by oppositely spinning electrons, since both these conceptions require definite orientations of the atoms. In fact the only way in which it seems possible to reconcile the formation of a definite lattice by atoms free to revolve in that lattice, is to consider the free electrons as negative ions, and the lattice as an ionic one. In this case the theory is essentially that of the electron lattice, with the added assumption that the ions are electrical di-poles. As previously stated, such a marked degree of polarization appears improbable; it would, for example, lead us to expect a considerable electro-striction effect, analogous to magneto-striction.

We have already seen that the Bridgman theory distinguishes between two classes of metals—namely, those in which the conducting electrons pass through the atoms, and those in which they pass between the atoms. For the latter class of metals the theory differs little from the other theories which have been considered, but for the metals in which the electrons are regarded as passing through the atoms a different picture is required. This conception would seem to demand that the electrons are passing from one atom to another not merely when a current flows, but when the metal is not carrying a current; for, as pointed out by Bridgman, a motion through the atom with no resistance is only likely to occur in some kind of a quantized orbit or path. Unless this kind of motion exists before the current is passed, we should expect a discontinuous current—E.M.F. curve (analogous to ionization potentials) in place of the continuous Ohm's Law. But since the Bridgman theory requires the conducting electrons to be few (though constant)

in number compared with the atoms*, it is clear that we cannot regard these conducting electrons as producing the crystal lattice; and the formation of the lattice will again have to be regarded as due to the sharing of, or the magnetic fields produced by, the non-conducting electrons, which we have already shown to be improbable.

Of all the theories of the metallic state, therefore, the electron lattice theory is the only one which gives a rational explanation of the formation of the crystal lattice. It is not intended to deal here with the applications of the theory to alloys and metallic solid solutions, but we may note that the formation of the substitutional type of solid solution is more readily understood on the basis of the electron lattice theory than on any of the other theories; for the fact that substitutional solid solutions are formed by metals in which the ions have entirely different electronic structures (*e.g.*, copper and aluminium) appears incomprehensible if we regard the lattice as due to the orbits of non-valency electrons, but can be understood if we regard the lattice as ionic. We may now see whether the same theory is in agreement with the tensile properties of metals.

SECTION V.

(1) We may note in the first place that our picture is in some ways like that of the older crystallographers, who regarded the metals as built up of closely touching spheres. The difference is that whereas the older view regarded the spheres as held together by direct attraction towards the spheres themselves, the present view regards the "spheres" as mutually repulsive, and held in contact by attraction towards the interpenetrating electron lattice. Of course, the term "sphere" is not to be taken too literally. It merely implies that the ions are drawn together until the attractive and repulsive forces balance, and that any further closing-up involves entry into a zone in which repulsion predominates. It will be shown later that these zones of repulsion are probably not strictly spherical; but little error is likely to result in considering them as approximately spherical at ordinary temperatures, since the thermal oscillations will tend to obliterate the non-spherical characteristics, although at lower temperatures the non-spherical nature of the repulsive zones may become more pronounced. For the present, therefore, in representing the structure of metallic crystals, it will be

* We have already noted the improbability of this.

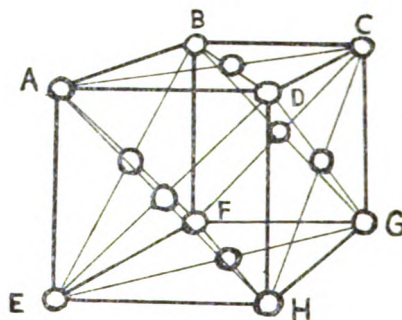
assumed that the ions are drawn into contact by attraction towards the electron lattice, and that the zones of repulsion can be represented by spheres of radius equal to half the closest distance of approach; *but this is not to be taken as implying the existence of any sharp bounding surface.*

It is at once apparent that this type of structure, in which comparatively large, mutually repulsive particles are held in contact by attraction towards much smaller particles interpenetrating the larger ones, is a structure very suited for plastic deformation when the larger particles are subjected to thermal oscillation and a stress is applied; for in the first place, as we have already shown, the great difference in the relative sizes of the positive ions and the negative electrons results in the structure being much less tightly bound together than in the case of the salts, where the ions are of comparable size (see page 1026); whilst, secondly, since the attractive forces between the atoms and electrons are of an electrostatic nature, we can understand their persisting after deformation has occurred, which is almost impossible if we regard the crystal forces as being directional in nature.

(2) We may consider first the case of the *face-centred cubic structure* in which so many metals crystallize. It is significant that three of the principal types of cubic salts, represented by the sodium chloride, zinc sulphide, and calcium fluoride types of lattice, all correspond to a face-centred cubic arrangement of cations; and so we can understand this type of lattice being formed by both uni- and di-valent metals. However we regard the electrons as being situated, we are to regard them as attracting the positive metallic ions until the latter are in contact. The closest approach is along the diagonals of the cube sides, the ions being in contact on the octahedral planes (cubical close packing). Further, whether we regard the electrons as occupying the positions of the chlorine ions in sodium chloride, of sulphur ions in zinc sulphide, or of fluorine ions in calcium fluoride, they will lie between the octahedral planes of the atoms. We have, therefore, a structure in which the relatively large metallic ions lie on close-packed octahedral planes, and it is clear that a glide or slip along an octahedral face is the type of motion which will take place most easily, and will cause the zones of repulsion of the ions to overlap least. Another way of looking at the matter is that if the deformation takes place by the ions rolling over each other, a slip on a octahedral plane will

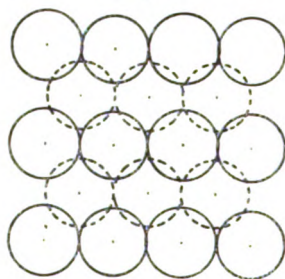
involve the least upward or downward motion. Fig. 2 shows a perspective view of the face-centred cubic structure, fig. 3 a view in the 110 direction, and fig. 4 a view in the 111 direction, which gives a direct plan of the octahedral faces.

Fig. 2.



The Face-centred Cubic Structure.

Fig. 3.

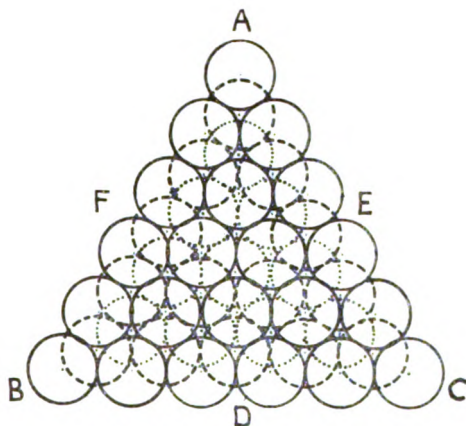


The Face-centred Cubic Structure: view in the (110) direction, *i.e.* at right angles to a plane such as $ACGE$ in fig. 2. The first plane of atoms is shown in full circles, and the second in broken lines. The third is again directly behind the first.

When we inquire as to the direction in which slipping will take place in any one octahedral plane, we should again expect the direction in which the atoms are brought into least contact, which is clearly when the atoms in the one layer pass directly over the middle points of the lines joining the centres of the atoms in the next layer—that is to say, in the direction of a line such as AD in fig. 4. But if this is so, the slip on this individual plane cannot proceed by more than one unit or step in this direction, since the

triangular arrangement of the atoms or ions on these planes is such that, whilst the first step in this direction will bring the ions in one plane into least close contact with those in the next layer, the next step in the same direction will bring them into the closest contact, since the centres of the ions in the one layer will pass directly over, instead of between, those in the next layer. One possibility is therefore that the deformation will take place by single steps on a very large number of planes. For many reasons, however, it is probable that the units which slip in crystals are large compared with the interatomic distances, or, in other words, that slip continues on the planes on which it starts. This is

Fig. 4.



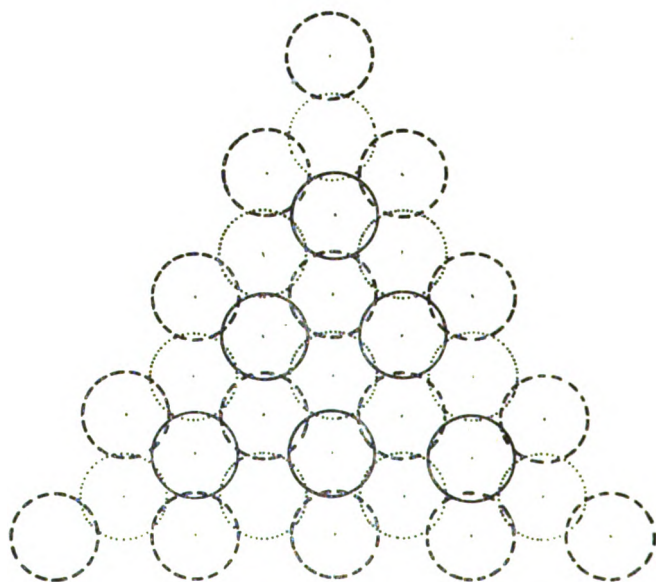
The Face-centred Cubic Structure: view in the (111) direction, *i.e.* along a diagonal such as DF in fig. 2. The first closely-packed layer is shown in full circles, the second in broken lines, and the third in dotted circles. The fourth layer is vertically under the first.

indicated by many facts, such as the comparatively small change in resistance, density, etc., produced by deformation. If this is so, it is clear that if this first step in the gliding on the particular octahedral plane is in the direction AD, the second step will have to be in one of the crystallographically similar directions such as BE or CF, after which a further step in the direction AD is possible, and will occur if the direction of the stress is unaltered, the process

Phil. Mag. S. 7. Vol. 4. No. 25. Suppl. Nov. 1927. 3 X

repeating itself. The net result is therefore a motion in the direction of one of the sides of the triangle ABC, *i. e.* in the direction of one of the diad (110) axes lying in the octahedral plane; and this is the motion which will be observed, since any actual measurement involves a very large number of such steps. Out of the crystallographically similar alternatives, the particular octahedral planes and directions chosen for slip will be those for which the component of stress is greatest in the particular case. This kind

Fig. 5.

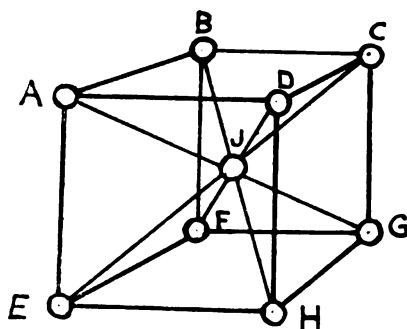


The Body-centred Cubic Structure : view in the (111) direction.

of motion in the (110) direction on the (111) plane is, in fact, that found by Taylor and Elam in the distortion of single crystals of aluminium, which crystallizes in the face-centred cubic system. This deduction in no way requires the ions to have a rigidly spherical shape, but depends on the assumption that gliding takes place so as to bring the ions into least close contact, and that slip continues on the planes on which it begins, the actual individuals out of innumerable parallel planes being determined presumably by slight flaws or inhomogeneities.

(3) We may next consider the hexagonal close-packed structure in which zinc, cadmium, magnesium, and other metals crystallize. This structure is very like the face-centred cubic, the difference being that in the close-packed layers each layer is vertically over the next layer but one, whereas in the face-centred cubic structure the repetition is at every fourth layer. Applying our previous argument, we should expect the gliding to take place along the close-packed layers in the same direction relative to these layers as before. This corresponds to motion on the basal plane in the direction of a closely-packed line of atoms, which is the exact kind of motion found by Mark and Polyani in the deformation of zinc crystals. In these two cases our deduction does not depend on giving the ions a rigidly

Fig. 6.



The Body-centred Cubic Structure.

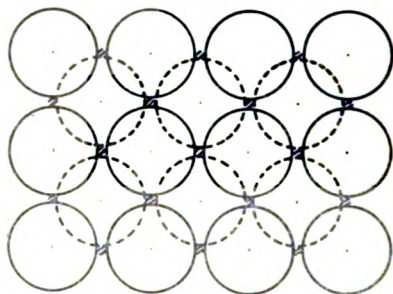
spherical shape, but merely demands that they are drawn into contact along the directions of closest approach.

(4) The body-centred cubic structure may now be dealt with, since it is here that the results are most interesting. In this case we are in some doubt as to the position of the electrons. Symmetry conditions will clearly place them symmetrically in the centres of the cube edges or faces according as the metal is uni-, di-, or possibly tri-valent. In fact this seems the only way in which one or two electrons per atom can be symmetrically arranged. But if this is the case, the most densely packed layers, which are those of the rhombic dodecahedron, contain both ions and electrons, and we no longer have a case of close-packed atomic layers interleaved with planes of electrons. In these circumstances we find that an entirely different type of deformation is

3 X 2

possible. Fig. 7 shows a view of the body-centred cubic structure in the (100) direction. It is interesting to note that if the ions are assumed spherical, there are channels right through the structure*, and that an electron lattice could pass down these without "touching" the atoms, although the thermal oscillations will tend to obliterate this characteristic. Fig. 5 shows a view down the (111) axis. This last is very remarkable. Referring to the small sketch (fig. 6), the ion D and others in its plane are shown in full circles; the ions J and F appear vertically under D when we look down the (111) diagonal, and each full circle in the figure represents a vertical pile of ions in mutual contact. Ions A, C, and H are shown with broken lines, which again represent vertical piles, and ions B, G, and E are shown in

Fig. 7.



The Body-centred cubic structure; view in the (100) direction.

dotted circles, which once more represent vertical piles of ions. In the figure the zones of repulsion of the ions are drawn as spheres of diameter equal to the closest approach of the ions in the structure, which equals $\frac{a\sqrt{3}}{2}$ if a is the side of the cube. It can be seen that when looked at in this way the structure consists of a series of vertical piles of ions, and that each pile only very slightly overlaps the domain of the surrounding piles. We are thus led to the conclusion that in this structure deformation may result, not in the gliding of one plane over another, since closely-packed planes do not exist, but by the sliding of these long rows or piles of ions over one another, as though the structure consisted of bundles of rods. Improbable as this

* Reference to the literature showed that this point had been previously noted by Bridgman.

may at first sight appear, it is precisely the type of deformation which Taylor and Elam * were forced to assume as the only possible explanation of their results for the distortion of single crystals of iron, which crystallizes in the body-centred cubic structure. The exact words of these authors are as follows † : "The particles of the metal stick together along certain crystallographic directions, and the resulting distortion may be likened to a large bundle of rods which slide over one another." They showed further that the direction was that of a normal to a (111) plane, *i.e.* the (111) direction, just as the above reasoning indicated. This conclusion does not depend entirely on the assumption of rigidly spherical ions, but merely demands that the atoms occupy the positions of the body-centred cubic lattice, and that the zone within which the repulsion predominates is approximately that of the closest distance of approach in the unstrained structure.

On the other hand, in cases in which the zones of repulsion of the ions were markedly non-spherical, the above deduction would no longer be strictly justified, and movement in certain planes might be favoured.

If it is objected that the above treatment is really nothing more than the older method involving piles of spheres, it may be emphasized that the fundamental point in the present method is to consider the comparatively large atoms or ions as held in contact, not by attractions between each other, but by attraction to the much smaller electrons in between, and that a hard bounding surface is not being assumed. On the other hand, the electron lattice theory, and this theory alone, gives us justification for considering the atoms in metals as ions drawn together until a zone is reached in which repulsion predominates.

(5) We see, therefore, that the electron lattice theory, as interpreted above, is capable of predicting absolutely the type of deformation found for crystals of the face-centred cubic, body-centred cubic, and close-packed hexagonal structures. For the present it is not considered justifiable to carry the simple argument further. On the old assumption of closely-fitting spheres this could have been done, since the spheres were regarded as attracting one another, and a rolling-over process need not affect this attraction. But in the point of view adopted here the attraction is not between the "spheres," which are considered mutually repulsive, but between these and the interpenetrating

* Proc. Roy. Soc. A, cxii. p. 337 (1926).

† *Ibid.* p. 359.

electron lattice, and the deformation will clearly affect the relative position of the two lattices. It is clear that the mobility of the structure will be greatest at the exact equilibrium position where everything is symmetrical and balanced, and we can understand that any movement from this position with its resultant effect on the relative positions of the atomic and electron lattices will cause the attractive and repulsive forces to come into play so that hardening results. We can further see that change of temperature will act oppositely on the mechanical properties and the electrical conductivity. For in connexion with the deformation process, the chances of the comparatively large atoms, or rather ions, passing over one another will increase with the amplitude of their oscillations. But the electrical conductivity depends on the passage of the small electrons between the atoms, and thus takes place with little or no resistance at the absolute zero, although increasingly interfered with as the amplitude of the atomic vibrations increases.

(6) The fact that deformation produces so much more marked an effect on the hardness than on the electrical conductivity may now be referred to. In the first place it has already been noted that change of temperature acts oppositely on the electrical conductivity and the plasticity, and it may not be justifiable to compare these at the ordinary temperatures where the thermal oscillations have already reached a considerable magnitude. In the second place the deformation process depicted above involves the movement of planes or rows of ions which are in contact. If this is correct a comparatively small obstacle may hold up the movement of a large number of atoms. For example, in the type of deformation shown by iron, where the rows of ions glide over one another, a single obstacle at the end of a row will hold up the movement of a whole row, but it will only impede the passage of the electrons between the ions in the immediate vicinity of the obstacle itself. In this way the disorganization produced by a very small amount of slip may prevent further slip over a wide area, but may only affect the passage of the electrons between the ions over a small area.

It is doubtful whether any of the other theories of the metallic state can give such a complete picture of the deformation processes as the above, for they nearly all require, to a greater or less extent, that the forces producing the crystals are definitely orientated attractions between the atoms, which appear incompatible with plastic deformation.

On the other hand, the type of structure suggested above, with comparatively large mutually repulsive particles held in contact by attractions to much smaller particles, is admirably suited for the plastic deformation so characteristic of the metals.

The criticism of the electron lattice theory on the grounds of instability has lost much of its force in view of the recent discoveries of the remarkable properties of the single crystals of metals. In the case of aluminium* and copper, for example, the single crystals possess no elastic tensile strength at all at the ordinary temperatures, and in this sense it may be said that the single crystal is unstable.

SECTION VI.

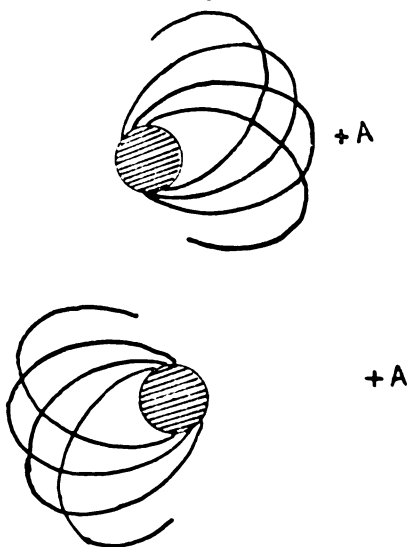
We may now discuss briefly the mechanism by means of which the electron lattice passes through the atomic lattice. We have noticed how in the comparatively open body-centred cubic structure there are channels straight through the crystal, if the ions are assumed spherical. In other structures this is not the case, and a more complex motion is required; but it may be emphasized that, although the positively-charged ions may be in "contact," there may still be room for the electrons to pass between them; for the zone of repulsion of a positively-charged ion for one of an opposite sign, or for an electron, will be smaller than its zone of repulsion for an ion of its own charge, on account of the opposing or reinforcing effects of the electrostatic charges in the two cases. It is therefore quite easy to understand how the electrons penetrate the ionic lattice, but it is not so easy to see how to reconcile the supra-conductivity motion at low temperatures with the conception of the formation of the lattice by the attractions of opposite charges. The explanation may perhaps be found in the nature of the ions themselves, and of the repulsive forces produced by their electrons. On the basis of the Bohr theory the electronic orbits are of two kinds, circular and elliptical. The circular orbits are comparatively simple, but the eccentric elliptical orbits are more complex. In that part of the orbit where the electron is far from the atom, the motion is that of a point charge moving round a massive nucleus. But when the electron comes round to the point where it is near to the nucleus, it plunges into the space occupied by the inner electrons, and undergoes a

* Phil. Trans. No. A, 636.

violent deviation from the simple motion. The result is a "central motion" which may be considered roughly as an elliptical motion with a violent precession of the major axis. Now up to the present we have regarded the repulsive fields of force of the ions as constant, but, strictly speaking, this would not seem correct.

Consider, for example, the effect of a single elliptical orbit at a point A as in fig. 8. It is clear that the position is very different at the different intervals of the precessional motion. We should therefore regard the spheres of repulsion of the ions, not as fixed, but as oscillating periodically. A motion

Fig. 8.



To show the effect of the precessional motion of the electrons upon the zones of repulsion of an ion.

of this kind may help the passage of the electrons between the atoms, just as, to give a crude illustration, a number of marbles may be pushed along a plane by a number of revolving elliptical cams. The motions of all the different ions will, of course, have to be in phase, and at ordinary temperatures this will be prevented by the thermal oscillations, which, however, die away as the temperature is lowered. A motion of this sort will be a kind of constitutional motion, distinct from the thermal oscillation, and its energy may correspond to the "Nullpunkt Energie" of the Quantum Theory which exists at the absolute zero

and cannot be given up. Whether the fundamental frequencies of the solids may be connected with a motion of this type is a matter which cannot be discussed here, but a conception of this sort seems to explain the way in which the electron lattice penetrates that of the atoms, and enables us to reconcile the conception of the ionic lattice with the fact of supra-conductivity.

It is to be noted that all metals do not show supra-conductivity at the temperatures of liquid helium, and in attempting to see which metals should show this effect on the basis of the above theory, the following factors have to be considered :—

(1) *The Crystal Structure.*—In general we should undoubtedly expect some structures to be more favourable than others. At present this point cannot be examined in detail owing to the lack of data for the crystal structures at very low temperatures, since the possibility of polymorphic changes makes it dangerous to argue from the structures at ordinary temperatures.

(2) *The Eccentricity of the Elliptical Orbits of the Ions.*—Here we should expect the effect of the precessional motion described above to be most marked in the case of the very eccentric orbits, or, in other words, in the elements of high atomic number, where the outer groups of electrons in the ions include the very eccentric 4_1 , 5_1 , or even 6_1^* orbits. This is quite in agreement with the fact that the elements which have been found to show supra-conductivity (indium, tin, mercury, thallium, and lead) are all of high atomic numbers.

(3) *The Symmetry of the Ion as a whole.*—In this connexion we should expect the above effect to be most pronounced where the ions in the metal were very unsymmetrical. Now, on the generally-accepted Stoner-Main-Smith modification of the Bohr theory, the first two electrons in a group form the N_{11} sub-grouping, and have the character of a more or less complete sub-group. On both chemical and spectroscopic grounds this is especially marked in lead and tin, and to a slightly less extent in thallium and indium. It is therefore highly probable that in these metals the whole of the valency electrons are not free, or ionized, in the solid metal, but that only those electrons which are not in the N_{11} groups are lost. In this case in tin and lead only two, and in indium and thallium only one, of the valency electrons will be free or ionized in the metal, and the

* See below for the case of lead and thallium.

resulting metallic ion will have a highly unsymmetrical structure such as (60) (18) (2)⁺⁺ for lead. It is, in fact, just these metals which show supra-conductivity.

On the other hand, the metals with symmetrical ions containing completed groups of 8 or 18 electrons, such as sodium, potassium, gold, silver, copper, zinc, and cadmium, do not show supra-conductivity, and neither do those in which the ions contain nearly complete 18 groups such as nickel and iron *; and we can quite understand that in a symmetrical ion with numerous similar orbits symmetrically disposed the above effect will be less pronounced. Mercury, however, is an exception to the above rule, if we regard the ion as having a structure (60) (18)⁺⁺ with two free electrons. Possibly this is connected with the other abnormalities of the mercury atom with its great reluctance to form the mercuric ion †; but whilst this particular point remains in doubt, it may be emphasized that the electron lattice theory as extended above is quite in agreement with the fact that some metals show supra-conductivity whilst others do not, since the factors (1), (2), and (3) just described will clearly vary greatly in different cases.

The electron lattice theory thus seems to have much to recommend it. It is in general agreement with the thermal and electrical properties, and in this connexion it can certainly hold its own with any of the rival theories. But in other connexions it seems to give a picture more comprehensive and more satisfactory than any of the other theories of the metallic state.

The author wishes to express his gratitude to Prof. Lindemann for his most kind interest and criticism.

Magdalen College,
Oxford.

APPENDIX.

The Dimensions of Ions in Salts and in Metals.

In 1920 the conception of the constant radii of ions was first put forward by W. L. Bragg ‡. The experimental evidence was that the substitution of one given cation for another in the alkali halides produced a practically constant change in the interatomic distances, irrespective of the nature of the anion, and similarly when one anion was

* For data see Onnes and Woltjer, Proc. 4th Int. Congress Refrigeration, i. p. 183 (1924); and Meissner, *Phys. Zeit.* xxvi. p. 689 (1925), *Z. Physik*, p. 38 (1926).

† The mercuric salts are almost unionized in solution.

‡ Phil. Mag. xl. p. 169 (1920).

substituted for another. The actual "radii," however, cannot be obtained from the interatomic distances, since however these are combined there is always one less equation than unknown quantity. The various methods of overcoming this difficulty are open to objection, since they involve assumptions either (as in the iron sulphide method) that the "radius"* of a positive ion in a metal is the same as in an ionized salt, which is certainly not true, or (as in the caesium di-chloro-iodide method) that the negative ions have the same radii in electro-valent as in co-valent compounds. These methods have been effectively criticized by Wyckoff †.

An alternative and more satisfactory method would appear to be as follows. The electronic configurations of the Cs^+ and I^- ions are identical (54 electrons), the only difference being that the nuclear charges are 55 and 53 in the two cases respectively. We may therefore as an approximation put the radius of these two ions as equal to half the distance between them in caesium iodide, and in this way obtain one more equation and so derive the whole of the radii of the different ions. The fact that the change in interatomic distance when one ion is substituted for another in both the caesium chloride and sodium chloride types of structure is the same, shows that we are justified in assuming that the "radii" of these alkali and halogen ions are the same when they are surrounded by either six or eight neighbours. In this way, using the interatomic distances given in Table II., we obtain the radii of the ions shown in Table III.

TABLE II.†
Interatomic Distances in Å. in the Alkali Halide Crystals.

	F.	Cl.	Br.	I.
Li^+	2.007	2.566	2.745	3.015
Na^+	2.310	2.814	2.968	3.231
K^+	2.664	3.164	3.287	3.526
Rb^+	3.172?	3.286	3.434	3.663
Cs^+	3.015?	3.563	3.713	3.947

* The conventional term "radius" is used here, but of course this really only means the distance at which the attraction and repulsion balance, and does not imply a sharp surface.

† Proc. Nat. Acad. Sci. ix. p. 30 (1923).

‡ These figures are taken from work by Davey (Phys. Rev. xxi. p. 143, 1923) and Havighurst (J. Amer. Chem. Soc. xlv. p. 2388, 1924). A critical selection has been made, and a mean value is taken where the two results appear of equal value. The differences are, however, very small. The value for CsF is from Wyckoff (J. Washington Academy Sci. xiii. p. 393, 1923).

TABLE III.

Ionic Radii deduced on the assumption that
 $\text{Cs}^+ = \text{I}' = 1.974 \text{ \AA.}$

$\text{Li}^+ = 1.041$	
$\text{Na}^+ = 1.257$	$\text{F}' = 1.041 ?$
$\text{K}^+ = 1.552$	$\text{Cl}' = 1.589$
$\text{Rb}^+ = 1.689$	$\text{Br}' = 1.739$
$\text{Cs}^+ = 1.974$	$\text{I}' = 1.974$

From these tables it can be seen that the single assumption that the radii of the caesium and iodine ions are equal gives us within 0.05 \AA. the relations $\text{Rb}^+ = \text{Br}'$, and $\text{K}^+ = \text{Cl}'$. Unfortunately the results for the fluorine ion are uncertain, as for both caesium and rubidium fluorides there is a wide discrepancy between the densities calculated from the X-ray data and those obtained by direct measurement, and this point is not yet decided*. But the relation between the potassium and chlorine ions on the one hand, and the rubidium and bromine ions on the other, is one quite apart from the simple additive law, and very strikingly confirms the truth of the fundamental assumption.

Reference to the literature showed that a somewhat similar suggestion had previously been made by Davey †, who, however, made four independent assumptions: namely, that $\text{Na}^+ = \text{F}'$, $\text{K}^+ = \text{Cl}'$, $\text{Rb}^+ = \text{Br}'$, and $\text{Cs}^+ = \text{I}'$. In view of the fact that the relative difference in atomic numbers becomes greater as the atomic number decreases, and that the additive law itself holds more closely among elements of high atomic number, it would seem that the above method is more accurate.

TABLE IV.

Salts of uni- and di-valent ions of identical electronic structure, forming the same type of crystal structure.		Interatomic distance in the rock-salt type of structure.		Ratio.
KF	CaO	2.664	2.395	1.112
KCl	CaS	3.164	2.843	1.113
KBr	CaSe	3.287	2.957	1.112
RbBr	SrSe	3.434	3.117	1.102
RbCl	SrS	3.286	2.933	1.120
NaCl	MgS	2.814	2.539	1.108
NaF	MgO	2.310	2.09	1.105

* See Wyckoff (*ibid.*) for a criticism of this point for rubidium fluoride.

† Phys. Rev. xviii. pp. 102-104 (1921).

Additional support for this is found in the fact that where the rock-salt structure is formed by uni- and di-valent ions having the same electronic structure, *e.g.* sodium chloride and magnesium sulphide, the ratio of the interatomic distances is approximately constant, as is shown in the above table (Table IV.).

As pointed out in the above paper, the alkali metals crystallize in the body-centred cubic structure in which each atom is surrounded by eight others, and it is therefore justifiable to compare the interatomic distances in these with the dimensions of the ions deduced above. For lithium, sodium, and potassium direct X-ray data are available, but not for rubidium or caesium. In papers by Bridgman on the effect of pressure on electrical resistance, the results are taken to indicate that rubidium and caesium have the body-centred structure; and on this assumption the interatomic distances can be calculated from the densities, since if a is the side of a unit cube (in Å.),

$$a^3 = \frac{K \times \text{atomic weight}}{\text{density}}.$$

For lithium, sodium, and potassium the values of K are 3.28, 3.35, and 3.10 respectively (from the X-ray data and densities), and taking a mean value of 3.24, we find the closest distances of approach to be 4.90 Å. for rubidium (density 1.53) and 5.28 Å. for caesium (density 1.90). Theoretically these values for K should be constant, and could be calculated, the differences being due chiefly to errors in the density determinations. But as these errors are likely to be in the same direction for all the alkali metals, it is thought better to use the above mean value. We have, therefore :

TABLE V.

	One-half closest approach in metal.	Radius of ion in halides.	Ratio.
Lithium.....	1.515 A.	1.041 A.	1.45
Sodium.....	1.86	1.257	1.48
Potassium.....	2.25	1.552	1.45
Rubidium.....	2.45	1.689	1.45
Caesium.....	2.64	1.974	1.34

With the exception of caesium, for which the constants are imperfectly known, the constancy of the ratio is very striking.

XCVI. *On the Application of the Aitken Effect to the Study of Aerosols.* By HENRY L. GREEN. M.A. (Cantab.), A.Inst.P.*

[Plate XXII.]

Introduction.

FOR the quantitative study of a disperse system in air or, as it has been more generally termed, an aerosol, a knowledge of the number of particles existing at any time is of fundamental importance.

Several methods have been employed for the accurate counting of the particles in dusts, smokes, and similar systems. Aitken† determined the number of "dust" particles in air by condensing moisture on them and counting the water-droplets thus formed, after they had settled on a glass plate. Whytlaw-Gray and others‡, using a slit ultra-microscope of the Zsigmondy-Siedentopf type, made direct counts on the number of particles in smokes, and were able to follow the changes taking place during rapid coagulation. It was realized, however, that the method was subject to certain limitations; amongst others, the limit of smallness of particle which could be seen depended upon the particular optical system used and the sensitiveness of the retina of the observer. At the time when their experiments were carried out it was thought that many amicroscopic particles existed in the smokes that were examined. With the view to extending the range of the ultra-microscope the idea has been developed of combining Aitken's method, which is capable of revealing particles of exceedingly small dimensions, with that used by Whytlaw-Gray.

Aitken§ found that, when moist air is cooled by a rapid expansion, water will condense into droplets only if there are nuclei present for their formation and the degree of supersaturation attained has been sufficiently high. This effect has been termed, for the purpose of this paper, the "Aitken" effect. His apparatus in its original form is not directly adapted for the continuous examination of aerosols, which may be rapidly coagulating, but the form of rapid expansion apparatus developed by C. T. R. Wilson|| can be

* Communicated by the Author.

† Collected Scientific Papers of John Aitken. Ed. by C. G. Knott, p. 187.

‡ R. Whytlaw-Gray, J. B. Speakman and J. H. P. Campbell, Proc. Roy. Soc. A, cii. p. 600 (1923).

§ *Loc. cit.* p. 199.

|| C. T. R. Wilson, Proc. Roy. Soc. A, lxxxvii. p. 277 (1912).

used successfully for producing expansions in the cell of an ultra-microscope, and the water-droplets formed by condensation on nuclei, such as are provided by the particles in a smoke, can be counted. For the more accurate counting of the droplets a photographic method in conjunction with a mechanical type of Wilson apparatus has been developed, and it is the purpose of this paper to describe this method and to show how it has been applied to the study of certain smokes.

Before dealing with the experimental methods in detail it is desirable to discuss the theoretical considerations underlying the application of the Aitken effect.

Theoretical Considerations.

The theory of the application of the Aitken effect has been worked out in detail by C. T. R. Wilson * ; here, the theoretical aspects have been merely summarized and data calculated in accordance with the particular experimental conditions holding in this investigation.

If air, saturated with water-vapour, is subjected to an adiabatic expansion of a given ratio, *i. e.* becomes supersaturated to a given degree, moisture will condense round any nuclei present, provided they are larger than a certain size.

Now there is a relationship between the minimum radius of an uncharged droplet, which could exist and grow, and a given degree of supersaturation which is expressed by the equation developed by Kelvin † and applied by Helmholtz ‡ to the case of droplets ; Kelvin's equation is

$$\log_e \frac{p_1}{p_2} = \frac{2S}{RT\rho r}, \quad . \quad . \quad . \quad . \quad (1)$$

where p_1 is the vapour-pressure over droplet, p_2 the vapour-pressure over a plane surface, $\frac{p_1}{p_2}$ the degree of supersaturation, S the surface-tension of liquid, r the radius of droplet, R the gas constant, T the absolute temperature, and ρ is the density of the liquid.

But a droplet will not form even with this supersaturation unless a nucleus of at least the same radius is present. So that it is possible to calculate the minimum size of uncharged

* C. T. R. Wilson, Phil. Trans. A, clxxxix. p. 265 (1897).

† Kelvin, Proc. Roy. Soc. Edin. vii. p. 63 (1870).

‡ K. R. von Helmholtz, Wied. Ann. xxvii. p. 508 (1886).

nuclei which must be present in order to produce a cloud of droplets with a given degree of supersaturation.

Now in an adiabatic expansion,

$$v_1\gamma^{-1}\theta_1 = v_2\gamma^{-1}\theta_2, \quad . \quad . \quad . \quad . \quad (2)$$

where v_1 is the volume before expansion, v_2 the volume after expansion, θ_1 the temperature before expansion, θ_2 the temperature at instant after expansion, and γ is equal to C_p/C_v .

Therefore, given the volume change, the theoretical instantaneous lowering of temperature can be calculated and the degree of supersaturation existing found after reference to vapour-pressure tables (see Column IV., Table I.).

From this value and by using the Kelvin equation the minimum sizes of uncharged nuclei for the formation of droplets have been derived (see Column V.). It must be noted that, in order to make these calculations, it is necessary to assume that the gas laws may be applied to water-vapour.

To gain an idea of the size of droplets formed it is necessary to calculate the mass of water deposited after a given expansion. When condensation takes place the process will continue until the heat liberated causes the temperature to rise to an equilibrium value and the remaining water-vapour is just saturated. Under these conditions

$$L(\rho_2 - \rho_3) = MC_v(\theta_3 - \theta_2), \quad . \quad . \quad . \quad . \quad (3)$$

where L is the latent heat of water at the mean temperature, ρ_2 the density of water-vapour at temperature θ_2 , ρ_3 the density of water-vapour at equilibrium temperature θ_3 , M the density of moist air at the same temperature, C_v the specific heat of air at constant volume, θ_3 the equilibrium temperature, and θ_2 is the temperature at the instant after expansion.

The point of intersection of the curve given by this equation (derived values of ρ_3 being plotted against given values of θ_3) with the curve for the variation of density of water-vapour with temperature must give the values of ρ_3 and θ_3 attained for a given expansion, *i. e.* given value of θ_2 . The difference between ρ_2 and ρ_3 gives the mass of water deposited per c.c. (see Column VI.).

For the purpose of detecting particles in aerosols an expansion ratio greater than about 1.38 probably cannot be used, since a general cloud is formed for expansions greater than this, even with perfectly dust-free air. In the case of smokes it is hardly necessary to use an expansion ratio

TABLE I.

Initial Temperature 15° C. Expansion Ratio.	Instantaneous Temperature. ° C.	Initial Pressure 760 mm. Hg. Equilibrium Temperature. ° C.	Degree of Super-saturation.	Radius of Nucleus revealed. cm.	Mass of Water condensed. gm./c.c.	Radius of Droplets. cm. (Water divided amongst 10 ⁷ particles/c.c.).
1.05	9.5	13.0	1.34	3.89×10^{-7}	0.94×10^{-6}	2.86×10^{-5}
1.10	4.1	10.6	1.84	1.93×10^{-7}	2.07×10^{-6}	3.67×10^{-5}
1.15	0.7	8.7	2.40	1.38×10^{-7}	2.80×10^{-6}	4.06×10^{-5}
1.20	- 5.4	6.2	3.25	1.05×10^{-7}	3.38×10^{-6}	4.32×10^{-5}
1.30	- 13.8	2.2	5.56	7.55×10^{-8}	4.28×10^{-6}	4.67×10^{-5}
1.40	- 21.4	- 1.9	9.05	6.14×10^{-8} *	4.91×10^{-6}	4.90×10^{-5}
1.50	- 28.4	- 5.5	13.80	5.37×10^{-8} *	5.29×10^{-6}	5.02×10^{-5}
1.60	- 34.6	- 9.2	20.05	4.86×10^{-8} *	5.57×10^{-6}	5.10×10^{-5}

* It is probable that the Kelvin formula no longer holds for droplets formed with these expansions owing to the variation of surface-tension, when the diameter of droplet becomes very small.

All physical data have been taken from the Smithsonian Tables (1918).

approaching this value. At a ratio of say 1·30, if the theory holds, a spherical uncharged nucleus $7\cdot55 \times 10^{-8}$ cm. in radius should be detectable at 15°C.; actually, particles in smokes are not necessarily spherical and many may be electrically charged, but these factors would tend, practically in every case, to favour deposition of water-vapour. The case in which charged particles of very small dimensions would not be revealed was not likely to arise in connexion with any of the aerosols it was desired to investigate by this method.

If the water deposited at the expansion ratio 1·30 were equally divided amongst 10^7 nuclei per c.c. (a number far greater than that attained in any aerosol so far examined), droplets of radius of the order $4\cdot67 \times 10^{-5}$ cm. would be formed. This size is well within the range of the ultra-microscope. It would be expected, however, that the water-droplet clouds would be heterogeneous since nuclei of different sizes would probably condense water at different rates.

The Visual Method of Counting.

The method of directly counting particles in aerosols was based on that developed by Zsigmondy for obtaining the number of particles in colloidal solutions. The original procedure adopted by Whytlaw-Gray was to pass a slow stream of the aerosol through an ultra-microscope cell illuminated by a beam of light of known depth. The particles were viewed through a microscope in which the field of vision was cut down by a square diaphragm in the eyepiece, so that the number of particles seen at any moment could be estimated at a glance; most observers find it difficult to estimate with accuracy more than six to eight particles in the field at once. Fifty instantaneous counts were taken on the slowly moving stream. The arithmetic mean of these counts multiplied by a factor, calculated from measurement of the volume of aerosol viewed, gave the number of particles per unit volume.

The above method, which formed the basis of the procedure for counting water-droplets produced by the condensation of moisture on the particles of a cloud, suffered from the defect that particles or droplets outside the beam of light, faintly illuminated by scattered or reflected light from those within the beam, were liable to be counted. This was pointed out in the first instance by Whytlaw-Gray, and he explains the high values he obtained for his original number counts as

being due to counting particles outside the beam, *i. e.* to an under-estimation of the effective depth of the beam.

Hence it is evident that this particular visual method of counting the droplets can only give roughly quantitative results, although relative values may be fairly accurate. It was decided, therefore, to develop a method of photographing the droplets formed in a mechanical or continuous-action Wilson apparatus and of counting their images on the negative with a low-power microscope. It was considered that there would be sufficient contrast between droplets within the beam of light and those without, to enable differentiation to be made in counting on the photographic plate. Further, a much deeper beam could be used, enabling more droplets to be counted and more observations to be taken in a given time.

Before giving an account of the photographic method a brief account will be given of the visual method, as this has a certain quantitative value.

Adiabatic expansions were obtained by the well-known plunger method due to Wilson*. An expansion chamber, diameter $2\frac{1}{2}$ cm., was connected directly to an ultra-microscope cell $\frac{1}{2}$ cm. in diameter and 3 cm. long, similar to the one used by Whytlaw-Gray†. A vertical scale was fixed to the expansion chamber so that the height of the plunger could be read; the apparatus was calibrated and a given height of the plunger corresponded to a certain expansion ratio. Wherever possible, the cell was lined with damp blotting-paper to keep the air inside thoroughly saturated with water-vapour.

The apparatus was mounted on a bench ultra-microscope of the slit type, a 1000-c.p. pointolite lamp being employed as the source of illumination. In using the apparatus, the plunger was roughly adjusted to slightly below the position to give the desired expansion, and a sample of the aerosol to be examined was drawn in by aspiration. The height of the plunger was then finally adjusted to the required height and all taps were shut. After an interval of 30 seconds, to allow the air to become saturated, the expansion was made. With air containing particulate matter a cloud would be formed and the droplets could be seen falling in the field of view. By using a sufficiently shallow beam and a suitable diaphragm the number of droplets in the field of view could be cut down, so that, as they fell, the number at any instant

* C. T. R. Wilson, *loc. cit.*

† R. Whytlaw-Gray and others, *loc. cit.*

could be estimated. At least 25 counts could be made before there were any signs of evaporation. Hence two expansions were usually made to give 50 counts, which were averaged and the number of particles per unit volume deduced.

Apart from the errors inherent in the ultra-microscope itself, there were possible errors arising from the difficulty in counting droplets moving rather rapidly through the field of vision. These errors would be particularly noticeable when there were a large number of droplets in the field, and when there were very few, with numerous "blanks" appearing in the counts. A continuous-action Wilson apparatus, which obviated these errors, was designed; subsequently it was used for the photographic method, for which an easily operated mechanical type of apparatus was essential.

A Continuous-Action Wilson Apparatus.

In this apparatus, the idea has been to arrange for a continuous series of expansions each on a fresh sample of the cloud; one count or photograph only is taken, immediately after the completion of each expansion, when the droplets are retained for the moment stationary in the field.

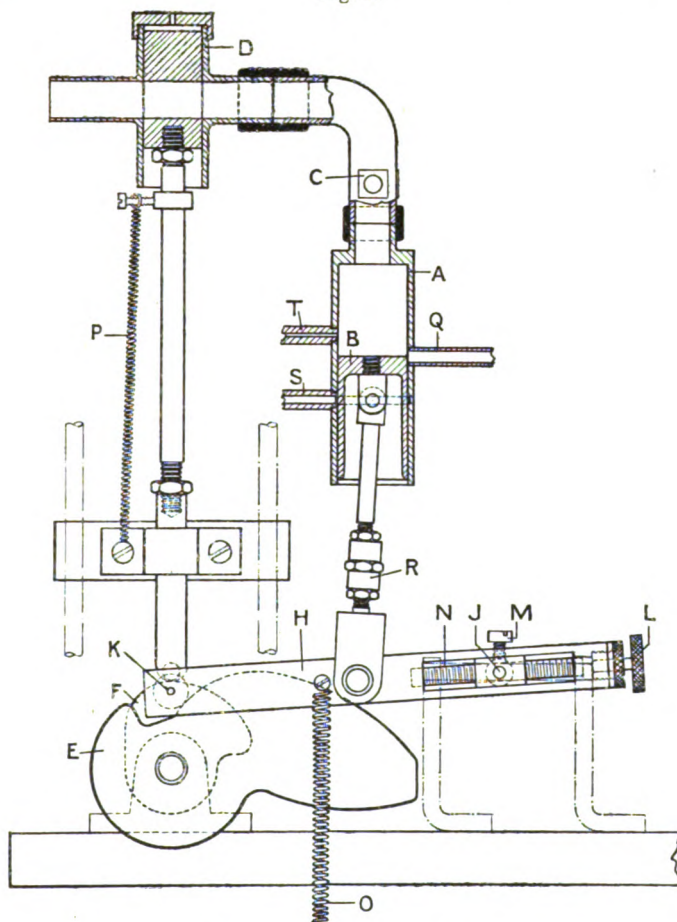
There were several necessary features which had to be borne in mind when the apparatus was designed. Expansions had to be very rapid, if not adiabatic, means had to be provided for changing the sample of aerosol after each expansion so as to guard against any possible diminution of numbers due to falling out of particles, and further, it was necessary to arrange for a pause in the action of the apparatus, just after the expansion, to enable a count or photograph to be taken.

A diagram of the apparatus is shown in fig. 1.

Expansions were caused by the motion of the piston (B) working in the cylinder (A). To the cylinder is attached by a rubber connexion an ultra-microscope cell (C), which in turn is connected to a shut-off valve (D). The motions of valve and piston are controlled indirectly by two cams (E) and (F) working on the same spindle, which is rotated by a 1/20 H.P. electric motor geared down through a gear-box (gear ratio 1:64).

The piston is linked with the rocker-arm (H), one end of which pivots at J and the other rests on the cam (E) through the roller (K). The pivotal point can be moved by the screw (L) so as to alter the length of the stroke of the piston and therefore the expansion ratio, as in the Ray Track

Fig. 1.

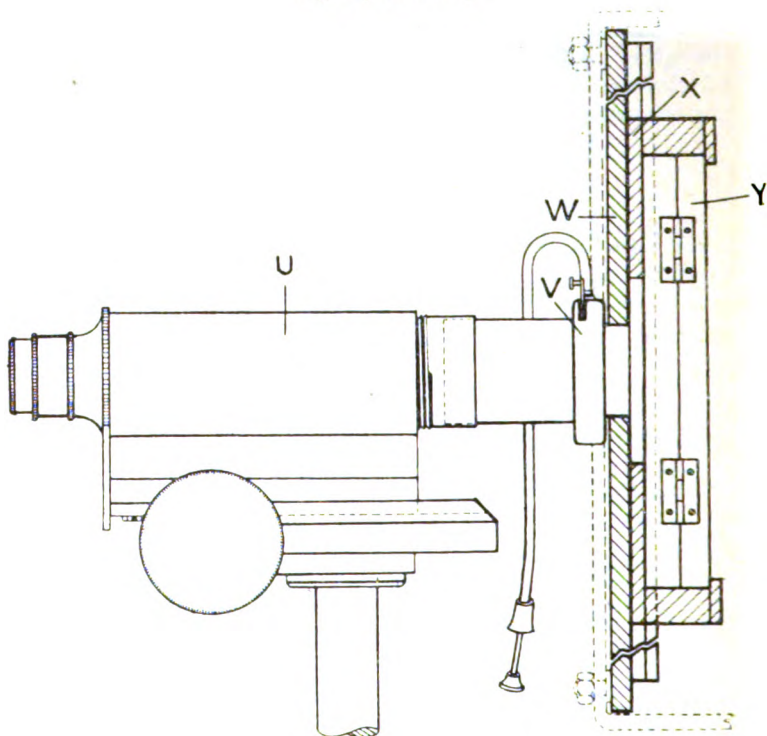


* T. Shimizu, Proc. Roy. Soc. A, xcix. p. 425 (1921).

second spring (P) keeps the slide of the shut-off valve bearing through its stem and roller on the other cam.

The apparatus was mounted with the ultra-microscope illuminating system and viewing microscope mutually at right angles, the axis of the latter being set in the same plane as the cell and cams shown in the diagram.

Fig. 1 (continued).



Action of Apparatus.

In practice the slide-valve was connected through about 40 cm. of glass tubing, diameter 1 cm., lined with damp blotting-paper, to the chamber containing the cloud, and the cylinder connected through the port (Q) to an aspirator. The cell was also lined with damp blotting-paper. The action of the apparatus is best described by tracing what happens during one revolution of the cams.

Consider the cams in the position shown in the diagram, when the port in the cylinder is uncovered and the shut-off valve is open. A sample of the cloud is being drawn through, and as the cams rotate the piston rises, shutting off the suction, the valve, however, remaining open. Just as the piston reaches its topmost position the valve shuts, and almost immediately afterwards the piston drops very suddenly, causing an almost adiabatic expansion of the air in the cell and cylinder; the roller of the rocker-arm falls on the circular portion of its cam. As the cams continue to rotate both valve and piston remain stationary, thus enabling a count to be taken of the droplets formed by condensation of moisture on any particles present. The valve now re-opens, and the piston drops, uncovering the port, and the cycle is thus started again. One revolution takes two seconds, and thus 50 counts are completed in 100 seconds.

In actual practice, certain difficulties, which were successfully overcome, were experienced with the apparatus. Leaks round the valve and piston were prevented by maintaining a film of castor oil over the working surfaces. In the case of the valve, a little oil was poured on the top of the slide from time to time and this was sufficient to keep the valve air-tight in its closed position. A reservoir of oil, feeding through the copper tube (S) on a ring cut in the walls of the cylinder below the port, maintained a film of oil on the piston and kept it air-tight.

The motion of the droplets after expansion was a source of considerable trouble. Partly owing to the peculiar construction of the cell and partly to convection, the droplets commenced to move downwards with a velocity greater than their terminal velocity immediately after each expansion, although the apparatus was perfectly air-tight. An upward current of air of suitable velocity would keep the droplets stationary. It was found that this could be obtained by allowing air to leak into the cylinder at a controlled rate after the rapid expansion had been completed. Accordingly a copper tube (T) of capillary bore, to which was attached a piece of rubber tubing and screw clip, was let into the cylinder. By regulating the screw, air could be admitted into the cylinder at a rate sufficient to correct the downward movement of the droplets in the ultra-microscope cell and cause them to remain stationary long enough for a single count to be made in the usual way.

There were two reasons for retaining the narrow cell :

- (a) The beam of light had only to pass through a small length of cloud before being brought to a focus ; thus losses of light due to absorption or scattering were reduced to a minimum.
- (b) The beam could be brought quite close to the front of the cell so that there was little "fogging" of the illuminated droplets by droplets between the beam and the objective.

The apparatus was calibrated for a particular expansion ratio by first of all determining the pressure change with a manometer connected to Q, when the piston was allowed to drop from its highest position to its lowest position, *i. e.* to the position where the port is uncovered, the valve (D) being kept shut. The actual pressure change was measured by a null method—that is by determining to what pressure the air in the tube (Q) must be adjusted in order that the manometer should show no change when the tube was opened to the cylinder after the expansion.

The internal diameter of the cylinder and the stroke of the piston, when the roller (K) fell to its various positions on the cam, were measured, and hence the pressure change could be calculated for the normal case when the roller dropped to the circular part of the cam. From this value and the value of the saturation pressure of water-vapour in the apparatus the expansion ratio was easily calculated.

Visual counting with this apparatus was found to be much easier and more accurate than with the earlier type. The adaptation of the apparatus for the photographic method is given below.

The Photographic Method of Counting.

Experiments have been carried out with various lens systems, plates and sources of illumination. The eventual arrangements evolved are as follows :—

The continuous-action Wilson Apparatus was set up in conjunction with the bench ultra-microscope and a 10 ampere Zeiss arc, with automatic feed, as source of illumination. The vertical reading microscope (U), normally used for counting, was arranged to throw an image of the droplets (magnification about $\times 2$) on the photographic plate. In order to do this, the 1-inch objective was replaced by one of 2½-inch focal length and an extensible tube, in place of the draw-tube and eyepiece, connected the microscope to a self-capping shutter (V), which was attached to a fixed

panel (W). A movable panel (X), holding a quarter-plate dark slide (Y), fitted into vertical grooves in the fixed one, thus permitting up and down movement of the plate. The slide could also be moved laterally so that, without undue crowding, it was possible to secure seven columns each of fourteen photographs on the one plate.

The procedure adopted has followed the same lines as in making visual counts except that a photograph could be taken of, practically speaking, the whole illuminated field, when, in the ordinary way, a count on only a very small portion could be made. By careful adjustment of the air-leak in the Wilson apparatus it has been possible to keep the droplets sufficiently steady after the expansion to allow an exposure of as much as one-fifteenth of a second to be made. The exposure is made by hand, but there is no difficulty in judging the moment when the shutter should be released. Ilford "Monarch" plates have been found quite satisfactory for this work.

A platinum wire was looped round the windows of the cell and maintained at just a sufficient temperature by an electric current to prevent condensation of moisture on them. The heat from the wire has a tendency to set up convection currents in the cell, but the number of photographs spoilt due to this cause is comparatively few. The top of the cell could be water cooled, if necessary, in order to slow down evaporation when the room temperature was high.

In Plate XXII. is shown a series of specimen enlargements of photographs taken during the history of an ammonium chloride cloud. The total magnification is $\times 23$, *i.e.* the magnification of the original photographs is $\times 5$, and the depth of the beam at its focus, 0.0263 cm.

The images of the droplets were counted on the photographic negative under a microscope using a $1\frac{1}{2}$ -inch objective and a $\times 4$ eyepiece, which gave a total magnification of about 20 diameters. A graticule ruled into 100 squares was set in the eyepiece. Only images in the central portion of each photograph were counted; these were of droplets within the beam of light and the depth of focus of the photographing objective, which gave clearly defined images. Droplets outside the beam illuminated by scattered light gave fainter images than those fully illuminated. These were comparatively few in number, and it was a matter of judgment whether or not they should be included in the counts. The magnification was such that the images covered by 24 (6×4) to 40 (4×10) squares in the graticule could be counted, just in the same way as the

ordinary ultra-microscope counts are taken with a square diaphragm. The counts from a number of successive photographs were averaged and multiplied by a factor to give the number of particles per c.c. in the cloud. The factor was obtained after calibration of the microscope and photographing objective, and determination of the expansion ratio in the Wilson apparatus and the depth of the beam of light.

Since the beam of light in the cell is shallower at the centre than at the sides, the depth was carefully measured over the whole area in which counts were made. This was done by turning the crossed slits through a right angle and taking photographs under the same conditions as in actual experiments. The depth was then measured on the plate by means of a reading microscope. It was necessary to take the mean of a number of readings on different photographs, as the confines of the beam are not *absolutely* sharp and there is a slight variation between one photograph and another.

A mean depth of as much as 0.5 mm. could be used, but, when the cloud contains a large number of particles, it is convenient to use a shallower beam, thus reducing the number of droplets photographed and preventing overlapping of images.

It is estimated that the various steps in the calibration may cause a total error in the calibration factor of as much as ± 10 per cent.

With the present apparatus a photograph can be taken at every revolution of the cams, *i.e.* every two seconds, and aerosols containing from 3×10^4 to 3×10^6 particles per cubic centimetre can be examined with it. An example of actual measurements in calibration is given below :—

Minimum depth of beam of light	=	0.0263 cm.
Mean depth of beam over area on photographic plate in which counts were made	=	0.0882 cm.
Area of plate covered by one graticule square of counting microscope	=	$(0.043)^2$ sq. cm.
Magnification of photographing objective	=	2.44.
For each photograph counts were made from 10 \times 4 graticule squares.		
Hence volume of cloud in Wilson apparatus in which counts were made	=	$\frac{40 \times (0.043)^2 \times 0.0882}{(2.44)^2}$ c.c.
Expansion ratio of Wilson apparatus	=	1.406
Therefore actual volume of cloud in which counts were made	=	$\frac{40 \times (0.043)^2 \times 0.0882}{(2.44)^2 \times 1.406}$ c.c.
Hence factor to convert number of particles per 40 counts to number of particles per c.c.	=	$\frac{(2.44)^2 \times 1.406}{40 \times (0.043)^2 \times 0.0882}$ = 2.97×10^3 .

*Application to the study of Ammonium Chloride
and Cadmium Oxide Clouds.*

Whytlaw-Gray and others * have studied various types of smokes of a high degree of dispersion and established that the initial rapid fall in the particulate number curves is due almost entirely to the coalescence of particles. In some of their subsequent work he and his co-workers have come to the conclusion that, owing to the inherent defects in the ultra-microscope itself, their original particulate number values were too high. They have since evolved a type of ultra-microscope cell which does not suffer from these defects, and by means of which they have made a fresh series of counts on ammonium chloride and cadmium oxide clouds. The application of the Aitken effect provides an independent means of counting the total number of particles and determining the rate of coagulation of such clouds.

Clouds were dispersed in an air-tight metre cube made of glass set in a wooden framework, which could be rendered dust-free by blowing through filtered air for about an hour.

The first series of determinations was made with ammonium chloride clouds. It was decided to disperse the substance under conditions which should be as simple as possible. Clouds were generated by comparatively slow sublimation from a platinum boat shaped to fit on a quartz U-tube, heated electrically. The heating element was a spiral of nichrome wire threaded through the tube and raised to a red heat by a current of about 1.6 amperes. The U-tube was sealed to glass tubes which carried the leads to the wire outside the chamber, so that no nuclei from the wire itself could reach the inside of the chamber. No nuclei were shot off by the boat or U-tube, and it was therefore possible to generate clouds, containing particles which were initially uncharged, in dust-free air. In no case was the air in the chamber dried, but was left at the ordinary humidity of the atmosphere.

The weight of ammonium chloride in the boat before an experiment was always the same, the amount sublimed being controlled by the length of time during which the boat was heated; this varied from one to three minutes according to the concentration desired. A fan set opposite the U-tube and about 12 inches from it was kept running for five minutes after the commencement of generation of the cloud.

The continuous-action Wilson apparatus was connected to the chamber as previously described. The expansion ratio

* Whytlaw-Gray and others, *loc. cit.*

was kept as high as 1.406, since it was necessary to make certain that all the particles were being revealed. As the expansions were not truly adiabatic this was below the limit of general cloud formation. With the plunger type of apparatus it was found by direct experiments that an expansion ratio of 1.10 will reveal all the particles in these aerosols. It was also possible to show by a direct comparison that the continuous-action Wilson apparatus was revealing all the particles.

Probable Errors of Observations.

The question of how many particles must be counted in order to deduce a reliable value for the number of particles per c.c. in the cloud at any time is considered in the case quoted below.

Three photographs were taken at intervals of two seconds of different samples from an ammonium chloride cloud in its initial stages. Forty counts were made from each photograph and the numbers of occurrences of 0's, 1's, 2's, etc., per square of the eyepiece graticule were plotted against their respective numbers. The curve (fig. 2) is a smooth and typical probability one. By applying the ordinary probability formula the probable error of the arithmetic mean of any forty observations was calculated. This amounted to ± 4.40 per cent., the average per square of the graticule being 5.37.

The probability that there should be n particles per square is given by $\frac{x^n}{n!} \cdot e^{-x}$, where x is the average number per graticule square and n may have any positive value from 0 to ∞ . Observed and calculated number of occurrences are given below:—

Average number per graticule square : 5.37.

Number of particles per graticule square :

0	1	2	3	4	5	6	7	8	9	10	11	12.
---	---	---	---	---	---	---	---	---	---	----	----	-----

Observed number of occurrences :

0	7	6	13	16	24	23	14	7	5	3	2	0.
---	---	---	----	----	----	----	----	---	---	---	---	----

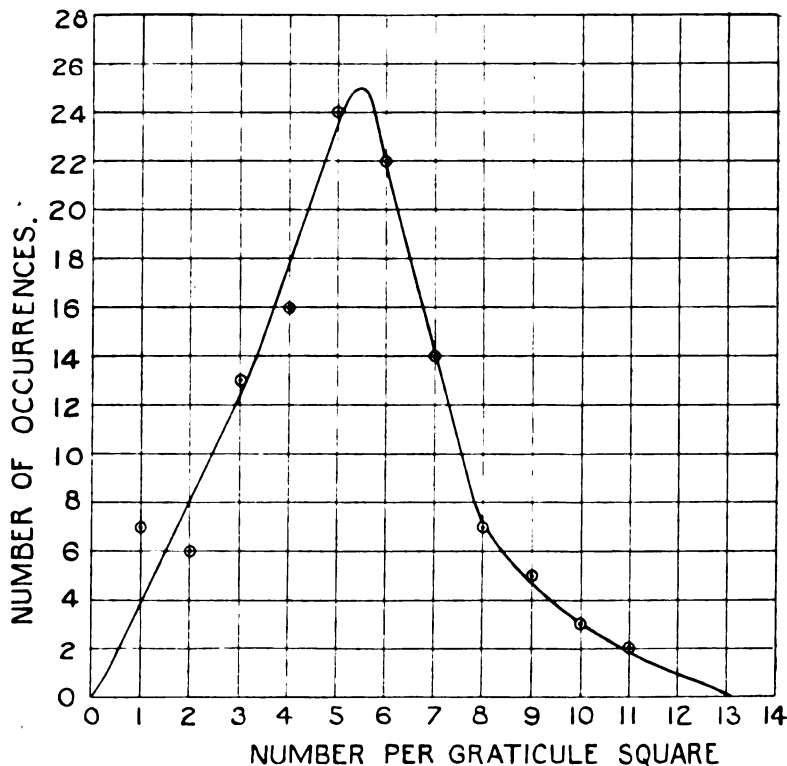
Theoretical number of occurrences :

1	3	8	14	19	21	19	14	10	6	3	1	1.
---	---	---	----	----	----	----	----	----	---	---	---	----

The agreement between the sets of figures is good, considering the small number of observations that were taken.

This procedure has been carried out for a number of clouds and in every case the theory of probability has been shown to hold. It appears therefore that the variation in individual counts, and in the average of forty counts between successive photographs, is such as would be expected from the random distribution of particles, and is not due to any inhomogeneity of the cloud, any fluctuation in its behaviour or in the action of the apparatus.

Fig. 2.



In order to deduce the number of particles in a cloud at any mean time sufficient photographs are taken to enable some five hundred droplets to be counted, thus reducing the probable error of the observation to ± 3 per cent. This convention has been adhered to in most of the subsequent work with the apparatus.

Results for Ammonium Chloride.

A number of clouds of various concentrations was dispersed by the method described, and their histories followed for about an hour and a half. The detailed figures for a typical cloud are given below and shown graphically in fig. 3. Enlargements of photographs taken from the negative for this cloud were shown in Plate XXII.

TABLE II.

No. of Photographs.	No. of Particles Counted.	Mean Time.	No. of particles per c.c. $n \times 10^{-5}$.	Particulate volume $1/n \times 10^5$.
		min. sec.		
3	592	6 40	5.86	0.171
4	667	9 5	4.95	0.202
4	523	15 15	3.88	0.258
5	558	19 30	3.34	0.302
6	559	27 35	2.76	0.362
6	540	30 35	2.67	0.375
7	567	38 47	2.42	0.413
9	591	49 0	1.98	0.505
9	532	55 47	1.75	0.571
6	314	63 11	1.55	0.645
6	331	68 47	1.64	0.610
8	364	82 8	1.35	0.741
6	246	89 15	1.22	0.820

It was found that the reciprocal of the number of particles per c.c. plotted against time gave a straight line in every case within the limits of experimental error*; that is, the rate of coagulation of the clouds followed the law

$$\frac{1}{n} = \frac{1}{n_0} + Kt, \quad (4)$$

where n is the number of particles per c.c. at time t , and n_0 is the initial number of particles.

It is therefore possible to tabulate the values for the initial number of particles per c.c., obtained by extrapolation, and the values for the coagulation constant as the

* This result has also been arrived at independently by H. S. Patterson, and the nomenclature suggested by him has been adopted

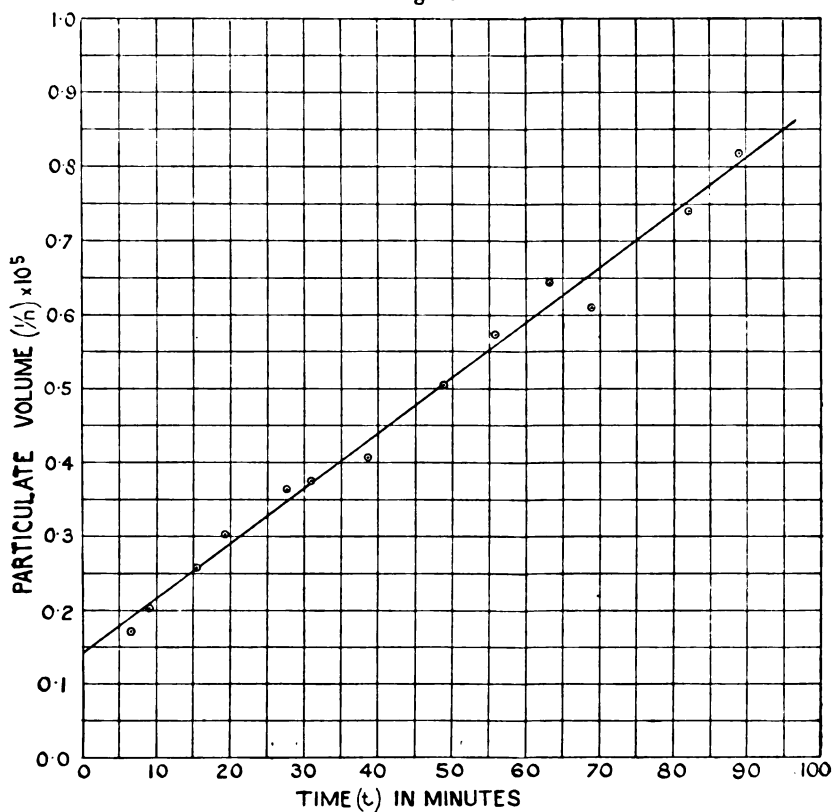
factor K will be termed, for a number of clouds thus :—

TABLE III.

Concentration (mg. per c. metre). c.	Initial number of particles per c.c. $n_0 \times 10^{-5}$.	K. cm. ³ /min. $\times 10^3$.
2.0	6.94	7.42
4.0	6.25	7.85
5.8	6.45	7.45
6.5	8.00	6.40
6.8	8.70	5.00
*15.0	9.35	5.12
*15.0	6.78	4.74
*15.0	6.67	4.20
18.6	8.70	3.90
23.6	9.44	4.70

* These clouds were generated from an open heater—nichrome ribbon wound on mica, heated electrically.

Fig. 3.



The values of K show a decrease as the concentration, *i. e.* initial size of particle, increases.

Although the conditions of generation of the clouds were kept constant as far as possible, the number of particles which may be formed initially for any given concentration may vary within rather wide limits, *e. g.* three clouds of 15 mg. concentration contained 9.35×10^5 , 6.78×10^5 , and 6.67×10^5 particles per c.c. respectively. It seems that small differences in the way the vapour coming off the boat condenses and is subsequently diluted by fanning may make a considerable difference in the number of particles initially formed, and, unless more precise methods of producing these clouds are adopted, more closely reproducible results are not likely to be obtained.

However, it is noteworthy that the initial numbers on the whole increase slowly with concentration, and considering that the concentration varied by ten-fold this increase is somewhat surprisingly small.

A hypothesis which provides an explanation for this result is that the degree of dispersion of a cloud formed from vapour depends upon the degree of supersaturation of the vapour and the number and size of nuclei present in the air.

The vapour pressure of ammonium chloride is very low at normal temperatures so that a high degree of supersaturation probably existed over the heated boat. Now the degree of supersaturation would be more or less the same in all the experiments since only the time of dispersal was altered and the other conditions were kept constant as far as possible. Further, the air probably contained a fairly constant number of nuclei, since it had been rendered dust-free by passage through a filter.

Possibly both these nuclei and single or complex molecules of ammonium chloride act as condensation centres for the vapour as it first comes off the boat, and the particles so formed are drawn over the boat time and time again with the net result that their size is increased and very few fresh nuclei are brought into play as the dispersal is continued: hence the number of particles formed initially would increase very slowly with the concentration.

It is doubtful whether the air itself contained sufficient nuclei to act as centres of condensation for the formation of all the particles. Wilson* showed that there is a large number of nuclei present even in dust-free air, and estimated

* C. T. R. Wilson, *Phil. Trans. A*, cxcix. p. 265 (1897).

their number as being of the order 10^8 per c.c. Andrén *, however, dealing with air which had been carefully purified by previous cooling to -78°C. , obtained a maximum figure of 10^4 per c.c. when the air was saturated with water-vapour. These nuclei were considered by him to be complex water molecules. He also concluded that Wilson's estimate was too high.

An attempt has therefore been made to estimate the number of nuclei in air, freed from dust particles and then saturated with water-vapour. A small plunger type of Wilson apparatus, similar to the one described in the first part of this paper but having an ultra-microscope cell 3 cm. in diameter, was set up and the number of nuclei revealed at various expansion ratios determined by the photographic method.

A wider cell was made since it was doubtful whether the original narrow cell would have given a truly adiabatic expansion when the ratio was increased to a high limit, but the photographic arrangements were the same as those employed with the continuous-action Wilson apparatus. One difficulty encountered was due to the droplets moving very rapidly downward with a velocity greater than their terminal velocity immediately after their formation, when the expansion ratio was high, i. e. the cooling was very great. The intensity of the light was not sufficient to allow exposures of less than 1/50th second to be made, so that it was necessary to wait until the droplets slowed up before taking a photograph, and a few may have been lost owing to evaporation. The following results were obtained :—

TABLE IV.

Expansion ratio.	Degree of Supersaturation.	No. of nuclei per c.c. $\times 10^{-14}$.	No. of nuclei per c.c. $\times 10^{-4}$ (Andrén).
1.330	6.50	0.56	0.10
1.375	8.05	2.24	0.70
1.416	9.67	4.45	4.00
1.468	12.15	5.32	10.00 ca.
1.570	18.18	9.95	10.50 ca.

These results are in fair agreement with those of Andrén,

* Andrén, *Ann. d. Physik*, lii. p. 1 (1917).

Phil. Mag. S. 7. Vol. 4. No. 25. *Suppl.* Nov. 1927. 3 Z

although there is no indication of a "saturation" value being reached, a discrepancy that may be due to differences in the experimental conditions.

However, they serve to give an estimate of the number of nuclei in moist dust-free air which may act as centres of condensation for the formation of the ammonium chloride particles.

Results for Cadmium Oxide Clouds.

It was necessary to shorten the connecting tube between the Wilson apparatus and the chamber to 10 cm., since owing to the greater density of cadmium oxide there were considerable losses of particles in the long connecting tube. Clouds were formed by arcing between cadmium electrodes for 45 seconds, a current of 3 amperes being employed.

The clouds showed similar behaviour to the ammonium chloride ones. Results have been tabulated in the same way as before and a typical particulate volume curve has been plotted in fig. 4.

TABLE V.

Cloud.	Initial number of particles per c.c. $n_0 \times 10^{-6}$.	K. cm. ³ /min. $\times 10^8$.
I.	1.25	5.28
II.	1.08	4.65
III.	0.94	4.36
IV.	0.95	4.84
V.	1.37	3.84

Comparison between the Results Obtained by applying the Aitken Effect and those by using the Ultra-microscope directly.

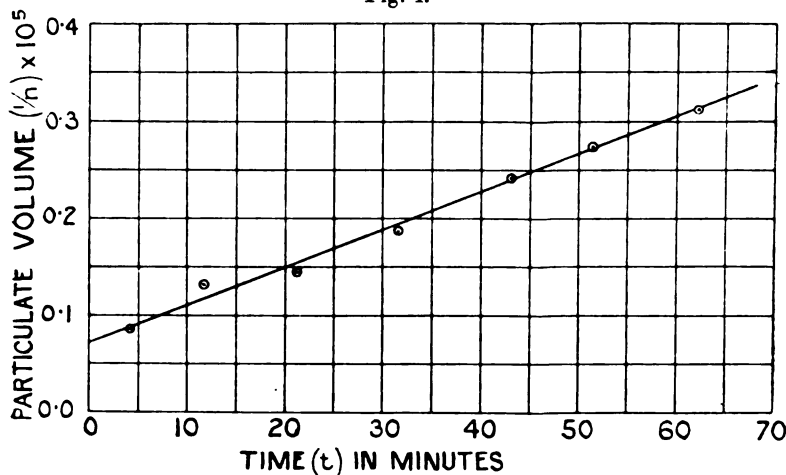
The writer has had the opportunity of comparing his results with recent ones obtained with a new type of visual ultra-microscope by Whytlaw-Gray. In this instrument the defects of the original type have been completely eliminated.

The limit of size of particle which can be detected visually is of the order 1×10^{-6} cm. radius, whilst the continuous-action Wilson apparatus would detect particles even smaller than 1×10^{-7} cm. in radius. A comparison

between the respective sets of results, particularly in regard to the slopes of the particulate volume curves, leads to the definite conclusion that the number of amicroscopic particles in these clouds is negligibly small.

In the case of cadmium oxide there do not appear to be any free ions of very small dimensions after the first few minutes; any such ions that are produced by the arc must be picked up by the visible particles within a very short space of time. No counts were made before three minutes

Fig. 4.



after dispersal of the clouds; there is a certain indication that the observations with the Wilson apparatus at this time are rather on the high side, and this may be due to the existence of free ions of a very small size.

Application of Smoluchowski's Theory.

The constant K has a wider significance if the coagulation of these clouds be considered from the point of view of Smoluchowski's theory of the mechanism of coagulation of sols. Smoluchowski*, by mathematical treatment of the chance collisions of particles owing to diffusion, derived an equation which can be expressed in the form

$$\frac{1}{n} = \frac{1}{n_0} + Kt, \quad (5)$$

where $K = 4\pi D \cdot Ra$, D being the diffusion coefficient and Ra the radius of sphere of action of a particle of radius r .

* Smoluchowski, *Zeit. f. Physik. Chem.* xcii. p. 129 (1918).

Whytlaw-Gray has calculated the value of K by substituting known values for the physical constants involved; putting in the constants for the conditions under which the clouds in these experiments were formed, it is found that

$$K = 8.63 \times 10^{-9} \frac{(1 + 9 \times 10^{-6}) R a}{r} \text{ cm.}^3/\text{min.}$$

Owing to the

fact that it is necessary to apply the Cunningham correction to the term for the mobility of the particles involved in the diffusion constant, K is no longer a constant but becomes a function of the radius of the particle. Assuming that the radius of sphere of action of a particle is twice its radius, it is possible to calculate the value for K for each of the ammonium chloride clouds in its initial stages. It is further necessary to assume an average value for the initial radii of the particles calculated from the weight of substance dispersed, the number of particles per c.c., and a density of the substance, taken as being that of the substance in bulk.

The figures for the series of clouds are tabulated below:—

TABLE VI.

Initial Average Radius of Particles. cm. $\times 10^5$.	K found. cm. ³ /min. $\times 10^9$.	K calculated. cm. ³ /min. $\times 10^9$.	K found/ K calculated.
0.75	7.42	3.78	1.96
1.02	7.85	3.26	2.41
1.07	5.00	3.18	1.65
1.08	6.40	3.17	1.93
1.12	7.45	3.12	2.38
1.36	5.12	2.88	1.84
1.49	3.90	2.77	1.41
1.52	4.74	2.76	1.72
1.53	4.20	2.76	1.52
1.56	4.70	2.73	1.74

No figures have been calculated for the cadmium oxide clouds since the concentrations were unknown.

The discrepancies between the actual and theoretical values of K for ammonium chloride are not any greater than might be expected, since the theoretical values were calculated on the simplest possible assumptions. There are several directions in which divergencies between the theoretical and practical conditions may arise.

(a) It has been assumed in making the calculations that the particles in the clouds are solid uncharged spheres and that coalescence takes place purely owing to particles coming into chance collision through diffusion. But it has been established by Patterson and Whytlaw-Gray * that particles are not necessarily spherical and that aggregates have a loose structure. The term "radius of sphere of action" cannot therefore have an exact significance, and its value may be several times that calculated on the basis that the original particles and complex particles are compact spheres.

(b) Although the majority of particles were uncharged when the clouds were generated, they picked up charges as the cloud aged owing to the natural ionization of the air. It is possible that the charges on particles exert some influence on the rate of coagulation of the cloud.

(c) No allowance has been made in these calculations for losses of particles due to falling out or diffusion to the sides of the chamber, but Whytlaw-Gray has shown that these would be small during the first hour and a half of the history of clouds of this type. Any such losses would tend to increase the apparent value of K .

(d) The density of the particles and of complexes in particular is likely to be less than that of the substance in bulk †, and therefore on this account the calculated values of K are possibly too high.

(e) All collisions have been considered effective in producing coalescence of particles, but if only a proportion are effective the theoretical values of K have again been over-estimated.

Until the influence of these factors has been investigated in detail it will not be possible to state definitely to what extent the Smoluchowski theory holds when applied to aerosols.

In conclusion, I should like to express my indebtedness to Professor R. Whytlaw-Gray, whose pioneer work on smokes was the inspiration of this research, and to Mr. J. D. Fry for their kind advice and criticism.

* H. S. Patterson and R. Whytlaw-Gray, Proc. Roy. Soc. A, cxiii, p. 302 (1926).

† H. S. Patterson and R. Whytlaw-Gray, *loc. cit.*

XCVII. *Atomic Structure and the Magnetic Properties of Coordination Compounds.*—Part II. By L. C. JACKSON, M.Sc., Ph.D., A.Inst.P., Henry Herbert Wills Research Fellow, Department of Physics, The University, Bristol*.

IT is proposed in the present paper to continue further the discussion of the magnetic properties of coordination compounds in the light of the schemes put forward by Welo and Baudisch, by Bose, and by Cabrera†. Special reference will be made to those compounds the properties of which appear to be anomalous and to present difficulties to the explanatory schemes suggested. In addition the discussion, which was confined in Part I. to the case of mononuclear coordination compounds, is extended to the case of those multinuclear compounds the magnetic properties of which are known.

Anomalies and Difficulties.

The theories discussed in Part I. set out to provide an explanation in terms of electronic distributions of the magnetic properties of coordination compounds, taking these properties to be such that compounds of Co^{+++} , Fe^{++} are diamagnetic, and those of Cr^{+++} , Fe^{+++} , Ni^{++} , Cu^{++} are paramagnetic with Weiss magneton numbers approximately equal to 19, 11, 16, and 10 respectively, except for the carbonyls, which received separate treatment. The majority of sixfold and fourfold coordination compounds which have been investigated actually possess the magnetic properties enumerated above, but there are various exceptions which do not fit directly into the scheme put forward. It is proposed to discuss these anomalies now.

In the first place, we may mention the iron and nickel carbonyls, $\text{Fe}(\text{CO})_5$ and $\text{Ni}(\text{CO})_4$. The theories of Welo and Baudisch and of Bose can give apparently satisfactory explanations of the magnetic properties of these compounds, both of which are diamagnetic. They were not, however, discussed in Part I., as the paper was limited to the material which is common to the three papers considered, and Cabrera does not deal with these compounds. It may be pointed out here that Cabrera's scheme is, however, able to give an explanation of the magnetic properties of the iron and nickel carbonyls in a manner not more arbitrary than the other

* Communicated by the Author.

† For a list of references see Part I. of this paper, Phil. Mag. ii. 86 (1926).

two schemes. If the two compounds are formulated as $[\text{Ni}(\text{CO})_3]\text{CO}$ and $[\text{Fe}(\text{CO})_4]\text{CO}$, and the two metals being divalent and each CO group involving the transfer of two electrons as assumed by Weio and Baudisch and by Bose, the Fowler scheme for the distribution of the "binding electrons" will hold. Then the iron carbonyl will be expected to be diamagnetic, as are other coordination compounds of ferrous iron, the electron distribution in the Fe^{++} ion being the same in the two cases. On the other hand, the nickel carbonyl, if supposed to have the same electron distribution in the Ni^{++} ion as in other nickel coordination compounds, would be expected to be paramagnetic. If, however, in this compound the electron distribution is

$$\begin{array}{ccc} \text{M}_{32} & \text{M}_{33} & \text{N}_{11} \\ 0 & 6 & 2 \end{array}$$

in place of that assumed for other (in Cabrera's scheme only for sixfold) compounds of nickel, viz.

$$\begin{array}{ccc} \text{M}_{32} & \text{M}_{33} & \text{N}_{11}, \\ 2 & 6 & 0 \end{array}$$

then the carbonyl would be diamagnetic, as is observed. This assumption may seem arbitrary, but something of the kind is necessary, as there are also nickel coordination compounds such as $\text{Na}_2\text{Ni}(\text{CN})_4$ which are diamagnetic and which present a difficulty to the three theories discussed in Part I. The case of these compounds will be discussed in a later section.

It may be mentioned that Bose states that in his scheme the coordination number appears as half the difference in the number of electrons in the normal ion and that in the coordinated atom. If, as it would appear, he takes the nickel and iron carbonyls as being fourfold and fivefold compounds respectively, then he must attribute the valency zero to the normal ion. This point is similar to the definite suggestion recently put forward by Weiss* that the metallic atom in these carbonyls has a valency zero; but this does not seem likely to be generally acceptable.

The next example of an apparently anomalous substance may be ferric acetylacetonate, the properties of which have been determined by Feytis† and Ishiware‡. In this case the magnetic moment corresponds to that in simple salts. It would then seem that the coordinated atoms in these

* *Comptes Rendus*, clxxxiv. p. 417 (1927).

† *Comptes Rendus*, clii. p. 708 (1911).

‡ *Sci. Rep. Tohoku*, iii. p. 303 (1914).

compounds have the same electronic distribution as in the ions of the corresponding simple salts. This requirement would raise a considerable difficulty for the theories of Welo and Baudisch and of Bose, in which the electrons from the coordinating groups pass into the structure of the central atom. It does not, however, present any such difficulty for Cabrera's scheme.

If each acetylacetonate group gave up only one electron, then the compound could theoretically be formulated as threefold in a manner consistent with the Fowler scheme and with the magnetic properties. However, each acetylacetonate group is regarded chemically as linked to the ferric ion by a principal and a subsidiary valency, and it does not seem satisfactory that these two bonds should be represented by the transference of a single electron. On the other hand, if each group gives up three electrons, the compound can be formulated as sixfold in the same way as $[\text{Co}(\text{en})_3]\text{Cl}_3$ is regarded as sixfold. The compound would then be expected to be paramagnetic with a magneton number of approximately 11. One might, however, reject the idea that the symmetry of the arrangement of the outer groups and their "binding electrons" is responsible for the rearrangement among the electrons of the M level of the central atom. If this is done then there will be no obvious reason why the electronic arrangement should not in some cases be the same as in simple salts. Cabrera's scheme, with the limitation mentioned, would thus be able to include also coordination compounds whose magnetic properties are those of simple salts rather than those associated with the majority of such compounds. It would then be proposed to accept the general scheme proposed by Cabrera; but there would still have to be found some more general reason for the distribution of the electrons than that originally suggested. On the other hand, one may not have to reject any part of Cabrera's scheme, for it may be that in ferric acetylacetonate, a compound of quite different class from the sixfold compounds such as $[\text{Co}(\text{NH}_3)_6]\text{Cl}_3$ with which Cabrera deals, the actual symmetry of the distribution of the "binding electrons" may be quite different from that in the other class of compounds mentioned. The tendency to redistribute the electrons of the M level of the Fe^{+++} ion would then be absent, so that ferric acetylacetonate would be expected to have the same magnetic properties as simple ferric salts.

Further examples of coordination compounds with magnetic properties differing from those usually found can be mentioned. Thus the complex nickel cyanides

$\text{Na}_2\text{Ni}(\text{CN})_4$ and $\text{K}_2\text{Ni}(\text{CN})_4$ are stated by Depold* to be diamagnetic. No immediate explanation of this anomaly seems to be possible on the schemes of Welo and Baudisch and of Bose, but, by applying to these compounds the idea previously mentioned when dealing with the carbonyls, a generalization of the scheme proposed by Cabrera does seem capable of furnishing an explanation.

One other point may be mentioned while dealing with difficulties encountered by the theories. At the end of Part I. it was mentioned that while generally compounds such as $\text{CoCl}_2 \cdot 6\text{H}_2\text{O}$ and $\text{NiSO}_4 \cdot 6\text{H}_2\text{O}$ would be regarded magnetically as examples of simple salts, they have been formulated by Werner as typical sixfold coordination compounds $[\text{Co}(\text{OH}_2)_6]\text{Cl}_2$ and $[\text{Ni}(\text{OH}_2)_6]\text{SO}_4$. It would seem necessary to consider whether there is any evidence from the magnetic data to enable one to distinguish between the two viewpoints and, in particular, to show that the latter is not in contradiction with the observed properties. It may be stated immediately that the magnetic data cannot decide the question, as we have seen that typical coordination compounds may either always have the same properties as the simple salts as in Cr^{+++} or may exceptionally possess them rather than those usually attributed to coordination compounds as in Fe^{+++} . To take, however, the particular examples cited above, $\text{CoCl}_2 \cdot 6\text{H}_2\text{O}$ and $\text{NiSO}_4 \cdot 6\text{H}_2\text{O}$, it would be expected with a large degree of certainty that $[\text{Ni}(\text{OH}_2)_6]\text{SO}_4$ would be paramagnetic with a magneton number of approximately 16, as is actually the case. One cannot say with equal certainty what would be the magnetic properties of $[\text{Co}(\text{OH}_2)_6]\text{Cl}_2$ as we have no data for sixfold coordination compounds of divalent cobalt. In all the coordination compounds of cobalt investigated by Rosenbohm this element was tervalent. In cobaltous acetylacetonate,

$\text{Co}(\text{CH}_3\text{CO} > \text{CH})_2$, we have, however, an example of a coordination compound of divalent cobalt. The susceptibility of this substance at atmospheric temperature has been determined by Feytis†. From the value given, it is seen that the assumption of a reasonable value for Δ would make the magneton number equal to that found in the simple salts of divalent cobalt. Thus, as far as the evidence goes, it seems probable that the majority of coordination compounds of divalent cobalt would have the same magnetic properties

* Dissertation, Halle (1913).

† *Comptes Rendus*, clii. p. 708 (1911).

as the simple salts, just as is the case with the corresponding salts of divalent nickel. It would therefore be expected that $[\text{Co}(\text{OH}_2)_6]\text{Cl}_2$ would be paramagnetic with a magneton number of approximately 24. The formulation of the hexahydrates as sixfold coordination compounds, at least in the cases considered, would then not be in disaccord with the observed magnetic properties.

Possible Experimental Test of the Theories.

It would seem to be just within the limits of possibility to make an experimental test of the various schemes that have been proposed for the explanation of the magnetic properties of coordination compounds. According to the schemes of Welo and Baudisch and of Bose, the number of electrons associated with the central coordinated atom is considerably greater than that of the normal ion in simple salts. In Cabrera's scheme the number of electrons associated with the central atom is the same as in the simple salts, the "binding electrons" forming a group associated with the molecule as a whole. It would therefore seem possible that a study of the intensity of the reflexion of X-rays from crystals of coordination compounds and simple salts of the same element would serve to determine whether the larger electron concentration in the central atom in the coordination compounds as postulated by the first two theories is actually present. On Cabrera's scheme the scattering power of the metallic atom should be very approximately the same in the two classes of compound, the change in scattering power due to the rearrangement of the electrons in the M level being probably too small to be detected experimentally. The proposed investigation would therefore seem able to serve as a definite test of the theories.

The Magnetic Properties of Multinuclear Coordination Compounds.

Of the data available concerning the magnetic properties of multinuclear coordination compounds, the majority are due to Rosenbohm. In addition, a few compounds have been measured by Feytis. The information given in Rosenbohm's paper relates only to compounds of cobalt and of chromium, and the measurements were carried out only at atmospheric temperature, so that the data available for discussion are as yet meagre and the magnetic moments of the molecules are uncertain.

BINUCLLEAR COMPOUNDS I.

Rosenbohm gives the values of the susceptibilities of a large number of "position" isomers of the type $[\text{Cr}(\text{NH}_3)_6]$ $[\text{Co}(\text{ON})_6]$, $[\text{Co}(\text{NH}_3)_6]$ $[\text{Cr}(\text{CN})_6]$. The data are reproduced below in Table I.

TABLE I.

Substance.	$\chi \times 10^6$.	$\chi_{\text{corr.}} \times 10^6$.	$M_{\text{corr.}} \times 10^6$.
$[\text{Cr}(\text{NH}_3)_6]$ $[\text{Co}(\text{ON})_6]$	17.78	17.05	6287
$[\text{Co}(\text{NH}_3)_6]$ $[\text{Cr}(\text{CN})_6]$	17.99	17.25	6364
$[\text{Cr}(\text{en})_3]$ $[\text{Cr}(\text{CN})_6]$	31.60	30.29	13340
$[\text{Cr}(\text{en})_3]$ $[\text{Co}(\text{CN})_6]$	14.64	14.04	6277
$[\text{Co}(\text{en})_3]$ $[\text{Cr}(\text{ON})_6]$	14.81	14.19	6364
$[\text{Cr}(\text{pn})_3]$ $[\text{Cr}(\text{ON})_6]$	28.67	27.48	13270
$[\text{Cr}(\text{pn})_3]$ $[\text{Co}(\text{CN})_6]$	13.43	12.87	6287
$[\text{Co}(\text{pn})_3]$ $[\text{Cr}(\text{CN})_6]$	13.61	13.05	6374
$[\text{Co}(\text{pn})_3]$ $[\text{Co}(\text{CN})_6]$	-0.332	-0.318	-154
$[\text{Cr}(\text{NH}_3)_6]$ $[\text{Cr}(\text{O}_2\text{O}_4)_3]$	29.57	28.34	13320
$\begin{bmatrix} (\text{NH}_3)_4 \\ \text{Cr} \\ (\text{C}_2\text{O}_4)_2 \end{bmatrix}$ $\begin{bmatrix} (\text{NH}_3)_2 \\ \text{Cr} \\ (\text{C}_2\text{O}_4)_2 \end{bmatrix}$	29.56	28.33	13320
$[\text{Cr}(\text{NH}_3)_6]$ $[\text{Co}(\text{C}_2\text{O}_4)_3]$	18.80	18.01	8597
$[\text{Co}(\text{NH}_3)_6]$ $[\text{Cr}(\text{C}_2\text{O}_4)_3]$	13.75	13.18	8597
$[\text{Cr}(\text{en})_3]$ $[\text{Cr}(\text{O}_2\text{O}_4)_3]$	25.41	24.35	13360
$\begin{bmatrix} (\text{en})_2 \\ \text{Cr} \\ (\text{C}_2\text{O}_4)_2 \end{bmatrix}$ $\begin{bmatrix} (\text{en}) \\ \text{Cr} \\ (\text{C}_2\text{O}_4)_2 \end{bmatrix}$	25.39	24.33	13330
$[\text{Cr}(\text{en})_3]$ $[\text{Co}(\text{O}_2\text{O}_4)_3]$	14.41	13.81	7640
$\begin{bmatrix} (\text{en})_2 \\ \text{Co} \\ (\text{C}_2\text{O}_4)_2 \end{bmatrix}$ $\begin{bmatrix} (\text{en}) \\ \text{Cr} \\ (\text{C}_2\text{O}_4)_2 \end{bmatrix}$	12.02	11.52	6384
$[\text{Co}(\text{en})_3]$ $[\text{Cr}(\text{O}_2\text{O}_4)_3]$	12.00	11.50	6374
$\begin{bmatrix} (\text{en})_2 \\ \text{Cr} \\ (\text{C}_2\text{O}_4)_2 \end{bmatrix}$ $\begin{bmatrix} (\text{en}) \\ \text{Co} \\ (\text{C}_2\text{O}_4)_2 \end{bmatrix}$	12.17	11.66	6509
$[\text{Cr}(\text{pn})_3]$ $[\text{Co}(\text{C}_2\text{O}_4)_3]$	11.74	11.25	6727
$\text{Co}(\text{pn})_3]$ $[\text{Cr}(\text{C}_2\text{O}_4)_3]$	10.93	10.48	6287
$[\text{Cr}(\text{en})_3]$ $[\text{Cr}(\text{SCN})_6]$	21.97	21.06	13320
$[\text{Cr}(\text{pn})_3]$ $[\text{Cr}(\text{SCN})_6]$	20.63	19.77	13350
$\begin{bmatrix} (\text{en})_2 \\ \text{Cr} \\ (\text{SCN})_2 \end{bmatrix}$ $[\text{Cr}(\text{SCN})_6]$ cis.	22.00	21.09	26720
	trans. 22.03	21.11	26760

In the above table the second column gives the values of

the susceptibilities direct from Rosenbohm's paper, the third and fourth columns the susceptibilities and molecular susceptibilities respectively corrected as mentioned below; *en* and *pn* stand for ethylenediammine and propylenediammine respectively.

Firstly, it may be pointed out that, formally at least, the ideas put forward by Fowler concerning the structure of mononuclear coordination compounds will apply also to these binuclear compounds. Taking both cobalt and chromium to be trivalent in these substances and calculating the number of electrons shared with or transferred to the coordinated atoms, we find that the total is always twenty-four.

On examining Table I. it will be seen that, as in the majority of other coordination compounds, those containing Co^{+++} are diamagnetic and those containing Cr^{+++} are paramagnetic. As will be seen later, the magnetic moment possessed by the chromium atom is the same approximately as that in the mononuclear compounds, and hence the electronic arrangements in the Co^{+++} and Cr^{+++} ions are respectively the same in the two classes of compounds, so that the points under discussion in Part I. will apply equally.

The corrected values in columns 3 and 4 of Table I. have been recalculated from Rosenbohm's data, using the now accepted value for the susceptibility of water 0.719×10^{-6} instead of 0.75×10^{-6} as used by Rosenbohm. On examining the last column of Table I. certain regularities pointed out by Rosenbohm will be apparent, constant differences in susceptibility occurring in pairs of "position" isomers, the values about 6287 and 6364 reappearing several times. Certain substances in the table, oxalate-compounds, appear to be anomalous, the molecular susceptibilities being considerably greater than in the other compounds in the list. This anomaly is in each case apparently due to the presence of the group $[\text{Co}(\text{C}_2\text{O}_4)_3]$. It must be mentioned that Feytis has also investigated some of the substances in question and did not obtain abnormally high values, but her values for the susceptibilities even of other compounds are consistently lower than those of Rosenbohm. The compounds are worthy of further study with a view to clearing up the present discrepancy in the information.

To obtain some idea of the magnitude of the magnetic moment carried by the chromium atoms in these binuclear compounds and of the probable order of accuracy of the data, the Weiss magneton numbers have been calculated for several of the compounds and are given in Table II. It is, however, to be emphasized that nothing is known of the

temperature variation of the susceptibilities of the compounds, and the supposition that they all obey Curie's law is a pure assumption. A study of the thermal variation is necessary before an adequate discussion of the data can be made. Before one can calculate the magneton number of the chromium atom, one must be able to evaluate the correction to be applied to the molecular susceptibilities to allow for the contributions due to the other parts of the molecule. Thus in the compound $[\text{Cr}(\text{NH}_3)_6][\text{Co}(\text{CN})_6]$ the diamagnetism of the NH_3 and CN groups can be allowed for, using Pascal's data; but one has also to bear in mind that the cobalt atom in such compounds carries a small but definite positive moment of as yet unknown origin. It is more convenient to treat the groups $[\text{Co}(\text{NH}_3)_6]$, $[\text{Co}(\text{CN})_6]$, etc., as a whole. Their properties can be deduced from Rosenbohm's data as follows. The molecular susceptibility of $[\text{Co}(\text{NH}_3)_6]\text{Cl}_3$ is known, and the contribution of the Cl_3 is obtained from Pascal's data; hence the part of the molecular susceptibility due to the $[\text{Co}(\text{NH}_3)_6]$ group can be calculated. The same process can be applied to $[\text{Co}(\text{en})_3]$ and $[\text{Co}(\text{pn})_3]$. That of $[\text{Co}(\text{CN})_6]$ cannot be obtained in the same way, but the molecular susceptibility of $[\text{Co}(\text{pn})_3][\text{Co}(\text{ON})_6]$ is given in Table I., and the required value can be obtained from this.

The corrected values of the molecular susceptibilities of such of the mixed chromium-cobalt compounds as can be treated in this way, and also of the compounds containing only chromium in which the diamagnetic proportion of the NH_3 , CN , etc., groups has also been allowed for, are given in Table II.

Table II.

Substance.	$M' \times 10^6$	n .
$[\text{Cr}(\text{NH}_3)_6][\text{Co}(\text{CN})_6]$	6690	
$[\text{Co}(\text{NH}_3)_6][\text{Cr}(\text{CN})_6]$	6770	
$[\text{Cr}(\text{en})_3][\text{Co}(\text{CN})_6]$	6737	19.3
$[\text{Co}(\text{en})_3][\text{Cr}(\text{CN})_6]$	6833	(From mean of previous column.)
$[\text{Cr}(\text{pn})_3][\text{Co}(\text{CN})_6]$	6780	
$[\text{Co}(\text{pn})_3][\text{Cr}(\text{CN})_6]$	6870	
$[\text{Cr}(\text{en})_3][\text{Cr}(\text{CN})_6]$	14139	19.7
$\left[\begin{smallmatrix} \text{Cr} \\ (\text{en})_2 \\ (\text{SCN})_2 \end{smallmatrix} \right][\text{Cr}(\text{CN})_6]$	28505	20.1

The values now do not show the regularities noticed in column 3 of Table I. The Weiss magneton numbers are

given in column 3 of Table II. They appear to increase with increasing molecular weight of the compound. This is possibly only apparent, and may be due to these substances not following Curie's law. The magneton numbers are, however, all of the same order of magnitude as those found in the mononuclear coordination compounds and in the simple salts of tervalent chromium, so that these compounds do not seem to show any new features of interest.

BINUCLEAR COMPOUNDS II.

A further class of compounds containing two coordinated atoms have been investigated by Rosenbohm. These are the diol compounds contained in Table III. All the values of the susceptibilities have been corrected to 0.719×10^{-6} for the susceptibility of water.

TABLE III.

Substance.	$\chi \times 10^6$.	$M \times 10^6$.	$M' \times 10^6$	n .
$\left[\begin{array}{c} \text{OH} \\ (\text{NH}_3)_4\text{Co} \end{array} \begin{array}{c} \text{Co}(\text{NH}_3)_4 \\ \text{OH} \end{array} \right] \text{Cl}_4 + 4\text{H}_2\text{O}$	-2.14			
" $\text{Br}_4 + 4\text{H}_2\text{O}$	-1.14			
" $(\text{SCN})_4$	-1.03			
$\left[\begin{array}{c} \text{OH} \\ (\text{en})_2\text{Co} \end{array} \begin{array}{c} \text{Co}(\text{en})_2 \\ \text{OH} \end{array} \right] \text{Br}_4 + 2\text{H}_2\text{O}$	-1.85			
" $(\text{NO}_3)_4$	-2.53			
$\left[\begin{array}{c} \text{OH} \\ (\text{en})_2\text{Cr} \end{array} \begin{array}{c} \text{Cr}(\text{en})_2 \\ \text{OH} \end{array} \right] \text{Br}_4$	14.66	10225	10545	17.4
" I_4	12.36	10948	11335	18.0
$\left[\begin{array}{c} \text{OH} \\ (\text{C}_2\text{O}_4)_2\text{Cr} \end{array} \begin{array}{c} \text{Cr}(\text{C}_2\text{O}_4)_2 \\ \text{OH} \end{array} \right] \text{Na}_4$	14.81	8620	8799	15.9

The cobalt compounds are diamagnetic and the chromium compounds paramagnetic, as was to be expected. The agreement among the values of the magneton numbers of the chromium compounds is not at all good, but may be due to the substances showing different deviations from Curie's law. The values for the first two compounds are, allowing a reasonable Δ in each case, sufficiently near to the value

found for simple salts and the mononuclear compounds to suggest that the chromium atoms possess the same electronic configuration in all the compounds.

TRINUCLEAR COMPOUNDS.

Rosenbohm gives the values of the susceptibilities of the chromium coordination compounds containing three chromium atoms, the formulæ of which are as follows :—

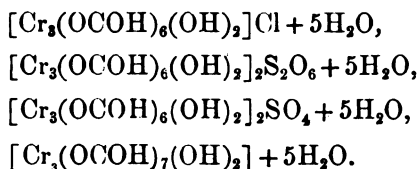


TABLE IV.

Substance.	$\chi \times 10^6$.	$M \times 10^6$.	$M' \times 10^6$.	n .
$[\text{Cr}_3(\text{OCOH})_7(\text{OH})_2] + 5\text{H}_2\text{O}$	23·76	14137	14344	16·6
$[\text{Cr}_3(\text{OCOH})_6(\text{OH})_2]\text{Cl} + 5\text{H}_2\text{O}$	24·83	14540	14748	16·8
$[\text{Cr}_3(\text{OCOH})_6(\text{OH})_2]_2\text{S}_2\text{O}_6 + 5\text{H}_2\text{O}$	23·51	27510	27885	16·3
$[\text{Cr}_3(\text{OCOH})_6(\text{OH})_2]_2\text{SO}_4 + 5\text{H}_2\text{O}$	22·51	24890	25240	15·5

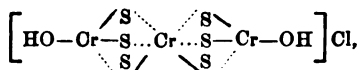
Rosenbohm's values have been corrected as before. The first three chromium compounds, on assuming Curie's law, give Weiss magneton numbers approximating to 16·5. (The fourth compound as it stands appears to be anomalous, giving 15·5. If, however, the figures 23·48 in the original paper were a misprint for 25·48, the compound would fall into line with the others.)

The absence of any knowledge of the actual temperature variation of the susceptibilities of these compounds prevents anything definite being stated with regard to the configuration of the paramagnetic atoms, but the value 16·5 for the chromic compounds suggests an idea which may not be too speculative to be mentioned here.

These magneton numbers are considerably different from those met with in other coordination compounds. This suggests that the three atoms in the molecule do not all carry the same magnetic moment so that the calculated magneton numbers are "effective" magneton numbers obtained by taking the root-mean-square of the values

1080 *Structure and Properties of Coordination Compounds.*

actually present. From a consideration of the configurations of the molecules, the formula of the dihydroxyhexaformato-chromi chloride being written



in which S stands for the formato group O·COH and full lines for principal valencies and dotted lines for subsidiary valencies, it seems not unlikely that the central chromium atom may be in a different state from the other two. If, now, it is assumed that there really exists a small negative Δ for all these compounds so that the actual magneton numbers are somewhat smaller than those calculated on the assumption of Curie's law, then the values obtained will be reproduced if the chromium atoms carry moments equal to 19, 0, 19 Weiss magnetons. The value usually found for chromium compounds is 19. This can easily be verified by a simple calculation; but the actual values are not given here, since there can be no question at present of any accurate numerical agreement between the observed and calculated values.

Summary.

The discussion of the magnetic properties of coordination compounds is continued in the light of the theories of Welo and Baudisch, of Bose, and of Cabrera. Particular attention is paid to those compounds which are apparently anomalous and which present various difficulties to the theories as yet proposed. The conclusion is reached that Cabrera's scheme is better able to account for the magnetic properties of coordination compounds in general than the other two schemes.

The discussion which was limited in Part I. of the present paper to the mononuclear coordination compounds is now extended to the multinuclear coordination compounds.

The H. H. Wills Physical Laboratories,
The University, Bristol.
May 1927.

XCVIII. *Resonant Circuits with Reactive Coupling.*
By R. T. BEATTY, M.A., B.E., D.Sc.*

1. *Introduction.*

IN this paper the fundamental equations considered are linear with constant coefficients, so that the discussion must be limited to the subject of amplification over a linear region of the characteristic curve and under conditions where the grid current is negligible: that is, the amplification is without distortion. The problem is simplified without using approximations by the introduction of equivalent circuits, and a representation by means of curves derived from a parabola is given, by help of which the behaviour of the circuits can be ascertained by inspection.

The geometry of the parabola is used to facilitate the discussion of amplification and resonance curves, and an attempt is made to give a quantitative basis for the treatment of selectivity by the introduction of two new terms—"tolerance" and "activity."

LIST OF SYMBOLS.

General Circuits.

Z_0	a_0	impedance, admittance of	grid-plate plate grid	circuit.
Z_1	a_1			
Z_2	a_2			
i_0	i_1	alternating currents flowing through Z_0 Z_1 Z_2 .		
e		alternating e.m.f. injected in grid circuit.		
e_1		alternating p.d. between	plate and filament grid and filament	
e_2				
S		internal	resistance admittance	from plate to filament.
s_x				
a_{g1}		equivalent total	grid input admittance.	
a_g				
$g = \mu s_x$		mutual conductance of valve.		
$K_0 - s_0$		capacity, inductance, conductance of	grid-plate plate grid	circuit.
K_1	L_1			
K_2	L_2			

* Communicated by the Author.

Equivalent Circuits.

$C_0 \sigma_0$	capacity, inductance, conductance of	grid-plate	circuit.
$C_1 L_1 \sigma_1$		plate	
$C_2 L_2 \sigma_2$		grid	
$\omega_1 \omega_2$	pulsatance at resonance	of plate circuit	of grid circuit.
$m_1 m_2$	maximum voltage		
	amplification		
* $\alpha_1 \alpha_2$	log of ratio of impressed pulsatance to that		
$t_1 t_2$	tangent of phase-angle		
$\sinh \alpha_1 = \partial \omega / \omega_1$	} approximately.		
$\sinh \alpha_2 = \partial \omega / \omega_2$			
g	mutual conductance of equivalent valve.		
ω	pulsatance of impressed frequency.		
ω_0	pulsatance to which whole circuit is tuned.		
m	m_1 or m_2 when $m_1 = m_2$.		
$p = C_0 \omega / g$.			
$N_1 = \sigma_0 g / \sigma_1 \sigma_2$.			
$N_2 = C_0 \omega g / \sigma_1 \sigma_2$.			
$N / \nu = N_1 + j N_2$.			
T	tolerance	of circuit or circuits : values in Table.	
Ac	activity		
$\partial \omega / \omega_0$	frequency departure		
y	ordinate of resonance curve.		
$A = C_2 \omega_2 g / \sigma_1 \sigma_2$	{ maximum voltage amplification for two circuits without reaction.		
F_0	reaction factor.		
F / ϕ	vector whose maximum modulus is F_0 .		
$t_0 = \tan \theta_0$	value of $t_1 = t_2$ corresponding to F_0 .		
$h = m_1 / m_2$.			
$\beta = 4h / (1 + h)^2$.			

Geometrical.

xy	coordinates of origin of vector N .		
$x_h y_h$	coordinates of a point corresponding to h .		
l	length of any line,	to parabola from xy	
n	length of normal	to parabola from $x_h y_h$	
$F / \phi, F_0, N / \nu, N_1, N_2, \beta, t_0, t_1, t_2$	also appear geometrically.		

* Thus $e^{\alpha_1} = \omega / \omega_1$.

2. General Equations for Two Circuits with Reactive Coupling.

The arrangement is shown in fig. 1. An impedance Z_1 is connected to the output side of a valve, while impedances Z_2, Z_3 are connected to the input side. The plate-filament and grid-filament capacities, together with any resistances which may be associated with them, are included respectively in Z_1 and Z_3 . Any impedance Z_0 may be connected between plate and grid, and will include the plate-grid capacity. S represents the internal plate-filament resistance of the valve: an e.m.f. e is injected in series with Z_2 .

The equations for the currents as derived by Miller are :

i_2	i_0	i_1
$Z_2 + Z_3$	$-Z_3$	0
$-Z_3[\mu + 1]$	$Z_3[\mu + 1] + Z_0 + S$	$-S$
$-Z_3$	$Z_0 + Z_3$	Z_1

$$\left. \begin{array}{c} \\ \\ \\ \end{array} \right\} = e \quad (1)$$

The determinant may be written :

$$\begin{vmatrix} 11 & 12 & 13 \\ 21 & 22 & 23 \\ 31 & 32 & 33 \end{vmatrix} \dots \dots \dots (2)$$

The relation between i_2 and e when $Z_2=0$ is given by

$$\frac{i_2}{e} = \frac{\Delta_{11}}{\Delta} = \frac{Z_1[\mu + 1] + S}{Z_1S + Z_3[Z_1 + S]} + \frac{1}{Z_3} \dots \dots (3)$$

Hence, as regards phenomena in the input circuit, the valve and the output circuit which is coupled to it may be replaced by an impedance in parallel with Z_2 and Z_3 . The reciprocal of this impedance is known as the equivalent grid input admittance, which will be referred to as a_{g1} : its value is given by the first term on the right side of equation (3).

Miller's equations (1) are not the most suitable for the development of this paper, and we will use instead equations corresponding to the scheme shown in fig. 2, where impedances are replaced by admittances and the variables are the potential differences e_1, e_2 .

It is easily shown that the following equations hold :—

e_1	e_2	= $e \cdot a_2$, . . . (4)
$-a_0$	$a_0 + a_2 + a_3$	
$s_x + a_0 + a_1$	$g_1 - a_0$	

where g_1 is the mutual conductance of the valve.

Figs. 1-5.

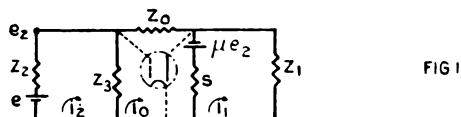


FIG 1

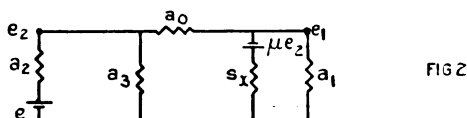


FIG 2

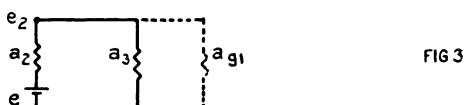


FIG 3

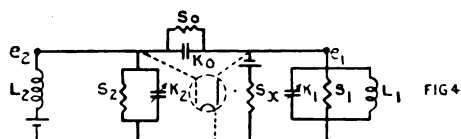
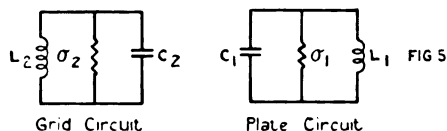


FIG 4



Grid Circuit

Plate Circuit

The equivalent grid input admittance a_{g1} (fig. 3) is given by

$$\frac{e \cdot a_2}{e_2} = a_2 + a_3 + a_{g1} \quad \dots \dots \dots (5)$$

But

$$\frac{e \cdot a_2}{e_2} = \frac{-\Delta}{\Delta_{12}} = a_2 + a_3 + a_0 + \frac{a_0[g_1 - a_0]}{s_x + a_0 + a_1} \quad \dots \dots (6)$$

Hence

$$a_{g1} = a_0 + \frac{a_0[g_1 - a_0]}{s_x + a_0 + a_1} \quad \dots \dots \dots (7)$$

The voltage amplification from grid to plate is

$$\frac{e_1}{e_2} = \frac{-[g_1 - a_0]}{s_X + a_0 + a_1} \cdot \cdot \cdot \cdot \cdot \quad (8)$$

The voltage amplification from input to grid is

$$\frac{e_2}{e} = \frac{a_2[s_X + a_0 + a_1]}{a_0[g_1 - a_0] + [s_X + a_0 + a_1][a_0 + a_2 + a_3]} \cdot \cdot \cdot \quad (9)$$

3. Two Resonant Circuits.

We will now develop the special case where both grid and plate circuits are tuned with reactive coupling, as shown in fig. 4.

Comparison with fig. 2 discloses the following identities:—

$$\left. \begin{aligned} a_0 &= s_0 + j\omega K_0, \\ a_1 &= s_1 + j\omega K_1' + \frac{1}{j\omega L_1}, \\ a_2 &= \frac{1}{j\omega L_2}, \\ a_3 &= s_2 + j\omega K_2. \end{aligned} \right\} \cdot \cdot \cdot \cdot \quad (10)$$

The voltage amplification is, by (8) and (9),

$$\frac{e_1}{e} = \frac{-a_2[g_1 - a_0]}{[s_X + a_0 + a_1][a_0 + a_2 + a_3] + a_0[g_1 - a_0]} \cdot \quad (11)$$

Substituting from (10) and using abridged notation, we have

$$\left. \begin{aligned} a_0 &= s_0 + jK_0\omega, \\ a_2 &= \frac{1}{jL_2\omega}, \\ s_X + a_0 + a_1 &= s_{10X} + j\left[K_{10}\omega - \frac{1}{L_1\omega}\right], \\ a_0 + a_2 + a_3 &= s_{20} + j\left[K_{20}\omega - \frac{1}{L_2\omega}\right], \end{aligned} \right\} \cdot \quad (12)$$

where, for example,

$$s_{10X} = s_1 + s_0 + s_X.$$

4. Simplified Notation and Equivalent Circuits.

The composite capacities and conductances which occur with multiple suffices in the preceding equations may now

be treated as single elements, and with this view the notation will be simplified as follows:—

Notation.

$$\left. \begin{array}{l} \text{OLD ... } L_1 \ L_2 \ K_0 \ K_{10} \ K_{20} \ s_{10x} \ s_{20} \ s_0 \ g_1 - s_0, \\ \text{NEW... } L_1 \ L_2 \ C_0 \ C_1 \ C_2 \ \sigma_1 \ \sigma_2 \ \sigma_0 \ g; \end{array} \right\} \quad (13)$$

and equivalent grid and anode circuits will be dealt with: these are shown in fig. 5.

The following symbols will be required to relate the frequency of the impressed wave to that of the resonance frequencies of the circuits in fig. 5:—

$$\left. \begin{array}{ll} \omega_1^2 = \frac{1}{C_1 L_1}, & \omega_2^2 = \frac{1}{C_2 L_2}, \\ m_1 = \frac{1}{\sigma_1 L_1 \omega_1}, & m_2 = \frac{1}{\sigma_2 L_2 \omega_2}, \\ \alpha_1 = \log \frac{\omega}{\omega_1}, & \alpha_2 = \log \frac{\omega}{\omega_2}, \\ t_1 = 2m_1 \sinh \alpha_1, & t_2 = 2m_2 \sinh \alpha_2, \end{array} \right\} \quad \text{. . . (14)}$$

together with the symbols:

$$p = \frac{C_0 \omega}{g}, \quad \text{. (15)}$$

$$N_1 = \frac{\sigma_0 g}{\sigma_1 \sigma_2}, \quad \text{. (16)}$$

$$N_2 = \frac{C_0 \omega_2 g}{\sigma_1 \omega_2} \quad \text{. (17)}$$

Using the new notation given in (13) and the symbols given in (15, 16, 17), equations (12) become

$$\left. \begin{array}{ll} a_0 = \sigma_0 + jC_0 \omega = \frac{\sigma_1 \sigma_2}{g} \left[N_1 + jN_2 \frac{\omega}{\omega_2} \right], \\ a_2 = \frac{1}{jL_2 \omega} = -jC_2 \omega_2 \cdot \frac{\omega_2}{\omega}, \\ s_x + a_0 + a_1 = \sigma_1 [1 + jt_1], \\ a_0 + a_2 + a_3 = \sigma_2 [1 + jt_2], \\ g_1 - a_0 = g - jC_0 \omega = g[1 - jp]; \end{array} \right\} \quad \text{. . . (18)}$$

and equation (11) becomes

$$\frac{e_1}{e} = \frac{jC_2\omega_2g}{\sigma_1\sigma_2} \cdot \frac{\omega_2}{\omega} (1-jp) \cdot \frac{1}{(1+jt_1)(1+jt_2) + [1-jp][N_1+jN_2\omega/\omega_2]} \quad (19)$$

This equation is exact.

5. Approximate Expression for Voltage Amplification.

When highly resonant circuits are used the variation of ω over the tuning range is small, and the ratio ω/ω_2 may be put equal to unity where it occurs explicitly in (19), but not where it occurs implicitly in t_1 and t_2 , since there the small quantity $\partial\omega/\omega$ is multiplied by a large quantity m . Again, when a valve is used whose grid-plate capacity is small, p may be neglected. Thus in a valve with the plate electrostatically shielded from the grid by a wire mesh we may have the values :

$$C_0 = 10^{-13} \text{ farad,}$$

$$g = 10^{-3} \text{ amp/volt ;}$$

hence, if $\omega = 10^7$,

$$p = \frac{10^{-13} \times 10^7}{10^{-3}} = 10^{-3}$$

and is negligible. Accordingly (19) may be written in the approximate form :

$$\frac{e_1}{e} = \frac{jC_2\omega_2g}{\sigma_1\sigma_2} \frac{1}{(1+jt_1)(1+jt_2) + N_1+jN_2} \quad (20)$$

Equation (20) * will form the basis of further development in this paper, but a preliminary discussion of the properties of a single resonant circuit and of two coupled resonant circuits will be necessary before this development can be taken up.

6. Standard Line Diagram.

If a single parallel circuit, such as either of the two shown in fig. 5, be connected to a course of alternating e.m.f. e by terminals placed at opposite ends of the inductance, then the

* In (20), σ_1 and σ_2 are regarded as independent of ω : this approximation may, according to the nature of σ_1 and σ_2 , increase or decrease the error due to putting ω_2 equal to ω .

total current flowing through the circuit is given by *

$$i = e\sigma[1+jt], \quad \dots \dots (21)$$

where the variation of t may be due either to change of capacity with fixed impressed frequency, or to change of impressed frequency with fixed capacity.

Hence the admittance is proportional to the lengths of lines drawn from a point P to a line QR (fig. 6, a). Let PQ, the perpendicular to QR, be the unit length, then PR represents the complex vector $1+jt$. A standard line diagram consists of a line QR associated with a point P at unit distance from it and graduated so that $QR=t$, the tangent of the angle by which the current is in advance of the e.m.f.

Similarly, for a single series circuit where the e.m.f. is injected in series with the inductance,

$$e = iR[1+jt], \quad \dots \dots (22)$$

and the impedance is proportional to PR.

Figs. 6-10.

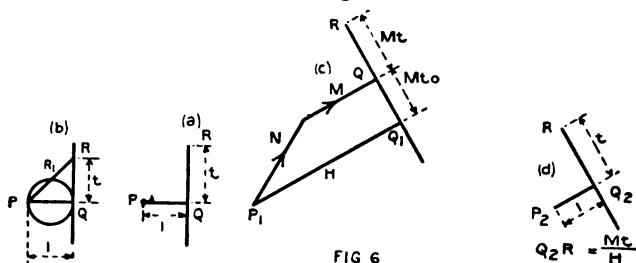


FIG 6

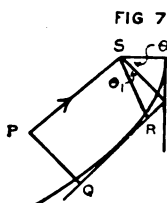


FIG 7

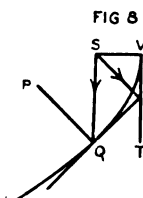


FIG 8

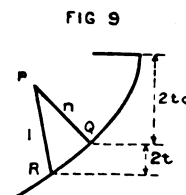


FIG 9

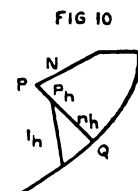


FIG 10

7. Standard Circle Diagram.

By inverting the line QR from the point P with reference to a circle of unit radius (fig. 6, b), a standard circle diagram

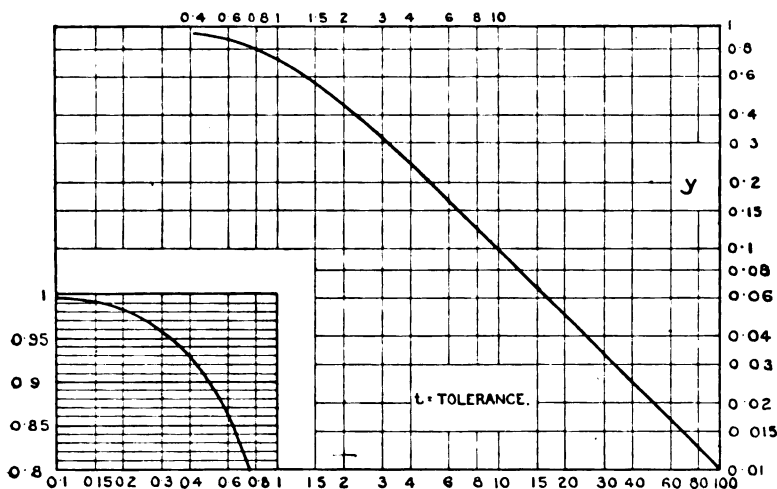
* When the frequency is varied, (21) and (22) are exact if R and σ are regarded as independent of ω : when the frequency is fixed and the capacity is varied, the equations are approximate. The circle diagram and resonance curve discussed in sections 7 and 8 are approximate to the same degree.

is obtained. In the case of a parallel circuit, PR_1 is proportional to the impedance corresponding to a phase-angle t , while for a series circuit PR_1 is proportional to the admittance, or, approximately, to the voltage amplification.

8. Standard Resonance Curve for Single Circuit.

For numerical calculation it is convenient to plot PR_1 as ordinate against t as abscissa (fig. 11). Since any single resonant circuit can be expressed by this curve, it will be termed a standard resonance curve for a single circuit. The

Fig. 11.



abscissa t is the tangent of the phase-angle: it is equal to $2m \sinh \alpha$, or, approximately, to $2m \partial \omega / \omega_0$, where $m \left(= \frac{L\omega}{R} \text{ or } \frac{1}{\sigma L \omega} \right)$ is the voltage amplification factor of the circuit at resonance.

9. Tolerance and Activity.

Since it will appear that standard resonance curves can be used for two circuits reactively coupled, with abscissa $T = Ac \partial \omega / \omega_0$ where T and Ac have no longer the simple signification of t and $2m$, the following nomenclature will be used:—

T = tolerance of circuit,

Ac = activity of circuit,

$$\partial \omega / \omega_0 = \frac{\omega - \omega_0}{\omega_0} = \text{frequency departure.}$$

In the case of a single circuit the tolerance is identical with the tangent of the phase-angle, and the activity is $\frac{2L\omega_0}{R}$ or $\frac{2}{\sigma L\omega_0}$.

10. Linear Transformation of Standard Line Diagram.

If the vector $1+jt$, corresponding to PR in fig. 6(a) be transformed to

$$M/\underline{\mu} [1+jt] + N/\underline{\nu}, \dots \dots \dots (23)$$

where M and N are complex vectors, a new vector diagram results (fig. 6, c), comprising a point P_1 and a line PQR. When this diagram is reduced to standard form (fig. 6, d) and the point Q_2 taken as the origin of t ,

$$Q_2R = T = \frac{Mt}{H}, \dots \dots \dots (24)$$

the line diagram and hence the resonance curve are of the form used for a single circuit, while the activity has been increased M/H times.

11. Application with Two Circuits reactively coupled.

Returning to equation (20), we write :

$$\frac{e_1}{e} = jA \cdot F/\underline{\phi}, \dots \dots \dots (25)$$

where

$$A = \frac{C_2\omega_2g}{\sigma_1\sigma_2}, \dots \dots \dots (26)$$

$$\frac{1}{F/\underline{\phi}} = (1+jt_1)(1+jt_2) + N_1+jN_2. \dots \dots (27)$$

A is the maximum voltage amplification obtainable without reaction, *e. g.* with C_0 zero. $F/\underline{\phi}$ represents the effect due to reaction which enters through N combined with the change of amplification due to detuning the grid and anode circuits, the latter effect entering through $t_1 t_2$.

F_0 , the maximum value of the modulus of $F/\underline{\phi}$, will be termed the reaction factor. F_0 can be found by varying t_1, t_2 being fixed, to give an intermediate maximum of F , and then varying t_2 to give the final maximum F_0 . Putting

$t = \tan \theta$, it is easy to show that

$$\frac{1}{F_0} = \sec \theta_0 + N_1 \cos \theta_0 + N_2 \sin \theta_0, \quad \dots (28)$$

where

$$t_0^2 + t_0[1 - N_1] + N_2 = 0 \quad \dots (29)$$

and

$$t_0 = t_1 = t_2. \quad \dots (30)$$

12. Graphical Construction for Amplification.

(a) *Fixed impressed frequency: one condenser varied.*

Equation (27) can be expressed graphically. To the parabola $y^2 = 4x$ (fig. 7) a tangent QT is drawn. If $TV = t_2$, ST represents the vector $1 + jt_2$, and if $\widehat{RST} = \theta_1$, SR represents $(1 + jt_1)(1 + jt_2)$. Draw PS to represent the vector N : vectorial addition gives

$$PR = PS + SR = \frac{1}{F \angle \phi}$$

by (27). PQ , the normal to QT , represents $\frac{1}{F_0}$.

When t_2 is fixed, R moves along TQ as t_1 is varied. Hence the line QT and the point P constitute a resonance line diagram of the type given by (23), and the tolerance is given by

$$T = \sec \theta_2 \cdot F_0 \cdot t_1 = \sec \theta_2 \cdot F_0 \cdot 2m_1 \cdot \frac{\partial \omega}{\omega}. \quad \dots (31)$$

The tolerance curve is that corresponding to a single circuit (fig. 11), and the activity is $\sec \theta_2 F_0$ times that of the anode circuit alone.

(b) *Fixed impressed frequency: both condensers varied.*

With both t_1 and t_2 varied, PQ is minimum when it is a normal to the parabola (fig. 8). It follows by geometry that $\widehat{QST} = \widehat{VST}$ or $t_1 = t_2$, agreeing with (30), and the ordinate of Q has the value $2t_0 = 2t_1 = 2t_2$ given by (29). Q is the point corresponding to the settings of the grid and anode condensers which give maximum amplification.

$PQ = \frac{1}{F_0}$ and its magnitude is given by (28) and (29) in terms of the coordinates of P .

As P moves towards Q , the activity and voltage amplification increase: instability sets in when P lies on the parabola.

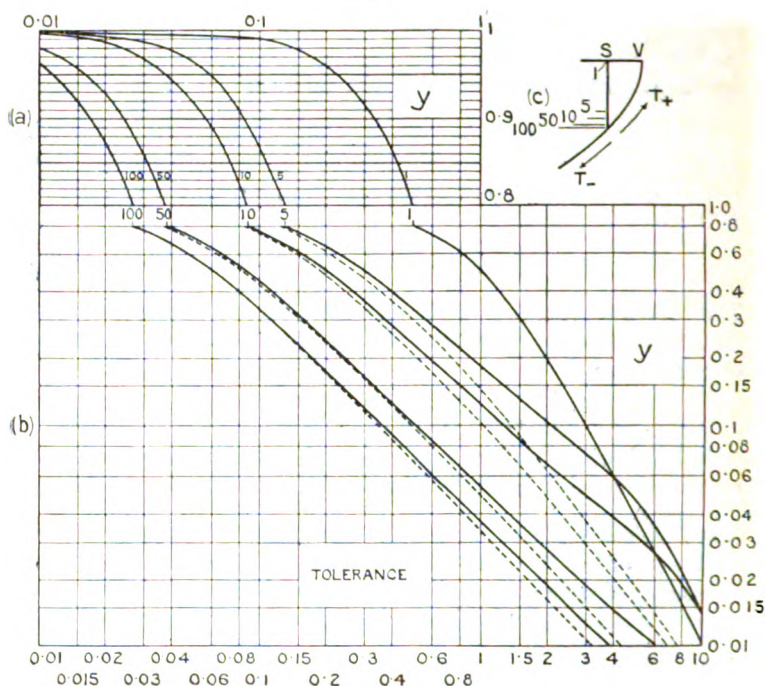
(c) *Impressed frequency varied : both condensers fixed : activities of grid and plate circuits equal.*

The point P being given, let the whole circuit be adjusted to the point Q (fig. 8). As the incoming pulsance is varied from ω_0 its value at Q to some other value ω , the product $(1+jt_0)^2$ will change to $1+j(t+t_0)^2$, where $t=2m \partial\omega/\omega_0$. The locus of the representative point R (fig. 9) will accordingly be the parabola. The resonance curve is obtained by plotting n/l against $t \left(= \frac{l}{n^{\frac{1}{2}}} = tF_0^{\frac{1}{2}} \right)$. The formula,

$$l_2 F_0^2 = \frac{l^2}{n^2} = T^4 + T^3 [F_0^{\frac{1}{2}} \cdot 4t_0] + T^2 F_0 [6t_0^2 + 4 - 2x] + 1 \dots, \quad (32)$$

can easily be derived *, and is suitable for computation.

Fig. 12.



In fig. 12 resonance curves are given for values of F_0 equal to 1, 5, 10, 50, 100. The locus of P is chosen to be

* The steps are similar to those by which equation (40) is derived from equation (33) when $h=1$.

the latus rectum (fig. 12, c): that is, the coupling is purely capacitive. The full lines correspond to positive, the broken lines to negative, values of T . In fig. 12 (a) the vertical scale is linear, since the logarithmic scale becomes inconveniently cramped near the value unity, and the ordinates are the mean values of the full and the broken lines.

It is evident that the curves are displaced to the left with increasing reaction and that their slope becomes smaller, the latter effect being less marked with negative tolerances. The reason is seen by inspection of the parabola (fig. 12, c). As T increases positively, the vertex is approached and the line l increases more slowly, that is its reciprocal decreases more slowly, than in the negative direction*. The curve $F_0=1$ is, of course, symmetrical.

(d) *Impressed frequency varied: both condensers fixed: activities of grid and plate circuits unequal.*

Let $h = \frac{m_1}{m_2}$, then

$$\frac{1}{F_{\phi}} = [1 + j(t_0 + t)][1 + j(t_0 + ht)] + N_1 + jN_2. \quad (33)$$

Therefore, putting

$$N_1 = x - 1$$

$$N_2 = -y,$$

$$\begin{aligned} l^2 = \frac{1}{F^2} &= t^4 h^2 + t^2 \cdot t_0 2h(1+h) \\ &\quad + t^2 [t_0^2 (1 + 4h + h^2) + (1+h)^2 - 2hx] \\ &\quad + 2t[1+h][t_0^3 + t_0(2-x) - y] \\ &\quad + [t_0^2 - x]^2 + [2t_0 - y]^2. \quad (34) \end{aligned}$$

If t_0 is chosen so that $t=0$ when l is minimum, the coefficient of t must vanish; hence

$$t_0^3 + t_0(2-x) - y = 0 \quad (35)$$

(cf. (29): hence t_0 is the parameter of the foot of the normal drawn to the parabola $y^2=4x$ from the point xy).

* This effect is inherent in the nature of reaction: it has no connexion with the asymmetrical resonance curve given by a single circuit of low activity. The activities here considered are so high that the resonance curve (fig. 11) of each constituent single circuit may be taken as symmetrical.

Put $T = t \cdot h^{\frac{1}{2}} F_0^{\frac{1}{2}}, \dots \dots \dots (36)$

$$\frac{1}{F_0^2} = [t_0^2 - x]^2 + [2t_0 - y]^2, \dots \dots \dots (37)$$

$$\beta = 4h/(1+h)^2, \dots \dots \dots (38)$$

$$t_0^2 - x_h = \beta[t_0^2 - x]. \dots \dots \dots (39)$$

Then (34) becomes, on multiplying each side by F_0^2 and eliminating t, x , and h ,

$$l^2 F_0^2 = l_h^2 / n_h^2 = T^4 + T^3 \cdot \left[\frac{F_0}{\beta} \right]^{\frac{1}{2}} \cdot 4t_0 + T^2 \cdot \frac{F_0}{\beta} \cdot [6t_0^2 + 4 - 2x_h] + 1, \quad (40)$$

which is of the same form as (32); so that the representative point lies on the parabola $y^2 = 4x$. Hence the construction is as follows (fig. 10).

From the point xy given by the chosen value of N draw the normal PQ to the parabola $y^2 = 4x$. $PQ = n = \frac{1}{F_0}$.

From Q cut off a length $P_h Q = \beta \cdot PQ$, where $\beta = \frac{4h}{(1+h)^2}$.

The resonance curve is now obtained by plotting n_h/l_h against T (T being reckoned from the point Q), where T is connected with the activities of the grid and anode circuits, and with F_0 by the formula

$$T = \sqrt{2m_1 \cdot 2m_2 \cdot F_0} \cdot \frac{\partial \omega}{\omega_0} \dots \dots \dots (41)$$

T , interpreted geometrically, is $F_0^{\frac{1}{2}}$ times the parameter of the parabola, reckoned from Q . The parameter is

$$\sqrt{2m_1 2m_2} \partial \omega / \omega_0,$$

and the coordinates of P, P_h are x, y, x_h, y_h .

For calculation, equation (40) may be used. The activity of the whole circuit is $\sqrt{2m_1 2m_2 F_0}$.

13. Tabulation of Results.

The Table summarizes the results so far obtained. If the phase-angle of either circuit changes as the resonance curve is described, the activity of that circuit will appear in the expression for the total activity: F_0 will appear in any case. Thus in the first row in the Table the phase-angle changes

TABLE.

Circuit.	Nature of Resonance Curve.	Tolerance = Activity $\times Q\omega/\omega_0$.	Maximum Voltage Amplification.	Maximum Mutual Admittance.	Parameter of Parabola reckoned from Tuning-point.
Single circuit, impressed frequency varied or condenser varied.	Standard curve for single circuit, derived from circle diagram (fig. 11).	$11 = 2m Q\omega/\omega_0$	m .		
Two circuits coupled, impressed frequency fixed: one condenser varied.	Standard curve for single circuit, derived from circle diagram (fig. 11).	$11 = 2m_1 \sec \theta_2 F_0 Q\omega/\omega_0$	$m_1 m_2 F_0 g/C_1 \omega$	$m_1 m_2 F_0 g$	
Two circuits coupled, impressed frequency varied: both condensers fixed.	Doubly infinite set of curves each defined by a point πy . A few curves shown in fig. 12.	$T = \sqrt{2m_1^2 m_2^2 F_0^2 Q\omega/\omega_0}$	$m_1 m_2 F_0 g/C_1 \omega$	$m_2 m_2 F_0 g$	$t = \sqrt{2m_1^2 m_2^2 Q\omega/\omega_0}$

and the activity appears in column 3; in the second row the phase-angle of the plate circuit only changes and the total activity contains the product $2m_1F_0$; in the third row the phase-angles of both circuits change and the product $2m_12m_2F_0$ appears*.

14. *Effects Due to Reaction.*

When a carrier wave modulated by speech frequencies is received, and it is desired simultaneously to cut out other carrier waves, the slope of the resonance curve should be small over the extent of the side bands due to speech and as steep as possible over the rest of the curve. Reaction in this case will either impair the quality of the speech or eliminate the other carriers less effectively. Further, the curves being asymmetrical, carriers of lower frequency will be more completely cut out than those situated at an equal frequency interval on the higher frequency side.

This effect is shown more clearly by taking for abscissa the ratio of the tolerance for any curve F_0 to the tolerance for the curve $F_0=1$ (fig. 13). As F_0 is increased, the curves become less steep and the asymmetry rises to a maximum and falls again.

When h differs from unity the asymmetry between the grid and plate circuits produces effects similar to those caused by increased reaction. In fig. 14, for any curve F_0 the abscissa is the ratio of the positive tolerance for a given value of h to the positive tolerance when $h=1$. The effect is more marked for small values of F_0 . For $F=100$ the curves are practically vertical lines.

In brief, selective reception from a broadcasting station is best achieved with symmetrical circuits and no reaction, provided that sufficient amplification can be obtained.

* The maximum mutual admittance of two reactively-coupled circuits given in column 5 of the Table is the current flowing across C_1 at resonance per unit e.m.f. injected in the grid circuit: it is obtained from (25) by multiplying each side by $C_1\omega$ and taking the maximum value: it bears a close relation to the expression for the activity given in row 4, column 3.

Under the conditions specified in row 4 the activity will remain constant during any change of the elements of the circuit which leaves the ratio of the mutual conductance of the circuit to that of the valve unaltered, and hence the abscissæ in fig. 12 when divided by this constant activity will represent frequency departures.

Fig. 13.

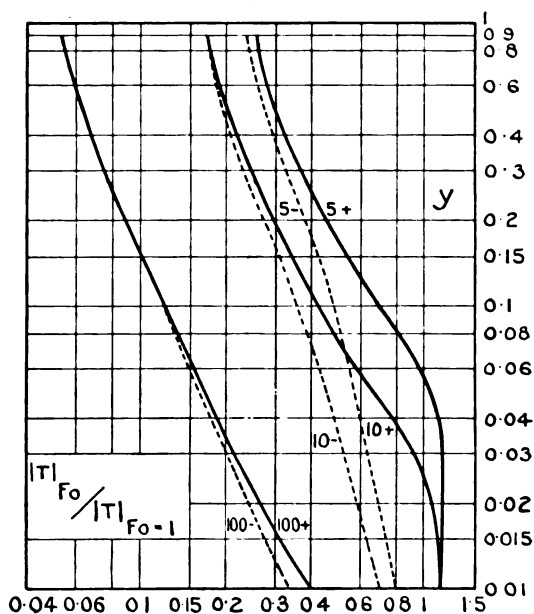
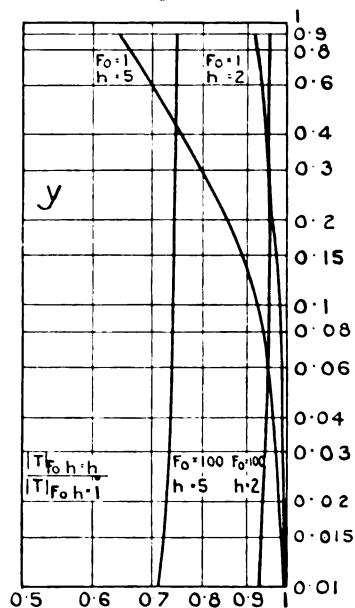


Fig. 14.



15. *General Remarks on Representation by a Parabola.*

For complete representation a doubly infinite set of resonance curves would be required, since one curve corresponds to each point xy . If, however, only one magnitude is required to characterize each curve, such as the ratio of the tolerance when $y=0.9$ to the tolerance when $y=0.01$, a single surface would suffice. In this paper, only a few curves have been drawn for the case of capacitive coupling; any other curve required can be plotted from eq. (40). It may be noted that with capacitive coupling xy lies on the latus rectum and only one normal can be drawn to the parabola, so that the resonance curve has a single peak. It is possible, though the case is of little interest, with values of $\sigma_0/C_0\omega$ of sufficient magnitude to place xy inside the evolute, in which case, since three normals can be drawn, two peaks will appear in the resonance curve*.

The method can also be used for two resonant circuits in a system which contains no source of energy. For example, when two resonant circuits are used with inductive coupling M , the series resistances being R_1, R_2 , the vector $N=M^2\omega^2/R_1R_2$, and is drawn along the axis of x to the focus. When the activities are equal the resonance curve is symmetrical: critical coupling occurs when $N=1$, and for closer coupling xy lies inside the evolute and the resonance curve shows a double peak.

16. *Explanation of the Systems of Co-ordinates.*

Positive directions of x are drawn towards the *left*, and positive directions of y are drawn upwards, from an origin which coincides with the vertex of the parabola. Vectors have their positive real components drawn to the *right* and their positive imaginary components drawn upwards. Angles increase positively in anti-clockwise direction.

It follows that in figs. 7-10 negative values of t_0 are shown and that the phase-angles θ_1 and θ_2 are negative.

* The value of $\sigma_0/C_0\omega$ may be far from negligible in the case of a valve whose plate is electrostatically shielded from the grid. Taking $\sigma_0=i10^{-6}$ mho, $C_0=10^{-13}$ F., $\omega=10^7$, we find $\sigma_0/C_0\omega=1$. Hence N may be inclined at 45° , as shown approximately in fig. 7.

XCIX. *The Effect of Various Flange Systems on the Open-end Correction of a Square Organ Pipe.* By S. A. HIGGS, B.Sc., and L. C. TYTE, B.Sc., Research Students, East London College*.

[Plates XXIII. & XXIV.]

Introduction.

§ 1. [N 1860, Cavaillé-Coll¹, a French organ builder, showed that the sum total of the lip and open-end corrections to the length of an organ pipe was $2b$, where b is the depth of the pipe—that is, the distance in centimetres from the front, *i.e.* the side containing the lip, to the back of the pipe. Later, in 1906, Brillouin² stated that the $2b$ was the aggregate of $0.4b$ due to the open end, and $1.6b$ due to the lip.

In 1877, R. H. M. Bosanquet³ found that the end correction for a square iron pipe 5 inches long and of 2 inch side was $0.44b$. It is important to note that the pipe he used had its outside edges cut away at each end, so that there was nothing in the nature of a flange on the pipe.

Rayleigh⁴ has calculated the correction for the open end for cylindrical pipes having an infinite horizontal flange to be between $0.82R$ and $0.78R$, where R is the radius, the actual value being nearer the upper limit. He⁵ found that the flange had the effect of increasing the end correction by $0.2R$. This experiment was repeated by R. H. M. Bosanquet⁶, who gives the more correct value of $0.25R$ for the increase in effective length of the pipe due to the horizontal flange. This gives the value of the open-end correction of the unflanged cylindrical pipe as about $0.6R$.

The main purpose of the following work was to test to what extent Rayleigh's analogy with the problem of electrical resistance is applicable to the case of square organ pipes.

Experimental Arrangements.

§ 2. A general view of the apparatus used throughout the whole course of the experiments is shown on Pl. XXIII. fig. 1. The hand-operated bellows in the left background was connected to the acid carboy on the extreme right. The air passed from this through each of the other carboys in turn to the last, which is the one nearest the bellows. From this issued three output pipes, one to the manometer seen on the left of the bellows, and one to each of the organ pipes situated

* Communicated by Prof. C. H. Lees, F.R.S.

about 10 feet apart. It will be seen that the pipes were quite symmetrical about the air-supply. The pressure used for blowing the pipes was 6 cm. of aniline throughout the whole range of experiments, and after some practice it was possible to keep this pressure constant to within about a millimetre. This point is important since it was found that, although the pipes were, for all practical purposes, exactly alike, and the arrangement was, as already mentioned, quite symmetrical, a variation of less than half a centimetre change in the pressure produced a noticeable change in the relative frequencies of the pipes—*i.e.*, the rate at which they were beating.

The pipes were made of wood and were of square cross-section. The approximate dimensions were:—

Length	40	cm.
Depth	3	„
Thickness of walls	1.0	„
Height of lip	0.9	„

It is interesting to note that when a pipe with height of lip 1.1 cm. was compared with one of nominally the same pitch, whose lip was 0.9 cm., the pipes required totally different pressures of blowing in order to sound the fundamental properly, and when thus sounding gave notes quite a semi-tone apart. When both pipes had 0.9 cm. lips, one pipe was about 4 vibrations per second sharper than the other. As some of the flanges which were placed on one of the pipes caused a change in frequency of 6 to 7 vibrations per second, the flanges were placed on the sharper of the two pipes. The flatter was used as the standard, and constant tests were made to see if the other pipe remained the sharper, or if the flange had made it pass through the unison point.

Frequency of the Standard Pipe.

§ 3. The determination of the changes in the open-end correction of the pipe necessitated an accurate knowledge of the frequency of the standard pipe. This was found by tuning a vertical monochord to the pipe. Twenty readings gave an accurate determination of the length of piano wire (60.99 cm.) which gave the same note as the pipe. The tension 8 kilograms weight was known accurately. The linear density of the wire (0.004304 gm. per cm.) was obtained by weighing the same length of wire as gave unison with the pipe measured under the same tension of 8 kilograms weight. This was done by cutting the wire at the

lower bridge, reattaching the weights and cutting at the upper bridge. Thus the linear density, under the conditions of the experiment, was found. The frequency of the pipe was given by the following expression :—

Frequency of pipe

$$n = \frac{1}{2l} \sqrt{\frac{T}{\sigma}}$$
$$= 350.0 \text{ vibrations per second.}$$

Hence we have the frequency of the standard pipe as 350.0 vibrations per second at 16°.2 C.

The Open-end Correction.

§. 4. Before proceeding to determine the change produced by various flanges, it was thought advisable to determine the actual end correction itself. The method employed was one suggested by Professor Lees.

One pipe was closed by a perfectly air-tight plunger and tuned to unison with the standard pipe. The plunger was a wooden rod, with a square block of wood, nearly the size of the pipe, on the end. This was covered on the sides by a piece of baize so that it was a tight fit. The bottom of the block was covered with a surface of matchwood. Before inserting the plunger in the pipe, vaseline was placed on the baize to secure a good air-tight joint. A scale was placed on the rod, and the distance of a cross-wire drawn across the top of the pipe, from a fiducial mark, was measured. The plunger was supported by means of a clamp stand, which was securely fastened to an ordinary adjustable screw table. It was found that there was a slight to-and-fro movement of the plunger, so two clamps and adjustable tables were used. This enabled the observer to adjust the position of the plunger with considerable accuracy, the pipes being tuned to less than 1 beat in 10 seconds. One hundred and forty readings of the length of the closed pipe, which was in unison with the other open pipe, were taken.

We then have, for the open pipe,

$$v/2n = L_1 + C_{(\text{lip})} + C_{(\text{end})},$$

where v is the velocity of sound in air, n the frequency of the pipe, L_1 is the length of the pipe, $C_{(\text{lip})}$ is the lip correction, and $C_{(\text{end})}$ is the open-end correction.

And for the closed pipe

$$v/4n = L_2 + C_{(\text{lip})},$$

where L_2 is the length of the closed pipe.

1102 Messrs. Higgs and Tyte : *Effect of Various Flange*

Assuming the lip corrections to be equal, since the pipes were similar, we have, on subtraction

$$v/4n = L_1 - L_2 + C_{(\text{end})}.$$

L_1 and L_2 could be determined accurately ; thus the accuracy of the value obtained depends upon the accuracy of the values of v and n used.

Now, in the experiments

$$L_2 = \mathcal{L} - (l + R - r),$$

where \mathcal{L} was the total length of the pipe when open, l is the distance from the lower surface of the plunger to the fiducial mark R , and r is the scale reading opposite the top of the pipe ; hence, $l + (R - r)$ is the distance from the bottom of the plunger to the top of the pipe.

Now, $\mathcal{L} = 40.68$ cm.

$$l = 9.67 \text{ ,,}$$

$$R = 80.00 \text{ ,,}$$

and an average value of $r = 67.69$,,

$$\therefore L_2 = 40.68 - (9.67 + 80.00 - 67.69) \\ = 18.70 \text{ cm.}$$

Now $L_1 = 40.59$ cm.

and $v/4n = 24.42$,, ;

since $v = 341.9$ metres per second

and $n = 350.0$ vibrations per second,

both measured at $16^{\circ}.2$ C.,

$$\therefore 24.42 = 40.59 - 18.70 + C_{(\text{end})}.$$

$$\therefore C_{(\text{end})} = 2.53 \text{ cm.,}$$

$$= 0.808 b,$$

where $b = 3.121$ cm., the mean depth of the pipes.

The mean of all the determinations gave the open-end correction of the square organ pipe to be

$$(0.8088 \pm 0.0013) b.$$

This is about double the value obtained by Bosanquet.

§ 5. It has been suggested that the closure of the open end changes the value of the lip correction. This is a problem which is very difficult to investigate, but certain conclusions can be drawn from the results of R. Kœnig's⁷ work on the position of anti-nodes in a large square organ

pipe. He used an open pipe, and also the same pipe closed ; hence from his results one can obtain values for the lip and open-end corrections for the open pipe, and for the lip and closed-end corrections for the closed pipe. It must be noted that he found a correction for the closed end ; but this was small, and would tend to make the above value a minimum. The values of the corrections are given in Tables I. and II.

TABLE I.—The Open Pipe.
Length of open pipe = 2.33 metres.
Depth of pipe = 0.12 „

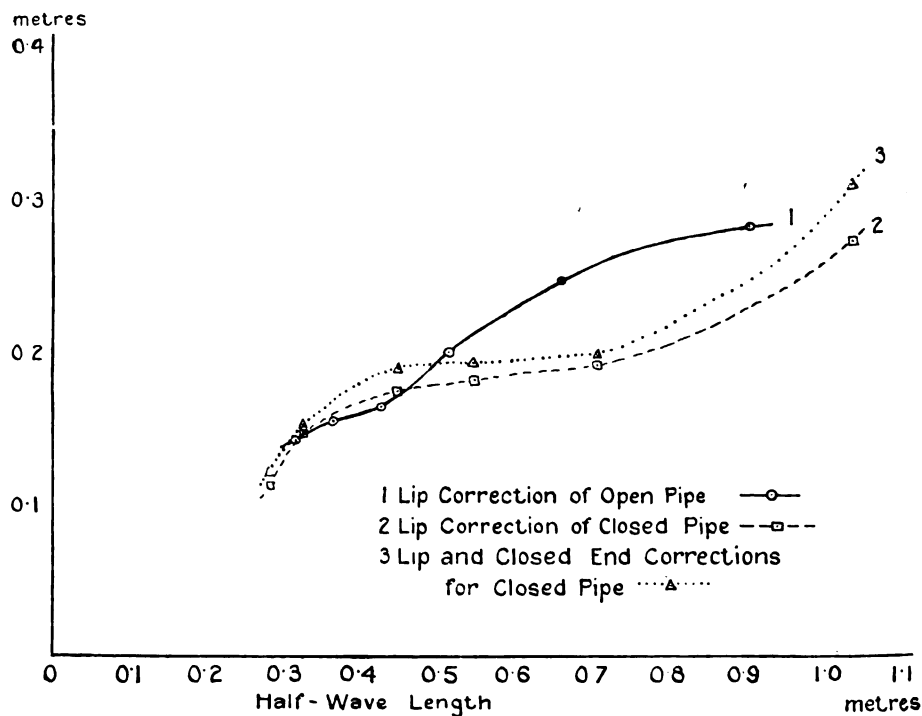
Order of partial.	Half-wave length.	Open-end correction.	Lip correction.
	metres.	metres.	metres.
III.	0.90	0.09	0.28
IV.	0.658	0.056	0.246
V.	0.513	0.036	0.198
VI.	0.425	0.057	0.162
VII.	0.365	0.067	0.157
VIII.	0.314	0.043	0.141

TABLE II.—The Closed Pipe.
Length of closed pipe = 2.28 metres.
Depth of pipe = 0.12 „

Order of partial.	Half-wave length.	Closed-end correction.	Lip correction.	Total end correction.
	metres.	metres.	metres.	metres.
V.	1.035	0.0375	0.270	0.3075
VII.	0.707	0.0035	0.191	0.1945
IX.	0.549	0.0095	0.182	0.1915
XI.	0.449	0.0145	0.174	0.1885
XV.	0.324	0.007	0.144	0.1510
XVII.	0.282	0.006	0.112	0.118

In fig. 2 the corrections are plotted against the half-wave length of the sound-wave used. In curve I. the lip corrections of the open pipe are plotted, in curve II. the lip corrections for the closed pipe, and in curve III. the lip and closed-end corrections of the closed pipe are plotted. These curves show that there is no considerable change produced in the lip correction by closing the open end of the pipe, and the method of § 4 is justified.

Fig. 2.



Curve plotted between half-wave length $\lambda/2$ as abscissæ and end corrections as ordinates.

The Effect of the "Hopper" Series of Flanges.

§ 6. The next series of experiments was made with "hopper"-shaped flanges, one of which is shown fitted to the pipe on Pl. XXIV. fig. 3. These were made of wood and covered with baize. They were constructed to have a solid angle ω , the semi-angle θ of the triangular section made by

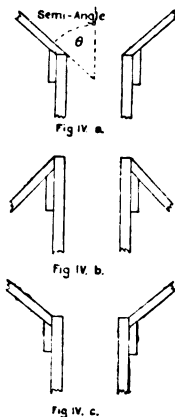
a plane passing through the axis and parallel to one edge being calculated from the formula

$$\omega = 4[2 \cos^{-1}(\sin \theta / \sqrt{2}) - \pi/2].$$

The following flanges were used :—

- (1) A flange of semi-angle 45° , giving a solid angle $2\pi/3$, and 2 feet square at the top ;
- (2) A flange of semi-angle 74° , giving a solid angle $3\pi/2$, and 4 feet square at the top ;
- (3) A plane horizontal flange, giving a solid angle 2π , and 3 feet square ;
- (4) A flange of semi-angle 135° , giving a solid angle $10\pi/3$, being (1) reversed ;
- (5) A flange of semi-angle 106° giving a solid angle $5\pi/2$, being (2) reversed ; and
- (6) A flange of 57° semi-angle, giving a solid angle π , and 2 feet 9 inches square.

Figs. 4 a-c.



The term "hood"-shaped flanges has been given to the reversed "hopper"-shaped flanges. Owing to the desirability of not cutting the pipes themselves, an important distinction existed between the "hopper" flanges and the "hood" flanges. Whereas, with one exception (flange 6), the former were constructed so that their sides met the inside of the square opening (see fig. 4 a), the latter could only have their sides meeting the outside edges of the top of the pipe (see fig. 4 b). Thus these flanges really consisted of

first a small horizontal flange, and then the "hood"-shaped flange round that. With regard to the exception mentioned above, this was the last flange to be made, and was constructed to come down to the outside edges of the pipe (fig. 4c). This flange was subsequently remade in the form 4a and the readings repeated, a slightly higher value for the change being obtained. The original reading obtained with this flange has been asterisked in Table IV.

As previously indicated, the effect of the flange on the end correction was determined by observing the rate at which the pipes were beating, both when they were in a normal condition and when the flange under consideration was placed on the sharper pipe. A hundred such observations were made for each flange.

It should be mentioned that the change in the open-end correction was calculated from the expression

$$\frac{\text{Change in frequency}}{\text{Frequency}} = \frac{\text{Change in end correction}}{\text{Effective length}}.$$

* In most cases the number of beats in an interval of 30 seconds was counted and the number of beats per second calculated. In the following table an extract from a typical set of readings is given, the flange in this case taking the pipes through the unison point:—

TABLE III.—Effect due to "Hopper"-shaped Flange of Semi-angle 45°.

Beats per second without flange.	Means. Beats per second.	Beats per second with flange.	Change. Beats per second.	Residuals. + -	$\frac{1}{2}$ square of residuals.
4.63	4.48	2.37	6.85	0.12	0.0036
4.33	4.46	2.38	6.84	0.11	0.0030
4.60	4.50	2.07	6.57	0.16	0.0064
4.40	4.45	2.05	6.50	0.23	0.0132
4.50	4.50	1.97	6.47	0.26	0.0169
4.50	4.40	2.27	6.67	0.06	0.0009
4.30	4.34	2.53	6.87	0.14	0.0049
4.38	4.49	2.42	6.91	0.18	0.0081
4.60	4.31	2.47	6.78	0.05	0.0006
4.02					
	503.22	—	807.96	23.67 23.31	6.5203

A.M. of change of frequency = 6.733 beats per second.

$\Sigma \frac{1}{4}$ square of residuals = 6.5203.

$\therefore [vv] = 4 \times 6.5203 = 26.0812.$

\therefore P.E. of a single determination = $0.6745 \sqrt{\frac{26.08}{119}}$
 = 0.31576 ;

P.E. of A.M. of 120 readings = $\frac{0.3157}{\sqrt{120}}$
 = 0.0288.

\therefore Change = (6.733 ± 0.029) vibrations per second.

Now, the mean number of beats per second without the flange

$$= 4.1935.$$

\therefore Mean frequency of B pipe

$$= 354.19 \text{ vibrations per second.}$$

Effective length of pipe

$$= \frac{34190}{2 \times 354.19} = 48.27 \text{ cm.}$$

\therefore Change due to flange

$$\begin{aligned} &= \frac{48.27}{354.2} \times \frac{b}{3.116} \times \text{Reduction in frequency,} \\ &= 0.04374 \{6.733 \pm 0.029\} b, \\ &= (0.2945 \pm 0.0013) b. \end{aligned}$$

Further details of the method of calculating the probable error will be found in 'The Combination of Observations' by D. Brunt (Cambridge University Press).

The results obtained with this series of flanges are given in Table IV. In this first line the value of the open-end correction is given ; the walls of the pipe can be considered to be a flange of solid angle 4π .

Approximate Mathematical Theory.

§ 7. Now let us, following Rayleigh, consider these cases from the electrical standpoint. Firstly, we will consider the pipe as cylindrical and to have on its end an infinite conical conductor, the circle of intersection of cylinder and cone

TABLE IV.—Summary of Results.

 b = depth of pipe = 3.116 cm.

Description of flange.	Semi-angle θ of flange.	Angle subtended by flange at opening.	No. beats/sec. without flange (mean).	No. beats/sec. with flange (mean).	Change in no. of beats/sec. due to flange.	Change in end correction as increase in length of pipe.	Total end correction.
"Hopper"	45°	4π	4.194	2.539†	6.733	$(0.2945 \pm 0.0013)b$	0.8088 b
"Hopper"	57°	π	3.891	0.241	3.650	$(0.1599 \pm 0.0014)b$	1.1033 b
"Hopper" *	57°	π	4.143	1.029	3.114	$(0.1363 \pm 0.0006)b$	0.9687 b
"Hopper"	74°	$3\pi/2$	4.330	2.894	1.436	$(0.0627 \pm 0.0005)b$	0.9451 b
Plane horizontal	90°	2π	3.771	2.798	0.973	$(0.0427 \pm 0.0005)b$	0.8715 b
"Hood"	106°	$5\pi/2$	4.260	3.315	0.945	$(0.0413 \pm 0.0009)b$	0.8515 b
"Hood"	135°	$10\pi/3$	4.447	3.834	0.613	$(0.0268 \pm 0.0006)b$	0.8501 b
							0.8356 b

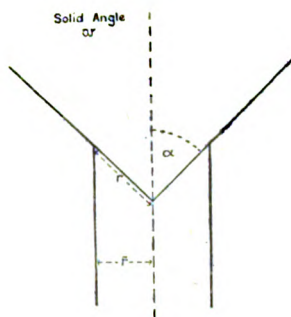
* Reference to this at top of p. 1106.

† With this flange the sharper pipe was flattened through the union point.

lying on a spherical surface of radius r , whose centre is the apex of the cone (see fig. 5).

Let ρ be the specific resistance of the material, ω the solid angle of the cone, and α the generating angle of the cone.

Fig. 5.



Now the resistance of the cone from the spherical surface r to infinity $= \rho/\omega r$.

Now, if \bar{r} is the radius of the cylindrical pipe, the resistance

$$= \frac{\rho}{\omega \bar{r}} \cdot \sin \alpha,$$

$$= \frac{\rho}{\omega \cdot r} \cdot 2 \sin \alpha/2 \cdot \cos \alpha/2.$$

Now, by spherical trigonometry, we know that

$$\omega = 2\pi(1 - \cos \alpha)$$

$$= 4\pi \cdot \sin^2 \alpha/2.$$

Hence

$$\sin^2 \alpha/2 = \omega/4\pi$$

and

$$\cos^2 \alpha/2 = 1 - \omega/4\pi.$$

Hence the resistance

$$= \frac{\rho}{\omega \bar{r}} \cdot 2 \cdot \sqrt{\frac{\omega}{4\pi}} \cdot \sqrt{1 - \frac{\omega}{4\pi}},$$

$$= \frac{\rho}{\bar{r}} \cdot \frac{1}{\sqrt{\pi}} \sqrt{\frac{1}{\omega} - \frac{1}{4\pi}}.$$

Now the pipe was actually a square one of side b ; so a close approximation is obtained by assuming the cylindrical pipe to be of the same area of cross-section--i. e., $b^2 = \pi \bar{r}^2$.

1110 Messrs. Higgs and Tyte : *Effect of Various Flange*

Hence the end correction E is the length of the pipe to have the same resistance, and is given by

$$\frac{E\rho}{\pi r^2} = \frac{\rho}{r\sqrt{\pi}} \sqrt{1 - \frac{1}{4\pi}};$$

$$\therefore E = \sqrt{\pi} \cdot \bar{r} \sqrt{1 - \frac{1}{4\pi}}.$$

But $\sqrt{\pi} \cdot \bar{r} = b$;

$$\therefore E = b \sqrt{1 - \frac{1}{4\pi}}.$$

The values are calculated for each flange in the following table :—

TABLE V.

Generating angle α .	Solid angle ω .	$\sqrt{1 - \frac{1}{4\pi}}$	End correction.
45°	$2\pi/3$	$\sqrt{\frac{5}{4\pi}}$	0.6308 b
57°	π	$\sqrt{\frac{3}{4\pi}}$	0.4886 b
74°	$3\pi/2$	$\sqrt{\frac{5}{12\pi}}$	0.3642 b
90°	2π	$\sqrt{\frac{1}{4\pi}}$	0.2821 b

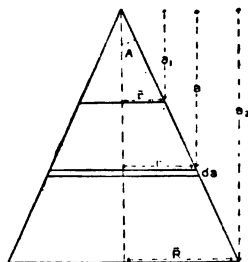
§ 8. Now, secondly, we will consider the electrical analogy of the flange system to be the resistance of a truncated cone of the same dimensions and having its smaller end flush with the pipe.

The resistance is determined as a mean of the lower limit, which is obtained by considering the frustrum of the cone to consist of an infinite number of layers separated by infinitely thin, infinitely conducting disks parallel to the flat ends; and the upper limit, which considers it to be constructed of infinite conical shells separated by infinitely thin, non-conducting layers.

(a) *Lower Limit.*

Consider a frustrum of a cone of generating angle A and of resistivity ρ . Let \bar{r} be the radius at a distance a_1 along the axis, measured from the apex, and \bar{R} at a distance a_2 (see fig. 6).

Fig. 6.



Now the resistance of a disk of thickness da at distance a along the axis

$$= \frac{\rho}{\pi} \cdot \frac{da}{(a \tan A)^2},$$

$$= \frac{\rho}{\pi \tan^2 A} \cdot \frac{da}{a^2}.$$

Hence the resistance of the frustrum of the cone between a_1 and a_2

$$= \frac{\rho}{\pi \tan^2 A} \int_{a_1}^{a_2} \frac{da}{a^2},$$

$$= \frac{\rho}{\pi \tan^2 A} \left\{ \frac{1}{a_1} - \frac{1}{a_2} \right\},$$

which is the lower limit of the resistance of the cone.

(b) *Upper Limit.*

As before, consider a cone of generating angle α , solid angle ω , and of resistivity ρ . Now the resistance from a spherical surface of radius r to infinity is

$$\frac{\rho}{\omega r} = \frac{\rho}{2\pi(1 - \cos \alpha)} \cdot \frac{1}{r},$$

since

$$\omega = 2\pi(1 - \cos \alpha).$$

Hence the conductance

$$= \frac{2\pi(1 - \cos \alpha)r}{\rho};$$

therefore the conductance of a conical shell of generating angle α , and of angular thickness $d\alpha$, from the spherical surface of radius r to infinity

$$= \frac{2\pi r \cdot \sin \alpha \cdot d\alpha}{\rho}.$$

Hence the resistance of this shell from spherical surface of radius r_1 to infinity

$$= \frac{\rho}{2\pi r_1 \sin \alpha \cdot d\alpha}.$$

And the resistance of part of it from the spherical surface of radius r_2 to infinity

$$= \frac{\rho}{2\pi r_2 \sin \alpha \cdot d\alpha}.$$

Resistance of shell between spherical surfaces of radii r_1 and r_2

$$= \frac{\rho}{2\pi} \left\{ \frac{1}{r_1} - \frac{1}{r_2} \right\} \frac{1}{\sin \alpha \cdot d\alpha},$$

hence its conductance

$$= \frac{2\pi}{\rho} \cdot \frac{r_1 \cdot r_2}{(r_2 - r_1)} \sin \alpha \cdot d\alpha.$$

Now let us apply this result to the frustrum of the cone. Let C be the apex of the cone of generating angle α , A_1 a point on the right section distance a_1 from the apex, and A_2 a similar point on the right section a distance a_2 from C (see fig. 7).

The conductance of a shell of angular thickness $d\alpha$ between surface A_1 and surface A_2

$$= \frac{2\pi}{\rho} \cdot \frac{CA_1 \cdot CA_2}{(CA_2 - CA_1)} \cdot \sin \alpha \cdot d\alpha,$$

but $CA_1 = a_1 \sec \alpha$

and $CA_2 = a_2 \sec \alpha$;

so the conductance of the shell

$$= \frac{2\pi}{\rho} \cdot \frac{a_1 a_2}{(a_2 - a_1)} \cdot \frac{\sin \alpha \cdot \sec^2 \alpha \cdot d\alpha}{\sec \alpha},$$

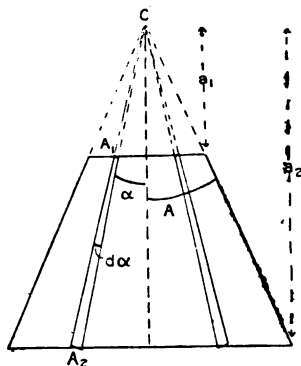
$$= \frac{2\pi}{\rho} \cdot \frac{a_1 a_2}{(a_2 - a_1)} \cdot \frac{\sin \alpha}{\cos \alpha} \cdot d\alpha;$$

\therefore conductance of frustrum of cone of generating angle A

$$= \frac{2\pi \cdot a_1 a_2}{\rho(a_2 - a_1)} \int_0^A \frac{\sin \alpha}{\cos \alpha} \cdot d\alpha,$$

$$= \frac{2\pi a_1 a_2}{\rho(a_2 - a_1)} \cdot \log_e \sec A.$$

Fig. 7.



Hence resistance of frustrum of cone

$$= \frac{\rho}{2\pi} \cdot \left\{ \frac{1}{a_1} - \frac{1}{a_2} \right\} \log_e \sec A,$$

which is the upper limit of resistance of the cone.

(c) *Mean Value.*

Now we may assume that the tendency for the lower limit to be approached is roughly proportional to the surface area of the plane ends, *i. e.* to

$$\pi \bar{r}^2 + \pi \bar{R}^2$$

$$= \pi(\bar{R}^2 + \bar{r}^2),$$

while the tendency for the upper limit to be approached is

Phil. Mag. S. 7. Vol. 4. No. 25. *Suppl.* Nov. 1927. 4 C

1114 Messrs. Higgs and Tyte : *Effect of Various Flange*
roughly proportional to the curved surface, *i. e.* to

$$2\pi\bar{R} \operatorname{cosec} A \cdot \frac{1}{2}\bar{R} \operatorname{cosec} A - 2\pi\bar{r} \operatorname{cosec} A \cdot \frac{1}{2}\bar{r} \operatorname{cosec} A \\ = \pi \operatorname{cosec}^2 A (\bar{R}^2 - \bar{r}^2).$$

Hence resistance of lower : upper

$$= (\bar{R}^2 + \bar{r}^2) : (\bar{R}^2 - \bar{r}^2) \operatorname{cosec}^2 A, \\ = L : U.$$

Thus we may write an approximate value of the resistance of the frustrum of the cone as

$$\frac{\rho}{\pi} \cdot \left\{ \frac{1}{a_1} - \frac{1}{a_2} \right\} \left(\frac{1}{\tan^2 A} \right)^{\frac{L}{L+U}} \left(\frac{1}{2 \log_e \sec A} \right)^{\frac{U}{L+U}},$$

but $a_1 = \bar{r} \cot A$
and $a_2 = \bar{R} \cot A.$

Hence the resistance is

$$\frac{\rho}{\pi} \cdot \tan A \cdot \left\{ \frac{1}{\bar{r}} - \frac{1}{\bar{R}} \right\} \left(\frac{1}{\tan^2 A} \right)^{\frac{L}{L+U}} \left(\frac{1}{2 \log_e \sec A} \right)^{\frac{U}{L+U}}$$

and the end correction is

$$E = \frac{b^2}{\pi} \cdot \tan A \left\{ \frac{1}{\bar{r}} - \frac{1}{\bar{R}} \right\} \left(\frac{1}{\tan^2 A} \right)^{\frac{L}{L+U}} \left(\frac{1}{2 \log_e \sec A} \right)^{\frac{U}{L+U}} \\ = \frac{b}{\sqrt{\pi}} \cdot \tan A \left\{ 1 - \frac{\bar{r}}{\bar{R}} \right\} \left(\frac{1}{\tan^2 A} \right)^{\frac{L}{L+U}} \left(\frac{1}{2 \log_e \sec A} \right)^{\frac{U}{L+U}}.$$

The calculation of the end correction from this formula is shown in the following tables. Table VI. gives the calculation of the "weight," Table VII. the calculation of the weighted portion of the lower limit, Table VIII. that of the upper limit, Table IX. the calculation of the mean value of the end correction, and Table X. a summary of the theoretical and experimental values.

TABLE VI.—Calculation of "Weights."
 $r = 1.756 \text{ cm.}$ $r^2 = 3.084.$

A.	cosec A.	$\bar{R}.$	$\bar{R}^2.$	$\bar{R}^2 + r^2.$	$\bar{R}^2 - r^2.$	$(\bar{R}^2 - r^2) \text{ cosec A.}$	$\frac{L}{L+U}.$	$\frac{U}{L+U}.$
46°	1.414	34.4 ^{cm.}	1183	1186	1180	2360	$\frac{1186}{3546} = 0.3344$	$\frac{2360}{3546} = 0.6656$
57°	1.192	47.3	2237	2240	2234	3174	$\frac{2240}{5414} = 0.4138$	$\frac{3174}{5414} = 0.5862$
74°	1.040	68.8	4733	4736	4730	5123	$\frac{4736}{9859} = 0.4804$	$\frac{5123}{9859} = 0.5196$

TABLE VII.—Weighted Portion of Lower Limit.

$\tan A.$	$\tan^2 A.$	$\left(\frac{1}{\tan^2 A}\right).$	$\left(\frac{1}{\tan^2 A}\right) \frac{L}{L+U}.$
1.000	1.000	1.000	1.000
1.540	2.372	0.4216	0.6027
3.467	12.16	0.08224	0.2730

TABLE VIII.—Weighted Portion of Upper Limit.

sec A.	$\log_e \text{ sec A.}$	$2 \log_e \text{ sec A.}$	$\frac{1}{2 \log_e \text{ sec A.}}$	$\left(\frac{1}{2 \log_e \text{ sec A.}}\right) \frac{U}{L+U}$
1.414	0.34635	0.69270	1.437	1.277
1.836	0.60757	1.21514	0.8250	0.8936
3.628	1.2887	2.57732	0.3880	0.6114

TABLE IX.—Calculation of Mean Value of End Correction.

$\frac{\bar{r}}{\bar{R}}$	$\left(1 - \frac{\bar{r}}{\bar{R}}\right)$	$\left(\frac{1}{\tan^2 A}\right) \frac{L}{L+U}$	$\left(\frac{1}{2 \log_e \sec A}\right) \frac{U}{L+U}$	$\frac{b}{\sqrt{\pi}} \cdot \tan A \left\{1 - \frac{\bar{r}}{\bar{R}}\right\} \left(\frac{1}{\tan^2 A}\right) \frac{L}{L+U} + \left(\frac{1}{2 \log_e \sec A}\right) \frac{U}{L+U}$
0.05105	0.94895	1.0000	1.277	0.6837 <i>b</i>
0.03713	0.96287	0.6027	0.8936	0.4506 <i>b</i>
0.02552	0.97448	0.2730	0.6114	0.3200 <i>b</i>

TABLE X.—Summary of Results.

Solid angle ω .	Infinite cone theory.	Truncated cone theory.	Experimental results.
$2\pi/3$	0.6308 <i>b</i>	0.6837 <i>b</i>	1.1033 <i>b</i>
π	0.4886 <i>b</i>	0.4506 <i>b</i>	0.9637 <i>b</i>
$3\pi/2$	0.3642 <i>b</i>	0.3200 <i>b</i>	0.8715 <i>b</i>
2π	0.2821 <i>b</i>	—	0.8515 <i>b</i>

§ 9. The above calculations only hold for the "Hopper" flanges, and, of course, the truncated cone theory is not even applicable to the horizontal flange. However, the infinite cone theory can be extended, with considerable error due to the spherical cap at the top of the pipe, to the "hood" flanges.

From the above theory the resistance of the infinite cone of solid angle ω is

$$\frac{\rho}{R \sqrt{\pi}} \sqrt{\frac{1}{\omega} - \frac{1}{4\pi}},$$

R being the equivalent external radius of the pipe, which is now involved.

Hence the end correction E is given by

$$\frac{E\rho}{\pi \bar{r}^2} = \frac{\rho}{R \sqrt{\pi}} \cdot \sqrt{\frac{1}{\omega} - \frac{1}{4\pi}},$$

$$E = \frac{\bar{r}}{R} \sqrt{\pi \bar{r}} \cdot \sqrt{\frac{1}{\omega} - \frac{1}{4\pi}}.$$

$$\text{Now } \sqrt{\pi \bar{r}} = b \quad \text{and} \quad \frac{\bar{r}}{R} = \frac{b}{B},$$

where B is the external thickness of the pipe.

$$E = \left(\frac{b}{B} \cdot \sqrt{\frac{1}{\omega} - \frac{1}{4\pi}} \right) b.$$

$$\text{And } \frac{b}{B} = \frac{3.116}{5.083} = 0.613,$$

and therefore the end correction

$$= \left(0.613 \sqrt{\frac{1}{\omega} - \frac{1}{4\pi}} \right) b.$$

The calculation of the end corrections for the two "hood" flanges are given in the following table:—

TABLE XI.—End Corrections of "Hood" Flanges.

ω .	$\sqrt{\frac{1}{\omega} - \frac{1}{4\pi}}$.	$\left(0.613 \sqrt{\frac{1}{\omega} - \frac{1}{4\pi}} \right) b$.
$5\pi/2$	$\sqrt{\frac{2}{5\pi} - \frac{1}{4\pi}} = \sqrt{\frac{3}{20\pi}} = 0.218$	$0.134 b$
$10\pi/3$	$\sqrt{\frac{3}{10\pi} - \frac{1}{4\pi}} = \sqrt{\frac{1}{20\pi}} = 0.126$	$0.077 b$

In the theory of the "hood" flanges no account has been taken of the compound nature of the flange, due to the small plane horizontal flange at the top of the pipe caused by the thickness of the walls, which considerably complicates the conditions for the mathematical problem.

We also have for the infinite plane horizontal flange the value given by Lord Rayleigh for cylindrical pipes, which is $0.82 \bar{r}$.

Now $\pi r^2 = b^2$, and hence this value is $.82 b / \sqrt{\pi} = 0.463 b$.

In spite of the incompleteness of the theory of the "hopper" flanges due to mathematical difficulties and the almost total lack of theory for the "hood" flanges, some correspondence between theory and experiment can be traced.

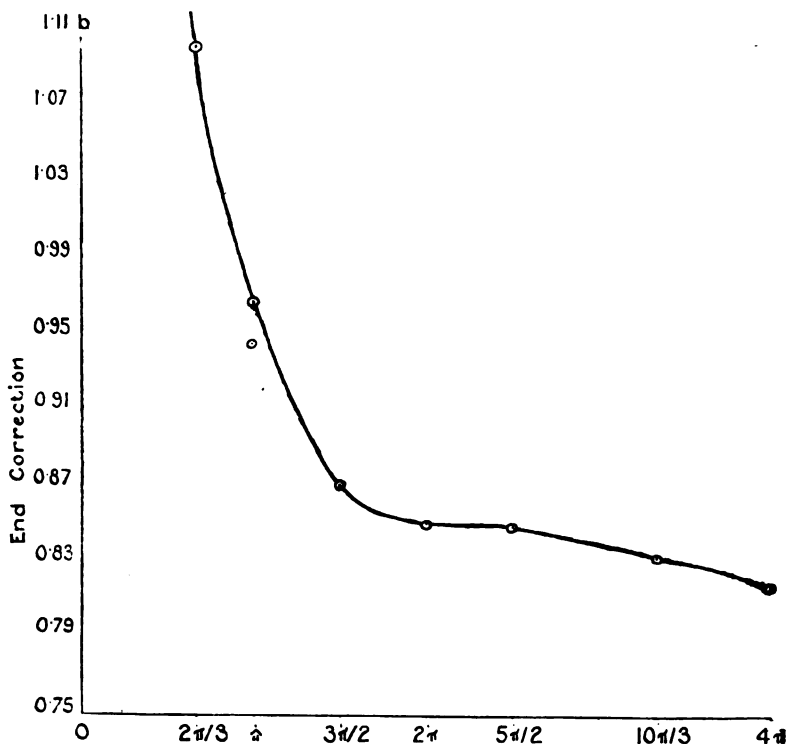
Discussion of Results for the "Hopper" Series of Flanges.

§ 10. It has been shown in Table IV. (p. 1108) that a considerable difference exists in the values of the end correction for the same flange, when firstly it makes contact with the inside of the pipe, and secondly when there is the small plane horizontal flange due to the thickness of the walls of the pipe and then the flange. This emphasizes the importance of the shape of the flange in the near vicinity of the open end of the pipe.

In fig. 8 the experimental values of the end correction have been plotted as ordinates against the solid angles of the flanges as abscissæ. From general considerations it can be seen that for a solid angle 0 the end correction is infinite, and that for a solid angle 4π the flange coincides with the walls of the pipe, and the correction is the ordinary open-end correction. The curve possesses these general characteristics, but the most striking feature is the point of inflexion in the region of the infinite plane horizontal flange. As the thickness of the walls of the ordinary pipe always act as a small horizontal flange, the value of the open-end correction will be higher than it otherwise would be; consequently the value of the change in the end correction will be smaller than it should. Now this effect will not be very serious with a flange of small solid angle, as it will only be a small percentage error; but as the angle of the flange increases, the effect will be more important. When the flanges have solid angles greater than that of the infinite plane horizontal flange, the effect of the small plane flange will play a prominent part, and the observed values of the end correction will be much greater than they should be. Thus the point of inflexion

on the curve is probably due to the effect of the wall of the pipe, and if that had been cut away or a thin pipe had been used, the curve would have been simple with one direction of curvature.

Fig. 8.



Curve plotted between end corrections and solid angle ω .

In fig. 9 the experimental values of the end correction for the three "hopper" flanges are plotted as abscissæ against the theoretical values as ordinates. If the arithmetical mean of the two sets of theoretical values is taken, a straight line can be drawn through the points. Let E be the experimental value and T the mean value on the electrical theory; we have, then, the relationship

$$E = C + kT,$$

both sides of the equation being in terms of b .

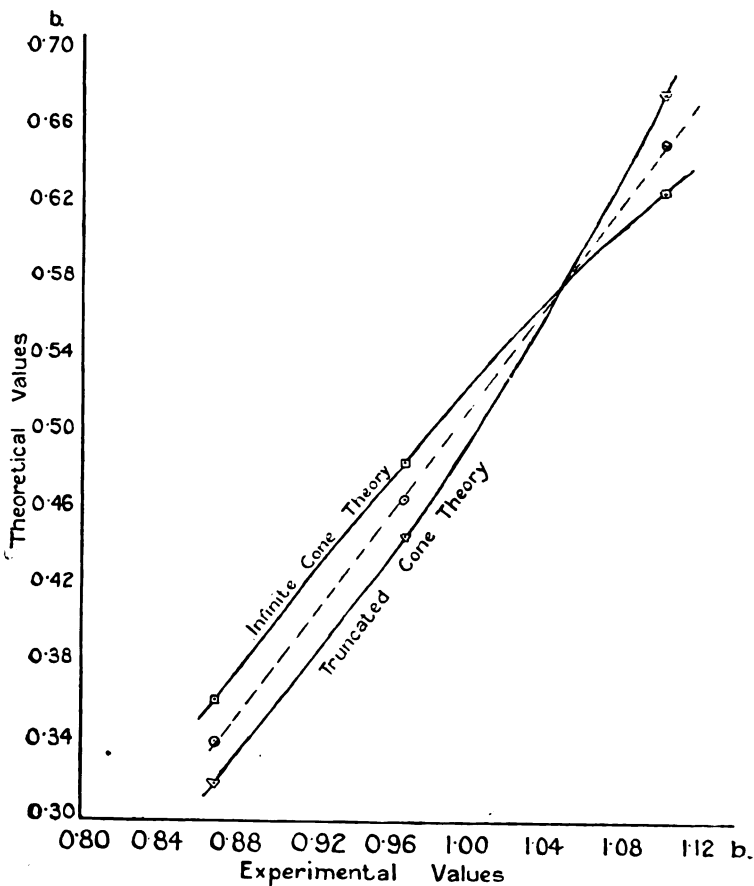
On solving for the constants,

$$C = 0.62 \text{ and } k = 0.735 ;$$

hence the expression becomes

$$E = 0.62 + 0.735 T.$$

Fig. 9.



Curve plotted between theoretical and experimental values of end correction.

This gives the relation between the acoustical measurements and the electrical theory. For the open-end correction of the unflanged pipe, whose solid angle is equivalent to 4π , the electrical theory gives the value 0, which is contrary to

common experience. The equation, however, becomes

$$E = 0.62,$$

and hence $0.62b$ can be taken as the open-end correction for an unflanged pipe. [It is lower than the experimental value, as it is the value for the ideal case of a pipe with infinitely thin walls.]

The electrical theory was worked out for cylindrical pipes of equivalent cross-sectional area to the square pipes, on which the acoustical measurements were made; thus the constant $k = 0.735$ may be considered to be the factor necessary to bring the theory into line with the conditions of the experiment.

If this value $0.62b$ is taken as the open-end correction, together with the experimental value of $0.85b$ for the end correction of the pipe with the infinite plane horizontal flange, the change caused by the horizontal flange is $0.23b$; it is interesting to note the correspondence with the values of the end corrections for the cylindrical pipe, which are $0.85r$ for the pipe with an infinite plane horizontal flange, $0.60r$ for the unflanged pipe, and $0.25r$ for the change produced by the flange.

The Effect of the Plane Flanges on the Sides of the Pipe.

§ 11. The final piece of work was an investigation of the effect produced by infinite plane flanges when they were placed on the sides of the pipes, as shown in fig. 1. The flanges used were flat wooden boards 3 feet long by 1 foot 10 inches wide, and covered with baize.

As before, the experiment consisted of counting for a given interval the beats between the pipes alternately without and with the flange in position, one hundred such double readings being taken for each flange.

The first experiment of this series was performed with the vertical flange on and extending 30 cm. down the back of the pipe. An extra piece was fitted on the face of the flange in contact with the pipe to rectify the fact that the flange was not flush with the inside of the pipe, due to the thickness of the wall. [It may be noted in passing that this wedge-like piece was observed to have nearly the same effect as the whole flange.]

It was found that the effect of the flange on the back of the pipe was to increase the effective length of the pipe by

$$(0.1127 \pm 0.0004)b.$$

This experiment was repeated with the same flange on the

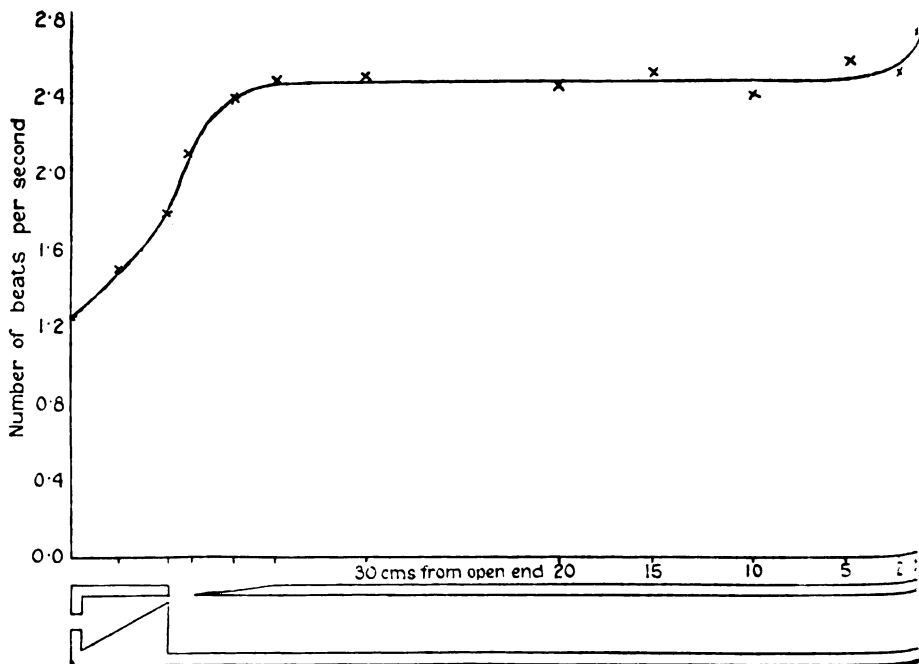
1122 Messrs. Higgs and Tyte : *Effect of Various Flange*

side of the pipe. It was found that the effect of this flange was to increase the effective length of the pipe by

$$(0.1248 \pm 0.0009) b.$$

It was suspected from this difference in values that when the flange was on the side of the pipe it might affect the lip in some way. To test this, determinations of the frequency—by counting the beats with the standard pipe—were made for the flange in various positions down the side of the pipe.

Fig. 10.



Curve plotted between number of beats per second and distance of flange along pipe.

The results obtained are given in Table XII. In fig. 10 the number of beats per second between the two pipes, for the flange in different positions, are plotted as ordinates, against the position of the lower edge of the flange, measured in centimetres from the top of the pipe, as abscissa.

This portion of the work was completed by investigating the effect of a flange system on one of the back corners of the pipe. It consisted of two flanges joined together at

right angles, each being of the same dimensions as that used in the previous experiments. As in the case of a single flange, a wedge was used to eliminate the effect of the thickness of the walls of the pipe. The effect was observed to be an increase in the effective length of the pipe of

$$(0.2524 \pm 0.0011) b.$$

This value is only 6 per cent. different from the sum of the single flange effects, which is 0.2375 *b*.

TABLE XII.—Number of Beats per Second for Different Positions of the Flange.

Position of bottom of flange.	No. of beats per second.
Bottom of pipe	1.25
Midway between bottom and mouth	1.51
At mouth	1.78
Bottom of lip.....	2.10
Half-way up lip.....	2.41
Top of lip	2.48
30 cm. down from top of pipe.....	2.51
20 " " " " "	2.46
15 " " " " "	2.52
10 " " " " "	2.41
5 " " " " "	2.59
2 " " " " "	2.52
Top of pipe	2.73

Discussion of Results for the Plane Flanges.

§ 12. Let us now consider fig. 10. Firstly, it will be observed that at the 30-cm. point, the position of the flanges in the former experiments, the curve has become quite horizontal; thus we can conclude that when in this position the flange has no effect on the lip. Hence a real difference exists between the effects for a flange on the back and on the side of the pipe; possibly this is due to the fact that at the mouth of the pipe the air moves from the lip in sheets parallel to the front of the pipe, and thereby introduces an inequality in the distribution of the air-flow which still exists at the open end of the pipe. It also shows that the short sleeve connected to the "hopper" flanges had no effect on the lip.

Secondly, it will be noted that the curve slopes steeply upwards in the region corresponding to positions between the bottom and mouth of the pipe. This large change would seem to indicate that the vortices issuing from the lip of the pipe curved right down below the mouth—a fact not generally recognized.

Lastly, the upward sweep of the curve at points corresponding to positions close to the open end points to the fact, previously demonstrated, that the frequency of the pipe is very largely affected by the configuration of its walls close to the open end.

The two sets of flange systems used in this section of the work are the acoustical equivalents of semi and quarter infinite conductors on the electrical theory; and although some of the “hopper” flanges (those of solid angle 2π and π) correspond to these same values, the effects in the acoustical cases are entirely different. Hence we are forced to conclude that the effect depends not only on the solid angle, *i.e.* the amount of free space, but also on the configuration of that free space about the open end of the pipe.

Conclusion.

§ 13. The results can be summarized as follows :—

(1) The value of the open-end correction for a square organ pipe was found experimentally to be $(0.809 \pm 0.001)b$; this value, which is really the one occurring in practice, being higher than that obtained by Bosanquet for a pipe open at both ends. This discrepancy between the results is probably due in part to the effect of the thickness of the walls, and partly to the fact that the length of the pipe used by Bosanquet was $2\frac{1}{2}$ times its breadth, while in the present experiments the length was 13 times the breadth. The estimate of $0.62b$, deduced from the results of the experiments on the “hopper” series of flanges, is probably very near the true value of the open-end correction for an ideal unflanged organ pipe.

(2) In spite of the great difficulties in the mathematical calculations of the electrical resistances, it is possible to make some test of the truth of Rayleigh's analogy between the acoustical and electrical problems. A study of fig. 9 leads to the conclusion that a linear relation exists between them, and, allowing for the open-end correction, the value in the acoustical case is directly proportional to its electrical equivalent. However, the fact that the effect of the flange system depends not only on the amount of free space it

encloses, but also on the distribution of that free space about the open end of the pipe, shows that in the electrical calculation precautions must be taken to have the lines of flow the same as in the acoustical problem.

(3) The experiments have shown quite definitely that the shape of the flange very close to the opening is very important, suggesting that the transition from the plane waves inside the pipe to the spherical waves, which travel out into free space, takes place rapidly and very near the opening, at a short distance from which the waves have taken up their ultimate form.

In conclusion, these experiments were carried out in the Physical Laboratories of the East London College under the supervision of Professor C. H. Lees, F.R.S., to whom we are greatly indebted for suggesting this work and also for much advice and encouragement during the course of the experiments.

References.

- (1) Cavaillé-Coll, *Comptes-Rendus*, l. p. 176 (1860).
- (2) M. Brillouin, *Journal de Physique*, Sept. 1906, vol. v. p. 569.
- (3) R. H. M. Bosanquet, *Phil. Mag.* 5th series, vol. iv. p. 216 (1877).
- (4) Lord Rayleigh, 'Theory of Sound,' ii. p. 176; or 'Collected Papers,' i. p. 61.
- (5) Lord Rayleigh, 'Collected Papers,' i. p. 319.
- (6) R. H. M. Bosanquet, *loc. cit.*
- (7) R. Koenig, "Méthode pour observer les vibrations de l'air dans les tuyaux d'orgue," p. 206, 'Expériences d'Acoustique,' 1882; or *Annalen der Phys.* 1881.

C. The Freezing-Points of Concentrated Solutions.—Part III. Solutions of Phenol. By EDWARD R. JONES, Ph.D. (Wales), and C. R. BURY *.

THIS is a continuation of previous work (*Phil. Mag.* (7) iv. p. 841, 1927) on the activity of associated substances in aqueous solution. In this paper are recorded the freezing-points and activities of solutions of phenol, which is unfortunately the only common member of its class which is sufficiently soluble to be suitable for this work.

The phenol used was fractionally crystallized three times, and was then distilled from anhydrous copper sulphate. The purified product was colourless, non-hygroscopic, and

* Communicated by the Authors.

melted at 40.71° C. Solutions were analysed by the method of Redman, Weith, and Brock (J. Ind. Eng. Chem. v. p. 389, 1913) : it was found, however, that analyses of the necessary accuracy were only obtained when the phenol solutions used were less than N/20 (*i. e.*, half the strength recommended by these authors). All solutions obtained during the course of our work were stronger than this; hence, after a rough preliminary analysis, weighed quantities were diluted to a known volume so that the resulting solution was as nearly as possible N/20. Duplicate analyses were made in every case, and these usually agreed to within 0.1 per cent.

The method of determining freezing-points has been fully described in a previous communication (Phil. Mag. (7) iii. p. 1032, 1927).

The results are given in the table, where m is the concentration in gram molecules per 1000 grams of water, θ is the depression of the freezing-point, and γ is the activity coefficient (*i. e.*, γm is the activity).

m .	θ .	γ .	M.	z .	K.
0	0		(94.1)	0	
0.1422	0.257	0.948	98.7	0.041	0.765
0.2322	0.412	0.915	98.5	0.067	0.516
0.3065	0.534	0.886	100.3	0.093	0.445
0.3696	0.631	0.858	102.4	0.122	0.439
0.4603	0.768	0.825	104.7	0.153	0.397
*0.5133	0.843	0.804	106.5	0.174	0.391
0.5386	0.881	0.797	106.9	0.179	0.373
0.6213	0.990	0.764	109.7	0.214	0.379
0.6903	1.073	0.737	112.5	0.245	0.399
†0.7803	1.174	0.702	116.2	0.285	0.428

* Eutectic: Ice-phenol hydrate-solution.

† Eutectic: Ice-solid phenol-solution.

The activities have been calculated by the method of Lewis and Randall ('Thermodynamics,' 1923, chap. xxiii.) : these authors observe that, in the cases they have studied, the quantity j/m (where $j = 1 - \frac{\theta}{1.858 m}$) is independent of concentration at low concentrations, and base their method of extrapolation to zero concentration on this fact. With phenol, j/m appears to be a linear function of the concentration down to the lowest concentration studied : a method

of extrapolation described by one of us (J. Amer. Chem. Soc. *xlvi*. p. 3123, 1926) is, however, applicable.

It must be remembered that phenol is a weak electrolyte : whilst ionization is quite inappreciable in the range of concentrations studied, it must be perceptible in very dilute solutions. There must therefore be a maximum in the activity coefficient-concentration curve in dilute solution, as with acetic acid, and it is dangerous to extrapolate to more dilute solutions from the data given in the table.

Previous determinations have been made by Peddle and Turner (J. Chem. Soc. *xcix*. p. 685, 1911) which, except for one point, are in fair agreement with ours ; and by Endo (Bull. Chem. Soc. of Japan, *i*. p. 25, 1926), whose freezing-point in dilute solutions are lower than ours, but agree at higher concentrations. Measurements have also been made by Arrhenius (*Zeit. phys. Chem.* *ii*. p. 491, 1888) and Rozsa (*Zeit. für Electrochemie*, *xvii*. p. 934, 1911). Activities have been calculated by Goard and Rideal (J. Chem. Soc. *ccxvii*. p. 1668, 1925) from the freezing-points of Peddle and Turner : they differ considerably from our values.

Endo (*loc. cit.*) has suggested that the abnormality of phenol is due to association to triple molecules. To test this hypothesis, we have calculated firstly the apparent molecular weight (*M*) from van't Hoff's equation, taking 1.858 as the molecular lowering of the freezing-point of 1000 grams water. Assuming the change of molecular weight to be solely due to formation of triple molecules, we then calculated the fraction associated (*x*) and the Law of Mass

Action constant $K = \frac{x}{3(1-x)^3 m^2}$, values for which are given in the table. The constancy of *K* is hardly satisfactory.

From the data given in the table, it follows that the free energy of formation of one gram molecule of phenol hydrate, $(C_6H_5OH)_2, H_2O$, from ice and solid phenol at about $-1^\circ C$ is $2RT \log_e \frac{0.5133 \times 0.804}{0.7803 \times 0.702}$ or -306 cal. Free energy is used in the sense defined by Lewis and Randall (*op. cit.*).

One of us (E. R. J.) acknowledges his indebtedness to the University of Wales for a Postgraduate Studentship.

Edward Davies Chemical Laboratories,
University College of Wales, Aberystwyth.
July 19th, 1927.

CI. *The Electrodeless Discharge through Gases.*

By Sir J. J. THOMSON, O.M., F.R.S.*

ABSTRACT.

THIS paper contains a discussion of the theory of the electrodeless discharge produced when a vessel containing gas at a low pressure is placed inside a solenoid, through which rapidly alternating currents produced by the discharge of Leyden jars are passing. It is shown that to produce the discharge the maximum magnetic force inside the solenoid must reach a value which depends (1) on the nature of the gas, (2) on its pressure, (3) on the frequency of the currents, (4) on the size of the vessel. This value is infinite when the pressure is either zero or infinity, it is a minimum when the pressure is such that $\lambda p = c$, where λ is the free path of the electron in the gas, p the frequency of the alternating current, and c the velocity of the electron when its energy is that required to ionize the gas. Thus there is a critical pressure when the discharge passes most easily, and this depends on the frequency of the currents. Experiments are described which confirm the truth of the theory. It is shown, too, that in the electrodeless discharge very large currents may pass through the gas without producing visible luminosity, so that luminosity of this kind involves processes in addition to the passage of a current. Within a certain range of pressures the gas is in a "sensitive" state, and the discharge has peculiar properties. Within a limited range of pressure and current density striations occur in the electrodeless discharge in hydrogen.

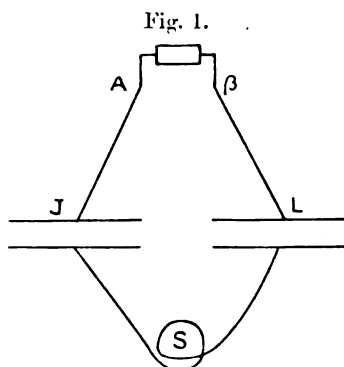
The luminosity at low pressures is not, as it is at high, confined to a ring, but extends on either side forming a double cone with the ring as base; the study of this outlying luminosity leads to very interesting results in connexion with the origin of visible radiation. It is found that the luminosity is quenched by a supply of electrons from a hot wire, and that when a solid is put into it the solid is surrounded by a dark space, which is much thinner than the Crookes' dark space, being only a millimetre or so thick. In many respects it resembles the dark space discovered by Dr. Aston, as it is more freely developed in helium and hydrogen than in other gases, and its thickness does not depend on the pressure of the gas.

Remarkable effects on the discharge itself are produced when certain solids are placed at the centre of the ring

* Communicated by the Author.

discharge. Thus, when a thin deposit on a thin glass rod of platinum or silver, sulphur, or many other substances is placed at the centre of the ring, the discharge is much weakened and may be entirely stopped. On the other hand, other substances such as fused potash, soda, sodium or lithium chlorides facilitate the discharge instead of stopping it; a theory of this effect is discussed, and various chemical effects which are ascribed to very absorbable radiations produced by the discharge are described. Since this type of discharge is exceedingly sensitive to the presence among the normal molecules of a very small number of a different character, whether this difference is due to their being molecules of a different element or to a different energy content of molecules of the same element, it supplies a useful method for studying the properties of these abnormal molecules.

THE type of electrical discharge discussed in this paper was described by me many years ago in the *Philosophical Magazine*, Series 5, xxxii. pp. 321-445. A solenoid S is placed in the circuit connecting the outer coatings of two Leyden jars, J, L, whose inner coatings are connected with *a*, *b*, the terminals of an induction coil. When sparks pass between these terminals electrical



oscillations are started in the circuit, and the solenoid is traversed by rapidly alternating currents; these produce by electromagnetic induction intense electric forces in the neighbourhood of the solenoid. If a glass bulb filled with gas at a low pressure is placed inside the solenoid,

Phil. Mag. S. 7. Vol. 4. No. 25. *Suppl.* Nov. 1927. 4 D

these forces produce, when conditions are favourable, a luminous discharge in the form of a ring; this is often exceedingly brilliant and very convenient for many types of investigations.

Mathematical Theory of the Discharge.

Currents passing through the long solenoid produce inside it a magnetic force H parallel to its axis. If no currents pass through the gas H will be constant across the section of the solenoid. In many cases, however, such large currents pass through the gas that they modify the distribution of the magnetic force, screening off as it were from the inside of the discharge tube the magnetic force, due to the currents through the solenoid.

Regarding the gas as a conductor of electricity and assuming for the moment that the conduction follows Ohm's Law, then H satisfies the differential equation

$$\frac{d^2 H}{dr^2} + \frac{1}{r} \frac{dH}{dr} = \frac{4\pi}{\sigma} \frac{dH}{dt}, \quad \dots \quad (1)$$

where r is the distance from the axis of the solenoid and σ the specific resistance of the gas.

If the periodic currents due to the discharge of the jars vary as e^{ipt} , equation (1) becomes

$$\frac{d^2 H}{dr^2} + \frac{1}{r} \frac{dH}{dr} = \frac{4\pi ip}{\sigma} H;$$

the solution of this is

$$H = AJ_0(inr),$$

where $n^2 = 4\pi ip/\sigma$, and J_0 denotes Bessel's function of zero order. At the outer boundary of the gas, when $r = a$, the magnetic force must be that due to the current through the solenoid, i. e. it must be equal to $4\pi NI$, where N is the number of turns per unit length of the solenoid, and I the current produced by the discharge of the jars. Let $H_0 \sin pt$ denote this magnetic force, then

$$H = H_0 \sin pt \frac{J_0(inr)}{J_0(ina)}. \quad \dots \quad (2)$$

The number of lines of magnetic force passing through a circle of radius r is equal to

$$\int_0^r H 2\pi r dr.$$

The electromotive force round the circuit is equal to

$$\int_0^r 2\pi r \frac{dH}{dt} \cdot dr,$$

so that the tangential electric force at a point is equal to

$$\frac{1}{r} \int_0^r r \frac{dH}{dt} \cdot dr.$$

The tangential force acting on an electron is due (1) to this force, and (2) to the motion of the electron in the magnetic field: this component is equal to $eH \frac{dr}{dt}$, hence the tangential force acting on an electron is

$$e \int_0^r r \frac{dH}{dt} dr + eH \frac{dr}{dt} = \frac{e}{r} \frac{d}{dt} \int_0^r rH dr.$$

Substituting the value of H from (2) and remembering that

$$xJ_0(x) = \frac{d}{dx} (xJ_1(x)),$$

we see that the tangential electric force on the electron

$$= \frac{e}{r} \frac{d}{dt} \frac{H_0 \sin pt r J_1(nr)}{n J_0(na)}.$$

Hence, if r and θ are the co-ordinates of an electron of mass m and charge e ,

$$\frac{m}{r} \frac{d}{dt} \left(r^2 \frac{d\theta}{dt} \right) = \frac{e}{r} \frac{d}{dt} \frac{H_0 \sin pt r J_1(nr)}{n J_0(na)};$$

hence

$$r^2 \frac{d\theta}{dt} = \frac{e}{m} \frac{H_0 \sin pt r J_1(nr)}{n J_0(na)}, \quad \dots \quad (3)$$

if $d\theta/dt$ vanishes when $t = 0$.

We have also the equation

$$m \left(\frac{d^2 r}{dt^2} - r \left(\frac{d\theta}{dt} \right)^2 \right) = -H e r \frac{d\theta}{dt};$$

hence

$$\begin{aligned} \frac{d^2 r}{dt^2} &= H_0^2 \frac{e^2}{m^2} \frac{\sin^2 pt}{(J_0(na))^2} \frac{J_1(nr)}{n} \left(\frac{J_1(nr)}{nr} - J_0(nr) \right) \\ &= -H_0^2 \frac{e^2}{m^2} \frac{\sin^2 pt}{J_0(na)^2} \frac{J_1(nr) J_1'(nr)}{n}, \quad \dots \quad (4) \end{aligned}$$

We shall now apply these equations to the solution of some special problems.

The first of these is to find the criterion that any discharge should occur in the gas. When the conditions are such that the discharge is only just beginning, the currents passing through the gas are very small, the gas is a very bad conductor, σ is very large, and n very small. When x is small

$$J_0(x) = 1,$$

$$J_1(x) = \frac{x}{2}.$$

Hence from (3) we get

$$\frac{d\theta}{dt} = \frac{e}{2m} H_0 \sin pt,$$

and from (4)

$$\frac{d^2r}{dt^2} + \frac{H_0^2 e^2}{4m^2} r \sin^2 pt = 0.$$

For the discharge to pass, the gas must be ionized; hence the electrons must acquire from the electric field sufficient energy to ionize the gas, and since they lose their energy when they come into collision with a molecule they must get this energy while travelling over a distance less than the mean free path of an electron. Hence, if W is the ionizing potential of the gas, λ the mean free path of the electron, the electrons in a space not greater than λ must acquire a velocity not less than q , where

$$eW = \frac{1}{2}mq^2.$$

But

$$\frac{d\theta}{dt} = \frac{H_0 e}{2m} \sin pt;$$

hence when the velocity $a d\theta/dt$ is equal to q ,

$$q = a \cdot \frac{H_0 e}{2m} \sin pt. \quad . \quad . \quad . \quad . \quad (5)$$

The space passed over in time t is $a\theta$, and thus is equal to

$$\frac{a \cdot H_0 e}{2mp} (1 - \cos pt).$$

This must be equal to λ_1 where λ_1 is not greater than λ ; hence

$$\lambda_1 = \frac{a H_0 e}{2mp} (1 - \cos pt). \quad . \quad . \quad . \quad . \quad (6)$$

From (5) and (6) we get

$$\frac{\lambda_1 p}{q} = \tan \frac{pt}{2},$$

$$\frac{q^2 + (\lambda_1 p)^2}{\lambda_1 p} = \frac{aH_0 e}{m} \quad (7)$$

Thus H_0 , the magnetic force required to produce discharge, will be infinite if λ_1 is either zero or infinite, *i. e.* if the pressure is infinite or zero. It has a minimum value when $\lambda_1 p = q$, and this value is given by the equation

$$2q = \frac{aH_0 e}{m} \quad (8)$$

We see from equation (7) that λ_1 and p only occur in the combination $\lambda_1 p$, so that the magnetic force required for discharge is a function of $\lambda_1 p$, or since λ_1 varies inversely with the pressure P , the magnetic force required for discharge is a function of p/P . This may be compared with Paschen's law for the spark potential when the discharge is between electrodes, *i. e.* that the spark potential is a function of the product of the pressure and the spark length.

This, however, is not the only condition which must be satisfied if the discharge is to occur, for if the electron is to ionize it must after acquiring a certain velocity retain it when under the action of the electric force long enough to enable it to make a collision. Let us suppose that the electric currents through the solenoid are so rapidly damped that only the first vibration is effective. The velocity of the electron will not be less than q from the interval given by the equation

$$q = \frac{aH_0 e}{2m} \sin pt_1 \quad (9)$$

to a time t_2 , where $pt_2 = \pi - pt_1$. During this interval the electron passes over a distance equal to

$$\begin{aligned} \frac{aH_0 e}{2mp} (\cos pt_1 - \cos pt_2) \\ = \frac{aH_0 e}{mp} \cos pt_1, \end{aligned}$$

and if it is to make a collision while its energy is great enough to ionize, this distance must be greater than λ , the mean free path of the electron. Hence we must have

$$\frac{aH_0 e}{mp} \cos pt_1 = \lambda, \quad (9)$$

where λ_2 is greater than λ_1 . From (8) and (9) we have

$$\tan pt_1 = \frac{2q}{\lambda_2 p},$$

$$a \cdot H_0 \frac{e}{m} = \sqrt{4q^2 + (\lambda_2 p)^2}. \quad . \quad . \quad . \quad (10)$$

This, again, makes the minimum value of $aH_0 e/m = 2q$. This, however, only occurs when $\lambda_2 p$ vanishes, and this from equation (7) would make H_0 infinite. Both equations (7) and (10) can be satisfied if we put $\lambda_1 p = \lambda_2 p = q/\sqrt{2}$; this gives for $aH_0 e/m$ the value $3q/\sqrt{2}$, which is only a little greater than $2q$. When there is no damping the conditions expressed by equations (10) and (9) are not required, as if the electron does not make a collision in one oscillation it will do so in another. In this case the discharge will occur when $aHe/m = 2q$. We see from this that even when the damping is so large that only a few vibrations occur very little increase is produced in the magnetic force required to produce discharge.

Since H_0 is given by the equation

$$aH_0 \frac{e}{m} = \frac{3}{\sqrt{2}} q,$$

when the ionizing potential is 12 volts

$$q = 2.1 \times 10^8 \text{ cm./sec.}$$

Since $e/m = 1.8 \times 10^7$; if $a = 5 \text{ cm.}$,

$$H_0 = 4.7.$$

Thus it does not require a very intense magnetic field to produce the discharge.

It is interesting to compare the *electric* force in the electrodeless discharge with that required to produce the spark discharge between electrodes. If F is the electric force for the spark discharge, then the condition that the electron should acquire enough energy to ionize the gas is

$$Fe\lambda = \frac{1}{2}mq^2;$$

if F' is the electric force for the electrodeless discharge

$$F' = \frac{1}{2}a \frac{dH}{dt} = \frac{1}{2}apH_0 \cos pt,$$

the maximum value is

$$F' = \frac{1}{2}apH_0;$$

and since $aH_0 = 2qm/e$ approximately,

$$\frac{F}{F'} = \frac{q}{2\lambda p},$$

when the electrodeless discharge passes most easily,

$$q = \lambda p.$$

Hence $F/F' = \frac{1}{2}$. So that the force in the spark discharge is half the maximum value of the force in the electrodeless.

Variation of the Magnetic Force required to produce the Electrodeless Discharge with the Pressure.

When the pressure is very high $\lambda_1 p$ will be small compared with q , and then from equation (7),

$$aH_0 \frac{e}{m} = \frac{q^2}{\lambda_1 p},$$

since λ_1 is inversely proportional to the pressure of the gas, H_0 will be proportional to the pressure. At low pressures, when $\lambda_2 p$ is large compared with q , we see from equation (10) that

$$aH_0 \frac{e}{m} = \lambda_2 p,$$

so that at very low pressure H_0 varies inversely as the pressure. Thus both at very high and at very low pressures H_0 is very large, the minimum value being at the pressure defined by $\lambda p = q$.

We have supposed that the magnetic force could be represented by the expression $H_0 \cos pt$. In the more general case, when a magnetic field is suddenly produced in the gas, it is easy to see that if this field reaches the value $2qm/ea$ in a time less than λ/q , and persists at this or a greater value for a time greater than λ/q , the conditions for the discharge will be satisfied whatever may be the pressure. Thus the magnetic force required for discharge might remain unaltered over a wide range of pressure, but would increase as soon as the pressure was great enough or low enough to make λ/q either small or large compared with the time taken to establish the magnetic field. Comparatively weak magnetic fields may produce the discharge if they are rapidly established, but however rapidly established they may be they cannot produce the discharge if the maximum value of the magnetic force falls below that given by equation (8).

Electromotive Force round the Circuit.

The electromotive force round the circuit, when $H = H_0 \sin pt$, is equal to

$$\frac{d}{dt} (\pi a^2 H_0 \sin pt) \\ = \pi a^2 H_0 p \cos pt.$$

The maximum value of this is $\pi a^2 H_0 p$. When the discharge passes most easily, $a H_0 \frac{e}{m} = 2q$. Thus the minimum electromotive force which can produce the discharge is

$$2\pi q p a (m/e). \quad . \quad . \quad . \quad . \quad . \quad (11)$$

It is thus proportional to the product of the frequency and the radius of the tube.

If C is the capacity of the Leyden jars used to produce the alternating currents through the solenoid, V the potential to which they are charged when the spark passes, I the current through the solenoid will be given by the equation

$$I = pCV \sin pt.$$

The magnetic force inside the solenoid $= 4\pi NI$, where N is the number of turns of wire per unit length of the solenoid.

$$\text{Hence} \quad H_0 = 4\pi N p C V,$$

and since $a H_0 \frac{e}{m} = 2q$,

$$V = \frac{qm}{2\pi e p N C a}.$$

An approximate value for p is $1/\sqrt{LC}$, where L is the self-induction of the circuit. Substituting this value,

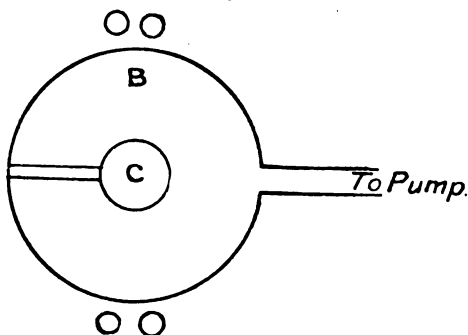
$$V = \frac{q}{2\pi e a N} \sqrt{\frac{L}{C}}.$$

We have hitherto supposed that the currents through the gas were so small that the magnetic forces due to them were negligible compared with those due to the alternating currents through the solenoid; when, however, the electric force due to these currents is much greater than that required to initiate the discharge, the currents through the gas may be comparable with those through the solenoid; the magnetic force produced by the gaseous currents is of the opposite sign to that produced by those through the solenoid, so that the total magnetic force towards the centre

of the tube may be very much less than that due to the currents through the solenoid alone. The following experiment shows this in a striking way.

A bulb C, containing gas at a pressure at which the ring discharge is very easily produced, is placed at the centre of another larger bulb B which is connected with a pump, so that the pressure inside it may be altered. The solenoid is placed round B. When the gas in B is at atmospheric pressure and no ring discharge is visible through it, the ring discharge is very bright in C. On reducing the pressure in B until a bright ring discharge passes through the outer portion of the gas inside it, the ring discharge through

Fig. 2.



C stops. When the pressure in B is still further reduced so that the ring discharge no longer passes through it, the discharge begins again in C. Thus, when the ring discharge is passing through B, the magnetic effect due to the gaseous current is sufficient to neutralize at C the magnetic force due to the current through the solenoid. There is a stage when though there is no discharge in C there is very little luminosity in B, showing that it is possible to have very intense currents with very little luminosity.

The equations already given enable us to calculate the effect of the currents in the gas. The case we have hitherto considered where these effects have been neglected corresponds to very small values of na ; when these effects are very large na is large. Now, if x is large,

$$J_0(\iota x) = \sqrt{\frac{2}{\pi x}} \epsilon^x, \text{ approximately,}$$

and

$$J_1(\iota x) = iJ_0(\iota x).$$

Hence the equation

$$H = H_0 \sin pt. \frac{J_0(\iota nr)}{J_0(\iota na)}$$

becomes, when na and nr are large,

$$H = H_0 \sin pt. \epsilon^{-n(a-r)} \left(\frac{a}{r}\right)^{\frac{1}{2}};$$

as n is very large $\epsilon^{-n(a-r)}$ is very small unless $a-r$ is small, so that the magnetic force will diminish very rapidly with the distance from the surface of the tube.

The equation

$$r \frac{d\theta}{dt} = \frac{e}{m} \frac{H_0 \sin pt. J_1(\iota nr)}{\iota n J_0(\iota na)}$$

becomes, when nr is large,

$$\begin{aligned} r \frac{d\theta}{dt} &= \frac{e}{m} \frac{H_0 \sin pt}{n} \frac{J_0(\iota nr)}{J_0(\iota na)} \\ &= \frac{e}{m} \frac{H_0 \sin pt}{n} \epsilon^{-n(a-r)} \left(\frac{a}{r}\right)^{\frac{1}{2}}. \end{aligned}$$

In order that the electron should be able to ionize the gas the maximum value of $r \frac{d\theta}{dt}$ must not be less than q , hence the condition for the self-sustained discharge is that

$$\frac{e}{m} \frac{H_0}{n} \ll q.$$

The electromotive force round a circuit of radius r

$$\begin{aligned} &= \int_0^r 2\pi r. \frac{dH}{dt}. dr \\ &= 2\pi p H_0 \cos pt \int_0^r \frac{r. J_0(\iota nr)}{J_0(\iota na)} dr \\ &= 2\pi p H_0 \cos pt \frac{r. J_1(\iota nr)}{\iota n J_0(\iota na)}; \\ &= 2\pi p H_0 \cos pt \frac{r. J_0(\iota nr)}{n J_0(\iota na)}, \end{aligned}$$

when nr is large.

Hence the electromotive force round the circuit whose radius is a is

$$2\pi p H_0 \cos pt. (a/n).$$

The maximum value of this is

$$2\pi p H_0 (a/n).$$

The minimum value of H_0 required to sustain the discharge is given by the expression

$$H_0 = \frac{m}{e} nq,$$

hence the maximum value of the E.M.F. round the circuit must not fall below

$$2\pi qap(m/e).$$

This is the same value as when na is small, see equation (11).

Though the E.M.F. round the circuit is the same when na is large as when it is small, the magnetic force is much larger when na is large. For when na is large

$$H_0 = \frac{mnq}{e},$$

and when na is small

$$H_0 = \frac{2mq}{ea};$$

the ratio of the first of these values to the second is $na/2$ and is large since na is large.

Let us now consider the path of an electron. To determine it when na is very small we have the equations

$$\frac{d\theta}{dt} = \frac{H_0 e}{2m} \sin pt,$$

$$\frac{d^2 r}{dt^2} + \frac{H^2 e^2}{4m^2} \sin^2 pt \cdot r = 0.$$

The second equation is a particular case of Hill's or Mathieu's equation, and the solution is not expressed by any simple function. We can, however, from physical considerations get some idea of the path of the electrons.

An electron acted upon by a steady magnetic force at right angles to the direction of projection will describe a circle with an angular velocity equal to $H(e/m)$. Thus, if the frequency p of a variable magnetic force is small compared with $H(e/m)$, the path of the electron will approximate to that which would be described if the magnetic force were constant. In the case we are considering the magnetic force is expressed by $H_0 \sin pt$, hence when $(e/m) H_0 \sin pt$ is large compared with p , the paths of the electrons will be circles. If C is the centre of the cross-section of the

tube an electron starting tangentially from P will, unless interfered with by collision with other molecules, describe a circle on PC as diameter. Thus as the paths of all electrons pass through C, we should expect to find a considerable excess of electrons in the region adjacent to C. The electrons if not in collision move with constant velocity, and thus are just as likely to ionize by collision at one part of the circle as at another. Thus when the pressure is so low that the free path of an electron is an appreciable fraction of the radius of the discharge-tube, the ring discharge may extend to a considerable distance towards the centre of the tube: this is a well-marked phenomenon with the ring discharge. When the pressure is high and the mean free path of the electron a very small fraction of the radius of the solenoid the ring discharge will be confined to a thin ring close to the surface. We see, however, that in any case the electrons will tend to get diffused through the tube, so that when once the discharge has been started other discharges following in rapid succession may expect to find a supply of electrons over the cross-section of the tube. The energy which these stray electrons acquire under the action of the field due to the alternating current through the solenoid will be proportional to the square of the distance from the centre, since their angular velocity is independent of that distance. Thus the electrons nearest the glass of the tube will acquire the greatest energy, and this energy, if the ring discharge is to take place at all, must be not less than the ionizing potential of the gas in the tube. But the electrons nearer the centre of the tube, though they may not acquire enough energy to ionize the gas, may acquire energy greater than that of some of the resonance potentials and so produce luminosity in the gas. As the energy acquired by the electrons decreases as we approach the centre, the luminosity produced in the tube will vary in character with the distance from the centre, the luminosity corresponding to the highest resonance potential occurring nearest the glass of the tube, while at the inner boundary of the luminosity the light will correspond to that with the lowest resonance potential. This effect in some gases is obvious to the most casual inspection, the discharge consisting of rings of different colours at different distances from the centre. When the discharge is examined by a spectroscope the effect is shown by most gases, lines which are prominent in the spectrum of the outer part of the discharge disappearing more or less abruptly as the distance from the centre diminishes.

We have supposed hitherto that the frequency of the electrical vibrations is small compared with $h e/m$. Let us now consider the case where the frequency is very great in comparison with this value. The value of $d\theta/dt$ will now change signs with great rapidity, and so the electron will oscillate from one side to another of a fixed radius, never making more than a small angle with it. We see from the equation that d^2r/dt^2 is always negative, so that the electron will have an acceleration towards the centre of the tube. Thus, the path of an electron in this case will be along a wavy line drawn from its original position to the centre of the tube. This will lead again to a motion of electrons to the centre and their distribution over the cross-section of the tube.

Effect of a Superposed Magnetic Field on the Discharge.

When the magnetic force is that due to the currents through the solenoid, there is a constant phase relation between the direction of the magnetic force and the direction of motion of the electron; the result is, as we see from the equation, that d^2r/dt^2 is always negative, so that the electrons tend to move away from the walls of the tube towards the centre. When, however, there is an external magnetic field parallel to the axis of the solenoid, the radial force on the electron is sometimes in one direction and sometimes in the opposite. It is thus sometimes away from the centre, and when it is so the electrons may be pushed against the walls of the tube before they can ionize the gas; this would stop the discharge from going in one direction. As we shall see, an external magnetic field has a very pronounced effect on the discharge, as this effect is not marked until the magnetic field exceeds a critical value. We can, from experiments on this effect, get some idea of the magnetic forces developed by the currents through the solenoid, as this will presumably be of the same order as the critical external magnetic force.

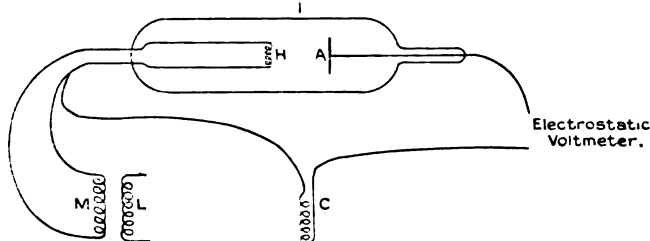
Experiments made to test the Validity of the Preceding Theory.

To test the theory I have made a large number of experiments to see how the electromotive force round the circuit in the discharge-tube when the ring discharge was passing varied with the pressure of the gas, the frequency of the currents through the solenoid, the dimensions of the discharge-tube, and the nature of the gas.

To measure the electromotive force round the circuit, a few turns of thin wire carefully insulated were wound on the outside of the discharge-tube; these were in contact with the outer wall of the discharge-tube and between it and the solenoid. To measure the E.M.F. round this circuit when the discharge was passing, I began by connecting the ends of the circuit to a spark-gap made of two brass balls carefully polished—the distance between the balls was altered by means of a screw, and the distance between them measured by a micrometer. I found, however, that this method was not satisfactory; it was not very sensitive and was somewhat irregular. I discarded it in favour of the method shown in fig. 3.

One end of the circuit was connected with the hot wire H of a large valve, which was very kindly lent to me by the Osram Company. The valve was carefully insulated and

Fig. 3.



the wire was heated by sending an alternating current through the coil *L*, which induced currents in the insulated coil *M*, which was in series with the wire. The other terminal *A* of the valve was connected with one pair of quadrants of an electrometer; the other pair were connected with the other end of the circuit and with earth. The solenoid had a wire soldered to it near the circuit and connected with earth. When the electromotive force round the circuit was in the direction tending to drive negative electrons from the hot wire, electrons would be driven from the wire to *A* and lower the potential of *A* and the quadrants of the electrometer connected with it. This process continues until the potential difference between *A* and earth equals the maximum electromotive force round the circuit in this direction. The reading of the electrometer gave the magnitude of the E.M.F. round the circuit in one direction; the E.M.F. in the opposite direction is not indicated by this arrangement. The electrical oscillations produced by the

Leyden jars are very appreciably damped, so that the E.M.F. in the first oscillation is considerably greater than that in the opposite direction in the second ; thus, when the circuit was connected up so that the first oscillation made the hot wire negative, the reading of the electrometer was considerably greater than if the first oscillation made the hot wire positive; thus, reversing the induction coil made a considerable difference in the reading, as did also reversing the connexions of the circuit with the hot wire valve. In fact, this arrangement gives a very convenient method for measuring the damping of the electrical vibrations. This damping, as has been already stated, is sometimes quite large; it is not uncommon for the electromotive force in the first oscillation to be twice that in the second.

It is essential when using this method to take great precautions to shield the apparatus from external disturbances. Unless this is done it has an uncanny knack of picking up any stray electromotive forces wandering about in the Laboratory ; these, if not eliminated, make the readings irregular. The hot wire valve and the electrometer were placed inside a large box covered with sheet-iron, and the leads from the circuit were surrounded by metal tubes connected with the earth. When these precautions were taken the method worked quite satisfactorily, and gave much more regular results than the spark-gap method.

The following table gives in volts the least E.M.F. round the circuit which will produce at different pressures the electrodeless discharge in air, hydrogen, and helium ; the pressures are given in mm. of mercury, the radius of the bulb was 5 cm.

Air.		Hydrogen.		Helium.	
Pressure. mm. of Hg.	E.M.F. volts.	Pressure. mm. of Hg.	E.M.F. volts.	Pressure. mm. of Hg.	E.M.F. volts.
·018	800	·04	750	·03	920
·13	210	·05	620	·04	920
·185	200	·08	440	·126	720
·280	168	·14	160	·75	120
·410	160	·20	150	1·4	116
·87	200	·32	120	2·1	83
4·0	420	·50	130	3·5	81
		2·1	150	5·4	100
		5·4	300	7·6	108

It will be seen from these figures that graphs representing these results would have very flat maxima, flatter than we should expect if the currents through the solenoid could be accurately represented by the expression $A \cos pt$. The damping of the oscillations is so great that the currents, instead of being represented by a sine curve, are more accurately expressed by a graph, where we have a sudden increase followed by a slower rate of decay. We have seen (p. 1136) that this would give rise to a flat maximum. The minimum E.M.F. round the circuit is found to depend upon the size of the Leyden jars used to produce the alternating currents: it is greater when the jars are small than when they are large. This is in accordance with equation (11), for p is larger with small jars than with large ones. The flatness of the maximum makes it difficult to determine the pressure at which the discharge passes most easily, but the results given above show quite clearly that it is very much higher for helium than for air or hydrogen. The measurements with different sized jars show that this critical pressure increases with the frequency, and measurements with discharge-tubes of different sizes show that the critical pressure does not depend upon the size of the tube.

The effect of pressure and frequency on the discharge can be shown qualitatively in the following way:—A battery of 12 equal small inductances is arranged so that any number from 0 to 12 can be thrown in series with the solenoid; this alters the inductance in the discharging circuit of the Leyden jars, and therefore the frequency of the electrical oscillations. The brightness of the electrodeless discharge is observed when 0, 1, 2, 3, 4, ... inductances are added to the circuit. There is a wide range of pressures when the brightness of the discharge increases as the first few coils are added, but begins again to decrease when the number added exceeds a certain value; thus we see that at a constant pressure there is a certain frequency at which the discharge passes most easily. Again, we find that the number of coils when the discharge is brightest depends on the pressure of the gas: the lower the pressure the greater the number of coils, and therefore the smaller the value of p when the discharge is brightest. This is in accordance with the equation $p\lambda = q$, where p is the frequency, λ the mean free path, and q the ionizing velocity.

According to equation (11) the minimum value of the E.M.F. which can produce discharge is $2\pi qpa(m/e)$. In the experiments recorded in the table $a = 5$ cm.; the minimum

voltage in hydrogen seems to be about 120 volts. If the ionizing potential for hydrogen is taken as 12 volts, $q = 2 \times 10^8$, since $e/m = 1.8 \times 10^7$, p must be 4×10^7 , which is not an unreasonable value as the jars were large and the leads long.

Estimation of the Amount of Ionization Produced in the Gas by the Electrodeless Discharge.

The shielding effect described on p. 1137 enables us to form some estimate of the number of electrons in the gas, and hence of the extent to which the gas is ionized. For we find that when the gas is showing this effect the magnetic force due to the solenoid may be increased to a considerable multiple of the value which would produce discharge in the inner bulb if there were no shielding without any discharge occurring. This shows that the shielding due to the currents passing through the gas reduces the magnetic force in the inside of the bulb to a fraction of that due to the current through the wires of the solenoid; but to do this, the gas currents must be pretty nearly as big as those through the wire.

If n is the number of electrons per unit volume, v their velocity, the current flowing through unit area of the gas is nev ; if H is the magnetic force, v is of the order $rHe/2m$; hence the current through unit area of the gas is $ne^2rH/2m$, but H , the force due to the solenoid, is $4\pi I$, where I is the current flowing through the wires of unit length of the solenoid. Hence the current through unit area of the gas must be of the order $4\pi I ne^2r/2m$; but since these currents are nearly as large as I , $4\pi ne^2r/2m$ cannot be a small quantity if the area through which currents flow is comparable with 1 sq. cm.; as e^2/m is about 3×10^{-13} , n must be of the order 10^{-13} to account for the shielding.

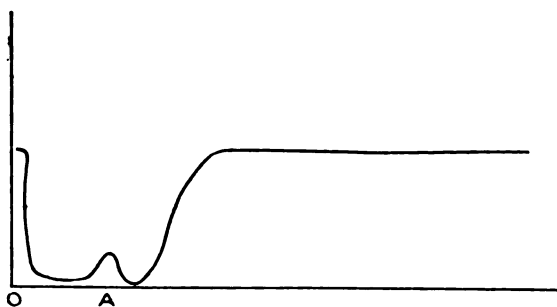
Thus when the shielding occurs at pressures comparable with .001 mm., the number of electrons is of the same order as the number of molecules in the gas, so that a large proportion of these must be ionized.

The effect of pressure on the shielding effect may be shown by the apparatus represented in fig. 2. Beginning with the gas in the outer bulb at atmospheric pressure and gradually reducing the pressure, there is no visible change in the brightness of the discharge in the inner bulb and no visible discharge in the outer until the pressure in the outer tube is of the order of a millimetre. This pressure depends on the nature of the gas: it is much higher for helium than

for hydrogen and higher for hydrogen than for air. On diminishing the pressure below this value the discharge in the inner bulb disappears, though there is but little luminosity in the outer. When the pressure is still further reduced there is often a recrudescence of the luminosity in the inner bulb; this, however, only extends over a small range of pressure. On further reduction the luminosity in the inner bulb disappears again, the luminosity in the outer begins to increase and soon becomes very bright, disappearing again when the pressure gets very low, when the discharge appears again in the inner bulb.

The relation between the luminosity in the inner bulb (the ordinate) and the pressure (the abscissa) is of the type represented in fig. 4. We see that at A there is a range of pressure

Fig. 4.



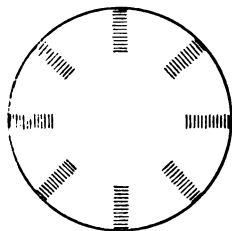
where the currents through the gas are less than at pressures on either side of the range. The properties of the gas in this range of pressure are peculiar: the gas is in the "sensitive" state, of which more will be said later on, and the discharge in this stage, and in this stage only, spreads from the outer bulb through all the tubes connected with it and also through the pump. One fact brought out very clearly by these experiments is that there is very little connexion between the brightness of the electrodeless discharge in the outer tube and the shielding it produces. The shielding effects depend on the currents through the gas. The fact that there may be large shielding with very little luminosity shows that large currents can pass through the gas without producing visible light, and that the production of this depends upon something in addition to the passage of the current. This is borne out by many familiar effects produced when the

ordinary discharge passes between electrodes, for though the average current passing through the different parts of the discharge-tube must be the same, the visible luminosity may be small in some places such as the dark space next the cathode and the dark spaces between the striations, and quite bright in others such as the negative glow and the positive column.

Striations in the Electrodeless Discharge.

On many occasions when the ring discharge was passing through hydrogen it was observed that the luminosity in the ring was not uniform but showed periodic variations, giving it a striated appearance as in fig. 5, the divisions between the

Fig. 5.



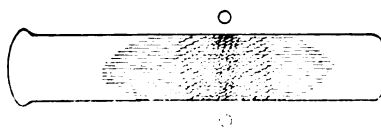
bright and dark portions being radial. This phenomenon only occurs within narrow limits both of pressure and of the intensity of discharge; the bright and dark portions are not steady, but flicker about so that it is not possible to photograph them. The striations are much more pronounced in hydrogen than in any other of the gases I have tried—indeed, I have not been able to feel sure that the phenomenon occurs in other gases.

Another quite different type of striation occurs at suitable pressures and intensities when two equal coils in series are placed at some distance from another on a straight tube containing gas at a low pressure. When the alternating current passes through the coils each coil gives rise to a ring discharge; by adjusting the distance between the coils and the pressure of the gas the luminosity between the coils can in hydrogen be got to show several alternations in brightness. Between the coils the discharge appears to be striated. It is not, however, easy to get the discharge into this state.

Another very interesting effect is observed much more easily. When the pressure of the gas is low the luminosity

in the neighbourhood of the coil of wire carrying the alternating current has the appearance represented in fig. 6: brightly luminous cones stretch out to a considerable distance on either side of the coil. If now two such coils are placed in series along a straight cylindrical tube, at a distance less than twice the length of a cone, the two cones will not blend unless the two coils are very close together, but will be

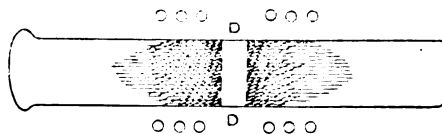
Fig. 6.



separated by a well-defined dark space D, the discharge having the appearance shown in fig. 7. The effect is not so plain at very low pressures as it is at somewhat higher ones.

If, instead of using two coils, we use one coil which can be moved along the tube, and put across one part of the tube a solid plate, either metallic or non-conducting, then, when the coil is moved so that the cone would strike against the plate if it retained its original length, it is found that the cone will never reach up to the plate but will be separated from it by a well-defined dark space. This is more striking in hydrogen and helium than it is in other gases, but I have seen it quite distinctly in air and oxygen. The thickness of this dark space does not, like the Crookes' dark space, increase as the pressure diminishes; it resembles the much thinner dark space discovered by Dr. Aston in helium and hydrogen in

Fig. 7.



being little affected by the pressure. It is, however, much more definite when the pressure is a considerable fraction of a millimetre of mercury than when it is much less than this. The thickness of the dark space depends on the intensity of the ring discharge: it is greater when the intensity is small than when it is great. The dark spaces produced in this way are only a millimetre or less in thickness. We can produce much more extensive dark spaces by letting the luminous

cone strike against a thin tungsten filament which can be raised to incandescence. When the filament is cold the luminosity envelopes the filament, and the only dark space is a very thin layer surrounding the thin filament. When, however, the filament is raised to incandescence and made to emit electrons, the luminosity disappears from a considerable volume around the filament, and there is a large dark space which disappears when the filament gets cold. This experiment suggests that free electrons can destroy the luminosity of the discharge. I think that the dark spaces we have described are due to an effect of this kind rather than to one of a hydrodynamical character due to the presence of the solids or to opposing streams of gaseous molecules. Let us take first the dark space between two cones. Outside each cone there seems to be a distribution of free electrons, so that when one cone is pushed up against a second the first brings a swarm of electrons against the luminosity of the second and destroys it in the front layer, while the electrons accompanying the second cone act in a similar way on the luminosity of the front layer of the first cone. Again, in the case of the solids there may be two effects present: the electrons in front of the cone may strike against the solid and rebound into the luminosity of the cone and destroy it; in addition to this, the electrodeless discharge is the source of very intense ultra-violet radiation. When this falls upon the solid it will make it emit electrons, and these will tend to destroy the luminosity in the neighbourhood of the plate.

The electrons on this view act as absorbers of the energy in the atoms or molecules, which in their absence would be converted into visible radiation.

This effect of electrons on luminosity is in accordance with the view, for which there is much experimental evidence, that the luminosity of a gas depends (1) on its atoms or molecules being put in a state, the "excited" state, in which, though they have more energy than when in the normal state, they are in quasi-stable equilibrium, and (2) on the atoms returning from this state to the normal one and giving out the excess of energy in the form of radiation.

When the atom is in the excited state it is probable that it is more active chemically than when it is in the normal one. One reason for this is that its electrostatic moment is greater; it is more polar, and therefore more likely to unite with an electron. If, however, it forms an association with an electron, which need only last for the very short time during which the atom remains in the excited state, the system with the attached

electron, differing fundamentally from the uncharged excited atom, will not emit radiation of the same type—indeed, it may not give out any visible radiation at all. This effect of electrons on luminosity seems analogous to the very remarkable effects discovered some years ago by Professor R. W. Wood. He found that traces of foreign gas, especially strongly electromagnetic ones, diminish to a remarkable extent the luminosity excited in other gases by resonance. They might, on the view just given, be expected to do this if they formed temporary compounds with the excited molecules of the luminous gas.

Sensitive State of the Ring Discharge.

The electrodeless discharge at certain pressures and intensities is very much affected by the approach of a conductor, though in general this produces very little effect. I have found this effect especially conspicuous in cyanogen, though it exists to some extent in all the gases I have tried. The following description relates to a bulb about 5 cm. in radius filled with cyanogen. When the pressure was much less than .1 mm. of Hg, the ring discharge was very bright and was not sensitive to the approach of a finger. When the pressure was raised to a pressure approaching .1 mm. a stage was reached when the appearance of the discharge suddenly changed with the pressure. Luminosity spreads through the tubes connecting the discharge-vessel with the pump, and if a finger is placed against one of these tubes the luminosity is repelled and there is a dark space under the finger. As I have already stated the shielding effect is abnormal when the gas is in this state. The ring became much less sharply differentiated from the rest of the bulb than it was at lower pressures, and in addition to the ring a bright line of light passing through the centre of the bulb and at right-angles to the ring appeared. When the pressure was still further increased the bright line through the centre broke up and several ill-defined luminous pencils, symmetrically distributed round the axis of the tube, took its place. At still higher pressures these beams disappeared.

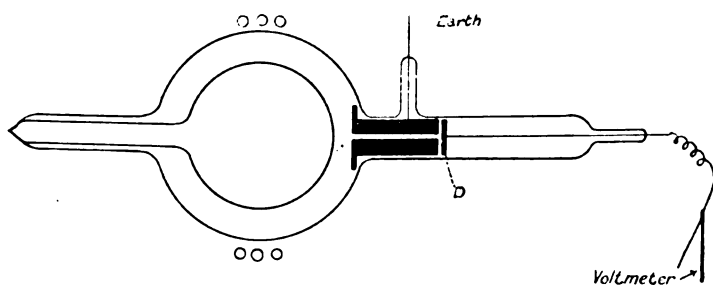
When the bright line was present the discharge was very sensitive to the approach of a finger; it was much brighter when the finger was held near the tube than when it was taken away. If the finger touched the glass the bright beam seemed to reach the glass too, but if the finger stopped short of the glass the beam stopped short too, and could be made

to contract or elongate by moving the finger backwards and forwards. At pressures of about $\cdot 05$ mm. the discharge was in such a sensitive state that unless the finger approached within a certain distance of the bulb there was no discharge of any kind, ring or straight line; a difference of half an inch in the position of the finger would make all the difference between a very bright discharge and none at all.

The bright line through the centre was bent by a magnet, showing that there is a stream of electrons along it. The direction of bending showed that the electrons were moving from the walls of the tube towards the centre.

When the discharge is sensitive the luminosity spreads from the vessel through which the discharge takes place through all the tubes connecting this vessel with the pump.

Fig. 8.



The finger appeared to repel this luminosity from the part of the tube to which it was applied.

If, when the discharge is in this state, a finger be placed against the outer bulb in the apparatus shown in fig. 2, a patch of green phosphorescence, due to cathode rays, will appear on the glass of the inner bulb. The luminous ring in the outer bulb is less differentiated in luminosity from the gas in its neighbourhood than it is outside this range of pressure, and the glass surface of the inner bulb is covered with a luminous glow. Again, as the following experiment shows, the electrical condition of the gas in the outer tube is exceptional over this range of pressure. A tube fitting round a metal rod with a hole in it was fused on to the outer bulb; behind the tube was a disk D connected with a gold leaf electroscope. When the electrodeless discharge was passing at pressures on either side of the sensitive state it discharged with great rapidity any charge, either positive or negative,

in the electroscope, even though this was connected with a Leyden jar to give it greater capacity, but when the discharge was sensitive, though the electroscope lost with great rapidity a negative charge, it did not lose a positive one unless this was in excess of a certain value, and if the electroscope was uncharged to begin with it soon acquired a positive charge. The conditions indicated that this was due to charged ions rather than to a photoelectric effect. There thus seems to be a range of pressure in which there is an excess of positive over negative ions. This would explain the phosphorescent patch produced when the finger is placed against the glass and the glow on the inner bulb, and in fact all the properties of the sensitive state.

The excess of the positive charge over the negative can be explained by the diffusion of electrons to the walls of the tube being more rapid than that of the positive ions. The electrons and the ions disappear from two causes, diffusion and recombination, but since the combination of an electron and a positive ion does not alter the total charge of electricity in the gas, the rate at which the excess of positive charge in the gas increases is equal to the rate at which electrons diffuse to the walls of the vessel. This rate vanishes when the pressure vanishes because then the number of electrons vanishes; it also vanishes when the pressure is very high because then the coefficient of diffusion vanishes. The rate must therefore be a maximum at some intermediate pressure, and it is in the neighbourhood of this pressure that the discharge is in the sensitive state.

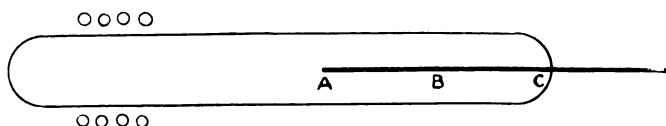
*Influence on the Discharge of various Solid Bodies
in the Discharge-Tube.*

I have observed some curious and suggestive effects produced by the presence of various substances in the discharge-tube. Thus, when making the experiment (described on p. 1149) on the effect of the hot tungsten filament on the luminosity of the discharge in its neighbourhood, I noticed that often when the solenoid produced a bright discharge when at one end of the tube, yet when it was moved down towards the other end of the tube so as to enclose the leads of the filament, which were two wires parallel to the axis of the tube and close together, the discharge stopped completely. This effect differs from the local effect produced by the filament on the luminosity in that the complete stoppage of the discharge is more marked when the tungsten filament is cold than when it is hot, whereas the effect on the luminosity is very much greater for the hot filament than for the cold.

I next tried the following experiment. The discharge-tube was a long cylindrical tube along which the solenoid could be moved from end to end. A thin cylindrical rod of aluminium, about 2 mm. in diameter, ran along the axis of a portion of the tube. When the solenoid did not enclose the rod the discharge went quite freely, but was dimmed when the solenoid was moved down the tube so as to surround the rod. It was easy to adjust the spark-gap in the primary circuit so as to make the discharge quite bright when the solenoid did not enclose the circuit and vanish when it did.

I next replaced the aluminium rod by a fine glass one; one half (AB) of this rod was silvered, the other half (BC) was platinized. It was found, within certain limits of pressure and spark length in the primary circuit, that a bright discharge occurred when the solenoid did not enclose the glass rod, but ceased when it came over the silvered or

Fig. 9.



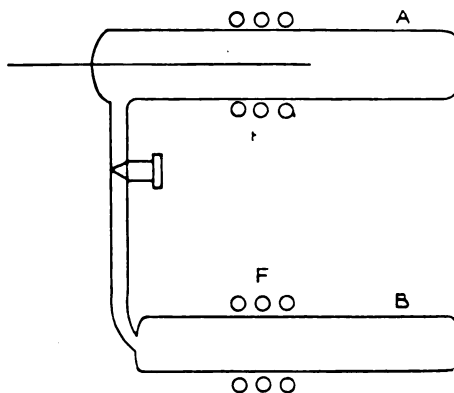
platinized portion. The platinized portion seemed more active than the silver, for when the discharge was quite extinguished when the coil was over the platinum it sometimes still lingered when it was over the silver.

I next, instead of coating the glass rod with metal, used one, half of whose length was clean while the other half was covered with sulphur. I found this produced even more marked results than the platinized one. For the discharge was brightly luminous when the solenoid did not enclose the rod, stopped when it enclosed the sulphur portion, and went again when the solenoid came over the uncovered part of the rod. When the gas in the tube was either hydrogen, air, or nitrogen there was a rapid diminution in the pressure, showing that chemical combination was going on, but the effect just described occurred also when the tube was filled with helium, when there was no change in the pressure.

With this rod in the tube it was found impossible, whatever might be the gas filling, to maintain the discharge for long, even though the solenoid did not encircle the rod. Though the discharge might be bright to begin with it gradually got fainter, and in a few minutes disappeared. Sometimes it was found impossible to get the discharge to

start again however much the spark-gap in the primary circuit was increased. If the tube was left for some hours, or if a current of gas was drawn through it for some minutes, it recovered its power of giving a luminous discharge. The effect seems to be connected with something condensed on the glass walls of the tube, for if the tube be heated for some minutes with a gas flame it recovers its power of giving a bright discharge. If one-half the tube has been heated, while the other half has been left cold, the discharge will often pass when the solenoid is over the part which has been heated, but will not do so when the solenoid is over the other portion. This experiment illustrates the large effects which may be produced by the walls of the tube. To investigate the matter further I tried the experiment represented in fig. 10.

Fig. 10.



A and B are equal cylindrical tubes round which solenoids E and F, equal in every respect, are placed in series. A and B are connected by a piece of quill tubing with a tap between A and B, so that the two tubes can either be shut off from each other or put in communication. The tube A contains a thin glass rod, half of which is coated with sulphur. The tube B contains nothing but the gas with which the tube is filled. Before the discharge begins the apparatus is filled with a gas at a suitable pressure, and the tap turned so as to cut off the connexion between A and B. Then when the currents are sent through the solenoids discharges pass through both tubes, but while the discharge in B continues indefinitely, that in A soon stops. If after this has occurred, and while the discharge is passing through B, the tap is turned so as to open the communication, the first effect is that the dis-

charge recommences in A. (The two solenoids are in series, so that an alternating current is passing through the solenoid round A.) If the tap is turned again so as to cut off the connexion between the tubes the discharge immediately stops. It will start again immediately if the tap between the two tubes is opened. The starting of the discharge in A is not due to electrons passing from B to A, for it occurs with undiminished intensity if a strong electromagnet is placed under the tube connecting A and B. This would prevent any electrons passing from one tube to the other. When the tap is open a faint luminous discharge can be seen passing from B through the piece of quill tubing and the tap. If the tap is kept open the discharge in A soon stops and that in B diminishes and after some little time stops, so that no discharge passes through either tube. If now the tap is turned so as to cut off the connexion between the tubes the discharge in B will slowly re-establish itself, and finally be as bright as it was originally. The spectrum, however, shows lines due to sulphur, so that some vapour of sulphur has leaked into this tube from A. The bulb A remains persistently dark, and no discharge passes through it, even after its temperature falls to that of the room. When the discharge passes through A the parts near the solenoid get appreciably warm, and some sulphur distils from the glass rod on to the walls of the tube.

If, after the discharge has stopped in A, a small quantity of fresh gas is let into this tube, the discharge starts again, though it only lasts for a short time. Anything that produces a current of gas in the tube seems to lead to a temporary revival of the discharge. When the gas in the tube is hydrogen the admission of fresh gas shows some interesting effects. When first the gas is admitted, the discharge in A shows the brilliant red cones characteristic of hydrogen emitting the Balmer lines, the red only persists however for a few seconds, the cones become white and the Balmer lines feeble, and after a short time the discharge stops. If the tap between A and B is open the discharge in B also shows the red cones when fresh hydrogen is admitted, but these persist much longer than in A and are visible after all discharge in A has stopped. The cones in B, however, gradually lose their red colour, become white, and ultimately, as was stated before, the discharge in B also stops provided the tap is kept open. If the tap is turned after the discharge in B has lost its redness but before it has ceased, the brightness of the discharge in B will increase but the red cones will not reappear.

I have tested the effect of different substances on the discharge by depositing a thin layer of the substance of about the same length as the solenoid at the middle of a thin glass rod placed along the axis of the discharge-tube. I have used, in addition to sulphur, silver, platinum, cadmium, the filament of an incandescent mantle, graphite, and found with all these that it was possible to get the discharge bright when the solenoid was not over the covered portion and to cease when it came over it; the effect was very distinctly less marked with the graphite than with the other substances—it required careful adjustment of the pressure to get it at all, and even then it was not nearly so well marked as for the other substances.

The effect is most marked when the pressure is only a few hundredths of a millimetre and gets much less at considerably higher pressures; it does not seem to depend upon the nature of the gas, as I have obtained it in air, hydrogen, oxygen, and helium. If, after the discharge has been running for some time, the tube is strongly heated in the neighbourhood of the place where the substance is deposited on the glass rod, it often happens that immediately after the heating the discharge will pass when the solenoid is over the patch of substance, the place where it was stopped before the heating, but that it is now stopped at some other part of the tube where it went before. This looks as if the effect is due to a deposit of something on the walls of the tube which is driven off at a high temperature. In a short time, however, the discharge stops again when the solenoid is over the patch.

Quite recently I have found that when patches of fused salts, such as potash, soda, sodium chloride, lithium chloride, are placed on the glass rod, the discharge at low pressure goes more easily when the solenoid is over the patch of salt than when it is in the other parts of the tube: this effect is opposite in sign to that produced by patches of metal or sulphur.

Theory of the Effects of Foreign Bodies on the Discharge.

The following considerations may help us to understand the influence of foreign bodies on the discharge:—In order that the discharge should occur the gas has to be ionized. For this energy is required; this comes from electrified bodies which have acquired high velocities under electric force. To start the discharge there must be some electrified bodies to begin with. In a gas in which there was nothing

but neutral molecules it would be impossible to produce a discharge unless the electric field was so intense that it was able to tear the electrons out of the molecule. To do this the field would have to be so strong that the fall of potential in a length equal to the diameter of a molecule is not less than the ionizing potential of the molecule; this requires a field where there is a fall of about 12 volts in 10^{-8} cm., or 1.2×10^9 volts per cm. This is quite a different order of intensity from that in discharge-tubes. It is to stray electrified atoms or electrons, and to stray electrons in particular, that we must look for the initiation of the discharge. Under normal conditions there is always a certain amount of ionization going on in a gas apart from that due to the action of the electric field or visible radiation. This residual ionization, as it is called, gives rise to some 10 or 12 pairs of ions per second per cubic centimetre of gas at atmospheric pressure. This ionization in its initial stage gives rise to free electrons. Before these electrons can ionize the gas, a time must elapse which must be very large compared with the interval between one collision of the electron with a molecule of the gas and the next. For before the electron can ionize it has to get from the electric field energy greater than the ionizing potential of the gas, and it has to convey this energy to an electron in a molecule before that electron can be liberated. When the electric field is not much more intense than the limit which will produce discharge, it may be only one out of a very large number of collisions which will result in the transfer of a sufficient amount of energy. Thus, anything which reduces the life of the electron below the time necessary for it to make these collisions will diminish its efficiency as an ionizer. The electron loses its power of ionization when it unites with a molecule to form a negative ion. In many gases we know from the experiments of Loeb that an electron makes a very large number of collisions before it gets linked up with a molecule, and this number varies greatly with the nature of the gas; thus it is certainly many millions if it is not infinite for pure nitrogen or helium; for oxygen, in which the electron has a comparatively short life, the number of collisions is about 30,000, while in chlorine the number is less than 300. Thus for the electronegative gases this number is exceptionally small. Now, sulphur is a very strongly electronegative element, and presumably a sulphur molecule would be very likely to capture an electron striking against it. If every collision of a sulphur molecule with an electron resulted in the capture of the electron, then even if the partial pressure

of the sulphur molecules was only $1/30,000$ of that of the molecules of oxygen the presence of the sulphur would halve the free life of the electron; if the gas were hydrogen or nitrogen instead of oxygen it would reduce it very much more. Though the vapour pressure of sulphur is exceedingly small, being only 0.003 mm. of Hg at 50°C ., it is more than $1/30,000$ of the pressure in the experiments we have described. It must be remembered, too, that when the discharge passes the temperature and therefore the vapour pressure of the sulphur increase. As a matter of fact, we find that there is a deposit of sulphur on the walls of the tube after the electrodeless discharge has been going for some time. It is thus, I think, probable that there may be enough sulphur vapour present in the discharge-tube to curtail seriously the life of the electron and thus diminish its ionizing power and thereby increase the difficulty of producing the discharge.

The experiments described on p. 1153 show that when the tube contains nitrogen, hydrogen, or air, these gases combine with the sulphur, if the compounds so formed are gaseous, or even though they are solids or liquids; if they are more volatile than sulphur they may produce effects which persist after the discharge has stopped if they, like sulphur, possess the power of capturing electrons. This would explain the effects observed with nitrogen, hydrogen, and air where, after the discharge has been passing for some time, the bulb gets into a state when the discharge stops and cannot be started again until a considerable time has elapsed or the bulb been washed out with fresh gas. In helium, where no combination occurs, this permanent effect is not produced; the sulphur diminishes the discharge for the time being, but does not lead to a state in which for some time it is impossible to get a discharge through the tube.

Anything that shortens the life of the electron will increase the difficulty of getting the self-sustained discharge; on the other hand, anything that reduces the number of collisions required by one electron to detach another from a molecule will facilitate the discharge. Thus, if the discharge produces complexes formed by the aggregation of several molecules, it may well be that an electron striking against one of these is more likely to detach an electron than if it struck against a single molecule; thus the presence of such aggregates would facilitate the discharge. We saw that with the apparatus shown in fig. 10, after the discharge had stopped in A and was passing in B, opening the tap between A and B caused the discharge to start in A and

persist for a short time, even though electrons were prevented by a strong magnetic field from passing from B to A. This suggests that aggregates, or agencies which have the power of producing aggregates or which give out radiations which ionize the gas, pass from B to A and help the electric field produced by the solenoid round A to ionize the gas. I found, in the earlier experiments referred to at the beginning of this paper, great difficulty in getting the electrodeless discharge to start in gases which had been very carefully dried; this is intelligible if we suppose that traces of moisture facilitate the formation of aggregates, the moisture acting as a catalyst for the electric discharge as it does in many cases of chemical combination. If this view is correct, the passage of the discharge may be made more difficult by agencies which remove from the gas certain products of the discharge. The discharge, besides producing chemical decompositions and combinations which are permanent, produces other modifications of the gas which only persist for a short time. In some cases, *e.g.* nitrogen or oxygen, the existence of these is shown by after-glows, which may persist for several seconds after the discharge stopped. In other gases the duration of their products is too short for them to produce visible after-glows, but their existence may be inferred from the changes which occur in the properties of the gas through which the discharge has passed. If the E.M.F. round the circuit in the electrodeless discharge is increased from zero to a high value and then diminished again to zero, the E.M.F. when the discharge first begins is nearly always considerably greater than that at which the discharge stops. It does not require as large an E.M.F. to maintain the discharge as to start it. The simplest explanation is that the discharge produces systems which are more easily ionized than the normal molecules. The experiment (fig. 11) supports this explanation strongly, for it shows that an E.M.F. which cannot produce discharge in a normal gas may do so if that gas is put into connexion with a gas through which a discharge is passing. If any substance which has a strong affinity for these easily ionized molecules is introduced into the gas it will remove them from the gas as fast as they are formed, and thus make the passage of the discharge more difficult. The presence of certain metals destroys the after-glow in gases which in their absence give intense glows. The metals destroy the compounds which produce the glows; these compounds are quite probably analogous to the easily ionized ones produced by the discharge—if the metals destroy these

as they do the glow-forming compounds their presence will make the discharge more difficult. The experiments already described show that the presence of metals may retard the discharge and that some metals are more effective than others.

The electrodeless discharge offers great advantages for the study of the effect of impurities on the passage of electricity through gases, for it starts close to the surface of the glass, which is where the impurities might be expected to congregate.

It might seem remarkable that a metal so little volatile as platinum should give off vapour able to affect the discharge.

Lenard (*Wied. Ann.* xxxvii. p. 443, 1889) and Rubens and Ladenburg (*Ber. Deutsch. Phys. Gesell.* ix. p. 749, 1907) have brought forward evidence that under the action of ultra-violet light many substances, including gold, evaporate. Since the electrodeless discharge produces very intense radiation of a very absorbable kind, we might expect that it would make the substances exposed to it evaporate. Again, the "sputtering" of the metal from the cathode in ordinary discharge-tubes shows that under certain conditions metals evaporate at temperatures much below that at which they give out visible radiation.

This may be the explanation of an effect I observed when studying the photoelectric emission produced by the radiation inside the discharge-tube. I found (*Phil. Mag.* ii. p. 687, 1926) that when a metal plate was exposed to the radiation there was, as might be expected, a large leak of negative electricity from the plate. What was remarkable, however, was that when the plate was strongly electrified positively there was a small leak of positive electricity from the plate. It was shown that this was not due to the ionization of the gas around the plate or to the incidence of radiation reflected from the plate on to neighbouring conductors, causing them to emit electrons which found their way to the plate and produced the effect of a leak from it of positive electricity. I have not, however, succeeded in getting direct evidence of the evaporation of thin films of gold exposed to these radiations.

The electrodeless discharge supplies, I think, a convenient method for investigating the effects of various physical agents on the ionizing potential of a gas, and whether or not these produce in the gas molecules more easily ionized than the normal ones; for, as the preceding experiments show, this discharge is very sensitive to anything which alters the ease with which a gas can be ionized.

I have much pleasure in thanking my assistant, Mr. Everett, for the help he has given me in this investigation.

CII. *The Analysis of the Copper Spectrum.*

By W. M. HICKS, F.R.S.*

II. COMPLEX SEPARATIONS AND QUARTET RELATIONS.

Summary.

THE paper begins with a short discussion of the inverse D lines, the result of which is to indicate the possibility that these and 5105, with the separation 2042, may not belong to doublet systems as generally supposed. Evidence is given for the existence of quartet systems depending on d terms with separations 2042, 1412, 894, and with separations completely following Landé's separation rules. Several other quartet examples are given, but no general discussion of the whole spectrum on this basis is attempted. Shenstone's lists of fundamental lines with 2042 separations are then discussed. An attempt is made to allocate them on the basis of the maps of [I] and to test these allocations by quartet arrangements and summation sets. In spite of the appearance of perfect quartet sets in which the separations follow Landé's rules, the evidence seems to lead to a suspicion that the 2042, 1412, 894 are composite, depending on association of links and term displacements. The quartic arrangements given by Beals, adopted later by Shenstone and by Sommer, are then specially considered and certain difficulties connected with their two-term theory of line constitution discussed. The evidence from the Zeeman effect appears on the whole to contradict the allocations suggested by them, but the conclusion is drawn that Landé's rules for Zeeman patterns do not apply to these systems. The majority of their quartet separations appear also to be composite, and the quartets involved are not real ones. It would appear, however, that as many new questions arise as are definitely settled.

The present paper is a sequel to that on the "Analysis of the Copper Spectrum" appearing in vol. ii. p. 194 of this journal †—referred to here as [I.]. It deals chiefly with the question of multiplicity in the spectrum of this element. It had been intended to begin with a consideration of the collaterals of the ordinary S, D series ‡ lines and a more complete discussion of the F and various P series. These are specially interesting, as collaterals enter in

* Communicated by the Author.

† The reader must be acquainted with the results of this paper, and especially must have its maps and Table A at disposal for continual reference. References to papers are given in three sets of numbers, of which the first gives the volume, the second the page, and the third the last two digits of the year, thus 12 means 1912, but a year of the previous century would be given in full.

‡ Shenstone, Phys. Rev. 28, 462, 26, appears not to have known that these series had already been allocated up to $m=10$. (Phil. Mag. 39, 457, 20, referred to later as [A] and 'Analysis of Spectra' (1922), p. 252.).

considerable numbers concurrently with a sudden diminution of intensity and change of character at S (4), D (4). Thus for successive orders $m=2, 3, 4$ the intensities of S, are 10, SR, 2n and of D₁₁ are 10 R, 10, 2n. The length to which the quartic discussion has extended has, however, compelled me reluctantly to exclude this portion.

The "Inverse D" Lines.

1. **T**HE sets of line pairs with the doublet separation which occur in analogous positions in the elements of this group, were allocated by Runge and Paschen as inverse doublet D sets, without D₁₁ representatives, since their Zeeman patterns as determined for Cu* and Au† seemed, with the knowledge of the Zeeman effect at that date, to point to corresponding D relations. Corresponding D₁₁ lines were later suggested by me [A. p. 469]. The great advance in our knowledge since then, due to Landé, calls for a re-discussion and re-statement, especially as the allocation of the D₁₁ does not seem to have met with general acceptance. Their appearance in the spectrum of each element gives opportunity for a comparative discussion. The following table gives a conspectus of their appearance to different observers and under different conditions:—

	Copper.									Silver.				Gold.					
	K.R.	A. a.	A. s.	H. a.	H. s.	E.V. a.	E.V. s.	E.H. a.	E.H. s.	K.R.	K. ⁽¹⁾	W.	E.V. s.	K.R.	E.H. a.	E.H. s.	E. a.	E. s.	E.V. s.
D ₂₂	8	6r	6	8	10	8	8	50	10r	4r	ft.	3	1?	4	4	1	4	6	3
D ₁₁	1n	1		1n	1n	3	1n	1	1	2r	2r	-	-	4	2	2	1n	5	8
D ₁₂	8	5	4	6	8	8	6	8	8	1r	1	-	-	2	2	1	2n	2	2

(1) Remeasured from K.R.'s old plates.

Here K.R. denotes Kayser and Runge. A., Aretz. H., Hasbach. E.V., Eder and Valenta. E., Eder. E.H., Exner and Haschek. K., Kaspar. W., Walters. a=arc. s=spark. These initials are used throughout this paper.

The only normal march of intensities is that given in Au by E.V. in the spark or K.R. in the arc. The outstanding facts are:—

(1) The apparent reversal of the order of intensities in the D₁₁, D₁₂.

(2) Their independence of arc or spark conditions except in Au, where the spark enhances them.

* Hartmann, *Ann. d. Phys.* 38, 43, 12. Runge and Paschen, *Berl. Sitz.* (1902) p. 720.

† Hartmann, *loc. cit.* Purvis, *Proc. Cam. Phil. Soc.* 14, 217, 07.

(3) The extreme faintness of the whole set in Ag (only observed by K.R.) and their considerable intensity in Au. The relation of this to the abnormal double valency of Cu, the normal valency of Ag, and the abnormal of Au, strikes the eye at once, suggesting connexion of these sets with the additional electrons transferred from the core.

It might be objected that the allocation of D_{11} in Cu is not correct, but this is met by the facts that in Cu and Ag the separations exactly fulfil the own conditions, the D_{11} in Cu comes essentially into the relations of map V., starting with the Y_2 link, whilst a reference to [I. pp. 207, 208] shows that, in Ag, D_{11} has the Y_1 link back, and, in Au, the X_1 forward, and finally the fact that in Au the observed Zeeman pattern fits the D_{11} allocation. As possible explanations may be suggested:—

(1) The D_{11} has been disrupted almost wholly into other collaterals.

(2) A normal D set has been displaced or linked so that, while the normal $p_1 d_1$ transitions have nearly all taken place and a few displaced (obs. D_{11}), the majority of the $p_1 d_2$, $p_2 d_2$ have been displaced to the set in question, and a few only or none of the normal transitions have occurred (see example below). Indeed, the spark nature of the set suggests displacement or linkage.

(3) In Cu the D_{11} line belongs to the system of the faint companions of the known complex lines D_{12} , D_{22} , and the main lines are an independent type.

In connexion with his research on the ultra-red spectrum of Cu, Randall * denoted by x (later by me d_2') the unknown term combining with p_1 , p_2 to give the doublet, and at the same time allocated lines to combinations with it, of $f(3)$, $f(4)$, $d_1(2)$, $p_1(2)$, $p_2(2)$ of which, however, that with $d_1(2)$ cannot be sustained, nor can one at least of the last two.

2. Shenstone has adopted a suggestion by Ruark and taken in Cu the strong line 5105.543 (F.B.), $n=19581.115$ as the corresponding D_{11} . If it be written $y-p_1$, the value of y , since $p_1=31524.53$ is 51105.65. He has given a long list of combinations of this y and x with several other terms, which he has arranged in sets in the form

$$\begin{aligned} s-q_1, \quad x-q_1, \quad y-q_1, \\ s-q_2, \quad x-q_2. \end{aligned}$$

These have formed the starting-point for quartet allocations

* *Ann. d. Phys.* 33, 739, 10.

by himself and by others. It must be admitted that as they stand, *i.e.*, if q_1, q_2 are *related* terms, the selection rules require j values of 2, 1 for q_1, q_2 (*i.e.*, p terms) and 3, 2 for y, x , or y is a real d_1^2 term. But there is nothing to show *a priori* that a particular pair chosen is to be taken as related. If, however, the connexion of q_1, q_2 be allowed it follows that y must be a d_1^2 or 233 term. Other evidence, however, seems to be definitely against y being the d_1^2 of the inverse set, quite apart from the reasons given above, that they already possess a different d_1^2 term of their own.

(1) In all the immense number of known cases, the satellite separation is a small fraction of the doublet separation. Here it is $2042/248 = 8.2$ times larger.

(2) In only a few cases do we find the satellite term less than that of the main lines. Here it is 49062 as against 51105.

(3) The satellite separation of a doublet depends exactly on our displacements in all known definite cases. Here the separation is 2042.876 (error certainly $< .01$). We have then

$$\begin{array}{ccc} 49062.77 & 2042.88 & 51105.65 \\ R/(1.495151)^2 & 30188 & R/(1.464963)^2 \end{array}$$

The displacement $30188 = 4\Delta + 26\delta_1 + 10.5$.

The 30188 is correct within unity in the last significant figure, and the greatest possible error in $4\Delta + 26\delta_1$ does not exceed .5. Thus the displacement definitely cannot be an *own* multiple. The result is fatal against 51105, 49062 being d_1^2, d_2^2 terms of the *same* system. This argument holds only if the d are to be doublet terms. If the multiplicity is higher than 2, we may expect from analogy something similar to the well-established triplet modification, where the *own* rule never applies exactly to each of the separations, but is absolute for their sum.

(4) In the red region King finds 5105 the only line seen in the furnace spectrum, whereas the two D_1' 5782, 5700, should also have been visible if they also were furnace lines. This we should expect if they belonged to the same system. It may be noted that 5105 is a single line of "great sharpness" (Janicki) whereas the other two are complex.

(5) To compare the respective effects of the arc and spark excitations we may take the observations of Hasbach.

	arc.	spark.
$x - p_2$	8	10
$x - p_1$	6	8
5105	$8n$	4

This clearly shows a remarkable difference in their reactions

to arc and spark. Whereas 5105 behaves as if it were a normal series line, the other two behave as if they were linked lines, *i. e.*, enhanced by the spark. Indeed, here the separation 2042·88 suggests at once a $3u$ link = 2041·89, with a displacement on the x or y term. If such displacement occurs in x the own shift is 2·40, if in y it is 2·55. If we take the Rydberg $u' = 680\cdot11$, $3u' + (-\delta_1)$ on $x = 2040\cdot33 + 2\cdot40 = 2042\cdot73$ and $3u' + (-\delta_1)$ on $y = 2042\cdot88$. As these numbers are all accurate to the last decimal, the latter, which reproduces the exact separation, must, if this linkage relation be real, be taken, and the former cannot be admitted. It would mean, a case already suggested, a possible normal inverse D set with a satellite separation 2·55, inverted as in the F series, in which the D_{12} , D_{22} lines in the actual excitation are shifted by $-3u'$. Thus for illustration

5782	17289·80	$3u'$	(19330·13)	} 248·44
5105			19581·12	
5700	17538·24	$3u'$	(19578·57)	

the lines in brackets denoting the supposed normal unlinked D_{22} , D_{12} . Against an explanation of this kind may be placed the fact that, as a rule, linkage separations are very frequently accompanied by term displacements, which vary with the terms involved, whilst in the seven examples given by Shenstone with reliable readings, all the separations involved agree within ·01 of their mean. On the other hand, we do find a very considerable number of $3u$ linking, *e. g.*, amongst others,

1. (8 vi) 27664·185 **2041·877** 29706·062 exact $3u$.
2. (3 vi) 27401·610 **2040·92** (31 vi) 29442·534 with complete chain, viz. (3 vi) $+M+X+e+L+u+u-L-M-e-X+u$ (31 vi) $=3u$.
3. 1n, 3883·73; 25744·29 **2040·96** 27785·25 $S_1(5)$.

This, as attached to $S_1(5)$, can have no relation to the y x separations here considered. It is $2u' + u = 2040\cdot85$ within O.E. of either line

E.H. {	20128·41	$3 \times 680\cdot46$	22169·77	(8 viii)
	29·46	$3 \times 680\cdot10$		
5.	24973·92	$3 \times 680\cdot52$	27015·48	$3 \times 680\cdot53$ 29057·08 (22, 18, 19 xiii).

Another possible allocation for the 5105 must not be passed over without notice. As a fact numerically it is $D_{11}^2(2) \cdot Y_1 \cdot Y_2$. Both lines have been measured by interferometer methods by Fabry and Buisson to three places of decimals (say possible O.E. $d\lambda = \cdot002$, $dn = \cdot005$). They give $19581\cdot115 - 19158\cdot370 = 422\cdot745 \pm \cdot01$; whilst $Y_1 + Y_2 = 210\cdot21 + 212\cdot54 = 422\cdot75$. The agreement is exact, and it

appeals to me as very strong evidence for the reality of the relation indicated. The two suppositions, however, correspond to essentially different constitutions. In this, p_1 enters as a positive term, in the former, as negative. Nevertheless, in the present paper I have discussed the data on the basis of the assumption made by Ruark, Shenstone, Beals, and Sommer, *i. e.*, as $y - p_1$.

The Evidence from the Zeeman Effect.

3. Let us now see what information the Z.P. can offer as to the term-types of these three lines, in view of the new knowledge since 1920 given by Landé's rules. The theoretical patterns involved for the D^2 , D^4 lines are as follows, the displacements being given as ratios to the standard shift. The strongest components in ϖ , σ and the smallest ϖ only are entered, other components being indicated by dashes. The intervals between components are twice the smallest ϖ . The first two figures in each case give the j values for the p , d terms respectively.

1, 2 D_{22}^2	·07/-, ·87	2, 2 D_{12}^2	·80, ·27/-, 1·07, -
2, 3 D_{22}^4	-, ·18/·83, ---	3, 3 D_{12}^4	·57, -, ·11/- - 1·49 - -
	2, 3 D_{11}^2		-, ·07/1·00 - - -
	3, 4 D_{11}^4		-, ·09/1·00, - - - - -

— D_{22}' , $\lambda = 5782$ was examined by Hartmann and by Runge and Paschen. Both give 0·83, but Hartmann also states "further decomposition into 6 or 9 components possible." Omitting F and higher order lines the only types capable of giving this not fully resolved pattern are D_{22}^2 and D_{22}^4 , either of which is capable of producing a merge 0·83, but D_{22}^2 has at most only six components, and the separation of the components (·13 or $d\lambda = \cdot 03$) is too small to have allowed them to be seen as separate by Hartmann. On the contrary D_{22}^4 has the exact ·83, and the component separation (·36, $d\lambda = \cdot 1$) is large enough to have enabled the separate components to have been recognised as such.

— D_{12}' , $\lambda = 5700$. Hartmann shows "a quite complicated decomposition. Under specially favourable conditions only four parallel could be certainly established of which the outer pair showed three times the intensity of the inner. With the four parallel, twelve components on the whole were ordinarily to be concluded." Runge and Paschen found the D_{12}^2 pattern without the internal ϖ pair, not to be unexpected perhaps in view of Back's * more recent observations that the corresponding components in the D_{12}^2 lines in Th, Ba, Cu are extremely faint. The eight σ of Hartmann cannot possibly be met by the doublet type, and it would

* *Ann. d. Phys.* 70, 333, 23.

seem that the lines observed by him were of quartic type. This carries with it the necessity that in these lines at least the p terms are also quartic, for their j values must be 3, 2 and they cannot be intercombination. In the case of Au, Hartmann gives for $-D_{22}'$, 0.885, none for $-D_{12}'$ and 0.111 for $-D_{11}$. These are not decisive as between doublet and quartet.

$\lambda=5105$. Hartmann gives 0.110 and recently Sommer 0.110. It is noticeable that these agree with that for AuD_{11}' . The strongest σ should be 1.00 in both doublet and quartet types, but as Back (*l. c.*) finds intensity ratios 9 : 7 : 3 : 1 and the components are only separated by about .18 in either case, a merge at 1.11 is to be expected. There are, however, other observations which fit the observed more exactly ; in fact, $f_1'^2 f_1'^2$ ($j=4$) requires 0.114, or $g_1'^2 g_1'^2$ ($j=5$) 0.111. In any case, even if y is a d_1 term, there is nothing to decide whether it is doublet or quartet. One apparent way to avoid the quartet decision is to suppose that the extra components are caused by the complex nature of the inverse D lines. Their companions, however, are so faint, compared with the main lines, that any effect due to them would be too weak to affect the observations. But another supposition, however upsetting according to our present ideas, might be mentioned, viz., that the doublet and quartic term values for $m=1$ are practically the same, and that the observed multiplicity depends on the excitation. On this basis the complex nature of these lines would be explicable, the main belonging to the doublet and the weak to the quartet or *vice versa*. In this connexion see the discussion as to the nature of $s-p_u$ in § 6, p. 1173.

However, let us accept for a moment the quartet allocation, and see to what it leads. The j for d^4 are 4, 3, 2, 1. Hence we should expect separations in the ratio 7 : 5 : 3 with the first = 2042. The other two should then be about 1450, 875. The j for p^4 are 3, 2, 1 requiring separations in the ratios 5 : 3 with the first = 248, so that the next should be about 150. A search gives at once the following quartet :—

j	4	3	2	1
1.			$2rr, 15723.63$	894.05
			153.57	6, 14829.58
2.	$6rv, 17289.797$	1412.60	$2, 15877.20$	893.85
	248.44		249.46	$5rv, 14983.35$
3.	8, 19581.115	2042.88	$5, 17538.238$	1411.58
			$1, 16126.66^{(1)}$	

(¹) By Aretz, who gives no re notation.

Moreover, the P doublet is completed thus:

$P_1(1)$ 10, 30783.592 248.375 $P_2(1)$ 10, 30535.217 153.876 $P_3(1)$ 4, 30381.341

As they stand, these form a perfect fourfold triplet and quartet—order of intensities, of separations and characters. Nevertheless, the $P_2(1)$ has been quite definitely shown by Purvis* to be of doublet type. The P_1^2, P_1^4 might possibly not be distinguished, with Z.P. = $\cdot 33/1\cdot 00$ — and —, $\cdot 20/1\cdot 00$ — —, but there can be no question as between P_2^2, P_2^4 with Z.P. = $\cdot 67/1\ 33$ and $\cdot 40$ —/— $1\cdot 87$ —. How is the difficulty to be met? Possibly the explanation is that the “ d ” separations are mixtures of links and displacements, whilst the p sep. = 153 depends on the $-3b$ displacement on p_2^2 . We have already seen how $2042\cdot 88$ can be explained by the $3u$ link and $d_2 = d_1(\delta_1)$. Also $3u - 3X_1 = 1412\cdot 25$ and $u + Y_2 = 893\cdot 17$ with small displacements might meet the 1412 and 894 separations. The three d separations above occur, as will be seen later, so frequently and in multiplet association, that the conclusion seems forced on us that these multiplets are not pure, *i. e.*, depend on displacements only, but are compounds of links and displacements. We shall see below that the same phenomena appear in the quartets which have been proposed by several recent writers. If so we are met with the problem as to the effect of displacement and linkage on Zeeman patterns. Displacement produces new terms and a change in the Z.P. may be expected, not subject to Landé’s rules unless such new term is a normal one (*e. g.*, in the above instance where a d_2 term is produced by one own displacement in a d_1). In the case of linkage further experiment is required to show whether any change is produced or if so what. In the above example, $3u$ —or $Y_1 + Y_2$ on D_{11} on alternative supposition—seems to have produced no change †. On the other hand, we find examples of such change, *e. g.*, the two lines (1 n) $46173\cdot 55$, (6R) $44173\cdot 68$ linked by $1999\cdot 87 = 2e + \cdot 27$ ($d\lambda = \cdot 01$) have quite different Z.P., viz. $\cdot 45/\cdot 66$ (Shenstone) and $0/\cdot 79$ (Sommer). It would be instructive also to learn whether the Z.P. of a summation line is to be obtained from Landé’s rules by adding the term components instead of subtracting. It would mean very greatly increased spreads in the patterns observed, so that even weak fields would resolve them. Unfortunately, summation lines must, as a rule, by the nature of the case, lie in the ultra-violet, and they are generally of small intensity.

* Proc. Camb. Phil. Soc. 14, 225, 07.

† We have a similar result in a pp' multiplet in Ba which is bodily linked by e to its normal position, *membra disiecta* of this latter being also in evidence. Here also the Z.P. of all the lines remain the $0/3/2$ for this type. See ‘Analysis,’ pp. 223, 278.

The Shenstone Lines.

5. The further consideration of multiplet systems on the basis of the quartet (A) above must involve a discussion of the list of lines with separations 2042, 13245, which we shall denote by ϕ , θ , given by Shenstone* in his first paper. Those writers—Beals†, Sommer‡, Shenstone* himself—who have used the latter's list as a starting-point for the allocation of multiplets, have accepted the doublet d type for the y , x terms, and naturally have taken this to hold for the corresponding sets in his list. For some of these we have data as to their Z.P. by one or other of these authors. We shall postpone consideration of further multiplets until these magnetic data and the constitution of these lines have been discussed. The lines are reproduced as to their wave numbers in table i. together with other information as explained at the foot. It is followed by table ii. containing a list of some other lines and sets involving the same separations and which we shall require later.

TABLE I.

		s	13240+	x	2042+	y
221	$P_2(1)$	10R, 30535.217	5.420	8, 17289.797		
248		Z. A. D. E. K. i. _a ⁽¹⁾		Z.		
222	$P_1(1)$	10R, 30783.592	5.354	6, 17538.238	862	8 <i>n</i> , 19581.100
		Z. A. D. E. K. i. _a ⁽²⁾		Z.		
422	p_a	8, 40114.024	5.487	2, 26868.537	868	3, 28911.405
829		Z. A. B. ii.		(38 vi) S'.		Z. S'.
421	p_b	6, 40943.241 ⁽⁶⁾	4.909	2, 27698.332		
		Z. A. B. iii.		Z.		
432	p_c	2, 44544.659	5.982	6, 31298.677	931	2, 33341.608
371		Z. B. C. i. _a		Z. C. S. (17 ii)		Z. C. S'.
431 ^b	p_d	2R, 44916.378	6.094	3, 31670.284		
		Z. A. B. E. i.		Z. C. S' (23 ii)		
221	p_e	1 <i>n</i> , 45821.84	6.44	2, 32575.399		
58		Z. A. E. i.		(16 iii)		
222 ⁶	p_f	1 <i>n</i> , 45880.08	6.24	6, 32633.841	859	4, 34676.700
		Z. A. C. i.		Z. A. S. (30 ii)		Z. A. S.
232 ⁷	p_g	1 <i>n</i> , 46173.55	6.17	6, 32937.382	851	3, 34970.233
3209		Z. A. B. E. i.		Z. A. S. (3 iii)		S'.
222	p_h	4 <i>n</i> , 49383.07	5.50	8, 36137.572	582	10R, 38180.15
		C. E.		A. (1 ix)		Z. A. iii. (2 ix)

* Phil. Mag. 49, 952, 25. Phys. Rev. 28, 449, 26.

† Proc. Roy. Soc. 111, 168, 26.

‡ Zeits. f. Phys. 39, 711, 26.

TABLE I. (*continued*).

	<i>s</i>	13240+	<i>x</i>	2042+	<i>y</i>
243 A			3, 30480·697	·872	4, 32523·569
680·10			Z. S. (6 i)		Z. C. S. (5 iii)
433 B			4, 31160·804	·873	5, 33203·677
			Z. C. S. (5 i)		Z. A. S'. (7 iii)
233 ^a E			4, 33352·963	·709	8, 35395·672
			Z. C. S. (13a iii)		Z. A. v. S'.
F			6, 41538·701	1·02	8R, 43581·72
					C. ii.
Q	1, 55028·5	6·2	2R, 41782·287	1·23	2, 43825·52
			C.		
M	2, 56358·9	20·6	4, 43098·34	·67	6R, 45141·014 ^(b)
	5, 13206·25 (·02)	(29892·09)	9·62 (·37)		C. i. K.
				[13249·79	4n, 29848·55]
K	6, 57426·38	12·70	6R, 44173·68		
iv 2	1n, 14281·74 (·10)	(... 91·94)	·47 (·4) Z. C. i. a	[13234·03	4, 30939·65]
J	3, 57942·7	(-1·7)	1n, 44704·40	·74	1n, 46747·14 ⁽⁴⁾
iv 49	2b, 14812·29 (·10)	(... 92·11)	3·20 (·30) C. v.		C.
				[13249·22	1, 31455·16]
233 ¹⁰ N			6R, 44874·55	1·51	1, 46918·062
	3, 14983·36 (·02)	(... 91·19)	3·94 (·20) Z. C. i. K.		K.
				[13238·58	2, 31635·97]
221 ¹¹ R			4R, 45119·39	(-2·11)	0, 47159·28 ⁽⁵⁾
iv 5	3n, 15226·841 (·07)	(... 92·55)	Z. C. i. K.		

The columns under *s*, *x*, *y* give the wave numbers; the second gives Shenstone's notation for the supposed second term, and the first the quantum numbers adopted by him in the order *rkj*; the fourth and fifth give the separations as additional to those entered at the top. The letters underneath have the following meanings:—Z. the Z. P. has been observed, S. denotes a *satelloid*, S'. one observed as such by Stücklen; A., B., C. denote Shenstone's classes, A. excited by bombardment, B. absorbed by vapour, C. excited by arc of 8 volts and not A.; E. absorbed by vapour, Zumstein (Phys. Rev. 25, 523, 25), K. Do. Kichlu (*Zeits. f. Phys.* 39, 572, 26); i. ii. ... v. Stücklen's classes of absorption in underwater spark.

(¹) Absorbed by vapour above 1080°.

(²) Do. above 1050°, Grotrian.

(³) By Wolfsohn, *Ann. d. P.* 80, 415, 26. (⁴) Dreblow. H. gives 46748·26 or

(⁵) Pina de Rubies.

2*y* larger.

Other allocations 5, 232—6, 232—7, 432—8, 433, all by B.

9, 221—10, 243—11, 232, all by S.

The numbers in [] have been added for later reference.

It should be noted that whilst in the first sets down to A (μ excepted) the ϕ are equal, the θ vary outside O.E., but it is remarkable that the variations seem to depend on the *y*. Thus, taking $\theta = 13245·40$, the deviations are ·02, -·05, ·09, -*y* + ·08, *y* + ·01, *y* - ·12, 2*y* - ·10, ·84, *y* + ·20, ·10.

TABLE II.

θ , ϕ represent the separations $s - \mathbf{x}$, $\mathbf{y} - \mathbf{x}$, also stand for abbreviations:
thus, θ 5·61 stands for 13245·61; ϕ 4·51 for 2044·51.

1.	{	1, 25329·27	θ 5·64	2, 11836·11 (7 iv)	247·42		
2.	1n,	25401·67	θ 4·21	1, 12083·53 (8 iv)			
3.	{	2, 27660·66	θ 6·69	1, 12157·47	ϕ 4·51	3, 14201·98 (39 iv)	
		680·06		2n, 14413·97 (3 iv)	211·99		
4.	{	4, 28340·72					
		1, 25468·74	θ 5·61	2, 12223·13 (1 iv)			
		2n, 26271·71 (53 vi)		6, 14829·58	249·82	1n, 15079·40	
		1000·18				995·1	
5.	{	2, 27271·89 (4 vi)	θ 40·00	1, 14031·89 (4 iv)	ϕ 2·6	4n, 16074·5 (s)	
		249·09		249·85			
		1, 27520·98	θ 39·24	1n, 14281·71 (2 iv)			
		680·01					
		2, 28200·99					
6.	sat.	56·39	θ 6·43	2, 14509·96 (12 iv)	ϕ 2·30	2, 16552·26 (22 iv)	
2·22	{	6, 2·7754·17 (51 vi.)	θ 6·28	2, 14507·89	246·79	2n, 14754·68 (11 iv)	
				2n, 13897·48			
1·71	{	1, 28552·60	θ 6·26	1408·86			
7.	{	1, 28550·89	θ 4·55	1, 15306·34 (9 iv)	$[\phi$ 9·07]	1n, 17355·41 (s, 19 vii)	
		241·61		247·35		247·71	
		3, 28792·50 (24 vi)		2, 15553·69	$[\phi$ 9·43]	3, 17603·12 (s, 8 v)	
		Note, 1·71 = 3y probably satelloid.					
8.	{	1. 3, 29384·15		6. 1n, 18330·93 s		11. 1n, 17704·43	
		2. 2n, 29535·26 (i)		7. 2n, 16537·79		12. 1n, 17706·92	
		3. 2, 16293·87 (51 iv)		8. 3, 18580·23 (s 8 vii)		13. 1n, 17712·37 s	
		4. [90·00]		9. 3, 16045·04 (43 iv)		14. 1, 19754·62 s	
		5. 0, 18335·7s		10. 1, 17456·13 (5 v)		15. 1n, ... 59·62	
		See map XI.					
9.	{			4n br, 21282·02 (9 viii)		16. 5, 15148·06	
				251·60			
10.	{	1, 34777·40	θ 3·78	2n br, 21533·62 (11 viii)			
		1, 37845·30 s	θ 1·66	4n br, 24603·64 D ₁₂ (3)	ϕ 39·86	2n, 26643·50 s	
				6n br, 07·29 D ₁₁ (3)			
11.	1n,	42302·54 (17 xiii)	θ 5·46	3, 29057·08 ¹ (43 vi)			
12.	1n,	42334·26	θ 3·45	1n, 90·81 (20 vi)			
13.	{	1, 42386·85					
		62308·4 = s(1)					
		(McL) 82230·1	θ 46	1n, 68984·07			
						diff. summation.	
14.	{			2n, 16251·51	3·80	1, 16255·31 (45 iv)	ϕ 3·31
					243·24	243·29	4n, 18298·65 s
						243·57	
		2n, 16490·99	3·86	2n, 16494·75 (48 iv)	3·85	16498·60	ϕ 3·52
							2n, 18542·13 (15 v)
				6, 21249·87 (sat. 5 viii)			
					248·11, 4·27		
15.	{				97·98		

(¹) With two successive — ϕ , see No. 5, p. 1165, and map XIII., 19.

6. The following statement gives the Z.P. according to Landé's rules for the suggested allocations of the terms and those actually observed. B., Sh., S. stand respectively for Beals, Shenstone, and Sommer. The allocations given in the first column are to be supposed combined with $s=211$, $x=232$, $y=233$.

p_a	13/160, 1·86 *		·27, ·80/·40, ·93, -- *
422	·39/1·52		B. ·25, 79/·33, ·84
	Sh. 0/1·69; S 0/1·80		
p_b	·33/2·33 §	·93/·13, 1·73 *	
421	B. 0/2·27; Sh. 0/2·34	B. ·91/0; S. ·97/0	
p_c	·40/·80, 160 †	·20, ·60/·60, 1·00, 1·40 §	0/1·20 †
432	Sh. ·45/1·66	B. ·39/1·18; S ·44/1·05	Sh. 0/1·7
431	1·00/1·00 †	·40/·40, 1·20 †	
p_d	Sh. ·91/1·11	B. ·31/1·10	
B. 232	= ·60/·20, 1·40 †	= 0/·80 †	
p_e	·67/1·33 †		
221	Sh. ·77/1·21		
222	·33/1·00, 1·67 †	·27, ·80/·53, 1·07, 1·60 †	·07, ·20/1·00 --- §
p_f	Sh. ·43/·70, 1·5	B. ·50/1·13; S ·52/1·18	B. 0/1·22; S 0/1·16
B. 232		0/·80 †	-, ·20/-, -, 1·80 †
232	·60/·20, 1·40 †	0/·80 †	
p_g	Sh. ·45/·66	B. 42/-	
B. 432	= ·40/·80, 1·60 †	·20, ·60/·20, ·60, 1·00	
p_h			·07, 20/1·00 --- *
222			S 0/1·12
A		·03, ·09/·77, -- ·94 †	·17, -- ·86/-- 1·03 --- †
243		B. 0/1·56	B. ·30/1·10; S 64/1·51
B		·29, ·86/-- -- 2·23 †	·09, -, ·43/-- 1·29 --- †
433		B. ·19, ·57/1·67	B. 0/1·19; S 0/1·15
E		·20, ·60/1·00, -, 1·80 *	0/1·20 * §
233		B. ·21, ·68/1·85;	B. 0/1·24; S 0/1·23;
		S ·21, ·68/1·85	Sh. 0/1·2
K		·07/·73, ·87 §	
2·1		S 0/·79	
Sh. 233		(Sh.) ·20, ·60/1·00 - 1·80 †	
N		S 0/·79	
S 243		(S) ·03, 09/·77 -- ·94 †	
Sh. 221		(Sh.) ·07/·73, ·87 †	
R		S 0/96	
S 232		(S) = 0/·80 §	

In discussing these results, unfortunately we cannot proceed with complete certainty, for the lines may belong to

Landé's types of higher degree, or they may be subject to the link and displacement modifications already referred to. Also very few of the observations give fully resolved patterns. We should probably be justified in assuming that Landé's rules either hold or do not hold for all the lines in the same horizontal set, *i. e.*, for combinations of the same term with *s*, *x*, *y*. The observations, however, are not sufficiently exact to enable any reliable determination of the splitting factor to be made.

In the above statement I have attached signs to indicate where, as it seems to me, agreement or otherwise is shown between the allocations and the observed Z.P. * denotes agreement, † definite disagreement, § doubtful. In sp_a there is an unaccountable difference between the observations of B and the others. It is curious that while the others agree with $s^2 - p_1^4$, B is compatible with $s^4 - p_1^4$, Z.P. = .20, .60/1.00, 1.40, 1.80, 2.20, provided the intensities are not very different. In the case of p_k the observed Z.P. is precisely the same as that of the 5105 or $y - p_1(1)$, which is as it should be, since we know on other evidence that p_k is $p_1(2)$. sp_b has been marked § because the π separation of .67, although large, here corresponds to $d\lambda = .04$, and may possibly be allowed as unresolved 0. yE is marked *§ because there are several cases with Z.P. = 0/1.20, and the observed are closer to others. An examination of the table shows that agreement between the proposed allocations and the corresponding Landé formula fails in the majority of cases. It may be noted that one in nine support $x = 232$, and possibly three in six support or do not exclude $y = 233$.

7. Let us now examine the observed Z.P. and possible allocations on the basis of the Landé formulæ.

p_a, p_b as above with four-fold p .

sp_c is better met by $P_1^4 = .20, 60/1.00 - - 2.20$ †, $x p_c$ by $p_2^4 p_3^4 (j=2, 1) = .47/1.27, 2.20$ †. A very considerable number G^1 fit $y p_c$, *e. g.*, G_{13}^4 or $445-454 = - - .08/ - - - 1.69$ *.

sp_d agrees exactly with G_{23}^4 or $444-454 = .89, - - - / - - - 1.11 - - -$; $x p_d$ none.

sp_e agrees exactly with G_{12}^4 or $445-455 = .73, - - - .08/ - - - - 1.25 - - - -$.

sp_f agrees with $s^2 d_3^4$ or $211-432 = .40/80, 1.60$; $x y_f$ none; $y p_f$ satisfies $d_1^2 d_3^4$ or $211-432 = 0/1.20$.

p_g none.

$y p_A$ may also be D_{11}^4 .

xA. $d_1^4 d_2^4$ or $434-433 = \cdot 03 - - / - - - - - 1\cdot 57$ agrees exactly and gives $x = d_2^4$ and $A = d^4$, or 434 , but then yA as $434-434$ does not give either of the observed patterns. $p_2^2 p_2^4 = \cdot 20, \cdot 60 / - 1\cdot 53 -$ agrees well with S, and $d_1^2 \frac{1}{2}^4$ or $233-443 = \cdot 09, \cdot 26, \cdot 43 / - - 1\cdot 11 - -$ with B.

xB. $232-233 = \cdot 20, \cdot 60 / 1\cdot 00, 1\cdot 40, 1\cdot 80$, requiring for yB or $233-233 = 0 / 1\cdot 20$. Both fit, making $B = d_1^2, x = d_2^2, y = d_1^2$.

xE. This and **xB** agree closely, but definitely differ. They look like modified Landé formulæ. It is remarkable that in **xE** both B and S give exactly the same measures.

xK, also $F_{33}^4 = \cdot 09, \cdot 26 / \cdot 77 - -$, is good—N same as K.

R. There is an extremely large number of combinations which will satisfy the observed $0 / \cdot 96$ —the best again with F or G, *e. g.*, $G_{22}^2 = \cdot 02 - - / - - - - - \cdot 97$; $g_3^4 g_3^4 = 0 / \cdot 984$ etc., etc.

Collecting the results, we have

1. Good evidence that $p_a = 422$, whilst $p_b = 421$ is not excluded.
2. No evidence for the constitution of $p_c p_d p_e p_f$, A, E, K, N, R.
3. p_f is 431 with **sxy** two-fold.
4. B is 233 with **xy** two-fold.

Although many of the lines are completely met by F, G combinations, these would be excluded if *s, x, y* are of the nature of *s d d* terms.

The conclusion so far must be, not that the allocations by B. S. Sh. are necessarily wrong, but that Landé's rules do not apply. That consequently the sets are either those of his higher degree or the lines are not simple but involve more than two terms (links or other term differences).

Constitution of the Shenstone lines.

8. We now return to the discussion based on observed inter-relations in the spectrum. We shall begin by an independent discussion of the fundamental sets given by Shenstone in his first paper (table i.). We have already seen in [I.] how a large part of the spectrum is formed of linkages—many of them very long—attached to definite

series lines and involving the well-established e, u, v links with new ones X, Y based on d (1). The maps there given are not, however, exhaustive, and the new Shenstone separations 13245 and 2042 had not then been recognized. Both these separations, or the very closely related ones of $13e + v = 13245.84 \pm .6$ and $3u = 2041.8$, occur also in large numbers throughout the whole spectrum from the ultra-red to the ultra-violet (see table ii. for some examples). There is also an exceedingly large number near the doublet value 248, as indeed Rydberg had noticed, and this is found also in the ultra-red region observed since his time.

The very great equality of all the corresponding separations found in table i. has already been referred to as affording strong evidence, taken alone, in favour of s, x, y being definite terms common to all the sets. But the large number of similar, but not exactly equal, values found throughout the spectrum, some examples of which have been given above, would seem to indicate that they also occur with qualities analogous to those of links. We shall leave the question of their real nature at present open, and simply regard them as constant quantities which, by being added to or deducted from the wave-number of one line, give that of another. It will not then follow that lines separated by these $\theta\phi$ must all have s, x, y as limit terms, although, of course, such a supposition would appear at first sight justified. That the numerical values of x, y in the p_{12} set are correct there can be no doubt, but it does not follow that they represent true terms. This may be illustrated by Ex. 8 of table ii., represented in map XI., which shows a set shifted from the $p_{1,2}$ set by the e link, even from the $P_3^4(1)$. The close lines shown there seem to represent displacements 2.49, 5.00, 4.81 being shifts on p (1) terms due to two and four own displacements. The line [4] is a supposed normal line producing (3) by displacement, $3\delta_1$ on p_2 shifts 3.75. It is seen that the small shift required produces three correct links v, θ , and $2u' + u$ to (6). It is interesting to notice that (5, 6) are spark lines shifted e from a forbidden $D_{21}(j=1 \text{ to } 3)$, while that corresponding to P_1 is wanting. The significant point here is that we have a case where the $\theta\phi$ occur, and yet the limits must definitely be e less than s, x, y . The set is considered in more detail in § 10 in connexion with quartet B. Another illustration occurs in map XII., where the A, B (1, 2, 5, 6) sets are found with another corresponding one e ahead, consequently with limits e larger, although the ϕ separation is reproduced.

We can only settle the limits in each case by determining

one term from other considerations, such as, for instance, the linkage maps or summation lines. We shall, however, refer to the three columns of table i. respectively as the s , x , y columns.

We have this term indication for the sets p_1, p_2-p_k-Q . p_1p_2 . They give the values $s=63208\cdot12$, $x=49062\cdot77$, $y=51105\cdot64$. Any summation lines belonging to this set will lie in the unobserved region between the shortest of Bloch and the longest of Millikan and Bowen*.

p_k . This is generally regarded, after Randall, as the $p_1(2)$ corresponding to the preceding $p_1(1)$. Indeed the Z.P. for the y lines are the same, $0/1\cdot10$ for $y-p(1)$ and $0/1\cdot12$ for $y-p_k$. The limits are then the same x, y . Moreover, the $y-p_k$, $x-p_k$ behave similarly as to absorption by vapour (see (4), p. 1165), for whilst $x-p_k$ does not show the effect, $y-p_k$ is in Stücklen's class iii. With $x-p_12=36137$ there is no indication for $x-p_2^2$, which should be about 67 behind it. For a summation scheme we find :

(10 r) 38180·15	2042·58	(8) 36137·57	13245·50 (4 x)	49383·07
51105·23		49057·3-19 $d\lambda$		
(1) 64030·32	2053·2+38 $d\lambda$	(2) 61977·1-33 $d\lambda$		beyond obs. region

Note.—Ultra-violet W.N. given to two decimal places are from observations by L. and E. Bloch; observations by Handke and others are given to one decimal place.

Here the y -summation is exact within O.E. The x -summation is also within the possible errors ($d\lambda=0\cdot25$) of McLennan's measure $\lambda=1613\cdot5$, but this is possibly a merge (see quartet I. below).

The defect $\cdot30$ in the 2042·58 is real, and can be explained by our shift on $p_1(2)=0\cdot326$.

Q. If the allocation † of $s-Q$ to P (3) is justified, the limits should be the actual x, y . In agreement with this we find the following summation set :

2, 43825·52	2043·24	8R, 41782·28	13246·2	1, 55028·5 -30
51102·3+17 $d\lambda$		49059·04		62298·8 +25
2, 58379·0+34 $d\lambda$	2043·2	00, 56335·81	13233·29	00, 69569·10 -30
Coll.: { 0, 56291·41 44·40 00, ... 335·81 35·56 00, ... 371·37 39·11 0, ... 410·48 Bl.				
{ 6, 56317·7 41·2 2, ... 358·9 44·5 3, ... 403·4 44·6 4, ... 448·0 Hke.				
{ 00, 69569·10 33·40 00, ... 602·50 37·80 00, 640·30 Bl.				

* Phys. Rev. 23, 1, 24.

† Phil. Mag. 39, 479, 20; 'Analysis, p. 254. This $p(3)$ is not in the same sequence as p_k .

Here the first two sets gives mean limit about 3 too small. The agreement of Handke's defective y -limit with that of Bloch's x is a curious coincidence, as the former's possible errors are considerable. The x , y limits definitely show a depression of 3.7. The s limit shows a further depression of 5.6 ($d\lambda = .2$ excessive for B/).

Round the x , s summation lines are seen successive close lines (given above) separated by roughly equal amounts. In general such successions indicate the presence of collaterals, in which case the summation lines may themselves be displaced, or the displacement may occur in the difference lines, the shift required in the x -line being 7.46. The latter supposition is supported by the succeeding F discussion.

If the displacement takes place in the Q term the own shift is the same for all three lines; if in the limits that for s would be 1.43 times larger than that for x , but the O.E. are too large to get any definite decision: $3\delta_1$ on x shift 7.20.

F. The F lines are 243.59, 243.80 behind Q, mean = 243.70. We find

8R 43581.72	2043.52	6, 41538.70
(50854.14)		48811.25
(58126.57)	(2042.76)	3, 56083.81

Here the x -limit is $x - 251.52$ with good measures. As the c -link is 251.39 [I. p. 200], it means that F is linked to a normal Q by $c = Q - c$. The limit is 247.79 less than that given by the Q summation set above, and this cannot be 248.44 within O.E. If Q be displaced 7.46, as indicated above, the normal $F - Q = 243.70 + 7.46 = 251.16$, in striking agreement. Thus $x F = c \cdot x Q + 7.46 = c \{x - p_1 3\}$. There is no observed line for $y + F$, but there are two—sep. 127.37—equally and oppositely displaced from it, viz., 58062.91, 58190.28. Treating the displacement as $25\delta_1$ on a y term, direct calculation gives for the undisplaced line

$$58062.91 + 63.68 = 58126.59$$

$$58190.28 - 63.72 = \dots\dots 6.56.$$

The mean is entered above, and the resulting limit is $y - 251.52$, corresponding to the observed $x - 251.52$.

9. In the three preceding cases we have quite definite indications from summation lines that in them we are dealing with pure difference lines in which 49062, 51105 behave as single terms. Moreover, the presence of displacements

Phil. Mag. S. 7. Vol. 4. No. 25. Suppl. Nov. 1927. 4 G

exactly depending on 51105 as a single term $= R/(1.464963)^2$ practically proves that y at least is a real term. But in none of the other lines in Shenstone's list do we find any summation lines corresponding to s, x, y limits. That such lines have not been seen does not, of course, prove that the limits are not s, x, y , but taken in combination with the fact that, as we shall see, summation lines for other allocations do occur in considerable numbers, we are left to suspect that for these sets the true limits are different from s, x, y .

To allocate these lines recourse must be had to the maps of [I.]. We begin with the $x-A, x-B$ lines, which are satelloids 5, 6 of map I. These are linked or collaterally related with the p_c and E sets. The inter-connexion—with some other linking—is shown in map XII., which explains itself. We note again here the repetitions of the e, u links found in the maps generally, especially in map VI. The separations 11 (at 3, 7) correspond to changes of a link from u to v or *vice versa*. The separation 149 is the old familiar $3b$ displacement on a p term. If we use the notation xA, yB , etc., to distinguish the sets, we note that in the x -chain—1, 2, 3, 4—we get first a $u'.v$ interchange 12.02 and then the $3b$ displacement, whereas in the y -chain—5, 6, 7, 8—we find the same in reversed order, with u, v interchange 11.45.

From 6 i [I. p. 223]

$$xB = e.P_1.v + 10x - y - .02,$$

the x, y^* having definitely entered through actual satelloids. We shall take $u' = u - y = 680.06$ to represent Rydberg's separation.

$$\text{Then } xB = e.P_1.u'.v + 10x - y + .03.$$

The line indicated by (3) on the map is less by 11.97 = change of v to $u' + .05$. Hence

$$(3) = e.P_1.2u' + 10x - y + .08.$$

Note that the v already existed in the xB , to be changed to u . The first red satellite of xp_c is 147.53 ahead. It is therefore $e.P_1.2u' + 10x - y + 147.61$.

Now $3b$ on p_1 shifts 147.64 [I. p. 236]. Hence the satellite is $e.P_1(3b).2u' + 10x - y - .03$. It is a y -satelloid

* x, y are not arbitrary, but definite modifications, entering through satelloids, due to an unknown source in $s(1)$ or $p(1)$ terms; y can also enter through $u' = u - y$. Numerically $xA = e.P_1(\delta).v - .13$.

with the first red satellite at a distance $4y + \cdot 03$ [I. p. 198]. Hence

$$\begin{aligned} \mathbf{x}p_c &= e.P_1(3b).2u' + 10x + 3y + 0 \text{ (direct calc. gives } +\cdot 02) \\ &= e.P_1(3b).2u + 10x + y + \cdot 02. \end{aligned}$$

Now $\mathbf{x}p_c$ appears in 17 ii in a false cycle [I. p. 224]. The present argument shows that the separation 129.54 between satellites in the map is not an "L" separation as taken in [I.], but, with various satellite differences and u, v interchanges, corresponds to a (3b) displacement. Map II., as developed from this, then proceeds with 18 ii, which is $u + \cdot 14$ ahead, and gives

$$18 \text{ ii} \equiv 31979.44 = e.P_1(3b).3u + 10x + y + \cdot 16. (d\lambda = \cdot 01).$$

Note that the $3u$ link here enters implicitly.

$sp_c(18)$ is $\theta + y + 0$ ahead of $\mathbf{x}p_c$. We find thence in 24 xii a line $e + 11.60$ ahead, the 11.60 changing $2u$ to $u.v^*$, and giving

$$(24) = P_1(3b).u.v.\theta + 10x + 2y + \cdot 17 (d\lambda = \cdot 008).$$

The important result follows that with A, B, p_c the " \mathbf{x} " limit is not \mathbf{x} , but contains $s(1)$; the A, B terms are both $p_1(1)$, and p_c is $p_1(1)(3b)$. Coming now to the \mathbf{y} column, it is seen that the chain appears as in map III., Nos. 5, 7, 13 a, 13. This map is a composite of three distinct chains without definitely indicated relation to one another or to map I. We see now that this was due to the neglect of the 2042 separation. The guess which was attempted in the discussion of map III. is not therefore sustained. Also the limit in $\mathbf{y}A$ is not \mathbf{y} , but that of $\mathbf{x}A + \phi$, where now $\phi = 2042.87$ behaves as a link, or as the difference of two terms $\mathbf{y} - \mathbf{x}$. It means a complicated change taking place in the atom represented by the simultaneous fall of two electrons, one from $p(1)$ to $s(1)$, the other from \mathbf{y} to \mathbf{x} , and at the same time the configuration changes producing the u, e links. The formulæ are

$$\begin{aligned} \mathbf{y}A &= e.P_1.v.\phi + 10x - y - \cdot 02, \\ \mathbf{y}B &= e.P_1.u.v.\phi + 10x - 2y + \cdot 03. \end{aligned}$$

Any summation lines would lie in unobserved regions.

The map also shows that E belongs to the same system,

* For other examples of $u.v$ interchange, see sp_c below; also 8, 9 iii, amongst many others.

which explains why A, B, E show no θ -linked lines. $\mathbf{x}E$ is $\phi + 11.41$ ahead of $\mathbf{x}p_c$, where $v-u=11.45$. Hence

$$\mathbf{x}E = e.P_1(3b).u.v.\phi + 10x + y - .02.$$

$\mathbf{y}E$ is $\phi - .17$ ahead, definitely not $\mathbf{y}-\mathbf{x}$; $\mathbf{x}E$ is an x -satelloid [I. p. 198], and $\mathbf{y}E$ a Stücklen satelloid :

$$\begin{aligned}\mathbf{y}E &= e.P_1(3b)u.v.2\phi + 10x + y - .19 \\ &= (...10y + .08 \text{ per sat.}).\end{aligned}$$

$\mathbf{x}p_d$ is 371.607 ahead of $\mathbf{x}p_c$. This separation occurs very frequently not only in the B. Sh. quartet systems, but in many other instances. Intermediate lines in many of these cases (§ 15) show that it is a composite of 2X links forward and a displacement $-b$ on a p_1 term. The X links are generally distorted, but form a series inequality. Here the chain given in the diagram contains the two separations 221.49, 200.50 with the lines $1n, 31520.17$, $1n, 31720.66$. They would certainly not be recognized as X links*, but the character of the lines ($1n$) suggests displacement, and the 371 being a composite. The other cases suggest that they are the distorted representatives. But there is some evidence, given below in p. 1197, that 371 may be a true term difference. Whether that is the case or not, we shall take the 371.61 as formed in the same way as in other cases, as indeed the associated chain from sp_c to sp_d also shows. Now p_c depends on $P_1(3b)$ and $-b$ on $p_1(3b)$ shifts 49.10, so that $2Y_1$ and the $-b$ give $420.42 - 49.10 = 371.32$. Hence

$$\begin{aligned}\mathbf{x}p_d &= \mathbf{x}p_c + 371.61 \\ &= e.P_1(2b).2u.2Y_1 + 10x + y + .31(d\lambda = 0.3)\end{aligned}$$

(if exchanges of x, y were permissible, the residual might be $11y + .01$).

The observed 50.38 from $\mathbf{x}p_d$ is an extra own displacement, making 50.33.

p_g . This is 3209.52, 3210.190, 3209.921 behind p_h , of which 3210.19 is the best measure. The θ value suggests the y for the variation in sp_g , and $\mathbf{x}p_g$ is a satelloid. $3e + Y_1 = 3209.61$ and $+y = 3210.18$.

An intermediate $3e$ exists, viz.,

$$\mathbf{x}p_g \quad 3e + .04 \quad 3n, 35926.89 \quad Y_1 + y - .10 \quad 36137.57.$$

Also it is 425.58, .44 behind E. $2Y_2 = 425.05$ and

* [Added in proof. Distortion met by (25) being $\mathbf{x}p_c + Y_1 + \text{change of } 2u \text{ in } p_c \text{ to } u.v$].

$+y = \dots \cdot 65$. There is no intermediate; but they cannot both be right, for p_k depends on $p(2)$ and E on $p_1(1)(3b)$. We shall get quartet and summation evidence below (see notes to quartet J) for the first supposition, in which case

$$\mathbf{x}p_g = \mathbf{x} - 3e - Y_1 - y - \cdot 01 - p_1(2) \text{ or } 45852\cdot 59 - p_1(2),$$

but the evidence here for this is not conclusive. It brings the p_g into the same category as p_1, p_2, p_k, Q, F .

p_a . $\mathbf{x}p_a$ is 38 vi, but it enters by a link $u - 1\cdot 66 = a - 3y$, and cannot be regarded as certain. If the arrangement in the map be admitted—and the own multiple law considered below (quartet J) supports it—

$$\begin{aligned} \mathbf{x}p_a &= 2X_2 \cdot e \cdot Q^*(-a-b-\delta) \cdot u' - \cdot 06 \\ &= 2X_2 \cdot 4e \cdot P_1(-a-b-\delta) \cdot v + \cdot 19, \end{aligned}$$

$$a + b + \delta = 37\delta = (6^2 + 1)\delta,$$

and the Z.P. shows that p_a is probably a p^4 term.

p_b . p_b is 829·217, ·794 ahead. The difference of the two values is real, and is met precisely by y . We shall find other examples of this separation (§ 15), which is $u + 3b$ on a p term. Indeed, here we find an intermediate for xp , viz., 27015·48, with separations 682·85 and 146·92. Here p_a depends on $p_1(-37\delta)$ and $3b$ on this shifts 148·97, so that $u + 3b$ shift = 680·63 + 148·97 = 829·60. Hence

$$\begin{aligned} \mathbf{x}p_b &= 2X_2 \cdot 4e \cdot P_1(-a + 2b - \delta)u \cdot v + \cdot 39 = \dots + y - \cdot 18, \\ \mathbf{s}p_b &= 2X_2 \cdot 4e \cdot P_1(-a + 2b - \delta)u \cdot v \cdot \theta - \cdot 10. \end{aligned}$$

There is, however, here also some evidence in favour of 829 being a true term difference (see quartet J below).

In passing we note here some further instances of exchange of u, v links:—

$\mathbf{s}p_b$ 40943·24	125 89	$1u, 41069\cdot 13$;	$\mathbf{x}p_b$ 27698·33;	$\mathbf{y}p_a$ 28911·40
11·33	12·32		-11·55	-13·10
$1u, 40954\cdot 57$	126 88	$1u, 41081\cdot 45$;	$2, 27686\cdot 78$;	$1, 28898\cdot 30$

These are $v - u - 12, +y + \cdot 30, + \cdot 10, 3y - \cdot 06$. The first two lines are the corresponding p_b with $2v$ for $u \cdot v$ and residuals $- \cdot 22, 2y + \cdot 22$; the third changes $u \cdot v$ to $2u$; the last changes v to u with $-3y + \cdot 25$. We can get either interchange in p_b , since it involves $u \cdot v$, but in p_a the change v to u only can take place, and the observations meet these conditions. Moreover, the entrance of the y is explained by $\mathbf{y}p_a$ and $\mathbf{x}p_b$ being satelloids.

* Q of map VI. and p. 219 [I.].

The sets M, K, J, N, R. We note : (1) The lines suggested by Shenstone for the s column for M, K, J show O-C errors greater than the possible, except just possibly for J. We conclude that M, K, N, R do not show the θ separations. (2) The intensities and characters of $x(K, N, R)$ and yM are the same, and all in Stücklen's class i. like the s lines, whilst the J are of intensity 1n and xJ is in class v. (3) K has no y representative, and those suggested for N, R are very doubtful, with intensities abnormally small. (4) In the case of M it is the y -line which is analogous in character to x of K, N, R.

We must draw the conclusion that the K, N, R are of closely allied nature, and possibly M (or yM placed in the x -column) may belong to the same category, whilst J is entirely unrelated to them.

$$xJ(2') \text{ xii) is } sp_d - 211.98 = e.P_1(2b).2u.X_1.\theta + 7x + 3y + .01.$$

K. xK is $1999.87 = 2e + .27$ behind $sp_g = 5e + Y_1 + .18$ behind sp_A .

$$\therefore xK = 5e.Y_1.P_1(2) - .18.$$

Any summation line would lie about 70024, amongst the extreme lines of Bloch.

N. H. and K.R. make this 700.87 ahead of xK , and the recent more accurate values of Wolfsohn make it 700.19. This is $Y_1.2Y_2 + (\Delta)$ on $P_1(2)$, where the Δ shifts 64.60. Taking W.'s wave-number in air, 44873.825 gives

$$xN = 5e.P_1(2)(\Delta).2Y_2 + .07.$$

R. Here W. agrees with H. (.32 for .39), and makes it 245.50 ahead. Now the "a" link is 245.54 [I. p. 200]. Hence

$$xR = 5e.P_1(2)(\Delta).2Y_2.a + .03.$$

M. xM is 1075.34 behind K. (2b) on $P_1(2)$ shifts 25.88, and $-u - 2Y_1 + 2b$ on $P(2) = -1101.05 + 25.88 = 1075.17$.

$$\therefore xM = 5e.Y_1.P_1(2)(2b) - u - 2Y_1 - .07 \\ = 5e.u.3Y_1.P_1(2)(2b) - .07$$

$$\text{or } = 5e.u.3X_1P_1(2)(2b - \delta) + .23.$$

$$yM \text{ is } 2042.67 = 3u + .78 \text{ ahead,}$$

$$= 5e.3X_1P_1(2)(2b).2u - .28 \text{ (W.) or } +.30 \text{ (H.).}$$

Either of the alternative forms for xM will meet the case, but the second explains why xM is of abnormal character,

and the vapour-absorption of \mathbf{yM} is seen as a consequence of its dependence, like K, N, R, on pure multiple b displacements. All these lines M ... R must therefore be transferred to the s -column.

p_s, p_f . Difficulties occur in the allocation. The θ separations are too large, and the intensities of the (s) lines ($1n$) compared with the (\mathbf{x}, \mathbf{y}) show a distinct anomaly when compared with those of the other sets. We cannot be certain, therefore, that the (s) and the (\mathbf{x}, \mathbf{y}) belong to the same system. sp_s is 680.83 ahead of \mathbf{yM} , so that

$$sp_s = 5e.3X_1.P_1(2)(2b).3u - .08,$$

with the same authority as \mathbf{yM} . sp_f is 58.24 ahead, which we naturally regard as due to a new term, *i.e.*, to displacement on $p_1(2)(2b)$. Now 45 δ on this shifts 58.00, so that

$$sp_f = 5e.3X_1.P_1(2)(65\delta).3u + .16.$$

It is not dependent on the a, b multiples which we have found so prevalent. On the other hand, as $65 = 8^2 + 1$, it is an example of a δ multiple condition already frequently met with. With these allocations the (\mathbf{x}, \mathbf{y}) lines fall in by interchange of \mathbf{x}, \mathbf{y} for s , and we get a very satisfactory system. But certain difficulties appear. xp_s is 16 iii; it is 49.02 from the outer satellite of 5 iii—*i.e.*, of \mathbf{yA} , which depends on $P_1(1)$ and b on $p_1(1)$ shifts 49.31. Now although exact links frequently depend on satellites, pure displacement shifts are rather exceptional, so that this allocation is in itself doubtful, apart from the magnitude of the residual. If not accepted, the link 50.75 in map III. must be marked false. If accepted, it gives $xp_s = e.P_1(b)v.\phi + 15x - y - .18$. Also xp_f is connected to \mathbf{xB} by a chain from xii to xiii, viz.,

$$\mathbf{xB}, 11, 35 \text{ xii} = 14 \text{ iii}, xp_f,$$

$xp_f, 11, \mathbf{xB}$ all being satelloids. The result is

$$xp_f = X_1.P_1(1).2u.v + 12y + 02.$$

This has clearly no connexion with the former xp_s . If it be accepted, the -58.44 to xp_s would be met by a change of v to u and a displacement $-b + 2\delta_1$

$$\text{and } xp_s = X_1.P_1(1)(-b + 2\delta_1).3u + 12y + .03.$$

The symmetry of the map speaks strongly for the reality of the whole chain. If it is not real, the false link must be the 208.27 between 11, 35 xii, but the successive X links are of great frequency in this map, and we get here a series

inequality $208.27 + 211.50 = 2X_1 + 0$. The question must be left open at present.

The results are here collected (satellite y etc. omitted).

- i. The s column contains $s(1)$ in the limit value, and the others are found by putting x, y for s . The s value only is given.

$$\begin{aligned} p_1, p_2 &= P_1(1), P_2(1) & p_s &= 5e.3X_1.P_1(2)(2b).3u \\ p_A &= P_1(2) & p_{s'} &= 5e.3X_1.P_1(2)(65\delta).3u \\ p_g &= 3e.Y_1.P_1(2) & Q &= (3\delta_1)P_1'(3) \\ & & F &= c.P_1'(3) \end{aligned}$$

Here P' refers to that P series, which produces also the lines $p1-pm$ (Analysis, pp. 254, 256).

- ii. The lines are to be transferred to the s column.

$$\begin{aligned} A &= e.P_1(1).v & yM &= 5e.3X_1.P_1(2)(2b).2u \\ B &= e.P_1(1).u.v & K &= 5e.Y_1.P_1(2) \\ E &= e.P_1(1)(3b).u.v.\phi & N &= 5e.P_1(2)(\Delta).2Y_2 \\ J &= e.P_1(1)(2b).2u.X_1.\theta & R &= 5e.P_1(2)(\Delta).2Y_2.a \end{aligned}$$

- iii. Lines apparently forming s lines by addition of θ link to x lines. The x lines are given.

$$\begin{aligned} p_a &= 2X_2.4e.P_1(1)(-a-b-\delta).v & p_c &= e.P_1(1)(3b).2u \\ p_b &= 2X_2.4e.P_1(1)(-a+2b-\delta).u.v & p_d &= e.P_1(1)(2b).2u.Y_1 \end{aligned}$$

The abnormality in this last class means that the s lines contain $2s(1)$ or that θ is a pure link. This is not easy to believe; but that θ, ϕ do appear in a way similar to that of links is shown by the existence of successive θ and ϕ values, although the evidence for θ is not very satisfactory, since the lines involved lie in the far ultra-violet with poor measures. Some cases are seen in map XIII., viz., $x p_e$, $s p_e(3)$, and $x p_c$, $s p_c(15)$. There are several successive ϕ and θ from ϕ separated lines difficult to explain if ϕ is a pure term separation. For one very definite instance of $\theta\phi$ see note to 26, 30, 42 of line-list for map XII.

A possible source of θ should perhaps here be put on record. Of the P' series referred to above, $P_1'(2)$ is 2037.22 (K.R.), 30 (McL.), $n=49068.73$ (McL.), close to x . We saw above that Q indicated a value about 7 smaller, and there is independent evidence which cannot be taken now. It gives

$$p_1'(2) = 13239.40 + 24 d\lambda \quad \text{or} \quad +7 = 13246. = \theta \text{ within O.E.}$$

So $x p_1 = s - p_1'(1) - p_1'(2)$, indicating a fall of one electron from $p(1)$ or $p(2)$ to s , accompanied by a simultaneous expulsion of one from $p(2)$ or $p(1)$ to a peripheral level. On the contrary, in class iii. the s column is formed by adding $p(2)$ to the x column, and the second electron falls from the periphery to $p(2)$ or $p(1)$. In passing, it is interesting to note that opposite own displacements on $p(1)$, $p(2)$ produce shifts about $\pm .59$ or y .

With this would go the assumption that y is a true term limit, and we should understand why the $x p$ lines are enhanced by the spark and the $y p$ weakened.

Quartets.

10. It is noticeable that, amongst the ultra-violet spark lines of Handke and of W. and E. Bloch, a very considerable number show not only the neutral atom links, but also separations 2042, 1412, and even 13245, or values close to them. They are therefore radiated by the neutral atom, and can have no relation to the ionized atom. We shall later have occasion to notice some of these 2042, 1412 separations, but it may be useful * here to give some examples of the presence of neutral links. The examples are taken from measures of L. and E. Bloch only, whose O.E. amount to only a few units of the second decimals in ångströms. The $d\lambda$ on the links are given in ().

TABLE III.

3, 56083.81	e+1.83	4, 57085.44 (.05)	5, 58722.66	e-.65	6, 59721.81 (.02)
1, 56975.18	e-.26	1, 57974.72 (.008)	5, 58752.34	u+.98	3, 59433.95 (.03)
3, 58436.47	v-.15	0, 58684.76 (.00)	1, 59219.51	e-.11	1, 60219.20 (.00)
6, 58518.20	v+.20	3, 59210.48 (.00)	0, 59455.15	2042.82	4, 61497.97 (.00)
			13236.69		1, 72691.84 (-.17)
1, 60986.77	-u'+0	4, 60306.71	e-.07		1, 61306.44 (.00, .00)
3, 62275.80	u+1.20	1, 62957.63	v-.04		1, 63649.67 (.03, .00)
3, 62219.24	e+.47	00, 63219.51	2048.68	$2\nu\nu$, 65268.19	(.01, .14)
4, 62247.12	e-.61	$2\nu\nu$, 63246.31	2042.76	00, 65289.07	(.01, .00)
4, 64790.76	-2040.55	5, 62750.21	e-.51		1, 63749.50 (.05, .01)
1, 64043.04	v-.98	1, 64734.14	X_2 +.04		0, 64946.45 (.02, .00)
1n, 6.146.25	v-1.05	2ν , 69837.28	-2040.67		1, 67796.61 (.02, .04)

The number of examples giving values exact within O.E. excludes an explanation of chance coincidences. Several of these ultra-violet lines almost at sight fall into quartet

* In view of the current obsession that "spark spectra" and "spectra of ionized atoms" are convertible phrases.

arrangements. From their high wave-number they must correspond to summation sets, and in some cases the corresponding difference quartets can be indicated. The ease with which they are recognized depends on the fact that neutral lines amongst them can consist of summation lines alone, and are only confused by the presence of radiations due to ionized atoms. But it is curious that some of these lines—especially in Handke's longer wave-lengths—are much more intense than others and than the corresponding difference sets. This is perhaps explained by the fact that these latter show irregular separations, small intensities, and parallel repetitions which suggest that they are not of a fundamental type, but are displacements from such. *E.g.*, in the quartets C, D below we clearly get two of similar nature mutually shifted by an amount of about 24.6.

We consider first the lines involved in map XI.. linked to our first quartet A (§ 4). That it contains a few spark lines is explained by the linking. We have seen that the P, D' lines have a parallel set at a distance $-e$ (4, 6, 7, 8, 2), even the "forbidden" line D_{21} being so reproduced. But the quartet depending on these is not found. Traces, however, of such a quartet appear shifted a distance $-e + 1412.7 - 243$, the 243 being the doublet separation 248.44 with a displacement $-\delta$ in $p_1(1)$ shifting 4.94 (obs. = 4.81). They are arranged here in quartet form, the lines being represented by the numbering in the map.

	(10)	1411.09	(9)	896.98	(16)	
	248.30		248.83			B.
(14)	2042.25	(13, 11, 12)	1413.05	(3)		

(16) is too strong; it does not reproduce the 894, and should probably be omitted. It is noticeable that, while the P are parallelized by $-e$ excluding P_1 , and the doublet D set by $-e$ including the forbidden D_{21} , the quartet D are parallelized by $-e - \nu + 1412 = 164$.

The next instance we take is one which is specially interesting because it gives indications of a series which closely follows an exact Rydberg sequence. Consider the $m=3$ set in the following list of difference-summation lines.

$m.$	$y.$	$x.$	$s.$
2	4n, 30825.261	3, 28792.500	—
		2032.75	
	51093.27	49063.10	
	00, 71361.29	00, 69333.70	outside obs.
		2027.59	

<i>m.</i>	<i>y.</i>	<i>x.</i>	<i>s.</i>
	1 <i>n</i> , 41201·65	1 <i>r</i> , 39153·26	0 <i>d</i> , 52398·82
	2048·39		13245·56
3.	51177·2	49062·2	62305·65 - 26 <i>dλ</i>
	1, 61012·8 (McL.)	1, 58971·2 (Hke.)	00·72212·49 - 52 <i>dλ</i>
	2041·6		13241·3
	45242·09 (P.R.)	[43204]	4, 56448·0 (Hke.)
	2038		13244
4	51106·49	(49058·8 - 15 <i>dλ</i>)	
	1, 56975·18	1, 54913·7 - 30 <i>dλ</i> (Hke.)	—
	2061·5 + 30 <i>dλ</i>		
	0, 47236·60 (P.R.)	[45197·34]	—
	2039·3		
5	51105·3		
	1, 54974·0 (Hke.)	—	—

Possibly for $s \mp t(6)$; calc. [59568] 62308·5 1, 65049·1 (McL.)

Here K.R. = Kayser and Runge. Hke. = Handke. McL. = McLennan.
P.R. = Pina de Rubies.

$m=2$. The 71361 of Bloch agrees with the calculated with $d\lambda = -06$.

$m=3$. 41201 comes in a long sequence of 1*n* lines suggesting displacement.

$m=4$. The 54913 by Hke. requires a possible correction $d\lambda = -2$. 56975 occurs also in quartet D below.

$m=5$. The *y* lines give exact mean limit, but require corrections $d\lambda = -16$, 09 to agree with the Rydberg formula. Pina de Rubies gives a series of successive lines at regular intervals before and after $y-t(5)$, viz.:—omitting the 47,

0, 133·93 0, 159·28 0, 185·77 3, 211·17 0, 47236·60 2*n*, 263·62 4, 286·65 4, 308·57
25·35 26·490 25·40 25·43 27·02 23·03 21·92

If the *y* be a true term, 10 δ , displacement shifts 25·49, whilst δ on $t(5)$ shifts 212. The shift 27·02 is $(-10 \delta_1)/(7 \delta) + 05$, but as the line involved is of a different character (2*n*) from that of the others, it possibly does not belong to the system. If we denote 47236 by Z the series of lines are:

$$(40 \delta_1)Z(-4 \delta), (30 \delta_1)Z(-4 \delta), (20 \delta_1)Z, (10 \delta_1)Z, Z, [(-10 \delta_1)Z(7 \delta)], \\ (-20 \delta_1)Z(-4 \delta), (-36 \delta_1)Z.$$

Direct calculation shows the first to be 102·66 behind Z as against observed 102·67 and $(-36 \delta_1)Z$ as 91·86 ahead as against observed 91·97 ($d\lambda = 005$).

Here we find the *s*, *x*, *y*, limits exact within O.E., and the exact θ separation. The O.E. in 39153 is small, and the mean limit is very close to exact *x*. Taking it as $x-t$, *t* is found to be

$$t = 9909·51 = R/\{3·326863\}^2.$$

Now the denominator for S(1) is 1·326748, the same mantissa within O.E. If *t* be corrected to the same mantissa, the wave number should be 68 less or K.R.'s measure 04 A

larger. It suggests the existence of series with current term following the Rydberg formula,

$$t(m) = R/\{m + \cdot 326748\}^2.$$

The calculated values for the x series are entered in the list in [] for $m=4, 5$. No observed lines are found for these, but they exist for y , in $m=4, 5$, for s in $m=4$, and possibly $m=6$.

The calculated values for $x \mp t(2)$ are 28803.53, 69322.01. They are not found, but $y + t(2)$ is given by Bloch with error $d\lambda = -\cdot 06$. The lines in the list, however, are close to these and give the true x limit within O.E. The $x - t(2) = 28792.50$ has a very small O.E. and gives mantissa $a = 326114$ or 634 too small. Thus either the Rydberg is not exact or displacements occur in $m=2$, indicated, indeed, by the defective ϕ separations. We leave the matter here as it has little bearing on our present discussion apart from the summation evidence. Details are given in the notes appended to the list. We should expect the forbidden column $s(1) - t(m)$ to show lacunæ. But the most interesting point is that the x, y set in $m=3$ form the starting-point of a quartet, accompanied by a collateral one. They are:

C.

j	4.	3.	2.	1.
1			2, 38312.88 s	1n, 37413.35 (E.H.)
			899.53	
			263.33	242.18
2	1n, 39468.57 s		1, 38049.55	4n, 37171.17 (Hp.)
			1419.02	878.38
		315.31	322.63	
3	1n, 41201.65 *	1r, 39153.26 *	1, 37726.92	
	2048.39	1426.95		
		66.73	55.55
	51107.2	490	476 44.57	46765.03
		62.23	39.71	
3	1, 61012.8 *	1, 58971.2 *	7, 57552.5 (Hke.)	
	2041.6	1418.7		
		318.3	312.9	
2		2, 58652.9	6, 57239.6	2, 56358.9
		1413.3	880.7	
			241.4	
1			6, 56998.2	[56098.8]

D.				
j	4.	3.	2.	1.
			2, 38312·87 s ?	1, 37425·25 *
			887·62	
			252·2	230·56
	1n, 39480·89 s	1n, 38060·7 (E.H.)	1n, 37194·69 K.R.*	
	1420·2	866·0		
	307·7			
1n, 41226·28 *	1n, 39173·2 s (E.V.)	—		
51106·52	490 59·25 64·78	476 44·02 35·61	4675 4·53 6·20	
1, 60986·77 *	0, 58956·36	3, 57535·74		
2030·41	1420·62			
	318·75	325·21		
	6, 58637·61	3, 57210·53	6, 56317·7 * (Hke.)	
	1427·08	892·8		
		235·35	233·9	
		1, 56975·18	3, 56083·81 *	
		891·37		

The limit means are entered in the order corresponding to the difference lines above.

The normal values of the limits are

51105·64 49062·77 47650·0 46756·1

These were first recognized in the summation sets, and the difference indicated by them. We notice that the two difference quartets (say, Q_1 , Q_2) are composed of weak lines with some spark representatives, the second more affected by the spark than the first, also that the Q are more intense, and that while Handke observes the Q_1 , the stronger excitation of Bloch produces the Q_2 . The presence of spark lines in the Q also suggests displaced lines, and this is further sustained by those lines in the neighbourhood of the same character already given (p. 1176).

Those sets giving mean limits close to the normal y , x are indicated by an asterisk. Our discussion would be much simplified if we could be sure that the corresponding difference-summation pairs were real, *i.e.*, that any displacement present were common to both lines. Unfortunately, here with good measures in Q_1 we have Handke's considerable O.E. in Q_1 , whilst the good measures of Bloch in Q_2 are combined with irregular and defective observations in Q_2 ; also the own shift in the $t(3)$ term (·217) is so small that definite conclusions cannot be drawn. Nevertheless it will be instructive to test the observations on this supposition. Where the mean limit is normal within O.E. we may be justified in taking these limits as not displaced. In the first (C), for instance, the mean 49062·2 is correct within Hke.'s O.E. In other words, the lines 39153, 58971 may be taken

as correctly allocated as Z_{12} , \mathbf{Z}_{12} (say) and may be taken as our starting-point. As the small oun shift ($\cdot 217$) in $t(3)$ renders the small details of any scheme not fully convincing, it will be sufficient here merely to give the result. It is shown in the annexed table, the first scheme indicating the displacements which the observed lines in the first quartet have experienced, and the second giving the wave numbers of the normal Z quartet of which the observed are collaterals.

The numbers in brackets before the W.N. denote the $d\lambda$ corrections to be applied to the observed to make exact agreement (0 means $< \cdot 01$). It will be seen that this is complete within O.E., but in the Q other values involving oun shifts in $t(3)$ might be taken, and the results be still within Handke's O.E., but no such latitude is allowable in the far more accurate Q lines. The significant point is that all the corresponding pairs are each true difference-summation lines (*i. e.*, displacement the same). In the calculations the d separations have been regarded as composite and depending on the limit term \mathbf{y} (oun shift 2.549). If all the limits be regarded as single terms, the shift per oun would be 2.549, 2.398, 2.295, 2.230. The agreement is definitely upset, again in accordance with several previous indications that \mathbf{y} is a real term, and 2042, etc., are composite; in other words, all the real limit terms differ only slightly from \mathbf{y} . The discussion of this set has one very important result in fixing more closely the normal values of the 1412, 894, which as given in the first quartet (A) are uncertain within a few decimals owing to their dependence on Aretz's measures. The modifications by the oun shifts can be exactly determined, and it is then seen that we get perfect agreement for 1412.70 and 894.00 within very small O.E. in all the lines.

Displacements in C.

$$\begin{array}{cccc} & & (-2\delta_1)Z_{38}(2\delta_1) & Z_{34} \\ (-2\delta_1)Z_{11}(2\delta_1) & (\delta_1)Z_{22} & (2\delta_1)Z_{23}(-4\delta_1 - 2\delta_1) & (-\delta)Z_{34}(-4\delta) \\ & Z_{12} & (\delta)Z_{13}(4\delta) & \end{array}$$

with the same scheme for \mathbf{Z} , but no \mathbf{Z}_{34} .

Resulting normal quartet:—

	2042 87	1412 7	89 4	
248 9		(0) 38307.35	(0) 37413.35	
		(0) 39471.12	(01) 38058.42	(0) 37164.4
317 86				
Z	(0) 41196.13	(0) 39153.26	(0) 37740.56	
\mathbf{Z}	(-2) 61015.15	(-03) 58972.28	(0) 57559.58	
317 86				
		(03) 58654.42	(-01) 57241.75	(-08) 56347.75
248 9				
		(02) 56992.82		[56098.82]
317 86 : 248 9	$= 5 \times 63.5 : 4 : 62.2 = 5 : 4$			

In the second quartet the characters of the lines suggest that it and the first are collaterals, that is are displaced from a common normal one. The first, second, and fourth mean limits are so close to normal values that any displacement must lie in the current term. The equal and opposite shifts in Z_{11} , Z_{34} from those of the normal quartet— $30\cdot15$,— $28\cdot38$; $30\cdot3$,— $30\cdot0$ —proves this for these lines. It means a displacement of -35δ , shifting $30\cdot54$, within one or two oons ($34\frac{1}{2}\delta$ shifts $30\cdot11$). But nothing is to be gained at present by following this out in more detail.

The $m = 2$ lines of the same $s(m)$ Rydberg series also show relation to quartet forms. We find :—

E.

			$2n, 27584\cdot18$	892 39	$2n, 26691\cdot79$ (C. T.)
				132 22	133 4
	$1n, 28864\cdot28$	1412 32	$2, 27451\cdot96$	893 06	$1, 26553\cdot90$ (C. T.)
	167 85		167 80		
$2, 30739\cdot38$	2042 95	$4, 28696\cdot43$	1412 27	$1n, 27284\cdot16$ (C. T.)	
		$7\cdot77$			
$51111\cdot29$		4906			
$00, 71483\cdot20$					
		$00, 69271\cdot27$			
167 83 : 132 3 = $5 \times 33\cdot56 : 4 \times 33\cdot1 = 5 : 4$					

This pd quartet has a defective summation, but those present both give y , x mean limits 5 too great (2δ , shift on $y = 5\cdot10$). We note also that both the $m = 2$, $m = 3$ quartets give the same separation ratio $5 : 4$.

We find a considerable number of sets throughout the whole spectrum separated by about 96. We find one here, for instance, with the observed $s(2)$, viz. (excluding the first line) :—

F.

	$4, 30939\cdot65$	2041 35	$1, 28898\cdot30$	1402 78	$3, 27495\cdot52$	903 73	$2, 26591\cdot79$
	85 60		105 80		112 51		109 4
$m=2$	$2n, 30825\cdot25$	2032 75	$3, 28792\cdot50$	1409 49	$1, 27383\cdot01$	900 67	$3n, 26482\cdot36, s. (E. V.)$
	$51093\cdot29$		$49063\cdot10$		$47651\cdot95$		$46755\cdot15$
	$00, 71361\cdot29$	2027 59	$00, 69333\cdot70$	1412 76	$1, 67920\cdot94$	892 99	$3, 67027\cdot95$
	$00, 71264\cdot66$	96 63					

The difference lines are respectively $85\cdot8$, $95\cdot87$, $96\cdot07$. $98\cdot85$ ahead of the Z_{14} of the E quartet. The Z_{11} , Z_{11} give too small a limit by $12\cdot35$, the others normal within O.E.

The 96 separations would be therefore current term displacements. The "forbidden" line 26482 is a spark line also, as it should be.

The first horizontal line in the above gives another parallel set, interesting because $2041\cdot35 = 3u' - 17$ is a linkage value, and $1402\cdot78 + 903\cdot73 = 1412\cdot7 + 893\cdot8$, the true normal d -values. To further illustrate the 96 case, we may adduce the following fragmentary set:—

G.

		1, 34878·19 (E. H.)	
		98·21	
1n, 37012·22	2035·82	1, 34976·40	1409·90 2n, 33566·51
		2·25	
51102·54		4906	
		3·03	
0, 65192·87	2043·22	0, 63149·65	
96·20			96·66
00, 65289·07	2042·76	4nr, 63246·31	

H.

	—	4n, 21282·02	887·75	4, 22169·77
		312·51		
—	2, 19556·59	1412·92	2n, 20969·51	
	451·04			
1, 17068·77	2036·78	2, s, 19105·55		
552·08		(37, — vii)	(9, 15 viii)	(8 viii)
1, 16516·77				

$$552 : 451 : 312 = 9 \times 61 \cdot 3 : 7 \times 64 \cdot 4 : 5 \times 62 \cdot 5 = 9 : 7 : 5$$

Any summation lines with limits y, z are outside observed regions. The frame is of F^4 type. 22169 appears as F_{44}^4 . It appears also of the same type in a different quartet arrangement given by Beals, and by Shenstone. When later we discuss the latter we shall find that the Z.P. definitely sustains the allocation of this line. Further (though not in B. or Sh.), the f separations are in the correct ratios according to Landé's rule. The d separations are additive, *i.e.* the lines are of the form $f-d$, not $d-f$. Two constituents are missing. In other respects it is a good typical F quartet, except that the characters are not all alike or the intensities normally related. Also the F_{33}^4 , or 20969, has a Z.P. = $0\cdot69$ (Sh.) which agrees with that for F_{33}^4 , viz. $\cdot26, \cdot09/\cdot77, \cdot94, 1\cdot11$. Sommer allocates this line to $d_1^2 d_1^2$, Z.P. = $\cdot60, \cdot20/1\cdot00, 1\cdot40, 1\cdot80$, which it certainly is not:

Shenstone to 232-??3, which includes Sommer's. On the contrary, the Z.P. for 19556 or F_{23}^4 is given by both S. and Sh. as 0/0, *i.e.* is not affected by the magnetic field. This contradicts F_{23}^4 and is consonant with their allocation as $d_4^4 d_4^4 (j=1, 1)$ or indeed with any line not affected by the magnetic field.

11. We come now to the consideration of the quartet relations of Shenstone's lines, and begin with those which the previous discussion has shown to depend on the y, x limits, viz. :— $p_1, p_2; p_A; Q; F$ and probably p_Q .

p_1, p_2 . These give the original quartet A which has served for the discovery of the 2042, 1412, 894 separations.

p_A . As p_A is $p_1(2)$ we should not expect to find such a complete set as for $p(1)$. Also no corresponding $p_2^2(2)$ occurs. The following arrangement, not altogether satisfying, would seem to indicate that p_A is a fourfold term also :—

I.

			1, 34777·40 (E. H.)	894	[... 83·40]
			1330		(1 _{un} , 33873·5)
	1 R, 36172·63	1408·55	1, 34764·10 (E. H.)		[... 66·0]
		35·08			
10, 38180·15	2042·87	8, 36137·57	—		
51105·23		[49062·51]	47653·7—18 dλ		(·46759)
1, 64030·32	2042·87	[61987·45]	1412·7	—	+ 896·0 1, 59678—35 dλ
		2, 61977·1—38 dλ			
	[... 56·0]	1412·7	6, 60543·31	889·7	2, 59653—35 dλ
			(7, 60537·0—36 dλ)		

In this [61987, ... 56] are calculated respectively from 64030 and 60543. McLennan's 61977 is the mean, and would represent their merge, $d\lambda = 1\cdot4$. [33883, ... 66] are calculated respectively from 34777 and 36172. Again, their merge might be represented by 33873. 59653 gives the correct separation within O.E. It is "forbidden," but a spark line. Handke's 60537 may also be a merge of 60543 and Z_{33} , or it may just possibly be his measure for Bloch's line ($d\lambda = \cdot 17$).

Q.F. These belong to $p(3)$. There are no traces of either a difference or summation quartet, except a just possible 1, 54913·7 by Handke, giving a separation 1422 with $x+Q$, and requiring $d\lambda = -\cdot 3$.

Phil. Mag. S. 7. Vol. 4. No. 25. Suppl. Nov. 1927. 4 H

J.

			1, 31455·18	
			24·57	
	1, 32890·81	1411·06	3n, 31479·75	891·39 3, 30588·36
	36·57; 39·55		40·42	
pg 2, 34970·233	2042·85	6, 32927·382 (30·36)	1407·21; or 10·09	31520·17
	630·28	1412·57	120·96; 117·98	115·80
1, 34339·95		3, 33048·34	1412·37	2, 31635·972 896·59 2, 30739·38 ⁽¹⁾
			84·79	85·87
			1n, 31720·66	895·41 nn, 30825·25

⁽¹⁾ Appears also in quartet E.

We have here a double quartet, in one with direct terms 40, 24, the other with inverted 120, 84. The 32927 is a y satelloid, its extreme violet satellite in (). Indeed, the d separations seem affected with the y shifts. Thus

$$1411·06 + 3y = 1412·77 \quad 891·39 + 5y = 894·24$$

$$1407·21 + 10y = 1412·91 \quad 896·59 - 4y = 894·31$$

$$1412·37 + y = 1412·94 \quad 895·41 - 2y = 894·27$$

In both quartets the portions after this line seem to depend on the satellite, and better even on one $2y$ further out. With this

$$39·5 : 24·5 = 5 : 3 \text{ and } 120·96 : 84·7 = 7 \times 17·2 : 5 \times 16·9 = 7 : 5.$$

The line 34339 is introduced as it gives 1412·57 *back* from 32927. This must be a coincidence and due to the fact that $1412 = 2042 - 630$, and the line is linked $-3Y_1 + \cdot 35$ or $-X_1 - 2Y_1 + \cdot 02$ with 34970.

If p_g is taken as $p_A - (3e + Y_1)$, as in § 23, the limit for $x p_g$ is 45852·59, and the summation for $x p_g$ would be $91705·19 - 32927·38 = 58777·81$. There is no line here, but both Hke. and Bl. give a series of successive lines with nearly equal separations suggesting the presence of collaterals. Thus

Bl.		Hke.	
	39·68		37·6
58637·61	58752·34	58652·9	58763·2
47·15	39·71	44·80	48·4
684·76	792·05	697·7	811·6
37·90		37·9	
722·66		735·6	

The composite limit depends on y , in which $-10\delta_1$ shifts 25·47. Thus $(10\delta_1)58777·81 = 58752·34$, which is one of Bloch's lines. In the neighbourhood, however, is a very

suggestive copy of the difference quartet by Hke., exact within his O.E. Thus

		6, 56317·9	—
		85·5	
1, 57815·4	1412·0	3, 56403·4	—
	127·3	124·4	
—	3, 57942·7	1414·9	8, 56527·8

Fortunately, one of these is given by Bl., so that the absolute value of one can be fixed. Hke.'s 56527·8 is Bl.'s 4,56524·32. This gives the separation 120·9 with Hke.'s 56403. If we correct from Bl. by the correct separations as shown by the difference quartet, we get the following set, in which the figures in () give $d\lambda = \text{Bl.} - \text{Hke.}$:—

		6, 56318·7 (−04)	[55924·7]
		84·7	
1, 57816·06 (·02)	1412·7	3, 56403·3 (·00)	[55509·4]
	120·96	120·96	
[59979·89]	3, 57937·02 (·17)	1412·7	8, 56524·32 (·1)

Here 57937 is 840·81 below the supposed correct summation 58777. This is $4Y_1 - \cdot 03$. Thus, while p is shifted $3e + Y_1$ back from p_λ , this set is shifted a further $4Y_1$ or $3e + 5Y_1$ from $x + p_\lambda$. It is probable that other linked sets may be present, for there are a considerable number of $e, 2e, 3e$ links in this region. The importance of this pair of quartets lies in the support it gives to the dependence of the p_e lines on p_λ , *i. e.* on $p_1(2)$. If we could feel certainty as to the exactness of the two sets of separations 39·55, 24·57 and 120·96, 84·70, the own law would give practical proof of this dependence on p_λ , for the respective mantissæ differences and own relations are as follows :—

$$4441 = 30\frac{1}{2}\delta - 16\cdot3 ; 2755 = 19\delta + 15\cdot8 \quad \text{sum} = 49\frac{1}{2}\delta - \cdot 5$$

$$13727 = 94\delta - 10 ; 9728 = 66\frac{1}{2}\delta + 10 \quad \text{sum} = 160\frac{1}{2}\delta + 0,$$

showing both the systematic triplet effect and the exact sum.

The foregoing have all been shown to depend on x, y in their limits. Evidence has also been given to show that the remainder of Shenstone's p -lines depend on $P(1)$, *i. e.* involve s in their limit values. We have been led to regard the separations between the pairs arranged by Shenstone as probably complex and due to combined links and a displacement on a p term.

p_a, p_b . We find

K.

$$\begin{array}{rcll}
 & & 2, 26771\cdot70 & \mathbf{890\cdot72} \quad 1, 25880\cdot98 \text{ (E.H.)} \\
 & & \mathbf{487\cdot49} & \\
 & 2, 27698\cdot33 & \mathbf{1414\cdot12} & 1n, 26284\cdot21 \\
 & \mathbf{829\cdot795} & & \\
 3, 28911\cdot40 & \mathbf{2042\cdot86} & 2, 26868\cdot54 & \text{---} \\
 \text{with } sp_a & \mathbf{829\cdot217} & sp_b & \mathbf{492\cdot94} \quad 1n, 41436\cdot28 \\
 & \mathbf{829\cdot2 : 492\cdot9} & = 5 \times 165\cdot8 : 3 \times 164\cdot3 = 5 : 3
 \end{array}$$

With the allocations adopted for p_a, p_b any summation lines would lie beyond observed regions. If the limits are y, x the only near one is $71264\cdot66$, which gives with p_a a mean $49066\cdot6$ definitely not x itself. But there are no other near lines falling in with the rest of the scheme, and it belongs to another set. It is not a satisfactory quartet, since 26771 is 5 vi depending on $p(-a)$, whilst p_a, p_b depend on $p(-a-b-\delta)$ and $p(-a+2b-\delta)$; on the complex basis this would mean that of the three terms involved the second would be displaced $+3b$ on the first, and the third $-(2b-\delta)$ on the second, and therefore quite inadmissible. In the absence of an established second separation it is not possible to use the own-multiple law to test if 829 is a real term difference on $p(-37\delta)$.

Unfortunately, the 487 is not sufficiently definite to test this. It is interesting to note, however, that if 26284 be corrected to make the d separation the normal $1412\cdot70$, the separation becomes $486\cdot07$. The $829\cdot217$ will go with this, but not $829\cdot795$ which is exact y larger. The mantissæ differences based on $p_1(-17\delta)$ are

$$24867 = 169\frac{3}{4}\delta - 1; 15012 = 102\frac{3}{4}\delta - 1 \quad \text{sum } 272\frac{1}{2}\delta - 2;$$

all exact within O.E. but showing no triplet effect, or perhaps indicating a triplet transference of about one own when the true displacement would be $170\delta, 102\frac{1}{2}\delta$. Note again $170 = 13^2 + 1$; $102\frac{1}{2}\delta = 5(9^2 + 1)\delta_1$.

The 829 separation occurs in the Beals's quartets discussed later. Several are found also in the ultra-violet lines of Bloch, in connexion with others about 2046 , which latter are very numerous. They should be summation lines, and in fact there seems some slight evidence for difference lines on the basis of the x limit. The following three examples, in which the ultra-violet summations are placed first, illustrate this statement. The first arrangement also illustrates a not uncommon phenomenon in spark spectra, where successive

repetitions of slightly differing configurations and meshes appear :—

L.

	2047·26	1,58259·45	833·07
	4,60306·71 ⁽¹⁾	831·04	4,59475·67
	2049·29	6,57426·38	
	683·53	683·62	
	669·77	2046·59	3,59623·18
	831·13	4,58792·05	
	829·45		
1,64546·94	2047·72	4,62499·22	
	49065·30		
	1,35631·39		

⁽¹⁾ Also with $-u'$ and $+e$ (see table iii.).

M.

	00,63527·56	
	828·72	
	3,64356·28	
	49058·40	or ...60·11
		to 6y sat.
1,35806·73	2046·21	6,33760·52 (sat.)
		or 2042·77 to 6y sat.
		(see 26 xii)

N.

	00,67159·17
	829·19
00,70034·38	2046·02
00,67988·36	4·062·70
4,30137·04	

p_c, p_d

O.

	(sat.) 3,30480·70	(894·16)	1n, 29580·05
	223·12		216·96
p_d	3,31670·28	1412·7	[30257·58] 894·47
	871·61		2n, 29363·11
p_e	2,33341·61	2042·93	6,31298·68
	sp_c 371·72	sp_d 224·63	6R, 45141·01 (Wlf.)
	371·60: 223·1 = $5 \times 74·3 : 3 \times 74·3 = 5 : 3$		

Here 30480 is αA and an α -satelloid. Its red satellites at -10α , -15α give separations 895·29, 892·64. Stücklen gives four red. One at -12α would give 894·16. The 30257, though not observed, is substantiated by the observed sum of separations. The own test applied to the separations 371·61, 223·12 supports the basis of true term separations, for $x p_c$ depends on $(3b) p_1 = 31376·89 = R/(1·86932)^2$.

The resulting mantissa differences are

$11171 = 76\frac{1}{2}\delta - 8·5$; $6803 = 46\frac{1}{2}\delta + 7·6$ sum = $123\delta - 0·09$,
showing both the systematic triplet variation and exact sum.

If 371 is $2X + (-b)$ on p , we look for about -50 on p_c or $+50$ on p_d , and find

$$\begin{array}{rcl}
 3, 31635.97 & (1412.84) & 8, 30221.51(\text{sat.}) \quad \text{---} \\
 & \mathbf{34.31} & (\mathbf{34.45}) \\
 x p_d \ 31670.28 & \mathbf{1412.7} & [30257.58] \ \mathbf{894.47} \ 2n, 29363.11 \\
 \left\{ \begin{array}{l} 6, 33760.53 (\text{sat.}) \\ 63.48 \end{array} \right. & \mathbf{50.38} & \\
 & \mathbf{2042.82} & 1n, 31720.66 \\
 50.38 : 34.31 = 1.47 = \text{roughly } 5 : 3
 \end{array}$$

30221 is also an x -satelloid, the separations from a $3x$ satellite, but 31635 would be a forbidden line. Also the satelloid is $e.P_2.u$, and is too strong for this set. The evidence for a direct quartet depending on b is therefore weak.

In the preceding no attempt at a systematic discussion of quartet systems has been made. A few examples starting from observed ϕ -separations and some of the systems connected with the Shenstone lines only have been considered. In arranging these, starting from a ϕ -pair, the near lines giving the successive 1412, 894 separations have been sought, without reference to any theoretical ratios of the associated sets of separations (quartet A, of course, excepted). Nevertheless, these separations in all the examples show ratios of small integers with great exactness, $5:3-5:4-9:7:5$. Especially should it be noted that the p^4 ratio $5:3$ is shown by p_a, p_b for which there is independent evidence that they are fourfold terms, and the f^4 ratio $9:7:5$ is found in H with independent evidence from the Zeeman effect for at least the presence of F_{44}^4, F_{33}^4 . Also the abnormal ratio $5:4$ appears in both the related systems belonging to $m = 2, 3$ of the Rydberg $s(m)$ series. This, of course, is to be expected if we are dealing with real term differences, and considerable support is given to a real term theory by their fulfilling the own displacement law. But in several cases there is evidence that they are composite. In fact, it is difficult in at least the d^4 separations 2042, 1412, 894 to believe that they are other than almost pure linkages, although even here the proper d^4 ratios $7:5:3$ are in evidence. The question must be left open at present.

The quartets of Stücklen and of Beals.

12. We now pass to the consideration of the quartets which have been recently proposed: (1) two by Stücklen* in the violet, and (2) three with related intercombinations

* *Zeits. f. Phys.* 34, 562, 25.

by Beals*, independently later by Shenstone*, and implicitly by Sommer*. At a first glance, doubts as to their reality must be felt, for, as regards the quartets:—

1. The characters of the lines as arranged in their frames show complete dissimilarity between those in the central columns and those of the two extreme ones, as indeed was pointed out by Beals.

2. The separations involved seem excessive, and not only are they irregular, but they run even contrary to Landé's separation rules.

3. Many of these suggest at once the presence of compound links, as, *e. g.*, $636 = 3X$.

4. Each quartet consists essentially of lines of a single map; that is, the lines are link and collaterally related.

5. They have the fatal objection that negative terms are required. I have already in [I.] referred to these so-called negative terms. An electron describes a certain quantized orbit, which possesses a certain total energy value. Its "term" measures its energy-defect, *i. e.* the difference between the energy from infinity and the actual total energy. It is a measure of the work required to expel the electron out of the atom from that particular orbit, and it is this property which renders the determination of its exact value so important. It cannot be negative, or the electron would, so to say, expel itself. The reason why such negative values are given by certain writers is due to the fact that they are governed by the belief that all wave numbers are the difference of two terms only, and other phenomena are passed over, amongst which may be mentioned summation lines, and the possibility of an atom having two or more of its electrons raised to different levels and simultaneously falling in. This includes the case of links, every link being in fact due to a fall between two levels with the same k . For instance, if we find, say in Cu two lines at $n_1, n_2 = 30000, 30248$, the separation suggests that the lines are $p_1 - t_1, p_2 - t_1$, and that $30000 = p_1 - t_1$, producing a term $t_1 = 31524 - 30000 = 1524$. Suppose, now, a similar pair are found, 2041 ahead with $n_1 = 32041$. The two-term basis would give $t_1 = -517$, whereas the true value is $31524 + 2041 - t_1$ with $t_1 = 1524$ as before. In other words, if 1524 were a true term in the first case, it would remain so in the second, and no negative values be introduced. In all cases, repeated separations are due to term differences—*e. g.*, any link is a difference of two terms, and is so calculated. The error lies

* *Loc. cit.*

in the assumption that a wave number in all cases depends on two terms only. That the assumption is wrong is proved not only by the deduction of negative terms on that basis, but also from the actual existence of links, that is of separations, given by definite two-term differences in cases where neither of these terms can enter on a two-term line basis. Difficulties arising also from the existence of successive equal separations are specially considered below in the discussion of table iv.

Two remarks may be interpolated here:—(1) A link has hitherto been regarded as due to an electron fall between two near levels of the same azimuthal quality. But the presence of considerable multiples of the same link would on this explanation seem to require falls of several electrons between similar levels, a conception difficult to visualize. Another explanation might be that a rearrangement of electrons within the core would affect the values of the outer levels, and that such changes proceed by discrete steps, just as in displacement we find the discrete our steps. (2) The explanation of summation lines based on the simultaneous fall of two electrons in a doubly-ionized atom [I. p. 195] requires a very close simultaneity in independent events. This difficulty may be avoided by supposing that a singly-ionized atom is also highly excited, with an electron in one of its peripheral levels. The fall of an exterior electron might then precipitate the simultaneous fall of this peripheral electron. The actual peripheral level would be immaterial, provided its order is so high that successive values are practically equal. When they are lower the orbits may be sufficiently stable, so as not to be sensitive to the action of the entering one. If they are we should get displaced summation lines—unfortunately for our power of definite allocation.

The writers named—and indeed a large number of others—treat all wave numbers as given to one decimal place, whatever the accuracy of the observation, and they are satisfied with agreement in the various term-differences within a few units in the first decimal place, even when the accuracy of the measure is ten times or more larger. In many cases agreements are thus accepted where the more accurately observed would definitely exclude them. It would seem preferable always to give the wave number to a significant figure, one more than that of the observed wave-length. If not, when we come to additions or subtractions, both observation and calculation errors are altered in an unknown way. Then the results should be compared with possible O.E.

13. *Stücklen*.—The lines forming these quartets are of the same character, belonging practically all to her class i. of lines absorbed in the underwater spark. The corresponding separations are very closely equal, and in the first quartet (dp) they increase in roughly regular ratios 2 : 3 : 4 and 1 : 2 with the j values adopted by her. But these ratios belong to odd-fold systems, and there is the fatal objection that the j refer to a very unlikely combination. The 4, 3, 2, 1 belong uniquely to d^4 ; 4, 3, 2 to f^3 , p^7 , or p^8 . The only possible conclusion would be that the quartet is an intercombination $d^4 p^6$, in which we should expect separations in the ratios 3 : 5 : 7 and 7 : 5, and these they decidedly are not. The quartet frame would be preserved by taking for j 1, 2, 3, 4 in place of 4, 3, 2, 1 and 1, 2, 3 of 4, 3, 2, in which case they would form a D^4 quartet, with a better intensity arrangement, but the separations now decrease with increasing j . If this last anomaly is accepted as possible, the arrangement must also be accepted as a perfect dp quartet. But I am inclined to think that where such an anomaly is found, it is a sign that composite separations are present, that the lines involve linkages, and that negative terms will be allocated by those who hold that all wave numbers are the differences of two terms. Her second quartet has such irregular separations that to me it appears unacceptable as a pure quartet; but this objection will not appeal to many recent writers. The first quartet is reproduced here in outline, the lines being represented by their intensities in (). Stücklen's j values are also entered, with those suggested above in ().

j	1 (4)	2 (3)	3 (2)	4 (1)
4 (1)			(2 u) 724·11	(2) 629·85
3 (2)		(6R) 574·64	(6R) 724·36	(1 u) 574·71 (1 n)*
		329·89	329·70	
2 (3)	(6R) 370·98	(2)† 574·73	(4R)	

The line denoted by *, 46748, has been added, as it reproduces the same separation 574 in a series, so that they cannot be pure term displacements. Also we find a similar series with 371, viz. † is followed by the line 44916 in her second quartet, separated by 371·62.

371. The region 44173 to 46250 of these quartets is included in fig. 1. The 371 occur also in Beals's quartet. They are produced in all cases by 2X links and a (b) displacement on $p(1)$. They are discussed together later. Here they are represented by the aa , bb , cc pairs in fig. 1 : 370·98— a , a —does not show these intermediate lines, and is

probably not connected with the other 371. The fig. shows 5 chain representing it, $50 + v - X - X + 54$ or $v - 2X$, with (2*b*) on $p(1) = 370.86$. Whether real or not need not detain us. We consider in detail the first quartet only.

574.64; **.73**; **.71** is the composite $e - 2Y_2 = 999.80 - 425.08 = 574.72$.

The intermediates are (unobserved indicated by a ●) :

44874- 214.89	44659	997.11	45656- 207.58	45449
44544- 214.66	44330	999.80	● - 210.41	45119
46173- 210.23	45962	999.80	● - 213.86	46748

724.11; **.36**. $724.2 = 574.72 + 149.48$ and (3*b*) on $p_2(1)$ shifts 149.43.

For intermediates we find

46079- 208.88	45870- 213.64	45656	997.20	●	149.43	46803
45449	1006.27	46455- 205.87	46249- 218.25	46031	142.21	46173

These show considerable displacements, but the X pairs form series inequalities, $X_2 + Y_1 + .04$, $2X_2 - .42$. In the first we get another example of **574.71**.

630.10; **629.85**. These differ by more than O.E. and by too much if real separations. They depend on X_1 , Y_1 , and are analogous to the 636 of Beals, which depend on X_2 , Y_2 (see p. 1211). Here $3X_1 = 629.64$; $3Y_1 = 630.63$; $2X_1 + Y_1 = 629.97$, etc. For intermediates

45449	207.58	45656	213.64	45870	208.88	46079
46173	207.95	●	207.96	46589	213.94	46806

We find a similar set in 25, 8 i, 26, 27 of map II., viz. :—

$$31741.90 \quad \mathbf{211.11} \quad 31953.01 \quad \mathbf{206.48} \quad 32159.49 \quad \mathbf{218.29} \quad 32372.78 \\ = \mathbf{630.88} = 3Y_1 + .25$$

329.89; **.70**. Possibly a separation of two unrelated lines. The two values must necessarily be nearly equal, since the associated 574 are.

14. *The Beals quartets*. These are given as d, p ; d, f ; d, d quartets with common d^4 terms. They are reproduced below with the addition of certain intermediate lines in italics, which have been introduced for a purpose described below. Those enclosed in () in the third refer to a set which Beals attributed to an unknown term of probably f type. Their positions in the maps of [I.] are indicated either on the right of each line or collectively in the same column.

$Q_2 = F^4.$				
1.	2.	3.	4.	1.
2	207.6 207.6 208.53 680.0 215.33 -148.1	207.6 207.6 208.53 680.0 215.33 -148.1	(14, 16, 5, 7 viii)	212.13 212.133 8, 2149.4 S 675.619 4, 22169 -148.04 739.71
3	2, 20840 + 212.20 2s, 21052 197.30	544.91 203.84 409.50 205.44		212.13 212.133 8, 2149.4 S 675.62 4, 22169 *
4	6, 21249 § S 244.277 8, 21494 § S	545.14 (-, 12, 11, 4 -- viii)		887.751 (7 viii)
5				(8 viii)

$Q_3 = dd.$

<i>j.</i>	4.	3.		2.	1.
1				$\left\{ \begin{array}{l} 1n, 18668 \quad 209.7 \quad 2, 1887.8 \quad \quad 887.65 \\ -50.22 \\ 3s, 18618 \quad 211.18 \quad 2s, 18829 \quad \quad 889.85 \\ 371.54 \quad 211.18 \quad 210.58 \quad 371.548 \\ 2s, 18829 \quad 210.58 \quad 0n, 19040 \\ 210.58 \end{array} \right\}$	$\left\{ \begin{array}{l} 2, 19556 * \\ -48.02 \\ 1ds, 19508 \\ 2X_2 - .09 \\ 3, 19928 * \end{array} \right\}$
2				$\left\{ \begin{array}{l} 2n, 18404 \quad 214.57 \quad 3s, 18618 \quad 211.18 \quad 2s, 18829 \quad 210.58 \\ 636.33 \\ 1ns, 18330 \quad 211.19 \quad 2n, 18542 \quad \quad 639.28 \\ 137.83 \quad -73.20 \\ 211.19 \quad 137.41 \quad 1s, 18970 \\ 207.68 \quad 1n, 19177 \end{array} \right\}$	
3 ⁽¹⁾	3, 17997† 545.24	2n, 18542		635.76	
	680.03	680.10		680.23	
892.268	(2, 18677†) 545.15 28	(1n, 19222) 210.02	1n, 19434	209.12 24s, 19643	214.76 (2n, 19858)
	212.23	212.02	(17, 15 v, 31 vii)	635.90	(-, 35 vii) (32, 31, 35, 39, 2, 3, 40 vii) (39, 35, 38 vii)
4	4, 18889 * 544.96	1n, 19434			(-, 36, 37 vii)

⁽¹⁾ Arelz measures for all three.

$$Q_1 = D^4.$$

<i>j.</i>	4	3.	2.	1.
1			3 <i>n</i> , 22640 (4 <i>x</i>)	887·88 4, 23528 *
			830·09	829·717
2		6 <i>n</i> , 22834 (3 viii) 636·7	2 <i>n</i> , 23470 (13 <i>x</i>)	887·51 4, 24358 *
			95·0	
		1095·6	1 <i>n</i> , 23565 (7 <i>x</i>)	1095·76
			1000·76	
3	6, 23384 § S 545·028	4 <i>n</i> , 23929 (12 <i>x</i>) 636·93	0 <i>n</i> , 24566 (14 <i>x</i>)	

Intercombination Lines (Beals).

<i>p</i> ² <i>d</i> ² .	2.	2042·87.	3.	<i>s</i> ² .	<i>f</i> ² <i>d</i> ²	2.	2042·87	3.	<i>s</i> ² .
3	[]	„	2, 27816 †		4			6, 29950 S *	
			1095·357					(409)	
2	<i>xpa</i>	„	<i>ypa</i> *	<i>spa</i> *.	3	6, 28317 S †	„	[]	
	829·795			829·889 ⁽¹⁾		739·64			
1	<i>xpb</i> *			<i>spb</i> §	2	3, 29057 ⁽²⁾	„	[]	
<i>d</i> ⁴					<i>f</i> ⁴				
4			6, 32311 S †		3	<i>xA</i> †	„	<i>yA</i> †	
			892·334		<i>p</i> ²				
3	<i>xB</i> †	„	<i>yB</i> †		1	<i>xpf</i> † ⁽³⁾	„	<i>ypf</i> §	<i>spf</i> †
	137·873		137·931		<i>d</i> ²				
2	<i>xpc</i> §	„	<i>ypc</i> †	<i>spc</i> †	3	<i>xE</i> *	„	<i>yE</i> *§	
	371·607			371·719		425·581		425·439	
1	<i>xpd</i> †			<i>spd</i> †	2	<i>xpg</i> †	„	<i>ypg</i>	<i>spg</i> †

$$3, 36104·93 † = d_1^2 d_1^4 \text{ (Beals)} = D_{22}^2(S_1).$$

⁽¹⁾ The value in table i. is 829·217. There are curious discrepancies in the measure here, especially in *spb*, $\lambda = 2441$. The decimals given are '625 H.; '651 Krebs; 665 Hamm, with '64 K.R.; '67 E.H.; '65 E.V.; '67 Hup. It would almost appear as if H. had made a MS. mistake, writing 625 for 665. The W.N. given in table i. is from this '665, that entered here from '625. From the fact that the W.N. of the two differ by '67, or *y*, within possible errors, it is possible that the two sets belong to differently observed lines separated by *y*. The two θ values for *p*, *p*_b differ by exactly *y*.

⁽²⁾ This comes in No. 5, p. 1165, and No. 11, table ii., whence it is seen that it has ϕ back, not forward as it should, and, moreover, has a true θ forward to a line which is "forbidden" if 29057 is *d*² *f*².

⁽³⁾ This set and the two following were given by Beals as *d*² *d*⁴. The allocations inserted are by S. and Sh., who agree.

For the sake of analogy with the others, the first, or D⁴, quartet is arranged with a same *d* term in the vertical columns in place of the usual D frame, in which the *p*-terms are in columns. S denotes a satelloid. Decimals in W.N. are omitted, but are given for the separations to three decimal places when the wave-lengths of both lines are given to three.

A glance at the list shows that each quartet consists practically of lines from a single map. Of the lines in the right column, depending on (434), and sustained, as we shall see, by their Z.P., only two occur on the maps. On the other hand, of those in the left—depending on (431)—and not well sustained by their Z.P., all but one occur in the maps. In the third quartet the two columns on the left both depend on map V., since those marked VII. belong to the centre of the map, and, as we already know, are not related to $D(2)$, but to the $y-p_1$ connected by $y-x$ to map V. Since the lines in each quartet belong practically to one map, it is clear that the separations involved can be considered as compounded of the links and the a, b displacements indicated by these maps. A few of the quartet separations differ by more than observation errors. This points to different sources or to different displaced p terms on which the a, b displacements have to act. We must discuss the origin of these separations in some detail. But we will begin by considering some difficulties in the explanation of certain observed effects on the basis of the usual current assumption that all lines depend on the difference of two terms. The most important, perhaps, is the existence of successions of two or more equal separations (σ). If the lines are given by the difference of two terms, they are of the form $A-t_1, A-t_2, A-t_3$, where $t_2 = t_1 - \sigma, t_3 = t_1 - 2\sigma$. Since any term is of the form $R/(\text{den.})^2$, where $\text{den.} = m + \text{definite function of } m \text{ and molecular and quantum constants}$, it would mean that the successive denominators must be so adjusted that the corresponding $R/(\text{den.})^2$ differ by equal amounts. One such case might be explained as a chance coincidence, but the large number of instances observed exclude this as a general explanation. Let us see how this is met in the present circumstances. For this purpose we select a few where the successive separations may be considered as equal within O.E. In other words no notice is taken of series inequalities or small displacements ordinarily occurring in linkage systems. Shenstone and Sommer are in general agreement as to the type of terms they adduce. As, however, this notation is extremely complex, those of Shenstone only are inserted below, and only differences between them indicated. Starting, from Shenstone's first list, assuming that the x, y are doublet d terms, and influenced by a common hypothesis, such general agreement is to be expected. In reproducing their allocations the usual term notation will be employed, different terms of the same ($r k j$) are represented by

Shenstone's prefix a, b, \dots , and barred and dashed letters by $(b), (c)$ inserted after the term symbol. The map places are also given; decimals in W.N. are omitted. *The term suffixes here are j values, contrary to the orthodox notation.*

TABLE IV.

1. (5, 2, 8 vi)	26771	680.11 ⁽¹⁾	27451	212.22	27664		
	$ad_3^4(c) - dp_3^4(c)$		$af_3^2 - dp_3^4(c)$	$(ad_3^4(c) - dd_3^4)$	$ad_1^4(c) - dp_3^4(c)$	3.52	$af_3^2 - d. d_3^4$
2. (11, 3, 9 vi)	27189	212.27	27401	212.22	27660	680.06	24340
			$af_3^2 - cg_1^4$		$ad_1^4(c) - cg_4^4$		
3. (33, 31, 32 iv)	15371	692.50	16063	692.06	16755		
			$f_1^2(c) - d_3^4(c)$, Sommer				
4. (14, 18 vi)	$ap_2^2 - df_3^4(c)$	27425	999.73	28425	$af_3^2 - dg_3^4$		
5. (29, 28 vi)	$ad_3^2 - n_4$	28974	999.88	29974	$af_1^4 - cg_4^2$		
Som.	$d_3^2 - f_1^2(c)$				$f_1^4 - f_1^2(c)$ (all (b)		
6.	$P_2(1) = s^2 - p_1^2$	30535	999.96	29535	$af_3^4 - d_3$ (map i.)		
7. (37, 11, 15 vi)	$ap_2^2 - dd_3^4$	26189	999.74	27189	999.85	28189	$ad_1^4(c) - cs^2$
8. 12, 16 vi)	$ap_2^2 - h_1(-f_3^4b)$	27319	999.08	23317 ⁴⁴	$(y\text{-sat.})$	$md_2^2 - af_3^4$	
				8.52			
9. (10, 9, 4 iv)	$bd_2^2(c) - df_3^4(c)$	14625	680.76	15306	680.61	15986	$hf_1^2 - dg_1^4$
10. (17, 18 ii)	$md_2^2 - ad_4^4(c)$	31298	680.76	31979	$ap_3^4 - c_3$	(Som. $-f_1^2(b)$)	
11. (13, 12, 11, 10 viii)		20640	212.63	20853	680.04	21533	680.56 22214
			$af_3^4 - cd_3^4$	The sum of the separations = $Y_2 + u' + u + 0$.			
			Sh.	Som.			
12. (6, 7 iii)	32991	212.69	33203	$ap_2^4 - cs^2, md_3^2 - ad_3^2$	$p_2^4 - p_1^4(c), d_3^4 - d_3^4(b)$		
(12, 13 iii)	33341	212.63	33554	$md_2^2 - ad_2^4, ad_1^4 - p_1$	$d_3^2 - d_3^4(b), d_1^4(b) - f_3^2(b, c)$		
(31, 32 vi)	29230	212.49	29442	$ap_2^2 - l_1, ap_1^2 - cp_2^2$	$p_2^2 - p_1^2(b), p_1^2 - s^2$		

⁽¹⁾ In map VI., 2, 5, this separation is given as 680.26, and was based on Hasbach's measure 3734.23, whose other lines here are to three places of decimals. E. H. gives 3734.20, $n=26771.91$, sep.=680.06. H.'s spark line is enhanced to (3) and = ... 382. This is equal to $dn=1.12$, or 1.33 from E. H., mean 1.23, or one on the $p_1(1)$ term. Correcting his are thus from his more accurate spark line thus displaced, $n=26771.82$, and the mean of this and of E. H. is taken.

From (1) we learn that 680.06 is due to $af_3^2 - ad_3^4(c)$ and 212.23 to $ad_4^4(c) - af_3^2$. In other words, lines separated by 680.06 must be represented by $Z - ad_4^4(c)$, $Z - af_3^2$. Every repetition of the same separation requires therefore a new term for Z . The additional set 27660 should be added to map VI. The remark as to new Z may be illustrated by the last fourteen examples of Sommer (p. 746 of his paper), associated with the θ separations. For another precisely similar case see footnote (2) on p. 1205.

- (2) The first line is not allocated. As we get here two successive X_2 separations, it is $ad_4^4(c) - af_3^2$ less than $af_3^2 - cg_4^2$, and so cannot be allocated as a pure difference line.
- (3) Two successive v seps, and same difficulty.
- (4, 5, 6) These are three sources for the e separations. They give $e = af_3^2 + df_3^4(c) - ap_2^2 - dg_3^4 = af_4^4 + n_4 - ad_3^2 - cg_4^2 = s^2 + d_3 - p_1^2 - af_3^4$, or two numerical relations between terms. (6) is the first link in map I., the whole of which seems quite incompatible with difference lines. With the allocations of Sh., 2i and 4i give $v = 692.11 = af_4^4 - dd_3^4 - (af_3^4 - dg_6^4)$, whilst 4, 5i give the P-doublet, $p_2^2 - p_1^2 = md_2^2 - ad_3^4(c) - (af_4^4 - dd_3^4)$.
- (7) Another succession of two e separations $e = .06$ and $e = .05$, making with (4, 5, 6) a third numerical relation. Naturally the middle line has received no allocation.
- (8) Another e giving with the others a fourth numerical relation. The last is a y -satelloid with satellites at $-4y, \delta_1$ on $p_1, +2y, +4y$. The 999.08 is measured to the first violet satellite. To a $3y$ satellite the sep. would be $999.71 = e = .09$.
- (9) gives two successive u with no allocation for the central line.
- (10) gives another explanation for u and with (9) compels another numerical relation between terms.
- (11) has only an allocation for the first line.

The three examples in (12) again require four terms to express the value of Y_2 , and with (11) give a fresh set of four numerical relations between terms.

Similar difficulties appear from the general constitution of the second quartet. With a new line $2n, 21533.62$ they appear to contain two parallel doublet d sets separated by 636, which may be written thus:—

4n, 22021.73				6n, 21385.51
148.04				148.1
4, 22169.77	887.75	4n, 21282.02	636.22	2n, 21533.62
				887.6
				1n, 20646.0

The allocations are:—

$$\begin{array}{ll}
 af_3^4 - cd_4^4 & af_3^4 - cd_3^4 \\
 af_2^4 - cd_1^4, af_2^4 - cd_2^4 & \text{none} \quad af_2^4 - cd_3^4
 \end{array}$$

The left hand gives $887 = cd_2^4 - cd_1^4$, so that 21533 would be $af_2^4 + cd_2^4 - cd_1^4 - cd_3^4$, or not a difference line. This

quartet contains also two satelloids, in one of which, 21494, the first violet satellite, shows 3 u back to 19454.

Another kind of difficulty on the term basis may be illustrated from the chains in map XIII., connected with (18). No. (19) is Beals's $d_3^2 - f_2^4$, and is accepted by Sommer. The latter recognises the θ separation to (17), and is obliged to give it $s^2 - f_2^4$ or $k=1 \rightarrow 4$. At the same time (18) is ϕ behind (19), instead of ahead, so that this cannot enter by the allotted $\phi = d_3^2 - d_2^2$. It is given $f_4^2 - f_5^4$, the second f barred, a new term. (22) is $p_2^2 - d_2^2$, but here 2041.49 is not ϕ , but connected with 3 u . In any case, a new numerical relation between terms results.

15. We now return to the more detailed discussion of the constitution of the separations exhibited in the Beals quartets, and concurrently to consider the evidence from the Zeeman effect. To assist in this certain intermediate lines have been inserted in italics in the above reproduction of these quartets. They serve to indicate the actual presence of links and displacements which go to the constitution of the separations. We begin with the d -separations common to all the quartets.

887. Obs. 887.88, .51, — 887.751, — 887.65, .66. There is also the 887.6 given above. The (432) lines are very nebulous, so that all these values may be equal within O.E. It seems a composite of two diminished u and X links. The nature of the diminution is indicated in the second quartet, where the intermediate is a y -satelloid, in which Hasbach gives two red and two violet satellites and Stücklen states that there are four red and six violet. The set is (9, 7, 8 viii). Hasbach's readings give

88.75, (89.59) 90.20, (91.87) 21494.15, 96.00, 97.98 ($-9y, -7y, +3y, +7y$)
22169.77 680.18 | $-4y$ | 209.85 21282.02

If we suppose two extra satellites at $-8y, -4y$, their wave numbers are as entered in brackets and their separation from the two quartet lines are within O.E. of u' and X_1 , and the observed diminution is the $4y$. In fact

$$u' + X_1 - 4y = 887.66.$$

We get a similar indication, clearly seen in map VIII. 11, 12, 13, 13 a in the new separation above by the existence of another line 20640.95. Thus

21533.6 680.0 20853.6 212.7 20640.95 (13 viii)
5.0
207.6 20646.0

It is instructive to note that 20640 has been observed by *Phil. Mag. S. 7. Vol. 4. No. 25. Suppl. Nov. 1927.* 4 I

E.H. alone and 20646.0 by Hasbach alone in the arc, but .42 by E.H. in the spark, or y within O.E., whilst E.H. give separation = 5.47 or $9y$. It suggests that these two are of satelloidal nature. The 20640 gives $u' + Y_2$, and 20646 gives $X_1 - 4y = 209.88 - 2.28 = 207.6$, the complete separation being again $u' + X_1 - 4y$. Although these are the only indications directly of the presence of the y , the diminished u and X are also present in the third quartet between 18668 and 19556, as well as in the intermediates shown in this quartet. Other illustrations are found in (44, 43, 46 vi) and in the third quartet round 19177, viz. :—

$$208.63 + 678.93 = 887.56; \quad 207.68 + 680.23 = 887.91$$

In the former the first line is allocated to $d_3^2(b) - 4d_2^2$, and since the 887 is due to $d_2^4 - d_1^4$, the last line is expressed by the sum of these; i. e., by four terms. In the latter no allocation is given for the first line, probably because being a spark line it was not considered. That, however, is really a support of their system, as, taking their formula for the last line, that for this line should be $af_3^2 - cd_1^4$, and consequently be "forbidden." As another example take the following two lines with the allocations as given :—

$$af_4^4 - dd_1^4 \quad 4, 30114.65 \quad 887.52 \quad 3, 31002.17 \quad af_2^4 - df_3^4$$

The difference of these expressions (four terms) must equal $cd_2^4 - cd_1^4$; another example of a numerical relation between terms. The constitution suggested, $u + X - ny$, is, however, quite a common one. Indeed, if we examine the satelloids we shall find a very considerable proportion have relations of this kind. As this particular kind of modification is an essential in the explanation of the complex form of the 887 separation, the examples are here given.

Sat. 2 (9, 7, 8 viii) in d_f above.

Sat. 4 (50, 49, 51 ii) 26861 **680.12** 275.41 **212.23** 277.54.17 (6.39) $u' + X_2 + .03$ and $+4y - .03$.

Sat. 6 (42, 47, 26 vi) 29267.10 **679.94** ($-7x$) 29950.82 ($-13x$) **209.83** 30153.63;

$$886.53 = u' + X_1 - 6y + 0.$$

The satelloid seems a mixed x, y . It has satellites at $-3y, -4y, -10x, +2x, +3x$. The separations here given are those for supposed satellites at $-7x, -13x$. In addition 29057.08 **210.11** behind 29267 gives with 29950 a separation **893.74** = $u' + Y_2 + 2y + 0$.

Sat. 15 (32, 31, 30 ii) 31953 **680.83** 32633 (S) **207.79** 32841; **888.62** = $+Y_1 - 3y + .06$.

H gives single violet sat. Stücklen states $6r, 3v$.

Sat. 16 (2, 1, 3 iii) 32037 **212.18** 32249 **677.83** 32927.38, 29.72, 30.26; **890.01** = $u' + X_1 + .07$.

Stücklen gives 8r, 6v.

For examples with $n=0$ see under 892 (p. 1217).

636. Obs. 636.7; .93†—636.0; 22†—636.33†; 635.76†—635.90† with 636.1 in the new example of the two triplets. Those marked † are from moderately good measures. It is clear that they cannot all be equal, so that the allocation of immutable term systems is not applicable. The value suggests at once the constitution 3X. Thus $3X_2=636.81$, within O.E. of two sets, $3X_2-y=636.24$, $3X_2-2y=635.67$ meet the others, but there is no satelloid evidence for the introduction of y . The intermediate components are indicated in the third quartet, but not in the first, whilst other instances of the 636 occur in the intermediates. We find similar successions in map VII. nos. 25, 29, 31, 35, 29.

18193 210.63—214.56—211.08—210.64 19040

The sums of the first and last three are respectively 636.27, 636.33. We have already found examples of $3X_1$ in Stücklen's quartets.

545. Obs. 545.028—544.91; 5.14—545.24; .96—545.15. These can be equal within O.E. It is approximately met by $v=692.08$ and a $3b$ displacement on a p term, *e.g.* ($\pm 3b$) on p_1 shifting -147.64 , 148.74 , and there seem indications of this in Q_2 , Q_3 , viz. :—

(14, 11, 4 viii)	20840	693.2	21533	-148.1	21385	545.14
(10, 9 vii, 17 v)	18889	691.83	19581	-148.87	19434	544.96

If we accept the map VIII. 21385 in Q_2 depends on $(-\delta_1)S(3)$ or on $+p_1$, whilst 19581 is $y-p_1$. As $(-3b)$ on p_1 shifts 148.74 , $v+(-3b)$ on p_1 in both examples gives $692.08-148.74=543.34$ or one unit less $=544.58$. In other words, although the constitutions of the lines in the two cases are quite different, the $-3b$ displacement produces the same effect. As, however, in the new discussion of map VIII. below the 693 has been treated as a false link, this explanation of the origin of 545 can only be accepted as possible. I am inclined to think that this separation is a chance difference, repeated because all the other separations adduced in the quartet are equal amongst themselves.

We take now the separations of the current terms in the three quartets, including also the corresponding values in Beals's intercombination sets (adopted also by S., Sh.). After

the consideration of the separations of each quartet, the discussion of the Zeeman effect will follow.

$$Q_1 = D^4.$$

829. Obs. 829.717 ; 830.09—829.795 ; .889 * or .217 (intercomb.). The intercombination lines are Shenstone's p_a , p_b considered on p. 1181, where it was found that the separations were met by $u + (3b)$ on $p_1(-a-b-\delta)$, giving 829.60. In the quartet the line 22640.64 † is $2e.X_1.D_{21}(3)(-4\delta) + .02$, and the two sets of lines are connected by the 887 or $u' + X_1 - 4y$, giving evidence of the entry of y . In this case $(-3b)$ on p_2 shifts 150.50 and $u' + (-3b)$ on p_2 gives 830.56, within O.E. of the 830.09.

We find a similar example in association with the first of the sets adduced in connexion with the discussion of the origin of 545, by the addition of a u link to the middle line (4, 11, 10 viii).

$$u_1(-\delta_1) S_1(3), \quad 21385 \quad \mathbf{148\ 10} \quad 21533 \quad \mathbf{680\ 56} \quad 22214 \quad \mathbf{828\ 68}$$

Here $u' + (-3b)$ on p_1 gives 828.80. This is specially interesting as showing how the similar but slightly different values observed arise from the same displacement on differently modified p terms.

1095. Obs. 1095.76 ; .6—abs. 1095.357. The intermediate placed in the quartet suggests that the separation is e with $2b$ displacement. On the $D_2(3)$ basis of the map, 23470 contains $(-3b)p_2$ and $(-2b)$ on this shifts 100.93 or $e + (-2b)$ on $(-3b)p_2 = 1100.73$ or with $(-2b + \delta) = 1095.73$.

On the $p_a = -p_1(-a-b-\delta)$ basis $(+2b)$ shifts 99.47 and **sep.** = 1099.27.

Note. $(-a+b-\delta) = -17\delta = -(4^2+1)\delta$ in association with $-(6^2+1)\delta$ of p_a (see discussion of p_a (p. 1181)).

* See note (1) to intercombination list.

† This line is interesting since Hasbach gives the spark representative as less by $d\lambda = .67$ or $n = 3.44$ larger and equal therefore to $2e.X_1.D_{21}(3)(-4\delta)$; in other words, the spark line appears as the analogue to the "forbidden" D_{21} . The shifts at disposal are so small (δ shift on $d(3) = .5077$) that we can get no reliable evidence for any precise allocation, but with the above allocation we find a summation line by E.V. at $\lambda = 1, 2740.07$ $n = 36485.84$ giving a mean limit 29563.24 with 22640.64. The calculated limit $2e.X_1p_2 = 31772.97 - 1999.60 - 209.88 = 29563.49$, and so far sustains the allocation.

The Z.P.

The 1st col. gives n , the 2nd the line type with quartic index omitted, the 3rd the theoretic Z.P., and the 4th the obs. H. denotes Hartmann.

23528	$D_{3,4}^*$	1.33/1.33	1.30/1.30 B.; 1.31/1.31 S.
24358	$D_{4,4}^*$.87/.87, 2.60	.81/.81, 2.60 B. .87/.87, 2.62 S.
23384	$D_{1,1}^{\dagger}\S$.09 -- /1.00 -----	0/1.18 B. 0/1.13 S.; 0/1.16 H.

The first two must be taken quite definitely as established. These are the two lines which appear in no map, as in this case they should not. For the third the most that can be said is that it is just possible if 1.18 is a merge. But if so, we should expect the observed and components to show as a broad band. Really the observed points directly to a Z.P.=0/1.20, of which there are several cases, *e.g.* $d_1^2 d_1^2$; $d_1^2 d_3^4$; $d_3^4 d_3^4$. D_{11}^2 , F_{11}^2 , F_{11}^4 might give merges also like that supposed for D_{11}^4 . The allocation appears to me improbable, but I have marked it \S .

$$Q_2 = F^4.$$

739. Obs. 739.71; 9.5—739.64; abs. This is the 887.75—148, *i.e.* a (3*b*) on a p (1) term. If we accept map VIII., the set depends on $S_1(3)$, and 22021 is $u.S_1.3Y_2-.05$, on which (—3*b*) shifts 148.74 (see rediscussion of VIII. at end) and $u+X_1-4y+(-3b)=739.49$. As 21385 is only linked to 22021, its p sequent is the same, and the (—3*b*) displacement has the same shift. In the intercombination the $j=3 \rightarrow =3$, 2 are absent, whilst $2 \rightarrow 3$, 2 are 6, 28317.435.S, (16 vi) and 3, 29057.08 (43 vi) with anomalous orders of intensities. If the allocations in map VI. are accepted, the formulæ may be written

$$\begin{aligned} 28317, 2Y_2.2e.u P_1(-b) v-6y-.03 \\ 29037, 2Y_2.2e.v P_1.2v-10y+.34 \end{aligned}$$

The difference is seen at once as $v+(-b)$ on $p_1-4y+.37$ ($d\lambda=.04$). The reality is illustrated by an intermediate line 28366.83 (17 vi) separated $690.25=v-3y-.08$ and 49.40. The origin of the separation is thus $v+(-b)$ on p_1-4y , different from the former, as might be expected from the different nature of the terms involved. It may be noted also that the 2042 separations are wanting in this intercombination set. In fact 29057 has ϕ back and a θ which would require a forbidden $s-f$.

409. Obs. 409·50 ; 9·28—no intercombination. The 409·50 is accurate to the last decimal. Although the lines for 409·28 are nebulous, H. and K.R. both agree, and E.H. make it ·04 less and E.V. ·09 greater. They are therefore clearly different. We find intermediate spark lines for both, which, since $197 = 4 \times 49$, indicate the composition $X + (4b)$ on a p . Accepting map VIII., 20480 depends on $(b)S_1$, i. e. on $(b)p_1$, and $(-4b)$ on this shifts 198·05 or another one 199·29, so that $Y_1 + (-4b - \delta_1)$ on $(b)p_1 = 409·50$.

For the second set however 21385, p_1 enters as $(-\delta_1)p_1$, on which $(-4b)$ shifts 198·56 and

$$Y_1 + (-4b) \text{ on } (-\delta_1)p_1 + y = 409·34.$$

The Z.P.

22169 ⁽¹⁾ F_{44}^{4*}	·20/·20 ; 60	·23/·23, ·64 B ; ·21/·45 S.
21794 $F_{22}^{4\S}$	07 -- / 90 ----,	0/88 S. ; 0/97 Sh.
21494 ⁽²⁾ $F_{11}^{4\S}$	05 , --- / 100 ----	0/1·20 B. ; 0/1·30 S. ; 0/1·09 H.
21249 ⁽²⁾	·09, -- · 67 / --- 1·33 ---	·64/1·40 B. ; ·65/1·42 ; 4 comp. H.
20840 F_{13}^{4+}	·20, -- / ·43 ---- 2·43	0/2·20 B. ; 0/2·05 S.

⁽¹⁾ Lüttig states that H. has observed the Z.P. for $\lambda = 4507·6$ as a very faint normal triplet ; but this must be in error for 4509·60 (i. e. $n = 22169$), since 4507 is a very broad and weak line whose Z.P. could certainly not have been observed. Indeed, Kayser's 'Handbuch' notes 4509, and not 4507, as having had its Z.P. determined.

⁽²⁾ " Higher splitting not excluded." (H.)

F_{44} must be regarded as established.

F_{22} is possible but not absolute, since a very considerable number of allocations meet the observed equally well. In fact F_{22}^2 is better, requiring ·03—/·77, -- ·94 with G_{22}^2 as good ;—marked §.

F_{11} . H alone supports the allocation. It appears rather to belong to one of the 0/1·20 ;—marked §.

F_{12} . Possible, but the symmetric σ pattern should require the measure 1·33, even if they merge. The Z.P. for S_2^2 or P_2^2 are as good, ·67/1·33, but $D_{22}^4 = \cdot 27, \cdot 80/- , 1·47$,—is the nearest ;—marked §.

F_{13} . With a component separation of ·40 ($d\lambda = \cdot 1$), 2·43 should stand by itself without a merge, and the σ should have been seen as two. The pattern of S. is that for p_1^2, p_1^4 , viz. 13,—/1·20, -- 2·00 ;—marked †.

The evidence that the scheme of lines in Q_3 represents an F quartet is very slight. The remarks on p. 1208 make its reality very doubtful, and the corresponding intercombination are defective. The evidence from the Zeeman effect is weak, and the direct evidence for F_{44}^4 only points to the existence of an F quartet which has not yet been allocated.

$$Q_3 = d^4 d^4.$$

371. Obs. 371·548; 1·54—371·607; 1·719 (inter.). The intermediate lines shown in the quartet and (7, 8) below for the intercombination indicate that this separation is $2X$ with $-b$ displacement on p . Map VII. gives both 18668 and 19556 as depending on $(b)D_2(2)$, i. e. on $(b)p_2$, and b on this shifts by $-49·81$ or $b-\delta_1$ by $-48·56$. Thus $X_1 + Y_1 + (b-\delta_1)$ displ. gives 371·53. The point here is that the separation is met by $2X$ links and b on $(b)p_2$ whether that just given is real or not. Since the first and second columns are only link related, the same explanation holds for the first as for the second. The intercombinations have already been discussed under $p_2 p_2$. But there is this difference, that while here p_1 enters + in D_2 , it enters as $-p_1$ in $p_2 p_2$, and the composition is $2Y_1 + (-b)$ on $P_1(3b) = 371·32$.

There are very large numbers of instances of this $2X + (b)$ displ. with actual separations varying according to the particular X links and the terms in which the (b) displacement is taken. The following are instances:—

1, 376·96		2, 373·5 (three arrangements)	
17960·71 _s		19484·70 _s	
210·86	209·28	209·28	-50·46
17751·85	19693·98	19693·98	19434·24
213·61	209·84	-50·62	209·12
17538·24 _{p_1}	19903·82	19643·36 _s	19643·36 _s
-47·51	-45·6	214·8	214·8
17585·75 _s		19858·2	
3, 367·34		4, 367·08	
31741·90		33048·34	45229·81
211·11		-57·34	217·74
31953·01		32991·00 (6 iii, 37 xii)	45447·55
(208·25) 206·48		212·68	209·22
(61·28) 32159·47 (8 i)S		33203·68	45656·77
(-52·04) -50·25		211·75	-55·56
32109·24		33415·42	45601·21

6, 372.65	7, 371.607	8, 371.719
45449.19	31298.6778 πp_c	44544.659 πp_c
207.58		-54.40
45656.77	2x210.99	44490.26
213.64		214.14
45870.41	31720.66	44704.40
-48.57	-50.38	211.97
45821.84	31670.284 πp_d	44916.378 πp_d

There are several also with the (*b*) displacement added. Thus, in vi, 11, 3, 9, 8 and 11, 3, 2, 8 give **212.26 + 212.23 + 50.36** and **212.26 + 50.36 + 212.23**, and in vii, 25, 29, 31, 32 give **210.56 + 214.63 + 50.53**.

The continued repetition of these distorted X and (*b*) in regions where the spectrum is not crowded, shows that they form sets really associated with current distortion. Nos. 5, 6, 8 are *bb*, *cc*, *aa* in fig. 1 and 7, 8 refer to Beals's intercombination sets.

137. Obs. 137.83; 41—137.873; 931. For the first two the maps show 3 vii—39 vii and 29 vii—15 v. The 3 vii is very doubtful. The two must be of the same type since they are merely linked by 3X. The intermediates inserted in italics in the quartet seem to indicate $X + (a-b)$ on a *p* term. A $p_1(1)$ term would give for $X_2 + (a-b)p_1(1) = 212.54 - 75.15 = 137.39$, and $Y_2 + \dots = 137.66$. In the "intercombination" pair the origin appears to be different. It was discussed above in connexion with the interpretation of αA etc. (p. 1178). It was there found as a (*3b*) displacement and an interchange of *u*, *v* links.

892. Obs. 892.26; .26—892.334. These are given by the two links $u' + X_2 = 892.33$. Indeed the whole set of separations 887, 894, 892 and others near appear to belong to a single type $X + u + ny$ where *n* is a positive or negative integer. There are very many examples of the Rydberg separations remarkable for their exact agreement or exact within *y*-multiples. They and the 680, 212 are met by B., Sh., and S. by differences of three terms of the type (43'3), (243), (43'4), say, d_2^4, f_3^2, d_1^4 . A set of successive 680, 212 are produced by $d_2^4 - Z, f_3^2 - Z, d_1^4 - Z$, or successive 212, 680 by $Z - d_1^4$ etc., where *Z* denotes some common term for that set, and for other sets a new term *Z* has to be introduced. The following list contains the majority of sets. Where they have allocated no terms the wave number is in italics. The normal large separation is taken as $892.33 = R$. The last column on the right gives the

allocation of the above Z by Shenstone. An asterisk refers to the succeeding discussion.

1. (12, 11, 10 vii)	17997	$u' - \cdot 02$	18677	$X_2 - \cdot 04$	18889	R - 08	c^4D_4
2. (15, 16, 17 v)	18541	$u' + \cdot 16$	19222	$X_2 - \cdot 21$	19434	R - 05	c^4D_3
3. 31, 35, 36 viii)	18618	$X_2 - 2y - \cdot 05$	18829	$u' - 2y - \cdot 14$	19508	R - 4y - 19	
4. (13, 12, 11 viii)	20640	2127	20853	6800	21533	8927	
5. (6, 3, 9 vi)	26721	$u' + \cdot 05$	27401	$X_2 - \cdot 04$	27613	R + 01	c^4G_4
6. (5, 2, 8 vi)	26771	$X_2 - 3y - \cdot 03$	26932	$u' + 3y + \cdot 04$			*
7. (50, 49, 51 vi)	26861	$u' + \cdot 04$	27451	$X_2 - \cdot 09$	27664	R	d^4P_3
8. (48, 17, 21 vi)	27686	$u' + \cdot 06$	27541	$X_2 - \cdot 04$	27754(S4)	R + 02	d^4D_4
9. (21, 24, 25 vi)	28579	$u' - \cdot 02$	28366	$X_2 - \cdot 01$	28579 →	R - 03	d^4P_4
10. (25, 26, 26a vi)	29472	$X_2 + 2y + 0$	28792	$u' + 05$	29472 →	R + 2y + 05	*
11. (32, 31, 30 ii)	31741	68102	30153	21071	59344	R - y - 03	*
12. (2, 1, 3 iii)	32037	$X_2 - 2y - \cdot 02$	31953	$u' + y + 20$	32633(S15)	R - y + 18	*
		$X_2 - \cdot 10$	32249	677835	32927-382 } (S16)		m^2D_3 *
				$u' + \cdot 11$	972	R + 01	
13. (4, 5, 6, 7 iii)	32311(S13)	$X_2 - \cdot 04$	32523(S14)	$u' + 05$	33203 →	R	*
		$u' - y + \cdot 16$	32991	$X_2 + y - \cdot 16$			
14. (5, 7, 17 iii)	32523(S14)	$u' + 05$	33203	$X_2 - y + \cdot 04$	33415	R - y + 09	*
15.	45141	$u' + \cdot 19$	45821	$X_1 - \cdot 38$	46031	$u' + X_1 - 19$	*
16. (in v)	D_{11} 21255	(3) 67840	(14) 21119	15 68004	16 21223	17	
		89095	88959	89129	89227		

In the first place we notice that the *satelloids* occur in Nos. 7, 11...14, and that where the separations vary from their normal values outside their O.E., the changes are met by the ubiquitous y -multiples, remarkable in their completeness. In one case (12) the satellite is present, and the 892.35 is exact within .01. This effect is important as showing that any small variations from normal values arise from y -modifications and are not due to new terms.

3. The y rule shows that this belongs to the system. No allocations have been given, but on their basis a new Z term should be introduced.
4. The separations are correct within O.E. and a second new Z is required.
5. This gives a mesh, the line 26932 established by the very exact y relations. Sh. and S. disagree in its allocation with 232-211 and 232-421 respectively. The separations of the mesh are 680.11, 212.23 and 210.53, 681.81. The upper set are $d_2^4, f_3^2, d_1^4 - Z$. To represent the lower set requires $Z' - d_1^4, Z' - f_3^2, Z' - d_2^4$, and it is impossible for two such sets to co-exist*. (13) is another similar case, but is not so decisive, for the variation from a y -multiple in the 32991 ($dn=17, d\lambda=.016$) is close to its possible O.E. Sh. and S. again disagree, giving respectively 422-211 and 422-421. 8, 9, 10 give a double continuation, established as real by the y -relation, and quite impossible to explain on the term basis. Consequently both Sh. and S. exclude the $X_2 + 2y + 0$, and the 681.02 as representing real separations. Again they disagree in allocations, viz. :—

28792	433 - h_2	433 - 443
29472	243 - h_2	243 - 443
30153	not allocated.	
30364	443 - 422	443 - 412

here h_2 means some term whose $j=2$.

11. The line 32633 is given as a *satelloid*, but its single "satellite" given by H. is probably a two own displacement on p (1). Stücklen gives $6r$ and $5v$. It is

* In passing it may be noted that seps. $a, b; b', a'$ in parallel cannot be produced by difference terms of the above form. If, however, the terms involved are related, as, *e.g.*, in a diffuse triplet d_1, d_2, d_3 , they are successive displacements on one, say, $t, t(-a), t(-a-\beta)$. The separations a, b are $t(-a)-t, t(-a-\beta)-t(-a)$ and the b', a' are $t(-\beta)-t, t(-a-\beta)-t(-\beta)$, but in this case the mesh is not exact. But the deviation must be calculable. This kind of inequality is seen in the example. Whether (5) conforms or not is a question of the unknown Z . The y deviation points to its not being of this nature.

Shenstone's x_{pf} of his first paper. The allocations are 443-443 (i. e. $f_2 f_2$), 422-433, 232-222, i. e. neither accepts the lines as an R set.

12. Here the observed satellite gives exact R. The set must be accepted and requires a third new Z. Sh. and S. disagree for the first with 422-453, 422-432, and give 423-434, 232-232 for the others.
- 13, 14. See under 5. Also here we find a continuation, established by the y rule and the presence of two sateloids, 32523 is an x set. Expressed in x the seps. are $u' - x + \cdot 13$, $X_2 + x - \cdot 13$, and $X_2 + x + \cdot 01$. Naturally no allocation is given for 33415.
15. I have included this although not of the R type, but the analogous $u' + X_1$. Piña de Rubies has observed 48073.77, 2042.43 ahead of 46031, a clear $y-x$ separation. S. has recognized this and consequently allocated 232- e_2 , 233- e_2 , where e is some $j=2$ term. The others are 233-222, 211-221.

We have this $y-x$ link back from 18541 in (2), viz. 2043.39. If real, the link hypothesis requires a 233 term in 18541 given as 433-433. Also a forward 2041.97 from 27664 in (6), but here it is a clear $3u$ link. If the ϕ sep. is taken 27664 should contain the 223 term (given 423-434).

16. (3, 14) are spark lines by E.V. If they are each corrected by $\cdot 10(d\lambda = -\cdot 04)$ the four sets become $R - 4y + 0$, $R - 5y + 01$, $R - 2y$, $R - \cdot 06$.

The Z.P.

1. 19556 $d_1 d_1 * \S$ not affected not affected B. & S.
 2. 19928 $d_1 d_3 *$ 60/60, 1.80 55/55, 1.63 B.; 54/54, 1.63 S.
 3. 18889 $d_1 d_1 *$ 0/1.43 0/1.44 B.; 0/1.42 S.
 4. 17997 $d_1 d_2 +$ 03, - - - - - 1.57 0/1.88 B.
1. The allocation is met, but cannot be uniquely proved—marked * \S .
 2. The observations could be explained by an error of 1/12th in measuring the field, but the agreement by different observers puts this aside. Some disturbing effect (linkage?) has evidently occurred in the line itself—marked *.
 3. This is a good agreement, but $d_2 d_2$ has 0/1.37. The line appears in 10 vii as $y - p_1 - v = D_{11}^4 - v + \cdot 24$, but the Z.P. does not agree with D_{11}^4 . Either the link is not real or the link has affected the Z.P.

4. This is definitely wrong. It is nearer $p_2^4 p_2^4$ with $0/1\cdot73$; $d_1^2 d_1^4$ with $\cdot11 - - - - - 2\cdot00$; or $d_1^2 d_2^2$ with $\cdot20, - / - - - 1\cdot80$ —marked †.

Z.P. Intercombination (Beals).

The majority has been discussed above as entering in Shenstone's first list. Here follow the remainder :—

- | | | | | |
|----|-------|------------------------|---|--|
| 1. | 27816 | $p_1^4 d_1^2 \uparrow$ | $\cdot20, \cdot60, 1\cdot00 / - - 1\cdot40 - -$ | B. gives $\cdot99$, presumably $\cdot99/99$. |
| 2. | 29950 | $d_1^2 f_2^4 *$ | $\cdot02 - - / 1\cdot14 - - - - 1\cdot33$ | $0/1\cdot26$ B.; $0/1\cdot28$ S. |
| 3. | 28317 | $d_2^2 f_3^4 \uparrow$ | $\cdot12 - / 68 - - - 1\cdot39$ | $0/1\cdot20$ B.; $0/1\cdot14$ S. |
| 4. | 29057 | $d_1^2 f_4^4 *$ | $\cdot20, \cdot60 / 20, \cdot60, 1\cdot00$ | B. gives $\cdot60$, presumably $\cdot60/60$. |
| 5. | 32311 | $d_1^2 d_1^4 \uparrow$ | $\cdot11, - - / 86 - - - - 2\cdot00$ | $0/1\cdot78$ B.; $0/1\cdot7$ Sh. |
| 6. | 18677 | $d_1^4 f_2^2 \uparrow$ | $\cdot28 - - / 0 - - - - 2\cdot86$ | $0/2\cdot14$ B.; $0/2\cdot15$ S. |
| 7. | 19222 | $d_2^4 f_2^2 \uparrow$ | $\cdot26 - 1\cdot29 / - - 1\cdot11 - -$ | $0/73$ S. |
| 8. | 36104 | see note | | $0/96$ B. |

1. The σ forbids the allocation. This definitely rules out 1095 as a quartic p separation.
2. The components are too close to have been observed, but a merge at $1\cdot26$ would mean that all the six σ components are practically of equal intensity. It may be noted that the line $d_1^2 f_3^4 (j=3 \rightarrow 3)$, which should have been at least of the same intensity as this strong line, is not observed. $f_1^2 g_2^4$ with $\cdot01 - - - - - / 1\cdot07 - - - - - 1\cdot27$ is exact and the only possible even fold combination up to $k=5$.
3. The σ negative the allocation. It would be one of the many $0/1\cdot20$.
4. Is good if $\cdot60$ means $60/60$.
5. If this is accepted it would mean the falling out of the stronger σ component. The Z.P. points to $f_1^4 f_2^4$ with $\cdot05 - - - - - / - - - - - 1\cdot67$, or to $f_2^4 f_2^4$ with $\cdot10 - - - - - 1\cdot76$ exact.
6. Both π and σ forbid this. $D_{13}^4, \cdot20, \cdot60 / - - - 2\cdot20$ is better but not satisfactory, or $f_1^2 f_1^4$ or $f_2^2 f_2^4$ (best) $= \cdot19 - - - - - 2\cdot19$. But it is probably a non-Landé pattern.
7. Quite inadmissible.
8. Given by B. as $d_1^2 d_1^4 (\cdot11 - - - / \cdot86 - - - - 2)$ by S. as $D_{22}^2 (\cdot07/73, \cdot87)$. The Z.P. is that of $F_{22}^2 (\cdot03 - - - - - 94)$. The allocation by S. to $x-p_2(2)$ is that of Randall, but this will not fit in with 36137 as $x-p_1(2)$ for the separation is far too small, and the own law is not obeyed.

The result as to the supposed intercombination lines is collected here. A dot refers to a "forbidden line"; — denotes

that the line has not been observed ; 0 that no Z.P. has been observed.

d^2p^4	s^2p^4	d^2d^4	s^2d^4
— †	•	• †	•
0 *	*	† †	•
* •	§	† †	†
d^2f^4		† •	†
• *	•	d^2p^2	s^2p^2
† —	•	† §	(1) †
* —	•	d^4f^2	
$d \cdot d^2$	s^2d^2	† †	
† 0	†		
* *§	•		
•	36104 †		

It is seen Z.E. is distinctly unfavourable to the allocations which have been based on the supposition that 2042 is a separation due to the difference of two doublet terms.

16. The allocation of lines to $s(2) - M$ etc. by Shenstone must not be passed over without discussion, since if the constitution proposed is sustained, the relation of map IV. to the $S(2)$ linkage must be given up. The lines are given in table i. in the s -column. The separations from the corresponding x -lines are taken to be $x - s(2)$. The value of this can be obtained with extreme accuracy, since $x - s(2) = x - p_1 + p_1 - s(2) = D_{12}' + S_1(2)$, and these two lines have reliable measures. Hasbach agrees with the interferometer measures of F.B. for D_{12}' , and his measure for D_{12}' gives correct ν with this, say correct within $d\lambda = .002$. For $S_1(2)$ we get $8092.74 \pm .02$ by Meggers, $.78$ by both Meissner and Eder, say $.76 \pm .02$. Hence the wave numbers are $17538.238 \pm .006 + 12353.03 \pm .03 = 29891.57 \pm .04$. Or we may arrive at the value through F.B.'s interferometer measure of $y - p_1$ and $\phi = 2042.877$. Thus

$$x - s(2) = 19581.115 + .008 + 12353.33 \pm .03 - 2042.877 \\ = 29891.57 \pm .04.$$

The probable errors of the lines involved are given in (). Those for $s(2) -$ etc. are given by Meggers. In the x column, under those of Hasbach I have inserted what I think are more probable values with probable errors. The separations are

M, 29891.37 (.39)	N, 29890.58 (.29)
K, 91.73 (.5)	R, 92.55 (.47)
J, 90.91 (.40)	

Thus on the hypothesis of an unchanging two-term constitution these values allow real separations for M, K, but exclude J, N, R*.

On the broader basis of links and displacements, however, we can hardly refrain from recognizing the whole set of five pairs as thus related, *i. e.* separated by $\mathbf{x}-s(2)$. At the same time, on this basis it will not follow that the small wave numbers refer to combinations of the form $3(2)-t$. This supposition would give for the sets $s(2)-R/D^2$ with D respectively 4.290, 4.743, 5.017, 5.118, 5.275, with no relation to each other. Nothing analogous to this is known amongst other atomic emission lines. Moreover, all these lines lie in the same region as that of S(2), which we already know is distinguished by the number of lines linked and displaced from S(2). Indeed, this is also indicated at a glance by the large number of separations present close to the doublet separation 248.44, from which it may be concluded that the $p(1)$ term or its displacements must be present (see discussion below of 14281). Some of these doublet connexions are shown in table ii.

Again, the presence of $s(2)-t$ lines would point to the existence of much stronger $s(1)-t$, which have not been seen. This objection might perhaps be countered by pointing out that the observed lines by Handke and by L. and E. Bloch in this region are spark produced, and the $s(1)-t$ might be thus obliterated. But McLennan has observed the arc spectrum in this region, and has not seen them. Further doubt must be felt when it is seen that while at least \mathbf{x} (M, K, N, R) are definitely related with similar characters, those for the supposed $s(2)-t$ vary in no relation to them. This is clearly seen by the following comparison:—

	M.	K.	J.	N.	R.
\mathbf{x}	4	6R	1n	6R	4R
$s(2)$	5	1n	2b	3	3n

Here all the \mathbf{x} characters are by Hasbach and the $s(2)$ by Meggers. The relative behaviour of the $s(2)$ are quite out of step with those of the \mathbf{x} .

The succession of several equal separations would be easy to explain if the \mathbf{x} sets were merely link connected. It would only mean that the successive $s(2)$ lines were linked

* Below λ , 2300 Hasbach reads about $d\lambda = .02$ too small. For (J)—H., Hup., K.R. give a mean 2236.28 and Wolfsohn is .295 *in vacuo*, generally less in air. .28+.015 is taken. For (N)—Wolfsohn gives 2227.776 in air and quotes Bidder as .768; K.R. and E.V. both give .77, which must be correct within .01. For (R)—Wolfsohn in air 2215.654 agrees with H. .65—possible error taken = .01.

in the same way as the successive α . But we have seen that this is only the case as between N, R, connected by the α -link. If the dependence of M ... on $p(2)$ and its displacements is accepted, $p(2)$ must be placed in the same way in the $s(2)-t$, and this is certainly not the case.

The foregoing considerations produce a disposition to accept the exclusion of the J, N, R set, already indicated by the numerical comparison as definite. There remain the M, K to be considered. For the M, 13206 shows no clear relation to other lines, *e. g.* no links or α , β displacements, so that its constitution remains otherwise undetermined. There is no reason therefore, *a priori*, to doubt its constitution as α M— $x + s(2)$, or even as $s(2) - R/(\pm 290)^2$, except that with its strong intensity of 5 the $s(1)$ representative 56343.7 or $\lambda - 1774.8$ (vac.) should have been seen by McLennan.

In the case of K, 14281* is 2 iv, and occurs with its connexions in 5 of table ii.† Here the θ -separations shown deviate so largely from the values that they should probably be excluded, as not real. In this set we have the repetitions of 248.8 and the ϕ -separation. Map IV. gives $14281 = S_2(2) . e . u' + .08$ and $14031 = (\delta_1) S_1(2) . e . u' - .10$.

Map VIII.

The map as drawn in [I.] was in two parts with several clear pseudo links, and no attempt was made to obtain line formulæ. In the light of the reality of the multiple β displacements, afforded by the preceding discussion, it is possible to re-arrange the map in a more satisfying manner, with the introduction of a few extra lines. The former ordinal numbers are still attached to the old lines, and the new ones run from 16 to 22 and 13 α . The map was drawn starting from the S(3) lines, but it includes two satelloids, a clear θ , and the 887 separations. In no other cases are these associated with normal S or D lines, and it would seem necessary to exclude them. If so, the pseudo link must be the first 679.29 with 149. On the other hand, the

* As supporting the validity of map IV. we may take the 14413 and 14201 (in 2, 3 of table ii. and 3, 39 iv). In the discussion in [I.] the formula for 39 was not given, but starting from 2 iv we saw that 132 is due to displacement $(-a)$ and 211.6 (3 to 10 iv) to $(-2a+b)$ on this. Consequently the -211 of 39 to 3 is $(2a-b)$ on 3 iv or $(a-b)$ on 2 iv, *i. e.* on p_2 . This shifts -79.77 as against the observed -79.76 .

† In this set 27520, 28200 were not noted in map VI., but they should be added, with its additional 680. 27271 depends on $P_1(-2a-b)$, on which Δ shifts 249.14 (for obs. 249.00). 28200 may be linked to this by u' .

presence of 248, and the a , $2b$, $3b$ displacements require the presence of the $p(1)$ terms. But the relations beyond (8) fit in extremely well, and the formulæ have been worked out on the supposition of a continuous map. This doubt, however, should be kept in mind. The sep. 682·96 is clearly pseudo, and is marked so. The measures of $S_1(3)$, $S_2(3)$ give a separation ·09 too large. If the error is in S_1 , ·09 should be deducted from all the residuals, and it will be found that the greater number are improved. In any case, the residual in any line is due to the error in S_1 as well as to its own O.E. The own shift in $s(3)$ is ·203, and is so small as to allow any rough agreement to be made exact within O.E. by introducing them. Fortunately, however, the s -term is much less subject to displacement than the p , and agreement has been reached without introducing multiple displacements except in 10, 11, 12, 13, where a common 3δ (shift ·61) seems called for. It would be met numerically by y , but this part of the map appears to belong to $S(3)$, where the satelloids do not occur. This general agreement, arrived at without displacements on the current term, does not necessitate the supposition that the map belongs to $S(3)$. The p_1 term must enter, and the map may start from a line $= p_1(1) + \text{links} - \text{some other term}$. The Zeeman effect seems to indicate that this term is an f .

$$S_1(3) = 22064\cdot78 ; S_2(3) = 22313\cdot31.$$

The S denotes $S_1(3)$.

10, 22214·18, 149·39 ahead of S_1 ,

$$-3b \text{ on } p_1 \text{ shifts } 148\cdot74 = (-3b)S(3\delta_1) + \cdot04$$

4, 21385·50, is $u - 1\cdot34$ from S_1 $= u \cdot (-\delta_1)S + \cdot10$

11, 21533·6, 148·10 ahead $= u \cdot (-3b)S(3\delta_1) + \cdot09$

E.H. give ... 32·25 or a collateral δ_1 on p_1 .

12, 20853·6, $u' - \cdot06$ behind $= u \cdot u'(-3b)S(3\delta_1) + \cdot13$

13, 20640·95, 212·65 behind $= u \cdot u' \cdot Y_2 \cdot (-3b)S(3\delta_1) + \cdot04$

13a, $2n$, 4842·2 ; 20646·0 — see p. 1209.

1, 22021·73, 636·23 on (4) $= u \cdot S \cdot 3Y_2 - \cdot05$

8, 22169·77, 148·13 on (1) $= u \cdot (-3b)S \cdot 3X_2 + \cdot06$

2, 22151·04, 129·31 on (1), $-a$ on p_1 shifts 128·84 $= u' \cdot (-a)S \cdot 3Y_2 - \cdot13$

K.R. and E.H. agree with ... 50·89 $u \cdot (-a)S \cdot X_2 \cdot 2Y_2 - \cdot01$

7, 21494·15, red sat. ... 88·75 or if exact $9y = \cdot27$ larger

$$\text{corrected red satellite} = 2u \cdot (-3b)S \cdot 3X_2 - \cdot06$$

$$\text{main line} = 2u(-3b)S \cdot 3X_2 + 9y - \cdot06$$

$$\text{viol. sat.} = 7y - \cdot16 = 2u(-3b)S \cdot 3X_2 + 16y - \cdot22$$

6, 22179·0 $= u(-3b)S \cdot 3X_2 + 16y + \cdot17$

9, 21282·02, 212·13 behind (7) $= 2u \cdot (-3b)S \cdot 2X_2 - 9y - \cdot08$

5, 21249·876, 248·10 behind viol. of (7)

The 248 suggests a $5b$ displacement or the doublet ν as a

presence of 248, and the a , $2b$, $3b$ displacements require the presence of the $p(1)$ terms. But the relations beyond (8) fit in extremely well, and the formulæ have been worked out on the supposition of a continuous map. This doubt, however, should be kept in mind. The sep. 682·96 is clearly pseudo, and is marked so. The measures of $S_1(3)$, $S_2(3)$ give a separation ·09 too large. If the error is in S_1 , ·09 should be deducted from all the residuals, and it will be found that the greater number are improved. In any case, the residual in any line is due to the error in S_1 as well as to its own O.E. The own shift in $s(3)$ is ·203, and is so small as to allow any rough agreement to be made exact within O.E. by introducing them. Fortunately, however, the s -term is much less subject to displacement than the p , and agreement has been reached without introducing multiple displacements except in 10, 11, 12, 13, where a common 3δ (shift ·61) seems called for. It would be met numerically by y , but this part of the map appears to belong to $S(3)$, where the satelloids do not occur. This general agreement, arrived at without displacements on the current term, does not necessitate the supposition that the map belongs to $S(3)$. The p term must enter, and the map may start from a line $=p_1(1) + \text{links} - \text{some other term}$. The Zeeman effect seems to indicate that this term is an f .

$$S_1(3) = 22064\cdot78 ; S_2(3) = 22313\cdot31.$$

The S denotes $S_1(3)$.

- 10, 22214·18, 149·39 ahead of S_1 ,
 $-3b$ on p_1 shifts 148·74 $= (-3b)S(3\delta_1) + \cdot04$
 4, 21385·50, is $u - 1\cdot34$ from S_1 $= u \cdot (-\delta_1)S + \cdot10$
 11, 21533·6, 148·10 ahead $= u \cdot (-3b)S(3\delta_1) + \cdot09$
 E.H. give ... 32·25 or a collateral δ_1 on p_1 .
 12, 20853·6, $u' - \cdot06$ behind $= u \cdot u'(-3b)S(3\delta_1) + \cdot13$
 13, 20640·95, 212·65 behind $= u \cdot u' \cdot Y_2 \cdot (-3b)S(3\delta_1) + \cdot04$
 13a, $2u$, 4842·2 ; 20646·0 — see p. 1209.
 1, 22021·73, 636·23 on (4) $= u \cdot S \cdot 3Y_2 - \cdot05$
 8, 22169·77, 148·13 on (1) $= u \cdot (-3b)S \cdot 3X_2 + \cdot06$
 2, 22151·04, 129·31 on (1), $-a$ on p_1
 shifts 128·84 $= u' \cdot (-a)S \cdot 3Y_2 - \cdot13$
 K.R. and E.H. agree with ... 50·89 $u \cdot (-a)S \cdot X_2 \cdot 2Y_2 - \cdot01$
 7, 21494·15, red sat. ... 88·75 or if exact $9y = \cdot27$ larger
 corrected red satellite $= 2u \cdot (-3b)S \cdot 3X_2 - \cdot06$
 main line $= 2u(-3b)S \cdot 3X_2 + 9y - \cdot06$
 viol. sat. = $7y - \cdot16$ $= 2u(-3b)S \cdot 3X_2 + 16y - \cdot22$
 6, 22179·0 $= u(-3b)S \cdot 3X_2 + 16y + \cdot17$
 9, 21292·02, 212·13 behind (7) $= 2u \cdot (-3b)S \cdot 2X_2 - 9y - \cdot08$
 5, 21249·876, 248·10 behind viol. of (7)

The 248 suggests a $5b$ displacement or the doublet ν as a

presence of 248, and the a , $2b$, $3b$ displacements require the presence of the $p(1)$ terms. But the relations beyond (8) fit in extremely well, and the formulæ have been worked out on the supposition of a continuous map. This doubt, however, should be kept in mind. The sep. 682·96 is clearly pseudo, and is marked so. The measures of $S_1(3)$, $S_2(3)$ give a separation ·09 too large. If the error is in S_1 , ·09 should be deducted from all the residuals, and it will be found that the greater number are improved. In any case, the residual in any line is due to the error in S_1 as well as to its own O.E. The own shift in $s(3)$ is ·203, and is so small as to allow any rough agreement to be made exact within O.E. by introducing them. Fortunately, however, the s -term is much less subject to displacement than the p , and agreement has been reached without introducing multiple displacements except in 10, 11, 12, 13, where a common 3δ (shift ·61) seems called for. It would be met numerically by y , but this part of the map appears to belong to $S(3)$, where the satelloids do not occur. This general agreement, arrived at without displacements on the current term, does not necessitate the supposition that the map belongs to $S(3)$. The p_1 term must enter, and the map may start from a line $= p_1(1) + \text{links} - \text{some other term}$. The Zeeman effect seems to indicate that this term is an f .

$$S_1(3) = 22064\cdot78 ; S_2(3) = 22313\cdot31.$$

The S denotes $S_1(3)$.

- 10, 22214·18, 149·39 ahead of S_1 ,
 $-3b$ on p_1 shifts 148·74 $= (-3b)S(3\delta_1) + \cdot04$
 4, 21385·50, is $u - 1\cdot34$ from S_1 $= u \cdot (-\delta_1)S + \cdot10$
 11, 21533·6, 148·10 ahead $= u \cdot (-3b)S(3\delta_1) + \cdot09$
 E.H. give ... 32·25 or a collateral δ_1 on p_1 .
 12, 20853·6, $u' - 0\cdot6$ behind $= u \cdot u'(-3b)S(3\delta_1) + \cdot13$
 13, 20640·95, 212·65 behind $= u \cdot u' \cdot Y_2 \cdot (-3b)S(3\delta_1) + \cdot04$
 13a, $2n$, 4842·2; 20646·0 — see p. 1209.
 1, 22021·73, 636·23 on (4) $= u \cdot S \cdot 3Y_2 - \cdot05$
 8, 22169·77, 148·13 on (1) $= u \cdot (-3b)S \cdot 3X_2 + \cdot06$
 2, 22151·04, 129·31 on (1), $-a$ on p_1
 shifts 128·84 $= u' \cdot (-a)S \cdot 3Y_2 - \cdot13$
 K.R. and E.H. agree with ... 50·89 $u \cdot (-a)S \cdot X_2 \cdot 2Y_2 - \cdot01$
 7, 21494·15, red sat. ... 88·75 or if exact $9y = \cdot27$ larger
 corrected red satellite $= 2u \cdot (-3b)S \cdot 3X_2 - \cdot06$
 main line $= 2u(-3b)S \cdot 3X_2 + 9y - \cdot06$
 viol. sat. $= 7y - \cdot16$ $= 2u(-3b)S \cdot 3X_2 + 16y - \cdot22$
 6, 22179·0 $= u(-3b)S \cdot 3X_2 + 16y + \cdot17$
 9, 21282·02, 212·13 behind (7) $= 2u \cdot (-3b)S \cdot 2X_2 - 9y - \cdot08$
 5, 21249·876, 248·10 behind viol. of (7)

The 248 suggests a $5b$ displacement or the doublet ν as a

presence of 248, and the a , $2b$, $3b$ displacements require the presence of the $p(1)$ terms. But the relations beyond (8) fit in extremely well, and the formulæ have been worked out on the supposition of a continuous map. This doubt, however, should be kept in mind. The sep. 682.96 is clearly pseudo, and is marked so. The measures of $S_1(3)$, $S_2(3)$ give a separation .09 too large. If the error is in S_1 , .09 should be deducted from all the residuals, and it will be found that the greater number are improved. In any case, the residual in any line is due to the error in S_1 as well as to its own O.E. The own shift in $s(3)$ is .203, and is so small as to allow any rough agreement to be made exact within O.E. by introducing them. Fortunately, however, the s -term is much less subject to displacement than the p , and agreement has been reached without introducing multiple displacements except in 10, 11, 12, 13, where a common 3δ (shift .61) seems called for. It would be met numerically by y , but this part of the map appears to belong to $S(3)$, where the satelloids do not occur. This general agreement, arrived at without displacements on the current term, does not necessitate the supposition that the map belongs to $S(3)$. The p_1 term must enter, and the map may start from a line $= p_1(1) + \text{links} - \text{some other term}$. The Zeeman effect seems to indicate that this term is an f .

$$S_1(3) = 22064.78 ; S_2(3) = 22313.31.$$

The S denotes $S_1(3)$.

- 10, 22214.18, 149.39 ahead of S_1 ,
 $-3b$ on p_1 shifts 148.74 $= (-3b)S(3\delta_1) + .04$
 4, 21385.50, is $u - 1.34$ from S_1 $= u.(-\delta_1)S + .10$
 11, 21533.6, 148.10 ahead $= u.(-3b)S(3\delta_1) + .09$
 E.H. give ... 32.25 or a collateral δ_1 on p_1 .
 12, 20853.6, $u' - .06$ behind $= u.u'(-3b)S(3\delta_1) + .13$
 13, 20640.95, 212.65 behind $= u.u'.Y_2.(-3b)S(3\delta_1) + .04$
 13a, $2u$, 4842.2; 20646.0 — see p. 1209.
 1, 22021.73, 636.23 on (4) $= u.S.3Y_2 - .05$
 8, 22169.77, 148.13 on (1) $= u.(-3b)S.3X_2 + .06$
 2, 22151.04, 129.31 on (1), $-a$ on p_1
 shifts 128.84 $= u'.(-a)S.3Y_2 - .13$
 K.R. and E.H. agree with ... 50.89 $u.(-a)S.X_2.2Y_2 - .01$
 7, 21494.15, red sat. ... 88.75 or if exact $9y = .27$ larger
 corrected red satellite $= 2u.(-3b)S.3X_2 - .06$
 main line $= 2u(-3b)S.3X_2 + 9y - .06$
 viol. sat. $= 7y - .16$ $= 2u(-3b)S.3X_2 + 16y - .22$
 6, 22179.0 $= u(-3b)S.3X_2 + 16y + .17$
 9, 21282.02, 212.13 behind (7) $= 2u.(-3b)S.2X_2 - 9y - .08$
 5, 21249.876, 248.10 behind viol. of (7)

The 248 suggests a $5b$ displacement or the doublet ν as a

presence of 248, and the a , $2b$, $3b$ displacements require the presence of the $p(1)$ terms. But the relations beyond (8) fit in extremely well, and the formulæ have been worked out on the supposition of a continuous map. This doubt, however, should be kept in mind. The sep. 682.96 is clearly pseudo, and is marked so. The measures of $S_1(3)$, $S_2(3)$ give a separation .09 too large. If the error is in S_1 , .09 should be deducted from all the residuals, and it will be found that the greater number are improved. In any case, the residual in any line is due to the error in S_1 as well as to its own O.E. The own shift in $s(3)$ is .203, and is so small as to allow any rough agreement to be made exact within O.E. by introducing them. Fortunately, however, the s -term is much less subject to displacement than the p , and agreement has been reached without introducing multiple displacements except in 10, 11, 12, 13, where a common 3δ (shift .61) seems called for. It would be met numerically by y , but this part of the map appears to belong to $S(3)$, where the satelloids do not occur. This general agreement, arrived at without displacements on the current term, does not necessitate the supposition that the map belongs to $S(3)$. The p_1 term must enter, and the map may start from a line $= p_1(1) + \text{links} - \text{some other term}$. The Zeeman effect seems to indicate that this term is an f .

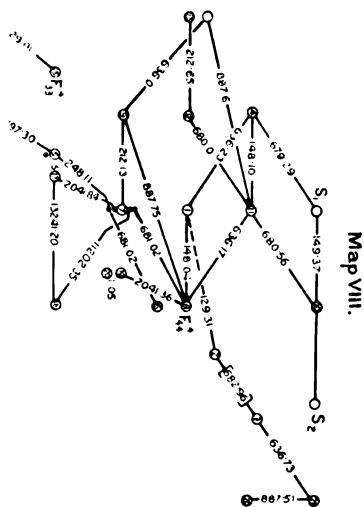
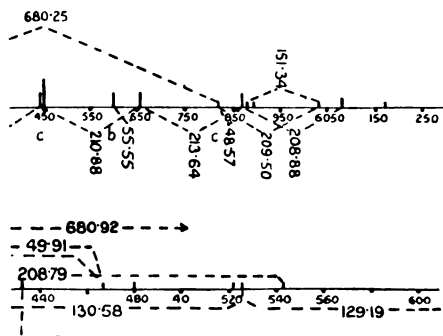
$$S_1(3) = 22064.78 ; S_2(3) = 22313.31.$$

The S denotes $S_1(3)$.

- 10, 22214.18, 149.39 ahead of S_1 ,
 $-3b$ on p_1 shifts 148.74 $= (-3b)S(3\delta_1) + .04$
 4, 21385.50, is $u - 1.34$ from S_1 $= u.(-\delta_1)S + .10$
 11, 21533.6, 148.10 ahead $= u.(-3b)S(3\delta_1) + .09$
 E.H. give ... 32.25 or a collateral δ_1 on p_1 .
 12, 20853.6, $u' - .06$ behind $= u. u'(-3b)S(3\delta_1) + .13$
 13, 20640.95, 212.65 behind $= u. u'. Y_2.(-3b)S(3\delta_1) + .04$
 13a, $2n$, 4842.2; 20646.0 — see p. 1209.
 1, 22021.73, 636.23 on (4) $= u. S. 3Y_2 - .05$
 8, 22169.77, 148.13 on (1) $= u.(-3b)S. 3X_2 + .06$
 2, 22151.04, 129.31 on (1), $-a$ on p_1
 shifts 128.84 $= u'.(-a)S. 3Y_2 - .13$
 K.R. and E.H. agree with ... 50.89 $u.(-a)S. X_2. 2Y_2 - .01$
 7, 21494.15, red sat. ... 88.75 or if exact $9y = .27$ larger
 corrected red satellite $= 2u.(-3b)S. 3X_2 - .06$
 main line $= 2u(-3b)S. 3X_2 + 9y - .06$
 viol. sat. $= 7y - .16$ $= 2u(-3b)S. 3X_2 + 16y - .22$
 6, 22179.0 $= u(-3b)S. 3X_2 + 16y + .17$
 9, 21292.02, 212.13 behind (7) $= 2u.(-3b)S. 2X_2 - 9y - .08$
 5, 21249.876, 248.10 behind viol. of (7)

The 248 suggests a $5b$ displacement or the doublet ν as a

[To face page 1225.



link; 5*b* on (−3*b*) shifts only 247·28. The two suppositions require respectively

$$2u.(2b)S.3X_2+14y+10$$

$$\text{and } v.2u.(-3b)S.3X_2+16y+12,$$

the first requiring the introduction of 2*y*. The succeeding lines support the second allocation.

16, 2*s*, 4748·85 E.V.; 21052·57 is 197·30 behind. (4*b*) on (2*b*) to (6*b*) *S* shifts 195·75; on (−3*b*) it shifts 198·05, and fits better the second allocation of (5). It gives

$$v.2u.(b)S.3Y_2-16y+06$$

14, 20840·37, 212·20 behind

$$v.u.u'(b)S.Y_2.X_2+16y+10$$

15, 20969·38, 129·01 ahead, −*a* on (6*p*) *S* shifts 129·15

$$=v.2u'(-a+b)S.Y_2.X_2+16y-03$$

−*a* on (6*b*) *p* shifts 127·08, again supports the second.

17, 2*ns*, 5139·03, E.V.; 19454·16, 2041·84=3*u*+·05 is a pure 3*u* link to a spark line

$$=5u(-3b)S.3X_2+12y+07$$

18, 1, 3057·65; 32695·36. The linked 3*u* line (17) is not φ. The line is separated from a 2*y* red sat. of (7) by 11202·35 or *s*(1)−*y*−1, which justifies its inclusion as a θ line

$$=(17)-2y+0$$

19, 1, 4966·72, E.H.; 20128·41. } The second is 2040·25 behind 8

$$=u.3u'(-3b)S.3X_2-01$$

20, 1, ... 66·46, E.H.; ... 29·46. } The first is then 2*y*−09 less

$$=3u.u'(-3b)S.3X_2+08$$

3, 22834·0. The 682 is probably not *u*. If real, formula

$$=(-a)S.3X_2+3·68$$

21, 2*nbr*, 4259·43; 23470·73

$$=(-a)S.6X_2+3·60$$

22, 2, 4104·223; 24358·24

$$=.....+u'+X_1-4y$$

Map XI.

(For lines, see No. 8 of table ii.)

Map XII.

1. 3, 3279·823	30480·697 S 6 i	22. 1 <i>n</i> , 2138·44	46748·26 H; 7·17 ⁽¹⁾
2. 4, 3208·236	31160·804 S 5 i	23. 3, 1725·9	57942·7 Hke.
3. 1 <i>n</i> , 3209·47	31148·83 S 5 ii	24. 2194·41	45556·06 P.
4. 6, 3194·103	31298·677 S 17 ii	25. 1 <i>n</i> , 3171·658	31520·163
5. 4, 3073·803	32523·569 S 5 iii	26. 1 <i>n</i> , 3151·61	31720·66 22 ii
6. 5, 3010·840	33203·677 S 7 iii	27. 3, 3156·625	31670·284 23 ii
7. 4, 2997·363	33352·963 13 <i>a</i> iii	28. 6, 3126·106	31979·438 18 ii
8. 2, 2998·384	33341·608 13 iii	29. 2 <i>n</i> , 2979·38	33554·22 12 iii
9. 8, 2824·373	35395·672	30. 6, 2961·177	33760·521 S 10 iii
10. 3 <i>n</i> , 3175·73	31479·757 i	31. 2 <i>n</i> , 2978·293	33566·508 12 <i>a</i> iii
11. 6 <i>n</i> , 3108·603	32159·491 S 8 i	32. 1 <i>n</i> , 2991·76	33415·42 17 iii
12. 1, 2982·16	33522·99 E.H.	33. 6, 3093·993	32311·342 S 4 iii
13. 1, 2922·87	34202·96 E.H.	34. 3, 3088·121	32372·781 25 ii
14. 2 <i>n</i> , 3014·84	33159·64 9 i	35. 4, 3128·692	31953·008 26 ii
15. 1 <i>n</i> , 3392·01	29472·61 11 i	36. 2, 3149·501	31741·899 27 ii
16. 2, 3391·09	29481·56 K.R. 11 <i>a</i> i	37. 2 <i>n</i> , 3030·25	32991·00 6 iii
17. 3, 3472·136	28792·500 12 i	38. 1, 3361·96	29738·05 46 vi
18. 2, 2244·240	44544·659	39. 2, 3068·912	32575·399 16 iii
19. 4, 2246·984	44490·275	40. 2 <i>n</i> , 3012·02	33190·68
20. 1 <i>n</i> , 2236·22	44704·40	41. 2 <i>n</i> , 3465·40	28848·45 44 vi
21. 2 <i>R</i> , 2225·665	44916·378	42. 1, 2791·95	35806·73

⁽¹⁾ Dreblow.

The measured satelloids of Hasbach are represented by dots vertically aligned with the main line. Additional satelloids by Stücklen (not measured) are denoted by dots south-west of the main line.

Phil. Mag. S. 7. Vol. 4. No. 25. Suppl. Nov. 1927. 4 K

The two ϕ , forward and back from (30), should be noted. They form an undoubted succession of equal ϕ separations from the satellite. K.R.'s reading for (42) is 35806.32 and gives 2042.84.

For general discussion, see §9:—39 is 1413.46 from the 1st satellite (2y) of 2 or 1412.89 from an unobserved 3y. Stücklen gives 3r, 5v. The chain 40 to 41 should be noted with the ϕ sep: = 3u link. The map is noted for the number of satelloids involved and the number of links made exact within O.E. by suitable choice of satellite. 35 is 14 xiii, which introduces another parallel set to 10, 11, 13, and gives a chain connecting p_f and B.

Map XIII.

- | | |
|---|-------------------------------|
| (1) 2, 1774.4, 56358.9. | (16) 1, 2483.27, 40257.33 |
| (2) 2, 1713.0, 58379.0. | (Hup.). |
| (3) 4, 1693.4, 59052.8 (McL.). | (17) 1n, 2363.20, 42302.54. |
| (4) 6, 1686.99, 59277.17. | (18) 2, 3700.532, 27015.482. |
| (5) 1, 1703.7, 58697.7. | (19) 3, 3440.52, 29057.08. |
| (6) 2, 2210.240, 45229.807. | (20) 2, 3517.029, 28424.990. |
| (7) 6R?, 2199.57, .73, 45449.19, 5.89. | (21) 2, 3671.969, 27225.621. |
| (8) 3, 2189.599, 45656.77. | (22) 2, 4003.038, 24973.993. |
| (9) 3n, 2179.37, 45870.41. | (23) 1n, 4242.26, 23565.73. |
| (10) 2n, 2169.49, 46079.29. | (24) 1n, 2701.01, 37012.22. |
| (11) 1n, 2356.80, 42417.42. | (24a) 2, 2630.002, 38011.47. |
| (12) 1n, 2171.75, 46031.34. | (25) 1n, 2911.21, 34339.95. |
| (13) 4n, 2079.47, 48073.79 (de Rubies). | (26) 1n, 3171.658, 31520.163. |
| (14) 4, 3128.692, 31953.008. | (27) 2n, 2979.38, 33554.22. |
| (15) 1, 1730.5, 57788.70. | (28) 2n, 2978.293, 33566.508. |
| | (29) 4, 1989.24, 50255.55. |

The n of the ultra-violet lines 1 ... 5 and 15 are subject to uncertainties about $-35d\lambda$, with $d\lambda$ considerable except in (4), where it is probably $< .05$. In the θ -separations, the 132 ... is represented by a —, thus 13260 is entered -60 etc. A comparison of Handke's with Bloch's measures of apparently the same line seem to show that the former's are from .3 to .5 Å too small. In other words, his wave numbers may be subject to a correction of the order ± 10 to ± 16 .

The map contains four different chains. To prevent confusion, they are distinguished by thick, thin, and dotted connexion lines.

27, 28 possibly correspond to a u, v interchange—in which case the separations shown to yp_g have no reference to 1412. 26. xp_g is a satelloid for which Stücklen gives 8r, 6v.

Hasbach gives $4y$ and $5y$; one at $10y$ would make the sep. = 1412.72.

The four separations 6-10 form a series inequality $= 2(X_2 + Y_2) - .14$ or replacing the 208.86 by the 209.50,

$$= 4Y_2 - .02,$$

pointing thus to link reality. So also

$$xM, yM, sp_s = \phi + u + 0.$$

14 is 35 xii—26 is 25 xii—27 is 29 xii.

Errata in [I].

P. 198. Sat. (12), the W.N. of the satellite should be corrected from .55 to .28. This necessitates the following alterations:—

Sat. (12). 1.79 for 2.06; $3y = 1.71$ for $4x =$; y for x .

P. 223. No. 8, .28 for .55; $3y - .05$ for $4x - .10$.

Map I. 5-8-10 read 999.35, 680.35.

Map II. 5i-8i-26 read 999.35, 208.27.

Map III. 8i-10i read 680.35.

P. 218, l. 12, read $-4a + b$ for $-4a$.

P. 230, l. 10, read .30 for .73.

P. 232. The formulæ were wrongly calculated on D_1 instead of D_2 .
Read respectively (a) $D_2 + .47$; e. (a) $D_2 + .46$; Y_2 . (a) $D_2 + .38$
and add, in place of footnote 7, residuals due to $d\lambda = .06$ in $D_2(4)$,
measured to .1.

Map IV. Between (40) (42), read 49.76 for 44.76.

Map VI. „ (6) (10) (9). read 210.53, 681.81.

„ „ (32) (31) (35), draw the 690.90 between (32) (35)
instead of (31) (35) and delete 133.07 (33).

Map VII. For links to (37) read 48.02, 678.02.

Map IX. Between (1) (4) append arrow pointing up.

Also Map VI. Between (5) (2) read 680.11.

See note to (1), table iv. of this paper.

Add. The addition referred to in note 2, p. 1223.

CIII. On the Scattering of Radiation from Atoms.

By IVAR WALLER*.

THE Kramers-Heisenberg dispersion formula gives the radiation scattered from an atom for wave-lengths long compared with atomic dimensions. This formula has been deduced from the principles of wave-mechanics by Schrödinger† and Klein‡. Following a procedure analogous to that of Klein, we deduce in § 1 of the following paper a dispersion formula, which also gives the radiation scattered from an atom for wave-lengths short compared with atomic dimensions. In § 2 we use this formula to find the gradual transformation of the scattering process as the wave-length varies. For long waves we have the dispersion given by the Kramers-Heisenberg formula, and, for sufficiently short waves, a pure Compton effect. In § 1 the approximation to the eigenfunctions of the continuous spectrum given by plane de Broglie waves is discussed, and also the expansion of the wave-functions of the stationary states in Fourier integrals. The corrections due to the spin of the electrons are neglected in this paper §.

§ 1. A wave-function u , corresponding to the motion of an electron in an electromagnetic field of vector potential \mathbf{A} and scalar potential V , must satisfy one of the equations ||

$$-\frac{\hbar^2}{4\pi^2} \left(\nabla^2 u - \frac{1}{c^2} \frac{\partial^2 u}{\partial t^2} \right) \pm 2 \frac{\hbar}{2\pi i} \frac{\epsilon}{c} \left(\mathbf{A} \nabla u + \frac{V}{c} \frac{\partial u}{\partial t} \right) + \left[\mu^2 c^2 + \frac{\epsilon^2}{c^2} (\mathbf{A}^2 - V^2) \right] u = 0, \quad (1)$$

where $-\epsilon$ is the charge and μ the mass of the electron. We consider an atomic field defined by $V = V_0$, $\mathbf{A} = 0$.*

Putting

$$u = \phi e^{\frac{2\pi i E t}{\hbar}} \quad \text{and} \quad E = E' + \mu c^2,$$

* Communicated by Prof. W. L. Bragg, F.R.S.

† E. Schrödinger, *Ann. d. Phys.* lxxxi. p. 108 (1926).

‡ O. Klein, *Zeits. f. Phys.* xli. p. 407 (1927).

§ A summary of the results arrived at in this paper has been given in a letter to 'Nature,' July 30, 1927, unfortunately without knowledge of a paper by G. Wentzel, *Zeits. f. Phys.* xliii. p. 1 (1927), who has used a dispersion formula for short waves to investigate the Compton effect of bound electrons. Some of the results given in that letter have already been obtained by Wentzel.

|| Cf. e. g., Klein, *loc. cit.*

we find on substitution in (1), taking the negative sign for the second term,

$$\nabla^2 \phi + \frac{8\pi^2 \mu}{h^2} (E' + \epsilon V_0) \phi + \frac{4\pi^2}{h^2 c^2} (E' + \epsilon V_0)^2 \phi = 0. \quad (2)$$

Let ϕ_n be a normalized eigenfunction ("Eigenfunktion") satisfying this equation, which is continuous and finite throughout space, and let the corresponding characteristic value ("Eigenwert") of E' be E_n' . We put

$$u_n = \phi_n e^{\frac{2\pi i E_n t}{h}} \quad \text{and} \quad E_n = E_n' + \mu c^2.$$

Corresponding to an atomic problem, we assume that all positive values of E' form a continuous set of characteristic values. For $E' < 0$ an infinite set of discrete characteristic values may be found. For the calculations made here it is formally important to have only discrete and not degenerated eigenfunctions. We may attain this by assuming the presence of distant boundary walls to which corresponds the boundary conditions $\phi = 0$.

The last term on the left side of (2) gives a relativity correction. Neglecting this term, we get the well-known equation

$$\nabla^2 \phi + \frac{8\pi^2 \mu}{h^2} (E' + \epsilon V_0) \phi = 0. \quad (2')$$

A light-wave falling on the atom can be defined by

$$V = 0, \quad \mathbf{A} = -\sigma \frac{c}{4\pi i \nu} \left[\mathbf{E}_0 e^{2\pi i \nu (t - \frac{\mathbf{nr}}{c})} - \bar{\mathbf{E}}_0 e^{-2\pi i \nu (t - \frac{\mathbf{nr}}{c})} \right]. \quad (3)$$

The vector \mathbf{r} may be drawn from the nucleus as origin. The sign \sim denotes the conjugate value. σ is a perturbation parameter. The electric field of the light-wave is

given by the real part of $\mathbf{E}_0 e^{2\pi i \nu (t - \frac{\mathbf{nr}}{c})}$. As a first approximation, the perturbed wave-functions may be written in the form $u_n + \sigma f_n$. In the equation for f_n , obtained in the usual way, we neglect the term containing $(E_n' \pm h\nu + \epsilon V_0)^2$, which gives a relativity correction. From a calculation which is analogous to the corresponding calculation for long waves given by Schrödinger, we find

$$f_n = -\frac{\epsilon}{8\pi^2 \mu \nu} \left[e^{\frac{2\pi i}{h} (E_n + h\nu)t} \sum_s \frac{\mathbf{E}_0 \mathbf{A}_{ns}}{\nu_{ns} + \nu} \phi_s + e^{\frac{2\pi i}{h} (E_n - h\nu)t} \sum_s \frac{\bar{\mathbf{E}}_0 \bar{\mathbf{A}}_{sn}}{\nu_{ns} - \nu} \phi_s \right],$$

. . . (4)

putting

$$\mathbf{A}_{ns} = \int \bar{\phi}_s e^{-\frac{2\pi i \nu}{c} \mathbf{nr}} \nabla \phi_n dv, \quad \nu_{ns} = \frac{E_n - E_s}{h}. \quad (4')$$

We now use the well-known formulæ of wave mechanics for charge-density and current-density* in a way closely analogous to that given by Klein†. Putting $\sigma=1$, we then find the following values of the charge-density ρ_n and the current-density \mathbf{I}_n , which determine the radiation scattered from an atom in the initial state n :

$$\left. \begin{aligned} \rho_n &= \sum_m^{\mathbf{E}_m < \mathbf{E}_n + h\nu} (\rho_{nm} + \bar{\rho}_{nm}) + \sum_m^{\mathbf{E}_m < \mathbf{E}_n - h\nu} (\rho_{mn} + \bar{\rho}_{mn}) \\ \mathbf{I}_n &= \sum_m^{\mathbf{E}_m < \mathbf{E}_n + h\nu} (\mathbf{I}_{nm} + \bar{\mathbf{I}}_{nm}) + \sum_m^{\mathbf{E}_m < \mathbf{E}_n - h\nu} (\mathbf{I}_{mn} + \bar{\mathbf{I}}_{mn}) \end{aligned} \right\} \quad (5)$$

putting

$$\left. \begin{aligned} \rho_{nm} &= \frac{e^2}{8\pi^2 \mu \nu} \sum_s (B_{ns} \vec{\phi}_s \phi_s - B_{sm} \phi_n \vec{\phi}_s) e^{2\pi i(\nu_{nm} + \nu)t} \\ \mathbf{I}_{nm} &= -\frac{ie^2}{4\pi^2 \mu \nu} \left[\mathbf{E}_0 \phi_n \vec{\phi}_m e^{-\frac{2\pi i \nu}{c} \mathbf{r} \cdot \mathbf{n}} - \frac{h}{8\pi^2 \mu} \sum_s (B_{ns} \mathbf{C}_{ms} \right. \\ &\quad \left. - B_{sm} \mathbf{C}_{ns}) \right] e^{2\pi i(\nu_{nm} + \nu)t} \end{aligned} \right\} \quad (5')$$

$$B_{ns} = \frac{\mathbf{E}_0 \mathbf{A}_{ns}}{\nu_{ns} - \nu}, \quad \mathbf{C}_{ns} = \vec{\phi}_n \nabla \phi_s - \phi_s \nabla \vec{\phi}_n. \quad (6)$$

It is easily confirmed that $\text{div } \mathbf{I}_{nm} + 2\pi i(\nu_{nm} + \nu)\rho_{nm} = 0$, and that the normalization conditions are fulfilled. From well-known formulæ of the Maxwell theory‡, one finds that the radiation scattered from the atom in a direction given by \mathbf{n}' , and corresponding to \mathbf{I}_{nm} (and ρ_{nm}) may, for great distances from the atom, be deduced from the dipol moment

$$\begin{aligned} \mathbf{d}_{nm} &= -\frac{1}{4\pi^2 \nu(\nu_{nm} + \nu)} \frac{e^2}{2\mu} \left[\mathbf{E}_0 \delta_{nm} \right. \\ &\quad \left. + \frac{h}{4\pi^2 \mu} \sum_s (B_{ns} \vec{\mathbf{A}}_{ms}' - B_{sm} \vec{\mathbf{A}}_{ns}') \right] e^{2\pi i(\nu_{nm} + \nu)t}, \end{aligned} \quad (7)$$

putting

$$\mathbf{A}_{ns}' = \int \vec{\phi}_s e^{-\frac{2\pi i}{c}(\nu_{nm} + \nu)\mathbf{n}' \cdot \mathbf{r}} \nabla \phi_n dv, \quad (7')$$

$$\delta_{nm} = \int \phi_n \vec{\phi}_m e^{\frac{2\pi i}{c}[(\nu_{nm} + \nu)\mathbf{n}' - \nu \mathbf{n}] \cdot \mathbf{r}} dv. \quad (7'')$$

* Cf. W. Gordon, *Zeits. f. Phys.* xli. p. 117 (1926).

† Klein, *loc. cit.*

‡ The formulæ (38), (40) and (41) in the paper by Klein, *loc. cit.* give

$$\mathbf{d}_{nm} = \int \mathbf{I}_{nm} e^{2\pi i(\nu_{nm} + \nu)\mathbf{n}' \cdot \mathbf{r}/c} dv / 2\pi i(\nu_{nm} + \nu).$$

The total radiation scattered from an atom in the initial state n may accordingly be derived from the following sum of dipol moments :

$$\sum_m^{E_m < E_n + h\nu} (\mathbf{d}_{nm} + \tilde{\mathbf{d}}_{nm}) + \sum_m^{E_m < E_n - h\nu} (\mathbf{d}_{mn} + \tilde{\mathbf{d}}_{mn}). \quad (8)$$

According to (6) it may be expected that, for large values of ν , only the term $\mathbf{E}_0 \delta_{nm}$ in the bracket [] of (7) is of importance. We shall investigate this point in § 2. The corresponding part of \mathbf{d}_{nm} comes from that part of the wave mechanical current-density which is formed by the product of the vector potential of the light-wave and the unperturbed wave-functions.

Assuming the unperturbed wave-functions to be real, one finds that the dipol moment \mathbf{d}_{nn} is given by

$$\mathbf{d}_{nn} = -\frac{1}{4\pi^2\nu^2} \frac{\epsilon^2}{2\mu} \left[\mathbf{E}_0 \delta_{nn} + \frac{h}{4\pi^2\mu} \sum_s \frac{\nu_{ns} (\mathbf{E}_0 \mathbf{A}_{ns}) \tilde{\mathbf{A}}_{ns}'}{\nu_{ns}^2 - \nu^2} \right] e^{2\pi i \nu t}. \quad (9)$$

For wave-lengths long compared with atomic dimensions, we must get the Kramers-Heisenberg dispersion formula*. In this limit all exponentials, except those containing the time, are to be put equal to unity. If

$$\mathbf{D}_{ns} = -\epsilon \int \mathbf{r} \phi_n \tilde{\phi}_s dv,$$

it then follows

$$\mathbf{A}_{ns} = \mathbf{A}_{ns}' = -\frac{4\pi^2\mu}{h\epsilon} \nu_{ns} \mathbf{D}_{ns}.$$

The relations †

$$\frac{\nu_{ms}}{\nu_{ns} + \nu} = 1 - \frac{\nu_{nm} + \nu}{\nu_{ns} + \nu}, \quad \frac{\nu_{ns}}{\nu_{ms} - \nu} = 1 + \frac{\nu_{nm} + \nu}{\nu_{ms} - \nu}. \quad (9')$$

$$\left. \begin{aligned} \sum_s [\nu_{ns} (\mathbf{E}_0 \mathbf{D}_{ns}) \mathbf{D}_{sm} + \nu_{ms} (\mathbf{E}_0 \mathbf{D}_{sm}) \mathbf{D}_{ns}] &= -\mathbf{E}_0 \frac{\epsilon^2 h}{4\pi^2 \mu} \delta_{nm} \\ \sum_s [(\mathbf{E}_0 \mathbf{D}_{ns}) \mathbf{D}_{sm} - (\mathbf{E}_0 \mathbf{D}_{sm}) \mathbf{D}_{ns}] &= 0, \end{aligned} \right\} \quad (9'')$$

then give

$$\mathbf{d}_{nm} = -\frac{1}{2h} \sum_s \left[\frac{(\mathbf{E}_0 \mathbf{D}_{ns}) \mathbf{D}_{sm}}{\nu_{ns} + \nu} + \frac{(\mathbf{E}_0 \mathbf{D}_{sm}) \mathbf{D}_{ns}}{\nu_{ms} - \nu} \right] e^{2\pi i (\nu_{nm} + \nu) t}.$$

In order to find a simple approximation to the wave-functions of the continuous spectrum we may assume \mathbf{E}' to

* About the existence of the incoherent radiation, cf. A. Smekal, *Naturw.* xi. p. 873 (1923).

† The relations (9'') follow directly from Heisenberg's matrix theory and are also easily obtained from (2').

be large compared with ϵV_0 . Neglecting ϵV_0 in (2), we get the wave equation for a free electron which has the solution

$$\phi_s = C_s e^{-\frac{2\pi i}{h} \mathbf{M}_s \cdot \mathbf{r}} \quad . \quad . \quad . \quad (10)$$

for $E = E_s$, if

$$\mathbf{M}_s^2 - \frac{1}{c^2} E_s^2 + \mu^2 c^2 = 0, \quad C_s = \frac{1}{\sqrt{v}} \sqrt{\frac{\mu c^2}{E}}; \quad . \quad (10')$$

v is the volume inside the boundary walls. The value of C_s follows from the relativistic normalization condition. The wave-function corresponding to ϕ_s represents the de Broglie wave of a free electron, having the energy E_s and the momentum \mathbf{M}_s . To each element h^3 of phase space must correspond one state of the electron. The number of eigenfunctions ϕ_s belonging to the element $d\tau = d\mathbf{M}_x d\mathbf{M}_y d\mathbf{M}_z$ of the momentum space is therefore $v h^{-3} d\tau$. Neglecting relativity corrections, we find instead of (10'),

$$E_s' = \mathbf{M}_s^2 / 2\mu, \quad C_s = \frac{1}{\sqrt{v}}. \quad . \quad . \quad . \quad (10'')$$

It is often useful to regard the wave-functions of any state n as a group of plane de Broglie waves. We may for that purpose put ϕ_n into the form of a Fourier integral

$$\phi_n = \int C_{\mathbf{M}}^{(n)} e^{-\frac{2\pi i}{h} \mathbf{M} \cdot \mathbf{r}} d\tau. \quad . \quad . \quad . \quad (11)$$

If n is a state for which relativity corrections in the normalization condition can be neglected, it then follows

$$\int |C_{\mathbf{M}}^{(n)}|^2 d\tau = h^{-3}. \quad . \quad . \quad . \quad (11')$$

A mean value $\overline{M_n^2}$ of the square of the momentum for the state n may be defined by the formula

$$\overline{M_n^2} = \overline{\mathbf{M}^2} = h^3 \int |C_{\mathbf{M}}^{(n)}|^2 \mathbf{M}^2 d\tau. \quad . \quad . \quad . \quad (12)$$

We then find from (2')

$$\overline{M_n^2} = 2\mu(E_n' + \epsilon \overline{V_0}) = 2\mu \overline{E_{\text{kin}}^{(n)}}. \quad . \quad . \quad (12')$$

Here $-\epsilon \overline{V_0}$ is the mean value (defined according to Schrödinger) of the potential energy in the state n . $\overline{E_{\text{kin}}^{(n)}}$ may therefore be regarded as the corresponding mean value of the kinetic energy.

For a Coulomb field ($V_0 = \frac{N\epsilon}{r}$) we have the relation of Bohr,

$$\overline{E_{\text{kin}}}^{(n)} = -\frac{1}{2} \overline{E_{\text{pot}}}^{(n)} = -E_n' = \frac{N^2 \epsilon^2}{2n^2 a_H}, \quad \left(a_H = \frac{h^2}{4\pi^2 \mu \epsilon^2} \right). \quad (13)$$

Therefore $M_n = \frac{Nh}{2\pi n a_H}$. For the normal state ($n=1$) we find

$$C_{\mathbf{M}}^{(1)} = \frac{2\sqrt{2}}{\pi} \frac{h^{-\frac{3}{2}} M_1^{\frac{5}{2}}}{(M_1^2 + \mathbf{M}^2)^2} \cdot \cdot \cdot \cdot \quad (13')$$

For a Coulomb field, it also follows, that $C_{\mathbf{M}}^{(n)}$ decreases at least as rapidly as $|\mathbf{M}|^{-4}$ if $|\mathbf{M}|$ tends to infinity. For any atomic field here considered, we may assume $C_{\mathbf{M}}^{(n)}$ to decrease so rapidly for increasing $|\mathbf{M}|$ that $C_{\mathbf{M}}^{(n)}$ is small, if $|\mathbf{M}|$ is much bigger than M_n . n then denotes a low state.

Taking relativity corrections into account, we can find a dispersion formula for very short waves in the following way:—Assuming $h\nu$ to be much bigger than $-E_1'$, we can neglect ϵV_0 in the equation giving f_n (cf. p. 1229). This equation may then be solved by expansions referring to the orthogonal functions (10). In this way* we find a dispersion formula which is similar to (7). Now, however, the quantities

$$[(E_n + h\nu)^2 - E_s^2]/2hE_s \quad \text{and} \quad [(E_n - h\nu)^2 - E_s^2]/2hE_s$$

have taken the place of the denominators $\nu_{ns} + \nu$ and $\nu_{ns} - \nu$. In the relations (4') and (7') ϕ_s is now a function (10). ϕ_n and ϕ_m are generally solutions of (2).

§ 2. We shall now enter upon a discussion of the distribution of intensities amongst the various frequencies of the scattered radiation. The initial state n is assumed to be a low state of the atom, for which relativity corrections may be neglected.

We shall investigate first the *coherent* radiation which is deduced from the dipole moment \mathbf{d}_{nn} . The wave-length λ of the incident radiation is first assumed to be large compared with D_n , a measure of the linear dimensions of the atom in the initial state n . \mathbf{d}_{nn} is then given by the Kramers-Heisenberg formula. The first term in the bracket [] of (7) is equal to E_0 . If, having due regard to the limits of λ , $h\nu$ can be chosen much bigger than the ionization energy

* In this case the normalization conditions are only approximately fulfilled.

$-E_1'$ of the normal state, the second term in that bracket will be small and can be neglected. It is easily found that the intensity of the scattered coherent radiation is then given by the classical formula of J. J. Thomson.

We then assume ν to be so big that λ is comparable with or less than D_n . δ_{nn} must now be less than unity, since the exponential factor in (7'') takes both positive and negative values in those parts of space from which some contribution to this integral is obtained. Using (11), we find

$$\delta_{nn} = h^3 \int C_{\mathbf{M}}^{(n)} \bar{C}_{\mathbf{M}+\mathbf{M}_R}^{(n)} d\tau. \quad \dots \quad (14)$$

Here $\mathbf{M}_R = \frac{h\nu}{c}(\mathbf{n} - \mathbf{n}')$ is the momentum imparted to the electron at the scattering of one light quantum. Now, according to a previous assumption, $C_{\mathbf{M}}^{(n)}$ is small if $|\mathbf{M}|$ is much greater than M_n . According to (14), δ_{nn} must therefore be small if $|\mathbf{M}_R| \gg M_n$. The second term in the bracket of (7) is to be neglected as before, if $h\nu \gg -E_1'$. For sufficiently high frequencies the coherent radiation therefore disappears*.

Since generally for $h\nu \gg -E_1$ only the first term $E_0\delta_{nn}$ in the bracket [] of (7) is to be taken into account, it also follows that the scattered radiation can in this case be directly calculated from the Schrödinger density of charge $\rho_n^{(0)} = -e|\phi_n|^2$, assuming each volume element dv to scatter classically as a free particle with the mass $-\mu\rho_n^{(0)}dv/e$ and the charge $\rho_n^{(0)}dv$.

The *incoherent* scattered radiation is given by those terms in the sum (8) for which $m \neq n$. The wave-length of the incident radiation is at first assumed to be large compared with D_n , so that $\delta_{nm} = 0$. If $h\nu$ is of the same order of magnitude as $-E_1'$ the second term in the bracket [] of (7) may sometimes be large enough to give a measurable incoherent radiation. If, taking the limits of λ into account, $h\nu$ can be chosen much bigger than $-E_1'$, this second term will generally be so small that the corresponding radiation—the intensity of which is proportional to the square of this term—can be neglected. For $h\nu > E_n - E_1$ only the first sum in (8) is to be taken into account.

If the frequency ν becomes so large that λ is comparable with, or less than D_n , the term $E_0\delta_{nm}$ must be taken into account. An incoherent radiation of various frequencies is

* Except, of course, in the direction of the incident wave.

then obtained. For states m belonging to the continuous term spectrum of the atom, the corresponding scattering frequencies $\nu_{nm} + \nu$ form a continuous spectrum. The scattering of a quantum of each of these frequencies is of course connected with the ejection of the electron from the atom. Assuming \mathbf{n} and \mathbf{n}' to be fixed, the distribution of intensity amongst these frequencies must, for sufficiently high frequency ν , show a hump which, as ν increases, goes over into the sharp peak corresponding to the pure Compton effect. We shall investigate this point, assuming that the approximation (10) may be used for the wave-functions ϕ_m , taking $s=m$. This implies the condition $E_n' \gg -E_n'$. It is easily seen that we may find the value of the second term in the bracket of (7) with fair accuracy by using the approximation (10) for ϕ_s . Taking for ϕ_n the expression (11), the sums and integrals occurring in the formula can be evaluated. The expression for d_{nm} thus found differs from that following from the relativistic formula mentioned at the end of § 1 only by relativity corrections. The last-mentioned expression must give a better approximation for high frequencies ν . This expression is * :

$$d_{nm} = -\frac{1}{4\pi^2\nu\nu'} \frac{\epsilon^2}{2\mu} \sqrt{\frac{\mu c^2}{E'}} \frac{h^2}{\sqrt{\nu}} C_{\mathbf{M}' + \kappa'\mathbf{n}' - \kappa\mathbf{n}}^{(n)} \left\{ E_0 + \right. \\ \left. + 2c^2 \left[\frac{[E_0(\mathbf{M}' + \kappa'\mathbf{n}')]\mathbf{M}'}{(E_n + h\nu)^2 - E_{\mathbf{M}' + \kappa'\mathbf{n}'}^2} + \frac{(E_0\mathbf{M}')(\mathbf{M}' - \kappa\mathbf{n})}{(E' - h\nu)^2 - E_{\mathbf{M}' - \kappa\mathbf{n}}^2} \right] \right\} e^{2\pi i \nu' t}. \quad (15)$$

Here $E' = E_m$, $\mathbf{M}' = \mathbf{M}_m$, $\nu' = \nu_{nm} + \nu = (E_n - E')/h + \nu$, $\kappa = h\nu/c$, and $\kappa' = h\nu'/c$. According to (10') we have the relation $\mathbf{M}'^2 - E'^2/c^2 + \mu^2 c^2 = 0$. Assuming ν , \mathbf{n} , and \mathbf{n}' to be fixed, these relations may be used to express ν' in terms of \mathbf{M}' . Since $E_m \gg -E_n$ and $E_m = E'$, we have approximately

$$h\nu = h\nu' + E'. \quad (16)$$

Let us now take a value of \mathbf{M}' , \mathbf{M}_c' say, satisfying the relation

$$\mathbf{M}' + \kappa'\mathbf{n}' - \kappa\mathbf{n} = 0. \quad (16')$$

We denote the corresponding value of ν' by ν_c . (16) and (16') are the relations expressing the conservation of energy and momentum for the Compton effect of a free electron. In this case \mathbf{M}_c is the momentum imparted to the electron

* This formula is not valid if any of the denominators vanish.

and ν , the frequency of the scattered radiation. Putting the corresponding frequency displacement $\nu - \nu_c = \Delta\nu_c$, we find, assuming $\mathbf{M}' - \mathbf{M}_c$ to be small compared with \mathbf{M}_c ,

$$\frac{\nu' - \nu_c}{\Delta\nu_c} = - \frac{(\mathbf{M}' - \mathbf{M}_c) \cdot \mathbf{M}_c}{\mathbf{M}_c^2 + \mu^2 c^2} \quad \dots \quad (17)$$

If $h\nu < \mu c^2$, \mathbf{M}_c is of course, to a first approximation, equal to $h\nu(\mathbf{n} - \mathbf{n}')/c$. If the direction of \mathbf{n}' is not the same as that of \mathbf{n} , it is always possible to satisfy the condition $|\mathbf{M}_c| \gg M_n$ by choosing ν big enough. According to (17), to values of $\nu' - \nu_c$ which are not small compared with $\Delta\nu_c$, correspond values of $|\mathbf{M}' - \mathbf{M}_c| = |\mathbf{M}' + \kappa' \mathbf{n}' - \kappa \mathbf{n}|$ large compared with M_n . According to previous assumptions, $C_{\mathbf{M}' + \kappa' \mathbf{n}' - \kappa \mathbf{n}}^{(n)}$ is then small. For values of $M_n/|\mathbf{M}_c|$ small compared with unity, the curve giving the distribution of intensity therefore shows a peak at $\nu = \nu_c$, whose sharpness increases as $M_n/|\mathbf{M}_c|$ diminishes.

Assuming $M_n/|\mathbf{M}_c|$ to be small, the incoherent radiation thus gives a Compton line which is only slightly broadened. We can easily find the intensity of this line. It follows from (16) and (16')* that only the first term \mathbf{E}_0 in the bracket $\{ \}$ of (15) is to be taken into account. According to § 1, there are $vh^{-3}d\tau$ eigenfunctions corresponding to the element $d\tau$ of the momentum space. The total intensity of the radiation scattered in the direction \mathbf{n}' is therefore

$$I = I_0 \frac{\epsilon^4}{\mu^2 c^4} \frac{\sin^2(\mathbf{E}_0, \mathbf{n}')}{R^2} \frac{\nu_c^2}{\nu^2} \frac{\mu c^2}{E_c} \cdot \frac{h^3}{v} \cdot \frac{v}{h^3} \int \left| C_{\mathbf{M}' + \kappa' \mathbf{n}' - \kappa \mathbf{n}}^{(n)} \right|^2 d\tau. \quad (18)$$

I_0 is the intensity of the incident radiation, R the distance from the atom, E_c the value of E' corresponding to \mathbf{M}_c . We make the transformation $\mathbf{M}' = \mathbf{m} + \mathbf{M}_c$ of the coordinates in momentum space. According to (16) and (16') the determinant $\frac{d(\mathbf{m}_x, \mathbf{m}_y, \mathbf{m}_z)}{d(\mathbf{M}'_x, \mathbf{M}'_y, \mathbf{M}'_z)}$ has the value $\mu c^2 \nu / E_c \nu_c$. Therefore (cf. (11'))

$$I = I_0 \frac{\epsilon^4}{\mu^2 c^4} \frac{\sin^2(\mathbf{E}_0, \mathbf{n}')}{R^2} \left(\frac{\nu_c}{\nu} \right)^3.$$

This is the intensity formula for the Compton effect of a free electron, given by Breit, Dirac, and Gordon†.

* Since $\mathbf{E}_0 \cdot \mathbf{n} = 0$ and $\mathbf{n}' \times \mathbf{n}' = 0$.

† G. Breit, Phys. Rev. xxvii. p. 362 (1926). P. A. M. Dirac, Proc. Roy. Soc. (A) iii. p. 705 (1926). Gordon, *loc. cit.*

We have found that the second term in the bracket [] of (7) does not give any contribution to the intensity of the pure Compton effect. Taking previous considerations into account it may be expected that this term can only give a small contribution to the scattered radiation if the condition $h\nu \gg -E_1'$ is fulfilled. Making the further assumption that the frequency displacement due to the Compton effect is small compared with ν , it is easily found that the total intensity of the radiation scattered in any direction is given by the formula of J. J. Thomson*.

This result is not valid if the atom contains more than one electron. It is a well-known fact that a good approximation to the motion of the electrons in an atom is often obtained by assuming the field acting upon each electron to be stationary. If this is the case the results given here may be applied to each electron separately. For frequencies ν high compared with the ionization energies of all electrons, divided by h , the coherent scattering may be deduced classically from that distribution of charge which is given by the sum of the Schrödinger densities for each separate electron.

Using general principles of quantum mechanics, a more complete examination of the scattering problem for an atom containing more than one electron may be given.

The general results given here in some respects ought to be completed. More definite results may be obtained for special atoms, *e. g.* for the hydrogen atom.

I wish to express my thanks to Prof. N. Bohr, Prof. C. G. Darwin, and Dr. O. Klein for their valuable interest in this work. I am also indebted to Prof. W. L. Bragg for discussions about this problem.

CIV. Cavitation in Screw Propellers.

To the Editors of the Philosophical Magazine.

GENTLEMEN,—

IN the July 1927 issue of the Philosophical Magazine a paper is presented by Mr. John Tutin entitled "A Theoretical Investigation of the Phenomenon of Cavitation in Screw Propellers," in which a new theory of flow about propellers is set forth. On page 23 it is stated that "the logical conclusion of this investigation is that an actuator cannot be made to deliver thrust by

* Cf. G. Wentzel, *loc. cit.*, and I. Waller, *loc. cit.*

the assumption of a perfect 'Bernouilli' flow and a discontinuity of pressure. It follows that the familiar Rankine-Froude theory and the corresponding vortex theory are incorrect. The inflow velocity and ideal efficiency deduced therefrom are misleading. This result is important, because these theories are extensively used in air-screw research in this country, France, Italy, Germany, and U.S.A."

We wish to call attention to the fact that the new theory rests upon an assumption which is not required in the Rankine-Froude theory, and which seems to us to have no experimental foundation. The assumption, not explicitly stated by the author, is contained in the left-hand member of equation 6 on page 21, which gives the longitudinal force acting on the inflow column. This force must be found by integrating the longitudinal component of the pressure over the entire boundary of the inflow column. The author's result is true only if the pressure is equal to p_0 everywhere on the boundary except at the propeller disk. In the general case the pressure outside of the slip-stream varies in such a way that $p + 1/2\rho V^2$ is constant as shown by Stanton and Marshall (see Repts. and Memo. No. 460 of the British Aeronautical Research Committee), and the longitudinal force depends on the shape of the boundary and on the area of the inflow column at a great distance from the screw. There is then no inconsistency with Equation 2. We know of no experiments which indicate that the pressure on the boundary of the inflow column is constant and equal to p_0 .

In connexion with the phenomenon of cavitation of water propellers, it may be of interest to call attention to the fact that the occurrence of a somewhat similar phenomenon in air propellers may be inferred from the results of our experiments on propeller sections at high speeds (see Technical Reports Nos. 207 and 255 of the National Advisory Committee for Aeronautics). It appears that a change of flow with speed takes place, which is dependent in some way on the flow very close to the surface—that is, in the "boundary layer." The lower limit of the pressure at any point on the surface seems to be of the order of one-half an atmosphere.

Yours faithfully,

Bureau of Standards,
Washington, D.C.
July 28, 1927.

L. J. BRIGGS,
H. L. DRYDEN.

CV. Cavitation in Screw Propellers.

To the Editors of the Philosophical Magazine.

GENTLEMEN,—

THE Phil. Mag. vol. iv. July 1927 contains a paper by Mr. J. Tutin dealing with the cavitation of screw propellers, in which the author puts forward a modified treatment of the actuator disk of Froude and Rankine and derives a different expression for the efficiency of the propeller. Mr. Tutin, however, is not correct in his statement that the modern vortex theory of air-screws depends on this assumption of an actuator disk.

The conception of the actuator disk is clearly a simplified assumption of the true characteristics of an air-screw, and Mr. Tutin has obtained a result in discordance with modern theory by applying the conception outside the limits of its validity. In estimating the increase of total pressure head in the air-screw slip-stream, it is legitimate to use Mr. Tutin's equations (2) and (3), which neglect the radial component of the velocity at the air-screw disk ; but this course is no longer sound when it is desired to consider independently the regions before and behind the air-screw. For a stream tube passing through the air-screw disk the equations should be

$$p_0 + \frac{1}{2}\rho V^2 = p + \frac{1}{2}\rho(V+u)^2 + \frac{1}{2}\rho w^2,$$

$$p + p_1 + \frac{1}{2}\rho(V+u)^2 + \frac{1}{2}\rho w^2 = p_0 + \frac{1}{2}\rho(V+v)^2,$$

where w is the radial component of the velocity. If the analysis is now continued on the lines suggested by Mr. Tutin, it follows that

$$u^2 = w^2 = (v-u)^2,$$

which is consistent with the modern theory that $v=2u$. Mr. Tutin's mysterious energy, which is lost in the inflow column and regained in the outflow column, is simply the kinetic energy of the radial velocity.

It follows that Mr. Tutin's modified expression for the air-screw efficiency cannot be accepted ; but his later remarks on the nature and cause of cavitation give a correct description of the phenomenon. Cavitation occurs when the suction on the back of a blade is too intense ; and to avoid cavitation it is necessary to obtain the thrust by pressure on the face of a blade rather than by suction on its back. Some such adjustment is possible by suitable choice of

the blade angles and camber of the blade sections. The problem, however, is further complicated by the rotation of the slip-stream which reduces the pressure at the core of the slip-stream.

Yours faithfully,
H. GLAUERT.

Royal Aircraft Establishment,
South Farnborough,
August 17, 1927.

CVI. *Cavitation in Screw Propellers.*

To the Editors of the Philosophical Magazine.

GENTLEMEN,—

I AM pleased to note that Messrs. Briggs and Dryden admit that my theory is correct if the pressure is equal to p_0 everywhere at the "boundary" except at the screw disk. That this assumption is implicit is quite clear from the equations, and it was not therefore considered necessary to state it separately. It is in my opinion a legitimate approximation to make. It is quite independent of the shape and extent of the slip-stream. It is doubtful whether in practice the "boundary" of the slip-stream can be precisely determined—certainly not by experiments in a wind tunnel, as I am sure Dr. Stanton would be the first to admit.

Indirectly, however, wind-tunnel experiments confirm the new momentum theory, because the mean experimental inflow ratios obtained independently by both Stanton and Fage are invariably greater than .5 (*e.g.* Fage, R. & M. No. 940, pp. 4 & 5 and Table 4).

In reply to Mr. Glauert, I am aware that the assumptions made in the Froude-Rankine theory differ ostensibly from the assumptions of the Vortex theory. In regard to inflow ratio, however, the two theories give the same result, and in this respect they must obviously sink or swim together.

It can be shown that for the Froude-Rankine actuator, the suction on the fore side of the disk must be equal to or less than the excess pressure on the after side. In an actual propeller, the suction on the back of the blades is usually more than double the pressure on the face of the blades. It is palpably absurd to suppose that the Froude-Rankine

actuator can in this respect represent even approximately the "true characteristics of an air-screw."

My amendments permit of an actuator having any required pressure distribution between the two sides, and for this reason alone it is likely to give results more consistent with experimental observations than are the deductions of existing theories.

There is certainly some difficulty in giving the correct physical interpretation to the additional terms introduced in the equations. As Mr. Glauert points out, the term in equation (11) labelled "energy dissipated at screw-disk" must be regarded as energy supplied at the screw-disk. This correction does not affect the applications of the theory, but the efficiency expressions should of course be amended accordingly. I do not agree with Mr. Glauert that these terms should be regarded as representing the radial component of the velocity. If this were so, at zero speed of advance the stream-lines at the screw-disk would be inclined at an angle of 45 degrees to the plane of the disk.

I invite exponents of the vortex theory to account for the following observed facts, which the amended momentum theory adequately interprets :—

1. Observed inflow ratios are normally greater than the value .5 indicated by the vortex theory.
2. Thrust and torque integrations by the vortex theory are normally in excess of the measured thrust and torque, which indicates overestimation of the angle of incidence by the vortex theory. This corresponds to too small an inflow.
3. The vortex theory indicates zero inflow at zero thrust. This cannot be reconciled with the experimental pitch ratios less than unity, as observed by Mumford and Schaffran (*loc. cit.*).
4. At high revolutions and positive nominal slip, Admiral D. W. Taylor, U.S.N., has obtained in the Washington Experiment Tank zero thrust from a cavitating propeller. This can be accounted for by the new momentum theory as being due to *excessive* inflow, when by the vortex theory the inflow would be zero.

Yours faithfully,

JOHN TUTIN.

Department of Naval Architecture,
The Technical College, Sunderland.

Phil. Mag. S. 7. Vol. 4. No. 25. *Suppl.* Nov. 1927. 4 L

To the Editors of the Philosophical Magazine.

GENTLEMEN,—

IN a communication on "The Effect of Radon on the Solubility of Lead Uranate" (Phil. Mag. vol. iv. p. 404, Aug. 1927), Dr. Kenneth C. Bailey ascribes to me the suggestion that in uranium minerals "most of the lead produced would probably form lead uranate, which is practically insoluble," while in thorium minerals "the relatively soluble lead thorate would be formed and partially removed by leaching." I wish to correct the erroneous impression that I contrasted the behaviour of lead uranate with that of "lead thorate." In the paper to which Dr. Bailey refers, I wrote (Phil. Mag. vol. i. p. 1068, May 1926):—"In thorium minerals the lead could not form a thorate, as thorium and oxygen do not constitute an acidic environment, and corresponding with this no thorates are known to exist. In thorianite the lead should be largely present as an oxide; and in thorite partly as oxide, and partly perhaps as a silicate. In both minerals the most probable lead compounds are therefore of a comparatively soluble type."

Dr. Bailey's experimental demonstration that under appropriate conditions lead from lead uranate may pass into solution must be taken into account in considering the alteration of radioactive minerals by weathering or ground-waters, but it does not effect the validity of my deduction that "lead present as oxide or silicate would be more easily removed by percolating waters and kinetic exchange than the lead in uranium minerals." Moreover, altered uraninites commonly give higher lead-ratios than the fresh materials associated with them, and at the same time have clearly lost a notable proportion of the uranium originally present. This indicates that under natural conditions leaching, when it occurs, removes uranium in greater proportion than lead. A repetition of Dr. Bailey's experiments B and C, using actual minerals instead of lead uranate, should provide a direct test of the principle of my preferential leaching hypothesis, and would probably give results that could be applied to the problem of interpreting discordant series of lead-ratios.

Yours faithfully,

ARTHUR HOLMES.

Science Laboratories,
The University, Durham.
August 12, 1927.

CVIII. *Notices respecting New Books.*

Thermionic Phenomena. By EUGÈNE BLOCH. Translated by J. R. CLARKE. (Methuen & Co. Price 7s. 6d. net.)

THE translation of Prof. Bloch's 'Les Phénomènes Thermioniques' should be of service as an introduction to one of the most important branches of modern physics. Reference is made to the researches of many investigators, in particular Prof. O. W. Richardson.

The first chapter gives interesting historical details of the subjects, the remaining part being devoted to electronic and positive ion emission in vacua and in gases, and the application of thermionic phenomena to the measurement of high vacua and to the rectification of alternating currents.

There are two useful indexes—one for authors, the other for subjects.

Light. By F. BRAY, M.A. (Edward Arnold & Co. Price 6s.)

THE author has successfully accomplished the task of providing an up-to-date text-book which will serve the purpose of general education, preparation for the Higher Schools Examinations, and the study of more advanced works on this subject. The historical treatment of the subject is a specially valuable feature, and will, without doubt, arouse the interest of the student.

The second part of the volume is devoted to the exposition of wave theory, with an introductory chapter on simple harmonic motion, interference, diffraction and polarization of light, and spectrum analysis.

The questions appended to each chapter serve to emphasize the most important points and to summarize the general results.

Mr. Bray has struck out a new line of treatment and produced a book noteworthy both for its freshness and utility.

History of Radio-Telegraphy and Telephony. By G. O. BLAKE, M.I.E.E., A.Inst.P. Pp. xix+425, with numerous figures. (London: Radio Press. 1926. n.p.)

THIS volume is not so much an historical account of the development of radio-telegraphy and telephony as a history of inventions connected with these sciences. The division into chapters is therefore mainly conditioned by the subjects under discussion: thus, for instance, one chapter deals with coherers, another with detectors, another with spark and arc generators of high-frequency currents, and so forth. The author has done his work with great thoroughness, and the reference list at the end of the volume contains 1125 entries. Many almost forgotten devices are recalled in the hope that, though of little practical use in their present form, they may contain ideas which may usefully be

adopted to some new invention. The volume is illustrated with over 200 illustrations of apparatus and circuits, 'extracted from patent specifications or technical journals. As a work of reference the volume should prove of considerable value, and its use will be facilitated by the detailed index at the end of it.

Spectroscopy. By E. C. C. BALY, C.B.E., M.Sc., F.R.S. Third Edition. In 4 volumes. Vol. II. Pp. viii+398, with 95 figures. (London: Longmans, Green & Co. 1927. Price 18s. net.)

THE numerous developments in spectroscopy during recent years are indicated by the fact that four volumes are required for the third edition of Prof. Baly's well-known work on 'Spectroscopy.' The first volume of the new edition appeared in 1924; the newer developments of the subject, arising in large measure from the application of quantum ideas by Bohr, will be dealt with in the two volumes which remain to be published. In the third volume it is proposed to include chapters on spectral series, the Zeeman and Stark effects and emission band spectra, whilst the fourth volume will deal with absorption spectra, the shift of spectral lines by pressure and by line-of-sight motion.

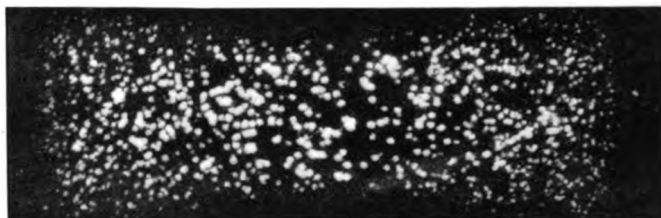
The volume under review contains an account of the application of interference methods to spectroscopy, including the theories of interferometers and special applications such as the determination of the angular diameters of stars, together with chapters on methods of illumination, the nature of spectra, fluorescence and phosphorescence, and the photography of the spectrum. Many investigations now demand a knowledge of the spectrum in the extreme infra-red and ultra-violet, and special plates and special methods of treatment are necessary. A great deal of valuable information is given on these matters, much of the information having been supplied by Dr. C. E. K. Mees.

The chapter on illumination includes an account of King's electric resistance furnace spectra and of the explosion of wires, and contains many practical details of great value for the experimental spectroscopist. The chapter on fluorescence and phosphorescence is very complete, and includes accounts of the most recent work on the subject.

Spectroscopists will look forward with eagerness to the appearance of the two remaining volumes, and we may venture a hope that publication will not be unduly delayed.

[*The Editors do not hold themselves responsible for the views expressed by their correspondents.*]

GREEN.



6 MINUTES.
 5.53×10^5 particles per c.c.

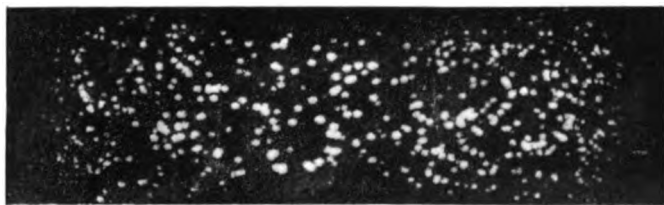


30 MINUTES.
 2.62×10^5 particles per c.c.



65 MINUTES.
 1.60×10^5 particles per c.c.

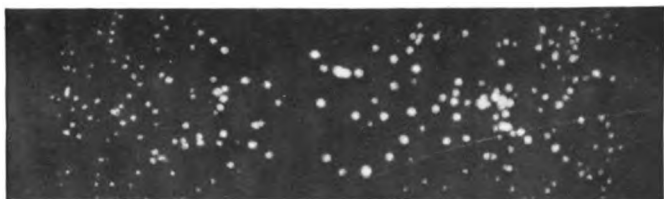
DROPLETS FORMED BY THE CONDENSATION OF MOISTURE ON THE 14



20 MINUTES.
 3.54×10^5 particles per c.c.

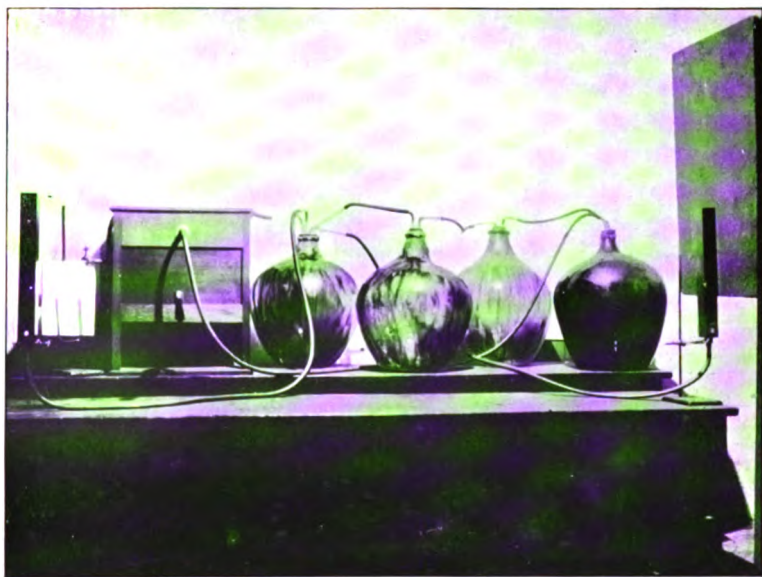


50 MINUTES.
 1.94×10^5 particles per c.c.



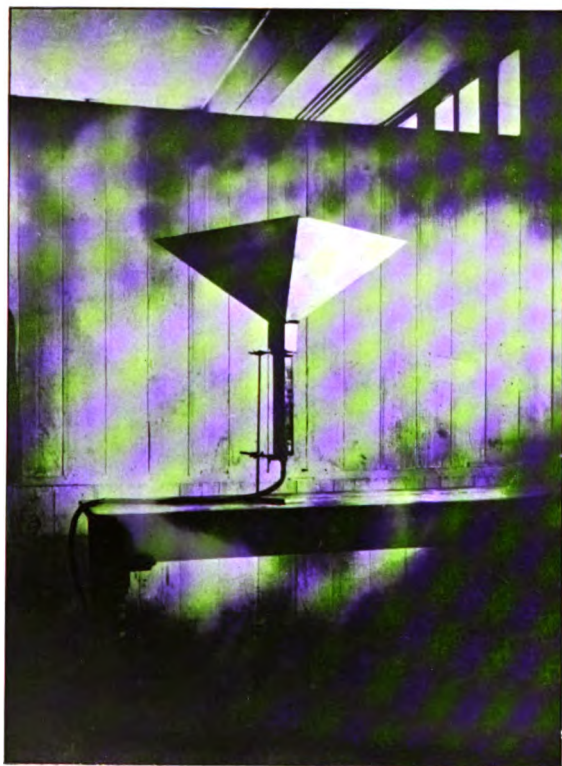
90 MINUTES.
 1.19×10^5 particles per c.c.

FIG. 1.



General view of apparatus used in experiments.

FIG. 3.



View of "Hopper" flange on pipe.

THE
LONDON, EDINBURGH, AND DUBLIN
PHILOSOPHICAL MAGAZINE
AND
JOURNAL OF SCIENCE.

[SEVENTH SERIES.]

DECEMBER 1927.

CIX. *Thermodynamic Integrating Factors.*
By Prof. A. PRESS*.

Introduction.

IT is rather generally believed that in any thermodynamic formula, or reasoning, it is sufficient to apply the universal integrating factor

$$\mu = \frac{1}{\theta} \quad . \quad . \quad . \quad . \quad . \quad . \quad (1)$$

in order to obtain a condition that must hold unquestionably. It is the object of the present paper to show in what respects the integrating factor (1) needs to be taken, and, secondly, to show that the universality of application of such integrating factor is far from justified. In fact, for every μ there corresponds a particular thermodynamic path function.

In this connexion it may be recalled that the writer made use of an integrating factor with two variables to prove the Grüneisen-Ratnowsky formulæ for specific heats, and, when corrected, also the elasticity coefficients would naturally follow without having to make use of the Quantum Theory. In fact, Trouton's formula when generalized is also obtainable in this way.

*The Integrating Factor and its Consequent
Equation of State.*

It has already been shown by the writer (see *Phil. Mag.* p. 431, Aug. 1926) that mathematically the condition for an

* Communicated by the Author.

Phil. Mag. S. 7. Vol. 4. No. 26. Dec. 1927.

4 M

integrating factor following from the fundamental equation

$$dQ = dU + p dv = dU + dW \quad . \quad . \quad . \quad (2)$$

is the equation :—

$$p + \frac{\partial U}{\partial v} + \frac{\mu}{\frac{\partial \mu}{\partial \theta}} \cdot \frac{\partial p}{\partial \theta} = \frac{\frac{\partial \mu}{\partial v}}{\frac{\partial \mu}{\partial \theta}} \cdot \frac{\partial U}{\partial \theta} \quad . \quad . \quad . \quad (3)$$

Naturally, if we assume an integrating factor of the form (1), then on the simplifying assumption that we make

$$\frac{\partial U}{\partial v} = 0 \quad . \quad . \quad . \quad . \quad . \quad (4)$$

it results that

$$p - \theta \frac{\partial p}{\partial \theta} = 0. \quad . \quad . \quad . \quad . \quad . \quad (5)$$

No other Equation of State can possibly follow from (5) than that (on integration)

$$\lg p = \lg \theta - \lg \left\{ \frac{a}{1} f(v) \right\} \quad . \quad . \quad . \quad . \quad . \quad (6)$$

$$p \cdot f(v) = a\theta$$

For the so-called “perfect gas,” writing for simplicity

$$f(v) = v \quad \text{and} \quad a = R, \quad . \quad . \quad . \quad . \quad . \quad (7)$$

we naturally have the “Equation of State”

$$pv = R\theta. \quad . \quad . \quad . \quad . \quad . \quad (8)$$

Yet the question may well be asked, how to obtain from (3) the characteristic equation for the adiabatic expansion of a “perfect gas” if μ is to be assumed as a possible universal integrating factor? Surely this question is an all-important one for Thermodynamic Science.

Without attempting to introduce the necessary integrating factor in (3) at this time, it will first be desirable to obtain the characteristic for adiabatic expansion without making use of the relation (1), or the assumption of a perfect gas.

The γ -Ratio and Adiabatic Expansion.

By the first law of thermodynamics we have

$$dQ = dU + p dv. \quad . \quad . \quad . \quad . \quad . \quad (2)$$

Quite generally, however, must we also have that

$$d(pv) = p dv + v dp. \quad . \quad . \quad . \quad . \quad . \quad (9)$$

Introducing the latter in (2) gives the equation

$$dQ = d(U + pv) + v dp. \quad (10)$$

The definition of adiabatic expansion is really determined by the relations

$$dQ = 0 = dU + p dv = d(U + pv) - v dp. \quad (11)$$

That is, by division in (11) we have

$$\frac{d(U + pv)}{dU} = -\frac{v}{p} \cdot \frac{dp}{dv} = 1 - \frac{d(pv)}{dU} = \gamma. \quad (12)$$

If then it should be found substantially that we can take

$$\frac{d(pv)}{dU} = \text{constant}, \quad (13)$$

though *not necessarily the same constant for all gases for example*, it will mean in (12) that

$$\gamma = \text{constant}. \quad (14)$$

Thus on integration we have that

$$\left. \begin{aligned} pv^\gamma &= \text{constant} \\ pv &= (1 - \gamma)U \end{aligned} \right\} \quad (15)$$

Of course, it is well known that the total heat of a body

$$I = U + pv \quad (16)$$

is not linearly related to the internal energy U , for we should then have

$$\frac{dI}{dU} = 1 + \frac{d(pv)}{dU}. \quad (17)$$

Ordinarily, anomalies occur. Thus (see Birtwistle, 'Thermodynamics,' p. 76), it was shown by Thomson and Joule in 1862 that the heat developed on compression may actually be more, or even less, than the corresponding amount of mechanical work on the compressing piston, depending on whether the substance was air, carbonic acid gas, or even hydrogen.

The Integrating Factor for Adiabatic Expansion.

To ease the mathematical work let us take then, as the fundamental conditions given, that

$$pv^\gamma = A; \quad \frac{\partial U}{\partial v} = 0^*; \quad pv = (1 - \gamma)U. \quad (18)$$

* This virtually implies that the potential due to molecular forces or aggregations does not occur.

It is required to determine the integrating factor μ that shall satisfy (3) even when the path taken by the substance involves the element of adiabatic expansion or compression.

Introducing (18) into (3) we have first to take note that we can obtain $\left(\frac{\partial p}{\partial \theta}\right)_v$ from (18) for it necessarily follows that

$$v\left(\frac{\partial p}{\partial \theta}\right)_v = (1-\gamma)\left(\frac{\partial U}{\partial \theta}\right)_v^*, \quad \dots \quad (19)$$

provided, and only provided, no anomalies occur as mentioned above with respect to (13). The equation (3) then reduces to

$$\frac{\partial \mu}{\partial \theta} \cdot \frac{A}{v^\gamma} + \frac{\mu(1-\gamma)}{v} \left(\frac{\partial U}{\partial \theta}\right)_v = \frac{\partial \mu}{\partial v} \left(\frac{\partial U}{\partial \theta}\right)_v. \quad \dots \quad (20)$$

To integrate the latter equation we can provisionally assume that

$$\left. \begin{aligned} \mu &= VT \\ \text{with } V &= F(v) \text{ only and } T = \phi(\theta) \text{ only} \end{aligned} \right\} \quad \dots \quad (21)$$

Introducing (21) into (20) gives, after reduction and rearrangement of terms that we need to satisfy the relation,

$$\frac{1}{T} \cdot \frac{dT}{d\theta} = \left(\frac{1}{A} \cdot \frac{\partial U}{\partial \theta} \right) \left\{ \frac{1}{V} \cdot \frac{dV}{dv} + \frac{(\gamma-1)}{v} \right\} v^\gamma. \quad \dots \quad (22)$$

For convenience we can write

$$\frac{1}{A} \frac{\partial U}{\partial \theta} = C \quad \dots \quad (23)$$

and assume that

$$\frac{\partial U}{\partial \theta} = \text{constant}. \quad \dots \quad (24)$$

Since the variables are separated we can equate each side to a constant α such that it follows

$$\frac{1}{T} \cdot \frac{dT}{d\theta} = \alpha; \quad T = e^{\alpha\theta}, \quad \dots \quad (25)$$

$$\frac{1}{V} \cdot \frac{dV}{dv} + \frac{(\gamma-1)}{v} = \frac{\alpha}{Cv^\gamma} = \frac{\beta}{v^\gamma}. \quad \dots \quad (26)$$

Solving (26) by bringing the v -terms to the right-hand side it is seen that we need to have V of the form

$$V = v^{1-\gamma} \cdot e^{\frac{\beta}{1-\gamma} \cdot v^{1-\gamma}} \quad \dots \quad (27)$$

* This is virtually the Grüneisen condition for solids, where v is substantially constant and $\frac{\partial p}{\partial \theta}$ connects with the elasticity coefficients.

Matrix Mechanics and a Radiating Harmonic Oscillator. 1249

In other words, the integrating factor *must* under the circumstances mentioned be given by

$$\mu = \mu_0 \frac{\epsilon^{1-\gamma} \nu^{1-\gamma}}{\rho^{1-\gamma}} \cdot \epsilon^{\alpha\theta} \dots \dots \dots (28)$$

Indeed, it necessarily follows that to each particular path thermodynamically pursued by a substance there corresponds a distinguishing thermodynamic integrating factor and not necessarily satisfying the relation $\mu = \frac{1}{\theta}$.

1314 18th St., N.W.
Washington, D.C., U.S.A.,
June 1st, 1927.

CX. Consequences of a Matrix Mechanics and a Radiating Harmonic Oscillator without the Quantum Postulate. By Prof. A. PRESS.*

SUMMARY.

IN order to avoid postulating quantum conditions from the start, as done in the Heisenberg-Born-Jordan-Dirac Matrix Mechanics, the writer conceived the idea of giving concrete visualization to the elements of the pq - qp matrix by relating them to a classical formula leading to an action (see paper published in the Phil. Mag. for Sept. 1924). This required a slightly modified way of defining the unit matrix.

If we consider a portion of a radiating gas capable of sending out a series of wave-lengths according to an observed law, then we may attribute to each periodicity a sine element and an associated cosine element of the p and q matrices. Such aggregates, when expressed in the form of an action matrix pq - qp , constitute a standard diagonal matrix. In the text it has been shown that there is an analogy also between $h/2\pi i$ of matrix mechanics and the χ -expression developed on the basis of the present matrix system.

An important distinction has also manifested itself. On account of the special character assigned to the p and q elements in the modified matrices employed, the squares of the $p(mn)$ elements rather than of the $q(mn)$ elements are associated with the frequencies $\nu(mn)$. It must also be said that the χ -function does not require the i -term to appear in the denominator. Nor is it necessary, for matrix processes, to assume that the value of all the diagonal elements in the unit matrix shall be unity or even equal to each other.

* Communicated by Prof. A. S. Eve, F.R.S.

The requirement of the i -factor in the numerator has naturally led to the minus sign appearing when doubly differentiating a matrix, as occurs when considering the problem of an harmonic oscillator. Nevertheless, it must be borne in mind that the harmonic oscillator functions, heretofore used, have not been strictly radiating systems*. This is especially true since the Hamiltonian H -function has been considered as constant and independent of the time. The radiating harmonic oscillator of the text, on the other hand, implies that only the mean H over the cyclic period is constant. Thus, during a quarter of a cycle absorption of energy is allowed for, and mathematically expressed, whereas during the next quarter of a cycle, radiation of energy is presumed to take place. Besides, for a radiating oscillator, the momentum is not wholly in phase with \dot{q} . Thus the observed frequencies are interpreted to indicate an upper level $n = +1$ and a lower level $n = -1$ with respect to a mean level of energy H_0 . Strangely enough the ratio of upper (or lower) level energy H_n to mean level energy H_0 is of the order of $1/3$ as against the $1/2$ obtained from the Heisenberg-Born mechanics for E_n . Considerable freedom, however, is left open for specifying the "orbital frequency" of the generators.

The evidence goes to show that the postulates of the Quantum Mechanics do not necessarily involve such bold assumptions as appear to be the case at first sight. Part of their strange character seems to be due to the use of non-radiating harmonic oscillators, whereas those of the radiating type are now made mathematically available.

It is significant that it should be possible to show from purely classical considerations that the non-radiating harmonic oscillator is only then capable of becoming of radiating type when a discrete amount of energy ($1/3$ of the non-radiating content) is continuously being absorbed and re-radiated. This appears to suggest that the radiating harmonic oscillator of the text is analogous in its properties to that of an ordinary organ-pipe.

THE equation of the non-radiating harmonic oscillator is

$$H = \frac{1}{2}p^2 + 2\pi\nu_0^2q^2, \quad . \quad . \quad . \quad . \quad . \quad (1)$$

where p is the generalized momentum and q is the generalized displacement. Consider, then, matrices of elements such as those of the Heisenberg-Born type :

$$q = (q_{mn}e^{2\pi i\nu(mn)t}); \quad p = (p_{mn}e^{2\pi i\nu(mn)t})^\dagger. \quad . \quad . \quad . \quad (2)$$

It is possible to get a correspondence between the matrices

* Attention should be directed to a very important contribution to the discussion and history of the Linear Oscillator by Prof. G. A. Schott F.R.S., in the Phil. Mag. for April 1927, p. 739.

† A different type of matrix will be further in question.

p and q and the true momenta and displacements \underline{p} and \underline{q} if we consider the following resultant matrix :

$$d = pq - qp = U. \quad . \quad . \quad . \quad . \quad . \quad (3)$$

Thus, let it be assumed that the process of differentiation with respect to the time can be performed in the following way :

$$\left(\frac{d}{dt}\right)d = \dot{d} = \left(\frac{d}{dt}\right)p \cdot q + p \cdot \left(\frac{d}{dt}\right)q - \left(\frac{d}{dt}\right)q \cdot p - q \cdot \left(\frac{d}{dt}\right)p,$$

or $\dot{d} = \dot{p}q + p\dot{q} - \dot{q}p - q\dot{p}. \quad . \quad . \quad . \quad . \quad . \quad (4)$

Let it be further assumed that we can have a matrix function H analogous to \underline{H} above, such that we can have corresponding canonical equations, viz. :

$$\frac{\partial H}{\partial p} = \dot{q}; \quad -\frac{\partial H}{\partial q} = \dot{p}. \quad . \quad . \quad . \quad . \quad (5)$$

It follows at once on substitution in (4) that

$$\dot{d} = -\frac{\partial H}{\partial q} \cdot q + p \cdot \frac{\partial H}{\partial p} - \frac{\partial H}{\partial p} \cdot p + q \cdot \frac{\partial H}{\partial q}$$

$$\dot{d} = \left\{ q \cdot \frac{\partial H}{\partial q} - \frac{\partial H}{\partial q} \cdot q \right\} + \left\{ p \cdot \frac{\partial H}{\partial p} - \frac{\partial H}{\partial p} \cdot p \right\}. \quad . \quad (6)$$

It can be shown quite generally in connexion with matrices that, adopting Dirac's Poisson-bracket notation *

$$-\left[\frac{\partial H}{\partial q} \cdot q\right] = -q \frac{\partial H}{\partial q} + \frac{\partial H}{\partial q} q = \left[q \cdot \frac{\partial H}{\partial q}\right] = \frac{\partial^2 H}{\partial p \partial q},$$

whereas

$$\left[\frac{\partial H}{\partial p} \cdot p\right] = p \cdot \frac{\partial H}{\partial p} - \frac{\partial H}{\partial p} \cdot p = \frac{\partial^2 H}{\partial q \partial p}. \quad . \quad . \quad . \quad . \quad (7)$$

There can therefore be a correspondence between the canonical equations of Hamilton and the canonical equations of Heisenberg for matrices generally, provided that the matrices are such that

$$\dot{d} = 0. \quad . \quad . \quad . \quad . \quad . \quad (8)$$

This means that the matrices must be of the type that

$$pq - qp = \text{constant (independent of } t). \quad . \quad . \quad (9)$$

The above two conditions can be met, first by interpreting the multiplication of matrices so that the time functions should not appear. This implies that a special meaning needs to be given to "multiplication," for by (4) it is presumed that the p 's and q 's are in fact functions of the time. Secondly, in order to meet the condition (9), a diagonal matrix condition is necessary. This can also be

* See Appendix.

satisfied by properly interpreting the elements of the resultant multiplication matrix.

Let us therefore form matrices and then develop their products. Thus let, for example,

$$q = \begin{pmatrix} q_{11} & q_{12} & q_{13} \\ q_{21} & q_{22} & q_{23} \\ q_{31} & q_{32} & q_{33} \end{pmatrix} \quad (10) \quad p = \begin{pmatrix} p_{11} & p_{12} & p_{13} \\ p_{21} & p_{22} & p_{23} \\ p_{31} & p_{32} & p_{33} \end{pmatrix} \quad (11)$$

$$pq = \begin{pmatrix} (p_{11}q_{11} + p_{12}q_{21} + p_{13}q_{31}) & (p_{11}q_{12} + p_{12}q_{22} + p_{13}q_{32}) & (p_{11}q_{13} + p_{12}q_{23} + p_{13}q_{33}) \\ (p_{21}q_{11} + p_{22}q_{21} + p_{23}q_{31}) & (p_{21}q_{12} + p_{22}q_{22} + p_{23}q_{32}) & (p_{21}q_{13} + p_{22}q_{23} + p_{23}q_{33}) \\ (p_{31}q_{11} + p_{32}q_{21} + p_{33}q_{31}) & (p_{31}q_{12} + p_{32}q_{22} + p_{33}q_{32}) & (p_{31}q_{13} + p_{32}q_{23} + p_{33}q_{33}) \end{pmatrix} \quad (12)$$

$$qp = \begin{pmatrix} (q_{11}p_{11} + q_{12}p_{21} + q_{13}p_{31}) & (q_{11}p_{12} + q_{12}p_{22} + q_{13}p_{32}) & (q_{11}p_{13} + q_{12}p_{23} + q_{13}p_{33}) \\ (q_{21}p_{11} + q_{22}p_{21} + q_{23}p_{31}) & (q_{21}p_{12} + q_{22}p_{22} + q_{23}p_{32}) & (q_{21}p_{13} + q_{22}p_{23} + q_{23}p_{33}) \\ (q_{31}p_{11} + q_{32}p_{21} + q_{33}p_{31}) & (q_{31}p_{12} + q_{32}p_{22} + q_{33}p_{32}) & (q_{31}p_{13} + q_{32}p_{23} + q_{33}p_{33}) \end{pmatrix} \quad (13)$$

It will be noticed that in pq , as well as in qp , the diagonal elements are either of the form

$$\sum p_{mn}q_{nm} \quad \text{or} \quad \sum q_{mn}p_{nm} \quad \dots \quad (14)$$

The condition then needs to be imposed by definition that

$$p_{mn}q_{rs} = 0 \quad \text{for} \quad m \neq s; \quad n \neq r. \quad \dots \quad (15)$$

The significance of this condition will be brought out later and will amount to ignoring term elements producing expressions in which the frequency of a p_{mn} element differs from the frequency of a q_{rs} element.

Forming now the subtraction of matrices (12) and (13), it is at once apparent that only diagonal elements need to be considered, and we have, subject to (15), that

$$pq - qp = \begin{pmatrix} \{(p_{11}q_{11} - q_{11}p_{11}) + (p_{12}q_{21} - q_{12}p_{21}) + (p_{13}q_{31} - q_{13}p_{31})\} & 0 & 0 \\ 0 & \{(p_{21}q_{12} - q_{21}p_{12}) + (p_{22}q_{22} - q_{22}p_{22}) + (p_{23}q_{32} - q_{23}p_{32})\} & 0 \\ 0 & 0 & \{(p_{31}q_{13} - q_{31}p_{13}) + (p_{32}q_{23} - q_{32}p_{23}) + (p_{33}q_{33} - q_{33}p_{33})\} \end{pmatrix} \quad (16)$$

The general term of any diagonal element is therefore seen to be of the form of

$$\Sigma(p_{mn}q_{nm}-q_{mn}\dot{p}_{nm}). \quad . \quad . \quad . \quad . \quad (17)$$

The multiplication of matrices has then to be so limited by definition that an expression such as (17) has no longer to involve the time function *per se*. It will then result that the canonical equations of classical mechanics can be translated in invariant form into the domain of general matrix mechanics. The first important thing, then, in a rationalization of matrix mechanics is to give a physical basis for the interpretation of (17).

By a theorem in classical generalized mechanics already deduced by the writer (see Phil. Mag. Sept. 1924), it was proved that if we have a component of generalized force defined by

$$\left. \begin{aligned} \dot{E}(mn) &= E_{nm} \sin \omega t + E_{mn} \cos \omega t, \\ \text{and a consequent generalized displacement} \quad &\left. \begin{aligned} \dot{D}(mn) &= D_{nm} \sin \omega t + D_{mn} \cos \omega t, \end{aligned} \right\} . \quad . \quad . \quad (18) \end{aligned}$$

the rate of doing work depended on the expression

$$\begin{aligned} \dot{E}(mn) \cdot \frac{d}{dt} \dot{D}(mn) &= \omega [\{ E_{mn} D_{nm} - D_{nm} E_{nn} \} \cos^2 \omega t \\ &+ E_{nn} D_{mn} \cos 2\omega t + \frac{1}{2} (E_{nm} D_{nm} - D_{mn} \cdot E_{mn}) \sin 2\omega t]. \quad (19) \end{aligned}$$

For a real activity (Force \times Velocity of Displacement) therefore, it is required that

$$E_{mn} D_{nm} - D_{mn} \cdot E_{nn} \neq 0. \quad . \quad . \quad . \quad . \quad (20)$$

The $2\omega t$ terms can contribute nothing to the real average activity. A similar expression will be developed for the action $p(mn) \cdot q(nm)$, and will be used for the interpretation of (17). One thing is certain, from (20) we can never have an expression

$$\frac{D_{nn}}{E_{nn}} = k = \frac{D_{nm}}{E_{nm}}, \quad . \quad . \quad . \quad . \quad (21)$$

where k has an ordinary real scalar value. Expression (20) would under those circumstances reduce to zero, which is contrary to hypothesis. In other words, $\dot{E}(mn)$ and $\dot{D}(mn)$ must, for real activity, be out of phase to some degree at least, and we should write instead

$$\dot{D} = k \dot{E}, \quad . \quad . \quad . \quad . \quad (22)$$

where k for complex operands is also complex*. That is, let

$$k = k_1 - k_2 j, \quad (23)$$

then with

$$\dot{D}(mn) = (D_{nm} + D_{mn}j) \cdot \sin \omega t, \quad . . . (24)$$

$$\left. \begin{aligned} (k_1 - k_2 j) \dot{E}(mn) &= (D_{nm} + D_{mn}j) \cdot \sin \omega t \\ \dot{E}(mn) &= (E_{nm} + E_{mn}j) \cdot \sin \omega t \end{aligned} \right\} . . . (25)$$

We have, by definition for the work done,

$$dW = \dot{E} \cdot d\dot{D} = \dot{E} dt \cdot \frac{d\dot{D}}{dt} = \dot{D} \cdot d\dot{P} = \frac{d\dot{P}}{dt} \cdot d\dot{D}. \quad . . . (26)$$

This follows, because for a generalized momentum \dot{P} the following obtains:

$$\frac{d\dot{P}}{dt} = \dot{E}; \quad \dot{P} = \int \dot{E} \cdot dt. \quad (27)$$

Yet it is to be borne in mind that with

$$\frac{d}{dt} = \omega j, \quad (28)$$

$$\dot{E} = \frac{D}{k} = \frac{d\dot{P}}{dt} = \omega j \dot{P}, \quad (29)$$

showing that the generalized momentum \dot{P} cannot be in time-phase with \dot{D} . To deduce the latter we have

$$\dot{P} = \frac{D}{k\omega j} = -\frac{1}{\omega^2} \cdot \frac{1}{k} \cdot \frac{d\dot{D}}{dt} = \frac{-(k_1 + k_2 j)}{\omega^2 k^2} \cdot \frac{d\dot{D}}{dt} \dagger, \quad (30)$$

where we define for convenience that

$$k^2 = k_1^2 + k_2^2. \quad (31)$$

A relation corresponding to (19) can be obtained for pq

* By k being complex is meant that a component $k_1 E$ of \dot{D} is in time-phase with \dot{E} , but the component of magnitude $k_2 E$ of \dot{D} is in time-quadrature with respect to \dot{E} . The Heaviside-Perry method of complexes, or Resistance Operators, was first extensively treated in Perry's 'Calculus for Engineers' (see pp. 236 *et seq.*). The method is much more powerful than that of Steimetz, since the latter has to do with the effective values of the variables, whereas the Heaviside operational method deals with instantaneous values throughout—an all important difference.

† See author's "Harmonic Algebra," Univ. of Calif. Publ's. Sept. 30, 1919. Also Heaviside, Elec. Mag. Theory, vol. ii. p. 228.

‡ This important result will be employed in developing the differential equation of a Radiating Harmonic Oscillator.

by noting first that

$$\frac{dD(mn)}{dt} = \omega(D_{nm} \cos \omega t - D_{mn} \sin \omega t) \quad . \quad . \quad (32)$$

$$E(mn) = E_{nm} \sin \omega t + E_{mn} \cos \omega t. \quad . \quad . \quad (33)$$

It is the multiplication of the right-hand expressions that leads to (19). For (32), (33), we can therefore substitute

$$\left. \begin{aligned} p(mn) &= (\omega p'_{nm}) \cos \omega t - (\omega p'_{mn}) \sin \omega t \\ q(mn) &= q_{nm} \sin \omega t + q_{mn} \cos \omega t \end{aligned} \right\} \quad . \quad . \quad (34)$$

These should lead to a form similar to (19) by using the substitution $\omega p'$ for D_{nm} and q_{nm} for E_{nm} , etc. However, if instead we write

$$p(mn) = p_{nm} \cos \omega t - p_{mn} \sin \omega t, \quad . \quad . \quad (35)$$

the result will be

$$\begin{aligned} p(mn) \cdot q(mn) &= [(q_{mn} p_{nm} - p_{mn} q_{nm}) \cos^2 \omega t \\ &\quad + q_{nm} p_{mn} \cos 2\omega t + \frac{1}{2}(q_{nm} p_{nm} - p_{mn} q_{mn}) \sin 2\omega t]. \end{aligned} \quad . \quad . \quad (36)$$

The mean action would thus depend on the expression

$$p_{mn} q_{nm} - q_{mn} p_{nm} = B \neq 0, \quad . \quad . \quad . \quad (37)$$

which will be plus or minus depending on whether radiation of energy or absorption exists. Expression (37) indicates in what manner the matrices for p and q are to be built up and moreover, indicates in what manner matrix multiplication is to be understood, and more especially with regard to d or U of (3).

Given that to each generator of a radiating system S are to be allocated a displacement coordinate $q(mn)$ and a momentum coordinate $p(mn)$, with reference to a unit or standard aggregation of generators (time $t=0$) acting as reference, then the two expressions are to be written in the form

$$q(mn) = q_{nm} \sin 2\pi\nu(mn)t + q_{mn} \cos 2\pi\nu(mn)t. \quad . \quad (38)$$

$$p(mn) = -p_{mn} \sin 2\pi\nu(mn)t + p_{nm} \cos 2\pi\nu(mn)t. \quad (39)$$

For simplicity we can write

$$\begin{aligned} q(mn) &= (q_{nm} + q_{mn}j) \sin 2\pi\nu(mn)t = q_{nm}s_{mn} + q_{mn}c_{mn} \\ &= q(nm) + q(mn), \quad . \quad . \quad . \quad (40) \end{aligned}$$

and for the momentum function

$$\begin{aligned} p(mn) &= (-p_{mn} + p_{nm}j) \sin 2\pi\nu(mn)t \\ &= -p_{mn}c_{mn} + p_{nm}s_{mn} = -p(mn) + p(nm). \quad . \quad (41) \end{aligned}$$

Writing out the matrix expressions for the S-system, we then have, for example,

$$p = \begin{Bmatrix} p(11) & p(12) & p(13) \\ p(21) & p(22) & p(23) \\ p(31) & p(32) & p(33) \end{Bmatrix}; \quad q = \begin{Bmatrix} q(11) & q(12) & q(13) \\ q(21) & q(22) & q(23) \\ q(31) & q(32) & q(33) \end{Bmatrix}. \quad (42)$$

Proper regard must, however, be paid to the fact that whereas any $q(mn)$ in q of (42) corresponds to the cosine function, such that

$$q(mn) = q_{mn} \cos 2\pi\nu(mn)t,$$

the $p(mn)$ of p corresponds to the sine function, so that

$$p(mn) = -p_{mn} \sin 2\pi\nu(mn)t.$$

In a similar way the following values hold: .

$$q(nm) = q_{nm} \sin 2\pi\nu(nm)t; \quad p(nm) = p_{nm} \cos 2\pi\nu(nm)t.$$

For convenience, we can set that

$$\nu(mn) = -\nu(nm). \quad . \quad . \quad . \quad (43)$$

We can then write

$$\left. \begin{aligned} q(mn) &= q_{mn} \cos 2\pi\nu(mn)t \\ q(nm) &= q_{nm} \sin 2\pi\nu(mn)t \end{aligned} \right\} . \quad . \quad . \quad (44)$$

$$\left. \begin{aligned} p(mn) &= p_{mn} \sin 2\pi\nu(nm)t \\ p(nm) &= p_{nm} \cos 2\pi\nu(nm)t \end{aligned} \right\} . \quad . \quad . \quad (45)$$

It is then the multiplication of two matrices of the form (10) and (11) rather than (42) that will give the resultant d according to (44) and (45), viz.:

$$\begin{aligned} & p q - q p \\ &= \left\{ \begin{array}{ccc} \{ (p_{11}q_{11} - q_{11}p_{11}) + (p_{12}q_{21} - q_{12}p_{21}) \\ \quad + (p_{13}q_{31} - q_{13}p_{31}) \} & 0 & 0 \\ 0 & \{ (p_{21}q_{12} - q_{21}p_{12}) + (p_{22}q_{22} - q_{22}p_{22}) \\ \quad + (p_{23}q_{32} - q_{23}p_{32}) \} & 0 & \\ 0 & 0 & \{ (p_{31}q_{13} - q_{31}p_{13}) + (p_{32}q_{23} - q_{32}p_{23}) \\ \quad + (p_{33}q_{33} - q_{33}p_{33}) \} \end{array} \right\} \end{aligned} \quad . \quad . \quad (46)$$

A simplified form of the bracket values represented by $p_{mn}q_{nm} - q_{mn}p_{nm}$ in (46) will now be in order.

It has already been pointed out in (30) that the generalized momentum P can be expressed in terms of the generalized displacement D and of \dot{D} . We have, in fact, that

$$P = \frac{D}{k\omega j} = \frac{k_1 + k_2 j}{\omega j k^2} (D_1 + D_2 j) \sin \omega t. \quad . \quad . \quad (47)$$

It follows, therefore, that

$$\begin{aligned} k^2 \omega \dot{P} &= (k_2 - k_1 j)(D_1 + D_2 j) \sin \omega t \\ &= (k_2 D_1 + k_1 D_2) s + (D_2 k_2 - k_1 D_1) c^*. \end{aligned} \quad (48)$$

Thus multiplying through with D to obtain the action, we have

$$\begin{aligned} k^2 \omega P \dot{D} &= [(k_2 D_1 + k_1 D_2) s + (D_2 k_2 - D_1 k_1) c] (D_1 s + D_2 c) \\ &= \{D_1(k_2 D_1 + k_1 D_2) \sin^2 \omega t + D_2(D_2 k_2 - D_1 k_1) \cos^2 \omega t\} \\ &\quad + \{D_1(D_2 k_2 - D_1 k_1) + D_2(k_2 D_1 + k_1 D_2)\} \sin \omega t \cdot \cos \omega t. \end{aligned} \quad (49)$$

It thus appears the average value of the action depends on the expression

$$\frac{1}{2\pi} \oint P \dot{D} dt = [P \dot{D}]_{\text{av.}} = \left\{ \frac{1}{2} \frac{(D_1^2 + D_2^2)}{\omega_{mn}^2} \cdot \frac{2\pi k_2}{k^2} \right\} \frac{1}{2\pi}. \quad (50)$$

Translated into the notation of (36), therefore, we have by (38) that

$$\begin{aligned} p(mn) \cdot q(mn) \big|_{\text{av.}} &= q_{mn} p_{nm} - p_{mn} q_{nm} \\ &= \left\{ \frac{2\pi k_2}{k^2} \cdot \frac{1}{2} \cdot \frac{(q_{mn}^2 + q_{nm}^2)}{\omega_{mn}^2} \right\} \frac{1}{2\pi} = \left\{ \frac{\pi k_2}{2k^2} \frac{|q(mn)|^2}{\omega_{mn}^2} \right\} \frac{1}{2\pi}. \end{aligned} \quad (51)$$

The latter brings out an analogy with the postulate of the quantum theory, for we can write (instead of h/i),

$$\chi_{mn} = \frac{\pi k_2}{\omega_{mn}^2 k^2} (q_{mn}^2 + q_{nm}^2)^\dagger, \quad (52)$$

where χ_{mn} would be a constant for an observation steady state. In any event (51) and (52) do not contain the time. There is then justification in regarding U of (3) as a "unit" matrix.

The following rule can therefore be enunciated. In forming a matrix product of elements the ordinary multiplication rule of algebraic matrices is understood, but in addition it is implied that average or mean time values be inserted in the resultant. As to differentiation with respect to time, it means that the differential of the resultant matrix is the same as the differential with regard to the individual matrices comprising the operand originally, and then taking average time values.

* Here s is employed for $\sin \omega t$ and c for $\cos \omega t$. When dealing with the double periodicity terms, as in the product $P \dot{D}$ of (49), the operators must be translated into c 's, and appropriate s 's introduced for the terms involving the sine functions of the time.

† A later improved form will be shown to involve the momenta rather than the coordinates divided by the frequency.

It is at once apparent from (26) that the amount of work done, as by radiation, can be put into two forms :

$$dW = \dot{D} \cdot dP ; \quad dW = \dot{P} \cdot dD,$$

indicating that W must be a function of P, \dot{P}, D, \dot{D} . If, then, by partial differentiation it is understood that

$$dW = \frac{\partial W}{\partial D} dD + \frac{\partial W}{\partial \dot{P}} d\dot{P}, \dots \dots \dots (53)$$

then this will lead to a solution

$$W = f(P, D), \dots \dots \dots (54)$$

provided that no \dot{P} 's or \dot{D} 's are presumed to appear in the last equation. If they are to appear at all they must do so by substitution only in the partial derivatives

$$\left. \begin{aligned} \frac{\partial W}{\partial D} &= \dot{P} \\ \frac{\partial W}{\partial \dot{P}} &= D \end{aligned} \right\} \dots \dots \dots (55)$$

The latter equations expressing radiation conditions, as a system, are more symmetrical even than the analogous Hamiltonian equations.

Transposing to the notation (5) we have for matrices

$$\frac{\partial W}{\partial q} = \dot{p} ; \quad \frac{\partial W}{\partial p} = \dot{q}, \dots \dots \dots (56)$$

with the reservation, as known from (30), that p is not in phase with \dot{q} . In fact, from (34), we have

$$\left. \begin{aligned} \dot{q}(mn) &= (q_{nm} + j q_{mn}) \sin \omega t ; \\ \dot{q}(mn) &= \omega j (q_{nm} + q_{mn} j) \sin \omega t \end{aligned} \right\} \dots \dots \dots (57)$$

On the other hand, from (30), we also note that

$$\dot{p}(mn) = - \frac{k_1 + k_2 j}{\omega^2 k^2} \cdot \frac{dq}{dt} \dots \dots \dots (58)$$

Thus

$$\dot{p}(mn) = - \frac{1}{\omega^2 k^2} \left\{ \frac{k_2}{\omega} \cdot \frac{d}{dt} + k_1 \right\} \dot{q}, \dots \dots \dots (59)$$

$$\dot{p}(mn) = - \frac{k_1}{\omega^2 k^2} \dot{q} - \frac{k_2}{\omega^3 k^2} \ddot{q}. \dots \dots \dots (60)$$

To develop the differential equation for the Radiating Harmonic Oscillator, the Hamiltonian canonical equations are

$$\frac{\partial H}{\partial p} = \dot{q} ; \quad - \frac{\partial H}{\partial q} = \dot{p}. \dots \dots \dots (61)$$

It was the above equations that were made the basis of

treatment for the Matrix Mechanics. We have, however, seen by (30) that as a condition for real activity (or action) we must have that

$$-\frac{\omega^2 k^2}{k_1 - k_2 j} \cdot p = \dot{q}. \quad \dots \quad (62)$$

This gives a clue for the possible form of \underline{H} . Thus by combining (61) and (62), we have

$$\begin{aligned} \frac{\partial \underline{H}}{\partial p} &= -\omega^2(k_1 - k_2 j)p = -\omega^2 k_1 p + k_2 \omega \frac{dp}{dt} \\ &= -\omega^2 k_1 p + k_2 \omega \dot{p}. \quad \dots \quad (63) \end{aligned}$$

On integrating the last equation, it follows

$$\underline{H} = -\frac{\omega^2 k_1}{2} p^2 + k_2 \omega p \dot{p} + f(q). \quad \dots \quad (64)$$

Applying now the second equation of (61) it is seen that

$$-\frac{\partial \underline{H}}{\partial q} = \dot{p} = \frac{\partial}{\partial q} f(q), \quad \dots \quad (65)$$

whence integrating, the form of \underline{H} must be

$$\underline{H} = -\frac{\omega^2 k_1}{2} p^2 + k_2 \omega p \dot{p} - \dot{p} q. \quad \dots \quad (66)$$

It is the latter equation and not (1) that applies to the problem of radiating systems.

Taking now the case of equation (30), we have, dropping subscripts,

$$p = \frac{q}{k\omega j}; \quad q = (k_1 - k_2 j)\omega j p. \quad \dots \quad (67)$$

If, then, for convenience, we let

$$p = P \sin \omega t', \quad \dots \quad (68)$$

$$q = \omega P(k_1 c + k_2 s). \quad \dots \quad (69) *$$

This means that

$$\dot{p} = \omega j P \sin \omega t' = \omega P c, \quad \dots \quad (70)$$

$$\dot{p} q = \omega^2 P^2(k_1 c^2 + k_2 s c). \quad \dots \quad (71)$$

Turning now to the next to the last term in (66), we likewise have

$$p \dot{p} = P s \omega P c = \omega P^2 s c,$$

so that on multiplying with $k_2 \omega$, we have

$$k_2 \omega p \dot{p} = k_2 \omega^2 P^2 s c. \quad \dots \quad (72)$$

* From (68) and (69) we note that for the absolute value $|p|^2 = P^2$, whereas $|q|^2 = \omega^2 P^2 k^2$. In other words $|q|^2 = 4\pi^2 \nu^2 k^2 |p|^2$. This is the result of (77).

The remaining term gives

$$p^2 = P^2 s^2, \\ \frac{\omega^2 k_1}{2} p^2 = \omega^2 P^2 \frac{k_1}{2} s^2. \quad . \quad . \quad . \quad . \quad (73)$$

Now, adding all the terms together, it follows that

$$-H = \omega^2 P^2 \left\{ \frac{k_1}{2} s^2 + k_1 c^2 \right\} \\ = \frac{3}{4} \omega^2 P^2 k_1 \{ 1 + \frac{1}{3} \cos 2\omega t' \}. \quad . \quad . \quad . \quad (74)$$

The latter equation it is seen indicates a constant component for the total energy \underline{H} , which is given by

$$-H_0 = \frac{3}{4} \omega^2 P^2 k_1. \quad . \quad . \quad . \quad . \quad (75)$$

This type of term means *no radiation*. Such radiation as does appear must come from the variable remainder represented by

$$-H_v = \frac{1}{4} \omega^2 P^2 k_1 \cos 2\omega t'. \quad . \quad . \quad . \quad . \quad (76)$$

The amplitude of the radiation is seen to fluctuate about a mean level H_0 of (75) with equal ranges (energy levels) plus and minus. This accords with the Heisenberg-Born Matrix Condition $n = \pm 1$. In (76) such amplitude has preferably been expressed in terms of the square of the momentum and the frequency.

To transform (76) as well as condition (52) use can be made of (69), which gives

$$|q|^2 = \omega^2 P^2 k^2 = \omega^2 k^2 |p|^2, \quad . \quad . \quad . \quad . \quad (77)$$

yet it is better to refer to the momenta amplitudes rather than the coordinate ones in order to emphasize the analogies with the quantum theory. We then have that

$$\chi = \frac{\pi}{2} k_2 P^2 = \frac{\pi}{2} k_2 |p|^2, \quad . \quad . \quad . \quad . \quad (78)$$

which is of the order of an energy (or quantum).

The ratio of the two energies above is given by

$$\frac{H}{H_0} = \frac{1}{3}. \quad . \quad . \quad . \quad . \quad (79)$$

It is significant that H_0 corresponds to the constant aggregate energy of the non-radiating harmonic oscillator heretofore employed, whereas H_v represents the amplitude of the fluctuating absorption and radiating component. Nothing is indicated about the "orbital periodicity" with which the potential and kinetic energies interchange in the

H_0 system. Whether there is a relationship of this latter with the half frequency component of the Nernst-Lindemann formula has yet to be determined, at least it is suggestive. In any case one thing is certain, equation (79) has been arrived at on purely classical lines, and it shows as a consequence of applying Hamilton's canonical equations that an unexcited harmonic oscillator, when caused to radiate by virtue of an impressed field of force, only then becomes radiating when it can absorb and re-radiate a definite discrete quantum of energy equal to $1/3$ of its normal unexcited content. This corresponds exactly with one of the conditions of the Planck-Bohr developments.

Indeed, an harmonic oscillator of the organ-pipe type does not give an appreciable increase of volume with increased blowing pressure. A point is soon reached when the dominant frequency takes a discrete jump in conformity with Bohr requirements.

APPENDIX.

Employing the bracket notation of Dirac, let

$$pq - qp = [q, p] = U,$$

$$- [q, p] = [p, q].$$

To interpret $[q, p^2]$, we note

$$[q, p^2] = p^2 q - qp^2 = p(pq) - (qp)p = p(pq - qp) + (pq - qp)p = pU + Up = 2p \cdot U.$$

In a similar manner it can be shown that

$$[q^2, p] = 2qU,$$

indicating quite generally

$$[q, p^n] = np^{n-1} \cdot U = \frac{\partial}{\partial p} p^n.$$

$$[q^n, p] = \frac{\partial}{\partial q} q^n.$$

In fact, as a simple extension for functions of q and p expressible as a series, we should have, dropping the unity matrix, that

$$[F(p, q), p] = \frac{\partial F}{\partial q}; \quad [q, F(p, q)] = \frac{\partial F}{\partial p} *.$$

* Kind acknowledgements are made to Dr. A. S. Eve, Director of the Physics Department of McGill University, to Professor A. H. S. Gillson, and to Dr. J. S. Foster, for their interest and criticisms.

CXI. *On the Behaviour of Small Quantities of Radon at Low Temperatures and Low Pressures.* By ALOIS F. KOVARIK, Ph.D., D.Sc., Professor of Physics, Yale University*.

THE temperature at which radon condenses or volatilizes was first investigated by Rutherford and Soddy †. They found that radon commences to volatilize at 120° absolute in their experiments in which a current of gas passed through the apparatus, and at 123° absolute in a stationary atmosphere. Boyle ‡, using the flow method, found the volatilization temperature at about 113° absolute. Laborde § found the same temperature of volatilization 120° to 122° absolute in spirals of copper, iron, tin, and silver, but about 20° lower in glass; Boyle's experiments, however, did not show any material difference for the metals and glass. Boyle and others have observed that radon at liquid-air temperature exhibits a vapour pressure, and Rutherford || was the first to measure the vapour pressure when radon condensed to form a liquid. This was later also done by Gray and Ramsay ¶. In these experiments large quantities of radon were used and a liquid radon was observed. Several observers, using small quantities of radon, have observed variations in the vapour pressure as a function of the quantity of radon used. The first of these observations are recorded by Russ and Makower** and by Boyle ††, and more recently by Fleck ‡‡ in his investigations of the condensation temperatures of radon and thoron. While Boyle's experiments bear out the general conclusion that a vapour phase of radon exists at any temperature, the numerical results were found to be irregular. It is also to be pointed out that since radon and thoron are isotopes, the temperatures of volatilization of radon and thoron should be the same; the problem was attacked by Fleck.

Rutherford, in his 'Radioactive Substances and their Radiations,' discusses these problems in some detail. Recently, while enjoying the hospitality of Cambridge

* Communicated by Prof. Sir E. Rutherford, O.M., P.R.S.

† Rutherford & Soddy, *Phil. Mag.* v. p. 561 (1903).

‡ Boyle, R. W., *Phil. Mag.* xx. p. 955 (1910).

§ Laborde, *Le Radium*, vi. p. 289 (1909); vii. p. 294 (1910).

|| Rutherford, E., 'Nature', lxxix. p. 457 (1909); *Phil. Mag.* xvii. p. 723 (1909).

¶ Gray & Ramsay, *Trans. Chem. Soc.* xcv. p. 1073 (1909).

** Russ & Makower, *Proc. Roy. Soc. A*, lxxxii. p. 205 (1909).

†† Boyle, R. W., *Phil. Mag.* xxi. p. 722 (1911).

‡‡ Fleck, A., *Phil. Mag.* (6) xxix. p. 337 (1915).

and the Cavendish Laboratory, the writer found Rutherford still much interested in these problems, and at his suggestion attempted the research which finally took the form embodied in this paper, and which is, briefly, an attempt to measure the vapour pressures of small quantities of radon at low temperatures under conditions of low pressure in the apparatus. Preliminary experiments were also carried out on the volatilization temperature under similar conditions of low pressure and small quantities of radon. Some experiments on the vapour pressure were repeated, extending the range of temperature, on my return to Yale.

From what we know of the equilibrium relations between the vapour-liquid and vapour-solid phases in the case of ordinary substances, we are forced to conclude that similar relations should hold in the case of radon, as indeed was shown for the vapour-liquid equilibrium by Rutherford and by Gray and Ramsay. When small quantities of radon are used, we cannot conclude that the condensed phase is either liquid or solid, for it is possible that it may be a condensation of single atoms into a layer which may not be even mon-atomic. In the latter case the work function may be quite different; and if the energy of "volatilization" of atoms of radon from a surface of glass should be greater than from solid radon, then the pressure of the radon vapour may be considerably smaller in the former case. The results of these experiments indicate this to be the case, but they also suggest that some radon may, at a very low temperature, also be solid radon, and that in different experiments the conditions for such dual condensation may vary, thus explaining the various irregularities that have been heretofore observed. In such a case one would expect that if sufficient time elapsed after the condensation took place, the phase with a higher vapour pressure would pass into the phase of lower pressure before real equilibrium was established. This, however, may not be observed in the ordinary procedure of the experiments. The observations are given in detail as the results may be found to have theoretical significance, for, if radon atoms could be condensed singly, the question arises whether or not the forces holding the atoms should be necessarily great since radon is inert and the explanations* of such forces in case of ordinary elements is based on action of valence electrons.

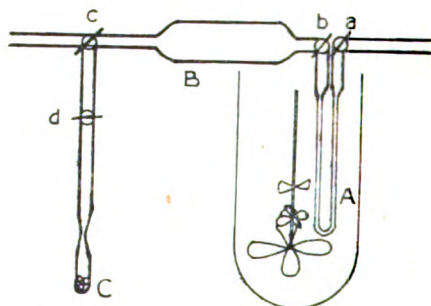
* Compare Langmuir, I., *Am. Chem. Soc. Journ.* xl. p. 1361 (1918).

Method and Apparatus.

Briefly the method of procedure to find the vapour pressure of radon at any temperature was as follows. Radon was condensed at liquid-air temperature in one part of the apparatus, which was then exhausted to a fairly low pressure. The radon was then subjected to a temperature desired, and after keeping it at this temperature for some time, it was allowed to diffuse into a known volume until a steady state was reached. The gaseous radon in the known volume was then collected in a charcoal tube immersed in liquid air. Similarly, the rest of the radon used was also collected. Later, the amounts of radon collected were measured, and from these measurements the pressure of the radon in the known volume was determined; and by using Knudsen's relation of pressures at different temperatures in the same vessel, the pressure at the experimental temperature was deduced.

The essential parts of the apparatus are shown in fig. 1.

Fig. 1.



A was a U-shaped tube of 0.336 cm. internal diameter, having Failla internally-sealed vacuum stop-cocks at the two ends. Radon was condensed in A. Through one of the stop-cocks, *a* (of large bore), radon was admitted into A; through the other, *b*, it could be allowed to diffuse into B, which in some experiments included the tubing *cd*. One arm of the three-way stop-cock, *c*, led to C through the stop-cock, *d*. C contained a small quantity of coconut shell charcoal, above which was a constricted portion of the tube for sealing-off purposes. When C was in the liquid-air bath the radon in B could be collected. Similarly, the radon in A—after removing A from its bath—could be collected into another similar tube, C, attached for this purpose. The third outlet from the three-way stop-cock led

to a rapidly-evacuating pump, a mercury pump, McLeod gauge, Plücker tube gauge, P_2O_5 bulbs, and charcoal bulbs used for evacuation purposes.

During an experiment, A was placed in a bath of pentane or of ligroïne (petroleum ether) contained in a pyrex glass tube, part of which extended into liquid air. The bath was kept constantly stirred. In some experiments this stirrer moved up and down about the U-shaped tube A, and in other experiments it was made of vanes on a rotating rod, two sets of vanes on the side of A being small and larger ones below A. A thermocouple of copper and constantan having one junction on the side of the lower part of A and the other in melting ice was used to measure the temperature.

The procedure in an experiment was as follows. The apparatus was exhausted and the radon was transferred by means of mercury into the apparatus, and by diffusion passed over P_2O_5 through the stop-cock *a* into A, the other stop-cock, *b*, being closed and A being immersed in liquid air. After about twenty minutes *a* was closed, *b* was opened, and *c* turned to shut off C, but allowing connexion with the pumps and gauges. By means of pumps the uncondensed gases with some radon were collected over mercury so as not to contaminate the laboratory with free radon. Exhaustion was carried on to a pressure of about 2 to 5×10^{-6} mm. Hg, and then the U-tube was closed off. Charcoal bulbs in liquid air in the pump-gauge system were then used to clear the vessel B of all radon. These charcoal bulbs were then closed, and the three-way stop-cock was turned to shut off the pumps, leaving B with *cd* connected or leaving B alone. A was now placed in its bath of ligroïne, and the desired temperature* of the bath was obtained by regulating the amount of immersion into liquid air, the stirrer being in operation. The temperature was read from the calibrated thermocouple, but an accurate pentane thermometer was always also used in the bath. After every experiment the temperature of boiling oxygen was obtained by the thermometers for checking purposes. When a desired temperature was kept constant for half an hour, A was connected to B, and the bath was kept continually at the desired temperature for another half-hour, after which A was again closed off. By trials it was found that one half-hour was sufficient time at the pressures used to get into what seemed to be an equilibrium state between A and B, as shown by the

* Bath for the very low temperatures was liquid air alone either freshly prepared or older.

fact that in a longer period no greater amount of radon apparently was diffused into B.

C having been previously heated and evacuated was now put into liquid air and the connecting stop-cock with B opened. Fifteen minutes was sufficient to collect the radon from B. While C was in liquid air it was sealed off. Another similar charcoal tube was sealed on, and the tube was heated and evacuated and made ready to collect the radon remaining in A. The time of the experiment was noted so as to be able to calculate the amounts of radon at the time of the experiment. The amount of radon was determined by γ -ray measurements with the following apparatus, which was found admirable for comparisons of any quantities. A large size cylindrical can, 64 cm. long and 44 cm. diameter, was fitted out as an ionization vessel. Along the axis was a lead tube of 1 cm. thickness and having an axial opening large enough to allow the introduction of the specimen to be tested or the radium standard to be used in the calibration. In this way the ionization was produced by γ -rays after passing through 1 cm. of lead. Half-way between the lead tube and the walls of the can was a cylindrical electrode of sheet iron, which was connected to an electroscope. Owing to the great length of the cylinder, the slight variations in the size of the specimens (the charcoal radon tubes) made no difference, and in fact a displacement of these from the middle point by as much as 2 cm. could not be detected in the ionization readings. Several hours after the charcoal radon tubes were sealed, measurements were made, several in number extending over several days; and in each case the instrument was standardized by taking measurements of the ionization current when one of three radium standards (0.15 mg., 1.305 mg., 5.00 mg.) was put in the middle of the lead tube, using in any particular case that standard which most nearly coincided with the γ -radiation effect of the radon tubes. All readings for a given specimen were extrapolated to zero time and averaged. The result is the amount of radon in curies collected in each case. The results for the various experiments are given in columns 2 and 5 (Table I.).

Precautions and Criticisms.

It might be supposed that the radon gas may be occluded on the walls of the glass tubes leading to the charcoal bulb, and that in this manner some radon would be lost and not be collected in the charcoal tube. This

was tested by filling the apparatus with about 16 millicuries of radon at the usual low pressure, A being initially at liquid-air temperature, and after reduction of pressure both A and B being brought to room temperature. The radon was left in the apparatus for two hours, after which it was collected in the usual way, and a new tube was sealed on and evacuated, A and B having been closed off during this process. The pump-gauge system was then closed off and A and B were connected to C, which was in liquid air and was collecting any residual gas. All the glass tubes were heated for half an hour by a Bunsen burner up to as high a temperature as possible without causing a caving-in at any place. C was sealed off, and measurements on it showed a trace of radon, but only of a magnitude comparable to the natural leak of the measuring apparatus. Consequently, no appreciable amount of radon could be lost by occlusion to the walls of the apparatus.

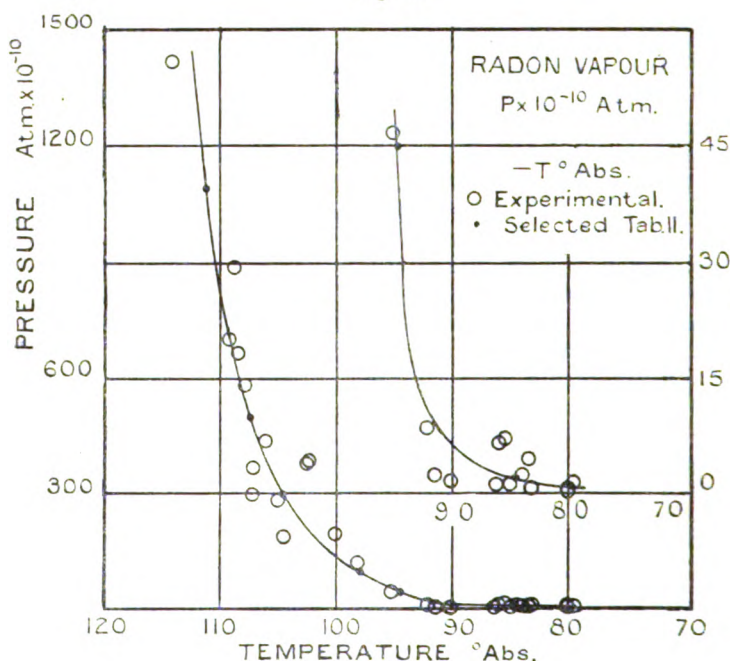
While the stop-cocks *a*, *b*, *c* were mercury sealed and graphite was used as a lubricant in most of the later experiments, small amounts of stop-cock grease of low vapour pressure were used in the first experiments. It is generally believed that radon is absorbed by the grease. Experiments were tried with large amounts of stop-cock grease put into the apparatus and exposed to 20 millicuries of radon for an hour. After collecting the radon and opening the apparatus, and collecting most of the grease so exposed and putting it along with the collectors (cleaners) into a test-tube and sealing it, it was found that the activity at the beginning was all due to radioactive deposit produced from the radon while this was in contact with it, and that after six hours a mere trace of activity could be detected. Consequently, in those experiments in which stop-cock grease was used no appreciable amount could have been lost by absorption by the grease.

Experiments were also tried to find the time necessary to collect in C all the radon in B. It was found that no residual radon could be collected from B after C had been collecting for ten minutes, even when one hour was allowed to collect any possible residual radon. It seems, therefore, that whatever gaseous radon was in the apparatus from which it was collected by C was for all practical purposes collected, and that the amount found in the charcoal collecting-tube represents the amount dealt with in the experiment. It would seem, therefore, that the radon in B which during an experiment was in apparent equilibrium with the radon in A was for all practical purposes all

collected in C. The determination of its quantity by the ionization method was certainly the most accurate part of the experiment.

The galvanometer used in connexion with the thermocouples gave a deflexion of the order of 4 divisions per degree, and each division could be estimated to at least one-fifth part. The actual temperature determinations were certainly correct to 1° centigrade, yet it will be noticed

Fig. 2.



from the curve (fig. 2) that the points do not lie on a smooth curve. The reasons for this must be looked for elsewhere, and these will be alluded to later.

Results.

The results of the experiments are given in Table I. The measured amount of radon collected from B is given in column 2, and the amount collected from A is given in column 5. Column 4 gives the radon in B in curies per cm^3 . B was at room temperature, which was taken in the calculations uniformly as 17°C . The pressure

TABLE I.

1.	OBSERVED VALUES.			CALCULATED VALUES.						
	2.	3.	4.	5.	6.	7.	8.	9.	10.	11.
T. Abs. temp.	Radon in B, 10^{-6} curie.	Volume of B, cm. ³	Radon in B, 10^{-6} curie cm. ³	Radon in A, 10^{-6} curie.	Radon compensated in A, 10^{-6} curie.	$p \cdot 10^{-10}$ atm. Pressure of B in B at 200 abs.	$P \cdot 10^{-10}$ atm. Equilibrium pressure in A at T, $P = P \cdot 200$	Log P.	$\frac{1}{T}$	
114.1	11130	31.21	357	5030	1730	2265	1122	-0.817	0.00877	C
109.4	5630	"	180.4	3095	1455	1114	705	-7.152	-0.00913	C
108.8	7300	31.65	230	7130	4408	1458	894	-7.040	-0.00919	Y
108.4	5380	31.21	172.2	3730	2187	1092	668	-7.175	-0.00923	C
108.1	4710	"	151	7320	6150	955	589	-7.250	-0.00925	C
107.1	2980	"	165.5	12500	11532	606	368	-7.134	-0.00934	C
107.1	7490	96.2	77.9	2195	16572	494	209	-7.524	-0.00934	Y
108.1	3600	31.21	115.3	17810	16662	731	444	-7.353	-0.00942	C
105.1	2330	"	74.6	15180	14802	478	286	-7.544	-0.00951	C
104.4	4830	96.2	50.2	1027	1332	318	191	-7.719	-0.00957	Y
102.6	3175	31.21	101.7	2255	1333	645	384	-7.416	-0.00974	C
102.5	3228	31.65	102	2000	1692	647	386	-7.413	-0.00975	C
100.1	1650	31.21	52.8	19762	19283	336	197.5	-7.704	-0.01001	Y
97.1	1087	"	31.8	6068	6652	221	127.4	-7.805	-0.01029	C
95.1	506	39.27	12.9	4365	4212	84.8	168	-8.330	-0.01052	C
92.1	75.5	31.21	2.12	12300	12278	15.4	808	-9.082	-0.01086	C
91.6	212	"	67.9	12375.5	12314	43.1	2.43	-9.614	-0.01101	C
90.1	188	39.27	4.8	4871	4814	30.4	1.71	-9.767	-0.01110	Y
86.3	122	31.21	0.301	12587.5	12584	2.48	1.36	-9.866	-0.01159	C
86.1	62.0	"	1.99	12230	12212	12.62	6.88	-9.161	-0.01161	C
85.6	65.6	"	2.10	8725	8706	13.32	7.23	-9.141	-0.01165	C
85.1	12.4	"	0.337	19750	19746	2.52	1.36	-9.865	-0.01175	C
84.6	6.35	"	0.204	4678	4678	1.295	0.70	-10.155	-0.01182	C
84.1	30.2	39.27	0.77	5059	5050	1.88	2.63	-9.589	-0.01189	Y
83.6	41.3	31.21	1.323	21412	21400	8.39	4.52	-9.345	-0.01196	C
83.1	8.3	"	0.266	9128	9128	1.70	0.91	-10.041	-0.01206	C
80.1	1673	96.2	0.174	771	769	1.105	0.53	-10.337	-0.01248	Y
80.1	4.3	31.65	0.136	12220	12218	0.86	0.46	-10.337	-0.01248	Y
79.6	1038	39.27	0.265	6128	6125	1.72	0.88	-10.056	-0.01256	Y
149.1	1820	31.21	58.3	186	None	C
117.1	9000	"	308	2006	"	C

produced by the radon in B at 290° absolute can be calculated by using the value for the volume of 1 curie at N.P.T. The mean of the experimental values of Rutherford, Debierne, and Gray & Ramsay, weighting their mean values equally, is $5.97 \times 10^{-4} \text{ cm}^3$. Using Geiger and Werner's* value for the number of α -particles emitted per second per gram radium, we get the same volume. Consequently, 1 curie per cm^3 at 290° absolute produces a pressure of

$$5.97 \times 10^{-4} \times \frac{290}{273} = 6.342 \times 10^{-4} \text{ atmosphere.} \quad \text{Column 7}$$

gives the pressure in B at 290 abs. calculated from the amount of radon per cm^3 as given in column 4. Now, the pressure in B at 290° absolute was in equilibrium with radon at a different pressure (Knudsen) in A, which was at the low temperature. Knudsen found that at low pressures, when the mean free path of molecules was very large in comparison with the size of the tube, the pressures at places of different temperature were connected by the relation

$$\frac{p}{\sqrt{T}} = \text{constant.} \quad \text{Consequently the pressure of the gaseous}$$

radon in A can be calculated from $\frac{p}{\sqrt{290}} = \frac{P}{\sqrt{T}}$, where p

and P are the pressures in B and A respectively. These values are given in column 8, and are the pressures of gaseous radon in equilibrium with condensed radon at a temperature T . The letters C and Y in the last column refer to the experiments performed at Cambridge and Yale respectively. The total volume of A was 11.86 cm^3 and 9.08 cm^3 for the C and Y experiments respectively, and the volume immersed in the bath at T temperature was 0.46 cm^3 and 0.52 cm^3 respectively. Using these data, a calculation can be made giving, at least approximately, the amount of gaseous radon in A, and by subtracting this amount from the amount of radon collected from A, one gets a value giving approximately the amount of radon condensed in A. These quantities are entered in column 6. The results given at the end of the table show according to such calculation that no radon was condensed in those experiments. Plotting the pressure in atmospheres against the absolute temperature, one gets the curve in fig. 2; and plotting the common logarithm of the pressure against the reciprocal of the absolute temperature, one gets the distribution of points shown

* Geiger & Werner, *Zs. f. Phys.* xxi. p. 187 (1924).

in fig. 3. The straight line drawn in fig. 3 is the nearest approach to a linear relation of the form $\log P = -a \cdot \frac{1}{T} + K$. In this case $a=970.15$, $K=1.787$. Selecting seven points from the smooth curve in fig. 2, as given in Table II. below, and assuming the form of relation between P and T

Fig. 3.

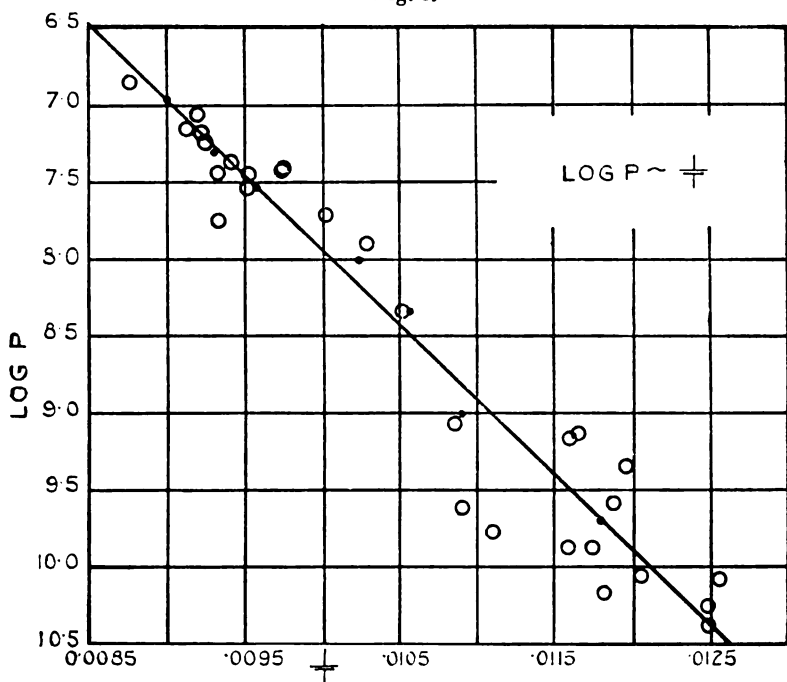


TABLE II.

P.	T.	$\frac{1}{T}$	$\log_{10} P$	
1100×10^{-10} atm.	111.1 abs.	0.00900	3.04139-10	-6.9586
500 "	107.4 "	.00931	2.69897-10	-7.3010
300 "	104.4 "	.00958	2.47712-10	-7.5229
100 "	97.8 "	.01023	2.00000-10	-8.0000
45 "	94.6 "	.01057	1.65321-10	-8.3468
10 "	91.7 "	.01091	1.00000-10	-9.0000
2 "	84.7 "	.0118	0.30103-10	-9.6990

1272 Prof. Kovarik *on the Behaviour of Small Quantities of*
to be $\log P = -a \frac{1}{T} + b \log T + C$, one gets the following
values of a , b and c : $-a = 968.479$, $b = 0.3021$, $c = 1.1579$;
and if natural logarithms are used, $a' = 2230.0$, $b' = 0.3021$,
 $c' = 2.6662$. If the form of the equation is

$$\log P = -a \frac{1}{T} + \frac{5}{2} \log T + C,$$

we get for the constants (common logarithms used)

$$a = -822.5 \text{ and } c = -4.77.$$

The best representation is given by

$$\log P = -968.479 \frac{1}{T} + 0.3021 \log T + 1.158.$$

Discussion of the Results.

Even though the points do not fall on a smooth curve and are somewhat irregularly spaced, the results give ample evidence that an equilibrium seems to exist between the gaseous state and the condensed state of small quantities of radon. It cannot be said that the condensed state represents solid radon. In fact, from what follows, one must conclude that the condensed state does not form uniformly and in the same way in the various experiments, and that it is probably a monatomic condensation and may be in parts also solid radon. In support of this idea the following deductions may be used. If Gray and Ramsay's results are plotted as $\log P$ against $\frac{1}{T}$, one gets a straight line which is well repre-

sented by the equation $\log P = -863 \frac{1}{T} + 4.083$. This equation gives the relation between gaseous radon and liquid radon in equilibrium. If we extrapolate to the temperature of solid radon which Gray and Ramsay give as 202° abs. (or to about 160° abs., which is probably more nearly correct *) and obtain the equilibrium pressure, and do likewise by using the equation representing the relation of radon and "condensed" radon as found in these experiments, we shall find that the extrapolated pressure from Gray and Ramsay's equation will be upwards of 500 times as great as the pressure obtained from the equation representing the results of these experiments. Assuming the permissibility of extrapolation in both cases, the pressures should be

* Paneth & Rabinowitsch, *Ber. d. Deut. Chem. Ges.* lviii. p. 1138 (1925).

the same. It seems justifiable to conclude that in the "condensed" state of the small quantities of radon in these experiments, the work function is greater than it would be if the condensed state represented truly a solid radon obtained by freezing liquid radon, and that probably all or part of the condensed radon is in a less-than-monatomic layer. If the U-tube in which the radon is condensed in liquid air is taken out of its bath and viewed, it is found to be luminous throughout, but shows some specks of greater brightness than the general luminosity. It is therefore possible that some radon may condense into a liquid and freeze at points which might for one reason or another be first cooled to the lowest temperature; and if this is so, and if these points may be different in different experiments, the relative amounts of solid radon and otherwise monatomic condensed radon will be different, and the average work function may be different in different experiments even if the temperature of the bath should be the same. This may explain the somewhat irregularly-spaced points along the curve, although here one may argue that the thermocouple junction, placed as it was on the outside lower end of the U-tube, may not give accurately the temperature of the radon in the tube. In the long time taken during each experiment for the bath to become constant, it would seem that only a slight shift along the temperature axis should result, whereas a varying force function will account for the greater irregularities observed. If these irregularities are due to a slightly wrong temperature reading, they should not be so pronounced as the curve (shown on enlarged scale) for the *low* temperatures shows them to be.

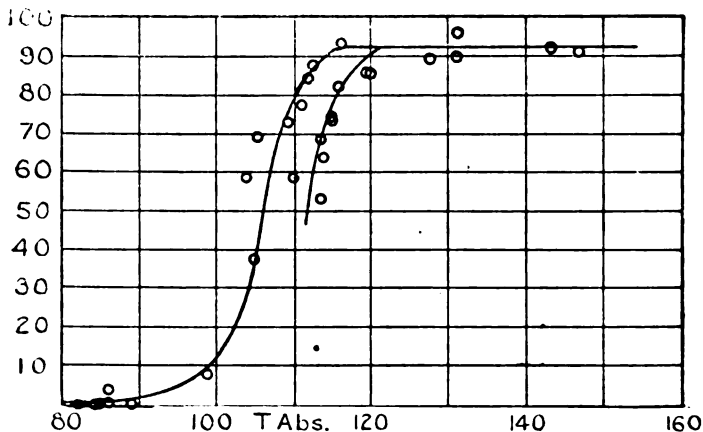
Also, if we assume the pressure from Gray and Ramsay's equation for the freezing temperature of radon, and substitute into the equation obtained from these experiments and solve for T , we shall get a temperature about twice as great as that assumed for the freezing temperature. This is quite in accord* with experiments on the temperature at which monomolecular layers of vapours may be driven off the surface on which they are condensed, the temperature being much above the boiling-point of the substance.

As a further support of the argument that the condensation is very likely not always of one kind, it is desired to refer to some preliminary experiments on the volatilization temperature of small quantities of radon in a glass tube, using the

* Becker, J. A., *Phys. Rev.* (2) xxviii. p. 341 (1926); but compare also Holst & Clausing, *Physica*, vi. p. 48 (1926).

apparatus of the preceding experiments. In the apparatus exhausted to a low pressure the radon in A was subjected to a definite temperature for at least half an hour. The vessel B was connected to A for half a minute. The radon diffusing into B was then collected in C, and so was also the remainder of the radon in A. The radon collected from B as a fraction of the total amount used is plotted against the temperature in fig. 4. It is desirable in these experiments to make the time of diffusion as short as possible, so as to prevent possible evaporation on account of the reduced pressure, and yet get the major part of the gaseous radon. Experimenting with radon in A at room temperature, it was found that in half a minute over 90 per cent. of the radon was diffused into B, and at low temperatures half a minute

Fig. 4.



was found to be the most suitable time for the diffusion. The radon collected becomes an approximate measure of the gaseous radon in A. A break in the curve should indicate the volatilization or condensation temperature. It will be noted from fig. 4 that for low temperatures the points can be arranged along two curves, one of which may be a variable one depending on the apparatus. The two volatilization temperatures seem to be about 116° and 121° absolute, the sort of values recorded by other investigators for the volatilization temperature.

If condensation of small quantities of radon may take place in these two ways—namely, to form at certain points of initial lowest temperature minute droplets of liquid radon, and these later freeze and at other points (the rest of the cooled surface) single atoms become attached to the surface

of the glass,—and if the vapour pressures of these two states are different, it would seem that if a sufficiently long time were allowed, that state which has the greater vapour pressure would change into the other. If the time required to effect this is long, intermediate values of vapour pressure would be measured in the actual experiment.

In connexion with the equation giving the relation between pressure and temperature, it may be of interest to note that the constant $C=1.158$ has a value which does not differ much from $\frac{3}{2} \log 222 - 1.622 = 1.898$, where 222 is the atomic weight of radon and -1.622 is the “universal constant” of Edgerton*.

Summary.

1. In summarizing, it can be said that the gaseous radon existing in actual or transient equilibrium with the condensed radon was collected and measured, and from such determinations for various low temperatures it was found that the deduced vapour pressure decreased with the lowering of temperature, and that its value is connected with the temperature by the equation

$$\log P = -968.479 \frac{1}{T} + 0.3021 \log T + 1.158.$$

2. The distribution of the points in the pressure-temperature curve shows irregularities far too great to be accounted for by experimental errors. This indicates a possible explanation that the condensation may be partly monatomic on the cooled surface and partly frozen minute droplets of radon. This argument is supported by various deductions and observations.

3. The volatilization temperatures of small quantities of radon condensed in a glass tube seem to be either 116° or 121° absolute.

In conclusion, I desire to thank Professor Sir Ernest Rutherford for the hospitality and continued friendship shown me, and suggesting the work on this interesting problem and for placing at my disposal the necessary equipment. I also wish to express my gratitude to the Memorial Hospital in New York City for their kindness in supplying me with the radon used in the experiments at Yale in checking up and extending the observations made at Cambridge.

Yale University, New Haven.

June 1, 1927.

* Edgerton, A. C., *Phil. Mag.* (6) xxxix. p. 1 (1920).

CXII. *The Crystallography of some Simple Benzene Derivatives.*
By W. A. CASPARI, D.Sc., Ph.D.*

THE investigation of crystals of organic substances of which the structural formulæ (as decided by chemical evidence) are based on the benzene ring has not, so far, brought any certainty as to the configuration of atoms in benzene and its derivatives in the crystal state. The hydrocarbons naphthalene and anthracene have indeed yielded to X-ray examination preliminary results of considerable interest†, and several other benzene and naphthalene derivatives have been studied. Advances in our knowledge of the crystal structure of such derivatives are to be expected either from advances in X-ray technique and interpretation or, as was found practicable in the case of naphthalene and anthracene, from comparisons of the X-ray data for different crystals. It may be well, therefore, to place on record the primary data for as many crystals as possible.

The substances here dealt with contain, chemically speaking, one benzene ring with no other substituent groups than hydroxyl, $-\text{OH}$, and the amino-group, $-\text{NH}_2$. The only mono-substituted body of this class which is solid at ordinary temperatures is phenol. Owing to its deliquescence and volatility, phenol is difficult of treatment by goniometric or X-ray methods, and only tentative data as to its crystallography have hitherto been published. Of the di-substituted derivatives, however, the three dihydroxybenzenes have been examined both goniometrically‡ and by X-rays§. Para-phenylene-diamine||, ortho-phenylene-diamine¶, and para-amino-phenol** have received attention from crystallographers, but no members of these two groups have been subjected to X-ray analysis.

The X-ray examination of the crystals described in the sequel has been carried out mainly by the rotating-crystal method, followed by indexing of the reflexion spots appearing on the photographs. The cell-dimensions, number of molecules in the cell, and space-group have been determined.

* Communicated by the Author.

† W. H. Bragg, *Proc. Phys. Soc. Lond.* xxxiv. p. 33 (1921).

‡ P. Groth, *Chem. Kristallographie*, iv. pp. 84-87.

§ W. H. Bragg, *J. Chem. Soc.* cxxi. p. 2766 (1922). W. A. Caspari, *ibid.* 1926, pp. 573, 2944; 1927, p. 1093.

|| C. Hintze, *Zeits. f. Krist.* iv. p. 552 (1884).

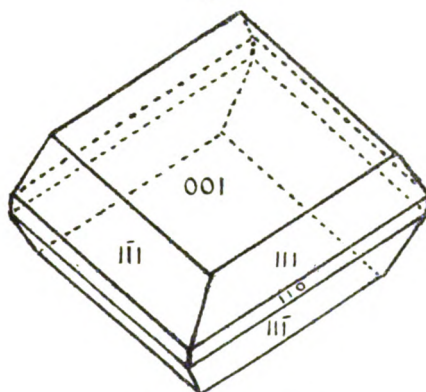
¶ P. Groth, *ibid.* iv. p. 276.

** W. Keith, *N. Jahrb. f. Min.* vi. p. 196 (1889).

Ortho-phenylene-diamine, Nc1ccccc1N, crystallizes from water,

chloroform, or benzene in flat plates of almost rectangular contour. With this crystal, as with many others, the rule was found to hold good that solvents of the water and alcohol type are apt to exaggerate tabular or acicular habit, whilst those of the chloroform and benzene type produce crystals of a more isometric tendency. The crystal is found to be monoclinic-prismatic, $\beta = 121^\circ 10'$, principal forms (001), (111), (11 $\bar{1}$), and (110), the latter feebly developed (fig. 1). Density, determined in this and the succeeding

Fig. 1.



o-Phenylene-diamine.

cases by flotation in a mixture of chloroform or carbon disulphide with petroleum spirit, 1.205. The X-ray photographs gave the following results:—

Cell-dimensions, $a = 7.74 \text{ \AA.}$

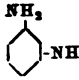
„ $b = 7.56 \text{ \AA.}$

„ $c = 11.76 \text{ \AA.}$

No. of molecules in cell, $n = 4$ (found, 3.98).

The c -axis diagram exhibits very markedly preponderating intensities in even layer-lines; a layer of molecules very similar to that in (001) is therefore to be expected halfway up the c axis of the cell. Reflexions from 40 planes in all were identified in the photographs, the strongest being from (001), (110), (112), (120), and (122). No halvings were apparent among the (hkl) planes, but in all the ($h0l$)

planes noted (ten altogether) h was even. Reflexions from (010) and (020) occur. The crystal must be placed in space-group C_{2h}^4 , with the simple lattice Γ_m (cf. Astbury and Yardley's Tables, Phil. Trans. 1924, cciv. p. 221).

Meta-phenylene-diamine, , is even more easily oxidizable than the other substances here dealt with, and should be freshly distilled before crystallization. Crystals may be obtained by slow evaporation of chloroform solutions, or by cooling of melted substance to which a little water has been added. They are orthorhombic-bipyramidal, and have the habit of rectangular parallelepipeds showing (100), (010), and (001), rarely also small dome and pyramid faces. Their general tendency is to be tabular along (001) and somewhat elongated along the b axis. Density 1.225. The X-ray data are as follows:—

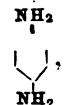
$$a = 11.97 \text{ \AA.}$$

$$b = 8.14 \text{ \AA.}$$

$$c = 23.61 \text{ \AA.}$$

16 molecules to the cell (found, 15.86).

The photographs are unusually well filled with reflexion spots. The greatest intensity is shown by (014), (024), (114), (124), (120), (200), (210), and (221). In all these diagrams the row-lines are for the most part occupied by spots without a gap up to the farthest layer-line. There are therefore no halvings, and the space-group can only be Q_h^1 , with the simple lattice Γ_0 . With this lattice, however, there cannot be more than eight asymmetric molecules to the cell. *Meta-phenylene-diamine*, therefore, would appear to be one of the examples, several of which are now known, of a crystal in which more than one molecule—in this case two—unite to form an asymmetric lattice unit.

Para-phenylene-diamine, , crystallizes from solvents of the acetone and alcohol type in monoclinic-prismatic plates tabular along (001) having the habit described by Hintze (*l. c.*). Petroleum spirit yields excessively thin leaflets of rhomboidal contour. From chloroform, compact all-round crystals are obtained in which several faces of the $h0l$ zone are well developed. Density 1.245. For the X-ray rotation photographs, Hintze's axes and β -angle

were taken and confirmed by the photographs themselves. The results are as follows :—

$$a = 8.29 \text{ \AA.}$$

$$b = 5.93 \text{ \AA.}$$

$$c = 24.92 \text{ \AA.}$$

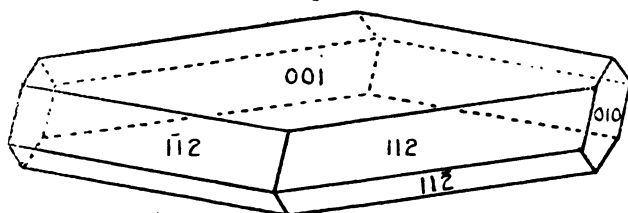
$$\beta = 112^\circ 58' \text{ (Hintze).}$$

8 molecules to the cell (found, 7.85).

The crystal reacts exceptionally well to the X-rays, and 57 planes were identified on the photographs, the strongest reflexions being from (004), (011), (110), (111), ($1\bar{1}\bar{1}$), ($10\bar{4}$), (200), and (201). No (hkl) or ($h0l$) halvings could be traced, but (010) and its higher orders do not appear. The space-group therefore appears to be C_{2h}^2 , simple lattice Γ_m . In the absence of (hkl) halvings, however, four asymmetric molecules suffice for the symmetry of the cell, whereas this cell, as we have seen, contains the substance of eight molecules. It must be concluded that here again the lattice-unit consists of two molecules so coupled as to form an asymmetric whole.

Ortho-amino-phenol, Nc1ccccc1O, forms flat plates of rectangular contour which are pseudo-tetragonal, but are actually found to be orthorhombic-bipyramidal (fig. 2),

Fig. 2.



o-Amino-phenol.

showing mainly (001) and ($1\bar{1}\bar{2}$), occasionally also (010) Density 1.328. The X-ray data are :—

$$a = 7.26 \text{ \AA.}$$

$$b = 7.71 \text{ \AA.}$$

$$c = 19.51 \text{ \AA.}$$

8 molecules to the cell (found, 8.07).

The strongest reflexions (among 39 planes identified) are

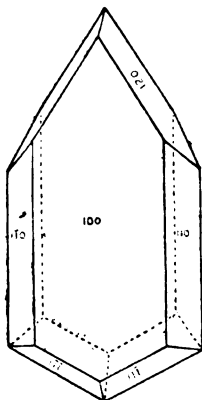
4 0 2

from (002), (120), (112), (211), (212), (221), and (222). There are no halvings in the (hkl) series. The base is represented by the second, fourth, and eighth orders; (020) and the whole series (021) to (026) occurs; the remaining planes parallel to axes are (200), (120), (220), (204), and (304). The inference is that $(hk0)$ and $(0kl)$ are halved when k is odd, and that $(h0l)$ is halved when l is odd. The crystal may therefore be assigned to the space-group Q_4^{15} , simple lattice Γ_0 .

OH

Meta-amino-phenol, Nc1ccccc1O, crystallizes from the various solvents with much the same habit, in characteristic orthorhombic-pyramidal crystals of pronounced hemimorphism

Fig. 3.

*m*-Amino-phenol.

(fig. 3), tabular along (100). Density 1.195. The X-ray data are:—

$$a = 6.14 \text{ \AA.}$$

$$b = 11.10 \text{ \AA.}$$

$$c = 8.38 \text{ \AA.}$$

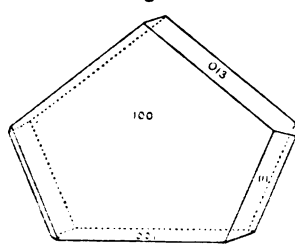
4 molecules to the cell (found, 4.09).

Among the 26 planes identified, (002) and (111) show the most intense reflexions. There are no (hkl) halvings. The reflexions from planes parallel to axes, of which 11 occur, indicate that $(0kl)$ is not halved, but that $(h0l)$ is halved when l is odd. The crystal may therefore be placed in space-group C_{2v}^4 , simple lattice Γ_0 .

Para-amino-phenol, Nc1ccc(O)cc1, was assigned by Keith (*l. c.*) to

the orthorhombic-bipyramidal class, with faces (100), (010), (110), and (011) developed. On looking more closely into the crystallization of this substance, it is found that there are at least two polymorphs, which we may call α and β . Of these, the more stable, or α -modification, appears to be the crystal examined by Keith, but it is distinctly hemimorphic and should be placed in the pyramidal class.

Fig. 4.

*p*-Amino-phenol.

Crystals may be obtained from solutions in alcohols, water, or ethyl acetate. From the latter solvents there is a tendency towards elongation along c , with a well-marked basal pedion; from alcohols, crystals elongated along a are deposited. In both cases (100), (013), and (111), are the principal other forms present, with occasional developments of (110) and (113). The density is 1.290, and the X-ray data are as follows:—

$$a = 8.25 \text{ \AA.}$$

$$b = 5.32 \text{ \AA.}$$

$$c = 13.06 \text{ \AA.}$$

4 molecules in the cell (found, 4.11).

The strongest reflexions, out of 27 noted, are from (110), (111), (201), and (211), and there are no (hkl) halvings. Fourteen planes parallel to axes are represented, such that ($h0l$) would appear to be halved when h is odd, and ($0kl$) when l is odd. The space-group C_{2v}^5 , simple lattice Γ_0 , is therefore indicated.

β -Para-amino-phenol.—When acetone is used as the crystallizing solvent, a second modification separates out in acicular crystals which, since on keeping they soon turn into

opaque pseudomorphs consisting of α -para-amino-phenol, are clearly a less stable form under ordinary conditions. The crystals are simple rectangular parallelopipeds bounded by the three pinacoids and elongated along c . Here and there small developments of (110) and (111) were noticed. Although the symmetry is very nearly tetragonal, Laue photographs showed it to be definitely orthorhombic and to be planar—that is, the crystal is either orthorhombic-bipyramidal or orthorhombic-pyramidal; the latter class is not excluded, even though no hemimorphism was revealed by microscopic examination. The X-ray results are:—

$$a = 12.07 \text{ \AA.}$$

$$b = 11.85 \text{ \AA.}$$

$$c = 5.82 \text{ \AA.}$$

6 molecules to the cell (found, 6.03).

The photographs are richer in spots than those of the α -modification, 43 planes being identified. On the c photograph the reflexions may be expected to be largely double spots, owing to the pseudo-tetragonal symmetry. The main difference in aspect between the a and b photographs lies in the presence of (210) and (410) in the former, and a strong (200) reflexion together with the absence of (120) and (140) in the latter. Intense reflexions are especially shown by (011), (101), (210), (220), and (211). No halvings of any sort could be traced, and the space-group Q_4^1 , simple lattice Γ_0 , is therefore indicated. Eight asymmetric molecules, however, is the smallest number required for a cell of this class. Since there are actually six molecules in the cell, it follows that the lattice-unit comprises the substance of three molecules, the cell containing only two such units. The major part of the crystal symmetry resides, therefore, in the lattice-units themselves, each of which must be symmetrical about two planes if the crystal is holohedral, or about one plane if it is hemimorphic. For a group of three molecules to possess this degree of symmetry, each individual molecule must possess it also. Now, it is unlikely that the molecule should be symmetrical about two planes, for the highest molecular symmetry hitherto met with in an aromatic compound is a centre. Probably, then, the crystal is really hemimorphic and comes under space-group C_{2v}^1 . The crystal is evidently of an unusual sort; but tri-molecular lattice-units are not unknown, and it is remarkable that such units occur in the fully-hydroxylated analogue of p -amino-phenol, namely quinol.

Summarizing the data now at hand for the present group of benzene derivatives, with the inclusion of those previously examined, we have:—

	<i>a.</i>	<i>b.</i>	<i>c.</i>	β .	<i>n.</i>
Catechol	17·46	10·74	5·48	94° 15'	8
Resorcinol	9·56	10·25	5·64	—	4
Quinol α	22·07	—	5·62	—	18
do. β	16·25	—	5·53	—	9
do. γ	13·24	5·20	8·11	107°	4
<i>o</i> -Amino-phenol	7·28	7·71	19·51	—	8
<i>m</i> -Amino-phenol	6·14	11·10	8·38	—	4
<i>p</i> -Amino-phenol	8·25	5·32	13·06	—	4
do. β ...	12·07	11·85	5·82	—	6
<i>o</i> -Phenylene-diamine	7·74	7·56	11·76	121° 10	4
<i>m</i> -Phenylene-diamine	11·97	8·14	23·61	—	16
<i>p</i> -Phenylene-diamine	8·29	5·93	24·92	112° 58'	8

It will be seen that, pending closer insight into the several structures, there are no such strikingly comparable data as in the case of naphthalene and anthracene. Taking the ortho-, meta-, and para-isomers of any one derivative, the dihydroxy-benzenes at least show one marked feature in common, in that one cell-dimension is about 5·5 Å. long in all three. Moreover, the intensities of the X-ray reflexions indicate that the planes corresponding to this spacing are in no case interleaved; hence this side of the cell would appear to be fully occupied by the spatial extent of one molecule. If we assume atoms to be actually grouped in molecules according to the structural chemical formulæ, and apply the known approximate atomic domains of carbon and hydrogen, this spacing would agree with the breadth of the hexagonal benzene ring. The thickness of a benzene ring can hardly exceed 3 Å., whilst the length of a molecule over any of the substituent groups must be not far from 7 Å.

On comparing different derivatives having substituents in the same position the similarity between *o*-amino-phenol and *o*-phenylene-diamine, as regards the *a* and *b* axes, attracts notice. On the basis of atomic domains, the spaces occupied by OH and NH₂ cannot differ greatly from one another, and the longest molecular dimension of any of the above ortho-compounds would correspond to this cell-side. Catechol, indeed, is wholly different, but its cell is a face-centred one; besides, it is always possible that there may be hitherto undetected polymorphs.

1284 *Crystallography of some Simple Benzene Derivatives.*

On comparing *para*-compounds, we find a remarkable connexion between the cell-dimensions if the cell of *p*-phenylene-diamine be cut in half along the *c* axis. The several cells may be written down thus:—

γ -Quinol	<i>a</i> , 13·24	<i>b</i> , 5·20	<i>c</i> , 8·11
α - <i>p</i> -Amino-phenol	<i>c</i> , 13·06	<i>b</i> , 5·32	<i>a</i> , 8·25
<i>p</i> -Phenylene-diamine	$\frac{1}{2}$ <i>c</i> , 12·46	<i>b</i> , 5·93	<i>a</i> , 8·29

The regular progression in these figures suggests that the molecules are arranged somewhat similarly in the three crystals, and that at least one of the cell-dimensions represents the span of a molecule. Since the overall length of any of the above molecules would work out, from atomic domains, at rather over 8 Å., the cell-sides in the last column may be so occupied. Some justification for treating the *p*-phenylene-diamine cell as a double one is to be found in the subdivision of the *c* axis of this crystal, mentioned above; also in the circumstance that the lattice-units are bimolecular.

For the present, any identification of a particular spacing with the “chemical” molecule can be no more than speculative. Certain arithmetical relations common to the cell-dimensions of all the simple benzene derivatives hitherto studied do, however, emerge. The cell-dimension 5·5 Å. and its integral multiples, as also $1\cdot5 \times 5\cdot5 = 8\cdot34$ Å. and its multiples, are observed to occur over and over again, as shown by the subjoined table:—

	Multiples of 5·5.			Multiples of 8·34.		
	<i>a.</i>	<i>b.</i>	<i>c.</i>	<i>a.</i>	<i>b.</i>	<i>c.</i>
Catechol	3·16	1·95	1·00	2·09	—	—
Resorcinol	—	1·87	1·02	—	—	—
Quinol α	4·00	—	1·02	—	—	—
do. β	2·96	—	1·01	1·95	—	—
do. γ	—	0·95	—	—	—	0·97
<i>o</i> -Amino-phenol	—	—	—	—	—	—
<i>m</i> -Amino-phenol	—	2·00	—	—	—	1·00
<i>p</i> -Amino-phenol	—	0·97	—	—	—	0·99
<i>o</i> -Phenylene-diamine ...	—	—	2·14	—	—	—
<i>m</i> -Phenylene-diamine ...	—	—	4·29	—	0·98	—
<i>p</i> -Phenylene-diamine ...	—	1·07	—	0·99	—	3·09
do. β ...	—	—	2·14	—	—	—
Benzene	—	—	1·05	—	—	—
Benzoic Acid	0·99	—	3·96	—	—	—

The figures represent the quotient of the various cell-dimensions by 5.5 and 8.34. Out of 80 cell-dimensions in all, 27 are found to be nearly integral multiples of one or the other length. The data for benzene and benzoic acid are taken from earlier X-ray work. Whatever the significance of these lengths may be, their occurrence seems too persistent to be merely accidental.

In conclusion, the author desires to express his acknowledgements to Sir Wm. Bragg, F.R.S., for the interest he has taken in this work, and to Dr. A. Müller for some valuable suggestions.

Davy-Faraday Laboratory,
The Royal Institution.

CXIII. *A Theory of Porous Flow.* By EARL E. LIBMAN,
Physics Department, University of Illinois *.

WHENEVER a material containing a fluid dries, the fluid is conducted from the interior to the surface. It is the purpose of this paper to develop mathematically the laws governing this flow.

Let

f_n = mass of fluid flowing in unit time through unit area normal to the direction n .

v = mass of fluid per unit mass of dry material. We will call this the "moisture density."

ρ = density of moist material.

σ = density of dry material.

τ = density of fluid.

w = mass of dry material in volume V of moist material.

E = mass of fluid evaporating in unit time from unit area of surface.

β = coefficient of compressibility of moist material.

Consider any closed surface lying wholly inside the given material. The rate at which fluid flows into the surface through the area dS is

$$-(\lambda f'_x + \mu f'_y + \nu f'_z) dS,$$

where $\lambda \mu \nu$ are the direction cosines of the outwardly

* Communicated by the Author.

directed normal to the surface. Hence,

$$-\iint (\lambda f_x + \mu f_y + \nu f_z) dS$$

is the rate of gain in fluid by the volume within the closed surface. If this volume is V , then

$$-\frac{1}{w} \iiint (\lambda f_x + \mu f_y + \nu f_z) dS$$

is the rate of gain in fluid per unit mass of dry material. But the rate of increase in fluid per unit mass of dry material is the rate of increase in v , where \bar{v} is the average value of v within the closed surface. Hence,

$$\begin{aligned} \frac{\partial \bar{v}}{\partial t} &= -\frac{1}{w} \iint (\lambda f_x + \mu f_y + \nu f_z) dS \\ &= -\frac{1}{w} \iiint \left(\frac{\partial f_x}{\partial x} + \frac{\partial f_y}{\partial y} + \frac{\partial f_z}{\partial z} \right) dx dy dz. \quad (1) \end{aligned}$$

by Green's Theorem, and this holds for any closed surface inside the material. Applying it to an element of volume surrounding the point $P(x, y, z)$, we have

$$\frac{\partial v}{\partial t} = -\frac{dx dy dz}{v} \left(\frac{\partial f_x}{\partial x} + \frac{\partial f_y}{\partial y} + \frac{\partial f_z}{\partial z} \right). \quad (2)$$

Now, the mass of fluid in the volume V is $w\bar{v}$ and the total mass of volume V is $w\bar{v} + w$. But the total mass of volume V is also ρV . Hence

$$w = \frac{\rho}{1 + \bar{v}} V. \quad (3)$$

When $V = dx dy dz$, then $\bar{v} = v$, and (2) becomes

$$\frac{\partial v}{\partial t} = -\frac{1+v}{\rho} \left(\frac{\partial f_x}{\partial x} + \frac{\partial f_y}{\partial y} + \frac{\partial f_z}{\partial z} \right) \text{ in the interior.} \quad (4)$$

On the bounding surface of the material consider an element of area dS . Upon dS , and within the solid, erect a small cylinder normal to the surface of height ϵ . Let p be the perimeter of dS and let n be the normal to the surface at dS . Then the rate of flow of fluid into the cylinder through the inside face is $f_n dS$. The rate of flow into the cylinder through the curved face is $f p \epsilon$, where f is the average rate of flow per unit area into the curved face. The rate of evaporation from dS is $E dS$. Hence the rate of gain in fluid by the cylinder is $f_n dS + f p \epsilon - E dS$. Now, the volume

of the cylinder is ϵdS , and by Eq. (3) the mass of dry material in this volume is $\frac{\rho}{1+v} \epsilon dS$. Hence the rate of gain in fluid by the cylinder per unit mass of dry material is

$$(f_n dS - f_p \epsilon - E dS) / \left(\frac{\rho \epsilon}{1+v} \right) = \frac{\partial \bar{v}}{\partial t}.$$

Thus we get

$$(f_n - E) dS + f_p \epsilon = \frac{\rho \epsilon}{1+v} \frac{\partial \bar{v}}{\partial t},$$

and taking the limit as $\epsilon \rightarrow 0$ gives

$$f_n - E = 0. \quad \text{Boundary condition} \quad \dots (5)$$

The flow of fluid in a porous material may be considered as due to three causes, first, the flow due to capillarity, second, the flow due to pressure gradient caused by shrinkage of the material, and third, the flow due to gravity.

If we consider a non-shrinking porous body, such as unglazed porcelain, and observe the flow in a horizontal direction so that gravity does not affect the results, we find that the flow takes place from points of higher to points of lower moisture content. There is little doubt that the rate of flow at any point is proportional to the moisture density gradient at that point, and we will make this assumption

$$f_{n \text{ cap.}} = -K \frac{\partial v}{\partial n} \dots \dots \dots (6)$$

It is well known (see Schlichter, Nineteenth Report of U.S. Geological Survey, 1897-98) that the rate of flow of a fluid through a porous material due to pressure is given by

$$f_{n \text{ press.}} = -k \frac{\partial p}{\partial n} \dots \dots \dots (7)$$

Finally, the flow due to gravity, which is always in the direction $-z$, is

$$f_{n \text{ gravity}} = -k g \tau \cos(zn) = -k g \tau \frac{\partial z}{\partial n} \dots \dots (8)$$

Consider now a small element of volume at $P(xyz)$ containing the mass δw of dry material. The volume of this element is, by Eq. (3) $\frac{1+v}{\rho} \delta w$, and, dividing this by the mass of dry material (namely, δw) we have for the volume

per unit mass of dry material at the point $P(x, y, z)$

$$V = \frac{1+v}{\rho} \quad . \quad . \quad . \quad . \quad . \quad . \quad (9)$$

Then

$$\frac{dV}{dv} = \frac{d}{dv} \left(\frac{1+v}{\rho} \right) \quad . \quad . \quad . \quad . \quad . \quad (10)$$

$$\frac{dp}{dv} = \frac{dp}{dV} \frac{dV}{dv} = \frac{d}{dv} \left(\frac{1+v}{\rho} \right) \cdot \frac{dp}{dV} \quad . \quad . \quad (11)$$

But

$$\beta = -\frac{1}{V} \frac{dV}{dp} \text{ by definition.}$$

Hence

$$\begin{aligned} \frac{dp}{dv} &= -\frac{d}{dv} \left(\frac{1+v}{\rho} \right) \cdot \frac{1}{V\beta} = -\frac{1}{\beta} \left[\frac{d}{dv} \left(\frac{1+v}{\rho} \right) \right] / \left(\frac{1+v}{\rho} \right) \\ &= -\frac{1}{\beta} \frac{d}{dv} \left(\log \frac{1+v}{\rho} \right), \quad . \quad (12) \end{aligned}$$

$$\frac{\partial p}{\partial n} = \frac{dp}{dv} \frac{\partial v}{\partial n} = -\frac{1}{\beta} \frac{d}{dv} \left(\log \frac{1+v}{\rho} \right) \cdot \frac{\partial v}{\partial n}, \quad . \quad . \quad . \quad (13)$$

and substituting Eq. (13) in Eq. (7), we have, adding Eqs. (6), (7), and (8),

$$f_n = - \left[K - \frac{k}{\beta} \frac{d}{dv} \left(\log \frac{1+v}{\rho} \right) \right] \cdot \frac{\partial v}{\partial n} - k g \tau \frac{\partial z}{\partial n}, \quad (14)$$

or, putting

$$\frac{d\phi}{dv} = K - \frac{k}{\beta} \frac{d}{dv} \left(\log \frac{1+v}{\rho} \right) \quad . \quad . \quad . \quad (15)$$

$$f_n = -\frac{\partial \phi}{\partial n} - k g \tau \frac{\partial z}{\partial n} \quad . \quad . \quad . \quad (16)$$

Note that ϕ , as a function of v only, is, for a given fluid, a property of the material. We will call it the "flow function."

From Eq. (16) we get

$$f_x = -\frac{\partial \phi}{\partial x}, \quad f_y = -\frac{\partial \phi}{\partial y}, \quad f_z = -\frac{\partial \phi}{\partial z} - k g \tau, \quad . \quad (17)$$

and putting this into Eq. (4) we get

$$\frac{\rho}{1+v} \frac{\partial v}{\partial t} = \frac{\partial^2 \phi}{\partial x^2} + \frac{\partial^2 \phi}{\partial y^2} + \frac{\partial^2 \phi}{\partial z^2}, \quad . \quad . \quad . \quad (18)$$

while from Eq. (15)

$$\frac{\partial \phi}{\partial n} + E + kg\tau \frac{\partial z}{\partial n} = 0. \quad \text{Boundary condition.} \quad (19)$$

Special Case of no Shrinkage.

In the special case where there is no shrinkage an element of volume δV does not change in volume. Hence the mass of dry material in δV is $\sigma \delta V$ and the mass of fluid is $\sigma v \delta V$. The total mass is then $\sigma \delta V + \sigma v \delta V$, and dividing this by the volume δV gives the density

$$\rho = \sigma(1 + v). \quad . \quad . \quad . \quad . \quad . \quad (20)$$

Thus $\frac{1+v}{\rho} = \frac{1}{\sigma}$, a constant, and Eq. (15) becomes

$$\frac{d\phi}{dv} = K. \quad . \quad . \quad . \quad . \quad . \quad (21)$$

Now, when there is no shrinkage, there is no change in the capillary structure of the material, and so K , which depends only on the structure, is constant. We have then

$$\phi = Kv + \text{const.} \quad . \quad . \quad . \quad . \quad . \quad (22)$$

and Eq. (18) becomes

$$\frac{\partial v}{\partial t} = \frac{K}{\sigma} \left(\frac{\partial^2 v}{\partial x^2} + \frac{\partial^2 v}{\partial y^2} + \frac{\partial^2 v}{\partial z^2} \right), \quad . \quad . \quad . \quad (23)$$

while Eq. (19) gives

$$K \frac{\partial v}{\partial n} + E + kg\tau \frac{\partial z}{\partial n} = 0. \quad \text{Boundary condition.} \quad (24)$$

Note that Eq. (23) is the equation of heat flow. *The flow of fluid within a non-shrinking porous body is analogous to the flow of heat.* For almost any problem in flow for the case of a non-shrinkable porous body we can find its analogue in heat flow solved in one of the numerous treatises on the subject and the transition is easily made.

Determination of the "Flow Function" ϕ .

In order to use the Eqs. (18) and (19) it is necessary to know the flow function ϕ as a function of v . We proceed to consider a method of determining ϕ experimentally.

Consider a bar of the material in question of length L . Let us prevent evaporation from the surface by painting the surface with wax or otherwise. Let one end of the bar be immersed in fluid and the other end kept in a constant

atmosphere. After a time equilibrium will be established and at any point the moisture density v will not vary with time. Then Eq. (18) becomes

$$\frac{\partial^2 \phi}{\partial x^2} = 1 \text{ when } 0 < x < L, \quad . \quad . \quad . \quad (25)$$

and Eq. (19) gives

$$\frac{\partial \phi}{\partial x} + E = 0 \text{ when } x = L. \quad . \quad . \quad . \quad (26)$$

These give

$$\phi = Ex + \text{const.} \quad . \quad . \quad . \quad (27)$$

Now, let us slice up our bar into slices perpendicular to its length and, by weighing each slice, drying, and weighing again, get v as a function of x , or x as a function of v . Putting this in Eq. (27) we have ϕ as a function of v if we know E as a function of v . The constant is arbitrary, since only the derivatives of ϕ enter into our equations. Knowing ϕ as a function of v , equation (18) must be solved for v as a function of t, x, y, z , with Eq. (19) as the boundary condition.

Determination of ρ and E .

If a piece of the material under investigation is taken and its dimensions and weight determined at intervals of time, while it is drying under the same atmospheric conditions as used in the experiment just discussed, we have data whereby to determine its density ρ and rate of evaporation per unit area E^* as functions of v .

The problem of drying is an important one in many industries, especially where, as in the pottery and brick industries, it is desirable to dry as quickly as possible and yet not cause cracking due to the shrinkage strains set up in the process. It is evident that the function ϕ is the governing entity in the procedure, and the writer hopes that data on the values of ϕ for different materials will be investigated. The problem of the distribution of stress due to drying is now under consideration.

* For clays E takes a very simple form, being constant and equal to the rate of evaporation from a free water surface. (Results of work soon to be published by Professor H. K. Hursh, Ceramics Department, University of Illinois.)

CXIV. *The Transparency of Turbid Media.*

By LUDWIK SILBERSTEIN.—(Communication No. 318.) *

IN a recent paper on the transparency of a developed photographic plate as observed under various conditions †, it was assumed that the total light scattered by each particle (grain) is sent forward, *i. e.* in the direction of and under acute angles with the incident light beam. It is well known that if the scattering particle, supposed to be spherical, is very small compared with the wave-length, then, according to Rayleigh's elementary theory and Mie's developed form of the electromagnetic theory ‡, one-half of the scattered light is sent forward and one-half backward §, the distribution of the intensity being perfectly symmetrical with respect to the plane passing through the particle and normal to the incident beam. For particles, however, whose size is comparable with the wave-length, there is a tendency of the scattered light to concentrate in the forward direction. This tendency, derived theoretically but tested also experimentally ||, is for gold particles, for instance, already very pronounced at a diameter of $160\mu\mu$ (with $\lambda=550$), while for somewhat larger particles ($180\mu\mu$) practically the whole scattered light is sent forwards, as a glance on Mie's figures (*l. c.* p. 429) will show. These and similar examples computed by Shoulejkin ¶, who pushed the ratio of particle size to wave-length up to the value of two or three units, have suggested the adoption of the said assumption in the case of the black silver grains of photographic emulsions, these grains being in general of the order of the wave-length of visible light. (Commonly, their diameters range from a few tenths to several whole microns.) The assumption of a unilateral spreading of the scattered light recommended itself also by the obvious simplicity of its consequences. Moreover, the object of that paper was only to correlate with each other the two kinds of photographic "density" (diffuse and specular) without studying each of them in detail as a function of the size and the number of particles, and for this purpose the assumption

* Communicated by the Author. From the Research Laboratory of the Eastman Kodak Company.

† L. Silberstein and C. Tuttle: "The Relation between the Specular and Diffuse Photographic Densities," *J. O. S. A. & R. S. I.* xiv. (1927).

‡ G. Mie, *Ann. der Physik*, xxv. pp. 377-455 (1908).

§ Unless the particle is a perfect conductor, when almost the whole light is scattered backwards. Cf. Mie, *l. c.* p. 430.

|| As, *e. g.*, by R. Gans, *Ann. der Physik*, lxxvi. p. 29 (1925).

¶ W. Shoulejkin, *Phil. Mag.* xlvii. p. 307 (1924).

turned out to be accurate enough. It has therefore been adopted in that connexion, although implying the rather uncertain extrapolation from Mie's spherical metallic particles to the generally larger, shapeless, and sponge-like silver grains of the photographic plate.

In the present paper the problem of light transmission through turbid media will be treated without this special simplifying hypothesis. It will be assumed that of the light scattered (or re-scattered) by each particle a certain fraction (ζ) is sent forward and the remainder backward, the numerical value of this fraction being left free. The equations corresponding to this general case are somewhat more complicated, but can be solved without trouble.

Consider a plane-parallel layer of absorbing and scattering particles which will be supposed to be all equal. Let I_0 be the intensity of the incident light collimated normally to the layer at its front surface ($x=0$) and I the intensity of the directly transmitted light which has penetrated to any depth x . The total energy scattered (per unit time) by a particle which is struck by this light can again be written AI , where A , the scattering coefficient, will be a function of wave-length, etc. Of this energy let the fraction

$$\zeta AI$$

be sent forward and the remainder $(1-\zeta)AI$ backward (along rays, that is, which make with the incident beam angles 0 to $\pi/2$ and $\pi/2$ to π respectively). Let κI be the energy absorbed by a particle, N the number of particles per unit volume, and $dn=Ndx$. Then, in the first place, we will have for the directly transmitted light

$$\frac{dI}{dn} = -(\kappa + A)I, \quad (1)$$

which is independent of the partition of the scattered light.

Next, if, at any depth x , S be the total flux of scattered light energy directed forward and S' that directed backward, a first contribution to dS/dn will be ζAI and $(1-\zeta)AI$ will be one to $-dS'/dn$, the role of x being for the retrograde flux S' replaced by $-x$. Further, of the scattered radiation S the amount κS will be absorbed and the amount AS will be re-scattered per particle; of the latter, however, the fraction ζAS is again sent forward so that only $(1-\zeta)AS$ is lost to the S -flux. Finally, the amount of S' re-scattered is AS' , and of this $\zeta AS'$ is sent in the negative and $(1-\zeta)AS'$ in the positive direction of the x -axis. Thus the

equation for S becomes

$$\frac{dS}{dn} = \zeta AI - \kappa S - (1 - \zeta) AS + (1 - \zeta) AS',$$

and similarly, the equation for S' ,

$$-\frac{dS'}{dn} = (1 - \zeta) AI - \kappa S' - (1 - \zeta) AS' + (1 - \zeta) AS,$$

or, collecting the terms

$$\frac{dS}{dn} = \zeta AI - \alpha S + (1 - \zeta) AS', \quad \dots \quad (2)$$

$$-\frac{dS'}{dn} = (1 - \zeta) AI - \alpha S' + (1 - \zeta) AS, \quad \dots \quad (3)$$

where $\alpha = \kappa + (1 - \zeta) A$.

(1), (2), (3) are the required differential equations for the three light fluxes*. In addition to these we have the boundary conditions, viz. at the front surface ($x=0$) of the layer, $I=I_0=1$, say, and

$$S=0, \text{ for } n=0, \quad \dots \quad (4)$$

and at the back surface,

$$S'=0, \text{ for } n=n, \quad \dots \quad (5)$$

where n is the total number of particles per unit area of the layer. (For $\zeta=1$ this system of equations reduces at once to our previous formulæ, *loc. cit.*)

By (1),

$$I = e^{-pn},$$

where $p = \kappa + A$. Thus the directly transmitted light would still obey Beer's simple law.

To satisfy the equations (2) and (3), put

$$S = re^{-pn} + ae^{\beta n} + be^{-\beta' n},$$

$$S' = r'e^{-pn} + a'e^{\beta n} + b'e^{-\beta' n},$$

where r, r' , etc. are constants to be determined. Substituting

* An explicit consideration of distinct light fluxes directed back and forth has already been introduced in A. Schuster's treatment of the problem of an incandescent "foggy atmosphere," *Astrophysical Journal*, xxi. p. 1 (1905). Schuster limits himself, however, to the special case of equal distribution (*i. e.* $\xi=\frac{1}{2}$), which would suit only very small particles. Moreover, he has no term representing the collimated radiation but, in accordance with the nature of his subject, considers only the scattered fluxes in either sense. This leads to two equations only, which (apart from the emission terms) differ somewhat from (2) and (3).

into (2), (3), and comparing the coefficients of the three exponentials, we find, first of all

$$r + \frac{1-\zeta}{\zeta} r' = -1,$$

$$r - \frac{\alpha + \beta}{(1-\zeta)A} r' = -1,$$

so that $r' = 0$ and $r = -1$.

Next,

$$\frac{a'}{a} = \frac{\alpha + \beta}{(1-\zeta)A} = \frac{(1-\zeta)A}{\alpha - \beta} = \lambda, \text{ say,}$$

and
$$\frac{b'}{b} = \frac{\alpha - \beta'}{(1-\zeta)A} = \frac{(1-\zeta)A}{\alpha + \beta'} = \mu, \text{ say.}$$

The first pair of these equations gives

$$\beta = \pm \sqrt{\alpha^2 - (1-\zeta)^2 A^2},$$

and the second pair gives exactly the same expression for β' . Thus, either $\beta' = \beta$ or $\beta' = -\beta$. But in the latter case we would have $\lambda = \mu$, and, by the boundary condition (5), $\alpha + b = 0$. This, however, would clash with the condition (4) which calls for $\alpha + b = 1$. We are left, therefore, with

$$\beta' = \beta = \sqrt{\alpha^2 - (1-\zeta)^2 A^2} = \sqrt{\kappa^2 + 2(1-\zeta)\kappa A}. \quad (6)$$

(Taking the negative square-root we would only interchange the roles of a and b .)

The two fluxes now become

$$S = ae^{\beta n} + be^{-\beta n} - e^{-pn}, \quad \dots \quad (7)$$

$$S' = \lambda ae^{\beta n} + \mu be^{-\beta n}, \quad \dots \quad (8)$$

where
$$\lambda = \frac{\alpha + \beta}{(1-\zeta)A}, \quad \mu = \frac{\alpha - \beta}{(1-\zeta)A}. \quad \dots \quad (9)$$

The coefficients a , b will be determined by the boundary conditions (4) and (5), i. e.

$$\alpha + b = 1, \quad \lambda ae^{\beta \bar{n}} + \mu be^{\beta \bar{n}} = 0,$$

whence, writing henceforth n instead of \bar{n} ,

$$a = \frac{\mu e^{-\beta n}}{\mu e^{-\beta n} - \lambda e^{\beta n}}, \quad b = \frac{-\lambda e^{\beta n}}{\mu e^{-\beta n} - \lambda e^{\beta n}}. \quad \dots \quad (10)$$

Thus, by (7),

$$S = \frac{\lambda - \mu}{\lambda e^{\beta n} - \mu e^{-\beta n}} - e^{-pn},$$

where λ , μ are as in (9).

Ultimately, therefore, the emergent scattered light flux,

proceeding forward, is

$$S = \frac{2\beta}{(\alpha + \beta)e^{\beta n} - (\alpha - \beta)e^{-\beta n} - e^{-(\kappa + A)n}}, \quad \dots \quad (11)$$

where

$$\alpha = (1 - \zeta)A + \kappa, \quad \beta = \sqrt{\kappa^2 + 2(1 - \zeta)A\kappa},$$

and the intensity of the directly transmitted, collimated light

$$I = e^{-(\kappa + A)n}.$$

Thus the total transmitted light flux $S + I$ or (since $I_0 = 1$) the *total transparency* of the layer, as recorded, say, by means of an integrating sphere, will be

$$S + I = \frac{2\beta}{(\alpha + \beta)e^{\beta n} - (\alpha - \beta)e^{-\beta n}}, \quad \dots \quad (12)$$

which contains the original three constants only through their two combinations, α and β *. It is this total transparency which is unambiguously observable, while it would be hard to isolate I from the superposition of some unknown fraction of S . In photographic nomenclature $-\log(S + I)$ would be the "diffuse density." Notice that in general only I itself satisfies Beer's law, while S and $S + I$ do not obey this law. (In the particular case $\zeta = 1$ we have $\alpha = \kappa = \beta$, so that $S = e^{-\kappa n} - e^{-\rho n}$, as in the first paper on this subject. In this case both I and $I + S$ obey Beer's law.) For small values of βn the total transparency (12) reduces

to $\frac{1}{1 + \alpha n}$, and for large βn to $\frac{2\beta}{\alpha + \beta} e^{-\beta n}$.

It may still be interesting to determine the total scattered light S' thrown *backward* and emerging at the front surface ($x = 0$) of the layer. This will be obtained by putting in (8) $n = 0$. Thus

$$S' = \lambda\alpha + \mu b,$$

* This differs, even for $\zeta = \frac{1}{2}$, from Schuster's result (*loc. cit.*) as regards the coefficients. In fact, Schuster's formula for the total emergent radiation R reduces, in absence of emission, to

$$R = 4c/[(1 + c)^2 e^{\beta n} - (1 - c)^2 e^{-\beta n}],$$

where, in our symbols $c = \sqrt{\frac{\kappa}{\kappa + A}}$, while $\beta = \sqrt{\kappa(\kappa + A)}$, identical with our β for $\zeta = \frac{1}{2}$. The difference in the structure of the coefficients is due to the fact that no collimated light (flux I) has been taken into account. The dependence on n , however, or equivalently on the thickness of the layer (*cf. infra*) is essentially the same. Schuster's type of formula has also been obtained by an entirely different reasoning by Channon, Renwick, and Storr, *Proc. Roy. Soc. p. 222 (1918)*.

i. e., by (10) and (9),

$$S' = (1 - \zeta) A \frac{e^{\beta n} - e^{-\beta n}}{(\alpha + \beta)e^{\beta n} - (\alpha - \beta)e^{-\beta n}}, \quad \dots \quad (13)$$

or, compared with the total forward flux,

$$\frac{S'}{S + I} = \frac{(1 - \zeta) A}{2\beta} (e^{\beta n} - e^{-\beta n}). \quad \dots \quad (14)$$

For indefinitely increasing n the emerging backward flux (13) tends to

$$S' = \frac{(1 - \zeta) A}{\alpha + \beta},$$

a finite value, as might have been expected.

In all these formulæ n or $\int N dx$ is the number of particles over unit area, whether their distribution in depth is uniform or not. If it is uniform ($N = \text{const.}$), the same formulæ hold good when n stands for the thickness of the layer, only that κ and A are then the original constants multiplied by N , i. e. the absorption and the scattering coefficients, not per particle but per unit volume.

Rochester, N.Y..

May 12, 1927.

CXV. *Some Comments on the Classical Theories of the Absorption and Refraction of X-Rays.* By F. K. RICHTMYER *.

Abstract.

THE assumptions usually made in the classical approach to the problem of the absorption of X-rays are summarized, and a relation is derived similar to that previously deduced by Kronig (J. O. S. A. and R. S. I. vol. xii. p. 554) between the index of refraction and the atomic absorption coefficient. It is shown that the relation is experimentally verified in so far as order of magnitude is concerned, but that an exact verification cannot be made because of the absence of data on absorption at long wave-lengths. However, it is doubtful whether a real verification of the formula is to be expected, since, by limiting the solution of the differential equation of motion of the electron oscillators to forced vibrations, expressions for scattering rather than for (fluorescent) absorption should result. It is pointed that all writers except Thomson introduce the λ^3 law of absorption as an experimental datum.

* Communicated by the Author. The author acknowledges with thanks his indebtedness to the Heckscher Research Council of Cornell University.

A different method of approach to a possible relation between absorption and refraction of X-rays is suggested by considering the equations of classical optics, which have led to an approximately correct expression for index of refraction of X-rays. It is shown that these equations, too, lead to expressions for scattering. The main part of X-ray absorption, namely fluorescent absorption—a photoelectric process on the basis of our modern quantum picture—is therefore, as might be expected, unexplained by these strictly classical methods.

THEORIES of the absorption of X-rays have been developed on strictly classical grounds by J. J. Thomson *, Houston †, A. H. Compton ‡, and, recently, Bothe §. These theories assume :—

- (1) That in the absorbing material there are (harmonic) electron oscillators of several kinds (K, L, M, ...), and that the natural frequencies of the oscillators of each kind extend from the frequency ν of the corresponding absorption limit to infinity.
- (2) That the electric moment f of any one oscillator of natural frequency ν_0 , when acted on by the periodic electric vector $\bar{E} = E_0 \sin 2\pi\nu t$ of a light-wave of frequency ν , can be represented by the equation

$$\ddot{f} + k\dot{f} + (2\pi\nu_0)^2 f = \frac{e^2}{m} E_0 \sin 2\pi\nu t, \quad \dots (1)$$

where e and m are the charge and mass respectively of the electrons.

- (3) That the term $k\dot{f}$, which ordinarily represents damping due to friction, is identified with the damping due to the radiation from the accelerated electron. If the rate dW/dt of radiation from an accelerated electron is given by the classical expression

$$\frac{dW}{dt} = \frac{2}{3} \frac{e^2 \ddot{x}^2}{c^3},$$

it follows that k in equation (1) is given by

$$k = \frac{2}{3} \frac{e^2}{mc^3} (2\pi\nu)^2.$$

* J. J. Thomson, 'Conduction of Electricity through Gases,' 2nd edition, p. 321.

† Houston, Proc. Roy. Soc. Edinburgh, xl. p. 34 (1919); Phil. Mag. (7th ser.) ii. p. 512 (Sept. 1926).

‡ A. H. Compton, National Res. Council, Bull. xx. p. 37 (1922).

§ Bothe, Zeits. f. Physik, xl. p. 653 (Jan. 1927).

- (4) *That transient effects have disappeared, and that the electron is executing forced vibrations of frequency ν .*

Now, the "friction" term, if we admit assumption 4, determines the rate at which energy is being extracted from the incident beam. The intensity of the incident beam is proportional to E_0^2 . Using these relations, and making reasonable approximations in the solution of equation (1), the following relation may be derived :

$$\int_{\nu_i}^{\infty} \tau_{i\nu} d\nu = \frac{\pi e^2}{mc} n_i, \quad . \quad . \quad . \quad . \quad (2)$$

where $\tau_{i\nu}$ is the absorption coefficient, at frequency ν , of the atom due to all its oscillator, n_i , of kind i . Houston* has used a relation of this kind to determine the number of K electrons per atom, obtaining the mean value for some 13 elements of 1.03 electrons per atom.

Equation (2) may be summed up for all the different kinds of oscillator in the atom by writing

$$\sum_i \int_{\nu_i}^{\infty} \tau_{i\nu} d\nu = \frac{\pi e^2}{mc} n, \quad . \quad . \quad . \quad . \quad (3)$$

where $n (= \sum n_i)$ is the total number of electrons per atom.

Numerous investigations † of the refraction of X-rays have shown that the classical theories of refraction may be extended to the X-ray region, and that the index of refraction \mathbf{n} is given to an approximation adequate for experimental purposes by

$$1 - \mathbf{n} = \delta = \frac{N n e^2}{2 \pi m \nu_r^2}, \quad . \quad . \quad . \quad . \quad (4)$$

where N is the number of atoms per unit volume and ν_r the frequency for which \mathbf{n} is determined. If we multiply both sides of the equation (3) by $cN(2\pi^2\nu_r^2)$, we have, using equation (4),

$$\frac{cN}{2\pi^2\nu_r^2} \sum_i \int_{\nu_i}^{\infty} \tau_{i\nu} d\nu = \delta. \quad . \quad . \quad . \quad . \quad (5)$$

This relation between index of refraction and absorption has been derived by Kronig ‡, using a slightly different procedure.

A rough check of equation (5) is, at least theoretically, possible. The value of δ for platinum, at $\lambda = 0.3 \text{ \AA.}$, is about

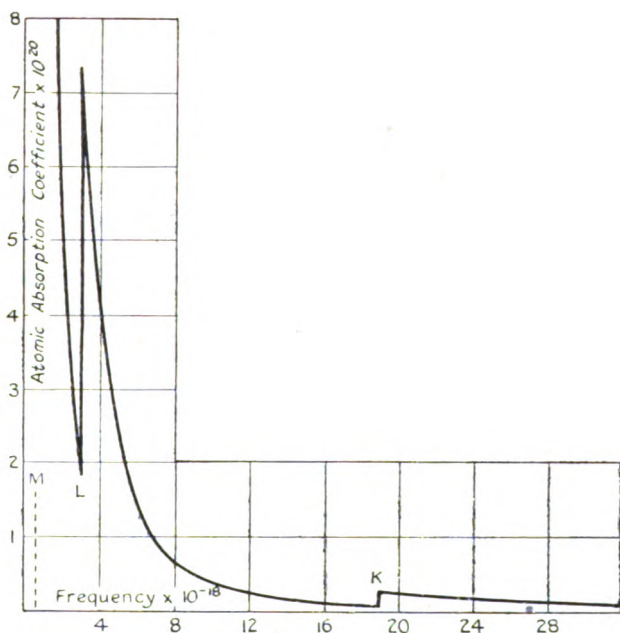
* *Loc. cit.* (Phil. Mag.).

† See A. H. Compton, 'X-Rays and Electrons,' p. 205.

‡ J. O. S. A. and R. S. I. vol. xii. p. 554 (June 1926).

$2 \cdot 10^{-6}$, as given by equation (4). The term $\sum_i \int_{\nu_i}^{\infty} \tau_{i\nu} d\nu$ is simply the area, call it S , between the coordinate axes and a curve plotted between the frequency and the *observed* values of (total) atomic absorption coefficient τ_{ν} . Such a curve is plotted to scale in fig. 1, from data compiled by Compton*. Because of our comparative ignorance of the numerical value of absorption coefficients for X-rays longer than about 2 \AA. , one can determine only *the order of magnitude* of S , and

Fig. 1.



not its actual value. But knowing that absorption coefficients in the region of long X-rays are very great, we may guess that S might be somewhere in the neighbourhood of $1 \cdot 2$. (Abscissæ are vibrations per second; ordinates are *atomic* absorption coefficients.) This gives a value for δ for Pt, as computed from equation (5) for $\lambda = 0 \cdot 3 \text{ \AA.}$, of about $1 \cdot 2 \cdot 10^{-6}$, considerably lower than the value given by equation (4), but at least of the right order of magnitude.

However, the relation between τ and δ is not quite so intimate as might be judged from equation (5) taken by

* 'X-Rays and Electrons,' p. 185.

itself. Equation (5) is, in fact, derived from equating the two values of n , given independently by equations (3) and (4) respectively. And equation (2), from which equation (3) is deduced, gives, as mentioned above, only one instead of two K electrons per atom. A similar result is pointed out by Kronig*. Hence equation (5) may be expected to yield too low a value for δ .

Indeed, the approximate numerical verification of equation (5) may even be fortuitous. For the limitation of the solution of equation (1) to the forced vibrations, after transients have disappeared, should lead to a determination of the *scattering* coefficient, rather than the *absorption* coefficient, which latter is given experimentally by the approximately correct relation

$$\tau_a = CZ^4\lambda^3,$$

where τ_a is the observed atomic absorption coefficient for wave-length λ , Z is the atomic number of the absorber, and C is a constant which depends on the spectral region. With the exception of J. J. Thomson's, the classical theories *do not lead to an independent theoretical justification for the law*

$$\tau_a \propto \lambda^3.$$

Rather this law is introduced *as an experimental datum*†, and an equation of the type

$$\tau_a = 2\pi \frac{e^2}{mc^2} \left(\sum_i \frac{n_i}{\lambda_i^2} \right) \lambda^3$$

results. But Thomson, by a procedure which amounts to taking transient effects into account, deduced theoretically the λ^3 law, although Thomson's complete formula,

$$\tau_a = \frac{\pi^3}{3} \frac{e^2}{mc^2} \left(\sum_i \frac{n_i}{\lambda_i^2} \right) \lambda^3,$$

gives values for τ_a about five times too large.

That the classical theories, when restricted to the forced vibration of the electrons, lead to a determination of scattering coefficients, is easily seen by considering the companion equation to the one from which equation (4) is derived. The well-known equations showing the relation, for frequency ν , between the index of refraction n and the

* *Loc. cit.*, p. 555.

† See, for example, Bothe (*loc cit.*).

extinction coefficient κ , are* :

$$n^2(1-\kappa) = 1 + \frac{4\pi m(\nu_0^2 - \nu^2) N n e^2}{4\pi^2 m^2(\nu_0^2 - \nu^2)^2 + p^2 \nu^2} \quad \dots \quad (6)$$

$$n^2 \kappa = \frac{N n e^2 p \nu}{4\pi^2 m^2(\nu_0^2 - \nu^2)^2 + p^2 \nu^2} \quad \dots \quad (7)$$

Here, as before, N is the number of atoms per unit volume, n the number of "mobile" electrons per atom, ν_0 is the natural frequency of the electron oscillators, and p is the constant of the so-called friction term $p\dot{x}$ in the ordinary equation of motion of the electron. If, as before, the damping be due to radiation, the numerical value of p is given by

$$p = \frac{8\pi^2 e^2}{3 c^3} \nu^2. \quad \dots \quad (8)$$

The relation between the extinction coefficient κ and the absorption coefficient μ is given by

$$\kappa = \mu \frac{\lambda}{4\pi}, \quad \dots \quad (9)$$

μ being expressed in cm.^{-1} †.

Now, in the X-ray region $\kappa \ll 1$, and n differs from unity by only a small quantity. Hence, assuming that damping is small (i. e., that $p^2 \nu^2 \ll 4\pi^2 m^2(\nu_0^2 - \nu^2)^2$), equation (6) at once reduces to equation (4), which in turn agrees with experiment. It might therefore be expected that a similar treatment of equation (7) would lead to a value of the absorption coefficient μ . Making these approximations, and using the values of p and κ from equations (8) and (9), one obtains from equation (7)

$$\mu = \frac{8\pi}{3} \cdot \frac{N n e^4}{m^2 c^4} \cdot \frac{\nu^4}{(\nu_0^2 - \nu^2)^2}, \quad \dots \quad (10)$$

which, for $\nu \gg \nu_0$, is identical with the Thomson expression for scattering. Therefore κ is related to the scattering coefficient σ rather than to the absorption coefficient μ .

Further, without making the approximation that $p^2 \nu^2 \ll 4\pi^2 m^2(\nu_0^2 - \nu^2)^2$, by combining equations (6) and (7) one obtains, using equations (8) and (9) as before,

$$\frac{\mu}{\rho} = \frac{16\pi^2}{3} \cdot \frac{e^2}{m \rho c^2} \cdot \frac{\lambda_0^2}{\lambda^2(\lambda^2 - \lambda_0^2)} \delta, \quad \dots \quad (11)$$

where μ/ρ should be the mass absorption coefficient for

* See, for example, Campbell's 'Modern Electrical Theory,' 2nd edition, p. 51.

† That is, μ is given by the equation $I = I_0 e^{-\mu x}$, which gives the intensity I of a beam of radiation of incident intensity I_0 after passing through a slab of the material x cm. thick.

X-rays of wave-length λ , ρ being the density of the absorber and λ_0 the characteristic wave-length emitted by its oscillators. Using this equation to compute the mass absorption coefficient for silver at $\lambda=1.297 \text{ \AA}$, for which $\delta=20 \cdot 16^{-6}$ as determined experimentally by Compton, one obtains

$$\left(\frac{\mu}{\rho}\right)_{\text{Ag}} = 2.3;$$

whereas μ/ρ for silver, at this wave-length, is approximately 150 *. Clearly, the value 2.3 corresponds more closely to the scattering coefficient. We have, however, no data on scattering with which to make even an approximate check of equations (10) and (11) at various wave-lengths.

These classical methods of approach to the problem of X-rays lead therefore to expressions for scattering, but leave untouched the main part of the absorption process—namely, the part which is proportional to the cube of the wave-length and which, in the modern quantum picture of the phenomenon, is associated with the expulsion of electrons. This failure is in entire harmony with the failure of classical theory to explain even qualitatively the essential facts of the photoelectric effect. It may, however, be a significant circumstance that Thomson, by considering the *potential* energy stored in the oscillator as a result of the passage of a light-wave, does succeed in deriving the λ^3 law, and thereby in giving a picture of the mechanism by which characteristic (*i. e.* fluorescent) radiation is emitted by the absorber.

Cornell University.
May 8, 1927.

CXVI. *The Crystal Structure of Cu_3Sn , and Cu_3Sb .* By
W. MORRIS JONES, *M.A., M.Sc.*, and Prof. E. J. EVANS,
D.Sc., University College, Swansea †.

IT is generally considered that a definite intermetallic compound is formed on the solidification of two liquid metals: (i.) if the solid so formed is of the same composition throughout; (ii.) if the solid contains the metal in approximately simple proportions; and (iii.) if the colour, density, hardness, electrical conductivity and other physical properties of the solid are in sharp contrast with those of the

* Computed from the writer's experimental equation (*Phys. Rev.* xxvii. p. 5, Jan. 1926). Allen (*Phys. Rev.* xxviii. p. 907) gives a slightly lower value.

† Communicated by the Authors.

component metals, or with those which might be expected if one metal was in a state of solid solution in the other.

Condition (ii.) has led to fixing a chemical formula for the compound with the inevitable association of a chemical molecule and the scheme of valency. In a large number of intermetallic compounds, however, the formulæ do not agree with the usual valencies assigned to the atoms. The X-ray study of the crystal structure of inorganic solids shows that in most crystals examined, the usually assumed chemical molecule cannot be distinguished, and that the unit of the solid state would appear to be a cell, the repetition of which in space makes up a crystal.

In the extension of the X-ray method to the investigation of the crystal structure of alloys, the nature of solid solution has, so far, been the main object of study. The results of these investigations show that when the end members of a continuous series of solid solutions have the same crystal structure, a unique and perfectly regular lattice is formed, the dimensions of the lattice gradually changing from those of the one to those of the other, as the atoms of one metal replace those of the other on the lattice. If the atoms of two metals are not structurally equivalent, two different structures co-exist over a range of composition, the initial and final structures being those of the two metals.

The crystal structure of very few intermetallic compounds has, so far, been examined*, though the number of such compounds is very large. A study of their crystal structure would, therefore, seem well worth while, especially as the evidence for the formation of a definite compound is not always as conclusive as seems desirable. We have, therefore, examined the crystal structure of a number of intermetallic compounds by the X-ray powder method, and the analyses of the photographs for two of the compounds, Cu₃Sn and Cu₃Sb, are given below.

The alloys were very carefully prepared at the Metallurgical Laboratory, under the direction of Professor C. A. Edwards, and their composition afterwards checked by chemical analysis.

X-ray Apparatus†.

The powder method of X-ray crystal analysis is well known, so the apparatus used in the present investigation need only be briefly described.

* Owen and Preston, *Phil. Mag.* ii. p. 1266 (1926); iv. p. 133 (1927).

† We are indebted to the Department of Scientific and Industrial Research for defraying the cost of part of the equipment.

The target of the X-ray tube was of copper and water cooled, whilst the cathode was a hot tungsten filament. A low vacuum was maintained by two mercury vapour pumps coupled up in series and working continuously. The voltage across the tube was kept at about 30,000 volts., as suitable for bringing out the characteristic radiation of copper with sufficient intensity. Under these conditions the milliamperes passing through the tube varied from 5 to 6, and the tube could be run continuously, the source of high potential being a high tension transformer.

The camera for taking the photographs was about 10 cm. in diameter, the powder being painted on a hair or fine wire and mounted at the centre. The film, placed round the circumference, was backed by an intensifying screen. Allowing for the thickness of the film and screen, the diameter of the camera was 9.96 cm., and this value was taken in the calculations.

A water-cooled aluminium window, within about 2 cm. of the target, enabled a strong beam of X-rays to issue from the tube. The camera could be brought up close to the window, with the powder about 7 cm. from the target. Good photographs were obtained with exposures ranging from $1\frac{1}{2}$ to 3 hours.

The camera was calibrated by taking a photograph of copper powder, measuring up the film, and seeing how the position of the lines of the pattern agreed with the calculated values from the known structure of copper. The correction for various distances from the centre of the film could then be ascertained. Some photographs were taken with powdered copper and the powdered alloy mixed together. The calibration of these films was, therefore, made from the copper lines on them. The films were measured by means of a travelling microscope, and lines on both sides of the centre were read. The readings agreed to within 1 per cent., and the calibration of the films, by means of the standard copper lattice, brought agreement within about 0.25 per cent.

These corrected readings were then reduced to glancing angles of reflexion, and the plane spacings calculated according to Bragg's law.

In order not to reduce the intensity of the X-ray beam, a nickel filter for the K_{β} radiation was not employed. Though the lines due to K_{α} and K_{β} appeared on the films, no confusion was caused, and a little familiarity with the films enabled the lines to be easily sifted out.

The results of the analysis of the photographs are given in the Tables below.

1. *The Crystal Structure of Cu₃Sn.*

TABLE I.—Cu₃Sn.

Copper K_α radiation. The value of λ_{K_α} is taken as 1·540 Å. Diameter of camera 9·96 cm. Close-packed hexagonal structure. Axial ratio 1·572.

Indices of form.	Distance of lines from centre in mm.			θ in degrees.	$\frac{\lambda}{2 \sin \theta}$ *	Theoretical spacing $c = 1·572$.	Observed intensity.	Calculated intensity.
	Film (1).	Film (2).	Mean.					
10 $\bar{1}$ 0	32·76	32·84	32·80	18° 52'	2·381 Å.	·381 Å.	·20	·23
0002	36·28	36·38	36·33	20 54	2·159	2·161	·40	·24
10 $\bar{1}$ 1	37·74	37·83	37·78	21 44	2·080	2·084	1·00	1·00
1012	50·08	50·00	50·04	28 47	1·599	1·599	·27	·18
11 $\bar{2}$ 0	59·07	59·17	59·12	34 1	1·377	1·375	·30	·26
10 $\bar{1}$ 3	67·22	67·20	67·21	38 40	1·233	1·235	·40	·29
2020	69·82	70·02	69·92	40 13	1·192	1·190 ₅	·05	·045
11 $\bar{2}$ 2	72·16	72·34	72·25	41 34	1·160	1·159	·30	·34
20 $\bar{2}$ 1	73·40	73·42	73·41	42 14	1·146	1·147	·17	·24
0004	79·16	79·27	79·21	45 34	1·079	1·080 ₅	·07	·05
2022	82·94	82·99	82·96	47 43	1·041	1·042	·07	·065
1014	89·88	89·90	89·89	51 42	·981	·983	·08	·058
2023	99·46	99·38	99·42	57 12	·916	·916	·20	·15
2130	102·43	102·48	102·46	58 56	·899	·899	·07	·046
21 $\bar{3}$ 1	106·27	106·28	106·27	61 8	·879	·880	·20	·26
1124	113·81	113·76	113·79	65 28	·846 ₅	·848	·24	·16
2132	—	118·83	118·83	68 21	·828 ₅	·830	·12	·08

Column 6 gives the plane spacings deduced from the observations, while column 7 gives the spacings calculated for a close-packed hexagonal structure with axial ratio 1·572.

The observed lines are thus accounted for by a close-packed hexagonal structure * for Cu₃Sn, with axial ratio 1·572.

The dimensions of the unit hexagonal prism deduced from the data are a_0 (base) = 2·749 Å., and c_0 (height) = 4·322 Å., corresponding to an axial ratio $c = 1·572$.

* Bain, Chem. Met. Eng. xxviii. p. 69, states that Cu₃Sn is close-packed hexagonal in type (like zinc), but gives no further information or any diffraction data.

It is clear from considerations of volume that with the alloy Cu_3Sn , in which the atoms are also as 3 : 1, it is impossible to associate a whole molecule with a cell of the above dimensions. If V is the volume of the cell, M the mass of the chemical molecule, ρ the density of the alloy, then the number of molecules associated with the cell is given by :

$$n = \frac{\rho V}{M}, \text{ where } V = \frac{\sqrt{3}}{2} a_0^3 c.$$

The density ρ of the alloy was determined by a standard method and yielded the value 8.998 for Cu_3Sn . This result is rather interesting, for the density of copper is 8.93 and that of tin is 7.29, and thus a marked contraction takes place on the formation of this alloy. This phenomenon, however, cannot alone be taken as evidence of the formation of an intermetallic compound, as the same phenomenon also occurs with solid solutions, but in the case of Cu_3Sn the density is greater than that of either component.

Returning to the above equation, and putting in the values of V , ρ , and M , we get $n = 0.495$, which means that with a cell of the above dimensions half a chemical molecule of Cu_3Sn is associated with it. Assuming the alloy to be a definite compound, such a cell repeated along the three co-ordinate axes would not make up a crystal of the substance, and this cell must, therefore, be a sub-unit of some larger crystal unit. Much time and trouble have been taken in searching the films and giving long exposures to discover additional faint lines which would give evidence of this. With exposures of eight hours and 6 milliamperes through the tube, and after a close search of the films, it could not be said with any degree of certainty that such additional lines were present. The number of atoms of copper and tin in the alloy is in the ratio of 3 : 1, whilst the squares of the atomic numbers of copper and tin are in the ratio of 1 : 3. This may account for the absence of some faint lines, taking the scattering effect of an atom as proportional to the square of its atomic number. In the well-known case of KCl , owing to the approximate equality of the atomic numbers of K and Cl , the diffraction data give a sub-unit of the true unit, and, for this compound, it is by comparison with the data for NaCl that the unit deduced is shown to be one-eighth of the true unit cell. We have prepared the compound Cu_3P , where the ratio of atoms is as 3 : 1, and of atomic numbers squared as 4 : 1. Consequently, if

the structure is hexagonal close packing, additional information might be obtained from powder photographs. A few films of this compound have been taken and additional lines can be seen on them, but as the films have not yet been analysed, nothing definite can be said as to the structure. A later paper will give an account of the study of these films.

If we assume all the atoms in the compound Cu_3Sn to be identical, or, better, if we assume a distribution of copper and tin atoms, as would be the case if the alloy was a solid solution, then M in the equation $n = \frac{\rho V}{M}$ should be taken as one-fourth of the mass of a Cu_3Sn molecule. If this is done, $n=2$, showing that two *mean* atoms are associated with the crystal unit. The relative intensities to be expected can be calculated on this basis and compared with the observed intensities of the lines on the photographs.

The intensities may be calculated from the formula * :

$$I \propto j \cdot d_{hkl}^{2/35} \cdot (A^2 + B^2),$$

where $A = \sum N \cos 2\pi(hx + ky + lz)$

and $B = \sum N \sin 2\pi(hx + ky + lz),$

j being the number of co-operating planes, and N atomic number, and the summation is to be taken over every atom contained in the crystal unit.

Placing a *mean* atom at points (000) and $(\frac{1}{3}, \frac{2}{3}, \frac{1}{2})$ in the cell, the other possible positions for the two atoms being eliminated owing to the absence of such simple reflexions as (0001) and (1121), and substituting the values of x, y, z , in the formula, the expression takes the form

$$I \propto j \cdot d_{hkl}^{2/35} \cdot N_m^2 [(1 + \cos 2\pi\{\frac{1}{3}h + \frac{2}{3}k + \frac{1}{2}l\})^2 + (\sin 2\pi\{\frac{1}{3}h + \frac{2}{3}k + \frac{1}{2}l\})^2],$$

where N_m is the atomic number of the *mean* atom.

The relative intensities calculated in this way are entered in Table I. column 9, and the observed intensities are given in column 8. The agreement between the observed and calculated intensities is good, and the relative intensities are the same as those obtained with a pure metal possessing a close-packed hexagonal structure. The cell is depicted in the figure.

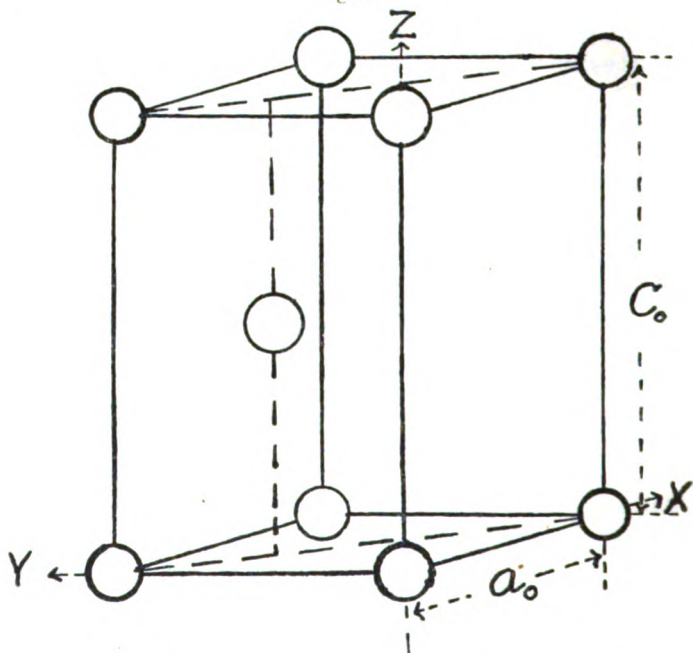
* Wyckoff, 'The Structure of Crystals,' p. 201.

In this cell the distance of closest approach of two atoms is that between atoms at (000) and $(\frac{1}{3}, \frac{2}{3}, \frac{1}{2})$. This distance is equal to

$$a_0 \sqrt{\frac{1}{3} + \frac{1}{4} \frac{c_0^2}{a_0^2}} = 2.68 \text{ \AA}.$$

The nearest distance between atoms in pure tin is 2.80 \AA ., and in pure copper, 2.54 \AA .*, so that the sum of the atomic radii of tin and copper is 2.67 \AA . This agrees closely with 2.68 \AA . obtained above for the shortest interatomic distance in the structure.

Fig. 1.



The information derived from the photographs is that which would be obtained if all the atoms of the alloy were identical, and the substance crystallized on an hexagonal lattice of the close-packed type. Lines which would enable a larger cell to be deduced are absent. This may be due either to the number of atoms of copper and tin being as 3 : 1, and their atomic numbers squared as 1 : 3, or, perhaps, to the compound Cu_3Sn not being a true compound but a solid solution.

* Bragg, 'X-rays and Crystal Structure,' p. 163.

2. The Crystal Structure of Cu_3Sb .

The photographs obtained with Cu_3Sb were exactly similar in pattern and in intensity of the lines to those of Cu_3Sn , but the distances of the lines from the centre of the films were slightly less.

The results of the analysis of these photographs are given in Table II.

TABLE II.— Cu_3Sb .

Copper K_α radiation. The value of λ_{K_α} is taken at 1.540 \AA . Diameter of camera 9.96 cm. Close-packed hexagonal structure, axial ratio 1.572.

Indices of form.	Distance of lines from centre in mm.			θ in degrees.	$\frac{\lambda}{2 \sin \theta}$	Calculated spacings.	Observed intensity.	Calculated intensity.
	Film (1).	Film (2).	Mean.					
10 $\bar{1}0$	32.50	32.41	32.46	18° 40'	2.406 \AA .	2.406 \AA .	.20	.23
0002	35.94	35.85	35.89	20 39	2.183	2.183	.40	.24
10 $\bar{1}1$	37.54	37.50	37.52	21 35	2.093	2.104	1.00	1.00
10 $\bar{1}2$	49.52	49.46	49.49	28 28	1.615	1.615	.27	.18
11 $\bar{2}0$	58.76	58.57	58.66	33 45	1.386	1.389	.30	.26
10 $\bar{1}3$	66.66	66.66	66.66	38 21	1.241	1.248	.40	.29
20 $\bar{2}0$	69.62	69.47	69.55	40 1	1.198	1.203	.05	.045
11 $\bar{2}2$	71.70	71.77	71.74	41 15	1.168	1.173	.30	.34
20 $\bar{2}1$	72.87	72.84	72.86	41 55	1.153	1.159	.17	.24
0004	78.21	78.27	78.24	45 1	1.089	1.092	.07	.05
20 $\bar{2}2$	82.67	82.68	82.68	47 35	1.043	1.052	.07	.065
1014	88.66	89.47	89.07	51 14	.988	.988	.08	.058
20 $\bar{2}3$	98.49	98.34	98.42	56 37	.922	.932	.20	.15
2130	101.91	101.83	101.87	58 36	.902	.909	.07	.046
2131	105.50	105.30	105.40	60 38	.884	.890	.20	.26
11 $\bar{2}4$	112.49	112.17	112.23	64 37	.852	.858	.24	.16
21 $\bar{3}2$	117.74	—	117.74	67 44	.832	.839	.12	.08
1015	122.79	—	122.79	70 29	.817	.819	.12	.074

The dimensions of the unit hexagonal prism calculated from the diffraction data are :—

a_0 (base) = 2.777 \AA . and c_0 (height) = 4.367 \AA .,
corresponding to an axial ratio

$$c_0 : a_0 = 1.572.$$

This cell is 3 per cent. larger in volume than the Cu_3Sn cell because of the larger antimony atom.

A determination of the density of the alloy gave the value 8.636. The density of antimony is 6.62, of copper 8.93, and, therefore, the density of the alloy is greater than 8.35 a value based on the proportion of antimony and copper present. A contraction takes place on the formation of the alloy, but the alloy is less dense than Cu_3Sn (8.998), though the atomic weight of antimony (120) is slightly greater than that of tin (119).

Taking the value 8.656 as the density of Cu_3Sb , we get $n=0.49$, so that half a molecule of Cu_3Sb is associated with the cell. If we assume a mean atom of mass one-fourth of the mass of the Cu_3Sb molecule as with Cu_3Sn , then $n=2$, and two such atoms would be associated with the cell. Placing such atoms at (000) and $(\frac{1}{3}, \frac{2}{3}, \frac{1}{2})$, the relative intensities of the lines on the photographs can then be calculated in the same way as for Cu_3Sn . The observed and calculated intensities are entered in Table II. columns 8 and 9. These are the same as those entered in Table I., since the atomic numbers of antimony and tin are 51 and 50 respectively, and the unit cells are exactly similar with the same axial ratio.

The distance of closest approach of atoms in antimony is 2.87 \AA^* , and in pure copper 2.54 \AA . The shortest inter-atomic distance for two atoms in the cell is 2.71 \AA ., which is almost exactly the sum, 2.705 \AA ., of the atomic radii of antimony and copper.

As copper itself is face centred cubic with a unit containing four atoms, it would appear that the substitution of one of these atoms by the much larger tin or antimony atom distorts the face centred cubic close-packing, with the result that the aggregate of atoms adjusts itself into the other close-packed arrangement—hexagonal close-packing.

As in the case of Cu_3Sn , the data for Cu_3Sb obtained in these experiments are the same as for a pure metal, such as zinc or magnesium, crystallizing on a close-packed hexagonal lattice containing one kind of atom.

Summary.

The crystal structures of Cu_3Sn and Cu_3Sb have been examined by the X-ray powder method.

Both compounds have close-packed hexagonal structures with axial ratio 1.572 in each case.

* Bragg, 'X-ray and Crystal Structure,' p. 173.

The diffraction pattern and the relative intensities of the lines are the same as obtained with a pure metal possessing a close-packed hexagonal structure. The absence of lines which would give a larger cell may be due to either:—

- (i.) that the diffraction effect of an atom is proportional to the square of its atomic number, and that in the above alloys the squares of the atomic numbers of copper and tin or antimony are as 1 : 3, whilst the ratio of the number of the respective atoms in the alloys is as 3 : 1; or perhaps
- (ii.) that the alloys may not be true compounds but solid solutions.

The dimensions of the hexagonal unit for Cu₃Sn deduced from the diffraction data are $a_0 = 2.749 \text{ \AA.}$, $c_0 = 4.322 \text{ \AA.}$

The shortest interatomic distance for the Cu₃Sn structure is 2.68 \AA. , agreeing closely with 2.67 \AA. , the sum of the atomic radii of copper and tin.

The dimensions of the hexagonal unit of Cu₃Sb are $a_0 = 2.777 \text{ \AA.}$, $c_0 = 4.367 \text{ \AA.}$

The shortest interatomic distance for the structure is 2.71 \AA. in almost exact agreement with 2.705 \AA. , the sum of the atomic radii of copper and antimony.

The Cu₃Sb cell is 3 per cent. larger in volume than that of Cu₃Sn, owing to the larger antimony atom.

Both cells are similar to that for a pure metal, such as zinc or magnesium, having a close-packed hexagonal crystal structure.

Powder photographs are being taken of the crystal structure of Cu₃P, where the ratio of the atomic numbers squared is as 4 : 1, and the ratio of the number of atoms as 3 : 1.

If Cu₃Sn and Cu₃Sb are true compounds, then further diffraction data from experiments with single crystals will doubtless be necessary before the distribution of atoms on the lattices and the space group can be determined.

In conclusion, we are grateful to Professor C. A. Edwards for his kindness in supplying us with the alloys and for the special interest he has taken in this research, and also to Professor W. L. Bragg for helpful criticism.

CXVII. *The Hall Effect in Aluminium Crystals in relation to Crystal Size and Orientation.* By PHYLLIS JONES, M.Sc.
(Research Student, University College of Swansea)*.

INTRODUCTION.

WHEN a metal plate carrying an electric current is placed in a magnetic field, so that the lines of force are normal to the plane of the plate and to the direction of flow of the electric current, a transverse galvanomagnetic potential difference is set up between the edges of the plate. This interesting result was discovered by Hall † in 1879, and from the time of its discovery much work has been done in an attempt to arrive at a satisfactory explanation of the phenomenon.

With this end in view, many experiments have been carried out to try and discover the factors which chiefly influence this effect.

The object of the present paper is to determine whether the Hall effect is in any way influenced by the dimensions and orientation of the crystal aggregates composing the metal. For this purpose experiments were performed with specimens of aluminium which were prepared and presented to the Metallurgical Department of the University College of Swansea by Professor H. C. H. Carpenter, and kindly loaned for the purpose of this research by Professor C. A. Edwards. The specimens were all of the same shape, and of approximately the same dimensions, viz. 23 cm. in length, 3 cm. in thickness, and 2.5 cm. in width. The size of the crystals varied in such a way that of the eight specimens examined, one contained a single crystal 16 cm. in length, while another contained very small crystals, 183 of which occupied an area of about 1 sq. mm. The remaining six specimens contained crystals of intermediate sizes.

Although aluminium crystallizes in the cubic system, it is still of some interest to determine whether the direction of the primary current with respect to the crystal face has any bearing on the Hall effect ‡.

Again, in the case of the crystalline aggregates, an opportunity is offered for testing whether the conditions at the

* Communicated by Prof. E. J. Evans, D.Sc.

† E. H. Hall, Amer. Journ. Math. vol. ii. p. 287 (1879).

‡ W. L. Webster (Proc. Camb. Phil. Soc. vol. xxiii. part 7, p. 800, July 1927) finds that the Hall coefficient in single crystals of iron is independent of the direction in the crystal, and that the effect is similar to that observed in ordinary soft iron.

crystal boundaries have any effect on the value of the Hall coefficient.

An absolute determination of the Hall coefficient in aluminium is, however, valuable owing to the uncertainty that exists concerning its magnitude. For some time, the value generally accepted for the Hall effect in aluminium was about 3.9×10^{-4} , but Smith * in 1910 obtained a lower value of 3.2×10^{-4} . Smith, however, states that the aluminium used by him for this determination was of unknown origin and that impurities may have influenced his results.

A little later, Alterthum † published a paper in which he quotes 3.9×10^{-4} as the value of the Hall coefficient for aluminium at room temperature. However, during the course of his paper, Alterthum points out that on increasing the primary current from 1 ampere to about 1.5 amperes the value obtained was 3.2×10^{-4} , which agrees with Smith's results. Raethjen ‡ recently examined the effect in aluminium foil, and obtained a value of 3.43×10^{-4} for the Hall constant. It is therefore evident that the value of the Hall coefficient for aluminium is somewhat uncertain.

DESCRIPTION OF APPARATUS AND METHOD.

It has been proved experimentally that for a given metal the Hall electromotive force E is given in absolute units by the formula $E = \frac{RHI}{d}$, where H is the magnetic field in gauss, I is the current in absolute units, d is the thickness of the plate in cms., and R is the Hall coefficient, which in general is a function of the temperature and of the strength of the field.

Aluminium happens to have a very low coefficient of the order of 3×10^{-4} ; and since the specimens used in the present experiments have an average thickness of .3 cm., it follows from the above formula that for a current of 4 amperes and a magnetic field of about 6000 gauss the Hall potential difference is an extremely small quantity of the order of 2.4×10^{-8} volt. A very sensitive instrument is therefore required for the measurement of such a small potential difference, and for this purpose a delicate Paschen galvanometer made by the Cambridge Scientific Instrument Company was used.

* *Phys. Rev.* xxx. p. 1 (1910).

† *Ann. d. Phys.* (4) xxxix. p. 933 (1912).

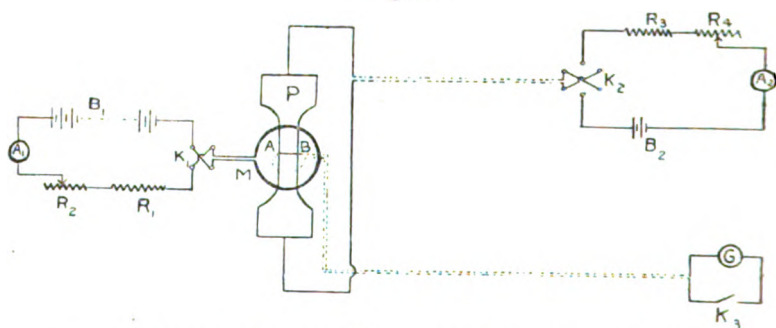
‡ *Phys. Zeits.* xxv. pp. 84-89 (1924).

The arrangement of the apparatus is shown in fig. 1, in which P represents one of the aluminium specimens.

The current through the specimen is supplied by a battery B_2 consisting of two storage cells. The remainder of the circuit consists of a rheostat R_3 , a fine adjustment rheostat R_4 , a reversing key K_2 , and a Weston ammeter A_2 , which had been calibrated against a large Weston standard ammeter, whose indications are correct to within one-tenth of 1 per cent. As the Weston ammeter A_2 enables the current to be read to within one part in 1200 of the current employed, the primary current through the plate could be measured correctly to within one-tenth of 1 per cent.

The specimen P was placed in a magnetic field, which was produced by a large circular electromagnet. The current through the coils of the magnet was supplied by the mains

Fig. 1.



from a storage battery B_1 . A resistance frame R_1 , an ammeter A_1 , a fine adjustment rheostat R_2 , and a reversing key K complete the magnet circuit. The magnetic fields corresponding to different currents through the coils of the electromagnet were measured by means of a Grassot fluxmeter and search coil. The absolute value of the magnetic field corresponding to a current of 2 amperes passing through the electromagnet was determined by means of a delicate ballistic galvanometer and a carefully constructed search coil whose mean area could be readily measured. In this way the corrections to be applied to the fluxmeter readings were determined, and the magnetic field measurements are considered to be correct to within about one-half per cent.

In fig. 1, K_3 in the secondary circuit represents a copper key and G represents the Paschen galvanometer. The galvanometer was mounted on a stone pillar, which was built into the concrete foundations of the laboratory. The

magnet system of the galvanometer was suspended between two pairs of coils, which could be connected in series or in parallel as required. When the coils were connected in series, as in the present experiments, the resistance of the galvanometer was 12.87 ohms. The terminals of the galvanometer were made of copper so as to eliminate thermoelectric effects. As the moving magnet system was easily influenced by external magnetic fields, it was found necessary to enclose the galvanometer in a double shield of soft iron. In this way the effect of external disturbing magnetic fields was very considerably reduced.

The Paschen galvanometer is characterized by its high sensitiveness corresponding to a comparatively quick period of motion of the magnet system. In the present experiments the control magnets were so arranged that for a period of about 3 seconds a microvolt applied to the terminals of the galvanometer produced a deflexion of about 38 cm. on a scale at a distance of 1 metre from the galvanometer.

The sensitiveness of the galvanometer varied slightly from day to day, probably owing to changes in the temperature of the room. The galvanometer was calibrated immediately before and after a series of readings of the Hall potential difference, and as was to be expected the calibration constant did not alter during that short interval of time.

The electromagnet was at a distance of $7\frac{1}{2}$ metres from the galvanometer, and was rotated into such a position that the direct effect of the permanent field of the excited electromagnet on the magnet system of the galvanometer was a minimum. This effect could be reduced to such an extent, that for a reversal of the magnetic field the change in the zero of the galvanometer as read on the scale 1 metre away was less than 1 mm. In this position of the electromagnet the sensitiveness of the galvanometer was found to be increased, and decreased respectively by about 1.2 per cent. on the application and reversal of the magnetic field for the maximum field employed. However, as will be shown later, a correction can be applied, if necessary, to eliminate any error on this account.

The galvanometer was connected to the specimen by means of long flexible wires, which were suspended overhead and were well insulated. The connecting wires were wound non-inductively, and kept taut to within a few inches of the galvanometer and aluminium plate respectively in order to avoid superimposed inductive effects in the galvanometer due to accidental vibrations.

The apparatus adopted for supporting the specimen in the

magnetic field consisted of a wooden frame, in which the specimen was rigidly supported in a vertical position in the air-space between the poles of the magnet. Brass clamps served as leads for the primary current, and the secondary electrodes consisted of spring copper contacts carried by thick strips of ebonite. In some cases the copper contacts were replaced by aluminium contacts, but the results were unaltered. By means of a screw arrangement the secondary electrodes could be moved along the edges of the specimen as required.

For a determination of the Hall coefficient an electric current was passed through the specimen, and the secondary electrodes were adjusted so that on closing the secondary circuit and reversing the current through the specimen, the deflexion indicated by the galvanometer was as nearly zero as possible. When this was the case, the secondary electrodes were practically on an equipotential line.

The magnetic field was then applied, and after a short interval of time, during which the inductive effects due to the application of the field had died down, the secondary circuit was closed and the reading on the scale of the galvanometer was observed. With the secondary circuit still closed, the primary current was quickly reversed and a second reading observed. The primary current was again reversed so as to pass in the original direction, and a third reading was noted. When the first and third readings agreed to within 1 mm., the mean of these two readings was taken and subtracted from the second reading to give a value of the deflexion produced by the field for a reversal of the primary current.

With the field still on, the primary current was reversed backwards and forwards so as to obtain several values of the deflexion, the mean of which shall be denoted by $2\theta_1$. Under good conditions it was found that for several reversals of the primary current through the plate the readings on the scale were identical for each particular direction of the primary current.

The secondary circuit was now opened, and the magnetic field was applied in the opposite direction. The primary current was again reversed a few times, in order to obtain an average deflexion $2\theta_2$ corresponding to the second direction of the field.

The mean of the two deflexions $2\theta_1$ and $2\theta_2$ on being halved gave a deflexion θ , which was proportional to the potential difference set up between the edges of the plate.

To be strictly correct, a small percentage correction should be applied so as to increase $2\theta_1$, and the same percentage correction so as to decrease the deflexion $2\theta_2$. This is due to

the fact that for one direction of the field the sensitiveness of the galvanometer was decreased by about 1.2 per cent. for the maximum field employed, whereas for the reverse direction of the field the sensitiveness of the galvanometer was increased by the same amount. Owing to the nature of the correction, however, it is clear that the result obtained on adding these slightly modified deflexions should agree with that obtained on adding the uncorrected deflexions. The difference between the results was calculated to be less than .1 per cent. for the maximum field employed.

The galvanometer was calibrated under exactly the same conditions as existed for the determination of the Hall effect, and the potential difference required to be applied to the terminals of the galvanometer to produce a deflexion θ was determined. Owing to the resistance of the long leads in the secondary circuit not being negligible, this potential difference was multiplied by a factor 1.091 in order to give the potential difference between the edges of the plate.

The determinations of the Hall effect for the various specimens were carried out at room temperature, which was registered on an accurate mercury thermometer placed with its bulb against the plate. The plates employed in these experiments were of such dimensions that the current passed through them did not produce an appreciable rise of temperature.

It should be mentioned at this point that when a plate carrying an electric current is placed in a magnetic field, so that the lines of force are normal to the plane of the plate and to the direction of the flow of the current, a transverse galvanomagnetic temperature difference is set up between the edges of the plate. If the secondary electrodes are made of a different material from the plate itself, this temperature difference, which is known as the Ettingshausen effect, gives rise to a thermo-electromotive force which is superimposed on the Hall potential difference.

The Ettingshausen effect, however, for copper electrodes can be calculated to be only of the order of 3×10^{-11} volt* for the magnetic field and primary current employed in the present experiment, and can therefore (within the limits of experimental error) be neglected in comparison with the Hall potential difference. In addition, when aluminium electrodes were used, there was practically no difference of potential to be expected due to the Ettingshausen temperature difference.

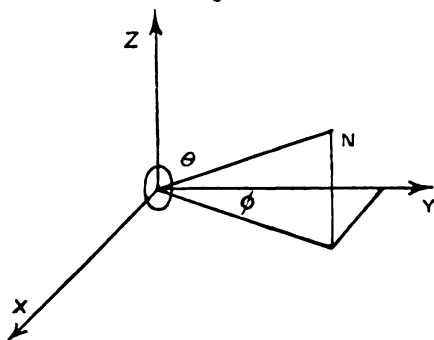
* Unwin found the Ettingshausen coefficient for aluminium at room temperature to be $+1.06 \times 10^{-9}$.

A DETERMINATION OF THE ORIENTATION OF CRYSTALS IN SPECIMENS.

The approximate orientation of the lattice planes of the single crystal in specimen A with respect to the face of the specimen was obtained by subjecting the crystal to an X-ray analysis. In specimen B the Hall effect was determined for the larger of the two crystals only, and this crystal was analysed by X-rays also. The method of procedure was somewhat similar to that described by Dr. Müller* in a paper published by him in 1924. The specimen under consideration was supported vertically and rotated in the path of a beam of X-rays from a copper target.

Following the method adopted by Dr. Müller, let X , Y , Z (fig. 2) represent the axes of a rectangular system of co-

Fig. 2.



ordinates in which the XY plane corresponds to the surface of the specimen, and the Z axis represents the direction of the long axis of the plate. The position of the line ON is then defined by the angles θ and ϕ , and the position of the cubic lattice is definitely fixed by the values of θ and ϕ for the normals to two known crystal planes.

In the present experiment the position of ON was determined only for the (111) planes in the lattice of each of the crystals A and B. Intense lines were obtained on the photographic plates, and from geometrical considerations were attributed to reflexions of the copper lines from the (111) planes of the crystals. From crystal B a reflexion was obtained from the (111) plane corresponding to the first order of the copper lines, but for crystal A a reflexion corresponding to the second order of the same lines was obtained.

* Roy. Soc. Proc. A, vol. cv, p. 500 (1924).

The value of θ was approximately determined from the nature of the photographs of these lines. In order to determine the angle ϕ it was necessary to know the angle of setting of the specimens for which the reflexions took place from the (111) plane. This was done by dividing into small ranges the whole of the range through which the specimen was originally turned, and determining for which of these ranges an intense (111) reflexion could be obtained. In this way the angle of setting for which the reflexion occurred could be determined to within a degree.

EXPERIMENTAL RESULTS.

The Hall coefficient was determined for eight specimens of aluminium, which are represented in Table I. by the letters A, B, ... H. These specimens contained 99.6 per cent. aluminium, the chief impurity being silicon 0.19 per cent. and iron 0.14 per cent. Specimen A consisted of a single crystal 16 cm. in length and 2.5 cm. in width; specimen B contained two crystals of the same width (2.5 cm.) and of about 6 and 8 cm. in length respectively. The lengths of the crystals in specimen C were approximately 6.7 cm., 2 cm., and 8 cm., the width being 2.5 cm. in each case. The approximate average dimensions of the crystals contained in specimens D, E, and F were 1.8 cm. by 1.7 cm., 1 cm. by .8 cm., and .6 cm. by .4 cm. respectively. Specimen G contained about 30 crystals per sq. cm., while specimen H, which was examined under a high-power microscope, was found to contain about 183 crystals per sq. mm.

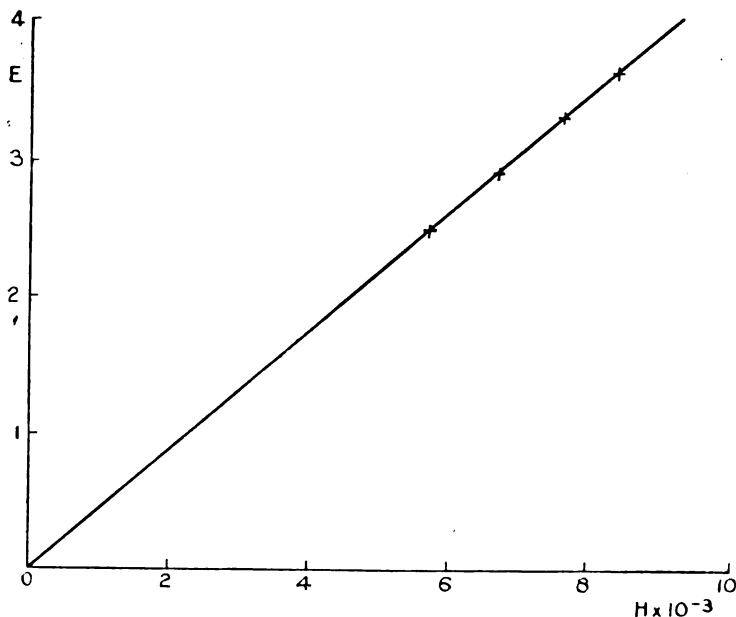
The Hall potential difference in these specimens was measured for magnetic fields ranging from 5724 gauss to 8414 gauss. The current passed through the plate for each determination of the Hall coefficient was 3.923 amperes. The deflexions produced in the present experiments for a reversal of the Hall e.m.f. ranged from 1.36 cm. for the lowest magnetic field to 2.83 cm. for the highest magnetic field. These deflexions could be read to one-tenth of a millimetre on the scale of the galvanometer.

A graph was plotted for each specimen, showing the relation between the Hall potential difference and the magnetic field employed. A graph for crystal A is shown in fig. 3, where the ordinates represent the Hall e.m.f. in absolute units, and the abscissæ represent the field in gauss. From fig. 3 it is seen that the Hall potential difference is proportional to the magnetic field.

1320 Miss P. Jones on the Hall Effect in Aluminium

Similar graphs were obtained for each of the other specimens.

Fig. 3.—Specimen A.



The results of the investigation of the Hall effect for each of the specimens are as follows:—

TABLE I.

$I = \cdot 3923$ absolute units.

$H = 8414$ gauss.

Specimen.	Number of grains per mm. ²	d , in cm.	Temperature.	E , in absolute units.	$R \times 10^4$.
A	0.00625	0.3147	15.8° C.	3.61	—3.44
B	0.00057	0.3150	16.4 „	3.59	—3.43
C	0.00072	0.3140	11.0 „	3.60	—3.42
D	0.0032	0.3114	15.2 „	3.66	—3.45
E	0.0125	0.3065	15.4 „	3.73	—3.46
F	0.042	0.3090	13.0 „	3.65	—3.42
G	0.3	0.3010	12.8 „	3.77	—3.44
H	183	0.3161	15.6 „	3.60	—3.45

In Table I., E is the value in absolute units of the potential

difference for a magnetic field of 8414 gauss, and R is the value of the Hall coefficient calculated from the formula

$$R = \frac{Ed}{IH}.$$

The negative sign attributed to the coefficient R means that the Hall effect in aluminium is in the same direction as that in bismuth.

An examination of Table I. shows that the values of the Hall coefficients for all the specimens are in good agreement with each other, the mean value of the constant being 3.44×10^{-4} at a mean temperature of 14.4°C . The Hall coefficient was also determined for another plate of aluminium of thickness .2605 cm., and for which the aluminium content amounted to at least 99.6 per cent. The Hall coefficient for this sample of aluminium was also found to be 3.44×10^{-4} , a value which is in good agreement with that obtained for each of the other specimens investigated. It is interesting to note that this value of the Hall coefficient for aluminium only differs by about .3 per cent. from that obtained by Raethjen*.

In order to compare the result obtained for aluminium with that obtained for a specimen of different material, the Hall coefficient was determined for a plate of electrolytic copper of the highest purity of thickness, .150 cm. The value of the coefficient for copper was found to be 5.27×10^{-4} at room temperature (21°C .), and this value agrees well with the value (5.28×10^{-4} at 18°C .) which was obtained by Alterthum†.

The results of the X-ray analysis in the case of the two specimens A and B are set down in Table II., where θ and ϕ are the angles referred to previously in connexion with fig. 2.

TABLE II.

Specimen.	θ .	ϕ .
A	86°	60°
B	68°	80°

These X-ray investigations do not lay claim to any great accuracy, but from the approximate results obtained it can be stated that the orientation of the crystal lattice with respect to the surface of the specimen differs in the case of the two crystals examined.

Although there is a difference in the orientation of the crystals, it is clear from Table I. (A and B) that the Hall

* *Loc. cit.*

† *Loc. cit.*

coefficient is the same in both cases, the small difference in the results being easily accounted for by experimental error. Since the primary current passes in a direction parallel to the surface of the specimen, it appears that the orientation of the lattice planes of the crystal with respect to the directions of the primary current does not in any way influence the Hall effect.

An examination of Table I. also shows that the Hall coefficient is the same within experimental error for all the crystalline aggregates, however large the number of crystals and the number of boundaries that exist in the specimen. Crystal size therefore has no influence on the magnitude of the Hall effect.

SUMMARY.

1. The Hall coefficient has been determined for eight specimens of single and aggregate crystals of aluminium for a current of 3.923 amperes and for magnetic fields ranging from 5724 to 8414 gauss.

2. The Hall coefficient in aluminium is independent of crystal size.

3. The Hall coefficient is independent of the orientation of the lattice planes in the crystal with respect to the primary current.

4. The absolute value of the Hall coefficient for aluminium is 3.44×10^{-4} .

I wish to express my gratitude to Professor E. J. Evans for his valuable advice, and to both Mr. W. Morris-Jones and Professor E. J. Evans for the use of their X-ray apparatus.

September 1927.

CXVIII. *On the Silvering of Glass Plates for Optical Instruments.* By J. J. MANLEY, M.A. (Fellow of Magdalen College, Oxford) *.

THE difficulties attending the preparation and renewal of plane-mirrors, such as those used in a Michelson interferometer, are well understood. Actual silvering is readily accomplished, but a chief difficulty arises from the uncertainty

* Communicated by the Author.

of obtaining a film sufficiently coherent and firm to endure the necessary polishing. Repeated failure led me to try some modifications of the usual procedure. Success was ultimately attained in two different ways, which are as follows :—

Method 1.—The glass plate, having been made chemically clean, is covered with distilled water and the containing-vessel placed in ice; the measured portions of the two silvering solutions are also similarly cooled. In due time the water is poured away from off the glass plate and the vessel at once replaced in ice. Next, the two ice-cold solutions are rapidly mixed and immediately introduced into the vessel containing the plate to be silvered. Silvering proceeds slowly, and apparently in consequence of this the film acquires a firmness rarely attained at ordinary temperatures. After some 8 or 10 hours the plate is removed from the bath, then washed and dried, and finally polished in the usual manner.

Method 2.—According to the second plan, whereby the lengthy and tedious process of polishing is eliminated, the silvering is effected at the prevailing temperature of the room. It is allowed to proceed for from 10–15 minutes only. When the plate has been immersed for the appropriate time a gentle stream of water is passed through the bath for some minutes. The silvering is thus arrested and the plate partially washed. Lastly, the plate is rinsed a few times with distilled water and then set up vertically upon white blotting- or filter-paper. Thus the mirror is rapidly dried and so made ready for immediate use.

Prepared according to method 2, the silver surface possesses a high reflecting power and scratches are entirely absent. It will, however, be obvious that such a mirror, the silver film of which has marked tenuity, must be handled with care and fingering avoided; but given proper treatment the permanence of the mirror is quite normal. The operation of renewing the reflecting silver film is simple in character and quickly performed, and the preparation of a new mirror is a commonplace, requiring but little experience or skill.

CXIX. The Accuracy of the Monochord as a Measurer of Frequency. By GEORGE E. ALLAN, D.Sc., Lecturer on Applied Physics, Glasgow University*.

CONTENTS.

Introductory.

Equation of motion of vibrating wire.

Corrections of Seebeck, Donkin, and Schaefer.

Apparatus: Monochord, standard metre, lead weights, standard vibrators, wire.

Monochord observations.

Effect of temperature on glass rule, forks, and wire.

Effect, on tension, of weight of monochord wire and upthrust on lead weights.

Effect of tension on linear density of wire.

Calculation of the Taylor frequency. Tables.

Form of correction. Logarithmic graphs.

Values found for m , c , p , q , and K .

Final form of correction.

Discussion.

ALTHOUGH the monochord is said to have been in use in the time of Pythagoras†, the elementary laws of vibrating strings were not made generally known till 1636, when Mersenne published them in a work entitled ‘L’Harmonie Universelle.’ These laws, expressed separately by Mersenne, were deduced as a whole from dynamical principles by Brook Taylor, who published them in his book on the ‘Method of Increments’ in 1715.

Galileo in 1638, Newton, Euler in 1729, D’Alembert in 1747, and Daniel Bernoulli in 1755‡ are also said to have studied the problem of vibrating strings.

When a uniform wire, of length l and linear density ρ_1 , is subjected to tension T , the frequency of its fundamental vibrations, as expressed by Taylor’s formula, is

$$n = \frac{1}{2l} \sqrt{\frac{T}{\rho_1}} \quad \dots \dots \dots (1)$$

The more complete equation of motion of the vibrating string indicates that Taylor’s formula is not exact, inasmuch

* Communicated by the Author.

† Helmholtz, ‘Sensations of Tone,’ 2nd English edition, p. 14 (1885).

‡ Rayleigh, ‘Sound,’ vol. i. p. 181. “It is to Daniel Bernoulli that we owe the general solution of the string equation.”

Accuracy of the Monochord as a Measurer of Frequency. 1325
as it makes no allowance for the "rigidity" of the wire.
The equation may be written* :

$$\frac{d^2y}{dx^2} = \frac{T}{\rho_1} \frac{d^2y}{dx^2} - \frac{k^2 E}{d} \frac{d^4y}{dx^4}, \quad \dots \quad (2)$$

where k is the radius of gyration of the section of the wire, E is Young's modulus, and d the volume density of the material of the wire. The last term in the equation introduces the correction for the resistance to bending, and the corrected frequency of the string then becomes †

$$n = \frac{1}{2l} \sqrt{\frac{T + \frac{EI\pi^2}{l^2}}{\rho_1}}, \quad \dots \quad (3)$$

where I is the moment of inertia of the cross-section of the wire. This correction is never applied in the ordinary use of the monochord, a fact which aids in causing the instrument to be regarded as a somewhat inaccurate means of measuring frequencies within the musical range.

A. Seebeck refers ‡ to Savart's correction for the rigidity of the wire, and to Duhamel's attempt to deduce the correction from theory. Seebeck also gives a form of correction which may, for our purpose, be modified so that in terms of the above symbols the observed frequency requires the addition of the quantity

$$\text{constant} \times \frac{n^2 \rho_1^{\frac{3}{2}}}{T},$$

where n is the frequency of the perfectly flexible string. He states that this correction may not be neglected in exact monochord work, and gives its amount in one instance as 1 vibration in 127, as observed in some tests with a thin steel wire.

W. F. Donkin § gives a correction which may be similarly reduced to the form

$$\text{constant} \times \frac{n^3 \rho_1^3}{T^{\frac{3}{2}}},$$

in which n is the frequency if the wire were perfectly thin. Schaefer's correction is the same as Donkin's. Donkin remarks that Seebeck found his correction to agree with experiment when the ends of the wire were clamped.

* See, for example, H. Lamb, 'Sound,' p. 132.

† O. Schaefer, *Ann. d. Physik*, vol. lxii. p. 156 (1920).

‡ *Ann. d. Physik u. Chemie*, vol. lxxvii. pp. 442-448 (18 8)

§ 'Acoustics,' 2nd edition, p. 179 (1884).

Donkin also found that his own form of the correction agreed with experiment in the case of a wire stretched over bridges *, but he gives no numerical data.

Both of the above authorities agree that the frequency as calculated by Taylor's formula is too low, that the deviation from the true frequency increases with the frequency and with the linear density, but diminishes with increased tension. These general conclusions are cited in the text-books on Sound by Rayleigh, Barton, and Lamb. The last-named author points out that the uncertainty of the correction for resistance to bending arises because of the uncertainty as to the nature of the terminal conditions of the wire. A wire where it passes over a bridge cannot be accurately regarded, he points out, as merely supported or as clamped.

Numerous researches have been made in which the monochord has played a part †; yet, so far as is known to the writer, no systematic experimental test of the monochord correction has been hitherto carried out.

The observations recorded here were made for the purpose of determining the magnitude of the correction and its dependence on frequency, linear density, and tension. Let n be the value of $\frac{1}{2l}\sqrt{\frac{T}{\rho_1}}$, or the Taylor frequency, and N the true frequency of the wire, then

$$N = n + \delta n, \quad . \quad . \quad . \quad . \quad . \quad (4)$$

where δn is the correction to be sought.

Apparatus.—Observations were made by means of a vertical monochord to which steel wires were attached and kept in definite tension by slotted weights placed on a brass

* *Loc. cit.* p. 187.

† J. Blyth, "Electric Sonometer," R.S.E. Proc. vol. xi. p. 28 (1880-81).

Barton and his co-workers, Phil. Mag. July 1905, p. 149; also Sc. Abstracts, 1907-12.

C. V. Raman, Phys. Rev. March 1911, p. 309. Motion at the nodes.

J. E. Ives, Phil. Mag. June 1911, p. 742. String in viscous medium.

J. A. Fleming, Phys. Soc. Proc. 1913. Loaded string and electrical analogue.

Kenelly and Manneback, Sc. Abstract No. 1915, Nov. 1921. Application of electric sonometer.

O. Schaefer, *loc. cit.* Measurement of expansion by monochord.

S. Ray, Phys. Rev. July 1926, p. 229. Investigation of wave-velocity.

carrier hung from the lower end of the wire. The wire made contact with two metallic bridges, and, as the upper bridge projected slightly beyond the lower one, satisfactory contact of the wire with both bridges was made by tilting the frame of the monochord back through about 1° . The length of the wire between the lower fixed bridge and the upper adjustable bridge was determined with a standard glass metre scale divided into centimetres and millimetres. The upper bridge had a screw for fine adjustment, and pads of cotton wool were used to stifle the vibrations of those parts of the wire which lay beyond the bridges. A small rimmed shelf below the lower bridge and a metal strap near the top of the monochord were fitted to carry the glass rule, so that the scale, when in use, was in contact with the wire, and the errors of parallax to which the readings of the bridge positions were liable were reduced to a negligible quantity. Length readings could thus be conveniently and accurately estimated, with the aid of a lens, to $1/10$ mm. By making 10 cm. the minimum length observed, an accuracy of at least 1 in 500 was obtained in the measurement of the length l .

The lead weights were about 500 gm. each, and the carrier weighed 169.4 gm. One lead weight, used as a standard, was carefully weighed, and the others were determined in terms of this standard.

The effect on the tension of the weight of the monochord wire below the upper bridge is small and variable. If the length of wire below the lower bridge is L , and W gm. is the weight supported, the tension is expressed accurately enough by

$$T = W + \rho_1(L + \frac{1}{2}l) - 0.108 \frac{W}{1000}, \quad \dots \quad (5)$$

where it is taken that the upthrust on the lead weights due to air displaced is 0.108 gm. wt. per kilo. of lead. Since the greatest error introduced by neglecting the two effects mentioned was 1 in 7000, namely in the case of the thinnest wire when carrying the smallest weight, these two sources of error were not taken into account, and it was found sufficient to express the other tensions to the nearest gramme.

Standard Vibrators.—The standards of frequency consisted of three forks of respective frequencies 255.6, 514.2, and 1024. Of these, the first and third were made by Kœnig of Paris; the highest fork was of massive form and was in good condition, and was assumed to be correct at

14° C., a little over the average temperature of the tests. When the second and third forks were sounded together beats were heard which had a frequency of 4.4 per second. By the use of small rubber bands as loads, the octave of fork No. 2 was found to have the higher pitch, and the frequency of the fundamental of this fork, as found from the beats, was 514.2. Forks Nos. 1 and 2, when sounded together, gave three beats per second, No. 2 being again higher in pitch, and a value 255.6 was found for the frequency of No. 1 fork.

Wire.—Ordinary steel piano wire was used in various sizes. The observations refer to wires having approximate linear densities, etc., as given in the following table. The diameters, as found by screw-gauge, were not always in conformity with those of the standard wire gauge system, and in nearly all cases there was a tendency to ellipticity of section. When not in use, the hanks of wire were kept in a tin box containing a quantity of dry slaked lime to prevent the rusting of the wires. The wires gradually rusted when hanging on the monochord, but readings were taken while the wires were fresh in order to discount this effect.

TABLE I.
Dimensions of Wires.

S.W.G. No.	Mean diameter. mm.	Linear density. gm./cm.	Approximate breaking- weight. kgm.
32	0.277	0.004930	17.7
28	0.351	0.007656	26.3
26	0.456	0.01278	40.0
23	0.616	0.02318	78.5

The figures in the last column are from one-reading tests, and are included to give a rough idea of the limiting tension which may be applied to these wires.

Monochord Observations.—Using a given wire and fork, a series of observations was taken for tensions varying from 668.9 gm. to 11,002 gm. weight, in all nine different tensions being employed. These tensions are specified in Table II.

TABLE II.—Monochord lengths, Taylor frequencies, and monochord errors. $\rho_0 = 0.004130$ gm. per cm.

Graph.	T.	668.9	1168	1667	2669	4164	5668	7175	8684	11002
		2.8254	3.0675	3.2219	3.4263	3.6195	3.7534		3.9387	4.0415
A 514.2	l	11.60	15.05	17.89	22.54	28.08	32.76			
	n	497.4	506.8	509.4	511.8	513.4	513.7			
	δn	16.8	7.4	4.8	2.4	0.8	0.5			
	$\log \delta n$	1.2253	.8692	.6810	.3802					
B 1024	l	9.10	11.41	14.17	16.50	18.54	20.40	22.95
	n	1001.5	1011.1	1017.4	1019.9	1021.8	1022.1	1023.6
	δn	22.5	12.9	6.6	4.1	2.2	1.9	0.4
	$\log \delta n$	1.3522	1.1106	.8195	.6128	.3424	.2788	

In the table above, the first column contains the letter by which the graph is denominated and the frequency of the standard fork. At the top are given the tensions in grammes and, for convenience, their logarithms. The spaces below contain the monochord lengths in cm., the Taylor frequencies, the monochord errors and their logarithms. In the graphs $\log \delta n$ is plotted against $\log T$. No points are plotted for errors less than unity.

TABLE III.— $\rho_0 = 0.007656$ gm. per cm.

Graph.	T.	668.9	1168	1667	2669	4164	5668	7175	8684	11002
		1866	2428	2886	3636					
C 255.6	l	248.2	252.0	253.4	254.6					
	n	7.4	3.6	2.3	1.1					
	δn	.869	.556	.362	.041					
	$\log \delta n$					
D 514.2	l	...	12.35	14.53	18.23	22.64	26.36	29.60	32.56	
	n	...	495.5	503.2	507.7	510.8	512.0	513.2	513.4	
	δn	...	18.7	11.0	6.5	3.4	2.2	1.0	0.8	
	$\log \delta n$...	1.272	1.041	.813	.532	.342	0		
E 1024	l	9.33	11.48	13.33	14.95	16.43	18.18
	n	992.0	1007.3	1012.4	1016.1	1017.5	1018.7
	δn	32.0	16.7	11.6	7.9	6.5	5.3
	$\log \delta n$	1.505	1.223	1.065	.898	.813	.724

TABLE IV.— $\rho_0=0.01278$ gm. per cm.

Graph.	T.	668.9	1168	1667	2669	4164	5668	7175	8684	11002
F 255.6	l	...	19.25	22.63	28.35	35.19	40.97			
	n	...	245.9	249.9	252.5	254.1	254.7			
	δn	...	9.7	5.7	3.1	1.5	0.9			
	$\log \delta n$987	.756	.491	.176				
G 514.2	l	14.40	17.77	20.56	23.06	25.30	
	n	497.2	503.3	507.6	509.4	510.8	
	δn	17.0	10.9	6.6	4.8	3.4	
	$\log \delta n$	1.230	1.037	.820	.681	.532	
H 1024	l	9.15	10.51	11.74	12.85	
	n	977.4	993.0	1000.5	1005.8	
	δn	46.6	31.0	23.5	18.2	
	$\log \delta n$	1.668	1.491	1.371	1.260	

TABLE V.— $\rho_0=0.02318$ gm. per cm.

Graph.	T.	668.9	1168	1667	2669	4164	5668	7175	8684	11002
I 255.6	l	21.70	26.58	30.76	34.56	37.86	42.49
	n	245.0	249.8	251.9	252.3	253.4	254.2
	δn	10.6	5.8	3.7	3.3	2.2	1.4
	$\log \delta n$	1.025	.763	.568	.519	.342	.146

With a given tension, six independent determinations were made of the monochord length of wire in unison with the fork, the bridge being put out of adjustment between the readings. In many cases the process was carried through three times, and in a few cases four times. The tuning was done by any or all of the methods: (a) by sense of tune, (b) by adjustment for maximum resonance, and (c) by reducing the beats to zero. The observations and results are given in Tables II. to VI. and in the accompanying graphs.

Calculation of the Taylor Frequency.—Before applying Taylor's formula, it is necessary to consider whether the readings require to be standardized for changes of temperature. Such changes will affect the standard metre, the standard forks, and the monochord wire. The range of temperature within which the tests were carried out was from $8^{\circ}5$ to $17^{\circ}5$ C., but most of the tests were made at temperatures between 11° and 13° C., and no corrections were applied for temperature effects. It is well known that the frequency of a fork undergoes a slight diminution with rise of temperature according to the formula

$$N = N_0(1 - \alpha t),$$

where t° C. is the temperature at which the frequency of the fork is N , and α is a coefficient which, for small temperature range, may be taken as 0.0001^* . A change of temperature of 10° would thus alter the frequency by about 1 in 1000. An endeavour was made to keep this error as low as possible by taking the tests when the room-temperature was between 11° and 13° C.

Effect of Tension on Linear Density.—Let a uniform steel wire of circular section, of radius r and of length l when unstretched, have mass m and density d . Then its linear density is given by

$$\rho_0 = \frac{m}{l} = \pi r^2 d. \quad \dots \quad (6)$$

When the wire is under tension T , let its length become $l + \delta l$. Its linear density ρ_1 is now

$$\rho_1 = \frac{m}{l + \delta l}. \quad \dots \quad (7)$$

Hence

$$\frac{\rho_1}{\rho_0} = \frac{l}{l + \delta l} = 1 - \frac{\delta l}{l} \text{ nearly.}$$

* E. C. Woodruff, Phys. Rev. xvi. pp. 325-55 (June 1903).

Also, by Hooke's law,

$$E \frac{\delta l}{l} = \frac{T}{\pi r^2} = \frac{Td}{\rho_0}, \text{ by (6).}$$

Therefore

$$\frac{\rho_1}{\rho_0} = 1 - \frac{Td}{E\rho_0} \text{ nearly,}$$

or

$$\rho_1 = \rho_0 - \frac{d}{E} T \text{ nearly. (8)}$$

From this approximation it appears that the correction is constant in amount for a given tension, and can be determined once for all for the series of tensions employed.

If we take for steel the values

$$d = 7.7 \text{ gm. per c.c.}$$

$$E = 2.2 \times 10^9 \text{ gm. wt. per sq. cm.,}$$

$$\rho_1 = \rho_0 - 3.5 \times 10^{-9} \times T,$$

where T is expressed in grammes weight. For a No. 32 wire under 8700 gm. weight tension, the correction amounts to more than 1 in 200. Lengths of the respective wires were accordingly measured under quite low tension, and weighed on a balance which had a sensitiveness of 0.20 mgm. per division. Tables were prepared giving the linear densities of each wire for the different tensions employed, and the Taylor frequencies were calculated by means of these tables, δn being then found from equation (4).

Form of the Correction.—Assume that the correction may be applied in the general form in which those of Seebeck and Donkin have been expressed, and let

$$\delta n = K \frac{n^p \rho_1^q}{T^m}, \text{ (9)}$$

where K is a constant. Then it remains to find values of p , q , m , and K which will satisfy the experimental results. It is to be noted that here n is the Taylor frequency, which is the only frequency available from the observations when an unknown frequency is being determined.

Beginning with the tension, the powers of T which appear in the corrections of Seebeck and Donkin are respectively 1 and 2. Neither of these powers fits the experimental results.

Assume, then, that $\delta n \times T^m$ is constant for a given frequency, then

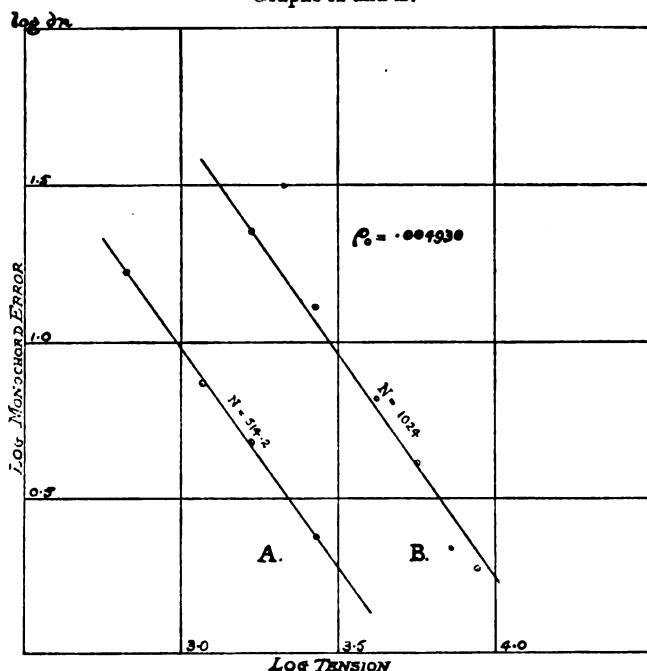
$$\log \delta n + m \log T = c, \quad \dots \dots (10)$$

and the graph of $\log \delta n$ and $\log T$ is a straight line of the type

$$y + mx = c.$$

The values of $\log \delta n$ were plotted against $\log T$, and straight lines were drawn through the mean positions of the points. An inspection of the graphs confirms the view that, apart from experimental error, the points lie on approximately

Graphs A and B.



parallel straight lines whose distance from the origin increases with the frequency and the linear density. The general conclusions of Seebeck and Donkin are thus verified within the scope of the experiments.

Value of m from the Graphs.—The power m was measured for each line from the ratio of the intercepts on the axes.

In general, the values differed from line to line, but an average has been taken as applicable over the whole range of observations.

Graphs C, D, and E.

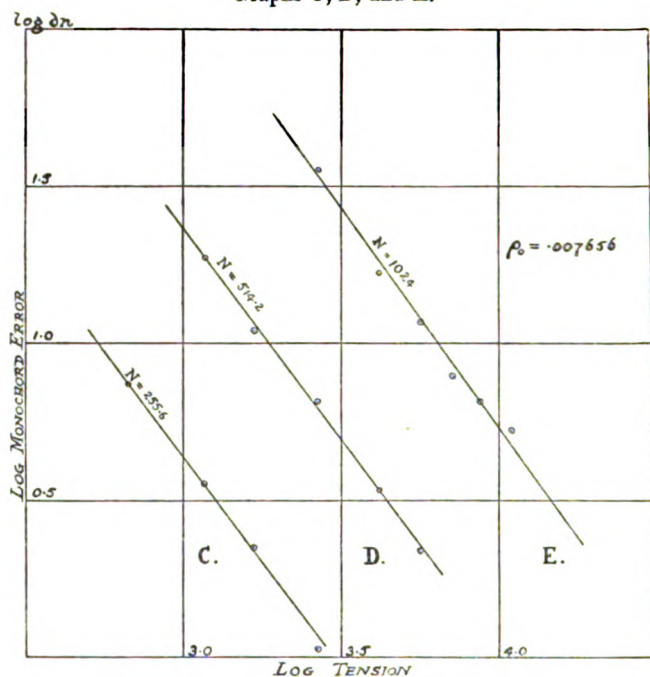


TABLE VI.

Values of m and c .

Graph.	Frequency.	Linear density.	m .	c .
A	514.2	.004930	1.406	5.072
B	1024	do.	1.420	5.719
C	255.6	.007656	1.297	4.733
D	514.2	do.	1.322	5.469
E	1024	do.	1.370	6.191
F	255.6	.01278	1.428	5.155
G	514.2	do.	1.412	5.940
H	1024	do.	1.284	6.627
I	255.6	.02318	1.357	5.714

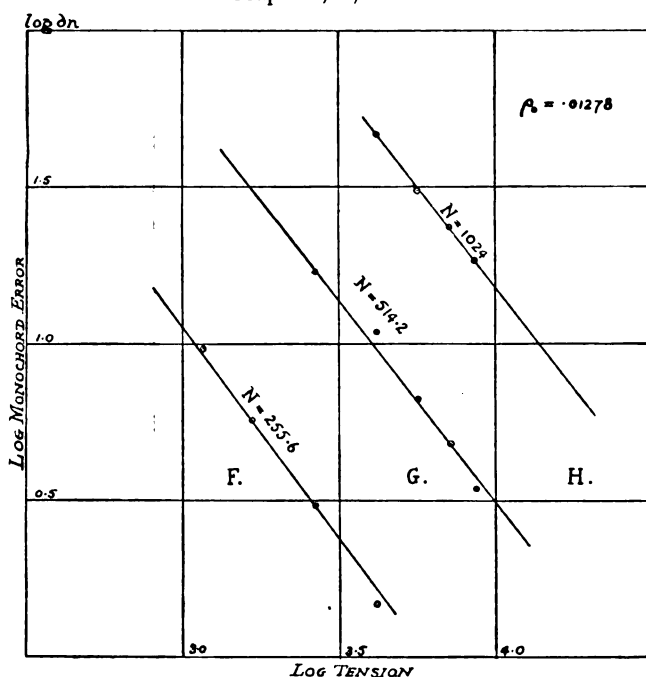
Mean $m = 1.366$

Values of c.—Placing in equation (10) the value found for m , along with a pair of values for $\log \delta n$ and $\log T$ respectively, mean values of c were found for each wire and each frequency. These mean values have been included in Table VI. above.

Evaluation of p , q , and K .—We get, from equations (9) and (10) above,

$$c = \log K + p \log n + q \log \rho_1. \quad . \quad . \quad . \quad (11)$$

Graphs F, G, and H.



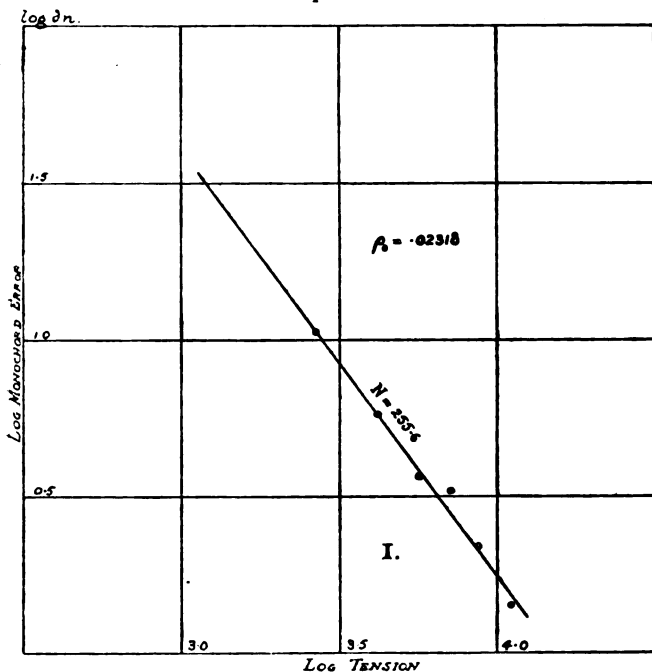
In this equation c and n are known, and if we employ the equation twice for the same wire with the same tension, but for different frequencies, K and $q \log \rho_1$ may be eliminated, giving

$$p = \frac{c_2 - c_1}{\log n_2 - \log n_1} \quad . \quad . \quad . \quad . \quad . \quad (12)$$

Corresponding values for c and n were taken for graphs A and B, C and D, D and E, F and G, and G and H from

Tables II.-VI., and inserted in equation (12), the mean value found for p being 2.391.

Graph I.



In a similar manner, using the data for different wires with the same frequency and same tension, we get

$$q = \frac{c_2 - c_1 - p(\log n_2 - \log n_1)^*}{\log \rho_1'' - \log \rho_1'} \quad , \quad . \quad . \quad . \quad (13)$$

where c_2 and c_1 refer to the values for, say, graphs D and A, and ρ_1'' and ρ_1' to the corresponding linear densities. Taking the appropriate values for graphs A and D, B and E, C and F, D and G, and E and H, twelve values of q were determined, of which the average was 2.070.

Value of K.—Substitution of the values found for c , p , and q in equation (11) gives $\log K$. Here one value was

* The Taylor frequencies are not exactly the same.

found for each graph, and the average of the nine was $\log K = 3.274$, from which $K = 1880$.

Final Form of the Correction.—The correction can now be stated in its numerical form, namely,

$\log \delta n = 3.274 + 2.391 \log n + 2.070 \log \rho_1 - 1.366 \log T$,
which is suitable for computation with four-figure logarithms.

Discussion.

In the determination of frequency by the monochord, the improvement to be obtained by using the correction stated above may be gauged if we consider first the degree of error involved in the use of Taylor's formula alone. With low tension the error may exceed 4 per cent., but with increased tension the error in measuring a low frequency, say round about 200 per second, may be reduced to the disappearing point. The correction is not important when low frequencies are measured with a thin wire under high tension, provided due allowance is made for the change of linear density with tension. With higher frequencies the error cannot be made to disappear, since, with the three largest wires used, the breaking weight is reached before the error is reduced to unity. This can be verified by noting where the graphs for $N = 1024$ cut the $\log T$ axis.

The wire No. 23 S.W.G. is too thick for monochord work. With thinner wires greater brilliance of tone is obtained; also the wires offer a greater length for measurement, and they respond visibly when in tune. As a measurer of frequency the monochord has a limited range of usefulness which may be regarded as including frequencies from 50 to 2000, the accuracy obtainable at the higher frequency being less than 1 in 500.

The above tests were made in the Applied Physics Department of the University of Glasgow, and the writer desires to thank Professor J. G. Gray for his friendly interest in the work.

July 10th, 1927.

CXX. *The Temperature-Electrical Resistivity Relationship in certain Copper Alpha Solid Solution Alloys.* By A. L. NORBURY, D.Sc., and K. KUWADA (both of University College, Swansea)*.

Experimental Methods.

THE alloys used were in the form of annealed wires (0.03 inch diam.). Their compositions are given in Table I. Their preparation is described in previous papers †. To measure their electrical resistivities at various temperatures, each wire was made into a spiral coil, about 1 cm. diam. by 4 cm. long, containing about 40 cm. of wire. A current of about 2 amps. was passed through each spiral via leads (about 30 cm. long) formed by the two free ends. A copper wire was fused on to each lead just outside the spiral. These two copper wires were connected to a Tinsley Vernier Potentiometer and the drop of potential compared with a known drop of potential in the main circuit. The arrangement was consequently similar to that in a platinum resistance pyrometer. The thermostats used were:—liquid air (-191°), solid CO_2 in alcohol (-78° to 0°), room temperature (17° to 21°), B.P. water (100°), B.P. naphthalene (218°), B.P. mercury (356°) and B.P. sulphur (444°) ‡. Each spiral and its leads was placed in a half-inch internal diameter glass tube closed at the lower end, which projected into the thermostat. Condensation of moisture at low temperatures caused errors, but this was overcome by drying and sealing up with paraffin wax.

Results obtained.

The results obtained are collected in Table I. and plotted in fig. 1, where it will be seen that a plotting of resistivity against temperature gives a linear relationship between -191° and 438° C., within the limits of experimental error, for all the alloys with the exceptions of the manganese-copper and nickel-copper alloys. The points for these alloys lie on curves which decrease in slope with increase in temperature. With these exceptions the linear relationship may be expressed by:

$$R_t = R_{t^0} + \alpha \times t^\circ C. \quad . \quad . \quad . \quad . \quad . \quad (i.)$$

* Communicated by the Authors.

+ Journ. Inst. Metals, vol. xxix. 1923 (ii.) p. 423. Phil. Mag. ii. p. 1188, Dec. 1923.

† The temperature in this thermostat was actually 438° C.

Electrical I

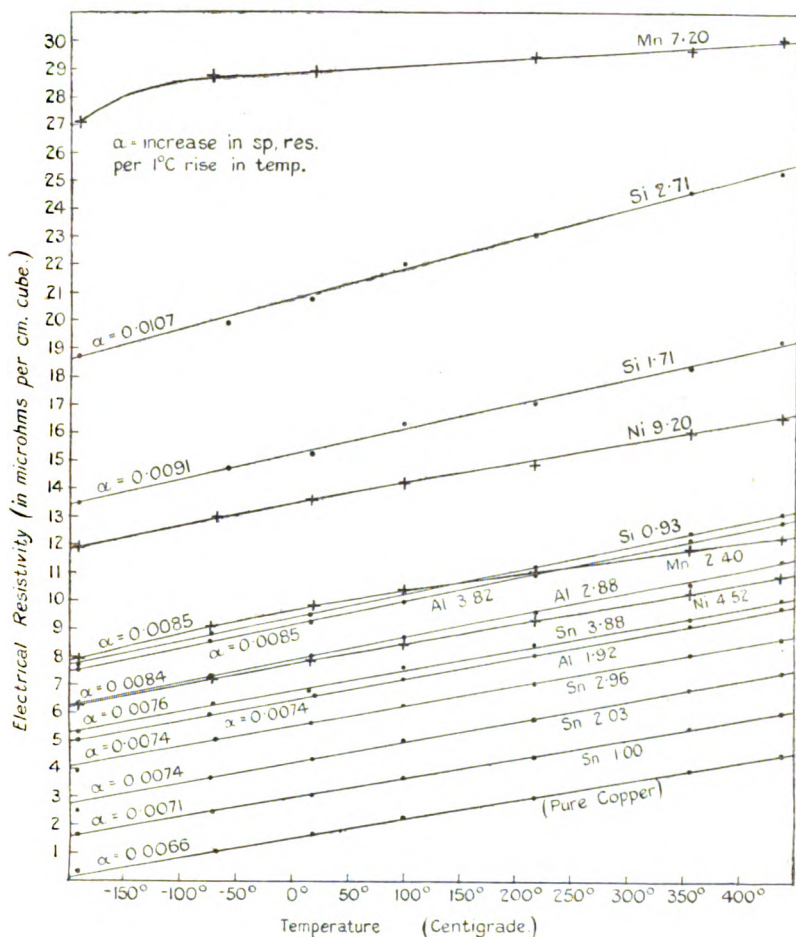
Added Element Weight per cent.	Liquid (-191°)
Pure Cu.	0.35
Al. 1.92	5.03
„ 2.88	6.33
„ 3.82	7.52
Mn. 2.40	7.92
„ 7.20	27.12
Ni. 4.52	6.27
„ 9.20	11.92
Sn. 1.00	1.65
„ 2.03	2.53
„ 2.96	3.79
„ 3.88	5.30
Si. 0.93	7.72
„ 1.71	13.46
„ 2.71	18.72

*
†

(where R_t = sp. res. at $t^\circ \text{C}$. R_0 = sp. res. at 0°C ., and α = increase in sp. res. per 1°C . rise in temperature).

It has previously been accepted that such lines, for dilute

Fig. 1.



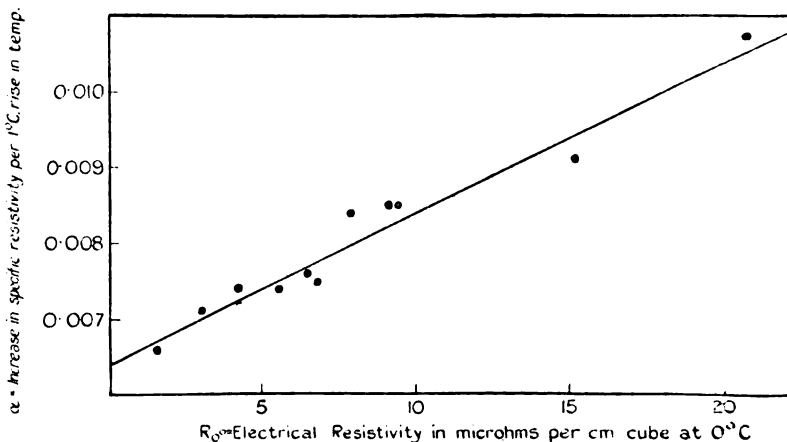
Electrical Resistivities of Certain Annealed Copper Alpha Solid Solutions at Temperatures between -191° and 438°C .

solid solution alloys, are parallel to one another, *i. e.* that they have a common value of α . A reference to the subject and to the work of Clay, Guertler, Bornemann, etc., will be

found in a previous paper by one of the authors*. The present data in fig. 1 show, however, that the lines are approximately, but not exactly, parallel to one another—in other words α is not the same for each.

By plotting the fig. 1 results on a large scale, values of α and R_0 for each alloy have been estimated and have been included in Table I. If these R_0 and α values are plotted against one another as shown in fig. 2, a linear relationship, within the limits of experimental error, is obtained, showing

Fig. 2.



Values of α plotted against values of R_0 .
(Relationship: $\alpha = 0.0064 + 0.0002 R_0$.)

that α increases in value when R_0 increases in value. The relationship in fig. 2 may be expressed by the equation:

$$\alpha = 0.0064 + R_0 \times 0.0002 \text{ microhms per cm. cube.} \quad (\text{ii.})$$

Hence a combination of equations (i.) and (ii.) gives:

$$R_{t^\circ} = R_0 + (0.0064 + R_0 \times 0.0002) t^\circ \text{ C.} \quad (\text{iii.})$$

which signifies that R_{t° (the sp. res. at any temperature t° between -191° and 438° C.) may be calculated from a knowledge of R_0 † (the sp. res. at 0° C.), and that this

* Trans. Faraday Soc. vol. xvii. p. 257 (1921).

† By suitably modifying the equation the sp. res. at any temperature may be used as a basis for calculating the sp. res. at any other temperature between -191° and 438° C.

equation holds for all the alloys used in the present research, with the exceptions of the manganese-copper and nickel-copper alloys.

The above results also have a bearing on the general relationship, found by one of the authors in a previous paper (*loc. cit.*), in which it was shown that the magnitudes of the "atomic effects" of solute elements in increasing the electrical resistivity of a metallic solvent were connected with the relative positions of the solvent and solute elements in the Periodic Table.

The bearing of the above results is that a higher or lower temperature of comparison than room temperature will give higher or lower values for the "atomic effects," but these will all be raised or lowered by the same percentage. Hence, a comparison of their relative "atomic effects" in a given solvent is independent of the temperature at which it is made.

The manganese-copper and nickel-copper alloys deviate somewhat from the above, since the comparison of their "atomic effects" is approximately, but not exactly, independent of the temperature of comparison.

In conclusion, the authors wish to thank Principal C. A. Edwards, D.Sc., for facilities for carrying out the present work and for his encouragement and advice; and acknowledge their indebtedness to the Royal Society Committee for a Government Grant.

CXXI. *Condenser Discharges in Discharge-Tubes.*—Part II.
The Intermittent Discharge. By WILLIAM CLARKSON,
M.Sc., A.Inst.P., *The Physical Institute of the University
of Utrecht* *.

I. INTRODUCTION.

THE intermittent discharge has been the subject of wide study during the past few years ⁽¹⁾.

Previous work has been largely on the timing relations. Both the empirical and the theoretical relations for the time of flash were quite early established ⁽²⁾, but it was found that if the sparking and the extinction potentials, or later even the maximum (peak) and minimum voltages as measured, were substituted in the relations, the timing agreement was not good.

* Communicated by Professor Ornstein.

Initially the time of duration of a flash was assumed to be negligibly small, but it was later seen that a lag at sparking was implied by certain phenomena and by timing graphs.

The large timing discrepancies at higher frequencies have been attributed⁽³⁾ to "clear-up" phenomena. Though this was mainly true over the region studied, it is shown here that appreciable lags both at "build-up" and "clear-up" of a discharge must be considered in a complete explanation.

2. METHODS.

Since all three variables—voltage, current, and time—were to be employed in calculations, it was necessary to determine their values accurately and to intercalibrate the various instruments used⁽⁴⁾.

The capacities and the voltmeter were correct, and the shunted galvanometer was calibrated against the latter. All parts of the circuit were thoroughly insulated.

It was necessary to determine exactly what error was caused by the potential-drop in the diode filament of the diode-voltmeter combination. A rotating commutator showed that small errors could occur. Corrections, when necessary, were easily made.

Suitable allowance was made when the circuit current could not be maintained at the saturation value for the circuit diode employed.

When it was desired to eliminate the leakage due to photo-electric currents, the tubes were worked in partial or complete darkness. Circuit currents down to $0.05 \mu\text{A}$. could then be measured.

A standardized rotating commutator was found to give satisfactory results for frequencies intermediate between those timable on a stop-watch and those determinable by a monochord.

3. GENERAL CONSIDERATIONS.

Neglecting the discharge-period, the time of flash (T) is given by

$$T = C(v_m - V_N)/i, \quad . \quad . \quad . \quad . \quad . \quad (4)$$

where i is the charging current, C the capacity, v_m the "striking" potential, and V_N the minimum potential attained.

Actually, since lag was present, the increase of current to a maximum and its subsequent fall to zero is gradual, and there is an interval at the beginning of "build-up" and the end of "clear-up" when the charging current i exceeds

the discharge current I and the voltage rises, even though a discharge is passing. The maximum and minimum voltages, V_C and V_B respectively, will be attained when $i = I$ (fig. 1, a)⁽⁴⁾.

The respective deviations of V_C and V_B from the starting voltage, ($\Delta_C = V_C - v_m$), and from that, V_N , to which the condenser would have fallen, ($\Delta_B = V_B - V_N$), will, of course, depend on the rate of charge (i/C) and on the current-time relations in discharge.

It is also apparent that a clear-up current may still be flowing when the corresponding striking voltage (v_m) as determined by threshold-current characteristic is reached. This is here denominated "overlapping"⁽⁵⁾. The reduction of v_m will become more pronounced as the time of flash is diminished.

Fig. 1 illustrates the phenomena just described. It will be seen that only the points V_C, i and V_B, i are known accurately, and that the values of v_m, i_m and v_n, i_n can merely be inferred.

4. V_C, V_B VARIATIONS.

These variations were systematically studied for constant capacity (C) and various currents (i), and *vice versa*. V_C, V_B curves obtained under similar conditions were of the same form for all tubes. Actually these V_C, V_B, i and the V_O, V_B, C curves correspond very closely to V_C, V_B, n (frequency) and V_C, V_B, T curves respectively. It was found that if all results were plotted on an n or a T basis, curves of precisely similar form to those given were obtained.

These results suggest that the V_C, V_B phenomena arise universally from similar causes: a general solution should therefore be possible.

It was most convenient to study the V_C, V_B, n changes with C constant, i variable.

a. C constant, i variable.—The changes described here are for a steady increase of charging current (fig. 3).

A steady corona discharge was obtainable for a certain range of small currents. Though this range corresponded to the major part of the corona characteristic for very small capacities ($< 0.001 \mu F.$), it was inappreciable for large values.

Corona flashes were then observed, with currents up to $1 \mu A.$, say, in the case of $C = 0.1 \mu F.$ Though very faint and slow at first, with V_C and V_B both of the value v_c (approx.), they became much quicker as i was increased,

and though V_0 remained almost constant V_B fell rapidly, as in single flashes, and finally normal flashes occurred. The succession of corona flashes discharges preliminary to a normal flash, described on a previous occasion⁽⁴⁾, would appear to be connected with lag phenomena of a more variable nature than present here.

Even with normal flashes V_c was approximately constant up to a frequency of 1-2 per second, but then rose in a regular manner, attaining, as a rule, a maximum (10-40 volts) at $n=20$, say (see figs. 5 & 6). dV/dn was then small, and at about $n=40$ V_c showed a progressive diminution, equalling v_c at about $n=100$ or so. The minimum value attained, generally with n equalling several hundreds per second, was frequently quite close to v_b in value. A steady discharge now occurred.

V_B changed in a reverse manner to V_c for normal flashes, being almost constant initially, then falling rapidly until attaining a minimum at about the maximum V_c , and finally rising slowly, with decreasing rate. It was generally approximately v_b just before the steady discharge was attained.

It is the purpose of this paper to show that the current-time relations in discharges, the "striking" and "clear-up" properties of the characteristic, and the variation of "build-up" with voltage serve to explain these phenomena, as well as those of single flashes. As is to be expected, the explanations developed here were found to apply to the other cases also.

b. V_c .—The voltage-time (V, t) relations assumed are given in fig. 1(a), where the effect of a constant charging current, tending to produce a steady increase of voltage, is shown. The voltage increases slowly to a maximum (V_c at a time τ), and then falls at an ever increasing rate (v_n at time θ).

With the rate of build-up constant, *i. e.* duration of discharge, θ , constant, τ and hence Δ_c ($\propto \tau$ and i/C) will increase with, though not more slowly than, i . The ratio τ/θ will also increase regularly, and though almost zero initially will be approximately unity for large values of i/C ⁽⁴⁾.

Actually, however, the rate of build-up is not constant, but increases with voltage, and though the voltage it corresponds to in intermittence is indeterminate ($< V_c, > v_m$), θ certainly becomes rapidly smaller as i/C and hence Δ_c become greater. The general variation of the ratio τ/θ will be unaffected; thus τ will increase rapidly with i/C , attain a maximum, and then change in a similar manner to θ .

The resulting Δ_c, i curve will be doubly inflected as in figs. 5 and 6. V_c , almost constant for corona and for the

Fig. 4.

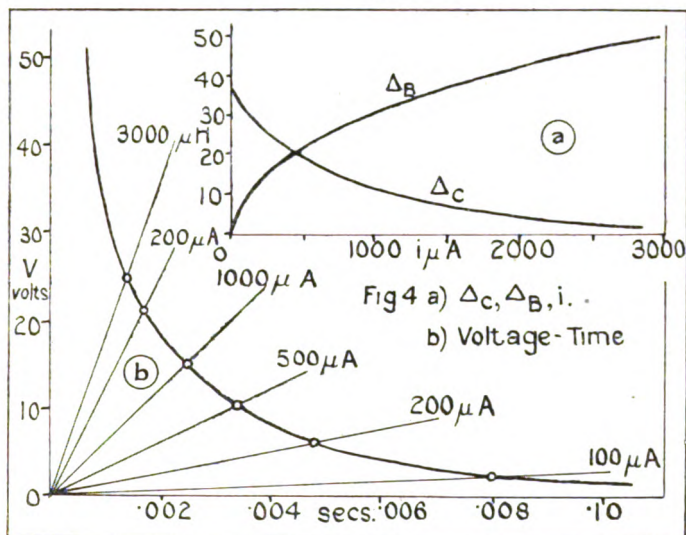
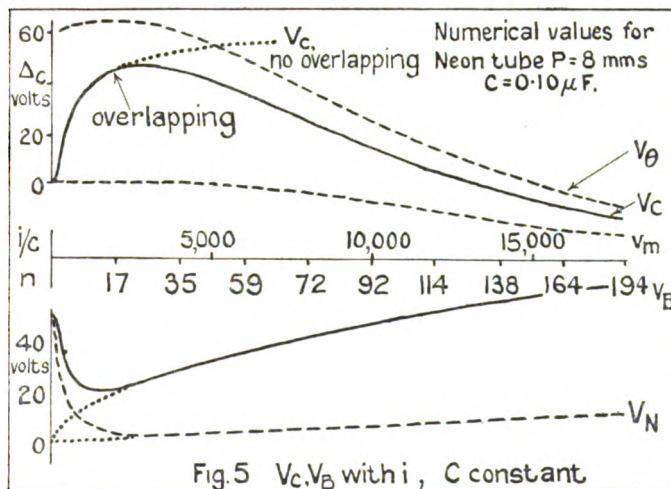


Fig. 5.

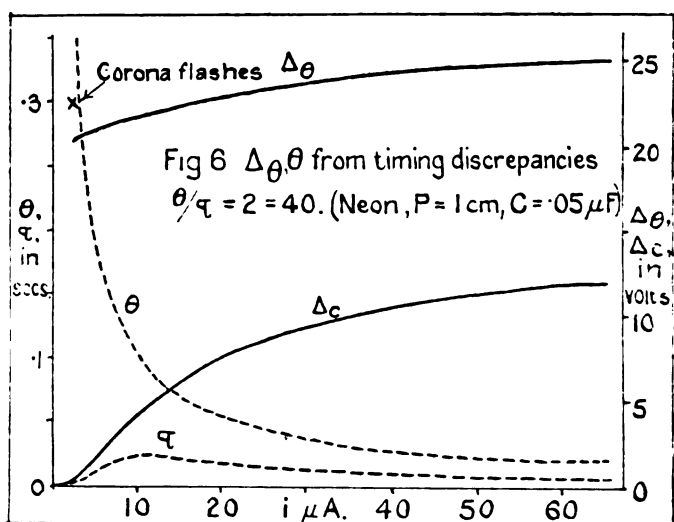


first normal flashes, should show a progressive rise at a diminishing rate. τ is a maximum at the second point of inflexion.

Fig. 6 shows that the agreement with observation, up to $n=10$ or so, is very satisfactory.

The results for various values of C ($0.002-1.0 \mu F$.) were equally good. The $V_c, i/C$ curves corresponded not only in form but quite closely numerically, changes of about 20 per cent. only being observed. In $\Delta_c, \log i/C$ curves, Δ_c rose very slowly for a small initial stage and then quite quickly at an (almost always) constant rate. Over this range Δ_c equalled $k \log i/C$, k only showing appreciable variation (decrease) when C became quite small. This should follow

Fig. 6.



from the foregoing considerations and from the fact, demonstrated earlier, that the voltage fall during the greater part of build-up is only a volt or two, save in the case of small capacities ($< 0.005 F$.), where it may approach 10 volts or so ($\Delta_c = 40$ volts). Thus for the greater part of τ the voltage-time relation at constant i/C will be essentially the same for most capacities, and Δ_c will be independent of C , with the foregoing exception of the small capacities, where decreases of the order observed are to be expected.

Beyond about $n=10$, conditions are different. Actually, though Δ_c should continue to increase with i , V_c attains a maximum at about $n=20-40$ and then decreases. This is attributable to "overlapping." Examination of V, n curves shows that in most cases this must first occur at about $n=10$.

The total duration of discharge at this stage must thus be of the order of one-tenth of a second. V_c , $\log i/C$ curves show a marked change in Δ_c at this value. This critical n is generally higher for small capacities.

c. θ , τ Values.—Sufficiently close values of τ (say $3/4$ to $2/3$) may be obtained from $\tau = \Delta_c C/i$, and of θ directly by a single-flash method, described previously⁽⁴⁾. Unfortunately this method is not applicable over the full range of values to be treated here. Experimental difficulties preclude the finding of the variation of θ with Δ_n , where the latter is small, as for low frequencies, and the conditions after “overlapping,” where Δ_c is largest, are not reproducible with sufficient accuracy. A further difficulty is, that for comparable values of τ and θ to be obtained the voltage variations during build-up should be the same in both cases. Despite this, however, sufficiently reliable results were obtained. They showed that the agreement over the range available was good. Timing relations (later) and single flash experiments confirm this. At overlapping θ was usually some three times greater than τ .

It is at least possible to give the variation of v_m and Δ_c after “overlapping” qualitatively. Single flashes showed that the lag was reduced by the presence of a quite small initial current. Thus on “overlapping,” though v would still be approximately equal to v_c until residual currents of $3\text{--}4\ \mu\text{A}$. were present, θ should decrease fairly quickly. v_m would fall as other points on the threshold characteristic were progressively realized, and there would also be rapid decrease of θ . If θ decreased less quickly than i/C increased, Δ_c need not decrease immediately, but could continue to increase for a certain range, though later it must fall, due to the simultaneous lowering of v_m and the reduction of θ . Fig. 5 shows the relations implied. They are in accord with observation.

d. *Clear-up*.—Fig. 1(a) shows the effect of a constant charging current superimposed on the V , t relations assumed to hold during clear-up. The voltage will fall rapidly at first (from v_n), reach a minimum value V_B , and then rise at a rate determined chiefly by the value of i/C . After clear-up the V , t curve will be linear; produced backwards it will intersect the time axis ($t=0$) at V_N . The voltage reduction, $v_n - V_N$, must be taken as that equivalent to a quantity transference equal to that actually occurring during clear-up.

The intersection of the charge-up and clear-up voltage curves will be intermediate between V_B and V_N . With

constant clear-up, Δ_B should increase with i/C . Fig. 4 (*a*) shows the form implied.

Fig. 4 (*a*) was obtained in the following way :— Δ_B variations are most easily studied with the V, t relations during clear-up, and hence V_N constant. In intermittence this condition at the best is only approximately realizable, and that only when the points V_c, i corresponding to the various rates of charge lie on the same discharge track (fig. 1, *a*).

In these experiments this condition was satisfied by limiting the driving voltage to a value approximately equal to that of the V_c corresponding to the i employed. These values of V_c were determined empirically (fig. 6, *a*). It is improbable that that v_n, i_n was not approximately constant. The charging current was constant throughout the clear-up period. It was measured at V_B .

In constructing the V, t curve for clear-up (fig. 4, *b*), the "charging" curves were drawn radially from the origin and a point on each midway between V_B and V_N was determined. The results were highly satisfactory. Current-time curves, obtained from these, were of similar form. In the case given the current falls to half value in 0.0005 sec., but the total duration of clear-up is about 0.02 second. The average current is of the order of $1/30$ of the initial current.

Similar curves were constructed for different parts of the characteristic by observing the V_c, V_B values for a given condenser charged to definite voltages, and discharged through the tube while known steady currents were flowing. The various values of r_n, i_n could be inferred from the V_c, i values, and clear-up curves drawn as previously. The apparatus defects were too great to permit of more than general confirmation of the results given.

In these experiments V_B was always less than v_b , even when i was many times greater than that for steady conditions. The increased negative glow showed that currents much greater than i could be obtained in flashes. This occurred even with very low values of V_N , though how close to R (fig. 1) has not yet been determined⁽⁵⁾. As suggested, either extinction or radical changes in the characteristic must have occurred in all these cases.

One aspect of fig. 4 (*b*) remains to be discussed. It has been assumed that V_N was not affected by voltage changes during clear-up. Previous considerations show that the quantity transference will be greater and V_N will diminish as i/C , and hence as V_B , is increased. The points plotted should therefore lie on a succession of clear-up curves tending to a decreasing V_N , and with an increasing time duration. Despite this, since

the voltage V_N utilized in the foregoing construction should be the one to which the condenser is tending at the moment V_B is reached, and as the changes up to this moment will not differ greatly in the various cases, the curve given will approximate quite closely to the one required.

Great changes, however, must be produced during the final, small current stage, particularly where n is greater than 6 or 7. Here the final voltage is of the order of v_c , and is many times higher than V_N . This point will be returned to later.

6. V_C, i_n, V_N, V_B VARIATIONS.

The i_n, v_n , and hence the V_N variations in intermittence can be deduced from the V_C, i values. The discharge tracks on leaving these points must be considered. Though almost constant at first ($V_C = v_c$), i_n will increase very rapidly as V_C increases. It will then slowly attain a maximum (near maximum V_C). From this stage i_n will show small changes, if any. They will be regular. These inferences are in agreement with observations on the extent of the negative glow.

V_N, i_n clear-up curves (fig. 2, *b*) show that V_N will fall rapidly after a small initial stage of constancy, will slowly pass through a minimum, and then remain constant or rise slowly.

Superimposing on these curves corresponding Δ_B changes (fig. 4, *a*), we find that V_B will be initially (almost) constant, will then fall rapidly, pass through a minimum, and then rise at a steadily diminishing rate.

As fig. 5 shows, these inferences are in complete accord with observations.

As V_N was almost constant, or changed regularly, for a wide range of frequencies ($n > 30$, say), the V_B curve produced backwards to $n = 0$ gave $V, i/C$ curves similar to that of fig. 4 (*a*) & (*b*).

The times of clear-up for the large neon-filled tube, $\theta_N = 0.015$ sec. for $\Delta_N = 40$ –50 volts, utilized earlier, were obtained in this way.

7. TIMING RELATIONS.

The time of flash, T , is usually expressed as a function of C, i , and a voltage difference (eqn. 4), say E .

In this paper the variations of E ,

$$E = Ti/C, \text{ i.e. } \propto i/n,$$

are determined, and it is shown that they may be explained in terms of build-up and clear-up phenomena.

Fig. 1 (a) shows that E equals $V_\theta - V_N$, where V_θ is the voltage that would be attained in a time θ after "striking," ($\Delta_\theta = V_\theta - v_m$), and $C(v_n - V_N)$ is the quantity transference actually taking place during clear-up up to the moment of "striking." It will be seen that where "overlapping" occurs the voltage intercept V_N will be higher than that V_N determined from V_B curves, by a voltage equal to that the condenser has yet to fall for complete clear-up. As this is only appreciable for large rates of charge (high n) where the variations of V_N are quite unambiguous, it may be neglected, more especially as the error at a maximum is only about 5 per cent. of $v_n - V_N$.

It has been shown that V_N may easily be determined from V_B , i curves, the error being smallest for low values of the frequency. This permits $V_\theta (= V_N + E)$ to be found accurately, and the observed variations of Δ_θ and Δ_c , and of θ and τ , to be compared with those required by theory.

a. V_θ Variations.—Consistent results for V_c , V_B , n and i relations were obtained in all cases. The variations of E are bound up with those of n with i . From $i=0$ n increased at a gradually increasing rate till a frequency of about 40 was reached. The rate then became constant, the n , i graph between $n=40-100$ (say) being a straight line, which produced to $n=0$ gave an intercept of low value on the i axis. Above $n=100$ the rate of increase of n again changed, increasing progressively with i . E was thus practically constant for an intermediate range, decreasing slowly for low and rapidly for high values of n .

Where V_c was maximum Δ_θ was from 2-6 times greater than Δ_c , but V_θ rapidly approached V_c for higher frequencies; this implies very small lags. No numerical results need be given (fig. 5). The weak subsidiary discharges sometimes occurring between flashes were not observed in these experiments. Their effect would probably have been inappreciable.

Table III. gives results for low values of n , where the Δ_θ and Δ_c variations are most pronounced and definite, and where the values calculated for θ are most capable of verification. They are for the large neon-filled tube, $C=0.05 \mu F$, and show the V_c , V_B , V_N , n variations already discussed.

The values obtained for Δ are as described (fig. 6). As previously⁽⁴⁾, θ varied somewhat hyperbolically with Δ_c . It had values of 0.6 sec. with V_c near v_c . The ratio of τ/θ increased as i/C was reduced. Values of from 2-50 were recorded.

Results obtained with $C=0.005 \mu F.$ were of precisely similar form and the Δ_c variations were of the same order, but the corresponding τ/θ ratios were some 2-3 times greater.

TABLE III.

i	3.0	4.3	6.0	9.4	14.7	21.9	35	40	70
n5	.67	.97	1.5	2.35	3.6	5.3	6.05	10.85
$V_c - V_s$	100	101.7	103.7	106.8	110.3	113.4	116.9	117.7	119.7
E	120+	121.3	122.5	124.1	126	128	130.7	132	133
$\Delta\theta$	20.4	20.8	21.2	21.4	22.0	22.8	24.1	24.5	25.5
θ34	.24	.18	.11	.075	.052	.034	.03	.018
τ008	.012	.017	.012	.021	.018	.014	.012	.009
Δ_c5	1.0	2.0	4.0	6.0	8.0	10.0	10.5	12.0
τ0044	.0060	.0081	.0100	.007	.0061	Upper, $C = .05 \mu F.$ Lower, $C = .005 \mu F.$ "Overlap," $\Delta_c = 10.5$ $\Delta_c = 7.0$		
θ36	.24	.16	.10	.072	.038			
$\Delta\theta$	41	40.2	40.2	41.9	44.5	49.6			

This, and the difference in θ , are due to the fact that the values of C where the fall of voltage during the initial stages (τ) of build-up have been reached.

Timing relations were obtained from corona flashes in an analogous manner. Some difficulty is experienced in measuring the currents accurately for this regime, but calculations are simplified by the fact that v_m and V_N closely correspond to v_c (V_c) and V_B respectively. Unfortunately, the actual voltage readings are rather unreliable. In all cases results were in close agreement with those for normal flashes, comparison being possible at the transition current for these two forms. A typical result is indicated in the diagram (fig. 6).

Though these considerations have also been extended to the case where the circuit includes a simple resistance, as in the previous work with which the author was associated, no comment is necessary in the absence of any conflicting evidence whatever.

b. "Overlapping" and θ_N .—An additional check to the results obtained is possible. The time of flash, T , at the first appearance of overlapping must correspond to the full duration of discharge and must equal $\theta + \theta_N$. θ is known. Two values

TABLE IV.

C.	θ .	T.	$T - \theta$.	θ_N^{graph} .	Ratio.
·05	·03	·15	·12	·018	7·0
·005	·04	·10	·06	·011	5·5

of θ_N so obtained (large neon-filled tube) are compared, in Table IV., with those determined from V_B , i and clear-up curves. The time for I to fall to $0\cdot01 \mu\text{A.}$ is taken, this being a reasonable limit to fix for the smallest current by which θ would be appreciably affected in the existing circumstances.

Marked discrepancies are seen to exist, but it will be shown that this is quite consistent with the arguments previously adduced.

The graphical construction employed is accurate for the small current (final) stage of clear-up, only if the voltage is V_N throughout. Actually V must vary between V_N and r_m during this period, being highest at the final stages. Thus it is certain that the clear-up, though not increased appreciably, will be considerably prolonged. The ratios given in the table accord quite well with this explanation. Unfortunately, it is impossible to apply the $\theta_N \propto 1/\Delta_N$ relation here (eqn. 3), since that was obtained only in the case of fully-developed

discharges, and the space-charge in overlapping corresponds to corona currents, for which numerical data are not available.

A further aspect of clear-up phenomena is also involved. The currents (I) in similar V, t graphs will vary as the capacity; "overlapping" depends on I . From the point of view of voltage changes θ_N varies as $1/\Delta N$, but from the point of view of current it will depend greatly on the size of the capacity. So far as they have been available, "overlapping" results support this. Table IV., where V_N varied from 40–50 volts, gives representative examples. The different time distribution of voltage must also be taken as playing a significant part in this connexion.

Quantitative examination of clear-up currents at overlapping have not yielded data of much significance up to the present, in the absence of any means of checking the results obtained.

c. Lag Variations.—The conclusiveness of these observations was apparently shaken by one fact—that, in some cases, especially in the region of the maximum V_C , E calculated was almost of the same value, or even less than $V_C - V_B$.

This fact is quite easy of explanation, if an erratic lag—as, indeed, was generally shown in other ways in such cases (*e. g.* preliminary discharges)⁽⁴⁾—is assumed. Owing to the measuring system employed, the values of V_C and V_B in these cases would be extreme values, whilst the frequency observed would be a mean value. E , and V_C and V_B , would then exhibit the relations recorded. Erratic variation of the frequency, as sometimes is observed, is explainable in a similar manner.

The fact that the lag and the characteristic may change during discharges is demonstrated by the frequently occurring phenomena of normal flashes being preceded by a varying succession of corona discharges. Also, in such tubes, the lag is much smaller after a long period of disuse, and v_c is appreciably lower. When the tube is put into use, v_m and V_C show a regular increase with time until the final, stable, value is attained. The lags, demonstrated by V_C , thus also increase regularly, until finally definite and repeatable values are recorded. The same effect is demonstrated when a tube is suddenly put into use, the frequency only becoming constant after a definite interval of time.

Mention of the effect of light on the lag was made previously. It was demonstrated in a marked manner with

corona flashes, the frequency and the conditions for transition to normal flashes being profoundly modified even by faint illumination. Such phenomena have been the subject of practical application⁽⁶⁾.

It will be seen that no definite distinction has been drawn between lag and corona characteristic changes; they are closely, if not indistinguishably, related.

The significance of the lag in the problem of stability is, of course, obvious.

CONCLUSION.

The foregoing experiments prove that considerable time-lags exist in discharge-tubes when quite appreciable currents, whether due to ionization factors or to the persistence of ionization during the clear-up, are flowing in the "dark period." These lags are at least one hundred times greater than those to be expected from an effect proceeding from the time required to build up a discharge in the gas. Further, the "chance electron" theory would appear to be disproved for these cases. The lags may be traced to a cathode-gas interface effect, which is modified by the action of radiation in such a way as to bring about a diminution of the lag, and either an actual change in the sparking potential, or a virtual change due to the production of a threshold current.

The results in either case are definitely that :

1. Though the sparking potential is lowered, the apparent sparking potential (peak voltage, V_c) will be greater than this statical sparking potential by an amount $\Delta_c = \tau i/C$, where τ is the effective lag and i/C the rate of charge. Thus V_c may correspond to an apparent increase in the sparking potential.
2. If the capacity is small, as for example in most discharge systems at high pressures, the properties of the corona characteristic are such that though discharges may occur they will not be sparks (or normal flashes) unless the lag is greatly reduced by the foregoing or other causes⁽⁷⁾. The occurrence of a spark is really only evidence that the transition stage from one type of discharge to another has been attained.

Finally, the writer would like to record with gratitude his indebtedness to Professor Ornstein for his sustaining interest in his researches and for the facilities so unreservedly placed at his disposal.

SUMMARY.

1. The sequence of phenomena and the variations of the maximum and minimum voltages (V_c and V_B) in the intermittent discharge are studied. The rate of charge is shown to be the significant variable.

2. The theory of the corona lag at "build-up" is discussed. It explains the V_c variations. The additional variations at higher frequencies are due to "overlapping" of discharges. Both the lag (θ) and the "striking" potential (v_m) are lowered.

3. V_B variations under constant clear-up conditions (constant final voltage, V_N) are examined. Current-Voltage-Time relations for clear-up are obtained. The current falls with time in a somewhat exponential manner. Times are of the order of 0.02–0.05 sec.

4. V_B variations in intermittence are shown to depend on the variation of clear-up with V_c and the rate of charge. The time of clear-up (θ_N) is obtained from the graphs.

5. The timing relation, $T = CE/i$, is discussed. E is the difference between $V_\theta (= v_m + \theta i/C)$ and the virtual V_N .

6. E is everywhere greater than $V_c - V_B$. The V_θ variations derived give results in both qualitative and quantitative agreement with prediction.

7. At "overlapping" $T = \theta + \theta_N$. θ_N values so derived differ from those determined graphically. This is shown to be in accord with theory, as are the apparent timing anomalies due to erratic lags.

8. Corona lag variations are briefly discussed.

References.

- (1) A bibliography of the subject is to be found in Taylor and Stephenson, *Phil. Mag.* xlix. p. 1083 (1925).
Valle, *Phys. Zeit.* xiv. p. 473 (1926).
- (2) Pearson and Anson, *Proc. Phys. Soc.* xxxiv. p. 204 (1922).
Taylor and Clarkson, *Journ. Sci. Insts.* i. p. 173 (1924).
Geffcken, *Phys. Zeit.* xxvi. p. 241 (1925).
- (3) Penning, *Phys. Zeit.* xxvii. p. 187 (1926).
- (4) Clarkson, *Phil. Mag.* iv. p. 121 (1927).
- (5) Clarkson, *Phil. Mag.* iv. p. 1002 (1927).
- (6) Taylor and Stephenson, 'Electrician,' Jan. 7th, 1925.
Campbell, *Phil. Mag.* iii. p. 1041 (1926).
- (7) Zelany, *Phys. Rev.* (1924).
Appleton, Emeleus, and Barnett, *Proc. Camb. Phil. Soc.* xxii. p. 447 (1925).
Wynn-Williams, *Phil. Mag.* i. p. 353 (1926).
Morgan, *Phil. Mag.* iv. p. 91 (1927).
- (8) Campbell, *Phil. Mag.* Oct. (1927).
Van der Pol, Letter 'Nature,' Sept. 10th. 1927.

CXXII. *A new form of Voltmeter for measuring the Average Voltage for Alternating Currents.* By JAMES TAYLOR, D.Sc., Ph.D., Mackinnon Student of the Royal Society, Trinity College, Cambridge*.

Introduction.

IN a previous paper (Journ. Scient. Instrs. iii. p. 113, 1925) the writer has considered an application of the diode to the measurement of A.C. voltages.

If a symmetrical alternating potential is applied to a hypothetical resistance R , which is characterized by the property of perfect unilateral conductivity, one-half of the voltage wave-form will be suppressed and an average current \bar{i} (as given by an A.C. instrument in series) will be registered; namely,

$$\bar{i} = \frac{\int_0^{\tau/2} \phi(t) \cdot dt}{\tau R}, \dots \dots \dots (1)$$

where the alternating potential form is given by the relation

$$V = \phi(t),$$

t being the time-phase and τ the total time-period.

The above ratio of the integral expression to the time-period is, by definition, half the value of the arithmetical average V , so that we may write

$$\bar{i} = \frac{V}{2R} \dots \dots \dots (2)$$

Such a system as imagined above could be applied to A.C. measurements.

Practical Method.

The above principle may be approximated to by use of a thermionic valve method.

A triode FGP, of which the grid and plate are short-circuited, is connected in series with a resistance R (of suitable magnitude, see later) and a microammeter A . The voltage to be measured is applied across the terminals $T_1 T_2$. R is adjusted to be about one megohm, if voltages of some 10 to 200 are being measured.

If $T_1 T_2$ are short-circuited, as a rule a small current is registered because of the pressure of the electrons emitted

* Communicated by Sir J. J. Thomson, O.M., F.R.S.

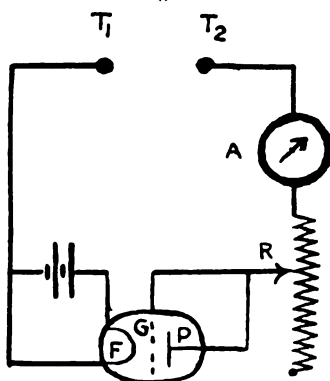
by the filament. This small current may be eliminated by including a small potentiometer in the circuit and adjusting so that no current flows when T_1 T_2 are short-circuited. The error arising from this electron pressure is usually less than a volt.

The instrument may be calibrated on D.C., and then applied to the measurement of average or R.M.S. values of A.C. voltages.

Theory of the Method.

The method depends upon the fact that the voltage taken across the valve is very small relative to that across the resistance R .

Fig. 1.



Assuming a valve volt-ampere characteristic of the form given by Langmuir,

$$i = k \cdot u^{3/2},$$

where u is the voltage across the valve and k is a constant, it was shown that the expression for the current for a D.C. voltage V is given by

$$i = \frac{V}{R} \left[1 - \frac{1}{V^{1/3}(kR)^{2/3}} - \frac{2}{3} \cdot \frac{1}{V^{2/3}(kR)^{4/3}} \right], \quad \dots (3)$$

and that for a S.H.A. voltage by (use of Γ -functions)

$$\bar{i} = \frac{V}{2R} \left[1 - \frac{1.04}{V^{1/3}(kR)^{2/3}} - \frac{0.73}{V^{2/3}(kR)^{4/3}} \right], \quad \dots (4)$$

\bar{V} being the average voltage of the S.H. wave.

Comparison of these equations shows that the ratio is very nearly one-half, since the second and last terms have

1358 *Voltmeter for measuring Alternating Currents.*

coefficients of almost equal value, and, further, the terms are themselves small compared with unity.

It is evident that the law of conductivity for the resistance R is approximately that given in the hypothetical case above.

In the previous work the method was applied only to the measurement of S.H.A. voltages, and it was found extremely satisfactory.

In the case of an arbitrary symmetrical alternating potential expressed by the relation $V = \phi(t)$ (see above), provided the average value,

$$\frac{\int_0^{\tau/2} \phi(t) \cdot dt}{\tau},$$

is great compared with the maximum value of u the voltage taken by the valve, the instrument gives an accurate half average value of the alternating voltage over the whole period. This condition for accurate performance is equivalent to the statement that the valve constant k must be sufficiently large to maintain a current of the value indicated by the D.C. microammeter at a voltage small compared with those being measured. In a general way this condition is satisfied.

The instrument is useful for the comparative measurement of square voltage wave-forms, such as are given by certain types of commutators supplied by direct voltage, and for those approximately square voltage forms associated with the condenser "flashing" in low potential intermittent discharges, a well-known example of which is the neon lamp intermittent discharge.

There is also the great advantage of an open and regular scale throughout the region. By the use of suitably chosen interchangeable resistances a very large range of possible voltage measurements may be obtained. This method of increasing the range has been utilized recently from voltages of about five volts to several hundreds.

Further, because of the small power consumption it is possible to utilize the voltmeter for the measurement of alternating current (for example, in parallel with a standard resistance).

There is no necessity for frequent calibration; indeed, a new valve may be substituted without the need of making a new calibration. Numerical data in connexion with this point were included in the previous paper which has been referred to.

CXXIII. *Notices respecting New Books.*

Manual of Meteorology. Vol. I.: *Meteorology in History.* By Sir NAPIER SHAW, with the assistance of ELAINE AUSTEN. Pp. xx + 339, with 18 plates. (Cambridge: At the University Press. 1926. Price 30s. net.)

THE fourth volume of this work appeared eight years ago, at a time when an account of the subjects dealt with was urgently required for aeronautics. The remaining volumes have been long awaited, and we may express the hope that the remaining two volumes will not now be long delayed.

The purpose underlying the whole work cannot be expressed better than in the author's own words: "The object of the book is to present the study of meteorology, not only as making use of nearly all the sciences and most of the arts, but also as a world study of a special and individual character, going back inevitably to the very dawn of history, and beyond that to the mazes of geological times."

In the present volume the author claims to "have tried to represent the knowledge which the reader of a paper on meteorology before a learned society of the present day will assume, perhaps unconsciously, to be in the possession of his audience." It is not a history of meteorology, but under the guise of the development of meteorological theories and observations through the centuries much valuable information is imparted to the reader, including details of instruments employed for investigations not only of the surface air but also of the upper air; instruments for special purposes are also described, such as pyrliometers, radiometers, dust-counters, thunderstorm recorders, etc. A chapter is devoted to the development of arithmetical and graphical manipulation.

The earlier chapters are devoted to an account of the meteorology of the world as known to the ancients; to the views of Herodotus, Aristotle, and others on meteorology; to weather-lore and to the question of variability of climate in historical times as far as the Mediterranean region is concerned. The dawn of meteorology as a science is illustrated by short biographies of seventy-four scientific worthies chosen as representing work which has helped to furnish the "instrumental, observational, and intellectual equipment of the exponents of the modern science of meteorology."

The beginnings of international co-operation in the study of meteorology are dealt with in a chapter giving an account of the first meteorological conferences.

The volume is excellently printed. Sir Napier Shaw writes in a stimulating manner, and the volume can be read with interest and pleasure not only by those who are workers in meteorology, but by a far wider circle.

Das Polarisationsmikroskop: seine Anwendung in der Kolloid-forschung und in der Färberei. Von H. AMBRONN und A. FREY. (*Kolloidforschung in Einzeldarstellungen*, Bd. 5.) Pp. x + 195, with 48 figures and 1 plate. (Leipzig: Akademische Verlagsgesellschaft m. b. H., 1926. Price 13.50 R.M.)

THIS volume is an elementary book written more especially for those with little mathematical knowledge, to enable them to use the powerful method of colloid investigation which is opened by the polarization microscope. It contains an elementary treatment of polarization and interference phenomena, which gives sufficient details for a working knowledge for the benefit of those to whom these subjects are new. This is followed by an account of various methods of investigation and determination of phase differences, and by practical details connected with the use of the polarization microscope. The second part deals with double refraction phenomena in dispersoid systems, and the third part with various optical methods which lead to information about the structure of such systems.

The polarization microscope is destined to play an increasingly important part in colloid investigation. This little handbook will serve as a useful introduction to the subject for those to whom it is new.

New Methods in Exterior Ballistics. Prof. F. R. MOULTON Pp. vi + 258, with 38 figures. (Chicago: University of Chicago Press. London: Cambridge University Press. 1926. Price 20s. net.)

THIS volume contains a brief account of some methods of external ballistics. It arises out of the duties imposed upon the author when he was placed during the war in charge of the Ballistics Branch of the Ordnance Department of the United States Army. He states in the preface that classical ballistic methods were wholly inadequate for current demands and not well suited to the solution of the problems involved. "Accordingly the subject was taken up anew by the author as a scientific problem requiring close co-ordination of adequate theory and well-conducted experiments. In view of the complete independence of the present developments from those that have gone before, no attempt has been made to treat the question historically, nor even to connect these results with those of earlier writers."

This claim is a large one, which does not appear to be fully justified, and the methods used are, in fact, not in general new. The differential equations of motion of a projectile are developed, the resistance function is then considered, and the effect of air resistance is treated by the methods of finite differences. The effects of abnormal air densities, of winds, of the rotation of the

earth, of variations in gravity, of curvature of the earth's surface, &c., are studied by the familiar method of differential variations. The motion of a rotating projectile is discussed by means of Euler's equations, and related problems, such as the oscillations of projectiles, are considered.

The treatment is mathematical throughout, and the volume is not intended for computers. It will be found of value to those interested in ballistics, though it is to be regretted that the work of earlier writers was not considered, and some of the results of recent independent researches included.

The Internal Constitution of the Stars. By A. S. EDDINGTON, M.A., LL.D., D.Sc., F.R.S. Pp. viii + 407, with 5 diagrams. (Cambridge: at the University Press. 1926. Price 25s. net.)

PROF. EDDINGTON has performed a valuable service in giving this connected account of the present state of the researches into the physical conditions in the interior of stars. The theory as it stands at present is largely his own work; as the theory has developed, various modifications have had to be made, and in referring to some of the earlier papers it is not infrequently difficult to ascertain exactly what assumptions are being used. The present volume overcomes this difficulty.

Although the theory is not free from serious difficulties, such as the explanation of the phase relationship between the light and velocity variations of Cepheid variables or the source of supply of energy in the interior of a star, it now commands general assent in its broader outlines, and fits in well with observational data. The time is therefore ripe for a connected mathematical account of the theory.

The book is characterized by the author's accustomed lucidity of style. The reader is also impressed by his physical intuition. Many of the mathematical problems to be faced can only be treated with the aid of simplifying assumptions; for these physical intuition is necessary in order to ascertain what approximations may be legitimately employed.

The introductory matter to the theory proper includes a general survey of the problem, and chapters on the thermodynamics of radiation and on the quantum theory. The concluding chapters are outside the main line of investigation, and deal with the outside of a star and with diffuse matter in interstellar space.

The methods and results of the theory have not been free from criticism. The value of the volume would have been enhanced if Prof. Eddington had considered these objections at greater length and the manner in which they may be met. To the onlooker, interested in the theory but taking no part in its development, some of the opposing views have at times proved rather puzzling, and a less cavalier treatment of rival views would have proved welcome.

The Elements of General Zoology. A Guide to the Study of Animal Biology, correlating Functions and Structure, with Notes on Practical Exercises. By WILLIAM J. DAKIN, D.Sc., Professor of Zoology in the University of Liverpool. 8vo. Pp. xvi + 496, text-figs. 252. (Oxford University Press. 1927. Price 12s. 6d.)

PROF. DAKIN has endeavoured to meet the criticism that Zoology is inferior to Botany as a subject for a school curriculum, owing to the difficulties in its experimental treatment. The mere study of structure as apart from function is uninspiring, but Prof. Dakin has shown that function and structure may be treated together, and that experiments are possible with a limited expenditure on apparatus and with material which is readily obtainable.

The subject-matter of the book does not follow the usual systematic arrangement, but is grouped under the headings of the various functions such as nutrition, respiration, blood-circulation, movement, sense, growth, reproduction, and others.

One difficulty has been to give sufficient information on structure to make intelligible the function without unduly increasing the size of the book. This has been done by means of clear annotated drawings and diagrams illustrating the anatomy of various types of animals.

In order to meet the needs of laboratory work where one type at a time will probably be studied throughout, the references in the index have been grouped under special headings; thus under Crayfish will be found references to this animal collected from all parts of the volume.

The book has been admirably produced by the Oxford Press, and is a marvel of cheapness. The illustrations call for special commendation, and the author is to be congratulated on having been able to borrow so many suitable from other works.

The Scientific Work of the late Spencer Pickering, F.R.S. Print for the Royal Society. (Harrison & Sons. 1927. Price 4s.)

PROF. A. HARDEN contributes an introductory biographical sketch of this remarkable investigator in widely different branches of Science, in physical chemistry and in the scientific and experimental study of the many problems connected with horticulture.

The first part of the volume, edited by Prof. Lowry, describes the researches in thermochemistry—Pickering's adjustable thermometer anticipating by two years that of Beckmann—theory of solution, colloid chemistry and valency.

The second part, edited by Sir John Russell, deals with Pickering's investigations on the growth of fruit-trees, the method of planting, the effect of grass, and the problems of the pests and diseases of fruit-trees.

His work on the Experimental Farm at Woburn has been described by Sir Daniel Hall "as the most substantial contribution of the last hundred years to the study of fruit-tree development."

Theory of Equations and the Complex Variable. By RAICHARAN BISWAS. (Chuckervetty, Chatterjee & Co., Calcutta.)

PROF. BISWAS has made a successful attempt to set out the Theory of Equations "from the standpoint of complex numbers." After the earlier chapters on the representation of complex numbers, Descartes' Rule, and the Theorems of Rolle and Sturm, the author introduces the "Biradical" transformation to derive the equation of the "squared differences" and the equation of the "semi sums" of the roots of an equation. Some interesting and useful applications to the solution of cubic and higher equations are given.

The approximation of the numerical roots of equations, determinants, and elimination are considered in later chapters.

Attention should be drawn to the numerous helpful exercises, some fully worked out by the author, others with answers only.

High Vacua. By G. W. C. KAYE. (Longmans, Green & Co. 1927. Price 10s. 6d.)

MANY researches in modern physics have been largely dependent for their success on the efficiency of vacuum pumps, and physicists are indebted to the author for producing a comprehensive, interesting and up-to-date treatise on this subject. Dr. Kaye traces the historical development from the mechanical pump of von Guericke and his "Magdeburg" hemispheres to the most recent high-speed pumps of Gaede and others—rotary mercury, molecular, and mercury-vapour pumps. Details of high-vacuum technique, joints, traps, leaks, cut-offs, "jetters," and backing pumps are set out.

A very complete account is given of the various high-vacuum gauges in use, the earlier instrument of McLeod and its later modifications, the radiometer and leaf-gauges of Knudsen, and other recently introduced gauges depending on gaseous, thermal, and electrical conductivities.

There is some satisfaction in noting that "during the last few years commercial high-vacuum technique of lamps and valves has made great strides" in England.

[The Editors do not hold themselves responsible for the views expressed by their correspondents.]

INDEX TO VOL. IV.

- ABSOLUTE** zero, on the properties of substances at the, 257.
- Acetic acid**, on the freezing-point of, 841.
- Activity coefficients**, on the calculation of, from conductivity measurements, 244.
- Aerosols**, on the application of the Aitken effect to the study of, 1046.
- Æther**, on the physical form of, 272.
- Aitken effect**, on the application of the, to the study of aerosols, 1046.
- Alexander** (Prof. L. M.) on the absorption of X-rays and multiple ionization of atoms, 670.
- Allan** (Dr. G. E.) on the accuracy of the monochord as a measurer of frequency, 1324.
- Alpha-particles**, on the scattering of, by helium, 605.
- Alpha-rays**, on the origin of the, 580.
- Alternating currents**, on a voltmeter for measuring the average voltage for, 1356.
- Aluminium crystals**, on the Hall effect in, 1312.
- Alums**, on the crystal structure of the, 688.
- Antennae**, on the constants of receiving and transmitting, 78.
- Antimony**, on the crystal structure of alloy of copper and, 1303.
- Antonoff** (Dr. G. N.) on the surface-tension of rock-salt, 792.
- Aqueous solutions**, on the equivalent conductivity of, 233, 300.
- Arc mercury lamp**, on a concentrated, 836.
- spectra of the oxygen group, on the, 486.
- Argon**, on the Geissler discharge in, 49.
- Artificial lines**, on a property of, 902.
- Atomic spectra**, on some new regularities in, 407.
- structure and the magnetic properties of coordination compounds, on, 1070.
- Atoms**, on the structure of radioactive, 580; on the absorption of X-rays and multiple ionization of, 670.
- AuSn**, on the automatic structure of, 133.
- Awbery** (J. H.) on the flow of heat in a body generating heat, 629.
- Bailey** (Dr. K. C.) on the effect of radon on the solubility of lead uranate, 404.
- Baker** (Capt. T. Y.) on the refraction of electromagnetic waves in a spherically stratified medium, 955.
- Balance**, on the surface-tension, 358.
- Barium**, on the spectrum of, 200.
- Barkla** (Prof. C. G.) on modified and unmodified scattered X-rays, 735.
- Bartlett** (A. C.) on an extension of a property of artificial lines, 902.
- Bateman-Herglotz equation**, on the, 531.
- Beatty** (Dr. R. T.) on resonant circuits with reactive coupling, 1081.
- Bending of thin strips**, on the, 348.
- Benzene derivatives**, on the crystallography of some, 1276.

- Beryllium, on the electrical conductivity of, at low temperatures, 386.
- Bisacre (F. F. P.) on the relativistic rule for the equipartition of energy, 949.
- Bismuth, on the arc spectrum of, 774.
- Blodgett (Dr. K. B.) on a method of measuring the mean free path of electrons in ionized mercury vapour, 165.
- Bond (Dr. W. N.) on bubbles and drops and Stokes's law, 889.
- Books, new:—Cavan's *Atoms and Molecules*, 250; Levi-Civita's *The Absolute Differential Calculus*, 250; Durell's *A Concise Geometrical Conics*, 251; Eddington's *Stars and Atoms*, 413; Clark's *Applied X-Rays*, 414; Forsyth's *The Calculus of Variations*, 415; Weatherburn's *Differential Geometry of Three Dimensions*, 415; Sommerfeld's *Three Lectures on Atomic Physics*, 416; Smithells's *Tungsten*, 638; Gifford's *Lens Computing*, 639; Darwin's *Recent Developments in Atomic Theory*, 639; Mellor's *Treatise on Inorganic and Theoretical Chemistry*, 640; *Collected Papers of Sir James Dewar*, 640; *Tables Annuelles de Constantes et Données Numériques de Chemie, de Physique, et de Technologie*, 867; Love's *Treatise on the Mathematical Theory of Elasticity*, 867; Saunders's *The Polarimeter*, 868; Bowman's *Elementary Algebra*, 868; Whitehead and Russell's *Principia Mathematica*, 868; Garrod's *The Upper Palaeolithic Age in Great Britain*, 869; Jones's *The Stone Age in Rhodesia*, 869; Hess's *Die elektrische Leitfähigkeit der Atmosphäre und ihr Ursachen*, 870; *Collected Researches: National Physical Laboratory*, 871; Forestier's *L'Énergie Rayonnante*, 871; Freundlich's *Colloid and Capillary Chemistry*, 872; von Laue's *La Théorie de la Relativité*, 1015; *Microskopische Physiographie der petrographisch wichtigen Mineralien*, 1010; Bloch's *Thermionic Phenomena*, 1243; Bray's *Light*, 1243; Blake's *History of Radio Telegraphy and Telephony*, 1243; Baly's *Spectroscopy*, 1244; Shaw's *Manual of Meteorology*, 1359; Ambronn & Frey's *Das Polarisationsmikroskop*, 1360; Moulton's *New Methods in Exterior Ballistics*, 1360; Eddington's *The Internal Constitution of the Stars*, 1361; Dakin's *The Elements of General Zoology*, 1362; *The Scientific Work of the late Spencer Pickering, F.R.S.*, 1362; Biswas, *Theory of Equations and the Complex Variable*, 1363; Kaye's *High Vacua*, 1363.
- Bowen (I. S.) on the spectral relationships of lines arising from the atoms of the first row of the periodic table, 561.
- Brentano (Dr. J.) on intensity measurements of X-ray reflexions from fine powders, 620.
- Briggs (L. J.) on cavitation in screw propellers, 1237.
- Bruce (W. W.) on the action in planetary orbits, 788.
- Bubbles, on the motion of, through viscous fluid, 889.
- Buckley (H.) on the radiation from the inside of a circular cylinder, 753.
- Bury (C. R.) on the freezing-points of concentrated solutions, 841, 1125; on the adsorption of butyric acid on water surfaces, 989.
- Butyric acid, on the freezing-point of, 841; on the adsorption of, on water surfaces, 980.
- Cadmium, on the fine structure of the spectrum lines of, in the ultraviolet, 112; on the spectrum of, 193; on the electrical conductivity of, at low temperatures, 386.
- Calcium, on the spectrum of, 200.
- Campbell (Dr. N. R.) on the characteristics of gasfilled photoelectric cells, 726.
- Carbon atom, on the reflecting power of the, for high-frequency rays, 232.
- Carr (A. J.) on Green's lemma and Stokes's theorem, 449.

- Caspari (Dr. W. A.) on the crystallography of some benzene derivatives, 1276.
- Cavitation in screw propellers, on, 17, 1237, 1239, 1240.
- Chadwick (Dr. J.) on the scattering of alpha-particles by helium, 605.
- Chromium, on the electrical conductivity of, at low temperatures, 386.
- Circuits, on resonant, with reactive coupling, 1081.
- Clarkson (W.) on the lag in electrical discharges, 121; on discharges and discharge-tube characteristics, 849; on condenser discharges in discharge-tubes, 1002, 1341.
- Cobalt, on the origin of terms of the spectrum of, 36.
- Cobbold (C. S.) on the geology of the Cambrian area of Comley, 251.
- Colloids, on the action of X-rays on, 325.
- Condenser discharge in discharge-tubes, on, 1002, 1341.
- Conductivity, on the equivalent, of strong electrolytes, 233, 300; on electrical, at low temperatures, 386.
- measurements, on the calculation of activity coefficients from, 244.
- Constantinesco torque converter, on the theory of the, 800.
- Coordination compounds, on atomic structure and the magnetic properties of, 1070.
- Copper, on the crystal structure of alloys of, with tin and antimony, 1303; on the temperature-electrical resistivity relationship in solid solution alloys of, 1338.
- spectrum, analysis of the, 1161.
- Corbino (Prof. O. M.) on the electronic theory of the voltaic cell, 436.
- Cork (Prof. J. M.) on the crystal structure of the alums, 688.
- Crowther (Prof. J. A.) on the action of X-rays on colloids, 325.
- Crystallography of some benzene derivatives, on the, 1276.
- Cylinder, on the radiation from the inside of a, 753.
- Davies (C. W.) on the calculation of activity coefficients from conductivity measurements, 244.
- Davis (Dr. A. H.) on the loud-speaker as a source of sound for reverberation work, 242.
- Dean (W. R.) on the motion of fluid in a curved pipe, 208.
- Deflexions, on a distant-reading instrument for measuring small, 269.
- Diffusion coefficients, on a method of determining, 873.
- Dilution formula, on a general, 1.
- law for strong electrolytes, on the, 831.
- Discharges and discharge-tube characteristics, on, 849, 1002, 1341; on electrodeless, through gases, 1128.
- Doan (Dr. R. L.) on the refraction of X-rays by the method of total reflexion, 100.
- Doublet laws, on the regular and irregular, 562.
- Drops, on the motion of, through viscous fluid, 889.
- Dryden (H. L.) on cavitation in screw propellers, 1237.
- Dufton (A. F.) on the warming of walls, 888.
- Earth's thermal history, on the, 338.
- Eckersley (T. L.) on the transmission of electric waves through the ionized medium, 147.
- Egnér (H.) on the effect of the acidity of the support on the structure of monomolecular films, 667.
- Elasticity, on the measurement of the, of thin strips, 348.
- Electric waves, on the transmission of, through the ionized medium, 147.
- Electrical conductivity at low temperatures, on, 386.
- discharges, on the, produced by two and three electrode systems in hydrogen, 64; on the lag in, 121.
- resistivity relationship, on the temperature-, in copper alpha solid solution alloys, 1338.
- Electrodeless discharge through gases, on the, 1128.

- Electrolytes, on the equivalent conductivity of strong, 233, 300; on the dilution law for strong, 831.
- Electromagnetic waves, on the refraction of, in a spherically stratified medium, 955.
- Electrons, on the mean free path of, in ionized mercury vapour, 165.
- Emeléus (Dr. K. G.) on the Geissler discharge in argon, 49.
- Emulsification, on the viscosity factor in, 820.
- Energy, on the absolute zero of the internal, of a substance, 257; on the relativistic rule for the equipartition of, 949.
- Entropy, on the absolute zero of, 257, 335.
- Equipartition of energy, on the relativistic rule for the, 949.
- Evans (Prof. E. J.) on the crystal structure of Cu_3 , Sn , and Cu_3Sb , 1302.
- Evaporation, on the rate of, of small spheres, 873.
- Everett (Miss A.) on the tangent lens gauge, 720.
- Fairbrother (J. A. V.) on the action of X-rays on colloids, 325.
- Ferguson (Dr. A.) on the Storch equation and the law of mass action, 1; on the equivalent conductivity of strong electrolytes, 233, 300.
- Films, on the effect of the acidity of the support on the structure of monomolecular, 667.
- Flange systems, on the effect of various, on the open-end correction of an organ pipe, 1099.
- Flashing, on the control of the, of a neon tube, 305.
- Fleming (N.) on the loud-speaker as a source of sound for reverberation work, 242.
- Fluids, on the motion of, in curved pipes, 208.
- Formic acid, on the freezing-point of, 841.
- Freezing-points of concentrated solutions, on the, 841, 1125.
- Gamma rays, on the origin of the, 599.
- Gases, on the effect of variable specific heats in, expanding through nozzles, 917; on the electrodeless discharge through, 1128.
- Geissler discharge in argon, on the, 49.
- Geological Society, proceedings of the, 251.
- Glass plates, on the silvering of, 1322.
- Glaucert (H.) on cavitation in screw propellers, 1239.
- Glenday (V. G.) on the Kateruk series of the Suk Hills, 252.
- Green (H. L.) on the application of the Aitken effect to the study of aerosols, 1046.
- Green's lemma, note on, 449.
- Hägg (G.) on the effect of the acidity of the support on the structure of monomolecular films, 667.
- Hall effect, on the, in aluminium crystals, 1312.
- Harmonic oscillator, on a radiating, without the quantum postulate, 1249.
- Harrington (Dr. E. L.) on a concentrated arc mercury lamp, 836.
- Harris (N. L.) on the Geissler discharge in argon, 49.
- Havelock (Prof. T. H.) on the dispersion of methane, 721.
- Heat, on the flow of, in a body generating heat, 629.
— regeneration and regenerative cycles, on, 526.
- Helium, on the scattering of alpha-particles by, 605; on the union of, with mercury, 699.
- Hicks (Prof. W. M.) on the analysis of the copper spectrum, 1161.
- Higgs (S. A.) on the effect of various flange systems on the open-end correction of an organ pipe, 1099.
- High-frequency sound-waves, on the effects of, 417.
- Holmes (Prof. A.) on the effect of radon on the solubility of lead uranate, 1242.
- Hume-Rothery (Dr. W.) on the metallic state, 1017.
- Hummel (F. H.) on the large bending of thin flexible strips, 348.
- Huxley (G. L. H.) on ionization by collision, 899.
- Hydrogen, on the discharges produced by two and three electrode systems in, 64.

- Hydrogen and hydroxyl ions, on the mobilities of the, 300.
- Indium, on the electrical conductivity of, at low temperatures, 386.
- Infra-red, on interference effects in the near, 682.
- Integral equations, on a class of, occurring in physics, 531.
- Integrating factors, on thermodynamic, 1245.
- Interference effects in the near infra-red, on, 682.
- Iodine, on the diffusion coefficient of, 873.
- Ionization, on multiple, 670, 763; on, by collision, 505, 899.
- Ionized medium, on the transmission of electric waves through an, 147.
- mercury vapour, on the mean free path of electrons in, 165.
- Ionizing potentials of the atoms of the first row of the periodic table, on the, 567.
- Iron, on the magnetic properties of, 641.
- J phenomenon, on the, 735.
- Jackson (Dr. L. C.) on atomic structure and the magnetic properties of coordination compounds, 1070.
- Joly (Prof. J.) on the earth's thermal history, 338.
- Jones (Dr. E. R.) on the freezing-points of concentrated solutions, 841, 1125.
- Jones (Miss P.) on the Hall effect in aluminium crystals, 1312.
- Jones (W. M.) on the crystal structure of Cu_3Sn and Cu_3Sb , 1302.
- Khastgir (Dr. S. R.) on modified and unmodified scattered X-rays, 735.
- Kichlu (P. K.) on the spectra of metals of group II., 193.
- Kleeman (Prof. R. D.) on the properties of substances in the condensed state at the absolute zero of temperature, 257.
- Kovarik (Prof. A. F.) on the behaviour of radon at low temperatures and pressures, 1262.
- Kuwada (K.) on the temperature-electrical resistivity relationship in copper alpha solid solution alloys, 1338.
- Lag in electrical discharges, on the, 121.
- Lamp, on a concentrated arc mercury, 836.
- Lathey (R. T.) on the dilution law for strong electrolytes, 831.
- Lead, on the electrical conductivity of, at low temperatures, 386.
- uranate, on the effect of radon on the solubility of, 404, 1242.
- Libman (E. E.) on a theory of porous flow, 1285.
- Lens gauge, on the tangent, 720.
- Leyshon (Dr. W. A.) on the control of the frequency of flashing of a neon tube, 305.
- Lines, on a property of artificial, 902.
- Light, on the molecular scattering of, in a liquid mixture, 447; on the transmission of, through turbid media, 1291.
- quanta and Maxwell's equations, on, 459.
- Liquid-mixtures, on the scattering of light in, 447.
- Loomis (A. L.) on the physical and biological effects of high-frequency sound-waves, 417.
- Loud-speaker, on the, as a source of sound for reverberation work, 242.
- McHugh (T.) on placing plane quadrilaterals in perspective, 28.
- McLay (Dr. A. B.) on regularities in atomic spectra, 407; on the arc spectra of elements of the oxygen group, 486.
- McLennan (Prof. J. C.) on electrical conductivity at low temperatures, 386; on regularities in atomic spectra, 407; on the arc spectra of elements of the oxygen group, 486.
- McLeod (J. H.) on the arc spectra of elements of the oxygen group, 486.
- Manley (J. J.) on the union of helium with mercury, 699; on the silvering of glass plates for optical instruments, 1322.
- Magnesium, on the spectrum of, 193.
- Magnetic properties of iron and other metals, on the, 641; on atomic structure and the, of coordination compounds, 1070.

- Martyn (D. F.) on frequency variations of the triode oscillator, 922.
- Mass action, on the validity of the law of, at limiting dilutions, 1.
- Mathur (S. B. L.) on the spectrum lines of cadmium in the ultra-violet, 112.
- Matrix mechanics without the quantum postulate, on, 1249.
- Maxwell's equations, on light-quanta and, 459.
- Meksyn (D.) on the physical form of æther, 272.
- Mercury, on the optical excitation of, 466; on the union of helium with, 699.
- lamp, on a concentrated arc, 836.
- vapour, on the mean free path of electrons in ionized, 165.
- Metallic state, on the, 1017.
- Metals, on the spectra of the, of group II., 193; on the magnetic properties of, 641.
- Methane, on the dispersion of, 721.
- Millikan (Prof. R. A.) on the spectral relationships of lines arising from the atoms of the first row of the periodic table, 561.
- Milner (Prof. S. R.) on Maxwell's stress and its time rate of variation, 943.
- Mirrors, on the silvering of, 1322.
- Mohammad (Prof. W.) on the spectrum lines of cadmium in the ultra-violet, 112.
- Monochord, on the accuracy of the, as a measurer of frequency, 1324.
- Monomolecular films, on the effect of the acidity of the support on the structure of, 667.
- Morgan (Dr. J. D.) on the three-point spark gap, 91.
- Morton (Prof. W. B.) on the large bending of thin flexible strips, 348; on the action in planetary orbits, 788.
- Moseley diagram in the field of optics, on the completed, 565.
- Neon, on the spectrum of, 223.
- tube, on the control of the flashing of a, 305.
- Networks, on the design of, for balancing telephone lines, 827.
- Nicholson (Dr. J. W.) on a class of integral equations occurring in physics, 531.
- Niven (C. D.) on electrical conductivity at low temperatures, 386.
- Norbury (Dr. A. L.) on the temperature-electrical resistivity relationship in copper alpha solid solution alloys, 1338.
- Nozzles, on the flow of gases through, 917.
- Optical excitation of mercury, on the, 466.
- Orbits, on the action in planetary, 788.
- Organ pipe, on the effect of various flange systems on the open-end correction of a square, 1009.
- Oscillator, on frequency variations of the triode, 922; on a radiating harmonic, without the quantum postulate, 1249.
- Owen (Dr. E. A.) on the atomic structure of AuSn, 133.
- Oxygen group, on the arc spectra of the, 486.
- Paris (Dr. E. T.) on resonance in pipes stopped with imperfect reflectors, 907.
- Parkinson (Dr. J.) on the Kateruk series of the Suk Hills, 252.
- Peak voltage in discharge-tubes, on the, 121.
- Perspective, on the placing of plane quadrilaterals in, 28.
- Phenol, on the freezing-points of solutions of, 1125.
- Phillips (F. C.) on the serpentines of the Shetland Islands, 253.
- Photoelectric cells, on the characteristics of gasfilled, 726.
- theory of sparking potentials, on a, 505.
- Physics, on a class of integral equations occurring in, 531.
- Pipes, on the motion of fluids in curved, 208; on resonance in, 907.
- Planetary orbits, on the action in, 788.
- Pocock (L. C.) on the design of networks for balancing telephone lines, 827.
- Ponte (M.) on the reflecting power of the carbon atom, 232.
- Porous flow, on a theory of, 1285.

- Potassium-sodium alloy, on the conductivity of, at low temperatures, 386.
- Powders, on intensity measurements of X-ray reflexions from, 620.
- Press (Prof. A.) on thermodynamic integrating factors, 1245; on consequences of a matrix mechanics and a radiating harmonic oscillator without the quantum postulate, 1249.
- Preston (G. D.) on the atomic structure of AuSn, 133.
- Propionic acid, on the freezing-point of, 841.
- Quadrilaterals, on the placing of plane, in perspective, 28.
- Quantum postulate, on the, 1249.
- Radiation, on the, from the inside of a circular cylinder, 753.
- Radioactive atom, on the structure of the, 580.
- Radon, on the effect of, on the solubility of lead uranate, 404, 1242; on the behaviour of, at low temperatures and pressures, 1162.
- Raman (Prof. C. V.) on the molecular scattering of light in a binary liquid mixture, 447.
- Rashevsky (Dr. N.) on light-quanta and Maxwell's equations, 459.
- Refraction, on the, of X-rays, 100; on the, of electromagnetic waves in a spherically stratified medium, 955.
- Regenerative cycles, on heat regeneration and, 526.
- Relativistic rule for the equipartition of energy, on the, 949.
- Relf (E. F.) on a distant-reading instrument for the measurement of small deflexions, 269.
- Resistivity relationship, on the, in copper alpha solid solution alloys, 1338.
- Resonance in pipes stopped with imperfect reflectors, on, 907.
- Resonant circuits with reactive coupling, on, 1081.
- Richey (J. E.) on the Mourn granite, 254.
- Richtmyer (Prof. F. K.) on the classical theories of the absorption and refraction of X-rays, 1296.
- Rideal (E. K.) on interference effects in the near infra-red, 682.
- Robinson (Prof. H. R.) on multiple ionization in X-ray levels, 763.
- Rock-salt, on the surface-tension of, 792.
- Rubidium, on the electrical conductivity of, at low temperatures, 386.
- Rutherford (Sir E.) on the structure of the radioactive atom and origin of the alpha-rays, 580; on the scattering of alpha-particles by helium, 605.
- Saha (Prof. M.) on the spectra of metals of group II., 193; on the spectrum of neon, 223.
- Sandeman (Dr. E. K.) on the torque converter, 800.
- Schrödinger's wave functions, on the application of, to the calculation of transition probabilities for the principal series of sodium, 495.
- Screw propellers, on cavitation in, 17, 1237, 1239, 1240.
- Shearer (J.) on a vacuum spectrograph and its use in the long X-ray region, 745.
- Silberstein (Dr. L.) on the transparency of turbid media, 1291.
- Silvering of glass plates, on the, 1322.
- Simmons (L. F. G.) on a distant-reading instrument for the measurement of small deflexions, 269.
- Smith (Dr. R. C.) on the viscosity factor in emulsification, 820.
- Sodium, on the transition probabilities for the principal series of, 495.
- chloride, on X-ray reflexion from, 620.
- potassium alloy, on the electrical conductivity of, at low temperatures, 386.
- Sollesnes (K.) on the structure of trimethylammonium iodide, bromide, and chloride, 985.
- Solutions, on the freezing-points of concentrated, 841, 1125.
- Sound-waves, on the effects of high-frequency, 417.
- Spark gap, on the three-point, 91.
- Sparkling potentials, on a photoelectric theory of the, 506.
- Specific heats, on the effect of variable, in gases expanding through nozzles, 917.

- Spectra, on the, of the metals of group II., 193; on some new regularities in atomic, 407; on the arc, of the oxygen group, 486.
- Spectral relationships of lines from the atoms of the first row of the periodic table, on the, 561.
- Spectrograph, on a vacuum, 745.
- Spectroscopic rules, on the new, 563.
- Spectrum of cobalt, on the, 36; on the ultra-violet, of cadmium, 112; on the, of neon, 223; on the arc, of bismuth, 774; analysis of the copper, 1161.
- Spheres, on the rate of evaporation of small, 873.
- Stokes's law, on, 449, 889.
- Storch equation, on the, 1.
- Stress, on Maxwell's, and its time rate of variation, 943.
- Strips, on the bending of thin, 348.
- Strontium, on the spectrum of, 200.
- Substances, on the properties of, at the absolute zero, 257.
- Sugiura (Y.) on the transition probabilities for the principal series of sodium, 495.
- Super-sonic vibrations, on the effects of, 417.
- Sur (N. K.) on the spectrum of cobalt, 36.
- Surface-tension of rock-salt, on the, 792.
- balance, on the, 358.
- Tangent lens gauge, on the, 720.
- Taylor (A. M.) on interference effects in the near infra-red, 682.
- Taylor (Dr. J.) on ionization by collision, 505; on a voltmeter for measuring the average voltage for alternating currents, 1356.
- Telephone lines, on the design of networks for balancing, 827.
- Temperature-electrical resistivity relationship in copper alpha solid solution alloys, on the, 1338.
- Tetramethylammonium: chloride, bromide, and iodide, on the structure of, 985.
- Thermodynamic integrating factors, on, 1245.
- Thomson (Sir J. J.) on the electrodeless discharge through gases, 1128.
- Thorium, on the electrical conductivity of, at low temperatures, 886.
- Three-point spark gap, on the, 91.
- Tin, on the crystal structure of alloy of copper and, 1303.
- Topley (B.) on the rate of evaporation of small spheres, 873.
- Torque converter, on the theory of the, 800.
- Toshniwal (G. R.) on the arc spectrum of bismuth, 774.
- Transition probabilities for the principal series of sodium, on the, 425.
- Transparency of turbid media, on the, 1291.
- Trevelyan (Miss B.) on the discharges produced by two and three electrode systems in hydrogen, 64.
- Triode oscillator, on frequency variations of the, 922.
- Turbid media, on the transparency of, 1291.
- Tutin (J.) on cavitation in screw propellers, 17, 1240.
- Tyte (L. C.) on the effect of various flange systems on the open-end correction of an organ pipe, 1099.
- Ultra-violet spectrum of cadmium, on the, 112.
- Vacuum spectrograph, on a, 745.
- Vegard (Prof. L.) on the structure of xenotime, 511; on the structure of trimethylammonium iodide, bromide, and chloride, 985.
- Verschaffelt (Prof. J. E.) on the absolute zero of entropy and internal energy, 335.
- Vibrator, on the control of the frequency of the flashing of a neon tube by a maintained, 305.
- Viscosity factor in emulsification, on the, 820.
- Vogel (I.) on the Storch equation and the law of mass action, 1; on the equivalent conductivity of strong electrolytes, 233, 300.
- Voltaic cell, on the electronic theory of the, 436.
- Voltmeter, on a, for measuring the average voltage for alternating currents, 1356.
- de Waard (Dr. R. H.) on the magnetic properties of iron and other metals, 641.

- Wadlow (Dr. E. C.) on the expansion of gases through nozzles, 917.
- Walker (Prof. W. J.) on heat regeneration and regenerative cycles, 526.
- Waller (I.) on the scattering of radiation from atoms, 1228.
- Wallis (Dr. F. S.) on the old red sandstone of the Bristol district, 254.
- Walls, on the warming of, 888.
- Warren (E. L.) on the surface-tension balance, 358.
- Waves, on the transmission of electric, through the ionized medium, 147; on the refraction of electromagnetic, in a spherically stratified medium, 955.
- Whittard (Dr. W. F.) on the Valentinian rocks of Shropshire, 255.
- Whytlaw-Gray (R.) on the rate of evaporation of small spheres, 873.
- Wilmotte (R. M.) on the constants of receiving and transmitting antennæ, 78.
- Wood (Prof. R. W.) on the physical and biological effects of high-frequency sound-waves, 417; on the optical excitation of mercury, 466.
- Wrinch (Dr. D. M.) on a class of integral equations occurring in physics, 531.
- Xenotime, on the structure of, 511.
- X-ray levels, on multiple ionization in, 763.
- reflexions, on intensity measurements of, from fine powders, 620.
- wave-length measurements, on, 745.
- X-rays, on the refraction of, by the method of total reflexion, 100; on the action of, on colloids, 325; on the absorption of, 670; on modified and unmodified scattered, 735; on the classical theories of the absorption and refraction of, 1296.
- Zinc, on the spectrum of, 193.
- Zircon, on the crystal structure of, 511.

END OF THE FOURTH VOLUME.

GAYLORD			PRINTED IN U.S.A.

GAYLORD

PRINTED IN U.S.A.